QUANTIFICATIONS OF THE DETRIMENTAL HEALTH EFFECTS OF IONISING RADIATION

A thesis submitted to the University of Manchester for the degree of
Doctor of Science (DSc)
in the Faculty of Medical & Human Sciences

2012

Linda Walsh (*formerly* Grimshaw) BSc, MSc, PhD

Dedication. *This thesis is dedicated to people who have had their quality of life diminished by the effects of ionising radiation from nuclear accidents or war. In particular to those affected: since 1945 by the World War II A-bomb attacks on Hiroshima and Nagasaki; since 1986 by the Chernobyl nuclear accident; and since 2011 by the Fukushima nuclear accident following the major earthquake and tsunami. I sincerely hope that some aspects of the global scientific effort invested in quantifying the detrimental health effects of ionising radiation may be of some direct benefit to these people, in addition to increasing our scientific knowledge in this area.*

"As has so often happened in epidemiology, clues may be discovered before the intimate processes of the disease are fully understood."

J.N. Morris, J.A. Heady, P.A.B. Raffle, C.G. Roberts & J.W. Parks,
Coronary heart-disease and physical activity of work,
The Lancet, page 111, Nov 28, 1953.

Contents   Page number

A note on the citation scheme applied in this thesis:
The references listed in the "General references" section are cited with the name of the first author and the year of publication. The publications involving the candidate, other than those listed for DSc consideration, as listed in section I of the "Main statement", are cited by number in square brackets. The journal publications involving the candidate, as listed for DSc consideration in section II of the "Main statement", are cited by number in curved brackets.

Abstract

This thesis, presented to The University of Manchester in 2012 by Dr. Linda Walsh, is in fulfilment of the requirements for the degree of Doctor of Science (DSc) and is entitled "Quantifications of the detrimental health effects of ionising radiation." A body of work and ensuing publications covering 2000–2012 are presented, predominantly concerning studies of various cohorts of people exposed to ionising radiation. The major areas cover epidemiological and statistical studies on the Life span study (LSS) cohort of Japanese survivors of the World War II atomic-bomb attacks on Hiroshima and Nagasaki and the mortality follow-up of German uranium miners.

Following the presentation of a very brief history of the effects of radiation exposure on humans, the background and context of the advances achieved by the candidate are described. The LSS provides the most studied cohort and a range of topics from cancer risks related to neutron and γ-ray doses, organ specific doses, and carcinogenesis have been explored covering about half of the candidate's publications. The cohort of German "Wismut" uranium miners exposed to radon and other potential carcinogens, which is the largest one of its kind, has enabled the development of epidemiological models for lung and extra-pulmonary cancers. The third distinct topic relates to analyses of data on cellular radiation damage relevant to the evaluation of both diagnostic radiation characteristics and the effects on cancer patients. Other studies have considered the incidence of malignant diseases in humans injected with radium-224 and development of epidemiological models for thyroid cancer risk in areas affected by the 1986 Chernobyl accident.

Fundamental contributions have been published in the application of mathematical methods for data analysis. The candidate has succeeded in going beyond the traditional statistical methods in radiation epidemiology by introduction of numerical techniques deriving from the field of information science and novel to the field. These methods, such as techniques for model selection and mitigation of strongly correlated quantities, have been presented as general tools and have demonstrated powerful results, such as in applications to data from LSS. The impact and relevance for public health of the epidemiological results is indicated by their frequent citation in recent reports by international bodies such as by the International Commission on Radiological Protection, the United Nations Scientific Committee on the Effects of Atomic Radiation, the World Health Organization (WHO) and WHO-International Agency for Research on Cancer.

Several topics, from among this broad coverage of radiation epidemiological themes, the development of novel statistical techniques and their application, are highlighted. Work on distinguishing the effect of neutrons and γ-rays in the Japanese LSS data has led to progress on quantifying their relative biological effectiveness with important consequences for the health effects of modern radiation diagnostics. A technique for combining risks from several risk models, called multi-model inference, has been shown to ease the dilemma of selecting between models with very different consequences, with particular relevance for major issues of public health concern connected with radiation exposure. The Wismut cohort has revealed for the first time the response characteristics of a significant effect of working underground on prostate cancer incidence, suggesting a relation with lack of exposure to light which remains unexplained.

Declaration

Candidate Name: Dr. Linda Walsh

Faculty: Faculty of Medical & Human Sciences

Higher Doctorate Title: Doctor of Science (DSc)

The publications on the detrimental health effects of ionising radiation on: Japanese A-bomb survivors (publication numbers 1-5, 7, 8, 11-13, 16, 20-23, 28-30, 37, 38, 41, 43, 44, 46-48); patients treated with radiation (10, 36); persons affected by the Chernobyl nuclear power plant accident (14, 27); German uranium miners (24, 26, 32-35, 39, 40, 42, 45, 49, 50); and radio-biological studies relevant to diagnostic radiation procedures (6, 9, 15, 17-19, 25, 31); have been either written by, or contain substantial contributions by, the candidate, Dr. Linda Walsh.

The specific nature of the contributions of the candidate to the papers in which she was not first author involved: the choice of methods and performance of the data analysis and risk analysis in the radiation epidemiological papers; the selection and application of statistical methods for data analysis including the fitting of mathematical functions to the experimental data; Monte-Carlo simulation (often for the assessment of uncertainties); and the selection and application of both parametric and non-parametric tests in the radiation biological papers. The candidate had the full responsibility for the risk analysis in all radiation epidemiological papers except in references 10, 36, 43 and 48. The candidate also contributed to the writing of the papers and often wrote the statistical methods and results sections and assisted in other sections.

In the papers where the candidate was the primary author (7, 8, 11, 21, 27, 29, 33, 34, 37, 38, 39, 41, 42, 44, 46, 47) the candidate concieved and wrote the publications and also performed the mathematical analyses that were double checked by co-authors.

The main primary scientific collaborators and co-authors (with a brief description of their contributions) were as follows:-
Prof. A. M. Kellerer (1-4, 7, 8, 11, 12, 13). Prof. Kellerer was the primary author of (1-4 and 13). The candidate was approximately equally contributing author in

all five papers and contributed to the ideas and their formalisation and development, did all the epidemiological data analysis and contributed to the writing of the papers.

Prof. W. Rühm (5, 7, 8, 11, 12, 13, 16, 20, 28). Prof. Rühm was the primary author of (5, 12, 16 and 20). The candidate was approximately equally contributing author for (5, 20) and made major contributions to all the other papers listed.

Dr. E. A. Nekolla (1, 4, 10, 16, 36). Dr. Nekolla was the primary author of (10 and 26) and the candidate made contributions to the double checking of results and the writing of the papers.

Dr. P. Jacob (14, 23, 27, 28, 43, 44). Dr. Jacob was the primary author of (14, 23 and 28). The candidate was approximately equally contributing author in (23 and 28) and contributed in all papers listed to the ideas and their formalisation and development, did all the epidemiological data analysis and contributed to the writing of the papers.

Prof. U. Schneider (22, 30, 46). Prof. Schneider was the primary author of (22 and 30). The candidate was approximately equally contributing author in (22 and 30) and contributed to the ideas and their formalisation and development, performed the epidemiological data analysis and contributed to the writing of the papers.

Dr. M. Kreuzer (24, 26, 32-35, 39, 40, 42, 45, 49, 50). Dr. Kreuzer was the primary author of (24, 26, 32, 35 and 49). The candidate was approximately equally contributing author in (24, 26 and 32) and contributed in all papers listed to the ideas and their formalisation and development, developed all the epidemiological data analysis programs and contributed to the writing of the papers.

Prof. E. Schmid (6, 9, 17, 31). Prof. Schmid was the primary author of (31) and the candidate was responsible for the data analysis, simulations and contributed to the the writing of the papers.

Dr. W. Göggelmann (6). Dr. Göggelmann was the primary author of (6) and was responsible for the main biological laboratory work. The candidate performed the data analysis and contributed to the writing of the paper.

Dr. M. Gomolka (9, 15, 17). Dr. Gomolka was the primary author of (9) and was responsible for the main biological laboratory work. The candidate was responsible the data analysis and contributed to the writing of the paper.

Dr. U. Oestreicher (19, 25). Dr. Oestreicher was the primary author of (25) and was responsible for the main biological laboratory work. The candidate was responsible for the data analysis and contributed to the writing of the paper.

Dr. G. Stephan (19, 25). Dr. Stephan was the primary author of (19) and did the main biological laboratory work. The candidate was responsible for the data analysis and contributed to the writing of the paper.

Dr. S. Hornhardt (9,15,17). Dr. Hornhardt was the primary author of (15) and did the main laboratory work. The candidate assisted with the data analysis and writing of the paper.

Dr. J. Yang (18). Dr. Yang was primary author of this paper and the candidate was involved in scientific discussions and the writing of the paper

Dr. F. Dufey (32-34, 39, 40, 42, 45, 49, 50). Dr. Dufey was primary author of (40 and 50). The candidate was equally contributing author for (40) and contributed ideas, analysis programs and to the writing of (50).
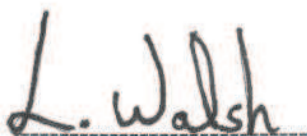
Dr. H. Schöllnberger (43, 44). Dr. Schöllnberger was the primary author of (43) and the candidate contributed the main idea behind the analysis and contributed to the writing of the paper.

Dr. J-C. Kaiser (27, 38, 44, 48). Dr. Kaiser was the primary author of (48) and the candidate contributed the idea behind the analysis, independent double checking of the epidemiological risk analyses and to the writing of the paper.

Mrs. M. Sogl (40, 42, 45, 49, 50). Mrs. Sogl was the primary author of (45) and the candidate contributed to the ideas behind the analysis, data analysis programs and independent double checking of risk analyses and to the writing of the paper.

I certify that none of the work contained in this thesis has been submitted in support of a successful or pending application for any other degree or qualification of this or any other University or of any professional or learned body.

I confirm that this is a true statement and that, subject to any comments above, the submission is my own original work.

L. Walsh

SIGNATURE

22nd November 2012

DATE

10

Copyright statement

i. The author of this thesis (including any appendices and/or schedules to this thesis) owns any copyright in it (the "Copyright") and she has given The University of Manchester the right to use such Copyright for any administrative, promotional, educational and/or teaching purposes.

ii. Copies of this thesis, either in full or in extracts, may be made only in accordance with the regulations of the John Rylands University Library of Manchester. Details of these regulations may be obtained from the Librarian. This page must form part of any such copies made.

iii. The ownership of any patents, designs, trademarks and any and all other intellectual property rights except for the Copyright (the "Intellectual Property Rights") and any reproductions of copyright works, for example graphs and tables ("Reproductions"), which may be described in this thesis, may not be owned by the author and may be owned by third parties. Such Intellectual Property Rights and Reproductions cannot and must not be made available for use without the prior written permission of the owner(s) of the relevant Intellectual Property Rights and/or Reproductions.

iv. Further information on the conditions under which disclosure, publication and exploitation of this thesis, the Copyright and any Intellectual Property Rights and/or Reproductions described in it may take place is available from the Head of School of Medicine (or the Vice-President) and the Dean of the Faculty of Life Sciences, for Faculty of Life Sciences' candidates.

Main Statement

I. Candidate's qualifications and research experience - curriculum vitae

Name:	Linda Walsh (formerly Grimshaw)
Date and Place of Birth:	22 February 1958, Bolton, Lancashire, England.
Nationality:	British
Family Status:	Married since 1983, with one son born in 1989.
Current Address:	Bettinastrasse. 28 D-81739 München Germany Tel: +49 89 601 3327 (home) +49 89 31603 2258 (work) E-mail: lwalsh@bfs.de

Academic Qualifications:
(*copies of certificates in appendix*.)

BSc (Hons.) Physics
Manchester University, 1979
MSc Title of thesis: Factors affecting the motion of
                    interplanetary dust particles
Manchester University, 1980
PhD Title of thesis: Numerical simulations of
                      ellipsoidal galaxies
Manchester University, 1985

Employment History:

Nov 2007 – present, Research Scientist
    BfS, Federal Office for Radiation Protection
    Ingolstaedter Landstrasse. 1
    85764 Neuherberg, Germany

Mar 2005 – Oct 2007, Research Scientist
     GSF, National Research Institute for
     Environment & Health,
     Ingolstaedter Landstrasse. 1
     85764 Neuherberg, Germany

Feb 2000 – Feb 2005, Research Associate
     Ludwig–Maximilians University
     Department of Radiobiology
     Schillerstrasse. 42
     80336 Munich, Germany

Oct 1993 – Jan 2000, Professor

European University Switzerland, European Business College
Berg-am-Laim Strasse. 47
81673 Munich, Germany

Aug 1992 – Jan 1995, Research Associate (part-time)
Department of Mathematics
Technical University of
Munich, Germany

Oct 1988 – Aug 1989, Research Associate
Department of Space Research
University of Groningen, the Netherlands

Oct 1985 – May 1988, Research Associate
Department of Applied Mathematics
University of New South Wales, Australia

May 1980 – Nov 1981, Research Assistant
Department of Polymer and Fibre Science
University of Manchester
Institute of Science and
Technology (UMIST), United Kingdom

Aug 1979 – May 1980, Dynamics Engineer
British Aerospace
Bolton, United Kingdom

Areas of Competence:

Since reading theoretical and experimental physics at the Schuster Laboratory, University of Manchester, U.K., international professional experience has been developed, in using computers as scientific tools. This experience is in statistical data analysis, mathematical modelling and computer simulation in the various research fields of Astrophysics, Space Science, Numerical Analysis and more recently, since the year 2000, Cancer Epidemiology and Radiation-Biophysics (health risk assessment). Substantial lecturing experience has also been gained in the areas of Statistics, Quantitative Methods and Epidemiology for both Bachelor and Master Students.

Research Experience:

The MSc by research, awarded in 1980, involved mathematical modelling to compute the radii of dust-free zones around the Sun. This modelling involved solving a set of stiff differential equations which represented the joint temporal

development in the dynamics and thermodynamics of interplanetary dust containing silicon and iron [1, 2]. The results of these models formed the scientific basis for a solar eclipse expedition to central Java, Indonesia in 1983 which was funded by the Royal Society, London.

The scientific computer programming and image processing experience which I gained whilst at the Department of Polymer and Fibre Science at UMIST was invaluable when I started a PhD project in the Astronomy Group of the Physics Department at Manchester University. The area of research was experimental stellar dynamics, involving the programming and analysis of N-body particle-mesh simulations (25,000 particles) of elliptical galaxies. Elliptical galaxies had been observed to rotate more slowly than theoretically expected and were suspected of being tri-axial ellipsoids. The computer simulations investigated many dynamical and observable properties of forty simulated galaxies which were allowed to evolve, for a time period equal to one quarter of the age of the Universe, from a wide variety of initial conditions. The computer models (which formed a parameter search) were subsequently image processed and compared to a wide range of relevant observations using many statistical analysis techniques. For this project, the most powerful vector processing computer then available (Cray 1) was needed and used to full potential. During this period of study as a doctorate student, I was also involved in observations of binary stellar systems and cataclysmic variable stars using the 60-inch (1.52m) infra-red telescope on Tenerife [3].

During the period of employment at the University of New South Wales, I researched lattice methods for multidimensional integration, in collaboration with Prof. I. H. Sloan in the School of Mathematics. The lattice rules are particular types of multidimensional non-random sets of points that form good abscissas for numerical integration. Computer searches were performed to find the 'best' such rules, according to a number-theoretic criterion, and a new class of lattice rules for the numerical integration of practical multidimensional integrals was identified [4, 6]. This new class was later confirmed by pure mathematicians working in the field of Number Theory. My contribution was to write the scientific programmes and perform the large scale extensive computer searches in Fortran with vector extensions for a Cyber 205 super-computer.

I was also employed by SRON (Space Research Organisation of the Netherlands) at the Rijksuniversiteit Groningen. This research work involved an investigation of the quantity and character of debris orbiting the earth which might be a hazard to spacecraft. The Infra Red Astronomical Satellite (IRAS) all-sky infra-red survey had produced maps of the sky in four wavebands separated by time intervals of minutes, hours and months. The sky maps were studied to determine efficient statistical signal-processing methods for locating the debris [5, 7 and 8]. I also spent time on the mathematical theory necessary for relating space debris orbital parameters to the IRAS signal detection measurements. The details of my research were included in a report to the European Space Agency which directly resulted in a five person-year research contract for SRON, Groningen, the Netherlands.

Research work done at the department of Mathematics of the Technical University in Munich, involved a detailed comparison study of two numerical methods applied in computer simulations of the Sun [9]. It was shown that, in order to achieve a precision which is equivalent to or higher than the relevant solar observations, a multiple shooting method is better suited than a differencing scheme for solving the set of differential equations describing the internal structure of the Sun.

During the period 2000–2012, scientific research work has been in the application of computer supported statistical and quantitative methods for evaluating the detrimental health risks from exposure to ionising radiation, i.e., radiation risk assessment. This research has been conducted mainly in Munich, Germany at the (former) Instiute of Radiobiology, Ludwig Maximillians University, the Helmholz Centre (formerly GSF) and the German Federal Office for Radiation Protection (BfS). It is the research conducted during this time-period that is presented in this thesis for consideration of the DSc degree (please see section II for the complete list of the publications submitted, and the copies of each of the publications at the end of the thesis). However the past experience gained in statistics, physics, programming and numerical analysis prior to entry into this research field has been invaluable in conducting the research detailed in the main body of this thesis.

I have recently been a World Health Organization panel member for the health risk assessment after the Fukushima nuclear power plant radiation realease in 2011. As a member of this panel, I made substantial contributions to the selection of risk assessment methodology, performed the actual risk calculations and wrote some major sections of the final report (WHO, 2012).

Since January 2012, I have been a partner, task leader and project board member of an international research project started under the seventh framework programme of the European Union, FP-7-EU-ANDANTE (Multidisciplinary evaluation of the cancer risk from neutrons relative to photons using stem cells and the analysis of second malignant neoplasms following paediatric radiation therapy)

I have also served as external expert journal reviewer for Radiation Research, Radiation & Environmental Biophysics, The British Medical Journals Occupational and Enviroinmental Medicine, BMJ open and some other journals.

Teaching and Lecturing Experience:

Teaching experience includes physics and computing tutorials at the University of Manchester, statistics, linear algebra and calculus tutorials and computer consulting for faculty of science students at the University of New South Wales, Australia. Many seminars have been presented, a few recent examples of which are tabulated below.

As a professor at the European University – European Business College, Munich, lectures were presented in statistics and calculus courses for the Bachelor of Business Administration, over a seven year period. In the Master of Business Administration (MBA, executive, degree programme), I lectured the Quantitative Business Methods course and supervised two MBA theses (T1, T2). From the beginning of 2005, I was invited to present annual lectures on the health risks associated with low doses of ionising radiation to students of the European Master of Science Degree in Radiation Biology (University College London & Gray Cancer Institute, U.K.). Since 2009, I am also an external lecturer for the MSc course in epidemiology at the Ludwig Maximillians University, Munich, Germany.

Publications (other than those listed for DSc consideration):

1. Grimshaw L. The origin of micrometeorites. Aerospace Dynamics. 3, 18-20, 1980

2. Grimshaw L. Factors affecting the motion of interplanetary dust particles. Moon and Planets. 26, 305-310, 1982

3. Elsworth Y, Grimshaw L & James JF. A possible outburst on AM Canem Venaticorum. Monthly Notices of the Royal Astronomical Society. 201, 45P-47P, 1982

4. Sloan IH & Walsh L. Lattice rules - classification and searches. In Proceedings of the Oberwolfach Conference on Numerical Integration, ed. Brass, H. & Hämmerlin, G., Birkhauser, 251-260, 1988

5. Walsh L & Wesselius PR. Detecting Space Debris above 900 km using IRAS. European Space Agency Report, March 1989, 1-30, 1989

6. Sloan IH & Walsh L. A computer search of rank 2 lattice rules for multidimensional quadrature. Mathematics of Computation. 54, 281-302, 1990

7. Walsh L, Wesselius PR & Olthof H. Detecting Space Debris above 900 km using IRAS (Infra-Red Astronomical Satellite). In Space Safety and Rescue 1988-1989. Volume 77. Science and Technology Series. Ed. Heath, G. W. (Ref. No. IAA-89-629), 345-354, 1990

8. Adorf H-M, Albrecht R & Walsh L. Space Debris: how serious is the situation? Hubble Space Telescope – European Coordinating Facilty Newsletter, No. 12, 13-14, 1990

9. Reiter J, Walsh L & Weiss A. Solar models: a comparative study of two stellar evolution codes. Monthly Notices of the Royal Astronomical Society. 274, 899-908, 1995

10. Walsh JR & Walsh L. Astronomy and astrophysics library: Tools of radio astronomy, 4th revised and enlarged edition, Book Review, Radiat Environ Biophys. 43, 141, 2004

11. Walsh JR & Walsh L. The orientation of the Greek temple of Epicurean Apollo. Astronomy and Geophysics. 47, p4.8, 2006

Supervised theses:

T1. Saldivar, Gilberto Romero. E-Commerce – An Opportunity for Developing Countries. A thesis presented to the European University in partial fulfillment of the requirements for the degree Master in Business Administration, 1998

T2. Andreeva, Petia. Production Applications of Management Science. A thesis presented to the European University in partial fulfillment of the requirements for the degree Master in Business Administration, 1999

Some Recent Lectures:

Walsh L	Epidemiology of the A-bomb survivors, Radiation Epidemiology course of the Master of Science in Epidemiology course, LMU Munich, 15.02.2012
Walsh L	Epidemiology of neutron risks, EU-ANDANTE project kick-off meeting, University of Pavia, Italy, 25.1.2012
Walsh L	Dose response models for the WHO Fukushima health risk assessment, Geneva, Switzerland, 14.12.2011
Walsh L (on behalf of Prof. H. Spiess – the invited speaker)	Life span study on Late Effects of Radium-224 in Children and Adults. HEIR09 conference Santa Fe, New Mexico 11.05.09
Walsh L	Non-skeletal Malignant Diseases in Patients Treated with Radium-224. HEIR09 conference Santa Fe, New Mexico 11.05.09
Walsh L	Radon and the risk of cancer Updated results of the German uranium miners cohort study, 1946–2003. HEIR09 conference Santa Fe, New Mexico 11.05.09

Membership of
Professional
Societies: Fellow, Royal Astronomical Society, London, U.K.

Areas of
Academic Interest: Physics, Mathematics, Statistics, Epidemiology
(medical data analysis, risk assessment and
 simulation),
Astronomy and Space Science.

Computer Skills: FORTRAN, Basic, C and C++, Mathematica,
IDL (Interactive Data Language), Kaleidagraph,
 MATLAB and epidemiological software – EPICURE.

Language Skills: English: mother tongue,
 German: fluent.

Professional references
may be obtained from:

Prof. emeritus Dr. Albrecht M. Kellerer
Former Radiobiological Institute,
University of Munich
Schillerstrasse 42,
80336 Munich, Germany.
Tel: +49-89-260 22084
Email: amkellerer@googlemail.com

Prof. Dr. Werner Rühm
Individual Dosimetry Group Leader
Institute for Radiation Protection
Helmholtz center Munich
Ingolstaedter Landstrasse 1
85764 Neuherberg, Germany
Tel: +49-89-3187 3359
E-mail: werner.ruehm@helmholtz-muenchen.de

Prof. Dr. Ernst Schmid
Former Radiobiological Institute,
University of Munich
Schillerstrasse 42,
80336 Munich, Germany.
Tel: +49-89-218075 820
Fax: +49-89-218075 840
Email: ernst.schmid@lrz.uni-muenchen.de

Dr. Thomas Jung
Head of Department
Department of Radiation Protection and Health
Federal Office for Radiation Protection
Ingolstaedter Landstrasse 1
85764 Oberschleissheim
Germany
Phone: +49-30-18333 2200
Fax: +49-30-18333 2205
Email: tjung@bfs.de

II. Complete list of the publications submitted for consideration for the DSc degree

The publications cover the time period 2001–2012 and are first given in chronological order according to type (journal and book publications and other works) and then the journal and book publications are re-grouped according to subject. The journal publications listed in this section are cited by number in curved brackets in the text. A publication matrix, including journal impact factors and the number of citations is included at the end of the reference list and is described in detail in the overall summary section.

Chronological order, journal and book publications

1. Kellerer AM, Nekolla E & Walsh L. On the conversion of solid cancer excess relative risk into lifetime attributable risk. Radiat. Environ. Biophys. 40, 249-257, 2001

2. Kellerer AM & Walsh L. Risk estimation for fast neutrons with regard to solid cancer. Radiat. Res. 156, 708-717, 2001

3. Kellerer AM & Walsh L. Solid cancer risk coefficient for fast neutrons, in terms of effective dose. Radiat. Res. 158, 61-68, 2002

4. Kellerer AM, Walsh L & Nekolla EA. Risk coefficient for γ-rays with regard to solid cancer. Radiat. Environ. Biophys. 41, 113-123, 2002

5. Rühm W, Walsh L & Chomentowski M. Choice of model and uncertainties of the gamma-ray and neutron dosimetry in relation to the chromosome aberrations data in Hiroshima and Nagasaki, Radiat. Environ. Biophys. 42, 119-128, 2003

6. Göggelmann W, Jacobsen C, Panzer W, Walsh L, Roos H & Schmid E. Re-evaluation of the RBE of 29 kV X-rays (mammography X-rays) relative to 200 kV X-rays using neoplastic transformation of human CGL1-hybrid cells. Radiat. Environ. Biophys. 42, 175-182, 2003

7. Walsh L, Rühm W & Kellerer AM. Cancer risk estimates for γ-rays with regard to organ specific doses Part I: All solid cancers combined. Radiat. Environ. Biophys. 43, 145-151, 2004

8. Walsh L, Rühm W & Kellerer AM. Cancer risk estimates for γ-rays with regard to organ specific doses Part II: Site specific solid cancers. Radiat. Environ. Biophys. 43, 225-231, 2004

9. Gomolka M, Rössler U, Hornhardt S, Walsh L, Panzer W & Schmid E. Measurement of the Initial Levels of DNA Damage in Human Lymphocytes induced by 29 kV X Rays (Mammography X Rays) Relative to 220 kV X Rays and γ Rays. Radiat. Res. 163, 510-519, 2005

10. Nekolla EA, Walsh L, Schottenhammer G & Spiess H. Malignancies in patients treated with high doses of radium-224. Proc, 9th Internat. conf. on Health Effects of Incorporated Radionuclides (HEIR 2004), Oeh U, Roth P, Paretzke HG (Eds.), GSF-Forschungszentrum GmbH, 67-74, 2005

11. Walsh L, Rühm W & Kellerer AM. Curvature in the dose response of the life span study cancer mortality data. Radiat. Res. 163, 477, 2005

12. Rühm W, Walsh L & Kellerer AM. Analysen der neusten LSS-Mortalitätsdaten (in German). Veröffentlichungen der Strahlenschutzkommission, Band 56, 43-56, Elsevier, Urban & Fischer, 2005

13. Kellerer AM, Rühm W & Walsh L. Indications of the neutron effect contribution in the solid cancer data of the A-bomb survivors. Health Physics. 90(6), 554-564, 2006

14. Jacob P, Bogdanova TI, Buglova E, Chepurniy M, Demidchik Y, Gavrilin Y, Kenigsberg J, Meckbach R, Schotola C, Shinkarev S, Tronko MD, Ulanovski A, Vavilov S & Walsh L. Thyroid Cancer Risk in Areas of Ukraine and Belarus affected by the Chernobyl Accident. Radiat. Res. 165, 1-8, 2006

15. Hornhardt S, Gomolka M, Walsh L & Jung T. Comparative investigations of sodium arsenate, arsenic trioxide and cadmium sulphate in combination with gamma-radiation on apoptosis, micronuclei induction and DNA damage in a human lymphoblastoid cell line. Mutation Res. 600, 165-176, 2006

16. Rühm W, Walsh L & Nekolla E A. The Cohort of the Atomic Bomb Survivors - Major Basis of Radiation Safety Regulations. CERN Yellow Series, Report 12, 319-329, 2006

17. Rössler U, Hornhardt S, Seidl C, Müller-Laue E, Walsh L, Panzer W, Schmid E, Senekowitsch-Schmidtke R & Gomolka M. The sensitivity of the alkaline comet assay in detecting DNA lesions induced by X-rays, gamma-rays and alpha particles. Proc. 14th International Symposium on Microdosimetry: Ionising radiation quality, molecular mechanisms, cellular effects and their consequences for low level risk assessment and radiation therapy, Nov 13-18, 2005, Venice, Italy, Radiat. Prot. Dosim. 122(1-4), 154-159, 2006

18. Yang Jianshe, Jing Xigang, Li Wenjian, Wang Zhuanzi, Zhou Guangming, Wang Jufang, Dang Bingrong, Gao Qingxiang & Walsh L. Correlation between initial chromatid damage and survival of various cell lines exposed to heavy charged particles. Radiat. Environ. Biophys. 45, 261-266, 2006

19. Stephan G, Schneider K, Panzer W, Walsh L & Oestreicher U. Enhanced yield of chromosome aberrations after CT examination in paediatric patients. Int. J. Radiat. Biol. 83(5), 281-287, 2007

20. Rühm W & Walsh L. Current risk estimates based on the A-bomb survivors data – a discussion in terms of the ICRP recommendations on the neutron weighting factor. Proc. of the Tenth Symposium on Neutron Dosimetry, Uppsala, Sweden June 12-16, 2006. Radiat. Prot. Dosim. 126(1-4), 423-431, 2007

21. Walsh L. A short review of model selection techniques for radiation epidemiology. Radiat. Environ. Biophys. 46, 205-213, 2007

22. Schneider U & Walsh L. Cancer risk estimates from the combined Japanese A-bomb and Hodgkin cohorts for doses relevant to radiotherapy. Radiat. Environ. Biophys. 47, 253-263, 2008

23. Jacob P, Walsh L & Eidemüller M. Modelling of carcinogenesis and cell killing in the atomic bomb survivors with applications to the mortality from all solid, stomach and liver cancers. Radiat. Environ. Biophys. 47, 375-388, 2008

24. Kreuzer M, Walsh L, Schnelzer M, Tschense A & Grosche B. Radon and risk of extrapulmonary cancers: results of the German uranium miners' cohort study, 1960-2003. Br. J. Cancer. 99, 1946-1953, 2008

25. Oestreicher U, Stephan G, Schneider K, Panzer W & Walsh L. Results of chromosome aberrations after computer tomography (CT) in children. In: Proceedings of the 36th Annual Meeting of the European Radiation Research Society, Tours 2008, Radioprotection. 43(5), 41, 2008

26. Kreuzer M, Walsh L, Schnelzer M, Tschense A & Grosche B. Radon and cancers other than lung cancer in uranium miners – Results of the German uranium miners cohort study, 1960–2003. In: Proceedings of the 36th Annual Meeting of the European Radiation Research Society, Tours 2008, Radioprotection. 43(5), 64, 2008

27. Walsh L, Jacob P & Kaiser JC. Radiation risk modeling of thyroid cancer with special emphasis on the Chernobyl epidemiological data. Radiat. Res. 172, 509-518, 2009

28. Jacob P, Rühm W, Walsh L, Blettner M, Hammer G & Zeeb H. Cancer risk of radiation workers larger than expected. Occ. Env. Med (BMJ). 66, 789-796, 2009

29. Walsh L. Heterogeneity of variation of relative risk by age at exposure in the Japanese atomic bomb survivors. Radiat. Environ. Biophys. 48, 345-347, 2009

30. Schneider U & Walsh L. Cancer risk above 1 Gy and the impact for space radiation protection. Advances in Space Research. 44, 202-209, 2009

31. Schmid E, Wagner FM, Romm H, Walsh L & Roos R. Dose-response relationship of dicentric chromosomes in human lymphocytes obtained for the fission neutron therapy facility MEDAPP at the research reactor FRM II. Radiat. Environ. Biophys. 48(1), 67-75, 2009

32. Kreuzer M, Grosche B, Schnelzer M, Tschense A, Dufey F & Walsh L. Radon and risk of death from cancer and cardiovascular diseases in the German uranium miners cohort study: follow-up 1946–2003. Radiat. Environ. Biophys. 49 (2), 177-185, 2010

33. Walsh L, Tschense A, Schnelzer M, Dufey F, Grosche B & Kreuzer M. The Influence of radon exposure on lung cancer mortality in German uranium miners, 1946-2003. Radiat. Res. 173, 79-90, 2010

34. Walsh L, Dufey F, Tschense A, Schnelzer M, Grosche B & Kreuzer M. Radon and the risk of cancer mortality – Internal Poisson models for the German uranium miners cohort. Health Physics. 99(3), 292-300, 2010

35. Kreuzer M, Schnelzer M, Tschense A, Walsh L & Grosche B. Cohort profile: The German uranium miners cohort study (WISMUT cohort), 1946-2003. Int. J. Epidemiol. 39(4), 980-987, 2010

36. Nekolla EA, Walsh L & Spiess H. Incidence of Malignant Diseases in Humans Injected with Radium-224, Radiat. Res. 174, 377-386, 2010

37. Walsh L, Radiation Protection in Occupational and Environmental settings, commissioned editorial, Occ. Env. Med (BMJ). 68, 387-388, 2011

38. Walsh L & Kaiser JC. Multi-model inference of adult and childhood leukaemia excess relative risks based on the Japanese A-bomb survivors mortality data (1950–2000). Radiat. Environ. Biophys. 50, 21-35, 2011

39. Walsh L, Dufey F, Möhner M, Schnelzer M, Tschense A & Kreuzer M. Differences in baseline lung cancer mortality between the German uranium miners cohort and the population of the former German Democratic Republic (1960–2003). Radiat. Environ. Biophys. 50, 57-66, 2011

40. Dufey F, Walsh L, Sogl M & Kreuzer M. Occupational doses of ionizing radiation and leukaemia mortality. Health Physics. 100(5), 548-550, 2011

41. Walsh L. Radiation exposure and circulatory disease risk based on the Japanese A-bomb survivor mortality data (1950–2003) – neglect of the healthy survivor selection bias. Letter to the editor of BMJ. 2011 http://www.bmj.com/content/340/bmj.b5349.full/reply#bmj_el_260742

42. Walsh L, Dufey F, Tschense A, Schnelzer M, Sogl M & Kreuzer M. Prostate cancer mortality risk in relation to working underground in the Wismut cohort of German uranium miners (1970–2003). BMJ open. 2012;2:e001002. DOI: 10.1136/bmjopen-2012-001002, 2012

43. Schöllnberger H, Kaiser JC, Jacob P & Walsh L. Dose-responses from multi-model inference for the non-cancer disease mortality of atomic bomb survivors. Radiat. Environ. Biophys. 51, 165-178, 2012

44. Walsh L, Kaiser JC, Schöllnberger H & Jacob P. Response to ''model averaging in the analysis of leukaemia mortality among Japanese A-bomb survivors'' by Richardson and Cole. Radiat. Environ. Biophys. 51, 97-100, 2012

45. Sogl M, Taeger D, Pallapies D, Brüning T, Dufey F, Schnelzer M, Straif K, Walsh L & Kreuzer M. Quantitative relationship between silica exposure and lung cancer mortality in German Uranium miners, 1946–2008, Br. J. Cancer. 107, 1188-1194, 2012

46. Walsh L & Schneider U. A method for calculating weights for excess relative risk and excess absolute risk in calculations of lifetime risk of cancer from radiation exposure. Radiat. Environ. Biophys. *accepted* October 2012, DOI: 10.1007/s00411-012-0441-x

47. Walsh L, Neutron relative biological effectiveness for solid cancer incidence in the Japanese A-bomb survivors – an analysis considering the degree of independent effects from γ-ray and neutron absorbed doses with hierarchical partitioning. Radiat. Environ. Biophys (*online first*). 2012, DOI: 10.1007/s00411-012-0445-6

48. Kaiser JC & Walsh L. Independent analysis based on the radiation risk for leukaemia in children and adults with mortality data (1950–2003) of Japanese A-bomb survivors. Radiat. Environ. Biophys (*online first*). 2012, DOI: 10.1007/s00411-012-0437-6

49. Kreuzer M, Sogl M, Dufey F, Schnelzer M, Straif K & Walsh L, Cardiovascular diseases in relation to gamma exposures in German uranium miners, 1946–2008. Radiat. Env. Biophys. *accepted* November 2012, DOI: 10.1007/s00411-012-0446-5

50. Dufey F, Walsh L, Sogl M, Tschense A & Kreuzer M. Radiation dose dependent risk of liver cancer mortality in the German uranium miners cohort 1946–2003 J. Radiol. Prot. *accepted* November 2012

Other works in chronological order, (only reviewed internally):-

A. Kellerer AM, Rühm W & Walsh L. Neutronen in Hiroshima – Lösung der dosimetrischen, aber noch nicht der strahlenbiologischen Kontroverse. GSF annual report 2003, 215–220, http://www.helmholtz-muenchen.de /fileadmin/GSF/pdf/publikationen/jahresberichte/2003/215_220_2003.pdf

B. Rühm W, Walsh L & Kellerer AM. The neutron effective dose to the A-bomb survivors. Technical report number TR 221 of the Radiobiological Institute, Ludwig-Maximilians University Munich, 2006

C. Kellerer AM, Rühm W & Walsh L. Accounting for radiation quality in the analysis of the solid cancer mortality among A-bomb survivors. Technical report number TR 223 of the Radiobiological Institute, Ludwig-Maximilians University Munich, 2006

D. Jacob P, Jacob V, Meckbach R and Walsh L. Implications of the effects of adaptive response, low-dose hypersensitivity and the bystander effect' for cancer risk at low doses and low dose rates. Final Report for the BFS project St.Sch 4367, 2006

E. Walsh L & Rühm W. Radiation-induced late detrimental health effects in cohorts exposed to ionising radiation – with special emphasis on the Japanese A-bomb survivours. Paper prepared for the Proc. of the Radiation and Environment Symposium on 29/30 June 2006 at the University of the Dardanelles, Turkey.

Journal publications re-grouped according to subject

Japanese A-bomb survivors
(1-5, 7, 8, 11-13, 16, 20-23, 28-30, 37, 38, 41, 43, 44, 46-48)

1. Kellerer AM, Nekolla E & Walsh L. On the conversion of solid cancer excess relative risk into lifetime attributable risk. Radiat. Environ. Biophys. 40, 249-257, 2001

2. Kellerer AM & Walsh L. Risk estimation for fast neutrons with regard to solid cancer. Radiat. Res. 156, 708-717, 2001

3. Kellerer AM & Walsh L. Solid cancer risk coefficient for fast neutrons, in terms of effective dose. Radiat. Res. 158, 61-68, 2002

4. Kellerer AM, Walsh L & Nekolla EA. Risk coefficient for γ-rays with regard to solid cancer. Radiat. Environ. Biophysics. 41, 113-123, 2002

5. Rühm W, Walsh L & Chomentowski M. Choice of model and uncertainties of the gamma-ray and neutron dosimetry in relation to the chromosome aberrations data in Hiroshima and Nagasaki, Radiat. Environ. Biophys. 42, 119-128, 2003

7. Walsh L, Rühm W & Kellerer AM. Cancer risk estimates for γ-rays with regard to organ specific doses Part I: All solid cancers combined. Radiat. Environ. Biophys. 43, 145-151, 2004

8. Walsh L, Rühm W & Kellerer AM. Cancer risk estimates for γ-rays with regard to organ specific doses Part II: Site specific solid cancers. Radiat. Environ. Biophys. 43, 225-231, 2004

11. Walsh L, Rühm W & Kellerer AM. Curvature in the dose response of the life span study cancer mortality data. Radiat. Res. 163, 477, 2005

12. Rühm W, Walsh L & Kellerer AM. Analysen der neusten LSS-Mortalitätsdaten (in German). Veröffentlichungen der Strahlenschutzkommission, Band 56, 43-56, Elsevier, Urban & Fischer, 2005

13. Kellerer AM, Rühm W & Walsh L. Indications of the neutron effect contribution in the solid cancer data of the A-bomb survivors. Health Physics. 90(6), 554-564, 2006

16. Rühm W, Walsh L & Nekolla E A. The Cohort of the Atomic Bomb Survivors - Major Basis of Radiation Safety Regulations. CERN Yellow Series, Report 12, 319-329, 2006

20. Rühm W & Walsh L. Current risk estimates based on the A-bomb survivors data – a discussion in terms of the ICRP recommendations on the neutron weighting factor. Proc. of the Tenth Symposium on Neutron Dosimetry, Uppsala, Sweden June 12-16, 2006. Radiat. Prot. Dosim. 126(1-4), 423-431, 2007

21. Walsh L. A short review of model selection techniques for radiation epidemiology. Radiat. Environ. Biophysics. 46, 205-213, 2007

22. Schneider U & Walsh L. Cancer risk estimates from the combined Japanese A-bomb and Hodgkin cohorts for doses relevant to radiotherapy. Radiat. Environ. Biophysics. 47, 253-263, 2008

23. Jacob P, Walsh L & Eidemüller M. Modelling of carcinogenesis and cell killing in the atomic bomb survivors with applications to the mortality from all solid, stomach and liver cancers. Radiat. Environ. Biophysics. 47, 375-388, 2008

28. Jacob P, Rühm W, Walsh L, Blettner M, Hammer G & Zeeb H. Cancer risk of radiation workers larger than expected. Occ. Env. Med (BMJ). 66, 789-796, 2009

29. Walsh L. Heterogeneity of variation of relative risk by age at exposure in the Japanese atomic bomb survivors. Radiat. Environ. Biophysics. 48, 345-347, 2009

30. Schneider U & Walsh L. Cancer risk above 1 Gy and the impact for space radiation protection. Advances in Space Research. 44, 202-209, 2009

37. Walsh L, Radiation Protection in Occupational and Environmental settings, commissioned editorial, Occ. Env. Med (BMJ). 68, 387–388, 2011

38. Walsh L & Kaiser JC. Multi-model inference of adult and childhood leukaemia excess relative risks based on the Japanese A-bomb survivors mortality data (1950–2000). Radiat. Environ. Biophysics. 50, 21-35, 2011

41. Walsh L. Radiation exposure and circulatory disease risk based on the Japanese A-bomb survivor mortality data (1950–2003) – neglect of the healthy survivor selection bias. Letter to the editor of BMJ. 2011 http://www.bmj.com/content/340/bmj.b5349.full/reply#bmj_el_260742

43. Schöllnberger H, Kaiser JC, Jacob P & Walsh L. Dose-responses from multi-model inference for the non-cancer disease mortality of atomic bomb survivors. Radiat. Environ. Biophys. 51, 165-178, 2012

44. Walsh L, Kaiser JC, Schöllnberger H & Jacob P. Response to "model averaging in the analysis of leukaemia mortality among Japanese A-bomb survivors" by Richardson and Cole. Radiat. Environ. Biophys. 51, 97-100, 2012

46. Walsh L & Schneider U. A method for calculating weights for excess relative risk and excess absolute risk in calculations of lifetime risk of cancer from radiation exposure. Radiat. Environ. Biophys. *accepted* October 2012, DOI: 10.1007/s00411-012-0441-x

47. Walsh L, Neutron relative biological effectiveness for solid cancer incidence in the Japanese A-bomb survivors – an analysis considering the degree of independent effects from γ-ray and neutron absorbed doses with hierarchical partitioning. Radiat. Environ. Biophys (*online first*). 2012, DOI: 10.1007/s00411-012-0445-6

48. Kaiser JC & Walsh L. Independent analysis based on the radiation risk for leukaemia in children and adults with mortality data (1950-2003) of Japanese A-bomb survivors. Radiat. Environ. Biophys (*online first*). 2012, DOI: 10.1007/s00411-012-0437-6

Patients treated with radiation
(10, 36)

10. Nekolla EA, Walsh L, Schottenhammer G & Spiess H. Malignancies in patients treated with high doses of radium-224. Proc, 9th Internat. conf. on Health Effects of Incorporated Radionuclides (HEIR 2004), Oeh U, Roth P, Paretzke HG (Eds.), GSF-Forschungszentrum GmbH, 67-74, 2005

36. Nekolla EA, Walsh L & Spiess H. Incidence of Malignant Diseases in Humans Injected with Radium-224, Radiat. Res. 174, 377-386, 2010

Persons affected by the Chernobyl nuclear power plant accident
(14, 27)

14. Jacob P, Bogdanova TI, Buglova E, Chepurniy M, Demidchik Y, Gavrilin Y, Kenigsberg J, Meckbach R, Schotola C, Shinkarev S, Tronko MD, Ulanovski A, Vavilov S & Walsh L. Thyroid Cancer Risk in Areas of Ukraine and Belarus affected by the Chernobyl Accident. Radiat. Res. 165, 1-8, 2006

27. Walsh L, Jacob P & Kaiser JC. Radiation risk modeling of thyroid cancer with special emphasis on the Chernobyl epidemiological data. Radiat. Res. 172, 509-518, 2009

German uranium miners
(24, 26, 32-35, 39, 40, 42, 45, 49, 50)

24. Kreuzer M, Walsh L, Schnelzer M, Tschense A & Grosche B. Radon and risk of extrapulmonary cancers: results of the German uranium miners' cohort study, 1960–2003. Br. J. Cancer. 99, 1946-1953, 2008

26. Kreuzer M, Walsh L, Schnelzer M, Tschense A & Grosche B. Radon and cancers other than lung cancer in uranium miners – Results of the German uranium miners cohort study, 1960–2003. In: Proceedings of the 36th Annual Meeting of the European Radiation Research Society, Tours 2008, Radioprotection. 43(5), 64, 2008

32. Kreuzer M, Grosche B, Schnelzer M, Tschense A, Dufey F & Walsh L. Radon and risk of death from cancer and cardiovascular diseases in the German uranium miners cohort study: follow-up 1946–2003. Radiat. Environ. Biophysics. 49 (2), 177-185, 2010

33. Walsh L, Tschense A, Schnelzer M, Dufey F, Grosche B & Kreuzer M. The Influence of radon exposure on lung cancer mortality in German uranium miners, 1946–2003. Radiat. Res. 173, 79-90, 2010

34. Walsh L, Dufey F, Tschense A, Schnelzer M, Grosche B & Kreuzer M. Radon and the risk of cancer mortality – Internal Poisson models for the German uranium miners cohort. Health Physics. 99(3), 292-300, 2010

35. Kreuzer M, Schnelzer M, Tschense A, Walsh L & Grosche B. Cohort profile: The German uranium miners cohort study (WISMUT cohort), 1946-2003. Int. J. Epidemiol. 39(4), 980-987, 2010

39. Walsh L, Dufey F, Möhner M, Schnelzer M, Tschense A & Kreuzer M. Differences in baseline lung cancer mortality between the German uranium miners cohort and the population of the former German Democratic Republic (1960–2003). Radiat. Environ. Biophysics. 50, 57-66, 2011

40. Dufey F, Walsh L, Sogl M & Kreuzer M. Occupational doses of ionizing radiation and leukaemia mortality. Health Physics. 100(5), 548-550, 2011

42. Walsh L, Dufey F, Tschense A, Schnelzer M, Sogl M & Kreuzer M. Prostate cancer mortality risk in relation to working underground in the Wismut cohort of German uranium miners (1970–2003). BMJ open. 2012;2:e001002. DOI: 10.1136/bmjopen-2012-001002, 2012

45. Sogl M, Taeger D, Pallapies D, Brüning T, Dufey F, Schnelzer M, Straif K, Walsh L & Kreuzer M. Quantitative relationship between silica exposure and lung cancer mortality in German Uranium miners, 1946–2008, Br. J. Cancer. 107, 1188-1194, 2012

49. Kreuzer M, Sogl M, Dufey F, Schnelzer M, Straif K & Walsh L, Cardiovascular diseases in relation to gamma exposures in German uranium miners, 1946–2008. Radiat. Env. Biophys. *accepted* November 2012, DOI: 10.1007/s00411-012-0446-5

50. Dufey F, Walsh L, Sogl M, Tschense A & Kreuzer M. Radiation dose dependent risk of liver cancer mortality in the German uranium miners cohort 1946–2003 J. Radiol. Prot. *accepted* November 2012

Radio-biological studies relevant to diagnostic radiation procedures
(6, 9, 15, 17-19, 25, 31)

6. Göggelmann W, Jacobsen C, Panzer W, Walsh L, Roos H & Schmid E. Re-evaluation of the RBE of 29 kV X-rays (mammography X-rays) relative to 200

kV X-rays using neoplastic transformation of human CGL1-hybrid cells. Radiat. Environ. Biophys. 42, 175-182, 2003

9. Gomolka M, Rössler U, Hornhardt S, Walsh L, Panzer W & Schmid E. Measurement of the Initial Levels of DNA Damage in Human Lymphocytes induced by 29 kV X Rays (Mammography X Rays) Relative to 220 kV X Rays and γ Rays. Radiat. Res. 163, 510-519, 2005

15. Hornhardt S, Gomolka M, Walsh L & Jung T. Comparative investigations of sodium arsenate, arsenic trioxide and cadmium sulphate in combination with gamma-radiation on apoptosis, micronuclei induction and DNA damage in a human lymphoblastoid cell line. Mutation Res. 600, 165-176, 2006

17. Rössler U, Hornhardt S, Seidl C, Müller-Laue E, Walsh L, Panzer W, Schmid E, Senekowitsch-Schmidtke R & Gomolka M. The sensitivity of the alkaline comet assay in detecting DNA lesions induced by X-rays, gamma-rays and alpha particles. Proc. 14th International Symposium on Microdosimetry: Ionising radiation quality, molecular mechanisms, cellular effects and their consequences for low level risk assessment and radiation therapy, Nov 13-18, 2005, Venice, Italy, Radiat. Prot. Dosim. 122(1-4), 154-159, 2006

18. Yang Jianshe, Jing Xigang, Li Wenjian, Wang Zhuanzi, Zhou Guangming, Wang Jufang, Dang Bingrong, Gao Qingxiang & Walsh L. Correlation between initial chromatid damage and survival of various cell lines exposed to heavy charged particles. Radiat. Environ. Biophysics. 45, 261-266, 2006

19. Stephan G, Schneider K, Panzer W, Walsh L & Oestreicher U. Enhanced yield of chromosome aberrations after CT examination in paediatric patients. Int. J. Radiat. Biol. 83(5), 281-287, 2007

25. Oestreicher U, Stephan G, Schneider K, Panzer W & Walsh L. Results of chromosome aberrations after computer tomography (CT) in children. In: Proceedings of the 36th Annual Meeting of the European Radiation Research Society, Tours 2008, Radioprotection. 43(5), 41, 2008

31. Schmid E, Wagner FM, Romm H, Walsh L & Roos R. Dose-response relationship of dicentric chromosomes in human lymphocytes obtained for the fission neutron therapy facility MEDAPP at the research reactor FRM II. Radiat. Environ. Biophys. 48(1), 67-75, 2009

Publication Matrix.

Index author: (Dr. **Walsh**, Linda)
data collected in October, 2012

Original publications (print-published, e-published or in press).
with one line references.

Please note: This table only includes post 2000 publications.

Journal	**Impact Factor** (2011)
Br. J. Cancer	5.042
Biophys.	1.696
Radiat. Res.	2.648
Health Physics	1.68
Mutation Res.	3.035
Int. J. Radiat. Biol.	2.28
Radiat. Prot. Dosim.	0.822
Radioprotection	1
BMJ-OEM	3.02
Int. J. Epidem.	6.414
BMJ-Open*	
J. Radiol. Prot.	1.388
Adv. Space Res.	1.178

* The Impact factor is not yet available because the journal was launched in 2011

number	First author, index author (if different) and last author	Journal		Journal impact factor (2011) Index author is first author or approximately equally contributing second author	Index author is last author or corresponding author	Index author is other author	Sum of year	Number of citations (from: Google Scholar) 19.10.12	(from: Thomson Reuters ISI web of science) 19.10.12
1	Kellerer, Nekolla & **Walsh**	Radiat. Environ. Biophys.	2001		1.7			24	15
2	Kellerer & **Walsh**	Radiat. Res.		2.6			4.3	17	16
3	Kellerer & **Walsh**	Radiat. Res.	2002	2.6				5	2
4	Kellerer, **Walsh** & Nekolla	Radiat. Environ. Biophys.		1.7			4.3	32	6
5	Rühm, **Walsh** & Chomentowski	Radiat. Environ. Biophys.	2003	1.7				7	7
6	Göggelmann, **Walsh** et al.	Radiat. Environ. Biophys.				1.7	3.4	37	35
7	**Walsh**, Rühm & Kellerer	Radiat. Environ. Biophys.	2004	1.7				31	17
8	**Walsh**, Rühm & Kellerer	Radiat. Environ. Biophys.		1.7			3.4	32	11
9	Gomolka, **Walsh** et al, Schmid	Radiat. Res.	2005			2.6		14	9
10	Nekolla, **Walsh** et al, Spiess	GSF publication							
11	**Walsh**, Rühm & Kellerer	Radiat. Res.		2.6					1
12	Rühm, **Walsh**, Kellerer	SSK publication in German					5.3		
13	Kellerer, Rühm & **Walsh**	Health Physics	2006		1.7			29	19
14	Jacob et al & **Walsh**	Radiat. Res.			2.6			53	37
15	Hornhardt et al, **Walsh** & Jung	Mutation Res.				3.0		17	13
16	Rühm, **Walsh** &Nekolla	CERN yellow series							
17	Rössler et al, **Walsh** & Gomolka	Radiat. Prot. Dosim.				0.8		12	5
18	Yang et al & **Walsh**	Radiat. Environ. Biophys.			1.7		9.9	7	3
19	Stephan et al, **Walsh** &Oestreicher	Int. J. Radiat. Biol.	2007			2.3		13	13
20	Rühm & **Walsh**	Radiat. Prot. Dosim.		0.8				4	4
21	**Walsh**	Radiat. Environ. Biophys.		1.7			4.8	20	16
22	Schneider & **Walsh**	Radiat. Environ. Biophys.	2008	1.7				24	19
23	Jacob, **Walsh** & Eidemüller	Radiat. Environ. Biophys.		1.7				5	3
24	Kreuzer, **Walsh** et al & Grosche	Br. J. Cancer.		5.0				28	15
25	Oestreicher et al & **Walsh**	Radioprotection			1.0				
26	Kreuzer, **Walsh** et al & Grosche	Radioprotection				1.0	10.4		
27	**Walsh**, Jacob & Kaiser	Radiat. Res.	2009	2.6				5	5
28	Jacob et al. **Walsh** & Zeeb	BMJ-OEM				3.0		24	19
29	**Walsh**	Radiat. Environ. Biophys.		1.7				8	4
30	Schneider & **Walsh**	Advances in Space Res.		1.2				1	2
31	Schmid et al, **Walsh** & Roos	Radiat. Environ. Biophys.				1.7	10.2	2	1
32	Kreuzer et al & **Walsh**	Radiat. Environ. Biophys.	2010		1.7			20	14
33	**Walsh** et al & Kreuzer	Radiat. Res.		2.6				18	13
34	**Walsh** et al & Kreuzer	Health Physics		1.7				10	5
35	Kreuzer et al, **Walsh** & Grosche	Int. J. Epidem.		6.4				13	5
36	Nekolla, **Walsh** & Spiess	Radiat. Res.				2.6	15.1	3	1
37	**Walsh**	BMJ-OEM	2011	3.0				1	1
38	**Walsh** & Kaiser	Radiat. Environ. Biophys.		1.7				7	5
39	**Walsh** et al & Kreuzer	Radiat. Environ. Biophys.		1.7				3	2
40	Dufey, **Walsh** et al & Kreuzer	Health Physics		1.7				1	1
41	**Walsh**	BMJ letter		13.7			21.8	1	1
42	**Walsh** et al & Kreuzer	BMJ-Open	2012	*launched 2011*				7	
43	Schöllnberger et al & **Walsh**	Radiat. Environ. Biophys.			1.7			1	
44	**Walsh** et al & Jacob	Radiat. Environ. Biophys.		1.7				1	
45	Sogl et al, **Walsh** & Kreuzer	Br. J. Cancer			5.0				
46	**Walsh** & Schneider	Radiat. Environ. Biophys.		1.7					
47	Walsh	Radiat. Environ. Biophys.		1.7					
48	Kaiser & **Walsh**	Radiat. Environ. Biophys.			1.7				
49	Kreuzer et al & **Walsh**	Radiat. Environ. Biophys.			1.7				
50	Dufey, **Walsh** et al & Kreuzer	J. Radiol. Prot.				1.4	15.2		
			Sum	68.8	13.8	27.0	108.2	537	345

III. Overall summary

This overall summary first presents a general description of the nature of the research field of radiation epidemiology, radiation biology and radiation protection and some historical details (Section 1). Radiation epidemiological and biological studies of exposed human groups are described and some of the major moot issues and sources of uncertainty related to the formulation of radiation dose limit recommendations for radiation protection are discussed (Section 1). A general summary of the candidate's contribution to the field is then given (Section 2). A specific summary of the candidate's contribution to the field is also given (Section 3) and the sub-sections of Section 3 review the current state of knowledge and describe the new developments that the candidate has been involved in, with more detail. This research includes: assessments of all solid cancer risks from γ-rays and neutrons; assessments of the incidence of malignant diseases in humans injected with radium-224; developments of epidemiological models for thyroid cancer risk in areas affected by the 1986 Chernobyl accident; development of epidemiological models for lung and extra-pulmonary cancers in the German "Wismut" uranium miners exposed to radon and other potential carcinogens; analysis of data on cellular radiation damage; and the introduction of model selection techniques and methods for multi-model inference into the field of radiation epidemiology.

Each detailed sub-section presents the aims, extent, nature and achievements of the research contained in the submitted publications and gives examples of how this work has contributed to the field and been cited in the epidemiological literature and by international bodies. In addition, interrelationships between the submitted publications are outlined and reference is also made to the work of other research scientists in the candidate's field.

A publication matrix is given, with the publication list in section II, that includes details of journal impact factors and the number of citations, with the aim of providing an indication of the standard of the journals and the reception of the publications.

1. Nature of the field

The assessment of detrimental health risks for humans, due to exposures from ionising radiation such as γ-rays, X-rays and neutrons, which penetrate deeply into the human body, has been an endeavour which has increased in magnitude

and effort over the last century, during a period where radiation epidemiology and biology have acquired a major role in science, medicine and public perception. It is instructive to briefly review the historical development of the field starting in 1895 when Roentgen announced the discovery of X-rays (Roentgen 1895, Glasser 1959). At this point in time, atoms and the atomic origins of the radiation were not understood. Sir Ernest Rutherford presented the first clear scientific results relating to the nature of the atomic radiation (Rutherford & Soddy 1902) and the nature of the atom (Rutherford 1911): this latter work was done during the time that Rutherford was a Professor at Manchester University (1907-1919).

Initially, X-rays were considered to be of universal benefit to society and a source of entertainment. "X-ray studios" opened in major cities to take "bone portraits", often on subjects who had no medical complaints. Newspapers competed with each other to publish the latest X-ray pictures first. Radioactive products such as toothpaste and pillows were very popular.

First indications of the danger associated with radiation began shortly after the discovery of X-rays when detrimental health effects associated with individual people were noticed. Thomas Edison reported stomach and eye injuries from X-rays in March of 1896 (Israel 1998, p.422). Shortly after, Henri Becquerel received accidental skin burns from radium, given to him by the Curies, which he had kept in his pocket. He is reported (Curie 1938, Chapter 15) to have told the Curies that: "I love this radium but I have a grudge against it!" The burns were subsequently reported to the Paris Academy of Science in 1901 along with other similar physiological effects discovered by Pierre Curie (Becquerel & Curie 1901).

Early radiography accidents are also known to have occurred – an example of which occurred in 1896 involving a Chicago patient with a fractured ankle who had radiographs done with exposure times of up to 40 minutes. The resulting skin injury eventually led to amputation and apparently the first malpractice lawsuit connected with radiography in the USA (Lichtenstein, 1996). Thomas Edison's assistant in the manufacture of X-ray tubes, Clarence Dally, died in 1904 after suffering from extensive skin cancer, burns and serial amputations – purportedly the first known death from radiation-induced cancer (Israel 1998, p.422). It is now almost certain that fatal aplastic anemia contracted by Marie Curie (see Curie 1938, p.372–373, for a historical documentation of the diagnosis) was a

consequence of her long-term scientific investigations into radium (which she discovered) and uranium.

Indications of danger associated with groups of people were first reported in 1911 when a cluster of leukaemia cases was found in a group of radiologists working in Berlin (von Jagie 1911). Evidence of the carcinogenic effects to the foetus, from diagnostic radiotherapy in obstetrics, was first reported by Stewart et al. 1956 and subsequently confirmed by many studies as a consistent association (see Wakeford 2008 for a review). An early major tragedy, in several countries, resulted in the use of ^{226,228}Ra on dials of watches and vehicle control panels to render them luminous. Hundreds of workers painted the dials with radium by tipping their paint brushes with their lips and thereby unknowingly incorporating large amounts of bone-seeking alpha and γ-ray emitters which ultimately caused bone-cancer (Rowland et al. 1978 & see the review by Fry 1998). This study provides one of the strongest epidemiological dose response curves ever seen, as illustrated in Figure 1. The upper dose group has 20 cases of bone cancers out of 44 subjects under investigation. Considering that the background incidence rate for bone sarcoma is about 1 in 20,000 persons per year this constitutes a massive radiation effect.
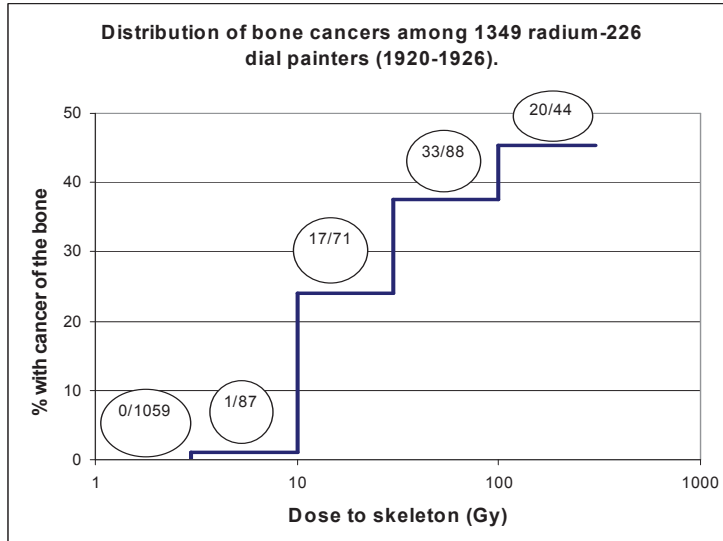
Figure 1. The distribution of bone cancers among 1349 radium-226 dial painters (1920-1926). The numbers in circles are the number of cases divided by the number of persons at risk in each dose category. (source: re-plotted with data from www.triumf.ca)

Many other studies have since been able to provide important information on radiation-related late detrimental health effects. Radiation epidemiological and biological studies of exposed human groups (G) are very varied and include:

G1) survivors of the World War II atomic bombings over Hiroshima and Nagasaki;

G2) patients treated with radiation for cancer and non-malignant diseases;

G3) workers exposed to occupational radiation;

G4) communities exposed to environmental sources of radiation;

G5) patients given diagnostic radiation;

G6) persons with intakes of radionuclides.

Many indicators of cellular damage and many detrimental health effects that could be attributed to exposures from ionising radiation have been investigated to date. Solid cancer and leukaemia incidence and mortality and cellular chromosomal aberrations are now known to have radiation as an important risk factor. Studies on Japanese A-bomb survivors, exposed mainly to γ-rays and neutrons, continue to provide valuable radiation epidemiological and biological data and quantitative assessments of the radiation related solid cancer and leukaemia risks (e.g. Preston et al. 2007). Results from this cohort have formed a basis for the construction of radiation protection guidelines that include the setting of various dose limits to the radiation received by occupationally exposed workers and the general public. Such dose limits come from assessments and recommendations that are issued and updated at regular intervals by international bodies, such as the International Commission on Radiological Protection (ICRP 2007) and the United Nations Scientific Committee on the Effects of Atomic Radiation (UNSCEAR 2008).

Some of the major moot issues (I) and sources of uncertainty related to the formulation of dose limit recommendations for radiation protection include the following points:

I1) the sensitivity of different organs to radiation and the relative tissue damaging effect of the various types of radiation are uncertain;

I2) the factors by which risks for children and young persons are higher than for adults;

I3) the magnitude, shape and statistical significance of the cancer risk when plotted as a function of dose are not very well-defined, particularly at the lower end of the dose range (where the associated error bars tend to be relatively wider than at higher doses);

I4) whether or not the cancer risks are similar for acute high-dose-rate exposures (as pertinent to the Japanese A-bomb survivors) and protracted low-dose-rate exposures (as relevant to a broad category of nuclear workers and the general population).

2. General summary of the candidate's contribution to the field

The following publications cited below, have either been written, or contain substantial contributions, by the candidate on the exposed human groups (G) listed above:

G1) Japanese A-bomb survivors:
   (1-5, 7, 8, 11-13, 16, 20-23, 28-30, 37, 38, 41, 43, 44, 46-48).

G2) patients treated with radiation: (10, 36).

G3) workers exposed to occupational radiation – German uranium miners:
   (24, 26, 32-35, 39, 40, 42, 45, 49, 50).

G4) persons exposed to environmental sources of radiation – Chernobyl:
   (14, 27).

G5) patients given diagnostic radiation:
   evaluation of diagnostic radiation characteristics: (6, 9, 15, 31);
   evaluation of effects on patients: (17-19, 25).

G6) persons with intakes of radionuclides – Chernobyl: (14, 27).

The following publications have either been written, or contain substantial contributions, by the candidate, on the major issues (I) listed above:

I1) organ radiation sensitivity and relative radiation tissue damaging effect:
   (6, 9, 13, 15, 17, 18, 20, 47).

I2) factors by which risks for children are higher than for adults: (19, 25, 38).

I3) magnitude and statistical significance of the cancer risk and shape of dose
   response: (2-4, 7-8, 10-12, 14, 22-24, 26-34, 36, 38, 40, 43, 45, 48, 50).

I4) comparison of cancer risks between acute and protracted exposures: (28, 37).

A publication matrix (located in section II, at the end of the complete list of submitted publications) demonstrates that the candidate has made original and substantial contributions to this major field of study over a whole range of sub-topics and is a leading authority in a number of areas outlined above (e.g., G1, G3, G5, I1 and I3). The "2011 impact factors" of the journals containing the papers accumulated over a 12 year period totals 108 (where over half of this value is from the candidate's contribution as first author or approximately equally

contributing second author). The papers had been cited in total between 345–537 times (depending on citation index source) up to mid-October 2012. Another indication of the reception of the candidate's publications can be gained by the inclusion and citation of the results from these publications in reports by International bodies such as ICRP, UNSCEAR, World Health Organization (WHO) and WHO-International Agency for Research on Cancer (IARC). Examples of such citations are given throughout the specific summary of the main statement (III. Section 3).

3. Specific summary of the candidate's contribution to the field

The sub-sections pertain to the detrimental health effects of ionising radiation on: the Japanese A-bomb survivors (3.1 and 3.6); patients treated with radiation (3.2); persons affected by the Chernobyl nuclear power plant accident (3.3); German uranium miners (3.4); and radio-biological studies relevant to diagnostic radiation procedures (3.5).

3.1 Assessments of cancer risks from γ-rays and neutrons based on the cohort of A-bomb survivors

3.1.1 A review of the current state of knowledge

Atomic bombs were detonated in 1945 over Hiroshima (350,000 inhabitants) and Nagasaki (270,000 inhabitants) on August the 6th and 9th respectively. The number of acute fatalities up to the end of 1945 is not known precisely, because of the destruction of records, but is estimated to be between 90,000 and 166,000 in Hiroshima and between 60,000 and 80,000 in Nagasaki (http://www.rerf.jp/general/qa_e/qa1.html). A master cohort including about 120,000 survivors was established to examine the effects of ionising radiation by the Atomic Bomb Casualty Commission (ABCC) in the late 1940s. From 1975 the tasks of epidemiological and medical data collection, maintenance and analysis was transferred to the Radiation Effects Research Foundation (RERF).

Figure 2 shows a chart of the sub-studies on the life span study (LSS) cohort of Japanese A-bomb survivors. Since 1950, biennial health examinations on about 20,000 survivors (The Adult Health Survey – AHS) have been carried out. There are studies on about 77,000 children of atomic bomb survivors (The F1 Study) and also on approximately 3,600 individuals who were exposed before birth (The In-utero Study). The main data sets pertain to the 86,000 survivors of the LSS cohort which form the basis for the analyses presented here.

This cohort is unique and characterized by: the large number of cohort members; the long follow-up period of more than 50 years; a composition that includes males and females, children and adults; whole-body exposures (which are more typical for radiation protection situations than the partial-body exposures associated with many medically exposed cohorts); a large dose range from natural to lethal levels; and an internal control group with negligible doses, i.e., those who survived at large distances (> 3km) from the hypocentres.

The Life Span Study Cohort
(www.rerf.or.jp)

Master cohort including 120,000 survivors established by

Atomic Bomb Casualty Commission (ABCC): 1947 - 1975

Radiation Effects Research Foundation (RERF): 1975 -

Since 1950 biennial health examinations on about 20,000* survivors (**AHS**)

Several mortality and incidence follow-ups of about 86,000 survivors (**LSS**) since 1950

In-utero study on 3,600* individuals

Children of atomic bomb survivors (**F1**) study on 77,000* individuals

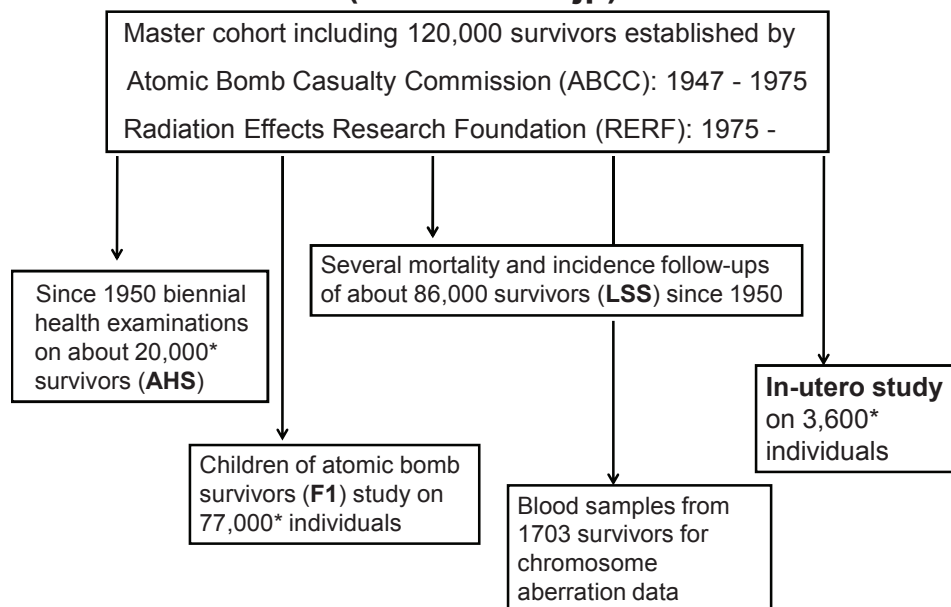Blood samples from 1703 survivors for chromosome aberration data

Figure 2. Chart of the various sub-studies on the LSS cohort of Japanese A-bomb survivors. *Numbers quoted from* Okubo 2012.

The limitations of the study include: the acute nature of the radiation exposure (i.e., not a continuous exposure as in many work places); the mainly external nature of the exposure (i.e., consequences of internal exposures cannot be investigated); the mixed radiation field (i.e., low linear energy transfer (LET) γ-radiation and high-LET neutron radiation); and the epidemiological results pertain to a Japanese population (i.e., transfer of results e.g., to western populations must be done carefully).

The positions of the individual LSS cohort members in the vicinity at the time of the A-bomb explosion over Hiroshima are given in Figure 3 with colour coded doses. About 44% of the LSS cohort is in the lowest dose group. The mean weighted colon dose received by the remaining 56% is approximately 0.2Sv. Basic data for solid cancers and leukaemia for a follow-up period from 1950 to 1990 and two more recent follow-up periods are given in Table 1. The recent paper by Ozasa et al. 2012, for the follow-up period 1950–2003, reports on 50,620 deaths and 10,929 fatal solid tumours (of which 527 are estimated to be radiation associated). According to detailed statistical modelling with the data, about 5% of the solid cancers and 30% of the leukaemia cases are associated with the A-bomb radiation exposures.
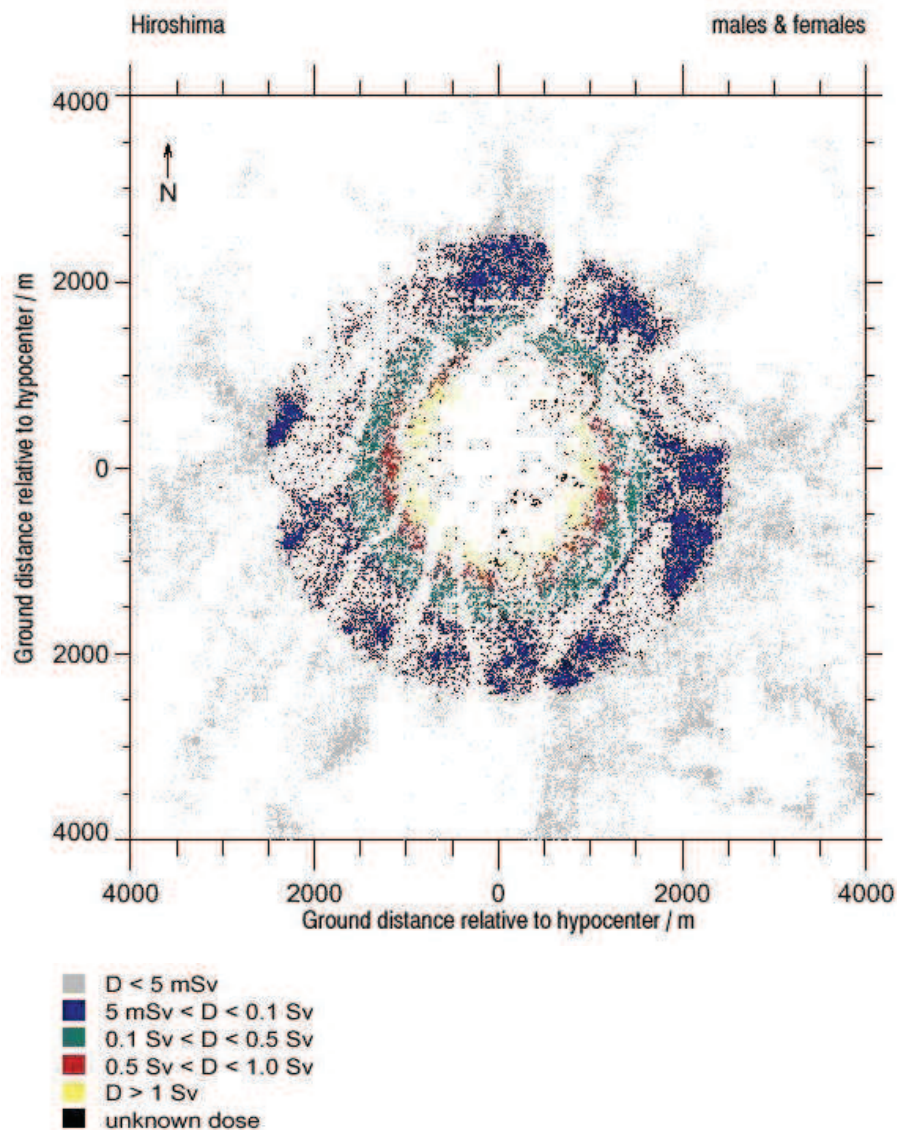
Figure 3. The positions of the individual victims (in the LSS) in the vicinity at the time of the A-bomb explosion over Hiroshima with colour coded weighted colon doses. (Source: M. Chomentowski, Radiobiological institute, University of Munich)

	Pierce et al. 1996			Preston et al. 2004	Ozasa et al. 2012
				1950-2000	1950-2003
1950-1990	Hiroshima	Nagasaki	Total	Total	Total
Survivors	58459	28113	86572	86611	86611
Deaths	26495	11175	37670	47685	50620
Solid tumours	5436	2142	7578	10127	10929
of which radiation associated	*247*	*87*	*334*	*479*	*527*
Leukaemia	196	53	249	296	318
of which radiation associated	*70*	*17*	*87*	*93*	*not given*

Table 1. Basic data for solid cancer and leukaemia mortality for a follow-up period from 1950 to 1990 and two more recent follow-up periods from 1950 to 2000 and to 2003.

The temporal patterns associated with the leukaemia and solid cancers are very different from each other, as can be seen from Figures 4 and 5 respectively, where the light coloured areas indicate the number of cancers that would have occurred without radiation exposure, and the red areas indicate the excess that has been attributed to the radiation exposure.
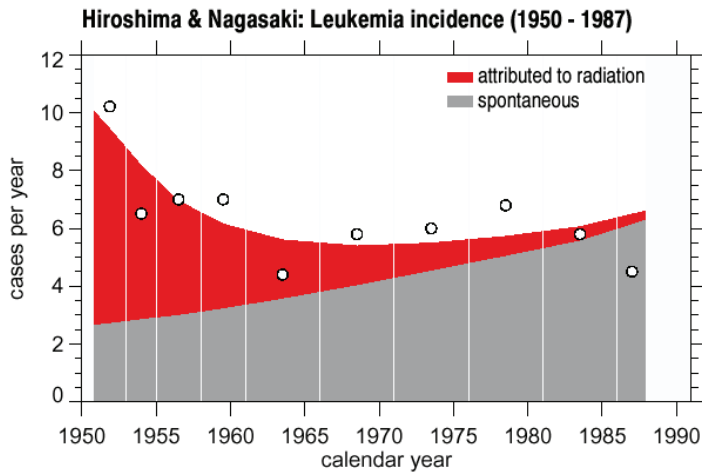

Figure 4. (Source: figure 2 of Kellerer 2001). The annual number of leukemia cases (circles) in the A-bomb survivors in both cities in the different time periods. The gray area represents the annual numbers that would have occurred without the radiation exposure. The red area represents the excess incidence rate attributable to radiation exposure. The increase of the spontaneous cases reflects the rise of the incidence rate with age of the A-bomb survivors. The excess rate was highest in the nineteen fifties and although no local leukemia registries existed before 1950, it is known from other radiation epidemiological studies that a certain excess rate may have already been present three to four years after exposure.
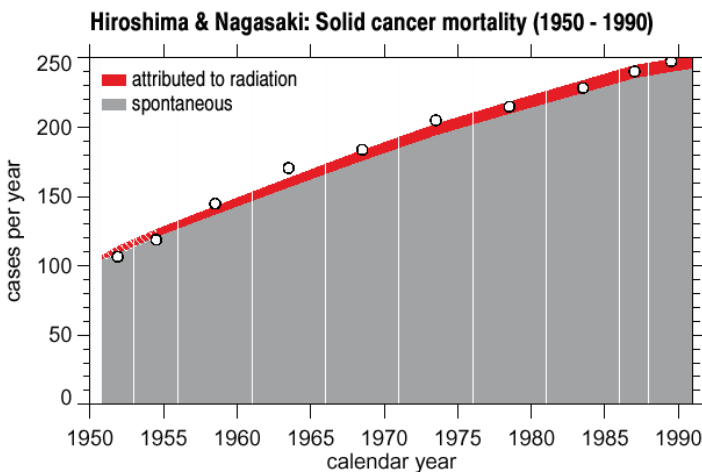
Figure 5. (Source: figure 3 of Kellerer 2001). The annual number of deaths from solid cancers (circles) in the LSS-cohort of the A-bomb survivors. The grey and red areas are defined as in Figure 4.

A summary of the organ specific mortality risks is given in Figure 6 which shows the excess relative risk (i.e., as described above, the ratio of the excess mortality to the spontaneous mortality), per Gy for various tumour sites. The dose responses associated with the excess mortality for solid cancer and leukaemia

are also rather different from each other being linear but admitting a slight curvature for all solid cancers and clearly curved for leukaemia. Recent dose response curves for all solid cancer mortality and incidence are reproduced in Figures 7 and 8 respectively:

Figure 6. (adapted from figure 1 of Ozasa et al. 2012). A summary of the organ specific excess relative risk (ERR) per 1Gy for various tumour sites.
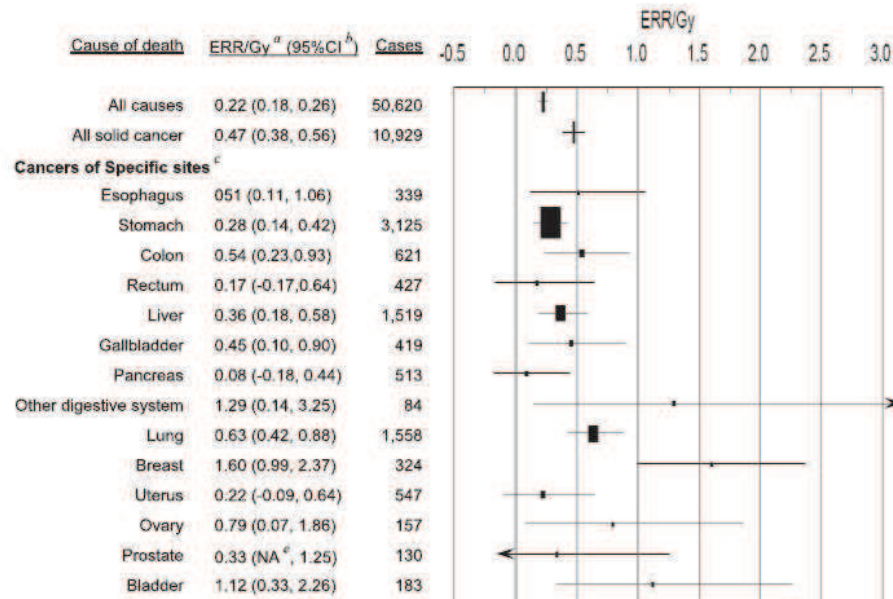[a] *ERR was estimated using the linear dose model, in which city, sex, age at exposure, and attained age were included in the background rates, but not allowing radiation effect modification by those factors.*
[b] *Horizontal bars show 95% confidence intervals.*
[c] *The size of the site-specific symbols is proportional to the number of cases.*
[d] *Not applicable to the part of the original figure shown here.*
[e] *The lower CI could not be calculated.*

Figure 7. (figure 4 of Ozasa et al. 2012). A dose-response curve for all solid cancers (mortality): Excess relative risk (ERR) for all solid cancer in relation to radiation exposure. The black circles represent ERR and 95% CI for the dose categories, together with trend estimates based on linear (L) with 95% CI (dotted lines) and linear-quadratic (LQ) models using the full dose range, and LQ model for the data restricted to dose < 2 Gy.
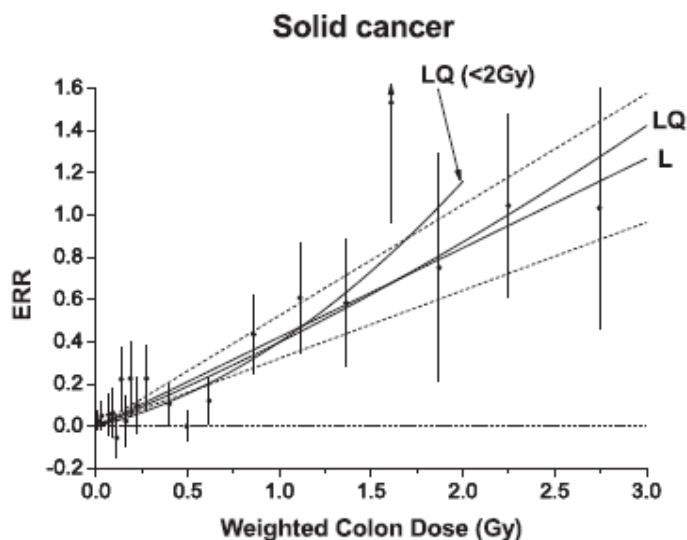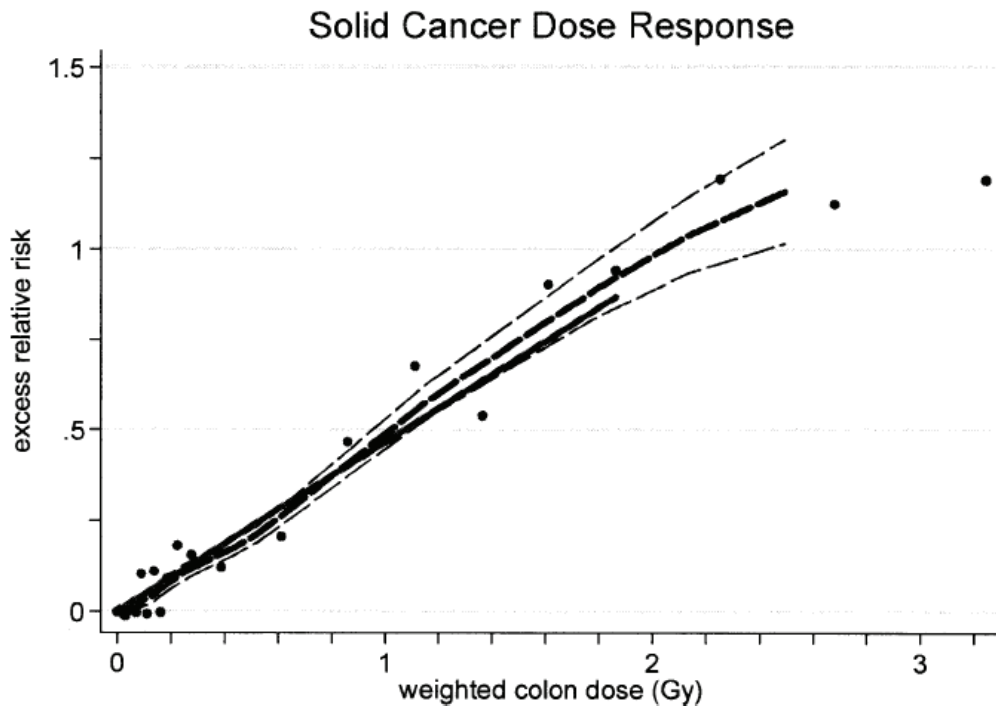
Solid Cancer Dose Response

Figure 8. (figure 3 of Preston et al. 2007). A dose-response curve for all solid cancers (incidence): Excess relative risk (ERR) for all solid cancer in relation to radiation exposure. The thick solid line is the fitted linear gender-averaged ERR dose response at age 70 after exposure at age 30 based on data in the 0 to 2 Gy dose range. The points are non-parametric estimates of the ERR in dose categories. The thick dashed line is a nonparametric smooth of the category specific estimates and the thin dashed lines are one standard error above and below this smooth.

3.1.2 The candidate's work

The cohort of the atomic bomb survivors forms a major basis for radiation safety regulations (16). Most major RERF analyses of the Japanese A-bomb data consider the cancer risk for all solid cancer with respect to the weighted colon doses, i.e., the γ-colon dose plus 10 times the neutron colon dose, where the factor 10 is assumed for the relative biological effectiveness (RBE) of neutrons relative to gammas. Consequently the late radiation effects are almost fully attributed to the γ-doses. This approach, although adopted consistently by RERF, is not entirely satisfactory because the attenuation of the gammas and neutrons by the human body are different (the neutrons are attenuated more) and the RBE of neutrons is associated with large uncertainty. Further a constant value of 10 is not consistent with the neutron weighting factors recommended by the ICRP and does not account for the increasing hardening of the neutron spectra with increasing distance from the bomb hypocentres in Hiroshima and Nagasaki (20).

Epidemiological data-sets for cancer incidence and mortality, in grouped form, are made available by RERF on their website, after the RERF papers are published. It has, therefore, been possible for the candidate to perform independent analyses with these data-sets based on Poisson regression (Breslow and Day 1988) for grouped data with either the EPICURE software (Preston et al. 1993) or self-written bespoke programs that interface with the MINUIT optimisation software (James 1994).

In a series of papers that refined the usual RERF approach, by developing new methods to either consider all solid cancer risks associated with γ-doses and neutron doses separately (1-4), or apply organ specific doses (7-8), some indications were found for a higher neutron relative biological effectiveness (RBE) with respect to gammas, than previously assumed (13). Such indications need to be treated very seriously since, for example, about 50% of proton therapy patients receive an additional neutron dose as an unwanted by-product. In January 2012 an international research project started under the seventh framework programme of the European Union, FP-7-EU-ANDANTE (Multidisciplinary evaluation of the cancer risk from neutrons relative to photons using stem cells and the analysis of second malignant neoplasms following paediatric radiation therapy): more information can be found at http://www.sciencenet-mv.de/index.php/kb_746/io_2905/io.html. The candidate is involved in ANDANTE with the development of a prospective international cohort of radiotherapy patients to further evaluate the cancer risk from neutrons relative to photons.

New neutron RBE values as a function of distance from the hypocentres have been presented (20). Since cancer risks for doses above 1 Gy are important for radiotherapy patients and for planning long-term manned space missions, such risks have also been presented (22, 30). A mechanistic model of carcinogenesis has also been applied to the A-bomb mortality data for all solid, stomach and liver cancer to examine the possible influence of radiation-induced cell inactivation on radiation risks (23). Comparisons of cancer risk following either chronic exposure or a single exposure have been made (28) and variations of cancer risk by age at exposure have been examined (29).

3.1.2.1 All solid cancer risks apportioned according to the associated γ-dose and neutron dose contribution

A method was developed (2) to uncouple the solid cancer mortality risk coefficient for neutrons from the low dose estimates of the relative biological effectiveness (RBE) of neutrons and the photon risk coefficient. This was achieved by relating the solid cancer risk in terms of organ averaged doses – rather than the colon doses – to two more directly assessable quantities: the excess relative risk (ERR_1) due to an intermediate reference dose D_1=1 Gy of γ-rays; and the RBE of neutrons, R_1, against this reference dose. It was concluded that the neutrons have caused 18% or 35% of the total effect at 1 Gy for tentatively assumed R_1 values between 20 and 50. The corresponding solid cancer mortality ERR for neutrons was found to be between 8/Gy and 16/Gy. A separate analysis (3) translated these values into risk coefficients in terms of the effective dose, E, by accounting for the γ-ray component produced by the neutron field in the human body.

This work was based on the Dosimetry System from 1986, DS86, (Roesch 1987) which was current at the time. Since then, DS86 has been updated to the dosimetry system from 2002, DS02, (Young & Kerr 2005) that included a reassessment of the neutron doses in Hiroshima. Preston et al (2004) reported on the effects of the changes of the dosimetry system on cancer mortality risk estimates and showed that at 1 Gy colon dose the doses did not change very much from DS86 in Hiroshima (i.e., a 3% decrease in neutron dose and an 8% increase in γ-dose). Consequently the risk estimates for neutrons (2, 3) remain essentially unaffected by the change in dosimetry system and are still currently applicable.

A further analysis (4) incorporated the new treatment for the explicit accounting of the neutrons (2, 3) to assess the risk coefficients for γ-rays with regard to solid cancer in terms of the ERR and the Lifetime Attributable Risk (LAR). The concepts and computations for deriving the factors for the conversion of ERR to LAR were described separately (1). Results from (1) were described and cited in BEIR VII–Phase 2 (2006) and the suggested methodology has been adopted (WHO 2012, Berrington et al. 2012). It was pointed out (4) that reference to the colon dose underestimates the average γ-ray dose to all relevant organs by only about 8.5%. On the other hand, it was noted that for neutrons the reference to the colon dose is not satisfactory. The organ averaging – with weight factors

accounting for the risk contribution of individual tumour sites (2) – results in neutron absorbed doses that are about twice as large as the colon doses. Figs. 9 and 10 illustrate the inferred response of the ERR (cancer mortality) to the total absorbed dose. The figures refer to the results obtained for an age attained of 60 years, with an attained age risk modification, but the dose responses for risk modification by age at exposure model are very nearly the same. Figure 9 gives results from the conventional analysis (with colon as reference organ and a neutron RBE (w) = 10). Figure 10 depicts the results obtained with the explicit accounting for neutrons. The solid curves show the effect contribution due to the γ-rays and the dotted curves represent the total effect. The abscissa values are the organ averaged absorbed doses (including the neutrons). The effect contribution of the neutrons increases more than proportionally to total dose, which reflects the fact that the neutron absorbed dose fraction increases with dose. The points (with standard errors) are direct fits to the data in the individual dose bins.
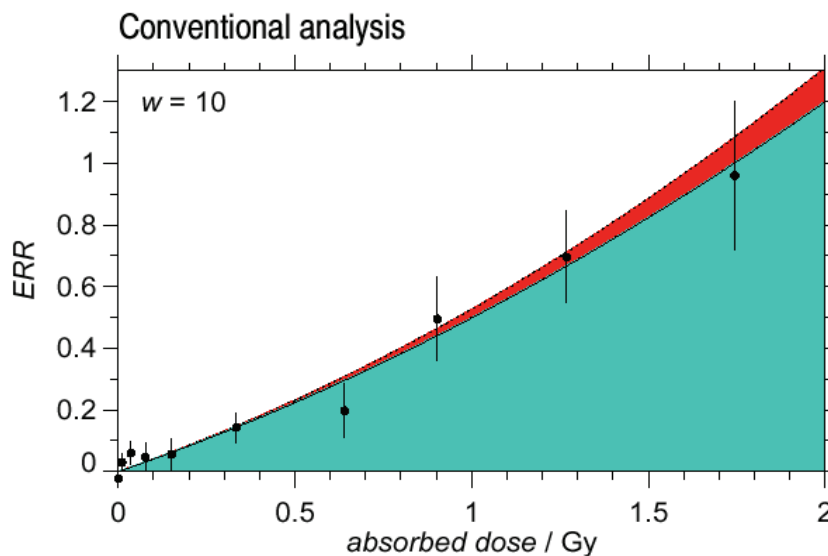
Figure 9. The inferred response of the ERR (cancer mortality) to the total absorbed dose from the conventional analysis (with colon as reference organ and a neutron RBE (w) = 10). The figure is for an age attained of 60 years, with an attained age risk modification. The points (with standard errors) are direct fits to the data in the individual dose bins.

Results from (2, 3 and 4) were described and cited in a recent monograph from the International Agency for Research on Cancer (chapter "Neutron radiation", p.231, IARC 100D, 2012) and results from (2 and 3) were described and cited in ICRP 92 (2003).
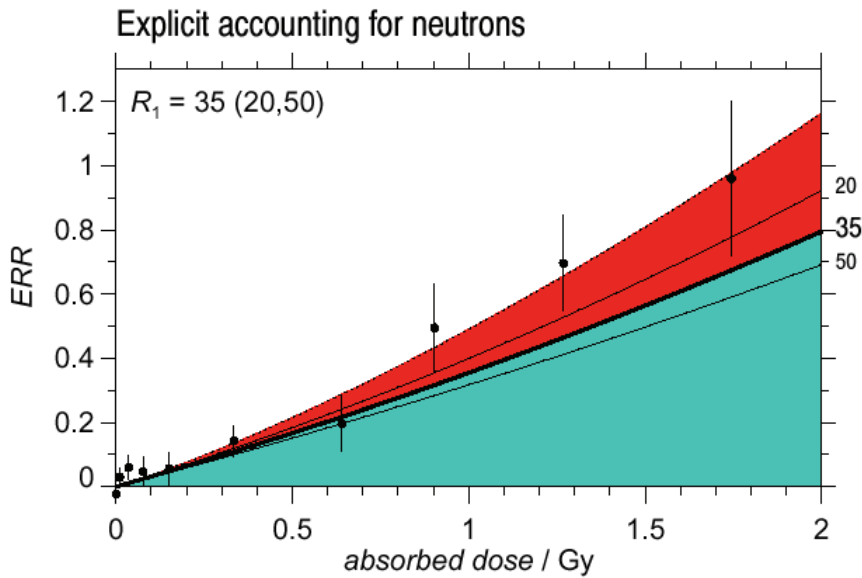
Solid cancer mortality (1950-1990), RERF

Figure 10. The inferred response of the ERR (cancer mortality) to the total absorbed dose, with the explicit accounting for neutrons (where R_1 is the RBE at 1Gy; the effects of setting R_1 to three values, 20, 35 and 50, can be seen on the right hand side of the dose response curve). The figure is for an age attained of 60 years, with an attained age risk modification. The solid curves give the effect contribution due to the γ-rays and the dotted curves represent the total effect. The abscissa values are the organ averaged absorbed doses (including the neutrons). The points (with standard errors) are direct fits to the data in the individual dose bins.

3.1.2.2 Application of organ specific doses

Further assessments (7, 8) repeated the earlier analysis (4) with two major extensions: by paralleling computations based on organ-average doses with new computations based on organ-specific doses; and updating the previous results by using the cancer mortality data for 1950–1997 which had just been released at that time. To apply organ-specific doses to the grouped publicly available solid cancer mortality data (file name: r13mort.dat) is not entirely trivial. Pierce et al. 1996 noted that "It is impossible to use more specific organ doses for solid cancers as a class, since there is no designated organ for those not dying of cancer."

This difficulty was resolved (7, 8) by formally treating each person as a set of 13 sub-units at risk, each belonging to 1 organ category. In terms of programming this meant creating a new organ category at the lowest level of the data structure where there are a total of 37,060 original data groups (for combinations of city, gender, age attained, age at exposure and colon dose category), each group

46

containing the number of cases of death from different types of solid cancer. For each of these original data records, 13 new organ-specific records were created to contain the numbers of deaths for each cancer type and the relevant organ-specific doses. This new data file was created with a computer program written by the candidate. The first 12 organ groups represented the specific sites with more than 100 deaths, while data group 13 contained the remaining widely varying sites which were assigned the organ-averaged doses. The refined risk coefficients were then computed by the maximum likelihood Poisson regression method.

While the application of organ-averaged doses (2, 3, 4) represents a distinct improvement over the traditional use of the colon doses, the organ-specific doses provide the best currently available dosimetric information. LAR values with respect to organ-specific doses (7) are up to about 20% higher than those obtained with exactly the same modeling techniques but in terms of the organ-averaged doses (4). The site-specific ERR/Gy as a function of RBE computed in (8) are suggestive of different radiation sensitivities for the various organs and this observation directly led to the idea for the analysis presented in the next section (13). Results from (8) were described and cited in a recent IARC monograph (IARC 2012, chapter "X- and γ-radiation", p.127) and in Annex A of UNSCEAR 2008.

3.1.2.3 Indications of a high neutron relative biological effectiveness (RBE) with respect to gammas

The Japanese A-bomb mortality data for the follow-up period (1950–1997), that was originally analysed by Preston et al. 2003, was re-analysed in (13) to obtained organ specific Excess Relative Risks (ERR) relative to the organ dose (γ-dose + RBE × neutron dose), ERR/Gy. These risks were then plotted against the average neutron fraction of the absorbed organ dose, defined as neutron organ dose/(neutron organ dose + γ-organ dose), which decreases with the depth of the organ in the human body because the neutrons are attenuated more than the gammas. It was found that the risks calculated with RBE=10, are larger for organs closer to body surface and that this trend, although inconspicuous, was highly statistically significant (see Figure 11, where three organs are marked explicitly in red as examples of organs at different depths in the human body, i.e.,

the colon has a higher body shielding and therefore a smaller average neutron fraction than the breast or lung).
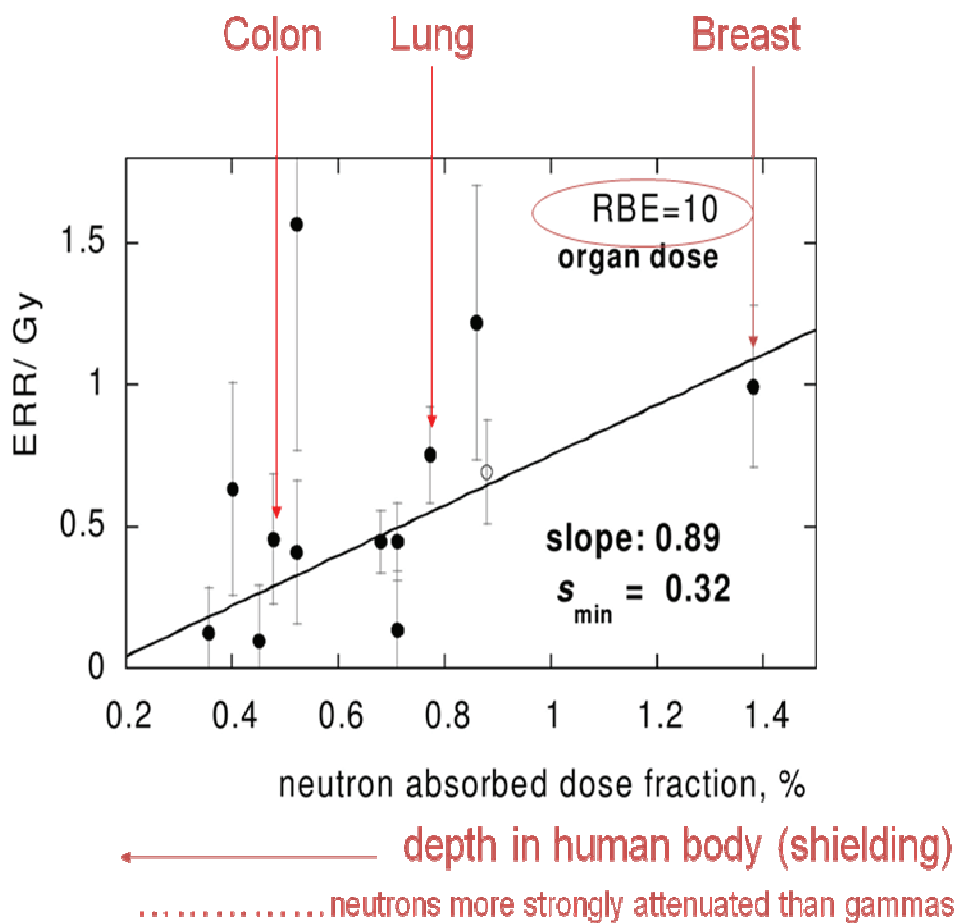
Figure 11. The ERR per Gy of weighted organ dose, calculated with an RBE = 10, as a function of the average neutron absorbed dose fraction (%) for different organs (each point represents a different organ). Three organs are marked explicitly in red as examples of organs at different depths in the human body, i.e., the colon has a higher body shielding and therefore a smaller neutron fraction than the breast or lung. The trend line has a slope of 0.89 with a lower 95% confidence limit (S_{min}) of 0.32.

This trend can be explained by underestimation of the neutron RBE since the statistical significance of the trend was found to decrease for larger RBE values. At an RBE of 35 the trend is still statistically significant. However the lower 95% confidence interval of the slope obtained with an RBE of 100 is just below zero (see Figure 12).

A similar trend was also apparent in the cancer incidence data for the follow-up period (1958–1987) available at the time from the original analysis of Thompson et al. 1994. Since the publication of (13), more recent incidence data has become available for the follow-up (1958–1998) as analysed in Preston et al. 2007. The trend described in (13) is also statistically significant in the new data (as yet unpublished analysis by the candidate). Results from (13) were described and

48

cited in a recent IARC monograph (chapter "Neutron radiation", p.231, IARC 100D, 2012)
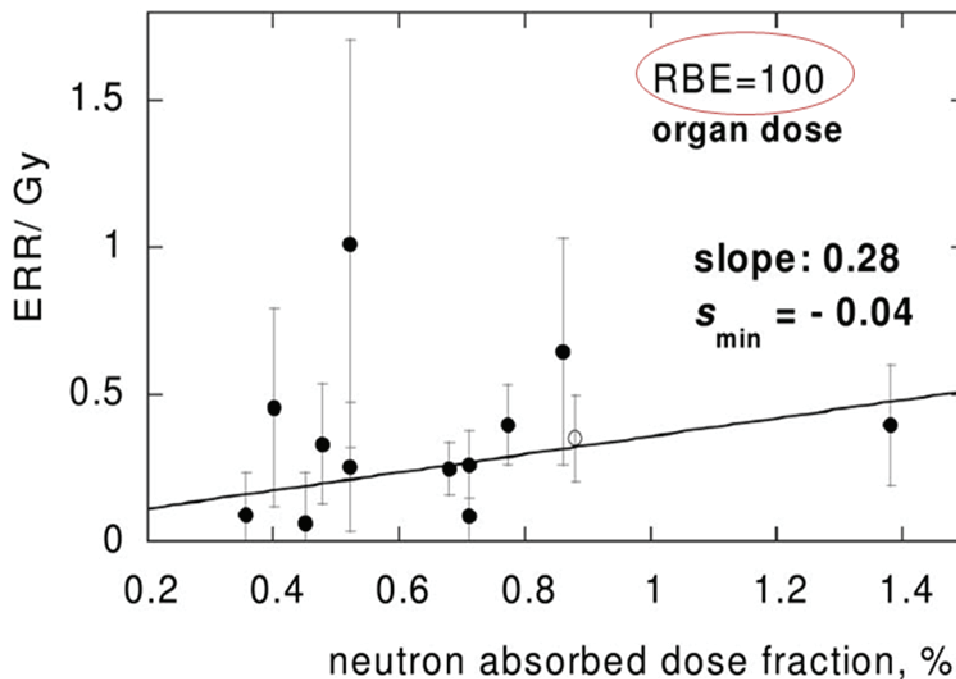
Figure 12. The ERR per Gy of weighted organ dose, calculated with an RBE = 100, as a function of the neutron absorbed dose fraction (%) for different organs (each point represents a different organ). The trend line has a slope of 0.28 with a lower 95% confidence limit (S_{min}) of -0.04.

This indication of high RBE values is automatically linked to a corresponding reduction in the risk estimates for γ-doses. Since Poisson regression log-likelihood computations were applied to fit the risk models to the solid cancer mortality data, the "goodness of fit" measure for this type of regression, i.e., the deviance, could also be plotted for different RBE values. This type of analysis resulted in a minimum deviance for RBE=100 with a 95% confidence lower limit of RBE=25. Since the ERR/Gy calculated assuming an RBE of 10 is widely adopted by international regulatory bodies, issues connected with organ sensitivity are also often based on this assumption. It would be interesting to do more work in the future to see if independent biological measures for organ radiation-sensitivity are correlated with the neutron absorbed dose fraction.

New calculations for neutron RBE, as a function of distance from the hypocenters for both cities that are consistent with the neutron weighting factor given in ICRP (1991), have been presented (20). Values of about 31 at 1000 m and 23 at 2000 m ground range in Hiroshima, and corresponding values for Nagasaki of 24 and 22, result from these calculations – if based on the neutron spectra from the DS86 dosimetry. If a neutron weighting factor consistent with ICRP 2003 is used,

the corresponding values are 23 and 21 for Hiroshima and 21 and 20 for Nagasaki, respectively. Consequently current risk estimates will be subject to some changes in view of the changed RBE values. This conclusion also holds if the more recent doses from the dosimetry system DS02 are applied instead of the older DS86 doses.

3.1.2.4 Cancer risks for doses above 1Gy

Assessments of radiation related risks for detrimental health effects obtained from analyses of the A-bomb survivors usually focus on the dose span between 0 and 1 Gy, since this is of chief interest for radiation protection purposes. However, since estimates of cancer risk for doses above 1 Gy are becoming more important for radiotherapy patients and for planning long-term manned space missions, such risks have also been presented (22, 30).

Very little is currently known about the shape of dose-response relationships for radiation-induced cancer in the radiotherapy dose range. The approach in (22) placed emphasis on doses relevant for radiotherapy with respect to radiation-induced solid cancer and could be regarded as a first attempt to acquire more information in this area. In (22) the analysis of the data from the A-bomb survivors was extended by including two extra high-dose categories (4-6 Gy and 6-13 Gy) and by an attempted combination of fit parameters from A-bomb survivors risk models and from risk models fitted to the secondary cancer data from patients receiving radiotherapy for Hodgkin's disease.

The recent indications for a high neutron dose contribution (13) were also incorporated into the analysis by considering three different values for the relative biological effectiveness (RBE) of the neutrons (10, 35 and 100) and a variable RBE as a function of dose. Linear, linear-exponential and plateau dose–response relationships were considered. The plateau model with a dose-varying RBE turned out to be the preferred model from the application of model selection techniques. It was concluded that, for doses above 1 Gy, there is a tendency for a nonlinear dose–response curve and further evidence of a neutron RBE greater than 10 for the A-bomb survivor data. Furthermore, the first direct evidence was provided that the bending over of the solid cancer excess risk dose response curve for the A-bomb survivors, generally observed above 2 Gy, is due to cell killing effects (22). Results from (22) were also given and cited in (IARC 2012, chapter "Neutron radiation", p.231)

One of the recognized limiting factors for long-term space missions is the health risk to the astronauts from cosmic radiation from galactic cosmic rays, the solar wind and solar particle events. Crew members on space missions are exposed to a dose-rate of about 1 mSv/day at solar maximum from cosmic radiation but this can increase drastically during solar particle events and the total effective dose received could be more than 1 Sv (Shiver 2008). Consequently, a similar analysis to the one in (22) was also performed with the specific aim of assessing the impact for space radiation protection in the planning of long-term manned space missions (30).

The work presented in (30) implied that the use of organ-averaged dose, a dose-dependent neutron RBE and the bending-over of the dose–response relationship for radiation-induced cancer could result in a reduction of radiation risk by around 50% above 1 Gy. This could have an impact on radiation risk estimates for space crews on long-term (>500 days) missions with possible exposures resulting in effective doses above 1Gy. The consequence of using a dose and dose-rate effectiveness factor (DDREF: a concept developed around 1980 to allow for perceived inadequacies in low dose or low dose-rate linear risk estimates from epidemiological studies, because radiobiological data suggested non-linear effects at low doses) of 1.0 instead of 2.0 increases cancer risk by about 40% and would therefore balance the risk decrease described above.

3.1.2.5 Mechanistic models of carcinogenesis

This work involved mathematical modelling in terms of both the empirical (descriptive) risk method and biologically based mechanistic methods for carcinogenesis which also result in risk estimates. A major report (D) was prepared on this work for the German Federal Office for Radiation Protection (BfS) and a paper contains the main results (23). The two-stage clonal expansion (TSCE) model of carcinogenesis of Moolgavkar & Knudson 1981 was applied to the A-bomb mortality data for all solid, stomach and liver cancer to examine the possible influence of radiation-induced cell inactivation on radiation risks (23). Different forms of cell survival curve i.e., either conventional or allowing for low-dose hypersensitivity (LDH) were investigated. LDH is an effect whereby, for some cell lines, the measured cellular survival can be lower than predicted if predictions are based on an extrapolation of surviving fractions generated at

higher doses to lower doses, using a linear quadratic dose response (see the early papers on this work by Lambin et al. 1993, Marples et al. 1993). Quality-of-fit tests for non-nested models (21) were used in comparisons between TSCE and descriptive models. The TSCE models were found to represent the data more economically (i.e., with fewer parameters for a similarly good description of the data) than descriptive risk models in general, but the data do not have enough statistical power to allow a firm determination of a preferred model type. Central excess relative and absolute risk estimates (at 1 Sv, for age at exposure 30 and age attained 70) from TSCE and empirical models were found to be in good agreement with each other and with previously published estimates.

3.1.2.6 Variation of cancer risk by age at exposure.

A recent conclusion that cancer risks for persons exposed in middle age may have previously been underestimated is based on modeling the cancer incidence data from the A-bomb survivors (figure 6 of Preston et al. 2007, reproduced below in the left-hand panel of Figure 13).
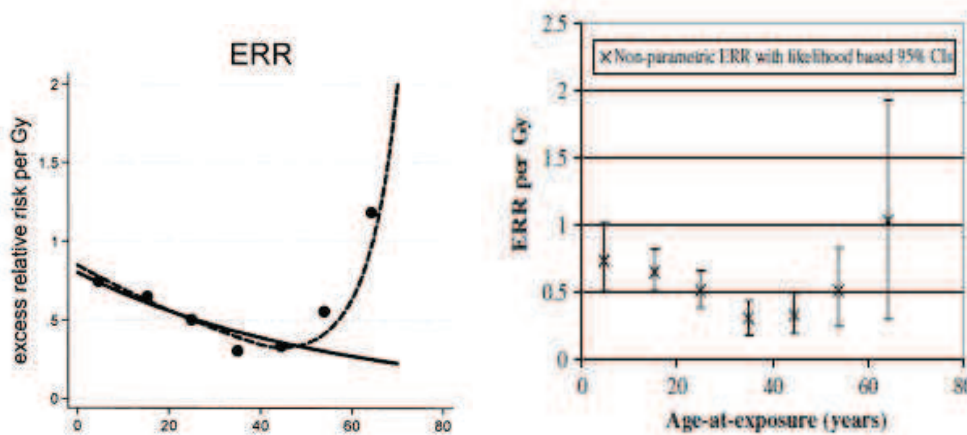
Figure 13. The left-hand side shows figure 6 of Preston et al. 2007, i.e., the excess relative risk per Gy plotted as a function of age at exposure in years. The right-hand side shows the independently constructed figure with 95% confidence interval (29).

However, as noted in (29), figure 6 of Preston et al. 2007 is difficult to interpret because the error bars associated with the non-parametric risks (the points in the left-hand panel of Figure 13) are very large. To illustrate this point the computations necessary for producing the Figure 6 of Preston et al 2007 were independently repeated and the results were re-plotted (see Figure 13, right-hand side) (29).

It was also noted in (29) that the evidence that risk increases at older ages at exposure is not as strong in the A-bomb mortality data (see figure 3 of (29)) as in the incidence data. This point was also later acknowledged in the major LSS paper on cancer mortality by Ozasa et al. 2012: "The nonparametric category-specific estimates of age-at-exposure effects on all solid cancer mortality risk in the current study were similar to the corresponding figures reported by Walsh 2009, in which an increased risk at an old age at exposure was less remarkable than in the figure reported by Preston et al 2007." These points were also described and cited in a recent editorial of the Journal of the National Cancer Institure, USA, (Boice 2010) which reproduced figure 3 of (29).

3.1.2.7 Comparisons of cancer risk following either chronic exposure or a single exposure

A current moot point is whether the cancer risk associated with chronic exposures accumulated over an extended period of time differs noticeably from the effects of a single exposure. In the currently recommended dose limits for occupational exposures (ICRP 2007), it has been assumed that solid cancer risk factors are a factor of two lower than for the A-bomb survivors (i.e., DDREF=2.0). In order to investigate this point further, twelve recent epidemiological analyses of eight studies on cancer after low-dose-rate, moderate-dose exposures with solid cancer or all cancer risk estimates were identified from a literature search and considered together. The reviewed studies included, among others, Chernobyl nuclear accident clean-up workers (Ivanov et al. 2001), residents of apartments built in Taiwan with accidently contaminated metal support structures (Hwang et al. 2006) and a pooled study of nuclear workers in 15 countries (Cardis et al. 2007). The twelve analyses were included in a meta-analysis of cancer risks related to such exposures and compared to risks from the A-bomb survivors (28). There were significant dose responses in 7 of the 12 analyses. For each of the twelve analyses, the risk for the same types of cancer among the A-bomb survivors with the same gender proportion and matched quantities for dose (e.g., A-bomb survivor skin dose was matched to the workers dose from a film badge reading), mean age attained and mean age at exposure were computed. A combined estimator of the ratio of the excess relative risk per dose from the low-dose-rate, moderate-dose exposures study to the corresponding value for the atomic bomb survivors was 1.21 (90% CI 0.51 to 1.90). This study provided

evidence that cancer risk factors for occupational exposures are not lower than for the A-bomb survivors.

A very similar study for leukaemia by Daniels & Schubauer-Berigan 2011 indicated that the spontaneous leukaemia risk (i.e., for a group of unexposed persons) was found to be increased by 19% due to a dose of 100mGy. The 19% increase was reported to agree well with the risk from acute exposure from the Japanese A-bomb survivors and is therefore an indication that leukaemia risks are similar for protracted and acute exposures (37). Consequently the analyses (28) and Daniels & Schubauer-Berigan 2011 indicate that there is little reason to use DDREF in radiation protection at this current stage of knowledge. Results from (28) have been described and cited in EPA 2011, WHO 2012 and are due to be cited in a new UNSCEAR report entitled "Uncertainties in risk estimates for cancer due to exposure to ionizing radiation" due for publication in 2013.

3.2 Life span study on late effects of [224]Radium in children and adults

3.2.1 Background and previous work

Just after World War II, [224]Ra, a short lived bone seeking α-emitter, was administered by a German physician, Dr. Paul Troch as a "remedy" for tuberculosis and ankylosing spondylitis. During the period from 1945 to 1955, several thousand patients were injected with [224]Ra in a solution, also containing traces of platinum and the red dye eosin, called Peteosthor. Prof. Heinz Spiess (Spiess 2010) endeavoured to put a stop to the Peteosthor injections and to initiate an epidemiological follow-up of the treated patients but Dr. Troch prohibited him from continuing his research.

A press release in 1947 caused the local government to request that further research on Peteosthor should be undertaken at the University of Göttingen, Germany. Consequently, Prof. Spiess was appointed there to assess the effect of Peteosthor in the treatment of tuberculosis. During the course of early experimental work in 1948 with animals in their growth phase (mice, guinea pigs and rabbits) using simple autoradiography on a photo-plate, it became clear to him that the [224]Ra becomes particularly concentrated in the bone growth-zones (see Figure 14). Histological proof was provided of irreversible injuries of the epiphysial cartilage with mitotic inhibition and cellular oedema and damage.

Prof. Spiess subsequently succeed in getting the injected doses of [224]Ra reduced and predicted a radiation-induced growth retardation in injected children, which was unfortunately later confirmed (see Spiess 2010 for a full description). Prof. Spiess issued the strong warning (1950 German Congress of Orthopaedics): **"Peteosthor is dangerous – following our extensive experimental studies, I feel obliged to warn against it, at least from the point of view of a paediatrician".** Further warnings were issued (German Congress of Surgery, Munich, 1951) and the injections of [224]Ra in children and juveniles were stopped soon after.
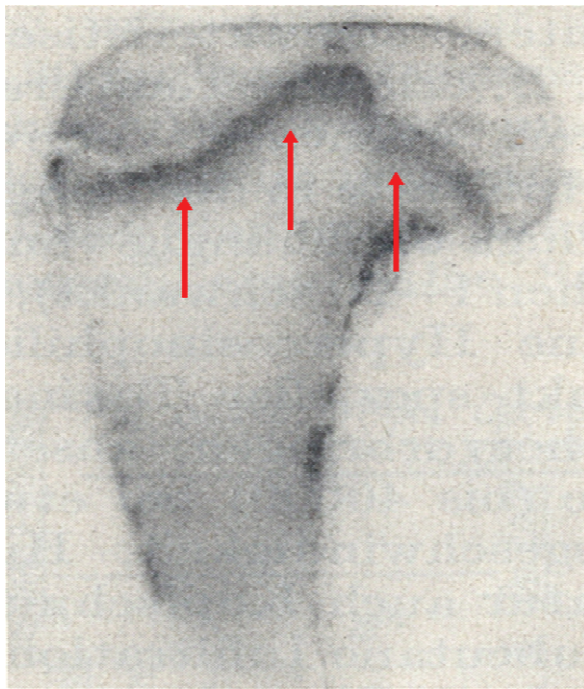
Figure 14. Photographic plate (courtesy of Prof. H. Spiess) – the red arrows indicate the deposition of [224]Ra in the bone of a young rabbit after 12 injections of [224]Ra.

Finance to follow-up the patients was initially refused but a first informal follow-up was initiated in 1954/55. Prof. Spiess and his wife visited 42 former patients, injected with [224]Ra as children, or their families. They were shocked by their observations on these visits due to their discovery of the predicted radiation induced growth retardation and 9 malignant bone tumours (7 of which were fatal). A formal follow-up programme began in 1955. The [224]Ra exposed patients were traced, warned and invited for examinations to the university hospital or offered a personal examination at home. Follow-up of 899 persons (including 217 children or juveniles) continued by questionnaire and telephone-interview at intervals of about 3 years, with excellent response rates. In December 2007, 124 persons were still alive and the follow-up period covered over 60 years.

The most striking observed detrimental health effect following ^{224}Ra injections was a large number of malignant bone tumours that occurred predominantly in childhood. This observation was the reason that Prof. Spiess was invited to the first conference on "Delayed Effects of Bone seeking Radionuclides" in Sun Valley, USA, in September 1967, where he reported on 50 ^{224}Ra induced bone tumors in children and adults, growth disturbances, osteochondroma and cataracts, and concluded that the younger the age at ^{224}Ra injection, the more severe the late effects (Spiess 1969).

3.2.2 The candidate's work

The candidate has been involved with the study since 2000 and has generally provided some support to Prof. Spiess and been involved in two publications (10, 36). Up to now 57 malignant bone tumours (38 and 19 in persons treated as children and adults respectively) have been observed where less than one case was expected (36). The peak occurred 8 years after the first Ra-224 injection and the last bone sarcoma occurred 46 years after injection (see Figure 15).

A significant excess of non-skeletal malignant diseases has also become evident. Expected numbers of cases were computed from the age, gender and calendar year distribution of person years at risk and incidence rates from a German Cancer Registry. Poisson statistics were applied to test for statistical significance of the standardized incidence ratios. Up to the end of December 2007, the total number of observed malignant non-skeletal diseases was 270 (248 specified cases of non-skeletal solid cancers, 22 other malignant diseases: 16 malignant neoplasms of lymphatic and hematopoietic tissue, 6 without specification of site) vs. 192 expected cases. Accounting for a five year minimum latency period and excluding 13 cases of non-melanoma skin cancer, 231 non-skeletal solid cancers were observed vs. 151 expected cases. Significantly increased cancer rates were observed for breast (32 vs. 9.7), soft and connective tissue (11 vs. 1.0), thyroid (7 vs. 1.0), liver (10 vs. 2.4), kidney (13 vs. 5.0), pancreas (9 vs. 4.1), bladder (16 vs. 8.0), and female genital organs (15 vs. 7.8) (36) – see Figure 16.
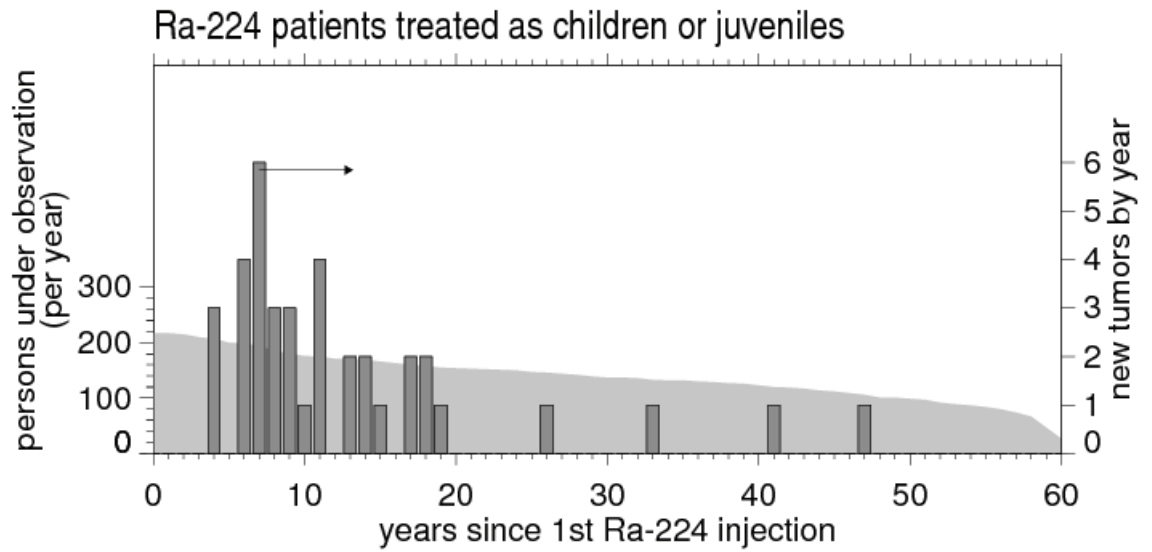
Figure 15. (graphics courtesy of Dr. Elke. A. Nekolla). The distribution of 38 cases of Malignant bone tumors in patients treated as children or juveniles (bars and right-hand ordinate, as indicated by the arrow) and the number of persons under observation (grey shaded area and left-hand ordinate).
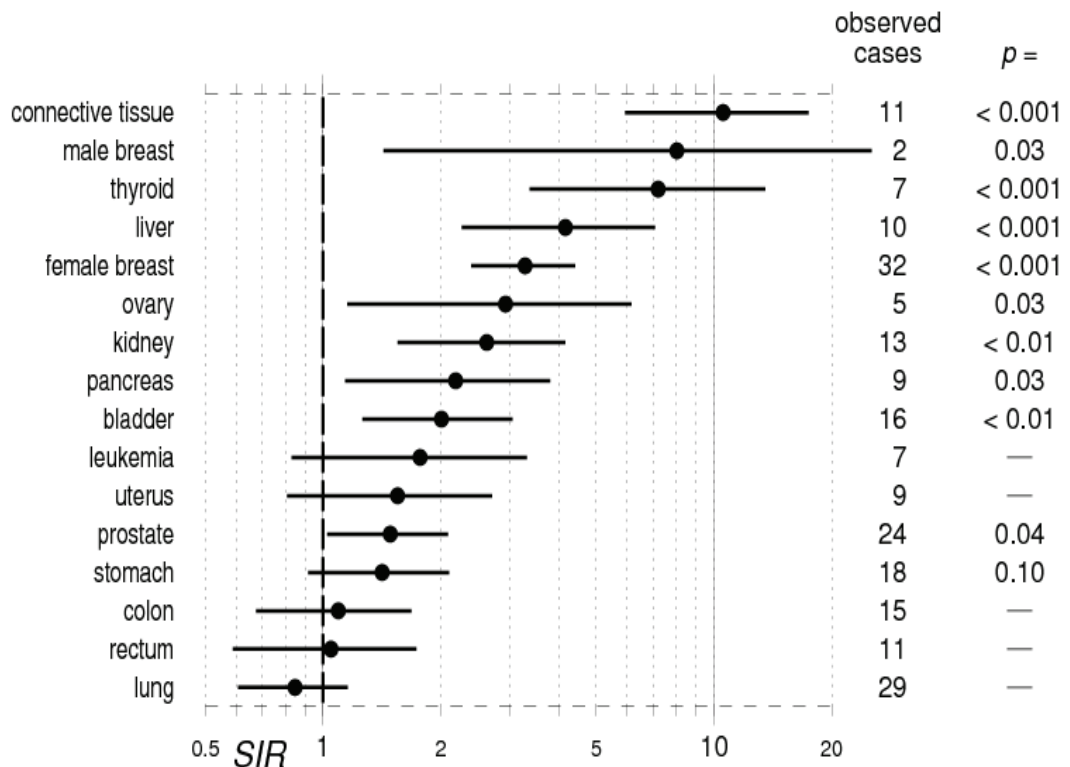
Figure 16. (figure 3 of (36)). Standardized Incidence ratios (SIR) for different types of cancer, as listed on the left-hand side, occurring up to December 2007. Two-sided 90% confidence intervals are given with the SIR central estimates (the dots) and the p-values associated with the SIRs are listed on the right-hand side

57

3.3 Development of epidemiological models for thyroid cancer risk in areas affected by the 1986 Chernobyl accident

3.3.1 Background and previous work

The Chernobyl nuclear power plant accident in April 1986 resulted in a large release of radio-nuclides, including thyroid-seeking radioactive iodine, ^{131}I, which formed the main component of post-accident thyroid doses in exposed persons. Subsequently, the incidence of thyroid cancer in Ukraine and Belarus was observed to increase significantly in 1990 amongst subjects who were children or adolescents at the time of the accident (Likhtarev et al. 1995, Kazakov et al. 1992). Over the subsequent decade, a further increase was observed in the incidence rates (Tronko et al. 1999).

3.3.2 The candidate's work

Detrimental health effects of ^{131}I exposures were assessed by analyses of epidemiological thyroid cancer data relating to this accident. Models were developed to fit epidemiological data on thyroid cancer incidence in young persons exposed to ^{131}I, with the specific aim of quantifying the risk per unit dose and the dependence of this risk on gender, time and age (14). The study (14) was based on 512 & 577 thyroid cancer cases in Ukraine and Belarus respectively. Based on these data, a model was presented in (14) with the feature of strongly decreasing excess relative risk (ERR) with increasing age-attained (see figure 6 of (14)). The results were given for various fixed ages-at-exposure and indicate a decrease of the ERR with time-since-exposure. A contrast to this result was found in the study of Likhtarov et al. 2006, where a trend of strongly increasing ERR with increasing time-since-exposure (see Table 6 in (14)) was reported.

Since a good understanding of the risks and their modification with time and age is important for assessing the future health care requirements and for developing the appropriate steps that must be taken in future accidents, a further study was done to investigate these conflicting results (27). The purpose of (27) was also to further refine these earlier models (14) and also to compare the Chernobyl risks with risks from the, then newly released, A-bomb data on thyroid incidence. The type of baseline modelling method was identified in (27) as the reason for the conflicting results. Various quality-of-fit criteria were found to favour a parametric

baseline model over various categorical baseline models. The model with a parametric baseline resulted in a decrease of the ERR by a factor of about 0.2 from an age-at-exposure of 5 years to an age-at-exposure of 15 years (for a time-since-exposure of 12 years), and a decrease of the ERR from time-since-exposure of 4 years to time since exposure of 14 years of about 0.25 (for an age-at-exposure of 10 years). Central ERR estimates (of about 20 at 1 Gy, for an age-at-exposure of 10 years and an age-attained of 20 years), and their ratios for females versus males (about 0.3) turned out to be relatively independent of the model types. Excess absolute risk estimates from the different models were predicted to be very similar.

Risk models with parametric and categorical baselines were also applied to thyroid cancer incidence among the atomic bomb survivors. For young ages-at-exposure, the ERR values in the model with a parametric baseline were found to be larger. Both data sets cover the period of 12 to 15 years since exposure. For this period, higher ERR values and stronger age-at-exposure modifications were found for the Chernobyl data set.

3.4 Epidemiological results for detrimental health effects in the German Wismut uranium miners exposed to radon and other potential carcinogens

3.4.1 Background to the development of the Wismut cohort study

Albert Einstein called for watchfulness in August, 1939 in a letter to President Franklin D. Roosevelt to warn him "that the element uranium may be turned into a new and important source of energy in the immediate future" and "that extremely powerful bombs of a new type may thus be constructed". By early 1941, Werner Heisenberg had turned to the Belgian Congo for uranium to fuel his research reactor, after the uranium stockpiles ran low in the Reich's army occupied Joachimsthal mines (then Czechoslovakia). At that stage in time, the main uranium seams beneath the German provinces of Saxony and Thuringia, including the Ore Mountains, had not yet been discovered. Although silver had been mined since the twelfth century in this area and it was known that pitchblende (containing uranium) often occurred just where the silver seams became exhausted.

There are reports that the Soviet Red Army (SRA) secretly began to collect information in 1944 on the uranium deposits in this region (Paul 1991). Immediately after the surrender of the Reich's army between late April and early May 1945, the SRA began to confiscate private documents pertaining to uranium deposits (Paul 1991). This region, spanning Saxony and Thuringia, was occupied by American forces at this time but the Americans appear not to have considered the mining possibilities. After World War II, the Soviet politicians very skilfully negotiated the right to occupy this German region at the Potsdam conference in August 1945 and immediately started intensive geological explorations to locate uranium seams (Wendt et al. 1988). The uranium was required to supply the Soviet Union's atomic industry which included fuelling the first Soviet nuclear bomb that was detonated in the Kazakh-steppe in 1949 (Grosche 2002).

Uranium seams were rapidly located, mined and the delivery of uranium to the Soviet Union began in 1946. It is markworthy that, in this same year, the amount of uranium won from the occupied territories in Germany exceeded the amount produced in the Soviet Union. The total yield of uranium from this region between 1946 and 1990 was 231,000 tonnes (Chronik der Wismut 1999). The uranium

mines in Saxony and Thuringia were run by the Soviet Stock Corporation from 1945 to the end of 1953 and then subsequently by a joint German and Soviet Stock Company. The company was known by the "undercover" code name of "Wismut" (German for bismuth) – a name chosen to distract from the real activities. An estimated 400,000 persons worked underground or in uranium ore processing facilities at the Wismut company at some stage between 1946 and 1990.

After German reunification, the German Federal Ministry for the Environment maintained the Wismut health data archives, thereby enabling the establishment of the cohort (Grosche et al. 2001, Kreuzer et al. 2002). The Wismut cohort, as recently profiled (35), is currently the largest single cohort of uranium mine workers with retrospective follow-up before 1999 and prospective follow-up from 1999. There were 64,311 former Wismut employees initially eligible for the cohort but it was decided to exclude from this number all women, persons born before 1900, persons with unknown radiation doses or implausible data and those who had either worked less than 180 days or started working after 1989. The final cohort consisted of 59,001 members, with 2,388 deaths from lung cancer for the first mortality follow-up period (1946–1998) and 58,987 members with 3,016 deaths from lung cancer for the second follow-up (1946–2003). Third follow-up (1946–2008) data was released in September 2012. It is envisaged to continue producing new follow-up data sets every 5 years. The subsequent follow-ups not only extend the previous follow-up by 5 years but also include any improvements in data-collection for the whole follow-up period (such as newly located death certificates or corrections for persons previously considered lost to follow-up and then located).

Job histories provide information for each cohort member on the period and type of employment on a daily basis. The exposure to radon and its progeny in Working Level Months (WLM)[1], effective doses from external γ-radiation (Sv) and exposures to long-lived radionuclides ($kBq \cdot h/m^3$) could be estimated retrospectively using job histories via a job-exposure matrix (JEM). A separate JEM calculated dust exposures in dust-years, i.e., an exposure to 1 mg/m^3 (for fine dust and silica dust) and 1 μg/m^3 (for arsenic), respectively, for 220 shifts of 8

---

[1] Exposure to radon and its progeny is expressed in WLM. One working level (WL) is defined as the concentration of short-lived radon daughters per litre of air that gives rise to 1.3×10^5 MeV of alpha energy after decay. One WLM of cumulative exposure corresponds to exposure to 1WL during 1 month (170 h) and is equivalent to 3.5 mJhm^{-3}.

hours each. Information on the causes of death is from death certificates and also in part from the Wismut pathology archives. Consequently the cohort is suitable for calculating risks for a wide variety of research issues connected with testing possible associations between disease mortality rates and exposures to radiation, dust and some other covariables. A reliable determination of baseline (sporadic) disease rates is generally unproblematic because the cohort includes a large number of cohort members who were not exposed to radiation or dust (e.g. office workers).

3.4.2 Previous work

Up to 1999, the best source of epidemiological data for evaluating cancer risks associated with radon in mines had been provided by combining data from 11 national studies (from China, Europe, Canada, USA and Australia) to give a total of 60,606 miners with 2,674 lung cancer deaths (Lubin et al. 1995, BEIR 1999, Darby et al. 1995). This collaborative analysis of 11 studies had already provided information on the risk for lung cancers (Lubin et al. 1995, BEIR 1999) and cancers other than lung cancer (Darby et al. 1995) associated with radon in underground miners. However there were heterogeneity issues related to demographic and genetic/racial characteristics, quality of exposure assessment, completeness of follow-up, accuracy of disease diagnosis, assessment of mine exposures other than radon, smoking and other lifestyle patterns. Therefore the creation of the single Wismut cohort, comparable in size to the combined 11 studies cohort, but more homogeneous, was a valuable addition to the research field. The first two major research publications to be based on the results of analysing the data from the first follow-up of the Wismut cohort were on lung cancer (Grosche et al. 2006) and cardiovascular diseases (Kreuzer et al. 2006). There have recently been interesting papers on the effects of smoking on the radon associated lung cancer risk (Schnelzer et al. 2010) and on stomach cancer mortality (Kreuzer et al. 2012).

3.4.3 The candidate's work: epidemiological results from the Wismut cohort

Since 2007 the candidate has been involved in an ongoing series of papers. The risks of extra-pulmonary cancers (24) and cardiovascular diseases (32) associated with radon exposures were evaluated. Refined models for lung cancer

(33) were developed and the effects of other potential carcinogens (particularly exposure to quartz dust) on the risk of lung cancer and all solid cancers with respect to radon were evaluated (34). No convincing associations between leukaemia mortality and occupational doses of ionizing radiation were found (40). In order to assess the scale and nature of the smoking epidemic in this cohort an indirect method involving smoking impact ratios was applied (39). Further analyses of site-specific risks for prostate cancer (42), cardiovascular diseases (49), liver cancer (50) and lung cancer (45) have been done. The candidate is heavily involved in ongoing work in this area including current analyses based on a detailed comparison of organ-specific cancer risks due to the γ-doses from the Wismut and A-bomb survivor cohorts and an evaluation of the relative biological effectiveness of alpha radiation with respect to γ-radiation.

3.4.3.1 The radon related risk of extra-pulmonary cancers

An analysis was done on the second follow-up data from 1960, based on 20,684 deaths to assess whether radon in ambient air can cause mortality from cancers other than lung cancer (24). Cohort death rates for 24 types of cancer were compared with age and calendar-year specific national death rates for the former German Democratic Republic (available from 1960) using Standardized Mortality Ratios (SMR). The Excess Relative Risk (ERR) per unit of cumulative exposure to radon in Working Level Months (WLM) was calculated using Internal Poisson regression (Breslow and Day 1988). The number of deaths observed (O) for all cancers other than lung combined was close to the expected (E) number calculated from national rates (n=3,340, O/E=1.02, 95% confidence interval (CI): 0.98; 1.05). The result for leukaemia mortality, indicated no association with exposure to radon progeny, and was cited by (IARC, 2012) and (WHO, 2010). Statistically significant increases in mortality for cancers of the stomach (O/E=1.15, 95% CI: 1.06; 1.25) and liver (O/E=1.26, 95% CI: 1.07; 1.48) and statistically significant decreases for oral and pharynx cancers combined and bladder cancer were found.

Evidence was provided for a positive relationship between mortality from cancers other than lung cancer and cumulative exposure to radon. A statistically significant relation with cumulative radon exposure was observed for all non-lung cancers combined (ERR/WLM=0.014%; 95% CI: 0.006%; 0.023%). This latter result persisted after adjustment for the potential confounders – long-lived

radionuclides, γ-radiation, arsenic and dust – and was also given and cited by IARC 2012, ICRP 2010 and WHO 2010.

3.4.3.2 The radon related risk of cardiovascular diseases and cancers of the extrathoracic airways

An analysis was performed on the full second follow-up data based on 5,141 deaths from heart diseases and 1,742 deaths from cerebrovascular diseases to assess whether radon in ambient air is associated with the risk of such diseases (32). Results from this work were also given and cited in WHO 2010. However, in line with a previous analysis on the first follow-up data (Kreuzer et al. 2006) and dosimetric calculations for radon-related organ doses, no statistically significant increase in risk was found for coronary heart diseases (ERR/WLM=0.0003%) or cerebrovascular diseases (ERR/WLM=0.001%). In the same paper (32) a statistically significant (p = 0.042) linear exposure response model for a group of 177 cancers of the extra-thoracic airways with ERR/WLM = 0.06%, was presented (see Figure 17).

3.4.3.3 Models for the radon exposure related lung cancer mortality risk

An analysis was done on the full second follow-up data based on 3,016 lung cancer deaths and 2 million person years (33). Other exposure covariables such as occupational exposure to external γ-radiation, long-lived radionuclides, arsenic, fine dust and silica dust were also considered. The SMR for lung cancer was found to be 2.03, (95% CI: 1.96; 2.10) and the simple cohort *ERR*/WLM for lung cancer was estimated to be 0.0019 (95% CI: 0.0016; 0.0022).

The BEIR VI model as developed for the analyses of the study on eleven miner-cohorts (Lubin et al. 1995; BEIR 1999) and previously applied to the first Wismut follow-up (Grosche et al. 2006) produced risks similar to those obtained with a mathematically continuous *ERR* model for lung cancer, newly developed by the candidate. The continuous model was characterized by a linear radon-exposure response with exponential effect modifiers for age at median exposure, time since median exposure and radon exposure rate. In this model the central estimate of *ERR*/WLM was found to be 0.0054 (95% CI: 0.0040; 0.0068) for an age at median exposure of 30 years, a time since median exposure of 20 years and a mean exposure rate of 3WL. The *ERR* decreased by 5% for each unit exposure rate increase. The *ERR* also decreased by 28% with each decade increase in

age at median exposure and decreased by 51% with each decade increase in time since median exposure. The method of radon-exposure determination (i.e., whether the exposures were estimated or measured) was found to play an unimportant role in the determination of the *ERR*.
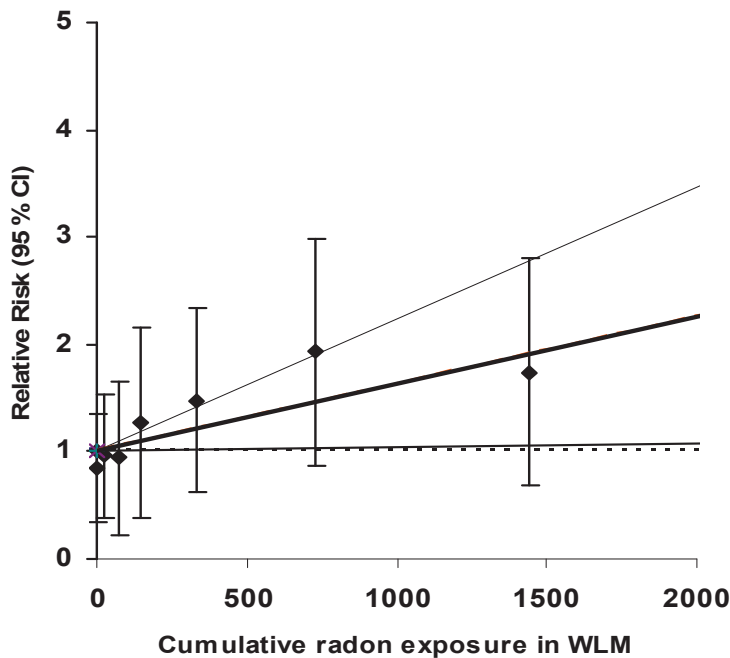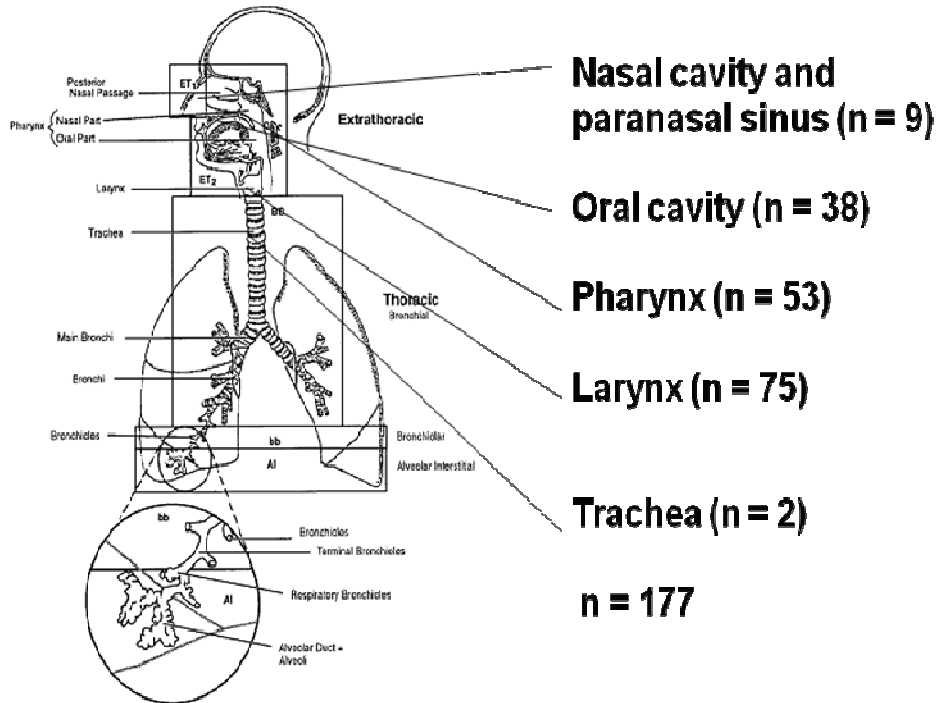
Figure 17. Upper panel: Schematic distribution of the numbers of mortalities (n) for a group of 177 cancers of the extra-thoracic airways. Lower panel (part of figure 3 from (32)): Simple risk models without risk modifying factors for the the exposure response of the extra-thoracic airway cancers (see upper panel). The square symbols represent the risks from the categorical analysis given with 95% confidence intervals. The bold line represents the simple linear risk model, ERR/WLM = 0.06%, with 95% confidence limits (i.e., the two finer lines).

The other exposure covariables were found to have only minor confounding influences on the *ERR*/WLM for the finally selected continuous model when included in the risk model in an additive way. Results from this work were also given and cited by WHO 2010.

3.4.3.4 Internal Poisson models for radon and the risk of cancer mortality

An analysis (34) was done on the full second follow-up data based on 20,920 deaths, 2 million person years and 6,373 cancers (3,016 lung cancers and 3,053 extra-pulmonary solid cancers). Internal Poisson regression was applied to estimate the excess relative risk (*ERR*) per unit of cumulative radon exposure in WLM for all major sites and for the follow-up period from 1946 to 2003 (see Figure 18). The *ERR*/WLM for all extra-pulmonary solid cancers combined without effect modification was found to be 0.014% (95% CI: 0.006%; 0.023%). An *ERR* model for extra-pulmonary solid cancer was developed that was linear in radon exposure with an exponential effect modifier which depends on age-attained. In this model the central estimate of *ERR*/WLM is 0.040% (95% CI: – 0.001%; 0.082%) for an age-attained of 44. The *ERR* decreases by 37% with each decade increase in age-attained. The highest *ERR*/WLM, after lung, was observed for cancers of the pharynx (0.16%), tongue/mouth (0.045%) and liver cancer (0.04%).

The effects of other potential carcinogens (particularly exposure to quartz dust) on the risk of lung cancer and all solid cancer with respect to radon were also evaluated. However the central *ERR*/WLM estimate for lung cancer was only found to be influenced to any notable degree, i.e., by an approximate 25% reduction, by the multiplicative inclusion of the covariable for quartz dust in the risk model (see Figure 19, left panel). The central *ERR*/WLM estimate for extra-pulmonary solid cancer was not found to be influenced to any notable degree by the inclusion of any of the covariables that were considered as potential confounders (see Figure 19, right panel). Results from this work were given and cited by IARC, 2012.

Site	n	ERR/100 WLM
Lung (C34)	3016	0.197 (0.170; 0.224)
Pharynx (C9-14)	53	0.163 (-0.042; 0.367)
Tongue/mouth (C1-6)	38	0.045 (-0.085; 0.175)
Liver (C22)	159	0.044 (-0.008; 0.095)
Non-Hodgkin (C82-85)	87	0.032 (-0.036; 0.101)
Rectum (C19-21)	241	0.028 (-0.008; 0.064)
Larynx (C32)	75	0.021 (-0.038; 0.080)
Stomach (C16)	595	0.022 (0.001; 0.042)
Gallbladder (C23-24)	81	0.021 (-0.035; 0.077)
Bladder (C67-68)	177	0.020 (-0.016; 0.056)
Kidney (C64-66)	171	0.017 (-0.023; 0.058)
Colon (C17-18)	301	0.016 (-0.012; 0.045)
Extrapul.(C0-C32; C35-C97)	3355	0.014 (0.006; 0.023)
Other/unspecified	462	0.009 (-0.014; 0.032)
Mult. Myeloma (C90)	55	0.007 (-0.056; 0.071)
Leukemia (C91-95)	128	0.005 (-0.034; 0.045)
Prostate (C61)	264	0.000 (-0.024; 0.024)
Pancreas (C25)	229	-0.001 (-0.029; 0.026)
Brain (C70-72)	115	-0.018 (-0.051; 0.018)
Esophagus (C15)	126	-0.025 (-0.053; 0.002)

Figure 18. The excess relative risk (*ERR*) per unit of cumulative radon exposure in Working Level Months (WLM) for all major sites with the number of deaths (n) given, for the follow-up period from 1946 to 2003. The error bars are for 95% CIs, the sites marked in yellow have a statistically significantly raised risk and the sites marked in pale blue have increased risks that are not statistically significant at the given level.
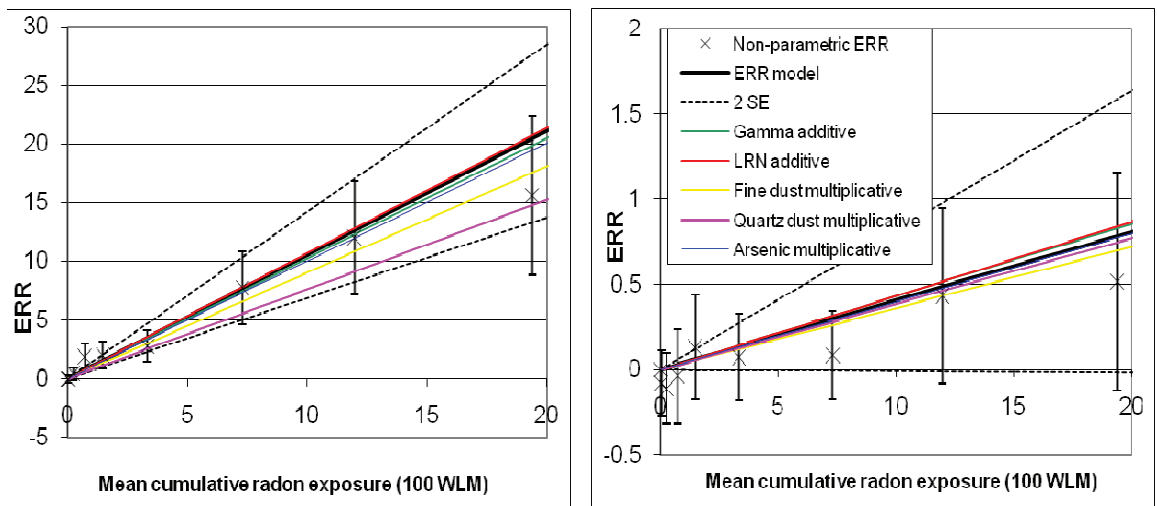
Figure 19. Left panel: Effects of the confounders (as colour coded in the key) on the Wismut model for lung cancer mortality centered at an age at median exposure of 33 years, 11 years since median exposure and an exposure rate of 2.7 Working Levels (WL). Right panel: Wismut model for extra-pulmonary solid cancer mortality centered at an age attained of 44 years.

3.4.3.5 Assessment of the scale and nature of the smoking epidemic in this cohort from differences in baseline lung cancer mortality between the Wismut cohort and the population of the former German Democratic Republic (1960–2003)

In order to assess the scale and nature of the smoking epidemic in this cohort (which has only very limited smoking data for a small fraction of persons), the candidate applied an indirect method involving smoking impact ratios (39). A previous analysis (33) noted external lung cancer mortality rates that were lower on average than the internal (spontaneous) baseline rates by 16.5% (95% CI: 9; 24%). The main purpose of (39) was to investigate the nature of, and possible reasons for, this difference by comparing patterns in spontaneous lung cancer mortality rates in the Wismut cohort with national male rates from the former German Democratic Republic (GDR). The analysis was based on 3001 lung cancers, 1.76 million person years for the period 1960–2003 and national rates covering the same period. Simple "Age Period Cohort" graphical analyses were applied to assess the main qualitative differences between the national and cohort baseline lung cancer rates. Some differences were found to occur mainly at higher attained ages above 70 years. Although many occupational risk factors may have contributed to these observed age differences, only the effects of smoking were assessed by applying the Peto-Lopez (Peto et al. 1992) indirect method for calculating the proportion of lung cancers attributable to smoking. It was inferred that the observed age differences could be due to the greater prevalence of smoking and more mature smoking epidemic in the Wismut cohort compared to the general population of the former GDR. In view of these observed differences between external population based rates and internal (spontaneous) cohort baseline lung cancer rates, it was strongly recommended to apply only the internal rates in future analyses of uranium miner cohorts.

3.4.3.6 Leukaemia mortality and occupational doses of ionizing radiation

Two papers (24, 34) included an analysis of the 128 leukemia deaths in the Wismut cohort for the second follow-up period and reported standardized mortality ratios and excess relative risks for leukemia mortality that indicated no elevated risk in connection with radon exposure. Another recent paper (Möhner et al. 2010) had reported a weak association between risks for leukemia incidence and exposure to ionizing radiation. Möhner et al. 2010 extended a previous case-control study of German uranium miners with 377 cases and 980 controls

(Möhner et al. 2006) to include medical exposures and organ doses to the red bone marrow (RBM). Analogous results for leukemia mortality in the Wismut cohort were presented (40).

Möhner et al. (2010) found an increased odds-ratio of 1.78 (90% CI 1.09; 2.91) in the highest dose category (their table 3) for all leukemia types combined assuming a lag-time of 15 years. Analogous results in (40), did not however indicate an increased relative risk (0.94, 90% CI 0.59; 1.49). The linear trends in leukemia excess relative risk (ERR) per unit absorbed RBM dose were not statistically significantly elevated (ERR/Gy = 2.7, 90% CI -0.2; 15.3, p = 0.15 and ERR/Gy = 1.1, 90% CI -0.6; 11.4, p = 0.49 for lag-times of 2 and 15 years respectively) but the central estimates were very close to those recently derived with techniques of multi-model inference for Japanese A-bomb survivors (38, gender averaged ERR at 1 Gy = 2.8, 95% CI 1.4; 3.8, for a 55 year old exposed at age 30 years).

Further preparatory work is currently underway to investigate leukaemia mortality in the third follow-up (1946–2008) and jointly with Möhner and colleagues in a Wismut case-cohort study.

Aside: There is a well known precedent, for disparate results between case-control and cohort studies from investigations of associations between obstetric X-rays and childhood leukaemia. An Oxford case-control study published by Alice Stewart and her colleagues (Stewart et al. 1956) had found an association, but a cohort study (Court Brown et al. 1960) had not. Sir Richard Doll had been one of the co-authors of the cohort study and he later conceded the point in the 1994 UNSCEAR report, but Stewart considered her work to have been temporarily devalued (Wakeford 2005).

3.4.3.7 Prostate cancer mortality risk in relation to working underground 1970–2003

A recent study and comprehensive literature review indicated that underground mining could be protective against prostate cancer (Girschik et al. 2010). This indication was explored further, by analysing data for 263 prostate cancer deaths in the Wismut cohort in relation to the number of days worked underground (42). Simple *SMR* analyses were applied, to assess differences between the national and cohort prostate cancer mortality rates, and complemented by refined analyses done entirely within the cohort. The internal comparisons applied Poisson regression excess relative prostate cancer mortality risk models with baseline stratification by age and calendar year and a whole range of possible explanatory covariables that included days worked underground, years worked at

high physical activity and radiation. The overall *SMR* was 0.85 (95% CI 0.75; 0.95). A linear excess relative risk model with the number of years worked at high physical activity and the number of days worked underground as explanatory covariables provided a statistically significant fit when compared to the baseline model (p=0.039) (see Figure 20). Results (with 95 % confidence intervals) for the ERR per day worked underground indicated a statistically significant (p=0.0096) small protective effect of -5.59 $(-9.81; -1.36) \times 10^{-5}$. Evidence was provided from the Wismut cohort in support of a protective effect from working underground on prostate cancer mortality risk. Additional computations were made on a large group of solid cancers that excluded prostate cancer and cancer sites with a radon related increased risk to examine the influence of biases due to either the healthy worker selection effect or the healthy worker survivor effect. These computations indicated no substantial biases in the given ERR, in these two respects, but the effects of such biases could not be entirely excluded.
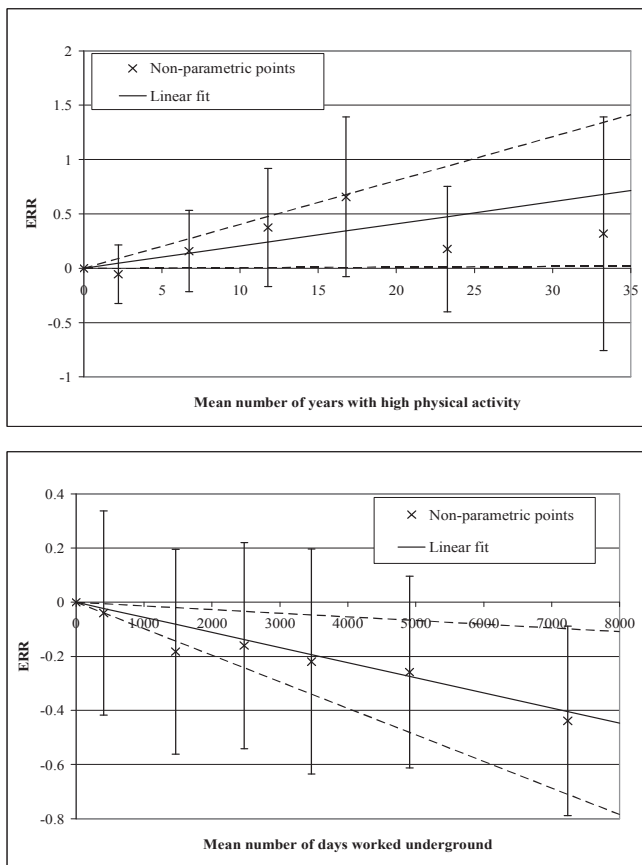
Figure 20. The upper panel shows the *ERR* and 95%CI as a function of mean number of years worked with high physical activity. The non-parametric points (crosses) with 95%CI are adjusted for mean number of days worked underground. The lower panel shows the *ERR* and 95% CI as a function of mean number of days worked underground. The non-parametric points (crosses) with 95% CI are adjusted for mean number of years worked with high physical activity.

3.4.3.8 Lung cancer mortality risk in relation to silica exposure 1946–2003

Although the International Agency for Research on Cancer classified silica as a carcinogen in both 1996 and 2009, the shape of the exposure-response relationship between excess lung cancer risk and silica exposures is still uncertain. Since the Wismut cohort data contains individual information on occupational exposure to crystalline silica in mg/m³-years, the nature of such an exposure-response relationship could be investigated further (45). The internal Poisson regression models with stratification by age and calendar year that had previously been developed for lung cancer risk with respect to radon exposures (33, 34) were extended and applied to estimate the ERR per unit of silica exposure. A preferred model for the excess risk of lung cancer from silica exposures, determined via model selection techniques, included a piece-wise linear spline function with a knot at 10 mg/m³-years of silica exposure. After full adjustment for radon (and also arsenic exposures) an ERR of 0.061 (95% CI: 0.039; 0.083) above 10 mg/m³-years with no increase in excess lung cancer risk below 10 mg/m³-years was determined (see Figure 21). The study confirmed a positive exposure-response relationship between silica exposures and excess lung cancer risk, particularly for high exposures.
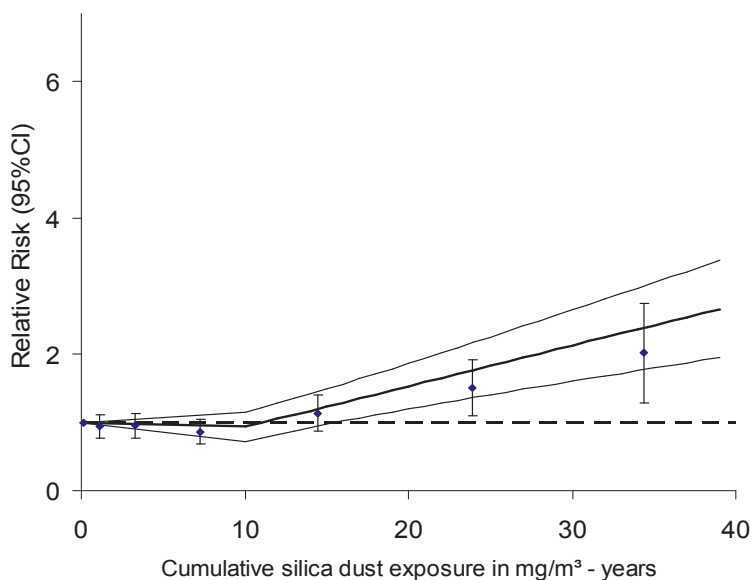
Figure 21. Relative risk of death from lung cancer (n = 2,995) in relation to cumulative silica dust with additive adjustment for radon (with the effect modifiers age at median exposure, time since median exposure and radon exposure rate) and arsenic. The points are from the non-parametric analysis (based on exposure categories 0-0.5, 0.5-2, 2-5, 5-10, 10-20, 20-30, 30+) and linear spline model (bold line) with 95% confidence limits (fine lines).

3.5 Statistical analysis of biological data on cellular radiation damage and radiation induced abnormal growth of tissue

Radiation is known to cause DNA damage, following which cellular repair mechanisms spring into action. DNA repair may proceed faultlessly, whereby the broken ends rejoin correctly and/or inconspicuously. Alternatively, following a faulty DNA repair, the cell can either have a mutated genome which may cause abnormal growth or the cell may die. Biological indicators of radiation damage at the cellular level depend strongly on: the mechanisms of biological cell responses after radiation exposure; the types of radiation; and the particulars of the exposure characteristics. Radiation induced cellular effects include:

• Alterations to DNA sequence caused by direct deposition of radiation energy or by radiation induced reactive oxygen species;

• Single or double DNA strand breaks and subsequent incomplete DNA repair resulting in different types of chromosome aberrations;

• Abnormal cellular growth;

• The induction of cell death by apoptosis or necrosis.

Biological indicators of radiation induced cellular damage provide indirect measurements of the effects produced by specific radiation types and depend on the energy deposition patterns from the radiation during cell traversal. Some types of high Linear Energy Transfer (LET) radiation, such as neutrons, protons and α-particles, deposit energy in dense tracks across the traversed cells. Low LET radiation, such as γ-rays and X-rays, may only deposit energy at one or a few places in each of the cells during traversal or may miss some cells altogether. Many techniques have been developed and applied to study radiation-induced indicators of cell damage. All result in a wealth of radiobiological data requiring analyses that often provide mathematical, computational and statistical challenges. The candidate has been active in selecting techniques and performing analyses in several radiobiological studies (5, 6, 9, 15, 17-19, 25, 31) that are described in the next few sub-sections.

3.5.1 Chromosome aberration data on blood samples from Japanese A-bomb survivors

A previous analysis by Stram et al. 1993 had shown an apparent city difference in the chromosome aberration dose responses for Hiroshima and Nagasaki A-bomb survivors, which is not apparent in the solid cancer or leukaemia epidemiological data. In order to investigate this difference further, data from the previous analysis on stable chromosome aberrations, consisting of mainly translocations and inversions (data-file CA1993.dat, available from www.rerf.or.jp), was reanalyzed to assess uncertainties in the gamma and neutron dosimetry (5). The data pertains to peripheral blood samples collected between 1968 and 1985 from 1,703 individuals in the LSS cohort of atomic bomb survivors. The data also includes individual information on city, year of assay, numbers of cells examined, number of cells with at least one aberration and DS86 bone marrow gamma and neutron doses.

Standard linear and parabolic dose response models were considered in addition to a model in which neutron and γ-doses were treated separately. Either a low-dose limiting value for the relative biological effectiveness (RBE) of neutrons relative to gammas of $R_0 = 70 \pm 10$ or an RBE value of $R_1 = 15 \pm 5$ at 1 Gy was applied. The use of R_1, as previously developed and applied to the analysis of solid cancer (2), incorporates the assumption that R_1 is known more precisely than R_0. Error-reducing transformations, based on the use of nearly orthogonal parameters, were also applied and resulted in a 50% reduction of the standard error of the fit parameter for the proportion of cells with at least one aberration at 1 Gy γ-dose. Several modifications, according to recent nuclear retrospective dosimetry measurements, to the DS86 doses were also investigated and were found to result in increasing non-linearity of the dose-response curve for Hiroshima, and a corresponding decrease for Nagasaki. However differences in the dose-response curves observed for both cities based on DS86 doses, although reduced by such modifications, could not be entirely explained by the applied dose modifications.

The extent to which the neutrons contribute to chromosome aberration induction in Hiroshima was found to depend significantly on the applied model. The model in which neutron and γ-doses were treated separately, including an R_1 value of 15 at 1 Gy, was the finally preferred model and predicted between 10% and 20% of the observed chromosome aberrations to be due to neutrons, at all doses.

Modifications applied to DS86 doses were relatively small because of the good agreement between DS86 predictions and the results of the retrospective gamma and neutron dosimetry. Consequently, the choices of model and RBE values were found to be the major factors dominating the interpretation of the chromosome data for Hiroshima and Nagasaki, with the dose modifications having a smaller influence.

3.5.2 The RBE of mammography X-rays (29 kV) relative to 220 kV X-rays using data on neoplastic transformations

Studies conducted during the past four decades have generally shown that low-energy photons are more effective, per unit absorbed dose, in inducing cellular damage than high-energy photons. However, Frankenberg et al. 2002 reported a higher than expected low-dose RBE for the 29 kV X-rays relative to the 220 kV X-rays (conventionally applied in general medical screening of chest and bone fractures), and claimed that the results were consistent with published data for various biological indicators of cellular damage. Since 29 kV X-rays are applied in screening mammography, these claims caused controversy and concern. Consequently, it was clear that further careful examinations were required (6, 9, 17) because of the important public-health implications from risk-to-benefit evaluations for mammography.

The study (6) on neoplastic transformation of human CGL1-hybrid cells was therefore designed to repeat the earlier investigation by Frankenberg et al. 2002, under well-defined irradiation and culture conditions, and to independently assess the validity of the high reported RBE values for 29 kV X-rays. The experiments with the two types of X-rays were performed simultaneously and shared the same controls. The transformation yields with both radiation qualities were fitted to the linear-quadratic dependence on absorbed dose. A corresponding analysis was performed for the data obtained earlier by Frankenberg et al. 2002. The transformation yields in (6) were found to substantially exceed those in Frankenberg et al. 2002. The difference in yields was attributed to inadequate feeding conditions of the cell cultures in the experiments of Frankenberg et al. 2002. A later study (Kühne et al. 2005) confirmed the results in (6).

The standard error bands of the dose response curves were derived and found to be considerably narrower in (6) than in Frankenberg et al. 2002. The lowest dose

considered in both studies of the 29 kV X-rays was 1 Gy, and at this dose the RBE relative to the conventional X-rays was determined to be 2 with a 95% confidence interval of 1.4–2.6. Frankenberg et al. 2002 reported an RBE of 3.2, but with a very broad 95% confidence. The estimated limit in (6) at low doses was RBE = 3.4 with a confidence interval that extends from less than 2 to large values (see Figure 22).
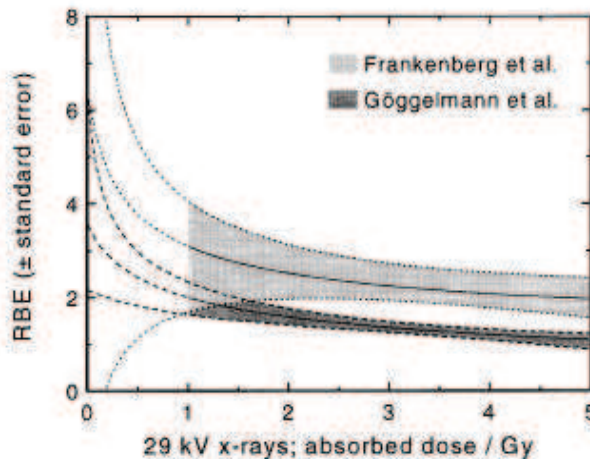
Figure 22. (figure 5 of (6)). The RBE of 29 kV X-rays relative to 200 kV or 220 kV X-rays. The region between the two dashed lines indicates standard errors obtained by Monte-Carlo simulation of 1000 RBE values at each of 18 dose points. The data of Frankenberg et al. 2002 are also plotted for comparison purposes.

Further experiments on human lymphocytes, involving alkaline comet assay (single cell gel electrophoresis) measurements of the initial levels of all single-strand DNA damage, regardless of origin, were also performed (9). It was found that the comet assay data did not indicate any differences in the initial radiation damage produced by 29 kV X-rays relative to the reference radiation types of either 220 kV X-rays or also ^{137}Cs and ^{60}Co γ-radiation. These results were found to be consistent with physical models of the possible energy deposition pattern and resulting damage in the DNA. Such models predicted an RBE for 29 kV X-rays relative to conventional X-rays of only 1.3 with an upper limit no greater than about 2 (Kellerer 2002). The results of (9) indicated that differences in biological effects must therefore arise through downstream processing of the damage.

Evidence supporting this same indication was also provided by a similar analysis (17) based on the same method and cell type, but extended by the inclusion of a consideration of radiation damage in human gastric cancer cells from ^{241}Am α-radiation in addition to the four types of radiation considered in (9). Preliminary

data for α-exposures of human gastric cancer cells only showed a statistically significant increase in DNA damage at high doses (>2 Gy ^{241}Am). However the damage at 2 Gy exceeded the damage induced at 2 Gy by ^{137}Cs gammas by a factor of 2.5. By contrast, other experiments involving different cell systems and DNA damage indicators, such as chromosomal aberrations (e.g. Schmid et al. 1996), have detected a significant increase in DNA damage at much lower doses of 0.02 Gy for ^{241}Am, resulting in a higher biological effectiveness. A reason for these differences could be that, in the lower dose ranges, only a small proportion of cells are hit by α-particles and the resulting initial damage is therefore too diluted to be observed with the comet assay. The results from (17) thus provided further indications that differences in biological effects must arise through downstream processing of the damage, i.e., the effects are more noticeable in biological indicators that show a radiation response at a later time since exposure.

3.5.3 Correlation between initial chromatid damage and survival of various cell lines exposed to heavy charged particles

Accelerated heavy ions have been successfully applied in the radiotherapy treatment of many patients with malignant tumours. Since it is of very great medical value to have information on the radiation sensitivity of individual patients, prior to radiotherapy treatment, much effort has been concentrated on developing methods to predict radio-sensitivity. The study (18) investigated the induction of chromatid breaks in four cancer cell lines (human hepatoma, gastric cancer, cervical carcinoma and melanoma) and one normal liver cell line. The cells were exposed to carbon ions accelerated by the heavy ion research facility in Lanzhou, China, using chemically induced premature chromosome condensation. Previous studies have reported the number of chromatid breaks to be linearly related to the radiation dose, but the relationship between cell survival and chromatid breaks is not clear. Cellular radiosensitivity, as measured by D_0 (the dose that reduces survival by $1/e$ in the final linear portion of the survival curve) is linearly correlated with the frequency of chromatid breaks per unit dose in these five cell lines. It was proposed (18) that premature chromosome condensation may be applied to predict individual radio-sensitivity in cancer patients before undergoing treatment with heavy ions.

3.5.4 Dose-response relationship of dicentric chromosomes in human lymphocytes obtained for the fission neutron therapy facility at the Munich research reactor

Experimental studies on the induction of dicentric chromosome aberrations in human lymphocytes have contributed to the current knowledge concerning the magnitude of the relative biological effectiveness (RBE) of neutrons relative to γ-ray or X-ray reference radiation. It is known that the neutron RBE increases with decreasing dose up to a constant value at doses where both the X-ray or γ-ray reference radiation and the neutron dose–response curves are linear.

The RBE of neutrons, with a mean energy of 1.9 MeV, from the neutron therapy facility MEDAPP at a relatively new German research reactor, (München Forschungs-Neutronenquelle Heinz Maier-Leibnitz, FRM II), was determined, at different depths in a phantom (31). Blood samples were exposed to total doses of 0.14–3.52 Gy at 2-cm depth, and 0.18–3.04 Gy at 6-cm depth in a phantom placed in the MEDAPP beam. The neutron and γ-ray absorbed dose rates were measured to be 0.55 Gy min^{-1} and 0.27 Gy min^{-1} respectively (at 2-cm depth), and 0.28 and 0.25 Gy min^{-1} respectively (at 6-cm depth).

Neutrons from both the MEDAPP beam and the beam of the former FRM I research reactor facilities were found to have a similar linear-quadratic dose-response relationship for dicentric chromosomes (at 2-cm depth), although the irradiation conditions were not identical. Different dose-response curves for dicentrics were obtained for the MEDAPP beam at 2 and 6 cm depth, suggesting a significantly lower biological effectiveness of the radiation with increasing depth. No obvious differences could be determined between the dose-response curves for dicentric chromosomes estimated under interactive or additive prediction between neutrons or γ-rays and the experimentally obtained dose–response curves.

The values for the neutron RBE at the MEDAPP beam relative to ^{60}Co γ-rays, decrease from 5.9 at 0.14 Gy to 1.6 at 3.52 Gy at 2-cm depth, and from 4.1 at 0.18 Gy to 1.5 at 3.04 Gy at 6-cm depth. A linear-quadratic dose–response relationship was obtained for the MEDAPP mixed neutron and γ-ray field, and also for the specific contribution of the fission neutrons. However it was concluded that further work is required to determine if the fission-neutron induced yield of dicentric chromosomes increases linearly with dose.

3.5.5 Enhanced yield of chromosome aberrations after computer tomography examinations in paediatric patients

A study on the yield of chromosome aberrations after computer tomography (CT) examinations in paediatric patients was considered to be necessary for two reasons: previous data on chromosome aberrations in peripheral lymphocytes after CT scans had only been obtained in adult patients; and the resulting organ doses, for a given instrumental setting of a CT-machine, are known to be higher in a child than in a larger adult. Therefore the study (19) was carried out to determine whether CT scans cause an increase in the yields of chromosome aberration in paediatric patients. Blood samples were taken from 10 children (5 girls and 5 boys) before and after their CT scans for accidental injuries (i.e., not diseases, as in earlier studies on adult patients). Chromosome analyses were carried out exclusively during metaphases of the first cell cycle of lymphocytes in-vitro using fluorescence plus Giemsa staining. The mean blood dose of the 10 children was 12.9 mGy. The frequencies of dicentrics and excess acentric fragments, based on more than 20,000 analyzed lymphocytic cells, were significantly increased in the samples collected after CT examination. On sub-dividing the patients into two age groups, i.e., 0.4 to 9 and 10 to 15 years, it was found that the observed increase in chromosome aberrations was mainly contributed by the younger age group. In this group the frequency of dicentrics was significantly increased whereas in the older group the observed increase was not significant. The results demonstrated that CT scans enhance the dicentric yields in lymphocytes of children aged up to 15 years and that those paediatric patients under 10 years of age may be more radiation sensitive than older patients.

3.6 Introduction of model selection techniques and methods for multi-model inference

The candidate has been active in introducing model selection techniques (21), evidence-based methods for multi-model inference (38, 43, 44, 48) and hierarchical partitioning methods (47) which had not previously been applied in this field.

3.6.1 Model selection techniques.

The need for the introduction of model selection techniques (7, *see footnote on p.148* of 25) became apparent to the candidate particularly after reading several papers by recognised experts on the analysis of the epidemiological data from the Japanese A-bomb survivors. In several cases, the candidate was convinced that more important information on the relative goodness of fit of non-nested radiation risk models could have been extracted from high-profile analyses. Consequently, a paper on model selection techniques for radiation epidemiology, with examples using the Japanese A-bomb epidemiological data was conceived and published (21).

For example, Pierce et al 1996 (on their p.19) used an indirect method involving the construction of nested-models and a standard likelihood ratio test, for comparing non-nested radiation risk models based on an age-attained explanatory covariable with risk models based on the age at exposure covariable. This comparison could have been achieved directly with techniques for non-nested models, as in the example given in (21).

Another example can be found in Preston et al (2002), a paper investigating breast cancer risks in 8 different cohorts. According to Preston et al (2002) "Formal statistical comparison of the fits of the excess relative risk and absolute excess rate models was not possible. An informal comparison of the deviance values for the various fitted models considered suggested that, while deviances for the ERR models tend to be slightly smaller than those for the EAR models, both types of models provide comparable fits to these data." (page 231, 2nd column, 2nd paragraph from the top, where EAR is Excess Absolute Risk). However there was enough information on the deviance of the final models of Preston et al (2002) for the pooled data to compute the relative goodness of fit. One can continue to read further in this paper that " final ERR model has deviance = 5849.3 and final EAR model has deviance of 5854.7 with two

parameters more". From this information the change in Akaike Information Criterion (AIC) is 9.4 which gives a calculated evidence ratio in favour of the ERR model over the EAR of 110 corresponding to a probability of model improvement of 0.991, i.e., see table 2 of (21). In this case formal comparisons of the fits were indeed possible as explained in (21).

3.6.2 Multi-model inference and hierarchical partitioning

The candidate realised that application of the established statistical technique of multi-model inference (MMI) (Burnham & Anderson 1998, 2002, 2004, Claeskens & Hjort 2008), often referred to as "model averaging", can generally lead to a better and more complete evaluation of the radiation risks per unit dose and their associated errors. This is achieved by taking account of not just one preferred model but a multiplicity of models that fit the data almost as well as each other. Use of the MMI terminology rather than "model averaging" is preferable since model averaging implies that the related uncertainties from model combinations are reduced. In reality, if MMI is applied, the uncertainties are increased to account for uncertainties between several models that describe the data almost equally well. Although MMI has been successfully applied in many other fields of research, the introduction and application in the field of radiation epidemiology began with the candidate's evaluation (38) of radiation related adult and childhood leukaemia mortality risks based on the Japanese A-bomb LSS data (1950–2000) with 296 leukaemia deaths.

In (38), MMI was applied to characterize model uncertainty amongst published radiation related leukaemia risk models, because there is low statistical power in the LSS data to discriminate between alternative model forms for the dose response. The candidate has been particularly interested in further applications and in refining and improving the initial approach (38) also by considering the extended follow-up mortality data (1950–2003, with 318 leukaemia deaths) made available just after the publication of (38). In particular, in (48), the reference set of models considered for the MMI of radiation-related leukaemia risks was changed from the set collected from previous studies in (38) to an independent set, selected by a rigorous statistical protocol from over 30 models.

Compared to (38), (48) reported similar central risk estimates and confidence intervals for the leukaemia central estimates for ERR from MMI for doses between 0.5 and 2.5 Sv. However, at lower doses the central estimates for ERR

from MMI were found to be lower by factors of 2 to 5, although the reduction was not statistically significant (see Figure 23). This reduction came mostly from the inclusion of a quadratic-exponential ERR model, not previously considered in (38) (i.e., the "Q-exp" model that has a Quadratic dose response form, slightly damped by an exponential factor at high doses and which contributed over 50% to the total multi-model weighting). The resulting central estimates for ERR from MMI were found to have a positive 2.5% percentile only above 300 mSv (see Figure 23).
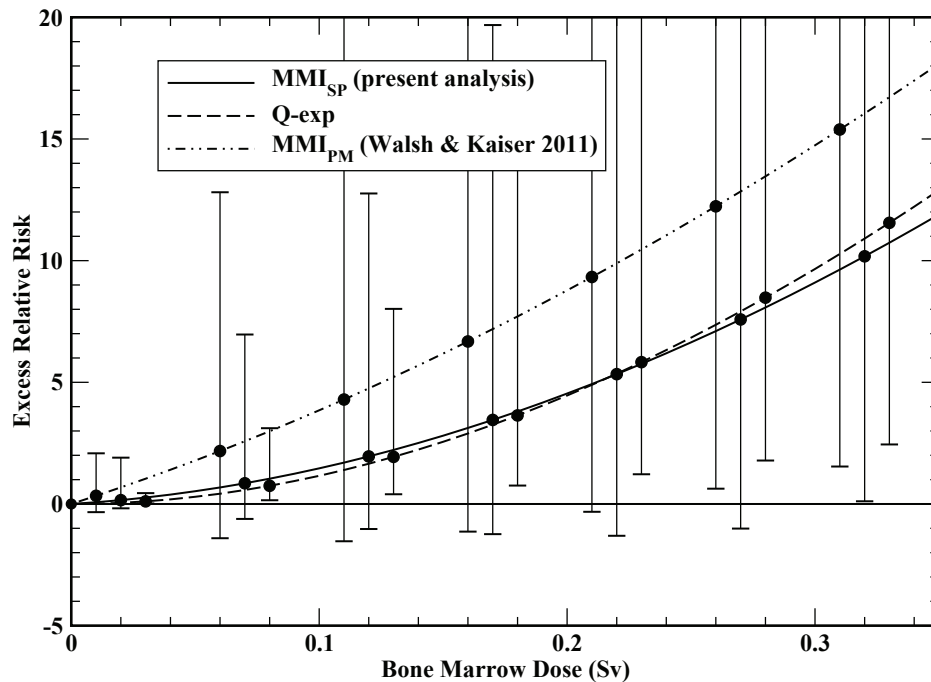
Figure 23. (figure 3 from (48)). Leukaemia mortality ERR dose response for a 7-year old child exposed at age 2 years, with 95% confidence intervals for the LSS data with a follow-up from 1950–2003. The full line is the MMI estimate from (48, marked as "present analysis" in the key), the dashed line is the best estimate for model Q-exp applied in (48) and the dot-dashed line is the MMI analysis based on the four models with the highest weights from (38) (i.e., Walsh and Kaiser 2011), but repeated for the LSS extended follow-up (1950–2003).

The candidate was informed that (38) will play a central role in a new UNSCEAR report entitled "Uncertainties in risk estimates for cancer due to exposure to ionizing radiation" due for publication in 2013. (38) has also been discussed and very positively evaluated by the German Radiation Protection Commission (SSK). There are already other papers, coauthored by the candidate and/or her direct collaborators, that are based on this method (43, see also 44 and Richardson & Cole 2012). A paper on breast cancer (Kaiser et al. 2012) by the candidate's collaborators acknowledges the candidate's input of the main idea. An evaluation of the risks of cardiovascular diseases associated with radiation (43) has recently been published and a paper on skin cancer is in preparation. Futhermore, a related method has been proposed for calculating evidence-based model weights

for excess relative risk and excess absolute risk in calculations of lifetime attributable risk of cancer from radiation exposure (46).

However, these approaches focus on comparisons among alternative models and not on the relative importance of the explanatory variables included in the models. Once a preferred model or set of models has been identified, radiation epidemiologists would often like to know which of the various possibly explanatory covariables included in the models has the strongest influence on the risk response variable. In addressing this problem the candidate had recently applied the hierarchical partitioning (HP) technique (Chevan & Sutherland, 1991) to a simple evaluation of the degree of independent effects from γ-ray and neutron absorbed doses on the all solid cancer incidence risk in the Japanese atomic bomb survivors LSS cohort (47).

The degree of correlation between the γ-ray and neutron absorbed doses was also considered with regression diagnostics. The partial correlation between the neutron and γ-ray colon absorbed doses (r=0.74) and the resulting variance inflation factor (2.2) are both below the levels beyond which remedial action is usually recommended. Applying HP to the models it was found that just under half of the drop in deviance resulting from adding the γ-ray and neutron absorbed doses to the baseline risk model, comes from the *joint* effects of the neutrons and γ-rays – leaving a substantial proportion of the deviance drop accounted for by *individual* effects. The average ERR/Gy γ-ray absorbed dose and the average ERR/Gy neutron absorbed dose were obtained directly here for the first time and agree well with previous indirect estimates (2-4). The average RBE of neutrons relative to γ-rays, calculated from fit parameters to the ERR all solid cancer model with both colon absorbed dose covariables is 65 (95% CI: 11; 170) also in agreement with previous indirect estimates (13). Therefore the determination of all solid cancer risks based on reference to the colon absorbed doses with a neutron weighting of 10, as applied in most RERF analyses (e.g., Ozasa et al 2012), may not be optimal and this practice should be reviewed. Any future improvements in neutron RBE precision could have important public-health consequences e.g., for the types of proton therapy that produce unwanted by-product neutron doses.

Future applications of HP and MMI could be very useful for statistical analyses in other cohort studies, e.g., on CT exposure and cancer incidence, and may

ultimately ease the dilemma of needing to choose between models with largely different consequences for major issues of public health concern.

Acknowledgements

General references

Becquerel H, Curie P. L'action physiologique des rayons du radium. Cr. Acad Sci. Paris. 132,1289–1291,1901

Berrington de Gonzalez A, Apostoaei AI, Veiga LHS, Rajaraman P, Thomas BA, Hoffman FO, Gilbert E, Land C. RadRAT: a radiation risk assessment tool for lifetime cancer risk projection. J. Radiol. Prot. 32, 205–222, 2012

Boice JD Models, models everywhere – is there a fit for lifetime risk? J. Natl. Cancer Inst., 102, 1606-1609, 2010

Breslow NE & Day NE. Statistical methods in cancer research, Vol. II. The design and analysis of cohort studies. IARC Scientific Publications No. 83. Lyon: International Agency for Research on Cancer, 1988

Burnham KP, Anderson DR. Model selection and inference: a practical information-theoretic approach. Springer-Verlag, New York, USA, 1998

Burnham KP & Anderson DR. Model Selection and Multimodel Inference. Springer, New York, 2nd edition, 2002

Burnham KP, Anderson DR. Multimodel inference. Understanding AIC and BIC in model selection. Sociol Meth Res 33(2): 261-304, 2004

Cardis E, Vrijheid M, Blettner M, et al. The 15-country collaborative study of cancer risk among radiation workers in the nuclear industry: Estimates of radiation-related cancer risks. Radiat. Res.167, 396–416, 2007

Chevan A & Sutherland M. Hierarchical Partitioning. The American Statistician. 45 (2), 90-96, 1991

Chronik der Wismut. Wismut GmbH, 1999

Claeskens G & Hjort NL. Model Selection and Model Averaging. Cambridge University Press, 2008

Court Brown WM, Doll R & Bradford Hill A. Incidence of leukaemia after exposure to diagnostic radiation in utero. BMJ (Nov 26), 1539–1545, 1960

Curie E. Madame Curie. Paris: Gallimard, 1938

Daniels RD & Schubauer-Berigan MK. A meta analysis of leukaemia risk from protracted exposures to low-dose gamma radiation. Occup. Environ. Med. 68, 457- 464, 2011

Darby SC, Whitley E, Howe GR., Hutchings SJ., Kusiak RA, Lubin JH, Morrison HI, Tirmarche M, Tomasek L, Radford EP & et al. Radon and cancers other than lung cancer in underground miners: a collaborative analysis of 11 studies. J. Natl. Cancer Inst. 87, 378- 84, 1995

EPA Radiogenic Cancer Risk Models and Projections for the U.S. Population, EPA 402-R-11-001,U.S. Environmental Protection Agency Office of Radiation and Indoor Air, Washington DC 20460, 2011

Frankenberg D, Kelnhofer K & Frankenberg-Schwager M. Enhanced neoplastic transformation by mammography X-rays relative to 200 kVp X-rays. Indication for a strong dependence on photon energy of the RBE_M for various endpoints. Radiat. Res. 157, 99–105, 2002 and Erratum: Radiat. Res. 158, 126, 2002

Fry SA. Studies of U.S. Radium Dial Workers: An Epidemiological Classic. Radiat. Res. 150 (suppl.) S21-S29, 1998

Girschik J, Glass D, Ambrosini GL & Fritschi L. Could mining be protective against prostate cancer? A study and literature review. Occup. Environ. Med. 67, 365-374, 2010

Glasser O. Wilhelm Conrad Röntgen und die Geschichte der Röntgenstrahlen. 2nd Edition, Springer Verlag, 1959

Grosche B, Kreuzer M, Brachner A, Kreuzer M & Brachner A. Investigation of health effects among German uranium miners: The design of three studies. Epidemiology 12 (Suppl 4): 74, 2001

Grosche B. Semipalatinsk test site: introduction. Radiat. Environ. Biophys. 41, 53-55, 2002

Grosche B, Kreuzer M, Kreisheimer M, Schnelzer M & Tschense A. Lung cancer risk among German male uranium miners: a cohort study, 1946-1998. Br. J. Cancer, 95, 1280-1287, 2006

Hwang SL, Guo HR, Hsieh WA, et al. Cancer risks in a population with prolonged low dose-rate γ-radiation exposure in radiocontaminated buildings, 1983–2002. Int. J. Radiat. Biol. 82, 849-858, 2006

International Agency for Research on Cancer (IARC), Monographs on the Evaluation of Carcinogenic Risks to Human Volume 100 part D: Radiation, Lyon France, 2012

International Commission on Radiological Protection. Recommendations of the International Commission on Radiological Protection. ICRP Publication 60. Ann. ICRP 21, Oxford: Pergamon Press, 1991

International Commission on Radiological Protection ICRP. Relative biological effectiveness (RBE), quality factor (Q), and radiation weighting factor (w_R). ICRP Publication 92. Ann. ICRP 33(4), Oxford: Pergamon Press, 2003

International Commission on Radiological Protection. The 2007 recommendations of the International Commission on Radiological Protection. ICRP–103 Annals of the ICRP, 37, Nos. 2-4, 2007

International Commission on Radiological Protection Statement, Lung cancer risk from radon and progeny. ICRP Draft report for consultation, ref 4843-4564-6599, 2010

Israel P. Edison: A Life of Invention, John Wiley & Sons, 1998

Ivanov VK, Gorski AI, Maksioutov MA, et al. Mortality among the Chernobyl emergency workers: estimation of radiation risks (preliminary analysis). Health Physics. 81, 514–21, 2001

James F. Minuit function minimization and error analysis, Version 94.1. Technical report, CERN, 1994

Kaiser JC, Jacob P, Meckbach R & Cullings HM. Breast cancer risk in atomic bomb survivors from multi-model inference with incidence data 1958–1998. Radiat. Environ. Biophys. 51, 1-14, 2012

Kazakov VS, Demidchik EP & Astakova LN. Thyroid cancer after Chernobyl. Nature. 359, 21, 1992

Kellerer AM. Invisible Threat – The risk of Ionizing Radiation, www.nupecc.org/iai2001/reports/B51.pdf, 2001

Kellerer AM. Electron spectra and the RBE of X rays. Radiat. Res. 158, 13–22, 2002

Kreuzer M, Brachner A, Lehmann F, Martignoni K, Wichmann HE & Grosche B. Characteristics of the German uranium miners cohort study. Health Physics. 83(1), 26-34, 2002

Kreuzer M, Kreisheimer M, Kandel M, Schnelzer M, Tschense A & Grosche B. Mortality from cardiovascular diseases in the German uranium miners cohort study, 1946-1998. Radiat. Environ. Biophys. 45, 159-166, 2006

Kreuzer M, Straif K, Marsh J, Dufey F & Sogl M. Occupational dust and radiation exposure and mortality from stomach cancer among German uranium miners, 1946-2003. Occup. Environ. Med. 69, 217-223, 2012

Kühne M, Urban G, Frankenberg D & Löbrich M. DNA double-strand break misrejoining after exposure of primary human fibroblasts to CK characteristic X rays, 29 kVp X rays and 60Co gamma rays. Radiat. Res. 164, 669-676, 2005

Lambin P, Marples B, Fertil B, et al. Hypersensitivity of a human tumour cell line to very low radiation doses. Int. J. Radiat. Biol. 63, 639–650, 1993

Lichtenstein JE. Forensic radiology. In Gagliardi RA, ed. A history of the radiological sciences. Reston, VA: American College of Radiology Radiology Centennial, 586-587, 1996

Likhtarev IA, Sobolev BG, Kairo IA, Tronko ND, Bogdanova TI, Oleinic VA, Epshtein EV & Beral V Thyroid cancer in the Ukraine. Nature, 375, 365, 1995

Likhtarov L, Kovgan L, Vavilov S, Chepurny M, Ron E, Lubin J, Bouville, A Tronko N & Bogdanova T. Post-Chornobyl Thyroid Cancers in Ukraine, Report 2: Risk Analysis. Radiat. Res. 166, 375-386, 2006

Lubin JH, Boice JDJr, Edling C, Hornung RW, Howe G, Kunz E, Kusiak RA , Morrison HI, Radford EP, Samet JM, Tirmarche M, Woodward A & Yao SX. Radon-exposed underground miners and inverse dose-rate (protraction enhancement) effects. Health Physics. 69, 494-500, 1995

Marples B & Joiner MC. The response of Chinese hamster V79 cells to low radiation doses: Evidence of enhanced sensitivity of the whole cell population. Radiat. Res.133, 41-51, 1993

Möhner M, Gellissen J, Marsh J W & Gregoratto D. Occupational and disgnostic exposure to ionizing radiation and leukemia risk among german uranium miners Health Physics. 99(3), 314-321, 2010

Möhner M, Lindtner M, Otten H & Gille HG. Leukemia and exposure to ionizing radiation among German uranium miners. Am. J. Ind. Med. 49, 238-248, 2006

Moolgavkar S & Knudson A. Mutation and cancer: a model for human carcinogenesis. J. Natl. Cancer Inst. 66, 1037-1052, 1981

Okubo T. Long-term epidemiological studies of atomic bomb survivors in Hiroshima and Nagasaki: study population, dosimetry and summary of health effects. Radiat. Prot. Dosim. 151(4), 671-673, 2012

Ozasa K, Shimizu Y, Suyama A, Kasagi F, Soda M, Grant EJ, Sakata R, Sugiyama H & Kodama K. Studies of the Mortality of Atomic Bomb Survivors, Report 14, 1950–2003: An Overview of Cancer and Noncancer Diseases. Radiat. Res. 177(3), 229-243, 2012

Paul R, Das Wismut Erbe, Verlag der Werkstatt, Göttingen, 1991

Peto R, Lopez AD, Boreham J, Thun M & Heath C Jr. Mortality from tobacco in developed countries: indirect estimation from national vital statistics. Lancet. 339,1268-1278, 1992

Pierce DA, Shimizu Y, Preston DL, Vaeth M & Mabuchi K. Studies of the mortality of atomic bomb survivors. Report 12, Part 1. Cancer 1950–1990. Radiat. Res. 146, 1-27, 1996

Preston DL, Lubin JH, Pierce DA. Epicure User`s Guide. HiroSoft International Corp., Seattle, 1993

Preston DL, Mattsson A, Holmberg E, Shore R, Hildreth NG & Boice JD. Radiation Effects on Breast Cancer Risks: A Pooled Analysis of Eight Cohorts. Radiat. Res. 158, 220-235, 2002

Preston DL, Shimizu Y, Pierce DA, Suyama A & Mabuchi K. Studies of Mortality of Atomic Bomb Survivors. Report 13: Solid Cancer and Noncancer Disease Mortality: 1950-1997. Radiat. Res. 160, 381-407, 2003

Preston DL, Pierce DA, Shimizu Y, Cullings HM, Fujita S, Funamoto S & Kodama K. Effects of recent changes in Atomic bomb survivor dosimetry on cancer mortality risk estimates. Radiat. Res. 162, 377-389, 2004

Preston, DL, Ron E, Tokuoka S, Funamoto S, Nishi N, Soda M, Mabuchi K & Kodama K. Solid cancer incidence in atomic bomb survivors: 1958-1998. Radiat. Res. 168, 1-64, 2007

Richardson D & Cole BS. Model averaging in the analysis of leukaemia mortality among Japanese A-bomb survivors. Radiat. Environ. Biophys. 51, 93-96, 2012

Roentgen WC. Über eine neue Art von Strahlen. Aus den Sitzungsberichten der Wuerzburger Physik.-medic. Gesellschaft, 1895

Roesch WC, Ed., US–Japan Joint Reassessment of Atomic Bomb Radiation Dosimetry in Hiroshima and Nagasaki, Vols. 1 and 2. Radiation Effects Research Foundation, Hiroshima, 1987

Rutherford E & Soddy F. The cause and nature of radioactivity. Philos. Mag., 4, 370-396 & 569-585, 1902

Rutherford E. The Scattering of α and β Particles by Matter and the Structure of the Atom. Philosophical Magazine, Series 6 21, 669-688, 1911

Rowland RE, Stehney AF & Lucas HF Jr. Dose-response relationships for female radium dial workers, Radiat. Res. 76, 368-383, 1978

Schmid E, Hieber L, Heinzmann U, Roos H & Kellerer A M. Analysis of chromosome aberrations in human peripheral lymphocytes induced by in vitro alphaparticle irradiation. Radiat. Environ. Biophys. 35, 179-184, 1996

Schnelzer M, Hammer G P, Kreuzer M, Tschense A, Grosche B. Accounting for Smoking in the Radon Related Lung Cancer Risk among German Uranium Miners: Results of a Nested Case-Control Study. Health Physics. 98, 20-28, 2010

Shiver L.Transport calculations and accelerator experiments needed for radiation risk assessment in space. Z. Med. Phys. 18 (4), 253-264, 2008

Spiess H. Ra-224-induced tumors in children and adults, in: Symposium on Delayed Effects of Bone-Seeking Radionuclides, Sun Valley (USA), September 11-14, 1967, in: Mays C.W. Salt Lake City: University of Utha Press 227-248, 1969

Spiess H. Life span study on late effects of radium-224 in children and adults. Health Physics. 99(3), 286-291, 2010

Stewart A, Webb J, Giles D & Hewitt D. Malignant disease in childhood and diagnostic irradiation in utero. Lancet. 268, 447, 1956

Stram DO, Sposto R, Preston DL, Abrahamson S, Honda T & Awa AA. Stable chromosome aberrations among A-bomb survivors: an update. Radiat. Res. 136, 29-36, 1993

Thompson DE, Mabuchi K, Ron E, Soda M, Tokunaga S, Ochikubo S, Sugimoto S, Ikeda T & Terasaki M. Cancer incidence in atomic bomb survivors. Part II: solid tumors,1958–1987. Radiat. Res. 137 (Suppl), S17-S67, 1994

Tronko MD, Bogdanova TI, Komisarenko IV, Epshtein OV, Likhtaryov IA, Markov VV, Oliynyk VA, Tereshchenko VP, Shpak VM & Voilleque P. Thyroid carcinoma in children and adolescents in Ukraine after the Chernobyl accident: statistical data and clinicomorphologic characteristics. Cancer. 86, 149-156, 1999

United Nations Scientific Committee on the Effects of Atomic Radiation UNSCEAR 1994 Report to the General Assembly, Sources and effects of ionizing radiation, 1994

United States National Research Council, Committee on the Biological Effects of Ionizing Radiation, Health Effects of Exposure to Radon: BEIR VI. United States National Academy of Sciences. National Academy Press: Washington DC,1999

United States National Research Council, Committee to Assess Health Risks from Exposure to Low Levels of Ionizing Radiation, Health Risks from Exposure to Low Levels of Ionizing Radiation: BEIR VII – Phase 2. United States National Academy of Sciences. National Academy Press: Washington DC, 2006

United Nations Effects of Ionizing Radiation. United Nations Scientific Committee on the Effects of Atomic Radiation UNSCEAR 2006 Report. Volume I. Annex A: Epidemiological studies of radiation and cancer. United Nations, New York, 2008

von Jagie N, Schwarz G, Siebenrock L. Blutbefunde bei Röntgenologen. Berliner Klinische Wochenschrift. 48, 1220-1222, 1911

Wakeford R. Obituary – Professor Sir Richard Doll J. Radiol. Prot. 25, 327-330, 2005

Wakeford R. Childhood leukaemia following medical diagnostic exposure to ionizing radiation in utero or after birth. Radiat. Prot. Dosim. 132 (2), 166-74, 2008

Wendt W, Kromer H, Schaarschmidt W & Vogel E. Zur Geschichte der Gebiets-parteiorganisation Wismut der SED, 1, Herausgeber: Gebietsleitung Wismut der SED, East Germany, 1988

WHO. World Health Organization (WHO). WHO Handbook on Indoor Radon: A Public Health Perspective. WHO Press, Geneva, 2009

WHO. World Health Organization (WHO). WHO Guidelines on Indoor air quality: selected pollutants, Ch 7 Radon, WHO Press, Geneva, 2010

WHO. World Health Organization (WHO). WHO Initial Health Risk Assessment from the Nuclear Accident after the 2011 Great East Japan Earthquake and Tsunami, WHO Press, Geneva, *in press* Dec. 2012

Young R, Kerr GD (eds) DS02: Reassessment of the Atomic Bomb Radiation Dosimetry for Hiroshima and Nagasaki, Dosimetry System 2002, DS02 Vols 1& 2, Radiation Effects Research Foundation, Hiroshima, 2005

4. Copies of each of the publications in published form

1. Kellerer AM, Nekolla E & Walsh L. On the conversion of solid cancer excess relative risk into lifetime attributable risk. Radiat. Environ. Biophys. 40, 249-257, 2001

ORIGINAL PAPER

Albrecht M. Kellerer · Elke A. Nekolla · Linda Walsh

On the conversion of solid cancer excess relative risk into lifetime attributable risk

Abstract Risk coefficients representing the lifetime radiation-induced cancer mortality (or incidence) attributable to an exposure to ionizing radiation, have been published by major international scientific committees. The calculations involve observations in an exposed population and choices of a standard population (for risk transportation), of suitable numerical models, and of computational techniques. The present lack of a firm convention for these choices makes it difficult to inter-compare risk estimates presented by different scientific bodies. Some issues that relate to a necessary harmonization and standardization of risk estimates are explored here. Computational methods are discussed and, in line with the approach utilized by ICRP, conversion factors from *excess relative risk* (*ERR*) to *lifetime attributable risk* (*LAR*) are exemplified for exposures at all ages and for occupational exposures. A standard population is specified to illustrate the possibility of a simplified standard for risk transportation computations. It is suggested that a more realistic perception of lifetime risk could be gained by the use of coefficients scaled to the lifetime spontaneous cancer rates in the standard population. The resulting quantity *lifetime fractional risk* (*LFR*) is advantageous also because it depends much less on the choice of the reference population than the lifetime attributable risk (*LAR*).

A.M. Kellerer (✉)
Radiobiological Institute, University of Munich,
Schillerstrasse 42, 80336 Munich, Germany
e-mail: AMK.SBI@LRZ.Uni-Muenchen.de
Tel.: +49-89-5996818, Fax: +49-89-5996840

Institute of Radiobiology,
GSF – National Research Center for Environment and Health,
Neuherberg, Germany

E.A. Nekolla · L. Walsh
Radiobiological Institute, University of Munich, Germany

Introduction

The derivation of nominal risk coefficients for ionizing radiation is a 2-step process. Epidemiological data from a *study population*, such as the observations of the solid cancer or the leukemia mortality (or incidence) rates among the A-bomb survivors, are first modeled to derive the excess absolute risk (*EAR*) or the excess relative risk (*ERR*) in their dependence on various parameters such as dose, D, sex, s, age at exposure, e, and/or age attained, a. The excess risk or excess relative risk is then, in a second step, "transported" to an idealized or real *reference population* and is expressed in terms of lifetime attributable risk per unit dose. This entails an integration over the ages at exposure that are considered and the periods at risk. The transport of *ERR* requires an integration also over the background cancer mortality (or incidence) rate, $m(a)$, in the reference population. Risk coefficients are, thus, dependent not only on the observation in an exposed population, but also on the background cancer rates and the life table data of the selected reference population.

The International Commission on Radiological Protection (ICRP) has introduced the notion of the nominal risk coefficient and has in the last general recommendations [1] presented risk estimates that were obtained from the observations on the A-bomb survivors and were then expressed, on the basis of computations by Land and Sinclair [2], in terms of average values for five reference populations, US, UK, Japan, China, and Puerto Rico. The United Nations Scientific Committee on the Effects of Atomic Radiation (UNSCEAR) in a major new assessment [3] has invoked the same five reference populations and has presented new risk estimates that will serve as guideline for regulatory decisions in radiation protection; the results will also be used as bench marks for comparisons with other numerical exercises. However, such exercises will be impeded by the lack of a clear convention on the population data to be used in the risk transport and on the definitions that are to be employed.

Land and Sinclair [2] have, in fact, in their computations for ICRP documented the input data in terms of the *equilibrium* survival functions (*actuarial* survival functions) for the five reference populations and the age-specific solid cancer mortality rates, and they have used a computational procedure that offers itself as a convention. By invoking the same five reference populations, UNSCEAR [3] has given the impression that it accepted the convention. But somewhat different and more complex input data were used, which have not been published. In addition, the concepts and quantities that were employed were similar but not equal. A current reevaluation [4], which explores new modeling procedures, highlights the resulting difficulty of arriving at a meaningful comparison of risk estimates that are based on different and only partly documented procedures. The subsequent considerations are meant to clarify some of the issues and to contribute towards the necessary harmonization of input data and of concepts and computational details.

Radiation-risk estimates tend to be scrutinized to a level of precision that is out of balance with their inherent degree of uncertainty. While unnecessary precision can be misleading, it is nevertheless essential in an often controversial discussion on risk coefficients to work with numbers that can be traced precisely to their computational origin and that can be reliably compared. The transport of risk from the study population to the reference populations contains inherent uncertainties and requires unproven assumptions. But this unavoidable uncertainty does not justify lack of rigor. When different studies make different *ad hoc* choices in the selection of population data and in the details of rather complex computations, the choices need not have major overall impact, but they need to be clearly defined unless they obscure the results and their dependence on various aspects of the risk modeling.

Concepts and quantities

The subsequent considerations can be kept on a fairly simple level. For a deeper analysis of the various concepts and quantities and their interrelation, the reader is referred to the treatment by Vaeth and Pierce [5], to the paper by Thomas et al. [6], and to the summaries in earlier UNSCEAR reports [7, 8].

Relative risk or absolute risk transportation

Before specific quantities are considered, one major issue needs to be determined. This is the choice whether the excess *relative* risk or the excess *absolute* risk is taken to be the same in the study population and in the reference population. When individual tumor sites are considered, the choice between *relative risk* (*RR*) *transportation* and *absolute risk* (*AR*) *transportation* will vary according to circumstances, and in some cases it may be necessary to employ intermediate procedures.

However, when all solid tumors are combined, the choice between the *RR* and the *AR* transportation is not critical; UNSCEAR [3] obtained with the *AR* transportation risk coefficients that are about 10% less than those obtained by the *RR* transportation. In the interest of simplicity only *RR* transportation will be considered here.

Lifetime attributable risk, *LAR*

The formal expression of the risk coefficient needs to be considered next. In radiation protection considerations the risk coefficient is usually taken to be the average of the coefficients for the two genders. However, to simplify the subsequent formulae, all quantities will be taken to be sex specific unless otherwise noted. Reference will here be made to the quantity *LAR* which is defined below. But more complicated quantities (*REID* and *ELR*) have been considered and while they may not be required in practice, their definitions and their relation to *LAR* are, nevertheless, explained in a subsequent section.

Most commonly, risk coefficients are expressed in terms of *lifetime attributable risk*, either for a specified age, *e*, at exposure (*LAR(e)*/Gy) or averaged over all ages at exposure (*LAR*/Gy). The quantity *LAR(e)* has earlier been termed *risk of untimely death* [*RUD(e)*], but this somewhat abstract name is here avoided in favor of the more familiar term. The equation for lifetime attributable risk has been given by Vaeth and Pierce [5]:

$$LAR(e) = \int_{e+L}^{a_{max}} m_E(a)S(a) / S(e)da$$
$$= \int_{e+L}^{a_{max}} ERR(a)m(a)S(a) / S(e)da \qquad (1)$$

where *e* and *a* are age at exposure and attained age, respectively, $m_E(a)$ is the excess cancer mortality (due to an exposure at age, *e*) while $m(a)$ is the spontaneous cancer mortality rate and *L* is the latent period. The *survival function*, i.e. the probability at birth to reach at least age *a*, is denoted by $S(a)$. The ratio $S(a)/S(e)$ is the conditional probability of a person alive at age *e* to reach at least age *a*.

The terms $S(a)$ and $S(e)$ in Eq.(1) refer to the survival function not of the exposed, but of the unexposed population. This simplifies the concept and makes *LAR* proportional to *ERR* and independent of the non-cancer excess mortality which is difficult to quantify. Use of the unreduced survival function also implies that at higher doses where there is substantial life shortening, *LAR* is somewhat larger than the actual number of attributable cancer deaths per exposed person. However, this difference is of little or no practical concern, since no summary risk coefficient is sufficiently specific and precise to serve as an accurate quantitative parameter at high doses. Moreover, it might be perceived as awkward if risk coefficients were marked down because irradiation "prevents" some cancers by causing people to die at earlier ages.

Formulae for *LAR*

The excess relative risk, which has been written in the abbreviated form, $ERR(a)$, in Eq.(1), can be factorized in a dose (D) dependent, but gender-averaged reference value, ERR_{ref}, and an age (a, e) and gender (s) dependent modifying function, μ:

$$ERR(D,s,a,e) = ERR_{ref}(D) \cdot \mu(s,a,e). \qquad (2)$$

Omitting the argument D in $ERR_{ref}(D)$ and in $LAR(e)$, Eq.(1) then takes the form:

$$LAR(e) = ERR_{ref} \int_{e+L}^{a_{max}} \mu(s,a,e)m(a)S(a)/S(e)\mathrm{d}a. \qquad (3)$$

A more specific formulation invokes one of the two familiar projection models. The traditionally applied *age at exposure model* postulates a modifying function μ that depends only on age at exposure, e, and does not decrease in time after exposure. The parameter ERR_{ref} is, in this model, usually related to age 30 at exposure; ERR_{ref} is, therefore, written ERR_{30}:

$$ERR(D,s,a,e) = ERR_{30} \cdot \mu(s,e)$$
$$= ERR_{30} \cdot \exp(-g \cdot (e-30)) \cdot (1 \pm s) \qquad (4)$$

(+ for females, – for males). In agreement with earlier analyses [9, 10, 11], typical parameter values are g=0.039/y and s=0.33 [4].

The more recent *attained age model* [12, 13] invokes a modifying function μ that depends only on age attained, a. In this model, the reference age 60 is a suitable choice; ERR_{ref} is, therefore, written ERR_{60}:

$$ERR(D,s,a,e) = ERR_{60} \cdot \mu(s,a)$$
$$= ERR_{60} \cdot \exp(-g \cdot (a-60)) \cdot (1 \pm s) \qquad (5)$$

(+ for females, – for males). ERR_{60} in the attained age model is numerically close to ERR_{30} in the age at exposure model. Typical parameter estimates are g=0.025/y and s=0.34 [4].

The computations for UNSCEAR with the attained age model invoke (rescaled to reference age 60):

$$\mu(s,a) = (a/60)^{-1.5} \cdot (1 \pm s) \qquad (6)$$

(+ for females, – for males; s=0.4). The power function leads to a rapid increase of *ERR* values at very young ages. A current reanalysis [4] retains, therefore, the somewhat more moderate exponential attained age modifier [Eq.(5)] that was used originally with the attained age model [12].

In subsequent formulae or statements, which apply both to ERR_{30} and ERR_{60}, the symbol ERR_{ref} stands for either quantity.

For a specified model, i.e. a specified modifying function, it is straightforward to compute *LAR* from an exposure that occurs either acutely with a given probability per year or with constant low dose rate throughout life. The two scenarios lead to the same result, since a linear dose relation independent of dose rate is assumed in the concept of the nominal risk factor [1]. The lifetime attributable risk is then obtained as the average of *LAR(e)* over life (see [5]). Using the abbreviation, c, for the life expectancy at birth,

$$c = \int_0^{a_{max}} S(a)\mathrm{d}a \qquad (7)$$

one obtains:

$$LAR = \frac{1}{c} \cdot \int_0^{a_{max}} LAR(e)S(e)\mathrm{d}e \qquad (8)$$

and the conversion factor between ERR_{ref} and *LAR* is:

$$LAR/ERR_{ref} = \frac{1}{c} \cdot \int_0^{a_{max}} LAR(e)/ERR_{ref} \cdot S(e)\mathrm{d}e. \qquad (9)$$

Alternative quantities, *REID* and *ELR*

More complicated concepts than *LAR* are not actually required, but one such concept, the quantity *risk of exposure induced (cause specific) death*, *REID* [7], deserves consideration, because it is used in the most recent report by UNSCEAR [3]. *REID* for solid tumor mortality differs from *LAR* in being defined with reference to the actual survival function after the radiation exposure. The formula in Eq.(1) is then replaced by:

$$REID(e) = \int_{e+L}^{a_{max}} ERR(a)m(a)S(a,D)/S(e,D)\mathrm{d}a \qquad (10)$$

where $S(a,D)$ and $S(e,D)$ represent the survival function of the population after exposure to dose D.

If *REID* were to be applied in radiation protection considerations, its values for different doses would be required. However, UNSCEAR has given only the values for 0.1 Sv, which do not differ appreciably from *LAR*, and the values for 1 Sv which are smaller than *LAR* at 1 Sv by about 10% for solid tumor mortality. Regardless of the question of practical applicability, it would be difficult to derive reliable values of *REID* because there is insufficient information to specify a dose-dependent survival function. Survival after a substantial radiation exposure is diminished due to radiation-induced cancer and non-cancer mortality. At doses of several Gy this also includes acute mortality. Recent studies among the A-bomb survivors show that there is late radiation-induced non-cancer mortality, but it remains difficult to quantify its dose dependence [14]. More is known about acute radiation mortality after high doses, but it is recognized to depend on the level of medical treatment which, in turn, varies with circumstances.

For these reasons it is unclear why UNSCEAR [3] refers, in spite of these various difficulties and limitations, to the quantity *REID*. There is an additional complication. In the absence of a specific statement on non-cancer mortality it seems likely that the calculations for UNSCEAR are actually directed not at *REID* but at an intermediate concept, *REID***(see Fig. 1) that disre-
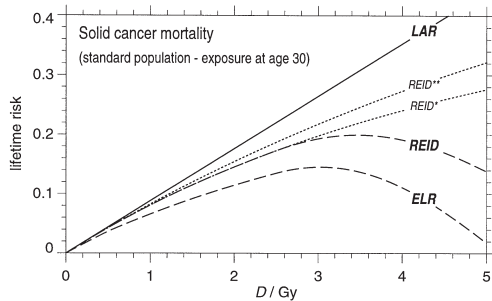
Fig. 1 Lifetime attributable risk, *LAR*, (*upper solid line*), *risk of exposure induced* (*cause specific*) *death, REID* (*upper dashed line*), and the intermediate quantities *REID*** that disregards all non-cancer mortality and *REID** that disregards merely acute mortality (*dotted lines*). The (cause specific) *excess lifetime risk, ELR,* is also included (*lower dashed line*). The quantities are given for a linear dose dependence and the solid cancer mortality in the standard population [see Eq.s (15) and (16)]

Fig. 2 The survival functions of the five reference populations chosen by ICRP (*light lines*) and, for comparison, the survival function for the tentative standard (*dashed lines*) discussed in the subsequent section [see Eq.(15)]

Fig. 3 The age-specific solid cancer mortality rates of the five reference populations chosen by ICRP (*light lines*) and, for comparison, the rates for the tentative standard (*dashed lines*) discussed in the subsequent section [see Eq.(16)]. The cancer death rate in the five reference populations is taken to be constant after age 87

gards both late and acute radiation-induced non-cancer mortality. To give a feeling for the different quantities, Fig. 1 presents the quantities *LAR* and *REID* (upper solid line and upper dashed line) for the standard population that is specified in a subsequent section. The intermediate quantities *REID*** that disregards all non-cancer mortality and *REID** that disregards merely acute mortality are indicated by the dotted lines. In this example an exposure at age 30 is assumed, and a linear dose-dependence with a gender-averaged *ERR*=0.5/Gy for solid cancer mortality. The dose dependence is taken not to bend downwards at high doses, which amounts to an overestimation. The late non-cancer mortality is – in the absence of better information – taken to have a threshold at 0.5 Gy and beyond this postulated threshold a slope of *ERR*=0.1/Gy is assumed. The acute radiation induced mortality is represented – again with unavoidable degree of arbitrariness – by a median lethal dose (LD_{50}) of 5 Gy and a half width of the distribution of lethal doses of 2.5 Gy. The main point is that *REID*, in its original definition [7], decreases rapidly at high doses and that the modification of the definition makes a considerable difference. It is also seen that the various quantities are not substantially different from *LAR* at low and intermediate doses.

The *(cause specific) excess lifetime risk, ELR,* is another quantity that has been adduced to express lifetime risk [15, 16]. It is the difference between the probability to die of cancer after the irradiation and the probability to die of cancer if unexposed. At high doses, i.e. when lifetime is considerably reduced, *ELR* assumes negative values. While there is little reason to invoke *ELR* in radiation protection considerations, it is included in Fig. 1 (lower dashed line) to show – as has been done with *REID* – its relation to the simpler and more suitable quantity *LAR*.
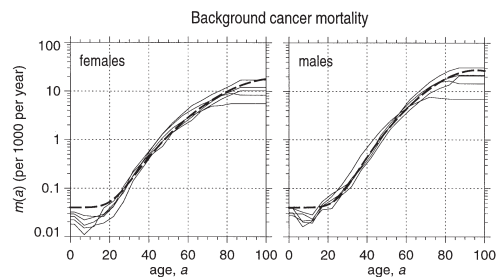
Conversion factors

ICRP data for the reference populations

In their risk computations [2] for ICRP [1] Land and Sinclair have chosen five reference populations. They have documented the input population data in terms of the actuarial survival curves, *S(a)*, and the age-dependent solid cancer mortality rates, *m(a)*, for each population and the two genders. These same data are summarily represented in Figs. 2 and 3. The heavy dashed lines represent a surrogate data set which will be discussed in the subsequent section; it can serve as an *ad hoc* substitute for the five ICRP reference populations to simplify risk transport calculations.

Table 1 Conversion factors, LAR/ERR_{ref}, for the five populations chosen by ICRP, and the averages of these factors. The results are given both for the attained age model [Eq.(5)] and the age at exposure model [Eq.(4)]. Using a power function in a with the attained age model [Eq.(6)] leads to average conversion factors that are larger by about 6%. The last column gives conversion factors that result for the tentative standard population defined in the subsequent section. Note that ERR_{ref} (i.e. ERR_{60} or ERR_{30}) is a gender-averaged value that depends only on dose

All ages at exposure	US	UK	Japan	China	Puerto Rico	**Average**	**Standard**
Mean lifetime							
Males	71.7	72.5	75.9	69.6	72.6	72.5	72.8
Females	78.5	78.3	81.8	71.9	79.6	78.0	78.1
Lifetime cancer mortality							
Males	0.21	0.25	0.23	0.13	0.18	0.20	0.20
Females	0.18	0.22	0.17	0.10	0.15	0.16	0.16
Both genders	0.20	0.24	0.20	0.12	0.17	0.18	0.18
Age attained model – LAR/ERR_{60}							
Males	0.099	0.115	0.100	0.066	0.082	0.092	0.092
Females	0.155	0.188	0.135	0.095	0.123	0.139	0.139
Both genders	0.127	0.151	0.118	0.081	0.102	**0.116**	**0.115**
Age at exposure model – LAR/ERR_{30}							
Males	0.153	0.179	0.155	0.095	0.132	0.143	0.145
Females	0.237	0.289	0.209	0.138	0.193	0.213	0.216
Both genders	0.195	0.234	0.182	0.116	0.163	**0.178**	**0.180**

Table 2 Conversion factors, LAR/ERR_{ref}, for the five populations chosen by ICRP, and the averages of these factors. The results are analogous to those in Table 1, but they refer to a working population (exposure ages 25 to 65 years)

Working population (ages at exposure 25 to 65)	US	UK	Japan	China	Puerto Rico	**Average**	**Standard**
Age attained model – LAR/ERR_{60}							
Males	0.104	0.120	0.108	0.067	0.088	0.097	0.096
Females	0.167	0.201	0.149	0.098	0.134	0.150	0.147
Both genders	0.136	0.161	0.128	0.083	0.111	**0.124**	**0.122**
Age at exposure model – LAR/ERR_{30}							
Males	0.091	0.106	0.095	0.054	0.081	0.086	0.086
Females	0.146	0.177	0.132	0.080	0.122	0.131	0.132
Both genders	0.119	0.141	0.113	0.067	0.102	**0.108**	**0.109**

Results in terms of the conversion factor *LAR/ERR*

Values for members of the public

The conversion factors obtained for the five reference populations of ICRP with the unchanged population data of ICRP [2] and their averages are listed in the first six columns of Table 1. Also included are the mean duration of life in each population and the lifetime cancer mortality. The conversion factors are given for the attained age model [Eq.(5)] and the age at exposure model [Eq.(4)]. The last column gives the conversion factors that result for a standard population that will be considered in the subsequent section. As explained, the conversion factors refer to a constant low dose rate exposure throughout life or to acute low dose exposures, at a random age.

The age at exposure model predicts – at the present stage of the follow-up of the A-bomb survivors – a substantially larger lifetime attributable risk from childhood exposures than from exposures at later age. This is reflected in the large difference of the conversion factors for the two projection models.

For considerations that relate specifically to occupational exposure, somewhat different values of conversion factors result which correspond to the exposure of a working population represented – in line with the choice of ICRP [1] – by an exposure period from age 25 to 65. The computations are changed only by the choice of the integration limits to 25 and 65 in Eq.(9). Table 2 gives the results.

The choice of the projection model is uncritical for occupational exposures; the conversion factors for the two models are similar in this case.

Reference to lifetime fractional risk, LFR

LAR specifies for a person exposed to a low dose the radiation-related excess probability for a fatal cancer. If, as is usual, the concept is applied to an exposed population, it specifies the expected number of fatalities, and such numbers – when they are not linked to the number of spontaneous cases – can be misleading. It is then more conducive for a realistic perception of risk to refer to a relative number. Such a number is obtained if *LAR* is scaled to the lifetime spontaneous cancer mortality (or incidence) in the reference population:

$$B = \int_0^{a_{max}} m(a) \cdot S(a)da. \tag{11}$$

The resulting overall excess relative risk is here termed *lifetime fractional risk*[1]

$$LFR = LAR / B. \tag{12}$$

The *LFR* per unit dose can serve as an alternative form of the nominal risk coefficient. Numerical values are not given since they can easily be derived from Tables 1 and 2 for a specified ERR_{ref}. Apart from being more suggestive of the actual level of a radiation risk than the *LAR* per unit dose, *LFR* has the added advantage that it is more stable with regard to changing population data.

LAR increases substantially with the longevity of a population. The risk coefficient, as now expressed in terms of *LAR*, is thus substantially larger for developed countries than developing countries. The largest value of *LAR* among the five ICRP reference populations exceeds the smallest value by a factor 2 for either of the projection models and equally for a population of all ages or a working population (see Tables 1 and 2). In fact, *LAR* would nearly vanish for the population in an underdeveloped country, and while this expresses, of course, the fact that other hazards are of dominant concern in such populations, it would still convey a wrong message with regard to radiation protection.

In contrast, *LFR* is the ratio of two quantities that increase both with the longevity of a population, which explains why the value of *LFR* for a specified ERR_{ref} does not vary greatly between the ICRP reference populations (either of all ages or of working ages). For a given projection model, *LFR* differs not by more than 20% between any of the ICRP reference populations. The lifetime relative risk coefficient, *LFR*, is thus a stable and meaningful parameter.

Expressed in terms of Eq.(12) and the average *LAR* and the average *B* for the five ICRP reference populations, *LFR* is:

$$LFR = 5.5 \cdot LAR. \tag{13}$$

Essentially the same relationship pertains if *LFR* is computed as an average of the *LFR* values of the five individual reference populations.

Divergent concepts:
collective risk versus *individual risk*

The definition of *LAR* or of the more complicated quantity *REID* invokes – as presented here [see Eqs.(1), (8), (10)] and previously [2, 5] the survival function $S(a)$. The resulting risk coefficient expresses the probability of harm for an *individual*, whether exposed at a specified age ($LAR(e)$) or

[1] In computations that refer to specific cases it can be more appropriate to use in the definition of *LFR* as denominator the spontaneous cancer mortality (or incidence) over a specified period. For example if the radiation risk from screening by mammography is to be assessed, it is natural to refer to the time interval from beginning of screening onwards.
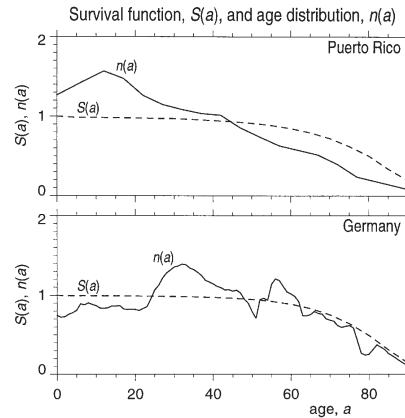
Fig. 4 Comparison of the equilibrium age distribution, $S(a)$, for two populations with the actual age distributions, $n(a)$. The data refer to both genders combined. The distributions for Puerto Rico are from [2, 17]. The data for Germany are from the national statistical office [18]. The distributions, $n(a)$, are normalized to the area under $S(a)$ [the life expectancy, see Eq.(7)] of the two populations

throughout life (*LAR*). The risk coefficient *LAR* can, for example, be invoked to express the presumed risk for an individual from lifelong exposure to natural background radiation or to a lasting elevated radiation level. Similarly the *LAR* can express the risk to a worker from exposures during his working life from age 25 to 65.

A somewhat different concept is related to the *collective* detriment, rather than the individual risk. One invokes in this case not the risk to a member of the population. Reference is, instead, made to the total detriment in an exposed population or a subgroup of a population. One uses, accordingly, in Eq.(8) the actual distribution of ages, $n(e)$, of the population or the subgroup of the population that is under scrutiny:

$$LAR = \int_0^{a_{max}} LAR(e)n(e)\mathrm{d}e \Big/ \int_0^{a_{max}} n(e)\mathrm{d}e. \tag{14}$$

Both concepts, the individual-related and the population-related measure of risk, are meaningful and have specific applications. But confusion must arise when the nature of the quantity is not spelled out. Thus, it is not sufficiently appreciated that ICRP [2] gives the individual-related risk quantity *LAR*, while UNSCEAR [3] has derived the population-related risk quantity *LAR*. Diverging definitions may not be entirely avoidable. However, it is necessary to state clearly the definitions and to bring out – at least in exemplary fashion – the general magnitude of the numerical differences between differently defined quantities.

Growing population numbers in most nations of the world imply that the actual age distributions, $n(a)$, differ substantially from the equilibrium age distributions,

Table 3 Conversion factors, LAR/ERR_{ref}, for Puerto Rico (an example of a young population with high birth rate) and Germany (an example of the opposite case). The results are given both, for the attained age model (a-model) [Eq.(5)] and the age at exposure model (e-model) [Eq.(4)]. The results refer to both age groups, i.e. all ages at exposure and a working population with exposure ages 25 to 65 years. The data for Puerto Rico are from [2, 17], the data for Germany from [18, 19]

LAR/ERR_{ref}		All ages at exposure		Working population (ages at exposure 25–65 years)	
		e-model	a-model	e-model	a-model
Puerto Rico	Individual-related	0.163	0.102	0.102	0.111
	Population-related	0.205	0.112	0.110	0.113
Germany	Individual-related	0.209	0.132	0.129	0.141
	Population-related	0.198	0.134	0.134	0.143

$S(a)$, with a significant shift towards younger ages. The age distribution that has been used in the UNSCEAR calculations for Puerto Rico can serve as an example. Figure 4 compares in the upper panel the distribution $n(a)$ with the equilibrium distribution $S(a)$ for Puerto Rico. An aging population with low birth rates is the opposite case; in the lower panel of Fig. 4, Germany is chosen as an example. For easier comparison with $S(a)$, $n(a)$ is normalized to the area under $S(a)$, i.e. to the life expectancy at birth [see Eq.(7)].

Table 3 gives the resulting conversion coefficients. The essential point is the substantial increase of LAR for a "young" population under the age at exposure model. In the example of Puerto Rico the conversion factor is LAR/ERR_{30}=0.163 in terms of the individual-related risk quantity, but LAR/ERR_{30}=0.205 in terms of the population-related risk quantity. For the attained age model the difference is substantially less: for the individual-related risk quantity the conversion factor is LAR/ERR_{60}=0.102, for the population-related risk quantity it is LAR/ERR_{60}= 0.112. For an "aged" population the differences are much smaller. In the example of Germany, for both risk models the individual-related risk quantity and the population-related risk quantity differ only slightly.

For occupational exposures, i.e. for exposures in the age range 25–65 the differences in the conversion factors are generally less. However, the population-related concept – if taken seriously – would require an even more detailed formulation in terms of gender-specific age distributions for the occupations in question. There appears to be little need for such exercises in accuracy. Generally speaking, the notion of the individual-related lifetime attributable risk as employed by ICRP appears to be more natural in relation to nominal risk coefficients than any concept that is sensitive to demographic variations.

Specification of a standard population

The tabulated conversion factors can facilitate the comparison of risk coefficients in terms of the five reference populations selected by ICRP. In the interest of stable numerical values and meaningful comparisons it appears advisable to retain, for the time being, the reference populations and the cancer and survival data specified by ICRP [2]. Eventually, however, it will be desirable to define a standard population that can serve as a simpler, more practical reference. The choice of a suitable convention ought to be made by an official scientific body, such as the ICRP.

As an interim solution, analytical expressions for the sex-specific population survival functions and the cancer mortality rates can be invoked that provide nearly the same LAR as the utilization of the five ICRP reference populations. The survival functions are in this *ad hoc* "standard" represented by a *Gompertz* expression:

$$ \tag{15} $$

with c_1=0.0015, c_2=0.0820 for males and c_1=0.0005, c_2=0.0905 for females.

The solid cancer mortality rates are modeled by the familiar power functions with some bending over at high ages:

$$ m(a) = k \cdot (a/60)^r \cdot \exp(-0.06 \cdot (a/60)^r) + 0.00004 \tag{16} $$

with k=0.0045, r=6 for males and k=0.0030, r=5 for females.

These dependencies are compared in Figs. 2 and 3 to the data for the five ICRP reference populations. To avoid unreadable diagrams the curves for the five reference populations have been indicated by light lines without identification of the countries. They are meant merely to indicate the bandwidth of the values and the rough agreement with the analytical expressions. The last columns in Tables 1 and 2 give the conversion factors that result for this tentative standard.

Conclusion

Deriving nominal risk coefficients is one of the major aims of modeling computations with epidemiological data, such as the information from the follow-up of the A-bomb survivors [9, 10, 11]. While risk coefficients are subject to considerable uncertainties, they are nevertheless a critical input into regulatory decisions.

256

The new risk estimates recently reported by UNSCEAR [3] attest to the continued effort at extending the data and improving the modeling computations. The results need to be compared to the current ICRP risk estimates, and future estimates will, in turn, be compared to the values presented by UNSCEAR [3]. The numerical comparisons have not been the object of the present considerations. They are considered elsewhere [4], and it is seen that the difference of conventions can have substantial impact on the resulting risk estimates. The present discussion has, instead, been focused on the concepts and computations that are required in the derivation of risk estimates and on the population data that are used to convert excess relative risk (*ERR*) into lifetime attributable risk (*LAR*) or lifetime fractional risk (*LFR*).

ICRP has selected five reference populations and has specified the required population data. This selection is of necessity arbitrary, and if some degree of arbitrariness is accepted, there is little reason to keep updating the survival and cancer data for the reference populations. Instead, the reference needs to be seen as a standard that makes the nominal risk coefficients insensitive to changing parameters that are unrelated to new insights on radiation risk. In this sense it appears desirable to adopt a standard population that can serve as an agreed upon component in the definition of nominal risk coefficients. A tentative standard has here been considered that is largely equivalent to the five ICRP reference populations. However, this is meant to be at best an *ad hoc* surrogate for the combination of the five standard populations. An actual standard would have to be chosen and adopted by an official scientific body, such as ICRP.

Adopting a standard will, of course, not exclude specific efforts that might be directed towards the derivation of estimates for national populations or specific critical subgroups of a population. But even then the standard values will remain a useful guideline; they will help to judge whether detailed computations are warranted or whether they are insignificant in comparison to the inherent uncertainty of the risk estimates.

Being summary parameters, the nominal risk coefficients are meaningful when they are applied to a broad group of cancers, such as all solid tumors taken together. For certain considerations it can be of interest to work out the contribution of specific tumor entities to the total risk. This involves the same type of computations that have been discussed here, but the assessments would be directed at specific national or ethnic populations, and there is, accordingly, less need or possibility for standardized computations. Similarly, it would be complicated to extend the present considerations to leukemia. The required computational detail appears to be unjustified in view of the relatively minor contribution of leukemia to the total cancer risk coefficient and also in view of the fact that nominal risk coefficients are, as the term indicates, general guidelines rather than firm numbers. While precise modeling computations are required in cases such as the derivation of probabilities of causation, it is sufficient with regard to the overall nom-

inal risk coefficient to account for leukemia in a summary fashion, as is the case in the current ICRP recommendations.

While the need for a standardization has been stated, it is perhaps equally important to emphasize the advantage that can be gained by moving away from stating risk coefficients (in terms of *LAR*) which specify the probability or the expected number of radiation-induced fatalities (or cases), and to turn, instead, towards the use of relative risk coefficients (in terms of *LFR*) which quantify the fractional increase of the cancer mortality. This quantity is – apart from being more suggestive of the factual impact of a risk – less dependent on the population data that enter the computation of the risk coefficients. But even risk coefficients expressed in relative terms, i.e. with reference to the lifetime fractional risk, will require a well defined computational convention to permit reliable comparisons and to ensure the necessary transparency of the underlying computations.

References

1. ICRP (1991) Publication 60. The 1990 recommendations of the International Commission on Radiological Protection. Annals of the ICRP. ICRP 21 (1–3). Pergamon Press, Oxford
2. Land CE, Sinclair WK (1991) The relative contributions of different organ sites to the total cancer mortality associated with low-dose radiation exposure. In: Risks associated with ionizing radiations. Annals of the ICRP 22 (1). Pergamon Press, Oxford, pp 31–58
3. UNSCEAR (2000) Sources and effects of ionizing radiation. United Nations Scientific Committee on the Effects of Atomic Radiation. Report to the General Assembly. Vol.II: Effects, Annex I. Epidemiological evaluation of radiation-induced cancer. United Nations, New York, pp 297–450
4. Kellerer AM, Walsh L, Nekolla EA (2001) Risk coefficients for γ-rays with regard to solid cancer. Submitted for publication
5. Vaeth M, Pierce D (1990) Calculating excess lifetime risk in relative risk models. Environ Health Perspect 87:83–94
6. Thomas D, Darby SC, Fagnani F, Hubert P, Vaeth M, Weiss K (1992) Definition and estimation of lifetime detriment from radiation exposures: principles and methods. Health Phys 63: 259–272
7. UNSCEAR (1994) Sources and effects of ionizing radiation. United Nations Scientific Committee on the Effects of Atomic Radiation. Report to the General Assembly, Annex A. United Nations, New York
8. UNSCEAR (1998) Sources and effects of ionizing radiation. United Nations Scientific Committee on the Effects of Atomic Radiation. Report to the General Assembly, Annex F. United Nations, New York
9. Pierce DA, Shimizu Y, Preston DL, Vaeth M, Mabuchi K (1996) Studies of the mortality of atomic bomb survivors. Report 12, Part 1. Cancer. Radiat Res 146:1–27
10. Pierce DA, Preston DL (2000) Radiation related cancer risks at low doses among atomic bomb survivors. Radiat Res 154: 178–186

11. Thompson DE, Mabuchi K, Ron E, Soda M, Tokunaga M, Ochikubo S, Sugimoto S, Ikeda T, Terasaki M, Izumi S, Preston DL (1994) Cancer incidence in atomic bomb survivors, Part II: Solid tumors, 1958–1987. Radiat Res 137:17–67

12. Kellerer AM, Barclay D (1992) Age dependences in the modelling of radiation carcinogenesis. In: DM Taylor, GB Gerber, JW Stather (eds) Age-dependent factors in the biokinetics and dosimetry of radionuclides. Radiat Prot Dosim 41:273–281

13. Pierce DA, Mendelsohn ML (1999) A model for radiation-related cancer suggested by atomic bomb survivor data. Radiat Res 152:642–654

14. Shimizu Y, Pierce DA, Preston DL, Mabuchi K (1999) Studies of the mortality of atomic bomb survivors. Report 12, part II. Noncancer mortality: 1950–1990. Radiat Res 152:374–389

15. BEIR IV (1988) Health risks of radon and other internally deposited alpha emitters. National Research Council, Advisory Committee on the Biological Effects of Ionizing Radiations. National Academy Press, Washington DC

16. BEIR V (1990) Health effects of exposure to low levels of ionizing radiation. National Research Council, Advisory Committee on the Biological Effects of Ionizing Radiations. National Academy Press, Washington DC

17. Ferlay J, Black RJ, Whelan SL, Parkin DM (eds) (1997) CI5VII: Electronic database of cancer incidence in five continents, vol. VII. International Agency for Research on Cancer, World Health Organization. IARC Press, Lyon

18. Statistisches Bundesamt (1998) Statistisches Jahrbuch. Metzler-Poeschel, Stuttgart, pp 62, 76

19. Statistisches Bundesamt (2000) Gesundheitswesen, Fachserie 12, Reihe 4: Todesursachen in Deutschland (Causes of death in Germany). Metzler-Poeschel, Stuttgart, pp 14–15

Note: Due to technical errors in the production, equation (15) is missing from the portable document file of reference (1).

Equation (15) should read as follows:

$S(a) = \exp(-c_1 \cdot \exp(c_2 \cdot a))$

2. Kellerer AM & Walsh L. Risk estimation for fast neutrons with regard to solid cancer. Radiat. Res. 156, 708-717, 2001

Risk Estimation for Fast Neutrons with Regard to Solid Cancer

Albrecht M. Kellerer[a,b,1] and Linda Walsh[a]

[a] *Radiobiological Institute, University of Munich, Germany; and* [b] *Institute for Radiation Biology, GSF-National Research Center for Environment and Health, Neuherberg, Germany*

Kellerer, A. M. and Walsh, L. Risk Estimation for Fast Neutrons with Regard to Solid Cancer. *Radiat. Res.* 156, 708–717 (2001).

In the absence of epidemiological information on the effects of neutrons, their cancer mortality risk coefficient is currently taken as the product of two low-dose extrapolations: the nominal risk coefficient for photons and the presumed maximum relative biological effectiveness of neutrons. This approach is unnecessary. Since linearity in dose is assumed for neutrons at low to moderate effect levels, the risk coefficient can be derived in terms of the excess risk from epidemiological observations at an intermediate dose of γ rays and an assumed value, R_1, of the neutron RBE relative to this reference dose of γ rays. Application of this procedure to the A-bomb data requires accounting for the effect of the neutron dose component, which, according to the current dosimetry system, DS86, amounts on average to 11 mGy in the two cities at a total dose of 1 Gy. With R_1 tentatively set to 20 or 50, it is concluded that the neutrons have caused 18% or 35%, respectively, of the total effect at 1 Gy. The excess relative risk (ERR) for neutrons then lies between 8 per Gy and 16 per Gy. Translating these values into risk coefficients in terms of the effective dose, E, requires accounting for the γ-ray component produced by the neutron field in the human body, which will require a separate analysis. The risk estimate for neutrons will remain essentially unaffected by the current reassessment of the neutron doses in Hiroshima, because the doses are unlikely to change much at the reference dose of 1 Gy.   © 2001 by Radiation Research Society

INTRODUCTION

Beginning with Report 26, the ICRP has linked recommendations for radiation protection to numerical risk estimates for the late, stochastic health effects of low radiation doses (*1, 2*). Continued investigations have developed these risk estimates further, and the 2000 UNSCEAR report (*3*) presents a detailed synopsis of current knowledge.

The late effects of high doses, such as 1 Gy or more, of sparsely ionizing radiation to the whole body are known reliably from various epidemiological observations, including

the follow-up of the A-bomb survivors (*4–6*). At lower doses, the observations are inevitably imprecise, and risk estimates must be based on extrapolations that cannot account for, nor are they intended to account for, the complexities in the response to very low doses that have been seen in radiobiological studies but that have not been related to health effects in humans.

Apart from the possible complexities at very low doses, any extrapolation remains uncertain, because varying degrees of curvature are seen in the dose–responses relationships from radiobiological investigations or epidemiological studies. This type of uncertainty is common in risk assessment and needs to be accepted. It applies equally, or in an even more complex manner, to chemical or biological carcinogens.

In the current treatment of this problem, the uncertainty is compounded for fast neutrons by an added and even more tentative extrapolation. In the absence of epidemiological data that are informative with regard to the late effects of neutrons, recourse is made to radiobiological studies. This is done by accepting the nominal risk coefficients for photons and multiplying them by presumed values, which are inferred from experimental investigations, of the maximum relative biological effectiveness, RBE_max, of neutrons at low doses or low dose rates. The resulting product of two nominal numbers, each the result of an extrapolation to effect levels below experimental observation, is subject to uncertainties that are difficult to assess. In controversial discussions on neutron risks, this procedure has been open to misuse when RBE_max values were taken from selectively chosen experimental systems.

It is argued here that, as far as the neutrons are concerned, the established procedure contains entirely unnecessary steps. In the absence of direct epidemiological evidence for neutrons, there is, of course, a need for linking epidemiological information for photons with appropriate information on the RBE of neutrons derived from experiments. However, there is no need to invoke low-dose extrapolations, i.e. the nominal low-dose risk estimate for photons and the putative RBE_max, since for neutrons, in contrast to γ rays or X rays, linearity in dose over a broad range is accepted for purposes of risk modeling. Accordingly, the dose coefficient is assumed not to decrease at low doses, and it can therefore be derived reliably from data at

moderate doses if such data are available. The simplified approach will be employed to infer the neutron risk coefficient from the solid cancer mortality data for the A-bomb survivors and from tentative values of the neutron RBE relative to an intermediate reference dose of γ rays.

The neutron risk estimate is of interest in itself, because neutron risks are discussed increasingly in radiation protection with regard to issues such as the transport of reactor fuel elements or exposures at aviation altitudes. However, it is also relevant for the risk estimates for γ rays from the data on the A-bomb survivors which have been developed by international risk assessment and protection committees such as ICRP (2) and UNSCEAR (3) as well as many national bodies such as NCRP (7, 8), NAS (9) and NRPB (10). The reason is that the radiation in Hiroshima especially, but also in Nagasaki, contained an admixture of fast neutrons that needs to be accounted for. In past computations, the contribution of the neutrons to the observed health effects has been considered to be minor. It has therefore been treated in a summary fashion, which has led to assertions that the inferences on the effects of low-dose γ rays might be seriously confounded by insufficiently understood contributions by neutrons (11, 12). The approach that is outlined here can contribute to a resolution of this issue, although this is not part of the present study.

THE CURRENT APPROACH

With the earlier A-bomb dosimetry system, TD65 (13), the neutrons were assumed to be a major contributor to the observed health effects (14, 15). When the dosimetry system currently employed, DS86, specified a substantially smaller neutron contribution at Hiroshima (16), these assumptions seemed to be disproved, and the data were subsequently deemed to be uninformative with regard to the contribution of neutrons. The neutron doses were accordingly accounted for crudely by assigning a weighting factor of 10 to the neutron absorbed dose to the colon. The resulting dose dependence for the excess relative risk (ERR) of all solid cancers combined was found to be indistinguishable from a linear relationship (4, 5).

At higher doses, the dependences have negative curvature; i.e., they bend down. In the analysis, this can be accounted for by an added term in dose, usually a negative exponential. If a sufficiently low cutoff in dose (2 Gy) is invoked, the added term can be disregarded.

In the majority of radiobiological experiments with X or γ rays, upward-curved dose dependences are obtained. This applies to cell studies (chromosome aberrations, transformation studies) as well as to animal experiments examining tumor incidence after radiation exposure (17). The upward curvature is taken to be a reflection of the fact that photon radiation has low efficiency at low doses and becomes more effective at higher doses, where sublesions produced by several ionizing particles (electrons) can interact to produce the critical damage. This interpretation is supported by the observation, in most experimental studies, of a time factor for sparsely ionizing radiation, i.e. by the fact that dose rate at higher doses is an important modifying factor, low dose rate being associated with more time for repair of sublesions and accordingly with reduced effect.

The data on leukemia for the A-bomb survivors (6) exhibit an upward-curved dependence of the ERR on dose; i.e., they agree with the radiobiological experience. The seemingly linear dependence for solid cancer, however, appears to be at variance with the majority of radiobiological observations. There are various factors that could mask an underlying linear-quadratic dose dependence. Thus it is conceivable that a quadratic component in dose is concealed, even at moderately high doses around 2 Gy, by the bending over that becomes clearly recognizable only at higher doses (18). A fit to a linear dose dependence thus would not necessarily overestimate the initial slope. It is equally possible that the initial slope is less than the overall slope up to 1 or 2 Gy, but that this is not detected due to the statistical uncertainty in the data (18). This latter interpretation has been adopted in the considerations that led to the risk estimates in ICRP 60 (2). For solid cancers, too, the nominal risk coefficient was therefore taken to be roughly half the value obtained from a purely linear fit. In ICRP terminology, a dose and dose-rate effectiveness factor, DDREF, was assumed and was set equal to 2 both for leukemia and for solid cancers. This factor has remained controversial, which reflects the fact that the risk coefficient for photons is subject to more uncertainty than the ERR from an intermediate γ-ray dose.

Since neutron risk estimates could not be based on direct epidemiological evidence, it was believed that they had to be obtained by multiplying the risk coefficient for photons by a factor that represents low-dose limiting values, RBE_{max}, of the neutron RBE. This procedure involves various extrapolations and unnecessary uncertainties. To reduce these uncertainties, the risk coefficient for neutrons will be assessed here by a more direct approach.

THE MORE DIRECT APPROACH

Reference to Observable Quantities

The diagram in Fig. 1 serves to explain the different approaches to the derivation of the risk coefficient, α_n, of neutrons. The lower solid curve represents schematically a linear-quadratic dose dependence of the ERR as it may apply to epidemiological data for a cohort of persons exposed to γ rays alone. In reality, there is no such study for solid cancers combined. The most informative study is that of the A-bomb survivors, who were exposed to a field of γ rays with some admixture of neutrons. However, the logic of the present approach is best brought out in terms of a dose–response relationship for γ rays alone; the necessary correction for the neutrons will be worked out subsequently.

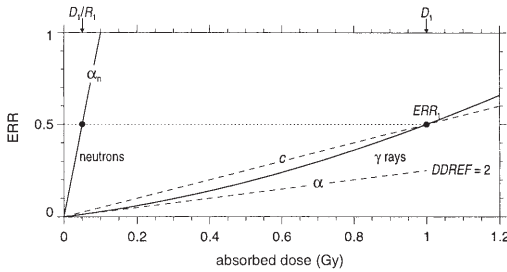The presumed initial slope of the dose dependence, i.e.

FIG. 1. Schematic diagram of a dose dependence of the excess relative risk after an acute γ-ray exposure and of the dependence for fast neutrons that is inferred in terms of the relative biological effectiveness, R_1, of neutrons relative to the reference γ-ray dose, $D_1 = 1$ Gy. The dose response for γ rays (solid curve) is represented as being linear-quadratic. The lower broken line indicates the initial slope of the dose response. The upper broken line indicates the reference slope $c = \mathrm{ERR}_1/D_1$.

FIG. 2. The ratio of neutron absorbed dose to γ-ray absorbed dose in Hiroshima as a function of total dose. The doses refer to the organ-averaged doses that equal the marrow dose (see Appendix). The solid curve corresponds to the current dosimetry system, DS86. The dotted line represents an earlier estimate (32) that was based on thermal neutron activation measurements but has now been discarded. The dashed curve represents an intermediate adjustment that is still consistent with preliminary ^{63}Ni measurements (34, 35). Three ground distances are indicated.

the risk coefficient for γ rays, is denoted by α (see lower broken line in Fig. 1). Because it is difficult to determine the effect of small doses in an epidemiological study, α is poorly known. A more reliable parameter is the effect, ERR_1, at an intermediate reference γ-ray dose, D_1, chosen here to be an acute dose of 1 Gy. The slope of the straight line from the origin to the point at D_1 (upper broken line) is termed the reference slope, $c = \mathrm{ERR}_1/D_1$. If the dose–response relationship is curved upward, its slope at D_1 exceeds the reference slope, but the reference slope will be roughly equal to the overall slope that is obtained when a linear dose–response model is fitted to data in a dose range that includes D_1 as an intermediate value. The reason is that a curved dose dependence may be fitted poorly at low and at high doses by a linear dose dependence, but the curve and the linear fit will nearly coincide at an intermediate dose. The ratio, c/α, of the reference slope to the presumed initial slope therefore corresponds to the DDREF; i.e., the photon risk estimate is $\alpha = c/\mathrm{DDREF}$.

The dose dependence in the diagram of Fig. 1 has a shape that corresponds to the DDREF of 2 that has been postulated by ICRP (2). In reality, there is no general rule as to the values of DDREF that are observed or estimated in radiation epidemiology and radiobiology. Examples are the apparent linearity (DDREF = 1) in the A-bomb data for solid cancer (4) and a DDREF of 6 for dicentric chromosome aberrations (19).

In the current approach, the risk coefficient, α_n, for neutrons is set equal to the risk coefficient, α (= c/DDREF), for the γ rays and the low-dose limit, $\mathrm{RBE_{max}}$, of the neutron RBE:

$$\alpha_n = \mathrm{RBE_{max}} \cdot \alpha = (\mathrm{RBE_{max}}/\mathrm{DDREF}) \cdot c. \qquad (1)$$

The formula involves, apart from the reference slope, c, for γ rays, the two extrapolated quantities, $\mathrm{RBE_{max}}$ and DDREF. With a bandwidth of 20 to 100 for $\mathrm{RBE_{max}}$ and 1 to 10 for DDREF, any neutron risk coefficient between $2c$

and $100c$ could thus be obtained. Carefully reasoned judgment and keeping the $\mathrm{RBE_{max}}$ close to the observations at intermediate doses have avoided bias in the recommendations of scientific committees (2, 20). But without formally stated constraints on the interrelationship of $\mathrm{RBE_{max}}$ and DDREF (see ref. 21), the equation has permitted both ambiguity and conflicting statements that have blurred the controversial discussions on the risk of low neutron exposures.

The ambiguity can be avoided. For purposes of risk modeling, the dose dependence is taken to be linear at low to moderate neutron doses. Hence it is sufficient to determine from epidemiological data the actually observed ERR_1 due to the reference γ-ray dose, D_1, and then to consider the neutron dose D_1/R_1 that might, in the light of experimental findings, be equivalent to the reference γ-ray dose. In this notation, R_1 is the RBE of neutrons relative to the reference γ-ray dose, D_1. The dose coefficient for the neutrons is then the product of two more tangible values:

$$\alpha_n = R_1\, c, \text{ with } c = \mathrm{ERR}_1/D_1. \qquad (2)$$

While R_1 is subject to the uncertainty that is inherent in consolidating a multitude of experimental results into a plausible range of representative values, and while any extrapolation from animals to humans must remain tentative, the estimate α_n is nevertheless more narrowly constrained by Eq. (2) than by Eq. (1).

D_1 needs to be a moderate dose, one large enough to permit a reliable determination of the ERR_1 in the epidemiological investigation, yet small enough to avoid the complication that results from the bending over of the dose–effect relationships at higher doses. For the A-bomb data, a reference dose of 1 Gy is a suitable choice and will be used in the subsequent analysis.

Choosing a Representative RBE

Equation (2) is less vulnerable to misinterpretation than Eq. (1), but, as stated above, it remains subject to the difficulty that radiobiological studies and animal experiments on tumor induction provide different values of R_1. In an extensive series of studies at the French CEA on male Sprague-Dawley rats, a fission-neutron dose of 20 mGy was consistently found to be equivalent to 1 Gy of acute γ rays with regard to both nonlethal (22) and lethal (23) tumors. This corresponds to an R_1 of 50. If the experiments were evaluated in terms of life shortening, as a proxy for the tumor mortality, the inferred value of R_1 was closer to 30 (23). Substantially smaller values of R_1 are suggested by the major studies of mice in which the results were evaluated in terms of life shortening, again as a reflection of increased tumor mortality (24–26), and the results indicate complicated dependences on the γ-ray dose rate (21). The broad range of experimental observations makes any choice of a representative value of R_1 judgmental. In line with an earlier assessment of an ICRP-ICRU liaison Committee and the synopsis (26) that was used by the Committee [ref. (27), Table D-1], a low value of $R_1 = 20$ may be taken to be representative for the experiments on life shortening in mice, while 50 is a high value based on the results obtained for tumor induction in rodents. The central value of R_1 of 35 in the tentative range of values of 20 to 50 is not inconsistent with the ratio of 46 of the quality factors for 0.5 MeV neutrons ($Q = 23$) and the quality factor for γ rays ($Q = 0.5$) proposed by the ICRP-ICRU Committee.

The induction of dicentric chromosomes in human lymphocytes is an example of an experimental system that has been prominent in discussions on the radiation weighting factor for neutrons. It exhibits a strongly curved dependence for γ rays, and, while it is doubtful whether this particular end point has much relevance to tumor induction in humans, it exemplifies the need to distinguish the two RBE values, RBE_{max} and R_1. For dicentric chromosomes, the observed RBE of neutrons at their most effective energy of about 0.5 MeV is $R_1 = 12$ relative to a γ-ray dose of 1 Gy,[2] while the maximum value at low doses is reported to be $RBE_{max} = 70$ (28, 29).

While the choice of any representative value of R_1 must remain uncertain, it appears reasonable to employ the low value of 20 and the high value of 50 as guidelines for the subsequent analysis and to quote the resulting neutron risk estimates for these values and for a central value of $R_1 = 35$. However, the dependence will be indicated for an even broader range of putative values of R_1.

The experimental radiobiological data refer to fission neutrons, with neutrons having different energy spectra in the various investigations. For the purpose of the present analysis, the values for R_1 are related to the energy range

[2] The coefficients in a linear-quadratic dose relationship for the induction of dicentric chromosome aberrations by γ rays were (19): $\alpha = (1.07 \pm 0.41) \times 10^{-2}/Gy$ and $\beta = (5.55 \pm 0.28) \times 10^{-2}/Gy^2$.

0.2 to 1 MeV where neutrons are seen to be most effective (27).

NEUTRONS IN THE A-BOMB DOSIMETRY

The procedure that has been outlined in the preceding section is straightforward, but it invokes the ERR_1 that has been caused by a *pure* γ-ray exposure. The A-bomb data, i.e. the major source of epidemiological information on radiation risk, relate to *mixed* photon and neutron irradiations. This does not change the essence of the argument, but it does require a correction and thus a slight modification of Eq. (2). Before this is dealt with, some dosimetric issues need to be considered.

It is still contested whether the dose dependence for Hiroshima is co-determined substantially, and perhaps in a complex manner, by the neutron component of the radiation which varies with distance and is different in the two cities (11, 12, 30). The contribution of neutrons had long been seen as a potentially critical issue (14, 15), and this was in fact a major driving force toward the dosimetry revision that led to DS86 (16). In a perhaps premature reaction to the lower neutron doses specified in DS86, it was then widely concluded that there was no way to infer and quantify the presumably small magnitude of the neutron contribution to the late health effects in Hiroshima and Nagasaki. This conclusion needs to be reassessed.

Pierce and Preston (31) have recently presented a new analysis in terms of the latest data on solid cancer incidence in the A-bomb survivors (follow-up to 1994). The neutron issue is not central to their work, but some of its aspects are considered, and the change in RBE with dose is treated realistically. In line with the usage in earlier RERF reports (4, 5), the analysis is related to the colon dose, i.e. the dose to the deepest-lying, most highly shielded organ.

For the γ rays, the choice of the reference organ is not critical. The doses to the more superficial organs are only a few percent higher; e.g., they are higher by 8% for the lung than for the colon. For the neutrons, the difference is much more critical, with the factor between lung and colon being about 1.9. Short of accounting for each organ individually, an appropriate organ-averaged dose must therefore be specified. This requires the shielding factors for the different organs and weighting factors that account for the contribution of the organs to the excess cancer mortality (or incidence). A suitable convention falls within the purview of RERF or ICRP. In the absence of such a convention, computations are employed in the Appendix. If the UNSCEAR organ-specific risk contributions are used as weighting factors, the organ-averaged γ-ray doses exceed the colon doses by a factor of 1.09, while the neutron doses exceed the colon doses by a factor of 2.1. These are the values for ages older than 12, and they happen to be almost exactly in line with the bone marrow doses for this age range. In the present computations, the organ-averaged dose is therefore obtained for all age-at-exposure groups with the
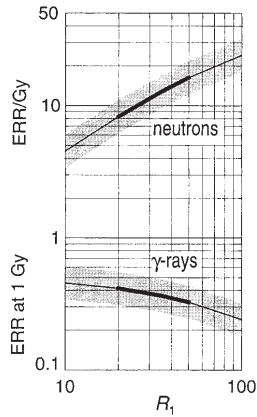
FIG. 3. The risk factor, α_n, for fast neutrons in terms of the excess relative risk, ERR/Gy, for solid cancer mortality. ERR is taken here to be an average for the age at exposure and the age attained model (see text). The lower curve represents the inferred reference slope, i.e. ERR from 1 Gy γ rays. The values are shown with their dependence on the assumed neutron RBE, R_1, as a function of an acute γ-ray dose of 1 Gy. The gray band represents the 95% confidence interval in the fit to the solid cancer mortality data.

city- and age-at-exposure-dependent conversion factors from the colon dose to the bone marrow.

An alternative averaging over organs uses either the number of cancer deaths in the LSS as weighting factors or the number of attributable cancer deaths per organ. As shown in the Appendix, this would lead to the somewhat smaller ratios of 1.8 or 2.0 for the organ-averaged neutron doses relative to the colon. The corresponding ratios for the γ rays are 1.06 and 1.08.

The diagram in Fig. 2 represents, in terms of the organ-averaged doses that equal the marrow dose, the neutron/γ-ray dose ratio, ρ, i.e. the (average) ratio of neutron absorbed dose to γ-ray absorbed dose. The solid line shows the dependence of ρ on the total γ-ray dose in Hiroshima according to the current dosimetry system, DS86. The neutron/γ-ray dose ratio for Nagasaki runs parallel to that for Hiroshima, but is lower by a factor of 3 (*16*). Because of this simple proportionality, the dependence for Nagasaki is not shown separately in the figure. There is no indication at present that the DS86 estimates for Nagasaki need to be modified.

To establish the context of the current discussions, the dotted line shows the relationship originally proposed by Straume (*32*) to account for the Hiroshima neutron discrepancy, i.e. for apparent inconsistencies between measurements of thermal neutron activation and the DS86 computations. In view of its inconsistency with the DS86 computations, and in light of current work to resolve the neutron discrepancy, this relationship is now discounted. Pierce and Preston (*31*) address a more plausible modification of

DS86 that would correspond to a roughly constant neutron/γ-ray dose ratio of about 0.04 when rescaled to the organ-averaged dose. Even this modification now appears to exceed the possible changes that are still consistent[3] with the available ^{63}Ni measurements in samples from Hiroshima (*35, 38*). The broken line therefore indicates an analogous but further reduced modification, with a neutron/γ-ray dose ratio close to 0.02 for the organ-averaged dose.

NEUTRON RISK ESTIMATES FROM THE A-BOMB DATA

Formulae for a Mixed Radiation Field

The derivation through Eq. (2) of the risk coefficient, α_n, for neutrons requires, apart from the assumed value R_1, the numerical value of the reference slope, $c = \text{ERR}_1/D_1$, for γ rays. The observations in Hiroshima and Nagasaki do not provide c directly, but the parameter can readily be inferred, with no further assumption, beyond Eq. (2), than additivity of the effect of the γ rays and the neutrons.

For both cities combined and averaged over all person years at risk in the cancer mortality data set, the neutron/γ-ray dose ratio is $\rho = 0.011$ at an organ-averaged γ-ray dose of 1 Gy. The observed excess relative risk, ERR_{obs}, at the γ-ray dose D_1, i.e. at the total absorbed dose $D_1 (1 + \rho)$, is the sum of the effect, $\text{ERR}_1 = c\, D_1$, of the γ rays and the effect, $\alpha_n\, \rho\, D_1$, of the neutrons. Let the observed slope, c_{obs}, be defined, in analogy to the reference slope, c, as $\text{ERR}_{obs}/[D_1(1 + \rho)]$. With $D_1 = 1$ Gy, one then obtains:

$$c_{obs} = (cD_1 + \rho D_1 \alpha_n)/(D_1 + \rho D_1) = (c + \rho \alpha_n)/(1 + \rho). \tag{3}$$

With $c = \alpha_n/R_1$ (see Eq. 2), this provides the risk coefficient for neutrons:

$$\alpha_n = R_1 c_{obs}\, (1 + \rho)/(1 + \rho R_1). \tag{4}$$

The term $(1 + \rho)/(1 + \rho R_1) = 1.011/(1 + 0.011\, R_1)$ distinguishes Eq. (5) from Eq. (2). It converts the observed slope, c_{obs}, i.e. the slope of the linear dose response for the actual A-bomb radiation, to the reference slope, c, for the γ rays alone. Accordingly, the γ-ray reference slope is

$$c = c_{obs}\, (1 + \rho)/(1 + \rho R_1), \tag{5}$$

the difference being that α_n increases but c decreases with R_1.

Table 1 gives, for different assumed values of R_1, the fraction, $f_n = \rho\, R_1/(1 + \rho R_1)$, of the observed effect that is due to the neutrons. It also gives in column 3 the ratio of the inferred slope, α_n, for neutrons to the observed slope c_{obs}. Column 4 gives the ratio of the inferred γ-ray reference slope to the observed slope, c_{obs}. To illustrate the less than proportional increase of α_n with increasing R_1, a broader range of values of R_1 is given in the table, beyond the values 20 to 50. The effect contributions of neutrons for the values 20 and 50 are 18% and 35%; i.e., the inferred

---

[3] W. Rühm, private communication.

TABLE 1
Fractional Effect Contribution by Neutrons at $(1 + \rho)$ Gy, Ratio α_n/c_{obs} of the Neutron Risk Coefficient to the Observed Slope c_{obs}, and Ratio c/c_{obs} of the γ-Ray Reference Slope to the Observed Slope c_{obs}

R_1	Effect fraction, f_n, due to neutrons	α_n/c_{obs}	c/c_{obs}
10	0.10	9.1	0.91
20	0.18	16.6	0.83
35	0.28	25.5	0.73
50	0.35	32.6	0.65
100	0.52	48.1	0.48

Note. The numbers are given in dependence on the assumed neutron RBE, R_1, relative to 1 Gy γ rays.

neutron contribution to the health effects is, even in these calculations which refer to both cities combined, substantial.[4]

The sensitivity of the results to the assumed neutron/γ-ray ratio is of interest with regard to both the uncertainty in the calculation of the organ-averaged dose and the eventual resolution of the Hiroshima neutron discrepancy, and it is therefore useful to consider a numerical example.

Assuming $c_{obs} = 0.5$/Gy (see the next section), then if ρ at 1 Gy increases from 0.011 to 0.015 due to a neutron dose revision, the neutron effect contribution for $R_1 = 20$ (50) increases from 18% (35%) to 23% (43%). However, the risk coefficient, α_n, for the neutrons decreases from 8.3/Gy (16.3/Gy) to 7.8/Gy (14.5/Gy), and the γ-ray reference slope, c, decreases proportionally from 0.41/Gy (0.33/Gy) to 0.39/Gy (0.29/Gy).

If, on the other hand, ρ at 1 Gy decreases from 0.011 to 0.007 due to an alternative organ dose averaging model, then the contribution of neutrons for $R_1 = 20$ (50) decreases from 18% (35%) to 12.3% (26%), while the risk coefficient, α_n, for the neutrons increases from 8.3/Gy (16.3/Gy) to 8.8/Gy (18.6/Gy). The γ-ray reference slope, c, increases proportionally from 0.41/Gy (0.33/Gy) to 0.44/Gy (0.37/Gy).

Risk Coefficients in Terms of ERR

With the present approach, the risk estimation for neutrons requires no detailed modeling of the dose dependence for solid cancers. It is sufficient to determine the excess relative risk, ERR_{obs}, at the γ-ray reference dose, D_1, of 1 Gy [i.e. total absorbed dose $(1 + \rho)$ Gy]. Reference to an intermediate dose around 1 Gy has the advantage that the ERR_{obs} can be estimated with the least relative uncertainty. As seen in nonparametric computations with the A-bomb solid cancer mortality data [e.g. Fig. 5 in ref. (33)], the fractional standard error of the ERR is smallest at around 1 Gy. It is also clear on general principles that different dose models, such as a linear or a linear-quadratic fit, provide different ERRs at low doses and at high doses near

<hr/>

[4] For Hiroshima alone, the values are 22% and 42%; for Nagasaki, they are 9% and 20%.

the dose cutoff, but will intersect at an intermediate dose level. At the intermediate dose level, the uncertainty due to the choice of the dose–response model is therefore the least. The value ERR_{obs} defines the slope, $c_{obs} = ERR_{obs}/1$ Gy, and the neutron risk coefficient, α_n, is then obtained in terms of c_{obs} from the values in Table 1.

Approximate values of ERR_{obs} can be taken from the analyses by RERF or by UNSCEAR. Those results were obtained in terms of colon dose, and a weighting factor of 10 was applied to the neutron absorbed dose component. Since the weighted colon dose is about 5% larger at 1 Gy than the colon absorbed dose, while the organ-averaged absorbed dose is about 10% larger than the colon absorbed dose (see the Appendix), it follows that, at 1 Gy, the organ-averaged absorbed dose exceeds the colon weighted dose by about 5%. The earlier results therefore provide values of ERR_{obs} that are about 5% larger than the values relative to the organ-averaged absorbed dose.

UNSCEAR (3) applies the two comparatively simple relative risk models with different time projections: the age-at-exposure model (e-model), with modifying factors that depend on age at exposure and gender; and the attained-age model (a-model), with modifying factors that depend on attained age and gender (39, 40). The age-at-exposure model provides a substantially higher lifetime relative risk for young ages at exposure. However, the difference does not appear in the parameter ERR_{obs} if it is expressed either as ERR_{30}, the gender-averaged ERR at 1 Gy for age at exposure 30, or as ERR_{60}, the gender-averaged ERR_{obs} at 1 Gy at age attained 60. With the above correction, i.e. reduced by 5%, the UNSCEAR results correspond to the values $ERR_{30} = 0.54$ and $ERR_{60} = 0.46$. For the subsequent considerations, the difference between these two values is immaterial, and reference will therefore be made to their average $c_{obs} = ERR_{obs}/1$ Gy $= 0.5$/Gy.

It is possible, of course, to derive, in terms of the publicly available RERF data on solid cancer mortality data (1950–1990) and the AMFIT routine of the Epicure software (36), the same results directly in terms of the organ-averaged absorbed dose. In a linear-quadratic dependence on organ-averaged absorbed dose, the quadratic component is then seen to be insignificant, and, as in the slightly different computations in terms of weighted dose (3, 4), the simple linear slope is therefore used. Our computations provide the value (and 95% confidence range) $ERR_{30} = 0.51$/Gy (0.37/Gy–0.65/Gy) for the e-model and $ERR_{60} = 0.48$/Gy (0.35/Gy–0.61/Gy) for the a-model. The slight numerical difference from the UNSCEAR results may reflect the choice of a relatively small dose cutoff at 2 Gy, but again the average value can be represented by $c_{obs} = ERR_{obs}/1$ Gy $= 0.5$/Gy.

With $c_{obs} = ERR/1$ Gy $= 0.5$/Gy and the values from Table 1, one obtains the risk coefficients, α_n, for neutrons in terms of the values of ERR for solid cancer mortality that are given in Fig. 3. For comparison, and to indicate the reciprocal relationship between the two quantities, the

figure also includes the ERR from 1 Gy γ rays; i.e., it indicates in its lower part the reference slope $c = \text{ERR}_1/1$ Gy. If a linear dose dependence without DDREF is assumed for the γ rays, and only under this condition, c equals the risk coefficient for γ rays.

The 95% confidence range for ERR_{obs} (ERR_{30} or ERR_{60}) in the fit to the data amounts to ±30%, and this is indicated by the shaded bands in Fig. 3. Possible errors in the dosimetry system should be somewhat less (38), and it is thus apparent from the figure that the uncertainty in R_1 has a similar impact on the inferred neutron risk estimate and a somewhat smaller impact on the inferred ERR_1 (and thus on the reference slope for γ rays) if the range of plausible values can be assumed to be 20 to 50.

The neutron risk estimate is expressed in the unit gray, but the magnitude of the relevant neutron doses is, of course, far below 1 Gy. The analysis invokes the neutron doses 1 Gy/R_1 = 20 mGy to 50 mGy, and 10 mGy happens to be of the same order of magnitude as the neutron dose at 1 Gy total dose to the A-bomb survivors. In common radiation protection situations, the neutron doses are of the order of fractions of 1 mGy, while a neutron dose of 1 Gy, if it is acute, is likely to be lethal.

It may seem somewhat artificial that reference is made here to absorbed dose (Gy) rather than to equivalent dose (Sv). However, there is no straightforward conversion. The risk coefficient α_n in Table 1 and Fig. 3 refers to a genuine neutron absorbed dose that equals essentially the neutron kerma (37) in the body. This is the dose from the charged recoil particles that are set free by the neutrons in the exposed organs. The ICRP equivalent organ doses, H_T, or the effective dose, E, from a neutron exposure are not defined in terms of the genuine neutron doses. They are instead derived by multiplying the recommended radiation weighting factor, w_R, by the sum of the genuine neutron dose and the γ-ray dose that is caused simultaneously in the human body by the incident neutrons (2). While this may appear to be a mere technical detail of the definition, it in fact makes a considerable difference at neutron energies of the order of 1 MeV or less. It follows, for example, that the mean effective neutron dose to the A-bomb survivors at 1 Gy is appreciably larger than the value 20 × 11 mSv = 220 mSv that would be obtained by a naive application of the ICRP radiation weighting factor, w_R = 20, for fission neutrons to the mean neutron absorbed dose of 11 mGy. It is therefore misleading to compare w_R to the values of R_1 invoked in the present analysis. The values R_1 are larger, because they relate to the genuine neutron dose component.

The comparison of the present results to the ICRP risk estimate for neutrons that is implicit in the adoption of their radiation weighting factor is, of course, of considerable interest. However, it requires an analysis of the γ-ray contribution from typical neutron exposures, and it must also include a consideration of the conversion of the excess rel-ative risk into lifetime attributable risk for solid cancer mortality. These issues need to be treated separately.

CONSIDERATION OF THE HIROSHIMA/NAGASAKI EFFECT RATIO

While the present approach avoids the extrapolations to low doses, it still requires an extrapolation from animal data to health effects in humans. The results that are obtained in this way remain subject to uncertainty. At the same time, contrary to current assumptions, these results suggest, a certain possibility of direct inference from the epidemiological data. A range of 20 to 50 has been considered here for plausible values of the neutron RBE, R_1, relative to 1 Gy of γ rays. This corresponds to a contribution of neutrons to the total radiation effect of between 23% and 43% at 1 Gy in Hiroshima, but only between 9% and 20% in Nagasaki. The city ratio, CR, i.e. the ratio of the ERR observed in Hiroshima and in Nagasaki at the same absorbed dose, assuming other factors to be equal, would then be substantially larger than unity (38). If the neutron/γ-ray dose ratios for Hiroshima and Nagasaki are denoted by ρ_H and ρ_N, the city ratio can readily be derived as

$$CR = [1 + (R_1 - 1)\rho_H]/[1 + (R_1 - 1)\rho_N]. \qquad (6)$$

With the DS86 values $\rho_H = 0.015$ and $\rho_N = 0.005$ at 1 Gy, the city ratio is CR = 1.17 or CR = 1.39 for R_1 = 20 or R_1 = 50. Computations in terms of the attained-age model[5] from the published data on solid cancer mortality and incidence provide values that lie within this range (cancer mortality: CR = 1.33 ± 0.39; incidence: CR = 1.26 ± 0.24), but the standard errors are too large to permit reliable conclusions, and the details of the computations therefore are not presented. Further computations with the most recent incidence data and with finer dose categories should provide more exact results. If the city ratio at 1 Gy were shown to be less than 1.5, and all other factors could be shown to be equal, this would exclude values of R_1 larger than 68, which is not far from the high value of 50 invoked here in view of the animal studies.

Any increase in the neutron doses in Hiroshima would further sharpen such conclusions. Furthermore, it will be worthwhile to examine whether computations in terms of the A-bomb data cross-tabulated for γ-ray and neutron doses can be helpful in identifying the contribution of neutrons.

CONCLUSION

The major new aspect in this analysis is the linkage of the risk coefficient for neutrons to quantities that can be

---

[5] The attained-age model has been invoked here, because high values up to about 2 have been obtained for the city ratio (4), but these values were biased. The bias and thus the high values are due, as pointed out by the authors of the report, to a substantial age difference between the populations in Hiroshima and Nagasaki. The attained-age model is much less sensitive to age at exposure and therefore provides more meaningful values of the city ratio.

TABLE A1
**Excess Absolute Risk for Solid Cancer Mortality
[REID (%)] due to 1 Gy of Acute Whole-Body
Exposure to γ Rays for Different Organs**

	Excess absolute risk		Organ dose/colon dose	
Organ	RR	AR	γ rays	Neutrons
Esophagus	1.13	0.61	1.18	2.56
Stomach	0.61	1.13	102	1.54
Colon	0.76	0.50	1	1
Liver	0.55	1.26	1.05	1.66
Lung	1.88	1.58	1.09	1.91
Breast	1.51	0.65	1.17	3.85
Bladder	0.28	0.22	1.05	1.17
Other solid cancer	1.95	1.72	(1.10)	(2.14)
Total	8.67	7.67		
RR average:			1.10	2.24
AR average:			1.08	2.00
Bone marrow			1.10	2.14

Notes. The values are averages of the values given by UNSCEAR (*3*) for the two genders and the five reference populations. Column 2 refers to relative risk transportation (RR), column 3 to absolute risk transportation (AR). Columns 4 and 5 give the ratio of the organ dose to the colon dose for γ rays and for neutrons.[6] In the absence of otherwise specified values, the dose ratios for the bone marrow are used for the organs that correspond to "other solid cancer".

TABLE A2
**The Ratio of the Organ-Averaged Dose to the
Colon Dose for γ Rays and for Neutrons**

	Organ average/ colon dose	
Weighting factors for the organ-specific dose coefficients[a]	γ rays	Neutrons
ICRP organ weighting factors [ref. (*2*), table S-2]	1.08	1.96
Number of cancer deaths in LSS (including ovary and pancreas)	1.06	1.79
Excess cancer deaths in LSS (4) (including ovary and pancreas)	1.08	1.98

Notes. The results given in the second and third columns result from different methods of weighting the individual organ-specific dose adjustment factors that have been provided by RERF.[6] The first column indicates the type of weights that have been applied to the organ specific neutron and γ-ray adjustment factors.

[a] For the organs in Table A1, with additional organs included, if specified.

observed at intermediate doses. The use of extrapolated values, such as the risk coefficient for γ rays and the low-dose limit, RBE_{max}, of neutrons, is unnecessary, and it introduces uncertainties that can be avoided. In line with the linearity in dose that is assumed for neutrons, their risk coefficient can be estimated in terms of the product of the ERR observed in a human population at an intermediate dose of γ rays, and the neutron RBE compared to this reference dose that is suggested by animal studies. Application of this procedure to the data from Hiroshima for solid cancers is slightly more complex, because it requires accounting for the neutron contribution at a total dose of 1 Gy, but it is otherwise straightforward and defines a fairly narrow range of values for the neutron risk coefficient.

Linking the dose coefficient for neutrons to observations at 1 Gy has the notable consequence that the result is insensitive to the eventual resolution of the neutron discrepancy in Hiroshima. [63]Ni measurements on samples from ground distances around 1000 m in Hiroshima (*34, 35*) suggest that there will be no major changes from the DS86 neutron doses at these distances, i.e. at total doses close to 1 Gy. If the DS86 neutron dose of 15 mGy in Hiroshima at a total dose of 1 Gy were moderately increased to, say, 20 mGy (see Fig. 2), the average neutron dose in the two cities at 1 Gy would increase from 11 mGy to 15 mGy, and the neutron risk coefficient, α_n, would, as stated with reference to Table 1, decrease by 6% to 11% for values of R_1 ranging from 20 to 50. There would thus be no major change. More substantial increases in the neutron dose at larger distances, i.e. at total doses below 0.5 Gy, cannot be excluded at present (*38*). They would not affect the neutron

risk estimate, but could have some impact on the risk estimate for γ rays.

The risk estimates for neutrons that are derived here apply to genuine neutron doses (neutron kerma in the body), while ICRP defines the effective dose of neutrons in terms of the radiation weighting factor multiplied into the total absorbed dose, including the contribution from the γ rays generated by the incident neutrons within the body. A comparison to the ICRP risk estimate therefore requires a separate analysis.

APPENDIX

Organ-Averaged Dose for Solid Cancer Mortality

Table A1 lists the cancer types for which the recent UNSCEAR report (*3*) gives lifetime attributable excess risks (REID) for five reference populations (China, Japan, Puerto Rico, UK, U.S.). Columns 2 (relative risk transportation, RR) and 3 (absolute risk transportation, AR) list the averages over the reference populations and the two genders. The organ doses relative to the colon dose are given in column 4 for the γ rays and in column 5 for the neutrons.[6] These dose factors are values for ages above 12 years and for the population in Hiroshima. Since the "other solid cancers" have not been specified by ICRP and there is accordingly no dose factor for this category, they are tentatively assigned the dose ratios for the bone marrow (values in parentheses).

The organ doses are averaged with weighting factors equal to the excess risk that they contribute (in either the RR or the AR calculations for UNSCEAR) to the solid cancer mortality. The organ average so obtained for ages above 12 corresponds closely to the bone marrow dose. Since the relative depths of the different organs do not change greatly with age, the conversion factors from colon to bone marrow dose are applicable in all age-at-exposure categories and for both cities.

Alternative models for organ dose averaging can be considered, and Table A2 gives the results for three different approaches. The first approach uses the ICRP organ weighting factors in the averaging; the second approach uses the total number of cancer deaths in the LSS (for the eight categories in Table A1 and, in addition, ovary and pancreas); the

third approach is analogous to the second, but uses the attributable numbers of cancer deaths as weighting factors. The resulting ratios of the organ-averaged neutron doses to the colon dose are somewhat smaller, but do not differ much from a factor of 2.

REFERENCES

1. ICRP, *Recommendations of the International Commission on Radiological Protection.* Publication 26, *Annals of the ICRP*, Vol. 1, No. 3, Pergamon Press, Oxford, 1977. [Reprinted (with additions) in 1987]

2. ICRP, *The 1990 Recommendations of the International Commission on Radiological Protection.* Publication 60, *Annals of the ICRP*, Vol. 21, No. 1–3, Pergamon Press, Oxford, 1991.

3. UNSCEAR, *Sources and Effects of Ionizing Radiation,* Vol. 2, Annex I, Epidemiological evaluation of radiation-induced cancer, pp. 297–450. United Nations, New York, 2000.

4. D. A. Pierce, Y. Shimizu, D. L. Preston, M. Vaeth and K. Mabuchi, Studies of the mortality of atomic bomb survivors. Report 12, Part I. Cancer. *Radiat. Res.* **146**, 1–27 (1996).

5. D. E. Thompson, K. Mabuchi, R. Ron, M. Soda, M. Tokunaga, S. Ochikubo, S, Sugimoto, T. Ikeda, M. Terasaki and D. L. Preston, Cancer incidence in atomic bomb survivors. Part II: Solid tumors, 1958–1987. *Radiat. Res.* **137**, 17–67 (1994).

6. D. L. Preston, S. Kusumi, M. Tomonaga, S. Izumi, E. Ron, A. Kuramoto, N. Kamada, H. Dohy, T. Matsuo and K. Mabuchi, Cancer incidence in atomic bomb survivors. Part III. Leukemia, lymphoma and multiple myeloma. 1950–1987. *Radiat. Res.* **137** (Suppl.), S68–S97 (1994).

7. NCRP, *Risk Estimates for Radiation Protection.* Report 115, National Council on Radiation Protection and Measurements, Bethesda, MD, 1993.

8. NCRP, *Uncertainties in Fatal Cancer Risk Estimates used in Radiation Protection.* Report 126, National Council on Radiation Protection and Measurements, Bethesda, MD, 1997.

9. National Research Council, Committee on the Biological Effects of Ionizing Radiation, *Health Effects of Exposure to Low Levels of Ionizing Radiation (BEIR V).* National Academy Press, Washington DC, 1990.

10. NRPB, *Estimates of Late Radiation Risks to the U.K. Population*, Vol. 4, no. 4. National Radiological Protection Board, Oxon, England, 1993.

11. H. H. Rossi and M. Zaider, Comment on the contribution of neutrons to biological effects at Hiroshima. *Radiat. Res.* **146**, 590–591 (1996). [letter to the Editor]

12. D. A. Pierce, Y. Shimizu, D. L. Preston, M. Vaeth and K. Mabuchi, Response to the letter of Drs. Rossi and Zaider. *Radiat. Res.* **146**, 591–593 (1996). [letter to the Editor]

13. R. C. Milton and T. Shohoji, *Tentative 1965 Radiation Dose (TD65) Estimation for Atomic Bomb Survivors.* Report TR 1-68, Atomic Bomb Casualty Commission, Hiroshima, 1968.

14. H. H. Rossi and A. M. Kellerer, The validity of risk estimates of leukemia incidence based on Japanese data. *Radiat. Res.* **58**, 131–140 (1974).

15. H. H. Rossi and C. W. Mays, Leukemia risk from neutrons. *Health Phys.* **34**, 353–360 (1978).

16. W. C. Roesch, Ed., *US–Japan Joint Reassessment of Atomic Bomb Radiation Dosimetry in Hiroshima and Nagasaki*, Vols. 1 and 2. Radiation Effects Research Foundation, Hiroshima, 1987.

17. NCRP, *Influence of Dose and its Distribution in Time on Dose–Response Relationships for Low-LET Radiations.* Report 64, National Council on Radiation Protection and Measurements, Bethesda, MD, 1980.

18. W. K. Sinclair, *Science Radiation Protection and the NCRP.* L. S. Taylor Lecture no. 17, National Council on Radiation Protection and Measurements, Bethesda, MD, 1993.

19. M. Bauchinger, E. Schmid, S. Streng and J. Dresp, Quantitative analysis of the chromosome damage at first division of human lymphocytes after ^{60}Co-γ-irradiation. *Radiat. Environ. Biophys.* **22**, 225–229 (1983).

20. ICRU, *The Quality Factor in Radiation Protection.* Report 40, International Commission on Radiation Units and Measurements, Bethesda, MD, 1986.

21. NRPB, *Relative Biological Effectiveness of Neutrons for Stochastic Effects*, Vol. 8, No. 2. National Radiological Protection Board, Oxford, England, 1997.

22. J. Lafuma, D. Chmelevsky, J. Chameaud, M. Morin, R. Masse and A. M. Kellerer, Lung carcinomas in Sprague-Dawley rats after exposure to low doses of radon daughters, fission neutrons, or γ rays. *Radiat. Res.* **118**, 230–245 (1989).

23. C. Wolf, J. Lafuma, R. Masse, M. Morin and A. M. Kellerer, Neutron RBE for tumors with high lethality in Sprague-Dawley eats. *Radiat. Res.* **154**, 412–420 (2000).

24. B. A. Carnes, D. Grahn and J. F. Thomson, Dose–response modeling of life in a retrospective analysis of the combined data from the Janus Program at Argonne National Laboratory. *Radiat. Res.* **119**, 39–56 (1989).

25. V. Covelli, M. Coppola, V. Di Majo, S. Rebessi and B. Bassini, Tumor induction and life shortening in BC3F1 female mice at low doses of fast neutrons and X rays. *Radiat. Res.* **113**, 362–374 (1988).

26. W. K. Sinclair, Fifty years of neutrons in biology and medicine: The comparative effects of neutrons on biological systems. In *Proceedings of the 8th Symposium on Microdosimetry* (H. G. Ebert, Ed.), Report EUR 8395. Commission of the European Communities, Brussels, 1982.

27. ICRU, *The Quality Factor in Radiation Protection.* Report 40, International Commission on Radiation Units and Measurements, Bethesda, MD, 1986.

28. R. L. Dobson, T. Straume, A. V. Carrano, J. L. Minkler, L. L. Deaven, L. G. Littlefield and A. A. Awa, Biological effectiveness of neutrons from Hiroshima bomb replica: Results of a collaborative cytogenetic study. *Radiat. Res.* **128**, 143–149 (1991).

29. E. Schmid, D. Regulla, S. Guldbakke, D. Schlegel and M. Bauchinger, The effectiveness of monoenergetic neutrons at 56 keV in producing dicentric chromosomes in human lymphocytes at low doses. *Radiat. Res.* **154**, 307–312 (2000).

30. A. M. Kellerer and E. Nekolla, Neutron versus γ-ray risk estimates. Inferences from the cancer incidence and mortality data in Hiroshima. *Radiat. Environ. Biophys.* **36**, 73–83 (1997).

31. D. A. Pierce and D. L. Preston, Radiation-related cancer risks at low doses among A-bomb survivors. *Radiat. Res.* **154**, 178–186 (2000).

32. T Straume, S. D. Egbert, W. A. Woolson, R. C. Finkle, P. W. Kubik, H. F. Grove, P. Sharma and M. Hoshi, Neutron discrepancies in the DS86 dosimetry system. *Health Phys.* **63**, 421–426 (1992).

33. M. Chomentowski, A. M. Kellerer and D. A. Pierce, Radiation dose dependencies in the atomic bomb survivor cancer mortality data: A model-free visualization. *Radiat. Res.* **153**, 289–294 (2000).

34. W. Rühm, A. M. Kellerer, G. Korschinek, T. Faestermann, K. Knie, G. Rugel, K. Kato and E. Nolte, The dosimetry system DS86 and

the neutron discrepancy in Hiroshima—Historical review, present status, and future options. *Radiat. Environ. Biophys.* **37**, 293–310 (1998).

35. W. Rühm, K. Knie, G. Rugel, A. A. Marchetti, T. Faestermann, C. Wallner, J. E. McAninch, T. Straume and G. Korschinek, Accelerator mass spectrometry of ⁶³Ni at the Munich tandem laboratory for estimating fast neutron fluences from the Hiroshima atomic bomb. *Health Phys.* **79**, 358–364 (2000).

36. D. L. Preston, J. H. Lubin and D. A. Pierce, *Epicure User's Guide.* HiroSoft International Corp., Seattle, 1993.

37. ICRU, *Fundamental Quantities and Units for Ionizing Radiation.* Report 60, International Commission on Radiation Units and Measurements, Bethesda, MD, 1998.

38. National Research Council, Committee on Dosimetry for RERF, *Status of the Dosimetry for the Radiation Effects Research Foundation (DS86).* National Academy Press, Washington DC, 2001.

39. A. M. Kellerer and D. Barclay, Age dependences in the modelling of radiation carcinogenesis. *Radiat. Prot Dosim.* **41**, 273–281 (1992).

40. D. A. Pierce and M. L. Mendelsohn, A model for radiation-related cancer suggested by atomic bomb survivor data. *Radiat. Res.* **152**, 642–654 (1999).

3. Kellerer AM & Walsh L. Solid cancer risk coefficient for fast neutrons, in terms of effective dose. Radiat. Res. 158, 61-68, 2002

Solid Cancer Risk Coefficient for Fast Neutrons in Terms of Effective Dose

Albrecht M. Kellerer[a,b,1] and Linda Walsh[a]

[a] Radiobiological Institute, University of Munich, Schillerstrasse 42, D-80336 Munich, Germany; and [b] Institute of Radiation Biology, GSF–National Research Center for Environment and Health, Ingolstädter Landstrasse 1, D-85764 Neuherberg, Germany

Kellerer, A. M. and Walsh, L. Solid Cancer Risk Coefficient for Fast Neutrons in Terms of Effective Dose. *Radiat. Res.* 158, 61–68 (2002).

Cancer mortality risk coefficients for neutrons have recently been assessed by a procedure that postulates for the neutrons a linear dose dependence, invokes the excess risk of the A-bomb survivors at a γ-ray dose D_1 of 1 Gy, and assumes a neutron RBE as a function of D_1 between 20 and 50. The excess relative risk (ERR) of 0.008/mGy has been obtained for $R_1 = 20$ and 0.016/mGy for $R_1 = 50$. To compare these results to the current ICRP nominal risk coefficient for solid cancer mortality (0.045/Sv for a population of all ages; 0.036/Sv for a working population), the ERR is translated into lifetime attributable risk and is then related to effective dose. The conversion is not trivial, because the neutron effective dose has been defined by ICRP not as a weighted genuine neutron dose (neutron kerma), but as a weighted dose that includes the dose from γ rays that are induced by neutrons in the body. If this is accounted for, the solid cancer mortality risk for a working population is found to agree with the ICRP nominal risk coefficient for neutrons in their most effective energy range, 0.2 MeV to 0.5 MeV. In radiation protection practice, there is an added level of safety, because the effective dose, *E,* is—for monitoring purposes—assessed in terms of the operational quantity *H**, which overestimates *E* substantially for neutrons between 0.01 MeV and 2 MeV. © 2002 by Radiation Research Society

INTRODUCTION

Neutron risk estimates are increasingly discussed with regard to issues such as the transport of reactor fuel. Their magnitude has been inferred in the past by multiplying risk coefficients for photon radiation by a low dose limit, RBE$_{max}$, of the relative biological effectiveness (RBE) of neutrons from cell or animal studies. With regard to solid cancer mortality, estimates of the low-dose excess relative risk (ERR) per gray for γ rays have varied roughly between 0.05 and 0.5 (*1*), while values of RBE$_{max}$ from experimental studies lie between 10 and 100 (*2*). The resulting values of the ERR

per gray for neutrons can thus range from 0.5 to 50, and even values beyond this range have in fact been claimed in the public debates on neutron risk. The preceding paper (*3*) derived more robust risk estimates for neutrons by postulating—as in the familiar approach—a linear dependence for neutrons, but using otherwise the less uncertain parameters, excess relative risk, ERR$_1$, derived from the A-bomb data at an intermediate γ-ray dose, $D_1 = 1$ Gy, and, from animal data, the RBE, R_1, of neutrons relative to the same γ-ray dose.

Table 1 shows the results from the preceding paper. They have been derived in terms of the common computational tool, i.e. the program AMFIT in the software system EPICURE (*4*), with the RERF data for solid cancer mortality (1950–1990). As in the most recent computations for UNSCEAR (*5*), the two comparatively simple relative risk models with different time projection are considered: the age-at-exposure model (*e*-model) with modifying factors that depend on age at exposure and gender, and the attained-age model (*a*-model) with modifying factors depending on attained age and gender. The age-at-exposure model provides substantially higher lifetime relative risk for the youngest ages at exposure, but the ERR per unit dose has roughly the same value, whether it is expressed in terms of ERR$_{30}$ (the gender-averaged ERR at 1 Gy for age at exposure 30) for the *e*-model, or in terms of ERR$_{60}$ (the gender-averaged ERR at 1 Gy at age attained 60) for the *a*-model.[2]

The risk coefficients in columns 2 and 3 are expressed in the appropriate unit, gray. However, it needs to be noted—and this also applies to subsequent figures—that the neutron doses of interest are much smaller, namely 1 Gy/R_1 = 20 mGy to 50 mGy in the analysis that led to Table 1 and fractions of 1 mGy in most radiation protection considerations.

---

[1] Author to whom correspondence should be addressed at Radiobiological Institute, University of Munich, Schillerstrasse 42, D-80336 Munich; e-mail: amk.sbi@lrz.uni-muenchen.de.

[2] The earlier paper was not concerned with the age dependence of the risk and it therefore used an average of the numerically similar values ERR$_{30}$ and ERR$_{60}$. The present analysis requires the lifetime attributable risk, which can depend critically on the projection model. For this reason, Table 1 spells out the separate values. They result from taking the product of the ratio α_n/c_{obs} listed in Table 1 of ref. (*3*) with the values ERR$_{30}$ = 0.51/Gy (0.37/Gy − 0.65/Gy) and ERR$_{60}$ = 0.48/Gy (0.35/Gy − 0.61/Gy) given in ref. (*3*).

TABLE 1
**The Risk Factor for Fast Neutrons in Terms of the
Excess Relative Risk, ERR$_{30}$/Gy, for the Age-at-
Exposure Model or the ERR$_{60}$/Gy
for the Attained-Age Model (3)**

	Solid cancer mortality (1950–1990)	
	Age-at-exposure model	Attained-age model
R_1	ERR$_{30}$/Gy	ERR$_{60}$/Gy
20	8.5 (6.1–10.8)	8.0 (5.8–10.1)
35	13.0 (9.4–16.6)	12.2 (8.9–15.6)
50	16.6 (12.1–21.2)	15.6 (11.4–19.9)

Note. The numbers (and 95% confidence regions) are for the different assumed values of the neutron RBE, R_1, relative to an acute γ-ray reference dose of 1 Gy.

ICRP (6) specifies the nominal risk coefficient in terms of lifetime attributable risk (LAR) per unit effective dose, E. The risk for solid cancer fatality is presently taken to be 0.045/Sv for a population of all ages and 0.036/Sv for a working population. Being primarily derived from the follow-up of the A-bomb survivors, these numerical values relate essentially to γ rays. However, equal effective doses of different types of radiation are deemed to carry equal risk, and through the choice of the radiation weighting factors, w_R, an implicit risk estimate is thus made for other types of radiation, such as neutrons. To determine whether this implicit risk estimate is consistent with the present risk estimate, the values in Table 1 need to be converted to LAR/Sv.

The transition from excess relative risk to LAR can be made in analogy to the ICRP procedure that led to the nominal risk coefficient. The conversion to effective dose is less straightforward. The neutron excess relative risk per gray relates to the organ-weighted genuine neutron dose, i.e. the absorbed dose from the recoil nuclei released by the neutrons (neutron tissue kerma). In contrast, the neutron effective dose is defined as the product of w_R and the organ-weighted total absorbed dose from neutrons incident on the body, which includes—especially at neutron energies below 1 MeV—a substantial γ-ray dose from neutron capture processes within the body.

The same peculiar convention applies to the organ equivalent doses. The radiation weighting factor must be applied to the sum of the genuine neutron absorbed dose in the organ and the absorbed dose due to γ rays released by the neutrons within the body (6).

CONVERSION FROM EXCESS RELATIVE RISK TO LIFETIME ATTRIBUTABLE RISK

For the conversion into LAR, the ERR needs to be "transported" to a population of all ages with a known distribution of lifetimes and with specified age-dependent solid cancer mortality or incidence rates. The selection of the reference population is, of course, arbitrary. But ICRP has established a precedent in the computations (7) for its

current recommendations (6). These computations derived averages for five reference populations, U.S., UK, Japan, Puerto Rico and China. For comparability to the ICRP risk estimates, the present computations are therefore performed with the same five populations and with the same survival functions and solid cancer mortality rates as used by ICRP.[3] The ICRP has employed the simple, unweighted average of the conversion factors for the five populations, and the same procedure is adopted here to derive the conversion factor, f, that links the ERR to the lifetime attributable solid cancer mortality risk, LAR:

$$LAR = f \cdot ERR. \qquad (1)$$

As detailed in a separate paper (8), the following conversion factors result for a population of all ages for the age-at-exposure and age-attained models:

$$f = LAR/ERR_{30} = 0.18 \text{ and } LAR/ERR_{60} = 0.12 \quad (2)$$

For occupational exposure, i.e. averaged over ages 25 to 65 at exposure (6), the conversion coefficients are not greatly different for the two projection models:

$$f = LAR/ERR_{30} = 0.11 \text{ and } LAR/ERR_{60} = 0.12 \quad (3)$$

LAR equals the quantity that had previously been termed risk of untimely death (RUD) (9). For low doses, it gives the expected number of excess cancer deaths. It is then equal to the more complicated quantity risk of exposure-induced death (REID) that has been used by UNSCEAR (5). For higher doses, LAR is slightly larger than REID, because it disregards life shortening due to the radiation exposure. In contrast to REID, the quantity LAR increases proportionally to ERR.

Figure 1 gives, as functions of the assumed neutron RBE, R_1, the risk coefficients LAR/Gy that are obtained with the conversion factors in Eq. (3) from the data in Table 1. The diagram stands for occupational exposure. Since the two projection models provide nearly the same values in this case, their average is plotted. The results are given for assumed values, R_1, of the neutron RBE that extend beyond the plausible range 20 to 50. This is done to indicate more clearly the dependence on R_1. The gray band represents the 95% confidence interval in the fit to the data for mortality from solid cancers. As pointed out with regard to Table 1, the appropriate unit of absorbed dose, gray, is used in the notation, but the doses of interest and, accordingly, the values of LAR are much smaller.

Figure 1 is analogous to the diagram that has been given in the preceding article (3) in terms of ERR. As in the earlier diagram, the lower curve and its confidence band represent the inferred reference slope, i.e. the LAR from an acute γ-ray dose of 1 Gy. If a linear dose dependence with no dose and dose-rate effectiveness factor (DDREF) is in-

[3] In its most recent report, UNSCEAR has invoked the same five reference populations but has used changed population data and somewhat different concepts, which has increased the risk estimates appreciably [see ref. (5)].
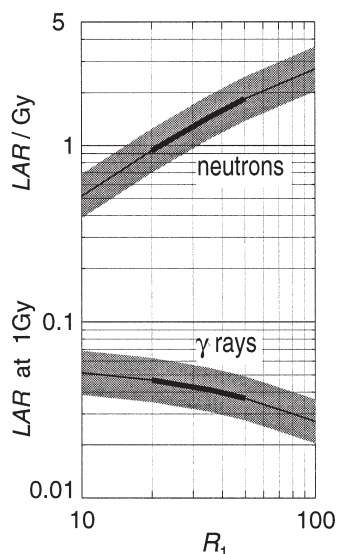
FIG. 1. The risk factor, LAR/Gy, for fast neutrons in terms of the lifetime attributable solid cancer mortality for a working population. The average is given of the nearly equal values for the age-at-exposure and attained-age models. The gray band represents the 95% confidence interval in the fit to the solid cancer mortality data. The values are given in dependence on the value, R_1, of the assumed neutron RBE relative to a reference γ-ray dose of 1 Gy. The lower curve represents the inferred reference slope, i.e. LAR from an acute γ-ray dose of 1 Gy. For a population of all ages, roughly the same values are obtained in terms of the attained-age model. The age-at-exposure model provides values that are higher by a factor 1.6.

voked, the lower curve represents the γ-ray risk estimate for a working population as inferred from the A-bomb solid cancer mortality data. The γ-ray risk estimate is not the subject of the present study, but it is of interest to note that the result—although it invokes no DDREF—is nevertheless close to the current ICRP risk estimate [LAR/Gy = 0.036/Gy for solid cancer mortality in a working population (6; table S-3)]. A more detailed assessment of the γ-ray risk coefficient (10) substantiates this conclusion.

With the attained-age model, the result for all ages at exposure equals essentially the estimates in Fig. 1 for occupational exposures [see Eqs. (1) and (3)]. However, the age-at-exposure model provides substantially larger values, which reflect the considerably larger risk projection for exposures in childhood. No separate diagram is given for this case, because the values are readily obtained by applying a factor of 1.6.

As stated in the Introduction, one cannot simply multiply the neutron absorbed dose (unit Gy) by the radiation weighting factor, w_R, to obtain the neutron effective dose (unit Sv). This calculation would provide values of the neutron effective dose that are significantly smaller than the

correct values, and it would lead to the conclusion that ICRP has substantially underestimated the neutron risk.

TRANSITION FROM NEUTRON ABSORBED DOSE TO EFFECTIVE DOSE

The Neutron and the γ-Ray Component of the Neutron Effective Dose

Up to this point, reference has been made to the absorbed dose from the charged recoil particles liberated by the neutrons, which is essentially the neutron kerma in the exposed tissue. For the purpose of the present discussion, this is termed the genuine neutron dose. No dose component from γ rays due to neutron capture inside or outside the exposed object—whether a small animal or a human body—is included in this quantity. In experiments with small animals, for example with rodents, the issue of the γ-ray component from neutron capture within the body does not arise, because this contribution is insignificant (11). Depending on the exposure geometry, some γ-ray component is, of course, due to neutron capture *outside* the animal, but in experiments with careful dosimetry, this γ-ray dose is treated separately; i.e.; it is not taken to be part of the "neutron absorbed dose". The situation is different when the human body is exposed to fast neutrons. The γ-dose from neutron capture within the body can be substantial because of the larger dimensions that are involved. This γ-ray component is clearly due to the incident neutron field, but it is a matter of choice whether one defines the "neutron absorbed dose" to include or exclude the γ-ray component. In this paper, the γ-ray component is taken to be excluded, and to avoid confusion the expression genuine neutron dose is used.

In radiobiology and in radiation epidemiology, the γ-ray component is usually not included; i.e., the term neutron absorbed dose refers to the genuine neutron dose. This makes sense, because the γ-ray component can substantially increase the value of the absorbed dose, while it does not add appreciably to the biological effect. The dosimetry for the A-bomb survivors follows the same convention; i.e., the contribution by γ rays from neutron capture within the body is not counted in the neutron dose, but it is included in the total γ-ray dose. In the computations for DS86, the neutron dose is derived in terms of the tissue kerma factors and the local neutron flux spectrum in the organs of interest (12).

In defining the organ equivalent doses and the effective dose for purposes of radiation protection practice, the ICRP has taken a different approach (6). Specifying the energy-dependent radiation weighting factor, w_R, for the external neutron field, ICRP stated that it needs to be applied to the total organ absorbed dose, $D_T = D_{T,\gamma} + D_{T,n}$, that is due to the neutrons incident on the human body. To distinguish D_T from the genuine neutron dose, $D_{T,n}$, for the purpose of the present discussion, D_T will be termed the inclusive neutron dose to the organ. The organ equivalent dose from a

monoenergetic neutron field is then the product of the in-
clusive neutron dose to the organ and the radiation weight-
ing factor for the neutrons:

$$H_T = w_R D_T = w_R (D_{T,\gamma} + D_{T,n}). \quad (4)$$

The neutron effective dose is obtained by averaging this over
the organs in terms of the organ weighting factors, w_T:

$$\begin{aligned} E &= w_R \sum_T w_T D_T \\ &= w_R(\sum_T w_T D_{T,\gamma} + \sum_T w_T D_{T,n}). \end{aligned} \quad (5)$$

It is helpful to write this equation in the simpler form:

$$E = w_R D' = w_R(D'_\gamma + D'_n). \quad (6)$$

w_R is thus a weighting factor for the organ-weighted inclu-
sive neutron dose D' that consists of a sparsely ionizing γ-
ray component, D'_γ, and the densely ionizing genuine neu-
tron component, D'_n:

$$\begin{aligned} D'_\gamma &= \sum_T w_T D'_\gamma = \sum_T w_T D_{T,\gamma,} \\ D'_n &= \sum_T w_T D_{T,n}. \end{aligned} \quad (7)$$

Equation (6) sets w_R apart from a neutron RBE which is
related to the genuine neutron dose alone. Misconceptions
arise when this difference is overlooked.

Let F_n be the fraction of the organ-weighted inclusive
neutron dose that is due to the genuine neutron dose:

$$F_n = \sum_T w_T D_{T,n}/\sum_T w_T D_T = D'_n/D'. \quad (8)$$

F_n, as computed by Leuthold *et al.* (*13*) for an anthropo-
morphic phantom, is given in Fig. 2 for rotationally sym-
metrical (ROT) exposure to fast neutrons of the specified
energies, E_n (solid line). The neutron fraction decreases rap-
idly with decreasing neutron energy. Typical moderated
neutron fields contribute a major fraction of the dose
through neutrons below 1 MeV. The γ-ray component is
therefore a substantial part of the inclusive neutron dose.

Rotational symmetry is typical for workplace exposure
conditions. For anterior–posterior (AP) exposure, the neu-
tron fraction is somewhat larger (see Fig. 2, dashed line).
Dose computations in aviation usually assume isotropic ex-
posure, which gives almost the same result as the rotational
geometry. In this paper, we do not address the high neutron
energies that are associated with aviation exposures.

NEUTRON RISK COEFFICIENT IN TERMS OF EFFECTIVE DOSE

Formula for the Risk Coefficient

The risk coefficient LAR/Sv in terms of the neutron ef-
fective dose is computed by deriving first the inclusive neu-
tron absorbed dose, D', that corresponds to the neutron ef-
fective dose $E = 1$ Sv:

$$D' = (D'_\gamma + D'_n) = E/w_R = 1/w_R \text{Gy}, \quad (9)$$

with the γ-ray and the neutron components:
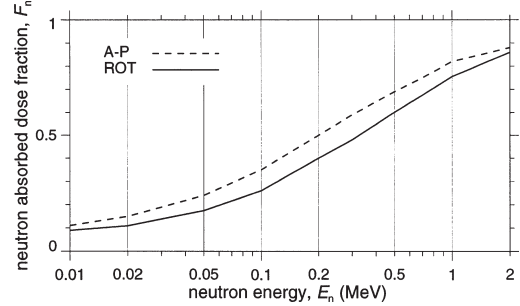
FIG. 2. The fraction, F_n, of the organ-weighted absorbed dose due to
neutrons as a function of neutron energy, E_n (*13*). A-P, anterior–posterior;
ROT, rotationally symmetrical.

$$D'_\gamma = (1 - F_n)/w_R \text{Gy}, \quad D'_n = F_n/w_R \text{Gy}.$$

The radiation weighting factor, w_R, for neutrons has been
specified in terms of a step function in neutron energy, E_n,
but ICRP (*6*) has offered a continuous approximation that
is favored in most computations:

$$w_R = 5 + 17 \exp[-\ln(2 E_n)^2/6] \; (E_n \text{ in MeV}). \quad (10)$$

To facilitate comparison to other computations, this depen-
dence (see dashed line in Fig. 3) is considered here, rather
than the step function. As expressed in Eq. (6), w_R is the
weighting factor for the inclusive neutron dose, i.e. for the
mixture of the γ-ray dose component and the genuine neu-
tron dose.

In a second step, the neutron risk coefficient LAR/Gy
from Fig. 1 needs to be applied to the neutron component,
while the risk coefficient, c_γ, for photons is to be applied
to the γ-ray component:

$$\text{LAR/Sv} = [c_\gamma \cdot (1 - F_n) + (\text{LAR/Gy}) \cdot F_n] \cdot w_R. \quad (11)$$

Since the neutron risk estimate, LAR/Gy, is much larger
than the photon risk coefficient, the exact value of c_γ is not
very critical. It is therefore an adequate approximation to
set c_γ equal to the LAR for photons at 1 Gy (see lower
curve in Fig. 1), i.e. the photon risk estimate under the
assumption DDREF = 1. This quantity equals the risk co-
efficient (LAR/Gy) for the neutrons divided by R_1, and con-
sequently Eq. (11) takes the form:

$$\text{LAR/Sv} = (\text{LAR/Gy}) \cdot [(1 - F_n)/R_1 + F_n]/w_R. \quad (12)$$

Dependence of RBE on Neutron Energy

Up to this point, neutron RBE values, R_1, have been con-
sidered that relate to the energy range, about 0.2 MeV to
0.5 MeV, where neutrons have been shown to have highest
efficiency. Dealing with a broader energy range, as in Figs.
2 and 3, one needs to account for the decrease of the RBE
at lower and at higher neutron energies.

Experimental studies provide different absolute values of
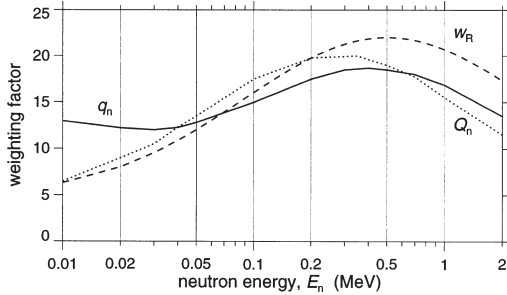
FIG. 3. Radiation weighting factor, w_R (dashed curve) (*6*), the organ-averaged quality factor, q_n (solid curve), and Q_n (dotted curve) (*13*) as a function of neutron energy, E_n.

the neutron RBE. However, the majority of results show a consistent energy dependence with a broad maximum, roughly between the neutron energies 0.2 MeV and 0.5 MeV (*14–16*). The position of the maximum on the energy scale is well explained in terms of microdosimetric data. The essential observation is that neutrons in this energy range tend to release recoil protons just beyond their Bragg peak energies, i.e. protons with maximum LET and with ranges comparable with the cell nucleus.

The general shapes of the dependence of RBE on neutron energy in the assessment of Hall *et al.* (*14*) and also in the chromosome study of Pandita and Geard (*16*) are reasonably well in line with the dependence of the quality factor on neutron energy (dotted line in Fig. 3). However, this dependence relates to the exposure of small objects and is not directly applicable to the neutron exposure of the human body, which is large enough to degrade the neutron spectrum appreciably. The solid line in Fig. 3 gives the shallower curve that results from the organ-weighted integration of the quality factor (*13*); the computations were for an anthropomorphic phantom and for rotational symmetry of the field.[4] The scaled form of this curve, $q' = q_n(E_n)/q_{n,\max}$, is used here as a modifier for R_1 to obtain a plausible neutron energy dependence.

Internal consistency between the quantity effective dose and the operational quantity ambient dose equivalent requires that w_R—since it relates to the mixed γ-ray and neutron dose—be substantially smaller than q_n. Figure 3 shows that this condition is not met. The radiation weighting factor w_R is in fact somewhat larger than q_n at the higher neutron energies, which shows that there is a lack of numerical consistency between the conventions for the radiation weighting factor and the quality factor. This point lies outside the scope of the present study. Nevertheless, in view of the importance of the radiation weighting factor and the quality factor in the current system of radiation protection, the issue is treated briefly in the Appendix.

---

[4] q_n is substantially larger at low energies than Q_n, because it accounts for the protons released due to thermal neutron capture by nitrogen.

Numerical Result

Figure 4 gives the coefficient LAR/Sv that results from Eq. (12) with the above assumption on the neutron RBE. As was the case with Fig. 1, the diagram stands for occupational exposure, i.e. for exposure age 25 to 65. Since the two projection models provide almost the same values [see Table 1 and Eq. (3)], their average is plotted. The solid line indicates the value that results with the assumed value $R_1 = 35$. The gray band represents all values that correspond to the values of R_1 between 20 (lower border) and 50 (upper border).

Neutron risks are an issue predominantly with regard to the exposure of adults, e.g. nuclear workers or other persons who handle or guard nuclear fuel. In normal radiation protection practice, i.e. apart from rare accident situations, the neutron risk estimates LAR/Sv for a population of all ages are of comparatively less importance and, as is the case with risk estimates for photons—they are subject to more uncertainty from risk projection into older age. With the attained-age model, the result for all ages at exposure is essentially the same as the estimate for occupational exposures [see Eqs. (2) and (3)]. However, the age-at-exposure model provides substantially larger values, which expresses the considerably larger risk projection in this model for exposures in childhood. As with Fig. 1, no separate diagram is given for this case, because the values are readily obtained by applying a factor of 1.6.

The diagram in Fig. 4 shows that, under the assumption that $R_1 = 35$, there is little disagreement between the current ICRP nominal risk coefficient and the risk coefficients of neutrons that are derived here. At neutron energies below roughly 0.3 MeV, the present estimates lie below the ICRP solid cancer fatality estimate 0.036/Sv for occupational exposure. Above this energy, they exceed the ICRP estimate somewhat. Neutron energies below 0.5 MeV dominate in the moderated neutron fields encountered in occupational
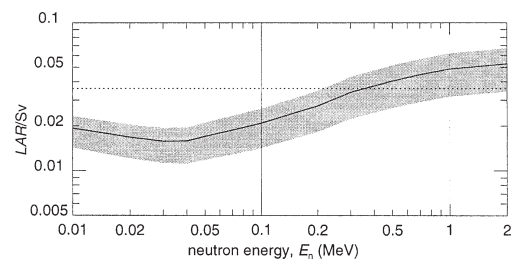
FIG. 4. Lifetime solid cancer mortality risk (LAR/Sv) relative to neutron effective dose for a working population. The values are given in their dependence on neutron energy, E_n. The solid curve results with $R_1 = 35$. The gray band represents the possible values that result for R_1 between 20 and 50. The assumed RBE values between 20 and 50 refer to the energy range 0.2 MeV to 0.5 MeV where the neutrons are most effective; outside this region, the neutron RBE is taken to decrease (see text). The current ICRP nominal risk coefficient for solid cancer mortality (0.036/Sv; working population) is indicated by the dashed line.
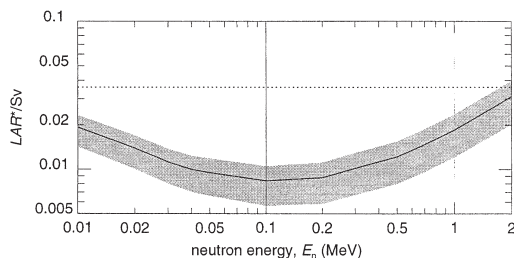
FIG. 5. Lifetime attributable risk (LAR*/Sv), relative to ambient dose equivalent of neutrons (H^*), in its dependence on neutron energy, E_n. The diagram is, apart from the difference between LAR/Sv and LAR*/Sv, analogous to Fig. 4.

radiation protection. In a neutron spectrum outside a transport container for spent nuclear fuel, more than half of the absorbed dose is due to neutrons below energy 0.2 MeV (*17*).

Risk Coefficient Relative to Ambient Dose Equivalent, H^*

The coefficient LAR/Sv specifies the lifetime attributable solid cancer mortality risk from fast neutrons in relation to the basic ICRP reference quantity effective dose, *E*. In radiation protection practice, neutron doses are usually estimated and documented in terms of measurements of the ambient dose equivalent, H^* (*18*), which substitutes as operational quantity for the effective dose. The ratio of H^* to *E* depends on neutron energy and on the directional distribution of the incident radiation, but in most cases—with the major exception of neutron energies in excess of 40 MeV—the ambient dose equivalent overestimates the effective dose. The risk coefficient, LAR*/Sv, relative to unit ambient dose, H^*, is therefore smaller than LAR/Sv in most cases. Results are given in Fig. 5 for a planar rotationally averaged exposure [(*18*), p. 98, Fig. 56)] which is, as stated before, a realistic assumption for occupational settings.

The results lie safely below the ICRP solid cancer mortality risk coefficient of 0.036/Sv. This confirms that the current radiation weighting factor for neutrons ensures adequate protection from neutron exposures.

CONCLUSION

Solid cancer mortality risk estimates for fast neutrons have been derived in the preceding paper (*3*) in terms of ERR and absorbed dose. They were based on the A-bomb data on solid cancer mortality data and on assumed values 20 to 50 of the neutron RBE relative to a reference γ-ray dose of 1 Gy. The comparison of the results to the ICRP nominal risk coefficient requires a conversion to lifetime attributable risk and to effective neutron dose, which has been the objective of the present analysis.

For neutron energies from 0.01 MeV to 2 MeV and for occupational exposure, i.e. for exposure ages 25 to 65, the

resulting risk coefficients are found to be largely in line with the ICRP nominal risk coefficient for solid cancer fatality (0.036/Sv). At neutron energies below 0.3 MeV, they are lower than the ICRP risk factor, which reflects the conservative character of the radiation weighting factor, w_R, at low neutron energies.

At neutron energies in excess of 0.2 MeV, risk estimates for all ages at exposure exceed the ICRP estimate 0.045/Sv for solid cancer mortality. They are larger by a factor of 1.6 than the estimates for occupational exposure, or for all ages at exposure under the attained-age model. The increased values reflect the (still insufficiently ascertained) high lifetime risk projection for childhood exposure, which needs to be substantiated in the continuing follow-up of the youngest cohort of A-bomb survivors. When the attained-age model was first suggested (*19*) as an alternative to the age-at-exposure model, the difference between the two models amounted to a factor of about 2. While the difference in the projection models is about 1.6 [see also ref. (*5*)] in the present analysis, it is bound to diminish further with the continued follow-up.

The neutron risk coefficients and the related question of the appropriateness of the radiation weighting factor for neutrons are of interest predominantly with regard to occupational radiation exposure. The inherent uncertainties in the risk coefficients and their use as a guideline, rather than a precise yardstick, should preclude any fine tuning of w_R in view of slightly changing risk estimates. However, if the radiation weighting factors for neutrons were to be reconsidered and a better agreement with the quality factor were aimed for, a decrease of w_R at low neutron energies may be advisable (see Appendix). Neutron energies above 2 MeV have not been considered here, and—especially for the much higher neutron energies at aviation altitudes—radiobiological data may be insufficient to allow reliable conclusions.

At the neutron energies that have been considered here, there is a considerable level of conservatism in practice, because the operational quantity ambient dose equivalent, H^*, is commonly used as a substitute for effective dose. H^* tends to overestimate *E* for fast neutrons, and this is reflected in the fact that the risk coefficients, LAR*/Sv, relative to H^* are consistently smaller than the ICRP nominal risk coefficient.

The present analysis has been restricted to the neutron risk coefficient for cancer mortality excluding leukemia. Leukemia is assumed to contribute only 10% to the total cancer mortality risk (*5, 6*). Its consideration would therefore be unlikely to change the overall conclusion. In addition, animal studies tend to suggest values of the neutron RBE that are lower, at a specified dose, than the values determined for solid tumors. It is therefore unlikely that the leukemia risk from neutrons exceeds current assumptions.

It is perhaps surprising that the neutron risk coefficients that are derived here do not substantially exceed the ICRP nominal risk coefficient. They might have been expected to

exceed it, because they are not linked to the nominal risk coefficient for photons and are therefore free of the reduction factor DDREF = 2. They would also be expected to exceed the current estimate, because RBE values for neutrons are considered that relate to a sizable γ-ray dose of 1 Gy, but are nevertheless fairly high (R_1 = 20 to 50). A partial explanation lies in the explicit accounting, in the preceding paper (*3*), for the contribution of neutrons to the effects observed at an intermediate dose in Hiroshima and Nagasaki. Any increased attribution to neutrons decreases, as had been pointed out earlier (*20*), the attribution to γ rays, i.e. the γ-ray risk estimate. An increased neutron RBE is therefore less than proportionally reflected in the increased neutron risk estimate. The second and even more important reason is the numerical adjustment for the fact that the effective dose, *E*, from a neutron exposure includes the substantial γ-ray component that is generated by neutrons in the human body. This particularity of the ICRP definition of effective dose makes the implied weighting factor for the genuine neutron dose substantially larger than the radiation weighting factor w_R (see the Appendix).

The neutron risk coefficient has been derived here in a way that uncouples it from the debatable issue of the dose and dose-rate effectiveness factor (DDREF) for photons. The absolute value of the risk coefficient for neutrons is, in this sense, more fundamental than the radiation weighting factor, which represents the ratio of the two risk coefficients.

APPENDIX

Relationship between w_R and the Quality Factor

All dose-equivalent quantities were defined in terms of the quality factor, $Q(L)$, until ICRP 60 (*6*) changed this by introducing the radiation weighting factor, w_R, into a new definition of the organ equivalent dose and the effective dose. The quality factor is retained in the definition of the operational quantities ambient dose equivalent and personal dose equivalent (*21*). The operational quantities are used to verify compliance with the limits for effective dose. In view of this interrelationship, the numerical conventions for w_R and $Q(L)$ are expected to be coherent, but this is currently not the case.

The Implied Radiation Weighting Factor for the Genuine Neutron Dose

w_R is the radiation weighting factor for the inclusive neutron dose, which consists of the genuine neutron dose and the γ-ray dose from neutron interactions in the body. If considered separately, the γ-ray dose needs to be assigned the weighting factor unity and the genuine neutron dose needs to be assigned a weighting factor ω_R that must be chosen so that w_R results for the mixed field.

Using the definition of the neutron fraction F_n [see Eq. (8)], one can rewrite Eq. (6) as a sum of the γ-ray component of the effective neutron dose, which equals D'_γ, and the remaining term that represents the effective dose from the genuine neutron component alone:

$$E = D'_\gamma + (w_R - 1)D'_\gamma + w_R D'_n \qquad (A1)$$
$$= D'_\gamma + [(w_R - 1)/F_n + 1]D'_n.$$

This provides the weighting factor for the genuine neutron dose that is implied in the ICRP definition of the neutron effective dose:

$$\omega_R = (w_R - 1)/F_n + 1. \qquad (A2)$$
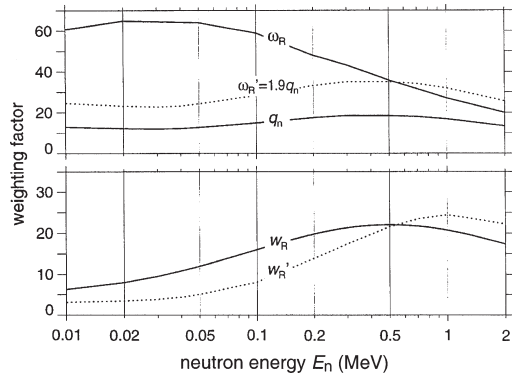
FIG. A1. Upper panel: The implied radiation weighting factor ω_R and the effective quality factor q_n (solid curves) in their dependence on neutron energy, E_n. The dotted curve represents an implied weighting factor ω'_R that corresponds to the potential modification w'_R in the lower panel (dotted line); numerically it equals $1.9 \cdot q_n$. Lower panel: The radiation weighting factor, w_R, for neutrons (solid line) and the modified radiation weighting factor w'_R that would correspond to the dotted line in the upper panel.

The implied weighting factor, ω_R, is represented in the upper panel of Fig. A1 by the upper solid line. It is the parameter that needs to be compared to neutron RBEs observed in experimental studies. ω_R is substantially larger than w_R for neutron energies below 1 MeV, which confirms that w_R—being a weighting factor for a mixed γ and neutron radiation—must not be seen as an RBE value for neutrons. ICRP has emphasized this point consistently, but in the absence of numerical quantification, it may not have been sufficiently appreciated.

The values of the implied weighting factor, ω_R, lie roughly between 50 and 25 in the most effective energy range (0.2 MeV to 1 MeV) of the incident neutrons. This happens to be in fair agreement with the values between 50 to 20 of R_1 that have been assumed in the present analysis on the basis of experiments on tumor induction in rats and in mice with fission neutrons. The further increase of ω_R with decreasing neutron energy makes no sense. It is an artifact of the numerical convention for w_R.

Numerical Interrelationships

The effective quality factor q_n, as given in Fig. 3, is included in the upper panel of Fig. A1 as the lower solid line. It corresponds to the ICRP convention for the quality factor, $Q(L)$ (*6*). If ICRP had chosen the values of the radiation weighting factor w_R for neutrons to be coherent (for rotational symmetry of the neutron field) with the quality factor, then ω_R would have to be equal to q_n. This is clearly not the case; w_R gives considerably more weight to the neutrons than the quality factor would if it were applied to the genuine neutron dose.

The lack of coherence between w_R and $Q(L)$ is currently compensated by another inconsistency: The application of the quality factor is essentially restricted to its use in the ambient dose equivalent, H^*, and the personal dose equivalent, H_p (*10*), and these two quantities refer to a depth in the ICRU sphere or in the body of 10 mm (*21*), which is so shallow that it corresponds to an absorbed dose from the neutron exposure that is considerably larger than the organ-averaged absorbed dose. The low value of the quality factor is thus more than offset by the poor selection of the reference depth, and, accordingly, the ambient neutron dose overestimates the effective neutron dose (*18*) at neutron energies between 0.1 MeV and 1 MeV.

In the present paper, the neutron RBE has been approximated by the effective quality factor, q_n, rescaled to reach a maximum value R_1 between

20 and 50. The resulting function $R_1 q'$ is inserted with $R_1 = 35$ into the upper panel of Fig. A1 as a dotted line; numerically this curve equals $1.9 \cdot q_n$.

If one intended to give the radiation weighting factor w_R a more meaningful energy dependence w'_R, one might define it so that the corresponding values ω'_R equal $1.9 \; q_n$, i.e. so that they coincide with the dotted line in the upper panel of Fig. A1. The dotted curve in the lower panel of Fig. A1 gives this modified radiation weighting factor ω'_R. The comparison to the current convention for w_R (solid line) shows that the difference is not large at neutron energies around 0.2 to 2 MeV. For the usual broad energy spectra of neutrons, the differences would tend to cancel in this energy range. At lower energies, the modified convention would decrease the radiation weighting factor considerably.

Analogous considerations would be required to make the quality factor consistent with the radiation weighting factor. But the issue would necessitate a modification of the quantities ambient dose equivalent and personal dose equivalent.

REFERENCES

1. United Nations Scientific Committee on the Effects of Atomic Radiation, *Sources and Effects of Ionizing Radiation, Annex F, Influence of Dose and Dose Rate on Stochastic Effects of Radiation*, pp. 619–687. United Nations, New York, 1993.

2. W. K. Sinclair, Fifty years of neutrons in biology and medicine: The comparative effects of neutrons on biological systems. In *Proceedings of the 8th Symposium on Microdosimetry* (H. G. Ebert, Ed.), p. 1. Report EUR 8395, Commission of the European Communities, Brussels, 1982.

3. A. M. Kellerer and L. Walsh, Risk estimation for fast neutrons with regard to solid cancer. *Radiat. Res.* **156**, 708–717 (2001).

4. D. L. Preston, J. H. Lubin and D. A. Pierce, *Epicure User's Guide.* HiroSoft International Corp., Seattle, 1993.

5. United Nations Scientific Committee on the Effects of Atomic Radiation, *Sources and Effects of Ionizing Radiation, Vol. 2, Annex I,* *Epidemiological Evaluation of Radiation-Induced Cancer*, pp. 297–450. United Nations, New York, 2000.

6. ICRP, *The 1990 Recommendations of the International Commission on Radiological Protection.* Publication 60, *Annals of the ICRP*, Vol. 21, No. 1–3, Pergamon Press, Oxford, 1991.

7. ICRP, *Risks Associated with Ionising Radiations. Annals of the ICRP,* Vol. 22, No. 1, Pergamon Press, Oxford, 1991.

8. A. M. Kellerer, E. A. Nekolla and L. Walsh, On the conversion of solid cancer excess relative risk into lifetime attributable risk. *Radiat. Environ. Biophys.* **40**, 249–257 (2001).

9. M. Vaeth and D. A. Pierce, Calculating lifetime risk in relative risk models. *Environ. Health Perspect.* **87**, 83–94 (1990).

10. A. M. Kellerer, L. Walsh and E. A. Nekolla, Risk coefficient for γ-rays with regard to solid cancer. *Radiat. Environ. Biophys.,* in press.

11. G. Dietze and B. R. Siebert, Photon and neutron dose contributions and mean quality factors in phantoms of different size irradiated by monoenergetic neutrons. *Radiat. Res.* **140**, 130–133 (1994).

12. W. C. Roesch, Ed., *US–Japan Joint Reassessment of Atomic Bomb Radiation Dosimetry in Hiroshima and Nagasaki*, Vols. 1 and 2. Radiation Effects Research Foundation, Hiroshima, 1987.

13. G. Leuthold, V. Mares and H. Schraube, *Monte-Carlo Calculations of Dose Equivalent for Neutrons in Anthropomorphic Phantoms using the ICRP 60 and Stopping Power Data of ICRU 49.* GSF–German National Research Center for Environment and Health, Technical Report 20/2001, 2001.

14. E. J. Hall, J. K. Novak, A. M. Kellerer, H. H. Rossi, S. Marino and L. J. Goodman, RBE as a function of neutron energy. *Radiat. Res.* **64**, 245–255 (1975).

15. ICRU, *The Quality Factor in Radiation Protection.* Report 40, International Commission on Radiation Units and Measurements, Bethesda, MD, 1986.

16. T. J. Pandita and C. R. Geard, Chromosome aberrations in human fibroblasts induced by monoenergetic neutrons. *Radiat. Res.* **145**, 730–739 (1996).

17. German Commission on Radiation Protection (Strahlenschutzkommission), *Berechnungsgrundlage für die Ermittlung von Körperdosen bei äußerer Strahlenexposition,* Veröffentlichungen der Strahlenschutzkommission Band 43, Urban und Fischer, München, 2000.

18. ICRP, *Conversion Coefficients for Use in Radiological Protection against External Radiation. Annals of the ICRP*, Vol. 26, No. 3/4, International Commission on Radiological Protection, Pergamon Press, Oxford, 1996.

19. A. M. Kellerer and D. Barclay, Age dependences in the modelling of radiation carcinogenesis. *Radiat. Prot. Dosim.* **41**, 273–281 (1992).

20. A. M. Kellerer and E. Nekolla, Neutron versus γ-ray risk estimates. Inferences from the cancer incidence and mortality data in Hiroshima. *Radiat. Environ. Biophys.* **36**, 73–83 (1997).

21. ICRU, *Quantities and Units in Radiation Protection Dosimetry.* Report 51, International Commission on Radiation Units and Measurements, Bethesda, MD, 1993.

4. Kellerer AM, Walsh L & Nekolla EA. Risk coefficient for γ-rays with regard to solid cancer. Radiat. Environ. Biophys. 41, 113-123, 2002

ORIGINAL PAPER

Albrecht M. Kellerer · Linda Walsh · Elke A. Nekolla

Risk coefficient for γ-rays with regard to solid cancer

Abstract A previous investigation has uncoupled the solid cancer risk coefficient for neutrons from the low dose estimates of the relative biological effectiveness (RBE) of neutrons and the photon risk coefficient, and has related it to two more tangible quantities, the excess relative risk (ERR_1) due to an intermediate reference dose D_1=1 Gy of γ-rays and the RBE of neutrons, R_1, against this reference dose. With tentatively assumed RBE values between 20 and 50 and in terms of organ-averaged doses – rather than the usually invoked colon doses – the neutron risk factor was seen to be in general agreement with the current risk estimate of the International Commission on Radiation Protection (ICRP). The present assessment of the risk coefficient for γ-rays incorporates – in terms of the unchanged A-bomb dosimetry system, DS86 – this treatment of the neutrons, but is otherwise largely analogous to the evaluation of the A-bomb data for the ICRP report and for the recent report of the United Nations Scientific Committee on the effects of ionizing radiation, UNSCEAR. The resulting central estimate of the lifetime attributable risk (*LAR*) for solid cancer mortality is 0.043/Gy for a working population (ages 25–65),and is nearly the same whether the age at exposure or the attained age model is used for risk projection. For a population of all ages 0.042/Gy is obtained with the attained age model and 0.068/Gy with the age at exposure model. The values do not include a *dose and dose rate effectiveness factor* (*DDREF*), and they are only half as large as the new UNSCEAR estimates of 0.082/Gy (attained age model and all ages) and 0.13/Gy (age at exposure model and all ages). The difference is only partly due to the more explicit treatment of the neutrons. It reflects also the fact that UNSCEAR has converted *ERR* into *LAR* in a way that differs from the ICRP procedure, and that it has summed the overall risk coefficient for solid tumor mortality and incidence from separate estimates for eight solid tumor categories, whereas the present study employs a combined computation for all solid tumors and uses the ICRP procedure for the conversion of *ERR* into *LAR*. The appendix gives results for the solid cancer incidence data.

Introduction

The most recent report [1] of the United Nations Scientific Committee on the effects of ionizing radiation (UNSCEAR) contains, in Annex I, an informative and complete reanalysis of the cancer mortality and incidence data of the A-bomb survivors. Its updated set of risk estimates for sparsely ionizing radiation is going to be widely used in considerations of radiation protection regulations. The present paper deals with a number of aspects that need not change the basic conclusions or alter the risk estimates greatly, but might nevertheless be part of a continued discussion toward their further improvement.

A still unresolved issue is the proper accounting for neutrons in the analysis of the A-bomb data. On the basis of the earlier dosimetry system, *TD65*, for the A-bomb survivors [2] it had been surmised [3, 4] that neutrons were responsible for a substantial fraction of the late health effects observed at Hiroshima. This assumption was abandoned when the current dosimetry system, *DS86*, specified considerably lower neutron doses in Hiroshima [5]. It was then concluded – against some dissenting arguments [6] – that the neutrons are, even in Hiroshima a minor potential contributor to the observed health effects, and that their role, although uncertain, is not critical to risk estimation. In subsequent analyses the neutrons were, therefore, accounted for crudely by a weighting factor 10 applied to their absorbed dose con-

A.M. Kellerer (✉)
Radiobiological Institute, University of Munich,
Schillerstrasse 42, 80336 Munich, Germany
e-mail: AMK.SBI@LRZ.Uni-Muenchen.de
Tel.: +49-89-5996818, Fax: +49-89-5996840

Institute of Radiobiology
GSF – National Research Center for Environment and Health,
Neuherberg, Germany

L. Walsh · E.A. Nekolla
Radiobiological Institute, University of Munich, Germany

tribution [7, 8]. The sum of the γ-ray absorbed dose and the weighted neutron dose was termed *weighted dose* and was expressed in terms of Sv. This approach was used in the computations that provided the current nominal risk coefficient for photon radiation [9, 10] and it has been equally employed for the new evaluation by UNSCEAR [1].

In contrast to the prevailing assumption, there is evidence that even under the current dosimetry system, DS86, the neutrons have contributed a substantial fraction of the late health effects among the A-bomb survivors [11, 12, 13]. An explicit accounting for the neutrons is thus required in the assessment of the γ-ray risk coefficient, and it will be based here on the unchanged dosimetry system DS86. Various conclusions in a previous article [12] can be referred to without being repeated in detail. These include the considerations on neutron RBE from experimental studies [14, 15, 16, 17] and the relevant dosimetric aspects.

A critical point with major impact on the present computations is the specification of the organ dose that is used in the analysis of the combined data for all solid cancers. In previous studies of the mortality or incidence of all solid cancers combined, reference has been made to the colon dose, i.e. the dose to the deepest lying, most highly shielded organ. This is, of course, an underestimation of the average dose to all relevant organs. For the γ-rays the underestimation is not very critical, because the suitably weighted average organ dose is only somewhat less than 10% larger than the colon dose. However, for neutrons the reference to the colon is unsatisfactory. The averaging – with weighting factors proportional to the risk contribution of individual tumor sites (see [12]) – results in a neutron absorbed dose that is twice as large as the neutron absorbed dose to the colon. As has been done in the preceding article [12], the subsequent considerations will accordingly employ the *organ-averaged dose* that exceeds the colon doses by the factors 1.1 for γ-rays and 2.1 for neutrons.

The present analysis makes use of the same data as UNSCEAR [1], the solid cancer mortality (1950–1990) and incidence data (1958–1987) published by the Radiation Research Effects Foundation (RERF). It is not primarily aimed at the derivation of somewhat modified risk coefficients, but focuses instead on the exploration of certain changes in the modeling calculations that can be employed in future analyses of data from the continued follow-up and results from the current dosimetry revision.

Pierce and Preston [18] have published a first evaluation in terms of extended incidence data (1958–1994) and also in terms of more narrow dose categories. Their work includes a realistic treatment of the neutron RBE in an approach that is employed in the present paper with some modifications. To facilitate the comparison, a notation is used here that parallels largely the notation adopted by Pierce and Preston.

Pierce and Preston also addressed the current reassessment of the dosimetry system, DS86. While DS86 appears to be well supported at intermediate doses of 1 Gy–2 Gy, it is still possible that – apart from a moderate revision of the γ-ray doses – the neutron doses will need to be somewhat increased for Hiroshima at lower total doses [13]. The subsequent analysis utilizes the unchanged DS86.

The conventional treatment

Realistic modeling of the dose-effect dependence for a mixed field of γ-rays and neutrons must account for the fact that the RBE of neutrons tends to increase with decreasing dose. As long as it was presumed that neutrons contributed little to the excess cancer rates among the A-bomb survivors, it seemed acceptable to disregard this dependence and to account for the neutrons roughly in terms of a constant weight factor, $w=10$, applied to their absorbed dose contribution in the colon. This approach postulates *a priori* a linear dose dependence both for γ-rays and neutrons, an assumption that is at variance with a wide range of radiobiological observations. While the subsequent modeling will utilize a more explicit treatment, computations according to the conventional treatment will be included to facilitate the comparison to previous risk calculations and, especially, the most recent UNSCEAR results.

The excess relative risk is factorized into a dependence on dose, d, and a modifying function, μ, that depends on the variables gender, s, age at exposure, e, or age attained, a:

$$ERR(d,s,e,a) = \mu(s,e,a) \cdot \rho(d) \tag{1}$$

where d is the "weighted dose" defined in terms of the γ-ray absorbed dose, D_γ, and the neutron absorbed dose, D_n:

$$d = D_\gamma + w \cdot D_n$$

The dose dependence $\rho(d)$ has usually been taken to be linear for solid cancers combined, and linear-quadratic for leukemias. The present computations employ the more general linear-quadratic fit in terms of weighted dose:

$$\rho(d) = \alpha \cdot (d + \theta \cdot d^2) \tag{2}$$

This is irrelevant for the maximum likelihood results, because they happen to be close to linear dose dependencies, but it is essential because it permits the derivation of the lowest initial slope, i.e. the minimum risk estimate that is compatible with the data in terms of a linear-quadratic dose dependence. Knowledge of this minimum value is necessary for an assessment of the *dose and dose rate effectiveness factor* (*DDREF*) that has been postulated by ICRP [9].

If the fitted data extend to large doses (say >2 Gy), it is common to include an added negative exponential term that accounts for the "bending over", i.e. the re-

duced slope of the dose dependence at higher doses. In the subsequent modeling a low dose cut-off of 2 Gy total absorbed dose will be chosen, and there will, accordingly be no need to include the negative exponential term, nor will there be a need to apply the corrections for random errors in dosimetry [19, 20].

A modified approach

The linear, linear-quadratic dose dependence

The explicit treatment employs, as has been done before [11, 18], a linear-quadratic dose dependence for the γ-ray dose, D_γ, and a linear relation for the neutron dose, D_n:

$$ERR\left(D_\gamma, D_n, s, e, a\right) = \mu(s, e, a) \cdot \rho\left(D_\gamma, D_n\right) \quad (3)$$

with the dose dependent term:

$$\rho\left(D_\gamma, D_n\right) = \alpha \cdot \left(D_\gamma + \lambda \cdot D_n + \theta \cdot D_\gamma^2\right) \quad (4)$$

As pointed out in previous analyses [7, 8, 11, 18], it is impossible to infer from a fit to the solid cancer or the leukemia data both parameters, α, the linear dose coefficient for γ-rays, and λ, the low dose limit of the neutron RBE. A wide range of values of the limiting RBE of neutrons at low doses, $\lambda = RBE_{max}$, fits the data equally well.

Extraneous information is therefore required, and to this purpose reference has usually been made to the maximum RBE of neutrons. This value, $\lambda = RBE_{max}$, is inferred by extrapolating RBE values from cell or animal studies to *low doses*. To avoid the uncertainty inherent in extrapolating to a limit at low doses, the previous article [12] invoked the neutron RBE, R_1, against an intermediate *reference γ-ray dose*, $D_1 = 1$ Gy, rather than the less tangible RBE_{max}.

The risk coefficient, $\alpha \cdot \lambda$, for neutrons that has been deduced in this way [12] could, in principle, be inserted into Eq.(4) to eliminate λ. However, the treatment is more coherent and transparent, if the tentatively assumed value R_1 of the neutron RBE against the γ-ray dose D_1 is introduced directly into Eq.(4). For this purpose R_1 needs to be expressed in terms of the parameters of Eq.(4).

Equation (4) determines the relationship between the neutron and γ-doses that have equal effect:

$$\lambda \cdot D_n = D_\gamma + \theta \cdot D_\gamma^2 \quad (5)$$

which provides the neutron *RBE* as a function of the γ-ray dose:

$$RBE = D_\gamma / D_n = \lambda / \left(1 + \theta \cdot D_\gamma\right)$$
and :
$$\lambda = R_1 \cdot \left(1 + \theta \cdot D_1\right) \quad (6)$$

Therefore, Eq.(4) takes the form:

$$\rho\left(D_\gamma, D_n\right) = \alpha \cdot \left(D_\gamma + R_1 \cdot \left(1 + \theta \cdot D_1\right) \cdot D_n + \theta \cdot D_\gamma^2\right) \quad (7)$$

The choice of R_1

As pointed out, the linear-quadratic dose dependence for γ-rays needs to be considered in order to gain information on the maximum curvature in the dose dependence that is still compatible with the data. However, the RERF solid cancer data exhibit – in contrast to the leukemia data – a seemingly linear dependence on dose, and this makes it difficult to appreciate the difference between using RBE_{max} or R_1. If linearity is accepted both for neutrons and γ-rays, RBE_{max} and R_1 are indeed equal. But it is evident that the case for or against linearity must not be made in terms of a treatment that postulates *a priori* that the γ-ray dose dependence is linear. The two parameters RBE_{max} and R_1 must, therefore, be distinguished even if the ultimate result suggests that their values do not differ appreciably.

Reference to R_1, i.e. the neutron RBE at intermediate doses – instead of the more elusive limit value RBE_{max} – reduces the systematic uncertainty that is inherent in the choice of a parameter to represent the relative effectiveness of neutrons in causing late effects in man. But uncertainty remains, because animal data on rodents vary considerably and need not be representative for man. A large series of experiments on male Sprague-Dawley rats with fission neutrons provides, both for non-lethal and for lethal tumors, values of R_1 close to 50 [14, 15]. Extensive experiments on mice where life shortening was used as a proxy for tumor induction [16, 17] have suggested lower values, but rather complex dependencies on γ-ray dose-rates. In view of the wide range of experimental results [21, 22], any assumption of a plausible range of values remains judgmental. Roughly in line with the recommendation of a joint task group of ICRP and ICRU [23] and as in the previous article on neutron risks [12], the high and low values 50 and 20 are considered for R_1, and $R_1 = 35$ is taken as a central reference value. The values R_1 that are assumed here may appear to be large in comparison to the ICRP radiation weighting factor w_R of about 20 for fission neutrons. However, it must be noted that w_R does not stand for the RBE of a pure neutron dose, but for the substantially lower RBE of the mixed neutron and γ-ray dose that is caused by an external neutron field in the human body [24]. In contrast, R_1 is the weighting factor that relates to the true neutron component of the dose. All resulting risk coefficients are reported for the different values of R_1. This permits an approximate judgment, even if values of R_1 outside the range 20–50 are considered.

Choosing two nearly orthogonal parameters

Both parameters α and θ in Eq.(7) are subject to considerable statistical error. The uncertainty in the initial slope of the dose relation, i.e. the error of α, is of particular interest. However, the second parameter, θ, is strongly (negatively) correlated with α. Its error specifies, therefore, essentially the same uncertainty and thus

provides no additional information. Rescaling θ to a parameter that is roughly "orthogonal" to α is, therefore, more informative. A suitable parameter[1], subject to considerably smaller error than either α or θ, is the effect level at an intermediate acute γ-ray dose, D_1, divided by this dose:

$$c = \rho\,(D_1, 0) = \alpha \cdot (1 + \theta \cdot D_1) \tag{8}$$

where c is the slope through the point D_1 on the dose relation for γ-rays; it will here be called the *reference* (γ-*ray*) *slope*. The effect at the intermediate γ-ray dose D_1 is reliably determined by the epidemiological observations. The reference slope c is, accordingly, a meaningful parameter; in fact, it is essentially equal to the slope of the dose dependence in a linear model.
With:

$$\theta = \frac{c/\alpha - 1}{D_1} \tag{9}$$

Equation (7) takes the form:

$$\rho\,(D_\gamma, D_n) = \alpha \cdot (D_\gamma - D_\gamma^2/D_1) + c \cdot (R_1 \cdot D_n + D_\gamma^2/D_1) \tag{10}$$

As explained in the preceding article, D_1=1 Gy is – in computations with the solid cancer data – a suitable choice for the intermediate γ-ray dose. Equation (10) reduces then (written as a value equation with unit Gy) to the form that is actually used in the computations:

$$\rho\,(D_\gamma, D_n) = \alpha \cdot (D_\gamma - D_\gamma^2) + c \cdot (R_1 \cdot D_n + D_\gamma^2) \tag{11}$$

Specifics of the modeling computations

Numerical values of the maximum likelihood fit parameters for the *ERR* models were obtained using the AMFIT routine in the EPICURE software [25]. In line with the approach for the RERF solid cancer mortality report [7] and the computations for UNSCEAR [1], the background rates were not modeled in parametric form, but were stratified by gender and by 5-year intervals of both attained age and age at exposure.

The modifying factor [see Eq.(1)] has been modeled either in terms of the *attained age model* [26, 27] or in terms of the traditionally applied *age at exposure model* which postulates an *ERR* that does not decrease in time after exposure. The use of these two comparatively simple models parallels the approach in the UNSCEAR report [1] and makes it unnecessary to invoke more complicated intermediate models. The results conveniently bracket the likely true values.
The modifying functions for the two models are:

$$\mu(s,a) = \exp\left(-g \cdot (a - 60)\right) \cdot$$
$$(1 \pm s) \ (+ \text{ for females}, \ - \text{ for males}) \tag{12}$$

---

[1] The notation θ and λ is adopted from Pierce and Preston [18]. The choice of the familiar symbol α (rather than β) for the initial slope with regard to γ-rays is the same as in the preceding article [12], so is the notation c for the reference slope c.

$$\mu(s,e) = \exp\left(-g \cdot (e - 30)\right) \cdot$$
$$(1 \pm s) \ (+ \text{ for females}, \ - \text{ for males}) \tag{13}$$

UNSCEAR [1] uses a power function for the attained age model instead of the exponential dependence:

$$\mu(s,a) = \left(a/60\right)^{-1.5} \cdot (1 \pm s) \tag{14}$$

The power function leads to very high *ERR* values at young ages and makes the computations rather dependent on the assumed latent period. In the absence of epidemiological evidence that favors Eq.(14) over Eq.(12), the somewhat more moderate exponential attained age modifier that has been used originally with the attained age model [26], is retained here.

The dose dependent term, $\rho(D_\gamma, D_n)$, in Eq.(4) equals the excess relative risk scaled to the reference attained age 60 in the attained age model [Eqs.(12) and (14)] or scaled to the reference age at exposure 30 in the age at exposure model [Eq.(13)]. It is also scaled to the average of the genders. The gender averaged relative risks, $\rho(D_\gamma, D_n)$, are – in agreement with the familiar notation [7, 8] – denoted by ERR_{60} and ERR_{30}. Other reference ages have actually been employed by RERF and by UNSCEAR, but here all results are rescaled to a=60 and e=30.

Numerical results in terms of *ERR*

Comparison to earlier linear estimates

To verify that the present computations are – apart from the more explicit treatment of the neutrons – in line with the earlier assessments, the results from RERF [7, 8] and UNSCEAR [1] are first compared in Table 1 with the coefficients that are obtained in the present analysis through the conventional approach, i.e. with a simple linear fit in weighted colon dose (w=10). The terms ERR_{60}/Gy and ERR_{30}/Gy stand for the dose coefficient (parameter α in the subsequent Table 2), and refer to the attained age and age at exposure model, respectively. All values in the table are derived from the same data sets, the RERF solid cancer mortality (1950–1990) and incidence data (1958–1987) and, being derived by the same computational procedure, they are very nearly equal. The slight differences reflect the choice of a relatively low dose cut-off (2 Gy) in the present computations. A further particularity is that parametric modeling of the background rates has been used by RERF in the computation of the ERR_{30} for the incidence data [8].

Results of the explicit treatment

The results of the explicit modeling computations are given in Table 2 for the solid cancer mortality data. Analogous results for the solid tumor incidence are given in terms of diagrams in the appendix. The numerical

Table 1 Comparison of dose coefficients obtained through the conventional approach, i.e. with a linear model in weighted ($w=10$) colon dose. ERR_{60} refers to the attained age model, ERR_{30} to the age at exposure model. The present results are obtained with a dose cut-off 2 Gy. RERF [7, 8] and UNSCEAR [1] employed a larger cut-off. All results, except the ERR_{30} for solid cancer incidence were derived with stratified background rates

Source	Solid cancer mortality		Solid cancer incidence	
	ERR_{60}/Gy	ERR_{30}/Gy	ERR_{60}/Gy	ERR_{30}/Gy
RERF	–	0.57	–	0.58
UNSCEAR 2000	0.48	0.57	0.57	0.59
Present analysis, conventional approach	0.50	0.53	0.57	0.58

Table 2 Results of the maximum likelihood fits to the solid cancer mortality data. The estimated parameters relate to acute γ-irradiation. α is the initial slope (ERR_{60}/D_γ for the attained age model, ERR_{30}/D_γ for the age at exposure model), c is the slope to ERR_{60} or ERR_{30} due to 1 Gy γ-rays; it corresponds closely to the dose coefficient in a linear dose model. The 95% confidence limits are given in brackets. c/α_{min} (=$1+\theta_{max}$) is the largest DDREF consistent with the data on the 95% confidence level, g and s are the age and the gender modifiers [see Eqs.(12) and (13)]

Solid cancer mortality 1950–1990 (df=13,201)

	α (Gy^{-1})	c (Gy^{-1})	c/α_{min}	g	s	deviance
Attained age model						
w=10	0.40 (0.11–0.69)	0.50 (0.36–0.64)	4.7	0.0254	0.339	6642.6
R_1=20	0.34 (0.06–0.62)	0.41 (0.29–0.52)	6.4	0.0252	0.339	6642.0
R_1=35	0.31 (0.04–0.59)	0.36 (0.26–0.46)	8.7	0.0250	0.340	6641.6
R_1=50	0.29 (0.02–0.56)	0.32 (0.23–0.41)	14.3	0.0249	0.341	6641.4
Age at exposure model						
w=10	0.48 (0.18–0.78)	0.53 (0.39–0.68)	2.9	0.0403	0.335	6633.1
R_1=20	0.42 (0.14–0.71)	0.43 (0.31–0.55)	3.2	0.0397	0.333	6632.4
R_1=35	0.40 (0.11–0.68)	0.38 (0.28–0.49)	3.4	0.0392	0.333	6632.1
R_1=50	0.37 (0.09–0.65)	0.34 (0.25–0.44)	3.7	0.0387	0.333	6631.9

values are specified here to more digits than is warranted by their statistical uncertainty; this is done to make the computational details traceable and to facilitate the comparison to the earlier analyses that are based on the same input data.

The rows labeled w=10 give the results obtained with the linear-quadratic dose model, but with the conventional approach in terms of weighted dose to the colon [see Eq.(2)]. These results are included to highlight the difference to the present computation with the change from colon to organ-averaged dose and the more explicit treatment of the neutrons.

The *reference slope*, c, corresponds closely to the γ-ray dose coefficient in a linear dose model. The estimate, α, of the initial slope of the dose dependence for the γ-rays differs to varying degrees from c, but the difference is never significant. Linearity can, therefore, be accepted and the parameter c with its smaller uncertainty (95% confidence interval ±28%) serves then as a better estimate of the dose coefficient than the coefficient α with its larger uncertainty (average 95% confidence interval ±80%). The parameter, c, is also suitable for a comparison to the risk estimates of RERF [7, 8] and UNSCEAR [1] which have been based on linear dose models.

With R_1=35, the value c=ERR_{60}/Gy=0.36 (attained age model) or c=ERR_{30}/Gy=0.38 (age at exposure

model) is obtained. The value of c decreases, of course, with increasing R_1, i.e. with higher effect attribution to the neutrons. However, the results are not highly sensitive to the assumed value of R_1.

Implications on *DDREF*

While c is the main reference parameter, the parameter values α are informative because their general consistency with c confirms the agreement of the data with linearity in γ-ray dose. The fairly large confidence intervals of α indicate, on the other hand, that the true value of the initial slope might deviate considerably from the best estimate.

The apparent linearity in γ-ray dose is, of course, at variance with the majority of dose-effect relations obtained for γ-rays in experimental radiobiology. These relations tend to be curvilinear, with ratios c/α (=$1+\theta$) substantially larger than unity. ICRP has, in view of the conflict between the epidemiological data and the general radiobiological evidence, adopted the *dose and dose rate effectiveness factor*, *DDREF*=2. This factor was taken to be a ratio of the apparent slope to the initial slope that would still be consistent with the epidemiological data. For leukemia the choice of a *DDREF* was natural because the RERF data for leukemia are actually sugges-
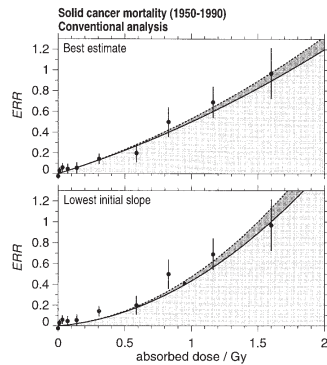
Fig. 1 Dose dependencies for solid cancer mortality inferred from the A-bomb survivors data in terms of the *attained age model* against total absorbed dose to the colon. The data points (with standard errors) represent the ERR_{60} for separate dose categories. The curves result from the *conventional analysis* in terms of a constant neutron *RBE*=10. The *dotted curves* represent the best fits to the data points. The *solid curves* represent the effect attributed to the γ-rays, the dark shaded areas represent the effect attributed to the neutrons. *Upper panel*: maximum likelihood fits. *Lower panel*: best fits with the minimum value of the initial slope, α, consistent with the data on the 95% confidence level (see Table 1)

Fig. 2 Dose dependencies for solid cancer mortality inferred from the A-bomb survivors data in terms of the *attained age model* against total organ-averaged absorbed dose. The data points (with standard errors) represent the ERR_{60} for separate dose categories. The curves result from modeling computations with *explicit treatment of the neutrons*. The *dotted curves* represent the best fits to the data points. The *solid curves* represent the effect attributable to the γ-rays. In each panel, the results are given for the values R_1=20, 35, and 50 (from top to bottom; the dotted curves coincide for the assumed values of R_1). The dark shaded areas represent the effect attributable to the neutrons (R_1=35). *Upper panel*: maximum likelihood fits. *Lower panel*: best fits with the minimum value of the initial slope, α, consistent with the data on the 95% confidence level (see Table 1)

tive of considerable curvature. For the solid cancers any assumed *DDREF* must be measured against the lowest value c/α_{min} (=1+θ_{max}) that is statistically still consistent with the data. This ratio is, therefore, separately tabulated in column 4 of Table 2.

The results show that substantial values of *DDREF* (=c/α_{min}) are statistically consistent with the solid cancer mortality data. Computations with the published incidence data (1958–1987) indicate a considerably more narrow range of possible values, the maximum admissible value being c/α_{min}=1.7 (see Appendix). Pierce and Preston had already pointed this out in their recent analysis [18] of the new incidence data (1958–1994).

Diagrams of the dose dependencies

Graphic representations of the risk estimates and their uncertainties will be given in the next section in a form that relates also to lifetime attributable risk. Before this issue is dealt with, diagrams are given in Figs. 1 and 2 to illustrate the observed data points (with standard errors) and the inferred dependencies of the *ERR* (cancer mortality) on total absorbed dose. The figures refer to the results obtained with the attained age model, but the dose dependencies for the age at exposure model are very nearly the same. Figure 1 gives results from the conventional analysis (with colon as reference organ and *w*=10). Figure 2 depicts the results from the present treatment, i.e. modeling computations with explicit accounting for neutrons [see Eqs.(3) and (11)]. The solid curves give the

effect contribution due to the γ-rays in terms of the model parameters from Table 2; the dotted curves represent the total effect. The abscissa values are the organ-averaged absorbed doses (including the neutrons). The effect contribution of the neutrons increases more than proportional to total dose, which reflects the fact that the neutron absorbed dose fraction increases with dose. The points (with standard errors) are direct fits to the data in the individual dose bins.

The upper panels of Figs. 1 and 2 give the maximum likelihood results, the lower panels give the dependencies with the lowest value of the initial slope (highest *DDREF*) on the 95% confidence level.

The effect attribution to neutrons is, of course, unrealistically low in the conventional treatment (Fig. 11), since it corresponds to a constant RBE of neutrons of only 10. In fact, in the conventional treatment the weighting factor *w*=10 [Eq.(1)] is applied to the colon, where the neutron contribution is least; this would correspond to using the weighting factor 5 with the organ-averaged dose [12].

In Fig. 2 the results from the explicit treatment are given for the intermediate value R_1=35 and for the high and low values 50 and 20 that are here invoked. The triplets of curves thus indicate the uncertainty in the inferred relation for γ-rays that is due to the choice of the neutron RBE, R_1. They do not represent the statistical uncertainty of the estimates in Table 2. This uncertainty is visualized in the comparison of the upper and lower panels.

The fit to the actual mixed radiation depends so little on the assumed value R_1, that the dotted curves coincide for the assumed values 20, 35, and 50 of R_1. The main purpose of the diagrams is to illustrate the substantial attribution to neutrons (dark shaded areas) in the explicit treatment (Fig. 2) and the fairly low initial slopes that are still consistent with the mortality data in terms of the attained age model.

Numerical results in terms of *LAR*

Risk coefficients are usually expressed in terms of expected numbers of fatalities (or cases) per unit dose.[2] Comparing the present results with such risk coefficients thus requires a conversion of excess relative risk per Gy into lifetime attributable risk per Gy.

As in the preceding paper [12], *lifetime attributable risk*, *LAR*, will be expressed in terms of the excess solid cancer mortality integrated over the survival function of the reference population. While this quantity has earlier been termed *risk of untimely death* (*RUD*) [28], the simpler name *lifetime attributable risk* is used here. This quantity corresponds to the risk coefficients derived earlier by ICRP and – apart from some numerical differences in the derivation of the conversion coefficients – to those more recently presented by UNSCEAR for low doses (0.1 Sv).[3]

The present considerations are restricted to the "transport" of excess relative risk (*ERR*) from the study population – here the A-bomb survivors – to the reference populations. This leads, as seen in the UNSCEAR results, to risk estimates that are roughly 10% higher than in the transport of excess absolute risk (*EAR*).

The computation of *LAR* involves integrating the excess relative risk over the background cancer mortality rates and the survival function of the selected reference population. In their computations for ICRP, Land and Sinclair [10] have invoked the populations US, UK, Japan, China and Puerto Rico and have computed the conversion factor from *ERR* to *LAR* for each of these five populations. They have then used the average of these factors to derive the nominal risk coefficient. While this procedure is to some degree arbitrary, it defines a usable standard that permits exact comparison. For this reason the same approach and the same population data as used for ICRP [9, 10] are employed here. The concepts and computations for deriving the factors for the conversion of *ERR* to *LAR* are described separately [29]. It is here sufficient to list the numerical results (for an assumed latency period of 5 years, and the modifying factors given in Table 1).

---

[2] Reference is made to Gy in the present treatment. This is done to avoid misinterpretations that can arise when computations are performed with different *RBE* values which must not be confused with the *quality* or *radiation weighting factors*.
[3] UNSCEAR uses a somewhat more complicated quantity, *REID*, which equals *LAR* at low doses. Since there is no need for summary risk coefficients relative to high doses, it is sufficient to consider the simpler quantity, *LAR* (for details see [29]).
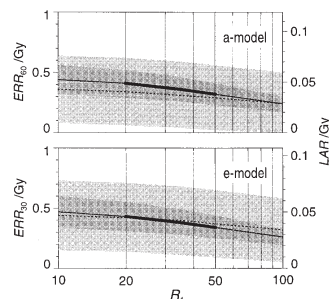
Fig. 3 The solid lines and the dark shaded bands represent – for the two projection models – the parameter *c*, i.e. the *ERR* for solid cancer mortality due to an acute γ-ray dose of 1 Gy and its 95% confidence range. The *broken lines* and the *light shaded bands* give the estimate of the initial slope, α, and its 95% confidence range in a linear-quadratic dose dependence for the γ-rays. The results are given in dependence on the assumed neutron RBE, R_1, vs. an acute γ-ray dose 1 Gy (see Table 2). The right ordinate gives the same quantities expressed in terms of the lifetime attributable risk for solid cancer mortality for a population of working ages. The confidence bands express only the statistical uncertainty in the *ERR*, not the uncertainty of the conversion coefficient *LAR/ERR*

Averaged over all ages one obtains:

$$LAR/ERR_{60} = 0.116 \quad \text{(attained age model)}$$
$$LAR/ERR_{30} = 0.178 \quad \text{(age at exposure model)} \tag{15}$$

If the power function [Eq.(14) instead of Eq.(12)] is used in the age attained model a somewhat larger conversion factor is obtained.

For a gender averaged working population of age range 25–65 (as specified in [9]) the conversion factors are similar for the two different projection models:

$$LAR/ERR_{60} = 0.124 \quad \text{(attained age model)}$$
$$LAR/ERR_{30} = 0.108 \quad \text{(age at exposure model)} \tag{16}$$

Figure 3 depicts, with reference to the left ordinate, the results from Table 2, i.e. the risk estimates in terms of *ERR* depending on the assumed value R_1 of the neutron RBE. The solid lines and the dark shaded bands give the reference slope, *c*, i.e. the slope through the *ERR* due to 1 Gy γ-rays, together with its 95% confidence ranges. This quantity, essentially the γ-ray slope in a linear dose dependence, is – as stated in the preceding section – fairly narrowly defined. It is given as a bold line in the range 20–50 of plausible values R_1. The results are not substantially different for the two projection models, the attained age model and the age at exposure model.

The broken lines and the light shaded bands give the estimates of the initial slope and their 95% confidence ranges. The essential point here is the broad range of initial slopes in the linear-quadratic dose dependence that are statistically consistent with the data. In this context it must be noted that the confidence ranges represent the uncertainty of the excess relative risk, *ERR*, but not the uncertainty of the conversion factors from Eq.(16).

The right ordinate gives the risk coefficient in terms of the lifetime attributable risk, *LAR*, for solid cancer mortality for a working population. For a population of all ages the values are higher by the factor 1.65 with the age at exposure model, and slightly smaller by the factor 0.94 with the attained age model.

Comparison to ICRP

The current ICRP solid cancer fatality coefficient is 0.045/Gy for a population of all ages, and 0.036/Gy for a working population [9]. These values were derived in terms of the age at exposure model. If the factor *DDREF*=2 is omitted, the values are 0.09/Gy and 0.072/Gy. The present computations provide – with the same conventional approach (*w*=10 and reference to colon dose), but with the 1950–1990 data (instead of the 1950–1987 data) – the coefficients 0.094/Gy and 0.057/Gy.

With the explicit treatment of neutrons the estimates are notably lower. The central estimates (R_1=35) in terms of the present explicit computations are 0.068/Gy (all ages) and 0.041/Gy (working ages) with the age at exposure model. For the attained age model, the result is 0.045/Gy for occupational exposures. For a population of all ages, the attained age model provides the value 0.042/Gy. However, the age at exposure model fits the data somewhat better. Thus the true value for a population of all ages may be closer to 0.068/Gy than to 0.042/Gy.

Comparison to UNSCEAR

UNSCEAR [1] quotes separate risk estimates for the five different reference populations. As averages over these populations and for all ages at exposure one obtains *LAR*=0.13/Gy for the age at exposure model, and 0.082/Gy for the attained age model. These values are twice as large as the central estimates 0.068/Gy and 0.042/Gy that are obtained here with the same solid cancer mortality data.

The difference is not entirely a matter of the more explicit treatment of the neutrons. UNSCEAR translates the *ERR* values for total solid cancer mortality (see [1], Annex I, Table 2 : ERR_{60}/Gy=0.48 and ERR_{30}/Gy=0.57) into the risk coefficients *LAR*/Gy=0.082 (attained age model) and *LAR*/Gy=0.13 (age at exposure model). This corresponds to the conversion coefficients LAR/ERR_{60}=0.171 and LAR/ERR_{30}=0.228. These values are larger by factors of 1.5 and 1.3 than the conversion factors in Eq.(15). One reason for the difference is that UNSCEAR has utilized somewhat more recent population data for the US, the UK, and Japan than ICRP and that they have employed actual age distributions of the populations, rather than the equilibrium distributions that correspond to the actuarial survival functions. This has increased the conversion factors somewhat (see [29]). A further part of the difference results

from the fact that the UNSCEAR Committee chose to derive the overall risk estimate for solid cancers not through a joint *ERR* (for each sex). Instead it determined it by deriving individual *ERR*s for eight cancer categories and by summing the estimated contributions. While the effect is not large, it is difficult to quantify the uncertainty that is associated with this less direct procedure.

LFR as an alternative expression of attributable risk

The lifetime attributable risk, *LAR*, specifies the probability of a fatal cancer due to the radiation exposure or the expected number of fatalities in a reference population. Such numbers can be misleading, if they are given without a reference scale. A relative parameter can be more meaningful, and a suitable quantity is the lifetime attributable risk, *LAR*, divided by the spontaneous lifetime cancer mortality risk, *B*, in the reference population, i.e. the fraction of deaths due to cancer. The modified quantity has tentatively been termed *lifetime fractional risk*, *LFR* [29], which is the fractional increase over the spontaneous lifetime cancer mortality. Besides being more indicative of the actual magnitude of the radiation risk, it has the attractive feature of depending little on the particularities of the reference population. In contrast to *LAR* (and the familiar risk coefficient), *LFR* is not larger for populations with high life expectancy, but is fairly equal for different reference populations [29].

The average of the ratio *LFR/LAR* for the five ICRP reference populations is 5.5, almost equally for the two projection models and both for a population of all ages and a working population [29]. This makes it a simple matter to translate *lifetime attributable risk* into *lifetime fractional risk*. Thus, for a working population, one can either specify the lifetime attributable solid cancer fatality as 0.043/Gy, or the lifetime fractional risk as 0.23/Gy.

Conclusions

Risk estimates for solid cancer mortality and incidence have here been obtained in terms of a treatment that includes an explicit accounting of the neutron effect contribution. The resulting estimates are lower by about a factor 1.4 than the values obtained in the conventional analysis that refers to the colon doses and utilizes a constant weighting factor *w*=10 for the neutrons.

The treatment is similar to the approach Pierce and Preston have taken in their recent analysis of the new incidence data [18]. They postulate – as was done here – a linear (neutrons), linear-quadratic (γ-rays) dose dependence, and they consider a low dose limit, RBE_{max}=λ =40, of the neutron RBE. The neutron RBE against the reference γ-ray dose D_1 equals R_1=λ/(1+θ ·D_1), where θ is the ratio of the quadratic to the linear dose coefficient for γ-rays (inverse of the *cross-over dose*). For dose dependencies with little or no curvature it would appear that the value 40 invoked by Pierce and Preston is

roughly in line with the range 20–50 for R_1 in the present computations. However, it is a major difference that the value λ=40 in the analysis of Pierce and Preston refers to the colon dose. Since the neutron to γ-ray absorbed dose ratio is larger by about a factor 2 for the organ-averaged dose than for the colon dose, the assumption RBE_{max}= λ=40 by Pierce and Preston is, in fact, equivalent to RBE_{max}=λ=20 with reference to the organ-averaged doses.

Averaged over the five populations that were invoked by ICRP, UNSCEAR derives the nominal risk coefficients LAR=0.13/Gy (age at exposure model) and LAR=0.082/Gy (attained age model) for solid cancer mortality. This exceeds the results LAR=0.068/Gy and 0.042/Gy from the present analysis (with R_1=35) by a factor of 2. The change from the conventional approach to the more explicit treatment of the neutrons accounts for about half of the difference. The remaining difference results partly from the fact that the UNSCEAR has invoked – for the transport of the ERR into LAR – the same reference populations as Land and Sinclair in their computations for ICRP [10], but has employed somewhat different population data and has used actual age distributions instead of the equilibrium distributions. A further difference is that UNSCEAR has not simply transported the overall ERR for all solid tumors to the reference populations, but has added up individually estimated contributions from different tumor sites to derive the overall solid cancer mortality risk.

The choice of the correct projection model in age is still open, and a definitive projection model will have to await the completion of the follow-up of the A-bomb survivors. The age at exposure model leads with the present solid cancer mortality data (1950–1990) to risk estimates for a population of all ages that are larger by a factor of about 1.6 than the estimates from the attained age model. This fairly large difference reflects a markedly elevated ERR in the youngest age at exposure cohorts. Whether these high values are real, has major implications with regard to the risk due to radiation exposure of children and juveniles.

The evidence for the elevated risk at young ages of exposure rests, at present, on a relatively small number of excess cancer cases (or cancer deaths) in these age cohorts. In this context it is of interest that the stratified treatment of the background of cancer mortality implies a somewhat peculiar secular trend of decreasing rates below age 60 and increasing rates above this age. With a parametric modeling of the background rates which does not include this complexity, the age at exposure dependence of the ERR is less marked. A similar reduction of the difference between the models results, if absolute risk – rather than relative risk – is transported in the computation of the LAR. Definitive conclusions on the dependence of LAR on age at exposure will require the continued follow-up of the A-bomb survivors. The attained age and the age at exposure model can in the meantime – in line with the approach chosen by UNSCEAR – be useful references that bracket the likely true value of the solid cancer risk coefficient.

The dose limits to the population are so low that a comparison to natural background radiation is more meaningful than a comparison to nominal risk numbers. In this sense the nominal risk coefficients are primarily of interest with regard to occupational exposures. For a gender averaged working population (age 25–65) the two projection models provide almost the same LAR, i.e. the choice of the projection model has ceased to be critical. With an assumed neutron RBE R_1=35, the solid cancer fatality risk coefficient 0.043/Gy is obtained. With a lower assumed value R_1=20 the coefficient is only moderately increased to 0.048/Gy.

Fairly large values of $DDREF$ are – as shown in Table 2 and Fig. 3 – consistent with the data for the solid cancer mortality. Considerably smaller risk coefficients than the central estimates can, therefore, not be ruled out. The incidence data define – as shown in Appendix, Fig. 4 – a more narrow range of the initial slope of the dose dependence for γ-rays. The maximum likelihood estimates of the ERR are moderately – although not with statistical significance – larger than the values for solid cancer mortality. The major difference is that the incidence data appear to be inconsistent with a $DDREF$ larger than about 1.7.

The result of the present analysis is remarkable insofar as the derived risk coefficient for occupational exposure corresponds closely to the current ICRP nominal risk coefficient, although it does not invoke the ICRP reduction factor $DDREF$=2. The risk coefficient could, therefore, remain largely unchanged if the $DDREF$ were abandoned.

The $DDREF$ remains a somewhat controversial issue. Radiobiological studies suggest a $DDREF$ both for x-rays and γ-rays. ICRP has, therefore, adopted $DDREF$=2 and has applied it to the risk estimates derived from the A-bomb data. On the other hand, there is evidence from radiobiological studies [30] that the RBE of x-rays compared to γ-rays is about 2 at low doses. Since the nominal risk coefficient is intended to be applicable not only to γ-rays, but also to x-rays, the two possible modifying factors would cancel out. This would tend to suggest that the $DDREF$ ought to be abandoned. Radioepidemiology, likewise, fails to provide strong support for a $DDREF$. There is no evidence for a $DDREF$ in the A-bomb data and no consistent evidence from other cohorts. At the same time, there is no indication of higher risk coefficients for x-rays than γ-rays in the epidemiological data. In this sense there appears to be little justification, both on the grounds of biology and epidemiology, to adopt a $DDREF$.

However, as stated at the outset, the present study is not aimed at deriving a new nominal risk coefficient. It focuses, instead, on methodological aspects that can be taken into account in future analyses based on a more recent follow-up of the A-bomb survivor data and an updated dosimetry.

A preceding paper [12] deduced the risk coefficient for neutrons in terms of a Poisson regression which required – in addition to an assumed R_1 – only the ERR_{obs}

at a dose of 1 Gy from the A-bomb radiation. An attractive feature of this approach is – apart from its simplicity – the fact that it is insensitive to uncertainties of the neutron dosimetry that still exist at lower doses. The present, more detailed modeling provides, of course, also a risk estimate for neutrons, $\alpha_n = c \cdot R_1$, and it is of interest to examine the consistency of the two results. The preceding paper derived (with $R_1 = 35$) the risk coefficients for neutrons ERR/Gy=12.8. The present, more explicit computations provide – in terms of the values c in Table 2 – the values ERR/Gy=13.0 as an average of the two different projection models. The degree of numerical equality may be accidental, but the comparison confirms the consistency of the two similar approaches.

Appendix

Results obtained from the solid cancer incidence data

Figure 4 gives the results for the solid cancer incidence data (1958–1987) in analogy to those for the solid cancer mortality data (Fig. 3). Only the results for the age at exposure model are given, because the two projection models (in terms of ERR_{30} and ERR_{60}) give almost precisely the same results. As with the mortality data, the incidence data fit the e-model better than the a-model. The maximum likelihood estimates of the initial slope α is somewhat larger – although not significantly so – than the maximum likelihood value of c. This implies – in agreement with an analysis of the more recent incidence data [18] – that the incidence data are inconsistent with a $DDREF$ in excess of about 1.7. Since there is no standard for the incidence rates, the diagram does not give a right ordinate with lifetime attributable incidence.
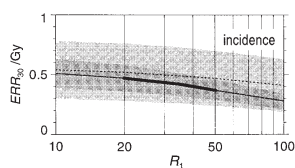
Fig. 4 The *solid line* and the *dark shaded band* represent – for the age at exposure model – the parameter c, i.e. the ERR_{30} for solid cancer incidence due to an acute γ-ray dose of 1 Gy and its 95% confidence range. The *broken line* and the *light shaded band* gives the estimate of the initial slope, α, and its 95% confidence range. The diagram is analogous to the diagrams in Fig. 3

References

1. UNSCEAR (2000) Sources and effects of ionizing radiation. United Nations Scientific Committee on the Effects of Atomic Radiation. Report to the General Assembly. Vol.II: Effects, Annex I. Epidemiological evaluation of radiation-induced cancer. United Nations, New York, pp 297–450
2. Milton RC, Shohoji T (1968) Tentative 1965 radiation dose (TD65) estimation for atomic bomb survivors. ABCC report TR 1–68, Radiation Research Effects Foundation, Hiroshima
3. Rossi HH, Kellerer AM (1974) The validity of risk estimates of leukemia incidence based on Japanese data. Radiat Res 58:131–140
4. Rossi HH, Mays CW (1978) Leukemia risk from neutrons. Health Phys 34:353–360
5. Roesch WC (ed) (1987) US-Japan joint reassessment of atomic bomb radiation dosimetry in Hiroshima and Nagasaki – final report, Vols.1 and 2, Radiation Research Effects Foundation, Hiroshima, Japan
6. Rossi HH, Zaider M (1996) Comment on the contribution of neutrons to the biological effect at Hiroshima. Radiat Res 146:590–593
7. Pierce DA, Shimizu Y, Preston DL, Vaeth M, Mabuchi K (1996) Studies of the mortality of atomic bomb survivors. Report 12, Part 1. Cancer. Radiat Res 146:1–27
8. Thompson DE, Mabuchi K, Ron E, Soda M, Tokunaga M, Ochikubo S, Sugimoto S, Ikeda T, Terasaki M, Izumi S, Preston DL (1994) Cancer incidence in atomic bomb survivors, Part II: solid tumors, 1958–1987. Radiat Res 137:S17–S67
9. ICRP (1991) Publication 60. The 1990 Recommendations of the International Commission on Radiological Protection. Annals of the ICRP. ICRP 21 (1–3). Pergamon Press, Oxford
10. Land CE, Sinclair WK (1991) The relative contributions of different organ sites to the total cancer mortality associated with low-dose radiation exposure. In: Risks associated with ionizing radiations. Annals of the ICRP 22 (1). Pergamon Press, Oxford, pp 31–58
11. Kellerer AM, Nekolla E (1997) Neutron versus γ-ray risk estimates. Inferences from the cancer incidence and mortality data in Hiroshima. Radiat Environ Biophys 36:73–83
12. Kellerer AM, Walsh L (2001) Risk estimates for fast neutrons with regard to solid cancer. Radiat Res 156:708–717
13. NAS/NRC (2001) Status of the dosimetry for the Radiation Effects Research Foundation (DS86) Committee on Dosimetry for RERF, Board on Radiation Effects Research, Division on Earth and Life Studies, National Research Council. National Academy of Sciences Press, Washington DC
14. Lafuma J, Chmelevsky D, Chameaud J, Morin M, Masse R, Kellerer AM (1989) Lung carcinomas in Sprague-Dawley rats after exposure to low doses of radon daughters, fission neutrons, or γ-rays. Radiat Res 118:230–245
15. Wolf C, Lafuma J, Masse R, Morin M, Kellerer AM (2000) Neutron RBE for tumors with high lethality in Sprague-Dawley rats. Radiat Res 154:412–420
16. Carnes BA, Grahn D, Thompson JF (1989) Dose-response modeling of life in a retrospective analysis of the combined data from the Janus program at Argonne National Laboratory. Radiat Res 119:39–56
17. Covelli V, Coppola M, Di Majo V, Rebessi S, Bassini B (1988) Tumor induction and life shortening in BC3F1 female mice at low doses of fast neutrons and x-rays. Radiat Res 113:362–374
18. Pierce DA, Preston DL (2000) Radiation related cancer risks at low doses among atomic bomb survivors. Radiat Res 154:178–186
19. Gilbert ES (1984) Some effects of random dose measurement errors on the analyses of atomic bomb survivor data. Radiat Res 98:591–605
20. Pierce DA, Stram DO, Vaeth M (1990) Allowing for random errors in radiation dose estimates for the atomic bomb survivor data. Radiat Res 123:275–284

21. Edwards AA (1997) Relative biological effectiveness of neutrons for stochastic effects. Documents of the National Radiological Protection Board, NRPB, Vol. 8, No.2, Chilton, Didcot
22. Sinclair WK (1982) Fifty years of neutrons in biology and medicine: The comparative effects of neutrons on biological systems. In: Ebert HG (ed) Proceedings of the 8th Symposium on Microdosimetry, Report EUR 8395. Commission of the European Communities, Brussels
23. ICRU (1986) The quality factor in radiation protection. International Commission on Radiation Units and Measurements, ICRU, Report 40, Bethesda, Md.
24. Kellerer AM, Walsh L (2002) Solid cancer risk coefficient for fast neutrons in terms of effective dose. Radiat Res (in press)
25. Preston DL, Lubin JH, Pierce DA (1993) Epicure User's Guide. HiroSoft International Corp. Seattle
26. Kellerer AM, Barclay D (1992) Age dependences in the modelling of radiation carcinogenesis. In: Taylor DM, Gerber GB, Stather JW (eds) Age-dependent factors in the biokinetics and dosimetry of radionuclides. Radiat Prot Dosim 41:273–281
27. Pierce DA, Mendelsohn ML (1999) A model for radiation-related cancer suggested by atomic bomb survivor data. Radiat Res 152:642–654
28. Vaeth M, Pierce D (1990) Calculating excess lifetime risk in relative risk models. Environ Health Perspect 87:83–94
29. Kellerer AM, Nekolla EA, Walsh L (2001) On the conversion of solid cancer excess relative risk into lifetime attributable risk. Radiat Environ Biophys 40:249–257
30. Borek C, Hall EJ, Zaider M (1983) X rays may be twice as potent as gamma rays for malignant transformation at low doses. Nature 301:156–158

5. Rühm W, Walsh L & Chomentowski M. Choice of model and uncertainties of the gamma-ray and neutron dosimetry in relation to the chromosome aberrations data in Hiroshima and Nagasaki, Radiat. Environ. Biophys. 42, 119-128, 2003

ORIGINAL PAPER

W. Rühm · L. Walsh · M. Chomentowski

Choice of model and uncertainties of the gamma-ray and neutron dosimetry in relation to the chromosome aberrations data in Hiroshima and Nagasaki

Abstract Chromosome data pertaining to blood samples from 1,703 survivors of the Hiroshima and Nagasaki A-bombs, were utilized and different models for chromosome aberration dose response investigated. Models applied included those linear or linear-quadratic in equivalent dose. Models in which neutron and gamma doses were treated separately (LQ-L model) were also used, which included either the use of a low-dose limiting value for the relative biological effectiveness (RBE) of neutrons of $R_0=70\pm10$ or an RBE value of $R_1=15\pm5$ at 1 Gy. The use of R_1 incorporates the assumption that it is much better known than R_0, with much less associated uncertainty. In addition, error-reducing transformations were included which were found to result in a 50% reduction of the standard error associated with one of the model fit parameters which is associated with the proportion of cells with at least one aberration, at 1 Gy gamma dose. Several justifiable modifications to the DS86 doses according to recent nuclear retrospective dosimetry measurements were also investigated. Gamma-dose modifications were based on published thermoluminescence measurements of quartz samples from Hiroshima and on a tentative reduction for Nagasaki factory worker candidates by a factor of 0.6. Neutron doses in Hiroshima were modified to become consistent with recent fast neutron activation data based on copper samples. The applied dose modifications result in an increase in non-linearity of the dose-response curve for Hiroshima, and a corresponding decrease in that for Nagasaki, an effect found to be most pronounced for the LQ-L models investigated. As a result the difference in the dose-response curves observed for both cities based on DS86 doses, is somewhat reduced but cannot be entirely explained by the dose modifications applied. The extent to which the neutrons contribute to chromosome aberration induction in Hiroshima depends significantly on the model used. The LQ-L model including an R_1 value of 15 at 1 Gy which is recommended here, would predict between 10% and 20% of the observed chromosome aberrations to be due to neutrons, at all doses. Because of the good agreement between DS86 predictions and the results of retrospective gamma and neutron dosimetry, the modifications applied here to DS86 doses are relatively small. Consequently, the choices of model and RBE values were found to be the major factors dominating the interpretation of the chromosome data for Hiroshima and Nagasaki, with the dose modifications resulting in a smaller influence.

W. Rühm (✉) · L. Walsh · M. Chomentowski
Radiobiological Institute,
University of Munich,
Schillerstrasse 42, 80336 Munich, Germany
e-mail: w.ruehm@lrz.uni-muenchen.de
Tel.: +49-89-5996838
Fax: +49-89-5996840

Introduction

The A-bomb survivors from Hiroshima and Nagasaki have been extensively monitored, and radiation-induced late effects such as leukemia, solid tumors, or non-cancer diseases have been carefully modeled (e.g. [1, 2, 3, 4]). Further studies have dealt with chromosome aberrations in peripheral blood lymphocytes, and dose-related increases continued to be detectable even decades after exposure (e.g. [5, 6, 7, 8]). Successively improved dosimetry systems have been developed as the investigations evolved.

The first dosimetry system, T57D (tentative 1957 doses), was published in 1960 [9] and was replaced by the tentative 1965 doses (T65D) in 1968 [10]. In 1978 Rossi and Mays [11] noted that a significant difference between the dose-response curves for leukemia in Hiroshima and Nagasaki could be explained—in terms of T65D doses—by the high relative biological effectiveness (RBE) of neutrons which had been found in various radiobiological studies. Later Loewe and Mendelsohn [12] pointed out that the differences in the dose-response curves for Hiroshima and Nagasaki disappeared when modified dose estimates were used. These developments motivated

a large international effort that resulted in the creation of the current dosimetry system DS86 [13]. For a more detailed description of these developments, see e.g. [14].

The similarity between the leukemia dose response in Hiroshima and Nagasaki that resulted with the DS86 doses was subsequently seen as a confirmation of DS86. Nevertheless, there have been a number of continued uncertainties.

A major change brought about by DS86 was a substantial reduction of the neutron doses in Hiroshima. However in the final report of DS86 [13] it was noted that neutron doses for Hiroshima should be seen as tentative. Subsequent neutron activation measurements on samples exposed to thermal neutrons from the Hiroshima bomb seemed to confirm this statement. They suggested considerably larger neutron doses than specified by DS86 at large ground ranges[1] (e.g. [15, 16, 17, 18]).

A second discrepancy relates to thermoluminescence measurements on quartz samples from Hiroshima. These measurements suggest that close to the hypocenter the gamma doses are smaller by a factor of about 0.6 compared to DS86, whereas they are larger by a factor of about 1.6 for ground ranges close to 2 km [19].

A subgroup of Nagasaki survivors exposed in factories ("Nagasaki factory workers") were added to the cohort in an extension of the dosimetry system although shielding calculations were difficult for them. Subsequent indications, from both chromosome aberration and cancer data, were that their doses (in the range 0.5–1.5 Gy)[2] might have been too large [3, 8].

The potential implications of the dosimetric uncertainties for risk estimation have been assessed in a number of studies [20, 21, 22, 23]. The present paper considers, based on the more recent developments, implications of the uncertainties and of potential dosimetric changes in the light of the chromosome aberration data.

In contrast to the leukemia and solid cancer data there continued to be in terms of the DS86 doses substantial differences in the dose response curves for chromosome aberrations in Hiroshima and Nagasaki (see Fig. 1). Stram et al. [7] concluded that in DS86 " ... either neutrons were underestimated in Hiroshima or gamma-rays were overestimated in Nagasaki". The abovementioned current issues of uncertainty with regard to DS86 are in apparent accordance with this statement.

As far as neutron doses are concerned, past studies primarily addressed the large discrepancy to the DS86 neutron doses that was suggested by the thermal neutron

---

[1] Ground range denotes the distance between the location of interest and the hypocenter of the explosion; the hypocenter being the vertical projection of the actual location of the explosion (burst height: 580±15 m [13]), i.e. the epicenter, onto the ground. Slant range denotes the actual distance of the location of interest to the epicenter.
[2] The special name Sievert (Sv) is here exclusively used with dose equivalent quantities that are defined in terms of the *officially* adopted values Q or w_R; in all other cases, the special name Gray (Gy) is used for the unit J/kg.

Fig. 1 Non-parametric excess relative rate per 0.2 Gy, as function of bone-marrow dose (with data from [7]); data are corrected for a weighted mean background rate of 1.218×10^{-2} aberrations per cell for Hiroshima and 1.322×10^{-2} aberration per cell for Nagasaki obtained from those surivors with estimated zero dose

activation measurements. However, in the meantime, working groups in the US, Japan, and Germany have initiated new measurement programs to detect thermal and fast neutron activation products in samples from Hiroshima. The joint US-Japanese working group on reassessment of A-bomb dosimetry publicly announced recently that after analysis of all available data, no major changes of the DS86 neutron doses are expected [24]. For this reason, any modifications of DS86 neutron doses discussed in this paper are not based on published thermal neutron activation data. Instead, we used new data on ^{63}Ni which had been produced in copper samples from Hiroshima by fast neutrons from the A-bomb via the reaction ^{63}Cu(n,p)^{63}Ni [25, 26, 27]. The ^{63}Ni can be detected by means of a dedicated chemical procedure [28] and accelerator mass spectrometry [29, 30, 31]. These data appear to be consistent, within their experimental uncertainties, with DS86 fast neutron fluences [32].

Though statistically compatible with DS86 calculations, the ^{63}Ni data are used here to slightly modify the DS86 bone marrow neutron doses. DS86-based bone marrow gamma doses were modified for Hiroshima as suggested by *in situ* thermoluminescence data [19]. Bone marrow gamma doses to Nagasaki factory workers were decreased by a factor of 0.6, in the dose range 0.5–1.5 Gy.

The work is focussed on three aspects:

– The apparent difference between the two cities which is seen in the chromosome data, but not for solid cancers and leukemia,
– The influence of the applied dose modifications on dose-response relationships, for different models,
– The potential role of neutrons on chromosome aberration induction in Hiroshima and Nagasaki.

Materials and methods

Chromosome aberration data

The present paper makes use of data for stable chromosome aberrations (CA1993.dat) previously analyzed by Stram et al. [7]. This data set is based on stable chromosome aberrations (primarily translocations and inversions) collected between 1968 and 1985 by the Radiation Effects Research Foundation (RERF) on 1,703 individuals from the Life Span Study (LSS) cohort of atomic bomb survivors—1,043 from Hiroshima and 660 from Nagasaki—with estimated DS86 shielded kerma less than 4 Gy when the neutron component of dose is weighted with a constant RBE of 10. For each individual the data set includes information on city, year of assay, numbers of examined cells and number of cells with at least one aberration, as well as DS86 bone marrow gamma and neutron doses. Fig. 1 visualizes the data in terms of the observed number of stable aberrations per investigated cell, corrected for a weighted mean background rate and for dose intervals of 200 mGy ("excess relative rate"). For further details see [7].

Models

For this study the chromosome data from Hiroshima and Nagasaki have been fitted in terms of a number of special forms (see Appendix A) of the generic model:

$$p_{i,t} = \alpha_t \cdot \left(1 + \rho\left(D_{\gamma,i}, D_{n,i}\right)\right) \qquad (1)$$

where $p_{i,t}$ is the expected proportion of cells with stable chromosome aberration(s); i is the survivor index; t is the time interval index; α_t is the background frequency of aberrations; $D_{\gamma,i}$ is the bone-marrow gamma dose for the ith survivor (Gy); $D_{n,i}$ is the bone-marrow neutron dose for the ith survivor (Gy); and $\rho(D_{\gamma,i}, D_{n,i})$ is a linear or linear-quadratic expression in the gamma and neutron dose.

The statistical models for the expected proportion, $p_{i,t}$, of cells with at least one aberration as a function of dose, were fitted using iterative re-weighted least-squares regression with the software package EPICURE [33]. Maximum likelihood calculations based on a simple binomial model are not suitable here because these data exhibit considerably larger variance at higher doses than a simple binomial model would imply [6]. Thus, regression techniques incorporating iterative re-weighted least-squares were applied, with weights chosen to compensate for the increased variability. As pointed out by Preston et al. [6], the over-dispersion observed in the aberration data appears to be adequately described by the equation:

$$\mathrm{var}\left(p_{i,t}\right) = p_{i,t}\left(1 - p_{i,t}\right)/N_i + (1 - 1/N_i) \cdot \theta \cdot p_{i,t}^2 \qquad (2)$$

where N_i is the number of cells examined for the ith survivor; θ is the over-dispersion parameter.

The first term represents the binomial variance, the second term models the over-dispersion. The variance $\mathrm{var}(p_{i,t})$ is used as weight in the regression analysis.

The various special models are described in Appendix A and the derived model parameters are listed in Table A1. The results and the essential conclusions on city differences, the impact of dosimetry modifications, and the potential influence of the neutrons are discussed in the Results and Discussion section.

Modifications applied to DS86 neutron and gamma doses

Gamma-ray doses in Hiroshima

DS86 gamma doses for Hiroshima were tentatively modified for part of the present computations, in line with data summarized by Nagatomo et al. [19]. In Fig. 2 of their paper Nagatomo et al. show thermoluminescence data for quartz samples from Hiroshima, in terms of the ratio of measured gamma dose to its value in DS86. A

Table 1 Modification factors c_γ (Eq. 3) and c_n (Eq. 4) applied to the DS86 gamma and neutron doses for Hiroshima; slant range as a function of absorbed gamma marrow dose was taken from [36]; c_γ is based on published thermoluminescence data [19], c_n is based on recent assessment of fast neutrons by determination of ^{63}Ni in copper samples [32]. The c_n factors are based on a weighted fit through the ^{63}Ni point estimates. In spite of the modification that is here applied it must be noted that the ^{63}Ni data are, within their uncertainties, compatible with the DS86 fast neutron fluences

Absorbed bone marrow gamma dose (Gy)	Slant range (km)	c_γ	c_n
0.2	1.63	1.26	1.93
0.4	1.47	1.16	1.49
0.6	1.37	1.10	1.29
0.8	1.30	1.06	1.16
1.0	1.25	1.03	1.07
1.2	1.20	1.00	1.00
1.4	1.17	0.98	0.94
1.6	1.13	0.97	0.90
1.8	1.11	0.95	0.86
2.0	1.08	0.94	0.83

least-squares regression through those data results in a functional dependence on slant range as given in Eq. 3:

$$c_\gamma(sl) = 0.528 \exp(0.534\, sl) \qquad (3)$$

where sl is the slant range (in km) to the bomb. For locations close to the hypocenter, c_γ=0.72. For a ground range of about 2 km, i.e. the largest distance for which thermoluminescence measurements were performed, c_γ equals about 1.6 (see also Table 1).

Neutron doses in Hiroshima

Recently improved methods have made it possible to detect very small amounts of ^{63}Ni in copper samples from Hiroshima and Nagasaki [28, 29, 30, 31]. The ^{63}Ni has been produced by fission neutrons from the A-bomb via the reaction ^{63}Cu(n,p)^{63}Ni. Since neutron doses are predominantly due to fast neutrons, ^{63}Ni is a better indicator of the magnitude of the neutron doses than activation products of thermal neutrons previously measured. The available results on ^{63}Ni for Hiroshima are compatible with the DS86 fast neutron fluences. Due to the uncertainties of the results from distant samples some deviation from DS86 estimates cannot be excluded [32], but these are far smaller than the discrepancy which had been reported in the literature for thermal neutrons. Essential agreement with DS86 has also recently been established for ^{36}Cl which was produced by thermal neutrons from the A-bomb explosion via the reaction ^{35}Cl (n,γ) ^{36}Cl in granite samples from Hiroshima [34, 35].

For the present computations the measured ^{63}Ni activities [32] have been normalized to the activities expected on the basis of DS86 (S. Egbert, private communication, 2001). A weighted least squares regression on the results has then provided the modification factor c_n for the neutron doses as function of slant range sl (in km):

$$c_n(sl) = 0.157 \exp(0.534\, sl) \qquad (4)$$

Close to the hypocenter the modification factor is 0.4, which reflects mainly a single data point at slant range 686 m. At a slant range of about 1.6 km, c_n equals about 1.9.

Both for the modification of the gamma dose and the neutron dose, it is necessary to assign a distance, sl, to each of the survivors in the study. This distance is not part of the data set. Therefore it is estimated from the bone marrow gamma dose for the person and the overall relation between the DS86 bone marrow gamma dose and distance [36]. Table 1 lists the modification factors for neutron and gamma dose vs. slant range and vs. the bone-marrow gamma dose in Hiroshima.

Gamma-ray doses to factory workers in Nagasaki

The publicly available data set includes Nagasaki factory workers but does not identify them as such. To apply tentative dose modifications the gamma doses were, therefore, reduced by a factor of 0.6 for 100 "factory worker candidates" [8]. The factory worker candidates were selected via Monte-Carlo techniques to attain a gender and age distribution and a mean dose as close as possible to the actual factory workers in the new solid cancer incidence data (D. Pierce, private communication).

Results and discussion

Four different forms of the generic model of Eq. 1 have been employed in the computations. The first two cases are the familiar linear (L) and the linear-quadratic formulation (LQ)—as originally utilized by [7]—in terms of a weighted dose $D = D_\gamma + 10 D_n$ with weighting factor 10 for the neutron absorbed dose. If ρ is the excess relative rate as in:

L : $\rho = \beta_1 D$

LQ : $\rho = \beta_1 D + \beta_2 D^2$

An assumed constant RBE of neutrons is, of course, an approximation which is not in agreement with the known decrease of RBE with increasing dose. Therefore we have used in addition the linear-quadratic model in gamma dose with linear term in neutron dose. In vitro studies suggest for Hiroshima-like neutrons against ^{60}Co γ-rays a low-dose limiting RBE value of $R_0 = 70$ [38] and a value of about $R_1 = 15$ at a gamma dose of $D_1 = 1$ Gy (see Appendix A). To postulate both of these values for the present study leads to a poor fit for the Hiroshima data. Models with $R_0 = 70$ and $R_1 = 15$ are, therefore, tested separately:

LQ − L$_0$: $\rho = \beta_1 D_\gamma + \beta_2 D_\gamma^2 + 70 \beta_1 D_n$

LQ − L$_1$: $\rho = \beta_1 D_\gamma + \beta_2 D_\gamma^2 + 15 (\beta_1 + \beta_2 D_1) D_n$

The computations are done to explore which form of the models provides the best agreement between the two cities and, furthermore, to determine the impact of the comparatively modest dosimetric changes which have been discussed in the preceding section. Accordingly each of the four models is employed under four conditions:

A No changes from DS86
B Modified gamma dose
C Modified neutron dose (no change in Nagasaki)
D Modified neutron and gamma dose.

Altogether there are, thus, 16 solutions for Hiroshima. For Nagasaki there are only 8 solutions, because no change of the neutron doses is considered. Some further explanations on the computations, are given in Appendix A. The numerical results are listed in Table A1.

Table 2 Background proportion of aberrations α_t for Hiroshima, and standard errors using the linear model given in Eqs. 1, 5 and 6, and DS86 neutron and gamma marrow doses

Time period	α_t (Hiroshima)
1968–1969	0.0071±0.0005
1970–1971	0.0107±0.0013
1972–1973	0.0158±0.0013
1974–1980	0.0147±0.0014
1980+	0.0156±0.0010

Change of background frequencies

The background frequencies, α_t, of aberrations (see Eq. 1) have long been noted to increase with calender year in the investigation, which may reflect improvements in laboratory technique over time [7]. In the present computations the α_t were estimated in terms of the linear model (Eqs. A$_1$ and A$_2$) and the unchanged DS86 doses. Table 2 gives the results which agree closely with those obtained by Stram et al. [7]. The values remained almost unchanged when they were derived in terms of the modified DS86 doses or when a linear-quadratic model was used.

Results for the remaining parameters and corresponding standard errors that were obtained utilizing the abovementioned models are given in Table A1, for both DS86 doses and for the discussed dose modifications. The X^2 overall goodness-of-fit parameters are not tabulated, because their associated values were all similar enough to show a statistically indistinguishable goodness-of-fit to the data for all the applied models. It should be noted that the results for β_1 and β_2 (LQ model of Eq. 7) for the unmodified DS86 bone marrow doses (column 2) agree, as expected, with those obtained by Stram et al. [7].

Slope for low gamma exposure

Figure 2 represents the values obtained for the linear coefficients for Hiroshima and for Nagasaki, i.e. for the low-dose yield of aberrations. The results indicate for the majority of the model formulations some upward curvature ($\beta_2 > 0$) in the dose response for both cities. This is reflected also in the fact that the initial slope is less in the linear-quadratic fits than in the purely linear fit, and it is in line with the earlier analysis (see Fig. 1). Furthermore it is clear that, for Hiroshima, the smallest initial slope is found for the gamma ray response in the model LQ-L$_0$ which postulates the high RBE of neutrons at low doses.

For Hiroshima the dose modifications tend to reduce the initial slope, because the modifications increase doses at large distances, i.e. at low exposure levels. For Nagasaki only the reduction of the comparatively high gamma doses between 0.5 Gy and 1.5 Gy to the factory workers is considered. Here there is the opposite effect, i.e. the initial slope increases by up to a factor 2, and the initially linear-quadratic dose-response curve becomes more linear after the dose modification.
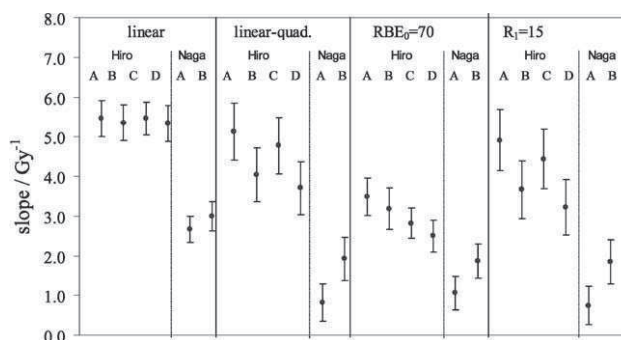
Fig. 2 Results for the linear slope at low doses, for different models and dose modifications (linear: Eq. 6; linear-quad.: Eq. 7; $RBE_0=70$: Eq. 8; $R_1=15$: Eq. 9): **A** DS86 neutron dose, DS86 gamma dose; **B** DS86 neutron dose, modified gamma dose; **C** modified neutron dose (consistent with recent [63]Ni data), DS86 gamma dose; **D** modified neutron dose (consistent with recent [63]Ni data), modified gamma dose (consistent with TLD data)

The initial slope is always significantly less for Nagasaki then for Hiroshima, except for the models LQ-L_0 and LQ-L_1 which account explicitly for the neutron RBE that changes with dose. But even with these models the differences remain large unless the DS86 dose values are subjected to the modifications.

Excess relative rate at 1 Gy gamma-ray dose

To assess the consistency of the chromosome data from the two cities it is not sufficient to consider the linear coefficients alone, i.e. the initial slopes at low doses. It is necessary to examine the overall agreement, and a suitable measure is, in addition to β_1, the parameter $c=\beta_1+\beta_2D_1$ which equals the slope to the excess relative rate at 1 Gy gamma-rays. The ratio c/β_1 indicates the non-linearity of the dose response. It is analogous to the dose and dose rate effectiveness factor, *DDREF*, i.e. it is the effectiveness ratio between a substantial dose of 1 Gy and a low dose. As explained in Appendix B, the parameter c can be derived directly in the model calculations, which has the advantage that its standard error is also obtained directly, rather than being inferred from the variance and covariance of the parameter estimates β_1 and β_2. Figure 3 lists the resulting values c in analogy to the representation of the linear coefficients in Fig. 2.

Due to the small modifications applied at 1 Gy gamma-rays for Hiroshima (see Table 1), the effect of the
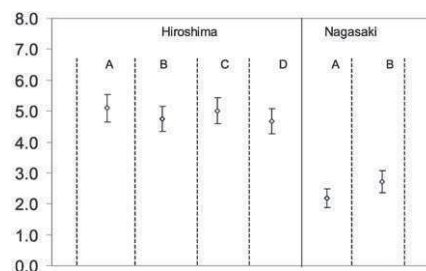
Fig. 3 Results for the slope to the excess relative rate c at 1 Gy gamma-rays (Appendix B), for different dose modifications: *A* Hiroshima and Nagasaki—DS86 neutron dose, DS86 gamma dose, *B* Hiroshima and Nagasaki—DS86 neutron dose, modified gamma dose, *C* Hiroshima—modified neutron dose (consistent with recent [63]Ni data), DS86 gamma dose, *D* Hiroshima—modified neutron dose (consistent with recent [63]Ni data), modified gamma dose (consistent with TLD data)

modifications on c are only small. However, the result confirms the continued disagreement between the results for Nagasaki and the larger values for Hiroshima which is now, i.e. for the model with the roughly orthogonal parameters, statisitically significant. As found with regard to the initial slope (Fig. 2), the disagreement is least if all dose modifications are taken into account.

The ratios c/β_2 which can be inferred from the LQ-L_1 model are shown in Table 3. For Hiroshima, the applied

Table 3 Ratios c/β_2 and standard errors inferred from the LQ-L_1 model; A–D as in caption of Fig. 2

Ratio	Hiroshima								Nagasaki			
	A		B		C		D		A		B	
c/α	1.04	+0.26 −0.18	1.30	+0.31 −0.24	1.13	+0.30 −0.18	1.45	+0.28 −0.44	2.93	+2.73 −1.39	1.47	+0.47 −0.40

124

Fig. 4a–d Resulting dose re-
sponse curves, for Hiroshima: **a**
LQ-L$_0$ DS86 doses, **b** LQ-L$_0$
modified neutron and gamma
doses, **c** LQ-L$_1$ DS86 doses, **d**
LQ-L$_1$ modified neutron and
gamma doses. The neutron
contribution lies between the
solid and dotted lines for R$_1$=15
(or R$_0$=70), and between the
dashed and dotted lines for
R$_1$=10 or 20 (or R$_0$=60 or 80)
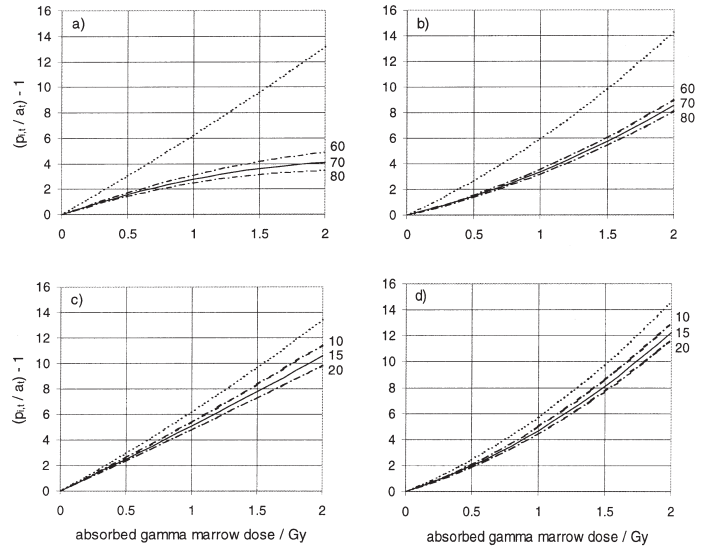
Fig. 5a–d Resulting dose re-
sponse curves, for Nagasaki: **a**
LQ-L$_0$, DS86 doses, **b** LQ-L$_0$,
modified gamma doses, **c** LQ-
L$_1$, DS86 doses, **d** LQ-L$_1$,
modified gamma doses. The
neutron contribution lies be-
tween the solid and dotted lines
for R$_1$=15 (or R$_0$=70), and be-
tween the dashed and dotted
lines for R$_1$=10 or 20 (or R$_0$=60
or 80)
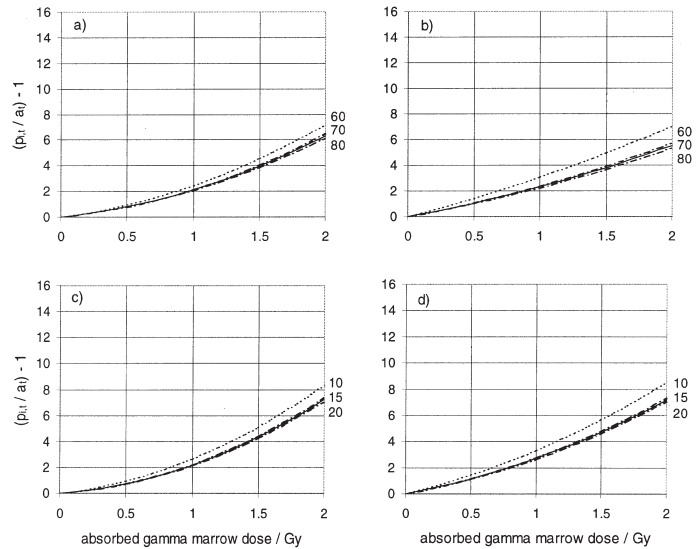
dose modifications tend to increase the c/β_2 ratios, i.e. the non-linearity of the dose-response. The differences are, however, not statistically significant. When the dose modifications to the factory worker candidates are applied the high ratio for Nagasaki decreases considerably. The non-linearity of the dose-responses becomes very similar for both cities, if all dose modifications are applied.

The effect contribution of the neutrons

An appreciable effect contribution by the neutrons is suggested by the high neutron RBE at low doses (R_0=70) that is found in vitro for chromosome aberrations. It is also supported by the fact that the modeling in terms of high neutron RBE minimizes the apparent difference between the Hiroshima and the Nagasaki data. However, it must be kept in mind that the value of 70 for R_0 was obtained from an interpolation to small doses and that, accordingly, the associated uncertainties are expected to be large. Figures 4 and 5 compare the fit to the data in the two cities for the two LQ-L models, with and without the applied dose modifications. For R_0 values of 60 and 80 were also used, to account for uncertainties associated with the estimated value of R_0. For the same reason, values for R_1 of 10 and 20 were also used in the LQ-L$_1$ model. The neutron contribution lies between the solid and dotted lines for R_1=15 (or R_0=70), and between the dashed and dotted lines for R_1=10 or 20 (or R_0=60 or 80).

For Hiroshima, the LQ-L$_0$ model would predict a considerable effect from neutrons. For example, with DS86 doses only about 30% of the induced stable chromosome aberrations is attributed to gamma radiation, at an absorbed bone-marrow gamma dose of 2 Gy (Fig. 4a). Even after the dose modifications were applied, the contribution from neutrons is still considerable and on the order of 30–50% depending on dose (Fig. 4b). On the contrary, the role of the neutrons is considerably smaller when the LQ-L$_1$ model is used (Fig. 4c, d). For Nagsaki the role of neutrons is less important, for all models used. Here, the applied modification to the bone marrow gamma dose clearly results in a more linear dose-response curve, for both LQ-L models (Fig. 5a–d).

While the results shown in Figs. 4 and 5 indicate the importance of an appropriate model it must be noted, however, that the inferences on the neutron contribution are indirect and, accordingly, rather uncertain.

Conclusions

Chromosome aberration data on a sample of the Life Span Study cohort which includes 1,703 survivors from Hiroshima and Nagasaki were analyzed and different models for the chromosome aberration dose-response investigated. The impact of several tentative bone marrow neutron and gamma dose modifications on the shape of the dose dependence obtained from the Hiroshima and Nagasaki data was quantified.

For a model linear in equivalent dose, both the applied gamma and neutron dose modifications have only a slight influence on the slope of the dose-response curve. A model linear-quadratic in equivalent dose or an LQ-L model appears to be more able to track the applied dose modifications. The prominent feature of any LQ-L model is that it implicitly allows for a dose dependence of the RBE for neutrons, i.e. for decreasing RBE values with increasing dose. As for the LQ-L$_0$ model, the choice of

the best low-dose limiting RBE value R_0, however, might be difficult and for example in the case of cancer and leukemia induction in man almost impossible due to lack of direct experimental data. As for the induction of chromosome aberrations, it might be reasonable to use data obtained in vitro, although any extrapolation from in vitro to in vivo situations is of course a second-choice scenario. Since any use of low-dose limiting values R_0 generally is associated with very wide confidence intervals, due to extrapolation of available data to low doses, the use of the LQ-L$_1$ is recommended here. This model circumvents this problem by use of R_1 values at an intermediate dose of 1 Gy where the associated uncertainties are much smaller and, at the same time, employs a transformation resulting in lower standard errors for one of the model parameters.

The major difference in the results obtained from the LQ-L$_0$ and LQ-L$_1$ models concerns the role of neutrons in Hiroshima. While the LQ-L$_0$ model would predict, for Hiroshima, a significant induction of stable chromosome aberrations due to neutrons (40–50%), the LQ-L$_1$ model suggests an effect from neutrons between 10% and 20%, for all doses. This difference in the interpretation of the chromosome aberration data shows the fundamental importance of the choice of an adequate model.

It is of interest to compare the resulting dose-response curves obtained for Hiroshima with those for Nagasaki. As already noted by Stram et al. there is a statistically significant city difference in the dose-response curves for Hiroshima and Nagasaki when DS86 doses are used [7]. Although the applied dose modifications tend to diminish this difference, they are not able to eliminate it completely. The model most sensitive to the applied dose modifications is the recommended LQ-L$_1$ model, and it is conlcuded that dosimetric issues could partly explain the apparent inconsistency between Hiroshima and Nagasaki.

The analysis described here for chromosome aberrations demonstrates how dose modifications discussed in the literature for Hiroshima might influence the shapes of the dose-response curves fitted to data from the A-bomb survivors. In principle, a similar analysis can also be performed on cancer or leukemia incidence and mortality epidemiological data collected from the A-bomb survivors [3]. It is expected that the consequences of dose adjustments on the functional form of the dose dependence for such endpoints will be qualitatively similar to those obtained here for chromosome aberrations. In particular, linear risk coefficients for gamma radiation could probably decrease and the curvature may increase somewhat for Hiroshima. A quantitative agreement between different data sets for different endpoints, however, cannot necessarily be expected. It is worthwhile considering that the present results were obtained for bone marrow doses. For organs located deeper down inside the human body, such as the colon, where body shielding is more effective for neutrons than for gamma radiation, any adjustment to gamma doses will become more important relative to dose modifications for neutrons.

Finally it is emphasized that the results presented here, although they appear to contribute to an overall improvement in the consistency of the chromosome data obtained from the A-bomb survivors from both cities, must not be interpreted as proof that the employed dose modifications are actually true. In order to draw firmer final conclusions, on any modifications that might be needed to be applied to DS86 gamma and neutron doses, additional thermoluminescence and neutron activation measurements–especially at large distances from the hypocenter in Hiroshima—would be very useful. It must be also noted that in a major international effort, neutron and gamma doses to the A-bomb survivors from Hiroshima and Nagasaki are currently being re-evaluated. The working groups involved have already announced that major changes to DS86 dose estimates are not to be expected [24].

If the final choice for dose modifications are close to those applied here then the functional form of the dose dependence for chromosome aberrations based on DS86 doses will be somewhat affected. However, the choice of model and RBE values are the major factors dominating the interpretation of the chromosome aberration data.

Appendix A: Linear and linear-quadratic models

Conventional analysis

D_i is the weighted bone-marrow dose for the ith survivor, with weighting factor 10 for the neutron absorbed dose:

$$D_i = D_{\gamma,i} + 10 \cdot D_{n,i} \qquad (5)$$

Linear model (L)

The linear model is the simplest option:

$$\rho(D_{\gamma,i}, D_{n,i}) = \beta_1 D_i \qquad (6)$$

Linear-quadratic model (LQ)

The linear-quadratic model has been utilized by Stram et al. [7]:

$$\rho(D_{\gamma,i}, D_{n,i}) = \beta_1 D_i + \beta_2 D_i^2 \qquad (7)$$

LQ-L model with a limiting low-dose RBE value RBE_0 of 70

The LQ-L model is linear-quadratic in the gamma-ray dose and linear in the neutron dose:

$$\rho(D_{\gamma,i}, D_{n,i}) = \beta_1(D_{\gamma,i} + 70D_{n,i}) + \beta_2 D_{\gamma,i}^2 \qquad (8)$$

As pointed out in previous analyses [1, 3, 23, 37], it is impossible to infer the two parameters for the gamma-rays, and at the same time the parameter for the neutrons. Extraneous information is therefore required and reference is, therefore made to the maximum RBE of neutrons.

This value RBE_0 is inferred by extrapolating RBE values from cell studies to *low doses*. It is defined as the ratio of the slope of the neutron curve to the linear coefficient of the gamma-ray curve. In this section, RBE_0 is estimated from in vitro experiments, where chromosome aberration data obtained with neutrons from the Little Boy Replica Reactor [38] are compared to those obtained with ^{60}Co γ-rays [39, 40]. With a_n of 1.18 ± 0.02 Gy^{-1} [38], and with a_γ 0.01735 Gy^{-1} (mean of 0.0199 Gy^{-1} given by Littlefield et al. [40] and of 0.0148 Gy^{-1} given by Lloyd et al. [39]), a value for RBE_0 of $68.0_{-9.7}^{+13.1}$ can be calculated which compares well with recently published values of RBE_0 obtained for mono-energetic neutrons with an energy of 565 keV [41]. A value of 70 is used here together with the third function of dose (Eq. 8). Values of 60 and 80 were also used to account for uncertainties associated with the estimated value of RBE_0.

LQ-L model with a neutron RBE 15 against 1 Gy of gamma-rays

To avoid the uncertainty inherent in extrapolating to a limit at low doses, a previous article [42] invoked the neutron RBE, R_1, against an intermediate *reference gamma-ray dose*, $D_1=1$ Gy , rather than the less tangible RBE_0:

$$\rho(D_{\gamma,i}, D_{n,i}) = \beta_1 D_{\gamma,i} + \beta_2 D_{\gamma,i}^2 + R_1(\beta_1 + \beta_2 D_1)D_{n,i} \quad (9)$$

For R_1, a value of 15 is adopted as a central reference value for $D_1=1$ Gy. This value was obtained as an unweighted average from publications reporting dose effect coefficients for dicentric aberrations caused by acute exposure of human whole blood to ^{60}Co γ-rays [39, 40, 43, 44, 45, 46]. Only data from scoring first division metaphases or from cultures with less than 5% second division metaphases were considered. Since the values for R_1 deduced from the cited references range between 11.5 and 17.8, calculations for $R_1=10$ and $R_1=20$ were also performed in order to span an associated range of uncertainty. All RBE data used here are summarised in [47].

Table A1 Resulting model parameters as obtained from EPICURE-GMBO [33] for the five different dose functions with standard errors

HIROSHIMA				NAGASAKI	
	DS86 bone-marrow neutron dose & DS86 bone-marrow gamma dose	DS86 bone-marrow neutron dose & modified bone-marrow gamma dose	Modified bone-marrow neutron dose (based on ^{63}Ni data) & DS86 bone-marrow gamma dose	Modified bone-marrow neutron dose (based on ^{63}Ni data) & modified bone-marrow gamma dose	DS86 bone-marrow neutron dose & DS86 bone-marrow gamma dose	DS86 bone-marrow neutron, DS86 bone-marrow gamma dose reduced by a factor of 0.6 for FW candidates
1. Linear model (Eq. 6) and constant RBE value of 10 (Eq. 5)					
β_1 [Gy^{-1}]	5.464±0.451	5.351±0.445	5.449±0.450	5.336±0.444	2.674±0.326	2.987±0.367
2. Linear-quadratic model (Eq. 7) and constant RBE value of 10 (Eq. 5)					
β_1 [Gy^{-1}]	5.124±0.716	4.045±0.676	4.770±0.707	3.708±0.669	0.817±0.468	1.918±0.548
β_2 [Gy^{-2}]	0.241±0.390	0.966±0.414	0.491±0.405	1.223±0.428	1.329±0.325	0.811±0.355
3. LQ-L model with implicit dose-dependent RBE and a limiting low-dose value from in vitro experiments of R_0=70 (Eq. 8)					
β_1 [Gy^{-1}]	3.487±0.476	3.183±0.521	2.819±0.386	2.495±0.407	1.061±0.419	1.872±0.430
β_2 [Gy^{-2}]	−0.725±0.628	−0.257±0.754	0.347±0.512	0.881±0.598	1.045±0.395	0.445±0.389
4. LQ-L model (Eq. 9) with R_1=15					
β_1 [Gy^{-1}]	4.909±0.772	3.668±0.725	4.439±0.745	3.226±0.700	0.745±0.484	1.846±0.560
β_2 [Gy^{-2}]	0.188±0.541	1.085±0.546	0.576±0.536	1.451±0.542	1.433±0.362	0.870±0.395
c [Gy^{-1}]	5.097±0.437	4.754±0.4118	5.015±0.429	4.678±0.405	2.180±0.301	2.716±0.356

Appendix B: use of nearly orthogonal parameters

Computations in terms of the parameter $c=\beta_1+\beta_2 D_1$

Both parameters β_1 and β_2 in Eq. 9 are subject to considerable statistical error. The uncertainty in the initial slope of the dose relation for gamma radiation, i.e. the error of β_1, is of particular interest. However, the second parameter, β_2, is strongly (negatively) correlated with β_1. Its error specifies, therefore, essentially the same uncertainty and provides, thus, no additional information. Re-scaling β_2 to a parameter that is roughly "orthogonal" to β_1 is, therefore, advantageous. A suitable parameter (see Kellerer and Walsh [42]), subject to considerably smaller error than either β_1 or β_2, is the slope to the effect level at an intermediate acute gamma-ray dose, D_1:

$$c = \beta_1 + \beta_2 D_1 \tag{10}$$

where c is the slope through the point at D_1 on the dose relation for gamma rays; it is here called the *reference (gamma-ray) slope*. The effect at the intermediate gamma-ray dose D_1 is reliably determined by the experimental observations, i.e. its relative standard deviation is less than that of β_1. The reference slope c is, accordingly, a meaningful parameter; in fact it is essentially equal to the slope of the dose dependence in a linear model. For D_1=1 Gy, Eq. 9 reduces then to the form that is actually used in the computations (Eq. 11):

$$\rho(D_{\gamma,i},\, D_{n,i}) = \beta_1\left(D_{\gamma,i} - D_{\gamma,i}^2/D_1\right) + c\left(R_1 D_{n,i} + D_{\gamma,i}^2/D_1\right) \tag{11}$$

All modeling computations were carried out with the routine GMBO of the software package EPICURE [33].

References

1. Thompson DE, Mabuchi K, Ron E, Soda M, Tokunaga M, Ochikubo S, Sugimoto S, Ikeda T, Terasaki M, Izumi S, Preston DL (1994) Cancer incidence in atomic bomb survivors. Part II: Solid tumors, 1958–1987. Radiat Res 137:17–67
2. Preston DL, Kusumi S, Tomonaga M, Izumi S, Ron E, Kuramoto A, Kamada N, Dohy H, Matsui T, Nonaka H, Thompson DE, Soda M, Mabuchi K (1994) Cancer incidence in atomic bomb survivors. Part III: Leukaemia, lymphoma and multiple myeloma, 1950–1987. Radiat Res 137:68–97
3. Pierce DA, Shimizu Y, Preston DL, Vaeth M, Mabuchi K (1996) Studies of the mortality of atomic bomb survivors. Report 12, Part I. Cancer: 1950–1990. Radiat Res 146:1–27
4. Shimizu Y, Pierce DA, Preston DL, Mabuchi K (1999) Studies of the mortality of atomic bomb survivors. Report 12, Part II. Noncancer mortality: 1950–1990. Radiat Res 152:374–389
5. Awa AA, Sofuni T, Honda T, Itoh M, Neriishi S, Otake M (1978) Relationship between radiation dose and chromosome aberrations in atomic bomb survivors in Hiroshima and Nagasaki. J Radiat Res 19:126–140
6. Preston DL, McConney ME, Awa AA (1988) Comparison of the dose-response relationship for chromosome aberration frequencies between the T65D and DS86 dosimetries. TR7–88, Radiation Effects Research Foundation, Hiroshima
7. Stram DO, Sposto R, Preston DL, Abrahamson S, Honda T, Awa AA (1993) Stable chromosome aberrations among A-bomb survivors: an update. Radiat Res 136:29–36
8. Kodama Y, Pawel D, Nakamura N, Preston DL, Honda T, Itoh M, Nakano K, Ohtaki K, Funamoto S, Awa AA (2001) Stable chromosome aberrations in atomic bomb survivors: results from 25 years of investigation. Radiat Res 156:337–346
9. Arakawa ET (1960) Radiation dosimetry in Hiroshima and Nagasaki atomic-bomb survivors. N Engl J Med 263:488–493
10. Milton RC, Shohoji T (1968) Tentative 1965 radiation dose estimation for atomic bomb survivors. Atomic Bomb Casualty Commission. Technical report TR 1–68
11. Rossi HH, Mays CW (1978) Leukaemia risk from neutrons. Health Phys 34:353–360
12. Loewe WE, Mendelsohn E (1981) Revised dose estimates at Hiroshima and Nagasaki. Health Phys 41:663–666
13. Roesch WC (ed) (1987) US-Japan joint reassessment of atomic bomb radiation dosimetry in Hiroshima and Nagasaki—final

report. Radiation Effects Research Foundation, vol.1, 2, Hiroshima, Japan

14. Rühm W, Kellerer AM, Korschinek G, Faestermann T, Knie K, Rugel G, Kato K, Nolte E (1998) The dosimetry system DS86 and the neutron discrepancy in Hiroshima—historical review, present status, and future options. Radiat Environ Biophys 37:293–310

15. Hoshi M, Yokoro K, Sawada S, Shizuma K, Iwatani K, Hasai H, Oka T, Morishima H, Brenner DJ (1989) Europium-152 activity induced by Hiroshima atomic bomb neutrons: comparison with the ^{32}P, ^{60}Co, and ^{152}Eu activities in dosimetry system 1986 (DS86). Health Phys 57:831–837

16. Straume T, Egbert SD, Woolson WA, Finkel RC, Kubik RC, Gove HE, Sharma P, Hoshi M (1992) Neutron discrepancies in the DS86 Hiroshima dosimetry system. Health Phys 63:412–426

17. Shizuma K, Iwatani K, Hasai H, Hoshi M, Oka T, Morishima H (1993) Residual ^{152}Eu and ^{60}Co activities induced by neutrons from the Hiroshima atomic bomb. Health Phys 65:272–282

18. Shizuma K, Iwatani K, Hasai H, Oka T, Endo S, Takada J, Hoshi M, Fujita S, Watanabe T, Imanaka T (1998) Residual ^{60}Co activity in steal samples exposed to the Hiroshima atomic-bomb neutrons. Health Phys 75:278–284

19. Nagatomo T, Hoshi M, Ichikawa Y (1995) Thermoluminescence dosimetry of the Hiroshima atomic-bomb γ rays between 1.59 km and 1.63 km from the hypocenter. Health Phys 69:556–559

20. Straume T (1993) Neutron discrepancies in the dosimetry system 1986 have implications for radiation risk estimates. RERF Update 4:3–4

21. Straume T (1996) Risk implications of the neutron discrepancy in the Hiroshima DS86 dosimetry system. Radiat Prot Dosim 67:9–12

22. Preston DL, Pierce D, Vaeth M (1993) Neutron and radiation risk: a commentary. RERF Update 4:5

23. Kellerer AM, Nekolla E (1997). Neutron versus γ-ray risk estimates—Inferences from the cancer incidence and mortality data in Hiroshima. Radiat Environ Biophys 36:73–83

24. Joint US-Japanese Working Groups on Reassessment of A-Bomb Dosimetry (2002) Press releases: consensus statement April 4, 2002, and consensus statement September 12, 2002 (in English and Japanese)

25. Shibata T, Imamura M, Shibata S, Uwamino Y, Ohkubo T, Satoh S, Nogawa N, Hasai H, Shizuma K, Iwatani K, Hoshi M, Oka T (1994) A method to estimate the fast-neutron fluence for the Hiroshima atomic bomb. J Phys Soc Jpn 63:3546–3547

26. Straume T, Marchetti AA, McAninch JE (1996) New analytical capability may provide solution to the neutron dosimetry problem in Hiroshima. Radiat Prot Dosim 67:5–8

27. Marchetti AA, Straume T (1996) A search for neutron reactions that may be useful for Hiroshima dose reconstruction. Appl Radiat Isot 47:97–103

28. Marchetti AA, Hainsworth LJ, McAninch JE, Leivers MR, Jones PR, Proctor ID, Straume T (1997) Ultra-separation of nickel from copper metal for the measurement of ^{63}Ni by AMS. Nucl Instrum Methods Phys Res B 123:230–234

29. McAninch JE, Hainsworth LJ, Marchetti AA, Leivers MR, Jones PR, Dunlop AE, Mauthe R, Vogel JS, Proctor ID, Straume T (1997) Measurement of ^{63}Ni and ^{59}Ni by accelerator mass spectrometry using characteristic projectile X-rays. Nucl Instrum Methods Phys Res B 123:137–143

30. Rugel G, Faestermann T, Knie K, Korschinek G, Marchetti AA, McAninch JE, Rühm W, Straume T, Wallner C (2000) Accelerator mass spectrometry of ^{63}Ni using a gas-filled magnet at the Munich tandem laboratory. Nucl Instrum Methods Phys Res B 172:934–938

31. Rühm W, Knie K, Rugel G, Marchetti AA, Faestermann T, Wallner C, McAninch JE, Straume T, Korschinek G (2000) Accelerator mass spectrometry of ^{63}Ni at the Munich tandem laboratory for estimating fast neutron fluences from the Hiroshima atomic bomb. Health Phys 79:358–364

32. Straume T, Rugel G, Marchetti AA, Rühm W, Korschinek G, McAninch JE, Carroll K, Egbert S, Faestermann T, Knie K, Martinelli R, Wallner A, Wallner C (2003). Measuring fast neutrons in Hiroshima at distances relevant to atomic bomb survivors. Nature (accepted for publication)

33. Preston DL, Lubin JH, Pierce DA, McConney ME (1991) EPICURE. Generalized regression models for epidemiological data. Software from Hirosoft International Corporation, Seattle

34. Rühm W, Huber T, Kato K, Nolte E (2000) Measurement of ^{36}Cl at Munich—a status report. SBI 212/11.2000, Radiobiological Institute, University of Munich

35. Huber T, Rühm W, Hoshi M, Egbert SD, Nolte E (2003) ^{36}Cl Measurements in Hiroshima granite samples as part of an international intercomparison study. Radiat Environ Biophys 42:27–32

36. Preston DL (1998) DS86 γ and neutron colon dose estimates for LSS survivors by distance. RERF Update 9(1):8

37. Pierce DA, Preston DL (2000) Radiation related cancer risks at low doses among atomic bomb survivors. Radiat Res 98:178–186

38. Dobson RL, Straume T, Carrano AV, Minkler JL, Deaven LL, Littlefield LG, Awa AA (1991) Biological effectiveness of neutrons from Hiroshima bomb replica: results of a collaborative cytogenetic study. Radiat Res 128:143–149

39. Lloyd DC, Edwards AA, Prosser JS (1986) Chromosome aberrations induced in human lymphocytes by in vitro acute X and γ radiation. Radiat Prot Dosim 15:83

40. Littlefield LG, Joiner EE, Hubner KF (1990) Cytogenetic techniques in biological dosimetry: overview and example of dose estimation in 10 persons exposed to γ radiation in the 1984 Mexican ^{60}Co accident. In: Mettler FA Jr, Kelsey CA, Ricks RC (eds) Medical management of radiation accidents. CRC Press, Boca Raton, Florida

41. Schmid E, Regulla D, Guldbakke S, Schlegel D, Bauchinger M (2000) The effectiveness of monoenergetic neutrons at 565 keV in producing dicentric chromosomes in human lymphocytes at low doses. Radiat Res 154:307–312

42. Kellerer AM, Walsh L (2001) Risk estimation for fast neutrons with regard to solid cancer. Radiat Res 156:708–717

43. Bauchinger M (1984) Cytogenetic effects in human lymphocytes as a dosimetry system. In: Eisert WG, Mendelsohn ML (eds) Biological dosimetry. Springer, Berlin, p 15

44. Fabry L, Leonard A, Wambersie A (1985) Induction of chromosome aberrations in G_0 human lymphocytes by low doses of ionizing radiations of different quality. Radiat Res 103:122

45. Vulpis N, Scarpa G (1986) Induction of chromosome aberrations by ^{90}Sr β-particles in cultured human G_0 lymphocytes. Mutat Res 163:277

46. Matsubara S, Kuwabara Y, Horiuchi J, Suzuki S, Ito A (1988) Dose distribution of neutron beam and chromosome analysis. Int J Radiat Oncol Biol Phys 14:503

47. National Council on Radiation Protection and Measurements (1990) The relative biological effectiveness of radiations of different quality. NRCP report 104, Bethesda MD

6. Göggelmann W, Jacobsen C, Panzer W, Walsh L, Roos H & Schmid E. Re-evaluation of the RBE of 29 kV X-rays (mammography X-rays) relative to 200 kV X-rays using neoplastic transformation of human CGL1-hybrid cells. Radiat. Environ. Biophys. 42, 175-182, 2003

ORIGINAL PAPER

W. Göggelmann · C. Jacobsen · W. Panzer · L. Walsh ·
H. Roos · E. Schmid

Re-evaluation of the RBE of 29 kV x-rays (mammography x-rays) relative to 220 kV x-rays using neoplastic transformation of human CGL1-hybrid cells

Abstract Neoplastic transformation of human CGL1-hybrid cells was examined after exposure to 29 kV x-rays (mammography x-rays) and conventional 220 kV x-rays. The study was designed to repeat, under well-defined irradiation and culture conditions, an earlier investigation by Frankenberg et al. (Radiat Res, 2002), and to assess the validity of the high RBE values of 29 kV x-rays that had been reported. The experiments with the two types of x-rays were performed simultaneously and shared the same controls. The transformation yields with both radiation qualities were fitted to the linear-quadratic dependence on absorbed dose, and a corresponding analysis was performed for the data earlier obtained by Frankenberg et al. The transformation yields in the present study exceed those in the earlier investigation substantially, and it appears that the difference reflects inadequate feeding conditions of the cell cultures in the early experiments. The standard error bands of the dose response curves are derived and are seen to be considerably more narrow in the present results. The lowest dose of the 29 kV x-rays was 1 Gy in both studies, and at this dose the RBE vs. the conventional x-rays has now been found to be 2 with a 95% confidence interval of 1.4–2.6. The previous result was about 3.2, but the 95% confidence is very broad for these data. The estimated limit at low doses is 3.4 in the present experiments with a confidence interval that extends from less than 2 to large values.

The co-authors and the editors of this Journal have the sad task to announce that Dr. Göggelmann died after submission of this manuscript.

W. Göggelmann · C. Jacobsen
Institute of Toxicology,
GSF–National Research Center for Environment and Health,
85764 Neuherberg, Germany

W. Panzer
Institute of Radiation Protection,
GSF–National Research Center for Environment and Health,
85764 Neuherberg, Germany

L. Walsh · H. Roos
Radiobiological Institute,
University of Munich,
80336 Munich, Germany

E. Schmid (✉)
Institute of Radiobiology,
GSF–National Research Center for Environment and Health,
P.O. Box 1129, 85764 Neuherberg, Germany
e-mail: eschmid@gsf.de
Fax: +49-89-31873551

Introduction

During the last three decades several efforts were made to determine—in terms of different kinds of cell damage—the relative biological effectiveness (RBE) of x-rays in its dependence on photon energy. Although there are considerable variations of RBE for specified photon energies, the studies in general showed that low-energy photons are more effective, per unit absorbed dose, in inducing cell damage than high-energy photons. In ICRP 60 [1] the dependence of RBE on photon energy is documented for the end-points carcinogenesis in animals, neoplastic transformation of mammalian cells, and chromosome aberrations in human cells. Particularly detailed observations have been published for the induction of dicentrics in human lymphocytes and for a broad range of photon energies [2].

In recent publications, Frankenberg et al. [3, 4, 5] have reported data on neoplastic transformation induced in a human hybrid cell line (CGL1) by 29 kV x-rays and by conventional 200 kV x-rays. Their finding of a higher than expected low-dose RBE for the 29 kV x-rays relative to the conventional x-rays, and their claims that these results are consistent with published data for various biological end-points have raised a critical debate. Since the 29 kV x-rays are used in screening mammography, there are implications for risk estimation that require careful examination. A recent evaluation [6] has not supported the selection of data from the literature that Frankenberg et al. [3] have made to confirm the high RBE of 29 kV x-rays relative to weakly filtered 200 kV x-rays

or to ^{60}Co γ-rays. It is, accordingly, of considerable interest to re-examine the transformation data and to substantiate them where necessary by additional investigations.

The dose-dependence of the neoplastic transformation rate obtained by Frankenberg and colleagues was fitted by the authors to the linear-quadratic [3] or linear [4] models. However, the derived RBE values varied, and different statistical treatments have provided different and rather wide standard errors. An improved replication experiment was, accordingly, called for.

Material and methods

Cell line

The CGL1 cell line (kindly provided by Dr. L.B. Hieber, GSF and originally obtained by Dr. Leslie Redpath) is a human hybrid cell line which was isolated from a fusion of a cell of a tumorigenic HeLa cell subline, D98/AH-2, and a non-tumorigenic normal human skin fibroblast cell. The CGL1 cell contains on average four copies of each chromosome, two of fibroblast and two of HeLa origin [7]. It is negative for the HeLa cell tumor-associated antigen, the cell surface protein intestinal alkaline phosphatase (p75-IAP), and therefore does not induce tumors when injected into nude mice [8, 9]. The neoplastic phenotype of HeLa cells is suppressed by the presence of normal fibroblast chromosomes 11 and 14. The complete loss of one fibroblast chromosome 11 and one fibroblast chromosome 14 or one copy of the tumor suppressor alleles from both fibroblast chromosomes 11 and 14 leads to neoplastic transformation [10]. The transformed cells re-express the Hela cell tumor-associated antigen p75-IAP which is used for their identification. This has allowed the human hybrid system to be developed into a quantitative in vitro model for radiation-induced neoplastic transformation of human cells [11].

Cell culture and chromosome analysis

CGL1 cells were grown in flasks containing Auto Pow essential medium (Eagle modified, ICN) supplemented with 5% calf serum (ICN), 2 mM glutamax (Gibco), non-essential amino acids (Gibco), 100 U/ml penicillin and 100 μg/ml streptomycin (Gibco) and 20 mM sodium bicarbonate (Sigma) was added to maintain the pH at 7.2. Cells were cultured at 37°C in a humidified atmosphere containing 5% CO_2. For all experiments the same batch of serum was used. Under these growth conditions, the cells have a doubling time of 22±2 h.

Prior to the irradiation experiments as well as after the end of all sets of experiments, the cytogenetic status of the CGL1 cells was examined. Slide cultures were set up in Quadriperm dishes (Heraeus). CGL1 cells were seeded at a density of 2×10^5 cells per slide in 5 ml medium and incubated for 24 h. During the last 3 h colcemid (0.5 μg/ml) was present. The preparation of cells and FISH staining with composite whole chromosome-specific DNA probes for the target chromosomes 11 and 14 was performed according to our standard technique [12].

Irradiation and dosimetry

The culture flasks, in an upright position with the CGL1 cells attached to the front wall, were irradiated in horizontal beams at air-kerma rates of ~0.42 Gy/min. During irradiation the nutrition medium filled the flasks to a height of less than 5 mm only and its influence was considered to be negligible.
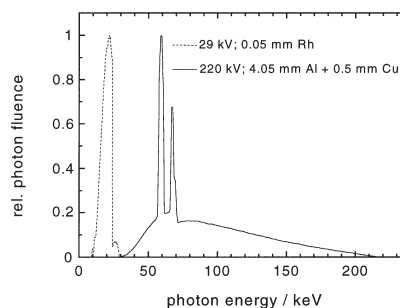
Fig. 1 X-ray spectra from tungsten anodes at a tube voltage of 29 kV with 0.05 mm Rh filtration and at a tube voltage of 220 kV with 4.05 mm Al+0.5 mm Cu filtration

Mammography radiation (29 kV x-rays)

To generate a radiation quality typical for mammography, a soft x-ray therapy unit Dermopan (Siemens) with an AEW50/25ö x-ray tube (anode material tungsten; anode angle 45°) was used. The unit was operated at a nominal tube voltage of 29 kV and a tube current of 20 mA. Since the Dermopan unit contains a rather simple one-peak high-voltage generator, with a strong dependence of tube voltage on primary voltage, tube current and duration of irradiation, the tube current and primary voltage at the transformer were manually held constant during irradiation. Under these conditions a tube voltage of 29 kV was maintained, as determined by means of a high purity germanium x-ray spectrometer.

The beam filtration consisted of 1 mm beryllium (tube window) and 0.05 mm rhodium (Rh) (RH000210, Goodfellow). The x-ray spectrum, characterized by the Rh-K edge at 23.2 keV, is shown in Fig. 1. Its mean photon energy amounts to 19.4 keV and its half-value layer (HVL) to 0.51 mm Al and both values are calculated from the photon spectrum. HVL values in mammography range typically from 0.34 to 0.56 mm Al [13]. The Rh-filter was bent cylindrically around the longitudinal axis of the tube through the focus to assure that the photons had to pass the same filter thickness, at least along the vertical field mid-line.

Two 0.02 cm^3 soft x-ray chambers (type M 23342, PTW) were used for dosimetry, one of which was connected to an electrometer IQ4 (PTW) mounted directly beside the culture flasks and served as a monitor chamber during irradiation. For the other chamber connected to a Unidos electrometer (PTW), an air-kerma calibration factor from PTB of the quality T30 (30 kV, 0.5 mm Al, E_m=19.6 keV, HVL=0.36 mm Al) was available. By means of this chamber the monitor was calibrated. To consider the absorption of the x-rays by the front wall of the flasks, the calibration occurred behind the front wall of a flask.

To achieve the air-kerma rate of ~0.42 Gy/min, it was necessary to select a distance to focus of only ~15 cm, which implied some inevitable field inhomogeneity. Consequently, prior to the experiments the field homogeneity at the front side of the flasks was tested by scanning the field in 1 cm steps in the vertical and horizontal direction. The test revealed that in the outermost corners of the flask, the air-kerma decreased to 91% of the central value and averaged over the whole flask area, the air-kerma dropped to 97%. In view of the small magnitude of this effect, it was decided to use the air-kerma value in the center of the field.

The absorbed dose to the cells was calculated according to

$$D_{cell} = K_{air} \times \overline{(\mu_{en}/\rho)}_{cell} / \overline{(\mu_{en}/\rho)}_{air} \qquad (1)$$

with $\overline{(\mu_{en}/\rho)}_M$ being the spectral mean value of the mass energy absorption coefficients of the respective material M calculated along

$$\overline{(\mu_{en}/\rho)}_M = \int\limits_0^{E_{max}} \Phi(E) \times E \times (\mu_{en}(E)/\rho)_M$$
$$\times dE / \int\limits_0^{E_{max}} \Phi(E) \times E \times dE \qquad (2)$$

from the spectral photon distribution $\Phi(E)$. Values for $(\mu(E)/\rho)$ were taken from Hubbell and Seltzer [14].

$$D_{cell} = K_{air} \times 1.02 \qquad (3)$$

Reference radiation (220 kV x-rays)

The reference radiation was generated by a highly stabilized MG 320 x-ray unit (Philips) with an MCN 323 x-ray tube (anode material tungsten, anode angle 22°) operated at a tube voltage of 220 kV and a tube current of 15 mA. The beam filtration consisted of 3 mm beryllium (tube window) and 4.05 mm Al+0.5 mm Cu added filtration. The x-ray spectrum is shown in Fig. 1. The mean photon energy amounts to 95.6 keV and the HVL to 1.39 mm Cu, both values calculated from the photon spectrum.

A transmission chamber (type 24366, PTW) connected to an IQ4 electrometer served as monitor chamber. A 1-cm³ thimble chamber (type M23331, PTW) connected to a Unidos electrometer, with an air-kerma calibration factor from PTB for the quality T200 (200 kV, 4 mm Al+1 mm Cu, HVL=1.6 mm Cu) was used to calibrate the monitor. The irradiation occurred at a distance of 70 cm to focus. Field inhomogeneity and absorption in the front wall of the flasks was negligible.

The absorbed dose to the cells was calculated in the same way as described above in Eqs. 1–3:

$$D_{cell} = K_{air} \times 1.087 \qquad (4)$$

Survival and transformation assay

For each experiment a frozen aliquot from the same stock culture of CGL1 cells was thawed and seeded into a 75 cm² flask which was filled with 15 ml medium and incubated for 3 days. From the culture 1×10^5 cells were seeded in 25 cm² flasks, filled up with 5 ml medium and incubated for 3 days. These flasks containing subconfluent cultures of 0.9–1.7×10^6 CGL1 cells were used either as controls or were irradiated at room temperature by 29 or 220 kV x-rays.

After an incubation time of 6 h, the cells were detached by trypsin and replated at densities of 2,500–10,000 cells per 75 cm² flasks for the transformation assay and at densities of 250–1,000 cells per 58 cm² dishes for the survival assay. The dishes were incubated at 37°C for 11 days, fixed with 70% ethanol for 10 min and stained with Giemsa for 15 min. For the transformation assay, cells were seeded at a density of about 30 survivors per cm² in the flasks which were incubated for 21 days, fixed with 2% paraformaldehyde/PBS for 20 min and stained with western blue for 10 min according to the method of Mendonca et al. [15]. During the postirradiation incubation period cells were re-fed on days 11, 14

and 18, with the medium used on day 18 supplemented with the antimycotic patricin (0.5 µg/ml medium).

Plating efficiencies for unirradiated cells were calculated by dividing the average number of colonies in 10 dishes by the number of cells initially plated. Survival rates of irradiated cells were calculated by dividing the average number of colonies in 10 dishes by the average number of colonies in the control. Data for the transformation assay were obtained by controlling each flask and signing all blue-colored areas which were checked using a stereomicroscope to score only foci according to the description of Mendonca et al. [15]. The transformation frequency (TF) is expressed as:

$$TF = -\frac{\ln(N_0 / N)}{n_{surv}} \qquad (5)$$

where N is the total number of flasks, N_0 is the number of flasks without foci, and n_{surv} is the number of survivors per flask.

The range of observed cell densities was 21–42 survivors per cm². Since the transformation frequencies (TF) are cell density-dependent they were scaled to a standard density of 30 cells per cm² by application of the formula previously used by Sun et al. [16] and Bettega et al. [17]. This rescaled transformation frequency is in the following sections denoted by T.

Determination of cell transformation frequencies

At each dose, two or three sets of experiments were carried out and the empirical standard deviations were found to be in line with those of the binominal distribution. The data in terms of N and N_0 were, therefore, pooled before the transformation frequencies were calculated. There are only two mutually exclusive outcomes (a flask either contains transformed cells or not) in each trial (or flask) and the outcomes in the series of trials (or flasks) constitute independent events (i.e. the probability of finding transformed cells is the same in different flasks at specified dose). Therefore binomial statistics apply and the standard errors (SE) were calculated accordingly.

Results

The cytogenetic status of the CGL1 hybrid cells was examined in a total of 200 metaphases using FISH in situ painting with DNA probes specific for the target chromosomes 11 and 14. The data in Table 1 indicate the variability of the intercellular distribution of the target chromosomes. Excluding the markers for HeLa chromosome 11 [11] and chromosome 14 [10], only 73% or 80% of the analysed cells—dependent on the timing of cytogenetic analysis—contained four copies of each target chromosome, whereas 27% or 20% of the analysed cells, showed loss or gain of the target chromosomes, repectively. This result is remarkable, because as already mentioned the complete loss of one fibroblast chromosome 11 and one fibroblast chromosome 14 results in neoplastic transformation.

Table 1 Intercellular distribution of the target chromosomes 11 and 14 in CGL1 hybrid cells determined by FISH-painting	Time point of cytogenetic analysis	Cells scored	Intercellular distribution of target chromosomes		
			<8	8	>8
	Prior to transformation experiments	100	23	73	4
	After the transformation experiments	100	18	80	2

Table 2 Neoplastic transformation of CGL1 cells by 29 kV x-rays

Dose (Gy)	PE of control	Survival rate	Cells seeded	Survivors per flask	Survivors per cm^2	Total number of flasks (N)	Number of flasks with foci	Number of flasks without foci (N_o)	Transfer freq. per 10,000 cells	Transfer freq.[a] per 10,000 cells
0	0.924	1.000	2,500	2,310	31	110	4	106	0.16	0.16
1.02	0.824	0.907	3,000	2,241	30	60	17	43	1.5	1.5
1.02	0.860	0.787	3,000	2,031	21	60	189	41	1.9	1.8
2.04	0.969	0.475	4,000	1,840	25	50	22	28	3.2	2.9
2.04	0.950	0.521	4,000	1,980	26	50	24	26	3.3	3.1
3.06	0.906	0.423	6,000	2,298	31	40	24	16	4.0	4.0
3.06	0.846	0.547	6,000	2,778	37	40	27	13	4.0	4.4
3.57	0.956	0.334	7,000	2,230	30	40	26	14	4.7	4.7
3.57	0.900	0.356	7,000	2,240	30	40	28	12	5.4	5.4
4.08	0.924	0.411	8,000	3,040	41	30	24	6	5.3	5.9
4.08	0.957	0.277	8,000	2,120	28	40	28	12	5.7	5.6
4.08	0.956	0.301	8,000	2,300	31	30	23	7	6.3	6.4
5.10	0.846	0.226	10,000	1,910	26	30	22	8	6.9	6.5
5.10	0.900	0.246	10,000	2,210	29	30	25	5	8.1	8.0

[a] rescaled to 30 survivors/cm^2 [16]

Table 3 Neoplastic transformation of CGL1 cells by 220 kV x-rays

Dose (Gy)	PE of control	Survival rate	Cells seeded	Survivors per flask	Survivors per cm^2	Total number of flasks (N)	Number of flasks with foci	Number of flasks without foci (N_o)	Transfer freq. per 10 000 cells	Transfer freq.* per 10 000 cells
0	0.924	1.000	2500	2,310	31	110	4	106	0.16	0.16
1.09	0.824	0.860	3000	2,379	32	60	8	52	0.6	0.6
1.09	0.962	0.814	3,000	2,100	28	60	9	51	0.8	0.8
2.17	0.969	0.527	4,000	2,044	27	50	16	34	1.9	1.8
2.17	0.950	0.624	4,000	2,372	32	50	20	30	2.1	2.1
3.26	0.906	0.483	6,000	2,510	35	40	19	21	2.6	2.7
3.26	0.846	0.591	6,000	3,000	42	40	20	20	2.3	2.6
3.81	0.956	0.387	7,000	2,590	35	40	27	13	4.3	4.6
3.81	0.900	0.384	7,000	2,420	32	40	23	17	3.5	3.6
4.35	0.924	0.421	8,000	3,112	41	30	24	6	5.2	5.9
4.35	0.957	0.329	8,000	2,520	34	40	28	12	4.8	5.0
4.35	0.956	0.310	8,000	2,370	32	30	19	11	4.2	4.3
5.44	0.846	0.257	10,000	2,170	29	28	20	8	5.8	5.7
5.44	0.900	0.274	10,000	2,470	33	30	24	6	6.5	6.8

[a] re-scaled to 30 survivors/cm^2 [16].
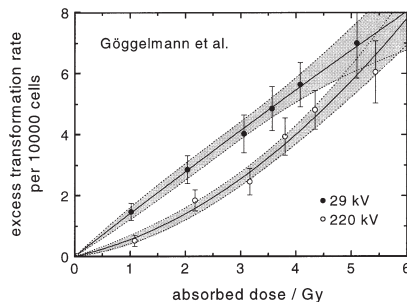
Fig. 2 Transformation frequency per 10,000 cells as a function of dose for 29 and 220 kV x-rays. The dots and the associated binomial standard error bars correspond to the data in Tables 2 and 3. The solid lines are the weighted least squares fits to the data. The dashed lines represent the borders of the standard error bands as calculated in terms of orthogonal parameters [18, 19]

Detailed results from the individual experiments of the transformation assay are given in Tables 2 and 3 for the 29 and 220 kV x-rays. The points in Fig. 2 represent the pooled data in Tables 2 and 3 for the transformation frequency per 10,000 cells (T) at the various doses. The standard error bars given correspond to the binomial distribution.

T in its dependence on dose has been fitted to the linear-quadratic model:

$$T = c + aD + bD^2 \tag{6}$$

For the 29 kV x-rays, and with the unit Gy for the absorbed dose, D, the resulting parameter estimates and their standard errors are:

$$T = (0.164 \pm 0.080) + (1.41 \pm 0.266)D$$
$$+ (-0.012 \pm 0.074)D^2 \tag{7}$$

For 220 kV x-rays the corresponding results are:

$$T = (0.155 \pm 0.080) + (0.394 \pm 0.180)D$$
$$+ (0.151 \pm 0.049)D^2 \qquad (8)$$

The weighted least squares regression curves that correspond to Eqs. 7 and 8 are shown in Fig. 2 as solid lines. The experiments with the two types of x-rays were performed simultaneously and they shared the same controls. It would, therefore, have been appropriate to perform a joint fit to obtain Eqs. 7 and 8. However, as it happened, the two independent fits provided very closely the same point estimate (and standard error) for the parameter $c=0.161\pm0.080$ and this estimate can, thus, be used as the joint value.

The standard error bands of the dose-effect relations cannot be derived from the standard errors of the parameters in Eqs. 7 and 8. The reason is that these parameters are correlated, so that their errors are not independent and cannot, therefore, be combined in the usual way, i.e. by summing the error squares, to quantify the uncertainty of T. Error bands for the dose-effect relations must, accordingly, be obtained by specific methods. The applicable methods range from Monte Carlo simulations to numerical procedures, either in terms of the *co-variances* of the model parameters or in terms of *orthogonal parameters*, i.e. parameters which are suitably transformed to become uncorrelated. A recently described method [18, 19] simplifies the use of orthogonal parameters considerably. It has here been applied to derive the standard error bands of the dose-effect relations. The results are given in Fig. 2 and in subsequent figures.

RBE of 29 kV x-rays relative to 220 kV x-rays

The RBE of 29 kV x-rays relative to 220 kV x-rays can be calculated as a function of absorbed dose, here chosen to be the dose of the mammography x-rays. The parameter estimates in Eqs. 7 and 8 and the method of orthogonal parameters provide the curves and standard error bands in Fig. 2. From these curves and error bands the estimate of the RBE and its dependence on dose are obtained as is shown in Fig. 3. The standard error band for the RBE results from combining the independent standard errors shown in Fig. 2. As also treated in [18, 19] this involves first a change from the uncertainty of the transformation rate at specified dose (vertical width of the error bands) to the uncertainty of the dose to reach the specified transformation rate (horizontal width of the error bands), and subsequently the combination of uncertainties by adding the squares of the relative errors. In some of the earlier analyses different and partly uninformative error estimates were given. The present procedure provides meaningful standard error bands. Even these are, as seen in Fig. 3, fairly broad.

The solid line represents the part of the estimated relation that corresponds to doses, both of the reference radiation 220 kV x-rays and of the 29 kV x-rays, but not
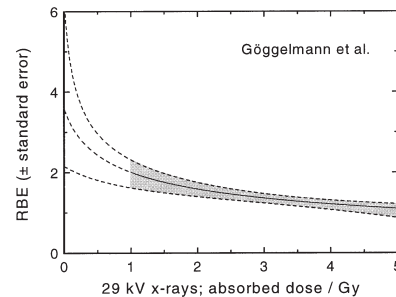
Fig. 3 The RBE of 29 relative to 220 kV x-rays as a function of the absorbed dose of 29 kV x-rays

below the smallest doses used in the experiments. The remainder of the curve represents an extrapolation in terms of the linear-quadratic model. The lowest dose, 1 Gy, of the 29 kV x-rays corresponds, according to the least square fit, to the dose 2 Gy of the reference radiation, i.e. the 220 kV x-rays. The point estimate of the RBE and standard error at this dose is 2±0.3; the 95% confidence interval is 1.4–2.6. The extrapolation to zero dose provides a point estimate of 3.4, and a confidence interval ranging from less than 2 to large values.

Comparison to the earlier results by Frankenberg et al. [3]

Figure 4 permits a comparison of the present results with the corresponding earlier observations published by Frankenberg et al. [3]. The comparison shows for the two experimental investigations a striking discrepancy of the results. In spite of the identical design of the two experimental studies the outcome is widely divergent. Although the standard error bands in the earlier experiment are broad, it is evident—even without statistical testing—that the transformation rates in the earlier experiment were substantially lower than in the experiments now reported. A minor difference would have been expected, because Frankenberg et al. have standardized their results to 50 surviving cells per cm^2 (against 30 cells per cm^2 in the present study); according to Sun et al. [16] this can explain a difference of about 20%. In actuality the difference amounts, for standard x-rays to a factor between 3 and 5. Apart from this striking discrepancy the decisive point is that the difference between the dose relations for the two types of x-rays is far less in the current experiments than in the earlier publication.

For a quantitative comparison of the results and their uncertainties the same statistical techniques as used in the preceding section have been applied to the earlier data. The analysis results, again with the unit Gy, in the estimated dose-effect relations for the 29 kV x-rays:

180
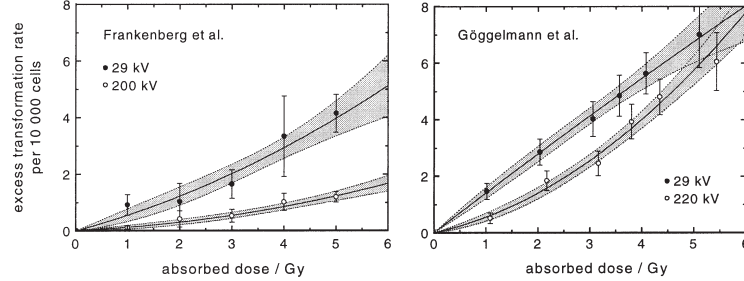
Fig. 4 Pooled transformation frequency per 10,000 cells as a function of dose for 29 kV and 200 kV x-rays observed by Frankenberg et al. [3] plotted analogously to the present data as a function of dose for 29 kV and 220 kV x-rays. The dots and the associated standard error bars (binomial rescaled to pooled empirical standard errors) correspond to the data in Table 4. The solid lines are the weighted least squares fits to the data. The dashed lines represent the borders of the standard error bands as calculated in terms of orthogonal parameters [18, 19]

Table 4 Parameter estimates (with standard errors) for the linear-quadratic dose response relations (with standard errors) for neoplastic transformation of CGL1 cells obtained by parallel analysis of the present data and the earlier data from Frankenberg et al. [3]

Parameter	Present data		Frankenberg et al. [3]	
	29 kV x-rays	220 kV x-rays	29 kV x-rays	200 kV x-rays
c	0.164±0.080	0.155±0.080	0.161±0.0366	0.1575±0.036
a/Gy	1.410±0.266	0.394±0.180	0.493±0.291	0.0754±0.080
b/Gy^2	−0.012±0.074	0.151±0.049	0.0605±0.072	0.0334±0.0182

$$T = (0.161 \pm 0.0366) + (0.493 \pm 0.291)D$$
$$+(0.0605 \pm 0.072)D^2 \tag{9}$$

while the result for the 200 kV x-rays is:

$$T = (0.1575 \pm 0.036) + (0.0754 \pm 0.080)D$$
$$+(0.0334 \pm 0.0182)D^2 \tag{10}$$

For easier comparison, the parameter estimates and standard errors are listed jointly in Table 4.

The far lower transformation yields in the earlier experiments appear to be due to different and inadequate culture conditions. In the experiments by Frankenberg et al. [3] there was, during the 21 day post-irradiation incubation, only 1 single exchange of medium after 10 days. In the present experiments the cells were re-fed on days 11, 14, and 18. Recent experiments in Redpath's group have been performed with twice weekly re-feeding of the cell cultures after the first week of the post-irradiation incubation period [20, 21]. This attests to the fact that frequent change of medium is a critical point within the culture conditions of CGL1 cells.

In order to quantify the effect of the mode of medium change, additional experiments have been carried out in the present study with 4.35 Gy of 220 kV x-rays. In these experiments Frankenberg's and our culture conditions were examined in parallel. As demonstrated in Table 5, the observed yields of neoplastic transformations in the CGL1 cells do not differ significantly when the experiments are repeated with adequate culture conditions, while uncontrolled differences by a factor in excess of 10
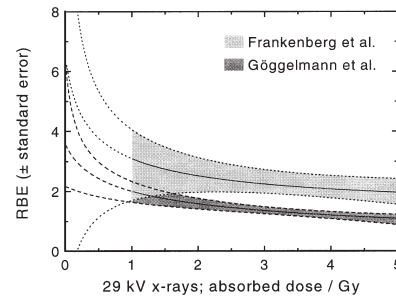
Fig. 5 The RBE of 29 kV x-rays relative to 200 kV or 220 kV x-rays. The region between the two dashed lines indicates standard errors obtained by Monte-Carlo simulation of 1000 RBE values at each of 18 dose points. These data of Frankenberg et al. [3] are analogously plotted to the data given in Fig. 3

were obtained under the culture conditions described by Frankenberg et al. [3].

Figure 5 gives for the data by Frankenberg et al. [3] the RBE vs. absorbed dose of the mammography radiation in the same type of diagram as in Fig. 3. For easy comparison the result from the present experiment—i.e. the diagram in Fig. 3—is superimposed on the earlier result. It is apparent that the earlier experiments suggest an RBE of 29 kV x-rays that is—especially at higher doses—substantially in excess of the one obtained in the current experiment. However it is apparent, in view of the

Table 5 Neoplastic transformation of CGL1 cells by 4.35 Gy of 220 kV x-rays

Dose (Gy)	PE of control	Sur-vival rate	Cells seeded	Culture condi-tion	Sur-vivors per flask	Sur-vivors per cm^2	Total number of flasks (N)	Number of flasks with foci	Number of flasks without foci (N_o)	Transfer freq. per 10,000 cells	Transfer freq.[a] per 10,000 cells
0	0.924	1.000	2,500	present	2,310	31	110	4	106	0.16	0.16
4.35	0.880	0.372	8,000	[3]	2,620	35	30	5	25	0.7	0.7
			8,000	present	2,620	35	30	22	8	5.0	5.3
			40,000	[3]	13,100	175	30	1	29	0.026	0.053
			40,000	present	13,100	175	30	28	2	2.1	4.3
4.35	0.912	0.332	8,000	[3]	2,420	32	33	2	31	0.26	0.27
			8,000	present	2,420	32	30	22	8	5.5	5.7
			40,000	[3]	12,100	161	27	5	22	0.18	0.36
			40,000	present	12,100	161	30	29	1	2.8	5.6

Culture condition during post-irradiation incubation. As in [3] cells were re-fed only on day 11, or in the present study, cells were re-fed on days 11, 14 and 18

[a] re-scaled to 30 survivors/cm^2 [16].

results in Table 5, that this finding is an artefact of the inadequate culture conditions.

Discussion

Most of the published information on radiation-induced neoplastic transformation of cells in culture relates to rodent-derived fibroblasts [1]. A major part of the quantitative studies has been performed with the clone 8 of C3H/10T1/2 derived from a mouse embryo by Reznikoff et al. [22]. It was, therefore, a significant new development when, recently, similar research on neoplastic transformations became possible with human hybrid cell lines [7, 23, 24]. There was, accordingly, considerable interest when Frankenberg et al. reported results determined with the new method on high RBE values for mammography x-rays [3, 4, 5]. The results seemed to considerably exceed the RBE values for mammography x-rays for transformation of C3H/10T1/2 cells subsequently reported by Brenner et al. [25]. They were also at variance with biophysical and microsimetric assessments [26, 27, 28] which all predicted RBE values of the mammography x-rays vs. conventional x-rays not larger than about 2.

In the present study, we have utilized the neoplastic transformation of the human hybrid cells CGL1 to reassess under well defined experimental conditions the RBE of 29 kV x-rays relative to 220 kV x-rays. An advantage of the CGL1 cell system lies in the fact that growth to confluence is not required for observation of neoplastically transformed colonies, and that the yields of such colonies can adequately be expressed as transformations per surviving cells [24]. On the other hand, it has been shown in the present study that culture conditions in the post-irradiation period are highly critical, and that infrequent medium change, as applied in the experiments by Frankenberg et al. [3, 4, 5], causes extreme fluctuations of the transformation rates.

The results of the present study are, indeed, strikingly different from those reported for the earlier investigation and they appear to invalidate the earlier reports. In particular there is a very marked difference of the present results for the conventional x-rays to the earlier findings with transformation rates which were lower by a factor of 3–5.

While the RBE values of the mammography x-rays are substantially smaller in the present study than the earlier values, they are nevertheless higher than the results with C3H/10T1/2 cells [25] and the microsimetric analyses [27, 28] would suggest. However, in spite of the considerably more narrow error bands in the present study, the findings are not statistically inconsistent with a predicted value of less than 2 for the low dose RBE of the mammography radiation.

The experiments that have here been reported were designed to parallel, in essence, the earlier study which indicated high RBE values for the 29 kV x-rays. Accordingly, they employed fairly high doses, 1 Gy being the lowest dose value for the mammography x-rays. Together with the assessment of the critical impact of inadequate feeding of the cells during the expression period, the study design was sufficient to invalidate the conclusions from the earlier investigation. However, added low-dose experiments would be required to arrive at more precise estimates of the low-dose RBE of mammography x-rays against conventional x-rays.

References

1. ICRP (1991) 1990 Recommendations of the International Commission on Radiological Protection. Publication 60, Annals of the ICRP, Vol. 21. Pergamon Press, Oxford
2. Schmid E, Regulla D, Kramer HM, Harder D (2002) The effect of 29 kV X-rays on the dose response of chromosome aberrations in human lymphocytes. Radiat Res 159:771–777
3. Frankenberg D, Kelnhofer K, Bär K, Frankenberg-Schwager M (2002) Enhanced neoplastic transformation by mammography

X-rays relative to 200 kVp X-rays. Indication for a strong dependence on photon energy of the RBE_M for various endpoints. Radiat Res 157:99–105. Erratum (2002) Radiat Res 158:126

4. Frankenberg D, Kelnhofer K, Garg I, Bär K, Frankenberg-Schwager M (2002) Enhanced mutation and neoplastic transformation in human cells by 29 kV$_p$ relative to 200 kV$_p$ X-rays indicating a strong dependence of RBE on photon energy. Radiat Prot Dosim 99:261–264

5. Frankenberg D, Frankenberg-Schwager M, Garg I et al. (2002) Mutation induction and neoplastic transformation in human and human-hamster hybrid cells: dependence on photon energy and modulation in the low-dose range. J Radiol Prot 22:A17–20

6. Schmid E (2002) Commentary. Is there reliable experimental evidence for a low-dose RBE of about 4 for mammography X rays relative to 200 kV X rays? Radiat Res 158:778–781

7. Stanbridge EJ, Flandermeyer RR, Daniels DW, Nelson-Rees WA (1981) Specific chromosome loss associated with expression of tumorigenicity in human cell hybrids. Somat Cell Genet 7:699–712

8. Der CJ, Stanbridge EJ (1981) A tumor-specific membrane phosphoprotein marker in human cell hybrids. Cell 26:429–438

9. Mendonca MS, Antoniono RJ, Latham KM, Stanbridge EJ, Redpath JL (1991) Characterization of intestinal alkaline phosphatase expression and the tumorigenic potential of gamma-irradiated HeLa x fibroblast cell hybrids. Cancer Res 51:4455–4462

10. Mendonca MS, Howard K, Fasching CL, Farington DL, Desmond LA, Stanbridge EJ, Redpath JL (1998) Loss of suppressor loci on chromosomes 11 and 14 may be required for radiation-induced neoplastic transformation of HeLa x skin fibroblasts human cell hybrids. Radiat Res 149:246–255

11. Mendonca MS, Fasching CL, Srivatsan ES, Stanbridge EJ, Redpath JL (1995) Loss of aputative tumor suppressor locus after gamma-ray-induced neoplastic transformation of HeLa x skin fibroblast human cell hybrids. Radiat Res 143:34–44

12. Schmid E, Zitzelsberger H, Braselmann H, Gray JW, Bauchinger M (1992) Radiation-induced chromosome aberrations analysed by fluorescence in situ hybridization with a triple combination of composite whole chromosome-specific DNA probes. Int J Radiat Biol 62:673–678

13. EUR 16263 (1996) European protocol on dosimetry in mammography. European Commission, Brussels

14. Hubbell JH, Seltzer S (1996) Tables of X-ray mass attentuation coefficients and mass energy-absorption coefficients from 1 keV to 20 MeV for elements Z=1 to 92 and 48 additional substances of dosimetric interest. NISTIR 5632, Gaithersburg. http://physics.nist.gov/PhysRefData/XrayMassCoef/cover.html

15. Mendonca MS, Antoniono JR, Sun C, Redpath JL (1992) A simplified and rapid staining method for the HeLa x skin fibroblast human hybrid cell neoplastic transformation assays. Radiat Res 131:345–350

16. Sun C, Redpath JL, Colman M, Stanbridge EJ (1988) Further studies on the radiation-induced expression of a tumor-specific antigen in human cell hybrids. Radiat Res 114:84–93

17. Bettega D, Calzolari P, Piazzolla A, Tallone L, Redpath JL (1997) Alpha-particle-induced neoplastic transformation in synchronized hybrid cells of HeLa and human skin fibroblasts. Int J Radiat Biol 72:523–529

18. Kellerer AM (2003) Error bands for the linear-quadratic dose-effect relation. Radiat Environ Biophys 42:77–85

19. Kellerer AM (2003) Error bands for the linear-quadratic dose-effect relation—A simplified use of orthogonal polynomials. Technical Report, University of Munich, SBI 222

20. Redpath JL, Liang D, Taylor TH, Christie C, Elmore E (2001) The shape of the dose-response curve for radiation-induced neoplastic transformation in vitro: evidence for an adaptive response against neoplastic transformation at low doses of low-LET radiation. Radiat Res 156:700–707

21. Redpath JL, Lu Q, Molloi S, Elmore E (2003) Low doses of diagnostic energy X-rays protect against neoplastic transformation in vitro. Int J Radiat Biol 79:235–240

22. Reznikoff CA, Bronkow DW, Heidelberger C (1973) Establishment and characterization of a cloned line of C3H mouse embryo cells sensitive to postconfluence inhibition of division. Cancer Res 33:3231–3238

23. Stanbridge EJ, Der CJ, Doersen CJ, Nishime RY, Peehl DM, Weissman BE, Wilkinson JE (1982) Human cell hybrids: analysis of transformation and tumorigenicity. Science 215:242–259

24. Redpath JL, Sun C, Colman M, Stanbridge EJ (1987) Neoplastic transformation of human hybrid cells by γ radiation: a quantitative assay. Radiat Res 110:468–472

25. Brenner DJ, Sawant SG, Hande MP, Miller RC, Elliston CD, Fu Z, Randers-Pehrson G, Marino SA (2002) Routine screening mammography: how important is the radiation-risk side of the benefit-risk equation? Int J Radiat Biol 78:1065–1067

26. Brenner DJ, Amols HI (1989) Enhanced risk from low-energy screen-film mammography X rays. Br J Radiol 62:910–914

27. Kellerer AM (2002) Electron spectra and the RBE of X rays. Radiat Res 158:13–22

28. Kellerer AM, Chen J (2003) Comparative microdosimetry of photoelectrons and Compton electrons: an analysis in terms of generalized proximity functions. Radiat Res 160:324–333

7. Walsh L, Rühm W & Kellerer AM. Cancer risk estimates for γ-rays with regard to organ specific doses Part I: All solid cancers combined. Radiat. Environ. Biophys. 43, 145-151, 2004

ORIGINAL PAPER

Linda Walsh · Werner Rühm · Albrecht M. Kellerer

Cancer risk estimates for gamma-rays with regard to organ-specific doses

Part I: All solid cancers combined

Abstract A previous analysis of the solid cancer mortality data for 1950–1990 from the Japanese life-span study of the A-bomb survivors has assessed the solid cancer risk coefficients for γ-rays in terms of the low dose risk coefficient ERR/Gy, i.e. the initial slope of the ERR vs. dose relation, and also in terms of the more precisely estimated intermediate dose risk coefficient, $ERR(D_1)/D_1$, for a reference dose, D_1, which was chosen to be 1 Gy. The computations were performed for tentatively assumed values 20–50 of the neutron RBE against the reference dose and in terms of *organ-averaged doses*, rather than the traditionally applied colon doses. The resulting risk estimate for a dose of 1 Gy was about half as large as the most recent UNSCEAR estimate. The present assessment repeats the earlier analysis with two major extensions. It parallels computations based on *organ-average doses* with computations based on *organ-specific doses* and it updates the previous results by using the cancer mortality data for 1950–1997 which have recently been made available. With an assumed neutron RBE of 35, the resulting intermediate dose estimate of the lifetime attributable risk (*LAR*) for solid cancer mortality for a working population (ages 25–65 years) is 0.059/Gy with the *attained-age model*, and 0.044/Gy with the *age-at-exposure model*. For a population of all ages, 0.055/Gy is obtained with the *attained-age model* and 0.073/Gy with the *age-at-exposure model*. These values are up to about 20% higher than those obtained in the previous analysis with the 1950–1990 data. However, considerably more curvature in the dose-effect relation is now supported by the computations. A dose and dose-rate reduction factor *DDREF*=2 is now much more in line with the data than before. With this factor the *LAR* for a working population is—averaged over the age-at-exposure and the age-at-
tained model—equal to 0.026/Gy. This is only half as large as the current ICRP estimate which is also based on the assumption *DDREF*=2.

Introduction

The exposure of the human body to ionising radiation is never completely uniform. The high energy γ-radiation from the A-bombs has produced only slightly different doses in the various organs, depending on their depth in the body, but for the fast neutron component of the radiation the differences are substantial. The specification of doses to the A-bomb survivors, for purposes such as the analysis of total cancer mortality or incidence has, accordingly, not been trivial. In keeping with the convention utilised in their fundamental series of assessments [1, 2], the Radiation Effects Research Foundation (RERF) continues to use the γ-ray absorbed dose to one of the deepest lying organs, the colon, plus the neutron absorbed dose to the colon multiplied by 10 as "weighted dose" in the computation of risks for all solid cancers combined.

Continuity in the method of dose specification is essential in order to ensure comparability of the increasingly complete results that are obtained as the follow-up of the life-span study of the A-bomb survivors continues. However, as this study approaches its ultimate conclusion, it is also important to explore those issues that can still be refined. The availability of the data that are now extended to the year 1997 [2] and the recent reassessment of the neutron dosimetry [3] make this a suitable occasion to examine the impact of a more detailed dosimetric specification.

In a previous paper [4] it has been pointed out that reference to the colon dose, underestimates the average γ-ray dose to all relevant organs by only about 8.5%. On the other hand, it was noted that for neutrons the reference to the colon is not satisfactory. The organ averaging—with weight factors accounting for the risk contribution of individual tumour sites [5]—results in neutron absorbed doses that are about twice as large as those to the colon.

L. Walsh (✉) · W. Rühm · A. M. Kellerer
Radiobiological Institute,
University of Munich,
Schillerstrasse 42, 80336 Munich, Germany
e-mail: Linda.Walsh@LRZ.uni-muenchen.de
Tel.: +49-89-218075821
Fax: +49-89-218075840

Table 1 Sites with more than 100 cancer deaths in the report 12 [1] solid cancer mortality data of 1950–1990 compared with the report 13 [2] data of 1950–1997 and the organ-specific dose applied to these sites in the computation of risk coefficients for all solid cancers combined

Sites with >100 deaths	Organ specific dose applied to the mortality data	Number of cancer deaths (1950–1990)	Number of cancer deaths (1950–1997)	Neutron adjustment factor	Gamma adjustment factor
Female breast	Breast	211	272	3.85	1.17
Oesophagus	Marrow	234	291	2.14	1.1
Lung	Lung	939	1264	1.91	1.09
Liver	Liver	893	1236	1.66	1.05
Gallbladder	Liver	228	328	1.66	1.05
Stomach	Stomach	2529	2867	1.54	1.02
Rectum	Bladder	298	370	1.17	1.05
Bladder	Bladder	119	150	1.17	1.05
Colon	Colon	347	478	1	1
Pancreas	Pancreas	297	407	0.94	0.98
Ovary	Ovary	120	136	0.83	1.01
Uterus	Uterus	476	518	0.7	1

The last two columns give the Hiroshima adult dose adjustment multiplication factors for conversion from colon dose to organ-specific dose. The order of organs in the table is based on their depth in the body.

For surface organs, such as the female breast, neutron absorbed doses can be nearly 4 times larger than those to the colon (see Table 1). It was likewise noted that, at least at low doses, the neutron RBE appears, from the available radiobiological evidence, to be substantially larger than 10, which increases the importance of the correct specification of the neutron dose contribution.

The previous articles [4, 5] employed the *organ-averaged doses*. The risk coefficient, *ERR*/Gy, for photons was derived in terms of a linear-quadratic dose dependence for γ-rays and a linear dose dependence for neutrons (LQ-L model) for a range of tentatively assumed RBE values of between 20 and 50. Both the *age-at-exposure* and the *age-attained* models were employed. In addition to estimating the *initial slope*, α, in the linear-quadratic dose dependence, with its comparatively large relative error, the *reference slope*, *c*, was determined which equals the ratio $ERR(D_1)/D_1 = \alpha + \beta D_1$ in the LQ-model, with D_1 set at 1 Gy. Using the two parameters α and *c* or the two parameters α and β is, of course, equivalent, but α and *c* have the advantage that they are nearly orthogonal, i.e. independent. The relative standard error of *c* is considerably smaller than that of α, and is comparable to that of the *slope*, α_L, *in a linear fit* to the data. The parameter *c* is similar to α_L, but it has the advantage that—where the LQ-model applies—it does not inherently depend on the dose cut-off that is chosen in the fit to the data. The slope, α_L, in a linear fit lacks this invariance; if there is positive curvature in the dose relation, the estimate of α_L will increase with increasing dose cut-off.

The present assessment updates the previous results by using the cancer mortality data for 1950–1997 which have recently been made available. In addition it extends the earlier assessment by applying, in addition to the organ-averaged doses, also the organ-specific doses.

Details of the modelling procedures

Parallel computations in terms of organ-averaged and organ-specific doses provide a test to the suitability of the application of the *organ-averaged dose* in risk estimation for all solid cancers combined. The present analysis applies the *organ-specific dose* to sites with more than 100 solid cancer deaths in the older mortality data set (Table X, p 15 in [1]). Table 1 shows the organ sites specially considered here and the *organ-specific doses* that were applied in the computation of risk coefficients for all solid cancers combined. The multiplication factors for conversion from the colon doses, given in the solid cancer mortality data 1950–1997, to organ-specific doses were taken from the publicly available (http://www.rerf.or.jp) data set *ds86adjf.dat*. These dose adjustment factors depend on radiation type, age at exposure and city; they are included for Hiroshima adults and both radiation types in Table 1. The remaining sites associated with less than 100 solid cancer deaths and, in most cases, with no available dose adjustment factor, include a wide range of organs and tissues; they were accordingly assigned the *organ-averaged doses*.

As stated above, *organ-specific doses* were applied to the grouped publicly available solid cancer mortality data (file name: *r13mort.dat*). To do this is not entirely trivial. Pierce et al. [1] noted that "It is impossible to use more specific organ doses for solid cancers as a class, since there is no designated organ for those not dying of cancer." However, this difficulty is resolved here by formally treating each person as a set of 13 sub-units at risk, each belonging to 1 organ category. In terms of programming this meant creating a new organ category at the lowest level of the data structure where there are a total of 37,060 original data groups (for combinations of city, gender, age attained, age at exposure and colon dose category), each group containing the number of cases of death from different types of solid cancer. For each of these original data records, 13 new organ-specific records were created

to contain the numbers of deaths for each cancer type and the relevant organ-specific doses and, solely for numerical cross checking purposes, the original colon doses. This new data file was created, in terms of a specially written program, with a total of 481,780 new records (>300 Mb). The first 12 organ groups represented the specific sites with more than 100 deaths (as detailed in Table 1), while data group 13 contained the remaining widely varying sites which were assigned the *organ-averaged doses*. The risk coefficients were then computed in EPICURE-AMFIT [6] by the maximum likelihood Poisson regression method with baseline cancer rate subtraction achieved through stratification on gender, age attained, age at exposure and the new organ category. In this stratification mode, the fitting procedure via AMFIT emulates a partial likelihood procedure (D. Pierce, private communication).

The models applied here were the same as those already considered and explained in detail [4] with γ-ray absorbed dose, D_γ, and a neutron absorbed dose, D_n, based on the dosimetry system DS86 [7]. The only differences between [4] and the present work is that the input data cover an extra 7 years of follow-up and that the *organ-specific doses* are used in part of the calculations. The excess relative risk is factorised into a function of dose and a modifying function that depends on the variables gender (s) and age at exposure (e) or age attained (a):

$$ERR\left(D_\gamma, D_n, s, e, a\right) = \mu(s, e, a)\, \rho\left(D_\gamma, D_n\right) \quad (1)$$

with the modifying functions for the *age-attained* and the *age-at-exposure models*:

$$\mu(s, a) = \exp\left(-g \cdot (a - 60)\right) \cdot (1 \pm s) \quad (2)$$

$$\mu(s, e) = \exp\left(-g \cdot (e - 30)\right) \cdot (1 \pm s)\, (+\text{for females},$$
$$-\text{ for males}) \quad (3)$$

and with the dose-dependent term:

$$\rho\left(D_\gamma, D_n\right) = \alpha\left(D_\gamma - D_\gamma^2\right) + c\left(R_1 D_n + D_\gamma^2\right) \quad (4)$$

As explained in the earlier paper [4], this dose-dependent term results from the relation:

$$\rho\left(D_\gamma, D_n\right) = \alpha\left(D_\gamma + R_M D_n\right) + \beta D_\gamma^2 \quad (5)$$

by using in the formula the neutron RBE, R_1, against an intermediate γ-ray *reference dose* D_1, rather than the low dose limit, R_M, of the neutron RBE, and by using the *reference slope*, $c = \rho(D_1, 0)/D_1$, i.e. the slope to the effect level at D_1, instead of β.

R_1 is used, instead of R_M, because animal experiments do not provide reliable values of the neutron RBE against γ-ray doses less than about 1 Gy. As stated, using the parameter c, instead of β, provides the same dose dependence. However, it has the advantage of providing the uncertainty of c, i.e. the effect level at dose D_1, while this information cannot be obtained from the parameters α and β and their standard errors.

The parameters α and c are not perfectly orthogonal, but the standard error of c or of the effect level, cD_1, is—together with the standard error of the initial slope, α,—sufficiently informative to judge the uncertainty of the fit to the data.[1] The initial slope, α, and its uncertainty are of specific interest with regard to low dose risk estimates. The parameter c and its uncertainty, on the other hand, are most relevant to the assessment of probability of causation at higher doses. For this purpose it is desirable to assess risks on an organ-specific basis, even though some details have already been presented [1, 2]. These previous analyses did not consider the influence of the assumed RBE values on the risk estimates for the various organs at different depths in the body. The modified data set described here is highly suitable for such an analysis, details of which will be presented in a subsequent companion article [9].

Although past and current RERF [1, 2] analyses of the LSS mortality data use an RBE value for the neutrons of 10, a different approach is chosen here with values of between 20 and 50, and a central value of 35 being in line with animal experiments [4]. It may be noted that this central value is compatible with current ICRP radiation weighting factor recommendations [10] which correspond to an RBE=31 of the neutrons alone at 1 km from the Hiroshima hypocenter, if the role of secondary γ-rays produced by interaction of the incident neutrons with the human body is accounted for separately [11, 12]. In order to illustrate the potential impact of the neutrons, some of the graphics have been extended to include extreme values of 100.

Numerical results for pooled solid cancers in terms of *ERR*

Table 2 (for the *age-at-exposure* model) and Table 3 (for the *age-attained* model) show the main results of the computations. The results which are directly comparable to [4], apart from the extra follow-up period, are given under *"organ-averaged dose"*, while the new computations are given in the table sections marked *"organ-specific dose* applied to organs with >100 tumours".

Results for α and c from Tables 2 and 3 are given and extended in Figs. 1 (for the *age-at-exposure* model) and 2 (for the *age-attained* model) as a function of R_1, the RBE of neutrons against an intermediate reference dose $D_1 = 1$ Gy of γ-rays. The associated lifetime attributable risk (*LAR*) for solid cancer mortality is added on the right ordinate axis of the figures. The method applied for the

---

[1] As has been discussed earlier [4, 8], a value of the reference dose D_1 can be chosen that makes the parameters α and c strictly orthogonal. The estimates of α and c and their standard errors then permit the determination of the standard error of the effect level at any dose. Orthogonality of α and c, for the A-bomb survivors life span study (LSS) data up to 2 Gy, would be achieved with a reference dose 1.2 Gy. However, it is convenient to use the same standard reference dose for different data sets. From this point of view the plain choice $D_1 = 1$ Gy appears natural.

Table 2 Results of the maximum likelihood fits to the solid cancer mortality data

	$\alpha(\text{Gy}^{-1})$	$c(\text{Gy}^{-1})$	c/α_{min}	g	s	Deviance
Solid cancer mortality 1950–1997						
Age-at-exposure model						
Colon dose (df=33,952)						
R=10	0.33 (0.10–0.55)	0.51 (0.38–0.64)	4.4	0.0463	0.2630	13562.8
Organ-averaged dose (df=33,952)						
R_1=20	0.27 (0.05–0.48)	0.41 (0.31–0.52)	7.2	0.0453	0.2603	13562.9
R_1=35	0.24 (0.03–0.46)	0.37 (0.27–0.46)	11.4	0.0443	0.2612	13563.1
R_1=50	0.22 (0.01–0.44)	0.33 (0.24–0.41)	31.8	0.0435	0.2624	13563.5
Organ-specific dose applied to organs with >100 tumours (df=441,424)						
R_1=20	0.27 (0.05–0.5)	0.45 (0.34–0.57)	8.4	0.0458	0.2669	35701.5
R_1=35	0.26 (0.03–0.48)	0.41 (0.31–0.51)	12.1	0.0450	0.2677	35700.3
R_1=50	0.24 (0.01–0.46)	0.37 (0.28–0.46)	23.4	0.0444	0.2686	35699.7

The estimated parameters relate to acute γ-irradiation, α is the initial slope (ERR_{30}/D_γ for the age at exposure model), c is the slope to ERR_{30} due to 1 Gy γ-rays; it corresponds closely to the dose coefficient in a linear dose model.

The 95% confidence limits are given in brackets, c/α_{min} (=1+θ_{max} in [13]) is the largest *DDREF* consistent with the data on the 95% confidence level, g and s are the age and the gender modifiers (see Eqs. 2 and 3).

The central estimates for c/α are from top to bottom 1.55 and 1.52, 1.54, 1.5 and 1.67, 1.58, 1.54 for rows 1–7 in the table.

conversion of *ERR* to *LAR* has already been fully described [14].

As seen in Tables 2 and 3, the age-at-exposure model (*e*-model) is associated with somewhat smaller deviance than the age-attained model (*a*-model). The age-at-exposure and the age-attained effect modifiers are not actually alternatives, but may jointly apply with relative weights that are difficult to assess due to the statistical limitations of the data. Which of the two age modifiers fits the data best, is therefore, a somewhat academic question. Since the two models are not nested, it is also a question that can not be readily answered in terms of the usual concepts of statistical significance.[2]

Discussion

Numerical cross checks

Two numerical cross checks were carried out:

1. The results from [4] were recomputed and reliably reproduced by selecting the time periods to 1990 in the standard data set (*R13mort.dat*).

[2] Akaike [15] has developed an alternative criterion for comparing models based on information theory. This is the Akaike Information Criterion score (AIC) which is the deviance plus twice the number of fit parameters—the model with the lowest AIC score is most likely to be correct, with the difference in AIC score giving information on how much more likely one model is compared to the other. From Tables 2 and 3 it can be seen that the differences in AIC score for analogous *a* and *e* models are between 12 and 13 providing strong evidence in favour of the age-at-exposure model over the age-attained model. For this reason—and also because the results are very similar for the two models—only the age-at-exposure model results will be employed in a subsequent paper [9] that deals with the individual organ risk estimates.

2. The results in Tables 2 and 3 under the section marked *organ-averaged doses* and computed with the full time span in the standard data set (*r13mort.dat*), were also recomputed and reliably reproduced by replacing, in the new data file for the additional stratification on organ category, the 13 organ-specific doses by the average organ doses. For the R_1 values of 20, 35, and 50 the resulting deviancies were—now also with 441,424 degrees of freedom—35,708.7, 35,708.9 and 35,709.3 for *the age-at-exposure* model, and 35,721.4, 35,721.2, and 35,721.3 for *the age-attained* model. The associated changes in deviance are between 7.2 and 9.6, with the lower deviance values being associated with the organ-specific dose data set.

Effect of additional follow-up

Only the data obtained in terms of the organ-averaged doses can be directly compared to the earlier results [4]. The reference slopes are now slightly lower than the earlier values for the age-at-exposure model (for example, for R_1=35 the earlier value was 0.38/Gy and is now 0.37/Gy), while they are larger by about a standard error range, for the age-attained model (for example, for R_1=35 the earlier value was 0.36/Gy and it is now 0.42/Gy). For both models there is now substantially more evidence for positive curvature of the dose-effect relation.

The degree of curvature indicated by the data can be seen in Figs. 1 and 2, from the extent to which the long-dashed line (representing the estimate of the initial slope, α) and the solid line (the *ERR* for solid cancer mortality due to an acute γ-ray dose of 1 Gy, i.e. the reference slope, c, which corresponds closely to the dose coefficient, α_L, in a linear dose model) deviate from each other. A greater deviation is indicative of more curvature in the dose response. The top diagrams (labelled a) in Figs. 1

Table 3 Results of the maximum likelihood fits to the solid cancer mortality data

Solid cancer mortality 1950–1997

Age-attained model

	$\alpha(\text{Gy}^{-1})$	$c(\text{Gy}^{-1})$	c/α_{min}	g	s	Deviance
Colon dose (df=33,952)						
R=10	0.33 (0.06–0.59)	0.60 (0.47–0.73)	8.1	0.0339	0.2688	13575.7
Organ-averaged dose (df=33,952)						
R_1=20	0.26 (0.01–0.51)	0.48 (0.37–0.58)	54.7	0.0337	0.2668	13575.6
R_1=35	0.23 (-0.02–0.48)	0.42 (0.33–0.51)	∞	0.0334	0.2687	13575.4
R_1=50	0.20 (-0.04–0.45)	0.37 (0.29–0.46)	∞	0.0332	0.2705	13575.5
Organ-specific dose applied to organs with >100 tumours (df=441,424)						
R_1=20	0.27 (0.00–0.53)	0.53 (0.42–0.64)	∞	0.0336	0.2759	35714.5
R_1=35	0.24 (-0.02–0.50)	0.47 (0.37–0.58)	∞	0.0333	0.2787	35713.2
R_1=50	0.22 (-0.04–0.48)	0.43 (0.34–0.52)	∞	0.0330	0.2812	35712.5

The estimated parameters relate to acute γ-irradiation, α is the initial slope (ERR_{60}/D_γ for the age attained model), c is the slope to ERR_{60} due to 1 Gy γ-rays; it corresponds closely to the dose coefficient in a linear dose model.

The 95% confidence limits are given in brackets, c/α_{min} (=1+θ_{max} in [13]) is the largest *DDREF* consistent with the data on the 95% confidence level, g and s are the age and the gender modifiers (see Eqs. 2 and 3).

The central estimates for c/α are from top to bottom 1.82 and 1.85, 1.83, 1.85 and 1.96, 1.96, 1.95 for rows 1–7 in the table.
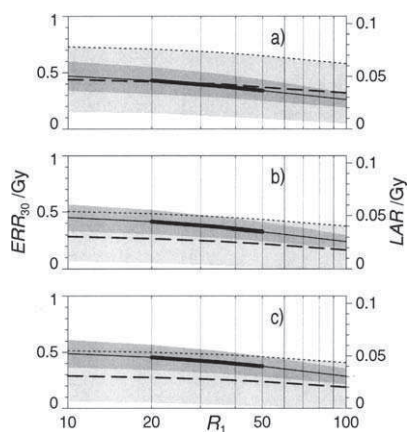
Fig. 1 A*ge-at-exposure* model. **a** For report 12 data (1950–1990) [1] with organ-averaged doses, graphics reproduced from [4]. **b** For report 13 data (1950–1997) [2] with organ-averaged doses. **c** For report 13 data (1950–1997) [2] with organ-specific doses. The *solid lines* and the *dark shaded bands* represent the parameter c, i.e. the *ERR* for solid cancer mortality due to an acute γ-ray dose of 1 Gy and its 95%-confidence region. The *long-dashed lines* and the *light shaded bands* give the estimate of the initial slope, α, and its 95%-confidence region in a linear-quadratic dose dependence for the γ-rays. The upper limit of the confidence region for α is emphasised with a *dotted line* since the associated shading is partially obscured in panels **b** and **c** by the darker shading associated with c. The results are given as functions of the assumed neutron RBE, R_1, vs. an acute γ-ray dose 1 Gy. The *right ordinate* gives the same quantities expressed in terms of the lifetime attributable risk of mortality for a population of working ages. The confidence bands express only the statistical uncertainty in the *ERR*, not the uncertainty of the conversion coefficient *LAR/ERR*
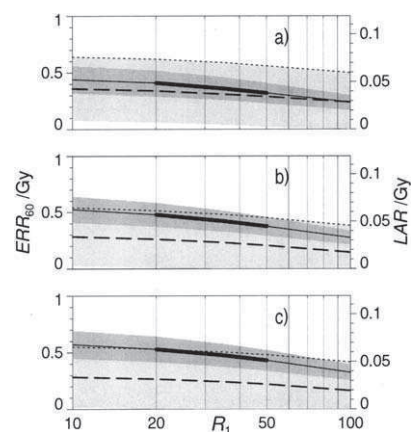
Fig. 2 *Age-attained* model. Diagrams analogous to Fig. 1

and 2 give the results for the report 12 data of 1950–1990 with organ-averaged doses; they are reproduced, for comparison purposes, from [4]. In these results there is little indication of curvature. The difference between the top diagrams and the intermediate diagrams (labelled b) is that the latter extend the follow-up by 7 years, but the modelling procedure is exactly the same. The greater deviation between the broken line (initial slope, α) and the solid line (*ERR*/1 Gy γ-ray dose) is quite notable. The difference is due to the extra 7 years follow-up time, and it is of considerable interest, because it suggests more curvature and, accordingly, admits a considerably larger dose and dose-rate reduction factor (*DDREF*).

The ratio c/α, which can be seen as the best estimate of *DDREF*, is now about 1.5 with the age-at-exposure model, and about 1.8 with the age-attained model. This

compares with values of 1.0 and 1.2, respectively, for the shorter follow-up period covered by the earlier data of 1950–1990 [1]. In this respect the present analysis does not confirm a recent statement that "There is little evidence against a simple linear dose response, with the only apparent curvature being a flattening for those dose estimates above 2 Sv that is not statistically significant" [2]. The values for the ratio c/α_{min}, i.e. the maximum *DDREF* still consistent with the data on the 95% level, are now very large[3]; with the age-attained model even a zero initial slope cannot be excluded.

That the attained-age model now suggests more curvature in the dose-effect relation than the age-at-exposure model might indicate less persistence of the *ERR* in time after exposure for low doses; but this issue is not explored further here.

Effect of using organ-specific doses

As one would expect, the risk estimates do not change greatly when the organ-specific doses (Figs. 1c and 2c) are used instead of the organ-averaged doses (Figs. 1b and 2b). With the organ-specific doses, risk estimates are obtained in terms of the reference slopes that are somewhat larger—by up to one standard deviation—than those obtained in terms of the organ-averaged doses. No difference is seen for the more uncertain estimates of the initial slopes. Only a slight further increase of curvature is notable.

The use of organ-averaged doses is thus seen to be a tolerable approximation to the use of the actual organ-specific doses when the total cancer mortality is assessed. In view of the singular importance of the data of the A-bomb survivors it is, nevertheless, justified to apply the optimal procedure. The extra computational effort presents no problem, especially since the same composite data set and only a slightly modified computational procedure are required in the subsequent Part II of this study [9] to obtain the organ-specific risk estimates.

To reiterate and summarise the main results presented so far:

1. More curvature is now supported by the mortality data in the maximum likelihood *ERR* dose-response curve. This is mainly due to the extra data for the additional 7 year follow-up. To a minor degree it is caused by the transition from *organ-averaged doses* to *organ-specific doses.*
2. The resulting central estimate of the *LAR* (including the additional follow-up and the use of site-specific organ doses) for solid cancer mortality for a working population (ages 25–65 years) is 0.059 at 1 Gy, obtained with the *attained-age* model and 0.044 with the *age-at-exposure* model. For a population of all ages,

0.055 at 1 Gy is obtained with the *attained-age* model and 0.073 with the *age-at-exposure* model. These values are up to about 20% higher than those obtained previously with exactly the same modelling techniques but in terms of the *organ-averaged doses* and the former data 1950–1990.
3. The new computations with respect to *organ-specific doses* result in risk coefficients showing a *reference (γ-ray) slope, c,* that is approximately up to one standard error higher than the values obtained with organ-averaged doses.

Conclusions

The central estimates for lifetime attributable risk (*LAR*) from γ-rays in this analysis are 30–45% lower than the most recent UNSCEAR estimates [16]. On the other hand, the estimates, $c=(0.41\pm0.05)$/Gy (*e*-model) and $c=(0.47\pm0.05)$/Gy (*a*-model) that are obtained here for all solid cancers combined, happen to be close to the recent RERF value *ERR*/Gy=(0.47 ± 0.06) [2]. However, this must not be taken to imply that the explicit treatment of the neutrons has little impact. The fairly low value obtained by RERF is a result of using a linear dose-response model with a rather high dose cut-off (the last dose category cut-off point being quoted as 3 Sv [2]). Because of the flattening out of the solid cancer data at doses beyond 2 Gy, the inclusion of the high dose data causes a substantial reduction of the estimated slope. Cut-off values from 1.5 to 2 Gy (as applied here) are more appropriate for an analysis in terms of the *LQ*-model. As has been shown in Tables 2 and 3, the larger values $c=0.51$/Gy (*e*-model) and 0.60/Gy (*a*-model) are obtained, if—in line with the analysis of RERF—the colon doses and *RBE*=10 are used with a dose cut-off of 2 Gy.

With a sufficiently low cut-off the risk estimates in terms of the parameter *c* are quite reliable. This is so because, up to 2 Gy, the *LQ*-model appears to be adequate and, within the applicability of the *LQ*-model, the estimate of *c* is essentially independent of the chosen dose cut-off. An artefact of the linear model with a high dose cut-off [2] is the fairly low value it suggests for the maximum applicable *DDREF* (=$1+\theta_{max}$). The present analysis indicates more curvature in the dose-dependence. Accordingly a *DDREF*=2 is now well in line with the mortality data, and—averaged over the *e*-model and the *a*-model—a low dose γ-ray risk coefficient, *ERR*/Gy, of about (0.22 ± 0.05)/Gy can now be recommended, instead of the value (0.47 ± 0.06) [2]. Translated into lifetime attributable risk and expressed in Sv, rather than Gy, this corresponds, for a working population, to the value *LAR*=0.026/Sv, which is appreciably less than the current ICRP value *LAR*=0.04/Sv (Table S-3, p 70 in [10]).

While the application of *organ-averaged doses* represents a distinct improvement over the traditional use of the colon doses, the *organ-specific doses* provide the best currently available dosimetric information. As demonstrated here, *LAR* values with respect to *organ-specific*

---

[3] This ratio corresponds roughly to the parameter $(1+\theta_{max})$ employed by Pierce and Preston in their analysis of the solid cancer incidence data (1958–1994) [13].

doses are up to about 20% higher than those obtained previously with exactly the same modelling techniques but in terms of the *organ-averaged doses*. However even the organ-specific doses applied here are not the best possible representation of the actual individual organ-specific doses. This is because only the grouped data are publicly available and with this data set some dose averaging is unavoidable.

Presumably the results are influenced not just by crude dose specifications, but equally by the data grouping and averaging procedures routinely applied as part of the standard data processing with the Japanese LSS data. The most accurate risk coefficients should be attainable with the unpublished individual data, rather than the publicly available grouped data, since forming groups out of individual data always results in some degree of loss of accuracy [17]. Consequently, it is urged that future risk assessments should utilise individual data and that these should be made available in a form that ensures the protection of individual personal privacy (for example—without name and with date of birth given as calendar year only). The availability of individual data would also facilitate the development of several other innovative data analysis methods which should lead to refinements in risk assessment. Two examples of these are: the application of orthogonal transformation methods which allow the error bands of the dose response curves to be evaluated more precisely and without over-inflation by covariance of the data [8]; the assessment of random dosimetry errors using Bayesian Markov Chain Monte Carlo methods, where a detailed knowledge of the individual dose distributions is required [18, 19].

References

1. Pierce DA, Shimizu Y, Preston DL, Vaeth M, Mabuchi K (1996) Studies of the mortality of atomic bomb survivors. Report 12, Part 1. Cancer: 1950–1990. Radiat Res 146:1–27
2. Preston DL, Shimizu Y, Pierce DA, Suyama A, Mabuchi K (2003) Studies of mortality of atomic bomb survivors. Report 13: Solid cancer and noncancer disease mortality: 1950–1997. Radiat Res 160:381–407
3. Bennett B, Young R (eds) (2004) DS02: a revised system for atomic bomb survivor dose estimation. Radiation Effects Research Foundation, Hiroshima, Japan
4. Kellerer AM, Walsh L, Nekolla EA (2002) Risk coefficients for γ-rays with regard to solid cancer. Radiat Environ Biophys 41:113–123
5. Kellerer AM, Walsh L (2001) Risk estimation for fast neutrons with regard to solid cancer. Radiat Res 156:708–717
6. Preston DL, Lubin JH, Pierce DA (1993) Epicure User's Guide. HiroSoft International Corp., Seattle
7. Roesch WC (ed) (1987) US-Japan joint reassessment of atomic bomb radiation dosimetry in Hiroshima and Nagasaki—final report, vols. 1 and 2, Radiation Research Effects Foundation, Hiroshima, Japan
8. Kellerer AM (2003) Error bands for the linear-quadratic dose response by application of orthogonal polynomials. Radiat Environ Biophys 42:77–85
9. Walsh L, Rühm W, Kellerer AM (2004) Cancer risk estimates for γ-rays with regard to organ specific doses, part II: Site specific solid cancers. Radiat Environ Biophys (in press)
10. ICRP (1991) Publication 60. The 1990 Recommendations of the International Commission on Radiological Protection, Ann. ICRP 21 (1–3). International Commission on Radiological Protection. Pergamon Press, Oxford
11. Rühm W, Walsh L, Kellerer AM (2004) The neutron effective dose to the A-bomb survivors. Technical report number TR 221 of the Radiobiological Institute, Ludwig-Maximilians University Munich. Radiat Environ Biophys (in press)
12. Kellerer AM, Rühm W, Walsh L (2004) Accounting for radiation quality in the analysis of the solid cancer mortality among A-bomb survivors. Technical report number TR 223 of the Radiobiological Institute, Ludwig-Maximilians University Munich. Radiat Environ Biophys (in press)
13. Pierce DA, Preston DL (2000) Radiation related cancer risks at low doses among atomic bomb survivors. Radiat Res 154:178–186
14. Kellerer AM, Nekolla E, Walsh L (2001) On the conversion of solid cancer excess relative risk into lifetime attributable risk. Radiat Environ Biophys 40:249–257
15. Akaike H (1973) Information theory and an extension of the maximum likelihood principle. In: BN Petrov, F Caski (eds) Proceedings of the Second International Symposium on Information Theory. Akademiai Kiado, Budapest Hungary, pp 267–281
16. UNSCEAR (2000) Sources and effects of ionizing radiation, vol.2, Annex I. Epidemiological evaluation of radiation-induced cancer. United Nations, New York, pp 297–450
17. Chomentowski M, Kellerer AM, Pierce DA (2000) Radiation dose dependences in the atomic bomb survivor cancer mortality data: a model-free visualization. Radiat Res 153:289–294
18. Bennett J, Little MP, Richardson S (2004) Flexible dose response models for Japanese atomic bomb survivor data: Bayesian estimation and prediction of cancer risk. Radiat Environ Biophys (in press)
19. Pierce DA, Stram DO, Vaeth M (1990) Allowing for random errors in radiation dose estimates for the atomic bomb survivor data. Radiat Res 123:275–284

8. Walsh L, Rühm W & Kellerer AM. Cancer risk estimates for γ-rays with regard to organ specific doses Part II: Site specific solid cancers. Radiat. Environ. Biophys. 43, 225-231, 2004

ORIGINAL PAPER

Linda Walsh · Werner Rühm · Albrecht M. Kellerer

Cancer risk estimates for gamma-rays with regard to organ-specific doses

Part II: Site-specific solid cancers

Abstract Part I of this study presented an analysis of the solid cancer mortality data for 1950–1997 from the Japanese life-span study of the A-bomb survivors to assess the cancer risk for γ-rays in terms of the organ-specific dose for all solid cancers combined. Compared to earlier analyses, considerably more curvature in the dose-effect relation is indicated by these computations, which now suggests a dose and dose-rate effectiveness factor of about 2. The computations are extended here in order to explore the *site-specific* solid cancer risks for various organs. A computational method has been developed whereby the site-specific cancer risks are all simultaneously computed with global age and gender effect modifiers. This provides a more parsimonious representation with fewer parameters and avoids the large relative standard errors which would otherwise result. The sensitivity of site-specific risks to the choices of the neutron *RBE* is examined. The site-specific risk estimates are quite sensitive to the neutron *RBE* for the least shielded organs such as the breast, bladder and oesophagus. For the deeper lying organs, such as the gallbladder, pancreas and uterus, the impact of the neutrons is much lower. With an assumed neutron *RBE* of 35, which is in line with results on low neutron doses in major past studies on rodents and which corresponds approximately to the current ICRP radiation weighting factor for neutrons, the neutrons appear to contribute about 40% of the observed excess cancer risk in the breast, i.e. the organ that is closest to the body surface. However, this neutron contribution fraction is only about 10% for deeper lying organs, such as the colon.

L. Walsh (✉) · W. Rühm · A. M. Kellerer
Radiobiological Institute,
University of Munich,
Schillerstrasse 42, 80336 Munich, Germany
e-mail: Linda.Walsh@LRZ.uni-muenchen.de
Tel.: +49-89-218075-821
Fax: +49-89-218075-840

Introduction

The Life Span Study (LSS) of cancer in the Japanese A-bomb survivors provides the best currently available data for evaluating the variation of radiation-induced cancer risk with cancer site. The reason is that survivors suffered irradiation of the whole body, which differs from the situation in most medical studies, where just a few organs are significantly exposed. Nevertheless, there are considerable variations of the γ-ray doses, and more so of the neutron doses, at different depths in the human body.

The fundamental assessments of radiation-induced health effects [1, 2] from the Radiation Effects Research Foundation (RERF) employ the "weighted dose" which is taken to be the γ-ray absorbed dose to one of the deepest lying organs, the colon, plus the neutron-absorbed dose to the colon multiplied by 10. Continuity in the dose specification method is essential for keeping the increasingly complete results comparable as the follow-up of the LSS survivors continues. However, as the study comes closer to its ultimate completion, it is also important to explore those aspects that can still be refined. The availability of cancer mortality data up to the end of 1997 [2] and the recent reassessment of the A-bomb dosimetry [3] have led to an examination of the impact of a more detailed dosimetric specification on the cancer risks for all solid cancers combined [4]. The influence of the assumed neutron *RBE* values on the risk estimates for the various organs at different depths in the body has not been considered in previous RERF [1, 2] analyses and is, therefore, considered here.

As recently pointed out [5] reference to the colon dose underestimates the average γ-ray component to all relevant organs by only about 8.5%, while it is not satisfactory for the neutron component for the following reasons:

– The organ averaging – with weight factors for the risk contribution of individual tumour sites [6] – results in neutron absorbed doses that are about twice as large as those to the colon. For surface organs, such as the

Table 1 Sites with more than 100 cancer deaths in report 12 [1] solid cancer mortality data (1950–1990) compared with the report 13 [2] data (1950–1997) and the reference organs used for scaling the colon doses to the organ-specific doses

Sites with >100 deaths	Reference organs for scaling the colon doses	Number of cancer deaths (1950–1990)	Number of cancer deaths (1950–1997)	Neutron adjustment factor	γ-ray adjustment factor
Female Breast	Breast	211	272	3.85	1.17[#]
Oesophagus	Marrow	234	291	2.14	1.1
Lung	Lung	939	1264	1.91	1.09
Liver	Liver	893	1236	1.66	1.05
Gallbladder	Liver	228	328	1.66	1.05
Stomach	Stomach	2529	2867	1.54	1.02
Rectum	Bladder	298	370	1.17	1.05
Bladder	Bladder	119	150	1.17	1.05
Colon	Colon	347	478	1	1
Pancreas	Pancreas	297	407	0.94	0.98
Ovary	Ovary	120	136	0.83	1.01
Uterus	Uterus	476	518	0.7	1

[#] A recent experimental simulation of A-bomb γ-ray spectra [7] has confirmed this particular value.
The order of organs in the table reflects their depth within the human body.
The last two columns give the dose adjustment factors for conversion from colon absorbed dose to organ-specific absorbed dose for Hiroshima adults.

female breast, neutron absorbed doses can be nearly 4 times larger than those to the colon (see Table 1).

– At the low neutron doses received by the A-bomb survivors, of only up to several 10 mGy, the neutron *RBE* appears from the available radiobiological evidence, to be substantially larger than 10, which increases the importance of the correct specification of the neutron dose contribution.

Previous articles [5, 6] employed the *organ-averaged doses*. The risk coefficient, *ERR*/Gy, for photons was derived in terms of a linear-quadratic (LQ) dose dependence for the γ-rays and a linear dose dependence for the neutrons, with a range of tentatively assumed *RBE* values of the small neutron dose component against a γ-ray dose (D_1) of 1 Gy. The *age-at-exposure* and the *age-attained model* were applied. In addition to estimating the *initial slope*, α, in the linear-quadratic dose dependence, with its comparatively large relative error, the *reference slope*, c, was determined. This parameter equals the ratio $ERR(D_1)/D_1 = \alpha + \beta D_1$ in the LQ-model. The estimates of c and of the coefficient, α_L, in an assumed linear model as well as their standard errors, are similar. But c, rather than the more familiar α_L, has been employed in the previous analysis for all solid cancers combined, since – under the assumption of the LQ-model – it does not inherently depend on the dose cut-off that is applied in the fit to the data. The slope, α_L, in a linear fit lacks this invariance. However, it is felt that the data for the individual organs are not sufficiently powerful enough to justify a linear-quadratic analysis for each organ and accordingly a linear model is applied here.

Part I of the investigation [4] has updated previous results [5] by using the cancer mortality data for 1950–1997 (which have recently been made available on the RERF web-site) and extended the earlier assessment by applying the *organ-specific doses* in order to compare the analysis for all solid cancers combined with that in terms of *organ-averaged doses*. Considerably more curvature in the dose-

effect relation was found to be supported by the updated and extended computations, which suggest now – even without reference to radiobiological investigations – a dose and dose-rate effectiveness factor (*DDREF*) of about 2. The modified data set described and applied in [4] is also highly suitable for assessing the influence of the assumed neutron *RBE* values on the risk estimates for the various organs at different depths in the body. This is the objective of this paper which forms Part II of the investigation.

Details of the modelling procedures

The present analysis, in common with the previous analysis for all solid cancers combined [4], applies the *organ-specific doses* to sites which had more than 100 solid cancer deaths in the older mortality data set (Table X in [1]). Table 1 shows the organ sites considered here and the reference organs used in the scaling of colon doses to the corresponding *organ-specific doses* that were applied in the computation of organ-specific risk estimates. The *dose-adjustment factors* for conversion from the colon absorbed doses (as given in the solid cancer mortality data 1950–1997) to organ-specific absorbed doses were taken from the publicly available (http://www.rerf.or.jp) data set ds86adjf.dat. They depend on radiation type, age-at-exposure and city and are included in Table 1 for both radiation types, but only for Hiroshima adults. The remaining sites, associated with less than 100 solid cancer deaths and, in most cases, with no available dose-adjustment factor, include a wide range of organs and tissues, they were accordingly assigned the *organ-averaged doses*.

As stated above, *organ-specific doses* were applied to the grouped publicly available solid cancer mortality data (file name: r13mort.dat). To do this is not entirely trivial. Pierce et al. [1] noted that "It is impossible to use more specific organ doses for solid cancers as a class, since there is no designated organ for those not dying of cancer". However, this difficulty has been resolved here and

in [4] by formally treating each person as a set of 13 sub-units at risk, each belonging to 1 organ category. In terms of programming this meant creating a new organ category at the lowest level of the data structure where there are a total of 37,060 original data groups (for combinations of city, gender, age-attained, age-at-exposure and colon dose category), each group containing the number of cases of death from different types of solid cancer. For each of these original data records, 13 new organ-specific records were created to contain the numbers of deaths for each cancer type and the relevant *organ-specific doses*. The first 12 organ categories (i=1,..12) represented the specific sites with more than 100 deaths (as detailed in Table 1), while category i=13 contained the remaining widely varying sites, such as thyroid, kidney, urinary tract, bone, oral cavity, connective tissue, skin, prostate, brain, central nervous system and other male and female genital sites, which were assigned the *organ-averaged doses*. The risk coefficients were then computed in EPICURE–AMFIT [8] by the maximum likelihood Poisson regression method with background cancer rate subtraction achieved through stratification on gender, age-attained, age-at-exposure and the new organ category.

The models applied here are the same as those already considered and explained in detail for all solid cancers combined [4, 5] with γ-ray absorbed dose, $D_{\gamma,i}$, and neutron absorbed doses, $D_{n,i}$, based on the dosimetry system DS86 [9]. It is noted that the A-bomb dosimetry has recently been reevaluated in a major international effort [3]. While the new dosimetry system DS02 is expected to replace the former DS86 in the near future, it has not been used in the present study since DS02 is not yet published. The differences between [5] and the present work is that the input data cover an extra 7 years of follow-up, the *organ-specific doses* were taken into account, and the site-specific risks for 12 different organs are now explicitly considered. The excess relative risk is factorised into a function of dose for the 13 organ categories and a joint modifying function that depends on the variables gender (s) and age at exposure (e) or age attained (a):

$$ERR(D_{\gamma,i}, D_{n,i}, s, e, a) = \mu(s, e, a) \, \rho_i(D_{\gamma,i}, D_{n,i}) \qquad (1)$$

with the modifying functions for the *age-attained* and the *age-at-exposure model:*

$$\mu(s, a) = \exp(-g(a - 60))(1 \pm s) \qquad (2)$$

$$\mu(s, e) = \exp(-g(e - 30)) \, (1 \pm s)$$
$$(+ \text{forfemales}, - \text{ formales}) \qquad (3)$$

The calculations can be performed in terms of either the *age-attained model* or the *age-at-exposure model* as in [4]. However, the earlier computations [4] have shown that the *age-at-exposure model* results in lower scores for the Akaike Information Criterion [10] (and is therefore more likely to be correct) than the *age-attained model*, while the resulting parameters were very similar. For this reason, most of the results presented in the next sections are for the *age-at-exposure model*.

In the dose-dependent term the same neutron *RBE* is used for all organs in a common model that is linear both in the γ-rays and the neutrons:

$$\rho_i(D_\gamma, D_n) = \alpha_{L,i}(D_{\gamma,i} + RBE \times D_{n,i}) \qquad (4)$$

The model does not account for the fact that, as described in [4], the data are now indicative of substantial curvature in the dose-effect relation for all solid cancers combined. However, it is felt that the data for the individual organs are insufficiently powerful to justify a linear-quadratic analysis for each organ, nor does it seem justified to postulate, in a linear-quadratic model, that all organs exhibit the same curvature corresponding to a *DDREF* of about 2 that has been found for all solid cancers combined [4]. Furthermore, it is felt that the linear model provides reasonably representative values for intermediate doses on the order of 1 Gy, which are particularly relevant with regard to specified sites because they are required in probability-of-causation computations. While site-specific cancer risks [1, 2] have already been variously assessed for probability-of-causation computations, the influence of the assumed neutron *RBE* values on the risk estimates for the various organs at different depths in the human body has not been considered.

The paucity of data for any one site alone makes it desirable to minimise the number of organ-specific parameters in the analysis. The fits are, therefore, performed with global, i.e. non-organ-specific, effect modifiers s and g. The advantage of using global effect modifiers is that it avoids the large relative standard errors (SE) which would otherwise result. Furthermore it is convenient that the same data set, with 13 organ categories, that has been used in Part I can also be employed here.

While current RERF [1, 2] analyses of the LSS mortality data apply a neutron *RBE* of 10, values for the *RBE* between 20 and 50, and a central value of 35 are used here. Information on the *RBE* of small neutron doses of up to several 10 mGy – which equals the range of neutron doses received by the A-bomb survivors at about 1 Gy total dose – has mainly been obtained in major past experiments on rats by Shellabarger et al. [11] and by Lafuma and colleagues [12]. Life shortening or tumour incidence were assessed in these experiments and *RBE* values of 35 to about 100 were found for low neutron doses. Also an *RBE* of 35 agrees approximately with current ICRP recommendations for radiation weighting [13], if correct account is taken of the fact that secondary γ-rays due to neutron capture within the body are included in the ICRP definition of effective dose, while they are not part of the neutron doses specified for the A-bomb survivors [14, 15]. In order to il- lustrate the potential impact of the neutrons, some of the graphics are extended to include neutron RBE values up to 100.

Site-specific estimates ERR/Gy

The numerical values of the age-at-exposure effect modifier, g, quoted in [1] but now given with SE, are

Table 2 *ERR*/Gy site-specific dose response coefficients $\alpha_{L,i}$ (with standard errors) computed with *RBE*=10 and 2 dose cut-off values

Organ	Dose cut-off	
	2 Gy	3 Gy
	α_L/Gy	α_L/Gy
Breast	1.31±0.37	1.23±0.33
Others	0.69±0.18	0.61±0.16
Oesophagus	1.22±0.48	0.99±0.40
Lung	0.75±0.17	0.67±0.15
Liver	0.45±0.14	0.31±0.11
Gallbladder	0.14±0.21	0.32±0.22
Stomach	0.45±0.11	0.43±0.10
Rectum	0.41±0.25	0.23±0.20
Bladder	1.57±0.80	1.32±0.69
Colon	0.46±0.23	0.64±0.23
Pancreas	0.10±0.19	0.06±0.16
Ovary	0.87±0.50	0.80±0.45
Uterus	0.16±0.21	0.18±0.19
Weighted average	0.47±0.05	0.42±0.05

The values apply to an age-at-exposure of 30 years; the gender and age modifiers are given in the captions of Fig. 1 and Table 3.

−(0.029±0.022)/year for lung and (0.079±0.034)/year for breast cancer. Thus, it is not clear whether there is a significant difference in the age-at-exposure effect modifier even between these two sites which are frequently considered to show the most notable difference in the age dependence. The global *g* value from the present analysis of the non-gender-specific sites is (0.039±0.008)/year.

Site-specific results from the computations with AM-FIT [8] are shown in Tables 2 and 3. A dose cut-off at 2 Gy is used in the present calculations, while 3 Gy or somewhat higher values have been used in earlier evaluations at RERF [1, 2]. Table 2 shows that – in line with the "bending down" of the dose relation that is evident at higher doses – the α_L values are mostly somewhat smaller for the cut-off at 3 Gy.

Table 3 gives the coefficients *ERR*/Gy for an age-at-exposure of 30 years, for various cancer sites that are obtained with a dose cut-off at 2 Gy and for different assumed *RBE* values. To facilitate the comparison to the earlier results from RERF [1, 2] the values are given in terms of $\alpha_{L,i}$, i.e. for a linear fit. Results are also included for an *RBE* of 10 and for the earlier follow-up period for comparison purposes. The results are further illustrated and extended in Fig. 1 for both the gender-averaged and female site-specific *ERR*/Gy values.

Discussion of the results

Effect of the additional follow-up

The first two columns of Table 3 show that the site-specific risk estimates do not change significantly with the added follow-up period. There is a slight decrease in the point estimates for some organs (breast, oesophagus, gallbladder, rectum, ovary), for other organs the values have not changed or they have become somewhat larger (liver, others). As expected, the uncertainties have decreased with the extension of the follow-up to 1997.

Table 3 Gender-averaged and female site-specific *ERR*/Gy for an age-at-exposure of 30 years and a linear dose response, i.e. parameters $\alpha_{L,i}$ (with standard errors)

Organ	*ERR*/Gy from linear fit with dose cut-off 2 Gy				
	RBE=10	*RBE*=10	*RBE*=20	*RBE*=35	*RBE*=50
	(1950–1990)	(1950–1997)	(1950–1997)	(1950–1997)	(1950–1997)
Breast	1.51±0.47	1.31±0.37	1.13± 0.32	0.93±0.26	0.79±0.22
Others	0.54±0.20	0.69±0.18	0.63±0.17	0.55±0.15	0.49±0.13
Oesophagus	1.63±0.74	1.22±0.48	1.11±0.44	0.98±0.39	0.88±0.34
Lung	0.75±0.22	0.75±0.17	0.69±0.15	0.61±0.14	0.54±0.12
Liver	0.35±0.18	0.45±0.14	0.42±0.13	0.38±0.11	0.34±0.10
Gallbladder	0.38±0.32	0.14±0.21	0.13±0.19	0.12±0.17	0.11±0.16
Stomach	0.43±0.12	0.45±0.11	0.41±0.10	0.37±0.09	0.33±0.08
Rectum	0.50±0.34	0.41±0.25	0.39±0.24	0.35±0.22	0.32±0.20
Bladder	1.63±0.99	1.57±0.80	1.48±0.75	1.37±0.69	1.27±0.64
Colon	0.45±0.32	0.46±0.23	0.44±0.22	0.42±0.20	0.39±0.19
Pancreas	0.10±0.27	0.10±0.19	0.09±0.18	0.09±0.17	0.08±0.16
Ovary	1.21±0.66	0.87±0.50	0.84±0.48	0.79±0.45	0.74±0.43
Uterus	0.22±0.25	0.16±0.21	0.16±0.20	0.15±0.19	0.14±0.18
Weighted average	0.47±.068	0.47±.055	0.43±0.05	0.40±0.046	0.36±0.049

The values are obtained with different neutron *RBE* values. For non-gender site-specific cancers, the age-at-exposure parameter is *g*=(0.039±0.008)/year and the gender parameter *s*=0.30±0.11. For the female sites, the age-at-exposure parameter is *g*=(0.036±0.009)/year. The parameters *g* and *s* were not fixed during optimisation but remained stable at about these values for each evaluation with different *RBE* values. Again the ordering of organs down the table is based on their depth in the body.
The "others" category includes a wide range of cancers, less frequent than the ones tabulated (i.e. with less than 100 deaths recorded in the data set associated with report 12 [1]), such as thyroid, kidney, urinary tract, bone, oral cavity, connective tissue, skin, prostate, brain, central nervous system and other male and female genital sites.
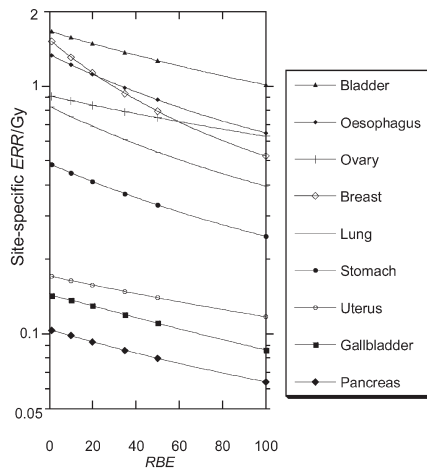
Fig. 1 *ERR*/Gy in terms of the parameters $\alpha_{L,i}$ as a function of the assumed *RBE* (*RBE* 1, 10, 20, 35, 50, 100) for an age-at-exposure of 30 years. The values for colon, liver and rectum are not shown here because they are very similar to those for the stomach. The *ERR*/Gy values for non-gender-specific cancers are gender-averaged where the age-at-exposure parameter is $g=(0.039\pm0.008)$/year and the gender parameter $s=0.30\pm0.11$. The female cancer sites have an age-at-exposure parameter of $g=(0.036\pm0.009)$/year. The parameters g and s were not fixed during optimisation, but remained stable at about these value for each evaluation with different *RBE* values

Table 4 Results from statistical procedures, involving likelihood ratios, to test if the models with separate linear risks, for each of the 12 main organs considered here, fit the data significantly better than the linear risk models for all solid tumours combined

RBE	χ^2-value	p
Age-at-exposure model		
10	23.6	0.023
20	22.0	0.038
35	20.1	0.065
50	18.7	0.095
Age-attained model		
10	29.9	0.003
20	28.2	0.005
35	26.3	0.010
50	24.9	0.015

With *RBE*=35 the coefficient α_L for all solid cancers combined was found to be (0.42 ± 0.05) and (0.49 ± 0.05)/Gy for the *age-at-exposure* and *age-attained-models,* respectively. In such likelihood ratio tests the change in deviance due to the transition from the separate organ model to the model for all solid cancer combined (i.e. nested models) is χ^2 distributed with respect to the associated change in degrees of freedom (Δdf). The resulting χ^2-values are given in column 2, where Δdf=12 here. The probabilities, p, associated with these χ^2-values, are given in column 3.

In general the differences between the models with separate linear risks for each organ and the models for all solid tumours combined become less statistically significant as the *RBE* increases. The differences are significant at or below the 5% (p=0.05) level for the age-attained models at all *RBE* values considered and for the age-at-exposure models with *RBE* values of less than 35

The decrease of the organ risk estimates with larger assumed values of *RBE*

The dose-response coefficients given in Table 3 and Fig. 1 are suggestive of different radiation sensitivities for the various organs. To examine whether the differences are statistically significant, the likelihood ratios were determined for the linear model with separate site-specific dose coefficients, $\alpha_{L,i}$, and for the linear model with all solid tumours combined. As seen from Table 4, the assumption of separate *ERR*/Gy values appears to be significantly better for both the *age-attained* and the *age-at-exposure models* at the lower values of *RBE*, while, at least for the age-at-exposure model, the significance is lost for the *RBE* values 35 and 50. The plausible reason is that low values of *RBE* cause somewhat inflated *ERR*/Gy estimates for the organs most substantially exposed to neutrons, which enhances the differences between the site-specific risk estimates. Since the site-specific risk estimates and their uncertainties are of considerable interest with regard to radiation protection standards [13, 16], they are shown in a more detailed diagram in Fig. 2. Starting on the left with the most shallow, i.e. least shielded organs, the diagram gives four different site-specific values, *ERR*/Gy, from a linear fit in dose. The first value (shown as a separate point) is obtained by using colon doses and an *RBE* of 10 for the neutrons. Values

Fig. 2 The diagram illustrates some of the data given in Fig. 1 for the $\alpha_{L,i}$ parameters and associated standard error bars at *RBE* 20, 35 and 50. In addition and for comparison purposes, the corresponding parameters for colon dose and *RBE*=10, i.e. the situation considered in [1, 2], are also given. For each organ there is an associated group of 4 points with standard error bars. In each group of four, on reading from left to right, the ordering is *1* Colon dose and *RBE*=10 (*square symbol*), *2* Organ-specific dose and *RBE*=20 (*connected circular symbol*), *3* Organ-specific dose and *RBE*=35 (*connected circular symbol*), *4* Organ-specific dose and *RBE*=50 (*connected circular symbol*). The organs are ordered from *left* to *right* according to increasing depth in the body

given in the main part of Reports 12 and 13 from RERF [1, 2][1] have been obtained in this way; they are, of course,

---

[1] The appendices of these reports give also results obtained in terms of organ-specific doses. But the numerical values are not readily comparable to each other or to the present results, because there have been further differences between the computations.

the largest and are given here only for comparison purposes. The three subsequent estimates of *ERR*/Gy (connected in each case by solid lines) are obtained in terms of *organ-specific doses* (or their weighted averages in the case of the pooled group containing "other" organs). The three estimates relate to assumed values 20, 35, and 50 for the neutron *RBE*. The purpose of the diagram is to show – in a direct comparison of values obtained in the same type of computation with the same data set – firstly the influence of the reference doses and, secondly, the influence of the assumed neutron *RBE*. While numerical values obtained in earlier assessments show considerable variations depending on other details of the analysis, such as the dose cut-off or the age and sex-dependent effect modifiers, the diagram in Fig. 2 brings out the two central aspects, namely dose specification and *RBE*.

It should be noted that – in view of the evidence in Part I [4] of the present study – the numerical values in Table 2 and in Figs. 1 or 2 can be tentatively reduced further by a *DDREF*=2 if they are referred to low doses.

Apart from the importance of using *organ-specific doses*, the essential point illustrated in Figs. 1 and 2 is the sensitivity of site-specific risk estimates to the assumed neutron *RBE*. It is apparent that – in line with the relatively higher dose contribution of neutrons – the risk estimates for sites close to the surface of the body, such as the breast, oesophagus and bladder, are much more dependent on the choice of *RBE* than deeper lying sites, such as the uterus and pancreas. Changing the *RBE* from 10 to 35 results in a decrease of the risk coefficient for the breast by the factor 1.31/0.93=1.41, while the reduction factor is only 0.16/0.15=1.07 for the uterus (Table 3).

The risk estimate for the breast must be based not only on the A-bomb data, but also on information from medical exposures, and both sources provide results with considerable uncertainty. However, the risk coefficient for the breast is particularly relevant to risk/benefit considerations for mammography screening, and a decrease of the estimate from *ERR*/Gy=1.51±0.47 to 1.31±0.37, and then to *ERR*=0.93±0.26 is, therefore, not without interest.

A more direct look at the effect contribution
by the neutrons

The solid curve in Fig. 3 gives the ratio of the weighted (*RBE*=35) neutron dose to the *γ*-ray dose to the breast for adult women in Hiroshima. As already pointed out, an *RBE* of 35 for the "genuine" neutron dose (i.e. the contribution of the neutron recoils) corresponds approximately to the current radiation weighting factor for neutrons (including the *γ*-rays from neutron capture in the body) as specified by ICRP. The solid line in the figure represents, accordingly, also the ratio of the effective dose from neutrons to the *γ*-ray absorbed dose. For other organs the values change proportionally in line with the neutron adjustment factor (see values in Table 1). The dotted line gives as an example, the values for the colon
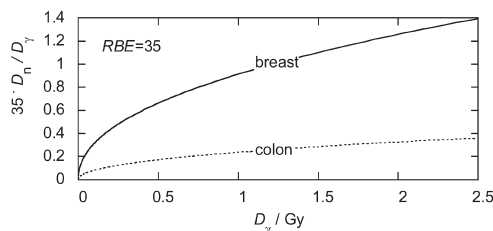

Fig. 3 The ratio of the *RBE* weighted neutron dose to the *γ*-ray dose versus the *γ*-ray dose to the organ. The *solid line* refers to the breast and to an assumed neutron *RBE* of 35 for Hiroshima female adults. The *broken line* represents the ratios for the colon at the same *RBE*=35. At other values of the neutron *RBE* the values change proportionally

and for *RBE*=35. Likewise the values change proportionally for other assumed values of *RBE*. An important feature of the dosimetry is the fact that the neutron fraction is larger close to the hypocentre (at large doses), and smaller at large distances (small doses).

Under the assumption of *RBE*=35, the neutrons contribute about 40% and 50% to the weighted dose to the breast at 0.5 and 1.5 Gy gamma absorbed dose, respectively. Under a linear model this equals the fractional contribution of the neutrons to the observed *ERR*. The dosimetric considerations explain well, why the risk estimates for the more superficial organs decrease substantially, when in the computations organ-specific neutron doses are used and are weighted with a larger *RBE* than the conventional factor 10. The trend of the data in Table 2 and Figs. 2 and 3 is, thus, understandable even without the details of the computation.

Conclusions

A computational method has been developed to derive site-specific risk coefficients for *γ*-ray-induced cancer with respect to *organ-specific doses*. A linear model in dose and the use of common age and gender effect modifiers for all organs has permitted a parsimonious representation with relatively few parameters, avoiding the large relative standard errors that result from the familiar approach.

The site-specific risk estimates are found to be quite sensitive to the assumed neutron *RBE* for the less shielded organs such as the breast, bladder and oesophagus. For the deeper lying organs, such as the gallbladder, pancreas and uterus the impact of the neutrons is much less. The dosimetry for the A-bomb survivors includes, in the neutron-absorbed dose, only the contribution of the protons and other heavy charged particles released by the neutrons and not the contribution of *γ*-rays due to neutron capture in the body. If this difference in the specification of the effective dose by ICRP is taken into account, a neutron *RBE* of 35 is roughly in accordance with the current ICRP radiation

weighting factor for fission neutrons. The inferred effect contribution by neutrons then ranges from 40% for the breast, as the least shielded organ, to 9% for a deep lying organ, such as the colon.

In view of the substantial role of the neutrons it would be highly desirable to use more specific information on the neutron doses to the A-bomb survivors in the computation of risks. Data on the orientation of the survivors with respect to the bomb exists in the dosimetry systems DS86 [9] and DS02 [3], but they have not been included in past computations nor have they been made publicly available. Only isotropic irradiation conditions have been considered in the publicly available epidemiological data up to now. In view of the substantial impact of the small neutron absorbed dose contribution this approximation appears now to be too crude.

In Part I of this work it was urged that the individual data be made generally available and several reasons were given. The current assessment suggests as a further refinement, the use of person-specific neutron dose estimates that are based on individual data on location and orientation relative to the hypocentre of the explosion.

References

1. Pierce DA, Shimizu Y, Preston DL, Vaeth M, Mabuchi K (1996) Studies of the mortality of atomic bomb survivors. Report 12, Part 1. Cancer: 1950–1990. Radiat Res 146:1–27
2. Preston DL, Shimizu Y, Pierce DA, Suyama A, Mabuchi K (2003) Studies of mortality of atomic bomb survivors. Report 13: solid cancer and noncancer disease mortality: 1950–1997. Radiat Res 160:381–407
3. Bennett B (2003) DS02: the new dosimetry system DS02 (in Japanese). Hiroshima Igaku (Journal of the Hiroshima Medical Association) 56:386
4. Walsh L, Rühm W, Kellerer AM (2004) Cancer risk estimates for gamma-rays with regard to organ-specific doses. Part I: All solid cancers combined. Radiat Environ Biophys 43:145–152
5. Kellerer AM, Walsh L, Nekolla EA (2002) Risk coefficients for γ-rays with regard to solid cancer. Radiat Environ Biophys 41:113–123
6. Kellerer AM, Walsh L (2001) Risk estimation for fast neutrons with regard to solid cancer, Radiat Res 156:708–717
7. Pattison JE, Payne LC, Hugtenburg RP, Beddoe AH, Charles MW (2004) Experimental simulation of A-bomb γ-ray spectra: revisited. Radiat Prot Dosim 109:175–180
8. Preston DL, Lubin JH, Pierce DA (1993) Epicure User's Guide. HiroSoft International, Seattle
9. Roesch WC (ed) (1987) US-Japan joint reassessment of atomic bomb radiation dosimetry in Hiroshima and Nagasaki—final report, vols. 1 and 2. Radiation Research Effects Foundation, Hiroshima, Japan
10. Akaike H (1973) Information theory and an extension of the maximum likelihood principle. In: BN Petrov, F Caski (eds) Proceedings of the second International Symposium on Information Theory. Budapest, Hungary, Akademiai Kiado, pp 267–281
11. Shellabarger CJ, Chmelevsky D, Kellerer AM (1980) Induction of mammary neoplasms in the Sprague-Dawley rat by 430 -keV neutrons and x-rays. J Natl Cancer Inst 64:821–832
12. Lafuma J, Chmelevsky D, Chameaud J, Morin M, Masse R, Kellerer AM (1989) Lung carcinomas in Sprague-Dawley rats after exposure to low doses of radon daughters, fission neutrons, or γ-rays. Radiat Res 119:230–245
13. ICRP (1991) Publication 60. The 1990 Recommendations of the International Commission on Radiological Protection. Ann ICRP 21 (1–3). Pergamon Press, Oxford
14. Rühm W, Walsh L, Kellerer AM (2004) The neutron effective dose to the A-bomb survivors. Technical report number TR 221 of the Radiobiological Institute, Ludwig-Maximilians University Munich. Radiat Environ Biophys (in press)
15. Kellerer AM, Rühm W, Walsh L (2004) Accounting for radiation quality in the analysis of the solid cancer mortality among A-bomb survivors. Technical report number TR 223 of the Radiobiological Institute, Ludwig-Maximilians University Munich. Radiat Environ Biophys (in press)
16. UNSCEAR (2000) Sources and effects of ionizing radiation, vol.2, Annex I. Epidemiological evaluation of radiation-induced cancer. United Nations, New York, pp 297–450

9. Gomolka M, Rössler U, Hornhardt S, Walsh L, Panzer W & Schmid E. Measurement of the Initial Levels of DNA Damage in Human Lymphocytes induced by 29 kV X Rays (Mammography X Rays) Relative to 220 kV X Rays and γ Rays. Radiat. Res. 163, 510-519, 2005

Measurement of the Initial Levels of DNA Damage in Human Lymphocytes Induced by 29 kV X Rays (Mammography X Rays) Relative to 220 kV X Rays and γ Rays

M. Gomolka,[a,1] U. Rössler,[a] S. Hornhardt,[a] L. Walsh,[b] W. Panzer[c] and E. Schmid[b,d]

[a] Federal Office for Radiation Protection, Department of Radiation Protection and Health (SG1.1), 85764 Oberschleissheim, Germany;
[b] Radiobiological Institute, University of Munich, 80336 Munich, Germany; and [c] Institute of Radiation Protection and [d] Institute of Radiobiology, GSF-National Research Center for Environment and Health, 85764 Neuherberg, Germany

Gomolka, M., Rössler, U., Hornhardt, S., Walsh, L., Panzer, W. and Schmid, E. Measurement of the Initial Levels of DNA Damage in Human Lymphocytes Induced by 29 kV X Rays (Mammography X Rays) Relative to 220 kV X Rays and γ Rays. 163, 510–519 (2005).

Experiments using the alkaline comet assay, which measures all single-strand breaks regardless of their origin, were performed to evaluate the biological effectiveness of photons with different energies in causing these breaks. The aim was to measure human lymphocytes directly for DNA damage and subsequent repair kinetics induced by mammography 29 kV X rays relative to 220 kV X rays, ^{137}Cs γ rays and ^{60}Co γ rays. The level of DNA damage, predominantly due to single-strand breaks, was computed as the Olive tail moment or percentage DNA in the tail for different air kerma doses (0.5, 0.75, 1, 1.5, 2 and 3 Gy). Fifty cells were analyzed per slide with a semi-automatic imaging system. Data from five independent experiments were transformed to natural logarithms and fitted using a multiple linear regression analysis. Irradiations with the different photon energies were performed simultaneously for each experiment to minimize interexperimental variation. Blood from only one male and one female was used. The interexperimental variation and the influence of donor gender were negligible. In addition, repair kinetics and residual DNA damage after exposure to a dose of 3 Gy were evaluated in three independent experiments for different repair times (10, 20, 30 and 60 min). Data for the fraction of remaining damage were fitted to the simple function $F_d = A/(t + A)$, where F_d is the fraction of remaining damage, t is the time allowed for repair, and A (the only fit parameter) is the repair half-time. It was found that the comet assay data did not indicate any difference in the initial radiation damage produced by 29 kV X rays relative to the reference radiation types, 220 kV X rays and the γ rays of ^{137}Cs and ^{60}Co, either for the total dose range or in the low-dose range. These results are, with some restrictions, consistent with physical examinations and predictions concerning, for example, the assessment of the possible difference in effectiveness in causing strand breaks between mammography X rays and conventional (150–250 kV) X rays, indicating that differences in biological effects must arise through downstream processing of the damage.   © 2005 by Radiation Research Society

INTRODUCTION

The dependence of the biological effects for different kinds of cell damage on photon energy is well documented. Cross comparisons of dose–response curves, which relate indicators of cellular damage such as chromosomal aberrations, mutation induction, cell survival and neoplastic cell transformation (in human and mouse cell lines) to absorbed doses of photons, e.g. at energies from 29 kV (mammography X rays) to about 200 kV (conventional X rays) or to 1.25 MeV (^{60}Co γ rays), have resulted in low-dose relative biological effectiveness (RBE) values ranging from 1 to 10 (*1–8*). However, it is uncertain whether the marked dependence of RBE on photon energy for these biological indicators is also representative of the complete biological effectiveness for the photon-induced initial DNA damage to late radiation effects in humans. This problem has gained particular attention with regard to risk–benefit considerations for mammography, because such findings are partly inconsistent with values predicted from microsimetric analyses for the low-dose RBE of mammography radiation (*9–11*). Whereas conventional X rays interact with cellular systems through Compton electrons and photoelectrons, the 29 kV X rays interact primarily through the photoelectric effect. Due to the low energy of the 29 kV photons, low-energy secondary electrons are released, which leads not only to a different energy deposition pattern in the cellular system but also to greater biological effects than those produced by higher-energy photons. Physical models describing the possible energy deposition pattern in the DNA and the resulting DNA damage predict an RBE of only 1.3 with an upper limit no greater than about 2 for 29 kV X rays relative to conventional X rays (*9*).

The cellular damage indicators depend strongly on the mechanisms of biological cell responses after radiation damage, e.g. DNA repair and the induction of cell death by apoptosis or necrosis. The dose response for every bi-
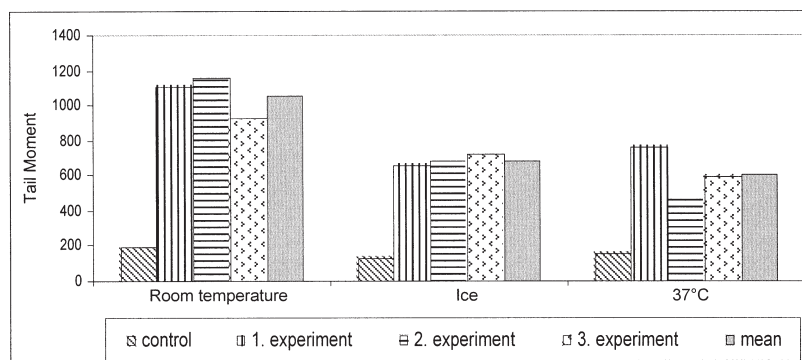
FIG. 1. Effect of temperature on damage induced during irradiation. Damage at room temperature (20°C) is increased compared to irradiation on ice or at 37°C.

ological indicator is an indirect measurement of the effect produced by the specific radiation type. The direct action of radiation on DNA can be detected by measuring single- or double-strand breaks or base changes caused by direct deposition of the radiation energy or by induced reactive oxygen species. Several techniques have been applied to study such radiation-induced DNA single-strand and/or double-strand breaks with different sensitivities to the specific lesions. These include alkaline or neutral filter elution (*12, 13*), alkaline unwinding (*14, 15*), sucrose gradient centrifugation (*16–18*), pulsed-field gel electrophoresis (*19–22*), and nucleoid sedimentation (*23, 24*). These techniques have the disadvantage that DNA damage is investigated in a population of cells and not at the single cell level.

The alkaline comet assay provides an excellent test for detecting direct DNA damage with respect to single-strand breaks, regardless of their origin, at the single cell level. In contrast to the neutral comet assay, which detects specifically double-strand breaks (DSBs), the alkaline assay is performed at doses that are relevant to physiological effects. It has been used widely to measure both *in vitro* and *in vivo* DNA damage and repair after the exposure of mammalian cells to various genotoxic agents such as chemicals and ionizing and non-ionizing radiation (*25–28*). For example, it has been reported that the alkaline comet assay is a useful biological technique to assess the biological effectiveness of different types of high-LET radiation such as neutrons (*29–32*). However, as recently observed for the induction of dicentric chromosomes in human lymphocytes (*33*), the RBE of neutrons depends on the choice of the low-LET reference radiation. So far no attempt has been made to test the usefulness of the alkaline comet assay for distinguishing between different types of low-LET radiation, which differ only slightly in energy deposition patterns.

Consequently, the purpose of the present study was to compare, in simultaneously performed comet assay exper-

iments, both the initial radiation damage and the associated subsequent DNA temporal repair patterns induced by 29 kV X rays with those of their reference radiation types: 220 kV X rays, ^{137}Cs γ rays and ^{60}Co γ rays.

MATERIALS AND METHODS

For the present study, peripheral blood was taken with informed consent from two healthy donors: one male (age 64) and one female (age 38) donor. This was considered to be necessary for such a systematic investigation to minimize interindividual variations in sensitivity. All experiments were performed at room temperature (~20–22°C), because exact dosimetry for irradiation on ice with 29 kV X rays was not possible. However, a preliminary experiment showed that the magnitude of the initial DNA damage in human lymphocytes induced by 3 Gy of ^{60}Co γ rays at 37°C and 20°C and on ice was greatest at 20°C (Fig. 1). Therefore, it can be assumed that the DNA repair processes did not result in an underestimation of the initial DNA damage under the chosen temperature conditions. Irradiation was performed simultaneously with all four radiation sources per experimental set to decrease possible variations due to different experimental conditions. Immediately after irradiation, whole blood aliquots were set on ice prior to embedding the blood cells in agarose. To study DNA repair, blood samples were incubated at 37°C for defined times before setting them on ice.

Irradiation and Dosimetry

Due to dosimetric demands, the blood irradiation occurred in different blood containers. For the soft mammography X rays, the containers had to be very thin, with thin walls, to minimize the dose decrement within the blood volume and the distortion of the X-ray spectrum by the walls. For the highly energetic γ rays, secondary electron equilibrium had to be established. The air kerma rates were ~0.42 Gy/min for the X rays and ^{60}Co γ rays and ~0.66 Gy/min for the ^{137}Cs γ rays.

Mammography Radiation (29 kV, tungsten anode, 50 μm rhodium filtration)

The blood was irradiated in flat cylindrical containers (2.2 mm thick, 23.9 mm in diameter) with 20 μm polyethylene terephthalate (Mylar) windows at the entrance and exit side. To generate a typical radiation quality for mammography, a Dermopan soft X-ray therapy unit (Siemens) with an AEW50/25ö X-ray tube (anode material tungsten; anode angle

45°) was used. The unit was operated at a nominal tube voltage of 29 kV and a tube current of 20 mA. Since the Dermopan contains a rather basic one-peak high-voltage generator, with a strong dependence of tube voltage from primary voltage, tube current and duration of irradiation, tube current and primary voltage at the transformer were kept constant manually during irradiation. Under these conditions a tube voltage of 29 kV could be achieved, as determined by means of a high-purity germanium X-ray spectrometer. The beam filtration consisted of 1 mm beryllium (tube window) and 50 μm rhodium (Rh) (RH000210, Goodfellow). The X-ray spectrum, characterized by the rhodium K edge at 23.2 keV, had a mean photon energy of 19.4 keV and a half-value layer (HVL) of 0.51 mm aluminum, both values calculated from the photon spectrum. HVL values in mammography range are typically from 0.34 to 0.56 mm aluminum (*34*).

Two 0.02-cm³ soft X-ray chambers (type M 23342, PTW Company, Germany) were used for dosimetry. One, connected to an electrometer IQ4 (PTW) and mounted directly beside the blood container, served as a monitor chamber during irradiation. For the other chamber, connected to a Unidos electrometer (PTW), an air kerma calibration factor from PTB (German National Metrology Institute) for the quality T 30 (30 kV; 0.5 mm aluminum; E_m = 19.6 keV; HVL = 0.36 mm aluminum) was available. By means of this chamber, the monitor was calibrated in terms of air kerma at the container-to-focus distance ($\sim$15 cm). More details on the X-ray source and the dosimetric procedures were given by Göggelmann *et al.* (*4*).

The mean absorbed dose to blood, D_{blood}, was determined, using Eqs. (1) and (2), from the measured air kerma at the position of the entrance window (K_{entr}), measured air kerma behind the exit window (K_{exit}) and a backscatter factor (BSF = 1.033) calculated by Monte Carlo methods for the above, filled blood container and spectrum. (The calculation of BSF was performed by M. Zankl, GSF-Institute for Radiation Protection.)

$$D_{blood} = \frac{1}{2} \times (BSF \times K_{entr} + K_{exit}) \times \frac{\overline{(\mu_{en}/\rho)}_{blood}}{(\mu_{en}/\rho)_{air}}; \quad (1)$$

$$D_{blood} = K_{air} \times 0.966; \quad (2)$$

where $\overline{(\mu_{en}/\rho)}_m$ is the mean spectral mass energy absorption coefficient for the materials m (blood, air). $\overline{(\mu_{en}/\rho)}_m$ was calculated using Eq. (3);

$$\overline{\left(\frac{\mu_{en}}{\rho}\right)}_m = \frac{\int_E \Phi(E) \times E \times [\mu_{en}(E)/\rho]_m \, dE}{\int_E \Phi(E) \times E \, dE}, \quad (3)$$

from the photon spectrum $\Phi(E)$ and fitted $(\mu_{en}(E)/\rho)_m$ values, taken from Hubbell (*35*).

Reference Radiation (220 kV, tungsten anode, 4.05 mm aluminum + 0.5 mm copper filtration)

The blood was irradiated in 1-ml syringes (7 mm in diameter). The reference radiation quality was generated by a highly stabilized MG 320 X-ray unit (Philips) with an MCN 323 X-ray tube (anode material tungsten; anode angle 22°) operated at a tube voltage of 220 kV and a tube current of 15 mA. The beam filtration consisted of a 3-mm beryllium (tube window) and 4.05 mm aluminum + 0.5 mm copper added filtration. The X-ray spectrum is characterized by a mean photon energy of 95.6 keV and a half-value layer of 1.39 mm copper; both values were calculated from the photon spectrum.

A transmission chamber (type 24366, PTW) connected to an IQ4 electrometer served as a monitor chamber. A 1-cm³ thimble chamber (type M23331, PTW) connected to a Unidos electrometer with an air kerma calibration factor from PTB for the quality T 200 (200 kV; 4 mm aluminum + 1 mm copper; HVL = 1.6 mm copper) was used to calibrate the monitor in terms of air kerma in the focus-to-syringe distance (70 cm).

Absorbed dose to blood was calculated from the measured air kerma according to

$$D_{blood} = K_{air} \times \frac{\overline{(\mu_{en}/\rho)}_{blood}}{(\mu_{en}/\rho)_{air}} \times T; \quad (4)$$

$$D_{blood} = K_{air} \times 1.067; \quad (5)$$

where $\overline{(\mu_{en}/\rho)}_m$ is the mean spectral mass energy absorption coefficient, analogous to Eq. (3) (*35*), and T = 0.97 is a correction factor for the dose decrement within the syringe.

Reference Radiation (⁶⁰Co γ rays)

Blood samples were irradiated in 2-ml syringes (11 mm in diameter) in the center of a Perspex phantom (thickness 22 mm, width 70 mm, height 117 mm) at an Eldorado 78 therapy unit (Atomic Energy of Canada Ltd). Air kerma was measured by means of a 1-cm³ thimble chamber (type M23331, PTW) connected to a Unidos electrometer (PTW) in an identical phantom. For the chamber an air kerma calibration factor for ⁶⁰Co γ rays from PTB was available. Absorbed dose to blood was determined from measured air kerma in source-to-syringe distance ($\sim$160 cm) using Eqs. (6) and (7),

$$D_{blood} = K_{air} \times \frac{\overline{(\mu_{en}/\rho)}_{blood}}{(\mu_{en}/\rho)_{air}}; \quad (6)$$

$$D_{blood} = K_{air} \times 1.102; \quad (7)$$

where $(\mu_{en}/\rho)_m$ is the mass energy absorption coefficient of blood and air for ⁶⁰Co γ rays (*35*).

Reference Radiation (¹³⁷Cs γ rays)

Blood (10 μl) was irradiated in 20-μl Eppendorf caps placed in a tart-shaped holder in a closed HWM D2000 irradiation facility (Wälischmiller). In spite of its unfavorable properties with regard to field homogeneity and consequently for dosimetry, this source was the only one available that provided dose rates similar to those of the other sources. For this source, an earlier calibration already existed already in terms of absorbed dose to water in the midline plane of the irradiation chamber of the source, where the Eppendorf caps were placed. Air kerma was determined by condenser-type chambers (PTW) evaluated with an integrating electrometer (Condiometer, PTW). The condenser chambers were again calibrated by means of a Farmer Dosimeter 2570 with a 0.6-cm³ thimble chamber (type 2571) at an open Caesa-Gammatron source (Siemens), and the results were converted into absorbed dose to water. A manufacturer's calibration existed for the ¹³⁷Cs ionization chamber.

Absorbed dose to blood was finally determined from absorbed dose in the midline plane using Eqs. (8) and (9):

$$D_{blood} = D_{water} \times \frac{\overline{(\mu_{en}/\rho)}_{blood}}{(\mu_{en}/\rho)_{water}}; \quad (8)$$

$$D_{blood} = D_{water} \times 0.991. \quad (9)$$

Due to field inhomogeneity and the multiple steps involved, the error in the dose measurements for the ¹³⁷Cs γ radiation was 10%, whereas the errors for the three other radiation types were less than 3%.

DNA Repair

DNA repair was assessed by incubation of the samples at 37°C immediately after irradiation. Aliquots were taken after certain intervals, usually from 10 to 60 min after irradiation, and set on ice. In parallel, sham-irradiated controls were also collected after the same intervals.

Comet Assay

For the comet assay, a modification of the original protocol of Singh *et al.* (*36, 37*) was applied to whole blood. Special microscope slides

(ESW-370; Erie Scientific, Portsmouth, NH) with frosted edges and a clear window were precoated with 200 μl of 0.1% low-melting agarose (Sigma) and dried at 40°C on a warming plate. Then 10 μl of whole blood was mixed with 100 μl of 0.5% warm agarose (Amresco, Solon, OH) at 50°C and immediately transferred onto prewarmed precoated slides. A cover slip was placed gently over the agarose prior to chilling the slide for 5 min at 0°C on a cooling plate. For further treatment the cover slip was removed.

The microscope slides were immersed in a freshly prepared cold lysis buffer (2.5 M NaCl, 100 mM Na$_4$EDTA, pH 10, 10 mM Tris HCl, pH 10, 1% SDS, and 1% Triton X-100). Lysis was performed over night. Afterward, most nuclear proteins were removed by incubation in the second lysis buffer (2.5 M NaCl, 100 mM Na$_4$EDTA, pH 10, 10 mM Tris HCl, pH 10) for 1 h at 37°C. Slides were transferred to a specially adapted tray to prevent movement of slides during electrophoresis (Amersham Pharmacia HE100 Supersub). Twenty-one slides could be electrophoresed in one electrophoresis chamber. Unwinding was performed for 20 min in electrophoresis buffer (300 mM NaOH, 2% DMSO, and 10 mM Na$_4$EDTA, pH 10; pH >13). The temperature during electrophoresis (0.8 V/cm; 300 mA; 30 min) was kept constant at 20°C by a temperature control unit. After electrophoresis, the DNA was precipitated and fixed by incubation in 1% ammonium acetate in ethanol (5 ml of 10 M ammonium acetate and 45 ml of 100% ethanol) for 30 min at room temperature. After dehydration in 100% ethanol overnight, the slides were rehydrated with 70% ethanol for 5 min (to avoid the agarose cracking during drying), air-dried and stored at room temperature prior to staining. Slides were incubated for 15 min in double-distilled water and then stained with 50 μl of a solution containing 950 μl water, 60 μl DMSO, 200 μl Vectashield (Vector Laboratories, Burlingame, CA), and 1 μl SYBR-green (Molecular Probes, Eugene, OR). Slides were evaluated immediately after staining.

Hardware and Software for Image Acquisition and Comet Analysis

Fifty comets per slide were examined under an epifluorescence microscope (Axiovert 135, Zeiss, Germany; 40× air objective) equipped with an adequate set of filters for SYBR-green and a monochromator (T.I.L.L. Photonics, Munich, Germany) as a light source for the image analysis. Excitation was performed at 461 nm and emission at 510 nm. Images were acquired with a Sony Video Camera (XC-7500) and evaluated by special software for comet image analysis (VisCOMET, Impuls GmbH, Gilching, Germany).

Statistical Evaluation

In total, results from five independent experiments were analyzed to detect the dose effect of the four different types of photon radiation and three independent experiments concerning DNA temporal repair patterns. DNA damage was determined by analyzing the Olive tail moment or percentage DNA in tail. The Olive tail moment was calculated by (center of gravity of tail profile − center of gravity of head profile) × tail intensity/total intensity and expressed in arbitrary units since length calibration is defined in pixels rather than micrometers.

The original data set was computed in box plots (Statistica Version 6, StatSoft). The data were transformed to natural logarithms to achieve a greater degree of normality in the data set distributions. The justification for the use of such natural logarithm transformations to achieve a greater degree of normality in the distribution function for tail moment is given in the Appendix. Linear fits by multiple regression analysis were applied to the dose–response curves.

RESULTS

A clear dose–response relationship for initial DNA damage was observed in human lymphocytes exposed to 29 kV X rays and the reference radiation types within the dose
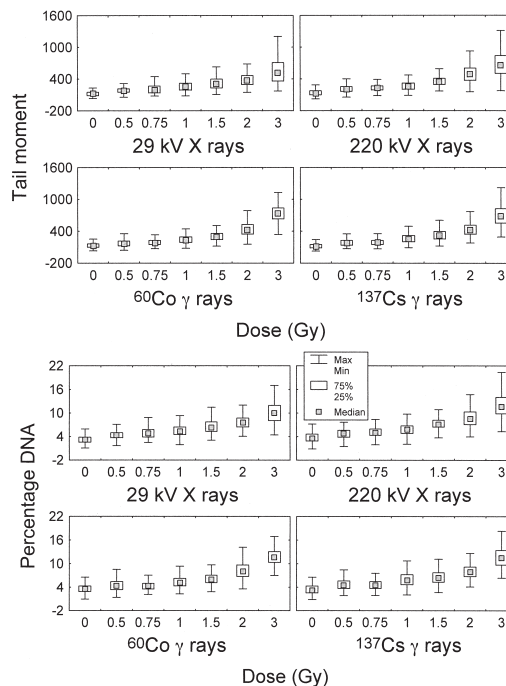
FIG. 2. Damage distribution demonstrated by box plot analyses of two damage parameters, tail moment and percentage DNA in the tail, as a function of free in air kerma dose.

range from 0.5 to 3 Gy. As shown in Fig. 2, the results for the two damage parameters analyzed, tail moment and percentage DNA in tail, are rather similar and are not normally distributed. The tail moment values were transformed by natural logarithms for all five independent experiments (Fig. 3a), while for percentage DNA in tail, means of 50 individual cells for five independent experiments were computed (Fig. 3b). There were only minor variations in the values obtained in the different experiments. The best-fit parameters indicate a linear dose–response relationship for all four radiation types (Fig. 4a, b) for tail moment as well as for percentage DNA. The slopes did not differ significantly from each other over the total dose range investigated. To determine whether 29 kV X rays were able to increase DNA damage in the low-dose range, we focused on the dose range from 0 to 1 Gy (Fig. 5). In this case too, the slopes did not differ significantly from each other. When tested by multiple regression analysis with the overparameterized coding method and separate slope design (Table 1), no significant effect could be detected amongst either the experiments or the radiation types. Since two out of five experiments were performed with blood from a female donor, the model was also investigated for gender effects.
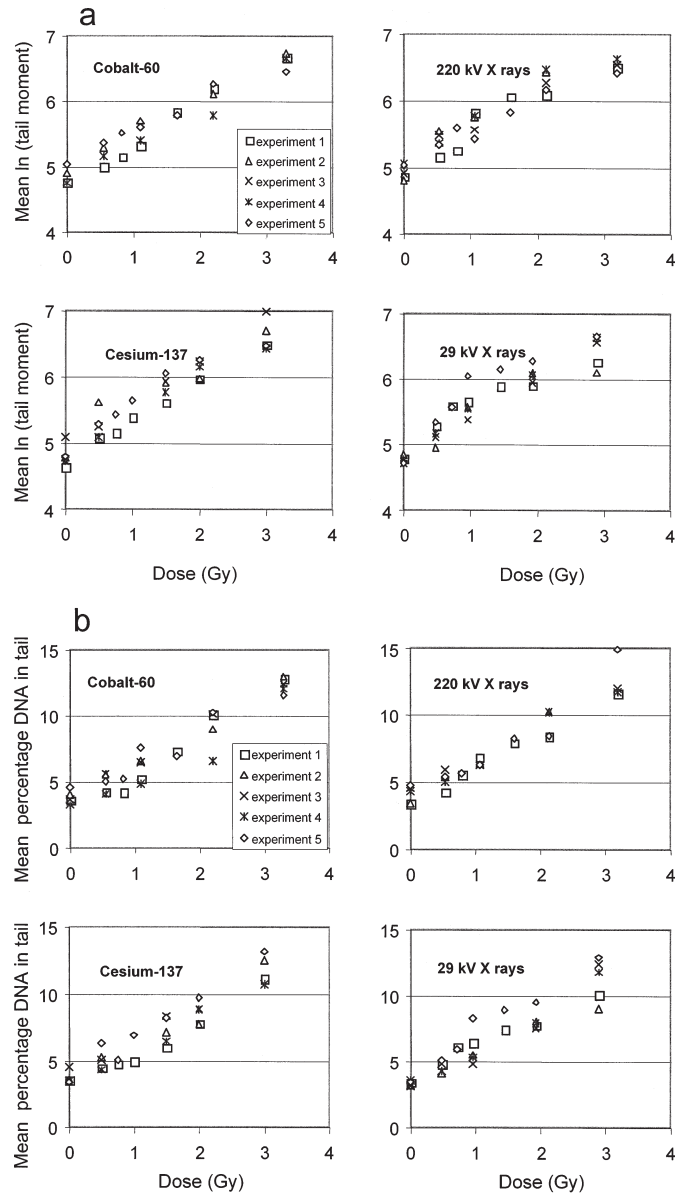
FIG. 3. Panel a: The mean natural logarithm of the tail moment as a function of blood dose for four different types of photon radiation. Each mean was computed from 50 individual ln(tail moment) values. Panel b: The mean percentage DNA in tail as a function of blood dose for four different types of photon radiation. Each mean was computed from 50 individual values.
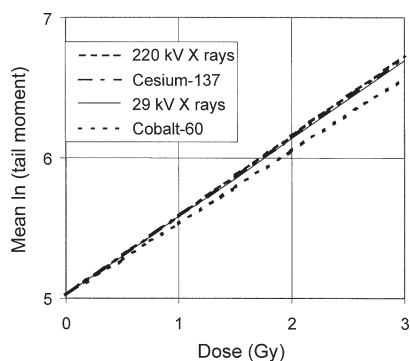
FIG. 4. Best-fit lines from the multiple regression for mean ln(tail moment) as a function of mean blood dose and as detailed in Table 1. The slopes are not significantly different; the intercept shown is for one experiment.

FIG. 5. The best-fit lines from a similar regression to that described in Table 1 but with a restricted mean blood dose range of 0 to 1 Gy. The trends in gradient are different from above, but not statistically significantly so. The intercept shown is for one experiment

No significant effect of this parameter on the data could be detected.

After irradiation of blood cells with an air kerma dose of 3 Gy, DNA repair was investigated after set intervals of 10, 20, 30 and 60 min. The experiments were repeated three times. The fraction of remaining damage was calculated by subtraction of the control tail moment from the corresponding tail moment at the various times. Initial damage at time zero was set to 100%. High variation in the experimental data can be seen during the fast repair period during the first 20 min after irradiation (Fig. 6). At repair times longer than 20 min, the residual damage showed only minor interexperimental differences. The best-fit calculation for the results obtained for the four radiation types did not detect any significant difference for the remaining damage after 60 min or for the repair half-time (Tables 2 and 3). However, there was a tendency that for irradiation with 29 kV X rays, repair of damaged DNA proceeded slightly more slowly in the first 10 to 20 min compared to the other reference radiation types (Fig. 7). In this time range, the experimental data are so variable that, for the X rays, a difference in half-time of only about 7 min [$1.645 \times (2.84 + 1.53)$] would have been detected in the fit function parameters with 90% confidence. This is because of the many sources of uncertainty due to dosimetry errors and intraexperimental and interexperimental variation.

DISCUSSION

The present study examines, for the first time, at the single cell level, the initial DNA damage and the subsequent time-dependent DNA repair in human lymphocytes after irradiation with photons of different energies. The comet assay data did not indicate any difference in the initial radiation damage produced by 29 kV X rays relative to the reference radiations, i.e. 220 kV X rays and ^{137}Cs and ^{60}Co

γ rays, either for the total dose range or in the low-dose range. It appeared that the 29 kV X rays tended to slow down DNA repair more than the reference radiation types, but this effect was not significant.

These results are, with some restrictions, consistent with physical examinations and predictions concerning, for ex-

TABLE 1
Multiple Regression with the Overparameterized Coding Method and Separate Slope Design: Results for the Categorical (Radiation Type and Experiment Number) and Continuous (Mean Blood Dose) Predictor Variables with Interaction between Dose and Radiation Type

Parameter	Best estimate	Standard error	t ratio
a	5.019	0.040	124.582
b_1	0.557	0.025	21.867
b_2	0.011	0.029	0.382
b_3	−0.040	0.029	−1.409
b_4	0.009	0.030	0.297
b_5	−0.145	0.049	−2.969
b_6	−0.033	0.053	−0.627
b_7	−0.028	0.053	−0.518
b_8	−0.103	0.053	−1.930
Standard error of mean ln(tail moment)		0.182	
Coefficient of determination		0.917	
df		107	
F value		147.35	
SS regression		39.12	
SS residual		3.55	

Notes. The model is: mean ln(tail moment) = $a + x_1 (b_1 + b_2 x_2 + b_3 x_3 + b_4 x_4) + b_5 x_5 + b_6 x_6 + b_7 x_7 + b_8 x_8$, where x_1 is the mean blood dose in grays; x_2 is either 0 or 1 and indicates a differential effect of 220 kV X rays relative to 29 kV X rays, x_3 is either 0 or 1 and indicates a differential effect of ^{60}Co relative to 29 kV X rays, x_4 is either 0 or 1 and indicates a differential effect of ^{137}Cs relative to 29 kV X rays, x_5 is either 0 or 1 and indicates a differential effect of experiment 1 relative to experiment 5, x_6 is either 0 or 1 and indicates a differential effect of experiment 2 relative to experiment 5, x_7 is either 0 or 1 and indicates a differential effect of experiment 3 relative to experiment 5, x_8 is either 0 or 1 and indicates a differential effect of experiment 4 relative to experiment 5. The various sums of squares (SS) and degrees of freedom (df) are given with the other usual measures for goodness of fit.
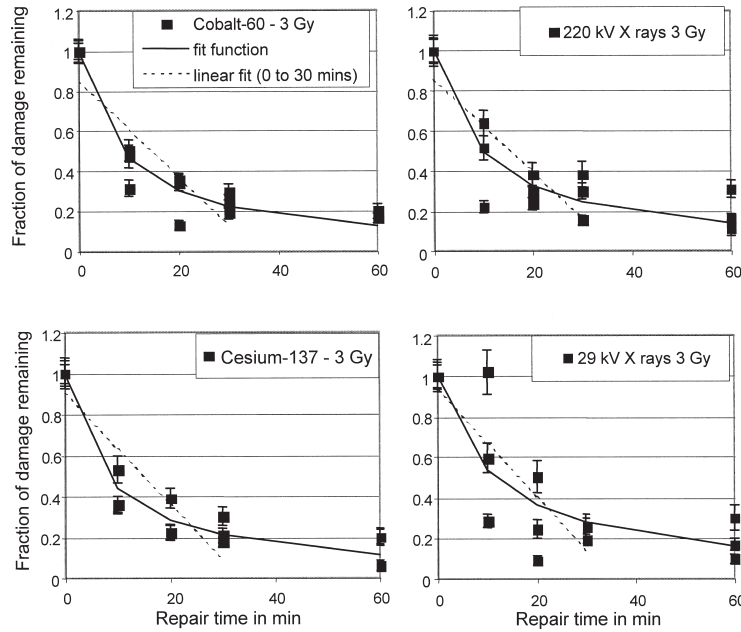
FIG. 6. The fraction of damage, mainly due to single-strand breaks, remaining after an initial irradiation with a free-in-air kerma dose of 3 Gy for four radiation types and for various repair times. Two points almost coincide for ^{137}Cs γ rays at 10, 20 and 60 min repair time.

ample, the assessment of the possible difference in effectiveness between mammography X rays and conventional X rays. As stated by Kellerer (*9*), Kellerer and Chen (*10*), and the ICRP (*38*), an analysis in terms of the explicit electron spectra at different photon energies leads to the conclusion that the RBE of mammography X rays compared with conventional X rays will, regardless of the underlying mechanisms, be between 1 and 2; this includes a consideration of a potential contribution of the 0.5 keV Auger electrons from oxygen that accompany all photoelectrons in water but only a minority of the Compton electrons that predominate at the higher photon energies. This suggestion is well in line with the RBE of about 1.3, as deduced by

Brenner and Amols (*11*) from microdosimetric data. This very low RBE value for primary lesions may be responsible for the present observation of a tendency of slowing down DNA repair after exposure of human lymphocytes to mammography X rays, indicating more complex DNA damage than after exposure to conventional X rays. The present analysis, which primarily assessed single-strand breaks, was consistent with the recent microdosimetric results. However, the present results are not consistent with recent reports (*1–8, 39*) that mammography X rays are more than twice as effective as conventional X rays or γ rays at intermediate doses or even more effective at small doses. There are two plausible explanations for this disparity: (1)

TABLE 2
Results of the Best Least-Squares Linear Fit Parameters for the Repair Time Data
between 0 and 30 min as Displayed in Fig. 5

Radiation type	Gradient	SE of gradient	Intercept	SE of intercept	χ^2	df	P	α	$T_{1/2}$ (min)
29 kV X rays	−0.0265	0.0055	0.93	0.10	0.46	10	1	4×10^{-6}	16.41
220 kV X rays	−0.0232	0.0048	0.86	0.09	0.34	10	1	1×10^{-6}	15.40
^{60}Co γ rays	−0.0242	0.0044	0.85	0.08	0.29	10	1	5×10^{-7}	14.44
^{137}Cs γ rays	−0.0270	0.0043	0.90	0.08	0.15	10	1	2×10^{-8}	14.97

Note. The fit function was $F_d = \text{gradient} \times t + \text{intercept}$, where F_d is the fraction of damage remaining and t is the time allowed for repair in minutes.

TABLE 3
Results of the Best Least-Squares Fit Parameters for the Repair Time Data between 0 and 60 min as Displayed Separately in Fig. 5 and Together in Fig. 6

Radiation type	A	SE of A	χ^2	df	P	α
29 kV X rays	11.52	2.84	0.44	13	1	2.5×10^{-8}
220 kV X rays	9.62	1.53	0.17	13	1	5×10^{-11}
^{60}Co γ rays	8.50	1.02	0.09	13	1	8.5×10^{-13}
^{137}Cs γ rays	8.00	0.85	0.07	13	1	1.4×10^{-13}

Notes. The fit function was $F_d = A/(t + A)$, where F_d is the fraction of damage remaining at t, the time allowed for repair in minutes. The major advantage of this parameterization is that there is only one fitted parameter, and this is designed to be the repair half-time in minutes.

The biologically relevant DSBs are masked by the prevailing SSBs, since DSBs contribute only about 2% to the total amount of breakage. If 29 kV X rays produce more DSBs by a factor of 2–4, this would not be detectable in the experimental system applied here, but it could be responsible for the delayed repair kinetics observed here for the 29 kV X rays. (2) On the other hand there are no, or only minor, differences in RBE for the initial biological effects, the quantity of primary lesions in DNA as detected by the comet assay, compared to the later effects detected by other assays. However, the higher RBE values obtained in studies of later biological damage indicators within the complete biological effectiveness range, i.e. from the photon-induced initial DNA damage to the late radiation effects in humans may then be due to the involvement of cellular processes acting on DNA as the first target of exposure to ionizing radiation. Measurements of the initial yield of DNA DSBs as a function of LET indicated only modest increases of 2–3, even at LETs that have an RBE for cell killing as high as 10, but when comparing the ratio of point mutations, high-LET radiation produces 12 times more. Thus Ward (*40*) suggested mechanisms whereby complex damage to intracellular DNA is caused by multiple radical attacks on local sites producing locally multiply damaged sites or clustered lesions. He concluded that the higher RBE for cell killing must be associated with the cell's response to the initial damage. Tanaka *et al.* (*31*) compared results from both the comet assay and studies of chromosomal aberrations and found the latter to be two to three times more sensitive and in good agreement with results from cell transformation experiments. They also suggested that primary DNA damage is amplified during cell proliferation after irradiation. If repaired, even in SSBs that are offset by several base pairs, loss of sequence information may occur and thus lead to errors in base sequences (*41*). A recent investigation (*42*) demonstrates that during DNA replication abasic sites, which are also created during radiation exposure, may result in the loss of a base triplet and give rise to proteins lacking a single amino acid. Proteins lacking a single amino acid have
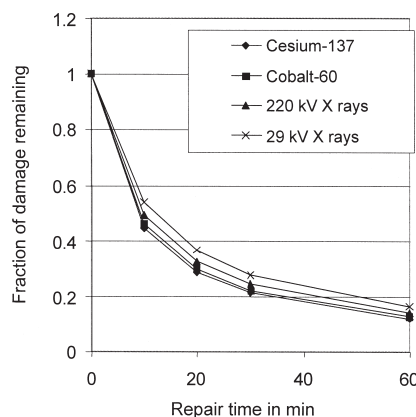
FIG. 7. The best fit to the fraction of damage remaining after irradiation with 3 Gy free-in-air kerma photon radiation as a function of repair time between 0 and 60 min (also displayed separately in Fig. 6). The fit function was $Fd = A/(t + A)$, where Fd is the fraction of damage remaining at t, the time allowed for repair in minutes. The major advantage of this parameterization is that there is only one fitted parameter, and this is designed to be the repair half-time in minutes.

been implicated in cancer and other diseases in which oxidative stress is a causative factor. Thus different repair pathways and DNA replication are steps in the downstream processing where initial DNA damage may be amplified.

CONCLUSION

The results from the present comet assay experiments illustrate that the yields of the initial DNA damage in human lymphocytes exposed to 29 kV X rays (mammography X rays) do not differ significantly from the corresponding yields obtained simultaneously for conventional X rays or ^{137}Cs and ^{60}Co γ rays. Especially because of the revived debate on the different magnitudes of the biological effects induced by photons with different energies, it is important to obtain information on the relative effects of low photon energy and reference radiations such as higher-energy X rays or γ rays. The present results are in essence consistent with physical models concerning the primary lesions at the DNA. On the other hand, it has long been recognized that, especially at different low doses, low-LET radiation types do not have the same biological effectiveness. In chromosome aberrations or cell transformation studies, there can be some biological factors that enhance the difference between mammography X rays and the reference radiation types. These differences in the downstream processing of primary lesions to produce late radiation effects lead to different RBE values.
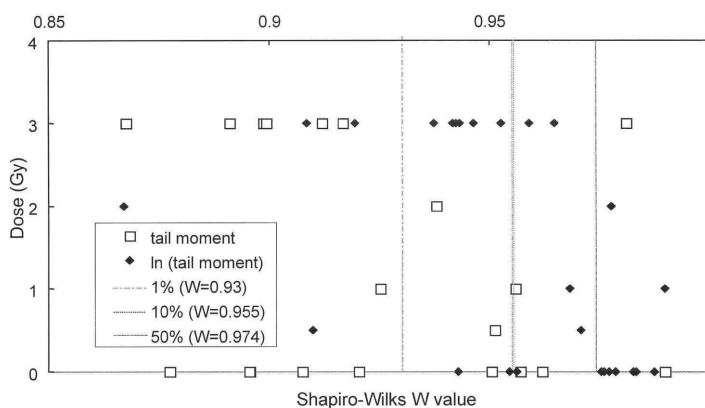
FIG. A1. Results for 52 *W* tests, 26 for tail moment and 26 for ln(tail moment); the percentage points are also represented as three vertical lines. Plotted values of *W* to the right of the vertical lines can be accepted for the hypothesis of normality at one of the three percentage points given. Critical values for normality hypothesis testing for *n* = 50 are *W* = 0.93, 0.955 and 0.974 for the percentage points 1, 10 and 50, respectively.

APPENDIX

The Underlying Distribution for Tail Moment

Each of the points in Fig. 3 represents the mean value of *n* = 50 individual ln(tail moment) values, one from each cell. There are 96 such sets of 50 data points contributing to Fig. 3, and part of the data analysis procedure involved identifying the best representation of the underlying distribution. A qualitative assessment of some of the individual distributions revealed a wide spectrum of shapes including symmetrical, skewed and weakly bimodal. Previous work has identified the form to be best represented by log-normal (*43*) or χ^2 (*44*).

To assess the statistical form for the present data sets, a detailed analysis has been done for a subset of the data for one experiment from the middle of the data collection process and the two types of X radiation. This reduced the analysis to 26 data sets on which tests of normality for both tail moment and ln(tail moment) were performed (52 tests). Initially a χ^2 test was performed and indicated that the distributions were closer to log-normal than normal. However, the disadvantage of the χ^2 test for normality is that the data must be grouped, and with 50 points the maximum number of bins allowed is only 10. A comparative study of various tests for normality (*45*) has evaluated the sensitivity of nine different tests and found the Shapiro-Wilks *W* test (*46*) to provide a generally superior measure of non-normality. The necessary Shapiro-Wilks *W* coefficients and percentage points for hypothesis testing for *n* = 50 are readily available in the literature (*46*), and this test was considered suitable for application to the comet assay data. The *W* statistic is obtained by dividing two different estimators for the variance, i.e. the squared slope of the probability plot regression line and the usual symmetric sample sum of squares about the mean, which should both be very similar for a normal distribution and result in *W* values close to unity, for *n* = 50, $0.14 < W \leq 1$. Small values of *W* are significant, i.e. indicate non-normality. Critical values for normality hypothesis testing for *n* = 50 are *W* = 0.93, 0.955 and 0.974 for the percentage points 1, 10 and 50, respectively.

Results for 52 *W* tests, 26 for tail moment and 26 for ln(tail moment), are presented in Fig. A1, where the percentage points are also represented as three vertical lines. Plotted values of *W* to the right of the vertical lines can be accepted for the hypothesis of normality at one of the three percentage points given. The choice of dose for the ordinate is not to indicate a dose response but merely to spread out the points better in the graphical representation. The general trend is that more ln(tail moment) tests can be accepted as normal than the corresponding tests for tail mo-

ment; i.e., there are more diamonds than open squares toward the right hand side of the graph. In fact, there are five tail moment *W*-test values off the scale below *W* = 0.85. The hypothesis that the distribution is normal can be rejected in a larger number of cases for tail moment than for ln(tail moment). On the basis of these results, it was concluded that the underlying distribution of tail moment was more closely represented by log-normal than by normal.

REFERENCES

1. D. Frankenberg, K. Kelnhofer, I. Garg, K. Bar and M. Frankenberg-Schwager, Enhanced mutation and neoplastic transformation in human cells by 29 kVp relative to 200 kVp X rays indicating a strong dependence of RBE on photon energy. *Radiat. Prot. Dosim.* **99**, 261–264 (2002).

2. E. Schmid, D. Regulla, H. M. Kramer and D. Harder, The effect of 29 kV X rays on the dose response of chromosome aberrations in human lymphocytes. *Radiat. Res.* **158**, 771–777 (2002).

3. E. Schmid, M. Krumrey, G. Ulm, H. Roos and D. Regulla, The maximum low-dose RBE of 17.4 and 40 keV monochromatic X rays for the induction of dicentric chromosomes in human peripheral lymphocytes. *Radiat. Res.* **160**, 499–504 (2003).

4. W. Göggelmann, C. Jacobsen, W. Panzer, L. Walsh, H. Roos and E. Schmid, Re-evaluation of the RBE of 29 kV x-rays (mammography x-rays) relative to 220 kV x-rays using neoplastic transformation of human CGL1-hybrid cells. *Radiat. Environ. Biophys.* **42**, 175–182 (2003).

5. R. Cox, J. Thacker and D. T. Goodhead, Inactivation and mutation of cultured mammalian cells by aluminium characteristic ultrasoft X-rays. II. Dose-responses of Chinese hamster and human diploid cells to aluminium X-rays and radiations of different LET. *Int. J. Radiat. Biol.* **31**, 561–576 (1977).

6. C. Borek, E. J. Hall and M. Zaider, X rays may be twice as potent

as gamma rays for malignant transformation at low doses. *Nature* **301**, 156–158 (1983).

7. L. Hieber, K. Trutschler, J. Smida, M. Wachsmann, G. Ponsel and A. M. Kellerer, Radiation-induced cell transformation: Transformation efficiencies of different types of ionizing radiation and molecular changes in radiation transformants and tumor cell lines. *Environ. Health Perspect.* **88**, 169–174 (1990).

8. D. Frankenberg, H. Kuhn, M. Frankenberg-Schwager, W. Lenhard and S. Beckonert, 0.3 keV carbon K ultrasoft X-rays are four times more effective than gamma-rays when inducing oncogenic cell transformation at low doses. *Int. J. Radiat. Biol.* **68**, 593–601 (1995).

9. A. M. Kellerer, Electron spectra and the RBE of X rays. *Radiat. Res.* **158**, 13–22 (2002).

10. A. M. Kellerer and J. Chen, Comparative microdosimetry of photoelectrons and Compton electrons: An analysis in terms of generalized proximity functions. *Radiat. Res.* **160**, 324–333 (2003).

11. D. J. Brenner and H. I. Amols, Enhanced risk from low-energy screen-film mammography x-rays. *Br. J. Radiol.* **62**, 910–914 (1989).

12. K. Eguchi, T. Inada, M. Yaguchi, S. Satoh and I. Kaneko, Induction and repair of DNA lesions in cultured human melanoma cells exposed to a nitrogen-ion beam. *Int. J. Radiat. Biol.* **52**, 115–123 (1987).

13. J. Heilmann, H. Rink, G. Taucher-Scholz and G. Kraft, DNA strand break induction and rejoining and cellular recovery in mammalian cells after heavy-ion irradiation. *Radiat. Res.* **135**, 46–55 (1993).

14. P. E. Bryant, R. Warring and G. Ahnstrom, DNA repair kinetics after low doses of X-rays. A comparison of results obtained by the unwinding and nucleoid sedimentation methods. *Mutat. Res.* **131**, 19–26 (1984).

15. J. H. Schwachofer, R. P. Crooijmans, H. Hoogenhout, H. B. Kal, R. Q. Schaapveld and J. Wessels, Differences in repair of radiation induced damage in two human tumor cell lines as measured by cell survival and alkaline DNA unwinding. *Strahlenther. Onkol.* **167**, 35–40 (1991).

16. D. Blocher, DNA double strand breaks in Ehrlich ascites tumour cells at low doses of x-rays. I. Determination of induced breaks by centrifugation at reduced speed. *Int. J. Radiat. Biol.* **42**, 317–328 (1982).

17. M. A. Ritter, J. E. Cleaver and C. A. Tobias, High-LET radiations induce a large proportion of non-rejoining DNA breaks. *Nature* **266**, 653–655 (1977).

18. K. Yamada, Y. Kameyama and S. Inoue, An improved method of alkaline sucrose density gradient sedimentation to detect less than one lesion per 1 Mb DNA. *Mutat. Res.* **364**, 125–131 (1996).

19. J. Dahm-Daphi and E. Dikomey, Rejoining of DNA double-strand breaks in X-irradiated CHO cells studied by constant- and graded-field gel electrophoresis. *Int. J. Radiat. Biol.* **69**, 615–621 (1996).

20. D. Frankenberg, H. J. Brede, U. J. Schrewe, C. Steinmetz, M. Frankenberg-Schwager, G. Kasten and E. Pralle, Induction of DNA double-strand breaks by ¹H and ⁴He ions in primary human skin fibroblasts in the LET range of 8 to 124 keV/micrometer. *Radiat. Res.* **151**, 540–549 (1999).

21. D. P. Garwood, L. L. Thompson and W. C. Dewey, Use of pulsed-field gel electrophoresis to measure X-ray-induced double-strand breaks in DNA substituted with BrdU. *Radiat. Res.* **128**, 210–215 (1991).

22. K. J. Weber and M. Flentje, Lethality of heavy ion-induced DNA double-strand breaks in mammalian cells. *Int. J. Radiat. Biol.* **64**, 169–178 (1993).

23. L. Weglarz, A. Koceva-Chyla, M. Drozdz and Z. Jozwiak, Single-strand breaks and repair in nuclear DNA in the presence of hydralazine assayed by the nucleoid technique. *Biochem. Mol. Biol. Int.* **43**, 513–519 (1997).

24. G. Ahnstrom, Techniques to measure DNA single-strand breaks in cells: A review. *Int. J. Radiat. Biol.* **54**, 695–707 (1988).

25. A. R. Collins, The comet assay. Principles, applications, and limitations. *Methods Mol. Biol.* **203**, 163–177 (2002).

26. P. L. Olive, DNA damage and repair in individual cells: Applications of the comet assay in radiobiology. *Int. J. Radiat. Biol.* **75**, 395–405 (1999).

27. P. L. Olive, The comet assay. An overview of techniques. *Methods Mol. Biol.* **203**, 179–194 (2002).

28. R. R. Tice, E. Agurell, D. Anderson, B. Burlinson, A. Hartmann, H. Kobayashi, Y. Miyamae, E. Rojas, J. C. Ryu and Y. F. Sasaki, Single cell gel/comet assay: Guidelines for *in vitro* and *in vivo* genetic toxicology testing. *Environ. Mol. Mutagen.* **35**, 206–221 (2000).

29. N. Gajendiran, K. Tanaka and N. Kamada, Comet assay to sense neutron 'fingerprint'. *Mutat. Res.* **452**, 179–187 (2000).

30. R. Mustonen, G. Bouvier, G. Wolber, M. Stohr, P. Peschke and H. Bartsch, A comparison of gamma and neutron irradiation on Raji cells: Effects on DNA damage, repair, cell cycle distribution and lethality. *Mutat. Res.* **429**, 169–179 (1999).

31. K. Tanaka, N. Gajendiran, S. Endo, K. Komatsu, M. Hoshi and N. Kamada, Neutron energy-dependent initial DNA damage and chromosomal exchange. *J. Radiat. Res.* **40**, 36–44 (1999).

32. I. Testard and L. Sabatier, Assessment of DNA damage induced by high-LET ions in human lymphocytes using the comet assay. *Mutat. Res.* **448**, 105–115 (2000).

33. E. Schmid, D. Schlegel, S. Guldbakke, R. P. Kapsch and D. Regulla, RBE of nearly monoenergetic neutrons at energies of 36 keV–14.6 MeV for induction of dicentrics in human lymphocytes. *Radiat. Environ. Biophys.* **42**, 87–94 (2003).

34. *European Protocol on Dosimetry in Mammography.* EUR-16263, European Commission, Brussels, 1996.

35. J. H. Hubbel, Photon mass attenuation and energy-absorption coefficients from 1 keV to 20 MeV. *Int. J. Appl. Radiat. Isot.* **33**, 1269–1290 (1982).

36. N. P. Singh, M. T. McCoy, R. R. Tice and E. L. Schneider, A simple technique for quantitation of low levels of DNA damage in individual cells. *Exp. Cell. Res.* **175**, 184–191 (1988).

37. N. P. Singh, R. R. Tice, R. E. Stephens and E. L. Schneider, A microgel electrophoresis technique for the direct quantitation of DNA damage and repair in individual fibroblasts cultured on microscope slides. *Mutat. Res.* **252**, 289–296 (1991).

38. ICRP, *Relative Biological Effectiveness (RBE), Quality Factor (Q), and Radiation Weighting Factor (wR).* Publication 92, *Annals of the ICRP*, Vol. 33, Pergamon Press, Oxford, 2003.

39. D. Frankenberg, K. Kelnhofer, K. Bar and M. Frankenberg-Schwager, Enhanced neoplastic transformation by mammography X rays relative to 200 kVp X rays: Indication for a strong dependence on photon energy of the RBE_M for various end points. *Radiat. Res.* **157**, 99–105 (2002).

40. J. F. Ward, The complexity of DNA damage: Relevance to biological consequences. *Int. J. Radiat. Biol.* **66**, 427–432 (1994).

41. A. A. Francis, R. D. Snyder, W. C. Dunn and J. D. Reagan, Classification of chemical agents as to their ability to induce long- or short-patch DNA repair in human cells. *Mutat. Res.* **83**, 159–169 (1981).

42. K. M. Kroeger, J. Kim, M. F. Goodman and M. M. Greenberg, Effects of the C4′-oxidized abasic site on replication in *Escherichia coli*. an unusually large deletion is induced by a small lesion. *Biochemistry* **43**, 13621–13627 (2004).

43. E. Bauer, R-D. Recknagel, U. Fiedler, L. Wollweber, C. Bock and K. O. Greulich, The distribution of the tail moments in single cell gel electrophoresis (comet assay) obeys a chi-square (χ^2) not a gaussian distribution. *Mutat. Res.* **398**, 101–110 (1998).

44. S. J. Wiklund and E. Agurell, Aspects of design and statistical analysis in the comet assay. *Mutagen* **18**, 167–175 (2003).

45. S. S. Shapiro, M. B. Wilk and H. J. Chen, A comparative study of various tests for normality. *J. Am. Stat. Assoc.* **63**, 1343–1372 (1968).

46. S. S. Shapiro and M. B. Wilks, An analysis of variance test for normality (complete samples). *Biometrika* **52**, 591–611 (1965).

10. Nekolla EA, Walsh L, Schottenhammer G & Spiess H. Malignancies in patients treated with high doses of radium-224. Proc, 9th Internat. conf. on Health Effects of Incorporated Radionuclides (HEIR 2004), Oeh U, Roth P, Paretzke HG (Eds.), GSF-Forschungszentrum GmbH, 67-74, 2005

Malignancies in Patients Treated with High Doses of Radium-224

E.A. Nekolla[1], L. Walsh[2], G. Schottenhammer[3], H. Spiess[3]

[1]Federal Office for Radiation Protection, BfS, Ingolstädter Landstraße 1, 85758 Neuherberg, Germany
[2]Radiobiological Institute, University of Munich; [3]Children's Hospital, University of Munich
e-mail: ENekolla@BfS.de

Abstract: Several thousand German patients suffering from ankylosing spondylitis, tuberculosis and some other diseases, received multiple injections of the short-lived α-emitter ^{224}Ra. The "Spiess study" was initiated in the early 1950s to follow the health of 899 persons (278 female, 621 male) who were treated mainly between 1945 and 1955. Most of the high dose patients and nearly all of those treated as children or juveniles (n=217) were included in the study. In June 2003, 152 persons were still alive. The most striking observed health effect, following ^{224}Ra injections, was a temporal wave of 56 malignant bone tumours with a maximum at about 8 years after exposure which has already been described in several publications. In 2000, a new analysis was performed because an improved dosimetry resulted in modified bone surface doses. The estimated risk coefficient, averaged over all ages at exposure, was found to be in agreement with earlier analyses. However, a statistically significant increase of bone tumour risk with decreasing age at exposure was found. The earlier results, which indicated a reversed protraction factor, were confirmed. A significant excess of *non-skeletal* solid malignancies has also appeared during the most recent observation decade. In 2004, significant increases of cancer rates were observed for several sites: for breast cancer (31 cases observed vs. 9.1 cases expected), soft tissue malignancies (11 vs. 1.0), thyroid carcinomas (7 vs. 0.9), liver (8 vs. 2.3), kidney (13 vs. 4.6), pancreas (8 vs. 3.9), and bladder cancer (14 vs. 7.7). The 8-fold excess relative risk of mammary cancers in those women exposed as children or juveniles is particularly striking; moreover, 2 cases of breast cancer occurred in men. In 1993, a control group of tuberculosis patients not treated with ^{224}Ra was established to rule out potential confounding factors – such as chest fluoroscopy – which might bias the breast cancer excess. From the comparison it appeared, that the ^{224}Ra treatment is responsible for most of the mammary cancer excess.

1. Introduction

During the 1940s and 50s the pharmaceutical *Peteosthor* was administered to patients suffering from ankylosing spondylitis, tuberculosis and some other diseases and was claimed to be an effective treatement of such diseases by the physician Dr. Paul Troch. Peteosthor was a mixture of the short-lived α-emitter radium-224 and traces of the red dye eosin and colloidal platinum where the latter was supposed to "guide" the ^{224}Ra to the affected tissue. In 1948, the paediatrician Heinz Spiess evaluated – as part of an inquiry by German universities – the effectiveness of *Peteosthor* therapy and demonstrated that a suppression of the growth of the tubercle bacillus would require doses of ^{224}Ra that are lethal. Spiess found that, in animal experiments, the distribution of radium in the organism was the same for Petcosthor and for pure ^{224}Ra. In addition he pointed out that ^{224}Ra caused growth retardation in young rabbits. Repeated warnings about Peteosthors very serious, detrimental side-effects were not heeded, until Spiess succeeded in stopping the treatment of children in the 1950s. The treatment of adults with ankylosing spondylitis continued, although with much lower doses.

The "Spiess study" (Study I) established the follow-up of 899 patients who received several injections of ^{224}Ra, mainly between 1945 and 1955 (see Fig. 1). This Study I includes most of the patients who were treated with high doses (mean bone surface dose: 30 Gy [1], mean specific activity: 0.66 MBq/kg), and almost all of those treated as children or juveniles. 455 patients (including 214 children and juveniles) were treated for tuberculosis, especially bone tuberculosis; 393, mostly adults and in the majority males, were treated for ankylosing spondylitis (see tab. I).

In June 2003, when the most recent follow-up was completed, a total of 152 study persons (70 women, 82 men) were still alive (see tab. I). In 2003, the mean attained age of those still alive was 69 years.
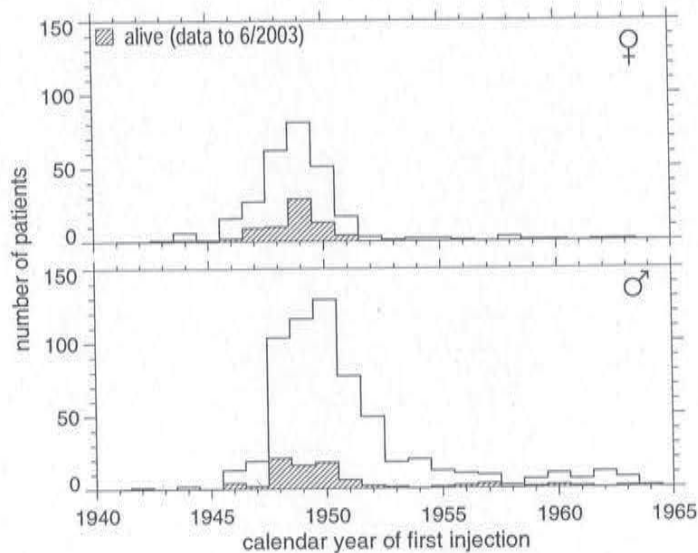
Fig. 1: Distribution of ^{224}Ra patients in calendar year of 1st ^{224}Ra injection, i.e. number of patients at specified calendar year (upper panel: female patients, lower panel: male patients); hatched area: patients still alive as of June 2003.

Tab. I: ^{224}Ra patients: current status (in June 2003) and distribution of sexes, ages at exposure and original diseases[a] (TB: tuberculosis; AS: ankylosing spondylitis)

total 899 (152)[b]							
females 278 (70)				males 621 (82)			
age at exposure ≤ 20 106 (42)		age at exposure > 20 172 (28)		age at exposure ≤ 20 111 (44)		age at exposure > 20 510 (38)	
TB	AS	TB	AS	TB	AS	TB	AS
105 (41)	–	124 (24)	24 (4)	107 (42)	1	117 (14)	368 (24)

[a] The numbers in last line do not add up to the totals because "other diseases" were not included
[b] The numbers in parentheses are the numbers of patients who are still alive

2. Results

2.1. Malignant bone tumours after ^{224}Ra injection

The most prominent detrimental side-effect of the ^{224}Ra injections were 56 malignant bone tumours which occurred in a temporal wave that peaked around 8 years after exposure. According to cancer registry data, the expected number of bone sarcomas in the Study I cohort would have been less than one over the entire observation period. Approximately half of the malignant bone tumours were osteosarcomas, the second most common histological type was fibrous-histiocytic sarcoma [1, 2]. The bone-sarcoma excess has been described in several publications (e.g. [3-7]). Recently, a new analysis

was performed [1], because a dosimetry reassessment by Henrichs et al. [8] led to changed bone sur-face doses. For those patients exposed at a young age, the new dosimetric calculations indicate doses substantially smaller than those previously assumed. Earlier analyses had led to the conclusion that the excess bone-tumour risk does not substantially depend on age at exposure. However, with the new dosimetric information, a significant increase of bone-tumour risk per unit dose with decreasing age at exposure was derived.

The earlier analysis [7] provided risk estimates that included a *reverse protraction factor* for the car-cinogenic effects of α-rays (i.e. higher bone-sarcoma risk for patients with longer exposure times at equal total dose). Such an effect has also been reported for lung cancers induced by the decay of ra-don and its daughters in the lungs of underground miners (see [9]). The new analysis confirms the result of a reverse protraction factor, however, whereas in the previous analysis the dependence on duration of exposure was postulated to be present even at low doses, a somewhat modified model has been employed here. In agreement with microdosimetric considerations and general radiobiological experience, the dependence of the excess bone tumour risk on dose-rate or duration is effective only at higher doses, i.e. the initial slope is independent of dose-rate or duration of the exposure [1]. The estimated risk coefficient, averaged over all ages at exposure, is in agreement with earlier analyses.

2.2. Non-skeletal malignancies following ^{224}Ra injections

Here, and in the following, the expected numbers of cases were computed from the age and calendar year distribution of study persons under observation and the calendar year and age specific incidence rates from the Saarland Cancer Registry.

As of June 2003, the total number of observed malignant diseases was 301 vs. 182 expected cases. During the most recent years of the follow-up, a significant excess of non-skeletal malignancies has become apparent, i.e. apart from the 56 malignant bone tumours, 225 specified cases of non-skeletal solid cancers have been observed and 20 other malignant diseases: 6 malignant neoplasms without specification of site, 8 cases of leukaemia, 3 Non Hodgkin lymphomas and 3 multiple myelomas.

In the following, a 5 years minimum latency period for radiation induced cases is assumed.

Four of the 225 non-skeletal tumours occurred less than 5 years after first ^{224}Ra injection. Assuming a 5 year lag period and excluding 12 cases of non-melanoma skin cancer, mainly basaliomas, 209 cases were observed vs. 143 expected cases.

In fig. 2, the rate ratios or standardised incidence rates, *SIR*, i.e. the quotients of the observed and the expected numbers of solid non-skeletal tumours (excluding non-melanoma skin cancer) with 90% confidence intervals, are given for the entire ^{224}Ra study cohort and for individual patient groups ac-cording to gender, age at exposure or original disease.

It should be noted that the relative rate for women is 2.6-times the expected, but the relative rate for men is close to 1. The rates are significantly increased both for women treated as adults and for women treated as children or juveniles,.

Especially for women exposed at younger ages, there is a marked excess: the number of observed cases is 5.5 times the number of expected cases. In this subgroup 19 breast cancer cases (vs. 2.4) have been observed (see below).

For male persons treated as children or juveniles, the rate ratio is more than twice that expected. On the other hand, the observed incidence rate of men exposed as adults is low compared to a "normal" population.

The relative rate in the sub-cohort of former tuberculosis patients is significantly increased as well because about half of these patients were below 21 years of age at the time of ^{224}Ra treatment.

However, in the cohort of ankylosing spondylitis patients or of persons who suffered from other dis-eases, the number of cases is less than expected.

Rate ratios for different groups of patients

	observed cases	p =
entire study cohort	209	< 0.001
female persons	88	< 0.001
male persons	121	—
age at treatment ≤ 20 years	61	< 0.001
female persons	39	< 0.001
male persons	22	< 0.001
age at treatment > 20 years	148	0.03
female persons	49	< 0.001
male persons	99	—
tuberculosis	132	< 0.001
ankylosing spondylitis	71	—
other diseases	6	—
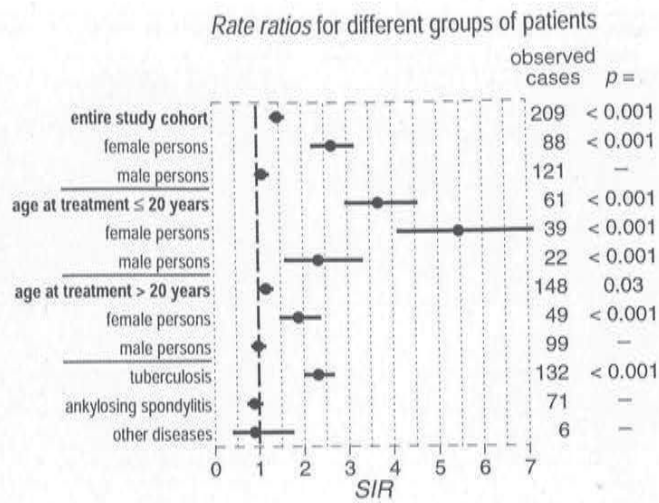
Fig. 2: Rate ratios (standardized incidence rates), i.e. quotients of the observed and the expected numbers of solid non-skeletal tumors (non-melanoma skin cancer excluded) with two-sided 90% confidence intervals, for the entire ^{224}Ra cohort, and different subgroups of patients according to gender, age at exposure or original disease (accounting for a 5 years lag period).

Rate Ratios for different types of cancer

	observed cases	p =
connective tissue	11	< 0.001
male breast	2	0.02
thyroid	7	< 0.001
liver	8	< 0.01
female breast	31	< 0.001
kidney	13	0.001
ovary	4	0.08
pancreas	8	0.04
leukemia	7	0.09
bladder	14	0.03
uterus	9	—
prostate	21	0.08
stomach	15	—
colon	13	—
rectum	9	—
lung	26	—
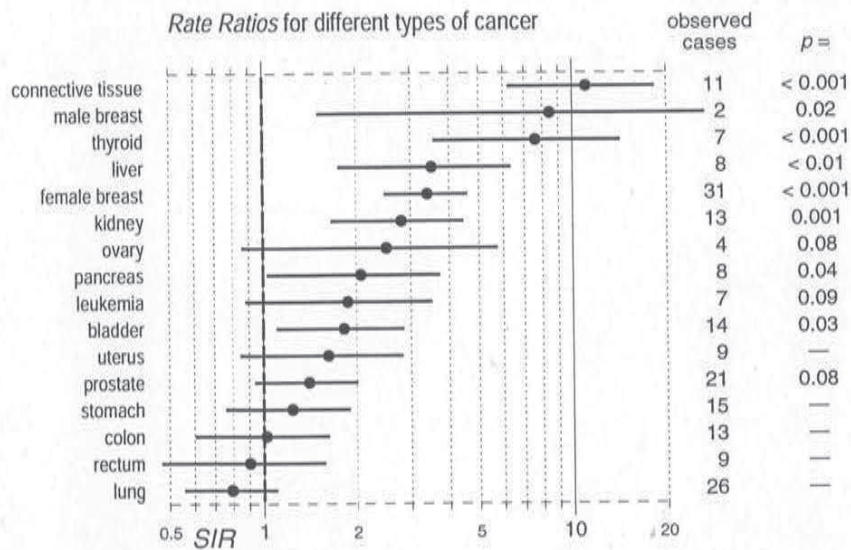
Fig. 3: Rate ratios for different sites of cancer with two-sided 90% confidence intervals (accounting for a 5 years lag period for solid cancers and soft tissue malignancies and a 2 year lag period for leukaemia).

A trend of overall enhancement can be recognised in fig. 3 which gives the rate ratios for different sites of cancer with 90% confidence intervals.

One of the most interesting and important results during the recent years of follow up was the significant increase of female breast cancer incidence (31 cases observed vs. 9.1 cases expected). Moreover, 2 cases of breast cancer occurred in men (vs. 0.2 expected cases). Furthermore, an apparent excess of

certain other non-skeletal solid tumours has also emerged in recent years: The rates of soft and connective tissue cancer (11 vs. 1), of thyroid carcinomas (7 vs. 0.9), of liver (8 vs. 2.3), of kidney (13 vs. 4.6), of pancreas (8 vs. 3.9) and of bladder cancer (14 vs. 7.7) appear to be significantly increased. On the other hand, the observed number of lung cancer cases is considerably lower than expected from a normal population (26 observed vs. 32.8 expected). The lung cancer "deficit" in the subgroup of ankylosing spondylitis patients (12 vs. 22.0, p=0.01) is likely to reflect their low level of smoking.

In the following sections, some details are given for those cancer sites where significantly enhanced rates have been observed. Reference is made to the revised dosimetry of Henrichs et al. [8] where estimates of excess relative risk (*ERR*) per Sv are given.

Female breast cancer:
In the sub-cohort of female ^{224}Ra patients treated as adults, breast cancer rates are less than 2fold, but significantly, increased (12 vs. 6.8). In the small subgroup of only 106 female patients treated as children or juveniles, the excess is striking – the relative rate being 8 (19 vs. 2.3).
Seven cases of breast cancer appeared relatively early, i.e. before the age of 45 years (see fig. 4). The youngest woman incurring breast cancer (with age at breast cancer diagnosis 28 years) was only 2 years old when treated with relatively high doses of ^{224}Ra.

For female breast cancer incidence, the point estimate of the *ERR* per Sv is estimated to be 0.8 for all women of the study cohort, 0.2 for women treated as adults and 2.2 for women who were treated with ^{224}Ra at younger ages. As in other epidemiological studies of radiation induced breast cancer, an obvious age at exposure trend was observed. The risk estimates are of the same order of magnitude as those e. g. for the A-bomb survivors where the *ERR* per Sv was estimated to be about 3 for those exposed when younger [10].

A control group of 182 tuberculosis (TB) patients not treated with ^{224}Ra was established to identify potential confounding factors – such as chest fluoroscopy – which might bias the breast cancer excess. The control group consists of patients treated at a German sanatorium between 1944 and 1954, with ages at treatment of between 8 and 21 years. Of the patients, 98 are female. In the TB comparison group, 8 mammary carcinomas were recorded, vs. 4.5 expected cases (p=0.09).
Strikingly, 4 of the 8 breast cancer cases in the controls received pneumothorax therapy, with correspondingly high numbers of fluoroscopies. Only 26 women of the entire comparison cohort received lung collapse treatment (with a mean number of 58 fluoroscopies per person). In this subgroup, 4 breast cancer cases were observed vs. 1 case expected (p=0.02). It is worth mentioning that another woman who was also treated by pneumothorax therapy was diagnosed with an angiosarcoma of the breast.
In the subgroup of persons *not* treated by pneumothorax therapy (with a mean number of 8 fluoroscopies per person), 4 breast cancer cases were observed vs. 3.5 cases expected. Therefore, the observed excess in the TB comparison group is probably attributable to repeated fluoroscopic x-ray examinations. In the ^{224}Ra cohort, TB patients were generally not treated by pneumothorax therapy. Hence it can be assumed that the ^{224}Ra treatment is responsible for most of the mammary cancer excess.
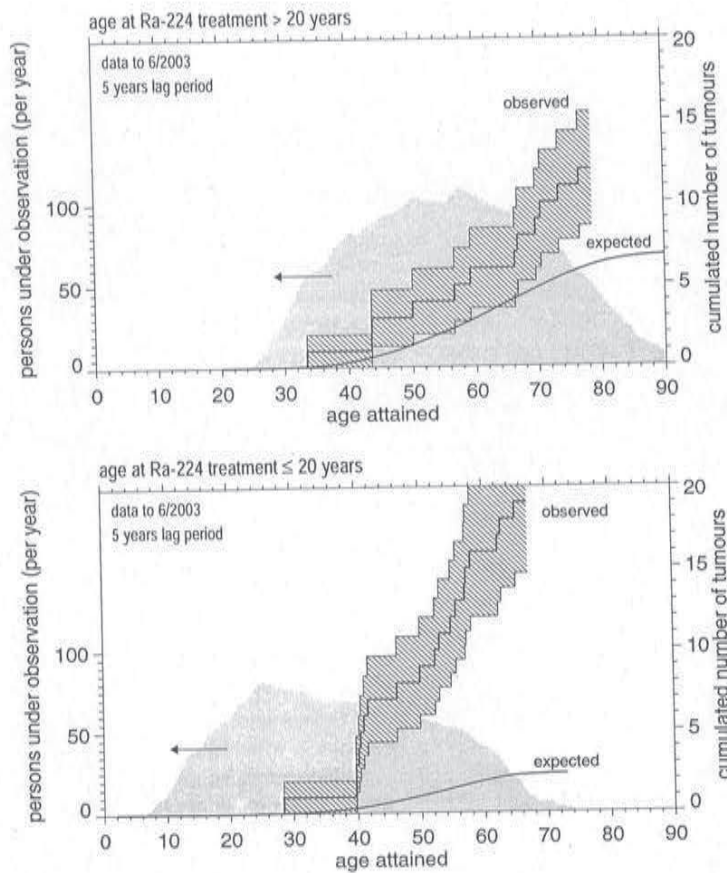
Fig. 4: Breast cancer incidence in the cohort of female ^{224}Ra-patients treated as adults (upper panel) and in the sub-cohort of those treated as children or juveniles (lower panel). The grey shaded areas give the number of patients under observation as a function of attained age (i. e. the person years at risk; left ordinate). The step function with the hatched range of standard errors represents the cumulative number of mammary carcinomas (right ordinate); the expected number of cases is indicated by the lower curve.

Malignant diseases of connective and other soft tissues:
Due to a reclassification of the malignant bone tumours in the ^{224}Ra cohort [11], 3 malignancies formerly classified as bone tumours, are now included in the group of soft tissue cancer (2 sarcomatoses, one myogenic sarcoma). The years of diagnosis date back several decades for these cases. In contrast, the other 8 soft tissue malignancies were diagnosed in the 1980s or later (3 leiomyosarcomas, 1 mesenchymal tumour, 1 neurofibrosarcoma, 1 neurilemoma, 1 fibrous histiocytoma and 1 soft tissue sarcoma). Considered separately, these 8 cases also amount to a significant excess (1.0 case expected, $p < 0.001$).

Thyroid cancer:
Seven cases of thyroid cancer were observed versus 0.9 expected cases. Again, it is remarkable that most of the thyroid cancer patients were treated with ^{224}Ra at younger ages, i. e. 4 of them were children during the ^{224}Ra treatment, and another 2 were in their early 20s when exposed. The *ERR* is high

and estimated to be about 3 per Sv. In the sub-group of patients treated as children or young adults (age at treatment ≤ 25 years), the point estimate of the *ERR* can be estimated to be about 7 per Sv.

For comparison: A-bomb survivors exposed when younger had a significantly higher risk than those exposed when older. In fact, among a-bomb survivors over 20 years of age at exposure there was no evidence of an excess of thyroid cancer at all. In the group of A-bomb survivors under 20 years of age at exposure, the *ERR* is estimated to be about 6 per Sv [10].

Liver cancer:

Liver carcinomas developed in 8 patients, vs. 2.3 cases expected. Seven of the 8 cases have been observed in male study persons.

However, liver cancer is frequently associated with pre-existing liver disease and it is known that many ^{224}Ra patients suffered from hepatitis during the ^{224}Ra treatment. Unfortunately, there is neither exact nor complete documentation. Three cases of liver cancer are associated with pre-existing liver cirrhosis and one case is connected with liver fibrosis.

Cancers of urinary organs:

Both rates of bladder cancer and kidney cancer are significantly increased. In the entire ^{224}Ra Study I cohort, 14 cases of bladder cancer cases (vs. 7.7 expected cases; $p=0.03$; *ERR* / Sv = 0.4), and 13 kidney cancer cases (vs. 4.6; $p=0.001$) have occurred. For female patients, the kidney cancer excess is even more pronounced: 4 cases observed vs. 0.8 expected cases ($p=0.01$).

Again, it is striking that age at ^{224}Ra exposure is a strong effect modifier, i.e. that persons treated with ^{224}Ra as children or juveniles are at a considerably higher risk of incurring kidney cancer compared to those who were older at ^{224}Ra treatment. The *ERR* is estimated to be 0.8 per Sv for the entire ^{224}Ra study cohort. The point estimate of the *ERR* for those exposed as children or juveniles is considerably higher, i.e. 2.6 per Sv (non-significant *ERR* for the older sub-group).

For comparison: In the A-bomb survivors' cohort, the number of kidney cancers is small. Therefore, there was no significant excess of kidney cancer. However, there was a significant trend for increasing risk of kidney cancer with decreasing age at exposure as has been observed in the ^{224}Ra study cohort [10].

Leukemias:

Leukemias have occurred in 8 patients vs. 3.8 expected cases ($p=0.04$) with one acute myeloid leukemia (in an ankylosing spondylitis patient) diagnosed as early as 1.7 years after the first ^{224}Ra injection. If a latent period of 2 years is assumed then the statistical significance is lost ($p=0.09$). In the sub-group of ankylosing spondylitis patients alone, 5 leukemia cases were observed vs. 2.2 expected ($p=0.07$) (latent period=2 years: 4 vs. 2.1; $p=0.16$). Two of the 8 leukemias are chronic lymphocytic leukemias which are not commonly assumed to be induced by radiation.

3. Conclusion

There is no doubt that the follow-up of the health of the ^{224}Ra patients has produced very important results connected with the detrimental side-effects of *Peteosthor* therapy. The study has already been conducted over some 50 years. Nevertheless, the follow-up of the remaining 17% of the cohort should be continued, so that a full evaluation of late effects of ^{224}Ra treatment can be completed. The completion is especially important since some of the side-effects (e.g. the increased rate of breast cancer incidence) have only become apparent during the last 10 to 15 years of follow-up. It is to be hoped that a continued follow-up into the future will not reveal any new side-effects but this must be thoroughly checked and monitored. Only when the complete story is known will it be possible to make a fully informed assessment of the risks and benefits of medical procedures involving lower doses of ^{224}Ra or similar substances.

4. References

1. Nekolla, E.A., Kreisheimer, M., Kellerer, A.M., Kuse-Isingschulte, M., Gössner, W., Spiess, H., *Induction of malignant bone tumours in radium-224 patients. Risk estimates based on the improved dosimetry.* Radiat. Res., 153: 93-103 (2000).

2. Gössner, W., *Pathology of radium-induced bone tumours: New aspects of histopathology and histogenesis.* Radiat. Res., 152: S12-S15 (1999).

3. Spiess, H., Mays, C.W., *Bone cancers induced by ^{224}Ra (Th X) in children and adults.* Health Phys., 19: 713-729 (1970).

4. Mays, C.W., Spiess, H., Chmelevsky, D., Kellerer, A.M., *Bone sarcoma cumulative tumour rates in patients injected with ^{224}Ra.* Strahlentherapie Suppl., 80: 27-31 (1985).

5. Chmelevsky, D., Kellerer, A.M., Spiess, H., Mays, C.W., *A proportional hazards analysis of bone sarcoma rates in German $^{224}radium$ patients.* Strahlentherapie Suppl., 80: 32-37 (1985).

6. Kellerer, A.M., Spiess, H., Chmelevsky, D., *Dose and dose rate dependence for bone sarcomas in radium-224 patients.* Int. J. Radiat. Biol., 58: 864-866 (1990).

7. Chmelevsky, D., Spiess, H., Mays, C.W., Kellerer, A.M., *The reverse protraction factor in the induction of bone sarcomas in radium-224 patients.* Radiat. Res., 124: S69-S79 (1990).

8. Henrichs, K., Bogner, L., Nekolla, E., Noßke, D., Roedler-Vogelsang, T., *Extended dosimetry for studies with ^{224}Ra patients,* in van Kaick, G., Karaoglou, A., Kellerer, A.M., (Eds.) *Health Effects of Internally Deposited Radionuclides: Emphasis on Radium and Thorium,* pp. 33-38. World Scientific, Singapore, (1995).

9. Lubin, J.H., Boice, J.D., Edling, C., Hornung, R.W., Howe, G., Kunz, E., Kusiak, R.A., Morrison, H.I., Radford, E.P., Samet, J.M., Tirmarche, M., Woodward, A., Xiang, Y.S., Pierce, D.A., *Lung Cancer and Radon: A Joint Analysis of 11 Underground Miners Studies.* NIH Publication No. 94-3644, U.S. Department of Health and Human Services, National Institutes of Health, Bethesda MD, (1994).

10. Thompson, D.E., Mabuchi, K., Ron, E., Soda, M., Tokunaga, M., Ochikubo, S., Sugimoto, S., Ikeda, T., Terasaki, M., Izumi, S., Preston, D.L., *Cancer incidence in atomic bomb survivors. Part II: Solid tumors, 1958-87.* Radiat. Res., 137: S17-S67 (1994).

11. Gössner, W., Wick, R.R., Spiess, H., *Histopathological review of Radium-224 induced bone sarcomas,* in van Kaick, G., Karaoglou, A., Kellerer, A.M., (Eds.) *Health Effects of Internally Deposited Radionuclides: Emphasis on Radium and Thorium,* pp. 255-259. World Scientific, Singapore, (1995).

This paper is respectfully dedicated to Prof. Wolfgang Gössner who always accompanied the "Spiess-Study" with great interest and commitment. He will always be remembered as a responsive, open and serious tutor. His efficiency of labour, cordiality and helpfulness were greatly appreciated.

11. Walsh L, Rühm W & Kellerer AM. Curvature in the dose response of the life span study cancer mortality data. Radiat. Res. 163, 477, 2005

LETTERS TO THE EDITOR

Curvature in the Dose Response of the Life Span Study Cancer Mortality Data: Comments on "Effect of Recent Changes in Atomic Bomb Survivor Dosimetry on Cancer Mortality Risk Estimates" by Preston *et al.* (*Radiat. Res.* 162, 377–389, 2004)

Linda Walsh, Werner Rühm and Albrecht M. Kellerer

*Radiobiological Institute, University of Munich,
80336 Munich, Germany*

We note with interest the latest analysis of cancer mortality in the Life Span Study (LSS) by Preston *et al.* that appeared in the October issue of *Radiation Research* (*1*). After further detailed examination, we feel obliged to pass comment on this paper.

The analysis of Preston *et al.* (*1*) was based on the Japanese A-bomb survivor mortality data collected between 1950 and 2000 that is not yet publicly available. However, the mortality data up to 1997 have been publicly available since February 2004, and we have conducted a careful analysis of these data that was published online recently and is now in print (*2*). The abstract of Preston *et al.* (*1*) discloses, to us, the surprising statement connected with the shape of the dose response for excess cancers: " . . . .but for solid cancers the additional 3 years of follow-up has some effect. In particular there is for the first time a statistically significant upward curvature for solid cancer on the restricted dose range 0–2 Sv." Our paper shows, however, that the statistically significant upward curvature was already present in the publicly available data to 1997. To quote the abstract of our paper: "However, considerably more curvature in the dose–effect relation is now supported by the computations. A dose and dose rate reduction factor DDREF = 2 is now much more in line with the data than before."

A dose cutoff at 2 Gy was also applied in our analysis, and it is suggested that the newly discovered curvature is due to the 2-Gy dose cutoff point and not just due to the additional 3 years of follow-up. The dose response exhibits a flattening above 2 Gy, which could explain that the previous RERF analysis (*3*) missed this effect because a dose cutoff at somewhere between 3 and 3.5 Sv was used. Considering that there has long been a question as to why the main epidemiological data (LSS) should have a linear dose response when the vast majority of data for biological indicators of cellular damage and animal experiments have mainly curved dose responses for γ radiation, this is not a trivial point. We are convinced that Preston and coauthors will take careful note of the conclusions of our paper.

Received: October 8, 2004

References

1. D. L. Preston, D. A. Pierce, Y. Shimizu, H. M. Cullings, S. Fujita, S. Funamoto and K. Kodama, Effect of recent changes in atomic bomb survivor dosimetry on cancer mortality risk estimates. *Radiat. Res.* **162**, 377–389 (2004)

2. L. Walsh, W Rühm and A. M. Kellerer, Cancer risk estimates for gamma-rays with regard to organ-specific doses. Part I: All solid cancers combined. *Radiat. Environ. Biophys.* **43**, 225–231 (2004).

3. D. L. Preston, Y. Shimizu, D. A. Pierce, A Suyama and K. Mabuchi, Studies of mortality of atomic bomb survivors. Report 13: Solid cancer and noncancer disease mortality: 1950–1997. *Radiat. Res.* **160**, 381–407 (2003).

Response to Letter on Curvature in the Dose Response of the Life Span Study Cancer Mortality Data by Linda Walsh *et al.*

Dale L. Preston,[a] Donald A. Pierce[b] and Yukiko Shimizu[b]

[a]Hirosoft International, Eureka, California, and [b]Radiation Effects Research Foundation, Hiroshima, Japan

We appreciate the interest of Walsh *et al.* in our recent papers (*1, 2*) and their careful analyses of the data from the first of these. However, we feel that suggestions in the final paragraph of their letter may lead to some confusion. It is true that failing to deselect some of the highest dose range, e.g. over 2 Sv, leads to small estimated upward curvature due to the leveling off of the dose response in the highest part of the dose range. Our remarks about the effect of increasing follow-up were in fact based on such a deselection.

In particular, what we intended to convey was the following. If analyses are restricted to survivors with dose estimates under 2 Sv, the apparent upward curvature increases with increasing follow-up time as shown below based on the data for solid cancer mortality. Here we use the modeling approach of our 2004 paper, including use of the entire dose range for estimation of the modifying effects of sex, exposure age, and attained age. The curvature is defined as the ratio of the quadratic to the linear parameter estimates in a linear-quadratic model.

	Follow-up from 1950 through		
	2000	1997	1995
Curvature estimate	0.951/Sv	0.460/Sv	0.344/Sv
Two-sided *P* value	0.015	0.114	0.210

However, as we noted in our 2004 paper, it is not clear that this curvature is either what has been long "expected" or that it is relevant to low-dose risks. That is, the ERR/Sv estimated directly from the dose range 0–0.5 Sv is closer to the linear estimate from the full dose range than to the low-dose slope in a linear-quadratic fit to the range 0–2 Sv. For this reason, as well as the leveling off at higher doses, results as shown in the table are sensitive to the dose range used. Further details on this, and results for solid cancer incidence data, will be presented in a forthcoming publication.

In reference (*2*) of their letter, the writers found statistically significant curvature for the solid cancer mortality follow-up through 1997 using a substantially different approach to the data than in our paper, including RBE assumptions and use of organ doses. In view of the result for that follow-up in the table here, where the curvature is marginally significant, this is not surprising.

Received: December 16, 2004

References

1. D. L. Preston, Y. Shimizu, D. A. Pierce, A. Suyama and K. Mabuchi, Studies of mortality of atomic bomb survivors. Report 13: Solid cancer and noncancer disease mortality: 1950–1997. *Radiat. Res.* **160**, 381–407 (2003).

2. D. L. Preston, D. A. Pierce, Y. Shimizu, H. M. Cullings, S. Fujita, S. Funamoto and K. Kodama, Effect of recent changes in atomic bomb survivor dosimetry on cancer mortality risk estimates. *Radiat. Res.* **162**, 377–389 (2004).

12. Rühm W, Walsh L & Kellerer AM. Analysen der neusten LSS-Mortalitätsdaten (in German). Veröffentlichungen der Strahlenschutzkommission, Band 56, 43-56, Elsevier, Urban & Fischer, 2005

Analysen der neuesten LSS-Mortalitätsdaten

Priv.-Doz. Dr. W. Rühm, Dr. L. Walsh, Prof. Dr. A.M. Kellerer
Strahlenbiologisches Institut, Universität München

Inhalt

1   Einleitung

Nach den Atombomben-Explosionen über Hiroshima und Nagasaki am 6. bzw. 9. August 1945 waren die akuten Folgen unmittelbar sichtbar: Weite Teile beider Städte waren beinahe vollständig zerstört und diejenigen, die sich zum Zeitpunkt der Explosionen nahe der Hypozentren aufgehalten hatten, hatten nur geringe Überlebenschancen. Aktuelle Schätzungen gehen davon aus, dass bis Ende 1945 in beiden Städten etwa 200.000 Betroffene an den akuten Folgen der Explosionen gestorben sind. Zu diesen akuten Folgen zählten nicht nur Verletzungen durch die Druckwelle und die Hitze der Explosionen, sondern auch Erkrankungen aufgrund der Exposition mit hohen Dosen ionisierender Gamma- und Neutronenstrahlung.

Erst Jahre später wurden die Spätfolgen sichtbar, zu denen die Exposition der Betroffenen mit niedrigen Dosen führte: Ende der 1940er Jahre sprachen erste Berichte von einem erhöhten Auftreten von Katarakten und Leukämie unter den Überlebenden. Grundlage für eine systematische Untersuchung legte dann eine 1950 durchgeführte Befragung von etwa 120.000 Überlebenden aus beiden Städten. Der Gesundheitszustand dieser Personen wurde bis 1975 im Rahmen der „Life Span Study" (LSS) von der „Atomic Bomb Casualty Commission" dokumentiert, eine Aufgabe, die danach der „Radiation Effects Research Foundation" (RERF) übertragen wurde. Unser heutiges Wissen über die durch ionisierende Strahlung beim Menschen verursachten Spätfolgen geht wesentlich auf diese Studie zurück, die seit mehr als 50 Jahren an den Überlebenden der Atombomben-Explosionen in Hiroshima und Nagasaki durchgeführt werden.

Im vorliegenden Artikel werden Ergebnisse zur Mortalität durch Krebserkrankungen der Atombomben-Überlebenden zusammengefasst, die in einigen kürzlich erschienenen Arbeiten beschrieben sind. Die hier vorgestellte Zusammenstellung dieser Ergebnisse ist bei weitem nicht vollständig und kann sich nur auf einige Aspekte beschränken, die für die Abschätzung der Risiken nach einer Exposition mit ionisierender Strahlung relevant sind. Besonderes Augenmerk wird dabei auf die abgeleiteten Dosis-Wirkungskurven sowie auf die Rolle der Neutronen bei der Induktion der beobachteten Spätfolgen gelegt.

2 Analysen der Radiation Effects Research Foundation

Vor kurzem wurde von RERF ein aktualisierter Follow-up (1950-1997) der Mortalität durch solide Tumoren abgeschlossen und eine eingehende Analyse veröffentlicht [1]. Die dieser Analyse zugrunde liegenden Daten sind in gruppierter Form verfügbar und können über das Internet heruntergeladen werden [2]. Sie beziehen sich auf 86.572 Überlebende, für die im Rahmen des Dosimetriesystems DS86 [3] Dosisabschätzungen vorhanden sind. Als „Referenzorgan" wurde in vielen Fällen das Colon benutzt und für die Berechnung gewichteter Colondosen wurden die von DS86 abgeschätzten Neutronen-Energiedosen mit 10 multipliziert, um der im Vergleich zur locker ionisierenden Gammastrahlung höheren biologischen Wirkung der Neutronen Rechnung zu tragen. Der Neutronenbeitrag zur gewichteten Colondosis beträgt in Hiroshima bei einem Abstand von 1000 m vom Hypozentrum etwa 10%, bei einem Abstand von 2000 m nur etwa 1%. Das bedeutet, dass die an den Überlebenden beobachteten Spätfolgen im Wesentlichen der Gammastrahlung zugeschrieben werden – was zwar allgemein akzeptiert ist, jedoch (wie weiter unten gezeigt wird) nicht zwingend aus den Daten hervorgeht.

Bei den in Preston et al. [1] beschriebenen Analysen werden Modelle zum zusätzlichen relativen Risiko (ERR – excess relative risk) und zum zusätzlichen absoluten Risiko (EAR – excess absolute risk) verwendet. Altersabhängigkeiten werden unter Benutzung der Parameter „Alter bei Exposition" und „erreichtes Lebensalter" beschrieben. Alle im Folgenden aus dieser Arbeit zitierten Risikoschätzungen gelten für eine 70jährige Person, die im Alter von 30 Jahren strahlenexponiert wurde. Während im vorangegangenen Follow-up (1950-1990) [4] unter 7.578 beobachteten Todesfällen durch solide Tumoren 334 strahleninduzierte Fälle abgeschätzt wurden, ergibt sich bei einer Verlängerung des Beobachtungszeitraums bis 1997 unter nun 9.335 beobachteten Todesfällen ein strahleninduzierter Exzess von 440 Fällen. Wird das ERR für die in der Studie verwendeten Dosiskategorien separat berechnet, ergeben sich mit zunehmenden gewichteten Colondosen zunehmende ERR-Werte (Abbildung 1, schwarze Punkte). In Bezug auf die Form der beobachteten Dosis-Wirkungskurve bemerken die Autoren der Studie: „There is little evidence against a simple linear dose response, with the only apparent curvature being a flattening for those with dose estimates above 2 Sv that is not statistically significant ($p>0.5$)" [1]. Einzig das Abflachen der Kurve oberhalb von 2 Sv stellt also eine Abweichung von einem linearen Verlauf dar, und diese Abweichung ist nicht signifikant. Weiter unten wird gezeigt, dass neuere Arbeiten zu einem etwas anderen Ergebnis kommen. Wird ein lineares Model für die Dosisabhängigkeit verwendet, ergibt sich für das ERR/Sv ein Wert von 0.47 ± 0.06 (Abbildung 1). Dabei ist anzumerken, dass in die Ableitung dieses Wertes alle soliden Tumoren eingingen und als Referenzorgan das Colon verwendet wurde.
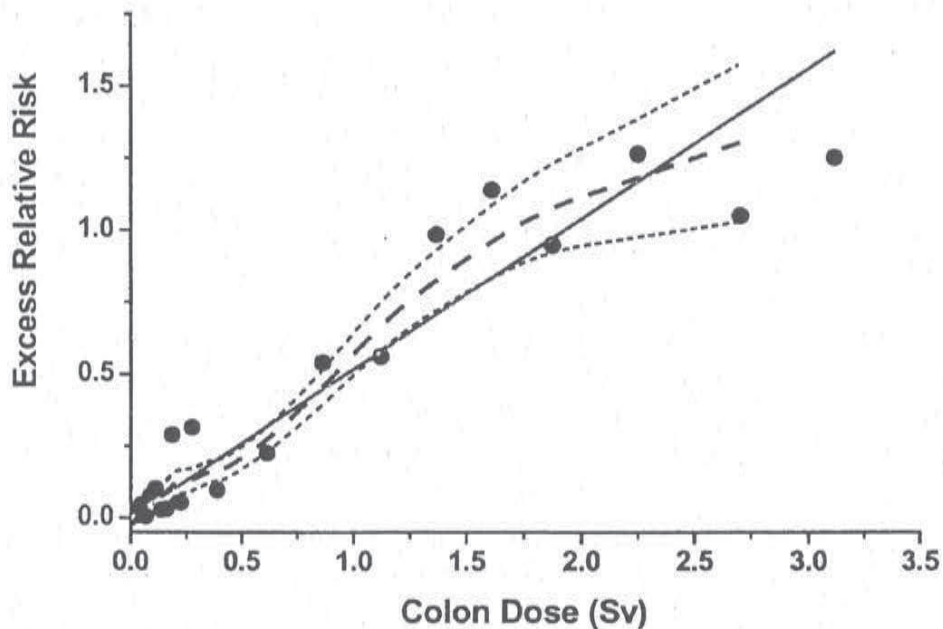
Abb. 1: Zusätzliches relatives Risiko für solide Tumoren (entnommen aus Preston et al. [1]); für die Berechnung der gewichteten Colondosis wurde zur Gamma-Energiedosis das zehnfache der Neutronen-Energiedosis addiert; für die Steigung der linearen Kurve ergibt sich ein Wert von (0.47 ± 0.06) pro Sv

Besonderes Augenmerk richten Preston und Mitarbeiter auf die niedrigste Dosis, bei der noch eine statistisch signifikante Erhöhung des zusätzlichen relativen Risikos beobachtet werden kann. Dazu beginnen sie die Auswertung bei der niedrigsten Dosiskategorie und beziehen dann sukzessive die nächsthöheren Dosis-Kategorien in die Auswertung mit ein, bis sich für das zusätzliche relative Risiko erstmals ein signifikant von null verschiedener Wert ergibt. Unter Anwendung dieser – theoretisch wenig begründbaren – Methode beobachten Preston und Mitarbeiter „... a statistically significant increase with dose when analysis is restricted to survivors with dose estimates less than about 0.12 Sv." Da die mittlere Dosis in diesem Dosisintervall etwa 50 mSv beträgt, wurde die Studie so interpretiert, dass bereits bei dieser Dosis ein signifikanter strahleninduzierter Effekt zu beobachten sei [5].

Etwa ein Jahr später veröffentlichte RERF einen weiteren Artikel zur Mortalität der Atombomben-Überlebenden [6]. Diese Arbeit war wesentlich motiviert durch die Tatsache, dass mittlerweile eine Revision der Dosimetrie in Hiroshima und Nagasaki stattgefunden hatte [7] und eine erste Einschätzung ihrer Auswirkungen auf die Risikoschätzungen gegeben werden sollte. Für diese Analyse bedienten sich die Autoren der Daten aus einem um drei Jahre verlängerten Follow-up (1950-2000) und beschränkten die Auswertung auf Überlebende mit einer gewichteten Colondosis kleiner als 2 Sv.

Erstmals seit 1990 wurden wieder die aufgetretenen Leukämiefälle analysiert. Die Zahl der in der Kohorte beobachteten Todesfälle durch Leukämie erhöhte sich seitdem von 249 auf 296, die der ionisierenden Strahlung zugeordneten Fälle von 87 auf 93. Dieser eher geringe Zuwachs ist Ausdruck der Tatsache, dass bei Leukämien eine relativ kurze Latenzzeit beobachtet wurde und das Gros der strahleninduzierten Leukämien bereits vor vielen Jahren aufgetreten ist. Für solide Tumoren stellt sich die Situation anders dar. Hier wurden durch den zusätzlichen Follow-up um nur 3 Jahre weitere 39 Fälle als strahleninduziert eingeordnet, so dass mittlerweile bei insgesamt 10.127 Todesfällen durch solide Tumoren von 479 strahleninduzierten Fällen ausgegangen wird.

Ein weiteres wichtiges Ergebnis der Studie ist, dass sich die für solide Tumoren abgeleiteten Risikokoeffizienten trotz des um 3 Jahre verlängerten Follow-ups kaum änderten. Einzig die Dosisrevision, die in beiden Städten zu etwa um 10% höheren Gammadosen geführt hat, zog um etwa 8% geringere Risikoschätzungen nach sich.

Besonders bedeutsam erscheint eine Beobachtung zur Form der Dosis-Wirkungskurve für Gammastrahlung: Während in der Vorgängerstudie noch von einem linearen Verlauf gesprochen wird (siehe oben), wird jetzt erstmals von einer Krümmung berichtet: „... there is for the first time a statistically significant upward curvature for solid cancer on the restricted dose range 0-2 Sv." Dieses Ergebnis wird von Preston et al. in erster Linie auf die um drei Jahre verlängerte Follow-up Periode zurückgeführt.

3 Weiterführende Arbeiten

Für eine Neubewertung der Neutronen in Hiroshima und Nagasaki, wie sie kürzlich vorgeschlagen wurde [8, 9], spielen zwei Aspekte eine zentrale Rolle: Zum einen gibt es Hinweise, dass zur Beschreibung der relativen biologischen Wirksamkeit (RBW) der Neutronen ein Wert von 10, der in den Analysen von RERF angenommen wird, zu niedrig ist. Darauf deuten beispielsweise Tierexperimente

hin [10, 11]. Auch die Anwendung des von der ICRP vorgeschlagenen Neutro-nen-Wichtungsfaktors w_R [12] auf Hiroshima und Nagasaki erfordert einen deutlich höheren Wert als 10, da die im menschlichen Körper durch die einfallenden Neutronen erzeugte Sekundär-Gammastrahlung [13] und die Här-tung der Neutronenspektren in Hiroshima und Nagasaki mit zunehmendem Ab-stand von den Hypozentren berücksichtigt werden muss [14]. Zum anderen führt die Wahl des Colons als Referenzorgan dazu, dass die Energiedosis durch die Neutronen für die meisten anderen Organe unterschätzt wird. Dies liegt daran, dass das Colon eines der am tiefsten im menschlichen Körper liegenden Organe darstellt und damit die Neutronen im Vergleich zur Gammastrahlung stärker ab-geschirmt werden, als es bei den meisten anderen Organen der Fall ist. Bei-spielsweise ist in Hiroshima die Energiedosis durch die Neutronen für die weib-liche Brust um den Faktor 3.85 größer als für das Colon, die Energiedosis durch die Gammastrahlung dagegen nur um den Faktor 1.17.

Da die LSS-Daten keine ausreichenden organspezifischen Dosisangaben enthal-ten, wurde in Walsh et al. [8] der verfügbare Datensatz des Follow-ups bis 1997 erweitert, indem auf der Grundlage der angegebenen Colondosen mittels Kor-rekturfaktoren Organdosen errechnet wurden. Dabei wurden diejenigen Organe berücksichtigt, für die mehr als 100 Todesfälle durch Krebs beobachtet wurden und Analysen für verschiedene RBW-Werte durchgeführt. Für alle solide Tumo-ren zusammen ergab sich – bei Verwendung eines linearen Dosismodells, eines RBW-Werts von 10 und bezogen auf das Colon (wie es RERF verwendet) – für die Steigung 0.51 ± 0.07 bzw. 0.60 ± 0.07, je nachdem ob ein Modell verwendet wurde, in das Alter bei Exposition oder erreichtes Lebensalter eingingen. Der (einer Mittelung zwischen beiden Altersabhängigkeiten entsprechende) in Re-port 13 von RERF abgeleitete Wert von 0.47 ± 0.06 (siehe oben) ist etwas nied-riger, da er auch Daten oberhalb von 2 Sv mit einschließt, was wegen des Abfla-chens der Dosis-Wirkungskurve zu einer niedrigeren Steigung führt (siehe Ab-bildung 1). Für einen höheren RBW-Wert von 35 dagegen ergibt sich (anders als bei einem RBW-Wert von 10) nur eine Steigung von 0.41 ± 0.05 (inkl. Stan-dardfehler) bzw. 0.47 ± 0.05 [8]. Dies demonstriert, dass bei höheren RBW-Werten für Neutronen die Risikoschätzungen für die Gammastrahlung abneh-men.

Bei Verwendung eines linear-quadratischen Dosismodells wurden RBW-Werte für Neutronen zwischen 20 und 50 verwendet, wie sie bei Tierexperimenten re-lativ zu Gammastrahlung bei einer Dosis von 1 Gy beobachtet wurden [10, 11]. Die Analysen ergaben, dass bereits für den Follow-up bis 1997 eine deutliche Krümmung der Dosis-Wirkungskurve für solide Tumoren beobachtet wird, so-fern die Auswertung auf den Dosisbereich 0 - 2 Sv beschränkt wird [8]. Dieses Ergebnis lässt sich auch im Hinblick auf den DDREF-Faktor („Dose and Dose

Rate Effectiveness Factor") interpretieren. Diesem Faktor wurde von der International Commission on Radiological Protection (ICRP) ein Wert von 2 zugeordnet [12], um die aus den LSS-Daten für hohe Dosen und Dosisraten abgeleiteten Risikoschätzungen auf den Bereich des Strahlenschutzes zu übertragen, der meist durch niedrige Dosen und Dosisraten charakterisiert ist. Der DDREF lässt sich berechnen aus dem Verhältnis der Steigung bei einem linearen Dosismodell zu der Anfangssteigung, die sich mit einem linear-quadratischen Dosismodell ergibt. Für RBW-Werte (1 Gy) zwischen 20 und 50 ergibt sich: „A dose and dose-rate reduction factor DDREF=2 is now much more in line with the data than before." [8].

Analoge Analysen führten Walsh und Mitarbeiter auch separat für diejenigen Organe aus, bei denen mehr als 100 Todesfälle durch solide Tumoren beobachtet worden waren, wobei auf eine Verwendung eines linear-quadratischen Modell aus statistischen Gründen verzichtet wurde [9]. Die wesentlichen Konsequenzen, die sich aus der Verwendung höherer RBW-Werte für Neutronen für die abgeleiteten organspezifischen Risikoschätzungen für Gammastrahlung ergeben, sind in Abbildung 2 beispielhaft für die Brust und den Colon veranschaulicht.

Für beide Organe reduziert sich mit zunehmendem RBW-Wert das zusätzliche relative Risiko pro Gy Gammastrahlung. Dieser Effekt ist jedoch deutlich geringer ausgeprägt für das Colon, da es tiefer im Körper gelegen ist als die Brust, sodass die Neutronen durch den Körper deutlich stärker abgeschirmt werden als es für die Brust der Fall ist. Interessanterweise sind die Unterschiede zwischen beiden Organe bei einem RBW-Wert von 100 deutlich geringer als bei niedrigen RBW-Werten. Sollten die RBW-Werte für Neutronen in Hiroshima und Nagasaki tatsächlich höher sein, hätte das also unter anderem zur Folge, dass sich die bisher für verschiedene Organe beobachteten ERR/Gy-Werte angleichen würden.
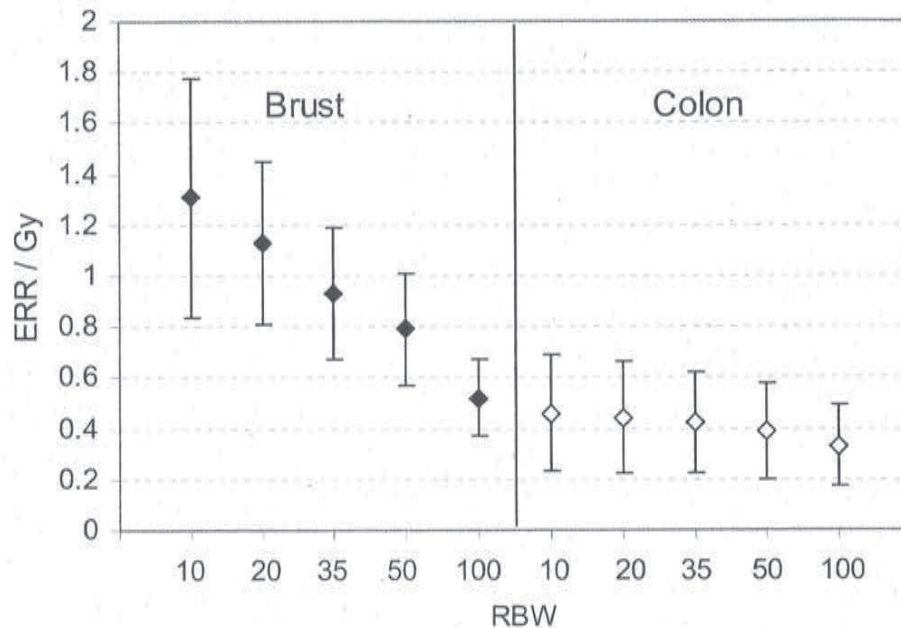
Abb. 2: Zusätzliches organspezifisches relatives Risiko pro Gy Gammastrah-
lung (ERR) für Brust und Colon inklusive Standardfehler. Die gezeigten
Werte beziehen sich jeweils von links auf RBW-Werte für Neutronen
von 10, 20, 35, 50 und 100. Die Auswertung basiert auf dem Follow-up
bis 1997, einem linearen Dosis-Wirkungsmodell und schließt alle Da-
ten bis zu einer gewichteten Colon-Dosis von 2 Sv ein

Dass die Neutronen wegen der unterschiedlichen Lage der Organe im menschli-
chen Körper in unterschiedlichem Maße zur Induktion von soliden Tumoren bei-
tragen, lässt sich veranschaulichen, wenn man das Produkt aus Neutronen-RBW
und Neutronen-Energiedosis mit der Gamma-Energiedosis vergleicht. Abbil-
dung 3 zeigt, dass die Neutronen bei einem RBW-Wert von 35 bei einer Gam-
ma-Energiedosis von 0.5 bzw. 1.5 Gy (was Abständen zum Hypozentrum in
Hiroshima von etwa 1000 m bzw. 1200 m entspricht) 40% bzw. 50% zur ge-
wichteten Gesamtdosis der Brust und somit zur Induktion von soliden Tumoren
beitragen, während die entsprechenden Werte für das Colon nur etwa 15% bis
25% betragen.
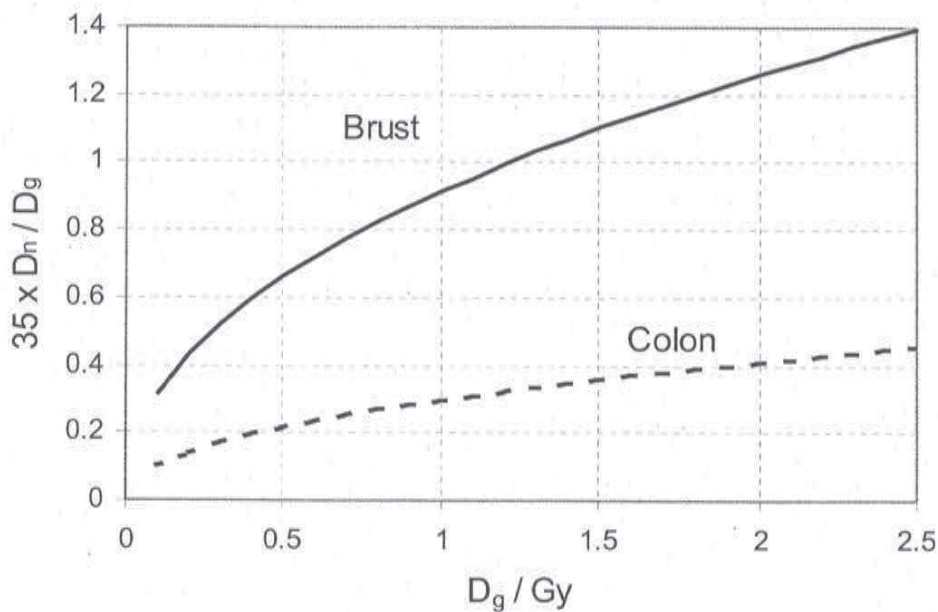
Abb. 3: Verhältnis von mit einem RBW-Wert von 35 gewichteter Neutronen-
Energiedosis   zur   Gamma-Energiedosis   für   Brust   bzw.   Colon
(Hiroshima)

4   Abschließende Bemerkung

Die gesundheitlichen Spätfolgen, die das gemischte Feld aus Neutronen- und Gammastrahlung bei den Überlebenden von Hiroshima und Nagasaki verursacht hat, werden seit mehr als 50 Jahren untersucht und sind in einer Vielzahl an Publikationen sorgfältig dokumentiert. Um die gewonnenen Erkenntnisse jedoch auf die Belange des Strahlenschutzes übertragen zu können, muss eine Analyse durchgeführt werden, bei der der Gammastrahlungsanteil und der Neutronenanteil getrennt betrachtet wird. Da es bis jetzt nicht gelungen ist, die relative biologische Wirkung der Neutronen aus den Daten der Atombomben-Überlebenden direkt abzuleiten, müssen dafür Annahmen getroffen werden, die sich auf Erkenntnisse aus anderen Bereichen stützen. In den von RERF durchgeführten Analysen wird meist davon ausgegangen, dass ein RBW-Wert von 10 die höhere biologische Wirksamkeit der Neutronen hinreichend beschreibt. Diese Annahme führt dazu, dass ein Großteil der bei den Überlebenden beobachteten strahleninduzierten Spätfolgen der locker ionisierenden Gammastrahlung zugeschrieben wird. Werden dagegen deutlich höhere RBW-Werte, wie sie beispielsweise in

Tierexperimenten beobachtet wurden, verwendet, dominieren die Neutronen in bestimmten Fällen (unabgeschirmte Exposition oberflächlicher Organe) sogar die beobachteten Effekte. Dies führt zu einer Verringerung der für die Gammastrahlung abgeleiteten Risikoschätzungen. Der Effekt ist für tief liegende Organe nicht besonders ausgeprägt, gewinnt jedoch für oberflächlich gelegene Organe an Bedeutung. Gleichzeitig verringern sich die Unterschiede bei den Risikoschätzungen, die für unterschiedliche Organe angegeben werden.

Das gegenwärtige Dogma, die bei den Überlebenden beobachteten Spätfolgen seien hauptsächlich durch locker ionisierende Gammastrahlung verursacht, erklärt sich aus der Tatsache, dass mit der Wahl eines RBW-Werts von 10 bereits vor Beginn der Analysen den Neutronen eine untergeordnete Rolle zugewiesen wird. Die Bewertung der Neutronen ist für die Ableitung von Risikoschätzungen für Gammastrahlung von zentraler Bedeutung und sollte daher in Zukunft verstärkt untersucht werden.

5 Literatur

[1]   Preston DL, Shimizu Y, Pierce DA, Suyama A, Mabuchi K: Studies of Mortality of Atomic Bomb Survivors. Report 13: Solid Cancer and Noncancer Disease Mortality: 1950-1997. Radiat. Res. 160, 381-407; 2003

[2]   Radiation Effects Research Foundation; 2004
       www.rerf.or.jp

[3]   Roesch WC (ed.): US-Japan Joint Reassessment of Atomic Bomb Radiation Dosimetry in Hiroshima and Nagasaki, Vols.1 and 2. Radiation Effects Research Foundation. Hiroshima; 1987

[4]   Pierce DA, Shimizu Y, Preston DL, Vaeth M, Mabuchi K: Studies of the mortality of atomic bomb survivors. Report 12, Part 1. Cancer. Radiat. Res. 146, 1-27; 1996

[5]   Brenner DJ, Doll R, Goodhead DT, Hall EJ, Land CE, Little JB, Lubin JH, Preston DL, Preston RJ, Puskin JS, Ron E, Sachs RK, Samet JM, Setlow RB, Zaider M: Cancer risks attributable to low doses of ionizing radiation: Assessing what we really know. PNAS 100 (24), 13761-13766; 2003

[6]   Preston DL, Pierce DA, Shimizu Y Cullings HM, Fujita S, Funamoto S and Kodama K: Effect of Recent Changes in Atomic Bomb Dosimetry on Cancer Mortality Risk Estimates. Radiat. Res. 162, 377-389; 2004

[7]   Young RW and Kerr GD (eds.): Report of the Joint US-Japan Dosimetry Working Group, Reassessment of the Atomic-Bomb Radiation Dosimetry for Hiroshima and Nagasaki - DS02. Radiation Effects Research Foundation, Hiroshima, Japan; 2004

[8]   Walsh L, Rühm W and Kellerer AM: Cancer risk estimates for γ-rays with regard to organ specific doses, part I: All solid cancers combined. Radiat Environ Biophys 43: 145-151; 2004

[9]   Walsh, L, Rühm W and Kellerer, AM: Cancer risk estimates for γ-rays with regard to organ specific doses, part II: Site-specific solid cancers. Radiat. Environ. Biophys. 43: 225-231; 2004

[10]   Sinclair WK: Fifty years of neutrons in biology and medicine: The comparative effects of neutrons on biological systems. In Proceedings of the 8th Symposium on Microdosimetry (H.G. Ebert, Ed.) Report EUR 8359. Commission of the European Communities, Brussels; 1982

[11]   Wolf D, Lafuma J, Masse R, Morin M, Kellerer AM: Neutron RBE for Tumors with High Lethality in Sprague-Dawley Rats. Radiat. Res. 154: 412-420, 2000

[12]   ICRP: Recommendations of the International Commission on Radiological Protection, ICRP Publication 60. Annals of the ICRP 21 (1-3), Pergamon Press, Oxford; 1991

[13]   Kellerer AM, Rühm W and Walsh L: Accounting for radiation quality in the analysis of the solid cancer mortality among A-bomb survivors. Technical report number TR 223 of the Radiobiological Institute, Ludwig-Maximilians University Munich; 2003

[14]   Rühm W, Walsh L and Kellerer AM: The neutron effective dose to the A-bomb survivors. Technical report number TR 221 of the Radiobiological Institute, Ludwig-Maximilians University Munich; 2003

13. Kellerer AM, Rühm W & Walsh L. Indications of the neutron effect contribution in the solid cancer data of the A-bomb survivors. Health Physics. 90(6), 554-564, 2006

INDICATIONS OF THE NEUTRON EFFECT CONTRIBUTION IN THE SOLID CANCER DATA OF THE A-BOMB SURVIVORS

Albrecht M. Kellerer, Werner Rühm, and Linda Walsh*

Abstract—Risk estimates for radiation-induced cancer are primarily based on the follow-up of the Japanese A-bomb survivors. Their exposures were due to gamma rays and neutrons, and, currently—with the assumed low RBE = 10 of neutrons and reference to the colon dose—the late radiation effects are almost fully attributed to the gamma rays. Solid cancer risk estimates for different organ sites are assessed here, and an inconspicuous but statistically highly significant trend of larger values is found for the organs closer to the body surface; i.e., the organs with less body shielding and, therefore, with larger neutron dose-fractions. Underestimation of the RBE of neutrons can explain this apparent correlation. The trend of *ERR*/Gy vs. depth ceases to be statistically significant for RBE values close to 100. The suggestion of high RBE values and the corresponding reduction of gamma-ray risk estimates is found to be in line with log-likelihood computations in terms of AMFIT, which provide for the solid cancer mortality of the A-bomb survivors the minimum deviance for RBE = 100 with a 95% confidence lower limit of 25. The present assessment had to use the data made publicly available by RERF. In this form they contain city-, sex-, age-, and dose-categories, but—instead of a separate neutron-dose category—only the mean neutron dose for each data cell. The tentative conclusions that are here obtained should, therefore, be examined by a more definitive analysis, either in terms of grouped data with a separate classification of neutron doses or, ideally, in terms of person by person calculations to be performed at RERF with individually estimated neutron doses.
Health Phys. 90(6):554–564; 2006

Key words: cancer; dose, organ; epidemiology; neutrons

INTRODUCTION

THE FOLLOW-UP of the A-bomb survivors is the major source of current knowledge on the risk of late radiation effects, especially of increased cancer mortality and incidence (Pierce et al. 1996a; Preston et al. 2003, 2004; Thompson et al. 1994). The absorbed dose to the survivors was predominantly due to the sparsely ionizing

gamma rays, but there has been a small densely ionizing dose contribution from fission neutrons. High linear energy transfer (LET)-radiation being very effective (Sinclair 1982), its contribution has found particular attention (Rossi and Mays 1978; Zaider 1991; Brenner 1996; Rossi and Zaider 1996; Pierce et al. 1996b). The issue seemed especially crucial after it was suggested (Straume et al. 1992) that the dosimetry system *DS86* (Roesch 1987) had underestimated the neutron absorbed doses. A major international effort has since produced the revised dosimetry system *DS02* (Young and Kerr 2005), which confirms largely the neutron-dose estimates in *DS86*. However, the issue remains of interest because microdosimetric considerations and radiobiological findings suggest values of the neutron relative biological effectiveness (RBE) that cause a higher neutron contribution to the late effects among the A-bomb survivors than currently assumed (Kellerer and Walsh 2001).

The assessments of solid cancer mortality by the Radiation Effects Research Foundation (RERF) employ the "weighted dose," which is the gamma-ray absorbed dose to the colon, as one of the deepest lying organs, plus the neutron absorbed dose to the colon multiplied by 10. Preston et al. (2004) have used this familiar dose specification also in their first assessment of the influence of *DS02* on solid cancer mortality-risk estimates, and they have found that the changes due to the dosimetry revision are comparatively minor.

Continuity in the method of dose specification is essential for keeping the increasingly complete results comparable, while the follow-up of the members of the life span study (LSS) continues. However, as the study comes closer to its ultimate conclusion, it is also important to explore possible refinements. The general availability of the solid-cancer-mortality data up to the end of 1997 (Preston et al. 2003) and the reassessment of the A-bomb dosimetry have motivated a recent analysis of the organ-specific risk coefficients and their dependence on dose specification (Walsh et al. 2004a and b). This included an exploration of the influence of the assumed neutron RBE on the risk estimates for the various organs.

Table 1. Sex-averaged and female-organ-specific *ERR*/Gy (with standard errors) for gamma rays and solid cancer mortality. The values refer to age 30 y at exposure. They are deduced in terms of AMFIT (Preston et al. 1993) from the 1950–1997 LSS data with the dosimetry *DS86* and the linear dose model (eqn 1). The computations used the dose cut-off 2 Gy and the specified neutron RBE values. The modifying factor for age at exposure is $g = 0.04$/y and the modifying factors for females and males are 1.3 and 0.7 (Walsh et al. 2004a).
The organs are listed in order of increasing depth in the body. The neutron absorbed dose fractions, f_n, are given in the first column of numbers, they equal the person-year weighted mean neutron dose divided by the person-year weighted gamma-ray dose.

Organ	Neutron absorbed dose fraction, $f_{n,i}$ (%)	*ERR*/Gy (organ specific doses)			
		RBE = 10	RBE = 20	RBE = 50	RBE = 100
Breast	1.38	1.31 ± 0.37	1.13 ± 0.32	0.79 ± 0.22	0.52 ± 0.15
Others	0.88	0.69 ± 0.18	0.63 ± 0.17	0.49 ± 0.13	0.35 ± 0.09
Oesophagus	0.86	1.22 ± 0.48	1.11 ± 0.44	0.88 ± 0.34	0.65 ± 0.25
Lung	0.77	0.75 ± 0.17	0.69 ± 0.15	0.54 ± 0.12	0.40 ± 0.09
Liver	0.71	0.45 ± 0.14	0.42 ± 0.13	0.34 ± 0.10	0.26 ± 0.08
Gallbladder	0.71	0.14 ± 0.21	0.13 ± 0.19	0.11 ± 0.16	0.09 ± 0.12
Stomach	0.68	0.45 ± 0.11	0.41 ± 0.10	0.33 ± 0.08	0.25 ± 0.06
Rectum	0.52	0.41 ± 0.25	0.39 ± 0.24	0.32 ± 0.20	0.25 ± 0.16
Bladder	0.52	1.57 ± 0.80	1.48 ± 0.75	1.27 ± 0.64	1.01 ± 0.51
Colon	0.48	0.46 ± 0.23	0.44 ± 0.22	0.39 ± 0.19	0.33 ± 0.16
Pancreas	0.45	0.10 ± 0.19	0.09 ± 0.18	0.08 ± 0.16	0.06 ± 0.13
Ovary	0.40	0.87 ± 0.50	0.84 ± 0.48	0.74 ± 0.43	0.63 ± 0.35
Uterus	0.36	0.16 ± 0.21	0.16 ± 0.20	0.14 ± 0.18	0.12 ± 0.15
Weighted average		0.47 ± 0.06	0.43 ± 0.05	0.37 ± 0.05	0.28 ± 0.03
χ^2 deviation from average		22.8	21.8	19.4	17.2

The resulting organ-specific risk coefficients are considered here in further detail. They will be seen to indicate an intriguing link to the effect contribution by the neutrons.

MATERIALS AND METHODS

The same organ sites are considered in the present study that were analyzed in the recent assessment of organ-specific risk estimates (Walsh et al. 2004b). The conversion factors from the colon doses (as given in the solid cancer mortality data 1950–1997) to organ-specific doses have been taken from the publicly available (www.rerf.or.jp) data set *ds86adjf.dat*. They depend on radiation type, age at exposure, and city and are listed in the earlier paper (Walsh et al. 2004a). Since the neutron dose contribution is particularly important for the subsequent considerations, its magnitude is indicated in the first column of Table 1 (see Results section) in terms of the organ-specific neutron absorbed dose fraction. As in the earlier study, the organs associated in RERF Report 12 with less than 100 solid cancer deaths have been combined. They include a wide range of organs and tissues and were, accordingly, assigned the organ-averaged neutron absorbed dose fraction. As will be shown, the inclusion of this category in the subsequent analysis is not critical.

The organ-specific risk estimates for gamma rays are obtained in computations with AMFIT (Preston et al.

1993). As in most earlier computations with the LSS data, the excess relative cancer mortality is quantified in terms of a model that is linear both in the gamma-ray absorbed dose, D_g, and the neutron absorbed dose, D_n:

$$ERR_i(D_\gamma, D_n) = \alpha_i(D_{\gamma,i} + RBE\, D_{n,i})\mu(s, a), \quad (1)$$

where the index i ($i = 1, 2, \ldots 13$) stands for the organ category, and $\mu(s, a)$ is the modifying function for sex and for age at exposure, e:

$$\mu(s, a) = \exp[-g(e - 30)](1 \pm s)$$

$$(+ \text{ for females, } - \text{ for males}). \quad (2)$$

The computations include, simultaneously, as explained in the earlier articles (Walsh et al. 2004a and b), the expressions for the different organ categories, which permit the use of common parameters, g and s, in the modifying function. The assumption of modifying factors that are not organ specific is, of course, a simplification, but it is required to make the values *ERR*/Gy for the various organs comparable. Apart from the modifying factors, the coefficients α_i for the various organs are equal to the excess relative risk per unit absorbed dose of gamma rays, *ERR*/Gy.[†]

[†] All values *ERR*/Gy in this paper represent the excess relative risk per unit absorbed dose of gamma rays. They do not stand for the ERR per unit absorbed dose of the A-bomb radiation, i.e., the mixture of gamma rays and neutrons.

The major, unavoidable limitation of the present analysis lies in the fact that the publicly available data set contains categories for city, sex, age and dose, but no separate category for neutron dose. Only average neutron doses are given for each cell, and these are used in the present analysis. The summary specification of the neutron doses in the published data set *ds86adjf.dat* reflects the accustomed judgment that the neutron effect contribution is comparatively minor and unimportant.

The linear model (*L*-model) is not strictly valid because it disregards the slight curvature that is now apparent in the dose-effect relation for the solid cancer mortality data up to 1997 (Walsh et al. 2004a) and which has also become evident in the more recent data set for all solid cancers combined, which has been publicly available since June 2005 (Preston et al. 2004; NAS/NRC 2005). It would, therefore, be more meaningful to employ a linear-quadratic dependence on gamma-ray dose and a linear dependence on neutron dose (*LQ*-model):

$$ERR(D_\gamma, D_n) = \alpha(D_\gamma + RBE\, D_n) + \beta\, D_\gamma^2. \quad (3)$$

This more complex relation is not usually invoked, and it would be particularly unsuitable in the organ-specific analysis because it provides estimates of α that have a much larger standard error than the coefficients α in the linear dose model. The dilemma has been resolved by showing (Walsh et al. 2004a) that the risk estimate at 1 Gy of gamma rays has (with a dose cut off of 2 Gy) very nearly the same value and standard error in the *L*-model as in the *LQ*-model (see Appendix, eqn A1). Regardless of the curvature in the dose-effect relation for gamma rays, the results of the present analysis therefore remain valid if the risk estimates are understood to refer to 1 Gy of gamma rays and not necessarily to the potentially less effective lower doses.

RESULTS

Organ-specific risk coefficients for solid cancer

The estimated values *ERR*/Gy for gamma rays are shown in Table 1 for age 30 y at exposure and for different assumed RBE values. They are based on the 1950–1997 follow-up data of the LSS-cohort. The results derived in terms of organ-specific doses and in terms of RBEs of 10, 20, 35, and 50 have already been given in the preceding article (Table 3 of Walsh et al. 2004b). The modifying factor for age, *e*, at exposure is $exp[-g(e - 30)]$ with $g = 0.04\ y^{-1}$. For the sites that are not gender specific the modifying factors for females and males are 1.3 and 0.7, i.e., the *ERR*/Gy needs to be multiplied by 1.3 for females and by 0.7 for males. The parameters *g* and *s* were not fixed but remained close to the above values for each evaluation with a different RBE. The organs are listed in order of

increasing depth in the body, i.e., increased shielding by the body. The first column of numbers gives for the various organs the person-year weighted sum of neutron absorbed doses divided by the corresponding sum of total absorbed doses. These average values are termed neutron dose fraction, f_n. Because the neutrons are more strongly attenuated than the gamma rays, the f_n are largest for the organs that are close to the body surface. For the same reason, the neutron contribution increases at closer distances to the A-bomb, i.e., at higher doses. For example, for the breast the (average) neutron dose fraction is $f_n = 1.38\%$, while at 1 Gy total breast dose the neutron contribution is 2.4%.

None of the organ-specific *ERR*/Gy differs with statistical significance from the average (listed in the penultimate row of Table 1). For the lower RBE values the weighted sum of squares of the differences, χ^2, exceeds considerably the critical value $\chi^2 = 19.7$ reached with 5% probability under the null-hypothesis of equal values of *ERR*/Gy for all organs. There is, of course, no reason to expect equality of the true organ-specific values of *ERR*/Gy. Accordingly, a large χ^2 is, by itself, not indicative of an incorrect modeling assumption.

On the other hand, the values of χ^2 decrease with increasing values of the neutron RBE, which implies that the *ERR*/Gy values for the various organ categories exhibit less spread. The smaller values of χ^2 could, thus, be indicative of the higher RBE values. This evidence is, of course, too indirect to be conclusive. A more specific analysis is required to quantify any actual trend of higher *ERR*/Gy values that are inferred if low values of the neutron RBE are assumed.

Trend of higher *ERR*/Gy for the less shielded organs

There is no reason to expect equal excess relative risk per unit absorbed dose for the various organs. But there are no currently known biological factors that should cause a systematic trend of the excess relative risk against depth. Accordingly, different values of *ERR*/Gy are expected, but not a statistically significant correlation between these and a location dependent parameter, such as the neutron absorbed dose fraction, $f_{n,i}$ (first column of numbers in Table 1). Some chance slope (negative or positive) must, of course, result, if the organ-specific values $(ERR/Gy)_i$ are plotted against the $f_{n,i}$, and a regression line is fitted to these data. The question is whether this slope lies within the range expected under the null hypothesis of no inherent correlation with depth.

The two diagrams in Fig. 1 represent the 13 organ-specific values $(ERR/Gy)_i$ vs. the neutron absorbed dose fractions, $f_{n,i}$. To render the values $(ERR/Gy)_i$ comparable, they are all given without the sex-modifying factor, i.e., to obtain the true values they need to be multiplied
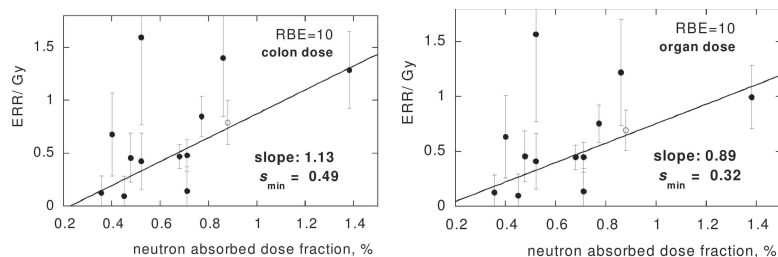
Fig. 1. Regression of the organ-specific risk coefficients $(ERR/\text{Gy})_i$ $(i = 1, 2, \ldots 13)$ against the absorbed dose fractions, f_i, due to neutrons. From left to right the points (and standard errors) represent the organs as listed, from bottom to top, in Table 1. The open dots represent the combined category of organs. The values $(ERR/\text{Gy})_i$ are given without the gender modifying factor (1 ± 0.3), i.e., they need to be multiplied by 1.3 for females and 0.7 for males. The slopes of the regression lines are positive with statistical significance better than 95%.
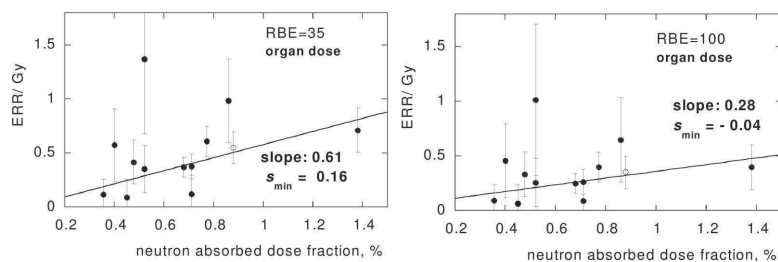
Fig. 2. Regression lines for organ-specific solid cancer ERR/Gy against the neutron absorbed dose fraction, f_i. The presentation is analogous to Fig. 1. The assumed values of the neutron RBE are 35 (left diagram) and 100 (right diagram). For RBE = 100, the minimum, $s_{\min}$, of the 95% confidence range reaches down to zero, i.e., the positive regression slope ceases to be statistically significant.

by 1.3 for females and by 0.7 for males.[‡] The visual inspection of the cloud of points may fail to indicate a trend, but the regression analysis accounts for the varying standard errors, and it provides regression lines with positive slope of high statistical significance. A systematic increase of the risk coefficients with the neutron absorbed dose fraction is, thus, suggested by the quantitative analysis. The lower limits, $s_{\min}$, of the regression slope on the 95% (two-sided) confidence level are noted in the diagrams. They are substantially larger than zero, i.e., the observed regression is statistically significant.[§]

The two diagrams in Fig. 2 give the results for the tentative values 35 and 100 of the neutron RBE. The

slopes of the regression lines are considerably less than in Fig. 1. For RBE = 35 the slope is still too large to be accepted as a random correlation. At RBE = 100, the 95% lower confidence limit, $s_{\min}$, is slightly less than zero; i.e., the trend of decreasing sensitivity with depth ceases to be statistically significant.

The open dot (second point from the right) in each of the correlation diagrams represents the combined category of organs labeled "others" in Table 1. The distinction is made because this category has been assigned the average, 0.88%, of the neutron absorbed dose fraction, which might introduce a bias.[**] On the other hand, it appeared desirable to use in the present analysis the same data set that has been used in the

---

[‡] This applies also to breast cancer; the values ERR/Gy in the diagrams are, thus, equal to the values for the breast in Table 1 divided by 1.3.

[§] The significance of the observed trend is crucial for the subsequent discussion. Since it is difficult to assess the applicability of the familiar regression test in terms of Student's t-statistic to a particular data set, a more transparent simulation procedure is described in the Appendix. It provides almost exactly the same results and confirms, thus, the conventional treatment.

[**] It could be argued that deaths from prostate cancer (80 cases in RERF Report 12, but 104 in Report 13) ought to be treated separately. However, the ERR/Gy for prostate cancer is similar in the mortality and incidence data, and the prostate is represented separately in the subsequent assessment of the incidence data (see next section, Fig. 3).
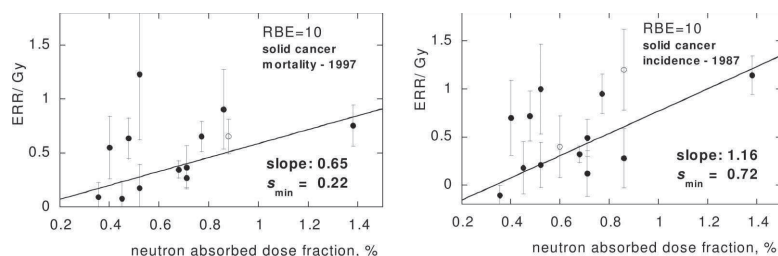
Fig. 3. Regression lines against neutron absorbed dose fraction for the organ-specific values $(ERR/Gy)_i$. The presentation is analogous to Figs. 1 and 2. The left diagram refers to the results obtained by RERF (Preston et al. 2003) for the latest solid cancer mortality data. These results were obtained with colon dose and a cut-off of 3 Gy or more. The right panel gives results obtained by Thompson et al. (1994) for the incidence data up to 1987. The solid circles represent the same organs as in Figs. 1 and 2. The open circle in the left diagram represents the category "others" (see Table 1); the open circles in the right diagram represent prostate (left point) and thyroid (right point).

previous assessments. The 1,015 deaths within the combined category (12% of all solid cancer deaths) relate to a large number of different organs or tissues so that the use of the average value of the neutron dose fraction appears acceptable. As it happens, the ERR/Gy for the combined group (the open symbols) lies, in all 4 diagrams, virtually on the regression line. This means that the removal of this group from the analysis would not greatly change the regression slopes and the confidence limits. To give an example, for RBE = 35 the slope would decrease from 0.61 ($s_{min} = 0.16$) to 0.59 ($s_{min} = 0.11$).

Consideration of related data

Finding numerical evidence for the effect contribution by neutrons in the solid cancer mortality data of the A-bomb survivors would be a major departure from current expectations. To ensure that the association is not merely a particularity of the present computations, one needs to check whether it is present also in the results obtained at RERF for the current solid cancer mortality data (Preston et al. 2003) and for the solid cancer incidence data (Thompson et al. 1994).

The left diagram in Fig. 3 shows that the trend of increasing ERR/Gy vs. the neutron dose fraction is present equally in the results obtained by RERF for the solid cancer mortality data up to 1997. The ERR/Gy values are lower and the slope is more shallow because RERF has used in their computations the colon dose with a cut-off at 3 Gy or more, which means that the "flattening" of the response at high doses already has some influence. The right panel refers to the results obtained by Thompson et al. (1994) for the incidence data, which are available only up to 1987. Instead of the "others" organ category, results are given separately for the prostate (left open circle) and for the thyroid (right open circle).[††] The regression is highly significant. The trend of increasing organ-specific estimates of ERR/Gy against the neutron absorbed dose fraction is, thus, generally present in the solid cancer data of the A-bomb survivors.

DISCUSSION

Possible explanations for the observed trend

The trend of higher ERR/Gy values for the less shielded organs can—in view of its high statistical significance—not be discounted as a mere chance occurrence. A true trend of less radiation sensitivity in the deeper lying organs cannot, of course, be ruled out, but currently there is no known theoretical or empirical basis to assume it. Little (2001) has compiled organ-specific risk estimates from a large number of radiation therapy studies and—with proper account for differences in sex and the age at exposure—has compared them to the LSS data. Unfortunately, the different studies on the same organs vary so substantially, and the uncertainties for many of the studies are so large, that there appears to be insufficient power to ascertain a possible trend of varying organ sensitivities with depth. An extension of this meta-analysis with inclusion of data from patients with diagnostic x-ray exposures may, nevertheless, be helpful to clarify the issue.

Underestimation of the neutron RBE has already been invoked as a potential explanation, but before this is explored further, alternative explanations need to be considered. A conceivable cause for lower risk estimates for the deeper lying organs could be underestimation of

---

[††] The anatomical position of the prostate being close to the urinary bladder, the somewhat larger neutron dose fraction 0.6 is used. The thyroid is assigned the same neutron dose fraction as the oesophagus.

the shielding of gamma rays by the body. If the gamma-ray doses to the colon, or other deep lying organs, were substantially smaller than currently assumed, the true risk coefficients for these organs would be larger than computed, i.e., the apparent trend might disappear. However, the dosimetric errors cannot nearly be large enough to make enough difference. The attenuation of the gamma rays will definitely not be twice as strong as currently assumed, but even if it were, the slope in the diagrams would change little. An alternative explanation would have been a large underestimation of the neutron doses, but the revised dosimetry system *DS02* has, by now, ruled out this possibility (Straume et al. 2003; Huber et al. 2003; Young and Kerr 2005). Short of a true correlation of organ sensitivity and depth in the body, underestimation of the neutron RBE remains, thus, the most credible cause of the higher risk estimates for the less shielded organs.

RBE values substantially larger than 10 cannot be rejected off-hand. Even the ICRP weighting factor for neutrons corresponds to an RBE of the A-bomb neutrons in excess of 20. The resulting difference to the conventional treatment is not trivial. The use of organ-specific dose, rather than colon dose, combined with the comparatively modest change from RBE = 10 to 20 increases, in the case of the breast, the relative effect contribution by the neutrons by a factor of more than 5 (Walsh et al. 2004b).

A survey of the relevant microdosimetry and the relatively few informative animal experiments with gamma-ray (or x-ray) doses around 1 Gy and with small neutron doses (Shellabarger et al. 1980; Lafuma et al. 1989; Wolf et al. 2000) is outside the scope of this article. Reference can, however, be made to the major assessment by Sinclair (1982), to NCRP Report 104 (1990), to ICRP 92 (2003), and to a recent report by the German Radiation Protection Commission (SSK 2005). A wide range of neutron RBE values between 20 and 100 is suggested, the major uncertainty lying in the potentially low carcinogenic efficiency of gamma-ray doses around 1 Gy.

The *ERR*/Gy for breast cancer

The observed trend of increasing risk estimates for the organs with higher neutron doses is not primarily driven by the breast cancer data. In fact, in all diagrams of Figs. 1–3 the value for the breast is slightly below the correlation line. The data for breast cancer lie, thus, within the trend of the other organ-specific values. On the other hand, one obtains with the accustomed assumption RBE = 10 an *ERR*/Gy for breast cancer that appears to be out of line with the lower values from medical

patients exposed to photon fields without the neutron component.

Of particular importance is the Massachusetts cohort study of tuberculosis fluoroscopy patients for which a much smaller *ERR*/Gy for breast cancer incidence has been derived than observed for the female A-bomb survivors (Little and Boice 1999). In fact, the same absolute excess breast cancer incidence (up to 2.5 Gy) has been found for the two cohorts, although the spontaneous incidence in Japan has been less by about a factor of 4. As discussed by Brenner (1999), the fluoroscopy exposures may have been less effective because they were fractionated, but they should have been more effective due to their much lower photon energies. Without going into details, it is noted that, in their important pooled analysis of breast cancer incidence in eight cohorts, Preston et al. (2002) consider as the most striking feature "the larger excess relative risk estimates in the LSS" compared to the other cohorts. The breast cancer incidence and mortality rates being lower in Japan than in Caucasian populations, they recommend—in order to attain better congruence of the results—absolute risk transfer, rather than the relative risk transfer or the mixed mode that is currently assumed for other cancer sites. The present considerations suggest that a higher neutron RBE reduces the *ERR*/Gy for the gamma rays sufficiently to render the postulate of absolute risk transfer unnecessary.

Implications of the explanation in terms of neutrons and possible objections

The analysis concerns a fundamental question: Are the late radiation effects among the A-bomb survivors almost exclusively due to the sparsely ionizing gamma rays, or do they reflect to a substantial degree the action of the densely ionizing neutron recoils? A clearly predominant role of the gamma rays is at present widely accepted. Likewise, it is assumed that the role of neutrons needs to be judged in terms of radiobiology alone and that no evidence can be found directly in the epidemiological data.

Fig. 4 summarizes the result of the computations. It gives—as a function of the assumed neutron RBE—the estimated slope (solid curve) of the regression of the organ-specific *ERR*/Gy values vs. the neutron dose fraction and, in addition, its lower confidence limit (dotted curve). The null hypothesis of no inherent trend of *ERR*/Gy vs. depth excludes, on the 95% (two-sided) confidence level, values of the neutron RBE below 100.

In the absence of other explanations for the observed trend, it is reasonable to see it as indication of high neutron RBE. This interpretation is, of course, tentative, and it is at variance with the current interpretation of the
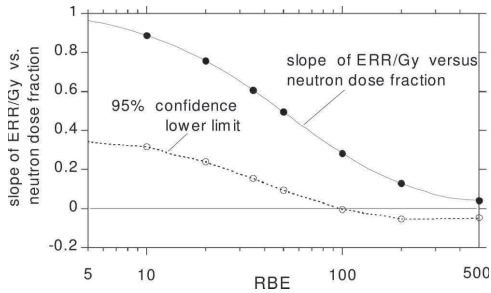
Fig. 4. Regression slope of the organ-specific *ERR*/Gy for gamma rays against neutron dose fraction with different assumed RBE (solid curve and full circles). The dotted curve (open circles) gives the minimum slope at the 95% (two-sided) confidence level. The slope differs with statistical significance from zero for RBE values less than 100.

Fig. 5. Nomogram, for breast cancer, of the *ERR*/Gy for gamma rays and for neutrons at various assumed values of the neutron RBE. The standard errors are given by the straight-line segments. The diagram shows that increasing values of the RBE correspond to less than proportional increases of *ERR*/Gy for neutrons and to substantial decreases of *ERR*/Gy for gamma rays. The data (Table 1) apply to the Japanese women in the LSS.

A-bomb data that assigns not more than about 10% of the excess cancer rates to the neutron dose contribution. But being potentially important, it deserves further examination and a careful consideration of the likely objections.

Improbability of high neutron RBE. The first objection is, of course, that values of the neutron RBE of 100 or more are too widely at variance with current assumptions to merit serious consideration. This argument ignores the fact that the major uncertainty is not so much the high effectiveness of neutrons, but the potentially low carcinogenic effect of gamma rays at doses around 1 Gy. The term *neutron* RBE tends to obscure this point; larger values are intuitively perceived to imply high neutron effectiveness, rather than low gamma-ray effectiveness.

A numerical example can help to rectify this misconception. If a high neutron RBE of 100 is considered, rather than 10, this might intuitively be perceived as an implausible 10-fold increase of the assumed neutron effectiveness. The nomogram in Fig. 5 corrects this impression. It plots the values for breast cancer from Table 1 (plus the results for RBE = 35 and 500) in such a way that—for the specified RBEs—the *ERR*/Gy can be read off both for the gamma rays and the neutrons. The diagram shows that an RBE of 100, instead of 10, implies—for breast cancer—a 4-fold increase of the neutron effectiveness and a 2.5 decrease of the effectiveness of gamma rays. It will be difficult to find firm evidence against these two changes among the epidemiological data outside the observations on the A-bomb survivors. The reduction of the risk estimate for the gamma rays is, in fact, in line with the information from medical cohorts (Little and Boice 1999; Little 2001).

Lack of direct evidence in terms of the log-likelihood computations. While high values of RBE imply no implausibly high absolute neutron efficiency, they will still appear unlikely as long as they are not supported more directly by the familiar log-likelihood computations in terms of AMFIT. This argument leads to an interesting observation. The major studies by RERF (Pierce et al. 1996a; Preston et al. 2003) have not assessed the influence of RBE on fitting the A-bomb data. A recent investigation (Walsh et al. 2004a) has, in terms of the linear-quadratic dose model, provided the least deviance for high values of RBE, but the issue was not further explored. The data were not expected to yield firm conclusions. Perhaps for the same reason, not much attention has been paid to results by Little (1997), who has, in fact, done computations with RBE as a free parameter. For the earlier solid cancer mortality data, and still with reference to the colon dose, Little found that the minimum deviance was attained for a neutron RBE between 100 and 150, but no RBE value could be excluded at the 95% confidence level.

In the computations now repeated with the current solid cancer mortality data and the linear dose model in terms of organ-specific doses, the minimum deviance is obtained, as shown in Fig. 6, at RBE = 100, and for Hiroshima alone at about 200. The 95% confidence range is RBE = 25 to 400 for both cities combined, and RBE = 28 with no upper bound for Hiroshima. While the uncertainties are large, the result is, nevertheless, important. To disregard it—because it is at variance with current assumptions—would mean that other results of

Fig. 6. Deviance increment obtained in fitting the solid cancer mortality data to a linear dose model with a dose cut-off of 2 Gy. For the combined data from both cities the best fit provides a neutron RBE slightly less than 100 and a 95% confidence range from RBE = 25 to about 400. For Hiroshima alone, the best fit is about 200, with confidence range down to 28 and no upper bound. For Nagasaki alone, the minimum likelihood is reached at about 400, but no values of the RBE can be excluded.

Fig. 7. The *ERR*/Gy for solid cancer mortality in a linear dose model for Hiroshima (solid curve) and for Nagasaki (broken curve). The symmetrical standard errors are inserted. The estimates for the two cities are equal for RBE = 50, but the difference becomes statistically significant (at the 95% confidence level) only for RBE larger than 400. The computations are performed with joint modifying factors for gender and age at exposure. If a separate age at exposure dependence is admitted for each of the cities, the resulting lifetime *ERR*/Gy is considerably smaller for Nagasaki.

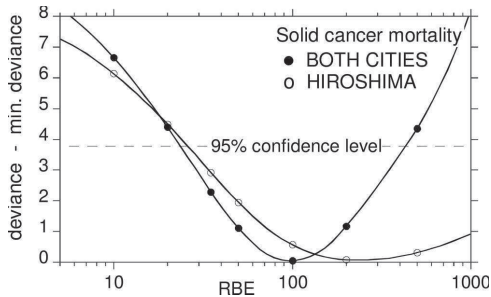the log-likelihood computations with AMFIT could likewise be accepted or ignored.

Absence of a city difference. There is a further likely objection. Earlier assessments by RERF (Pierce et al. 1996a; Preston et al. 2003) have concluded that there is no statistically significant difference of over-all response in Hiroshima and Nagasaki. Absence of a city difference in the RERF computations would, in fact, support the assumed low RBE. Since the relative dose contribution by neutrons was 2 to 3 times larger in Hiroshima than in Nagasaki, any substantial underestimation of RBE should cause a markedly larger overestimate of *ERR*/Gy in Hiroshima.

Fig. 7 depicts the dependence of *ERR*/Gy, the estimated gamma-ray risk coefficient for Hiroshima and Nagasaki, on the assumed RBE. There should ideally be no city difference with the correctly chosen RBE. The data confirm that there is—on the 95% confidence level—no statistically significant city difference up to an assumed RBE of about 200. Equality of the dose coefficients results at RBE = 50, but the statistical uncertainty is too large for firm conclusions to be drawn.

At this point it needs to be noted that the comparison between the two cities is somewhat uncertain because the published data do not permit a judgment of the influence that dosimetric adjustments for the Nagasaki factory workers may have. Assessing the impact of the current A-bomb dose revision, Preston et al. (2004) have noted that the use of *DS02* leads to roughly a 10% reduction of the risk coefficients for Hiroshima and a roughly 20% reduction for the Nagasaki survivors (without the factory

workers). These changes would increase the city difference that is seen in Fig. 7 at low assumed RBE and shift the intersection of the two curves to higher RBE. Likewise, the change would bring the deviance curve for both cities in Fig. 6 closer to the curve for Hiroshima alone.

The comparison between Hiroshima and Nagasaki is subject to another, more serious limitation. The computations have been performed, as in earlier studies, with common sex and age-at-exposure modifiers for Hiroshima and Nagasaki. The use of city specific spontaneous solid cancer mortality, and also of city specific sex-modifying factors, is found to make comparatively minor differences. However, if separate age-at-exposure modifiers are admitted, the age dependence is much steeper for Nagasaki. The comparison must then be made in terms of lifetime averaged *ERR*/Gy, and this value turns out to be much smaller for Nagasaki than Hiroshima. As long as this anomaly remains unexplained, the comparison between the two cities needs to be judged with great reservation.

Curvature in the dose response as a reflection of the gamma-ray effect. A final objection against a large effect contribution by neutrons relates to the curvature that has recently become apparent in the dose response for solid cancer mortality (Walsh et al. 2004a; Preston et al. 2004). Under the current interpretation the dose response is believed to reflect predominantly the effect of the gamma rays, and any upwards curvature is seen as the non-linear response that is characteristic for low-LET but not for high-LET radiation.

In reality the situation is more complex. Even if the dose response were linear both for gamma rays and neutrons, there would still be an upward, curved dose dependence on absorbed dose. This is so because the neutron dose fraction—and, thus, the effectiveness of the radiation—is larger at shorter distances from the bomb; between 0.2 Gy and 2 Gy the neutron fraction increases by roughly a factor 4 (Roesch 1987; Young and Kerr 2005). Apparent curvature in the dose-effect relation is, thus, by itself no proof that the gamma rays are predominant. The application of the linear-quadratic model to the solid cancer mortality data has, indeed, provided the minimum deviance at large values of the neutron RBE (Walsh et al. 2004a).

CONCLUSION

Various observations support the notion that neutrons have, in spite of their small absorbed dose fraction, contributed considerably to the excess solid cancer mortality among the A-bomb survivors in Hiroshima. If this is so, it implies substantially reduced risk estimates for gamma rays, especially for the less-shielded organs such as the breast. The reduction would bring the risk estimates derived from the LSS data closer to the generally lower estimates from the follow-up of cohorts exposed to x rays for medical reasons (Little 2001). The conclusions could affect the judgment of radiation risk and the choice of the ICRP organ weighting and radiation weighting factors. Issues, such as the dose reduction factor *(DDREF)* or the mode of risk transfer between a Japanese and a Western population would appear in a new light. The further implication is a certain increase of the risk estimates for neutrons.

Although they are potentially very important, the inferences are at present tentative. This is so because they are based on the currently available data set *ds86adjf.dat* (www.rerf.or.jp) from RERF, which is still linked to the former dosimetry, *DS86*, and specifies the neutron doses only crudely. Using a dosimetry system that is not fully up to date is a minor drawback; the major difficulty is that, instead of a separate classification of the neutron doses, there are only mean neutron doses for each data cell. Using mean values sacrifices valuable information because the ratio of neutron to gamma-ray dose varies not only with city and gamma-ray dose, but also with body weight, directional orientation of the exposed person and, most importantly, with shielding conditions. If—on the basis of this additional information—neutron doses were more explicitly specified, the analysis could become much more informative.

The essential point is that the issue of the neutron effect contribution is still open. Since the matter is of fundamental importance to risk assessment and radiation protection in general, all possible efforts need to be made to resolve it.

One possibility would be to explore other sources of relevant information. The A-bomb survivors are not the only large cohort exposed to gamma rays and neutrons. The nuclear workers from the Mayak Nuclear Complex are another similarly exposed group (Shilnikova et al. 2003). But, while the analysis of Mayak data may ultimately provide important information, it is still in progress and cannot yet corroborate or contradict the inferences from the data of the A-bomb survivors.

The A-bomb data offer, at this point, the most direct possibility to resolve the role of neutrons. The comparison of effects in Hiroshima to those in Nagasaki has long been seen as the most obvious possibility, but—as explained—it is subject to considerable uncertainty. The definitive analysis requires, therefore, computations with a separate specification of the neutron doses in terms of the new dosimetry system *DS02*.

RERF has set a high standard by making the epidemiological data from the Life Span Study of the A-bomb survivors generally available after publication of their own analyses. There have been good reasons in the past—both in terms of computing practicability and protection of privacy—to analyze and then to release the data in grouped format. Computing practicability has ceased to be an issue, and person-by-person computations should by now be a preferred procedure, at least in the computations by RERF. Restrictions will still be required for the release of ungrouped data. But it is likely that methods can be worked out to continue and extend RERF's policy of openness without compromising the privacy of the A-bomb survivors.

REFERENCES

Brenner DJ. Direct biological evidence for a significant neutron dose to survivors of the Hiroshima atomic bomb. Radiat Res 145:505–507; 1996.

Brenner DJ. Does fractionation decrease the risk of breast cancer induced by low-LET radiation? [Commentary]. Radiat Res 151:225–229; 1999.

Huber T, Rühm W, Hoshi M, Egbert SD, Nolte E. ^{36}Cl measurements in Hiroshima granite samples as part of an international intercomparison study: results from the Munich group. Radiat Environ Biophys 42:27–32; 2003.

International Commission on Radiological Protection. Recommendations of the International Commission on Radiological Protection. Oxford: Pergamon Press; ICRP Publication 92; Annals of the ICRP 33(4); 2003.

Kellerer AM, Walsh L. Risk estimation for fast neutrons with regard to solid cancer. Radiat Res 156:708–717; 2001.

Lafuma J, Chmelevsky D, Chameaud J, Morin M, Masse R, Kellerer AM. Lung carcinomas in Sprague-Dawley rats after exposure to low doses of radon daughters, fission neutrons, or gamma rays. Radiat Res 119:230–245; 1989.

Little MP. Estimates of neutron relative biological effectiveness derived from the atomic bomb survivors. Int J Radiat Biol 72:715–726; 1997.

Little MP. Comparison of the risks of cancer incidence and mortality following radiation therapy for benign and malignant disease with the cancer risks observed in the Japanese A-bomb survivors. Int J Radiat Biol 78:431–464; 2001.

Little MP, Boice JD. Comparison of breast cancer incidence in the Massachusetts tuberculosis fluoroscopy cohort and in the Japanese atomic bomb survivors. Radiat Res 151:218–224; 1999.

National Academy of Sciences, National Research Council. Committee on the Biological Effects on Ionizing Radiation. Health risks from exposure to low levels of ionizing radiation. Washington, DC: NAS/NRC; BEIR VII; 2005.

National Council on Radiation Protection and Measurements. The relative biological effectiveness of radiations of different quality. Bethesda: NCRP; Report 104; 1990.

Pierce DA, Shimizu Y, Preston DL, Vaeth M, Mabuchi K. Studies of the mortality of atomic bomb survivors. Report 12, Part 1. Cancer. Radiat Res 146:1–27; 1996a.

Pierce DA, Shimizu Y, Preston DL, Vaeth M, Mabuchi K. Response to the letter of Drs Rossi and Zaider. Radiat Res 146:591–593; 1996b.

Preston DL, Lubin JH, Pierce DA. Epicure user's guide. Seattle: HiroSoft International Corp; 1993.

Preston DL, Mattsson A, Holmberg E, Shore R, Hildreth NG, Boice Jr JD. Radiation effects on breast cancer risk: a pooled analysis of eight cohorts. Radiat Res 158:220–235; 2002.

Preston DL, Shimizu Y, Pierce DA, Suyama A, Mabuchi K. Studies of mortality of atomic bomb survivors. Report 13: Solid cancer and noncancer disease mortality: 1950–1997. Radiat Res 160:381–407; 2003.

Preston DL, Pierce DA, Shimizu Y, Cullings HM, Fujita S, Funamoto S, Kodama K. Effect of recent changes in atomic bomb dosimetry on cancer mortality risk estimates. Radiat Res 162:377–389; 2004.

Roesch WC. US–Japan joint reassessment of atomic bomb radiation dosimetry in Hiroshima and Nagasaki, Vols. 1 and 2. Hiroshima: Radiation Effects Research Foundation; 1987.

Rossi HH, Mays CW. Leukemia risk from neutrons. Health Phys 34:353–360; 1978.

Rossi HH, Zaider M. Comment on the contribution of neutrons to biological effects at Hiroshima [letter to the editor]. Radiat Res 146:590–591; 1996.

Shellabarger CJ, Chmelevsky D, Kellerer AM. Induction of mammary neoplasms in the Sprague-Dawley Rat by 430-keV neutrons and x rays. J National Cancer Inst 64:821–832; 1980.

Shilnikova NSD, Preston DL, Ron E, Gilbert ES, Vassilenko EK, Romanov SA, Kuznetsova ME, Okatenko PV, Kreslov VV, Koshurnikova NA. Cancer mortality risk among workers at the Mayak Nuclear Complex. Radiat Res 159:787–798; 2003.

Sinclair WK. Fifty years of neutrons in biology and medicine: the comparative effects of neutrons on biological systems. In: Ebert HG, ed. Proceedings of the 8th Symposium on Microdosimetry. Brussels: Commission of the European Communities; Report EUR 8359; 1982: 1–37.

Strahlenschutzkommision (SSK) des Bundesministeriums für Umwelt, Naturschutz und Reaktorsicherheit, Vergleichende Bewertung der biologischen Wirksamkeit verschiedener ionisierender Strahlungen. Veröffentlichungen der Strahlenschutzkommission, Bd. 53. Jena, Germany: Elsevier/Urban & Fischer; 2005 (in German).

Straume T, Egbert SD, Woolson WA, Finkel RC, Kubik PW, Grove HF, Sharma P, Hoshi M. Neutron discrepancies in the DS86 dosimetry system. Health Phys 63:421–426; 1992.

Straume T, Rugel G, Marchetti AA, Rühm W, Korschinek G, McAninch JE, Carroll K, Egbert S, Faestermann T, Knie K, Martinelli R, Wallner A, Wallner C. Measuring fast neutrons in Hiroshima at distances relevant to atomic-bomb survivors. Nature 424:539–541; 2003.

Thompson DE, Mabuchi K, Ron E, Soda M, Tokunaga S, Ochikubo S, Sugimoto S, Ikeda T, Terasaki M. Cancer incidence in atomic bomb survivors. Part II: solid tumors, 1958–1987. Radiat Res 137(Suppl):S17–S67; 1994.

Walsh L, Rühm W, Kellerer AM. Cancer risk estimates for gamma rays with regard to organ specific doses, part I: all solid cancers combined. Radiat Environ Biophys 43:145–151; 2004a.

Walsh L, Rühm W, Kellerer AM. Cancer risk estimates for gamma rays with regard to organ specific doses, part II: site-specific solid cancers. Radiat Environ Biophys 43:225–231; 2004b.

Wolf D, Lafuma J, Masse R, Morin M, Kellerer AM. Neutron RBE for tumors with high lethality in Sprague-Dawley rats. Radiat Res 154:412–420; 2000.

Young RW, Kerr GD. Report of the joint US–Japan working group. Reassessment of the atomic bomb radiation dosimetry for Hiroshima and Nagasaki: Dosimetry System DS02. Hiroshima: Radiation Effects Research Foundation; 2005.

Zaider M. Evidence of a neutron RBE of 70 ($\pm$ 50) for solid tumor induction at Hiroshima and Nagasaki and its implication for assessing the effective neutron quality factor. Health Phys 61:631–636; 1991.

APPENDIX

Accounting for the curvature in the dose relation for gamma rays

As stated in the main text, the two parameters α and β in the *LQ*-model of eqn (2) have fairly large standard errors. This problem has been removed in a preceding study (Walsh et al. 2004a) by using, instead of the parameter β, the effect level at a reference gamma-ray dose, D_1. With this substitution eqn (2) can be rewritten as:

$$ERR(D_\gamma, D_n) = \alpha(D_\gamma - D_\gamma^2/D_1 + RBE\, D_n) + cD_\gamma^2/D_1^2.$$

$$(A1)$$

With the dose cut-off of 2 Gy, the reference dose is taken to be 1 Gy. With the dose unit Gy, eqn (A1) then reads:

$$ERR(D_\gamma, D_n) = \alpha(D_\gamma - D_\gamma^2 + RBE\, D_n) + cD_\gamma^2.$$

(A2)

The advantage of the parameter change is that it provides—in addition to the estimated α with its relative large standard error—the parameter c, which has nearly the same numerical value and the same standard error as the parameter α in the linear model. The linear parameter in eqn (A2) has, of course, the same large standard error as obtained in the straightforward formulation of eqn (2). It is noted that the estimate of the dose and dose-rate reduction factor (*DDREF*) is c/α.

Using eqn (A2) for the individual organs, but as in the *L*-model with the joint gender and age modifying factors, has provided numerical estimates and standard errors of c which are roughly equal to the values a obtained with the *L*-model. Regardless of the curvature in the dose effect relation for gamma rays, all conclusions of the present analysis remain, therefore, valid when the risk estimates are related to 1 Gy of gamma rays, rather than the low doses that are less effective by the imprecisely estimated *DDREF*.

Simulation procedure as alternative to the *t* test

Student's *t* test for regression slope is widely used, but—as with other parametric tests—the preconditions for its applicability are difficult to verify. An alternative assessment in terms of a more transparent simulation procedure avoids this issue. The null-hypothesis is independent of the variables $(ERR/Gy)_i$ and f_i, i.e., the slope
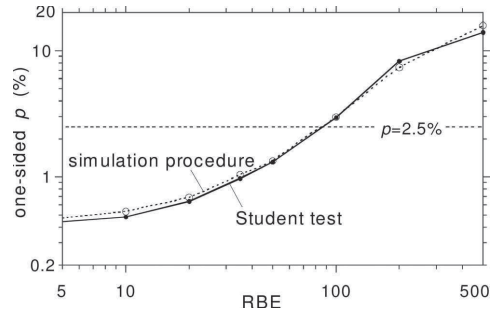
Fig. A1. The *p*-value to reach or exceed under the null-hypothesis the observed regression slope. The solid curve (full circles) gives the results of Student's *t* test, the dotted curve (open circles) those for the simulation procedure. For values of the neutron RBE <90 the null hypothesis can be rejected with less than 2.5% (one sided) error probability, i.e., under the 95% (two sided) confidence level.

of the regression line is taken to result from a mere random association of the two sets of numbers. The distribution under the null-hypothesis results then from the slopes for all possible permutations of the 13 values $(ERR/Gy)_i$ against the 13 values f_i. The total number of permutations being excessive ($13! > 6 \times 10^9$ for $I = 13$), a large number of random permutations is created for each data set. The fraction of the simulated slopes that exceed the observed slope then equals the probability value, *p*, for significance of the observed positive trend. In Fig. A1 the values are given for the various RBE values, and it is seen that the two test procedures agree very closely.

∎ ∎

14. Jacob P, Bogdanova TI, Buglova E, Chepurniy M, Demidchik Y, Gavrilin Y, Kenigsberg J, Meckbach R, Schotola C, Shinkarev S, Tronko MD, Ulanovski A, Vavilov S & Walsh L. Thyroid Cancer Risk in Areas of Ukraine and Belarus affected by the Chernobyl Accident. Radiat. Res. 165, 1-8, 2006

Thyroid Cancer Risk in Areas of Ukraine and Belarus Affected by the Chernobyl Accident

P. Jacob,[a,1] T. I. Bogdanova,[b] E. Buglova,[c,2] M. Chepurniy,[d] Y. Demidchik,[e] Y. Gavrilin,[f] J. Kenigsberg,[g] R. Meckbach,[a] C. Schotola,[a] S. Shinkarev,[f] M. D. Tronko,[b] A. Ulanovsky,[a] S. Vavilov[d] and L. Walsh[a]

[a] *GSF—Institute of Radiation Protection, Neuherberg, Germany;* [b] *Institute of Endocrinology and Metabolism of the Academy of Medical Sciences of Ukraine, Kyiv, Ukraine;* [c] *Research Institute of Radiation Medicine and Endocrinology, Minsk, Belarus;* [d] *Ukrainian Radiation Protection Institute, Kyiv, Ukraine;* [e] *Belarus State Medical University, Minsk, Belarus;* [f] *State Research Center—Institute of Biophysics, Moscow, Russian Federation; and* [g] *National Radiation Protection Commission, Minsk, Belarus*

Jacob, P., Bogdanova, T. I., Buglova, E., Chepurniy, M., Demidchik, Y., Gavrilin, Y., Kenigsberg, J., Meckbach, R., Schotola, C., Shinkarev, S., Tronko, M. D., Ulanovsky, A., Vavilov, S. and Walsh, L. Thyroid Cancer Risk in Areas of Ukraine and Belarus Affected by the Chernobyl Accident. *Radiat. Res.* **165**, 1–8 (2006).

The purpose of the present study was to analyze the thyroid cancer incidence risk after the Chernobyl accident and its degree of dependence on time and age. Data were analyzed for 1034 settlements in Ukraine and Belarus, in which more than 10 measurements of the ^{131}I content in human thyroids had been performed in May/June 1986. Thyroid doses due to the Chernobyl accident were assessed for the birth years 1968–1985 and related to thyroid cancers that were surgically removed during the period 1990–2001. The central estimate for the linear coefficient of the EAR dose response was 2.66 (95% CI: 2.19; 3.13) cases per 10^4 PY-Gy; for the quadratic coefficient, it was -0.145 (95% CI: -0.171; -0.119) cases per 10^4 PY-Gy^2. The EAR was found to be higher for females than for males by a factor of 1.4. It decreased with age at exposure and increased with age attained. The central estimate for the linear coefficient of the ERR dose response was 18.9 (95% CI: 11.1; 26.7) Gy^{-1}; for the quadratic coefficient, it was -1.03 (95% CI: -1.46; -0.60) Gy^{-2}. The ERR was found to be smaller for females than for males by a factor of 3.8 and decreased strongly with age at exposure. Both EAR and ERR were higher in the Belarusian settlements than in the Ukrainian settlements. In contrast to ERR, EAR increases with time after exposure. At the end of the observation period, excess risk estimates were found to be close to those observed in a major pooled analysis of seven studies of childhood thyroid cancer after external exposures. © 2006 by Radiation Research Society

INTRODUCTION

Thyroid cancer incidence in Ukraine and in Belarus started to increase significantly in 1990 among those who were children or adolescents at the time of the Chernobyl accident in April 1986 (*1, 2*). Since then, the incidence rate has increased further (*3, 4*). Analyses of thyroid cancer after the Chernobyl accident have a large potential for improving the understanding of the detrimental health effects of ^{131}I exposures, which were the main cause of thyroid doses after the accident.

Two case-control studies found an association of the increase in thyroid cancer incidence with radiation exposure due to the Chernobyl accident (*5, 6*). These studies have limitations in deriving risk estimates due to large dose uncertainties.

A cohort study is being performed here based on data for 25,161 Belarusian and Ukrainian children who had the ^{131}I content of the thyroid measured in May/June 1986 (*7*). Due to the intensive screening of the cohort members, the prevalence is considerably higher than in the general population. Consequently, estimates of the excess absolute risk (EAR) per dose for cohort members will not be the same as in the general population. It remains an open question as to what degree the intensive screening will influence excess relative risk (ERR) estimates.

Ecological studies have been performed for settlements in Belarus, Russia and Ukraine with relatively good dosimetry (*8, 9*). There is a general concern whether quantitative risk values can be derived with such an ecological study design (*10, 11*). Therefore, extensive simulation studies have been performed to explore the potential of ecological studies of thyroid cancer incidence in areas highly contaminated by the Chernobyl accident.[3] A main problem here is the potential for correlations between thyroid dose and increased case detection between the settlements. These simulations indicate that the ecological bias is relatively small in studies in which the ecological units are age groups in settlements with measurements of the ^{131}I content in the human thyroid. The reasons include:
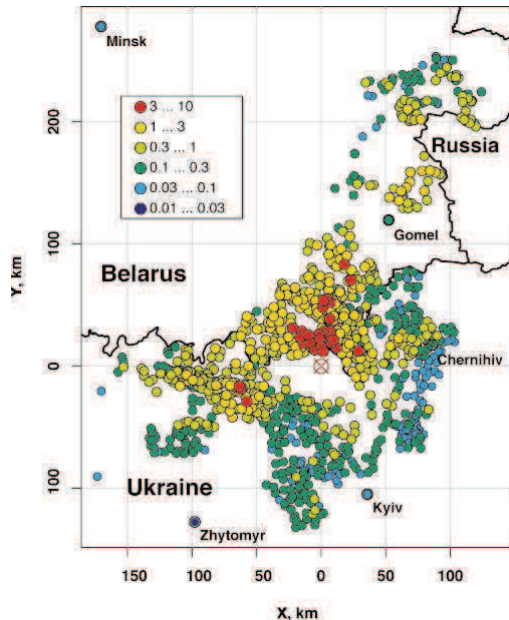
FIG. 1. Average thyroid dose (Gy) of the birth cohort 1968–1985 in the 608 Ukrainian and 426 Belarusian study settlements. The Chernobyl nuclear power plant is indicated in the center of the map.

1. There is a unique database of more than 200,000 measurements of the ^{131}I content in the human thyroid that were performed in May/June 1986 (*12, 13*).
2. Radiation is the dominant cause of thyroid cancer among those who were children or adolescents in the highly contaminated areas at the time of the accident, where the thyroid measurements were performed.
3. In general, there is no evidence for a correlation of thyroid dose and the main confounding factor, an increase in case detection and reporting, within the ecological units. In larger towns, there was a potential for such a correlation. Simulation calculations showed, however, that the ecological bias due to such a correlation is very small.[3]
4. There is no indication that the dose response for thyroid cancer after exposures during childhood is nonlinear in the dose range of 0.05–1.0 Gy (*9, 14*).

The purpose of this study was to derive risk estimates for those who were children or adolescents at the time of the Chernobyl accident and were living in settlements in which more than 10 measurements of the ^{131}I content in the human thyroid were performed in May/June 1986 (study settlements). Compared to earlier reports (*8, 9*) the risk analysis presented here is based on improved dose estimates and a longer follow-up (until the end of 2001), which
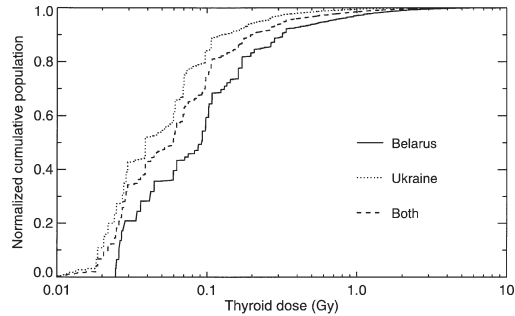
FIG. 2. Population weighed distribution of age-gender specific doses in the 608 Ukrainian and 426 Belarusian study settlements.

allows an evaluation of the degree of dependence on time. Relationships between the uncertainty of dose estimates, the variability of individual doses within the age-gender groups in the single settlements, and the range of average doses of the ecological units are discussed, because these are considered important criteria for the validity of the ecological study.

MATERIALS AND METHODS

The analysis presented here is based on registry data on thyroid cancer. To guarantee the privacy of the persons involved, the registry data were merged before analysis into groups of 2-year intervals of birth year and 2-year intervals of year of surgery. In total, the study uses data for 18,612 ecological units, which are defined by nine birth-year groups in the period 1968–1985, both genders, and 1034 study settlements (Fig. 1). For each of the ecological units, there are thyroid cancer data for six year-of-surgery groups in the period 1990–2001.

Dosimetry

Individual thyroid doses due to ^{131}I exposures were derived from measurements of the ^{131}I activity in the human thyroid that had been performed during the first few weeks after the Chernobyl accident. Short-lived radionuclides contributed less than 10% to the total thyroid dose (*15*). The doses were calculated as a product of the time-integrated activity in the thyroid, and a conversion factor, absorbed energy per ^{131}I decay and per thyroid mass (*16*).

Ukraine. Age-gender specific doses in 608 settlements were derived from a total of 75,313 individual dose estimates (*17*). Time-integrated activities in the thyroid were assumed to be the product of an average time-integrated activity in the settlement and age- and gender-dependent factors. Different factors were used for rural and urban areas. The 95% range of average age-gender specific thyroid doses was 0.014–0.33 Gy (Fig. 2). There were a few small settlements with considerably higher doses, up to 16 Gy for 1–2-year-old boys. Typically, the individual time-integrated activities within the ecological units (age-gender groups in the single settlements) had a coefficient of variation (CV) of 1.1, corresponding in a lognormal distribution to a geometric standard deviation (GSD) of 2.3. The spread of their distributions is a combined effect of the variability of the true individual doses and the uncertainties of the dose estimates.

Belarus, age-dependent doses. Previous estimates of individual thyroid dose estimates, based on measurements of the ^{131}I activity in the human thyroid (*13*), have been reviewed and improved (*18*). One main result of

this new analysis was that the ingestion pathway dominates the time dependence of the radioiodine intake not only for rural settlements but also for most of the inhabitants of the large cities Minsk and Gomel. Age-dependent thyroid doses were derived for 426 study settlements in Belarus based on 90,699 re-evaluated individual time-integrated activities. Typically, the individual time-integrated activities within the age groups of the single settlements had a CV of 1.2 (corresponding to a GSD of 2.6) (*19*). Uncertainty of the average integrated activities in the ecological units depends on the number and the quality of measurements in the settlement. It was assessed to correspond on average to a CV of 0.5 (GSD of 1.6). This value also applies to the dose estimates, because the uncertainty of the average value of the conversion factor is small compared to the uncertainties of the iodine measurements.

Belarus, age-gender dependent doses. Only estimates of gender-averaged doses were available for Belarus, so the following procedure was applied to estimate the gender specific doses. The gender-specific doses in Kyiv City (which was the Ukrainian city with the largest number of ^{131}I measurements) were used to derive gender-specific doses, $D_{s,i}^{city}$, for the birth cohort i in Minsk and Gomel City according to

$$D_{s,i}^{city} = D_{av,i}^{city} \cdot D_{s,i}^{K}/D_{av,i}^{K}, \quad \text{with} \tag{1}$$

$$D_{av,i}^{K} = (PY_{f,i}^{K}D_{f,i}^{K} + PY_{m,i}^{K}D_{m,i}^{K})/(PY_{f,i}^{K} + PY_{m,i}^{K}), \tag{2}$$

where PY is person-years, the index s can be either f for females or m for males, and the index K stands for Kyiv. In the same way, gender-specific doses for the rural settlements of Belarus were derived using the doses in Chernihiv Oblast (which was the Ukrainian oblast with the largest number of ^{131}I measurements). The 95% range of average age-gender specific doses in the 426 Belarusian study settlements was 0.025–1.11 Gy (Fig. 2). There were a few small settlements with considerably higher thyroid doses, of up to 18 Gy for 1–2-year-old boys.

Both countries. For settlements close to the boundary of the two countries, comparable values have been derived by the dosimetric approaches used for the two countries (Fig. 1). The distribution of the estimated individual doses within the ecological units was slightly wider in Belarus than in Ukraine because of a larger uncertainty of the measurements. The measurements in Ukraine were performed with collimators, which were less prone to error than the measurements taken without collimators for Belarus. Also, there were generally better measurement conditions in Ukraine (e.g., measurements were taken inside houses rather than outside, subjects were wearing clean clothes rather than contaminated ones, and subjects were asked to wash before measurements were taken). The 95% range of average age- and gender-specific thyroid doses in the 1034 settlements was 0.018–0.65 Gy (Fig. 2). The ratio of the two limiting percentiles of the range is 36 corresponding to a CV of 1.15 (GSD of 2.5) for a lognormal distribution.

Population

Ukraine. The age-gender structure according to the census data for 1989 and age-gender specific death rates were used to estimate the demographic structure in the study settlements in 1986 (*20, 21*). A linear interpolation of the census data for 1979 and 1989 gave similar results (*20, 22*), which was considered to be a confirmation of the method. Information on the total population in the study settlements in the years 1992–1994 was obtained from local authorities. Information on the population of the Ukrainian oblasts for 1991 and 1994 was received from the Ministry of Statistics of Ukraine (*23*). It was assumed that the number of inhabitants of each settlement changed during 1986–1994 proportionally to the changes in the whole rural/urban population of the oblast in which the settlement is located and that the age-gender structure also remained the same. In total, there were 997,000 children and adolescents in 1986 in the 18 age and gender groups of the 608 Ukrainian study settlements. Most of the children and adolescents (694,000) lived in Kyiv City.

Belarus. The derivation of the age-gender structure of the population in the Belarusian study settlements in 1986 is similar to the Ukrainian
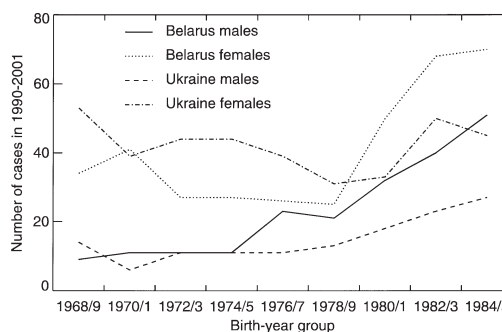
FIG. 3. Number of thyroid cancer cases in the period 1990–2001 in nine birth-year groups in the 608 Ukrainian and 426 Belarusian study settlements.

study settlements and has been described elsewhere (*24*). In total, there were 623,000 children and adolescents in 1986 in the 18 age and gender groups of the 426 study settlements. Most of the children and adolescents lived in either Minsk City (418,000) or Gomel City (132,000) at the time of the accident.

Both countries. The loss of follow-up during the period 1986 to 2001 was neglected because it was considered to be small compared to the other sources of uncertainties in the risk analysis. The loss of person-years due to death was relatively small because the members of the cohort were quite young during the period of observation. The loss of follow-up and cases due to migration was also considered to be small, because thyroid cancers of people who were exposed as children or adolescents by the Chernobyl accident and who underwent surgery in Belarus, Russia or Ukraine should be reported to the registry of the country where the person lived at the time of the accident. Migration to other countries has been neglected.

Thyroid Cancer Cases

Data on thyroid cancer cases in the period 1990–2001 for the birth cohort 1968–1985 were used. These data files contain the place of residence at the time of the accident for all cases. For some of the cases, only the year of birth was available; for this reason, only birth years were used for all cases here, and age at surgery is defined by the difference of the year of surgery and the birth year.

Ukraine. The clinical-morphological register at the Institute of Endocrinology and Metabolism of the Academy of Medical Sciences of Ukraine has been described elsewhere (*3*). According to the *Order of the Ministry of Public Health on the Improvement of Endocrinological Help to the Population* from 1992, all thyroid cancer cases among subjects who were up to 18 years old at the time of the Chernobyl accident and who were operated on in Ukraine must be reported to the register. The data were cross-checked with the Ukrainian Cancer Registry, and a few missing cases were added. For the 608 Ukrainian study settlements, 512 thyroid cancer cases were reported, 378 cases among females and 134 among males. There is no clear dependence of the cases among females on birth year (Fig. 3). For males, the incidence in the birth cohort 1984/1985 is larger than in the birth cohort 1968–1977 by a factor of 2.5. For both genders together, the incidence rate is 52 cases per 10^6 person-years for the youngest subjects (birth years 1982–1985), and about 40 cases per 10^6 person-years for the other birth-year groups. The ratio of female to male cases is about 2 for the younger subjects (1978–1985) and about 4 for the older subjects (birth years 1968–1977). There is a continuous increase of the incidence rate in the subsequent years (Fig. 4) compared to the first years after the accident. The screening of the Ukraine-American cohort started in 1998 (*25*). Up to the end of 2000, 43 cancer cases

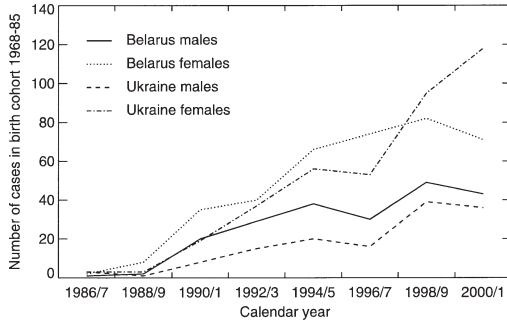**FIG. 4.** Number of thyroid cancer cases for nine calendar-year periods in the birth-year cohort 1968–1985 in the 608 Ukrainian and 426 Belarusian study settlements.

were detected, which contributed 20% to the number of cases in 1998–2000 in our 608 study settlements.

Belarus. A data exchange of the following three registers was performed, which resulted in consistent data sets in the registers:

1. The Belarusian State Chernobyl Register, which was established in 1993 according to a decree of the Council of Ministers of Belarus, containing data on liquidators and citizens of areas with ^{137}Cs contaminations exceeding 555 kBq m^{-2}.
2. The Belarusian Cancer Register, which was established in 1953 according to a directive from the Ministry of Public Health of the USSR. The register does not contain information about the place of residence at the time of the Chernobyl accident.
3. The medical history records of patients treated in the National Scientific and Practical Center of Thyroid Tumors in Minsk, where all thyroid cancers of Belarusian children are treated.

For the 426 Belarusian study settlements, 577 thyroid cancer cases have been reported, 368 cases among females and 209 among males. In contrast to the Ukrainian study settlements, the incidence among young subjects is considerably greater than for the older subjects (Fig. 3). The incidence rate is 133 cases per 10^6 person-years for the youngest (birth years 1984–1985), where this rate decreases initially with age at exposure and then has an approximately constant value of about 55 cases per 10^6 person-years for the birth-year cohorts of 1978–1969. The ratio of female to male cases is about 1.6 for the youngest subjects (1980–1985) and 1.2 for the birth-year cohort (1976–1979) and increases to 4 for the older subjects (birth years 1968–1971). As in Ukraine, the incidence rate increases continuously since the first years after the accident (Fig. 4).

Data Analysis

Poisson regressions were performed with EAR models,

$$\lambda(c, s, aae, age, d)$$
$$= \lambda_0(c, s, aae, age) + \alpha(c, s, aae, age, d), \quad (3)$$

and with ERR models

$$\lambda(c, s, aae, age, d)$$
$$= \lambda_0(c, s, aae, age)[1 + \alpha(c, s, aae, age, d)], \quad (4)$$

where λ is the total incidence rate, λ_0 the baseline incidence rate, α the EAR, β the ERR, c the country, s the gender, aae the age at exposure (birth year $-$ 1986), age the age attained (calendar year $-$ birth year), and d the thyroid dose. The baseline risk was modeled by

$$\lambda_0(c, s, aae, age)$$
$$= \exp[\eta_0 + \theta_c\eta_c + \eta_s\theta_s + \eta_{aae}(10 - aae) + \eta_{age}\ln(age/20)], \quad (5)$$

the EAR by

$$\alpha(c, s, aae, age, d)$$
$$= (\alpha_1 d + \alpha_2 d^2)\exp[\alpha_c\theta_c + \alpha_s\theta_s + \alpha_{aae}(10 - aae)$$
$$+ \alpha_{age}\ln(age/20)], \quad (6)$$

and the ERR by

$$\beta(c, s, aae, age, d)$$
$$= (\beta_1 d + \beta_2 d^2)\exp[\beta_c\theta_c + \beta_s\theta_s + \beta_{aae}(10 - aae)$$
$$+ \beta_{age}\ln(age/20)], \quad (7)$$

where $\alpha_{...}$, $\beta_{...}$ and $\eta_{...}$ are fit parameters, θ_c is -0.5 for Ukraine and 0.5 for Belarus, and θ_s is -0.5 for males and 0.5 for females.

The regressions were performed with the program AMFIT of the software package EPICURE (Hirosoft International Corporation, Seattle, WA). Results for subgroups were considered to be different if the 95% confidence range for the corresponding fit parameters did not include the value for equality.

RESULTS

Baseline Incidence Rate

The estimates of the baseline incidence rate in the EAR and the ERR models are nearly identical (Table 1). The central estimate of the baseline incidence rate is 14 cases per 10^6 PY. No significant difference is observed between the Ukrainian and the Belarusian settlements. The rate is assessed to be larger for females than for males by a factor of 5.9. For the same age attained, the baseline incidence rate in the year 2001 is estimated to be larger than in 1990 by a factor of 1.9. For fixed age at exposure, the rate increases with age attained to the power of 3.8 (Fig. 5). This increase is due to aging and to an improvement in case detection and reporting during the period of observation.

Excess Absolute Risk

The central estimate for the linear coefficient of the EAR dose dependence is 2.66 (95% CI: 2.19; 3.13) cases per 10^4 PY-Gy; for the quadratic coefficient, it is -0.145 (95% CI: -0.171; -0.119) cases per 10^4 PY-Gy^2 (Table 1). Thus the dose–response curve has a downward curvature for very high doses. The EAR is assessed to be higher in the Belarusian study settlements than in the Ukrainian settlements by a factor of 1.4 and higher for females than for males by a factor of 1.5.

For fixed attained age, EAR decreases with increasing *aae,* for a difference of 8 years in *aae* by a factor of 0.4 (Fig. 6, upper panel).

For fixed *aae,* EAR increases (a bit more than) proportionally with age attained. A non-parametric analysis indicates that the increase flattens with time after exposure (*26*). Models with quadratic terms in $\ln(age/20)$ in Eqs. (5) and (7), however, did not improve the quality of the fit.

TABLE 1
Best Estimates and 95% Confidence Intervals of Fit Parameters According to Equations (3–7)

	Excess absolute risk model		Excess relative risk model	
	Fit parameter	Value	Fit parameter	Value
Baseline incidence rate for age at exposure 10 and attained age 20	$\exp(\eta_0)$	14.0 (10.5; 18.7) $(10^6\ PY)^{-1}$	$\exp(\eta_0)$	14.0 (10.5; 18.6) $(10^6\ PY)^{-1}$
Ratio of baseline incidence rates in Belarusian and Ukrainian study settlements	$\exp(\eta_c)$	0.83 (0.64; 1.08)	$\exp(\eta_c)$	0.83 (0.63; 1.08)
Ratio of baseline incidence rates of females and of males	$\exp(\eta_s)$	5.93 (4.01; 8.77)	$\exp(\eta_s)$	5.97 (4.03; 8.84)
Slope of the logarithm of the baseline incidence rate with decreasing age at exposure[a]	η_{aae}	0.058 (0.010; 0.106) a^{-1}	η_{aae}	0.058 (0.010; 0.106) a^{-1}
Exponent of attained-age dependence of baseline incidence rate	η_{age}	3.76 (2.84; 4.69) a^{-1}	η_{age}	3.77 (2.84; 4.69) a^{-1}
Linear coefficient of dose response of excess risk	α_1	2.66 (2.19; 3.13) $(10^4\ PY\ Gy)^{-1}$	β_1	18.9 (11.1; 26.7) Gy^{-1}
Quadratic coefficient of dose response of excess risk	α_2	-0.145 $(-0.171;\ -0.119)$ $(10^4\ PY\ Gy^2)^{-1}$	β_2	-1.03 $(-1.46;\ -0.60)$ Gy^{-2}
Ratio of excess risks in Belarusian and Ukrainian study settlements with same dose	$\exp(\alpha_c)$	1.36 (1.12; 1.66)	$\exp(\beta_c)$	1.64 (1.14; 2.37)
Ratio of excess risks of females and of males for the same dose	$\exp(\alpha_s)$	1.55 (1.29; 1.86)	$\exp(\beta_s)$	0.260 (0.162; 0.415)
Slope of the logarithm of excess risk with decreasing age at exposure[b]	α_{aae}	0.106 (0.075; 0.137) a^{-1}	β_{aae}	0.048 (0.015; 0.111) a^{-1}
Exponent of attained-age dependence of excess risks	α_{age}	1.05 (0.71; 1.40) a^{-1}	β_{age}	-2.71 $(-3.76;\ -1.67)$ a^{-1}

[a] Equal to the slope of the logarithm of the baseline incidence rate with calendar year of observation.
[b] Equal to the slope of the logarithm of the excess risk with calendar year of observation.
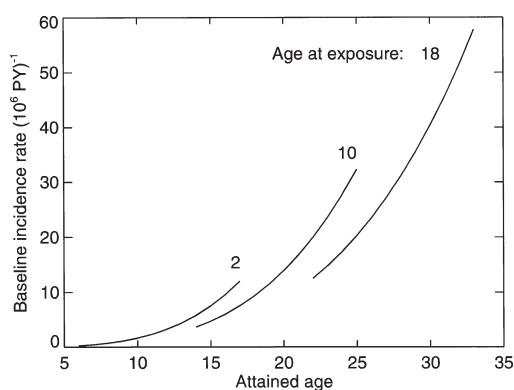
FIG. 5. Estimated baseline thyroid cancer incidence for different ages at exposure (birth year − 1986) in the 1034 study settlements.

Excess Relative Risk

The central estimate for the linear coefficient of the ERR dose dependence is 18.9 (95% CI: 11.1; 26.7) Gy^{-1}; for the quadratic coefficient, it is −1.03 (95% CI: −1.46; −0.60) Gy^{-2} (Table 1). The ERR is assessed to be higher in the Belarusian settlements than in the Ukrainian settlements by a factor of 1.6 and lower for females than for males by a factor of 3.8.

ERR depends mainly on age attained, with a small dependence on *aae* (Fig. 6, lower panel). In a period in which age attained doubles, ERR decreases by a factor of 6.5.

Results for Subpopulations

The numbers of baseline, excess and total cases predicted by the EAR and ERR models for the entire study population and for subgroups of the study population are similar (Table 2). For males in the Belarusian settlements, the ratio of excess to baseline cases, i.e. the excess relative risk, is estimated to be 8.5. For females in the Belarusian settlements and males in the Ukrainian settlements, it is about 2.2 and for females in the Ukrainian settlements 0.6.
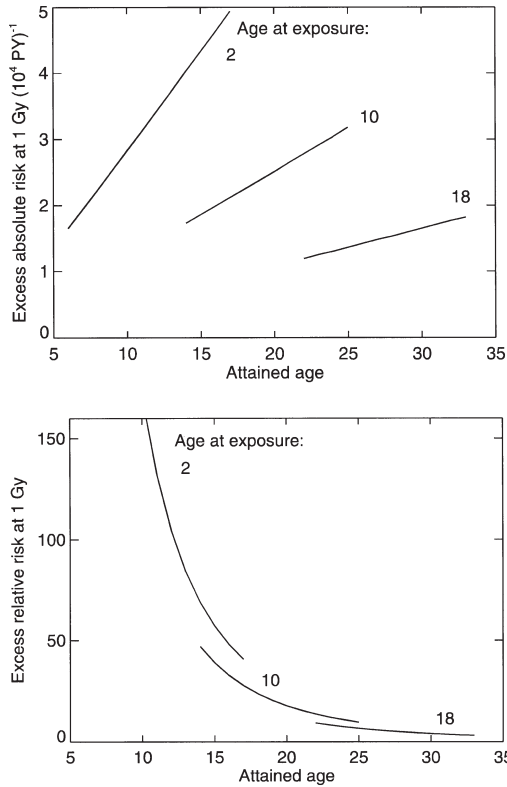
FIG. 6. Central estimate of EAR (upper panel) and of ERR (lower panel) after an exposure to 1 Gy for different ages at exposure (birth year − 1986) in the 1034 study settlements.

Separate risk analyses were performed in subpopulations. Best estimates of excess risks in towns with more than 10,000 children and adolescents and in the remaining smaller villages agree within 10% (results not shown).

DISCUSSION

Criteria for Quality Assessment of the Ecological Study

Average doses in the ecological units were estimated based on 166,012 individual dose estimates for persons with measurements of the ^{131}I activity in the thyroid. Thus, although the study is not based directly on individual dose estimates, there are on average nine individual dose estimates per ecological unit. There are 150 settlements with less than 18 individual dose estimates. Therefore, some ecological units have only one or even no individual dose estimate. The dose estimates for the ecological units, however, are based on at least 11 individual dose estimates and a generic age-gender dependence of the thyroid dose.

The range of average doses for the ecological units (GSD = 2.5) is larger than the uncertainty of the average dose in the ecological units (GSD = 1.6) and similar to the range of true individual doses within the ecological units (GSD of 2.1 to 2.6; see Appendix). Ideally, the range of average doses for the ecological units should exceed the other two ranges. The present study is close to fulfilling these conditions.

The major concern, that an ecological bias may exist in the present study, is due to an observed correlation of screening level and dose. Ecological studies have been simulated for four screening scenarios for thyroid cancer in settlements, in which the ^{131}I activity in the human thyroid was measured in May/June 1986 after the Chernobyl accident.[3] These simulations indicate that the ecological bias is small in the present study.

Dependence of Risk Estimates on Time after Exposure

In an earlier study (*27*) of Belarusian settlements with relatively good dosimetry, the EAR per dose was 2.8 (95% CI: 1.3; 6.0) cases per 10^4 PY-Gy for females and 1.7 (95% CI: 0.8; 3.6) cases per 10^4 PY-Gy for males in the period 1994–1996. This is in very good agreement with the results of the present work. In the birth-year cohort 1968–1985, the EAR increases and the ERR decreases with time after exposure. This is explained by a faster increase in the spontaneous thyroid cancer incidence than of the radiation-in-

TABLE 2
Baseline, Excess and Total Cases According to the EAR and ERR Models Compared with Observed Cases and Estimates of Average Dose

Cases	Model	Ukrainian settlements			Belarusian settlements			All settlements		
		Males	Females	Both	Males	Females	Both	Males	Females	All
Baseline	EAR	40.9	237.1	278.0	21.8	121.2	143.0	62.6	358.4	421.0
	ERR	40.7	238.1	278.8	21.7	122.0	143.7	62.4	360.1	422.5
Excess	EAR	97.8	136.2	234.0	185.1	249.3	434.4	282.9	385.5	668.4
	ERR	96.9	135.0	231.9	184.1	248.4	432.5	281.0	383.4	664.4
Total	EAR	138.7	373.3	512.0	206.8	370.6	577.4	345.5	743.9	1089.4
	ERR	137.6	373.1	510.7	205.7	370.5	576.2	343.3	743.6	1086.9
Observed cases		134	378	512	209	368	577	343	746	1089
Average dose (Gy)		0.083	0.075	0.079	0.189	0.171	0.180	0.124	0.112	0.118

duced incidence. The spontaneous thyroid cancer incidence increased due to the aging of the cohort and due to an increasing case detection and reporting rate.

The increase in the EAR with time after exposure occurs mainly before 1998 (26). It may be concluded that the additional cases detected in the cohort study (7), in which the screening started in 1998, have only a minor effect on the results of the present study. The continuing increase in the annual number of excess cases in the study settlements underlines the importance of longer-lasting studies of thyroid cancer in populations that have been exposed by the Chernobyl accident.

Dose Uncertainties

The risk analysis presented here does not take dose uncertainties into account. For a linear dose response and an additive classical error structure, an underestimation of the excess risk is expected if the dose uncertainty is neglected in the Poisson regression (28). This underestimation is expected to be small in the present analysis as indicated by the following two observations:

1. The dose uncertainty is small compared to the range of average doses used for the ecological units.
2. In an earlier analysis, calculations were performed that were similar from the methodological point of view to the present analysis (9). Results were compared with an independent method, a risk calculation with a Monte Carlo method, which took dose uncertainties into account. No large bias of the results was observed. Indeed, the EAR was found to be 10% higher in the Monte Carlo calculation than in the Poisson regression.

In summary, the bias on the risk estimates caused by neglecting the dose uncertainties in the analysis is not expected to be large. However, the confidence intervals are too small, and this should be kept in mind in the evaluation of the significance of differences discussed in the Results section.

Comparison with Risks after External Exposures

A pooled study of thyroid cancer after external exposures during childhood resulted in estimates of the EAR per dose of 4.4 (95% CI: 1.9; 10.1) cases per 10^4 PY-Gy and of the ERR per dose of 7.7 (95% CI: 2.1; 28.7) Gy^{-1} (14). The pooled study includes cohorts with observation times that extend to several decades after exposure. The observation period of the present study was 4 to 15 years after exposure. Results for the end of the observation period (central estimate for linear coefficient of EAR in 2001 is 3.4 cases per 10^4 PY-Gy and of ERR is 10.3 Gy^{-1}) are in good agreement with the results for external exposures.

APPENDIX

Combined Variability and Uncertainty of Estimated Individual Doses within the Ecological Units

The CV of the estimated time-integrated activities of the individuals within the ecological units has been estimated as 1.1 for Ukraine and 1.2

for Belarus. The variability of the dose factor that relates the time-integrated activity and the thyroid dose has been estimated to correspond to a GSD of 1.8 (29). Assuming a lognormal distribution of the dose factor, error propagation leads to a CV in the range of 1.4–1.6 for the estimated individual doses within the ecological units.

Variability of True Individual Doses within the Ecological Units

Main factors influencing the variability of true individual doses of a group of given age and gender in a study settlement are the variability in the thyroid mass, the ^{131}I concentration in milk, and the rate of consumption of contaminated milk.

Typically, these factors can be described by lognormal distributions with GSDs of 1.8, 1.3–1.8 and 1.6, respectively (15). Combination of these three sources of variability leads to distribution for the true doses with GSDs of 2.1 to 2.6, or coefficients of variability (CV) of 0.9 to 1.2. This is consistent with the range of estimated individual thyroid doses within the ecological units (see above), since the latter distribution is broadened by the uncertainties of the individual dose estimates.

REFERENCES

1. V. S. Kazakov, E. P. Demidchik and L. N. Astakova, Thyroid cancer after Chernobyl. *Nature* **359**, 21 (1992).
2. I. A. Likhtarev, B. G. Sobolev, I. A. Kairo, N. D. Tronko, T. I. Bogdanova, V. A. Oleinic, E. V. Epshtein and V. Beral, Thyroid cancer in the Ukraine. *Nature* **375**, 365 (1995).
3. M. D. Tronko, T. I. Bogdanova, I. V. Komisarenko, O. V. Epshtein, I. A. Likhtaryov, V. V. Markov, V. A. Oliynyk, V. P. Tereshchenko, V. M. Shpak and P. Voillequé, Thyroid carcinoma in children and adolescents in Ukraine after the Chernobyl accident: statistical data and clinicomorphologic characteristics. *Cancer* **86**, 149–156 (1999).
4. Y. E. Demidchik and E. P. Demidchik, Thyroid carcinomas in Belarus 16 years after the Chernobyl disaster. In *Proceedings of Symposium on Chernobyl-Related Health Effects,* pp. 66–77. Radiation Effects Association, Tokyo, 2002.
5. L. N. Astakhova, L. R. Anspaugh, G. W. Beebe, A. Bouville, V. V. Drozdovitch, V. Garber, A. I. Gavrilin, V. T. Khrouch, A. V. Kuvshinnikov and M. A. Waclawiw, Chernobyl-related thyroid cancer in children of Belarus. *Radiat. Res.* **150**, 349–356 (1998).
6. S. Davis, V. Stepanenko, N. Rivkind, K. J. Kopecky, P. Voillequé, V. Shakhtarin, E. Parshkov, S. Kulikov, E. Lushnikov and M. A. Waclawiw, Risk of thyroid cancer in the Bryansk Oblast of the Russian Federation after the Chernobyl power station accident. *Radiat. Res.* **162**, 241–248 (2004).
7. V. A. Stezhko, E. E. Buglova, L. I. Danilova, V. M. Drozd, N. A. Krysenko, N. R. Lesnikova, V. F. Minenko, V. A. Ostapenko, S. V. Petrenko and L. B. Zablotska, A cohort study of thyroid cancer and other thyroid diseases after the Chornobyl accident: Objectives, design and methods. *Radiat. Res.* **161**, 481–492 (2004).
8. P. Jacob, G. Goulko, W. Heidenreich, I. Likhtarev, I. Kairo, N. D. Tronko, T. I. Bogdanova, J. Kenigsberg, E. Buglova and V. Beral, Thyroid cancer risk to children estimated. *Nature* **392**, 31–32 (1998).
9. P. Jacob, Y. Kenigsberg, I. Zvonova, G. Goulko, E. Buglova, W. F. Heidenreich, A. Golovneva, A. A. Bratilova, V. Drozdovitch and H. G. Paretzke, Childhood exposure due to the Chernobyl accident and thyroid cancer risk in contaminated areas of Belarus and Russia. *Br. J. Cancer* **80**, 1461–1469 (1999).
10. H. Morgenstern, Ecologic studies. In *Modern Epidemiology* (K. J.

Rothman and S. Greenland, Eds.), pp. 459–480. Lippincott-Raven, Philadelphia, 1998.

11. J. H. Lubin, The potential for bias in Cohen's ecological analysis of lung cancer and residential radon. *J. Radiol. Prot.* **22**, 141–148 (2002).

12. I. A. Likhtariov, N. K. Shandala, G. M. Gulko, I. A. Kairo and N. I. Chepurnoy, Exposure doses to thyroid of the Ukrainian population after the Chernobyl accident. *Health Phys.* **64**, 594–599 (1993).

13. Y. I. Gavrilin, V. T. Khrouch, S. M. Shinkarev, N. A. Krysenko, A. M. Skryabin, A. Bouville and L. R. Anspaugh, Chernobyl accident: Reconstruction of thyroid dose for inhabitants of the Republic of Belarus. *Health Phys.* **76**, 105–119 (1999).

14. E. Ron, J. H. Lubin, R. E. Shore, K. Mabuchi, B. Modan, L. M. Pottern, A. B. Schneider, M. A. Tucker and J. D. Boice, Thyroid cancer after exposures to external radiation: A pooled analysis of seven studies. *Radiat. Res.* **141**, 259–277 (1995).

15. Y. Gavrilin, V. Khrouch, S. Shinkarev, V. Drozdovitch, V. Minenko, E. Shemiakina, A. Ulanovsky, A. Bouville, L. Anspaugh and N. Luckyanov, Individual dose estimation for a case-control study of Chernobyl-related thyroid cancer among children of Belarus. Part I: ^{131}I, short-lived radioiodines (^{132}I, ^{133}I, ^{135}I), and short-lived radiotelluriums (^{131m}Te and ^{132}Te). *Health Phys.* **86**, 565–585 (2004).

16. ICRP, *Age-Dependent Doses to Members of the Public from Intake of Radionuclides: Part 1. Ingestion Dose Coefficients.* Publication 56, *Annals of the ICRP,* Vol. 20, No. 2, Pergamon Press, Oxford, 1990.

17. I. Likhtarov, L. Kovgan, S. Vavilov, M. Chepurny, A. Bouville, N. Luckyanov, P. Jacob, P. Voillequé and G. Voigt, Post-Chernobyl thyroid cancer in Ukraine. Report 1: Estimation of thyroid doses. *Radiat. Res.* **163**, 125–136 (2005)..

18. S. Shinkarev and Y. Gavrilin, Post-Chernobyl thyroid doses in Belarus based on measurements of the ^{131}I activity in the human thyroid and on the semi-empirical model. In *Thyroid Exposure of Belarusian and Ukrainian Children due the Chernobyl Accident and Resulting Thyroid Cancer Risk.* GSF-Bericht 01/05, ISSN 0721-1694. GSF National Research Center for Environment and Health, Neuherberg, Germany, 2005.

19. R. Meckbach, S. Shinkarev, A. Ulanovsky and P. Jacob, Post-Chernobyl thyroid doses in Belarus based on measurements of the ^{131}I activity in the human thyroid and on a factorisation method. In *Thy-roid Exposure of Belarusian and Ukrainian Children due the Chernobyl Accident and Resulting Thyroid Cancer Risk.* GSF-Bericht 01/05, ISSN 0721-1694, GSF National Research Center for Environment and Health, Neuherberg, Germany 2005.

20. Ministry of Statistics of Ukrainian SSR, *Population age-gender structure of Ukrainian SSR at 12 January 1989 (According to All-Union Census of 1989).* Kyiv, 1991. [in Ukrainian]

21. Technika, *National Economy of Ukrainian SSR in the Year 1990.* Kyiv, 1990. [in Ukrainian]

22. USSR State Committee, *Summary of All Union Census of the Year 1979.* Moscow, 1989. [in Russian]

23. Statistics State Committee of Ukraine, *Population of Ukraine in 1996. Demography reference book.* Kyiv, 1997. [in Ukrainian]

24. J. Kenigsberg, E. Buglova, J. Kruk and E. Ulanovskaya, Chernobyl-related thyroid cancer in Belarus: Dose and risk assessment. In *Proceedings of Symposium on Chernobyl-Related Health Effects,* pp. 26–42. Radiation Effects Association, Tokyo, 2002.

25. N. D. Tronko, O. O. Bobylyova, T. I. Bogdanova, O. V. Epshtein, I. A. Likhtaryov, V. V. Markov, V. A. Oliynyk, V. P. Tereshchenko, V. M. Shpak and P. Voillequé, Thyroid gland and radiation (Ukrainian-American Thyroid Project). In *Radiation and Humankind* (Y. Shibata, S. Yamashito and M. Watanabe, Eds.), pp. 91–104. International Congress Series 1258, Elsevier, Amsterdam, 2003.

26. P. Jacob, J. Kenigsberg, S. Vavilov, M. Tronko, C. Schotola, S. Shinkarev, E. Buglova, M. Chepurniy, R. Meckbach and A. Ulanovski, Thyroid cancer risk in Ukrainian and Belarusian areas affected by the Chernobyl accident. In *Thyroid Exposure of Belarusian and Ukrainian Children due to the Chernobyl Accident and Resulting Thyroid Cancer Risk.* GSF-Bericht 01/05, ISSN 0721-1694, GSF—National Research Center for Environment and Health, Neuherberg, Germany, 2005.

27. P. Jacob, Y. Kenigsberg, G. Goulko, E. Buglova, F. Gering, A. Golovneva, J. Kruk and E. P. Demidchik, Thyroid cancer risk in Belarus after the Chernobyl accident: Comparison with external exposures. *Radiat. Environ. Biophys.* **39**, 25–31 (2000).

28. R. J. Caroll, D. Ruppert and L. A. Stefanski, *Measurement Error in Nonlinear Models.* Chapman & Hall/CRC, Boca Raton, FL, 1995.

29. ICRP, *Basic Anatomical and Physiological Data for Use in Radiological Protection*: *Reference Values.* Publication 89, International Commission on Radiological Protection, Pergamon, Oxford, 2003.

15. Hornhardt S, Gomolka M, Walsh L & Jung T. Comparative investigations of sodium arsenate, arsenic trioxide and cadmium sulphate in combination with gamma-radiation on apoptosis, micronuclei induction and DNA damage in a human lymphoblastoid cell line. Mutation Res. 600, 165-176, 2006

Comparative investigations of sodium arsenite, arsenic trioxide and cadmium sulphate in combination with gamma-radiation on apoptosis, micronuclei induction and DNA damage in a human lymphoblastoid cell line

Sabine Hornhardt [a,*], Maria Gomolka [a], Linda Walsh [b], Thomas Jung [a]

[a] *BfS-Federal Office for Radiation Protection, Department of Radiation Protection and Health, Ingolstädter Landstr. 1, 85764 Oberschleißheim, Germany*
[b] *GSF-National Research Center for Environment and Health, Ingolstädter Landstraße 1, D-85764 Neuherberg, Germany*

Abstract

In the field of radiation protection the combined exposure to radiation and other toxic agents is recognised as an important research area. To elucidate the basic mechanisms of simultaneous exposure, the interaction of the carcinogens and environmental toxicants cadmium and two arsenic compounds, arsenite and arsenic trioxide, in combination with gamma-radiation in human lymphoblastoid cells (TK6) were investigated. Gamma-radiation induced significant genotoxic effects such as micronuclei formation, DNA damage and apoptosis, whereas arsenic and cadmium had no significant effect on these indicators of cellular damage at non-toxic concentrations. However, in combination with gamma-radiation arsenic trioxide induced a more than additive apoptotic rate compared to the sum of the single effects. Here, the level of apoptotic cells was increased, in a dose-dependent way, up to two-fold compared to the irradiated control cells. Arsenite did not induce a significant additive effect at any of the concentrations or radiation doses tested. On the other hand, arsenic trioxide was less effective than arsenite in the induction of DNA protein cross-links. These data indicate that the two arsenic compounds interact through different pathways in the cell. Cadmium sulphate, like arsenite, had no significant effect on apoptosis in combination with gamma-radiation at low concentrations and, at high concentrations, even reduced the radiation-induced apoptosis. An additive effect on micronuclei induction was observed with 1 μM cadmium sulphate with an increase of up to 80% compared to the irradiated control cells. Toxic concentrations of cadmium and arsenic trioxide seemed to reduce micronuclei induction.

The results presented here indicate that relatively low concentrations of arsenic and cadmium, close to those occuring in nature, may interfere with radiation effects. Differences in action of the two arsenic compounds were identified.
© 2006 Elsevier B.V. All rights reserved.

Keywords: Arsenic; Cadmium; Gamma-radiation; Combined effects; Human TK6 lymphoblastoid cells

1. Introduction

Combined human exposure to environmental toxicants such as heavy metals and arsenic is frequently due to their ubiquity, wide use in industry and persistence in the environment. Many of these compounds are toxic, mutagenic and/or carcinogenic.

Arsenic is one of the most frequent, globally occurring, environmental toxins [1]. Although arsenicals are, if at all, only weak mutagenic in bacterial and mammalian test systems, epidemiological studies have clearly identified arsenic as a carcinogen to humans [1,2]. Arsenic acts on cells through a variety of mechanisms, influencing numerous signal transduction pathways and resulting in a vast range of cellular effects that include apoptosis, growth inhibition, promotion or inhibition of differentiation and angiogenesis [3,4]. Arsenic-induced responses vary depending on cell type, dose and its chemical form. Arsenic trioxide was detected as an active compound in an ancient Chinese therapy for leukemia and is currently under review in clinical approval process [5].

Cadmium is an important heavy metal environmental toxicant, also classified as a weakly mutagenic human carcinogen [6], and it has been related to several human carcinomas such as lung cancer, or prostate and renal cancer [6,7]. As in the case of arsenic, the mechanism of cadmium action is not clear, however, a competitive reaction with zinc has been shown. It is well known that cadmium affects cell proliferation, differentiation, apoptosis and other cellular activities such as antioxidative reactions and DNA repair [7].

Generally, ionising radiation arising from environmental and controlled occupational exposure situations contributes only to a small fraction of the life-long attack on DNA by genotoxins with exceptions such as areas with elevated naturally occurring radioactive materials [8]. For example, radon migrates from soils and rocks and accumulates in enclosed areas, such as underground mines and homes [9]. Especially in these elevated exposure situations, combined effects with other environmental toxins, such as arsenic or heavy metals, may be relevant [10]. To date it is well established that inorganic arsenic is causally associated with lung cancer via inhalation. Cohort studies of uranium miners on lung cancer [10,11] give some evidence that arsenic might interfere with radiation effects. However, the efforts so far to assess and quantify effects of radiation in vivo seldom take into account the concomitant presence of other toxins. These combined exposure situations may lead to health risk effects with a multiplicative or synergistic outcome differing from those expected by simply adding the effects of the single noxes [12]. The existing data are rudimentary and hardly give sufficient estimates of the present day low exposure situations [13].

In this study the effects of gamma-radiation together with the environmental contaminants cadmium, arsenic trioxide and arsenite on human lymphoblastoid cells were investigated. Important indicators of cellular damage such as: (i) apoptosis playing an important role in the elimination of damaged cells, (ii) genotoxicity measured by DNA damage induction using the comet assay and micronuclei formation and (iii) DNA repair investigated with the comet assay were examined. Radiation doses applied in this study were close to the detection limit of the damage indicators tested. In order to mimic the in vivo situation the cadmium and arsenic concentrations were kept close to naturally occurring concentrations.

2. Materials and methods

2.1. Cell culture

Frozen TK6 human lymphoblastoid cells from the same batch were thawed for each experiment and cultivated in RPMI 1640 medium (Biochrom, Germany) supplemented with 10% fetal calf serum, 1% sodium pyruvate [113-24-6] and 1% non-essential amino acids (Promocell, Germany). The suspension cultures were seeded at a concentration of 3×10^5 cells/ml and maintained in tissue culture flasks in a humidified incubator at $37\,^\circ C$ with 5% CO_2. Asynchronous cultures in the exponential phase of growth were used in all experiments. Dilutions $(0.1–10\,\mu M)$ were made from the stock solution of 0.01 M sodium arsenite ([7784-46-5], Fluka, Switzerland) or arsenic trioxide ([1327-53-3], Sigma–Aldrich, Germany) and 0.03 M cadmium sulphate ([10124-36-4], Fluka, Switzerland).

2.2. Cellular toxicity

Cytotoxicity was determined by the trypan blue ([72-57-1], Seramed, Germany) exclusion assay. After incubation of the cells for 24 h in arsenic or cadmium containing medium a sample of the culture was mixed with 0.1% trypan blue (dye:medium = 1:6) and viable cells were counted in a Neubauer chamber under a light microscope.

2.3. Cellular uptake of arsenic and cadmium

Cellular uptake of metals was determined by inductively coupled plasma (ICP)-emission spectroscopy according to Schramel et al. [14]. Exponentially growing cells were incubated for 22 h in a metal containing medium, washed three times in PBS (Biochrom, Germany), counted and samples of 3×10^6 cells together with the metal stock solution used were analysed (Dr. P. Schramel, GSF-Research Center, Germany). Concentrations of the stock solutions were determined to be 0.0311 for 0.03 M cadmium and 0.0095 for 0.01 M arsenite, respectively.

2.4. Irradiation

For apoptosis and micronuclei assays cell cultures were irradiated in cell culture flasks at room temperature with ^{137}Cs-gamma-rays (69 cGy/min; HWM-2000, Markdorf, Germany) using single doses of 1–4, 6 or 8 Gy in air. For the comet assay cells were incubated for 22 h in arsenic or cadmium containing medium, adjusted to a number of 30 000 cells per slide in 10 μl serum-free medium, then irradiated on ice in Eppendorf tubes with a single dose of 1 or 2 Gy and kept on ice until required.

2.5. Apoptosis assay

Apoptotic cells were determined with the APO2.7 antibody (Beckman Coulter Corporation, Germany) directed against the mitochondrial protein APO2.7, which is expressed specifically during apoptosis [15]. Exponentially growing TK6 cells were set in fresh medium supplemented with arsenic or cadmium (0.1–10 μM) and immediately gamma-irradiated (1, 2 or 4 Gy as single dose) and then incubated for 24 h. In each experiment samples without chemical supplement, with arsenite, arsenic trioxide or cadmium sulphate with or without irradiation were tested. About $0.5–1 \times 10^6$ TK6 cells per sample were permeabilized in 100 μl of digitonin solution ([11024-24-1], 12.5 mg/ml PBS), incubated on ice for 20 min, then washed twice in 2 ml PBSF. The cell pellet was mixed gently with 20 μl APO2.7 staining-solution and 80 μl FCS. After 15 min incubation at room temperature in the dark, cells were washed and finally mixed with 250–750 μl PBSF and stored on ice until measured with a Coulter EPICS-XL flow cytometer (Beckman Coulter Corporation, Germany). Bivariate plots of forward (FS) and sideward scatter (SS), SS and Apo2.7-phycoerythrin (logarithmic) signal distribution of cells were recorded to gate and calculate the apoptotic cell fraction.

2.6. Micronucleus assay

Micronuclei induction was determined by flow cytometry according to Nüsse et al. [16]. TK6 cells were seeded in arsenic or cadmium (0.1–10 μM) containing medium and immediately gamma-irradiated (1 or 3 Gy). For each experiment cell cultures without chemical supplement or with arsenite, arsenic trioxide or cadmium sulphate with or without irradiation were set up. After incubation of the cultures for 24 h about 10^6 exponentially growing cells were centrifuged and resuspended with 50–100 μl of the supernatant. The cell suspension was mixed with 1 ml of solution I containing 584 mg/l sodium chloride [7647-14-5], 1 g/l sodium citrate [68-04-2], 10 mg/l RNAse A from bovine pancreas (Merck, Germany), 0.3 ml/l Nonidet P-40 (Merck, Germany) and 10 μg/ml propidium iodide ([25535-16-4], Sigma–Aldrich, Germany). After incubation for 1 h at room temperature in the dark 1 ml of solution II (15 g/l citric acid ([77-92-9], Merck, Germany), 0.25 M sucrose ([57-50-1], Alpha-Aersar, Germany)) containing 10 μg/ml propidium

iodide was added and the suspension analysed with the flow cytometer. The analysis protocol determined the micronuclei due to size of stained DNA-containing particles.

2.7. Comet assay (single cell gel electrophoresis)

The procedure of Singh et al. [17] with minor modifications [18], was applied. Special microscopic slides (ESW-370; Erie Scientific, Portsmouth, NH) were pre-coated with 200 μl of 0.1% low-melting agarose [9012-36-6] (Sigma–Aldrich, Germany). About 10 μl of approximately 30 000 cells in serum-free RPMI-medium were mixed with 100 μl of 0.5% warm agarose (Amresco, Solon OH, USA) at 50 °C and then transferred immediately onto a pre-warmed pre-coated slide. A cover slip was placed over the agarose prior to chilling the slide for 5 min at 0 °C on a cooling plate. The microscope slides without cover slip were immersed in cold lysis buffer I (2.5 M NaCl, 100 mM Na-EDTA [60-00-4], pH 10, 10 mM Tris–HCl [1185-53-1], pH 10, and 1% SLS [151-21-3], 1% Triton X-100 [9002-93-1]) over night, followed by the second lysis in buffer II (2.5 M NaCl, 100 mM Na-EDTA pH 10, 10 mM Tris–HCl, pH 10) for 1 h, at 37 °C. About 20 min unwinding was performed in the electrophoresis chamber (Amersham Pharmacia HE100 Supersub) in electrophoresis buffer (300 mM NaOH [1310-73-2], 2% DMSO [67-68-5], and 10 mM Na-EDTA; pH > 13). Temperature during electrophoresis (0.4 V/cm; 300 mA; 60 min) was kept constant at 20 °C. After electrophoresis, the DNA was precipitated and fixed by incubation in 1% ammonium acetate [631-61-8] in ethanol [64-17-5] for 30 min at room temperature. After dehydration in 100% ethanol overnight, the slides were rehydrated with 70% ethanol for 5 min, air-dried and stored at room temperature. For staining, each slide was treated with 50 μl prestain-solution (5% DMSO, 5% sucrose, 10 mM NaH$_2$PO$_4$ [7558-80-7]) and then with 50 μl staining-solution containing 1 μl YOYO (Molecular Probes, Eugene OR, USA) in 1 ml H$_2$O, 5% DMSO, 20% Vectashield anti-fading (Vector Laboratories, Burlingame, USA). If not further indicated all reagents used were from Merck, Germany. After incubation at 4 °C for 2 days, the slides were evaluated under a Fluovert FU microscope (Leica, Germany) with a 40-fold magnification. Fluorescence images were acquired with a Sofcam Sensor Camera (itm) and 60 comets per slide were evaluated with VISCOM software (Impuls GmbH, Germany).

DNA protein cross-links were determined according to Merk and Speit [19]. After lysis, slides were washed three times in TE-buffer (100 μM Tris, 5 μM EDTA, pH 10), then covered with 100 μl proteinase K-solution (1 mg/ml TE, Sigma–Aldrich, Germany) and a cover slip, before incubation for 2 h at 37 °C. Control slides were incubated with 100 μl TE-buffer. After removing the cover slip, slides were processed as described above.

For DNA repair studies cells were incubated for time intervals of 30–90 min at 37 °C directly after treatment.

Statistical evaluation of the comet data (percent DNA in tail of 60 cells per slide, two parallel slides of three independent experiments) was performed with STATISTICA software

(StatSoft GmbH, Europe). Since DNA damage data (%DNA in tail) are not normally distributed, data were tested for statistical significance by U-test analysis.

3. Results

3.1. Cytotoxicity and intracellular concentrations of arsenic and cadmium

Toxicity of the compounds sodium arsenite, arsenic trioxide and cadmium sulphate in TK6 cells was examined to determine the highest non-toxic concentration on the induction of apoptosis, micronuclei and DNA damage. Cell viability was tested after 24 h with concentrations between 0.1 and 1000 μM (10^{-7} and 10^{-3} M) of arsenic or cadmium in cell culture medium (Fig. 1).
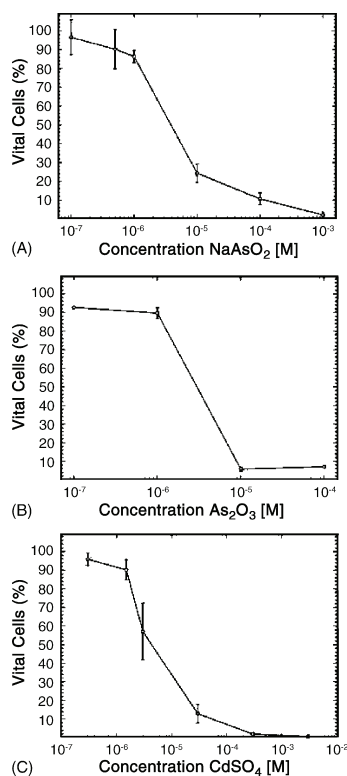
Fig. 1. Cytotoxicity of sodium arsenite (A), sodium trioxide (B) and cadmium sulphate (C). Viability determined by trypan blue exclusion assay after 24 h.

LD50 was determined between 3 and 4 μM for all compounds. For further experiments the concentration range between 0 and 10 μM ($0–10^{-5}$ M) was chosen.

Intracellular concentration of the test compounds sodium arsenite and cadmium sulphate was determined by ICP emission spectroscopy in samples of 3×10^6 cells after 22 h. In medium containing 0.1 μM arsenite the intracellular arsenic concentration in TK6 cells was increased to 849 ng/l (3.3 nmol/10^6 cells) compared to 105 ng/l in control cells incubated in medium not supplemented with arsenic or cadmium; in medium containing 1 μM arsenite the intracellular concentration was 7875 ng/l (34.3 nmol/10^6 cells). Intracellular cadmium concentration was 34.5 μg/l (15.9 nmol/10^6 cells) in 0.3 μM cadmium containing medium, 48.5 μg/l (22.2 nmol/10^6 cells) in 3 μM cadmium containing medium compared to 11 μg/l in control cells grown in medium not supplemented with cadmium.

3.2. Apoptosis

After irradiation and incubation for 24 h TK6 cells showed, in the dose range of 0–8 Gy, a linear dose effect relationship for apoptosis (Fig. 2). The apoptotic level of $16.6 \pm 3.8\%$ after 4 Gy irradiation found here is in good agreement with the apoptotic level in TK6 cells based

Fig. 2. The mean percentage induction of apoptosis after gamma-irradiation. Data points and their associated standard error of the mean are illustrated and the broken line represents the weighted least squares best fit: mean apoptosis (%) = $(3.65 \pm 0.32) \times$ dose (Gy) + (3.62 ± 0.27), given here with standard errors for the fit parameters. If the linear representation is replaced by a second degree polynomial fit in dose, the parameter multiplying the quadratic term in dose is insignificantly small (0.01 ± 0.17).
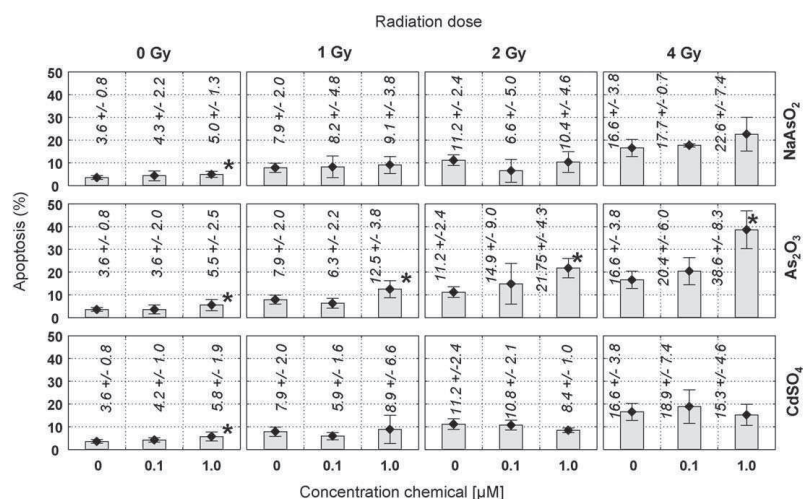
Fig. 3. Induction of apoptotic cells determined 24 h after combined treatment with the APO2.7 assay. Each data point (bars and diamonds) represents the mean of at least three independent experiments, error bars indicate the standard deviation, *significant deviation ($p < 0.05$, T-test) from control ($0 \mu M \pm$ irradiation).

on sub-G1 DNA content after 4 Gy gamma-irradiation [20].

Induction of apoptosis by arsenic or cadmium alone was comparatively low but dose-dependent (Fig. 3). A $10 \mu M$ concentration of arsenic or cadmium induced a very high percentage of dead cells (60–80%, data not shown). However, at this concentration it was not possible to differentiate between apoptotic and necrotic cell populations due to toxicity.

Arsenite alone, at concentrations of $1 \mu M$ or higher (not shown), caused a significant apoptotic effect in TK6 cells (Fig. 3). In combination with radiation, no significant additive effect was observed. Arsenic trioxide produced a similar small increase in apoptosis as arsenite, but interestingly, in combination with irradiation, the concentration of $1 \mu M$ arsenic trioxide resulted in an elevated level of apoptotic cells that was higher than the sum of the radiation effect and arsenic effect alone. The relative increase was 40% at 1 Gy compared to the radiation effect alone, but raised further to 90% and 130% at 2 and 4 Gy, respectively. Similar to arsenite, the effect of cadmium on apoptosis induction was only small. Also in combination with irradiation no significant additive effect was observed. In combination with 2 and 4 Gy cadmium even reduced the number of apoptotic cells (Fig. 3). This effect might be due to increasing toxicity of the combination or an inhibition of proliferation.

3.3. Micronuclei

After treatment with arsenic or cadmium and/or gamma-radiation TK6 cells were measured by flow cytometry for micronuclei induction. Micronucleation due to radiation was measured up to 8 Gy with a dose-dependent maximal amount of about 40% micronuclei compared to non-irradiated cells (Fig. 4). The best weighted least squares fit to the data in Fig. 4 is linear and the fit function is quoted in the caption of Fig. 4. The addition of a quadratic term to the weighted least squares fit does not lead to a significant improvement in the goodness of fit. On the other hand an unweighted least squares linear quadratic fit (also quoted in the caption of Fig. 4) to the data does follow the trends in the data at 6 and 8 Gy very well. In the unweighted case a linear quadratic fit has a lower χ^2-value than a linear fit. Therefore the question becomes one of whether the unanimous nature of the data up to 4 Gy (which indicate a linear dose–response) is more important than the rather inexact trends in the data at 6 and 8 Gy (which indicate a linear quadratic dose–response) which might reflect the toxicity of the irradiation doses.
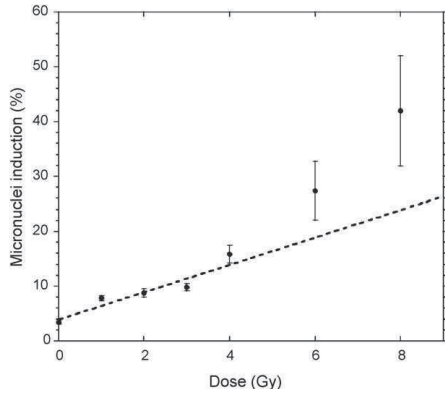
Fig. 4. The mean percentage of micronuclei induction after gamma-irradiation alone. Data points and their associated standard errors of the mean are illustrated and the broken line represents the weighted least squares best fit: mean micronuclei induction (%) = $(2.50 \pm 0.21) \times$ dose (Gy) + $(3.9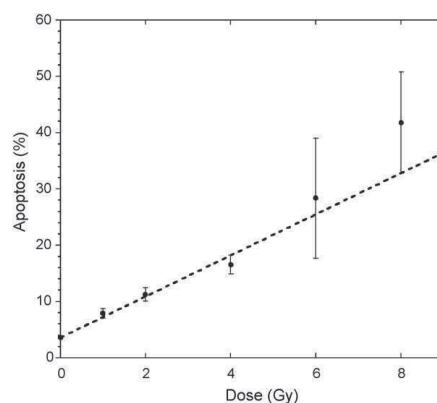4 \pm 0.35)$, with standard errors for the fit parameters. If the linear representation is replaced by a second degree polynomial fit in dose, the parameter multiplying the quadratic term in dose is insignificantly small (0.06 ± 0.14). The best UNWEIGHTED fit (not plotted) is: $(4.54 \pm 1.21) + (0.92 \pm 0.74) \times$ dose + $(0.47 \pm 0.09) \times$ dose_squared.

Sodium arsenite and arsenic trioxide had no significant effect on micronuclei induction in the non-toxic dose range from 0.1 to 1 μM (Fig. 5), while the toxic concentration of 10 μM arsenic caused a five- to eight-fold induction in micronuclei formation. However, at this high concentration it was difficult to distinguish between the micronuclei and necrotic cell fragments due to toxicity. A significant additive effect with non-toxic arsenite concentration (1 μM) could only be observed in combination with 3 Gy irradiation. This effect seemed to be even more than additive with arsenic trioxide. However, at 10 μM, the two arsenic compounds showed different reactions: whereas the micronucleation after arsenite treatment was further strongly increased, the effect with arsenic trioxide showed no further increase of the micronuclei level.

Similar to the arsenic compounds cadmium displayed a slight dose-dependent increase in micronuclei induction from 0.6% to 4.1% by 0.1–10 μM cadmium sulphate, respectively (Fig. 5). Interestingly, the combination of 1 μM cadmium and 1 Gy gamma-dose showed a more than additive increase of 80% in micronucleation (Fig. 5). This effect was less pronounced at 3 Gy. The combined treatment with 10 μM cadmium and radiation doses of 1 or 3 Gy resulted in a decrease in micronucleation.
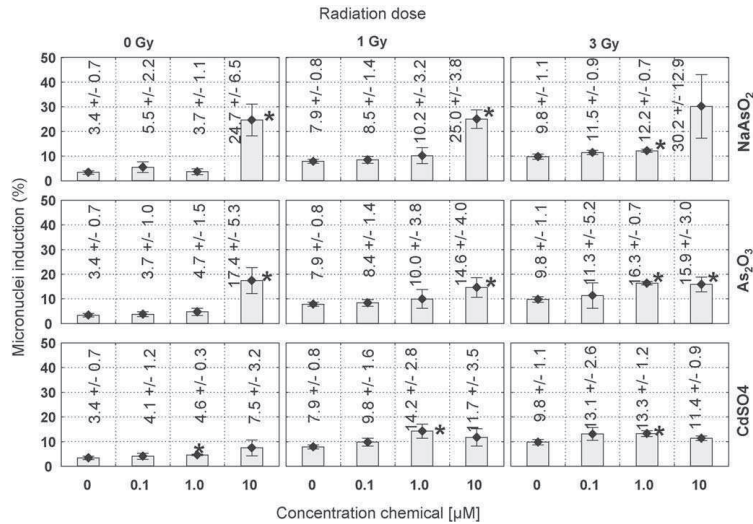
Fig. 5. Induction of micronuclei after combined treatment of different concentrations of arsenite, arsenic trioxide and cadmium sulphate with gamma-radiation doses 0, 1, and 3 Gy. Each data point (bar and diamond) represents the mean of at least three independent experiments, error bars indicate the standard deviation; *significant deviation ($p < 0.05$, T-test) from control (0 μM ± irradiation).
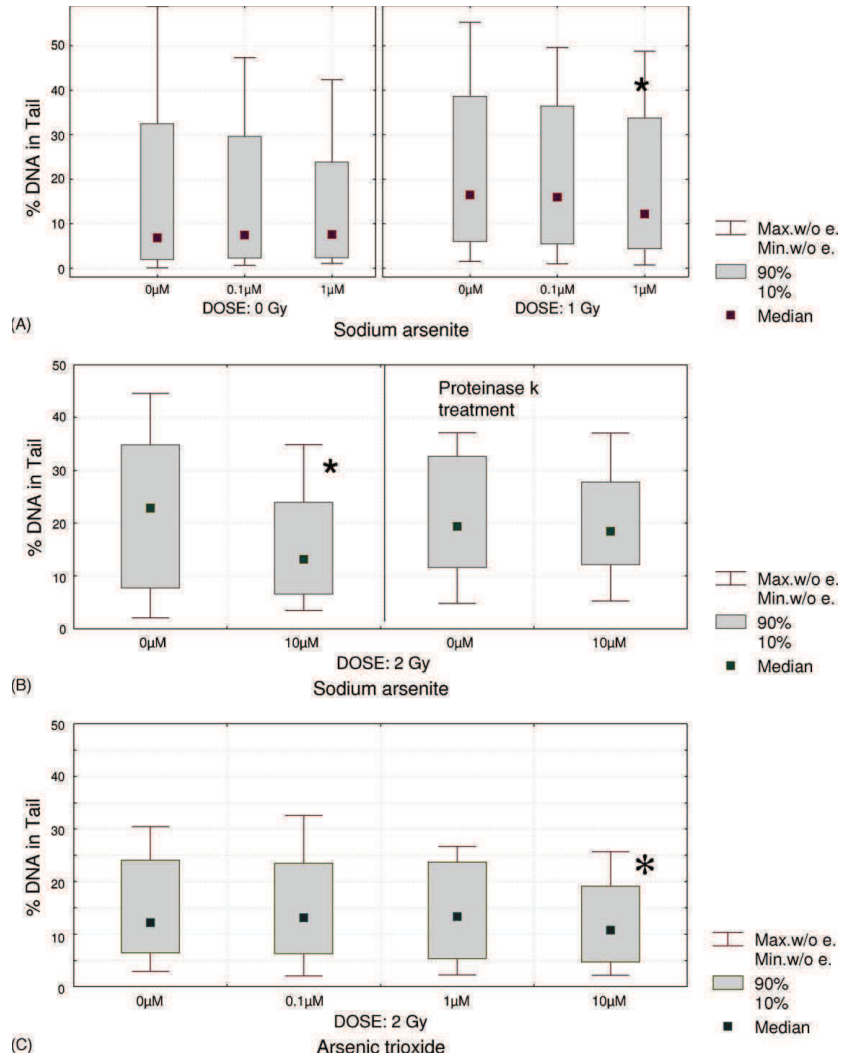
Fig. 6. Distribution and median of % DNA in tail measured with the comet assay shown as box plots. Each box contains data of three independent experiments, *statistically significant ($p < 0.005$ in U-test) from control (0 μM ± irradiation). (A) Effect of sodium arsenite on DNA damage with and without 1 Gy irradiation after 22 h preincubation of TK6 cells in arsenite containing medium. (B) Distribution and median of DNA damage with and without proteinase K treatment. TK6 cells set in arsenite medium were irradiated immediately without preincubation. The combined exposure to arsenite and 2 Gy resulted in a significant decrease in DNA damage (left), no statistically significant difference between control cells (0 μM) and cells with and without arsenite after proteinase K treatment (right). (C) Effect of arsenic trioxide on DNA damage after 22 h preincubation of TK6 cells in arsenic trioxide containing medium and 2 Gy irradiation.
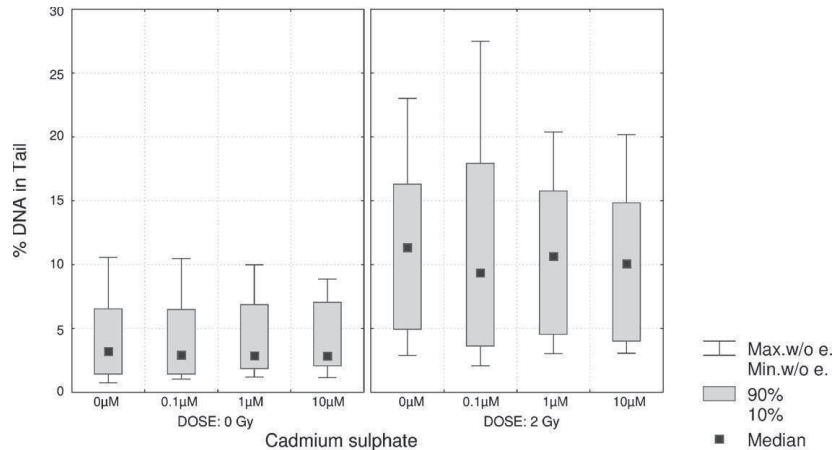
Fig. 7. Distribution and median of % DNA in tail after treatment of the cells with cadmium sulphate shown as box plots. Cells were irradiated with 2 Gy after 22 h incubation in medium with different cadmium concentrations. No statistically significant DNA damage by cadmium treatment or combined treatment with gamma-radiation compared to control (0 μM, 0 Gy ± irradiation).

3.4. Comet assay

The induction of DNA strand breaks by arsenic and cadmium alone or in combination with gamma-rays was investigated with the comet assay. After preincubation with arsenite for 22 h, DNA damage was not significantly affected with increasing arsenite concentrations. However, the combination of 1 Gy gamma-dose and 1 μM arsenite decreased DNA damage significantly in comparison to radiation alone (Fig. 6A). Similar results were obtained in combination with a 2 Gy dose. No significant effects on DNA repair were detectable in the presence of arsenite with and without gamma-irradiation after 30, 60 and 90 min repair times (data not shown).

To find out if the decrease of DNA damage was due to DNA protein cross-links, the cells were treated with proteinase K during the comet preparation. After eliminating DNA bound proteins no significant difference was seen between arsenite treated cells and untreated control cells regarding the median of damaged cells (Fig. 6B). Even 30 min incubation of the cells in serum-free medium supplemented with 10 μM arsenite significantly reduced the "apparent" DNA damage in combination with radiation probably due to a rapid arsenite uptake [21] in the cell. This result clearly shows that the decrease of DNA damage in the presence of arsenite is mostly due to DNA protein cross-links caused by arsenite preventing the damaged DNA to move during electrophoresis.

Arsenic trioxide was less effective in DNA cross-linking than arsenite. Significantly reduced DNA damage was only detectable at a concentration of 10 μM arsenic trioxide in combination with a 2 Gy gamma-dose, demonstrated in Fig. 6C. No detectable effect on DNA repair was found.

Cadmium showed no significant effects on DNA damage (Fig. 7) or DNA repair (data not shown) with or without radiation doses of 1 or 2 Gy.

4. Discussion

To date, there are only a few investigations on the combined effects of gamma-radiation and metal compounds and the results are not conclusive. The combined treatment of cadmium and gamma-radiation resulted in an increase of primary DNA damage due to inhibition of DNA repair and generation of reactive oxygen species [22]. Combined treatment of arsenite and gamma irradiation lead to an increase in chromosomal damage in lymphocytes [23], to inhibition of mitotic recombination in the *Drosophila* wing spot test [24], and DNA double strand repair in CHO cells [25]. Combined exposure of mouse embryos to gamma-radiation and arsenite corresponded to the effects obtained by the addition of the single effects [26]. Similar to TK6 cells, mouse embryos showed no effect at 0.1 μM arsenite on morphological development, proliferation and micronucleus formation. On the proteome level, combined treatment

Table 1
Summary of results

Endpoint	Compound	Single effect	Combined effect
Apoptosis	Arsenite	Very low apoptosis induction	No clear additive effect
	Arsenic trioxide	Very low apoptosis induction	More than additive effect
	Cadmium sulphate	Very low apoptosis induction	Reduction of apoptosis at concentration > 1 μM and doses > 1 Gy
Micronuclei	Arsenite	No significant effects in the non-toxic concentration range 0.1–1 μM	Significant additive effect only with 1 μM and 3 Gy
	Arsenic trioxide	Very low increase of micronuclei with concentration, no significant effects in the non-toxic concentration range 0.1–1 μM	Significant more than additive effect only with 1 μM and 3 Gy, 10 μM less effective than arsenite
	Cadmium sulphate	Very low increase of micronuclei with concentration, significant effects in the non-toxic concentration range > 0.1 μM	Significant more than additive effect with 1 μM, reduced effect with 10 μM
DNA damage	Arsenite	No significant effects	Significant reduction of DNA strand breaks at 1 μM
	Arsenic trioxide	No significant effects	Significant reduction of DNA strand breaks at 10 μM
	Cadmium sulphate	No significant effects	No additive effects
DNA repair	Arsenite	No inhibition	No inhibition
	Arsenic trioxide	No inhibition	No inhibition
	Cadmium sulphate	No inhibition	No inhibition

of TK6 cells with gamma-radiation and arsenite showed significant effects on the abundance of proteins such as glutathione transferase omega, proteasome and serine/threonine phosphatase PP1-A [27].

The investigations presented here (summarised in Table 1) show that, at non-toxic, close to naturally occurring concentrations, the environmental pollutants arsenic and cadmium alone did not significantly induce DNA damage, apoptosis and micronuclei. However, arsenic trioxide, in combination with gamma-rays, showed a synergistic enhancement of apoptosis induction. At high radiation doses both arsenicals showed, at a 1 μM concentration, a significant increase in micronuclei induction, arsenic trioxide exceeding the sum of expected addition of the single effects, but being less effective in inducing DPCs than arsenite. The data presented here indicate that the two arsenic compounds may interact through different pathways in the cell.

Arsenicals (arsenite and arsenic trioxide) themselves at non-toxic concentrations have only a very small effect on apoptosis induction in TK6 cells which is consistent with low-level induction of apoptosis by arsenite in HL-60 cells [28] and by arsenic trioxide in HL-60 cells and breast tumour cell lines [29]. Gamma-irradiation caused the expected rate in apoptosis induction [20] due to induction of direct DNA damage and ROS induction [30]. The combination of arsenic trioxide and gamma-radiation induced a synergistic apoptotic effect consistent with data from human HeLa cells [31] and is also

described for the combination with quinones [32]. ROS has been implicated as playing a pivotal role in arsenic-induced apoptosis [33–35] dependent on the cellular oxidation/reduction state [34,36,37]. One explanation for different action of arsenic compounds might be their differential influence on gluthathione redox status and antioxidative enzymes [38] that might interfere with radiation effects. The analysis of the proteome of TK6 cells after treatment with arsenite and gamma-radiation showed that the combined exposure had significant antagonising effects on the abundance of proteins such as glutathione-*S*-transferase omega (hGSTO1-1), which is identical with monomethylarsonic acid reductase, the rate limiting enzyme in arsenic biotransformation [39], proteasome and serine/threonine phosphatase PP1-A, interfering with apoptotic or transformation pathways [27]. At the same time, the induction of the ß4 precursor of the proteasome seen after arsenite or gamma-radiation alone was inhibited. An important role of the proteasome is to degrade oxidised proteins especially under conditions of oxidative stress. If arsenite is able to interfere with proteasome activity induced by irradiation, the cells may escape the apoptotic pathway. Other proteins affected were serine/threonine phosphatase hPP-1A and enzymes of the mitochondria, which also interfere with apoptosis. The effect on these enzymes might be different by arsenic trioxide.

Our results show that cadmium itself caused only a low apoptosis induction in TK6 cells in contrast to a

human T cell line [40]. Apoptosis induction by cadmium seems to depend strongly on the cell type used [41]. The tendency of decreased apoptosis after higher doses of gamma-radiation in the presence of non-toxic cadmium concentrations is in agreement with results of the combination with cadmium and other DNA damaging agents such as chromium [42], gamma-radiation, methylmethane sulphonate and H_2O_2 [43] or by inducing mechanisms against oxidative damage [44]. Suppression of apoptosis induced by other noxes may be an important non-genotoxic mechanism of cadmium carcinogenesis and explanation for co-carcinogenic effects.

The in vivo induction of micronuclei in human individuals by occupational or environmental arsenic exposure is well documented [4], whereas cytogenetic effects due to cadmium exposure are not yet fully elucidated [45]. In general, it was found here that the formation of micronuclei by non-toxic concentrations of arsenic compounds and cadmium sulphate was very low. Arsenicals at non-toxic 1 μM concentration showed a significant increase in combination with 3 Gy gamma-radiation. The effect of arsenic trioxide seemed to be more than additive with an increase of approximately 60%. However, this synergistic effect was less pronounced after treatment with 10 μM arsenic trioxide than with arsenite probably due to a high apoptotic rate or toxicity at this concentration. Cadmium sulphate itself induced a very low frequency of micronuclei in a concentration-dependent manner, confirming data of other human cell lines [46,47]. In contrast to the effect of arsenicals, 1 μM cadmium in combination with a dose of 1 Gy increased micronucleation significantly, but was less effective at higher concentrations and higher radiation doses. This effect might indicate that cadmium interferes with cell cycle components in presence of radiation-induced DNA damage [43] and is consistent with the data presented here on apoptosis induction.

The data on apoptosis and micronuclei induction are consistent with the comet assay data. Arsenic and cadmium showed no significant genotoxic effects by the compounds themselves. In contrast, it could be clearly demonstrated, in experiments with combined exposure of arsenicals and gamma-radiation, that arsenic induced DNA-protein cross-links, the covalent binding of DNA to proteins. The cross-linking effect was less significant with arsenic trioxide. The data found with arsenite are consistent with effects reported by other authors. A dose related induction of DNA–protein cross-links (DPC) in a similar dose range used here was observed in a human hepatic cell line [48]. DPCs were also detected with the comet assay in vivo in several organs of mice fed with an arsenic-containing diet [49] and in lymphocytes of

mice treated with arsenic [50]. The results of arsenite effects on DNA are not always consistent and seem to be concentration-dependent. Whereas very low arsenic concentrations (below 0.01 μM) showed an increase in DNA damage [51,52] and might be due to DNA repair processes to remove oxidative DNA adducts and DPCs [53], concentrations up to 5 μM caused a decrease due to DPCs [54], inducing an increase in micronucleation at the same time [51,52]. This increase in micronuclei is comparable to the micronuclei data presented here. Higher arsenic concentrations again caused an increase in DNA damage due to cytotoxicity [55,56]. However, especially effects of arsenic seem to depend on the concentration used whether DNA strand breaks or DPCs are formed.

Although no significant effects of cadmium on DNA damage were found here, DNA strand breaks and DPCs were detected in murine und human cells [56–58], mainly at high cadmium concentrations. Fatur et al. [46] found that the effect of cadmium at low concentrations might be dependent on the preincubation time of the cells and might be due to protective mechanisms of the cell such as the induction of metallothionine [59]. These results indicate that incubation time of the cells might be important for the outcome of the experiments and might explain inconsistent results.

Since the direct genotoxic effects of cadmium and arsenic are rather weak and/or restricted to comparably high concentrations, indirect genotoxic effects enhancing mutagenicity in combination with other DNA damaging agents like UV, alkylating agents BP and to disturbing DNA repair processes might be more relevant at low, non-toxic concentrations and may well explain comutagenic effects [60]. Thus, arsenic might enhance mutagenicity of other compounds not only by inhibition of DNA repair enzymes [61] but also by inducing DPCs [19,62], whereas cadmium might disturb DNA–protein interactions essential for the initiation of nucleotide excision repair most likely by the displacement of essential metal ions like zinc [63]. Consistent with these results, no significant effects on DNA repair in TK6 cells were found here with the comet assay. However, one reason may be that in the comet assay the total DNA repair is measured by the time dependent decrease of DNA strand breaks (predominantly single strand breaks). Effects on one repair system or specific enzymes are not detectable and fidelity of DNA repair cannot be controlled.

5. Conclusion

In summary the most pertinent findings were: (i) the synergistic enhancement of apoptosis by interaction

between arsenic trioxide and gamma-radiation, (ii) the ability of the two different arsenic compounds to induce DPCs despite of their low concentration and (iii) the different action mechanisms for arsenite and arsenic trioxide. Cadmium enhanced significantly the induction of micronuclei. These findings support the co-carcinogenic mechanisms of the compounds. In addition the interaction of arsenic compounds with radiation-induced apoptosis could have a clinical applicability via a combination therapy of cancer cells.

Acknowledgements

References

[1] IARC International Agency for Research on Cancer Monographs on the Evaluation of the Carcinogenic Risks to Humans—Overall Evaluation of Carcinogenicity; An Updating of IARC Monographs, vols. 1–42, Suppl. 7, Lyon, 1987.

[2] IARC International Agency for Research on Cancer Monographs on the Evaluation of the Carcinogenic Risks to Humans—Some Metals and Metallic Compounds, vol. 23, Lyon, 1980.

[3] W.H. Miller Jr., H.M. Schipper, J.S. Lee, J. Singer, S. Waxman, Mechanisms of action of arsenic trioxide, Cancer Res. 62 (2002) 3893–3903.

[4] T.G. Rossman, Review: mechanism of arsenic carcinogenesis: an integrated approach, Mutat. Res. 533 (2003) 37–65.

[5] W.-C. Chou, C.V. Dang, Acute promyelocytic leukemia: recent advances in therapy and molecular basis of response to arsenic therapies, Curr. Opin. Hematol. 12 (2005) 1–6.

[6] IARC monographs: beryllium, cadmium, mercury, and exposures in the glass manufacturing industry, in: International Agency for Research on Cancer Monographs on the Evaluation of Carcinogenic Risks to Humans, vol. 58, IARC Scientific Publications, Lyon, 1993, pp. 119–237.

[7] M. Waisberg, P. Joseph, B. Hale, D. Beyersmann, Review: molecular and cellular mechanisms of cadmium carcinogenesis, Toxicology 192 (2003) 95–117.

[8] M. Sohrabi, The state-of-the-art on worldwide studies in some environments with elevated naturally occurring radioactive materials (NORM), Appl. Radiat. Isot. 49 (1998) 69–188.

[9] S.C. Darby, D.C. Hill, Health effects of residential radon: a European perspective at the end of 2002, Rad. Prot. Dos. 104 (2003) 321–329.

[10] Y.T. Liu, Z. Chen, A retrospective lung cancer mortality study of people exposed to insoluble arsenic and radon, Lung Cancer 14 (Suppl. 1) (1996) S137–S148.

[11] I. Hertz-Picciotto, A.H. Smith, Observations on the dose–response curve for arsenic exposure and lung cancer, Scand. J. Work Environ. Health 19 (1993) 217–226.

[12] W. Burkart, G.L. Finch, T. Jung, Quantifying health effects from the combined action of low-level radiation and other environmental agents: can new approaches solve the enigma? Sci. Tot. Environ. 205 (1997) 51–70.

[13] United Nations Scientific Committee on the Effects of Atomic Radiation (UNSCEAR), Report to the General Assembly, Annex G: Combined Effects of Radiation and Other Agents, United Nations Publications, 2000.

[14] P. Schramel, B.-J. Klose, S. Hasse, Die Leistungsfähigkeit der ICP-Emissionsspektroskopie zur Bestimmung von Spurenelementen in biologisch-medizinischen und in Umweltproben, Fresenius Z. Anal. Chem. 310 (1982) 209–216.

[15] S.K. Koester, P. Roth, W.R. Mikulka, S.F. Schlossman, C. Zhang, W.E. Bolton, Monitoring early cellular responses in apoptosis is aided by the mitochondrial membrane protein-specific monoclonal antibody APO2.7, Cytometry 29 (1997) 306–312.

[16] M. Nüsse, W. Beisker, B.M. Miller, G.A. Schreiber, S. Viaggi, E.M. Weller, J.M. Wessels, Measurement of micronuclei by flow cytometry, Meth. Cell Biol. 42 (1994) 149.

[17] N.P. Singh, R.R. Tice, R.E. Stephens, E.L. Schneider, A microgel electrophoresis technique for the direct quantitation of DNA damage and repair in individual fibroblasts cultured on microscope slides, Mutat. Res. 252 (1991) 289–296.

[18] M. Gomolka, G. Lüke, E. Konhäuser, K. Hetzl, C. Schindewolf, K. Lobenwein, S. Hornhardt, R. Balling, M. Hrabe de Angelis, T. Jung, Variability in repair efficiencies of radiation-induced DNA strand breaks in two DBA/2 mouse lymphoma cell lines, Neoplasma 46 (Suppl.) (1999) 50–52.

[19] O. Merk, G. Speit, Significance of formaldehyde-induced DNA–protein cross-links for mutagenesis, Environ. Mol. Mutagen. 32 (1998) 260–268.

[20] Y. Yu, J.B. Little, p53 is involved in but not required for ionizing radiation-induced caspase-3 activation and apoptosis in human lymphoblast cell lines, Cancer Res. 58 (1998) 4277–4281.

[21] A. Hartwig, U.D. Gröblinghoff, D. Beyersmann, A.T. Natarajan, R. Filon, L.H.F. Mullenders, Interaction of arsenic(III) with nucleotide excision repair in UV-irradiated human fibroblasts, Carcinogenesis 18 (1997) 399–405.

[22] W. Burkart, B. Ogorek, Genotoxic action of cadmium and mercury in cell cultures and modulation of radiation effects, Toxicol. Environ. Chem. 12 (1986) 173–183.

[23] A.N. Jha, M. Noditi, R. Nilsson, A.T. Natarajan, Genotoxic effects of sodium arsenite on human cells, Mutat. Res. 284 (1992) 215–221.

[24] M.E. De la Rosa, J. Magnusson, C. Ramel, R. Nilsson, Modulating influence of inorganic arsenic on the recombinogenic and mutagenic action of ionizing radiation and alkylating agents, Mutat. Res. 318 (1994) 65–71.

[25] S. Takahashi, E. Takeda, Y. Kubota, R. Okayasu, Inhibition of repair of radiation-induced DNA double-strand breaks by nickel and arsenite, Rad. Res. 154 (2000) 686–691.

[26] W.-U. Müller, C. Streffer, C. Fischer-Lahdo, Toxicity of sodium arsenite in mouse embryos in vitro and its influence on radiation risk, Arch. Toxicol. 59 (1986) 172–175.

[27] S. Tapio, J. Danescu-Mayer, M. Asmuss, A. Posch, M. Gomolka, S. Hornhardt, Combined effects of gamma-radiation and arsenite on the proteome of human TK6 lymphoblastoid cells, Mutat. Res. 581 (2005) 141–152.

[28] T. Ochi, F. Nakajima, T. Sakurai, T. Kaise, Y. Oya-Ohta, Dimethylarsinic acid causes apoptosis in HL-60 cells via interaction with glutathione, Arch. Toxicol. 70 (1996) 815–821.

[29] M. Lu, J. Levin, E. Sulpice, A. Sequeira-Le Grand, M. Alemany, J.P. Caen, Z.C. Han, Effect of arsenic trioxide on viability, proliferation, and apoptosis in human megakaryotic leukemia cell lines, Exp. Hematol. 27 (1999) 845–852.

[30] R.K. Schmidt-Ullrich, P. Dent, S. Grant, R.B. Mikkelsen, K. Valerie, Signal transduction and cellular responses, Rad. Res. 153 (2000) 245–257.

[31] Y.-J. Chun, I.-C. Park, M.-j. Park, S.-H. Woo, S.-I. Hong, H.Y. Chung, T.-H. Kim, Y.-S. Lee, C.H. Rhee, S.-J. Lee, Enhancement of radiation response in human cervical cancer cells in vitro and in vivo by arsenic trioxide (As$_2$O$_3$), FEBS Lett. 519 (2002) 195–200.

[32] J. Yang, H. Li, Y.-Y. Chen, X.-J. Wang, G.-Y. Shi, Q.-S. Hu, X.-L. Kang, Y. Lu, X.-M. Tang, Q.-S. Guo, J. Yi, Anthraquinones sensitise tumour cells to arsenic cytotoxicity in vitro and in vivo via reactive oxygen species-mediated dual regulation of apoptosis, Free Rad. Biol. Med. 37 (2004) 2027–2041.

[33] M.D. Pulido, A.R. Parrish, Metal-induced apoptosis: mechanisms, Mutat. Res. 533 (2003) 227–241.

[34] Y. Jing, J. Dai, R.M.E. Chalmers-Redman, W.G. Tatton, S. Waxman, Arsenic trioxide selectively induces acute promyelocytic leukemia cell apoptosis via a hydrogen peroxide-dependent pathway, Blood 94 (1999) 2102–2111.

[35] Y. Nakagawa, Y. Akao, H. Morikawa, I. Hirata, K. Katsu, T. Naoe, N. Ohishi, K. Yagi, Arsenic trioxide-induced apoptosis through oxidative stress in cells of colon cancer cell lines, Life Sci. 70 (2002) 2253–2269.

[36] J. Dai, R.S. Weinberg, S. Waxman, Y. Jing, Malignant cells can be sensitized to undergo growth inhibition and apoptosis by arsenic tioxide through modulation of the glutathione redox system, Blood 93 (1999) 268–277.

[37] J. Yi, F. Gao, G. Shi, H. Li, Z. Wang, X. Shi, X. Tang, The inherent cellular level of reactive oxygen species: one of the mechanisms determining apoptotic susceptibility of leukemic cells to arsenic trioxide, Apoptosis 7 (2002) 209–215.

[38] J.Y. Yeh, L.C. Cheng, B.R. Ou, P.D. Whanger, L.W. Chang, Differential influences of various arsenic compounds on glutathione redox status and antioxidative enzymes in porcine endothelial cells, Cell. Mol. Life Sci. 59 (2002) 1972–1982.

[39] R.A. Zakharyan, A. Sampayo-Reyes, S.M. Healy, G. Tsaprailis, P.G. Board, D.C. Liebler, H.V. Aposhian, Human monomethylarsonic acid (MMA^v) reductase is a member of the glutathione-S-transferase superfamily, Chem. Res. Toxicol. 14 (2001) 1051–1057.

[40] B. El Azzouzi, G.T. Tsangaris, O. Pellegrini, Y. Manuel, J. Benveniste, Y. Thomas, Cadmium induces apoptosis in a human T cell line, Toxicology 88 (1994) 127–139.

[41] W. Wätjen, H. Haase, M. Biagioli, D. Beyersmann, Induction of apoptosis in mammalian cells by cadmium and zinc, Environ. Health Perspec. 110 (Suppl. 5) (2002) 865–867.

[42] C. Yuan, M. Kadiiska, W.E. Achanzar, R.P. Mason, M.P. Waalkes, Possible role of caspase-3 inhibition in cadmium-induced blockage of apoptosis, Toxicol. Appl. Pharmacol. 164 (2000) 321–329.

[43] C. Meplan, K. Mann, P. Hainaut, Cadmium induces conformational modifications of wild-type p53 and suppresses p53 response to DNA damage in cultured cells, J. Biol. Chem. 274 (1999) 31663–31670.

[44] J.D. Eneman, R.J. Potts, M. Osier, G.S. Shukla, C.H. Lee, J.-F. Chiu, B.A. Hart, Suppressed oxidant-induced apoptosis in cadmium adapted alveolar epithelial cells and its potential involvement in cadmium carcinogenesis, Toxicology 147 (2000) 215–228.

[45] V. Verougstraete, D. Lison, P. Hotz, A systematic review of cytogenetic studies conducted in human populations exposed to cadmium, Mutat. Res. 511 (2002) 15–43.

[46] T. Fatur, M. Tusek, I. Falnoga, J. Scancar, T.T. Lah, M. Filipic, DNA damage and metallothionin synthesis in human hepatoma cells (HepG2) exposed to cadmium, Food Chem. Toxicol. 40 (2002) 1069–1076.

[47] A.I. Seoane, F.N. Dulout, Genotoxic ability of cadmium, chromium and nickel salts studied by kinetochore staining in the cytokinesis-blocked micronucleus assay, Mutat. Res. 490 (2001) 99–106.

[48] P. Ramirez, L.M. Del Razo, M.C. Gutierrez-Ruiz, M.E. Gonsebatt, Arsenite induces DNA–protein cross-links and cytokeratin expression in the WRL-68 human hepatic cell line, Carcinogenesis 21 (2000) 701–706.

[49] R.R. Tice, J.W. Yager, P. Andrews, E. Crecelius, Effect of hepatic methyl donor status on urinary excretion and DNA damage in B6CF1 mice treated with sodium arsenite, Mutat. Res. 386 (1997) 315–334.

[50] B.S. Banu, K. Danadevi, K. Jamil, Y.R. Ahuja, K.V. Rao, M. Ishaq, In vivo genotoxic effect of arsenic trioxide in mice using comet assay, Toxicology 162 (2001) 171–177.

[51] T. Gebel, P. Birkenkamp, S. Luthin, H. Dunkelberg, Arsenic(III), but not antimony(III), induces DNA–protein cross-links, Anticancer Res. 18 (1998) 4253–4258.

[52] N. Schaumlöffel, T. Gebel, Heterogeneity of the DNA damage provoked by antimony and arsenic, Mutagenesis 13 (1998) 281–286.

[53] T.-S. Wang, T.-Y. Hsu, C.-H. Chung, A.S.S. Wang, D.-T. Bau, K.-Y. Jan, Arsenite induces oxidative DNA adducts and DNA–protein cross-links in mammalian cells, Free Rad. Biol. Med. 31 (2001) 321–330.

[54] J.-T. Dong, X.-M. Luo, Arsenic-induced DNA-strand breaks associated with DNA–protein cross-links in human fetal lung fibroblasts, Mutat. Res. 302 (1993) 97–102.

[55] E. Guillamet, A. Creus, J. Ponti, E. Sabbioni, S. Fortaner, R. Marcos, In vitro DNA damage by arsenic compounds in a human lymphoblastoid cell line (TK6) assessed by the alkaline comet assay, Mutagenesis 19 (2004) 129–135.

[56] A. Hartmann, G. Speit, Comparative investigations of the genotoxic effects of metals in the single cell gel (SCG) assay and the sister chromatid exchange (SCE) test, Environ. Mol. Mutagen. 23 (1994) 299–305.

[57] R.R. Misra, G.T. Smith, M.P. Waalkes, Evaluation of the direct genotoxic potential of cadmium in four different rodent cell lines, Toxicology 126 (1998) 103–114.

[58] S.A. Mouron, C.D. Golijow, F.N. Dulout, DNA damage by cadmium and arsenic salts assessed by the single cell gel electrophoresis assay, Mutat. Res. 498 (2001) 47–55.

[59] P. Lopez-Ortal, V. Souza, L. Bucio, E. Gonzalez, M.C. Gutierrez-Ruiz, DNA damage produced by cadmium in a human fetal hepatic cell line, Mutat. Res. 439 (1999) 301–306.

[60] A. Hartwig, Carcinogenicity of metal compounds: possible role of DNA repair inhibition, Toxicol. Lett. 102–103 (1998) 235–239.

[61] J.W. Yager, J.K. Wienke, Inhibition of poly(ADP-ribose) polymerase by arsenite, Mutat. Res. 386 (1997) 345–351.

[62] J.-T. Dong, X.-M. Luo, Effects of arsenic on DNA damage and repair in human fetal lung fibroblats, Mutat. Res. 315 (1994) 11–15.

[63] M. Hartmann, A. Hartwig, Disturbance of DNA damage recognition after UV-irradiation by nickel(II) and cadmium(II) in mammalian cells, Carcinogenesis 19 (1998) 617–621.

16. Rühm W, Walsh L & Nekolla E A. The Cohort of the Atomic Bomb Survivors - Major Basis of Radiation Safety Regulations. CERN Yellow Series, Report 12, 319-329, 2006

The cohort of the atomic bomb survivors – major basis of radiation safety regulations

W. Rühm[1], L. Walsh[1], E.A. Nekolla[2]
[1] Institute for Radiation Protection, GSF – National Research Center for Environment and Health, Neuherberg, Germany
[2] Federal Office for Radiation Protection, Neuherberg, Germany

Abstract

Since 1950 about 87 000 A-bomb survivors from Hiroshima and Nagasaki have been monitored within the framework of the *Life Span Study*, to quantify radiation-induced late effects. In terms of incidence and mortality, a statistically significant excess was found for leukemia and solid tumors. In another major international effort, neutron and gamma radiation doses were estimated, for those survivors (*Dosimetry System DS02*). Both studies combined allow the deduction of risk coefficients that serve as a basis for international safety regulations. As an example, current results on all solid tumors combined suggest an excess relative risk of 0.47 per Sievert for an attained age of 70 years, for those who were exposed at an age of 30 years. After exposure to an effective dose of one Sievert the solid tumor mortality would thus be about 50% larger than that expected for a similar cohort not exposed to any ionizing radiation from the bombs.

1   Introduction

After the atomic bomb explosions over Hiroshima and Nagasaki on August 6th and 9th 1945, both cities were almost completely destroyed. Those who were hit close to the hypocentres (the hypocentre is the vertical projection of the point of explosion (epicentre) to the ground) had almost no chance of survival. By end of 1945, about 200 000 inhabitants had died due to the detrimental health effects caused by the high doses of ionizing radiation, the blast wave and the heat.

Acute effects such as epilation, diarrhoea, central nervous system syndrome, etc., however, were not the only consequences of the exposure to ionizing radiation: A few years after the explosions, the first studies indicated an increase of cataracts and leukemia among the A-bomb survivors [1,2]. In the early 1950s a census was initiated by the joint US-Japanese Atomic Bomb Casualty Commission which was later replaced by the Radiation Effects Research Foundation (*RERF*), and about 120 000 survivors were identified. Based on these individuals, various studies have been made since 1950 to investigate any radiation-induced late effects on the health of these survivors.

There are other cohorts that provide important information on radiation-induced late effects such as, for example, (1) the dial painters in the US who incorporated ^{226,228}Rn and showed an excess in bone sarcomas [3], (2) the children in Russia, Belarus and the Ukraine who were exposed to ^{131}I and showed and excess in thyroid cancer after the Chernobyl accident [4], (3) the uranium miners who were exposed to ^{222}Rn and radon progenies and showed an excess in lung cancer mortality [5], (4) members of the tuberculosis Massachusetts cohort who were medically exposed to X-ray fluoroscopies and showed an excess in breast cancer [6], (5) the Mayak workers in Russia who incorporated ^{239,240}Pu and showed an excess of lung cancer [7], (6) the patients who where treated with ^{224}Ra against tuberculosis and ankylosing spondylitis and who showed an excess in bone sarcomas [8], or (7) those who were medically exposed in utero to X-rays in the UK and showed and excess in leukemia and solid tumors [9]. However, the cohort of the A-bomb survivors from Hiroshima and

Nagasaki is unique for various reasons. Those reasons include, for example, (1) the large number of cohort members investigated, (2) the long follow-up period of about 50 years, (3) a composition including males and females, children and adults, (4) a whole-body exposure which is more typical for radiation protection situations than partial-body exposures typical for many medically exposed cohorts, (5) a large dose range from natural to lethal levels, and (6) the fact that the cohort includes an internal control group with negligible doses, i.e. those who survived at large distances to the hypocentres. In spite of these advantages it is noted, however, that some issues must be kept in mind before the results obtained from the A-bomb survivors can be used for general radiation protection: (1) The A-bomb survivors were exposed to a high dose rate which is contrary to the situation involving low dose rates that are typical for many occupational exposures; (2) The consequences of internal exposures cannot be investigated since the survivors were predominantly exposed externally; (3) The results obtained on the Japanese cohort can not necessarily be transferred to western-type populations; (4) Risk estimates for gamma radiation depend somewhat on the biological effectiveness assumed for the neutrons because the survivors were exposed to a mixed neutron and gamma radiation field.

In general, any study on radiation-induced late-effects requires both, information on disease incidence and mortality in the investigated cohort, and information on the doses received by the affected individuals during the exposure to radiation. For the A-bomb survivors both are available – information on disease incidence and mortality is obtained within the framework of the Life Span Study (*LSS*) project [10-14], while individual doses are given in the dosimetry systems such as DS86 [15] and, more recently, DS02 [16]. If the observed health data such as the number of deaths due to solid cancer are plotted on the y-axis versus dose on the x-axis, any radiation-induced effect would appear as a positive correlation (Fig. 1). The slope of a linear correlation can be interpreted as a risk coefficient, i.e. as radiation-induced effect per dose of ionizing radiation.

Below, the *LSS* and the dosimetry of the A-bomb survivors are described in some detail, resulting risk estimates are briefly discussed, and some of the ongoing scientific discussions are sketched. Other studies conducted by *RERF* such as the Adult Health Study (biennial medical examinations of about 24 000 A-bomb survivors), the In-utero Study (investigations on about 3300 individuals who had been exposed in-utero), and the F1-Study (investigations on about 77 000 non-exposed children of A-bomb survivors) also provide valuable information, but are not further discussed here.
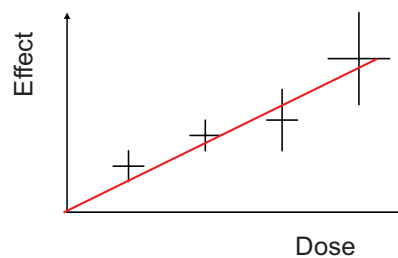
Fig. 1: Principle of a dose response relationship. The slope of a linear fit through the data represents a measure for the effect per dose.

2   Y-axis: the data from the life span study

In a continuous series of reports, *RERF* has published its findings on the incidence and mortality due to leukemia, solid cancer and other diseases, among the members of the *LSS* cohort. Report 12, for example, was based on the follow-up of 86 572 survivors from 1950-1990 [11]. During this period of time, 37 670 individuals died due to various reasons including 7578 individuals who died from solid cancer, and 249 who died from leukemia. While the number of radiation-induced excess cases was quite small compared to the spontaneous cases for solid cancer – in fact, about 334 of the total 7578 cases corresponding to 4.4% (8.2% among those with a nonzero dose) were attributed to the ionizing radiation – it was considerably larger for leukemia (about 87 of the total 249 cases corresponding to 35% [44% among those with a nonzero dose] were attributed to the radiation). Data given in the most recent *RERF* publication that is based on the follow-up 1950-2000 confirm this trend [14]: about 477 of the total 10,085 deaths due to solid cancer, and about 93 of the total 296 deaths due to leukemia were attributed to the radiation.

It is interesting to note that for leukemia, most of the radiation-induced excess cases occurred during the early phase of the follow-up in the 1950s and 1960s, due to the short latency period of this disease (Fig. 2). As mentioned above, extending the follow-up from 1990 to 2000 increased the number of observed leukemia cases from 87 to 93, i.e. by about 7%. Any new leukemia case observed in the *LSS* cohort today is thus rather spontaneous than due to the radiation. For solid tumors, however, the situation appears to be different: during the early phase of the follow-up the radiation-induced fraction of solid tumors was considerably smaller than that for leukemia, but did not decrease significantly in the following decades (Fig. 3). Extending the follow-up from 1990 to 2000 increased the number of excess solid tumor cases from 334 to 477, i.e. by about 43%. This may highlight why it is important to continue this study although more than half a century has already passed since its beginning: for solid tumors, a considerable number of radiation-induced cases is still to come. Those of the *LSS* cohort still alive (in fact, about 48% of the survivors were still alive in 1998 [13]) were exposed at very young ages. Thus, in the future the study is expected to provide new information on the late effects induced by ionizing radiation in children and adolescents.
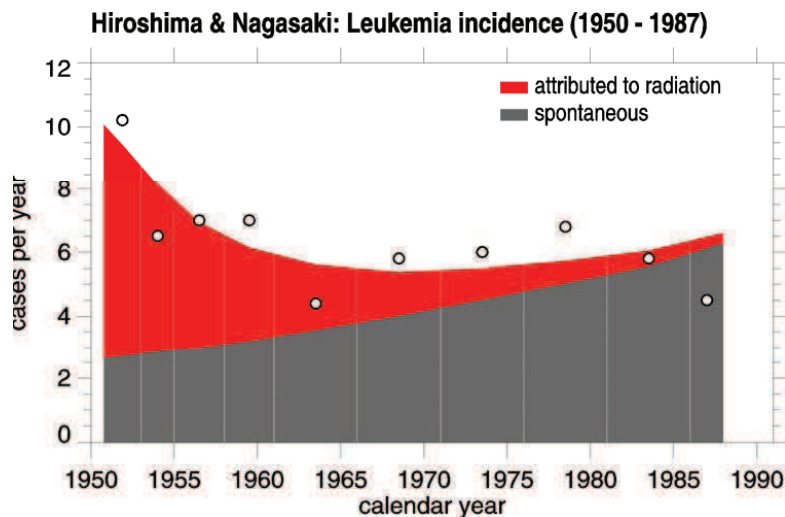
Fig. 2: Leukemia incidence in Hiroshima and Nagasaki, based on a follow-up 1950–1987
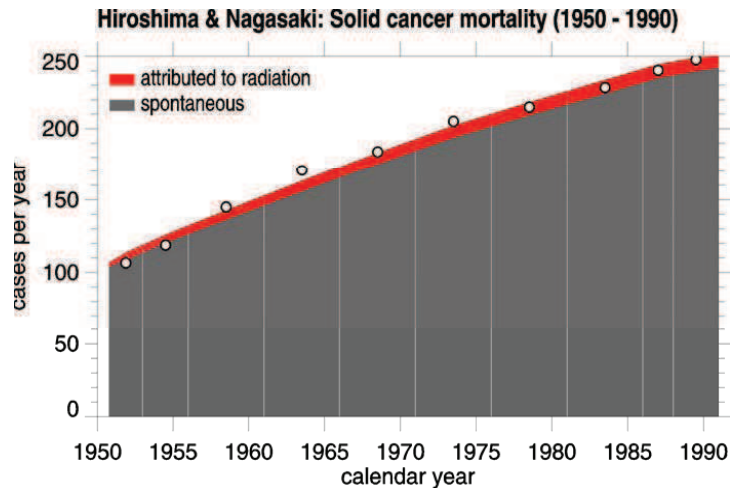
Fig. 3: Solid cancer mortality in Hiroshima and Nagasaki, based on a follow-up 1950–1990

3   X-axis: the dosimetry of the A-bomb survivors

While early dose estimates for the gamma and neutron radiation doses in Hiroshima and Nagasaki had been performed already in the 1950s and 1960s [17,18], it was in the early 1980s that extensive modelling allowed the estimation of organ doses to the survivors on an individual scale. The so-called DS86 model included, for example, calculation of the neutron and gamma radiation emitted by the exploding bombs ("source terms"), hydrodynamic simulation of the atmosphere disturbed by the explosions, coupled neutron and gamma ray transport calculations from the points of explosions ("epicentres") to the ground, quantification of the shielding by Japanese houses and other structures, and calculation of the shielding by the human body itself [15]. Figure 4 shows, as an example, the location of about 58 000 survivors from Hiroshima at the time of bombing (*atb*). The color code represents DS86 colon doses for these survivors. Figure 4 demonstrates the wide dose range to which the *LSS* cohort was exposed: doses of a few mSv for those who were located beyond about 2500 m from the hypocenter on the one hand, and doses up to several Sv for those few who could survive at a distance of less than 1000 m from the hypocenter on the other.

Results of various measurements that had been made in the 1950s and 1960s during test explosions on the Nevada Test Site proved the reliability of the DS86 methodology [15]. Measurements on environmental samples from Hiroshima containing quartz allowed the retrospective determination of the gamma radiation doses from the A-bomb by means of the thermoluminescence method. The results indicated somewhat lower experimental doses than calculated by DS86 close to the hypocenter, and slightly higher values at distances beyond 1000 m. For example, at a distance of about 1400 m from the hypocenter, the experimental data were about 20%-30% higher than those calculated [15]. In order to reconstruct the fast neutrons from the Hiroshima A-bomb that were responsible for the neutron doses to the survivors, early efforts concentrated on the detection of [32]P (half-life: 14.2 days) that was produced by fast neutrons in samples that contained sulfur [19,20]. Results of these studies showed reasonable agreement with DS86 calculations close to the hypocentre, but did not allow firm conclusion to be drawn at distances larger than about 700 m. Since these data were the only data on fast neutrons available until recently, an experimental corroboration of the neutron doses to the members of the LSS cohort who survived beyond about 1000 m from the

hypocenter (see Fig. 4) did not exist. From the 1960s until the mid 1990s, work on neutron fluence reconstruction concentrated on those radioisotopes that had been produced by thermal neutrons such as ^{60}Co [21], ^{152}Eu [22] and ^{36}Cl [23-25], due to a lack of alternatives. See [26] for a more complete list of references. Similar to the results on gamma radiation, most of the experimental results on thermal neutrons were somewhat lower close to the hypocentre of Hiroshima, compared to DS86 calculations. Contrary to the thermoluminescence data, however, the thermal activation measurements showed significantly higher results than DS86 approaching factors between 10 and 100 at distances beyond 1500 m. Interestingly, the few data available for Nagasaki appeared to support DS86 calculations even at large distances. A detailed description of the situation as it appeared by 1998 is given in [26].

D < 5 mSv
5 mSv < D < 0,1 Sv
0,1 Sv < D < 0,5 Sv
0,5 Sv < D < 1,0 Sv
D > 1 Sv
unknown dose
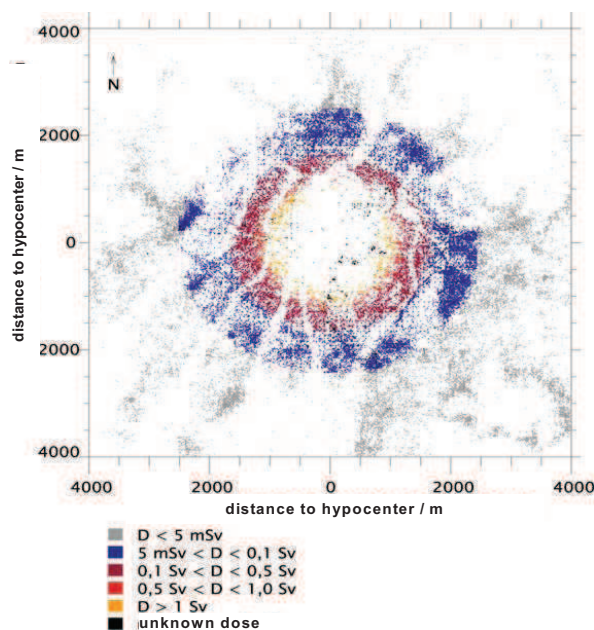
Fig. 4: Location of about 58 000 survivors in Hiroshima, at the time of bombing. The color code represents dose estimates for the colon obtained from the DS86 model (figure produced by M. Chomentowski, Radiobiological Institute, University of Munich, during a stay at *RERF* Hiroshima).

In the 1990s, the situation prompted major international efforts to improve the A-bomb dosimetry. Those efforts included novel approaches for measuring the radioisotope ^{63}Ni produced by fast neutrons in copper samples from Hiroshima, additional measurements of radioisotopes produced by thermal neutrons, and a complete re-evaluation of all computational aspects of the DS86 dosimetry model.

In a joint Japanese-US-German project, five copper samples could be identified in Hiroshima that had been exposed to fast neutrons from the A-bomb. The nickel in those samples was extracted by means of a specially developed chemical method [27], and the ^{63}Ni measured at the Munich MLL Laboratory by means of accelerator mass spectrometry [28]. The results indicated, within their experimental uncertainties, good agreement for four samples that were located at distances beyond about 1000 m where people had survived (Fig. 5). Thus, a major discrepancy that had been reported in the literature for thermal neutrons was not confirmed for fast neutrons [29].
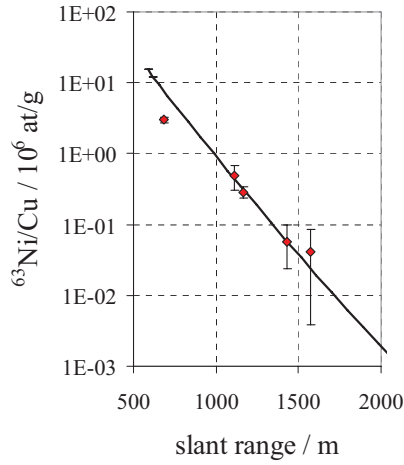
Fig. 5: Measured ^{63}Ni nuclei per gram copper (symbols) compared to DS86 calculation (solid line), as a function of distance from the epicentre

A joint Japanese-German collaboration was the first to show that new measurements of ^{36}Cl produced by thermal neutrons in Hiroshima were in agreement with DS86 calculations at distances beyond 1000 m from the hypocentre where previous measurements suggested a major discrepancy (Fig. 6) [30-33]. This finding was confirmed by other studies (for example, Ref. [16]). A detailed description of the work that was done to improve the dosimetry of the A-bomb survivors and that led to an updated Dosimetry System DS02 will soon be published [16].
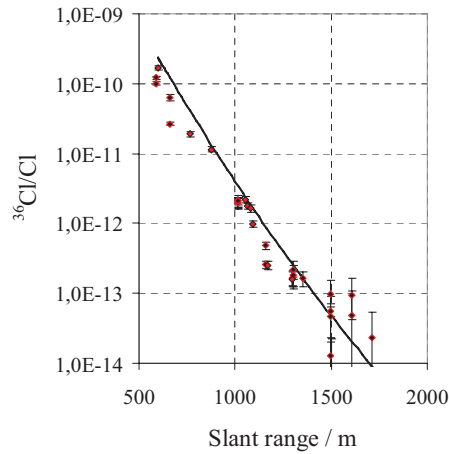
Fig. 6: Measured ^{36}Cl/Cl ratios (symbols) compared to DS86 calculation (solid line), as a function of distance from the epicentre

324

4 Dose-response relationships obtained from the LSS data

4.1 Shape of the dose-response curve for solid cancer

Recently, *RERF* published the results of a detailed follow-up of the *LSS* cohort, based on the period from 1950 to 1997 [13]. These results are summarized here in terms of the excess relative risk (*ERR*) as a function of weighted colon dose. The *ERR* is defined as the difference between the number of observed solid cancer cases (*O*) in the cohort, and the number of solid cancer cases expected for the cohort (*E*) if no additional exposure due to A-bomb radiation was present, normalized to this number (see Eq. 1). The *ERR* is a function of dose, sex, age-at-exposure, and age-attained. All data given here were calculated for those aged 70 years who were 30 years old *atb*, and are gender-averaged.

$$ERR = (O - E)/E \qquad (1)$$

where:

– O is the number of cases observed in the exposed cohort,

– E is the number of cases expected in an identical (hypothetical) cohort not exposed to A-bomb radiation.

The weighted colon dose as used by *RERF* is the sum of the colon absorbed dose from the gamma radiation, and the ten fold colon absorbed dose from the neutrons (Eq. 2). The factor 10 accounts for the increased relative biological effectiveness (*RBE*) of the densely-ionizing neutron radiation compared to that of the sparsely-ionizing gamma radiation.

$$D = D_\gamma + 10 \cdot D_n \qquad (2)$$

where:

– D is the weighted absorbed dose to the colon,

– D_γ is the absorbed dose to the colon due to the gamma radiation,

– D_n is the absorbed dose to the colon due to the neutrons radiation.

It is important to note that with the chosen value of 10 for the neutron weighting factor, the contribution of the neutrons to the weighted colon dose is relatively small. Based on *DS86* or *DS02*, for example, the contribution of the neutrons is less than 10%, at a distance of 1000 m from the hypocenter in Hiroshima, and about 1% at a distance of 2000 m. In other words, the major fraction of the late effects observed in the LSS is attributed to the gamma radiation if a value of 10 for the neutron weighting factor is used.

The dose-response relationship obtained by *RERF* for solid tumors is shown in Fig. 7. As a major finding is noted that for all solid cancer combined "There is little evidence against a simple linear dose response, with the only apparent curvature being a flattening for those with dose estimates above 2 Sv that is not statistically significant (p > 0.5)" [13]. Based on a linear dose-response curve, an ERR/Sv of 0.47 ± 0.06 is obtained for survivors who are 70 years old, and were exposed at an age of 30 years. Until recently, the linear dose-response curve was somewhat surprising since it was not observed for leukemia which showed a significant upward curvature [11]. Additionally, based on animal experiments, biological experiments and on theoretical considerations, a linear-quadratic rather than a pure linear dose-dependence was expected, for the sparsely-ionizing gamma radiation.
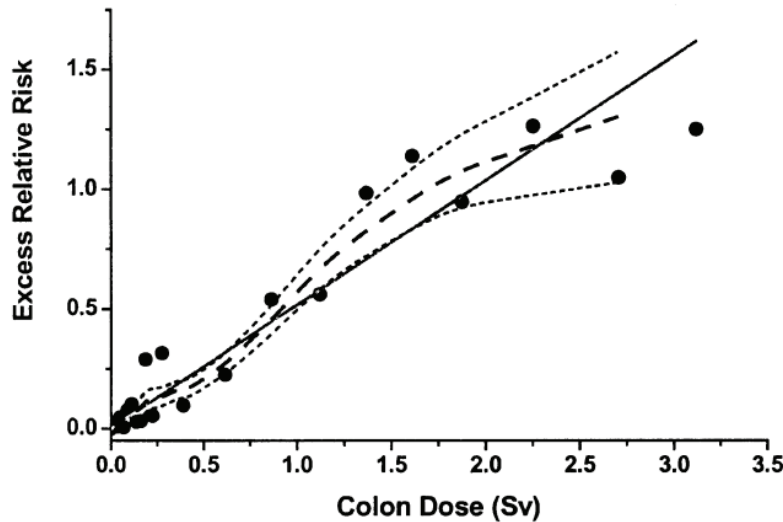
Fig. 7: Excess relative risk for all solid tumors combined versus weighted colon dose (Eq. 2). The linear fit through the data corresponds to a slope of (0.47±0.06)/Sv [13].

Preston and coworkers were able to find a statistically significant increase of the ERR with dose for those survivors whose doses were below 120 mSv. If the analysis was restricted to those whose doses were below 100 mSv, however, a statistically significant slope of the dose-response was not observed [13].

About one year later, *RERF* published a further report that included an additional three years follow-up. While the motivation of this article was primarily to provide a first discussion of the new *DS02* doses, it is also important for another reason: for the first time a significant upward curvature was found in the solid cancer mortality data [14]. This result was independently confirmed by Walsh and coworkers who used the earlier follow-up (1950-1997) for their analysis [34]

4.2 The role of the neutrons

As has been mentioned earlier, the chosen value of 10 for the *RBE* of the neutrons implies that most of the observed late effects are attributed to the gamma radiation. There are reasons to believe, however, that values greater than 10 provide a more realistic description of the biological effectiveness of the neutrons. In fact, animal experiments, chromosome aberrations measured in peripheral blood of about 1800 A-bomb survivors, and recommendations published by the International Commission on Radiological Protection (ICRP) [35] would suggest higher values [36–38], as well as a detailed analysis of organ-specific risk estimates obtained for solid cancers [39].

Qualitatively speaking, the use of higher *RBE* values for the neutrons implies that a larger fraction of the observed radiation-induced late effects (e.g. solid cancer or leukemia) is attributed to the neutrons. As a consequence, a smaller fraction is attributed to the gamma radiation and thus the risk estimates deduced from the LSS cohort for gamma radiation will also become smaller. This effect is demonstrated in Figs. 8 and 9. While Figure 8 shows the results of a conventional analysis of the solid cancer mortality data (1950-1990) with an assumed *RBE* value of 10 for the neutrons, Fig. 9 shows the results based on *RBE* values of 20, 35, and 50.
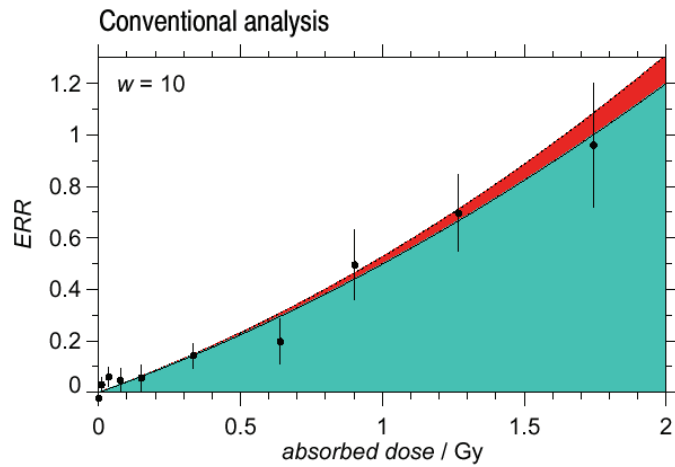
Fig. 8: Excess relative risk for solid cancer mortality, versus weighted colon dose; a value of 10 is used for the neutron *RBE* [40]
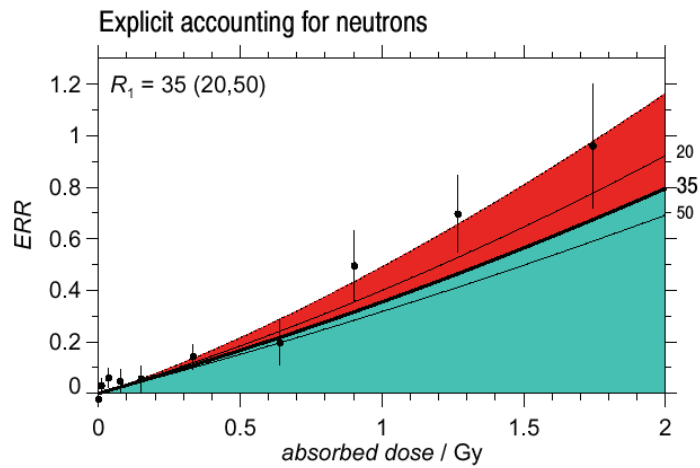
Fig. 9: Excess relative risk for solid cancer mortality, versus weighted colon dose; values of 20, 35, and 50 are used for the neutron *RBE* [40].

5   Conclusion

Data obtained on the A-bomb survivors from Hiroshima and Nagasaki serve as a major basis for radiation protection regulations. For more than half a century, considerable efforts have been made to quantify the morbidity and mortality of initially about 100 000 individuals. Recently, a major international effort came to an end that included re-evaluation of all aspects of A-bomb dosimetry. It was concluded that – while previous measurements suggested a significant discrepancy between neutron activation measurements and calculations for thermal neutrons – results of more recent measurements turned out to be in agreement with these calculations. While current analyses attribute most of the observed radiation-induced effects such as leukemia and solid tumors to the gamma radiation, more recent analyses suggest the neutrons having contributed considerably to these effects. It is expected that a final decision on how to interpret the effect contribution of the neutrons will be made in the next couple of years.

References

[1] J.H. Foley, W. Borges, T. Yamawaki, Jpn. Am. J. Med. 13 (1952) 311.

[2] D.G. Cogan, S.F. Martin, S.J. Kimura, Science 110 (1949) 654.

[3] S.A. Fry, Radiat. Res. 150 (Suppl.) (1998) S21.

[4] E. Cardis et al., J. Natl. Cancer. Inst. 97 (2005) 724-732

[5] BEIR VI., National Academy Press (ISBN 0-309-056454-4), 1999

[6] M.P. Little and J.D. Boice, Radiat. Res. 151 (1999) 218-224

[7] M. Kreisheimer et al., Radiat. Environ. Biophys. 42 (2003) 129-135

[8] E.A. Nekolla et al., Radiat. Res. 153 (2000) 93-103

[9] R. Wakeford and M.P. Little, Int. J. Radiat. Biol. 79 (2003) 293-309

[10] D.E. Thomson et al., Radiat. Res. 137 (Suppl.) (1994) S17.

[11] D.A. Pierce et al., Radiat Res. 146 (1996) 1.

[12] Y. Shimizu et al., Radiat. Res. 152 (1999) 374.

[13] D.L. Preston et al., Radiat. Res. 160 (2003) 381.

[14] D. L. Preston et al., Radiat. Res. 162 (2004) 377.

[15] W.C. Roesch (ed.) US-Japan joint reassessment of atomic bomb radiation dosimetry in Hiroshima and Nagasaki – final report. Radiation Effects Research Foundation, Hiroshima (1987).

[16] R.W. Young and G.D. Kerr (eds.) Reassessment of the Atomic-Bomb Radiation Dosimetry for Hiroshima and Nagasaki - DS02. RERF, Hiroshima, Japan, (2005) in press.

[17] E.T. Arakawa, N. Engl. J. Med. 263 (1960) 488.

[18] R.C. Milton and T. Shohoji, Tentative 1965 radiation dose estimation for atomic bomb survivors, Technical Report TR 1-68, Atomic Bomb Casualty Commission, Hiroshima and Nagasaki (1968).

[19] F. Yamasaki and A. Sugimoto, Collection of Investigative Reports on Atomic Bomb Disaster, Science Council of Japan, Tokyo (1953) p. 18.

[20] B. Arakatsu, Collection of Investigative Reports on Atomic Bomb Disaster, Science Council of Japan, Tokyo (1953) p. 10.

[21] T. Hashizume et al., Health Phys. 13 (1967) 149.

[22] T. Nakanishi, T. Imura, M. Sakanoue, Nature 302 (1983) 132.

[23] G. Haberstock et al., Radiocarbon 28 (1986) 204.

[24] T. Straume et al., Health Phys. 63 (1992) 421.

[25] T. Straume et al., Radiat. Res. 138 (1994) 193.

[26] W. Rühm et al., Radiat. Environ. Biophys. 37 (1998) 293.

[27] A.A. Marchetti et al., Nucl. Instr. Meth. B123 (1997) 230.

[28] W. Rühm et al., Health Phys. 79 (2000) 358.

[29] T. Straume et al., Nature 424 (2003) 539.

[30] T. Huber et al., Radiat. Environ. Biophys. 42 (2003) 27.

[31] T. Huber et al., Radiat. Environ. Biophys. 44 (2005) 75.

[32] E. Nolte et al., Radiat. Environ. Biophys. 44 (2005) 87.

[33] W. Rühm et al., In: Reassessment of the Atomic-Bomb Radiation Dosimetry for Hiroshima and Nagasaki - DS02. RERF, Hiroshima, Japan, (2005) in press.

[34] L. Walsh, W. Rühm, A.M. Kellerer, Radiat. Environ. Biophys. 43 (2004) 145.

[35] International Commission on Radiological Protection, ICRP Publication 60. Ann. ICRP 21 (1-3), Pergamon Press, Oxford (1991).

[36] D. Wolf et al., Radiat. Res. 154 (2000) 412.

[37] W. Rühm, L. Walsh, M. Chomentowski, Radiat. Environ. Biophys. 42 (2003) 119.

[38] A.M. Kellerer L. Walsh, Rad. Res. 156 (2001) 708.

[39] A.M. Kellerer, W. Rühm, L. Walsh, Health Phys. (2005) accepted.

[40] A.M. Kellerer, L. Walsh, E.A. Nekolla, Radiat. Environ. Biophys. 41 (2002), 113.

17. Rössler U, Hornhardt S, Seidl C, Müller-Laue E, Walsh L, Panzer W, Schmid E, Senekowitsch-Schmidtke R & Gomolka M. The sensitivity of the alkaline comet assay in detecting DNA lesions induced by X-rays, gamma-rays and alpha particles. Proc. 14th International Symposium on Microdosimetry: Ionising radiation quality, molecular mechanisms, cellular effects and their consequences for low level risk assessment and radiation therapy, Nov 13-18, 2005, Venice, Italy, Radiat. Prot. Dosim. 122(1-4), 154-159, 2006

THE SENSITIVITY OF THE ALKALINE COMET ASSAY IN DETECTING DNA LESIONS INDUCED BY X RAYS, GAMMA RAYS AND ALPHA PARTICLES

U. Rössler[1], S. Hornhardt[1], C. Seidl[2], E. Müller-Laue[1], L. Walsh[3], W. Panzer[3], E. Schmid[4], R. Senekowitsch-Schmidtke[2] and M. Gomolka[1,*]

[1]Federal Office for Radiation Protection, Department Radiation Protection and Health, Ingolstädter Landstrasse 1, 85764 Oberschleissheim, Germany
[2]Department of Nuclear Medicine, Technische Universität München, Ismaninger Strasse 22, 81675 Munich, Germany
[3]Institute of Radiation Protection, GSF-National Research Center for Environment and Health, 85764 Neuherberg, Germany
[4]Radiobiological Institute, University of Munich, 80336 Munich, Germany

Experiments were designed and performed in order to investigate whether or not the different cellular energy deposition patterns of photon radiation with different energies (29 kV, 220 kV X rays; Co-60, Cs-137-γ-rays) and alpha-radiation from an Am-241 source differ in DNA damage induction capacity in human cells. For this purpose, the alkaline comet assay (single cell gel electrophoresis) was applied to measure the amount of DNA damage in relation to the dose received. The comet assay data for the parameters '% DNA in the tail' and 'tail moment' for human peripheral lymphocytes did not indicate any difference in the initial radiation damage produced by 29 kV X rays relative to the reference radiations, 220 kV X rays and the gamma rays, whether for the total mean dose range of 0–3 Gy nor in the low-dose range. In contrast, when the 'tail length' data were analysed saturation of the fitted dose response curve appeared for X rays at about 1.5 Gy but was not apparent for gamma rays up to 3 Gy. Preliminary data for alpha exposures of HSC45-M2 cells showed a significant increase in DNA damage only at high doses ($>$2 Gy Am-241), but the damage at 2 Gy exceeded the damage induced at 2 Gy by Cs-137-γ-rays by a factor of 2.5. In contrast, other experiments involving different cell systems and DNA damage indicators such as chromosomal aberrations have detected a significant increase in DNA damage at much lower doses, that is at 0.02 Gy for Am-241 and depict a higher biological effectiveness. These results indicate that differences in biological effects arise through downstream processing of complex DNA damage.

INTRODUCTION

Several damage indicators such as cell death, neoplastic cell transformation, mutation induction and chromosomal aberrations have shown that radiations of low linear energy transfer (LET) (X rays and gamma rays) differ in their biological effectiveness[1–4]. Alpha particles, which are considered as high LET radiation show a high biological effectiveness[5]. Computational approaches for determining the spectrum of DNA damage induced by ionizing radiation have shown that the yield of strand breaks per unit absorbed dose is nearly constant over a wide range of LET[6]. For induced DNA fragments, it has been shown that DNA double-strand breaks in photon-irradiated cells are randomly distributed, whereas irradiation of intact K562 cells with high-LET nitrogen ions produced an excess of non-randomly distributed DNA fragments of 10 kbp–1 Mbp in size[7]. It has been postulated that this non-random pattern of breaks results in a higher complexity of induced breaks and finally leads to misrepair which cause the cellular responses mentioned above[8,9].

The comet assay provides an excellent method for detecting direct DNA damage and its subsequent repair at the single cell level[10]. If alkaline conditions are applied during electrophoresis, single strand DNA breaks are detected regardless of whether they result from DNA double strand lesions, abasic sites, or original single strand breaks. In contrast, if neutral conditions exist in the test system only DNA double strand breaks and damage at doses $>$3 Gy are detectable[11]. To investigate a physiological interesting dose range, the alkaline comet assay was applied to see how different radiation qualities vary in the initial radiation damage.

MATERIALS AND METHODS

Cell culture

Isolated human lymphocytes that had been stored in liquid N_2 were thawed quickly and incubated for 24 h at 37°C and 5% CO_2 in RPMI (L-Glutamat) and 10% FCS (1 million cells per ml medium). Cells were washed in 0.9% NaCl twice and centrifuged for 10 min at 300 g. Aliquots of 30,000–50,000 cells in 10 μl of 0.9% NaCl were set on ice prior to irradiation.

---

*Corresponding author: mgomolka@bfs.de

For alpha irradiation human gastric cancer cells (HSC45-M2) or human lymphocytes were used. About 2.0 million HSC45-M2 cells were grown in special metallic ring devices with a bottom hostafan foil of 2 μm thickness for two days in 3.5 ml of DMEM medium with 10% FBS and 1% penicilin/ streptomycin at 37°C and 5% CO_2 in an incubator. In order to achieve a better attachment of the cells, the foil was treated for 5 min with 3 ml of 0.8 mol NaOH and subsequently rinsed with water before sterilisation. Human lymphocytes were attached to hostafan foil according to conditions described in Schmid *et al.* (1996)[12]. Lymphocytes were cultivated for 3 h on the same type of sterile ring devices as used for HSC45-M2 cells but without alkaline treatment of the foil at 37°C and 5% CO_2 in an incubator. Before irradiation, the medium was carefully drawn off and cells were washed twice with 1 ml of PBS-solution.

Irradiation and dosimetry

Experiments involving the comparison of low LET radiations, were performed with whole human blood exposed either to X rays or to gamma rays. The other experiments involving a comparison with high LET alpha radiation were performed with HSC45-M2 and isolated human lymphocytes exposed to Am-241 alpha particles in a dose range of 0.5–3.0 Gy. In parallel, HSC45-M2 cells were irradiated with Cs-137-gamma rays applying the same cell cultivation conditions as for alpha particle irradiation. These experiments were only performed once, but with triplet slides. Data from 10 independent radiation experiments involving Cs-137-gamma rays and frozen human lymphocytes from one donor are shown as Cs-137-refer in Figure 3.

Low LET radiation

Whole blood was irradiated at room temperature with low energy mammography X rays (29 kV), 220 kV X rays, ^{60}Co gamma rays or ^{137}Cs gamma rays according to the conditions described in Gomolka *et al.* (2005)[13]. When ^{137}Cs irradiation was performed to compare the data with alpha irradiation, HSC45-M2 cells were grown on a hostafan foil as described above, but before irradiation, the medium was discarded, the cells were washed twice with 1 ml PBS and scraped off the foil with 50 μl of 0.9% NaCl solution. The foil was washed again with 50–100 μl of 0.9% NaCl-solution and cells were diluted finally in a total volume of 100–150 μl depending on cell density. Aliquots of 10 μl with 30,000–50,000 cells each were then irradiated on ice in eppendorf cups in a closed HWM D2000 facility (Wälischmiller 0.66 Gy per min) in a dose range of 0.5–3.0 Gy and subsequently subjected to the comet

assay. Aliquots of 30,000–50,000 cells in 10 μl of 0.9% NaCl of frozen lymphocytes were irradiated on ice.

High LET radiation

HSC45-M2 cells were grown on hostafan foil as described above. Before irradiation, the culture medium was removed and the cells were washed twice with 1 ml PBS to remove cells which had not attached to the foil. Cells were irradiated with a [241]Am source with a particle fluence of 5.2×10^9 alpha-particle $\times$ min^{-1} m^{-2} which corresponds to 0.1025 Gy/min. The dosimetry and details of the source are given elsewhere[14]. Dosimetry is only exact for cells <10 μm. In contrast to lymphocytes HSC45-M2 cells vary in cell size from 10 to 15 μm. At a distance of 15 μm the dose is only about 30% of the defined surface dose. Therefore physical dosimetry for this cell line is error prone. Experiments were carried out with this cell line since external alpha particle irradiation is compared with the DNA damage induced by [213]Bi labeled antibodies against a cellular antigen of the HSC45-M2 cells in future experiments. The cultivation ring was placed with the foil directly on the irradiation window of the source. Irradiation was performed on air, cells were cooled with ice on top of the ring devices during irradiation. After irradiation cells were scraped off the foil with 50 μl of 0.9% NaCl-solution. After washing the foil again with 50–100 μl of 0.9% NaCl-solution, the washing suspensions were combined to a final volume of 100–150 μl depending on cell density. Aliquots of 10 μl with 30,000–50,000 cells each were used for the comet assay. For attached human lymphocytes [241]Am irradiation was performed in the same way as described for HSC45-M2 cells.

Comet assay

The Comet Assay was performed as described in Ref. (13). Aliquots of whole blood, frozen or on freshly isolated lymphocytes and phythaemagglutinin (PHA) stimulated lymphocytes in case of alpha irradiation were used. Peripheral blood was taken with informed consent from healthy donors. Results were compared only for those experiments involving simultaneous irradiation, in order to achieve similar blood quality and cell growth conditions.

Hardware and software for image acquisition and comet analysis

Data for low LET radiation (X rays; Cs-137 and Co-60 gamma rays) were evaluated by a semiautomatic system as described in Ref. (13) using a special software for evaluating comet images (VisCOMET,

Impuls GmbH, Gilching, Germany). Fifty comets were evaluated for each slide.

For high LET radiation and the corresponding reference radiation Cs-137, data were evaluated by a fully automatic system using the software of Metafer-4 CometScan (Metasystems, Altlussheim, Germany). With the automated system, between 100 and 200 cells per slide were analysed, depending on the percentage of automatically detected false positive cells, which were discarded after evaluation of the comet image gallery. For a detailed description of the system see Ref. (15).

Statistical evaluation

Data were fitted and compared using a multiple linear regression model. For detailed statistical evaluation see Ref. (13).

RESULTS

Photon radiation

Comet assay experiments were performed with whole blood exposed to X and gamma rays (0.5 – 3.0 Gy). Three DNA damage parameters were evaluated for X (29 kV, 220 kV) and gamma (^{137}Cs, ^{60}Co) irradiation: '% DNA in the tail', 'tail moment (Olive)' and the 'tail length'. No difference in the induced initial radiation damage was detected for the parameters '% DNA in the tail' and 'tail moment (Olive)' (Figure 1). All radiation qualities showed a linear dose-effect relationship with the same slope when best-fit analyses were performed with the data. However, differences were found if the parameter 'tail length', in which the migration of the fragments in the electric field is reflected, was used. The X rays induced a significantly different

dose response than the gamma rays. At 1.0–1.5 Gy, the X ray dose response showed saturation (Figure 2; Table 1). The exponential term, which models the bending over the dose response in the fit, was significantly different from zero at the 90% level of confidence for the X rays but not for the gamma rays.

Alpha particle irradiation

When irradiating confluently grown human gastric cancer cells (HSC45-M2) on hostafan foil with an Am-241 source, DNA damage is detectable at doses ≥ 2 Gy (Figure 3). In contrast, DNA damage in attached lymphocytes can be visualised already at 1 Gy. In lymphocytes irradiated with X and gamma rays in suspension DNA damage is already visible at 0.5 Gy (Figures 1 and 3). However, at 2 and 3 Gy the damage induced by alpha particles is 2.6- and 2.5-fold higher, respectively, in comparison to Cs-137 irradiation. Preliminary data following irradiation of attached lymphocytes with X and gamma rays are in good agreement and show also a factor of 2- to 2.5 fold between alpha and gamma irradiation experiments. Attached lymphocytes will be used for future experiments, since the dosimetry here is very precise. The cell sizes range from 4 to 7 μm[12].

DISCUSSION

This study has demonstrated that the amount of DNA breaks detected with the Comet assay is similar among different photon radiations and different by a factor of 2.0–2.6 between alpha particle and gamma radiation. In contrast, other biological tests for assessment of radiation damage such as cell transformation or chromosomal aberrations indicate a much higher biological effect of alpha rays
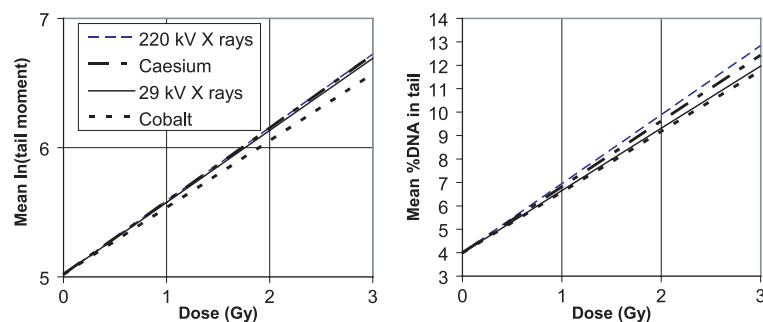
Figure 1. DNA damage induced by different low LET radiation is compared. Best fits from the multiple regression for both the mean natural logarithm of tail moment and the mean percentage of DNA in tail as a function of the mean-blood dose (Gy) from 5 independent experiments. The slopes are not significantly different for the four types of radiation. The original data and a description of the multiple regression method and the corresponding fit parameters for the left-hand diagram are given in Ref. (13).
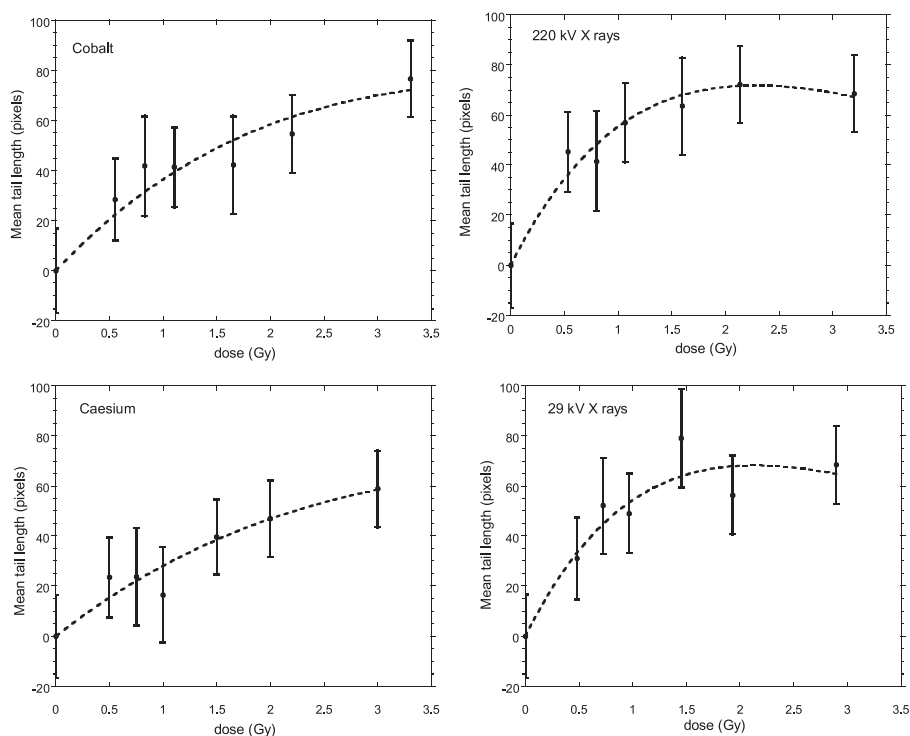
Figure 2. Best fits for the DNA damage parameter 'tail length' are demonstrated from the same experiments as in Figure 1. To correct for the experimental variance and to propagate errors systematically, the variance of the control values was calculated. Then the mean of the four zero values was substracted from the dose response values and the errors for each experiment were combined, to improve the signal to noise ratio of the five independent experiments. The four curves show that the saturation effect at 1.5 Gy is significant for X rays (220 kV, 29 kV) on the 90% level of confidence but not for gammas (Cs-137, Co-60). See Table 1.

Table 1. Results of the weighted least squares fits for the mean 'tail length' (T_1) dose response to the data shown in Figure 2.

Radiation type	Linear dose response		Exponentially modified linear dose response		
	Gradient m ($\pm$SE)	Coefficient of determination	α ($\pm$SE)	β ($\pm$SE)	Coefficient of determination
29 Kv	31.0 ± 4.0	0.54	86.9 ± 25.4	0.47 ± 0.15	0.95
220 Kv	29.6 ± 3.6	0.43	85.9 ± 23.4	0.44 ± 0.13	0.98
Cobalt	25.6 ± 3.5	0.88	45.6 ± 17.0	0.22 ± 0.15	0.96
Caesium	22.0 ± 3.8	0.93	33.7 ± 16.8	0.18 ± 0.21	0.96

The fit functions were: $T_1 = mx$(not shown) and $T_1 = ax.e^{(-\beta x)}$ (shown in Figure 2) where x is the mean blood dose in Gy.

compared to photon radiation and of 29 kV X rays compared to ^{60}Co or ^{137}Cs gamma rays[2–4,12]. In contrast to the Comet assay, where the initial DNA damage is detected, the biological effects measured in these test systems require DNA repair mechanism and cell division. Thus the qualities of DNA repair and further downstream processes have a major impact on the biological effectiveness of the

157
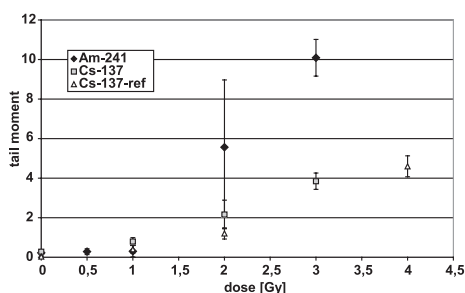
Figure 3. DNA damage of alpha particle irradiation (Am-241) compared to Caesium-137 (Cs-137) in a parallel experiment using human gastric cancer cells (HSC45-M2). For each radiation source/dose triplet slides were prepared. Median out of 'tail moment' of 100–200 cells was calculated for each slide. Computed are mean and standard deviation of the three measured median values. For comparison, mean of the median of 10 different radiation experiments with human frozen lymphocytes in suspension after irradiation with Cs-137 (Cs-137 ref) are given. Caesium irradiation experiments with HSC cells and human lymphocytes result in similar DNA damage. At doses >2 Gy damages induced by alpha particle irradiation are significantly higher by a factor of 2.5 than damages induced by caesium irradiation.

radiation type. Another key result of the analysis is that the complexity of the induced DNA breaks may be indicated by investigation of the parameter 'tail length' in the Comet assay and by a slightly different repair kinetic of the biologically more effective 29 kV X rays[13].

It was found that with the comet assay DNA damage induced by different low and high LET radiation types can be detected at the single cell level. For photon radiation, it was demonstrated by the parameters '% DNA in the tail' and 'tail moment' that the mere numbers of breaks do not differ significantly among the various photon radiation types used in this experiment. When the total amount of breaks is measured by these parameters a linear dose response curve can be fitted to the data. For the parameter '% DNA in the tail', the total amount of damaged DNA is reflected by its intensity compared to the total intensity of the comet. For 'tail moment (Olive)' migration distance of the DNA fragments is included by the multiplication of the intensity value with a migration distance value of the fragments. In contrast to the 'tail length' parameter, the total migration length of the DNA fragments is not captured, since the measurement is performed from the centre of gravity in the tail profile to the centre of gravity in the head profile. Therefore differences in DNA damage measured as 'tail moment (Olive)' should only be visible if there is a

clear difference in the amount of induced DNA breaks. This was not detected in the present study. However, by considering 'tail length', DNA fragments of both X rays showed an early saturation effect in their dose effect relationship. These observations can be best explained if the fragments initiated by X rays are different from the fragments induced by gamma rays, either in length or in the clustering of breaks close together, to change the migration behaviour of the DNA. For the first time it is demonstrated here, that 'tail length' indicates that the quality of the breaks among photon radiation with various LET may differ substantially. The results from repair experiments are in good agreement with these data[13] and show that 29 kV X rays tend to slow down DNA repair more than the reference radiation types, indicating more complex lesions induced by this radiation quality. However, this effect was not statistically significant.

Alpha irradiation experiments showed a significantly different dose response compared to gamma rays, but the effectiveness to induce DNA damage is lower than for chromosomal aberrations, where at 1 Gy the frequency of dicentric chromosomes was 0.277 compared to ^{137}Cs where the frequency was 0.062[12]. These results are consistent with data from neutron energy-dependent initial DNA damage as detected by the alkaline comet assay and chromosomal aberrations[16]. Chromosomal aberrations tend to be 2–3 times more sensitive than the initial DNA damage measured with the comet assay and they were in good agreement with cell transformation experiments. A striking difference between gamma irradiation and alpha irradiation in terms of mean 'tail moment' was found in this investigation for gastric cancer cells and for human lymphocytes attached to an hostafan foil. Surprisingly, the detection limit of the Comet assay was much higher for alpha irradiation than for gamma irradiation (2 Gy vs 0.5 Gy, respectively). This may be due to errors in dosimetry, because of the special growth conditions of this gastric cancer cell line, which tend to form cell foci, and the variation in cell size of the single irradiated cells, since damage induced in attached lymphocytes is already significant at 1 Gy. On the other hand when compared to another type of alpha particle irradiation, such as [213]Bi bound to antibodies against the cellular adhesion molecule E-cadherin, DNA damage was also detected only at high activity concentrations of 1.6 MBq [213]Bi with the comet assay (U. Rössler, Ch. Seidl and M. Gomolka, unpublished data). But heavy chromosomal aberrations and reduced survival occurred already at activities far below the detection limit of the Comet assay by a factor of 10.

In summary, using the Comet assay initial DNA damage can be detected for all investigated radiation types. It shows essentially a linear dose

effect relationship for the parameters 'tail moment' and '% DNA in the tail'. The results are in accordance with other physical and biological investigations, indicating that the difference in the amount of induced breaks by different LET radiations does not explain the biological consequences as detected after DNA repair and cell division. The parameters 'tail length' and 'DNA' repair indicate for photon radiation that the induced breaks differ by their quality. For alpha particles, it was found that the quantity of induced breaks is different when expressed in 'tail moment' between alpha and gamma irradiation, but the factor of 2.0–2.6 is lower than that found with cell survival or chromosomal aberrations.

REFERENCES

1. Borek, C., Hall, E. J. and Zaider, M. *X rays may be twice as potent as gamma rays for malignant transformation at low doses*. Nature **301**, 156–158 (1983).

2. Frankenberg, D., Kelnhofer, K., Garg, I., Bar, K. and Frankenberg-Schwager, M. *Enhanced mutation and neoplastic transformation in human cells by 29 kVp relative to 200 kVp X rays indicating a strong dependence of RBE on photon energy*. Radiat. Prot. Dosim. **99**, 261–264 (2002).

3. Schmid, E., Regulla, D., Kramer, H. M. and Harder, D. *The effect of 29 kV X rays on the dose response of chromosome aberrations in human lymphocytes*. Radiat. Res. **158**, 771–777 (2002).

4. Goggelmann, W., Jacobsen, C., Panzer, W., Walsh, L., Roos, H. and Schmid, E. *Re-evaluation of the RBE of 29 kV x-rays (mammography x-rays) relative to 220 kV x-rays using neoplastic transformation of human CGL1-hybrid cells*. Radiat. Environ. Biophys. **42**, 175–182 (2003).

5. ICRP, *Relative biological effectiveness (RBE), quality factor (Q), and radiation weighting factor (w_R)*. Publication 92, Annals of the ICRP 2003, Vol 33, Pergamon Press, Oxford, 2003.

6. Nikjoo, H., O'Neill, P., Wilson, W. E. and Goodhead, D. T. *Computational approach for determining the spectrum of DNA damage induced by ionizing radiation*. Radiat. Res. **156**, 577–583 (2001).

7. Radulescu, I., Elmroth, K. and Stenerlow, B. *Chromatin organization contributes to non-randomly distributed double-strand breaks after exposure to high-LET radiation*. Radiat. Res. **161**, 1–8 (2004).

8. Ward, J. F. *The complexity of DNA damage: relevance to biological consequences*. Int. J. Radiat. Biol. **66**, 427–432 (1994).

9. Rydberg, B., Lobrich, M. and Cooper, P. K. *Repair of clustered DNA damage caused by high LET radiation in human fibroblasts*. Phys. Med. **14**(Suppl. 1), 24–28 (1998).

10. Tice, R. R., Agurell, E., Anderson, D., Burlinson, B., Hartmann, A., Kobayashi, H., Miyamae, Y., Rojas, E., Ryu, J. C. and Sasaki, Y. F. *Single cell gel/comet assay: guidelines for in vitro and in vivo genetic toxicology testing*. Environ. Mol. Mutagen. **35**, 206–221 (2000).

11. Wojewodzka, M., Buraczewska, I. and Kruszewski, M. *A modified neutral comet assay: elimination of lysis at high temperature and validation of the assay with anti-single-stranded DNA antibody*. Mutat. Res. **518**, 9–20 (2002).

12. Schmid, E., Hieber, L., Heinzmann, U., Roos, H. and Kellerer, A. M. *Analysis of chromosome aberrations in human peripheral lymphocytes induced by in vitro alpha-particle irradiation*. Radiat. Environ. Biophys. **35**, 179–184 (1996).

13. Gomolka, M., Rossler, U., Hornhardt, S., Walsh, L., Panzer, W. and Schmid, E. *Measurement of the initial levels of DNA damage in human lymphocytes induced by 29 kV X rays (mammography X rays) relative to 220 kV X rays and gamma rays*. Radiat. Res. **163**, 510–519 (2005).

14. Roos, H. and Kellerer, A. M. *Design criteria and performance parameters of an alpha irradiation device for cell studies*. Phys. Med. Biol. **34**, 1823–1832 (1989).

15. Schunck, C., Johannes, T., Varga, D., Lorch, T. and Plesch, A. *New developments in automated cytogenetic imaging: unattended scoring of dicentric chromosomes, micronuclei, single cell gel electrophoresis, and fluorescence signals*. Cytogenet. Genome Res. **104**, 383–389 (2004).

16. Tanaka, K., Gajendiran, N., Endo, S., Komatsu, K., Hoshi, M. and Kamada, N. *Neutron energy-dependent initial DNA damage and chromosomal exchange*. J. Radiat. Res. (Tokyo) **40**, 36–44 (1999).

18. Yang Jianshe, Jing Xigang, Li Wenjian, Wang Zhuanzi, Zhou Guangming, Wang Jufang, Dang Bingrong, Gao Qingxiang & Walsh L. Correlation between initial chromatid damage and survival of various cell lines exposed to heavy charged particles. Radiat. Environ. Biophys. 45, 261-266, 2006

ORIGINAL PAPER

Correlation between initial chromatid damage and survival of various cell lines exposed to heavy charged particles

**Yang Jianshe · Jing Xigang · Li Wenjian ·
Wang Zhuanzi · Zhou Guangming · Wang Jufang ·
Dang Bingrong · Gao Qingxiang · Walsh Linda**

Abstract The biophysical characteristics of heavy ions make them a rational source of radiation for use in radiotherapy of malignant tumours. Prior to radiotherapy treatment, a therapeutic regimen must be precisely defined, and during this stage information on individual patient radiosensitivity would be of very great medical value. There are various methods to predict radiosensitivity, but some shortfalls are difficult to avoid. The present study investigated the induction of chromatid breaks in five different cell lines, including one normal liver cell line (L02), exposed to carbon ions accelerated by the heavy ion research facility in Lanzhou (HIRFL), using chemically induced premature chromosome condensation (PCC). Previous studies have reported the number of chromatid breaks to be linearly related to the radiation dose, but the relationship between cell survival and chromatid breaks is not clear. The major result of the present study is that cellular radiosensitivity, as measured by D_0, is linearly correlated with the frequency of chromatid breaks per Gy in these five cell lines. We propose that PCC may be applied to predict radiosensitivity of tumour cells exposed to heavy ions.

Introduction

Radiotherapy is one of the most effective methods for the treatment of malignant tumours. GSI in Germany and HIMAC in Japan have successfully treated hundreds of patients with carcinomas by using accelerated heavy ions [1]. Radiotherapy using heavy ions is expected to bear some advantages as compared to treatment involving X-rays and γ-rays, due to biophysical characteristics of heavy ions, such as high linear energy transfer (LET) at the Bragg peak region, low side-scattering, etc. Before clinical treatment can begin, the therapeutic regimen must be defined and during this stage information on individual patients' radiosensitivity would be of great medical value.

In the present study, we first evaluated the radiosensitivity of tumour tissue cells, because different cell types have different degrees of radiosensitivity depending on the source and type of radiation and associated physical characteristics such as LET. The evaluation of radiosensitivity in normal tissue cells is also important with regard to predicting the possible side effect of radiotherapy. Such side effects could limit the effective dose that should be delivered to the target volume. Several methods have been developed to measure cell radiosensitivity, for example, the colony assay [2–5] and the cytoplasm-blocked micronuclei assay [6]. Pre-

Y. Jianshe (✉) · J. Xigang · L. Wenjian · W. Zhuanzi ·
Z. Guangming · W. Jufang · D. Bingrong
Institute of Modern Physics,
Chinese Academy of Sciences,
Lanzhou 730000, China
e-mail: yangjs@impcas.ac.cn

J. Xigang
Graduate School of Chinese Academy of Sciences,
Beijing 100039, China

G. Qingxiang
Life Science School of Lanzhou University,
Lanzhou 730000, China

W. Linda
GSF National Research Center,
Institute of Radiation Protection,
85764 Neuherberg, Germany

vious data have shown that these two methods are not ideal. While the colony assay is a classic and precise method for detecting radiosensitivity, the formation of a colony takes at least 7 days. Conflicting views have been held concerning the detection of cell radiosensitivity with the cytoplasm-blocked micronuclei method. Some scientists find a good relationship between the number of radiation-induced micronuclei and cell radiosensitivity, but others do not agree [6, 7]. Consequently the authors decided to test if a quick and precise method for detecting tumour cell radiosensitivity could be developed based on chromatid damage scored immediately after irradiation.

Many researchers have found that chromosome damage is the main cause of cell death following irradiation [8]. In recent years, the chemically induced premature chromosome condensation (PCC) technique has been used to observe chromosome damage. This technique is effective and precise [9], and a maximum of 24 h is long enough to obtain the results. Durante et al. [10] and Kawata et al. [11–13] reported that the exposure of normal cells to radiation from heavy ions produced chromosome breaks, which were mainly of the chromatid and isochromatid types. The number of chromatid breaks was found to be linearly correlated with the absorbed dose of radiation. In comparison with experiments involving X-rays or γ-rays, more isochromatid breaks were produced by exposure to heavy ions, but no information was reported concerning the correlation between the cell survival fraction and the number of chromatid breaks. The reasoning behind the present study was that if a reliable relationship between these two indicators of cellular damage were to be found, then it may be possible to develop a quick method to quantify tumour radiosensitivity based on chromatid damage.

The heavy ion research facility in Lanzhou (HIRFL), a research centre for radiobiology, is currently preparing to accept the first cancer patients to receive radiotherapy using heavy ions. In the present study, several human cell lines of various tissues were selected for exposure to carbon ions generated by the HIRFL. The PCC technique was applied to investigate the quantity and nature of chromatid breaks induced by the radiation and the nature of relationship between the cell survival fraction and frequency of chromatid breaks.

Materials and methods

Cell culture and irradiation

Human hepatoma cell line SMMC-7721, normal liver cell line L02, gastric cancer cell line BGC-823, cervix carcinoma cell line HeLa, and melanoma cell line A375 (purchased from the Chinese Center for Type Culture Collection [CCTCC]) were grown in RPMI-1640 medium supplemented with 10% fetal calf serum at 37°C in 5% CO_2. For the L02 cell line 0.25 U/ml insulin (Sigma production) was added to the culture medium. Chromosome numbers of these cell lines were 46 (L02), 62 (SMMC-7721), 48 (BGC-823), 40 (HeLa), and 60 (A375).

Exponentially growing cells in plastic culture dishes were irradiated at room temperature with $^{12}C^{6+}$ ion beams generated by the HIRFL with a dose range from 0 to 8 Gy. The initial energy of $^{12}C^{6+}$ ions was 80.55 MeV/U, which was decreased by 13.58 mm Lucite ($\rho = 1.2$ g/cm^3) to 20 MeV/U before it reached the cells. The LET was calculated as 96 keV/μm at the position where the carbon ions interacted with the cells (Fig. 1). LET was calculated using the Trim Program 92, written by Bierstadt and Ziegler [14]. Dosimetry was performed with an air-ionizing chamber where the uniformity of the carbon ion beams was 85%, as measured by the CR39 technique.

Colony assay

After exposure to radiation, cells were washed three times using PBS (pH 7.0), treated with trypsin, and resuspended in 5 ml of culture medium; the cell titre was determined with a light microscope. At each dose, 200, 400, and 600 cells were seeded in duplicate into 60 mm diameter culture dishes, then 5 ml of RPMI-1640 medium supplemented with 10% fetal calf serum was added to the culture dishes, which were incubated
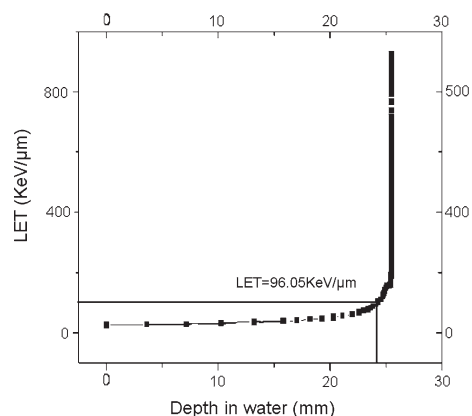
Fig. 1 The relationship between the range and LET of carbon ions generated from HIRFL, as calculated with TRIM

at 37°C in 5% CO_2 for 7–14 days to allow colony formation. Experiments were repeated three times. Results are given as mean ± standard error. The data were plotted using Origin 7.0 (Original lab, America). D_0 was calculated using $S = \exp - (\alpha D - \beta D^2)$.

Chromosome preparation

Calyculin A (BIOMOL America), used as the PCC inducer, was dissolved in 100% ethanol as a 1 mM stock solution. In order to induce PCC, calyculin-A was added to cell cultures 5 min before irradiation at a final concentration of 50 nM [15]. After irradiation, cells were incubated for a further 30 min at 37°C in 5% CO_2. For the chromosome spread cells were treated in 75 mM KCl for 20 min at 37°C and fixed with Carnoy's fixative. After a final wash and fixation with Carnoy's fixative, cells were dropped onto a glass slide and dried at 37°C and 85% relative humidity.

The cells were stained with 5% Giemsa (5 ml original Giemsa solution diluted with 47.5 ml 0.067 M Na_2HPO_4 and 47.5 ml 0.067 M KH_2PO_4) for 20 min. According to the standard criteria [16], more than 40 G_2-phase cells were scored for each dose level. Chromatid discontinuities, misalignments of the region distal to the lesion, and non-stained region longer than the chromatid width were considered as chromatid breaks. An isochromatid break was considered as two breaks that occurred at the same position on each of two sister chromatids, i.e. a lesion through the two q arms or p arms of the chromosome was regarded as an isochromatid break. A total of 20 non-irradiated cells were examined; Spontaneous chromatid breaks (mean ± SD) per cell were determined as: L02 (0 ± 0), SMMC-7721 (0.5 ± 0.01), BGC-823 (1.0 ± 0.01), HeLa (0.4 ± 0.02), A375 (0.5 ± 0.01). The mean number of chromatid breaks in non-irradiated cells was subtracted from the mean number observed in irradiated cells to provide the experimental data given in the next section.

Results

Cell survival fraction of five cell lines exposed to carbon ions

Figure 2 shows the survival curves of the five cell lines after irradiation with $^{12}C^{6+}$ carbon ions. An exponential survival curve without shoulder was observed. Among the five cell lines, L02 showed the highest survival after exposure, followed by SMMC-7721, BGC-823, HeLa, and A375. From the survival curves the D_0 values were determined (Table 1).
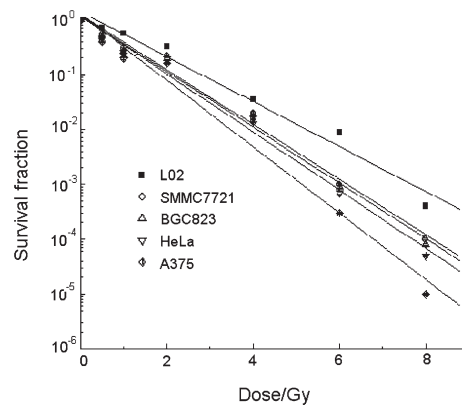
Fig. 2 Survival curves of five cell lines exposed to accelerated carbon ions. Curves were fitted with the Origin 7.0 software. The *error bars* represent standard errors of the mean. All experiments were repeated three times

Initial chromatid breaks induced by carbon ion irradiation

After exposure to carbon ion beams, both chromatid-type and isochromatid-type breaks were induced in chromosomes. The frequencies of chromatid and isochromatid breaks per cell are given in Table 2. Figure 3 illustrates the relationship between chromatid breaks and absorbed dose. The number of chromatid breaks increased linearly with increasing dose. The average number of isochromatid breaks at a given dose was much higher than that of chromatid-type breaks in all of the five cell lines; and the lowest number was seen for the L02 cell line.

The relationship between D_0 value and alpha coefficient

To determine the relation between cellular radiosensitivity and the frequency of chromatid breaks per cell

Table 1 D_0 values for the five cell lines exposed to carbon ions

Cell line	D_0 (Gy^{-1})	SD of D_0 (Gy^{-1})
L02	1.38	0.033
SMMC-7721	0.98	0.044
BGC-823	0.95	0.047
HeLa	0.86	0.032
A375	0.77	0.038

Table 2 Chromatid/isochromatid breaks of five cell lines exposed to carbon ions with different dose

Dose (Gy)	Chromatid breaks per cell					Isochromatid breaks per cell				
	L02	SMMC-7721	BGC-823	HeLa	A375	L02	SMMC-7721	BGC-823	HeLa	A375
0	0 ± 0	0 ± 0.01	0 ± 0.01	0 ± 0.02	0 ± 0.01	0 ± 0	0 ± 0.01	0 ± 0.01	0 ± 0.02	0 ± 0.01
0.5	1.0 ± 0	1.2 ± 0.01	1.5 ± 0.01	1.7 ± 0.02	2.1 ± 0.02	2.0 ± 0	3.0 ± 0.01	5.0 ± 0.1	7.0 ± 0.01	10 ± 0.02
1	1.8 ± 0	1.6 ± 0.02	2.9 ± 0.01	3.2 ± 0.2	4 ± 0.02	4 ± 0	6 ± 0.2	9 ± 0.01	12 ± 0.2	15 ± 0.02
2	4 ± 0	5.4 ± 0.01	6 ± 0.02	6.5 ± 0.02	7 ± 0.02	9 ± 0	12 ± 0.02	17 ± 0.04	21 ± 0.04	25 ± 0.02
4	9.2 ± 0	13 ± 0.04	15 ± 0.1	17 ± 0.02	16 ± 0.03	20 ± 0	26 ± 0.04	27 ± 0.02	29 ± 0.1	38 ± 0.06
6	14.6 ± 0	22 ± 0.03	24 ± 0.02	27 ± 0.2	32 ± 0.06	36 ± 0	40 ± 0.1	44 ± 0.5	49 ± 0.3	55 ± 0.02
8	19.5 ± 0.01	29 ± 0.02	32 ± 0.1	35.2 ± 0.04	39.6 ± 0.2	45 ± 0.02	54 ± 0.05	58 ± 0.2	61 ± 0.06	70 ± 0.04

Fig. 3 The relationship between chromatid breaks (*left*) and isochromatid breaks (*right*) and absorbed dose. The *error bars* are standard errors of the mean. Experiments were repeated three times
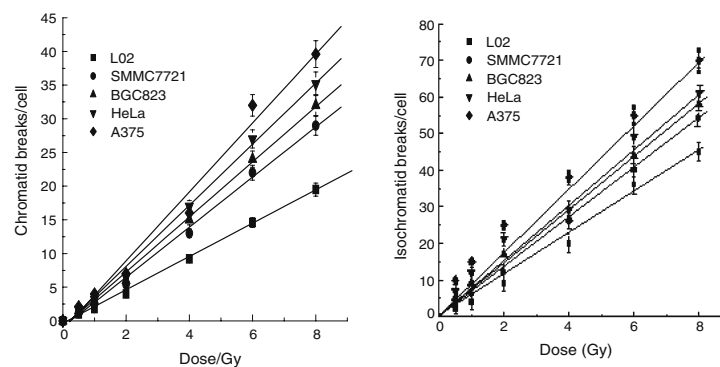
and per Gy, the alpha coefficients (slopes) of the chromatid and isochromatid break induction curves shown in Fig. 3 were plotted against the D_0 values determined in Fig. 2. The relevant data were fitted and it was found that D_0 value of the five cell lines was highly linearly correlated with alpha coefficients; meanwhile, a nearly linear relationship was also found when isochromatid breaks were considered.

Discussion

Chromosomes are the key targets when cells are exposed to radiation, and chromatid damage is linked directly to the biological fate of the cells. The PCC technique is one of the most reliable and sensitive methods available for measuring radiation-induced damage in cells. Recently, a chemically induced PCC technique using calyculin-A was introduced by Gotoh et al. [15] and Durante et al. [9]. Chromatid-type aberrations in G_2-phase rodent cells have been studied using this technique [17]. Kawata et al. [18] have studied human normal cells exposed to low LET radiation

and to accelerated heavy charged particles such as carbon ions and silicon ions. They found that heavy ions were much more effective than γ-rays at inducing isochromatid breaks. When one isochromatid break was scored as two breaks, the ratio of the number of isochromatid breaks to the total number of chromatid breaks increased with increasing LET. This result led them to conclude that increased induction of isochromatid breaks is a valid reflection of exposure to high-LET radiation.

Near 100 keV/μm, heavy ions have the largest RBE value. In the present study, the LET value of carbon ions was 96 keV/μm; the ion beam induced the greatest number of chromatid breaks, especially isochromatid breaks. The results of chromatid breaks induced by carbon ions in the present study were in good agreement with the results of Kawata et al. [11–13, 18]. Although these authors studied human normal fibroblast cells, the type and number of chromatid breaks of the five cell lines in the present study were nearly the same as in their results. Previous studies have reported that radiosensitivity correlates with the induction of DNA damage. Is there some inner relationship between the DNA
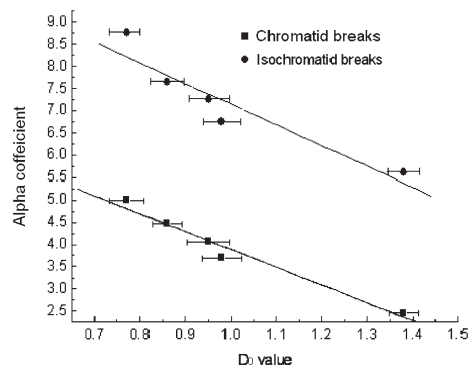
Fig. 4 The relationship between D_0 value and the alpha coefficient of fitted lines in Fig. 3. All data points from *left to right* represent L02, SMMC-7721, BGC-823, HeLa and A375 cell lines. The *error bars* are standard errors of the mean

damage and chromatid breaks when cells are exposed to different types of radiation? It is well known that the chromosome is the higher topological structure of DNA, and that radiation interacts with DNA resulting in chromatid breakages [19]. From Fig. 3 it can be seen that most of the chromatid breaks were of the isochromatid type, occurring almost twice as frequently as the chromatid-type breaks. Also, the relationship between absorbed dose and survival fraction (Fig. 2) and between absorbed dose and chromatid breaks (Fig. 3) was linear. All the data mentioned above support the suggestion that chromatid breaks exposed by the chemically induced PCC technique could be considered as a reflection of damage in cells exposed to heavy ions. In this study the relationship between cell survival fraction and chromatid breaks has been determined and found to be of potential usefulness in predicting cell radiosensitivity by the PCC method. While the D_0 value is a good marker reflecting the radiosensitivity of different cells to radiation, the alpha coefficient of the linear relation between chromatid/isochromatid breaks and absorbed dose reflects the capacity with which heavy ions induce chromatid/isochromatid breaks in different cell lines. The results in the present study show (Fig. 4) that the D_0 values of the five cell lines correlated linearly with the alpha coefficients. This result may lead to a possible method for predicting radiosensitivity of tumours exposed to heavy ions. More cell types will be investigated in future work in order to confirm and extend these results.

References

1. Kraft G (2000) Tumor therapy with heavy charged particles. Prog Part Nucl Phys 45:s473–s544
2. Girinsky T, Bernheim A, Lubin R, Tavakolirazavi T, Baker F, Janot F, Wibault P, Cosset JM, Duvillard P, Duverger A (1994) In vitro parameters and treatment outcome in head and neck cancers treated with surgery and/or radiation: cell characterization and correlation with local control and overall survival. Int J Radiat Oncol Biol Phys 30:789–794
3. West CM, Davidson SE, Burt PA, Hunter RD (1995) The intrinsic radiosensitivity of cervical carcinoma: correlations with clinical data. Int J Radiat Oncol Biol Phys 31:841–846
4. West CM, Davidson SE, Roberts SA, Hunter RD (1997) The independence of intrinsic radiosensitivity as a prognostic factor for patient response to radiotherapy of carcinoma of cervix. Br J Cancer 76:1184–1190
5. Rosenblum ML, Knebel KD, Wheeler KT, Barker M, Wilson CB (1975) Development of an in vitro colony formation assay for the evaluation of in vivo chemotherapy of a rat brain tumor. In Vitro 11:264–273
6. Eastham AM, Atkinson J, West CM (2001) Relationship between clonogenic cell survival, DNA damage and chromosomal radiosensitivity in nine human cervix carcinoma cell lines. Int J Radiat Biol 77:295–302
7. Guo GZ, Sasai K, Oya N, Shibata T, Shibuya K, Hiraoka M (1999) A significant correlation between clonogenic radiosensitivity and the simultaneous assessment of micronucleus and apoptotic cell frequencies. Int J Radiat Biol 75:857–864
8. Cornforth MN, Bedford JS (1993) Ionizing radiation damage and its early development in chromosomes. Adv Radiat Biol 17:423–427
9. Durante M, Furusawa Y, Gotoh E (1998) A simple method for simultaneous interphase–metaphase chromosome analysis in biodosimetry. Int J Radiat Biol 74:457–462
10. Durante M, Frusawa Y, George K, Gialanella G, Greco O, Grossi G, Matsufuji N, Pugliese M, Yang TC (1998) Rejoining and misrejoining of radiation-induced chromatin breaks. IV. Charged particle. Radiat Res 149:446–454
11. Kawata T, Durante M, Frusawa Y, George K, Takai N, Wu H, Cucinotta FA (2001) Dose–response of initial G_2-chromatid breaks induced in normal human fibroblasts by heavy ions. Int J Radiat Biol 77:165–174
12. Kawata T, Durante M, Furusawa Y, George K, Ito H, Wu H, Cucinotta FA (2001) Rejoining of isochromatid breaks induced by heavy ions in G2-phase normal human fibroblasts. Radiat Res 156:598–602
13. Kawata T, Ito H, Uno T, Saito M, Yamamoto S, Furusawa Y, Durante M, George K, Wu H, Cucinotta FA (2004) G_2 chromatid damage and repair kinetics in normal human fibroblast cells exposed to low- or high-LET radiation. Cytogenet Genome Res 104:211–215
14. Ziegler JF, Biersack JP, Littmark U (1985) The stopping and range of ions in solids. Pergamon Press, Oxford
15. Gotoh E, Kawata T, Durante M (1999) Chromatid break rejoining and exchange aberration formation following γ-ray exposure: analysis in G_2 human fibroblasts by chemical-

induced premature chromosome condensation. Int J Radiat Biol 75:1129–1135

16. Savage JR (1976) Classification and relationships of induced chromosomal structural changes. J Med Genet 13:103–122

17. Hieber L, Lücke-Huhle C (1983) PCC technique reveals severe chromatin lesions and repair in G_2-arrested cells after alpha irradiation. Exp Cell Res 144:57–62

18. Kawata T, Gotoh E, Durante M, Wu H, George K, Furusawa Y, Cucinotta FA (2000) High-LET radiation-induced aberrations in prematurely condensed G_2 chromosome of human fibroblasts. Int J Radiat Biol 76:929–937

19. Wurm R, Burnet NG, Duggal N, Yarnold JR, Peacock JH (1995) Cellular radiosensitivity and DNA damage in primary human fibroblasts. Int J Radiat Oncol Biol Phys 15:553–554

19. Stephan G, Schneider K, Panzer W, Walsh L & Oestreicher U. Enhanced yield of chromosome aberrations after CT examination in paediatric patients. Int. J. Radiat. Biol. 83(5), 281-287, 2007

informa
healthcare

Enhanced yield of chromosome aberrations after CT examinations in paediatric patients

G. STEPHAN[1], K. SCHNEIDER[2], W. PANZER[3], L. WALSH[3], & U. OESTREICHER[1]

[1]*Federal Office for Radiation Protection, Oberschleissheim,* [2]*Department of Pediatrics, University of Munich, and* [3]*Institute of Radiation Protection, GSF-National Research Center for Environment and Health, Neuherberg, Germany*

Abstract

Purpose: To determine whether computed tomography (CT) could enhance the chromosome aberration yields in paediatric patients.
Material and methods: Blood samples were taken before and after CT scans from 10 children for whom the medical justifications for CT examinations were accidental injuries and not diseases as investigated in earlier studies. Chromosome analysis was carried out in lymphocytes by fluorescence plus Giemsa (FPG) staining exclusively in metaphases of the first cell cycle *in vitro*.
Results: The mean blood dose of the 10 children was about 12.9 mGy which was determined by a newly developed dose estimation. Based on more than 20,000 analyzed cells it was found that after CT examination the frequencies of dicentrics (dic) and excess acentric fragments (ace) in lymphocytes were significantly increased. By subdividing the children into two age groups, those with an age from 0.4 years to 9 years and from 10–15 years, it became obvious that the observed increase in chromosome aberrations was mainly contributed by the younger age group. In this group the frequency of dicentrics was significantly increased whereas in the older group the observed increase was not significant.
Conclusion: Our results demonstrate that CT examinations enhance the dicentrics yields in peripheral lymphocytes of children aged up to 15 years. Since in particular significantly increased dicentric yields could be observed in children with an age from 0.4–9 years, it can be assumed that children younger than 10 years may be more radiation sensitive than older subjects.

Keywords: *Children, CT, x-rays, chromosome aberrations, low level effects*

Introduction

The rapidly increasing widespread use of computed tomography (CT) in the past two decades has led to scientific concern about its potential human health hazards. Although CT scans, especially paediatric examinations, have resulted in advantages in diagnostic radiology, it is well-known that they generally produce higher radiation doses than other medical x-ray examinations. Since the resulting organ doses are higher in a child than in a larger adult, for a given instrumental setting of a CT-machine, and due to the increased lifetime risk of a child per unit dose, Brenner (2002) suggested 'as the best available risk estimates that paediatric CT will result in significantly increased lifetime radiation risk over adult CT'.

Biological radiation effects induced by CT examinations can therefore be expected to be more pronounced in children than in adults. In particular, chromosome aberrations are of great concern as they are involved in the mechanism of cancer genesis. It has been shown that an increased level of chromosome aberrations in peripheral lymphocytes may be an indication of an enhanced cancer risk (Hagmar et al. 1998). If such cytogenetic effects are produced by CT examination, it is important to evaluate whether they can be attributed to the calculated blood dose in combination with the contrast medium effect. Iodised contrast media has been shown to enhance the radiation effect in a way that depends on the concentration of the contrast medium and on the energy of the x-rays (Hadnagy et al. 1982).

Correspondence: U. Oestreicher, Federal Office for Radiation Protection, Ingolstaedter Landstr. 1, D-85764 Oberschleissheim, Germany.
E-mail: uoestreicher@bfs.de

Compared with the extensive results on the induction of cytogenetic effects in human cells obtained *in vitro* and *in vivo* when iodized contrast media have been used concomitantly with medical x-ray examinations (summarized by Joubert et al. 2005), relatively little information is available on the corresponding effects of CT scans *in vitro* and *in vivo* (Weber et al. 1995, M'kacher et al. 2003). Moreover, up to now such an investigation of the cytogenetic effects in children after CT examinations in the presence of iodized contrast media has not been published. Consequently, the purpose of the present study was to investigate and quantify the detrimental cytogenetic effects in children undergoing CT examinations, using especially the frequency of dicentrics in peripheral lymphocytes as the most sensitive and characteristic bioindicator of human radiation exposure. A further important point was to investigate for the first time only children for whom the medical justifications for CT examinations were accidental injuries and not diseases, i.e., CT scans were considered necessary in order to establish a proper treatment. Due to this selection the results of such a study could be ranked higher than the findings in the earlier cases because it was not always determined whether similar biological effects occurred also in patients without diseases.

Materials and methods

Patients and blood sampling

Chromosome aberrations were investigated before and after the CT scan in 10 children (5 boys, 5 girls). They were between 5 months and 15 years of age (median: 8.4 years) and had no previous exposure to ionizing radiation before the diagnostic CT scan. In combination with the CT scan different contrast media were used: Accupaque (Amersham, UK),

Solutrast 300 (Altana, Konstanz, Germany), Imagopaque (Amersham, UK). Contrast medium of between 2.1 ml and 3.1 ml per kg body weight was administered intravenously. The patient data and CT exposure conditions are given in Table I. For chromosome analysis, blood samples were taken immediately before and after (about 20 min) the CT scans. From all parents a written informed consent to the participation of their children was obtained according to the declaration of Helsinki, and the design of the work has been approved by the ethical committee of the Paediatric Hospital of the University of Munich.

Blood culture conditions and chromosome analysis

Blood cultures were set up within 3 h after sampling. The technique used to culture the lymphocytes was similar to our standard conditions which have been fully described earlier (Stephan & Pressl 1999): 0.5 ml whole blood, 4.5 ml Roswell Park Memorial Institute (RPMI)-1640 medium (Biochrom, Berlin, Germany) supplemented with 10% (v/v) of foetal calf serum (Biochrom, Berlin, Germany), 2 mM glutamine and antibiotics (Biochrom, Berlin, Germany), 2% phytohaemagglutinin (PHA) (Biochrom, Berlin, Germany). The cultures were incubated for 48 h in the presence of 10 mM bromodeoxyuridine (BrdU) (Sigma-Aldrich, Munich, Germany). The cultures were incubated for 48 h at 37°C. For the final 3 h, 0.1 μg ml^{-1} Colcemid (Roche, Mannheim, Germany) was present. After hypotonic treatment with 75 mM KCL (Merk, Darmstadt, Germany), the cells were fixed in methanol-acetic acid (3:1).

These culture conditions ensured that the chromosome analysis was performed exclusively in metaphases of the first cell cycle *in vitro*. Chromosome preparation and fluorescence plus Giemsa (FPG) staining were carried out according to our

Table I. Patient data and exposure conditions.

Patient	Age (y)	Gender (m, f)	Weight (kg)	Examination	CT[a] scanner	Tube voltage (kV)	Q[b] (mAs)	Pitch	Length of scan (cm)	Contrast medium	ml
1	0.42	m	1.9	Thorax	Aura	120	50	1	2	Solutrast 300	5
2	2	m	13	Thorax	TS M	120	100	1	10	Accupaque	40
3	3	f	17	Thorax[c]	Aura	130	90	1	0.7	–	0
4	5	f	18	Thorax	TS M	120	90	1.3	21	Solutrast 300	42
5	9	m	29	Abdomen	TS M	120	60	1.5	27	Accupaque	75
6	11	m	43	Thorax	Aura	120	40	1.5	24	Imagopaque	70
7	11	m	48	Abdomen	Aura	120	60	1.5	35	Imagopaque	100
8	11	f	33	Thorax	Aura	120	35	1.5	23	Imagopaque	80
9	12	f	37	Thorax	TS M	120	60	1.5	22	Accupaque	85
10	15	f	41	Thorax	TS M	120	60	1.5	24	Solutrast 300	80

[a]Both multi slice spiral CT scanners were made by Philips; [b]Q = tube current × time per tube rotation; [c]high resolution CT, 7 slices with slice thickness of 1 mm.

laboratory procedures (Stephan & Pressl 1999) and all slides were coded. Although the frequencies of different structural aberrations of the chromosome-type (dicentrics, centric rings, excess acentrics) and of the chromatid-type (breaks, exchanges) were determined, in the present study only the data for dicentrics (dic) and excess acentrics (ace) were used in the quantitative analysis. For scoring of ace, only one acentric fragment (assuming a complete exchange process) was assigned to each exchange.

Statistical analysis

Statistical analysis was carried out for dicentrics and excess acentrics. The Wilcoxon test for paired observations (Wilcoxon & Wilcoxon 1964) was used to test the null hypothesis that the values in two populations are not different in level, or magnitude, for two samples collected as paired observations. It is a more powerful test than the sign test and can be applied here to test a hypothesis connected with a possible radiation effect on the cytogenetic status of the paediatric patients before and after CT scans. Statistical procedures associated with testing the difference between the means of two populations follows the basic steps in hypothesis testing where the relevant standard error is the standard error of the difference between two population means. Use of the normal distribution for testing the difference between mean aberration frequencies is appropriate here even though the aberrations are usually Poisson distributed because the central limit theorem can be invoked.

Determination of mean dose to blood by CT scan

The dosimetric task in this study was, to estimate the mean dose to the blood containing contrast medium for individual patients of different age and size, undergoing thorax or abdomen examinations under different exposure conditions (Table I). The mean dose to blood in this situation is the interesting quantity, because at the time when the blood after the CT-examination was withdrawn, a complete mixture of irradiated blood with non- irradiated blood had already occurred. A dosimetric approach was developed to estimate mean dose to blood. Blood in this approach is formally treated like an organ. The blood in the thoracic region receives a similar mean dose to the lungs and the blood in the abdominal region receives a similar mean dose to the small intestines. This is because lungs and small intestines are extended organs, which cover wide parts of the respective body regions and because the depth dose profiles from scanners with $360°$ tube rotation are comparatively flat.

The mean dose D(blood,c) to blood containing contrast medium was determined from Equation 1:

$$D(blood, c) = CTDI_{air}/p \times L \times f_c(organ)_m \times f_{blood} \times k_{CT} \times d_e \quad (1)$$

where $CTDI_{air}$ is airkerma free in air on the axis of rotation (mGy); p, pitch; L, length of the scan (cm); $f_c(organ)_m$, mean organ dose conversion coefficient per unit of $CTDI_{air}$ for the selected organ when the patient is exposed to a single slice of 1 cm thickness across this organ (cm^{-1}); f_{blood}, portion of blood in the body region (thorax, abdomen) in which the examination occurred; k_{CT}, correction factor typical for the used CT scanner; and d_e, factor describes the increase of absorbed dose in blood due to the presence of contrast agent.

$CTDI_{air}$ was determined from Equation 2:

$$CTDI_{air} = {}_nCTDI_{air} \times Q \quad (2)$$

$_nCTDI_{air}$ is an apparatus specific quantity. It amounts to 0.50 mGy/mAs for the CT scanner TS M operated at a tube voltage of 120 kV and to 0.43 mGy/mAs or to 0.50 mGy/mAs for the scanner Aura operated at 120 kV or 130 kV (Nagel et al. 2000, Stamm & Nagel 2002). Values for Q, the product of tube current and time per tube rotation, stem from the hospital records (Table I). The same holds for the values for p and L in Equation 1.

The mean organ dose conversion coefficient $f_c(organ)_m$ was derived from data sets containing calculated organ dose conversion coefficients $f_c(organ,z)$ from top to bottom for the mathematical human phantoms BABY /4/, CHILD (Zankl et al. 1993) and EVA (Zankl et al. 1991). Values $f_c(organ,z)$ express the mean organ dose per unit of $CTDI_{air}$, when the phantom is exposed to a 1 cm slice at position z of the phantoms length axis. $f_c(organ)_m$ was formed by averaging $f_c(organ,z)$ over those slices which contain more than 10% of the organ volume (5% in case of the lungs of EVA). For these slices the $f_c(organ,z)$ values vary only slightly, thus justifying the average formation. Table II shows the resulting values for $f_c(organ)m$ for the phantoms

Table II. Mean organ dose conversion coefficients $f_c(organ)_m$ for a single 1 cm slice. Tube voltage 125 kV, filtration 2.2 mm Al + 0.2 mm Cu, focus to axis distance 75 cm, no beam shaping.

	BABY (4.2 kg)	CHILD (21.7 kg)	EVA (59.2 kg)
Organ		$f_c(organ)_m$	
Lungs	0.13	0.078	0.039
Small intestines	0.15	0.069	0.050

BABY, CHILD and EVA. Since the patients age and weight (Table I) differ from the phantoms, the $f_c(organ)_m$ required in Equation 1, had to be interpolated from exponential decay curves, fitted to the $f_c(organ)_m$ as a function of weight (Table II). The values for the individual patients are listed in Table III.

The portion of blood in the respective regions is quantified by the factor f_{blood}. The International Commission on Radiological Protection (ICRP) reports in publication 23 (ICRP 23, 1975) that for adults 52% and 21% of the total blood volume can be apportioned to the thoratic and splanchnic blood pools, respectively. In ICRP publication 89 (ICRP 89, 2003) blood volumes in various organs and vessels are quoted itself of regional blood pools. Adding such blood volumes for adult thorax and abdomen results in 36% and 26% of the total blood volume being attributed to the thoracic and abdominal pools, respectively. Kozlik-Feldmann et al. (1998) report a thoracic blood volume of 30% for children of weight between 7.5 and 23 kg. Considering these discrepancies, it was decided to use a f_{blood} value of 0.3 for both the thoracic and the abdominal region.

The values for $f_c(organ,z)$ were calculated for a CT scanner with a focus to axis distance of 75 cm, a tube voltage of 125 kV and a filtration of 2.2 mm Al + 0.2 mm Cu, without beam shaping (Zankl et al. 1991, 1993). TS M (focus to axis distance 47.5 cm; beam filtration 3 mm Al) and Aura (focus to axis distance 51.5 cm; beam filtration 1.5 mm Al + 0.07 mm Cu) differ markedly from this scanner. However, there are correction factors k_{CT} available (Stamm & Nagel 2002), taking into account differences in scanner geometry and the effects of beam shaping and filtration for patient dose calculations. For TS M k_{CT} amounts to 0.8 and for Aura to 0.7.

Table III. Mean organ dose conversion coefficients, $f_c(organ)_m$; total blood volume; iodine concentration C in blood; absorbed dose enhancement factor, d_e and mean dose to blood D(blood,c).

Patient	$f_c(organ)_m$	Total blood (l)	C (g/g)	d_e	D(blood,c) (mGy)
1	0.139	0.15	0.0103	2.17	2.8
2	0.101	1.03	0.0117	2.33	28.3
3	0.090	1.34	–	1.00	1.2
4	0.088	1.39	0.0090	2.03	31.3
5	0.061	2.31	0.0097	2.11	16.7
6	0.050	3.20	0.0066	1.75	5.1
7	0.051	3.28	0.0092	2.04	13.3
8	0.061	2.25	0.0106	2.21	6.6
9	0.056	2.75	0.0093	2.06	12.3
10	0.052	3.05	0.0079	1.90	11.4

The determination of d_e is based on the fundamental dosimetric relation:

$$D(blood, c) = \frac{(\mu_{en}/\rho)_{blood,c}}{(\mu_{en}/\rho)_{blood}} \times D(blood) = d_e \times D(blood) \quad (3)$$

with D(blood) the dose to blood without contrast agent and $(\mu_{en}/\rho)_{blood,c}$ and $(\mu_{en}/\rho)_{blood}$ the respective mass energy absorption coefficients of blood with and without contrast agent. $(\mu_{en}/\rho)_{blood,c}$ can be calculated from $(\mu_{en}/\rho)_{blood}$ along:

$$(\mu_{en}/\rho)_{blood,c} = (1 - C) \times (\mu_{en}/\rho)_{blood} + C \times (\mu_{en}/\rho)_{iodine} \quad (4)$$

with $(\mu_{en}/\rho)_{iodine}$ the mass energy absorption coefficient of iodine and C the concentration of iodine in blood. From Equations 3 and 4 follows:

$$de = (1 - C) + C \times \frac{(\mu_{en}/\rho)_{iodine}}{(\mu_{en}/\rho)_{blood}} \quad (5)$$

The values for C in Equations 4 and 5 result from the amount of administered contrast medium (Table I), the concentration of iodine in the contrast agent (300 mg/ml for all the three agents) and the total blood volume of the patients. Total blood volume of the individual patients was derived from the weight of the patients (Table I) and from Linderkamp et al. (1977) where blood volumes per kg body weight (ml/kg), are provided for children of age 0 – 14 years and for both genders. The individual total blood volumes and iodine concentrations C are listed in Table III.

The mass energy absorption coefficients for blood and iodine in Equation 5 represent average values, which were calculated from the respective energy dependent $(\mu(E)_{en}/\rho)$ values for blood and iodine (Hubbell & Seltzer 1995) by integration over the energy fluence spectra emitted by the CT-units. These spectra are nearly identical, consequently the ratio $(\mu_{en}/\rho)_{iodine}/(\mu_{en}/\rho)_{blood}$ is the same for both units. It amounts to 115. The individual values for d_e, resulting from Equation 5, are listed in Table III. The finally resulting mean doses to blood D(blood,c) are presented in Table III. It should be mentioned, that for patient 3 the application of Equations 1 and 2 leads to a D(blood) value of only 0.6 mGy instead of the listed 1.2 mGy, but for such thin slices the irradiated slice is commonly broader than the recorded nominal slice thickness by a factor of 2.

Results

The results of the chromosome analysis of dicentrics and excess acentrics in 10 children before and after

CT examination are presented in Table IV. Centric rings could not be observed. Applications of the Wilcoxon procedure, described above, to test the hypothesis that there was no cytogenetic detrimental radiation effect at the 5% level of significance (a one-tailed test) for both aberration types yielded the following results. For dicentrics and excess acentric fragments (sample size of 9, critical value of the Wilcoxon statistic is 8) the calculated values of the Wilcoxon test statistics are 3 and 7 respectively leading to a rejection of the hypothesis. Note that the sample sizes used was 9 even though there were 10 children because tied observations must be dropped from the Wilcoxon test procedure and there were tied observations in subject number 7 and 8 for dicentric and acentric fragment data respectively. There were some difficulties associated with the cell sample size analysed for child number 1, where only

49 cells were examined before CT and 398 cells after CT. Since these sample sizes are much smaller than the others of about 1000 cells, the Wilcoxon test was also performed excluding this child. In this case, the test outcome did not change for dicentrics, but the null hypothesis of no cytogenetic detrimental radiation effect can not now be rejected at the 5% level of significance for the excess acentric fragments.

A total of 10,313 cells were analyzed before the CT examination (Table IV). The mean frequencies of dicentrics and excess acentric fragments were found to be 0.39 ± 0.19 dic/1000 cells and 1.65 ± 0.40 ace/1000 cells, respectively. All of the results here are quoted with standard errors of the mean, where these have been calculated by the usual method of error propagation where differences or quotients of aberration frequencies have been stated. After the CT examination which has resulted in a mean blood dose of about 12.9 mGy a total of 10,558 cells have been analyzed. The mean frequency for dicentrics is 1.33 ± 0.35 dic/1000 cells and for excess ace fragments is 2.75 ± 0.51 ace/1000 cells. In comparison to the corresponding frequencies of aberrations observed before the CT scan, a significant increase was only found for the dicentric yield ($p = 0.02$). The difference in the mean dicentric frequency observed before and after the CT scan represents the dicentric frequency which is caused by the CT examination, i.e., 0.94 ± 0.4 dic/1000 cells. The dose response curve for the individual differences in the dicentric yield observed before and after the CT scan is given in Figure 1. The data have been fitted by weighted least squares and give the following dose response which is marked as a dashed line: Mean number of dicentrics per cell $= (2.82 \pm 3.26) \times 10^{-5} \times$ mean blood dose in

Table IV. Frequencies of chromosomal aberrations in children who underwent computed tomography (CT).

Patient	D(blood,c) (mGy)	Before CT			After CT		
		Cells	Dic	Ace	Cells	Dic	Ace
1	2.8	49	0	0	398	1	2
2	28.3	1520	0	4	1527	1	4
3	1.2	1634	1	2	1330	1	4
4	31.3	934	0	1	899	2	1
5	16.7	1079	0	2	1543	4	7
6	5.1	1011	0	1	1052	1	3
7	13.3	1010	0	0	1024	0	1
8	6.6	1059	1	0	1034	0	0
9	12.3	1012	2	3	1010	3	6
10	11.4	1004	0	4	741	1	1
	mean 12.9 Σ	10313	4	17	10558	14	29

Dic, dicentrics; Ace, excess acentrics.
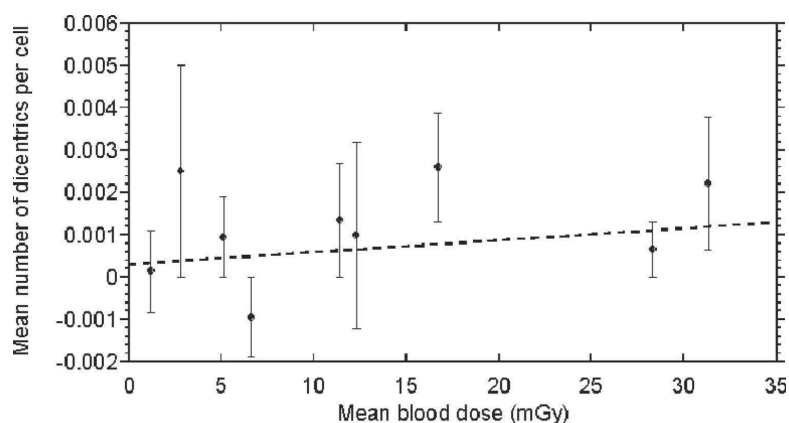
Figure 1. The difference in the mean number of dicentrics per cell as a function of mean blood dose with one standard error bars. For each child, the mean number of dicentrics per cell before CT scan has been subtracted from the mean number after CT scan.

mGy + (3.04 ± 6.06) × 10^{-4}. Note that the data for child number 7 with a mean blood dose of 13.3 mGy has been excluded from the plot and the weighted least squares fit. This is because no dicentrics were found before or after CT scan and so the Poisson error associated with this measurement can only be determined as zero and this would force the weighted fit to pass exactly through the point (13.3, 0). Although a tendency for increasing yields of dicentrics with the applied dose is recognisable, a significant increase could not be calculated.

When the 10 children, however, are subdivided into age groups of older and younger than 10 years it became clear that the younger age group show a more pronounced increase in chromosomal aberrations by CT scans than the older age group. In the age group 10 – 15 years (5 children with a mean age of 12 years), the increased frequency of dicentrics is not significantly different from 0.59 ± 0.34 dic/1000 cells to 1.03 ± 0.46 dic/1000 cells. However in the age group 0.4 – 9 years (5 children with a mean age of 3.9) a significant increase of the dicentric yield from 0.19 ± 0.19 dic/1000 cells to 1.58 ± 0.53 dic/1000 cells was observed ($p = 0.013$). In the frequencies of excess acentric fragments before and after CT examination there is no significant difference between the two age groups (older age group: 1.57 ± 0.55 and 2.26 ± 0.68; younger age group: 1.73 ± 0.58 and 3.16 ± 0.74). In consequence, the observed significant increase in chromosome aberrations produced by CT scan in all investigated children is mainly influenced by the younger age group. However, it has to be taken into account that the children in the younger age group have a calculated mean blood dose of 16.1 mGy, which is higher by a factor of 1.7 than the mean dose of 9.7 mGy for the children in the older age group.

Discussion

Earlier data on chromosome aberrations in peripheral lymphocytes after CT scans have only been obtained in adult patients. Unexpectedly high yields of dicentrics and centric rings were observed in five adult patients extensively exposed to diagnostic x-rays, i.e., many photographs and fluoroscopies were made in each case, partly combined with CT examinations and the use of iodised contrast media (Weber et al. 1995). Due to these combined diagnostic examinations a direct comparison of the chromosome aberration yields with those of the present study appears to be not justified. However, using premature chromosome condensation (PCC) combined with fluorescence in situ hybridization (FISH), a significant increase in the frequency of chromosomal fragments in peripheral blood lymphocytes of 10 adult patients with different carcinomas was also observed immediately after CT scans. In contrast, no significant increase in structural chromosome aberration yields could be observed by applying FISH technique to metaphase spreads (M'kacher et al. 2003). This cell cycle stage-dependent appearance of chromosome aberrations indicates that, in fact, CT scans produce chromosome alterations in interphases, but many of them may have been repaired before arriving at the metaphase stage. Therefore, the significantly enhanced dicentric yields obtained in the blood of the 10 children, especially of the younger age group, are not in agreement with the earlier results determined by FISH staining in metaphase spreads after CT examinations of adult patients.

The earlier observations together with the present findings, in particular the findings determined for the younger age group, require an additional consideration that is related to the problem of radiation sensitivity. There may be obviously a tendency that children are more radiation sensitive than adults undergoing CT examinations, even if one considers that in the present study the calculated mean blood dose of 16.1 mGy for children in the younger age group was higher by a factor of 1.7 than the mean dose of 9.7 mGy for the children in the older age group. Controverse observations to this assumption seem to be found by Leonard et al. (1995). They gave chromosome aberration data in lymphocytes of 9 children (aged 5 – 12 years) with different types of malignant diseases treated with total-body high-energy photon irradiation, and corresponding data in lymphocytes of 2 healthy adults and 2 children exposed under the same irradiation conditions. There was no significant difference in the dose-effect relationships for dicentrics after irradiation of lymphocytes of children *in vivo* and *in vitro* and those of the adults *in vitro*. However, these results should be considered with some restrictions, because the mean dicentric yield of 27.7 ± 5.5 dic/1000 cells (25 dicentrics in 901 analysed cells) observed before radiation exposure of the 9 children was extremely high. In contrast, for our 10 children for whom the medical justifications for CT examinations were accidental injuries and not diseases, only a mean dicentric yield of 0.39 ± 0.19 dic/1000 cells was observed before CT. This control value is only half of that previously observed in our laboratory in an adult control group, 0.95 ± 0.14 dic/1000 cells (Stephan & Pressl 1999). For example, similar low control values for children could be observed by Padovani et al. (1993). However, it should be taken into account that such low control values were found even in adults, as it was discussed by Stephan and Pressl (1999) by summarizing control values of the literature.

Conclusion

Our results demonstrate that CT examinations enhance the dicentrics yields in peripheral lymphocytes of children aged up to 15 years. Since in particular significantly increased dicentric yields could be observed in children with an age from 0.4 – 9 years, it can be assumed that children younger than 10 years may be more radiation sensitive than older subjects. Consequently, the investigated children < 10 years of age may be a group with an increased potential risk in accordance with Hagmar et al. (1998) and as proposed by ICRP 68 (1994), since the children show an increased level of chromosome aberrations and they have many proliferating tissues, which are necessary for the manifestation of a mutation to give rise of the development of a carcinoma.

References

Brenner DJ. 2002. Estimating cancer risks from pediatric CT: Going from the qualitative to the quantitative. Pediatric Radiology 32:228 – 231.

Hadnagy W, Stephan G, Kossel F. 1982. Enhanced yield of chromosomal aberrations in human peripheral lymphocytes in vitro using contrast media in x-irradiation. Mutation Research 104:249 – 254.

Hagmar L, Bonassi S, Stromberg U, Brogger A, Knudsen L, Norppa H, et al. and the European Study group on Cytogenetic Biomarkers and Health. 1998. Chromosomal aberrations in lymphocytes predict human cancer: A report from the European Study Group on Cytogenetic Biomarkers and Health. Cancer Research 58:4117 – 4121.

Hubbell JH, Seltzer SM. 1995. Tables of x-ray mass attenuation coefficients and mass energy-absorption coefficients 1 keV to 20 MeV for elements Z = 1 to 92 and 48 additional substances of dosimetric interest (NISTIR 5632) US Department of Commerce, Physics Laboratory, Gaithersburg.

ICRP Publication 23: Report of the Task Group on Reference Man. 1975. Oxford, UK: Pergamon Press.

ICRP Publication 68: Dose coefficients for intakes of radionuclides by workers. 1994. Oxford, UK: Pergamon Press.

ICRP Publication 89: Basic anatomical and physiological data for use in radiological protection: Reference values. 2003. Annals of the ICRP. Oxford, UK: Elsevier.

Joubert A, Biston MC, Boudou C, Ravanat JL, Brochard T, Charvet AM, Esteve F, Balosso J, Foray N. 2005. Irradiation in presence of iodinated contrast agent results in radiosensitization of endothelial cells: Consequences for computed tomography therapy. International Journal of Oncology, Biology and Physics 62:1486 – 1496.

Kozlik-Feldmann R, Konert M, Netz H. 1998. Normal values for the distribution volumes of less invasive circulation monitoring by double indicator measurement in pedriatic intensive care. Zeitschrift für Kardiologie 87(9):762.

Leonard A, Baltus I, Leonard ED, Gerber GB, Richard F, Wambersie A. 1995. Dose-effect relationship for *in vivo* and *in vitro* induction of dicentric aberrations in blood lymphocytes of children. Radiation Research 141:85 – 98.

Linderkamp O, Versmold HT, Riegel KP, Betke K. 1977. Estimation and prediction of blood volume in infants and children. European Journal of Pediatrics 125:227 – 234.

M'kacher R, Violot D, Aubert B, Girinsky T, Dossou J, Beron-Gaillard N, Carde P, Parmentier C. 2003. Premature chromosome condensation associated with fluorescence *in situ* hybridisation detects cytogenetic abnormalities after a CT scan: Evaluation of the low-dose effect. Radiation Protection Dosimetry 103:35 – 40.

Nagel HD, Galanski M, Hidajat N, Maier W, Schmidt T. 2000. Radiation exposure in computed tomography. Frankfurt: COCIR.

Padovani L, Caporossi D, Tedeschi B, Vernole P, Nicoletti B, Mauro F. 1993. Cytogenetic study in lymphocytes from children exposed to ionising radiation after the Chernobyl accident. Mutation Research 319:55 – 60.

Stamm G, Nagel HD. 2002. CT-Expo: Ein neuartiges programm zur Dosisevaluierung in der CT Fortschritte. Röntgenstrahlen 174:1570 – 1576.

Stephan G, Pressl S. 1999. Chromosomal aberrations in peripheral lymphocytes from healthy subjects as detected in first cell division. Mutation Research 446:231 – 237.

Weber J, Scheid W, Traut H. 1995. Biological dosimetry after extensive diagnostic X-ray exposure. Health Physics 68:266 – 269.

Wilcoxon F, Wilcoxon RA. 1964. Some rapid approximate statistical procedures. Pearl River, New York, USA: Lederle Laboratories.

Zankl M, Panzer W, Drexler G. 1991. The calculation of dose from external photon exposures using reference human phantoms and Monte Carlo methods. Part VI: Organ doses from computed tomographic examinations. Munich: GSF-Bericht 30/91.

Zankl M, Panzer W, Drexler G. 1993. Tomographic anthropomorphic models. Part II: Organ doses from computed tomographic examinations in paediatric radiology. Munich: GSF-Bericht 39/90.

20. Rühm W & Walsh L. Current risk estimates based on the A-bomb survivors data – a discussion in terms of the ICRP recommendations on the neutron weighting factor. Proc. of the Tenth Symposium on Neutron Dosimetry, Uppsala, Sweden June 12-16, 2006. Radiat. Prot. Dosim. 126(1-4), 423-431, 2007

CURRENT RISK ESTIMATES BASED ON THE A-BOMB SURVIVORS DATA – A DISCUSSION IN TERMS OF THE ICRP RECOMMENDATIONS ON THE NEUTRON WEIGHTING FACTOR

W. Rühm* and L. Walsh
Institute of Radiation Protection, GSF National Center for Environment and Health, Ingolstädter
Landstraße 1, D-85764 Neuherberg, Germany

Currently, most analyses of the A-bomb survivors' solid tumour and leukaemia data are based on a constant neutron relative biological effectiveness (RBE) value of 10 that is applied to all survivors, independent of their distance to the hypocentre at the time of bombing. The results of these analyses are then used as a major basis for current risk estimates suggested by the International Commission on Radiological Protection (ICRP) for use in international safety guidelines. It is shown here that (i) a constant value of 10 is not consistent with weighting factors recommended by the ICRP for neutrons and (ii) it does not account for the hardening of the neutron spectra in Hiroshima and Nagasaki, which takes place with increasing distance from the hypocentres. The purpose of this paper is to present new RBE values for the neutrons, calculated as a function of distance from the hypocentres for both cities that are consistent with the ICRP60 neutron weighting factor. If based on neutron spectra from the DS86 dosimetry system, these calculations suggest values of about 31 at 1000 m and 23 at 2000 m ground range in Hiroshima, while the corresponding values for Nagasaki are 24 and 22. If the neutron weighting factor that is consistent with ICRP92 is used, the corresponding values are about 23 and 21 for Hiroshima and 21 and 20 for Nagasaki, respectively. It is concluded that the current risk estimates will be subject to some changes in view of the changed RBE values. This conclusion does not change significantly if the new doses from the Dosimetry System DS02 are used.

INTRODUCTION

The survivors of the A-bomb explosions over Hiroshima and Nagasaki were exposed to a mixed neutron and gamma radiation field. The resulting doses are strongly inversely correlated with the distance of the survivors from the hypocentres, at the time of exposure. In the analyses of the solid cancer data performed by the Radiation Effects Research Foundation (RERF), the colon is used as the reference organ. Figure 1 shows the ratio of the colon absorbed doses due to neutrons and gamma radiation, based on the Dosimetry System DS86[1].

At first glance, Figure 1 seems to suggest the neutrons to be of minor importance compared to the gamma radiation, as far as any radiation-induced health effect is concerned. However, as neutron radiation is biologically much more effective than gamma radiation, neutron absorbed doses must be multiplied by their relative biological effectiveness (RBE), before their role on the health effects observed among the A-bomb survivors can be assessed. Currently, most of the analyses of the Life Span Study (LSS) incidence and mortality data are based on a neutron RBE value of 10 that is applied to all survivors independent of their distance to the hypocentre[2–5]. Even with an RBE value of 10, the effect contribution of the neutrons would be <10% at a distance to the hypocentre of 1000 m, and only ∼1% at a distance of 2000 m, for

Hiroshima (see Figure 1, if the neutron curve is multiplied by a factor of 10).

There is an ongoing discussion on the proper weighting of the neutron dose in the analysis of the A-bomb data. It has already been shown that the accustomed use of the low weighting factor 10 for the neutrons and, in addition, that the reference to the colon as the organ with the lowest neutron dose contribution suggest a very minor role of the neutrons. In a series of recent publications it has been suggested to use higher constant values for the neutron RBE than 10—either based on evidence from animal experiments[6] or based on analyses of the LSS data[7–9]. As a result of higher RBE values, the effect contribution of the neutrons would be further increased and, for minimally shielded organs close to the body surface, such as the female breast, neutron effect contributions of up to 40% could not be ruled out[10].

In view of the desired continuity of the studies on the A-bomb survivors, there is understandable reluctance to abandon earlier conclusions before all relevant radiobiological evidence is thoroughly reexamined. But even at this point it is useful to judge the issue in light of the common agreement that is reflected in the recommendations of the International Commission on Radiological Protection (ICRP).

The radiation weighting factors, w_R, are of course designed for simple use in the practice of radiation protection and not for application in rigorous risk assessment. They represent, nevertheless, the

*Corresponding author: werner.ruehm@gsf.de
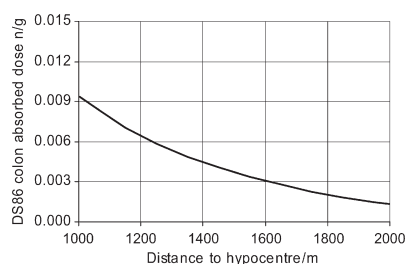
Figure 1. Ratio of neutron and gamma radiation absorbed dose for the colon versus distance to the hypocentre, Hiroshima[26].

summary of all essential information, and for this reason they will here be related to the weighting of neutrons in the analysis of the A-bomb data. As will be seen, there is considerable discrepancy. The ICRP weighting factor for neutrons imply a larger contribution role of the neutrons in the health effects to the A-bomb survivors than currently assumed.

In addition, the issue of a distant-dependent neutron RBE value in the LSS data analyses has—to the authors' knowledge—not been directly investigated before. There is at least one strong reason for questioning the use of a constant RBE for the LSS cohort: The RBE for neutrons is a function of neutron energy. In ICRP Report 60[11], a weighting factor w_R for neutrons at low doses was introduced. Given the energy dependence of w_R, it is interesting to note that the neutron spectra in Hiroshima and Nagasaki change with distance from the hypocentres. This is illustrated in Figure 2 which permits a

quantification of the percentage of neutrons below a specified energy. For example, it can be seen that only 3% of the neutrons had an energy above 1 MeV, at a distance of 1000 m to the hypocentre in Hiroshima, while this fraction increases to 10% at 2000 m, respectively.

Both the hardening of the neutron spectra in Hiroshima and Nagasaki with increasing distance from the hypocentres and the dependence of the neutron weighting factor w_R on neutron energy could result in the necessity of applying different values for w_R in the dose calculations for survivors whose locations at the time of bombing were different. This issue is quantified in more detail next.

RESCALED ICRP NEUTRON WEIGHTING FACTORS TO BE APPPLIED TO THE NEUTRON ABSORBED DOSE IN HIROSHIMA AND NAGASAKI

ICRP neutron weighting factors as a function of neutron energy

Although ICRP Report 60 introduced a step function for the radiation weighting factor w_R for neutrons at low doses, with a maximum value of 20 at an energy between 100 keV and 2 MeV[11], it gave also a smooth fit (Equation 1 and Figure 3) to the w_R values as function of energy of the incident neutrons that is more suitable for detailed calculations.

$$w_R(E_n) = 5 + 17 \cdot \exp\left(\frac{-(\ln(2E_n))^2}{6}\right) \qquad (1)$$

where E_n is the energy of the incident neutrons in units of MeV.

In the more recent ICRP Report 92[12], this approach was modified and Equation 2 was
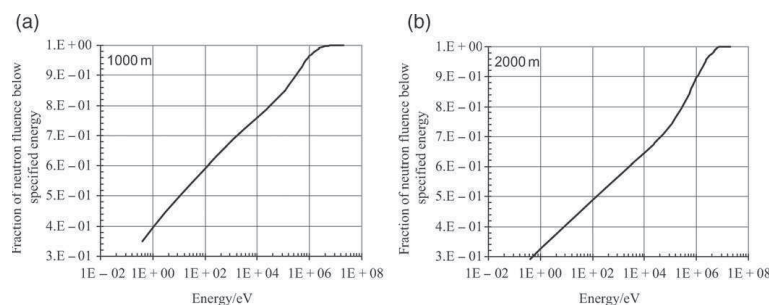
Figure 2. The fraction of free-in-air neutron fluence below specified energy, one meter above the ground, for (a) 1000 m (left panel) and (b) 2000 m (right panel) from the hypocentre in Hiroshima[1].

424
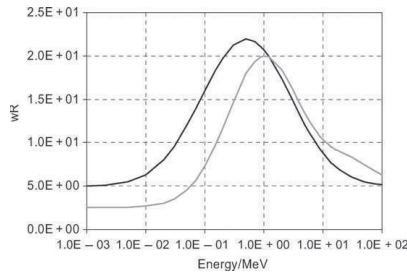
Figure 3. The neutron weighting function w_R as recommended by the ICRP Report 60 (black line) and the ICRP Report 92 (grey line).
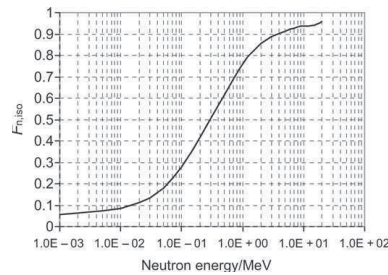
Figure 4. The fractional contribution, $F_{n,iso}$, of neutrons (recoils alone) to the total absorbed dose, for an adult anthropomorphic phantom under isotropic irradiation conditions with mono-energetic neutrons of the specified energy[14,15].

proposed as a better alternative to Equation 1 (see also Figure 3)[13].

$$w_R(E_n) = 2.5 \cdot (2 - \exp(-4 \cdot E_n)$$
$$+ 6 \cdot \exp\left(\frac{-(\ln(E_n))^2}{4}\right) + \exp\left(\frac{-(\ln(E_n/30))^2}{2}\right)\right)$$
$$(2)$$

The analysis described next involves the application of both functions.

Calculation of neutron weighting factors based on ICRP recommendations, corrected for secondary gamma-rays

The w_R is defined in terms of the incident neutron spectrum[12,13] and depends on the energy of the incident neutrons (Figure 3); however, w_R also includes an additional contribution from secondary gamma-rays produced by neutron capture reactions in the body. In contrast, the neutron absorbed doses specified for the A-bomb survivors are based on the neutron spectrum at the site of the investigated organ, excludes the contribution from the secondary gamma-rays. It is for this reason that w_R (Figure 3) must not be applied directly to the DS86 neutron absorbed doses in the calculation of the corresponding neutron effective doses D_n. The correct approach for the calculation of D_n involves the application of rescaled w_R values that take only the genuine contribution from the neutrons (recoils alone) into account.

The fractional contribution, $F_{n,iso}$, of the neutrons to the total absorbed dose (recoils alone) for an anthropomorphic adult phantom that is isotropically irradiated with neutrons of the specified energy is shown in Figure 4[14,15]. It can be inferred from this figure, for example, that after an isotropic irradiation of an anthropomorphic adult phantom with 1-MeV neutrons, $\sim$25% of the total absorbed dose is from secondary gamma-rays and 75% is from the neutrons.

The values for $F_{n,iso}$ that are visualised in Figure 4 were used to calculate a rescaled radiation weighting factor $w_{R,recoil}$ (recoils alone) (The term 'recoils' used here also includes the protons which are produced due to the ^{14}N(n, p)^{14}C reaction, on nitrogen in tissue.) that does not include any contribution from the secondary gamma-rays (Equation 3 and Figure 5).

$$w_{R,recoil} = \frac{w_R + F_{n,iso} - 1}{F_{n,iso}} \qquad (3)$$

Although the rescaled $w_{R,recoil}$ is close to that used by the ICRP for neutron energies above $\sim$5 MeV, it is significantly higher for neutron energies below $\sim$1 MeV and can assume values which are even larger than 60 below $\sim$100 keV, for the weighting factor based on the ICRP Report 60 (Figure 5a).

The pronounced increase of the rescaled ICRP60 neutron weighting factor as shown in Figure 5a is due to the fact that the ICRP60 neutron weighting factor approaches a value of 5, for low energies, while the recoil contribution of the neutrons to the total absorbed dose becomes very small, for these energies (see Figure 4).

425
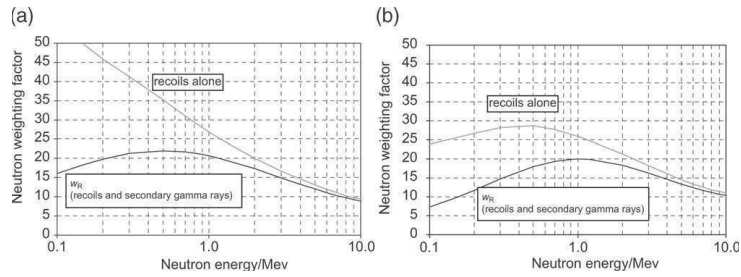
Figure 5. The neutron weighting factors used in this work: Left panel (a) w_R as suggested by (ICRP60)[11] which includes contributions due to neutron-induced secondary gamma rays (lower curve, following Equation 1 and shown in Figure 3), and $w_{R,recoils}$, which only includes the contribution due to recoils (upper curve); right panel (b) same for w_R as suggested by (ICRP92)[12].

EFFECT OF NEUTRON SPECTRUM HARDENING ON THE RESCALED MEAN WEIGHTING FACTORS FOR THE NEUTRONS IN HIROSHIMA AND NAGASAKI

Neutron fluence spectra used

Figure 6 shows an example of the DS86 free-in-air (fia) neutron fluence spectra at 1 m above ground for Hiroshima, at distances to the hypocentres of 1000 and 2000 m[1]. In this figure, the ordinate quantity, lethargy, is defined as the ratio of the neutron fluence, φ, and the difference in the natural logarithm of the top and bottom of each neutron energy group. In the chosen lethargy versus neutron energy presentation, equal areas below the curve represent equal neutron fluences (numbers of neutrons per cm^2 and kt). Neutron spectra for additional distances and those for Nagasaki are given elsewhere[1,16].

Figure 6 demonstrates that most of the neutrons per cm^2 and kt had an energy below 1 MeV. However, the fraction of neutrons with energy higher than ~1 MeV becomes greater at large distances from the hypocentre (see also Figure 2). In any case, the fraction of neutrons below 1 MeV is not negligible. Whether these neutrons need to be included into the calculation of average $w_{R,recoil}$ values and whether they would thus contribute towards increased $w_{R,recoil}$ values for those who survived close to the hypocentres, however, depends on the extent of their contribution to genuine neutron absorbed dose.

The fluence-to-neutron absorbed dose conversion coefficients

The following considerations are based on the reference conversion coefficients of effective dose as
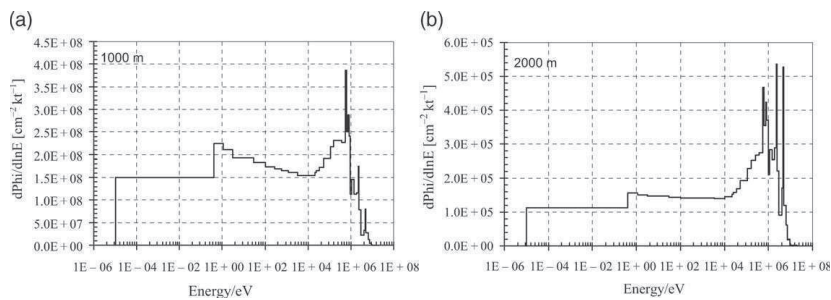
Figure 6. DS86 neutron fluence spectra, 1 m above ground and free-in-air, for (a) 1000 m (left panel) and (b) 2000 m (right panel) from the hypocentre in Hiroshima[1].

a function of neutron energy, $c(E_n)_{effdose}$, for an isotropic neutron exposure of an adult anthropomorphic phantom[17]. These coefficients specify the contribution of neutrons to effective dose (including the contribution due to secondary gamma-rays produced in the body) per incident neutron fluence. Since $w_{R,recoil}$ has to be averaged over the genuine neutron absorbed dose (see earlier), the ICRU reference conversion coefficients were first divided by the ICRP60 w_R to obtain the reference conversion coefficients of absorbed dose, $c(E_n)_{absdose}$, as a function of neutron energy. Because the $c(E_n)_{absdose}$ values obtained in this way still include the contribution from secondary gamma-rays to absorbed dose, they were multiplied with the $F_{n,iso}$ values (Figure 5) to calculate the corresponding conversion coefficients of genuine neutron absorbed dose per neutron fluence, $c(E_n)_{absdose,recoils}$ (Figure 7).

If the resulting neutron absorbed dose is given in terms of neutron energy fluences instead of the neutron fluences, Figure 7 changes to Figure 8. The plateau between 0.1 and 5 MeV represents the energy range in which the neutron energy is directly deposited into the tissue volume of interest and thus the absorbed neutron dose is directly proportional to the neutron energy fluence.

Distant-dependent mean neutron weighting factors for Hiroshima and Nagasaki

Multiplication of $c(E_n)_{absdose,recoils}$ (Figure 7) with the DS86 neutron fluence spectra leads then to the
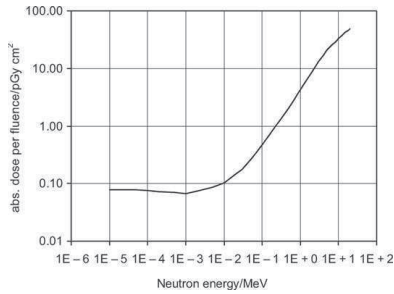
Figure 7. Conversion coefficients $c(E_n)_{absdose,recoils}$ (genuine neutron absorbed dose per neutron fluence) as a function of neutron energy, for an isotropic exposure of an adult anthropomorphic phantom (based on the reference conversion coefficients for effective dose for neutrons given in (ICRU57)[17], the ICRP60 radiation weighting factor for neutrons, w_R,[11] and the fractional contribution $F_{n,iso}$ (Figure 5) of neutrons due to recoils to the total absorbed dose).
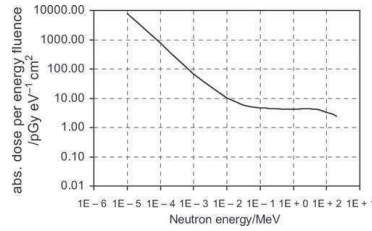
Figure 8. Similar to Figure 7, except that the neutron conversion coefficients $c(E_n)_{absdose,recoils}$ are given in terms of the neutron energy fluence.

genuine contribution of neutrons to absorbed dose as a function of energy (Equation 4), for survivors exposed in Hiroshima or Nagasaki, at different distances from the hypocentres.

$$D_{n,i}(E_{n,i}) = c(E_{n,i})_{absdose,recoils} \cdot \phi_{n,i}(E_{n,i})$$
$$= \frac{c(E_{n,i})_{effdose} \cdot F(E_{n,i})_{n,iso}}{w_R(E_{n,i})} \cdot \phi_{n,i}(E_{n,i}) \quad (4)$$

where the subscript i refers to the DS86 neutron energy group, $D_{n,i}$ is the contribution of the incident neutrons to the genuine neutron absorbed dose, $E_{n,i}$ is the mean neutron energy, $c(E_{n,i})_{effdose}$ is the reference conversion coefficient of effective dose[17], $F_{n,iso}$ is the fractional contribution of the neutrons to the total absorbed dose due to recoils (Figure 4), w_R is the ICRP neutron weighting factor (Equation 1) and Φ_n is the DS86 neutron fluence (see Figures 2 and 6).

Figure 9 presents the results of these calculations in terms of the fraction of genuine neutron absorbed dose due to recoils, from neutrons below the specified energy. For example, it can be inferred from the figure that $\sim$50% of the absorbed dose due to recoils is due to incident neutrons with an energy below 1 MeV, in Hiroshima at 1000 m from the hypocentre (Figure 9a), while it is only $\sim$20% at 2000 m from the hypocentre (Figure 9b).

On the basis of Equation 4, the average weighting factor for the neutrons was then calculated according to Equation 5, for DS86 neutron spectra for Hiroshima and Nagasaki at distances to the hypocentres of 5, 500, 1000, 1500 and 2000 m (Tables 1 and 2). Because the corresponding DS02 neutron spectra are not available in the DS02 final report[18], they were obtained from[19]. Accordingly, the average weighting factor for the neutrons was also calculated based on DS02 neutron spectra, and the results are also given in Tables 1 and 2 for the sake

(a)

(b)
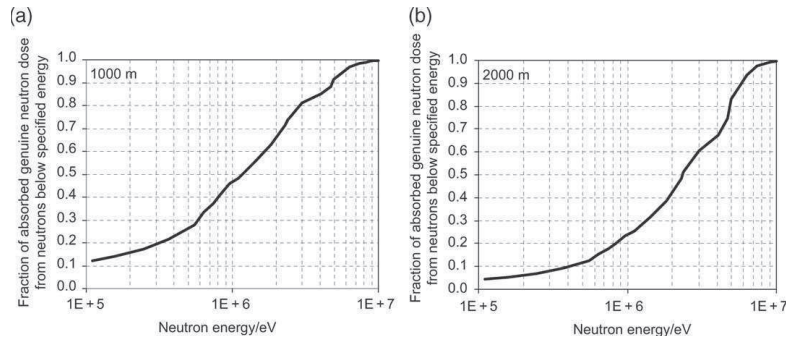
Figure 9. Fraction of neutron absorbed dose due to recoils, from incident neutrons below specified energy; the calculation was performed on the basis of the DS86 neutron spectra for Hiroshima given in Figures 2 and 6; for details see text.

of completeness.

$$\overline{w_{\mathrm{R,recoils}}} = \frac{\sum_i w_{\mathrm{R,recoil}}(E_{\mathrm{n,i}}) \cdot D_{\mathrm{n,i}}(E_{\mathrm{n,i}})}{\sum_i D_{\mathrm{n,i}}(E_{\mathrm{n,i}})} \quad (5)$$

The results in Table 1 indicate that the mean weighting factors for neutrons to be applied to the neutron absorbed doses of the A-bomb survivors depend somewhat on the distance to the hypocentre, being ∼30% larger at 1000 m compared to 2000 m in Hiroshima, and ∼10% larger at Nagasaki. This is due to a hardening of the neutron spectrum, as the distance to the hypocentres increases. As a result, the contribution of neutrons (recoils alone) with an energy below 1 MeV becomes less important at large distances and, correspondingly, the mean weighting factors decrease with increasing distance. From Table 1 one might deduce that the use of a constant neutron weighting factor is not justified at least for Hiroshima, and that a higher value than that of 10 used in the LSS risk analyses should be

applied if the analysis of the A-bomb life span study health data is to be consistent with current ICRP recommendations.

Compared to Hiroshima, the mean weighting factors deduced for Nagasaki are consistently lower at the same distance. This is because the Nagasaki neutron spectra are generally harder than those in Hiroshima, and include a higher fraction of MeV neutrons[1,16]. However, this difference in the mean weighting factors is not very large, and it may be considered acceptable to apply a mean weighting factor deduced from both cities in any quantitative analysis based on data from Hiroshima and Nagasaki combined.

The same procedure was also applied to calculate $w_{\mathrm{R,recoils}}$ values based on a modified neutron weighting factor[13,20] proposed in a recent ICRP publication[12] (Table 2).

While the general trend of increasing neutron weighting factors with decreasing distance from the hypocentre is still observable for both cities, it is somewhat smaller than that observed based on the ICRP Report 60 values (Table 1).

Finally, it should be noted that the mean weighting factors given in Tables 1 and 2 are based on

Table 1. Average $w_{\mathrm{R,recoils}}$ values (see Figure 5) based on ICRP Report 60 recommendations and on DS86 and DS02 prompt neutron spectra, as a function of distance from the hypocentres.

Averaged $w_{\mathrm{R,recoils}}$	5 m	500 m	1000 m	1500 m	2000 m
Hiroshima, DS86	44.0	38.7	30.6	25.8	23.1
Nagasaki, DS86	30.1	25.2	24.0	22.7	21.5
Hiroshima, DS02	44.8	40.2	33.2	28.1	25.1
Nagasaki, DS02	29.3	25.9	24.9	23.9	22.9

Note: For details see text.

Table 2. Same as Table 1, but for a rescaled w_{R} for the recoils as suggested in (ICRP 92[12], see also Ref. 20).

Averaged $w_{\mathrm{R,recoils}}$	5 m	500 m	1000 m	1500 m	2000 m
Hiroshima	25.5	24.9	23.3	21.8	20.7
Nagasaki	22.4	21.9	21.3	20.6	20.0
Hiroshima, DS02	25.8	25.3	24.0	22.7	21.6
Nagasaki, DS02	22.6	22.1	21.7	21.2	20.7

survivors who were located in the open air at the time of the bombing. This is because DS86 fia neutron spectra, published in the DS86 final report[1], had been used. Unfortunately, corresponding neutron spectra for typical shielding situations are not publicly available and, consequently, this issue could not be further investigated within the frame of the present study.

POTENTIAL IMPLICATIONS ON RISK ESTIMATES

Recently it was pointed out that the colon dose is not the best choice for analyses with all solid cancers combined, as it is one of the deepest lying organs in the human body. The human body shields the colon much more effectively against the neutrons than the gamma radiation. For example, colon neutron and gamma radiation absorbed doses must be multiplied by factors 2 (for the neutrons) and 1.08 (for the gamma rays) to calculate organ-averaged doses[21]. If the data shown in Figure 1 are plotted in terms of organ-averaged doses [i.e. multiplied by factors 2 (for the neutrons) and 1.08 (for the gamma rays)], and if the neutron absorbed dose is multiplied by the averaged neutron weighting factors as given in Tables 1 and 2, the neutrons contribute significantly to the total weighted dose of the survivors (Figure 10).

Figure 10 suggests that, compared to standard RERF evaluation, the use of mean w_R values based either on ICRP Reports 60 or 92 applied to organ-averaged doses, the neutrons could contribute much more to the total weighted dose than has been previously assumed. As a result, current risk estimated for gamma radiation would decrease[8,21]. It should

Figure 10. Similar to Figure 1, Hiroshima; dashed line: for colon and an RBE value of 10 (standard RERF approach); grey line: for organ-averaged doses (i.e. neutron absorbed doses for the colon multiplied by a factor 2, and gamma radiation absorbed doses for the colon multiplied by a factor 1.08, respectively) and mean w_R based on ICRP Report 92 (Table 2); black line: same as grey line, but for mean w_R values based on ICRP Report 60 (Table 1).

be emphasised, however, that the investigations described earlier are not final. The best possible analysis of any distant-dependent RBE values would require the individual data from the LSS cohort. Since these individual data are not publicly available, the analysis presented here was based on grouped data. It is therefore recommended that a more detailed analysis of the mechanisms mentioned earlier, based on the individual LSS data, should be performed before final conclusions can be drawn.

The analysis presented here is largely based on the dosimetry system DS86. Recently, this system was thoroughly revised to include all aspects of survivor dosimetry and involved different teams from Japan, the USA and Germany. The results published indicate ∼8% higher gamma radiation doses and 3–20% lower neutron doses for Hiroshima, and 7–11% higher gamma radiation doses and 25–40% lower neutron doses for Nagasaki, respectively, depending on distance from the hypocentres[18]. The resulting risk estimates for solid cancer and leukaemia, however, do not change significantly[22]. If further calculations are performed, which are based on the modified colon gamma and neutron absorbed doses as suggested by DS02 and the rescaled averaged $w_{R,recoils}$ values given in Tables 1 and 2 for Hiroshima, Figure 10 changes to Figure 11. It is evident that even with DS02, the neutrons would account for an appreciable effect contribution.

OTHER EVIDENCE FOR AN RBE VALUE HIGHER THAN 10

A striking trend of decreasing radiation sensitivity of various human tissues has been found with increasing depth in the human body, in the RERF risk estimates for different organs[8]. In the absence of any biological reason, this trend was suggested to be due to the choice of an RBE value of 10. Although there remained statistically significant differences between the different tissues, the trend with depth in the body could be made statistically insignificant if an RBE value for the neutrons of 100 was chosen. In the same publication it was also shown that if the RBE for the neutrons was treated as a fit parameter, the best fit of the solid cancer mortality data could be obtained for a neutron RBE of 100.

It was also shown recently that the striking intercity difference, i.e. different induction of chromosome aberrations in peripheral blood samples from survivors in Hiroshima and Nagasaki, which had been observed and discussed in several previous papers[23–25] becomes insignificant, if higher RBE values for the neutrons are chosen that were based on the *in vitro* induction of chromosome aberrations by neutron and gamma radiation[9].

Finally, studies on animal models also suggest high RBE values for the neutrons. For example, the
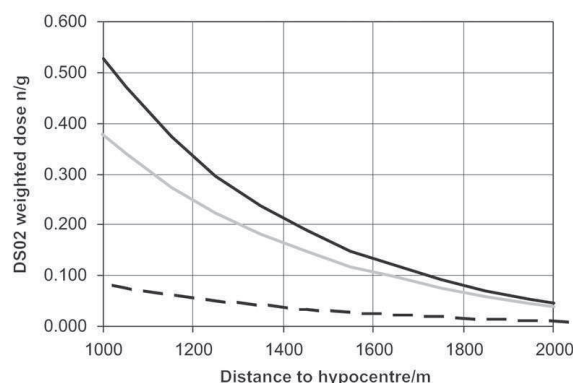
Figure 11. Similar to Figure 10, but based on DS02 colon doses, Hiroshima; dashed line: for colon and an RBE value of 10 (standard RERF approach); grey line: for organ-averaged doses (i.e. neutron absorbed doses for the colon multiplied by a factor 2, and gamma radiation absorbed doses for the colon multiplied by a factor 1.08, respectively) and mean w_R based on ICRP Report 92 (Table 2); black line: same as grey line, but based on ICRP Report 60 (Table 1).

effectiveness of fission neutrons was compared to that of X-rays and gamma rays, in terms of the induction of malignancies in male Sprague-Dawley rats. This study suggested a value for the RBE of fission neutrons of about 50, at neutron doses between 20 and 60 mGy[6].

CONCLUSION

Currently, most of the analyses of the LSS solid tumour incidence and mortality data are based on a constant neutron RBE value of 10[2–5].

Although there are various other reasons why a neutron RBE value of 10 might be too low, it is shown here that current ICRP recommendations on the neutron weighting factor for neutrons also suggest higher values. The ICRP radiation weighting factors are of course designed for simple use in the practice of radiation protection and not for application in rigorous risk assessment. They represent, nevertheless, the summary of all essential information, and for this reason they were here related to the weighting of neutrons in the analysis of the A-bomb data. Additionally, it was demonstrated here that the neutron RBE might depend on distance from the hypocentres, due to the hardening of the neutron spectra in Hiroshima and Nagasaki with increasing distance from the hypocentres. If the investigation is based on current ICRP recommendations for the RBE of neutrons[11], e.g. an RBE of about 31 should be applied to those who survived at a distance of 1000 m in Hiroshima, whereas an RBE of about 23 should be applied to those who survived at a

distance of 2000 m in Hiroshima (Table 1). This dependence on distance decreases if radiation weighting factors of the neutrons are used based on ICRP92. In any case, however, the resulting numerical values of the neutron RBE to be applied in Hiroshima and Nagasaki are at least twice as large as that currently used by the RERF for its analyses of the LSS data. Although slightly different results were obtained numerically, for the new dosimetry system DS02, the basic conclusions of the present analysis did not change. Finally, it is important to note that increasing the neutron RBE in the LSS analyses would result in decreased risk coefficients for gamma radiation.

The approach described here is suitable for further improvement by including small refinements in the ICRP92 model for the radiation weighting factor and applying these to the new RERF incidence data. However, since both the new ICRP model and the new epidemiological data are not yet finalised and are due for publication in the near future, such an improved analysis will need to be the subject of future work.

REFERENCES

1. Roesch, W. C. (ed). *US-Japan joint reassessment of atomic bomb radiation dosimetry in Hiroshima and Nagasaki–final report, Vols. 1 and 2*. Radiation Effects Foundation, Hiroshima, Japan (1987).
2. Thompson, D. E., *et al*. *Cancer incidence in atomic bomb survivors. Part II: Solid tumors, 1958–1987*. Radiat. Res. **137** (suppl), 17–67 (1994).
3. Pierce, D. A., Shimizu, Y., Preston, D. L., Vaeth, M. and Mabuchi, K. *Studies of the mortality of atomic bomb survivors. Report 12, Part 1. Cancer*. Radiat. Res. **146**, 1–27 (1996).
4. Shimizu, Y., Pierce, D. A., Preston, D. L. and Mabuchi, K. *Studies of the mortality of atomic bomb survivors. Report 12, Part II. Noncancer mortality*: 1950–1990. Radiat. Res. **152**, 374–389 (1999).
5. Preston, D. L., Shimizu, Y., Pierce, D. A., Suyama, A. and Mabuchi, K. *Studies of Mortality of Atomic Bomb Survivors. Report 13: solid cancer and noncancer disease mortality: 1950–1997*. Radiat. Res. **160**, 381–407 (2003).
6. Wolf, C., Lafuma, J., Masse, R., Morin, M. and Kellerer, A. M. Neutron RBE for induction of tumors with high lethality in Sprague-Dawley rats. Radiat. Res. **154**, 412–420 (2000).
7. Walsh, L., Rühm, W. and Kellerer, A. M. *Cancer risk estimates for gamma-rays with regard to organ-specific doses - Part I: All solid cancers combined*. Radiat. Environ. Biophys **43**, 145–151 (2004).
8. Kellerer, A. M., Rühm, W. and Walsh, L. *Indications of the neutron effect contribution in the solid cancer data of the A-bomb survivors*. Health Phys. **90**, 554–564 (2006).
9. Sasaki, M. S., Endo, S., Ejima, Y., Saito, I., Okamura, K., Oka, Y. and Hoshi, M. *Effective dose of A-bomb radiation in Hiroshima and Nagasaki as assessed by chromosomal effectiveness of spectrum energy photons and neutrons*. Radiat. Environ. Biophys., **45**, 79–91 (2006).
10. Walsh, L., Rühm, W. and Kellerer, A. M. *Cancer risk estimates for gamma-rays with regard to organ-specific doses - Part II: Site-specific solid cancers*. Radiat. Environ. Biophys. **43**, 225–231 (2004).
11. International Commission on Radiological Protection. *Recommendations of the International Commission on Radiological Protection*. ICRP Publication 60. Ann. ICRP 21 (Oxford: Pergamon Press) (1991).
12. International Commission on Radiological Protection ICRP. *Relative biological effectiveness (RBE), quality factor (Q), and radiation weighting factor (w_R)*. ICRP Publication 92. Ann. ICRP 33(4) (Oxford: Pergamon Press) (2003).
13. Kellerer, A. M., Leuthold, G., Mares, V. and Schraube, H. *Options for the modified radiation weighting factor of neutrons*. Radiat. Prot. Dosim. **109**, 181–188 (2004).
14. Mares, V. Private communication (2004).
15. Leuthold, G., Mares, V. and Schraube, H. *Monte-Carlo calculations of dose equivalents for neutrons in anthropomorphic phantoms using the ICRP 60 recommendations and the stopping power data of ICRU 49*. GSF-Report, Neuherberg (2003).
16. Rühm, W., Walsh, L. and Kellerer, A. M. *The neutron effective dose to the A-bomb survivors*. Technical Report TR221, Radiobiological Institute, Ludwig-Maximilians University Munich (2004).
17. International Commission on Radiation Units and Measurements. *Conversion coefficients for use in radiological protection against external radiation*. ICRU Report 57 (Bethesda, tMD: ICRU) (1998).
18. Young, R. W. and Kerr, G. D. (eds). *Reassessment of the atomic bomb radiation dosimetry for Hiroshima and Nagasaki – Dosimetry System 2002*. Report of the Joint US-Japan Working Group. Radiation Effects Foundation, Hiroshima, Japan (2005).
19. Egbert, S. SAIC, Private Communication (2005).
20. Kellerer, A. M., Rühm, W. and Walsh, L. *Accounting for radiation quality in the analysis of the solid cancer mortality among A-bomb survivors*. Technical Report **TR223**, Radiobiological Institute, Ludwig-Maximilians University Munich (2004).
21. Kellerer, A. M. and Walsh, L. *Risk estimation for fast neutrons with regard to solid cancer*. Radiat. Res. **156**, 708–717 (2001).
22. Preston, D. L., Pierce, D. A., Shimizu, Y., Cullings, H.M., Fujita, S., Funamoto, S. and Kodama, K. *Effect of recent changes in atomic bomb survivor dosimetry on cancer mortality risk estimates*. Radiat. Res. **162**, 377–389 (2004).
23. Stram, D. O., Sposto, R., Preston, D., Abrahamson, S., Honda, T. and Awa, A.A. *Stable chromosome aberrations among A-bomb survivors: an update*. Radiat. Res. **136**, 29–36 (1993).
24. Kodama, Y., Pawel, D., Nakamura, N., Preston, D., Honda, T., Itoh, M., Nakano, M., Ohtaki, K., Funamoto, S. and Awa, A. A. *Stable chromosome aberrations in atomic bomb survivors: results from 25 years of investigation*. Radiat. Res. **156**, 337–346 (2001).
25. Rühm, W., Walsh, L. and Chomentowski, M. *Choice of model and uncertainties of the gamma-ray and neutron dosimetry in relation to the chromosome aberrations data in Hiroshima and Nagasaki*. Radiat. Environ. Biophys. **42**, 119–128 (2003).
26. Preston, D. *DS86 gamma and neutron colon dose estimates for LSS survivors by distance*. RERF Update **9(1)**, (1998).

431

21. Walsh L. A short review of model selection techniques for radiation epidemiology. Radiat. Environ. Biophys. 46, 205-213, 2007

ORIGINAL PAPER

A short review of model selection techniques for radiation epidemiology

Linda Walsh

Abstract A common type of statistical challenge, widespread across many areas of research, involves the selection of a preferred model to describe the main features and trends in a particular data set. The objective of model selection is to balance the quality of fit to data against the complexity and predictive ability of the model achieving that fit. Several model selection techniques, including two information criteria, which aim to determine which set of model parameters the data best support, are reviewed here. The techniques rely on computing the probabilities of the different models, given the data, rather than considering the allowed values of the fitted parameters. Such information criteria have only been applied to the field of radiation epidemiology recently, even though they have longer traditions of application in other areas of research. The purpose of this review is to make two information criteria more accessible by fully detailing how to calculate them in a practical way and how to interpret the resulting values. This aim is supported with the aid of some examples involving the computation of risk models for radiation-induced solid cancer mortality fitted to the epidemiological data from the Japanese A-bomb survivors. These examples illustrate that the Bayesian information criterion is particularly useful in concluding that the weight of evidence is in favour of excess relative risk models that depend on age-at-exposure and excess relative risk models that depend on age-attained.

L. Walsh (✉)
Institute of Radiation Protection, GSF National Center
for Environment and Health, Ingolstädter Landstraße 1,
85764 Neuherberg, Germany
e-mail: Linda.Walsh@gsf.de

Introduction

Poisson regression, involving a multivariate analysis of numbers of uncommon events (e.g., the incidence of cancer or the mortality from cancer) in cohort studies, is often applied to the field of radiation epidemiology. With this method it is possible to determine several theoretical models given relevant epidemiological data, for example, for the relative risk of dying from lung cancer for smokers who live in areas associated with high radon levels. The decision concerning which of these models is the most plausible, without necessarily considering the preferred values of the model parameters, can be made with model selection techniques. Within each model, the parameters indicate the importance of particular effects, for example, the age dependence of the spontaneous death rate in the absence of radon and smoking, or the change in the death rate with radon exposure levels and/or smoking levels. Such parameters are not usually predicted by prior knowledge, but need to be estimated from the data in order to determine which combination of (explanatory) covariables, if any, is capable of adequately describing the total detrimental health risks. Current data may not be statistically powerful enough to constrain the parameters of the model at the required level. Alternatively, although less common in epidemiology than in other fields, the presence of good data may lead to the very different problem of determining when to stop adding extra useful parameters, or when to stop re-parameterisation procedures. In this case, it is possible then to arrive at several competing models that seem to fit the data approximately equally well. Occam's razor (also known as the principle of parsimony) provides a solution to model selection here—the simpler model should be preferred. A complicated model that explains the data slightly better than a simpler model needs to

be penalised for the extra parameters which tend to decrease the overall power of a model in making predictions. In contrast, a model that is too simple and unable to fit the data well needs to be discarded. Such considerations and problems associated with preferred model selection are widespread across many areas of research and form a common type of statistical challenge.

The standard approach to model fitting usually involves choosing one initial set of parameters to be varied and then using a likelihood method to determine the best-fit model and associated parameter confidence intervals. Eventually, the initial parameter set may be replaced by another set chosen ad hoc and the whole process repeated an ad hoc number of times. Typically, the introduction of extra parameters will often improve the fit to the data set, regardless of the relevance of these new parameters, and so a simple comparison of maximum likelihoods will generally tend to favour the model with the most parameters[1]. A less commonly adopted approach, which compensates for this effect by penalising models which have more parameters, and therefore counterbalances the improvement in maximum likelihood that the extra parameters may allow, is that of model selection.

A considerable wealth of the statistical literature is devoted to model selection (excellent text book accounts have recently been given [1–3]) and its use is widespread in many branches of science. In model selection, the data are involved in allowing the determination of which combination of parameters gives the preferred fit. Here, the emphasis is placed on the application of information criteria to aid in the elimination of parameters that do not play a sufficient role in improving the fit to the available data. These information criteria have led to considerable advances in the understanding of how statistical inference is related to information theory.

The model selection techniques reviewed here aim to determine which set of parameters the data support by computing the probabilities of the different models, given the data, rather than considering the allowed values of the fit parameters. Choice of the technique depends on the nesting properties of the competing models. Nested models are those where the more complicated model has additional parameters to those in the simpler model and where the latter may be interpreted as a particular case of the former with the additional parameters kept fixed at some fiducial values. Several techniques are reviewed that apply to linear and non-linear models including: ''Likelihood ratio'' tests, which *require the models to be nested* and were originally

proposed by Neyman and Pearson [4] (see, however, [5] for a modern textbook explanation); and two likelihood based information criteria [1–3] which *do not require the models to be nested*. These information criteria due to Akaike [6, 7] and Schwarz [8] arise from extending the likelihood-based methods by information theoretical and Bayesian considerations, respectively. These criteria have only recently been applied to the field of radiation epidemiology [9, 10], even though they have longer traditions of application in other areas of research (e.g. [11, 12]). Although the underlying theoretical considerations associated with information criteria are very involved (and are not covered in detail here—but just described and cited), the actual criteria have very simple expressions and are easy to derive from the standard output of most optimisation software. The purpose of this review is to promote the application of these techniques in the field of radiation epidemiology by aiming to increase their accessibility and by fully describing how to calculate them and how to interpret the resulting values. This is done with the aid of some practical examples involving the epidemiological data from the Japanese A-bomb survivors.

Model selection statistics

In Poisson regression, it is possible to specifically model rate functions for grouped survival data. Let d_i, P_i and x_i denote the number of deaths (or cases), the total number of person–years at risk and covariates (e.g., age and dose) for the ith data cell, respectively. Then the model for the expected number of deaths $E(d_i)$ in the cell can be written as:

$$E(d_i) = P_i \lambda(\beta, x_i),$$

where $\lambda(\beta, \mathbf{x})$ is the rate function model and β is the chosen set of fit parameters.

If $\hat{\beta}$ represents the computed optimised values of the fit parameter set, then the contribution of the ith data cell to the log likelihood is

$$L_i = d_i \ln(P_i \lambda(\hat{\beta}, x_i)) - P_i \lambda(\hat{\beta}, x_i)$$

and the log likelihood is simply the sum of L_i over the i data cells, ΣL_i.

The overall quality of a model fit to the data in Poisson regression is often quantified by the deviance, dev. The deviance contribution from the ith data cell is computed as twice the difference between the likelihood contribution, when d_i is used as the estimate of the cell mean, and the value of L_i for the current model. Thus, the total deviance is minus twice the natural logarithm of the maximum likelihood, $M = \max(\Sigma L_i)$.

---

[1] However, this should not give the impression that the standard model selection approach involving maximum likelihoods pays no attention to the number of fit parameters, which, in fact, determines the number of degrees of freedom, as explained below.

As indicated above, the general problem of choice of the procedure to use for selection of a preferred model in Poisson regression usually depends on whether the competing models are ''nested''. Model A is nested within model B, if model A is a special case of model B, i.e., if both contain the same model parameters and model B has at least one additional parameter.

Nested models

When two models are nested, it is known that the *difference* between their deviances, dev(B) − dev(A) is chi-square (χ^2) distributed [4, 5]. In this case, *the degrees of freedom for the difference* is equal to the difference in degrees of freedom for the two original test statistics, $df(B) - df(A)$. This suggests the most commonly used method for comparing the fit of two nested models to see if a particular parameter can be dropped from a model without substantially reducing the explanatory power of the model: one tests whether the resulting difference in deviance, dev(B) − dev(A) is significant or not, for the given degrees of freedom and a chosen level of statistical significance. If the difference is significant, then the extra parameters associated with model B are retained. This method is also known variously as partitioning the deviance and applying likelihood ratio tests [4, 5] and is not strictly applicable to non-nested models. Correspondingly, model B with one additional fit parameter than model A is considered to be an improvement over model A with 95% probability, if deviance is reduced by more than 3.84 points. This is because the χ^2-probability distribution with one degree of freedom leaves 5% of the total probability excluded, and consigned to the tail of the total distribution, at χ^2 = 3.84. This and a few other examples are given in Table 1.

Non-nested models

It is sometimes possible, with a little ingenuity, to create nested models from non-nested models in order to test whether a particular parameter can be dropped from a model without substantially reducing the explanatory power of the model. However, in the situation of fitting different types of models to the same data set, for example, when fitting biologically based mechanistic models, empirical excess relative risk models and excess absolute

risk models all to the same A-bomb data set, this is *often not* possible. The AIC and BIC information criteria (as explained below) allow many more inter-comparisons between totally different model types and provide guidance, for example, on whether biologically based models fit the data more economically, i.e., with fewer parameters, than the empirical models, or whether the ERR model fits better than the EAR model.

In general, if the models are not nested and cannot be reformulated as nested models, there is a tendency, in the field of radiation epidemiology, to just quote the change in deviance without interpretation (e.g. [13, p. 390]). This approach can be improved on by the application of information criteria.

The more general problem of choosing among non-nested models, with different numbers of parameters, can be approached with an information theoretic extension of the maximum likelihood principle, as originally suggested by Akaike [6, 7] and fully described in a dedicated textbook to Akaike information criterion statistics [14] and in [1]. Another information criterion involves evaluating the leading term in the asymptotic expansion of the Bayes solution as suggested by Schwarz [8]. An informative description of both methods has recently been given [15].

Akaike's [6, 7] suggestion amounts to maximising the likelihood function separately for each model *j*, obtaining the likelihood M_j and then choosing the model that minimises the Akaike information criterion (AIC),

$$AIC = -2\ln(M_j) + 2k_j, \qquad (1)$$

where k_j is the number of fit parameters in the model (i.e., the number of values that are estimated from the data) and the first term on the right-hand side of Eq. 1 is just the familiar deviance.

The AIC is derived by an approximate minimisation of the Kullback–Leibler information entropy, which measures the difference between the true data distribution and the model distribution. The full statistical justification is given in the original Akaike papers [6, 7] and in [1].

Adopting this formulation of AIC, the probability *P* for a model improvement can then be computed by the following equation [16]:

$$P = 1 - \exp(-0.5\,\Delta AIC)/(1 + \exp(-0.5\,\Delta AIC)) \qquad (2)$$

where ΔAIC is the change in AIC between two competing models.

Thus, an arbitrary model *A* is considered to be an improvement of another model B with 95% probability, if the AIC for model A is smaller than the AIC for model B by 5.9 points, i.e. $\Delta AIC = -5.9$ (see Table 2 for this and other examples).

Table 1 Probability and evidence ratio (ER) values connected with various model-to-model changes in deviance (i.e. ΔDeviance)

ΔDeviance (P = 0.05)	Δnumber of parameters
3.84	1
5.99	2
7.81	3
9.49	4

When comparing two models A and B, the probability that model A fits the data better than model B can be divided by the probability that model B fits better than model A (by invoking complementary probabilities) to obtain the evidence ratio, ER as given in Table 2, where

$$ER = 1/\exp(-0.5\ \Delta AIC). \qquad (3)$$

The other criterion for model selection, mentioned above, is a later product of early work on a Bayesian approach for comparing predictions made by two competing scientific theories [17, 18] and involves Bayes factors. If the prior probabilities of two competing models are equal, then the Bayes factor is just the posterior probability of one of these models. It is possible to avoid the introduction of the prior probabilities, and the associated numerical integrations associated with the full Bayesian method (as in [19] for example), by using a rough asymptotic approximation to the Bayes factors developed by Schwarz [8]. Then the relevant procedure for model selection involves choosing the model that minimises the Bayes Information Criterion (BIC), where the BIC is often defined to be minus twice the Schwarz criterion [8]:

$$BIC = -2\ln(M_j) + k_j \ln(n), \qquad (4)$$

where n is either the number of data points (for individual data) or the number of data groups or cells (for binned data).

In contrast to the AIC, the BIC involves an asymptotic approximation and does not have an information-theoretic justification—despite the name. The factor of two, just mentioned, has the function of putting the BIC on the same scale as the familiar deviance and likelihood ratio test statistic [4, 5] and so here again, the first term on the right-hand side of Eq. 4 is just the deviance. The evidence for model improvement is positive, strong or very strong, if the difference in the BIC values, between two competing models, lies in the ranges of 2–6, 6–10, and 10 and above, respectively [20] (Table 3).

Although approximate minimum t values for the different grades of evidence and sample size have been given in Table 2 of [20], the basic idea presented here is to rely on the BIC ranges for grades of Bayesian evidence for model selection among non-nested models, rather than on P or t values.

The presence of different information criteria in the literature naturally leads to the question of which one is best. Monte Carlo tests have indicated that the AIC has a tendency to favour models which have more parameters than the true model [20]. A formal proof [21] has shown the AIC to be "dimensionally inconsistent". This means that the probability of AIC favouring an over-parameterised model does not tend to zero even as the data set size tends to infinity. Nevertheless, the AIC has been considered here in addition

Table 2 Probability and evidence ratio (ER) values connected with various model-to-model changes in AIC (i.e. ΔAIC)

ΔAIC	Probability	Evidence ratio
–1.0	0.622	1.65
–2.0	0.731	2.72
–3.0	0.818	4.48
–4.0	0.881	7.39
–5.0	0.924	12.18
–5.9	**0.950**	**19.11**
–6.0	0.953	20.09
–7.0	0.971	33.12
–8.0	0.982	54.60

The bold values are for the 95% probability of model improvement

Table 3 Probability and evidence ratio (ER) values connected with various model-to-model changes in BIC (i.e. ΔBIC)

$|\Delta BIC|$	Evidence
0–2	Weak
2–6	Positive
6–10	Strong
>10	Very strong

Source [20]

to the dimensionally consistent BIC, which penalises over-parameterised models more harshly than AIC, as the data set size increases (due to the second term in its definition, Eq. 4).

Other statistics for model selection that are of general interest, but not applied to the examples of the next section, include: Mallows C_p [22]; the shortest length description principle [23, 24]; stochastic complexity (of a data string relative to a class of probabilistic models) [25]; the shortest data description [26]; and the deviance information criterion [27].

An example of applications of model selection: the A-bomb survivors

Data on cancer mortality

The cohort of the atomic bomb survivors from Hiroshima and Nagasaki is unique due to the large number of cohort members; the long follow-up period of more than 50 years; a composition that includes males and females, children and adults; whole-body exposures (which are more typical for radiation protection situations than the partial-body exposures associated with many medically exposed cohorts); a large dose range from natural to lethal levels; and an internal control group with negligible doses, i.e. those who survived at large distances (>3 km) from the hypocentres. The most recent data set on cancer mortality for the follow-up time periods from 1950 to 2000 with the new dosimetry system DS02 [28, 29] (data file: DS02CAN.DAT from http://www.rerf.or.jp) has been selected for the analysis here. DS02 was developed by a large international team of

scientists and included the calculation of the neutron and gamma radiation transport from the point of A-bomb explosion through the atmosphere, accounting for shielding due to buildings and the human body. Validation of these calculations involved neutron activation measurements performed on environmental samples from Hiroshima (e.g. [28–33]). The mortality data are in a grouped form and are categorised by sex, city, age-at-exposure, age-attained, the calendar time period during which the health checks were made and weighted survivor colon dose. This data set provides an opportunity for conducting analyses of the data with various risk models, e.g., for radiation induced all-solid-cancer mortality, as applied in the next section.

Weighted doses

Weighted organ doses are defined by

$$d = d_\gamma + \text{RBE} \, d_n, \qquad (5)$$

where d_γ and d_n are organ absorbed doses from γ-rays and neutrons, respectively. For RBE, the relative biological effectiveness of neutrons, the value 10 has been used.

Only the data groups with mean weighted colon dose categories corresponding to < 2 S_v were used. The two data subsets chosen for the modelling, the associated number of cancer deaths and the number n of data cells, are given in Table 4.

Since this analysis involves all types of solid cancers grouped together, weighted organ-averaged doses [34] are used in a place of the weighted colon dose. The organ-averaged doses are calculated with weighting factors accounting for the risk contribution of individual tumour sites. The weighted organ-averaged doses are larger than the colon doses (which are used in the radiation effects research foundation analyses) by factors of 1.085 and 2 for the gamma and neutron contributions, respectively [34].

The risk models

The risk models applied here, for radiation-induced solid cancer mortality, are very similar to those already considered and explained in detail [9, 13]. In the present work, all

Table 4 Some characteristics of the data sets of atomic bomb survivors with mean weighted colon doses <2 Sv: number of cancer deaths from all types of solid cancer and number of data cells (n, required in the calculation of BIC using Eq. 4) in the grouped mortality data which covers the time from 1950 to 2000

Data set	Number of deaths	Number of data cells (n)
Male, all solid, DS02	4,779	14,803
Female, all solid, DS02	5,234	15,139

analyses are sex-specific in order to facilitate the model-to-model comparisons here and to explore different functional forms for the age-related parameters, which may be different for males and females (an aspect to be included in a future paper). This approach deviates slightly from that in [13], where the analysis pertains to both sexes together but where the baseline model contains fit parameter values that are all sex-specific, with the only fit parameters that are really treated as common to both males and females, relating to the explanatory covariables of age-attained and age-at-exposure. Use is made of a general rate (hazard) model of the form

$$\lambda(d, a, e) = \lambda_0(a, e)[1 + \text{ERR}(d, a, e)], \qquad (6)$$

for the excess relative risk (ERR) and

$$\lambda(d, a, e) = \lambda_0(a, e) + \text{EAR}(d, a, e) \qquad (7)$$

for the excess absolute risk (EAR), where $\lambda_0(a, e)$ is the baseline cancer death rate, a is age-attained and e is age-at-exposure.

The ERR is factorised into a linear function of dose and a modifying function that depends either in terms of the age-attained model, ERR(d, a), [35, 36] or in terms of the traditionally applied age-at-exposure model, ERR(d, e), (which postulates an ERR that does not decrease in time). A more complicated mixed model which includes both age variables, ERR(d, a, e), can also be considered as a third alternative. The functional form is exponential for age-at-exposure in ERR(d, e) or a power function for age-attained in ERR(d, a) and the modifying factors (see, Eq. 6) have been modelled as

$$\text{ERR}(d, a, e) = k_d d \exp(-g_e(e - 30) + g_a \ln(a/70)), \qquad (8)$$

where k_d is the ERR per unit dose for an age-at-exposure of 30 years and an age-attained of 70 years, and g_e, g_a are fit parameters.

The model centering at age-at-exposure of 30 years and an age-attained of 70 years was chosen to match that adopted in previous analyses, e.g. [13]. Note that here ERR(d, e) and ERR(d, a) are nested within ERR(d, a, e); however, ERR(d, e) and ERR(d, a) are not nested models.

Similarly, the EAR is also factorised into a linear function of dose and a modifying function that depends either exponentially on age-at-exposure or on the natural logarithm of age-attained or on both age variables:

$$\text{EAR}(d, a, e) = k_d d \exp[-g_e(e - 30) + g_a \ln(a/70)] \qquad (9)$$

where k_d, g_e and g_a are fit parameters. However k_d is now the EAR in units of number of excess cases per 10,000 person years per S_v, for an age-at-exposure of 30 years and an age-attained of 70 years.

The nesting properties of the EAR models are also analogous to those of the ERR models.

Although the baseline rates can be dealt with by stratification, the main calculations in the next section adopt a fully parametric model:

$$\lambda_0(a,e) = \exp\{\beta_0 + \beta_1 \ln(a/70) + \beta_2 \ln^2(a/70)$$
$$+ \beta_3 \max^2(0, \ln(a/40)) + \beta_4 \max^2(0, \ln(a/70))$$
$$+ \beta_5(e - 30) + \beta_6(e - 30)^2\}, \qquad (10)$$

where $\beta_0,\ldots,\beta_6$ are fit parameters.

This is a simplified version of the model of Preston et al. [13]. Some terms, including a city parameter relating to differences in baseline cancer rates between Hiroshima and Nagasaki, were dropped from the full model of Preston et al. [13] in arriving at Eq. 10. This was because an application of the likelihood ratio test for nested models [4, 5], as described above, indicated that the extra terms did not significantly improve the fit in the current analysis.

Estimation of fit parameters and statistical analysis

The maximum likelihood technique is used to fit the models, as described in [37, 38]. Best estimates uncertainty ranges and correlations of the fit parameters were determined by minimising the deviance using the MIGRAD minimisation subroutine from the CERN LIBRARY MINUIT software for optimisation. MIGRAD implements a stable version of the Davidon–Fletcher–Powell variable-metric (a quasi-Newton method) [37]. The models were also computed in EPICURE/ AMFIT [38] as a double check on the numerical methods, associated convergence properties, resulting parameter values and uncertainty ranges. No inconsistencies were found.

The number of parameters in the age-at-exposure model, for example, was assumed to be equal to the number of parameters actually optimised (9 parameters) plus the two spline joins in the β_3 and β_4 parameters at 40 and 70 years, respectively, in the baseline model (Eq. 10), thus a total of 11 parameters.

The quality of model fits and associated information criterion values

Full details of the properties of interest in radiation epidemiology, i.e., ERR dose response curves with age effect-modifications and central estimates for the ERR/S_v, have already been given for these types of models [9, 13] and are not discussed here. However, for completeness, the parameter sets for four preferred models are given in Table 6, in the Appendix. Since the purpose here is to illustrate model selection techniques, the main results of relevance are given in Table 5. All inferences made in this

Table 5 Preferred models

Data set	Model	Number of parameters	Deviance	BIC	AIC
Male	**ERR(d, e)**	11	6,419	**6,525**	6,441
	ERR(d, a)	11	6,420	6,526	6,442
	ERR(d, a, e)	12	6,416	6,531	6,440
	EAR(d, e)	11	*6,447*	*6,553*	*6,469*
	EAR(d, a)	11	6,422	**6,528**	6,444
	EAR(d, a, e)	12	6,417	6,532	6,441
Female	**ERR(d, e)**	11	6,697	**6,803**	6,719
	ERR(d, a)	11	*6,704*	6,810	6,726
	ERR(d, a, e)	12	6,695	6,811	6,719
	EAR(d, e)	11	*6,742*	*6,848*	*6,764*
	EAR(d, a)	11	6,695	**6,801**	6,717
	EAR(d, a, e)	12	6,693	6,809	6,717

The bold text indicates the preferred models (i.e., minimum BIC value for each of the data sets). The models and numbers that are italicised indicate the models that are a particularly bad choice in terms of model-to-model changes in deviance or AIC or BIC

section come from an evaluation of model-to-model changes in the quantities given in Table 5 with the aid of Tables 1, 2, 3 for interpretation. Table 5 gives the values of Deviance, BIC and AIC associated with the two classes (ERR, EAR) of models considered here. The borderlines necessary for interpreting the model-to-model changes in these values can be seen from Tables 1, 2, 3. Among these models, comparisons can be made between two nested models in the same class (where the nesting properties have been explicitly given above) using the change in deviance, and between any two models using the model-to-model changes in AIC and BIC.

The full process of model selection would normally start with adding the explanatory variables one-by-one to the model i.e., add dose, then add one age related variable and then the other age related variable. However, the full process has not been described here since the aim is one of illustrations of model selection techniques rather than of detailing the complete model selection process. There are also intrinsic difficulties involving the evaluation of time-related effect-modification factors which are caused by collinearity (i.e. correlations) in the variables [39], but these are not considered here.

Considering the ERR age-at-exposure model, it can be seen from Table 5 that when the age-attained parameter is added to the model the deviance is reduced by 3 and 2 points for the male and female data sets, respectively. Here, the likelihood ratio test would indicate that inclusion of age-attained does not lead to a significant improvement in model fit. However, if one happened to start with the ERR age-attained model and then added the age-at-exposure parameter, the deviance is reduced by 4 and 9 points for the

male and female data sets, respectively, which does lead to a significant improvement in an overall model fit. This indicates the main problem in this type of model fitting—which age covariable describes the data best? Is it the age-at-exposure or the age-attained? This clearly cannot be answered with the conventional method of just looking for the change in deviance (because non-nested models are involved) and it is exactly here where the information criteria are of greatest value. It is also important to reiterate here that the inability to distinguish between two models could also arise because the data are not intrinsically powerful enough to fulfil this purpose.

There are several cases of model-to-model comparisons in Table 5 where the changes in deviance and AIC are very small (and therefore do not indicate model preferences) but where the changes in BIC indicate strong Bayesian evidence in favour of one model. For example, the comparisons between the ERR(d, e) and ERR(d, a, e) models for the female data set yield ΔDeviance = 2, ΔAIC = 0 and ΔBIC = 8. Given the theoretical considerations of the dimensional consistency of BIC mentioned above, this seems to be the more credible measure here and indicates strong Bayesian evidence in favour of ERR(d, e).

Comparisons between the three ERR models or between the three EAR models, for the male data generally yielded changes in AIC of 4 or less—except in the case of the EAR(d, e) model which stands out as a particularly poor choice. This is also true for the female data set with the additional qualification that ERR(d, a) is also a poor choice because AIC, in this case, is seven points more than the other two models in this class.

The preferred models in terms of BIC for both sets of data are ERR(d, e) and EAR(d, a). The female data supports the ERR(d, e) (ΔBIC = 7 and 8) and EAR(d, a) (ΔBIC = 8 and 47) models with strong to very strong Bayesian evidence (Table 3). However, the male data support the ERR(d, e) and EAR(d, a) models with Bayesian evidence that encompasses all four categories (in Table 3) for the various model-to-model comparisons that are possible in Table 5. The Bayesian evidence does not provide support for the mixed age models, ERR(d, a, e), EAR(d, a, e) in either data set, since the addition of a second age-related fit parameter was penalised with positive and strong evidence for the male and female data, respectively.

It is also possible to determine the relative quality of fit between the two model types ERR and EAR using AIC and BIC. Considering the changes in AIC and BIC between the preferred models in each class, i.e. ERR(d, e) and EAR(d, a), it can be seen from Table 5 that for males, ΔAIC = 3, indicating that ERR(d, e) is an improvement over EAR(d, a) with 82% probability (according to Table 2), and ΔBIC = 3, indicating positive Bayesian evidence in favour of ERR(d, e) (Table 3). For females, ΔAIC = 2 indicating that EAR(d, e)

is an improvement over ERR(d, a) with 73% probability (Table 2) and ΔBIC = 2, indicating weak Bayesian evidence in favour of EAR(d, e) for the female data set (Table 3).

Conclusion

An effort here has concentrated on explaining, applying and interpreting the outcomes of several techniques in the area of ''goodness of fit evaluations'' so that main conclusions drawn from model selection do not depend on just one type of statistical test, which could be associated with stringent assumptions (e.g. nested models). The usual comparison of deviance values and number of model parameters has been applied along with two other measures: two information criteria (AIC and BIC), not usually applied to radioepidemiology. The BIC appears to be the best method from theoretical considerations of dimensional consistency.

As examples, to illustrate the application of theses techniques, several types of radiation risk models have been fitted to the most recent mortality data for all solid cancers occurring in the Japanese A-bomb survivors. Model-to-model changes in the BIC have been seen, from these examples, to display more decisive properties in model selection than changes in AIC or changes in deviance considerations. Considering the results from all techniques together, the weight of evidence was in favour of excess relative risk models that depend on age-at-exposure and excess absolute risk models that depend on age-attained. There was positive Bayesian evidence that the excess relative risk models that depend on age-at-exposure fitted the male data better than the excess absolute risk models that depend on age-attained. However, the reverse trend was found with weak evidence for the female data. It has been demonstrated here that application of the two information criteria allows *interpretable* comparisons between non-nested models and indeed between different model types, which are not allowed by standard methods of likelihood ratio testing for nested models. This feature renders the information criteria to be particularly useful in the field of radiation epidemiology. Finally, it is probably of some importance to follow Box [40] in believing that ''all models are wrong, but some are useful''; actually, some are more useful than others.

Appendix

Table 6

Table 6 Fit parameters [with standard errors (SE)] for the four preferred models in Table 5 as defined by Eq. 6–10

Parameter	Males				Females			
	ERR(d, e)		EAR(d, a)		ERR(d, e)		EAR(d, a)	
	Fitted value	SE	Fitted value	SE	Fitted value	SE	Fitted value	SE
β_0	−3.50	0.52	−3.69	0.79	−6.90	0.64	−6.98	0.75
β_1	8.49	1.75	7.81	2.71	−1.72	2.18	−1.96	2.56
β_2	1.92	1.33	1.16	2.18	−4.05	1.74	−4.28	2.07
β_3	−2.98	1.66	−2.32	2.52	5.06	2.04	5.32	2.38
β_4	−6.96	1.90	−7.09	2.01	−0.61	1.54	−0.70	1.62
β_5	3.89×10^{-4}	1.28×10^{-3}	-9.25×10^{-4}	1.23×10^{-3}	1.38×10^{-2}	1.49×10^{-3}	1.26×10^{-2}	1.43×10^{-3}
β_6	-3.11×10^{-4}	5.28×10^{-5}	-3.00×10^{-4}	5.29×10^{-5}	-4.35×10^{-4}	5.55×10^{-5}	-4.38×10^{-4}	5.58×10^{-5}
k_d	0.3199	0.07185	26.32	6.054	0.4982	0.08104	24.03	3.484
g_e	0.0397	0.0138			0.04518	0.01135		
g_a			3.215	0.6272			2.76	0.443

k_d has units of ERR/S_v (at an age-at-exposure of 30 years) for the ERR models, and number of excess cases per 10,000 person years per S_v (at an age-attained of 70 years) in the EAR models. Note, however, that the baseline cancer rate parameter values for β_0 to β_7 will result in $\lambda_0(a, e)$ with units of number of cancer deaths per year

References

1. Burnham KP, Anderson DR (2002) Model selection and multi-model inference. 2nd edn. Springer, New York
2. MacKay DJC (2003) Information theory, inference and learning algorithms. Cambridge University Press, London
3. Gregory P (2005) Bayesian logical data analysis for the physical sciences. Cambridge University Press, London
4. Neyman J, Pearson ES (1928) On the use and interpretation of certain test criteria for purposes of statistical inference, part II. Biometrika 20A:263–294
5. Harrell FE Jr (2001) Regression modeling strategies: with applications to linear models, logistic regression and survival analysis. Springer Series in Statistics
6. Akaike H (1973) Information theory and an extension of the maximum likelihood principle. In: Petrov BN, Caski F (eds) Proceedings of the 2nd international symposium on information theory. Budapest, Hungary, Akademiai Kiado, pp 267–281
7. Akaike H (1974) A new look at the statistical model identification. IEEE Trans Autom Control 19(6):716–723
8. Schwarz G (1978) Estimating the dimension of a model. Ann stat 6:461–464
9. Walsh L, Rühm W, Kellerer AM (2004) Cancer risk estimates for γ-rays with regard to organ specific doses, part I: All solid cancers combined. Radiat Environ Biophys 43:145–151
10. Izumi S, Ohtaki M (2004) Aspects of the Armitage–Doll gamma frailty model for cancer incidence data. Environmetrics 15:209–218
11. Tavecchia G, Pradel R, Boy V, Johnson AR, Cezilly F (2001) Sex- and age-related variation in survival and cost of reproduction in greater flamingos. Ecology 82(1):165–174
12. Mukherjee S, Feigelson ED, Babu GL, Murtagh F, Fraley C, Raftery A (1998) Three types of gamma-ray bursts. Ap J 508:314–325
13. Preston DL, Shimizu Y, Pierce DA, Suyama A, Mabuchi K (2003) Studies of the mortality of atomic bomb survivors. Report 13 solid cancer and noncancer disease mortality1950–1997. Radiat Res 160:381–407

14. Sakamoto Y, Ishiguro M, Kitagawa G (1986) Akaike information criterion statistics. Kluwer Academic, Dordrecht
15. Yang Y (2005) Can the strengths of AIC and BIC be shared? A conflict between model identification and regression estimation. Biometrika 92:937–950
16. Motulsky H, Christopoulos A (2002) Fitting models to biological data using linear and nonlinear regression. A practical guide to curve fitting. GraphPad Software, Inc.
17. Jeffreys H (1935) Some tests of significance, treated by the theory of probability. Proc Camb Philo Soc 31:203–222
18. Jeffreys H (1961) Theory of probability, 3rd edn. Oxford University Press, Oxford
19. Radivoyevitch T, Hoel DG (2000) Biologically-based risk estimation for radiation-induced chronic myeloid leukemia. Radiat Environ Biophys 39:153–159
20. Kass RE, Raftery AE (1995) Bayes factors. J Am Stat Assn 90:773–795
21. Kashyap R (1980) Inconsistency of the AIC rule for estimating the order of autoregressive models. IEEE Trans Auto Control 25:996–998
22. Mallows CL (1973) Some Comments on C_p. Technometrics 15(4):661–675
23. Kolmogorov A (1968) Three approaches to the quantitative definition of information. Probl Inf Transmission 1:1–12
24. Ramos AA (2006) The minimum description length principle and model selection in spectropolarimetry. Online under arXiv:astro-ph/0606516 v1 21 June 2006
25. Rissanen J (1986) Stochastic complexity and modeling. Ann Stat 14(3):1080–1100
26. Rissanen J (1978) Modeling by shortest data description. Automatica 14:465–471
27. Spiegelhalter DJ, Best NG, Carlin BP, van der Linde A (2002) Bayesian measures of model complexity and fit. J R Stat Soc B 64, part 4, 583–639
28. Bennett B (2003) DS02: The new dosimetry system DS02. Hiroshima Igaku (Japanese). J Hiroshima Med Assoc 56:386

29. Young R, Kerr GD (eds) (2005) DS02: Reassessment of the atomic bomb radiation dosimetry for Hiroshima and Nagasaki, Dosimetry System 2002, DS02, vols 1, 2, Radiation Effects Research Foundation, Hiroshima

30. Straume T, Rugel G, Marchetti AA, Rühm W, Korschinek G, McAninch JE, Carroll K, Egbert S, Faestermann T, Knie K, Martinelli R, Wallner A, Wallner C, Fujita S, Shizuma K, Hoshi M, Hasai H (2003) Measuring fast neutrons in Hiroshima at distances relevant to atomic-bomb survivors. Nature 424:539–541

31. Straume T, Rugel G, Marchetti AA, Rühm W, Korschinek G, McAninch JE, Carroll K, Egbert S, Faestermann T, Knie K, Martinelli R, Wallner A, Wallner C, Fujita S, Shizuma K, Hoshi M, Hasai H (2004) Measuring fast neutrons in Hiroshima at distances relevant to atomic-bomb survivors. Nature 430:483

32. Huber T, Rühm W, Hoshi M, Egbert SD, Nolte E (2003) ^{36}Cl measurements in Hiroshima granite samples as part of an international intercomparison study: results from the Munich group. Radiat Environ Biophys 42:27–32

33. Huber T, Rühm W, Kato K, Egbert S, Kubo F, Lazarev V, Nolte E (2005) The Hiroshima thermal neutron discrepancy for ^{36}Cl at large distances; Part I: New ^{36}Cl measurements in granite samples exposed to a-bomb neutrons. Radiat Environ Biophys 44:75–86

34. Kellerer AM, Walsh L (2001) Risk estimation for fast neutrons with regard to solid cancer. Radiat Res 156:708–717

35. Kellerer AM, Barclay D (1992) Age dependences in the modelling of radiation carcinogenesis: age-dependent factors in the biokinetics and dosimetry of radionuclides. Radiat Prot Dosim 41:273–281

36. Pierce DA, Mendelsohn ML (1999) A model for radiation related cancer suggested by atomic bomb survivor data. Radiat Res 152:642–654

37. James F (1994) Minuit function minimization and error analysis, Version 94.1. Technical report, CERN

38. Preston DL, Lubin JH, Pierce DA (1993) Epicure User's Guide. HiroSoft International Corp., Seattle

39. Lagarde F (2006) Understanding estimation of time and age effect-modification of radiation-induced cancer risk among atomic-bomb survivors. Health Phys 91(6):608–618

40. Box GEP (1976) Science and statistics. J Am Stat Assoc 71:791–799

22. Schneider U & Walsh L. Cancer risk estimates from the combined Japanese A-bomb and Hodgkin cohorts for doses relevant to radiotherapy. Radiat. Environ. Biophys. 47, 253-263, 2008

ORIGINAL PAPER

Cancer risk estimates from the combined Japanese A-bomb and Hodgkin cohorts for doses relevant to radiotherapy

Uwe Schneider · Linda Walsh

Abstract Most information on the dose–response of radiation-induced cancer is derived from data on the A-bomb survivors who were exposed to γ-rays and neutrons. Since, for radiation protection purposes, the dose span of main interest is between 0 and 1 Gy, the analysis of the A-bomb survivors is usually focused on this range. However, estimates of cancer risk for doses above 1 Gy are becoming more important for radiotherapy patients and for long-term manned missions in space research. Therefore in this work, emphasis is placed on doses relevant for radiotherapy with respect to radiation-induced solid cancer. The analysis of the A-bomb survivor's data was extended by including two extra high-dose categories (4–6 Sv and 6–13 Sv) and by an attempted combination with cancer data on patients receiving radiotherapy for Hodgkin's disease. In addition, since there are some recent indications for a high neutron dose contribution, the data were fitted separately for three different values for the relative biological effectiveness (RBE) of the neutrons (10, 35 and 100) and a variable RBE as a function of dose. The data were fitted using a linear, a linear-exponential and a plateau-dose–response relationship. Best agreement was found for the plateau model with a dose-varying RBE. It can be concluded that for doses above 1 Gy there is a tendency for a nonlinear dose–response curve. In addition, there is evidence of a neutron RBE greater than 10 for the A-bomb survivor data. Many problems and uncertainties are involved in combing these two datasets. However, since very little is currently known about the shape of dose–response relationships for radiation-induced cancer in the radiotherapy dose range, this approach could be regarded as a first attempt to acquire more information on this area. The work presented here also provides the first direct evidence that the bending over of the solid cancer excess risk dose response curve for the A-bomb survivors, generally observed above 2 Gy, is due to cell killing effects.

Introduction

The dose–response relationship for radiation carcinogenesis up to 1 or 2 Gy has been quantified in several major analyses of the atomic bomb survivors data; recently papers have been published, for example, by Preston et al. [1, 2] and Walsh et al. [3, 4]. This dose range is important for radiation protection purposes where low doses are of particular interest. However, it is also important to know the shape of the dose–response curve for radiation-induced cancer for doses above 1 Gy. In patients who receive radiotherapy, parts of the patient volume can receive high doses and it is therefore of great importance to know the risk for the patient to develop a cancer which could have been caused by the radiation treatment. In addition, the health risk to astronauts from space radiation is recognized as one of the limiting factors for long-term space missions. During solar events astronauts can receive doses which are above 1 Gy [5, 6].

The shape of the dose–response curve for radiation-induced cancer is currently of much debate [7–16]. It is not

U. Schneider (✉)
Division of Medical Physics,
Department of Radiation Oncology and Nuclear Medicine,
The Triemli Hospital Zürich,
8063 Zürich, Switzerland
e-mail: uwe.schneider@psi.ch

L. Walsh
GSF National Research Center,
Institute of Radiation Protection,
85764 Neuherberg, Germany

known whether cancer risk as a function of dose continues to be linear or decreases at high dose due to cell killing or levels off due to, for example, a balance between cell killing and repopulation effects. The work presented here, aims to clarify the dose–response shape for doses above 1 Gy. In this dose range, data are available from the atomic bomb survivors from Hiroshima and Nagasaki, although the data pertaining to doses above 4 Gy have not usually been included in previous analyses, due to the associated large uncertainties. In addition, data are available from about 30,000 patients with Hodgkin's disease who were irradiated with localized doses of up to around 40 Gy. The aim of this paper is to attempt a combination of the epidemiological data from the atomic bomb survivors and the Hodgkin data, in order to determine a possible dose–response relationship for radiation-induced solid cancer for radiotherapy doses. Many problems and uncertainties (see "Discussion" section) are involved in combing these two datasets. However, since very little is currently known about the shape of dose–response relationships for radiation-induced cancer in the radiotherapy dose range, this approach could be regarded as a first attempt to acquire more information on this area.

Materials and methods

Modeling of the atomic bomb survivors data

The most recent data for all solid cancers incidences relating to the follow-up period from 1958 to 1998 and with DS02 doses (which is publicly available from the Radiation Effects Research Foundation—RERF, web site: http://www.rerf.or.jp) were analyzed here [1]. Computations were performed with respect to the organ-averaged weighted doses because reference to the colon weighted dose, which is supplied in the standard dataset for use in the analysis of all solid cancers combined, is known to underestimate the average dose to all organs [17]. The organ-averaged doses are calculated with weighting factors accounting for the risk contribution of individual tumor sites. The weighted organ-averaged doses are greater than the colon doses (which are used in the RERF analyses) by factors of 1.085 and 2 for the gamma and neutron contributions, respectively.

Data of 281 survivors (out of a total of 86,611) with doses varying from 4 to 13 Gy were included with the main data of doses between 0 and 4 Gy in the present analysis. The high-dose data were regrouped into organ-averaged absorbed dose categories of 4–6 Gy and 6–13 Gy. All doses were adjusted to allow for random errors in dose estimates by the method of Pierce et al. 1990 [18].

The excess absolute risk (EAR) models were optimized against the epidemiological data, by the maximum likelihood Poisson regression method employing the EPICURE-AMFIT software [3]. Although the baseline rates can be dealt with stratification, the main calculations here adopt the fully parametric baseline model of Preston et al. [1].

Since there are some recently discovered indications of a high neutron dose contribution [19, 20], the data were fitted separately for three different values for the relative biological effectiveness of neutrons (10, 35 and 100). In addition, a dose dependent RBE_D for neutrons determined by Sasaki et al. [21] using the kerma-weighted chromosomal effectiveness of A-bomb spectrum energy photons was used (Eq. 9 in [21]). When applying Sasaki's equation the maximum RBE of the neutrons at the low-dose limit is 75.1.

The EAR models applied here were the same as those already considered and explained in detail [1, 2]. Here organ-averaged weighted dose D is the sum of the γ-ray dose and the RBE-weighted neutron dose. The differences between the previous [2] and present work are that the input data include two extra high-dose categories; organ-average weighted doses are applied instead of colon-weighted doses; a range of neutron weighting factors (RBEs) are considered; and different forms of dose–response relationships, which are more suitable for the high-dose data, i.e. a linear-exponential and a plateau model are employed.

The excess absolute risk is factorized into a function of dose $f(D)$ and a modifying function that depends on the variables gender (s) and age at exposure (e) and age attained (a):

$$EAR(D, e, a, s) = \beta f(D)\mu(e, a, s) \qquad (1)$$

where β is the initial slope and μ the modifying function containing the population dependent variables:

$$\mu(e, a, s) = \exp\left(\gamma_e(e - 37) + \gamma_a \ln\left(\frac{a}{46}\right)\right)(1 \pm s) \qquad (2)$$
$$(+\text{for females}, -\text{for males})$$

In this form the fit parameters are gender-averaged and centered at an age at exposure (e) of 37 years and an attained age (a) of 46 years, since these are the characteristic ages of the Hodgkin's patient population as described in the next section. However, the centering is not critical to the fitting procedure and the resulting risks can be scaled to gender-specific values for any values of the two age variables.

It should be noted here that the dose-dependent part $f(D)$ of Eq. (1), which is, to a first approximation, population-independent is sometimes called organ equivalent dose (OED) [13], when averaged over the whole body volume. For highly inhomogeneous dose distributions, cancer risk is proportional to average dose only for a linear dose–response relationship. For any other dose–response

relationship the OED in the body is proportional to cancer risk, if it is defined as

$$\text{OED} = \frac{1}{V} \sum_i V_i f(D_i) \tag{3}$$

where V is the total body volume and the sum is taken over all volume elements V_i with homogenous dose. The OED is hence a dose–response weighted dose variable, which is proportional to cancer risk in one population (same gender, age at exposure and age attained). This quantity allows comparisons of, e.g. dose distributions in a radiotherapy patient with respect to radiation induced cancer.

Three different dose–response relationships are considered here. The first is a linear response over the whole dose range:

$$\text{OED} = \frac{1}{V} \sum_i V_i D_i \tag{4}$$

The second is a linear-exponential dose–response relationship of the form:

$$\text{OED} = \frac{1}{V} \sum_i V_i D_i \exp\left(-\alpha D_i\right) \tag{5}$$

and the third is a dose–response, which is flattening at high dose, a so-called plateau dose–response [9] described by:

$$\text{OED} = \frac{1}{V} \sum_i V_i \frac{(1 - \exp\left(-\delta D_i\right))}{\delta} \tag{6}$$

All of the dose–response curves defined by Eqs. (4)–(6) become, in the limit of small dose:

$$\lim_{D \to 0} \text{OED} = \frac{1}{V} \sum_i V_i D_i = \overline{D} \tag{7}$$

Hence the OED is, in the case of a homogenous distribution of small dose, average absorbed organ dose, which is consistent with radiation protection schemes.

It should be noted here that it is possible to define a homogenous organ dose, OHD, which would result in the same radiation-induced cancer rate as the inhomogenous dose distribution. OHD is then, for the linear-exponential model, simply the inverse function of Eq. (5):

$$\text{OHD} = -\frac{1}{\alpha} \text{LambertW}(-\alpha \text{OED}) \tag{8}$$

where *LambertW* is the Lambert-function. For a plateau dose–response relationship, the corresponding homogenous dose is:

$$\text{OHD} = -\frac{1}{\delta} \ln\left(1 - \delta \text{OED}\right) \tag{9}$$

When applying a dose–response model which is linear in dose, even for large doses Eq. (4), the OHD is simply the mean dose.

The data were also test-fitted using a linear-quadratic-exponential EAR model. However, the fit parameters relating to the quadratic term in dose were not found to be statistically significantly determined (in contrast to previous results for the lower dose range of 0–2 Sv for excess relative risk models, [3]) indicating that a linear-exponential dose–response curve may be a better representation of the dose response than a linear-quadratic-exponential dose–response, when the data pertaining to high doses are included in the analysis.

Modeling of the Hodgkin's patients

Cancer risk is only proportional to average organ dose as long as the dose–response curve is linear. At high dose it could be that the dose–response relationship is nonlinear and as a consequence, OED replaces average dose to quantify radiation-induced cancer. In order to calculate OED in radiotherapy patients, information on the three-dimensional dose distribution is necessary. This information is usually not provided in epidemiological studies on second cancers after radiotherapy. However, in Hodgkin's patients the three-dimensional dose distribution can be reconstructed.

For this purpose data on secondary cancer incidence rates in various organs for Hodgkin's patients treated with radiation were also included in this analysis. Data on Hodgkin's patients treated with radiation seem to be ideal for an attempted combination with the A-bomb data. These patients were treated at a relatively young age, with curative intent and hence secondary cancer incidence rates for various organs are known with a good degree of precision. Since the treatment of Hodgkin's disease with radiotherapy has been highly successful in the past, the treatment techniques have not been modified very much over the last 30 years. This can be verified, for example, by a comparison of the treatment planning techniques used from 1960 to 1970 [22] with those used from 1980 until 1990 [23]. Additionally, the therapy protocols do not differ very much between the institutions that apply this form of treatment. These factors make it possible to reconstruct a statistically averaged OED distribution for each dose–response model $f(D)$, which is characteristic for a large patient collective of Hodgkin's disease patients.

The overall risk of selected second malignancies of 32,591 Hodgkin's patients after radiotherapy has been quantified by Dores et al. [24]. They found, for all solid cancers after the application of radiotherapy as the only treatment, an excess absolute risk of 39 per 10,000 patients per year (with a 95% confidence interval ranging from 35.4 to 40.5). The total number of person years in these studies was 92,039 with a mean patient age at diagnosis of 37 years. In combining the Hodgkin data with the A-bomb

Table 1 Population-dependent variables with one standard deviation in brackets applying the EPICURE-AMFIT code to the atomic survivor data

	RBE			RBE_D
	10	35	100	
Gender s	0.1686 (0.070)	0.1707 (0.070)	0.1742 (0.071)	0.1704 (0.071)
Age at exposure γ_e	−0.0285 (0.006)	−0.0280 (0.006)	−0.0273 (0.006)	−0.0277 (0.006)
Attained γ_a	2.408 (0.273)	2.423 (0.274)	2.432 (0.277)	2.409 (0.274)

survivor data "age at diagnosis of Hodgkin's disease" was equated to "age at exposure to the A-bomb", and "age at diagnosis of Hodgkin's disease + follow-up-time" was equated to "attained age of A-bomb survivors". The follow-up time distribution of the Hodgkin's patients [24] can be used with the temporal patterns of the atomic bomb data of Eq. (2) to obtain the mean attained age (a = 46 years). The mean age at exposure and mean attained age for the Hodgkin population was then used to center the fit of the A-bomb survivor data.

In several studies, no increased risk of solid cancers overall was observed after the application of chemotherapy alone. Dores et al. calculated the solid cancer risk both, after radiotherapy alone and combined modality therapy, and found an excess absolute risk of 43 per 10,000 patients per year for the latter. As a consequence, the difference in risk between combined modality treatment and radiotherapy

Table 2 Results of the fit to the atomic bomb data only. In brackets one standard deviation is given

RBE	Model parameter	Linear	Linear-exponential	Plateau
10	β^b	9.572 (3.84)	14.201 (0.95)	14.348 (0.94)
	α^a	–	0.089 (0.024)	–
	δ^a	–	–	0.206 (0.027)
	P value	>0.5	>0.5	<0.01
35	β^b	7.093 (4.08)	11.815 (0.84)	12.259 (0.81)
	α^a	–	0.082 (0.021)	–
	δ^a	–	–	0.202 (0.023)
	P value	>0.5	>0.5	<0.01
100	β^b	4.030 (3.83)	8.365 (0.66)	8.873 (0.65)
	α^a	–	0.066 (0.017)	–
	δ^a	–	–	0.178 (0.018)
	P value	>0.5	>0.5	0.751
RBE_D	β^b	8.813 (2.33)	11.710 (0.74)	11.790 (0.76)
	α^a	–	0.064 (0.020)	–
	δ^a	–	–	0.143 (0.021)
	P value	>0.5	0.477	<0.01

The P value was calculated using a χ^2-statistic with 21 degrees of freedom

[a] in Gy^{-1}

[b] in $(10,000\ PY\ Gy)^{-1}$

alone (4 per 10,000 patients per year) can be tentatively attributed to either chemotherapy or a genetic susceptibility of the Hodgkin patient population with regard to cancer or both. For this reason, we used this risk difference as an error estimate for the subsequent analysis.

A statistically averaged dose distribution was reconstructed, which is characteristic for a large patient collective of Hodgkin's disease patients in the Zubal Phantom, a voxel-based anthropomorphic phantom [25]. Different treatment plans for the various patterns of lymph nodes involvement [26] were obtained. The dose distributions were converted into OED according to Eqs. (4)–(6), assuming a mechanistic approach of cancer risk, where it is assumed that the total risk is the volume-weighted sum of the risks of the partial volumes. A statistically averaged OED distribution was then obtained by combining the OED from different plans with respect to the statistical weight of the involvement of the individual lymph nodes [26]. Details of the treatment plans were taken from the review by Hoppe [23]. The Eclipse External Beam Planning system version 6.5 (Varian Oncology Systems, Palo Alto, CA) was used for treatment planning with corrected dose distributions for head-, phantom- and collimator-scatter also including the extremities. Three different treatment plans were computed which included a mantle field, an inverted-Y field and a para-aortic field. All plans were calculated with 6 MV photons and consisted of two opposed fields. The prescribed dose was 36 Gy. The OED representing the risk for all solid cancers was finally determined as the average OED in the whole Zubal phantom.

Combined fit of A-bomb survivor and Hodgkin's patients

Since the dose distribution in a Hodgkin's patient is highly inhomogenous and the dose–response relationships as described by Eqs. (5) and (6) are nonlinear, it is not appropriate to apply a straight forward fit to the data. An iterative fitting procedure needs to be used instead. For this purpose, as described in the last section, the whole three-dimensional dose distribution used for Hodgkin treatment was converted into an OED-distribution for given model parameters α or δ. In addition, the dose data of the atomic

Fig. 1 Plot of cancer incidence per 10,000 persons per year as a function of organ equivalent dose (OED) of the A-bomb survivors (*as squares*) and the Hodgkin's patients (*as a diamond*). **a**, **c**, **e** and **g** show the *fit to the A-bomb survivor data* using a linear-exponential model and **b**, **d**, **f** and **h** using a plateau-dose model. The data and fits are presented for four different neutron RBE models and for age at exposure of 37 years and attained age of 46 years
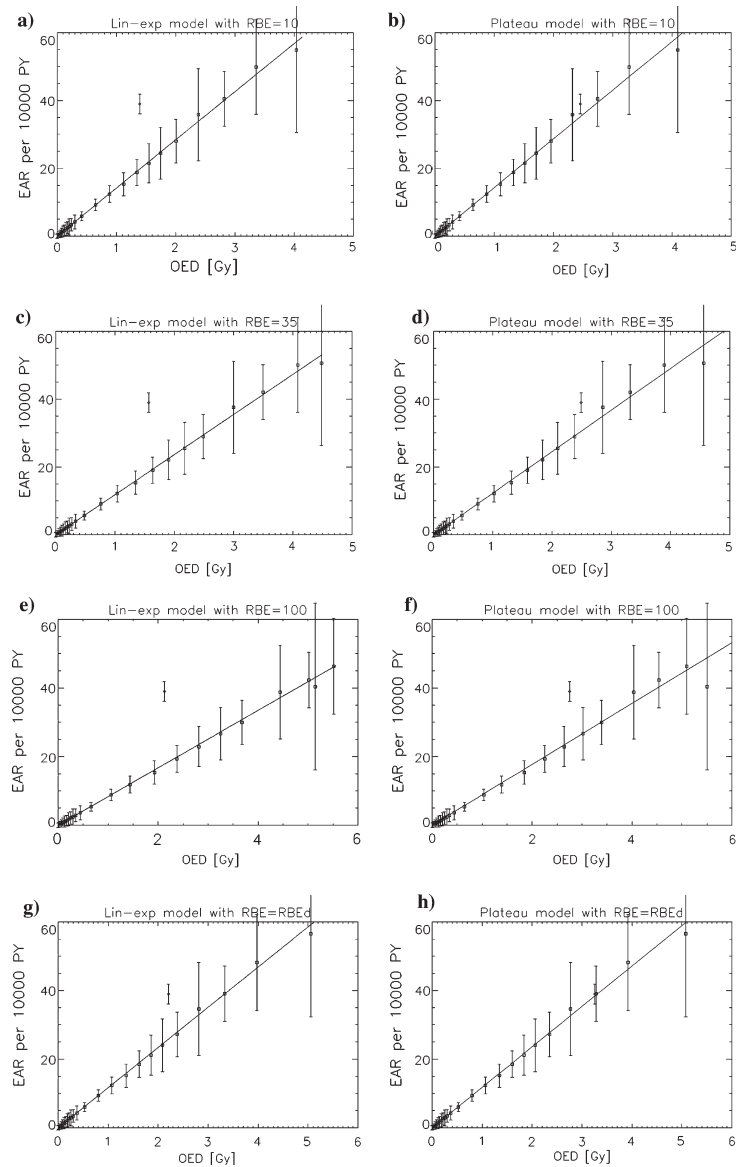
bomb survivors were converted to OED using Eqs. (5) and (6), and a homogenous whole body irradiation of the subjects was assumed. Since EAR as a function of OED is by definition linear Eq. (1), a linear curve was fitted to the combined dataset. The fitted EAR values were compared to the original data and weighted with the inverse of their variances. The α- and δ-values were fitted iteratively by minimizing χ^2

Table 3 Results of the fit to the Hodgkin's data only

RBE	Model parameter	Linear	Linear-exponential	Plateau
10	β^b	3.016 (0.31)	14.201 (0.82)	14.378 (0.90)
	α^a	–	0.055 (0.018)	–
	δ^a	–	–	0.180 (0.023)
	P value	>0.5	<0.01	<0.01
35	β^b	3.016 (0.31)	11.815 (0.69)	12.259 (0.75)
	α^a	–	0.047 (0.014)	–
	δ^a	–	–	0.150 (0.018)
	P value	>0.5	<0.01	<0.01
100	β^b	3.016 (0.31)	8.365 (0.51)	8.873 (0.54)
	α^a	–	0.034 (0.010)	–
	δ^a	–	–	0.100 (0.011)
	P value	>0.5	0.061	0.013
RBE_D	β^b	3.016 (0.31)	11.710 (0.70)	11.790 (0.75)
	α^a	–	0.047 (0.018)	–
	δ^a	–	–	0.140 (0.020)
	P value	>0.5	<0.01	<0.01

For the linear-exponential and the Plateau-model the initial slope of the atomic bomb data fit is used (Table 2). In brackets one standard deviation is given. The P value was calculated using a χ^2-statistic with 22 degrees of freedom

[a] in Gy^{-1}

[b] in $(10,000\ PY\ Gy)^{-1}$

$$\chi^2 = \sum \left(\frac{EAR_j - EAR_j^{fit}}{\sigma_j}\right)^2 \qquad (10)$$

where σ_j is the standard deviation of each data point and the sum includes both the A-bomb and the Hodgkin data.

The combination of the A-bomb survivor data with the Hodgkin's patients data made it necessary to use a fitting procedure other than the EPICURE-AMFIT software. To be consistent throughout β, α and δ for the A-bomb survivors data were re-fitted using the above-mentioned fitting routine. Since the re-fitted parameters agree within their standard errors with results using the EPICURE-AMFIT software, only the results of the re-fits are given here.

Results

Fits to A-bomb survivors data alone

Fitting the EAR model dose modifying function Eq. (2) with EPICURE-AMFIT to the atomic survivor data yields the population-dependent variables listed with the standard deviations in Table 1.

If a simple linear fit is optimized against the data, it is possible to determine the initial slope β for a neutron

RBE = 10, 35, 100 and RBE_D. The data are listed together with the corresponding standard deviations and P values in Table 2. The P values were obtained by applying a χ^2-statistic with 21 degrees of freedom applied to the complete dataset (A-bomb survivors and Hodgkin data). Values for β for a linear-exponential fit and for plateau-fit to the A-bomb survivors are also given in Table 2. The linear-exponential and plateau-fits for all four neutron RBE values considered here are plotted in Fig. 1.

Fits to the Hodgkin's data alone

Since in the limit of small dose both, the linear-exponential and the plateau-dose–response curve, as described by Eqs. (5) and (6), respectively, become linear with dose, the initial slope β is by definition the same as that required for application with small doses in radiation protection. For this reason, the initial slope is taken from the fits to the A-bomb survivors of Table 2. The remaining model parameters α and δ, were then determined by an iterative fit to the Hodgkin's data point. For the linear fit, an initial slope of 3.016 is obtained independently of the neutron RBE. The linear-exponential fit results in α and δ values, which are listed in Table 3 and plotted in Fig. 2 for the different values of the neutron RBE considered here.

Fits to A-bomb and Hodgkin's data combined

The combined dataset of A-bomb survivors data and Hodgkin's patients were fitted iteratively. The model parameters together with their standard deviations and the P values are listed in Table 4. The fitted functions are plotted in Fig. 3.

Discussion

The epidemiological data from the A-bomb survivors and the Hodgkin's patients are associated with large errors as discussed below. Nevertheless, some basic conclusion can be tentatively drawn from the analysis presented here. The quality of the applied fits measured by the P value (listed in Tables 2–4) shows that the linear model does not describe the data as well as the two other models. It seems that for doses above 4 Gy, the dose–response relationship is flattening. However, there is not much difference between the linear-exponential and the plateau-dose–response relationships, regarding their quality of fit. Both models fit the data well with a slight advantage for the plateau model.

It has been observed [17, 27] that cancer risks for patients exposed to ionizing radiation in the treatment of

Fig. 2 Plot of cancer incidence per 10,000 persons per year as a function of organ equivalent dose (OED) of the atomic bomb survivors (*as squares*) and the Hodgkin's patients (*as a diamond*). **a**, **c**, **e** and **g** show the *fit to the Hodgkin's patients* using a linear-exponential model and **b**, **d**, **f** and **h** using a plateau-dose model. The data and fits are presented for four different neutron RBE models and for age at exposure of 37 years and attained age of 46 years
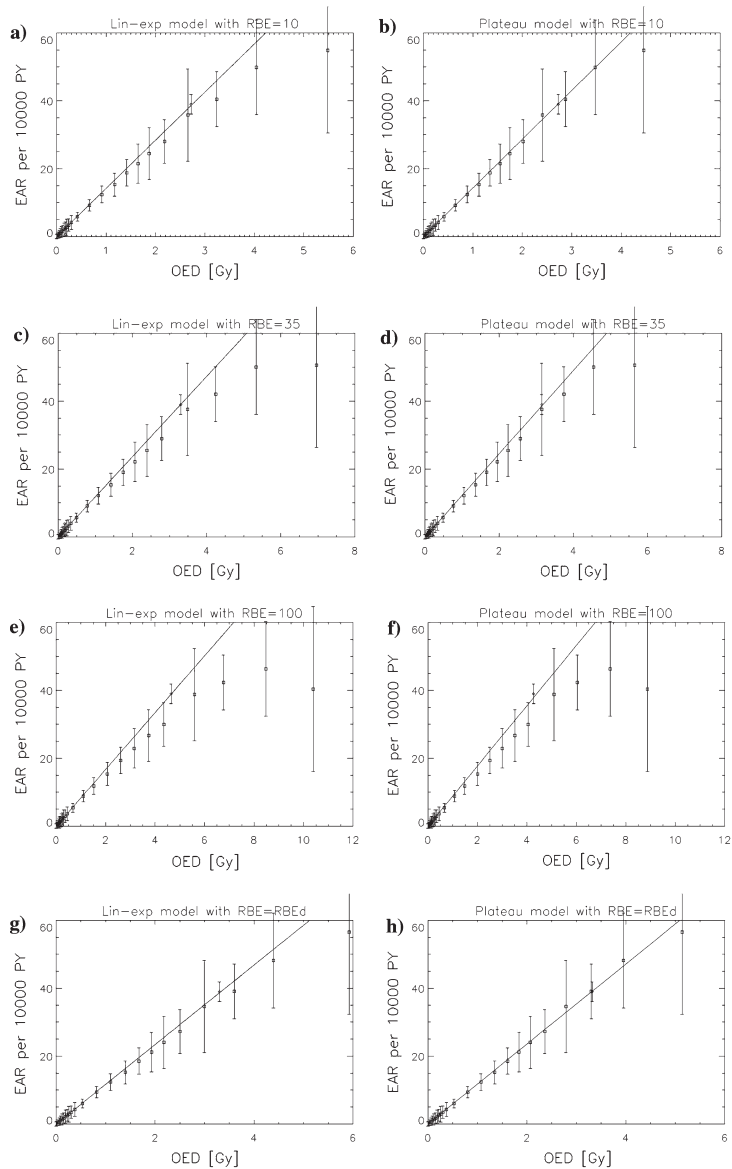
cancer, are generally lower (when plotted against average absorbed dose, not OED) than those estimated from the A-bomb survivors. It was suggested that cell sterilization, dose fractionation or a larger neutron RBE in the A-bomb data could account for this difference. The present analysis using OED, which includes cell sterilization effects, shows good agreement with the A-bomb data which are plotted as a function of absorbed dose for a RBE of 10

Table 4 Results of the fit to the atomic bomb data and the Hodgkin's data combined

RBE	Model parameter	Linear	Linear-exponential	Plateau
10	β[b]	4.170 (9.01)	12.367 (0.81)	13.824 (0.90)
	α[a]	–	0.050 (0.018)	–
	δ[a]	–	–	0.179 (0.023)
	P value	>0.5	<0.01	<0.01
35	β[b]	4.140 (6.86)	9.877 (0.68)	10.966 (0.75)
	α[a]	–	0.043 (0.014)	–
	δ[a]	–	–	0.146 (0.018)
	P value	>0.5	<0.01	<0.01
100	β[b]	3.522 (4.20)	6.689 (0.51)	7.205 (0.56)
	α[a]	–	0.034 (0.010)	–
	δ[a]	–	–	0.111 (0.012)
	P value	>0.5	0.053	0.168
RBE$_D$	β[b]	4.184 (6.72)	10.774 (0.70)	11.677 (0.70)
	α[a]	–	0.044 (0.017)	–
	δ[a]	–	–	0.139 (0.019)
	P value	>0.5	<0.01	<0.01

In brackets one standard deviation is given. The P value was calculated using a χ^2-statistic with 22 degrees of freedom

[a] in Gy^{-1}

[b] in $(10,000\ PY\ Gy)^{-1}$

and for Sasaki's RBE in Fig. 4. It has often been hypothesized that the bending-over, of the solid cancer excess risk dose–response curve for the A-bomb survivors, that has been observed to occur above 2 Gy, could be due to cell killing effects. The work presented here might provide the first direct evidence for this. The impact of dose fractionation and repopulation is not included in the present analysis.

The average doses in the two highest-weighted dose categories are increased from 5.4 and 8.9 Sv for a RBE 10 up to 12.7 and 22.1 Sv for a RBE of 100, respectively. Since the data in these high dose categories are subject to very large errors (standard deviation 0.8 and 2.3 Sv for RBE = 10, and 6.1 and 12.3 Sv for RBE = 100), it is not possible to assess the degree of dependability of the assumption of a large neutron RBE values such as 100, if the mean doses in these dose categories are compared with the lethal doses for humans (LD50). Additionally, it is worth noting that the last dose category employed here has been omitted in all previous analyses of these data, since the small chance of survival suggests that estimates of doses in this upper group could possibly be too large [18]. Sasaki's formulation of a neutron RBE which is variable with dose results in a dose–response curve which fits the data well and the average dose in the two highest dose categories is only increased to 5.7 and 9.0 Sv. This could be an additional indication for a dose-dependent neutron RBE.

Increased risks of solid cancers after Hodgkin's disease have been generally attributed to radiotherapy. An important question is whether chemotherapy for Hodgkin's disease also adds to the solid cancer risk, and if so, at which sites. If chemotherapy indeed affects induction of solid tumors, one would expect that patients receiving combined modality treatment would have a greater relative risk than patients treated with radiotherapy alone. Only one study has reported a significantly greater risk for solid cancers overall after combined chemo- and radiotherapy compared with irradiation alone [28], whereas no such difference has been found in the majority of investigations [28]. However, for selected solid cancer sites larger (e.g. lung) or lower (e.g. breast) risks were observed after combined modality treatment than after irradiation alone [28]. It can be tentatively hypothesized, for the analysis presented here, that cancer risk after chemotherapy of disparate sites is balanced in such a way that the risk for all solid tumors is not affected [28].

It is well known that genetic susceptibility underlies Hodgkin's disease [29]. It is not clear whether this genetic susceptibility would also affect the development of other cancers. There is the possibility of a cancer diathesis, the prospect that, for some reasons related to genetic makeup, a person who developed one cancer has an inherently increased risk of developing another. However, such cancer susceptibility would result in a minimal excess cancer incidence compared to the incidence of radiation related tumors, since such an excess cancer incidence of solid tumors should also be seen in Hodgkin's patients after treatment with chemotherapy alone. However, there is no statistically significant increase for all solid tumors combined. Therefore, such an effect will be hidden in the 95% confidence interval of the observed cancer incidence after chemotherapy.

In this work, EAR has been used to quantify radiation-induced cancer. Usually ERR is recommended for transferring risk from the Japanese population to other populations. EAR is used here, since the risk calculations of the Hodgkin's cohort are based on extremely inhomogenous dose distributions. It is assumed that the total absolute risk in the whole body is the volume-weighted sum of the risks of the partial volumes which are irradiated homogenously. Currently, there is no available method for obtaining analogous whole-body risk using ERR. Since the difference between the Japanese and the US population in EAR for all solid tumors is less than 10% and only all solid tumors together were analyzed here, the use of EAR is probably justifiable.

Fig. 3 Plot of cancer incidence per 10,000 persons per year as a function of organ equivalent dose (OED) of the atomic bomb survivors (*as squares*) and the Hodgkin's patients (*as a diamond*). **a**, **c**, **e** and **g** show the *fit to the combined dataset of A-bomb survivor data and Hodgkin's patients* using a linear-exponential model and **b**, **d**, **f** and **h** using a plateau-dose model. The data and fits are presented for four different neutron RBE models and for age at exposure of 37 years and attained age of 46 years
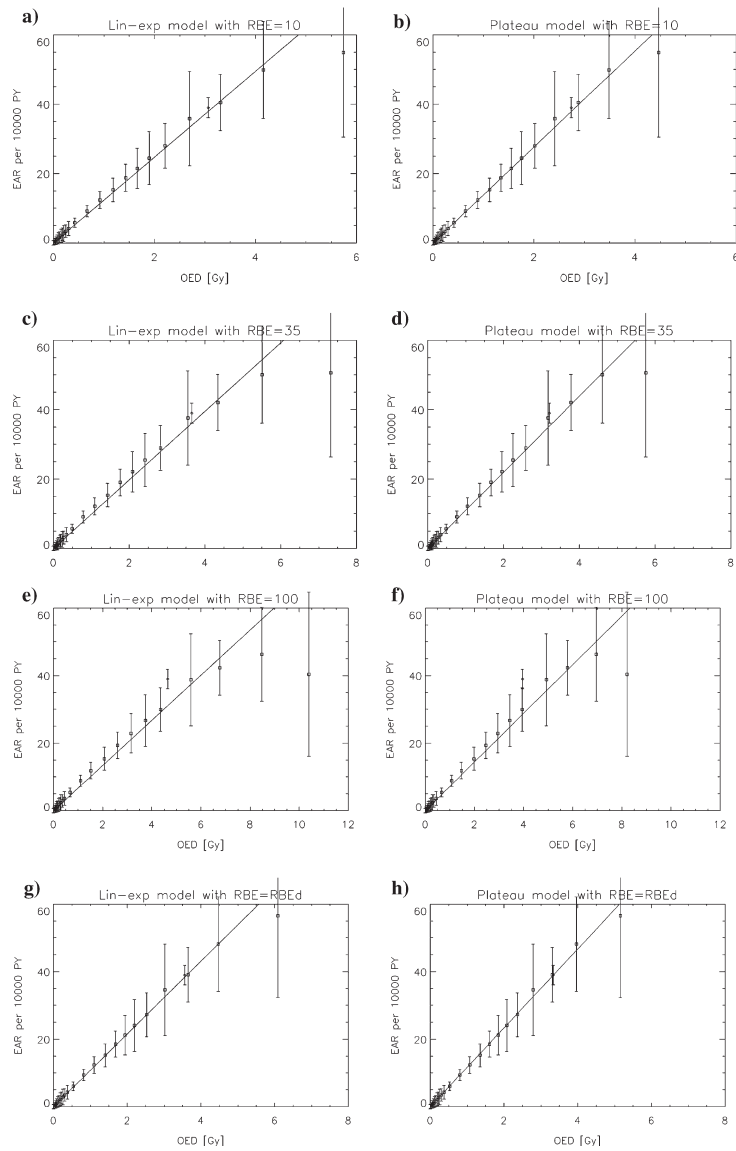
Conclusions

A comparison of dose distributions in humans, for example in radiotherapy treatment planning, with regard to cancer incidence or mortality can be performed by computing OED, which can be based on any dose–response relationship. In this work, OED was defined for a linear Eq. (4), a linear-exponential Eq. (5) and a plateau dose–response relationship Eq. (6). The model parameters (α and δ) were obtained by a fit of these OED models to A-bomb survivors

a)

b)
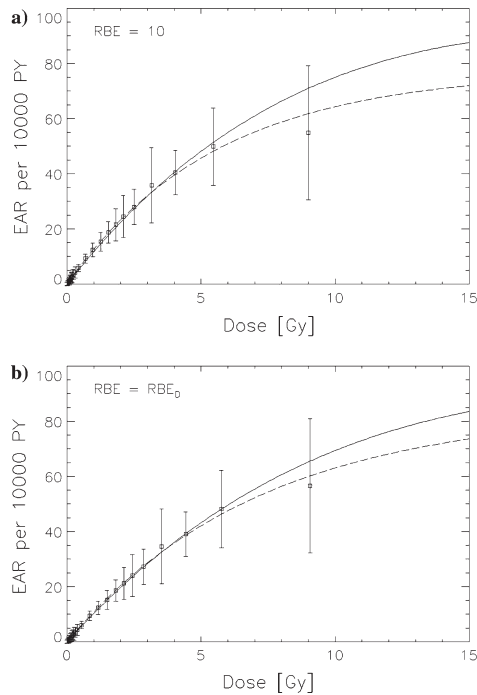
Fig. 4 Plot of cancer incidence per 10,000 persons per year as a function of *organ absorbed dose* of the atomic bomb survivors (*as squares*). Shown are the fits to the combined dataset of A-bomb survivor data and Hodgkin's patients using a linear-exponential model (*solid line*) and a plateau-dose model (*dashed line*). The data and fits are presented for a neutron RBE of 10 (**a**) and for a varying RBE$_D$ (**b**)

and Hodgkin's patients data and are listed in Table 3. For any three-dimensional inhomogenous dose distribution, cancer risk can be compared by computing OED using the coefficients obtained in this work.

For absolute risk estimates, EAR can be determined by taking additionally the fitted initial slope β from Table 3 and multiplying it with the population-dependent modifying function Eq. (1) using the fitted coefficients of Table 1. However, absolute risk estimates must be viewed with care, since the errors involved are large.

It has often been hypothesized that the bending over, of the solid cancer excess risk dose response curve for the A-bomb survivors, that has been observed to occur above 2 Gy, could be due to cell killing effects. The work presented here might provide the first direct evidence for this.

References

1. Preston DL, Ron E, Tokuoka S, Funamoto S, Nishi N, Soda M, Mabuchi K, Kodama K (2007) Solid cancer incidence in atomic bomb survivors: 1958–1998. Radiat Res 168:1–64
2. Preston DL, Pierce DA, Shimizu Y, Cullings HM, Fujita S, Funamoto S, Kodama K (2004) Effects of recent changes in Atomic bomb survivor dosimetry on cancer mortality risk estimated. Radiat Res 162:377–389
3. Walsh L, Rühm W, Kellerer AM (2004) Cancer risk estimates for X-rays with regard to organ specific doses, part I: all solid cancers combined. Radiat Environ Biophys 43:145–151
4. Walsh L, Rühm W, Kellerer AM (2004) Cancer risk estimates for γ-rays with regard to organ specific doses, part II: site specific solid cancers. Radiat Environ Biophys 43:225–231
5. Cucinotta FA, Wu H, Shavers M, George K (2003) Radiation dosimetry and biophysical models of space radiation effects. Gravit Space Biol Bull 16(2):11–18
6. Kim MH, Cucinotta FA, Wilson JW (2007) A temporal forecast of radiation environments for future space exploration missions. Radiat Environ Biophys 46(2):95–100
7. Lindsay KA, Wheldon EG, Deehan C, Wheldon TE (2001) Radiation carcinogenesis modelling for risk of treatment-related second tumours following radiotherapy. Br J Radiol 74(882):529–536
8. Hall EJ, Wuu CS (2003) Radiation-induced second cancers: the impact of 3D-CRT and IMRT. Int J Radiat Oncol Biol Phys 56(1):83–88
9. Davis RH (2004) Production and killing of second cancer precursor cells in radiation therapy. Int J Radiat Oncol Biol Phys 59(3):916
10. Schneider U (2005) Dose–response relationship for radiation-induced cancer-decrease or plateau at high dose. Int J Radiat Oncol Biol Phys 61(1):312–313
11. Dasu A, Toma-Dasu I (2005) Dose-effect models for risk-relationship to cell survival parameters. Acta Oncol 44(8):829–835
12. Dasu A, Toma-Dasu I, Olofsson J, Karlsson M (2005) The use of risk estimation models for the induction of secondary cancers following radiotherapy. Acta Oncol 44(4):339–347
13. Schneider U, Zwahlen D, Ross D, Kaser-Hotz B (2005) Estimation of radiation induced cancer from 3D-dose distributions: concept of organ equivalent dose. Int J Radiat Oncol Biol Phys 61: 1510–1515
14. Schneider U, Kaser-Hotz B (2005) A simple dose–response relationship for modelling secondary cancer incidence after radiotherapy. Z Med Phys 15(1):31–37
15. Sachs RK, Brenner DJ (2005) Solid tumor risks after high doses of ionizing radiation. Proc Natl Acad Sci USA 102(37):13040–13045
16. Schneider U, Kaser-Hotz B (2005) Radiation risk estimates after radiotherapy: application of the organ equivalent dose concept to plateau dose–response relationships. Radiat Environ Biophys 44(3):235–2399
17. Kellerer AM, Walsh L (2001), Risk estimation for fast neutrons with regard to solid cancer. Radiat Res 156:708–717

18. Pierce DA, Stram DO, Vaeth M (1990) Allowing for random errors in radiation dose estimates for the atomic bomb survivor data. Radiat Res 123:275–284
19. Kellerer AM, Rühm W, Walsh L (2006) Indications of the neutron effect contribution in the solid cancer data of the A-bomb survivors. Health Phys 90(6):554–564
20. Rühm W, Walsh L (2007) Current risk estimates based on the A-bomb survivors data—a discussion in terms of the ICRP recommendations on the neutron weighting factor. Radiat Prot Dosimetry. (Advance access, May 28, doi:10.1093/rpd/ncm087)
21. Sasaki MS, Endo S, Ejima Y, Saito I, Okamura K, Oka Y, Hoshi M (2006) Effective dose of A-bomb radiation in Hiroshima and Nagasaki as assessed by chromosomal effectiveness of spectrum energy photons and neutrons. Radiat Environ Biophys 45:79–91
22. Carmel RJ, Kaplan HS (1976) Mantle irradiation in Hodgkin's disease. An analysis of technique, tumor eradication, and complications. Cancer 37(6):2813–2825
23. Hoppe RT (1990) Radiation therapy in the management of Hodgkin's disease. Semin Oncol 17(6):704–715
24. Dores GM, Metayer C, Curtis RE, Lynch CF, Clarke EA, Glimelius B, Storm H, Pukkala E, van Leeuwen FE, Holowaty EJ, Andersson M, Wiklund T, Joensuu T, van't Veer MB, Stovall M, Gospodarowicz M, Travis LB (2002) Second malignant neoplasms among long-term survivors of Hodgkin's disease: a population-based evaluation over 25 years. J Clin Oncol 20(16):3484–3494
25. Zubal IG, Harrell CR, Smith EO, Rattner Z, Gindi G, Hoffer PB (1994) Computerized three-dimensional segmented human anatomy. Med Phys 21(2):299–302
26. Mauch PM, Leslie AK, Kadin M, Coleman CN, Osteen R, Hellman S (1993) Patterns of presentation of Hodgkin disease. Cancer 71(6):2062–2071
27. Little MP (2001) Comparison of the risks of cancer incidence and mortality following radiation therapy for benign and malignant disease with the cancer risks observed in the Japanese A-bomb survivors. Int J Radiat Biol 77(4):431–464 (Erratum in: Int J Radiat Biol 2001 77(6):745–60)
28. van Leeuwen FE, Travis LB (2005) Risk of second malignancy in patients with selected primary cancers. In: DeVita VT, Hellman S, Rosenberg SA (eds) Cancer: principles & practice of oncology, 7th edn. Lippincott Williams & Wilkins, Philadelphia, pp 2575–2602
29. Mack TM, Cozen W, Shibata DK et al (1995) Concordance for Hodgkin's disease in identical twins suggesting genetic susceptibility to the young-adult form of the disease. N Engl J Med 332(7):413–418

23. Jacob P, Walsh L & Eidemüller M. Modelling of carcinogenesis and cell killing in the atomic bomb survivors with applications to the mortality from all solid, stomach and liver cancers. Radiat. Environ. Biophys. 47, 375-388, 2008

ORIGINAL PAPER

Modeling of cell inactivation and carcinogenesis in the atomic bomb survivors with applications to the mortality from all solid, stomach and liver cancer

Peter Jacob · Linda Walsh · Markus Eidemüller

Abstract The two-stage clonal expansion (TSCE) model of carcinogenesis has been applied to cancer mortality data from the atomic bomb survivors, to examine the possible influence of radiation-induced cell inactivation on excess relative risk (ERR) and excess absolute risk (EAR) estimates. Cell survival curve forms being either conventional or allowing for low-dose hypersensitivity (LDH) were investigated. Quality-of-fit tests for non-nested models were used in comparisons with the types of empirical risk models applied at the Radiation Effects Research Foundation (RERF) in Hiroshima. In general the TSCE model was found to represent the data more economically (i.e., with fewer parameters for a similarly good description of the data) than the empirical risk model. However, the data are not strong enough to give a clear preference to one of the very different model types used. Central ERR and EAR estimates (at 1 Sv, for age at exposure 30 and age attained 70) from TSCE and empirical models were in good agreement with each other and with previously published estimates. However, the TSCE models including radiation-induced cell inactivation resulted in a lower estimate of the relative risk at young ages at exposure (0–15 years) than the empirical model. Also the TSCE model allowing for radiation-induced cell inactivation with a conventional cell survival curve resulted at 0.2 Sv in significantly lower risk estimates than the model with LDH. These model differences have been used here to suggest risk estimates which include model uncertainty as well as the usual statistical uncertainty. Model uncertainties were small for central estimates and larger for other values of the variables. Applying the proposed method to excess risk for all solid cancer at 1 Sv, age at exposure 10 and age attained 70, results in total uncertainty ranges that are wider than the pure statistical uncertainty range by about 30% for both ERR and EAR.

Introduction

The cohort of the atomic bomb survivors from Hiroshima and Nagasaki is unique for various reasons: the large number of cohort members; the long follow-up period of 50 years; a large dose range from natural to lethal levels; and an internal control group with negligible doses. Cancer mortality data from the atomic bomb survivors have a follow-up period beginning in 1950, i.e. 5 years after exposure and 7 years before the start of the corresponding cancer incidence data. Site-specific cancer mortality data are available for a follow-up period up to 1997 with the dosimetry system DS86 [1], all cancer mortality data for a follow-up up to 2000 with the recently revised dosimetry system DS02 [2, 3].

Epidemiological data-sets concerning the atomic bomb survivors provide an opportunity for conducting analyses of the data with biologically motivated models of carcinogenesis. The standard two-stage clonal expansion (TSCE) model for carcinogenesis [4, 5] has already been shown to model several important epidemiological datasets rather well, and is therefore an ideal candidate for further development to include non-linear low-dose effects.

P. Jacob (✉) · L. Walsh · M. Eidemüller
Helmholtz Zentrum München, German Research Center
for Environmental Health, Institute of Radiation Protection,
Ingolstädter Landstraße 1, 85764 Neuherberg, Germany
e-mail: Jacob@helmholtz-muenchen.de

L. Walsh
Federal Office for Radiation Protection, 85764 Oberschleißheim,
Germany

For acute exposures to γ radiation, such as those received by atomic bomb survivors, low-dose hypersensitivity in the cell survival response has been seen in many cell lines [6, 7]. For most cell lines, the number of inactivated cells per unit dose is higher for low doses (up to a few hundred mGy) than for high doses where an increase in radio-resistance is observed.

The purpose of this paper is to analyze the mortality from all solid cancers combined, stomach and liver cancer with the TSCE model, in order to examine the possible influence of radiation-induced cell inactivation on excess risk estimates. Conventional cell survival curves and curves with low-dose hypersensitivity are considered.

Stomach cancer is the most frequently occurring cancer in this cohort, with lung and liver cancer occupying second and third place in the frequency ranking, respectively. An analysis for lung cancer incidence that included consideration of low-dose hypersensitivity has already been presented [8]. Both statistical and biological considerations lead to the choice of stomach and liver for the special site-specific analysis presented here. New data for cell inactivation in liver cells has recently been published [9] and somewhat older data on cell inactivation in stomach cells [10] was found to be suitable for integration into the TSCE model with cell inactivation. Since no specific data for the low-dose hypersensitivity of liver or stomach cells are currently available, some general characteristics of the associated biological data for 26 different human cell types [7, 11] were integrated into the TSCE modeling procedure. All solid cancers together were also investigated because of the better statistical power.

Materials and methods

The data on cancer mortality on the atomic bomb survivors from Hiroshima and Nagasaki are analyzed with four types of models:

- TSCE models without explicit modeling of radiation-induced cell inactivation
- TSCE models with explicit modeling of radiation-induced cell inactivation in the form of a classical cell survival curve
- TSCE models with explicit modeling of radiation-induced cell inactivation taking account of low-dose hypersensitivity
- empirical risk models as used at the Radiation Effects Research Foundation (RERF) in Hiroshima.

Quality of fit criteria for non-nested models were applied in order to compare the preferred models of the four model types.

Data on cancer mortality

The two most recent datasets on cancer mortality in the cohort of atomic bomb survivors in Hiroshima and Nagasaki have been analyzed here. These cover the follow-up time periods from 1950 to 1997 and from 1950 to 2000 with the dosimetry systems DS86 and DS02, respectively (data files: R13MORT.DAT and DS02CAN.DAT from http://www.rerf.or.jp). Concerning all cancers combined, our analyses of the two data sets resulted in similar findings as they were reported for analyses with conventional excess risk models [3]. Therefore, we report here only results on the most recent data set. This data set, however, does not contain any details of organ specific cancer mortality. Therefore, the stomach and liver cancer modeling could only be performed with the DS86 dataset.

The data are in grouped form and are categorized by gender, city, age at exposure, age attained, calendar time period during which the mortality checks were made and weighted survivor colon dose. For each data group i, the record contains the mean age attained a_i, the mean age at exposure e_i, the mean colon weighted dose d_i, the number of person years PY_i and the number of cancer cases.

Weighted doses

Weighted organ doses are defined by

$$d = d_\gamma + \mathrm{RBE}\, d_\mathrm{n}, \qquad (1)$$

where d_γ and d_n are organ doses from γ-rays and neutrons, respectively. For RBE, the relative biological effectiveness of neutrons, the value 10 has been used if not otherwise specified.

Only the data groups with mean weighted colon dose categories corresponding to ≤ 2 Sv were used, in order to avoid the flattening of the dose response in the dose region >2 Sv. Age-attained and age-at-exposure dependences were found to be rather insensitive to the dose cut-off.

The colon doses were transformed to doses in other organs by applying conversion factors supplied in a separate RERF data set. The actual six data sets chosen for the modeling, the associated number of cancer deaths and the number n of data cells are given in Table 1.

In the calculations for all solid cancers combined, weighted organ-averaged doses [12] are used in place of the weighted colon dose. The organ-averaged doses are calculated with weighting factors accounting for the risk contribution of individual tumor sites. The weighted organ-averaged doses are larger than the colon doses (which are used in the RERF analyses) by factors of 1.085 and 2 for the gamma and neutron contributions, respectively.

Table 1 Data sets of atomic bomb survivors with colon doses ≤2 Sv: number of cancer deaths and data cells

Data set	Number of cancer deaths, n	Number of data cells
Male, all solid, DS02	4,779	14,803
Female, all solid, DS02	5,234	15,139
Male, stomach, DS86	1,544	16,928
Female, stomach, DS86	1,298	16,764
Male, liver, DS86	719	16,928
Female, liver, DS86	511	16,764

Cell inactivation

Conventional cell survival curves

The dose response of cell inactivation after exposure to low-LET radiation is conventionally modeled by cell survival curves of the form

$$S(d) = \exp[-a_r d - b_r d^2], \qquad (2)$$

where d is absorbed dose, and a_r and b_r are the parameter values of the linear and quadratic dose terms, respectively.

Cell survival curves for liver cells, stomach cells, and a mixture of cells from various organs used in the present analysis are shown in Fig. 1.

Cell survival curves with low-dose hypersensitivity

Low-dose hypersensitivity (LDH), observed for a number of cell lines for cell inactivation after exposure to low-LET radiation [7], has been modeled with the form

$$S(d) = \exp[-a_r(1 + (a_s/a_r - 1)\exp(-d/d_c))d - b_r d^2], \qquad (3)$$

where a_s is the coefficient of the linear dose term in the low-dose (sensitive) regime and d_c a dose characteristic for the transition from the low-dose to the high-dose regime.

Low-dose hypersensitivity is expressed by $a_s > a_r$ (Fig. 1). In the present analysis, the mortality data of the atomic bomb survivors do not have enough power to determine these additional parameters. Therefore, the parameters were estimated from experimental data.

No specific data for the low-dose hypersensitivity of liver or stomach cells are currently available. Therefore, general characteristics of the associated biological data obtained from more than 26 different human cell lines [7] were integrated into the modeling procedure: characteristic values for the ratio a_s/a_r were judged to be 5 and 20 (from Fig. 2 of [7]), whereas characteristic values for the d_c were judged (from Table IV of [11]) to be 0.1 and 0.2 Gy. All four combinations of these values for a_s/a_r and d_c were applied in the present analysis. The influence
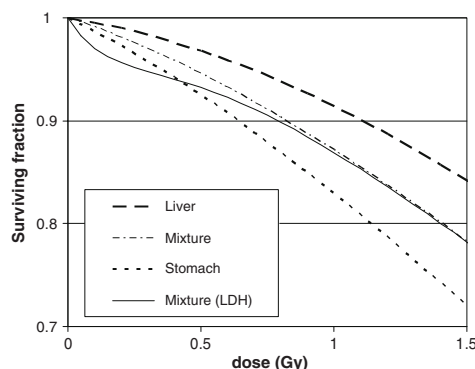
Fig. 1 Cell survival curves for liver cells (*dashed line*: $a_r = 0.0399$ Gy^{-1}, $b_r = 0.0500$ Gy^{-2} [9]), stomach cells (*dotted line*: $a_r = 0.1252$ Gy^{-1}, $b_r = 0.0624$ Gy^{-2} [10]), and combined sites: liver, stomach, colon and lung (*dot-dashed line*: $a_r = 0.0859$ Gy^{-1}, $b_r = 0.0520$ Gy^{-2} [9–11]), computed with the method of Hawkins [13]. The *solid curve* is for the combined sites with LDH, shown here for values of $a_s/a_r = 5$ and $d_c = 0.2$ Gy in Eq. (3)

of the actual values of these parameters on the results is negligible.

In the present application the absorbed dose in Eqs. 2 and 3 has been replaced by the weighted dose according to Eq. 1.

The TSCE model

The TSCE model (Fig. 2) gives a stochastic description of a simplified temporal process of carcinogenesis. It is assumed that at age a a set of mutations and/or epigenetic events initiates healthy stem cells with a rate $v(a)$ into intermediate cells. Intermediate cells can form clones as a net result of cell division with a rate $\alpha(a)$ and of differentiation or inactivation with a rate $\beta(a)$. A further set of mutations and/or epigenetic events converts intermediate cells with a rate $\mu(a)$ into malignant cells. Once a malignant cell is
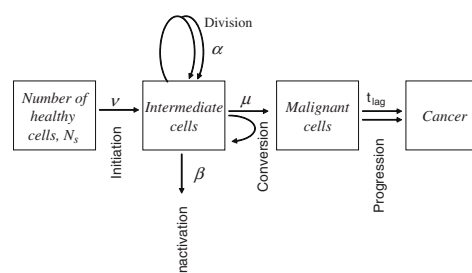
Fig. 2 Schematics of the two-stage clonal expansion (TSCE) model

produced, it causes death due to cancer after some lag time t_{lag}. As in previous analyses [8, 14, 15], the lag time was found not to have a major influence on the results. In the main calculations, the lag time is fixed to 5 years.

It is convenient to introduce a parameter $X(a)$, which is the product of the age-dependent creation rate of clones of intermediate cells and the malignant conversion rate μ_0 in the absence of any exposure:

$$X = \mu_0 \nu N_s \qquad (4)$$

Baseline cancer mortality in the TSCE model

Under the assumption that the five biological parameters (number of susceptible stem cells N_s, initiation rate ν, division rate α, differentiation and inactivation rate β, and malignant conversions rate μ) are independent of age, the TSCE model can be solved analytically [16, 17]. The cancer mortality rate can be determined from three parameters X_0, α_0 and β_0. The values of α_0 and β_0, however, depend on the value of μ_0 [18], which is set in the present calculations to 10^{-6} year^{-1}.

Secular trends in baseline cancer rates were described by a multiplicative factor for X_0.

Radiation action on parameters of the TSCE model

The radiation action was described by immediate actions on the initiation rate ν and on the malignant conversion rate μ, and by delayed actions by taking account of cell inactivation effects on the division rate α and the differentiation or inactivation rate β of intermediate cells. Spontaneous baseline parameters are used before and after these two time periods (Fig. 3). Within these four time periods the
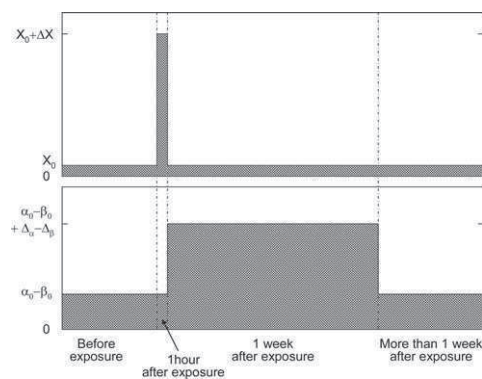
Fig. 3 Schematic representation of the TSCE model parameters X and α–β in four time periods: before exposure, during the first hour after exposure, during the following week after the exposure, and later

TSCE model parameters were assumed to be constant so that the exact hazard function could be calculated by a recursion formula [19].

The short-term action is assumed to last for $\Delta a_I = 1.14 \times 10^{-4}$ years (1 h), which is short compared to all other time periods in the model. In the TSCE$_{IT}$ model (i.e. the TSCE model with a linear effect of the radiation on the initiation and conversion rates) the parameters values during the first hour after exposure are expressed by:

$$X = \exp\left\{\beta_5(e - t_e) + \beta_6(e - t_e)^2\right\}[X_0 + X_d d/\Delta_{a_I}]$$
$$\mu/\mu_0 = 1 + \mu_d d, \qquad (5)$$

where e is the age at exposure, t_e is 30 years, and β_5, β_6, X_d and μ_d are fit parameters.

The delayed action is assumed to last for $\Delta a_P = 1.92 \times 10^{-2}$ years (1 week), which is the time period typically chosen in cell inactivation experiments between exposure and scoring. The effect of the radiation-induced cell killing is expressed by a change of α and β, assuming a dose dependence, which is proportional to the number of inactivated cells in in vitro experiments divided by the time of the observation period

$$\Delta\alpha = \alpha_d[1 - S(d)]/\Delta a_P$$
$$\Delta\beta = \beta_d[1 - S(d)]/\Delta a_P, \qquad (6)$$

where α_d and β_d are fit parameters.

The cell survival function $S(d)$ can either have the conventional form (Eq. 2) in the TSCE$_C$ model or the form for low-dose hypersensitivity (Eq. 3) in the TSCE$_L$ model. The hazard turned out to depend mainly on α_d–β_d, whereas the specific values of α_d and β_d have little influence on the hazard and could not be determined from the data. In the calculations the value of 1 was assumed for β_d. A cell killing effect on the number N_s of healthy stem cells has not be included in the model, because the killed fraction of cells is relatively small (see Fig. 1) and homeostasis is assumed to reconstitute the number of healthy stem cells.

In addition to the models described above, a TSCE$_P$ model, similar to what has been used in previous papers [e.g. 15] is considered. In the TSCE$_P$ model the delayed radiation action on a promotion rate of intermediate cells

$$\gamma = \alpha - \beta - \mu \qquad (7)$$

is defined in the first week after the short-term radiation action by

$$\Delta\gamma = \gamma_d d/\Delta a_P, \qquad (8)$$

while keeping $q = (\sqrt{\gamma 2 + 4\alpha\mu} - \gamma)/2$ constant; γ_d is a fit parameter. It may be noted that the TSCE$_P$ model can be derived from the models with radiation-induced cell inactivation (Eq. 8) by assuming that $1 - S(d)$ is proportional

to d, and by neglecting the effect of the radiation-induced cell inactivation on the parameter q.

The empirical models

Use is made of a general rate (hazard) model of the form

$$\lambda(a, e, d) = \lambda_0(a, e)[1 + \mathrm{ERR}(d, e)], \tag{9}$$

for the excess relative risk (ERR) and

$$\lambda(a, e, d) = \lambda_0(a, e)[1 + \mathrm{EAR}(d, a, e)] \tag{10}$$

for the excess absolute risk (EAR), where $\lambda_0(a, e)$ is the baseline cancer death rate. The ERR is factorized into a linear function of dose and a modifying function that depends exponentially on age at exposure (EMP$_E$ model):

$$\mathrm{ERR}(d, e) = \kappa_d d \exp\left(-\omega(e - t_e)\right), \tag{11}$$

where κ_d, the ERR per dose for age at exposure 30, and ω are fit parameters

Alternatively, models without an age-at-exposure modifier (EMP$_0$ model) were tested. It is also possible to fit an analogous age-attained model, however, a previous analysis concluded that the age-at-exposure model fitted the data somewhat better [20].

Similarly, the EAR is factorized into a linear function of dose and a modifying function that depends exponentially on age at exposure and the natural logarithm of attained age (EMP$_{EAR}$ model):

$$\mathrm{EAR}(d, a, e) = \kappa_d d \exp\left[-\omega(e - t_e) + \omega_a \ln(a/t_{a1})\right], \tag{12}$$

where t_{a1} is 70 years.

Although the baseline rates can be dealt with by stratification, the main calculations here adopt a fully parametric model:

$$\begin{aligned}
\lambda_0(a, e) = \exp\Big\{ &\beta_0 + \beta_1 \ln(a/t_{a1}) + \beta_2 \ln^2(a/t_{a1}) \\
&+ \beta_3(\max(0, \ln(a/t_{a2})))^2 + \beta_4(\max(0, \ln(a/t_{a1})))^2 \\
&+ \beta_5(e - t_e) + \beta_6(e - t_e)^2 \Big\},
\end{aligned} \tag{13}$$

where $\beta_0, \ldots, \beta_6$ are fit parameters, and t_{a2} is 40 years. This is a simplified version of the model of Preston et al. [1], in which some terms were dropped, because they were not found to significantly improve the fit in the current analysis.

Estimation of parameters and statistical analysis

The TSCE and the empirical models contain sets of parameters from which the cancer mortality rate λ_i can be computed in each data cell as a function of age a_i, age at

exposure e_i and dose d_i. The models predict the number of fatal cancers as a Poisson random variable with an expectation value of $PY_i \lambda_i$. In order to estimate the parameters in the model, the maximum likelihood technique is used, as described in a previous work [15]. Best estimates, uncertainty ranges and correlations of the parameters were determined by minimizing the deviance (minus twice the natural logarithm of the likelihood) using the CERN LIBRARY MINUIT minimizer called MIGRAD which implements a stable variation of the Davidon-Fletcher-Powell variable-metric (a quasi-Newton method) [21]. The empirical models were also computed in EPICURE/AMFIT [22] as a double check on the numerical methods.

The magnitude of the deviances and the number of parameters were used to assess the relative quality of the model fits. The number of parameters in the age-at-exposure model was assumed to be equal to the number of parameters actually optimized plus two for the spline joins t_{a1} and t_{a2} in the β_3 and β_4 terms of the baseline model (Eq. 13) (a total of 11 parameters for the EMP$_E$ model). The number of TSCE model parameters was assumed to be equal to the number of parameters actually optimized plus the lag time. For the TSCE models with an explicit modeling of cell inactivation, the parameter β_d, which was set to 1.0, was counted as a further model parameter.

For nested models, the likelihood ratio test was used to determine the preferred model. The quality of fit of the preferred models, which were non-nested, was assessed by two methods [23].

Based on information theory, Akaike [24] proposed to choose the model with a minimal value of the Akaike Information Criterion, AIC,

$$\mathrm{AIC} = \mathrm{dev} + 2k, \tag{14}$$

where dev is the deviance of the model and k the number of fit parameters.

The probability for a model improvement can then be computed by the following equation [25],

$$\mathrm{prob} = 1 - \exp\left(-0.5\Delta\mathrm{AIC}\right)/(1 + \exp\left(-0.5\Delta\mathrm{AIC}\right)). \tag{15}$$

Thus, a model A is considered to be an improvement of another model B with 95% probability, if the AIC for model A is smaller than the AIC for model B by 5.9 points.

Based on the Bayesian approach of Schwarz [26], we also use the Bayes Information Criterion,

$$\mathrm{BIC} = \mathrm{dev} + k \ln(n), \tag{16}$$

where n is the number of deaths from cancer, as proposed by Volinsky and Raftery [27].

The evidence for a model improvement is positive, strong or very strong if the difference in the BIC values is larger than 2, 6 and 10 points, respectively [28].

The BIC imposes a stricter penalty against extra model parameters than the AIC. A formal proof [29] has shown the AIC to be "dimensionally inconsistent", meaning that the probability of AIC favoring an over-parameterized model does not tend to zero even as the dataset size tends to infinity. Since, however, the AIC is closer to the maximum likelihood test for nested models than the BIC, the AIC has been considered here in addition to the dimensionally consistent BIC.

All significance tests reported here were performed as two sided.

Calculation of excess risk values

Parametric calculations

In the empirical models, central estimates of the ERR or the EAR, for example for age at exposure 30, are obtained directly by the fit procedure. Estimates and uncertainty ranges of the ERR or the EAR for other variable values, for example for other ages at exposures, were also obtained directly from the fit procedure by adjusting the centering (i.e. the values of t_e and t_{a1} in Eq. 12) and re-optimizing accordingly. In the TSCE models, none of the excess risk values are directly obtained by the fit procedure. The excess risk values are calculated here by a method already fully described by [8]. The best estimates are calculated from the optimized parameter values obtained from fitting the mortality data. The uncertainty bounds are calculated from the distributions and correlations of the model parameters. Crystal Ball (Crystal Ball. Forecasting and Risk Analysis for spreadsheet users, 1998, Decisioneering, Denver, Co, USA) is used to calculate 10,000 Monte-Carlo realizations from the parameter distributions. Alternative realization sets including correlation accounting and Latin hypercube sampling [30] were also computed using a computer program written by one of the coauthors (M.E.) as a double check. For each realization of the parameters a baseline mortality rate and a mortality rate at e.g. 1 Sv can be calculated which together provide a realization of either the ERR or EAR at 1 Sv. Uncertainty bounds are then obtained from the corresponding percentiles of the ordered set of the 10,000 ERR or EAR realizations.

Non-parametric calculations

Non-parametric estimates of the ERR in dose categories have been obtained by adjusting for age at exposure and age attained. Further adjustments for city (Hiroshima or Nagasaki) were not found to be necessary. These calculations have been performed with AMFIT/EPICURE.

Results

Preferred models for the four types of models

For each of the six data sets, all three types of preferred TSCE models included a radiation effect on the initiation rate (Table 2). For the preferred models with an explicit modeling of radiation-induced cell inactivation, allowing for an action of the radiation on other parameters generally did not improve the fit. Only for one data set (all solid cancer types among males) an additional effect of the radiation on the malignant conversion rate (TSCE$_{ICT}$ and TSCE$_{ILT}$ models) improved the fit (Table 2). In the models with low-dose hypersensitivity, the choices of different values for the ratio a_s/a_r and for the d_c had only minor influence on the deviance and on the parameters.

Among the empirical models, the exponential form of the age-at-exposure risk effect modifier of the ERR (Eq. 11) fitted the data for all cancer best (Table 2). However, the data on stomach cancer among males and for liver cancer for both sexes were best fitted with an empirical model without an age-at-exposure risk modification. Concerning the EAR models, all six data sets could be fitted equally well with either a linear age-at-exposure EAR effect modifier or with the exponential form (Eq. 12). The maximum observed change in deviance on switching between the two functional forms was only one point. The quality of the EAR model fits was not improved by the inclusion of an age-at-exposure risk modification in the cases of stomach cancers for both sexes and liver cancers among females.

A comparison of the ERR and EAR preferred models generally yielded changes in AIC of less than six, except in the case of male liver cancer where the ERR risk model fitted significantly better than the EAR model. The same type of comparison in terms of BIC yielded strong to very strong Bayesian evidence in favor of the ERR model, since the extra age-attained fit parameter in the EAR model was strongly penalized here.

Comparison of preferred models

The weight of evidence accumulated from the changes in BIC values given in Table 2 indicates that the TSCE models without an explicit modeling of radiation-induced cell inactivation generally fit the data better than the other TSCE models. The reason is that the BIC imposes a strict penalty on the inclusion of the additional parameter β_d in the model with explicit radiation-induced cell inactivation. It may, however, be argued that β_d should not be counted as a parameter, because in a wide range of values it does not influence the hazard. The differences of the AIC values for the various TSCE model types were generally small.

Table 2 Preferred models: empirical EMP (index "E"/"0": with/ without age-at-exposure modifier), TSCE without explicit radiation-induced cell inactivation (index "I" for radiation action on initiation rate, index "P" for radiation action on promotion rate, γ; index "T" for radiation action on malignant conversion rate), TSCE with radiation-induced cell inactivation with a conventional cell survival curve (index "C"), and TSCE with radiation-induced cell inactivation with low-dose hypersensitivity (index "L")

Data set	Model	Number of parameters	Deviance	BIC	AIC	Data set	Model	Number of parameters	Deviance	BIC	AIC
Male, all solid DS02	EMP$_E$	11	6,419	6,512	6,441	Female, stomach DS86	EMP$_E$	11	3,870	3,949	3,892
	TSCE$_{IP}$	**8**	**6,424**	**6,492**	**6,440**		**TSCE$_I$**	**7**	**3,878**	**3,928**	**3,892**
	TSCE$_{ICT}$	10	6,420	6,505	6,440		TSCE$_{IC}$	9	3,877	3,942	3,895
	TSCE$_{ILT}$	10	6,422	6,507	6,442		TSCE$_{IL}$	9	3,877	3,942	3,895
Female, all solid DS02	**EMP$_E$**	**11**	**6,697**	**6,791**	**6,719**	Male, liver DS86	EMP$_0$	10	2,679	2,745	2,699
	TSCE$_{IT}$	**8**	**6,717**	**6,786**	**6,733**		**TSCE$_{IP}$**	**8**	**2,678**	**2,731**	**2,694**
	TSCE$_{IC}$	**9**	**6,714**	**6,791**	**6,732**		TSCE$_{IC}$	9	2,683	2,742	2,701
	TSCE$_{IL}$	**9**	**6,712**	**6,789**	**6,730**		TSCE$_{IL}$	9	2,683	2,742	2,701
Male, stomach DS86	EMP$_0$	10	3,959	4,032	3,979	Female, liver DS86	EMP$_0$	10	2,137	2,199	2,157
	TSCE$_I$	**7**	**3,961**	**4,012**	**3,975**		**TSCE$_I$**	**7**	**2,140**	**2,184**	**2,154**
	TSCE$_{IC}$	9	3,960	4,026	3,978		TSCE$_{IC}$	9	2,139	2,195	2,157
	TSCE$_{IL}$	9	3,960	4,026	3,978		TSCE$_{IL}$	9	2,140	2,196	2,158

For each of the data sets, models with the minimum BIC value and models without strong evidence against them are indicated by bold letters

There is very strong evidence according to the BIC (ΔBIC $\geq$ 10) for five of the six data sets that the quality of fit is better for the preferred TSCE models than for the preferred empirical models. The reason is the smaller number of parameters in the TSCE models. There were generally only small differences in the quality of fit according to the AIC. For the remaining data set (all solid cancer among females), the BIC values are similar for all four types of models. The changes in AIC indicate that the empirical model fits this data set better than the TSCE models with more than 95% probability.

The all-cancer mortality as predicted by the four preferred models agreed well with the raw mortality rates for the atomic bomb survivors with doses smaller than 20 mSv (Fig. 4). The very small differences for males indicate that the baseline is slightly better described by the empirical model. On the other hand, there is a tendency that the TSCE models describe the data for the higher-dose group better.

The quality of fit was also evaluated by comparing the calculated number and the observed number of cancer fatalities in nine dose/age-at-exposure and in nine dose/ age-attained data categories. The actual χ^2 values are generally below the critical value of 15.5 (Tables 3, 4).

The TSCE and empirical models were also refitted with higher neutron RBE values of 35 and 100 [31], but only one of the data subsets (female, all solid) fitted to the empirical model showed an improvement in deviance of 6 points in the transition from an RBE of 10 to 100. Otherwise, the deviance profiles in this range of RBE values were found to be generally rather flat.

Parameters

The parameters which describe the baseline cancer mortality rates in the TSCE model (X_0, β_5, β_6, α_0, β_0) clearly depend on gender and on cancer site (Table 5). This may be related to differences in the processes of carcinogenesis. The division and inactivation rates of intermediate cells are the best determined parameters. Their difference, α_0–β_0, is about 0.1 year^{-1}, which is by five orders of magnitude larger than the assumed value of μ_0 (10^{-6} year^{-1}). This difference is independent of μ_0, as long as μ_0 is small. The values of α_0 and β_0, however, are approximately proportional to $(\mu_0)^{-1}$ [18, 32].

The effect of the radiation on the initiation rate, expressed by X_d, is significant (Table 5). The dose which creates the same number of clones as spontaneous processes during 1 year (i.e., X_0(1 year)/X_d) is in the range of 0.02 to 0.2 Sv.

A positive value of α_d–β_d indicates that the number of intermediate cells inactivated by the radiation is over-compensated by a stimulation of the proliferation of intermediate cells. The parameter α_d–β_d in the TSCE models with radiation-induced cell inactivation is significantly positive for all solid cancer among males and for liver cancer among females (Table 5). For the other four data sets, however, no significant result about a growth or anti-growth stimulating effect of the radiation could be obtained.

For one data set (male all solid cancers) the preferred among the models with radiation-induced cell inactivation contains an action of the radiation on the malignant
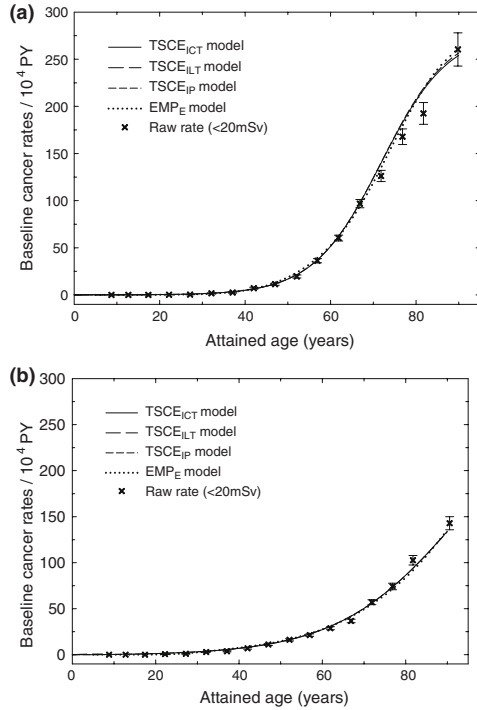
Fig. 4 Baseline all-cancer mortality rates **a** for males and **b** for females as predicted by the four preferred models, and raw rates among atomic bomb survivors with doses below 20 mSv

conversion rate. The value of the corresponding parameter μ_d, however, is not significant and has only a small influence on the excess risk.

The results obtained for the empirical models with EPICURE/AMFIT were practically the same as the results obtained with MINUIT.

Central estimates of ERR

Central estimates (age at exposure 30 and age attained 70) of the ERR at 1 Sv of all four model types are fully consistent with each other (Table 6). There is a tendency for the TSCE models to result in lower ERR at 1 Sv estimates than the empirical models but this effect is in general not statistically significant.

Estimates for the ERR at lower doses are more influenced by the modeling. Central estimates of the ERR at 0.2 Sv in TSCE models with a conventional dose dependence of cell inactivation tend to give lower risk estimates than TSCE models with low-dose hypersensitivity. For the

Table 3 Observed and calculated number of solid cancer fatalities in subsets of male atomic bomb survivors

Data subset	Dose (Sv)	All solid cancer fatalities, males		
		Observed	EMP_E model	$TSCE_{IP}$ model
$e = 0$–29	<0.005	692	699	705
	0.005–0.25	696	681	683
	0.25–2	272	259	253
$e = 30$–59	<0.005	1,295	1,254	1,252
	0.005–0.25	1,190	1,230	1,228
	0.25–2	396	403	406
$e = 60+$	<0.005	102	112	110
	0.005–0.25	116	115	114
	0.25–2	20	26	28
χ^2		–	6.2	7.6
$a = 0$–29	<0.005	1	3	6
	0.005–0.25	4	3	6
	0.25–2	1	1	2
$a = 30$–59	<0.005	418	444	424
	0.005–0.25	444	437	418
	0.25–2	166	158	157
$a = 60+$	<0.005	1,670	1,618	1,638
	0.005–0.25	1,554	1,586	1,601
	0.25–2	521	529	527
χ^2		–	6.0	9.1

Table 4 Observed and calculated number of solid cancer fatalities in subsets of female atomic bomb survivors

Data subset	Dose (Sv)	All solid cancer fatalities, females		
		Observed	EMP_E model	$TSCE_{IT}$ model
$e = 0$–29	<0.005	703	713	713
	0.005–0.25	681	697	696
	0.25–2	298	310	306
$e = 30$–59	<0.005	1,375	1,388	1,395
	0.005–0.25	1,531	1,454	1,458
	0.25–2	419	422	417
$e = 60+$	<0.005	103	113	110
	0.005–0.25	93	115	112
	0.25–2	31	23	27
χ^2		–	13.2	9.1
$a = 0$–29	<0.005	8	6	13
	0.005–0.25	2	6	14
	0.25–2	1	3	8
$a = 30$–59	<0.005	457	479	462
	0.005–0.25	534	490	473
	0.25–2	220	197	188
$a = 60+$	<0.005	1,716	1,730	1,743
	0.005–0.25	1,769	1,769	1,780
	0.25–2	527	555	554
χ^2		–	13.6	33.4

Table 5 Best estimates and 95% confidence intervals of parameters in the preferred TSCE models with radiation-induced cell inactivation ($\mu_0 = 10^{-6}$ year^{-1})

Parameter	Male, all solid, DS02 TSCE$_{ICT}$	Female, all solid, DS02 TSCE$_{iL}^{a}$	Male, stomach, DS86 TSCE$_{iL}^{b}$
α_0 (year^{-1})	3.515 (3.505; 3.525)	10.70 (10.65; 10.74)	15.69 (15.67; 15.71)
X_0 (year^{-2})	0.78 (0.68; 0.88) $\times 10^{-6}$	4.68 (3.71; 5.66) $\times 10^{-6}$	0.789 (0.591; 0.988) $\times 10^{-6}$
β_0 (year^{-1})	3.389 (3.379; 3.399)	10.63 (10.59; 10.67)	15.58 (15.56; 15.60)
X_d (year Sv)$^{-1}$	4.1 (1.1; 13.7) $\times 10^{-6}$	91 (50; 167) $\times 10^{-6}$	11.2 (2.3; 55.5) $\times 10^{-6}$
α_d–β_d	2.3 (0.5; 4.2)	1.0 (−0.2; 2.2)	−1.2 (−2.6; 0.2)
μ_d (Sv^{-1})	12.9 (−4.5; 34.1)	–	–
β_5 (year^{-1})	−0.04 (−0.3; 0.21) $\times 10^{-2}$	1.30 (1.01; 1.60) $\times 10^{-2}$	2.82 (2.25; 3.4) $\times 10^{-2}$
β_6 (year^{-2})	−2.81 (−3.53; −1.69) $\times 10^{-4}$	−4.40 (−5.48; −3.32) $\times 10^{-4}$	−5.42 (−7.35; −3.52) $\times 10^{-4}$

Parameter	Female, stomach, DS86 TSCE$_{IC}$	Male, liver, DS86 TSCE$_{IC}$	Female, liver, DS86 TSCE$_{IC}$
α_0 (year^{-1})	30.63 (30.61; 30.64)	1.86 (1.30; 2.42)	4.68 (4.44; 4.93)
X_0 (year^{-2})	3.01 (2.05; 3.96) $\times 10^{-6}$	0.03 (0.020 0.04) $\times 10^{-6}$	0.063 (0.033; 0.093) $\times 10^{-6}$
β_0 (year^{-1})	30.58 (30.57; 30.60)	1.70 (1.13; 2.26)	4.56 (4.32; 4.81)
X_d (year Sv)$^{-1}$	136 (37; 553) $\times 10^{-6}$	0.37 (0.09; 1.52) $\times 10^{-6}$	0.75 (0.09; 6.14) $\times 10^{-6}$
α_d–β_d	−1.6 (−4.4; 1.2)	1.8 (−3.7; 7.2)	5.9 (1.2; 10.5)
β_5 (year^{-1})	3.76 (3.09; 4.42) $\times 10^{-2}$	−2.64 (−3.31; −1.96) $\times 10^{-2}$	−0.00 (−0.98; 1.00) $\times 10^{-2}$
β_6 (year^{-2})	−4.29 (−6.39; −2.22) $\times 10^{-4}$	0.24 (−2.63; 3.07) $\times 10^{-4}$	−4.32 (−8.17; −0.59) $\times 10^{-4}$

[a] $a_s/a_r = 5$; $d_c = 0.2$ Sv
[b] $a_s/a_r = 20$; $d_c = 0.1$ Sv

Table 6 Central *ERR* estimates (±1 standard deviation) at 1 or 0.2 Sv for age at exposure $e = 30$ and age attained $a = 70$. The 95% confidence intervals were generally symmetrical around the best estimates

Data set	Empirical model	TSCE model without cell inactivation		TSCE model with conventional cell inactivation		TSCE model with LDH	
	at 1 Sv	at 1 Sv	at 0.2 Sv	at 1 Sv	at 0.2 Sv*	at 1 Sv	at 0.2 Sv*
Male, all solid, DS02	0.32 ± 0.07	0.23 ± 0.05	0.05 ± 0.01	0.26 ± 0.06	0.04 ± 0.01	0.26 ± 0.05	0.08 ± 0.02
Female, all solid, DS02	0.50 ± 0.09	0.40 ± 0.06	0.08 ± 0.01	0.46 ± 0.06	0.07 ± 0.01	0.47 ± 0.06	0.11 ± 0.01
Male, stomach, DS86	0.16 ± 0.11	0.12 ± 0.11	0.02 ± 0.02	0.12 ± 0.12	0.02 ± 0.03	0.11 ± 0.11	0.01 ± 0.04
Female, stomach, DS86	0.39 ± 0.23	0.55 ± 0.18	0.11 ± 0.03	0.56 ± 0.20	0.12 ± 0.06	0.54 ± 0.19	0.14 ± 0.07
Male, liver, DS86	0.64 ± 0.20	0.14 ± 0.47	0.04 ± 0.08	0.11 ± 0.07	0.02 ± 0.02	0.11 ± 0.08	0.03 ± 0.02
Female, liver, DS86	0.36 ± 0.21	0.11 ± 0.15	0.02 ± 0.03	0.21 ± 0.17	0.03 ± 0.02	0.19 ± 0.18	0.05 ± 0.05

* The differences between model types are generally largest here with p values of 0.03 and 0.01 for all solid cancer, male and female, respectively

analysis of all female solid cancer combined, e.g., the ERR value of 0.07 (95% CI: 0.05, 0.09) in the model with conventional cell inactivation differs significantly from 0.11 (95% CI: 0.08, 0.14) in the model with LDH ($p = 0.02$). The results of the empirical relative risk model and of the TSCE model without an explicit modeling of the radiation-induced cell inactivation are generally intermediate to the results of the TSCE models with conventional and with LDH cell survival curves.

The ERR is by construction proportional to dose in the empirical models and essentially proportional to dose in the TSCE models without radiation-induced cell inactivation (Figs. 5, 6). The fit of the TSCE models with radiation-induced cell inactivation for all solid cancer types together, however, shows an upward curvature of the ERR in the dependence of dose, which is modulated by a downward curvature in the low-dose range in the models with low-dose hypersensitivity. In general, the deviations from a linear dose response are small. Most of the nonparametric estimates agree within one standard deviation either with all four of the model types, or with none of the models. Thus, compared to the uncertainty of the non-

Fig. 5 Excess relative risk of mortality from all solid cancer types as a function of dose as calculated with the preferred models for age at exposure $e = 30$ years and age attained $a = 70$ years, and non-parametric estimations for dose groups and all ages together. The *error bars* indicate one standard deviation ranges

parametric estimates the four model types give consistent results.

Dependences of ERR on age

The TSCE models with conventional and with LDH cell inactivation result in a similar dependence of the ERR at 1 Sv on age at exposure (results not shown). There is, however, a systematic trend of lower age-at-exposure effect modification at young ages at exposure (0–15 years) in the TSCE models with radiation-induced cell inactivation than in the empirical model with an exponential age-at-exposure dependence. For age at exposure 5 and age attained 70, for example, the ERR at 1 Sv for all solid cancer types among females is by a factor of 2.1 lower in the TSCE$_{IL}$ model than in the EMP$_E$ model ($p = 0.05$). The difference between the TSCE models with radiation-

induced cell inactivation and the empirical model is especially expressed for stomach cancer among females. For age at exposure 5, the best estimate of the ERR at 1 Sv for stomach cancer among females is lower in the TSCE$_{IL}$ model than in the EMP$_E$ model by a factor of 8.6 ($p = 0.05$). The difference of the model types concerning the ERR for young ages at exposures decreases with decreasing age attained (results not shown).

Since the power of the data with regard to excess risks is higher at 1 Sv than at lower doses, model differences in ERR results are more expressed at lower doses. Again, for an age-at-exposure of 5 years the ERR in the TSCE models with radiation-induced cell inactivation is lower than in the empirical model (Fig. 7). For a dose of 0.2 Sv, the difference amounts to a factor of 2.4 for all solid cancer among females ($p = 0.02$).

Estimates of EAR

The empirical and the biologically based models result in EAR at 1 Sv central estimates that are fully consistent with each other (results not shown). Again, the modeling of radiation-induced cell inactivation has the largest implications in the low-dose region. In general, cell inactivation with conventional dose dependence causes a lower EAR estimate at low doses, and cell inactivation with low-dose hypersensitivity a higher EAR estimate. For females, all solid cancer types combined an EAR at 0.2 Sv of 3.6 (95% CI: 2.8, 4.4) cases per 10^4 PY Sv is obtained with a conventional cell survival curve, which is smaller than 5.5 (95% CI: 4.1, 6.8) cases per 10^4 PY Sv as obtained with a cell survival curve with low-dose hypersensitivity ($p = 0.014$). The result of the empirical model of 4.7 (95% CI: 3.3, 6.1) cases per 10^4 PY Sv is intermediate to the results of the two TSCE models.

In contrast to ERR, the age-at-exposure effect modification of EAR (at both 1 and 0.2 Sv) at young ages at exposure (<15 years) are fully consistent between the empirical and the TSCE model types with both forms of radiation-induced cell inactivation.

Discussion

A major effort here has concentrated on applying four techniques in the "goodness-of-fit evaluations" so that the main conclusions did not depend on just one type of statistical test: two information criteria (AIC and BIC) for non-nested models, a Chi-squared type consideration of observed and fitted values of the total number of deaths in age- and dose-group categories, and a comparison of dose response curves with non-parametric values of ERR in several dose groups. Considering all
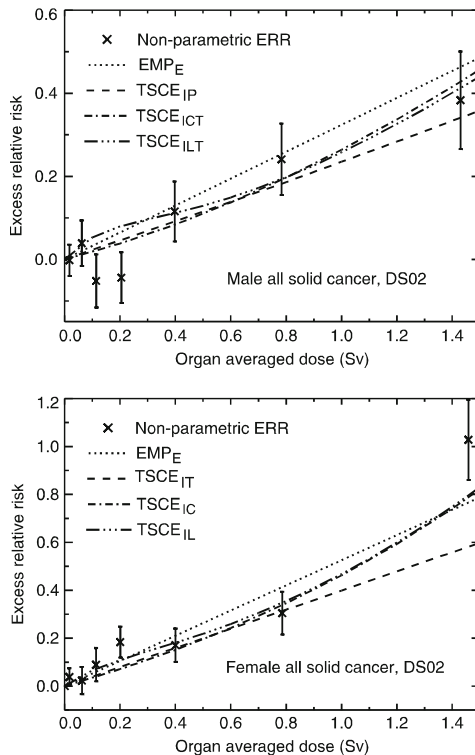
Fig. 6 Excess relative risk of mortality from stomach and liver cancer as a function of dose as calculated with the preferred models for age at exposure $e = 30$ years and age attained $a = 70$ years, and non-parametric estimations for dose groups and all ages together. The *error bars* indicate one standard deviation ranges
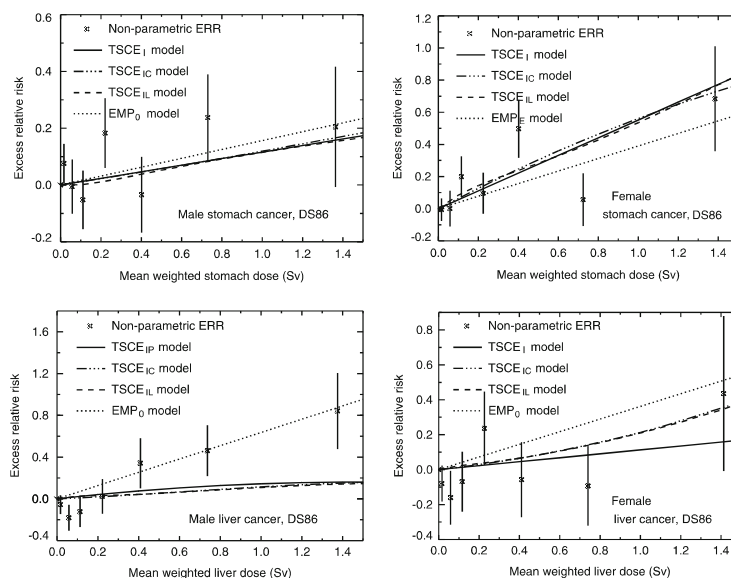
criteria together, none of the four model types studied could be ruled out.

In general, the TSCE models turned out to be more economical in terms of the total number of parameters required as compared to the empirical models. With the exception of the data set on all cancer types among females, a comparable deviance was achieved by all four types of models. Thus, the relatively small number of parameters in the TSCE models indicates that these models contain some plausible features of the process of carcinogenesis.

Radiation-induced processes in carcinogenesis

Radiation action on the initiation rate is found to be relevant for all six data sets. Effects on other processes of carcinogenesis could not be identified unequivocally by the present analysis of mortality data for the atomic bomb survivors from Hiroshima and Nagasaki. It may also be noted that the assumptions of the present analysis on the applicability of measured cell survival curves to the complex process of carcinogenesis in stem cells, which communicate in the tissue in a complex manner with other cell types, are not more then a simplified modeling approach. The approach is only justified by the present lack of a better understanding of the ongoing processes in the tissue.

For stomach cancer mortality, the dose required to initiate the same number of cells as spontaneous initiation processes during one year as found in this analysis

(according to Table 5 the best estimate is for males 0.07 Sv and for females 0.02 Sv) is very close to what has been derived Kai et al. [14] from stomach cancer incidence data among the atomic bomb survivors (for males 0.1 Sv, for females 0.02–0.05 Sv, depending on age at exposure). Also, the results of Kai et al. on the value of spontaneous growth rate of clones of intermediate cells of stomach cancer, γ_0, of 0.131 (95%CI: 0.115, 0.149) year^{-1} for males and 0.066 (95%CI: 0.048, 0.090) year^{-1} for females are very close to the results of the present analysis. Although the results on stomach cancer have to be treated with caution because of missing information on infections with helicobacter pylori and on smoking, it is interesting to observe that results of different analyses of epidemiological data with models of carcinogenesis are converging. Unfortunately, it is not yet possible to compare the models with experimental results, because pre-carcinogenic lesions in the stomach, which could be candidates for the clones of intermediate cells, have not yet been identified [33].

In the models with radiation-induced cell inactivation, a relatively strong effect of the kind of the survival curve (Eqs. 2, 3) on the promotion rate of initiated cells is found for all cancers combined. This promoting effect is assumed to be proportional to the number of inactivated normal cells. Since for cells with low-dose hypersensitivity, the number of inactivated cells per dose is especially high for low doses, this induces an especially high promotional effect for initiated cells at low doses as well. This explains why the slope of the dose-response curve is steeper at low
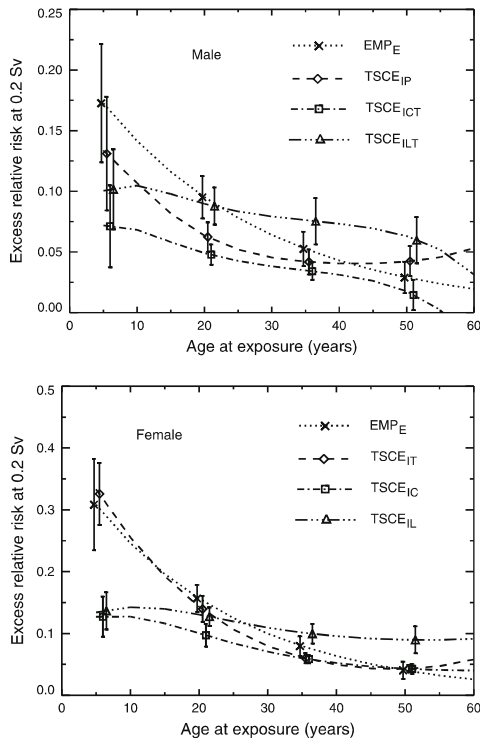
Fig. 7 Age-at-exposure modification to excess risks at 0.2 Sv for an age attained of 70 years for all solid cancer types. The *error bars* indicate one standard deviation ranges. The TSCE models with cell inactivation (TSCE$_C$ or TSCE$_L$) indicate smaller risks at low age at exposure than the empirical model (EMP$_E$)

doses than at higher doses in the models with low dose hypersensitivity.

Implications for risk estimates

The inclusion of low-dose hypersensitivity in radiation-induced cell inactivation did not improve the qualities of the model fits but rather provided an alternative biologically feasible model. In the models analyzed here, the implications of low-dose hypersensitivity on excess relative risk estimates at 1 Sv are rather small. At lower doses, however, risk estimates from the TSCE model with conventional cell survival curves and the TSCE model with LDH differ significantly from each other. This additional variation could be regarded as an expression of model uncertainty in the risk estimates, which in principle could be reduced by experiments demonstrating whether or not LDH plays a role in the radiation response of animals or humans.

One possible way to take the model uncertainty into account is to define the uncertainty range of results by the lowest and highest bounds of risk estimates in models with comparably high quality of fit. If this is done for the four preferred models, then according to Fig. 8

- the model uncertainty contributes only moderately to the total uncertainty of the risk estimates for intermediate ages of exposure (25–40)
- for ERR the total uncertainty range extends the uncertainty range of the empirical model for young ages considerably to lower risk values and for older ages at exposures mainly to higher risk values
- for EAR the total uncertainty range extends the uncertainty range of the empirical model for younger and for older ages at exposure mainly to higher risk values.

Applying the method outlined above to excess risk for all solid cancer at 1 Sv, age at exposure 10 and age attained 70 results in total uncertainty ranges that are wider than the pure statistical 95% uncertainty range according to the empirical model by about 30% for ERR and for EAR (Table 7).

The main influence of the inclusion of cell inactivation in the TSCE model was found to be a weakening of the age-at-exposure effect modification of the excess relative risk estimate as compared to the empirical model with an exponential dependence of the ERR on age at exposure (EMP$_E$ model). In this context it is notable, that except for all solid cancer among females an empirical model with an exponential age-at-exposure effect modifier did not describe the data sets significantly better as empirical models with a linear age-at-exposure effect modifier or even without an age-at-exposure effect modifier.

The most recent ERR values at 1 Sv published by Preston et al. [1] for age at exposure 30 in an age-constant linear ERR model are statistically consistent with the values found in the analysis presented here where small differences in risk estimation can be attributed to differences in modeling procedure (e.g. different dose cut-off values, the application of the more suitable organ-averaged doses applied here rather than colon doses in the analysis of all solid cancers). There was also consistency between the EAR values in [1] and those presented here. The TSCE model relative risk estimates generally tended to be lower than the risk estimates in the empirical models, the absolute risk estimates, however, were quite close.

Conclusion

In the present analysis, a comparably good description of the mortality data for the atomic bomb survivors was

Fig. 8 Excess risk estimates at 1 Sv for age attained of 70 years and for all solid cancer types together: Best estimates of the four preferred models, and one standard deviation statistical uncertainty bars of the empirical model and total uncertainty band including model uncertainty
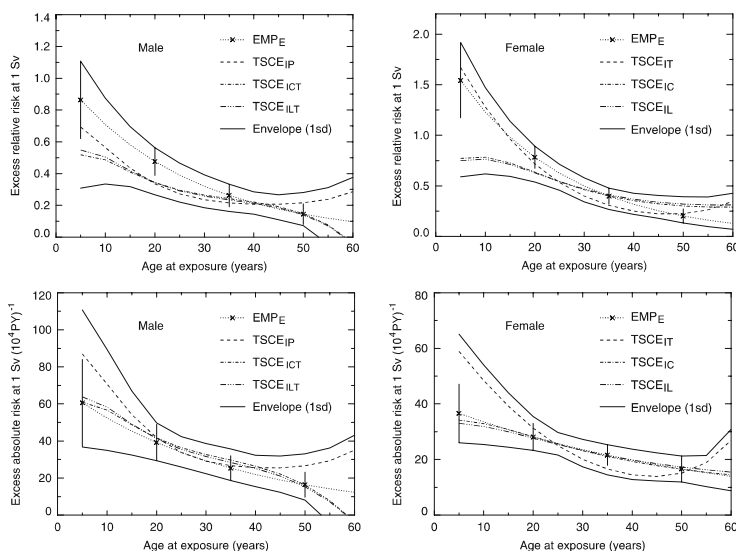
Table 7 Excess risk estimates at 1 Sv for all solid cancer for age at exposure 10 and age attained 70: comparison of the 95% statistical uncertainty range in the empirical model and the 95% uncertainty ranges including model uncertainty

Sex	Risk parameter	Empirical model	Lowest uncertainty boundary	Largest uncertainty boundary	Ratio of wideness of uncertainty ranges[a]
Male	ERR	0.71 (0.38; 1.03)	$TSCE_{ICT}$ model: 0.19	EMP_E model: 1.03	1.30
Female	ERR	1.23 (0.76; 1.70)	$TSCE_{IL}$ model: 0.48	EMP_E model: 1.70	1.30
Male	EAR (10^{-4} PY)	52.4 (18.3; 86.4)	EMP_E model: 18.3	$TSCE_{IP}$ model: 107.5	1.31
Female	EAR (10^{-4} PY)	33.5 (17.5; 49.5)	EMP_E model: 17.5	$TSCE_{IT}$ model: 59.4	1.31

[a] (largest uncertainty boundary − smallest uncertainty boundary)/(wideness of uncertainty range in empirical model)

achieved by application of TSCE models of carcinogenesis, requiring less fit parameters than the conventional ERR models. This may be taken as an indication that the TSCE model indeed reflects some main characteristics of the process of carcinogenesis.

The analyses with TSCE models that explicitly take into account radiation-induced cell inactivation showed three main effects:

- Radiation-induced cell inactivation resulted in an increase of the number of precancerous cells. Thus, radiation-induced cell inactivation is not necessarily a protective effect concerning the induction of cancer.
- In these models, excess relative risks after exposure at young age was smaller than in more conventional models. At the present time, the diverging results of the two model types express an unexpected uncertainty in our knowledge. Further research, possibly with data including a longer follow-up, is needed to clarify the

issue of cancer risks after radiation exposures at young age.
- Excess relative risks at low doses were lower in models with conventional cell survival curves than in models with low-dose hypersensitivity. Both models described the data equally well.

The results of the present study demonstrate the suitability to analyze radio-epidemiological data with models of carcinogenesis that explicitly take into account radiobiological effects. This approach may also be used to investigate, how radiation-induced genomic instability influences cancer risks after exposures to ionizing radiation.

References

1. Preston DL, Shimizu Y, Pierce DA, Suyama A, Mabuchi K (2003) Studies of mortality of atomic bomb survivors. Report 13: solid cancer and noncancer disease mortality: 1950–1997. Radiat Res 160:381–407

2. Young R, Kerr GD (2005) DS02: reassessment of the atomic bomb radiation dosimetry for Hiroshima and Nagasaki, Dosimetry System 2002, DS02, Vols 1& 2. Radiation Effects Research Foundation, Hiroshima

3. Preston DL, Pierce DA, Shimizu Y, Cullings HM, Fujita S, Funamoto S, Kodama K (2004) Effect of recent changes in atomic bomb survivor dosimetry on cancer mortality risk estimates. Radiat Res 162:377–389

4. Moolgavkar S, Knudson A (1981) Mutation and cancer: a model for human carcinogenesis. J Natl Cancer Inst 66:1037–1052

5. Moolgavkar SH, Luebeck EG (1990) Two-event model for carcinogenesis: biological, mathematical and statistical considerations. Risk Anal 10:323–341

6. Marples B (2004) Is low-dose hyper-radiosensitivity a measure of G_2-phase radiosensitivity? Cancer Metastasis Rev 23:197–207

7. Joiner MC, Marples B, Lambin PH, Short S, Turesson I (2001) Low-dose hypersensitivity: current status and possible mechanisms. Int J Radiat Oncol Biol Phys 49:379–389

8. Jacob V, Jacob P (2004) Modelling of carcinogenesis and low-dose hypersensitivity. An application to lung cancer incidence among atomic bomb survivors. Radiat Environ Biophys 42:265–273

9. Yang JS, Li WJ, Zhou GM, Jin XD, Xia JG, Wang JF, Wang ZZ, Guo CL, Gao QX (2005) Comparative study on radiosensitivity of various tumor cells and human normal liver cells. World J Gastroenterol 11:4098–4101

10. Jenkins VK, Barranco SC, Townsend CM, Perry RR, Ives KL (1986) Differential response to gamma radiation of human stomach cancer cells in vitro. Int J Radiat Biol 50:269–278

11. Wouters BG, Sy AM, Skarsgard LD (1996) Low-dose hypersensitivity and increased radioresistance in a panel of human tumor cell lines with different radiosensitivity. Radiat Res 146:399–413

12. Kellerer AM, Walsh L (2001) Risk estimation for fast neutrons with regard to solid cancer. Radiat Res 156:708–717

13. Hawkins RB (2000) Survival of a mixture of cells of variable linear-quadratic sensitivity to radiation. Radiat Res 153:840–843

14. Kai M, Luebeck EG, Moolgavkar SH (1997) Analysis of the incidence of solid cancer among atomic bomb survivors using a two-stage model of carcinogenesis. Radiat Res 148:348–358

15. Heidenreich WF, Jacob P, Paretzke HG (1997) Exact solutions of the clonal expansion model and their application to the incidence of solid tumors of atomic bomb survivors. Radiat Environ Biophys 36:45–58

16. Kopp-Schneider A, Portier CJ, Sherman CD (1994) The exact formula for tumor incidence in the two-stage model. Risk Anal 14:1079–1080

17. Zheng Q (1994) On the exact hazard and survival functions of the MVK stochastic carcinogenesis model. Risk Anal 14:1081–1084

18. Jacob P, Jacob V (2003) Biological parameters for lung cancer in mathematical models of carcinogenesis. Radiat Prot Dosimetry 104:357–366

19. Heidenreich WF, Luebeck EG, Moolgavkar SH (1997) Some properties of the hazard function of the two-mutation clonal expansion model. Risk Anal 17:391–399

20. Walsh L, Rühm W, Kellerer AM (2004) Cancer risk estimates for γ-rays with regard to organ specific doses, part I: all solid cancers combined. Radiat Environ Biophys 43:145–151

21. James F (1994) Minuit function minimization and error analysis, Version 94.1. Technical Report, CERN

22. Preston DL, Lubin JH, Pierce DA (1993) Epicure user's guide. HiroSoft International Corp., Seattle

23. Walsh L (2007) A short review of model selection techniques for radiation epidemiology. Radiat Environ Biophys 46:205–213

24. Akaike H (1973) Information theory and an extension of the maximum likelihood principle. In: Petrov BN, Caski F (eds) Proceeding of second international symposium on information theory. Akademiai Kiado, Budapest, pp 267–281

25. Motulsky H, Christopoulos A (2002) Fitting models to biological data using linear and nonlinear regression. A practical guide to curve fitting. GraphPad Software Inc

26. Schwarz G (1978) Estimating the dimension of a model. Annals Stat 6:461–464

27. Volinsky CT, Raftery AE (2000) Bayesian information criterion for censored survival models. Biometrics 56:256–262

28. Kass RE, Raftery AE (1995) Bayes factors. J Am Stat Assoc 90:773–795

29. Kashyap R (1980) Inconsistency of the AIC rule for estimating the order of autoregressive models. IEEE Trans Automat Contr 25:996–998

30. Iman RL, Conover WJ (1982) A distribution-free approach to inducing rank correlations among input variables. Commun Stat 11:311–334

31. Kellerer AM, Rühm W, Walsh L (2006) Indications of the neutron effect contribution in the solid cancer data of the A-bomb survivors. Health Phys 90:554–564

32. Hazelton WD, Luebeck EG, Heidenreich WF, Moolgavkar SH (2001) Analysis of a historical cohort of Chinese tin miners with arsenic, radon, cigarette smoking, and pipe smoke exposures using the biologically based two-stage clonal expansion model. Radiat Res 156:78–94

33. Rugge M, Russo VM, Guido M (2003) What have we learnt from gastric biopsy? Aliment Pharmacol Ther 17(Suppl. 2):68–74

24. Kreuzer M, Walsh L, Schnelzer M, Tschense A & Grosche B. Radon and risk of extrapulmonary cancers: results of the German uranium miners' cohort study, 1960-2003. Br. J. Cancer. 99, 1946-1953, 2008

Full Paper

Radon and risk of extrapulmonary cancers: results of the German uranium miners' cohort study, 1960–2003

M Kreuzer*,[1], L Walsh[1], M Schnelzer[1], A Tschense[1] and B Grosche[1]

[1]Federal Office for Radiation Protection, Department of Radiation Protection and Health, Neuherberg 85764, Germany

Data from the German miners' cohort study were analysed to investigate whether radon in ambient air causes cancers other than lung cancer. The cohort includes 58 987 men who were employed for at least 6 months from 1946 to 1989 at the former Wismut uranium mining company in Eastern Germany. A total of 20 684 deaths were observed in the follow-up period from 1960 to 2003. The death rates for 24 individual cancer sites were compared with the age and calendar year-specific national death rates. Internal Poisson regression was used to estimate the excess relative risk (ERR) per unit of cumulative exposure to radon in working level months (WLM). The number of deaths observed (O) for extrapulmonary cancers combined was close to that expected (E) from national rates ($n = 3340$, O/E = 1.02; 95% confidence interval (CI): 0.98–1.05). Statistically significant increases in mortality were recorded for cancers of the stomach (O/E = 1.15; 95% CI: 1.06–1.25) and liver (O/E = 1.26; 95% CI: 1.07–1.48), whereas significant decreases were found for cancers of the tongue, mouth, salivary gland and pharynx combined (O/E = 0.80; 95% CI: 0.65–0.97) and those of the bladder (O/E = 0.82; 95% CI: 0.70–0.95). A statistically significant relationship with cumulative radon exposure was observed for all extrapulmonary cancers (ERR/WLM = 0.014%; 95% CI: 0.006–0.023%). Most sites showed positive exposure–response relationships, but these were insignificant or became insignificant after adjustment for potential confounders such as arsenic or dust exposure. The present data provide some evidence of increased risk of extrapulmonary cancers associated with radon, but chance and confounding cannot be ruled out.
British Journal of Cancer advance online publication, 11 November 2008; doi:10.1038/sj.bjc.6604776 www.bjcancer.com
© 2008 Cancer Research UK

Keywords: epidemiology; radon; radiation; cohort study; U-miners

Although it is well established that occupational exposure to the radioactive gas, radon (^{222}Rn), and its progeny increases the risk of lung cancer (BEIR, 1999; Laurier et al, 2004; Tomasek, 2004; Brüske-Hohlfeld et al, 2006; Grosche et al, 2006; Villeneuve et al, 2007; Tomasek et al, 2008; Vacquier et al, 2008), little is known about any effects on other cancers (Tomasek et al, 1993; Darby et al, 1995a; BEIR, 1999; Moehner et al, 2006; Rericha et al, 2006). As it is estimated that doses from radon and its progeny to organs other than the lung are approximately $\geqslant$ 100 times lower (Kendall and Smith, 2002; Marsh et al, 2008), large-scale occupational radon studies are required to investigate this possible relationship.

The largest and most informative study on this subject to date is the pooled analysis of 11 miners' cohorts published by Darby et al (1995a). Overall, no statistically significant exposure–response relationship was observed, except for pancreatic cancer. The researchers concluded that high concentrations of radon in the air do not cause a material risk of mortality from cancers other than lung cancer. However, low statistical power, missing information on potential confounders and heterogeneity among the 11 studies were of concern. The aim of these analyses of the German Wismut uranium miners' cohort study is to further evaluate the relation-

ship between radon and extrapulmonary cancers. Compared with the pooled study, the Wismut cohort has a comparable size (58 987 vs 64 209), a longer average follow-up period (35 vs 17 years), a larger number of deaths from cancers other than lung cancer (3340 vs 1253), a longer mean duration of employment (12 vs 6 years) as well as a higher average cumulative exposure to radon (279 vs 155 working level months (WLM)). Moreover, information on occupational exposure to external γ-radiation, long-lived radio-nuclides (LRNs), arsenic, fine dust and silica dust is available.

MATERIALS AND METHODS

Cohort definition and follow-up

The cohort has been described earlier (Grosche et al, 2006; Kreuzer et al, 2002, 2006). In brief, it represents a stratified random sample of 58 987 males, employed for at least 6 months from 1946 to 1989 at the former Wismut uranium company in East Germany. The first follow-up ran up to the end of 1998 (Grosche et al, 2006; Kreuzer et al, 2006), and this study extends the follow-up by 5 years through 2003. Information on the vital status of individuals was obtained from local registration offices, whereas death certificates were obtained not only from the responsible Public Health Administrations but also from central archives and the pathology archive of the Wismut company. The underlying causes of death from death certificates or the autopsy files were coded

according to the 10th revision of the International Classification of Diseases (ICD-10).

Information on exposure to radiation and other variables

Radiation exposure was estimated by using a job-exposure matrix (JEM), which was originally generated for compensation purposes by the Miners' Institution for Statutory Accident Insurance and Prevention (Lehmann *et al*, 1998). This JEM has been developed further to meet scientific purposes (HVBG and BBG, 2005). It includes information on exposure to radon and its progeny, external γ-radiation and LRNs (^{235}U and ^{238}U) for each calendar year of employment (1946–1989), each place of work and each type of job. More than 900 different jobs and 500 different working places were evaluated for this purpose. Radon (^{222}Rn) measurements in the Wismut mines were carried out from 1955 onwards. For the period 1946–1954, radon concentrations were estimated by an expert group based on measurements from 1955, taking into account ventilation rate, vein space, uranium content and so on (Grosche *et al*, 2006; Kreuzer *et al*, 2006; Moehner *et al*, 2006). Complete information on job type, type of mining facility and periods of absence is available on a daily basis for all cohort members. The cumulative exposure to each of the three radiation sources was calculated as the sum of the annual exposures estimated by the JEM weighted by the duration of work in days. Exposure to radon and its progeny is expressed in WLM. One working level is defined as the concentration of short-lived radon daughters per litre of air that gives rise to 1.3×10^5 MeV of alpha energy after complete decay. One WLM of cumulative exposure corresponds to exposure to 1 WL during 1 month (170 h) and is equivalent to 3.5 mJh m^{-3}. Exposure to LRNs is given in kBqh m^{-3}, and exposure to external γ-radiation is given as an effective dose in mSv.

Information on arsenic, dust and silica is based on a JEM similar to that for radiation, providing annual dose values for each calendar year, each place of work and each type of job (Bauer, 2000; HVBG and BBG, 2005). These annual values are given in dust-years, where 1 dust-year is defined as an exposure to 1 mg m^{-3} fine dust or silica dust and 1 μg m^{-3} for arsenic over a time period of 220 shifts of 8 h. Differences in the number of shifts and daily working hours in the different calendar years were accounted for by multiplying with a correction factor. Cumulative exposure to each of the three sources is expressed in dust-years. Arsenic was present only in mines in Saxony. Thus, arsenic exposure was calculated only for cohort members who worked in areas with rock containing a sufficient concentration of arsenic. The threshold value for arsenic is 10 μg m^{-3} in air (inhaled particle fraction), corresponding to one-tenth of the technical guideline concentration value of arsenic, which was valid until 2004. Data on smoking are not included in this analysis because the relevant information is only available after 1972 from medical records for a small proportion of the cohort.

Statistical methods

Two statistical methods were applied, external comparisons with national rates and internal regression. In the first method, the mortality rates of the cohort were compared with those of the general male population in Eastern Germany, formerly the German Democratic Republic. External rates were available from 1960 onwards. For this reason, all analyses were limited to the follow-up period 1960–2003, with the 236 cohort deaths before 1960 being excluded. The number of man-years at risk for each miner was calculated as the time between entry into and exit from the cohort. In these analyses, the date of entry was defined as the start of employment plus 180 days or 1 January 1960, whichever comes later. The date of exit was defined as the earliest of the date of death, emigration, loss to follow-up or the end of the period of

follow-up (31 December 2003). The expected mortality rate was calculated by applying national mortality rates, grouped by calendar year and 5-year age bins, to the person-years in the grouped cohort data. The standardised mortality ratio (SMR) is given by the ratio of O/E, where O is the number of observed deaths in the cohort and E is the number expected from external rates. In common with other miners' studies (Tomasek *et al*, 1993; Darby *et al*, 1995a), a 5-year lag was used to calculate the cumulative exposure to radon for all sites of cancer other than leukaemia and a zero lag for leukaemia. The confidence intervals of the SMR were calculated on the basis of the poisson distribution (Breslow and Day, 1987). SMRs were corrected for missing causes of death by dividing O by the proportion of known causes of death, *P*, which is binomial distributed. In practice, it was found to be adequate to ignore the variability of *P* as, when methods were applied to account for this variability (Rittgen and Becker, 2000), the resulting SMR confidence intervals were not significantly affected.

The cancer sites examined were defined according to the pooled study by Darby *et al* (1995a), but the 10th ICD code was used instead of the 9th ICD code. Earlier revisions of the ICD (8 and 9) and the former codes of the German Democratic Republic were recoded to ICD-10. As no separate external rates had been available for the time period 1968–1979 for cancers of the tongue and mouth, salivary gland and pharynx, these cancers were combined in the external analyses. In a few cases, the external rates were not available for certain years and cancer types and hence were not included in the corresponding external analyses, which is why the total numbers are sometimes lower than those in the internal regression and do not sum to the total number of non-lung cancers. A separate analysis for time periods < or >10 years since first employment was performed, because earlier studies (Tomasek *et al*, 1993; Darby *et al*, 1995a) showed a lower mortality during the first period compared with the later period, most probably because of the selection of healthy men for employment in the mines. Owing to the long follow-up period in this cohort and the restriction of the follow-up period to 1960 and later, the proportion of cases occurring <10 years after the first employment was extremely low (1.7%) and thus did not affect the overall risk estimate.

Poisson regression was used to test for an association between cancer mortality risk and cumulative radon exposure. Tabulations of person-years at risk and cancer deaths were created with the DATAB module of the EPICURE software (Preston *et al*, 1998). Cross-classifications were made by age, *a*, in 16 categories (<15, 15–19, 20–24,..., 85+ years), individual calendar year, *y*, in 58 categories and cumulative radon exposure, *w*, in seven categories (0, >0–49, 50–99, 100–499, 500–999, 1,000–1,499, 1500+ WLM). The WLM categories were defined to be comparable with other studies (Darby *et al*, 1995a; Moehner *et al*, 2006), but with an added category of 0 WLM. The tabulated data were fitted to the following model – if *r(a, y, w)* is the age, year and exposure-specific cancer mortality rate and $r_0(a,y) = r(a,y,0)$ is the baseline disease rate for non-exposed individuals, $w = 0$ then

$$r(a, y, w) = r_0(a, y) \times \{1 + ERR(w)\} \qquad (1)$$

where ERR is the excess relative risk. A linear form for ERR(w) $= \beta w$, with no dependence of the slope β on *a* and *y*, was used to investigate the exposure–response relationship. In addition, a categorical analysis of the form ERR(w) $= \Sigma_{j=1,7}\beta_j w_j$ was performed, where *j* refers to the exposure class. To test for the five potential confounders, LRN, external γ-radiation, fine dust, quartz fine dust or arsenic, each of these variables (z_i), *i* = 1, 5 was added separately to the model (1) with ERR(w, z_i) $= \beta w + \gamma z_i$. Maximum likelihood with the AMFIT module of the EPICURE software (Preston *et al*, 1998) was used for estimation of the fit parameters: β, γ, β_j (*j* = 1, 7), and the internal baseline rates in

strata. Internal regression analyses were restricted to individual cancer sites with a total of >35 deaths.

RESULTS

In the follow-up period 1960–2003, a total of 57 199 persons were under observation, resulting in 1 762 208 person-years at risk and a mean duration of follow-up of 35 years. By the end of 2003, 35 294 (61.7%) men were alive, 20 684 (36.2%) had died, 233 (0.4%) had emigrated and 988 (1.7%) were lost to follow-up. The underlying cause of death was available for 19 501 (94.3%) of the deceased men, among them 6341 deaths from malignant cancers (2999 lung cancers plus two cancers of the trachea and 3340 non-lung cancers). A total of 49 268 individuals were exposed to radon at some time during Wismut employment, whereas 7931 had never been exposed (Table 1). Those exposed received a mean cumulative exposure to radon of 279.4 WLM (median = 30.8), a mean cumulative exposure to external γ-radiation of 48.6 mSv (median = 16.5) and an average cumulative exposure to LRN of 4.2 kBqh m^{-3} (median = 1.05).

Figure 1 shows the annual mean exposure values for radon and its progeny in WLM, and for external γ-radiation in mSv and LRN in kBqh m^{-3} for the exposed cohort members. Radon concentrations decreased sharply after 1955 because of the introduction of several ventilation measures, which led to conditions in accordance with the international radiation protection standards after 1970. In contrast to this, external γ-radiation and LRN show a different pattern, because their concentration was not affected by the improved ventilation. The annual mean exposure values for fine dust, silica dust and arsenic are given in Figure 2. Owing to the use of dry drilling, the concentrations of dust had been very high until 1955 and then decreased steadily with the implementation of wet drilling, reaching very low levels after 1970. A total of 17 554 miners were exposed to arsenic, with higher annual values in the early years compared with the later years.

Table 2 gives the numbers of O and E deaths based on the male Eastern German population, as well as the corresponding SMRs (O/E) with 95% CIs for all cancers other than lung cancer combined and for 24 individual cancer sites. The number of non-lung cancer deaths combined was close to expectation (O/E = 1.02; 95% CI: 0.98–1.05). Among 24 individual non-lung cancer sites, a

significant excess was found for stomach (O/E = 1.15; 95% CI: 1.06–1.25) and liver cancers (O/E = 1.26; 95% CI: 1.07–1.48), as well as a significant deficit of cancers of the tongue, mouth, pharynx and salivary gland combined (O/E = 0.80; 95% CI: 0.65–0.97) and those of the bladder (O/E = 0.82; 95% CI: 0.70–0.95). Overall mortality was significantly higher than in the general population (O/E = 1.03; 95% CI: 1.02–1.05), mainly because of lung cancer (O/E = 2.03; 95% CI: 1.96–2.10).

In the internal regression analyses shown in Table 3, there is a significantly increased mortality from all cancers other than lung cancer with cumulative radon exposure (ERR/WLM = 0.014%; 95% CI: 0.006–0.023%). The two highest exposure categories 1000–1499 WLM and >1500 WLM show a 1.2-fold (95% CI: 1.02–1.38) and 1.16-fold (95% CI: 0.94–1.76) higher risk compared with the reference category of 0 WLM, respectively. Among the 18 individual sites with >35 cases, a significant positive relation with radon is observed for stomach cancer (ERR/WLM = 0.021%; 95% CI: 0.0007–0.043%), whereas excesses with borderline statistical significance were found for cancers of the pharynx (ERR/WLM = 0.16%; 95% CI: −0.045 to 0.37%) and liver (ERR/WLM = 0.044%; 95% CI: −0.008 to 0.096%). No association between leukaemia and cumulative radon exposure is found.

Table 1 Characteristics of the German uranium miners' cohort, 1960–2003

	Mean (minimum–maximum)
Duration of follow-up (years)	35 (0.5–50)
Duration of employment (years)	12 (0.5–40)
Radon exposed miners (n = 49 268)	
Duration of exposure (years)	11 (1–44)
Age at first exposure (years)	22 (14–67)
Cumulative exposure (WLM[a])	279 (>0–3224)
Miners exposed to	
External γ-radiation (n = 49 256)	
Cumulative exposure (mSv)	48.6 (>0–908.6)
Long-lived radionuclides (n = 49 256)	
Cumulative exposure (kBqh m^{-3})	4.2 (>0–132.2)
Arsenic (n = 17 554)	
Cumulative exposure (dust-years[b])	122.5 (>0–1417.4)
Fine dust (n = 56 914)	
Cumulative exposure (dust-years[c])	36.7 (>0–315.2)
Silica dust (n = 56 878)	
Cumulative exposure in (dust-years[c])	5.8 (>0–56.0)

[a]WLM = working level months. [b]Dust-year is defined as exposure to 1 μg m^{-3} for arsenic over 220 shifts each at 8 h. [c]Dust-year = 1 dust-year is defined as exposure to 1 mg m^{-3} of fine dust or silica dust over 220 shifts each at 8 h.
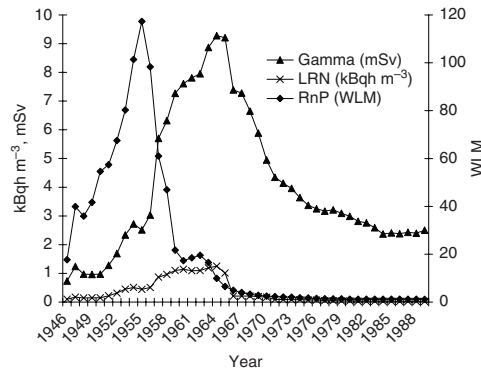

Figure 1 Mean annual exposure to radon and its progeny in working level months (WLM), external γ-radiation in mSv and long-lived radio-nuclides in kBqh m^{-3} among exposed miners.
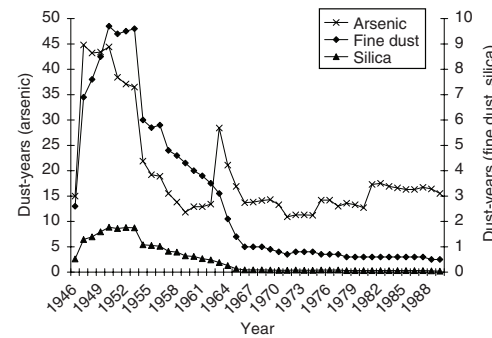
Figure 2 Mean annual cumulative exposure for exposed cohort members with respect to fine dust (n = 56 914), silica dust (n = 56 878) and arsenic exposure (n = 17 554) in dust-years.

Table 2 Number of deaths observed (O) and expected (E), ratio of observed to expected deaths (O/E), and 95% CI for selected cancer sites, 1960–2003

Cancer site (ICD-10 code)	O	O*	E	O*/E	95% CI*
Tongue, mouth, salivary gland and pharynx (C00–C14)	99	105.0	131.8	0.80	0.65–0.97
Oesophagus (C15)	125	132.6	120.1	1.10	0.92–1.31
Stomach (C16)[a]	588	623.7	542.2	1.15	1.06–1.25
Colon (C17–C18)	299	317.1	310.9	1.02	0.91–1.14
Rectum (C19–C21)	241	255.6	267.9	0.95	0.84–1.08
Liver (C22)[a]	154	163.3	129.3	1.26	1.07–1.48
Gallbladder (C23–C24)[a]	76	80.6	75.4	1.07	0.84–1.34
Pancreas (C25)[a]	223	236.5	225.2	1.05	0.92–1.20
Nose (C30–C31)[a]	8	8.5	8.0	1.06	0.46–2.09
Larynx (C32)	75	79.5	67.2	1.18	0.93–1.48
Bone (C40–C41)	13	13.8	21.4	0.64	0.34–1.10
Malignant melanoma (C43)[a]	33	35.0	48.0	0.73	0.50–1.02
Other skin (C44)	9	9.5	12.5	0.76	0.35–1.45
Connective tissue (C47 and C49)[a]	14	14.8	21.6	0.69	0.38–1.16
Prostate (C61)[a]	262	277.9	314.4	0.88	0.78–1.00
Testis (C62)	25	26.5	25.3	1.05	0.68–1.55
Kidney (C64–C66)[a]	162	171.8	161.6	1.06	0.91–1.24
Bladder (C67–C68)[a]	173	183.5	224.4	0.82	0.70–0.95
Brain and other nervous system (C70–C72)[a]	110	116.7	124.2	0.94	0.77–1.13
Thyroid gland (C73)[a]	18	19.1	13.9	1.38	0.81–2.17
Hodgkin's disease (C81)[a]	29	30.8	35.1	0.88	0.59–1.26
Non-Hodgkin's disease (C82–C85 and C91.4)[a]	85	90.2	91.6	0.98	0.79–1.22
Myeloma (C90)[a]	51	54.1	52.6	1.03	0.77–1.35
Leukaemia (C91–C95, except C91.4)	127	134.7	150.9	0.89	0.74–1.06
Leukaemia excluding chronic lymphatic (C91–C95, except C91.1 and C91.4)	71	75.3	83.9	0.90	0.70–1.13
Other and unspecified	295	312.8	312.5	1.00	0.89–1.12
All cancers other than lung cancer (C00–C32 and C35–C97)	3340	3543.7	3488.2	1.02	0.98–1.05

[a]Exclusion of some cases for specific years, as external rates are missing (in total 46 missing cases). O*, corrected for missing causes of death, O* = O/0.943; E = expected cases based on age and calendar year standardised national mortality rates from Eastern Germany.

This is also true for all leukaemia except chronic lymphatic leukaemia (non-CLL) ($n = 87$, ERR/WLM = 0.019%; 95% CI: −0.04 to 0.08%), CLL ($n = 40$, ERR/WLM = −0.013%; 95% CI: −0.067 to 0.040%) and acute myeloid leukaemia ($n = 31$, ERR/WLM = 0.036%; 95% CI: −0.076 to 0.149%).

Overall, there is a low correlation between exposure to radon and exposure to external γ-radiation, LRN or arsenic ($R < 0.28$), whereas fine dust ($R = 0.57$) and silica dust ($R = 0.63$) are relatively highly correlated with radon exposure. Additional adjustment for each of the five factors showed no substantial modifying effect on the overall ERR/WLM for all non-lung cancers combined. In contrast, the adjustment led to a decreased risk for certain sites (e.g., stomach, larynx and liver) (Table 4). Overall, none of the risk estimates for the different cancer sites were significant after adjustment for the potential confounders.

DISCUSSION

In this study, a statistically significant relation between cumulative radon exposure and risk of extrapulmonary cancers combined is observed (ERR/WLM = 0.014%). After adjustment for potential confounders, such as exposure to arsenic, dust, LRN and γ-radiation, the ERR/WLM is only marginally modified, values of the ERR/WLM ranging from 0.016 to 0.011%, with some of the borderline significance. No earlier miners' studies have reported a statistically significant result for this relationship (Tomasek *et al*, 1993; Darby *et al*, 1995a; Vacquier *et al*, 2008), and hence a non-causal chance result in our study cannot be ruled out. However, the earlier studies may have been limited by low statistical power. For example, in the pooled study by Darby *et al* (1995a) an ERR/WLM of 0.01% for the time period >10 years after employment was observed, in line with our findings, but it is not statistically significant (Table 5). In both studies, an excess of non-lung

cancers seems to be present only for exposure categories above 1000 WLM.

Dosimetric calculations indicate that extrapulmonary organs received very low doses compared with those received by the lung (Kendall and Smith (2002); Marsh *et al*, 2008). Marsh *et al* (2008) recently estimated the absorbed doses for specific organs for several exposure scenarios in mines. For example, wet drilling, medium ventilation and medium physical activities were associated with the following doses in mGy/WLM: bronchial region 7.3, red bone marrow 0.031, kidney 0.02 and liver 0.0065. In our analyses, the ERR/WLM for lung cancer is approximately 14 times higher ($n = 2999$; ERR/WLM = 0.20%; 95% CI: 0.16–0.22%) than for non-lung cancers ($n = 3,340$; ERR/WLM = 0.014%), which is compatible with the biokinetic models. For individual sites, the majority showed a positive exposure–response relationship (15 from 18), although this was significant only for stomach cancer (Figure 3). After adjusting for the five potential confounders, however, no individual sites showed a significant exposure–response relationship.

Specific sites

Liver The increased mortality of liver cancer in miners compared with the general population ($n = 158$, O/E = 1.26; 95% CI: 1.06–1.25) is consistent with other miners' studies (Tomasek *et al*, 1993; Darby *et al*, 1995a,b) and appears not to be a chance finding. It may be because of the high consumption of alcohol among miners, which, in the early years, was offered (with cigarettes) free of charge. Alcohol abuse, or cirrhosis, was mentioned on the death certificate for 8%, or 37%, of the liver cancers, respectively. The principal two studies provided no evidence of a relationship with increasing cumulative exposure to radon (Tomasek *et al*, 1993; Darby *et al*, 1995a). In contrast, a non-significantly elevated ERR/WLM of 0.044% ($P = 0.09$) is observed here. Adjustment for

Table 3 Relative risk for selected cancer sites by cumulative radon exposure based on internal poisson regression, 1960–2003

Cancer site (ICD-10 code)		Cumulative radon exposure in working level months (WLM)							Total	ERR/100 WLM[a]	P-value
		0	0–49	50–99	100–499	500–999	–1499	≥1500			
Tongue and mouth (C01–C06)	Cases	3	12	5	11	1	6	0	38	0.045	0.50
	RR[b]	1.00	1.30	3.10	3.12	0.43	6.15	0			
Pharynx (C09–C14)	Cases	6	16	2	10	12	6	1	53	0.163	0.12
	RR	1.00	0.97	0.54	1.27	2.85	3.33	1.18			
Oesophagus (C15)	Cases	19	38	7	37	15	6	3	125	−0.025	0.08
	RR	1.00	0.97	0.76	1.31	0.82	0.69	0.68			
Stomach (C16)	Cases	76	143	35	141	95	62	38	590	0.021[c]	0.04
	RR	1.00	1.21	1.42	1.34	1.16	1.51	1.77[c]			
Colon (C17–C18)	Cases	51	74	13	66	41	44	10	299	0.017	0.26
	RR	1.00	0.79	0.63	0.84	0.71	1.58	0.71			
Rectum (C19–C21)	Cases	39	55	16	53	39	22	17	241	0.028	0.13
	RR	1.00	0.77	0.97	0.91	0.89	1.03	1.58			
Liver (C22)	Cases	25	35	12	24	34	21	7	158	0.044	0.09
	RR	1.00	0.70	1.10	0.59	1.18	1.52	1.02			
Gallbladder (C23–C24)	Cases	15	17	3	19	12	9	6	81	0.021	0.46
	RR	1.00	0.70	0.57	0.85	0.70	1.05	1.37			
Pancreas (C25)	Cases	38	60	11	51	43	16	9	228	−0.001	>0.5
	RR	1.00	0.81	0.70	0.93	1.04	0.78	0.86			
Larynx (C32)	Cases	13	15	2	16	20	8	1	75	0.021	0.49
	RR	1.00	0.66	0.40	0.92	1.51	1.23	0.29			
Prostate (C61)	Cases	50	60	12	62	42	20	17	263	0.000	>0.5
	RR	1.00	0.85	0.81	0.88	0.75	0.71	1.20			
Kidney (C64–C66)	Cases	26	44	12	42	23	13	11	171	0.017	0.39
	RR	1.00	0.83	0.96	1.01	0.79	0.92	1.60			
Bladder (C67–C68)	Cases	22	34	10	42	39	22	8	177	0.020	0.28
	RR	1.00	1.03	1.47	1.26	1.44	1.60	1.15			
Brain and others (C70–C72)	Cases	15	41	9	18	22	10	0	115	−0.018	0.27
	RR	1.00	1.32	1.33	0.85	1.56	1.52	0			
Non-Hodgkin's disease (C82–C85 and C91.4)	Cases	14	22	8	18	13	9	3	87	0.032	0.35
	RR	1.00	0.71	1.34	1.00	1.05	1.54	1.05			
Myeloma (C90)	Cases	13	11	2	14	7	7	1	55	0.007	>0.5
	RR	1.00	0.40	0.37	0.82	0.56	1.22	0.34			
Leukaemia (C91–C95, excluding C91.4)	Cases	22	29	5	36	17	14	4	127	0.006	>0.5
	RR	1.00	0.75	0.57	1.13	0.75	1.26	0.71			
Other and unspecified	Cases	75	137	24	93	74	31	23	457	0.009	0.44
	RR	1.00	0.96	0.84	0.90	1.01	0.86	1.29			
All non-lung cancers (C00–C32, C35–C97)	Cases	522	843	188	753	549	326	159	3340	0.014[c]	<0.001
	RR	1.00	0.89[c]	0.94	1.00	0.99	1.20[c]	1.16			
Person-years at risk	0-year lag	256 264	781 696	102 726	290 243	191 867	92 371	47 019	1 762 208		
	5-year lag	363 845	693 782	95 229	287 756	191 037	86 643	43 913	1 762 208		
Mean cumulative radon exposure		0	11.1	71.9	263.4	732.1	1197.2	1940.8			

[a]ERR/WLM = excess relative risk per working level months. [b]RR = relative risk. [c]Statistically significant (P <0.05).

Table 4 Excess relative risk (ERR) per 100 WLM for specific cancer sites after accounting for various potential confounding factors, 1960–2003 – analyses restricted to individuals with available information on all considered confounders (*n* = 56 278)

Poisson regression model	ERR/WLM (95% Confidence limits)			
	All non-lung cancers	Stomach cancer	Larynx cancer	Liver cancer
Without adjustment	0.015 (0.006; 0.023)	0.022 (0.001; 0.043)	0.020 (−0.038; 0.078)	0.042 (−0.009; 0.092)
Adjusted for exposure to				
γ-Radiation	0.016 (0.007; 0.026)	0.012 (−0.011; 0.035)	−0.009 (−0.067; 0.050)	0.041 (−0.015; 0.098)
LRN	0.016 (0.007; 0.026)	0.011 (−0.013; 0.034)	−0.018 (−0.077; 0.014)	0.047 (−0.009; 0.103)
Arsenic	0.014 (0.005; 0.024)	0.009 (−0.013; 0.031)	0.009 (−0.053; 0.072)	NC
Fine dust	0.011 (−0.0002; 0.023)	0.007 (−0.022; 0.036)	−0.033 (−0.129; 0.063)	0.022 (−0.045; 0.09)
Silica dust	0.012 (−0.005; 0.024)	0.012 (−0.018; 0.043)	−0.055 (−0.161; 0.050)	0.034 (−0.035; 0.101)

ERR/WLM = excess relative risk per working level months; NC = not calculable.

Table 5 Risk of deaths from cancers other than lung cancer combined by cumulative radon exposure in WLM in the pooled 11 miner study and this study (categorical analyses and excess relative risk per WLM)

Cumulative exposure to radon in WLM	11 miners' cohort study (Darby *et al*, 1995a)[a]			Cumulative exposure to radon in WLM	Present Wismut study		
	Person-years	No. of cases	SMR[b]		Person-years	No. of cases	Relative risk	95% CI
	—	—	—	0	363 845	522	1.00	
<50	295 078	405	0.98	>0–50	693 782	843	0.89	0.79–0.99
50–99	87 286	183	1.04	50–99	95 229	188	0.94	0.77–1.10
100–499	222 305	515	0.99	100–499	287 756	753	1.00	0.88–1.12
500–999	42 231	93	1.02	500–999	191 037	549	0.99	0.86–1.11
1000–1499	10 686	25	1.11	1000–1499	86 643	326	1.20	1.02–1.37
1500+	12 108	32	1.10	1500+	43 913	159	1.16	0.94–1.76
Total	669 694	1253			1 762 208	3340		
ERR/WLM[c] (95% CI)	0.01% (−0.01 to 0.02%)				0.014% (0.006%–0.023%)			

[a]Risk estimates based on comparisons with external mortality rates for the time period of more than 10 years since employment. [b]SMR = standardised mortality ratio, no confidence limits had been given in the original publication. [c]ERR/WLM = excess relative risk per working level months.

exposure to external γ-radiation, LRN, arsenic and dust led to some decrease in the ERR/WLM. Confounding from other factors such as alcohol consumption cannot be ruled out.

Stomach A significantly elevated SMR for stomach cancer (*n* = 590, O/E = 1.15; 95% CI: 1.06–1.25) was observed here, as in other studies of radon-exposed miners (Kusiak *et al*, 1993; Darby *et al*, 1995a), and among coal miners (Rockette, 1977). Although not fully understood, it could be related to dust exposure (Cocco *et al*, 1996). In the pooled study, an elevated SMR (*n* = 217; SMR = 1.33; 95% CI: 1.16–1.52) was found with no exposure–response relationship (Darby *et al*, 1995a), whereas in our study, the risk increased significantly with increasing cumulative radon exposure (ERR/WLM = 0.022%). The highest exposure category (1500 WLM or more) was associated with a 1.8-fold (95% CI: 1.06–2.48) significantly higher risk of death compared with the reference category of 0 WLM. Adjustment for each of the five confounders, however, reduced the ERR/WLM by a factor of approximately 2, leading to insignificant values. Thus, part of the proportionate increase in risk because of radon might be explained by confounding.

Pharynx A significant deficit of cancers of the tongue, mouth, salivary gland and pharynx combined (*n* = 99, SMR = 0.8; 95% CI: 0.65–0.97) may be a chance finding because of multiple testing. There was a constant, but not significant, increase in pharyngeal cancer risk with increasing cumulative radon exposure (*n* = 53, ERR/WLM = 0.16%; 95% CI: −0.045 to 0.37%). It can be noted that this value was nearly as high as for lung cancer (ERR/WLM = 0.20%), but no such relationship was reported in other studies on miners, although the number of pharyngeal cases was

small (Tomasek *et al*, 1993; Darby *et al*, 1995a). Additional adjustment for the five possible confounders only led to a small reduction of the ERR/WLM. Some studies have provided estimates for organ doses after inhalation of radon and its progeny separately for the extrathoracic airways, and have reported a pharyngeal dose that was nearly as high as the lung dose (Kendall and Smith 2002; Jacobi and Roth, 1995).

Larynx The combined 11 studies on miners showed a 1.21-fold non-significantly increased SMR for larynx cancer that was not related to cumulative radon exposure (Darby *et al*, 1995a), but there were only 38 cases. In the first follow-up of the French uranium miners' study (1946–1985), a significantly increased SMR of 2.35 was observed on the basis of 17 cases (Tirmarche *et al*, 1993), which became insignificant after extension of the follow-up period to 1999 (SMR = 1.24, *n* = 29) (Vacquier *et al*, 2008). The SMR in this study (*n* = 75, SMR = 1.18; 95% CI: 0.93–1.48) is comparable with the findings of the pooled study (Darby *et al*, 1995a). ERR/WLM was elevated, but not significantly. Adjustment for the five potential confounders led to a substantial decrease in the observed ERR/WLM.

Kidney Animal experiments suggest an increased mortality of kidney cancer after inhalation of radon (Masse *et al*, 1992), but none of the miners' studies found any such excess (Tomasek *et al*, 1993; Darby *et al*, 1995a), apart from the French study (*n* = 20, SMR = 2.0; 95% CI: 1.22–3.09) (Vacquier *et al*, 2008). Moreover, none of these studies observed a trend with cumulative radon exposure. The same holds true in our data, there being no excess (*n* = 162, SMR = 0.91) or an exposure–response relationship.
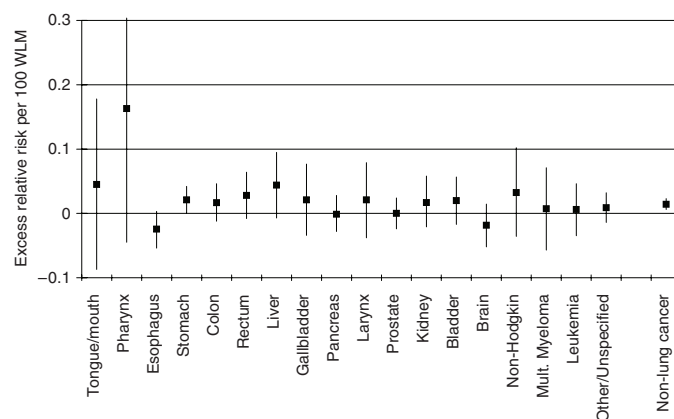
Figure 3 Excess relative risk (ERR) per 100 WLM and 95% confidence limits for all cancer sites with >35 cases and all cancers other than lung cancer combined, 1960–2003.

Leukaemia In our study, no association between cumulative radon exposure and leukaemia is found, or with CLL, non-CLL or AML, consistent with earlier studies (Tomasek *et al*, 1993; Darby *et al*, 1995a; Laurier *et al*, 2001; Vacquier *et al*, 2008), including a recent large case–control study with 377 leukaemia cases among former Wismut employees (Moehner *et al*, 2006). In contrast, Rericha *et al* (2006) noted, in a Czech uranium miner case–cohort study, a significantly increased relative risk of 1.75 (95% CI: 1.10– 1.75) for leukaemia incidence in the highest quintile of cumulative radon exposure (>100 WLM) compared with the lowest (<3 WLM). However, there was a very high correlation in the mines, between radon and exposure to γ-radiation, which could have introduced confounding bias.

Strengths and limitations

The major strengths of our study are the large cohort size, the large number of extrapulmonary cancers, the long follow-up period, the wide range of radon exposures and particularly the information available on other exposures such as arsenic, fine dust, silica, external γ-radiation and LRN. These advantages allowed the independent replication of the analysis of the 11 miners' cohort studies (Darby *et al*, 1995a), which may have suffered from heterogeneity problems. The potential limitations of this study include the accuracy of the underlying causes of death on death certificates, missing causes of death, exposure misclassification particularly in the early years of mining activities as well as missing information on other potential confounders such as alcohol consumption, smoking, occupational exposure to diesel exhaust or asbestos. Moreover, despite the large number of cancer cases overall, there is a low statistical power with respect to certain sites, and multiple testing could have led to some spurious findings.

Confounding

Within a nested case–control study of lung cancer in the Wismut cohort, information on smoking was collected from miners, their relatives and the medical Wismut archive. Most of the former Wismut employees had been smokers. Overall, the low correlation between smoking and cumulative radon exposure makes smoking an unlikely major confounder. It is known that Wismut employees in the early years had a relatively high alcohol consumption compared with the male general population. For approximately 5% of the deceased cohort members, alcohol abuse was noted on the death certificate. This rough surrogate for alcohol consumption was slightly negatively correlated with cumulative radon exposure.

Exposure misclassification

Inevitably, exposures in the very early years are associated with considerable uncertainty. To obtain some insight into potential bias by misclassification, the cumulated radon exposure was separated into two components according to other studies investigating the effect of the quality of exposure (Tomasek *et al*, 2008; Vacquier *et al*, 2008), one risk estimate for the period 1946–1954, the years with retrospectively estimated radon concentrations and the other for when the JEM was based on measurements in the shafts. As, for all non-lung cancers combined, there was only a non-significant difference in the estimates for these two periods, a major bias through misclassification of exposure is unlikely, but cannot be excluded. Another potential limitation is the use of the exposure to radiation instead of the actual organ dose. Recently, it has been suggested that several factors such as physical activity, ventilation in the mines, dry or wet drilling may influence the individual doses (Marsh *et al*, 2008). Work on these dose calculations is currently in progress within the European collaborative research project ALPHA-RISK (European Commission, 2006), which will also provide a method for calculating the dose to the various organs from combined exposure to radon and its progeny, LRN and external γ-radiation.

CONCLUSION

Some evidence of a very small radon-related risk of extrapulmonary cancers was found, compatible with dosimetric calculations for organ doses. However, the possibility of non-causal results because of chance and confounding cannot be ruled out.

REFERENCES

Bauer HD (2000) *Studie zur retrospektiven Analyse der Belastungssituation im Uranbergzbergbau der ehemaligen SDAG Wismut mit Ausnahme der Strahlenbelastung für die Zeit von 1946 bis 1990*. Hauptverband der gewerblichen Berufsgenossenschaften: Sankt Augustin

BEIR (1999) *Committee on Biological Effects of Ionizing Radiation (BEIR VI). Health effects of exposure to radon – BEIR VI*. National Academy Press: Washington DC

Breslow NE, Day NE (1987) *Statistical Methods in Cancer Research. Volume II – The Design and Analysis of Cohort Studies*. Scientific publication 82 IARC: Lyon

Brüske-Hohlfeld I, Schaffrath Rosario A, Wölke G, Heinrich J, Kreuzer M, Kreienbrock L, Wichmann HE (2006) Lung cancer risk among former uranium miners of the Wismut company in Germany. *Health Phys* **90:** 208–216

Cocco P, Ward MH, Buiatti E (1996) Occupational risk factors for gastric cancer: An overview. *Epidemiol Rev* **18:** 218–234

Darby SC, Radford EP, Whitley E (1995b) Radon exposure and cancers other than lung cancer in Swedish iron miners. *Environ Health Perspect* **103**(Suppl 2): 45–47

Darby SC, Whitley E, Howe GR, Hutchings SJ, Kusiak RA, Lubin JH, Morrison HI, Tirmarche M, Tomásek L, Radford EP (1995a) Radon and cancers other than lung cancer in underground miners: a collaborative analysis of 11 studies. *J Natl Cancer Inst* **87:** 378–384

European Commission (2006) Alpha-Risk: risks related to internal and external exposures. In: *Euratom Research Projects and Training Activities* ISBN 92-79-00064-0. EUR 21229 http://ec.europa.eu/research/energy/pdf/nuclear_fission_2_en.pdf (Volume II)

Grosche B, Kreuzer M, Kreisheimer M, Schnelzer M, Tschense A (2006) Lung cancer risk among German male uranium miners: a cohort study, 1946–1998. *Br J Cancer* **95:** 1280–1287

HVBG and BBG (2005) *Belastung durch ionisierende Strahlung, Staub und Arsen im Uranerzbergbau der ehemaligen DDR* (Version 08/2005) Bergbau BG (BBG): Gera; Hauptverband der gewerblichen Berufsgenossenschaften (HVBG) (CD-Rom): St Augustin

Jacobi W, Roth P (1995) *Risiko und Verursachungswahrscheinlichkeit von extrapulmonalen Krebserkrankungen durch die berufliche Strahlenexposition von Beschäftigten des ehemaligen Wismut AG*. GSF-Bericht 4/1995. GSF-Forschungszentrum für Umwelt und Gesundheit: Neuherberg

Kendall GM, Smith TJ (2002) Doses to organs and tissues from radon and its decay products. *J Radiol Prot* **22:** 389–406

Kreuzer M, Brachner A, Lehmann F, Martignoni K, Wichmann HE, Grosche B (2002) Characteristics of the German uranium miner cohort study. *Health Phys* **83:** 26–34

Kreuzer M, Kreisheimer M, Kandel M, Tschense A, Grosche B (2006) Mortality from cardiovascular diseases in the German uranium miners cohort study: 1946–1998. *Radiant Environ Health* **45:** 159–166

Kusiak RA, Ritchie AC, Springer J, Muller J (1993) Mortality from stomach cancer in Ontario miners. *Br J Ind Med* **50:** 117–126

Laurier D, Tirmarche M, Mitton N, Valenty M, Richard P, Poveda S, Gelas JM, Quesne B (2004) An update of cancer mortality among the French cohort of uranium miners: extended follow-up and new source of data for causes of death. *Europ J Epidemiol* **19:** 139–146

Laurier D, Valenty M, Tirmarche M (2001) Radon exposure and the risk of leukemia: a review of epidemiological studies. *Health Phys* **81:** 272–288

Lehmann F, Hambeck L, Linkert KH, Lutze H, Reiber H, Renner HJ, Reinisch A, Seifert T, Wolf F (1998) *Belastung durch ionisierende Strahlung im Uranerzbergbau der ehemaligen DDR*. Hauptverband der gewerblichen Berufsgenossenschaften: Sankt Augustin

Marsh JW, Bessa Y, Birchall A, Blanchardon E, Hofmann W, Nosske D, Tomasek L (2008) Dosimetric models used in the alpha-risk project to quantify exposure of uranium miners to radon gas and its progeny. *Radiat Prot Dos* **130**(1): 101–106

Masse R, Morlier JP, Morin M, Chameaud J, Bredon P, Lafuma J (1992) Animals exposed to radon. *Radiat Prot Dosim* **45:** 603–609

Moehner M, Lindtner M, Otten H, Gille HG (2006) Leukemia and exposure to ionizing radiation among German uranium miners. *Am J Ind Med* **49:** 238–248

Preston DL, Lubin JH, Pierce DA, McConney ME (1998) *Epicure, release 2.10*. HiroSoft: Seattle

Rericha V, Kulich M, Rericha R, Shore DL, Sandler DP (2006) Incidence of leukemia, lymphoma, and multiple myeloma in Czech uranium miners: a case-control study. *Environ Health Perspect* **114:** 818–822

Rittgen W, Becker N (2000) SMR Analysis of historical follow-up studies with missing death certificates. *Biometrics* **56:** 1164–1169

Rockette HE (1977) Cause-specific mortality of coal miners. *J Occup Med* **19:** 795–801

Tirmarche M, Raphalen A, Allin F, Chameaud J, Bredon P (1993) Mortality of a cohort of French uranium miners exposed to relatively low radon concentrations. *Br J Cancer* **67:** 1090–1097

Tomasek L (2004) Leukaemia among uranium miners – late effects of exposure to uranium dust? *Health Phys* **86:** 426–427

Tomasek L, Darby SC, Swerdlow AJ, Placek V, Kunz E (1993) Radon exposure and cancers other than lung cancer among uranium miners in West Bohemia. *Lancet* **341:** 919–923

Tomasek L, Rogel A, Tirmarche M, Mitton N, Laurier D (2008) Lung cancer in French and Czech uranium miners: Radon-associated risk at low exposure rates and modifying effects of time since exposure and age at exposure. *Radiat Res* **169:** 125–137

Vacquier B, Caer S, Rogel A, Feurprier M, Tirmarche M, Luccioni C, Quesne B, Acker A, Laurier D (2008) Mortality risk in the French cohort of uranium miners: extended follow-up 1946–1999. *Occup Environ Med* **65**(9): 597–604

Villeneuve PJ, Morrison HI, Lane R (2007) Radon and lung cancer risk: an extension of the mortality follow-up of the Newfoundland fluorspar cohort. *Health Phys* **92:** 157–169

25. Oestreicher U, Stephan G, Schneider K, Panzer W & Walsh L. Results of chromosome aberrations after computer tomography (CT) in children. In: Proceedings of the 36th Annual Meeting of the European Radiation Research Society, Tours 2008, Radioprotection. 43(5), 41, 2008

Results of chromosome aberrations after Computed Tomography (CT)in children

U. Oestreicher[a], G. Stephan[a], K. Schneider[b], W. Panzer[c] and L. Walsh[d]

[a] *Federal Office for Radiation Protection, Ingolstaedter Landstr. 1, 85764 Oberschleißheim, Germany;* [b] *University of Munich, Lindwurmstr. 4, 80337 München, Germany;* [c] *Helmholtz Zentrum München, Ingolstaedter Landstr. 1, 85764 Neuherberg, Germany;* [d] *Federal Office for Radiation Protection, Ingolstaedter Landstr. 1, D 85764 Neuherberg, Germany uoestreicher@bfs.de*

The use of CT scans has increased rapidly during the last years in adults and children as well. CT involves larger radiation doses than the more common conventional x - ray imaging procedures. To examine the biological effect in the peripheral blood of the paediatric patients chromosome analysis was carried out in 10 children for whom the medical justifications for CT examinations were accidental injuries and not diseases as investigated in earlier studies. Blood samples were taken before and after CT scans. Chromosome analysis was carried out in lymphocytes by fluorescence plus Giemsa (FPG) staining exclusively in metaphases of the first cell cycle in vitro. The mean blood dose of the 10 children was about 12.9 mGy which was determined by a newly developed dose estimation. Based on more than 20,000 analysed cells it was found that after CT examination the mean frequencies of dicentrics and excess acentric fragments in lymphocytes were significantly increased. By subdividing the children into two age groups, those with an age from 0.4 years to 9 years and from 10 years to 15 years, it became obvious that the observed increase in chromosome aberrations was mainly contributed by the younger age group. In this group the frequency of dicentrics was significantly increased whereas in the older group the observed increase was not significant. Further investigations will be necessary to confirm these results.

26. Kreuzer M, Walsh L, Schnelzer M, Tschense A & Grosche B. Radon and cancers other than lung cancer in uranium miners – Results of the German uranium miners cohort study, 1960-2003. In: Proceedings of the 36th Annual Meeting of the European Radiation Research Society, Tours 2008, Radioprotection. 43(5), 64, 2008

Radon and cancers other than lung cancer in uranium miners - Results of the German uranium miner cohort study

M. Kreuzer[a], L. Walsh[a], M. Schnelzer[a], A. Tschense[a] and B. Grosche[b]

[a] *Federal Office for Radiation Protection, Ingolstaedter Landstr. 1, D 85764 Neuherberg, Germany;* [b] *Federal Office for Radiation Protection, Ingolstaedter Landstr. 1, 85764 Oberschleißheim, Germany*

mkreuzer@bfs.de

Background It is well established that lung cancer is caused by radon, while uncertainty exists as to whether cancers other than lung might be related to exposure from radon. To investigate further the risk of extra-pulmonary cancers, mortality data from the German uranium miners cohort study are analysed.

Materials and methods The cohort includes 58,747 men who were employed for at least 6 months between 1946 and 1989 at the former Wismut uranium company in Eastern Germany. Exposure to radon and its progeny, long-lived radionuclides, external gamma radiation as well as exposure to arsenic and dust was estimated by using a detailed job-exposure matrix. A total of 20.680 deaths were observed in the follow-up period 1960 to the end of 2003. The different causes of death were compared with the age- and calendar-year specific national death rates of Eastern Germany, formerly GDR. Standardized mortality ratios (SMR) with 95% confidence limits (CI) were calculated. To investigate the exposure-response relationship an internal poisson regression using a linear model was applied and the excess relative risk (ERR) per unit of cumulative exposure to radon in Working Level Month (WLM) was calculated.

Results For 19.598 (94.3%) of the deceased cohort members causes of death had been available, among them 2.999 lung cancer deaths and 3.341 deaths from cancers other than lung. After adjusting for missing causes of deaths, for all cancers other than lung combined mortality in the cohort was close to that expected from national rates (SMR=1.02, 95% CI: 0.98-1.05). Among 23 individual cancer categories, statistically significant increases in mortality for cancers of the stomach (SMR=1.15, 95% CI: 1.06-1.25) and liver (SMR=1.26 , 95% CI: 1.07-1.45) and statistically significant decreases for cancers of the tongue, mouth and pharynx combined and bladder were observed. A statistically significant relation with cumulative exposure was observed for all non-lung cancers combined (ERR/WLM=0.014%) and stomach cancer (ERR/WLM=0.021%).

Conclusion Our findings suggest a weak evidence for a relationship between exposure to radon and mortality from cancers other than lung cancer. Chance, confounding by unconsidered risk factors and bias due to missing causes of deaths cannot be ruled out. If at all, the risk for extrapulmonary tumors associated with radon is appreciably lower than that for lung cancer.

27. Walsh L, Jacob P & Kaiser JC. Radiation risk modeling of thyroid cancer with special emphasis on the Chernobyl epidemiological data. Radiat. Res. 172, 509-518, 2009

Radiation Risk Modeling of Thyroid Cancer with Special Emphasis on the Chernobyl Epidemiological Data

L. Walsh,[a,1] P. Jacob[b] and J. C. Kaiser[b]

[a] *BfS – Federal Office for Radiation Protection, Neuherberg, Germany; and* [b] *HelmholtzZentrum München – German Research Center for Environmental Health, Institute of Radiation Protection, Neuherberg, Germany*

Walsh, L., Jacob, P. and Kaiser, J. C. Radiation Risk Modeling of Thyroid Cancer with Special Emphasis on the Chernobyl Epidemiological Data. *Radiat. Res.* 172, 509–518 (2009).

Two recent studies analyzed thyroid cancer incidence in Belarus and Ukraine during the period from 1990 to 2001, for the birth cohort 1968 to 1985, and the related ^{131}I exposure associated with the Chernobyl accident in 1986. Contradictory age-at-exposure and time-since-exposure effect modifications of the excess relative risk (ERR) were reported. The present study identifies the choice of baseline modeling method as the reason for the conflicting results. Various quality-of-fit criteria favor a parametric baseline model to various categorical baseline models. The model with a parametric baseline results in a decrease of the ERR by a factor of about 0.2 from an age at exposure of 5 years to an age at exposure of 15 years (for a time since exposure of 12 years) and a decrease of the ERR from a time since exposure of 4 years to a time since exposure of 14 years of about 0.25 (for an age at exposure of 10 years). Central ERR estimates (of about 20 at 1 Gy for an age at exposure of 10 years and an attained age of 20 years) and their ratios for females compared to males (about 0.3) turn out to be relatively independent of the modeling. Excess absolute risk estimates are also predicted to be very similar from the different models. Risk models with parametric and categorical baselines were also applied to thyroid cancer incidence among the atomic bomb survivors. For young ages at exposure, the ERR values in the model with a parametric baseline are larger. Both data sets cover the period of 12 to 15 years since exposure. For this period, higher ERR values and a stronger age-at-exposure modification are found for the Chernobyl data set. Based on the results of the study, it is recommended to test parametric and categorical baseline models in risk analyses. © 2009 by Radiation Research Society

INTRODUCTION

Thyroid cancer incidence in Ukraine and Belarus was observed to increase significantly in 1990 among subjects who were children or adolescents at the time of the Chernobyl accident in April 1986 (*1, 2*). Since then, the incidence rate has increased further (*3, 4*). Detrimental health effects of ^{131}I exposures, which formed the main component of post-accident thyroid doses, can be assessed by analyses of epidemiological thyroid cancer data relating to this accident.

The purpose of the present study was to examine the influence of the methods applied for modeling the baseline rates on the age and time effect modifications on the thyroid cancer incidence risk after the Chernobyl accident. A recent study by Jacob *et al.* (*5*) presented a model with the feature of strongly decreasing excess relative risk (ERR) with increasing attained age [see Fig. 6 of ref. (*5*)]. The results were given for various fixed ages at exposure and thus expressed a decrease of the ERR with time since exposure. In contrast to this result, in the study of Likhtarov *et al.* (*6*), a trend of strongly increasing ERR with increasing time since exposure [see Table 6 in ref. (*6*)] was found.

Different types of risk models for the ERR that differ mainly in the numerical treatment of the baseline risk assessment were applied. The baseline forms are either fully parametric as used by Jacob *et al.* (*5*), categorical (i.e. stratified with nuisance stratum parameters), or of a categorical form with a smaller number of subgroups due to the inclusion of interaction effects of attained age and gender (i.e., where each category has an explicit associated fit parameter), as applied by Likhtarov *et al.* (*6*). Comparisons of such models are also made here for the most recent incidence data, covering the period from 1958 to 1998, from the survivors of the A-bombs over Hiroshima and Nagasaki (*7*).

MATERIALS AND METHODS

Chernobyl Data

Data selected for the analysis presented here are the same as applied previously in Jacob *et al.* (*5*) and pertain to 1.62 million children inhabiting 1034 settlements in the countries of Ukraine and Belarus. Only de-identified and aggregated records were used. Individual dose estimates are based on a total of 174,000 measure-

ments of the ^{131}I content in human thyroids, consisting of at least 10 measurements in each settlement taken during May/June 1986 (*8*). Thyroid doses due to the Chernobyl accident were assessed for the birth years 1968–1985 and relate to thyroid cancers that were surgically removed during the period 1990–2001. The thyroid doses associated with this period cover a wide range from 8 mGy to 18.3 Gy with person-year weighted means of 0.19, 0.17, 0.09, 0.08 and 0.12 Gy for Belarusian males, Belarusian females, Ukrainian males, Ukrainian females and the total cohort, respectively. The data are in grouped form and are categorized on country, settlement, gender, birth year (with intervals of 2 years), and year in which thyroid surgery was performed (also with intervals of 2 years), hereafter referred to as operation year.

The analysis is based on a total of 1089 cases of thyroid cancer and approximately 19.4 million person years (PY). To quantify uncertainties in the modification of risk by age and time in the different models two ratios were considered:

1. The ratio of the ERR at age at exposure 15 years to the ERR at age at exposure 5 years for a fixed time since exposure of 12 years.
2. The ratio of the ERR at time since exposure of 4 years to the ERR at time since exposure of 14 years for a fixed age at exposure of 10 years.

These ratios are well suited, in the sense of falling within and characterizing the range of the main body of data, and form useful tools for comparing the age-at-exposure and time-since-exposure risk modification in the various risk model parameterizations applied here. To facilitate comparisons between the results obtained from the Chernobyl data and from the atomic bomb data, a fixed time since exposure of 12 years was chosen for the first ratio. This time is at the end of the observation period for the Chernobyl data and at the start of the observation period for the atomic bomb survivors' cancer incidence data.

A-Bomb Data

Recently released cancer incidence data from the survivors of the WW II A-bombs over Japan were selected for comparison with the Chernobyl data. The A-bomb data cover the period from 1958 to 1998 and contain 18,645 cancers, including 471 cases of thyroid cancer, among 111,952 persons contributing almost 3 million PY. A major analysis of these data can be found in ref. (*7*).

Types of Risk Models Applied to the Chernobyl Data

To summarize the main features associated with the age and time trends indicated by the model fit parameters, optimized against the Chernobyl data, four ERR models are considered with the general form

$$\lambda(c, s, e, a, d) = \lambda_0(c, s, e, a)[1 + \mathrm{ERR}(c, s, e, a, d)], \quad (1)$$

where λ is the total incidence rate and λ_o the baseline incidence rate. The covariables are c, the country; s, the sex; e, the age at exposure in years; a, the attained age in years; oy, the year in which thyroid surgery was performed, i.e. operation year; and d, the thyroid dose in Gy.

Three specific model types are considered in detail here:

1. Model P, as applied in ref. (*5*)[2] with

$$\lambda_0(c, s, e, a) = \exp[\eta_0 + \eta_c \ \theta_c + \eta_s \ \theta_s + \eta_e(10 - e) + \eta_a \ln(a/20)] \quad (2)$$

and

$$\mathrm{ERR}(c, s, e, a, d) = \\ [\beta_1 \ d + \beta_2 \ d^2] \exp[\beta_c \ \theta_c + \beta_s \ \theta_s + \beta_e(10 - e) + \beta_a \ln(a/20)], \quad (3)$$

where $\eta...$ and $\beta...$ are fit parameters with subscripts denoting the specificity, i.e., c for country, s for sex etc. θ_c and θ_s are indicator

variables for city and gender, respectively, with values of -0.5 for Ukraine, 0.5 for Belarus, -0.5 for males and 0.5 for females.

2. Model C, as in Eq. (3) but recomputed here with a categorical method for dealing with baseline rates, i.e. with baseline stratification on the covariable combination c, s, e, a instead of Eq. (2) above. Age at exposure and attained age were categorized in 5-year intervals.

3. Models CS1 and CS2, which are named to indicate their categorical simplified (CS) nature and which have a close correspondence to models 3 and 4 in the paper of Likhtarov *et al.* (*6*) [with parameters given in Table 6 of ref. (*6*)] but refitted to the data set described here. These models both have

$$\lambda_0(oy, c, s, a,) = \exp\{\beta_1 + \Sigma \ \beta_{i=2,3} \ c_{i=1,2} \\ + \Sigma\beta_{i=4,15} \ s_{i=1,2} \ a_{i=1,6} + \Sigma\beta_{i=16,21} \ oy_{i=1,6}\}, \quad (4)$$

where $oy_{i=1,6}$, $c_{i=1,2}$, $s_{i=1,2}$, $a_{i=1,6}$ and $e_{i=1,6}$ are the categorical variables for oy in 2-year intervals; c, s, a and e as defined above with the latter two variables in 5-year intervals with

$$\mathrm{ERR}(c, s, e, a, d) = \beta \ d \exp\Sigma\gamma_i Z_i, \quad (5)$$

where $\Sigma\gamma_i Z_i = \Sigma \ \gamma_{i=1,4} \ e_{i=1,6}$ or $\Sigma \ \gamma_{i=1,4} \ oy_{i=1,6}$ for model CS1 and CS2, respectively. These model forms are generally routinely used in radiation epidemiology, and specifically in Liktarov *et al.* (*6*), and are for interaction effects of dose with either age at exposure (CS1) or time since exposure (CS2).

The regressions for all model types were performed with the AMFIT module of the EPICURE software package (Hirosoft International Corporation, Seattle, WA).

Types of Risk Models Applied to the A-Bomb Data

A recent analysis of thyroid cancer incidence data for the atomic bomb survivors in Hiroshima and Nagasaki (*7*) provided the following gender-averaged excess risk models in terms of weighted thyroid dose, d, where the neutron dose component has been multiplied by 10 and added to the γ-ray component:

$$\mathrm{ERR}(d, a, e) = (1 \pm s(0.14 \pm 0.29)) \cdot (0.58 \pm 0.26) \\ \cdot d \cdot (a/70)^{(-1.45 \pm 0.82)} \cdot \exp[(-0.037 \pm 0.023) \cdot (e - 30)]. \quad (6)$$

The gender indicator variable, s, is $+1$ for females and -1 for males. Age-related covariables are: age attained, a, in years; age at exposure, e, in years. The units of d are in Sv. The fit parameters with standard errors have been inserted directly into the model forms [see www.rerf.or.jp filename: lss07siteahs.log, page 4 for the relevant EPICURE computer output that contains the results quoted in Eq. (6)].

[2] The Liktarov models and A-bomb models all produce central estimates for the risk that are unweighted with respect to gender and country effect modifiers. To achieve consistency in central risk estimates among all model types considered here, some simple adjustments to the models P and C were necessary. This is because models P and C incorporate the features of a directly fitted ratio of excess risks in Belarus and Ukraine at the same dose and a directly fitted ratio of excess risks in females and males at the same dose. These features are obtained by applying gender and city indicator variables [i.e. θ_s and θ_c in ref. (*5*)] set to either $+0.5$ or -0.5. This method has the effect of causing the fit parameters for the central estimates for models P and C to be means obtained with different weights for the two countries and both genders. Constant multiplication factors of 1.27 and 1.25 may be applied to the central risk estimate fit parameters of models P and C, respectively, to make them directly comparable to the central risk estimates from the other model types considered here.

TABLE 1
Goodness-of-Fit Measures for Model Types
Considered and Fitted to the Chernobyl Data

Model	Number of parameters	df	Deviance	AIC	BIC
P	11	107725	3837.9	**3859.9**	**3965.4**
C	54	107682	3772.9	*3880.9*	4398.6
CS1	22	107714	3859.6	3903.6	*4114.6*
CS2	24	107712	3875.0	3923.0	4153.1

Note. The bold numbers indicate the best *AIC* or *BIC*, the italicized numbers indicate the best *AIC* or *BIC* within classes of models with a categorial baseline method [see ref. (*10*) for an explanation of *AIC* and *BIC*].

Additional computations made here involved a replacement of the parametric baseline used in ref. (*7*) by a categorical baseline with stratification of baseline rates on gender, city (Hiroshima or Nagasaki), age attained, age at exposure (both in 5-year intervals), and an indicator variable for participation in the Adult Health Survey (AHS). This later inclusion, also made in ref. (*7*), was necessary because baseline thyroid cancer incidence rates for AHS participants have been estimated to be about 40% higher than those for other cohort members in a recent analysis based on a fully parametric baseline model (*7*).

RESULTS

Quality of Fit of the Chernobyl Data to the Various Models

Table 1 gives the degrees of freedom, the deviance and two indices for the goodness of fit for non-nested models (*9, 10*). The lowest deviance is achieved by the C model (54 parameters), the second best by the P model (11 parameters). The deviance of the CS1 and CS2 models (22 and 24 parameters, respectively) is considerably higher.

According to the Bayesian Information Criterion (*BIC*), there is strong evidence for model P generally fitting the data best. The reason is the smaller number of parameters, which is weighted strongly by the *BIC*. The Aikake Information Criterion (*AIC*) gives more weight to the deviance than the *BIC*. Thus, generally, the criteria for the quality of fit of non-nested models indicate a preference for the fully parametric models with relatively simple and smooth descriptions of the baseline incidence rates. Quality-of-fit criteria for non-nested models may not be totally adequate for intercomparisons between models with parametric and categorical baselines. Among the categorical models, model C is preferable to the CS1 and CS2 models by the AIC; model CS1 is preferred over the C and CS2 models by the BIC; both information criteria disfavor model CS2.

As independent measures of the quality of fit, the numbers of cases predicted for subgroups of the study population (that are deemed to be in the problematical covariable zones, from an examination of Figs. 1–3) are considered. The χ^2 values, given in Table 2, only have the purpose of indicating where the deviations are greatest and so they do not take the number of model parameters into account or form part of a hypothesis-testing

procedure. Again, the fully parametric model appears to describe the data best. The categorical models (C and CS1) have particular problems for the subgroups with young attained age (not shown) and young age at exposure. In the latter case, the numbers of cases in the intermediate-dose groups are overpredicted (by more than three standard deviations) and are underpredicted in the high-dose group (by more than two standard deviations). The categorical models (C and CS2) also have particular problems for early and intermediate times since exposure. The numbers of cases in the intermediate dose groups are overpredicted (by more than two standard deviations) and are slightly underpredicted in the high-dose group (by more than one standard deviation). However, the categorical model C actually does better than the P model for the two-dimensional projections into categories of age at exposure and age attained (not shown), where these correspond to the actual strata applied directly in the categorical C model.

In summary, the quality-of-fit criteria give rather more support to the fully parameterized model than the categorical models for young age at exposure and short times since exposure. Information on the parameter values and uncertainty ranges for the models discussed here are given either in refs. (*5, 6*) or in the Appendix (Tables A1–A3).

Excess Relative Risks from the Chernobyl Data

Central estimates of the parametric and categorical models for the ERR at 1 Gy for an age at exposure of 10 years and attained age of 20 years agree quite well. Best estimates with 95% confidence intervals are 22.8 (12.3; 33.3) and 18.0 (9.7; 26.3) for models P and C, respectively. Gender effects and country differences are in agreement between all model types: Females have a lower ERR than males; Ukrainians have a lower ERR than Belarusians.

All models predict a decrease of the ERR with age at exposure (Fig. 1). At 12 years since exposure, the age-at-exposure modification of the risk in the C and CS1 models is not as steep as that predicted by the parametric model P. The reason for the difference is that for young ages at exposure, the number of baseline cases in the exposed groups is considerably higher in the C and CS1 models than in the P model (Table 2). Preference is given here to the age-at-exposure dependences in the parametric model, because all quality-of-fit criteria considered here tend to favor the parametric model. At 12 years since exposure, the ERR after exposure at age 15 is predicted by the parametric model to be a factor of 0.17 (95% CI: 0.05; 0.29) lower than after exposure at age 5 (Table 3).

The age-at-exposure dependence of the ERR, for a fixed time since exposure, is steeper in the model with a parametric baseline than in the categorical models (see

FIG. 1. Time patterns in the Chernobyl data. The effect modification of ERR at 1 Gy by age at exposure for a fixed time since exposure of 12 years. The fit parameters for model CS1 are shown with one standard error. Results of ref. (7) for the atomic bomb survivors are shown for comparison.

above), while for fixed attained age, the age-at-exposure modification is steeper in the categorical model than in the parametric model (Fig. 2). Thus, when considering age-at-exposure effects, it is important to state whether time since exposure or attained age is fixed in the consideration.

The parametric model predicts a strong decrease of the ERR with time since exposure, whereas the ERR dependence is either rather flat or even increasing in the categorical models (Fig. 3). Again the difference could be related to a larger number of predicted baseline cases in the categorical models compared to the parametric model (Table 2). Considering the weaker predictions of the categorical models for the time-since-exposure groups (Table 2), the present works tends to favor the decrease of the ERR with time since exposure as predicted by the parametric model. For an age at exposure of 10 years, the parametric model predicts a decrease of the ERR from a time since exposure of 4 years to a time since exposure of 14 years by a factor of 4.4 (95% CI: 0.9; 7.8). The categorical model C predicts an increase (Table 3). In this latter respect, the models yield results that are not consistent, with only slightly overlapping confidence intervals. Though the result of the model CS2 for the data used in the present analysis is intermediate and is statistically compatible with the results of the other two models, the model turns out to be highly unstable when the results are compared to the results obtained in ref. (6) for a slightly different data set. The underperformance of the categorical models C and CS2, according to the quality-of-fit considerations (Tables 1 and 2), could be taken to indicate a preference for the result of the parametric model.

The ERR for females was assessed to be consistently lower than for males (by a factor of 0.3).

Excess Relative Risks from the A-Bomb Data

On replacing the fully parametric baseline model of ref. (7) with a categorical model that has stratification on gender, city (Hiroshima or Nagasaki), attained age, age at exposure (both in 5-year intervals), and participation in the AHS, i.e. a total of 912 strata, the following results were obtained here:

$$\mathrm{ERR}(d, a, e) = [1 \pm s(0.30 \pm 0.31)] \cdot (0.90 \pm 0.35) \\ \cdot d \cdot \exp[(-0.053 \pm 0.019) \cdot (e - 30)] \quad (7)$$

At 1 Sv, the central ERR estimate of 0.90 ± 0.35, obtained with a stratified baseline, is a factor of 1.6 higher than that of 0.58 ± 0.26 (see Eq. 6), obtained with the parametric baseline of ref. (7), and the confidence intervals overlap substantially. A further effect of

TABLE 2
Observed and Predicted Number of Total Cases (with the Number of Predicted Baseline Cases in Parentheses) for Four Models in Various Three-by-Three Covariable Subgroups of the Chernobyl Data

Subgroup/χ^2 value	Observed cases	Predicted cases (baseline cases)		
		Model P	Model C	Model CS1
Covariable subgroups for age at exposure, e and thyroid dose, d				
$e < 7$; $d < 0.06$	28	24 (12)	29 (18)	27 (15)
e < 7; $0.06 \leq d < 0.2$	177	208 (35)	228 (66)	225 (77)
e < 7; $0.2 \leq d < 20$	302	268 (8)	263 (15)	261 (20)
$7 \leq e < 13$; $d < 0.06$	138	138 (96)	132 (96)	135 (93)
$7 \leq e < 13$; $0.06 \leq d < 0.2$	71	67 (26)	63 (26)	66 (29)
$7 \leq e < 13$; $0.2 \leq d < 20$	73	75 (7)	67 (7)	74 (8)
$13 \leq e < 18$; $d < 0.06$	221	222 (199)	214 (188)	211 (184)
13 ≤ e < 18; $0.06 \leq d < 0.2$	39	43 (28)	45 (27)	45 (30)
13 ≤ e < 18; $0.2 \leq d < 20$	40	42 (10)	49 (10)	45 (11)
χ^2		10	22	19
Covariable subgroups for time since exposure, tsx and thyroid dose, d				
				Model CS2
$tsx < 7$; $d < 0.06$	67	65 (45)	69 (57)	57 (37)
$tsx < 7$; $0.06 \leq d < 0.2$	48	63 (10)	71 (29)	67 (24)
$tsx < 7$; $0.2 \leq d < 20$	88	86 (3)	77 (8)	78 (6)
$7 \leq tsx < 11$; $d < 0.06$	117	118 (92)	112 (90)	102 (72)
$7 \leq tsx < 11$; $0.06 \leq d < 0.2$	88	101 (25)	113 (40)	119 (49)
$7 \leq tsx < 11$; $0.2 \leq d < 20$	148	127 (7)	129 (11)	132 (14)
$11 \leq tsx < 15$; $d < 0.06$	203	202 (170)	194 (155)	201 (157)
$11 \leq tsx < 15$; $0.06 \leq d < 0.2$	151	154 (54)	152 (50)	167 (85)
$11 \leq tsx < 15$; $0.2 \leq d < 20$	179	172 (15)	172 (13)	166 (24)
χ^2	-	9	18	23
$\Sigma\chi^2$		19	40	42

Notes. χ^2 is a quality-of-fit measure that does not take the number of model parameters into account here. The units of dose, d, are in Gy, age at exposure, e, and time since exposure, tsx, are in years.

applying a stratified baseline here is that the attained-age modification [which had a P value of 0.076, according to the score test statistic, with the parametric model, Eq. (6)] has a P value of 0.412 and so has been dropped from the model given in Eq. (7) here. The age-at-exposure effect modification found here in Eq. (7) is strongly indicated, with a P value of 0.007 according to the score test statistic.

For the ages and times considered here, the ERR estimates in the parametric model are higher than in the categorical model. At the start of the observation period (12 years after exposure), the ERR for age at exposure 5 years is larger than for age at exposure 15 years by a factor of about 3 for the parametric baseline model (Fig. 1). In the first years of observation, the dependence of the ERR on time since exposure was rather flat (Fig. 3).

DISCUSSION

Parametric Compared to Categorical Modeling of the Baseline Thyroid Cancer Rates

Several modeling regimens have been applied to the Chernobyl data to assess the influence of three different methods for dealing with baseline risks. Generally good agreement was found for the central risk estimates and the effect modifiers gender and country.

The main pertinent results here, presented in Figs. 1–3, are that nature of the age-at-exposure and time-since-exposure effect modifications of the central excess relative risks were found to be strongly dependent on the form of the baseline model. A comparison of Figs. 1 and 2 indicates that the steepness of the age-at-exposure effect modification depends both on whether a para-

TABLE 3
Model-Specific Values Tabulated for Two ERR Ratios

ERR model	Baseline model	Data	ERR($e = 15$)/ERR($e = 5$)	ERR($tsx = 4$)/ERR($tsx = 14$)
P	parametric	Jacob *et al.* (5)	0.17 (0.05; 0.29)	4.37 (0.92; 7.82)
C	categorical	Jacob *et al.* (5)	0.33 (0.09; 0.57)	0.57 (0.17; 0.97)
CS1/CS2	categorical, simplified	Jacob *et al.* (5)	0.31 (0.12; 0.58)[a]	1.63 (0.09; 4.12)
CS1/CS2	categorical, simplified	Likhtarov *et al.* (6)	0.32 (0.08; 1.30)[a]	0.10 (0.03; 0.43)

Notes. The two ratios are the ratio of the ERR at age at exposure 15 years to the ERR at age at exposure 5 years (for a fixed time since exposure of 12 years) and the ratio of the ERR at time since exposure (tsx) of 4 years to the ERR at time since exposure of 14 years (for fixed age at exposure of 10 years, all obtained from the Chernobyl data. 95% confidence ranges are quoted in parentheses.
[a] $e = 5$ and 15 are at the lower bounds of the time intervals in these two cases.

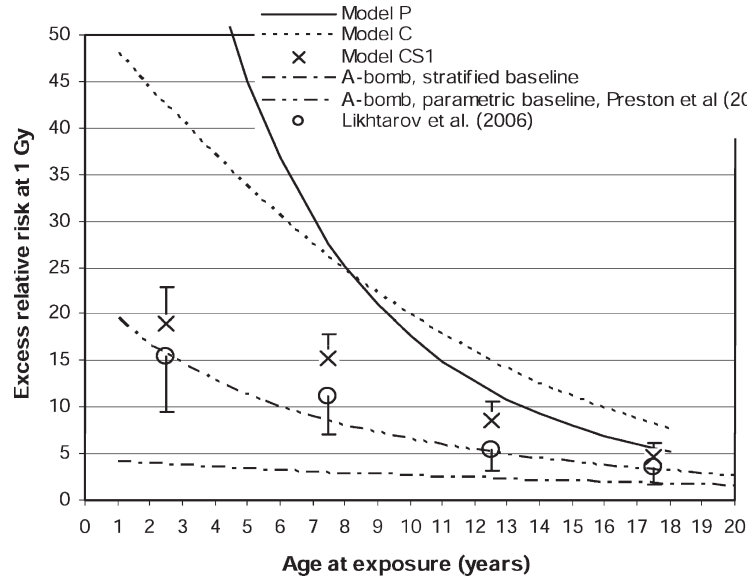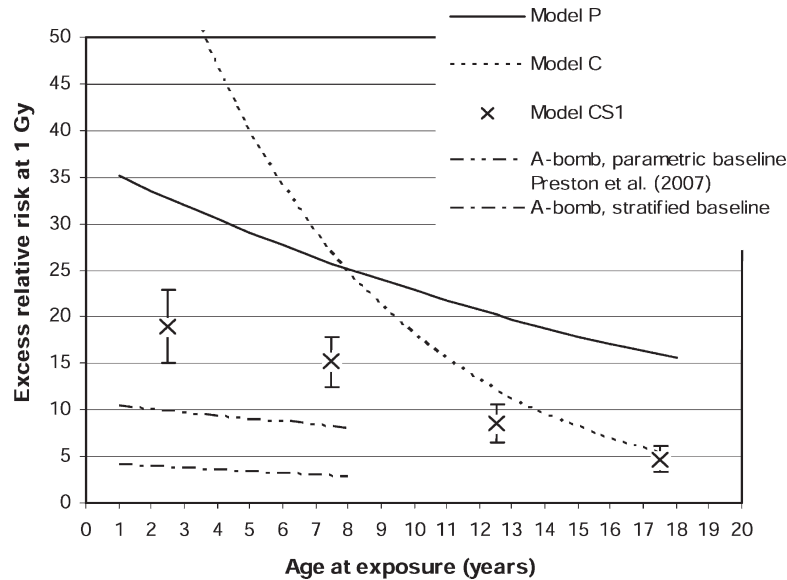**FIG. 2.** Time patterns in the Chernobyl data. The effect modification of ERR at 1 Gy by age at exposure for a fixed attained age of 20 years. The fit parameters for model CS1 are shown with one standard error. Results of ref. (7) for the atomic bomb survivors are shown for comparison.

metric or categorical baseline model was used and on whether this specific effect modification was considered for fixed time since exposure or for fixed attained age. This effect is pronounced for the Chernobyl data but not for the A-bomb data. Figure 3 indicates that the steepness of the time-since-exposure effect modification also depends on whether a parametric or categorical baseline model was used. Again, this effect is pronounced for the Chernobyl data but not for the A-bomb data.

The type of baseline modeling was also found to considerably influence the ERR results for thyroid cancer incidence among the atomic bomb survivors. Although the central estimate of ERR at 1 Sv for an age at exposure of 30 years, i.e. an adult, is higher with a stratified baseline than with the parametric baseline of ref. (7), the situation is reversed for persons exposed as children due to the different effect modifications indicated by the two different baseline methods.

In the case of the present Chernobyl data set, all quality-of-fit tests considered here tended to indicate a preference for the parametric representation of the baseline cancer rates. However, other known confounding risk factors for thyroid cancer such as genetic predisposition, iodine deficiency and iodine prophylaxis at the time of the accident could not be studied because of the current state of the data. Given the differences

found in the present work, it is strongly recommended to routinely test excess risk models for sensitivity to the method used for the determination of the baseline rates, and if there are no evident epidemiological indications for one method over another, any resulting differences should be included in the overall uncertainty evaluation.

The results of the present study cannot be taken as evidence that parametric baseline modeling is generally preferable to categorical baseline modeling.

Results for Two Different Chernobyl Data Sets

In the present work, the categorical models of Likhtarov *et al.* (6) were applied to the data set of Jacob *et al.* (5). Comparing the results obtained with the same models fitted to the data in ref. (5), which is for Ukraine and Belarus, and Likhtarov *et al.* (6), which is just for the Ukraine, showed generally lower risk estimates associated with the latter data. This is consistent with the country effects on risk estimates obtained from the data in ref. (5), which are higher for Belarus than for Ukraine. The reason for this systematic difference is not clear. It may be related to country differences in iodine deficiency (11) or to higher incidence rates and possibly to a more intensive surveillance of the thyroid during regular medical examinations in Belarus (12). The latter is indicated by a larger fraction of small carcinomas in Belarus compared to Ukraine.
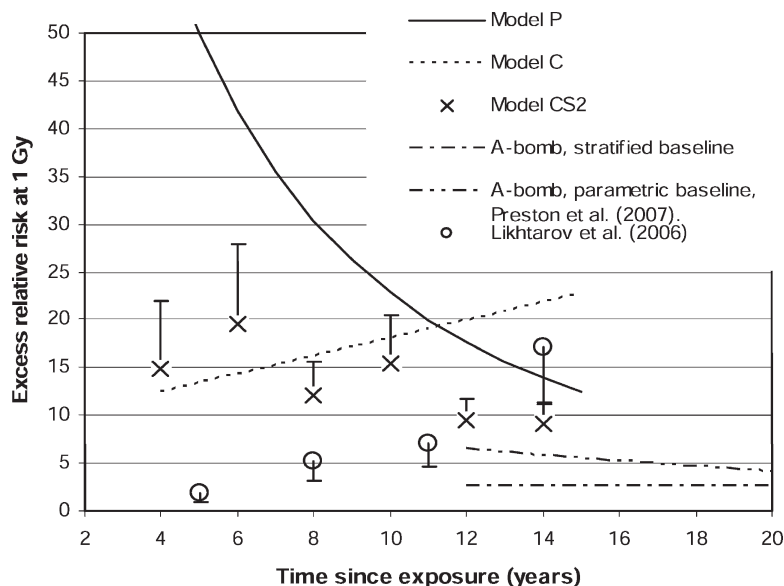
FIG. 3. Time patterns in the Chernobyl data. The effect modification of ERR at 1 Gy by time since exposure, at an age at exposure of 10 years. The fit parameters for model ERR-CS2 are shown with one standard error. Results of ref. (7) for the atomic bomb survivors are shown for comparison.

With two exceptions, the results obtained with the two data sets are quite consistent if the country effect is taken into account. The increase of the ERR with time since exposure reported by Likhtarov *et al.* (6) is only weakly reproduced by one of the other analyses. Part of the effect may be due to the use of a categorical baseline model, which does not seem to be fully supported by the data. Another possibly related discrepancy between the models of ref. (6) and those considered both here and in refs. (5, 7) can be found in the attained-age trends in the baseline models. The baseline risk reported by Likhtarov *et al.* (6) can be seen [in Table 4 of ref. (6)] to decrease with increasing attained age for males but to increase for females. This trend for males contradicts the trends found both here (in Table A2 of the Appendix) and in ref. (5) and also in general thyroid cancer incidence rates (13) as well as in the latest thyroid cancer incidence data[3] for the A-bomb survivors (7).

EAR Estimates

Analogous EAR forms of the ERR models used in this paper were also investigated. In contrast to the ERR results, the EAR estimates and associated trends in effect modification were found to be consistent in the various models. Also, there is a good agreement between

refs. (5) and (6) on a larger EAR for females than for males (factor 1.5) and a decrease of the EAR with age at exposure (factor 0.4 for ages at exposure of 15 and 5 and for an attained age of 20). Thus, for the age-at-exposure and time-since-exposure regimes considered here, EAR values can be estimated with a lower uncertainty and a higher reliability than ERR values. For a thyroid exposure of 1 Gy, the central estimate of the EAR is about 2 cases per 10^4 PY.

Similarities to and Differences from the Atomic Bomb Survivors

The Chernobyl data set and the data set for the atomic bomb survivors overlap in coverage for the period of just over 12 years to 15 years since exposure. For this period, higher ERR values and a stronger age-at-exposure modification are found in the parameteric model for the Chernobyl data. Considering the age-at-exposure modification of the ERR, however, the results for the atomic bomb survivors are generally consistent

---

[3] The increase in the A-bomb baseline rates with attained age for thyroid cancer incidence rises up to 1.4 and 2.5 cases per 10^4 PY at an age of 70 years for males and females, respectively (for a birth cohort corresponding to $e = 30$ years), according to the parametric baseline model of ref. (7).

with the results of the categorical model for the Chernobyl data. The real nature of the age-at-exposure effect modification remains an open question.

It should be noted that the results of the present study are not easily compared to the analysis by Ron *et al.* (*14*) of pooled data from five cohort studies data, because a major part of the pooled data relate to a follow-up time longer than 15 years.

Recommendation on Baseline Modeling

Based on the experience of the study, it is generally recommended to test parametric and categorical baseline models in risk analyses. If quality-of-fit criteria do not clearly favor one kind of model, then deviating results indicate a larger uncertainty of the results than the statistical uncertainty of either method.

APPENDIX

TABLE A1
ERR Best Estimates (Centered at $e = 10$ Years, and $a = 20$ Years) and 95% Confidence Ranges of ERR Fit Parameters for Model C (with Stratum-specific Background Rates)

Symbol	Model C, fit parameters Eq. (3)	Meaning
β_1 (Gy^{-1})	15.25 (8.97; 21.52)	Linear term: ERR per unit dose for $a = 20$ and $e = 10$
β_2 (Gy^{-2})	-0.83 (-1.17; -0.49)	Quadratic term: ERR per unit dose squared for $a = 20$ and $e = 10$
exp(β_c)	2.18 (1.07; 4.46)	Country ratio
exp(β_s)	0.33 (0.14; 0.75)	Sex ratio
β_e (a^{-1})	0.159 (0.100; 0.218)	Slope of the logarithm of ERR with decreasing age-at-exposure
β_a (a^{-1})	1.04 (0.23; 1.85)	Power of a central estimate risk modification

TABLE A2
Rate, Relative Risks and 95% Confidence Intervals for Background Variables (as Optimized with a Simple ERR Model Part that is Linear in Dose) for Models Very Similar to Those in Likhtarov *et al.* (*6*)

Symbol	Variable	Estimate	Lower 95% bound	Upper 95% bound
exp (β_1)	**Constant**	6.47×10^{-6}	3.87×10^{-6}	1.08×10^{-5}
	Country			
exp (β_2)	*Ukraine*	1.0		
exp (β_3)	*Belarus*	1.13*	0.99	1.29
	Age at risk, years			
	males			
exp (β_4)	–	1.0		
exp (β_5)	*10–14*	1.42	0.85	2.38
exp (β_6)	*15–19*	1.01	0.59	1.74
exp (β_7)	*20–24*	0.74	0.42	1.29
exp (β_8)	*25–29*	1.05	0.58	1.93
exp (β_9)	*30+*	1.10	0.55	2.20
	females			
exp (β_{10})	*5–9*	1.51	0.83	2.77
exp (β_{11})	*10–14*	2.49	1.50	4.12
exp (β_{12})	*15–19*	2.01	1.19	3.37
exp (β_{13})	*20–24*	2.26	1.34	3.81
exp (β_{14})	*25–29*	4.10	2.38	7.07
exp (β_{15})	*30+*	4.26*	2.39	7.61
	Calendar time			
exp (β_{16})	*1989–1990*	1.0		
exp (β_{17})	*1991–1992*	1.41	1.06	1.88
exp (β_{18})	*1993–1994*	1.90	1.44	2.52
exp (β_{19})	*1995–1996*	1.81	1.36	2.41
exp (β_{20})	*1997–1998*	2.75	2.08	3.63
exp (β_{21})	*1999–2001*	2.78	2.07	3.72

Notes. The parameters β_1 to β_{21} refer to the fit parameters defined in Eq. (4). *Note that the background fit parameters change somewhat when reoptimized for models CS1 and CS2, with the largest changes associated with the female relative risks. The latter change from having a maximum relative risk of about 4 in the baseline parameters here to a maximum of about 10 or 11 for model CS1 and CS2, respectively. The baseline risk for Belarus relative to Ukraine is also slightly model-dependent.

TABLE A3
Excess Relative Risks and 95% Confidence Intervals for Dose with Various Interaction Effects for Models Very
Similar to Those in Likhtarov *et al.* [ref. (*6*) and Eq. (5) of the Main Paper]

Model	Symbol	Variable	ERR/Gy	Lower 95% bound	Upper 95% bound
CS1			Age in 1986, years		
	$\exp(\gamma_1)$	*1–4*	18.93	11.27	26.60
	$\exp(\gamma_2)$	*5–9*	15.15	9.78	20.53
	$\exp(\gamma_3)$	*10–14*	8.56	4.70	12.43
	$\exp(\gamma_4)$	*15–18*	4.73	1.88	7.58
CS2			Mean calendar year (in each 2-year interval)		
	$\exp(\gamma_1)$	*1990.5*	14.93	1.34	28.52
	$\exp(\gamma_2)$	*1992.5*	19.60	3.51	35.70
	$\exp(\gamma_3)$	*1994.5*	12.01	4.89	19.12
	$\exp(\gamma_4)$	*1996.5*	15.43	5.72	25.13
	$\exp(\gamma_5)$	*1998.5*	9.41	4.93	13.88
	$\exp(\gamma_6)$	*2000.5*	9.18	4.82	13.53

REFERENCES

1. V. S. Kazakov, E. P. Demidchik and L. N. Astakova, Thyroid cancer after Chernobyl. *Nature* **359**, 21 (1992).

2. I. A. Likhtarev, B. G. Sobolev, I. A. Kairo, N. D. Tronko, T. I. Bogdanova, V. A. Oleinic, E. V. Epshtein and V. Beral, Thyroid cancer in the Ukraine. *Nature* **375**, 365 (1995).

3. M. D. Tronko, T. I. Bogdanova, I. V. Komisarenko, O. V. Epshtein, I. A. Likhtaryov, V. V. Markov, V. A. Oliynyk, V. P. Tereshchenko, V. M. Shpak and P. Voilleque, Thyroid carcinoma in children and adolescents in Ukraine after the Chernobyl accident: statistical data and clinicomorphologic characteristics. *Cancer* **86**, 149–156 (1999).

4. Yu . E. Demidchik and E. P. Demidchik, Thyroid carcinomas in Belarus 16 years after the Chernobyl disaster. In *Proceedings of Symposium on Chernobyl-related Health Effects*, pp. 66–77. Radiation Effects Association, Tokyo, 2002.

5. P. Jacob, T. I. Bogdanova, E. Buglova, M. Chepurniy, Y. Demidchik, Y. Gavrilin, J. Kenigsberg, R. Meckbach, C. Schotola and L. Walsh, Thyroid cancer risk in areas of Ukraine and Belarus affected by the Chernobyl accident. *Radiat. Res.* **165**, 1–8 (2006).

6. L. Likhtarov, L. Kovgan, S. Vavilov, M. Chepurny, E. Ron, J. Lubin, A. Bouville, N. Tronko and T. Bogdanova, Post-Chornobyl thyroid cancers in Ukraine, report 2: Risk analysis. *Radiat. Res.* **166**, 375–386 (2006).

7. D. L. Preston, E. Ron, S. Tokuoka, S. Funamoto, N. Nishi, M. Soda, K. Mabuchi and K. Kodama, Solid cancer incidence in atomic bomb survivors: 1958–1998. *Radiat. Res.* **168**, 1–64 (2007).

8. V. A. Stezhko, E. E. Buglova, L. I. Danilova, V. M. Drozd, N. A. Krysenko, N. R. Lesnikova, V. F. Minenko, V. A. Ostapenko and S. V. Petrenko, A cohort study of thyroid cancer and other thyroid diseases after the Chornobyl accident: Objectives, design and methods. *Radiat. Res.* **161**, 481–492 (2004).

9. F. E. Harrell, Jr., *Regression Modeling Strategies: with Applications to Linear Models, Logistic Regression and Survival Analysis*. Springer, Berlin, Heidelberg, New York, 2001.

10. L. Walsh, A short review of model selection techniques for radiation epidemiology. *Radiat. Environ. Biophys.* **46**, 205–213 (2007).

11. E. Cardis, A. Kesminiene, V. Ivanov, I. Malakhova, Y. Shibata, V. Khrouch, V. Drozdovitch, E. Maceika, I. Zvonova and

D. Williams, Risk of thyroid cancer after exposure to ^{131}I in childhood. *J. Natl. Cancer Inst.* **97**, 724–732 (2005).

12. P. Jacob, T. I. Bogdanova, E. Buglova, M. Chepurniy, Y. Demidchik, Y. Gavrilin, J. Kenigsberg, J. Kruk, C. Schotola and S. Vavilov, Thyroid cancer among Ukrainians and Belarusians who were children or adolescents at the time of the Chernobyl accident. *J. Radiol. Prot.* **26**, 51–67 (2006).

13. D. M. Parkin, S. L. Whelan, J. Ferlay, L. Raymond and J. Young, *Cancer Incidence in Five Continents*, Vol VII. IARC Scientific Publications No. 143, IARC, Lyon, 1997.

14. E. Ron, J. H. Lubin, R. E. Shore, K. Mabuchi, B. Modan, L. M. Pottern, A. B. Schneider, M. A. Tucker and J. D. Boice, Thyroid cancer after exposure to external radiation: a pooled analysis of seven studies. *Radiat. Res.* **141**, 259–277 (1995).

28. Jacob P, Rühm W, Walsh L, Blettner M, Hammer G & Zeeb H. Cancer risk of radiation workers larger than expected. Occ. Env. Med (BMJ). 66, 789-96, 2009

Is cancer risk of radiation workers larger than expected?

P Jacob,[1] W Rühm,[1] L Walsh,[2] M Blettner,[3] G Hammer,[3] H Zeeb[3]

ABSTRACT

Occupational exposures to ionising radiation mainly occur at low-dose rates and may accumulate effective doses of up to several hundred milligray.

The objective of the present study is to evaluate the evidence of cancer risks from such low-dose-rate, moderate-dose (LDRMD) exposures.

Our literature search for primary epidemiological studies on cancer incidence and mortality risks from LDRMD exposures included publications from 2002 to 2007, and an update of the UK National Registry for Radiation Workers study. For each (LDRMD) study we calculated the risk for the same types of cancer among the atomic bomb survivors with the same gender proportion and matched quantities for dose, mean age attained and mean age at exposure. A combined estimator of the ratio of the excess relative risk per dose from the LDRMD study to the corresponding value for the atomic bomb survivors was 1.21 (90% CI 0.51 to 1.90).

The present analysis does not confirm that the cancer risk per dose for LDRMD exposures is lower than for the atomic bomb survivors. This result challenges the cancer risk values currently assumed for occupational exposures.

What this paper adds

► Occupational exposures to ionising radiation occur normally at low-dose rate and may sum up to moderate doses in the order of 100 mGy.

► Limits of occupational exposures are based on the assumption that cancer risk factors are lower than for the atomic bomb survivors by a factor of two.

► Twelve recent epidemiological studies on cancer after low-dose-rate, moderate-dose exposures were included in this analysis of cancer risks related to such exposures.

► The studies provide evidence that cancer risk factors for occupational exposures are not lower than for atomic bomb survivors.

► The new evidence for cancer risks should be taken into account in optimisation procedures for the use of radionuclides and ionising radiation at the work place and in medicine.

Occupational and medical diagnostic exposures to ionising radiation are mainly due to Roentgen rays and gamma rays, which belong to so-called low-linear energy transfer (LET) radiation. The exposures may accumulate over a lifetime to doses of the order of 100 mGy. For example, in the 15-countries collaborative study on radiation workers in the nuclear industry, about 10% of the 407 000 study members received external doses exceeding 50 mGy, while only 0.1% received doses exceeding 500 mGy.[1] Exposures with doses in the range of 50–500 mGy are considered here to be moderate in comparison with the high-dose groups of the atomic bomb survivors from Hiroshima and Nagasaki.

Within an hour, which is the timescale for cellular repair processes, doses from occupational and medical diagnostic exposures do not generally exceed the order of 10 mGy. Thus, these exposures occur at low-dose rate.

It follows that estimates of health risks, in particular of cancer risks, related low-dose-rate, moderate-dose (LDRMD) exposures are of central importance for practical radiation protection.

Current estimates of cancer risks from LDRMD exposures are mainly based on risk coefficients derived from the Japanese atomic bomb survivors, that is, from persons with acute, high-dose exposures, which are then combined with a "dose and dose-rate effectiveness factor" (DDREF).[2] [3] Values for DDREF have mainly been deduced from experiments with laboratory animals and from radiobiological measurements. Specifically, the International Commission on Radiological Protection (ICRP) derived estimates of the excess cancer risk after low-dose exposures and after exposures with higher doses but low-dose rates by reducing the corresponding risk value for the atomic bomb survivors by a DDREF of 2.0.[2] The BEIR VII Committee of the US National Research Council used a DDREF of 1.5.[3]

During the past few years, a number of epidemiological studies have been published, which provide major information on cancer risk after LDRMD exposures. The statistical power of each of these studies is not strong because of the relatively low risks of the doses involved. Therefore, the present study focuses on studies of larger groups of cancers. More specifically, studies of all cancer, all cancer excluding leukaemia, all solid cancer and all solid cancer excluding bone cancer have been included.

In the present paper, values of the excess relative risk (ERR) per dose in LDRMD studies of cancer risks from exposures to low-LET radiation are compared with those calculated for the atomic bomb survivors for the same grouping of cancer types, gender distribution, average age at exposure, average age attained and dose quantity. A combined estimator of the resulting risk ratios is calculated. Based on this risk estimator, cancer lifetime risks are assessed.

In some of the LDRMD studies, ERR-per-dose distributions include a value of zero, which would correspond to an infinite value of the DDREF. In order to avoid resulting instabilities of the calculations, the inverse DDREF value, Q, that is, the ratio of the ERR-per-dose value in the LDRMD study to that for the atomic bomb survivors, is calculated here.

METHODS

Literature search

A systematic literature search for primary epidemiological studies was conducted in the PubMed database in January 2008, covering the period January 2002 to December 2007. The search terms "radiation" and "cancer" were combined with alternatives of the terms "occupation", "work", "personnel", and "environmental" or "emergency". A number of exclusion terms were specified to limit the findings to ionising radiation effects in the occupational, environmental or emergency setting. An initial selection of 714 papers was identified. The PubMed search was augmented by a manual search for references, by which a paper on Chernobyl emergency and clean-up workers[4] and a paper on Oak Ridge National Laboratory (ORNL) workers[5] were identified. Further, stimulated by a suggestion of a reviewer, a recent study on the UK National Registry for Radiation Workers[6] was included in the analysis, because of its outstanding importance. Results without inclusion of this study are also reported below.

The initial selection was then restricted to cohort and case-control studies and epidemiological reviews, which left 123 papers. Further eliminations were made of studies on exposures to alpha radiation (because most of the occupational exposures are due to external radiation), focused on children or individual cancer sites, or without dosimetry. Further, nine publications were not included in our analysis mainly because relative risk estimates and their standard deviations could not be derived,[7–11] because there were many cohort members with high exposures,[12 13] because no data of the Life Span Study (LSS) were available for the corresponding group of cancers among the atomic bomb survivors[14] or the required information on age at exposure and age at risk were not obtained.[15]

If a study contained results for different cancer outcomes, then the outcome closest to "solid cancer" was chosen. Especially, inclusion of leukaemia was avoided as far as possible because of differences in height of risk and in shape of dose response, if compared with solid cancer.

Concerning the 15-countries collaborative study of cancer risk among radiation workers in the nuclear industry,[16] the present analysis includes only results, which are not based on the Canadian data, because problems with the application of the Canadian data within the 15-countries study have been reported (Norman Gentner, personal communication, 2008).

ERR per dose for atomic bomb survivors

The publicly available atomic bomb survivor datasets for cancer mortality from 1950 to 2000 (DS02can.dat) and cancer incidence from 1958 to 1998 (lssinci07.csv) from the Radiation Effects Research Foundation (http://www.rerf.or.jp) were used to calculate ERR-per-dose values for acute exposures. Only survivors with doses below 4 Gy of shielded kerma were used in the risk analysis.

The atomic bomb survivor data for the cancer categories used in an LDRMD study, i were fitted with a model including an explicit ERR-per-dose parameter, $\beta_{\mathrm{lss}i}$, a male fraction, f_i, an age at exposure, e_i and an age-attained, a_i:

$$\lambda(d_i, s, e, a) = \lambda_0(s, e, a) \; [1 + \beta_{\mathrm{lss}i} \, d_i \, \rho_i(s, e, a)] \quad (1)$$

with

$$\rho_i(s, e, a) = \theta_i(s) \, \exp[\alpha_i \, (e - e_i) + \omega_i \, \ln \, (a/a_i)] \quad (2)$$

and

$$\theta_i(s) = 1 + \theta_{is} \, f_i, \text{ if } s = \text{ female}$$

$$(3)$$

$$\theta_i(s) = 1 - \theta_{is} \, (1 - f_i), \text{ if } s = \text{ male}$$

Here λ is the total mortality/incidence rate, λ_0 the baseline rate, d_i the dose (see below), s gender, e the age at exposure, a the age at risk and α_i, ω_i and θ_{is} are parameters. For e_i, the average age at start of follow-up in the LDRMD study was chosen as a surrogate for average age at exposure. The modelling of age-at-exposure and age-attained dependences in equation (2) is the way the age parameters are treated in recent A-bomb papers, for example, by Preston et al.[17]

We based the risk calculations for the atomic bomb survivors

- on the dose to that organ as it was used in the corresponding LDRMD study, if the study was based on an organ dose
- the skin dose, if the LDRMD study was based on film badge or TLD readings.

Neutron doses were weighed by a factor of 10.

The Poisson regressions were performed with the programme AMFIT of the software package EPICURE (HiroSoft International Corp., Seattle, Washington, USA).

Ratio of ERR-per-dose values

The ratio of the ERR-per-dose value, $\beta_{\mathrm{ldrmd}i}$, in an LDRMD study i and the corresponding value for the atomic bomb survivors was calculated as:

$$q_i = \beta_{\mathrm{ldrmd}i}/\beta_{\mathrm{lss}i}. \quad (4)$$

Normal distributions were assumed for $\beta_{\mathrm{ldrmd}i}$ and $\beta_{\mathrm{lss}i}$ with average values corresponding to the best estimates given in the publications (for $\beta_{\mathrm{ldrmd}i}$) or obtained in the Poisson regression (for $\beta_{\mathrm{lss}i}$). Standard deviations of the single estimates were estimated by dividing the width of their respective confidence interval by twice the appropriate quantile of the normal distribution. Percentiles and the variance V_i of q_i were calculated from 1000 samples from each distribution generated with the Monte Carlo software package Crystal Ball (Decisioneering, Denver, Colorado, USA).

Combined estimator of the risk ratio

A combined estimator of the ratio of the ERR-per-dose values for LDRMD and acute exposures was obtained by the inverse variance method for calculating a weighted average of the ratios for the single LDRMD studies.

$$Q = \left(\sum_{i=1}^{n} q_i / V_i \right) \bigg/ \sum_{i=1}^{n} 1/V_i \quad (5)$$

where n is the number of LDRMD studies considered.

The ratio Q was calculated separately for studies of cancer mortality and for studies of cancer incidence. Some of the LDRMD mortality studies had part of the data in common. In order to avoid a double counting of such mortality data, two analyses including only independent studies were performed. In the first analysis, LDRMD studies with the larger number of cancer mortality cases were used. In the second analysis, instead of these, LDRMD studies with the smaller number of cases were included. Out of the three analyses (two for cancer mortality and one for incidence) the combined risk estimator with the narrowest uncertainty range (the ratio of the upper and the lower boundary of the 90% confidence interval) was defined to

Table 1 List of cancer mortality studies, which were included in the analysis

No	Reference, country	Population	Follow-up, cancer cases	Type of exposure	Cancer outcomes	ERR per dose, β_{ldrmd} $(Gy)^{-1}$, best estimate and 90% CI
1	Boice 2006, USA[18]	Workers at Rocketdyne	−1999, 3066	External and internal	All cancer excluding leukaemia	0.0 (−1.9 to 2.4)*
2	Cardis 2007, 14 countries†[16]	Radiation workers in nuclear industry	Variable, 6119	External	All cancer excluding leukaemia	0.6 (−0.1 to 1.4)
3	Ivanov 2001, Russia‡[21]	Chernobyl clean-up workers	1991–1998, 515	External	Neoplasms ICD-9 140–239	2.1 (1.3 to 2.9)*
4	Ivanov 2006, Russia[4]	Chernobyl clean-up workers	1992–2002, 651	External	Solid cancer	1.5 (0.2 to 2.9)*
5	Krestinina 2005, Russia[24]	Techa River residents	−1999, 1842	External and internal	Solid cancer except bone cancer	0.9 (0.2 to 1.7)*
6	Muirhead 2009, UK[6]	Radiation workers	−2001, 6959	External	Malignant neoplasms excluding leukaemia	0.3 (0.02 to 0.6)
7	Stayner 2007, USA[5]	ORNL workers	−1984, 225	External	All cancer excluding leukaemia	4.8 (0.4 to 13.3)§
8	Telle-Lamberton 2007, France¶[19]	French nuclear workers	1968–1994, 721	External	All cancer excluding leukaemia	1.5 (−0.5 to 4.0)
9	Wing 2005, USA[20]	Hanford workers	−1994, 2265	External and internal	All cancer	0.3 (−0.3 to 1.0)

ERR, excess relative risk; ORNL, Oak Ridge National Laboratory.
*95% confidence interval.
†Canadian data excluded from 15-countries study.
‡Summarised by Ivanov et al[25] in 2007, and therefore included in our analysis.
§After correction for dose uncertainties. The result without this correction is 5.4 (0.5 to 12.6) Gy^{-1}.
¶Results for "all cancer excluding leukaemia" were supplied by personal communication with Telle-Lamberton (2008).

be the main analysis. Sensitivity analyses were performed by excluding single studies from the main analysis. Study heterogeneity was assessed by calculating Cochran's Q statistic and the corresponding p value.

Lifetime risks
The BEIR VII committee performed a probabilistic calculation of the lifetime-solid-cancer mortality and incidence risks per dose for low-dose-rate exposures to external radiation according to:

$$lr_{BEIRVII} = lr_{lss}/DDREF_{BEIRVII} \quad (6)$$

where lr_{lss} is the lifetime risk per dose for acute, high-dose exposures as derived for most cancer sites from the incidence data of the atomic bomb survivors from Hiroshima and Nagasaki, transferred to the American population.[3] $DDREF_{BEIRVII}$ has a mode of 1.5 and a 95% CI of 1.1 to 2.3.

Lifetime-solid-cancer mortality and incidence risks per dose for LDRMD exposures have been calculated here as:

$$lr_{ldrmd} = lr_{BEIRVII} DDREF_{BEIRVII} Q \quad (7)$$

In the calculation, $lr_{BEIRVII}$ and $DDREF_{BEIRVII}$ were assumed to be negatively correlated with a correlation coefficient of −0.5. In order to check the impact of this subjective choice, limiting calculations were also performed for values of the correlation coefficients of 0 and −1.

The ICRP has defined the detriment-adjusted nominal risk coefficient as a weighted sum of lifetime risks per dose for fatal and non-fatal cancer, severe heritable effects, and length of life lost. The coefficient is calculated by:

$$d_{ICRP} = d_{lss}/DDREF_{ICRP} \quad (8)$$

where d_{lss} is the detriment-adjusted nominal risk coefficient for cancer after acute, high-dose exposures as derived mainly from the incidence data of the atomic bomb survivors.[2] $DDREF_{ICRP}$ has the value of 2.

Taking account of the cancer risk per dose in LDRMD epidemiological studies, a detriment-adjusted nominal risk coefficient for cancer was assessed here according to:

$$d_{ldrmd} = d_{ICRP} DDREF_{ICRP} Q \quad (9)$$

RESULTS
Studies of low-dose-rate, moderate-dose exposures
All 12 studies selected for the analysis were cohort studies. The nine mortality studies (table 1) and three incidence studies (table 2) included seven studies on radiation workers,[5 6 16 18–20] three studies on emergency and clean-up workers after the Chernobyl accident[4 21 22] and two studies on the residents of villages located along the banks of the Techa River.[23 24] Although a number of Chernobyl liquidators have obtained high-dose-rate exposures, the studies are included here, because the vast majority had only low-dose-rate exposures. None of the 12 studies include a considerable number of cohort members with cumulative exposures exceeding a few hundred milligray.

The best estimates of the ERR were positive in all studies (in one study it was 0.0). In seven of the 12 studies the excess cancer risk was significantly related to the radiation exposure.

Table 2 List of cancer incidence studies, which were included in the analysis

No	Reference, country	Population	Follow-up, cancer cases	Type of exposure	Cancer outcomes	ERR per dose, β_{ldrmd} $(Gy)^{-1}$, best estimate and 90% CI
10	Ivanov 2004, Russia[22]	Chernobyl clean-up workers	1996–2001, 1370	External	Solid cancer	0.3 (−0.4 to 1.2)*
11	Krestinina 2007, Russia[23]	Techa River residents	1956–2002, 1836	External and internal	Solid cancer except bone cancer	1.0 (0.3 to 1.9)*
12	Muirhead 2009, UK[6]	Radiation workers	−2001, 10 855	External	Malignant neoplasms excluding leukaemia	0.3 (0.04 to 0.5)

*95% confidence interval.

Table 3 Datasets, parameters and risk per dose for the atomic bomb survivors corresponding to the low-dose-rate, moderate-dose studies of cancer mortality in table 1, and the risk ratios, q_i

No	Population	Male fraction	Average age at start of follow-up	Average age at end of follow-up	Dose quantity	ERR per dose (Gy^{-1}) in LSS, β_{lss}, best estimate and 90% CI	Risk ratio, q, best estimate and 90% CI
1	Workers at Rocketdyne	0.92	31	56	Skin dose	0.26 (0.16 to 0.35)*	0.00 (−7.25 to 7.33)
2	Radiation workers in nuclear industry	0.90	31	46	Colon dose	0.49 (0.30 to 0.67)	1.19 (−0.34 to 3.12)
3	Chernobyl clean-up workers†	1.00	35	47	Skin dose	0.47 (0.29 to 0.65)*	4.49 (2.79 to 7.17)
4	Chernobyl clean-up workers	1.00	35	50	Skin dose	0.23 (0.11 to 0.34)*	6.66 (1.67 to 14.7)
5	Techa River residents‡	0.40	28	63	Stomach dose	0.54 (0.42 to 0.65)*	1.71 (0.52 to 3.04)
6	UK radiation workers	0.90	29	52	Skin dose	0.30 (0.21 to 0.39)	0.91 (0.01 to 2.01)
7	ORNL workers	1.00	30	57	Skin dose	0.25 (0.16 to 0.33)	19.6 (−6.38 to 51.3)
8	French nuclear workers	0.79	31	49	Skin dose	0.33 (0.23 to 0.43)	4.59 (−2.34 to 12.6)
9	Hanford workers	0.76	31	55	Skin dose	0.41 (0.33 to 0.49)	0.73 (−0.87 to 2.35)

ORNL, Oak Ridge National Laboratory.
*95% confidence interval.
†Calculations performed for all cancer, because out of 515 neoplasms (ICD-9 140–239) there were only three non-cancer cases (ICD-9 208–239).
‡Calculations performed for all solid cancer, because mortality data with DS02 were not available for bone cancer.

ERR per dose for atomic bomb survivors

The ERR-per-dose estimates for the atomic bomb survivors matched by categories of cancer mortality, sex ratios, average ages at exposure and average ages at risk of the LDRMD studies vary by more than a factor of 2.5 (tables 3 and 4). The highest estimate corresponds to the conditions in the cancer incidence study of the Techa River residents: a value of 0.59 (95% CI 0.49 to 0.69) Gy^{-1} is obtained for relatively young average age at first exposure (25 years) and a large fraction of females (0.57). Also, the risk estimation is related to the dose in a relatively well-shielded organ (stomach). The lowest estimate corresponds to a mortality study of Chernobyl liquidators: a value of 0.23 (95% CI 0.11 to 0.34) Gy^{-1} is obtained for all solid cancer and a high male fraction (100% males). Further, the risk is related to the relatively high dose in skin.

Comparison of ERR-per-dose values for different types of exposure

Generally, the uncertainties of the ERR estimates in the LDRMD studies are much larger than the corresponding estimates for atomic bomb survivors (figs 1 and 2). In six of the 12 LDRMD studies, the best estimate of the ERR per dose is larger than that for the atomic bomb survivors by more than a factor of 1.5, in five studies it is comparable, and only in one study it is smaller by more than a factor of 1.5.

The risk ratio, q, is significantly larger than 1.0 for the two mortality studies of Chernobyl clean-up workers.[4 21] In the remaining 10 LDRMD studies, the cancer-risk-per-dose values are compatible with those from the study of the atomic bomb survivors.

Combined estimator of the risk ratio

No statistical heterogeneity was detected between the estimated ratios, q_i, included in each of the three analyses (table 5).

It should be noted, however, that the power of the test is not strong in view of the small number of studies included. The uncertainty range of the combined estimator for the larger mortality studies and for the incidence studies had the same width. The analysis of the larger mortality studies was chosen as the main analysis because it includes more studies.

The main analysis includes seven cancer mortality studies, five of nuclear workers,[5 6 18–20] one of Chernobyl emergency and clean-up workers[21] and one of Techa River residents.[24] A risk ratio, Q, of 1.21 (90% CI 0.51 to 1.90) is obtained. The best estimate for the smaller mortality studies is larger; the difference is, however, not significant (p = 0.16). The combined estimator for the incidence studies is relatively close to the result of the main analysis.

Leaving out one of the studies changed the best estimate of Q in the main analysis at most by 26%. The lowest risk ratio with a value of 0.96 (90% CI 0.12 to 1.80) was obtained when the study of the Techa River residents was excluded. The highest risk ratio with a value of 1.44 (90% CI 0.48 to 2.41) was obtained when the study of the UK radiation workers was excluded.

Lifetime risks

Based on assessments of BEIR VII for lifetime cancer risks after acute exposures and on the results of the present analysis (equation 7), a number of about 14 (90% CI 6 to 31) or 24 (90% CI 9 to 49) excess solid cancer cases among 1000 males or females, respectively, is obtained for LDRMD gamma-ray exposures with a dose of 100 mGy. It is further estimated that there would be about seven (90% CI 3 to 15) or 11 (90% CI 4 to 23) excess fatalities from solid cancer among males or females, respectively.

If $lr_{BEIRVII}$ and $DDREF_{BEIRVII}$ were assumed to be not or completely anti-correlated, then the best estimates of the

Table 4 Datasets, parameters and risk per dose for the atomic bomb survivors corresponding to the low-dose-rate, moderate-dose studies of cancer incidence in table 2, and the risk ratios, q_i

No	Population	Male fraction	Average age at start of follow-up	Average age at end of follow-up	Dose quantity	ERR per dose (Gy^{-1}) for acute exposure, β_{lss}, best estimate and 90% CI	Risk ratio, q, best estimate and 90% CI
10	Chernobyl clean-up workers	1.00	35	49	Skin dose	0.33 (0.21 to 0.46)*	0.99 (−1.10 to 3.25)
11	Techa River residents	0.43	25	65	Stomach dose	0.59 (0.49 to 0.69)*	1.70 (0.54 to 2.92)
12	UK radiation workers	0.90	29	52	Skin dose	0.37 (0.29 to 0.46)	0.71 (0.09 to 1.42)

*95% confidence interval.

Figure 1 Excess relative risk per dose for cancer mortality in nine studies of low-dose-rate, moderate-dose exposures (red symbols), as compared with acute, high-dose exposures (atomic bomb survivors of Hiroshima and Nagasaki) (blue symbols). The error bars indicate 95% CIs for the studies of workers at Rocketdyne, the Chernobyl emergency workers and the Techa River residents, and 90% CIs for all other studies.
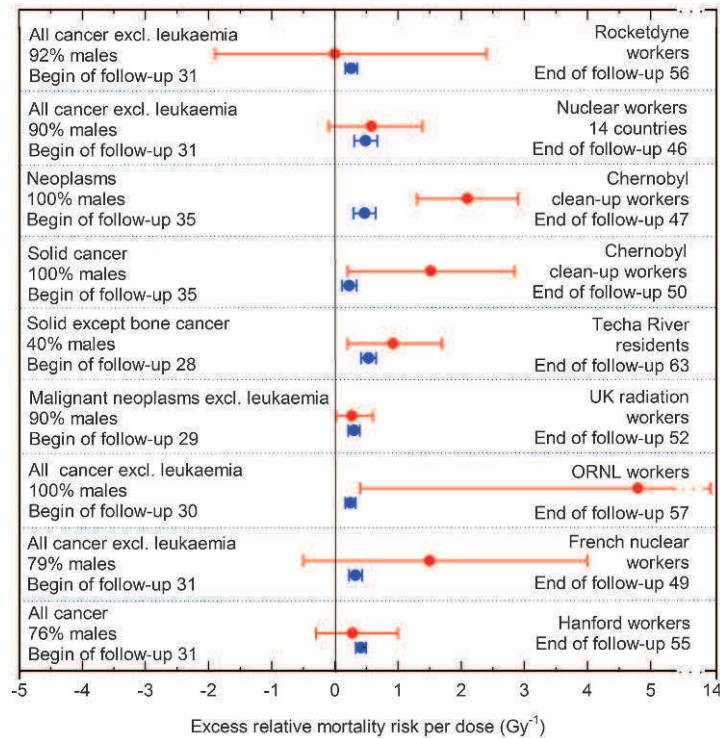
lifetime risks are essentially the same and the confidence intervals are increased or decreased by about 30%, respectively.

The radiation protection system of the ICRP is based on the effective dose. For whole body exposures with low-LET radiation, the effective dose in the unit Sievert (Sv) is numerically equal to the absorbed dose in the unit Gray (Gy) as it was used by BEIR VII. Based on the assessment of the ICRP for the detriment-adjusted nominal cancer risk coefficient for acute exposures and on the result of the present analysis (equation 9), an estimate of the detriment-adjusted nominal risk coefficient for workers of about 10 (90% CI 4 to 16) 10^{-2} Sv^{-1} is

obtained for LDRMD exposures. Representing essentially a sum of excess cancer fatalities and of weighted excess non-fatal cancer cases, this value is slightly larger than the sex-averaged result for the mortality risk as described above.

DISCUSSION

Strengths and limitations of the present study

It is the strength of the analysis to have extracted the following common information from a number of recent epidemiological studies of cancer after LDRMD exposures:

Figure 2 Excess relative risk per dose for cancer incidence in three studies of low-dose-rate, moderate-dose exposures (red symbols), as compared with acute, high-dose exposures (atomic bomb survivors of Hiroshima and Nagasaki) (blue symbols). The error bars indicate 95% CIs for the Chernobyl emergency workers and the Techa River residents, and 90% CIs for the UK National Registry for Radiation Workers.
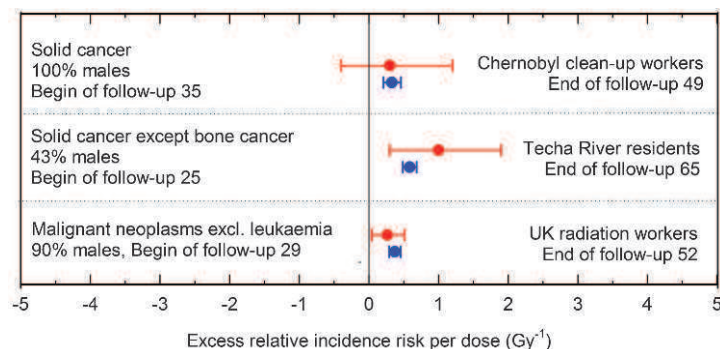
Table 5 Ratios of the excess relative risk per dose in low-dose-rate, moderate-dose studies and for the atomic bomb survivors as calculated in three analyses (main analysis in bold)

Endpoint	Criterion to select independent studies	Numbers of studies included*	Risk ratio, Q, best estimate and 90% CI	p Value for heterogeneity
Mortality	**Larger number of cancer cases**	**1, 4, 5, 6, 7, 8, 9**	**1.21 (0.51 to 1.90)**	**0.79**
Mortality	Smaller number of cancer cases	1, 2, 3, 5	2.08 (1.16 to 3.01)	0.21
Incidence	–	10, 11, 12	0.98 (0.41 to 1.54)	0.49

*Compare tables 1 and 2.

▶ There is evidence for an excess cancer risk after LDRMD exposures to ionising radiation.

▶ There is no indication that the excess cancer risk per dose for LDRMD exposures is smaller than for the atomic bomb survivors.

▶ These results still hold if single studies are excluded from the analysis.

Most of the studies included in the present analysis have methodological limitations especially concerning dosimetry. It is impossible to predict how improvements of dosimetry would or will change the results of the single LDRMD studies. A Monte Carlo simulation study incorporating uncertainty in the dose parameters estimated for study of ORNL workers found very little impact of these uncertainties on ERR-per-dose estimates.[5] Further, if future changes of the results of several LDRMD studies do not go in the same direction (increasing or decreasing the risk), then implications for the general results of the present analyses are expected to be low, because

▶ the risk ratios in the three different analyses presented in table 5 are quite consistent;

Figure 3 Ratio Q of excess relative risk-per-dose values for cancer after low-dose-rate, moderate-dose exposures and after acute, high-dose exposures as recommended by the International Commission on Radiological Protection (ICRP),[2] used by BEIR VII (95% CI),[3] and derived in the present analysis from epidemiological studies (epi-risk, 90% CI).

▶ the risk ratio of the main analysis is not strongly affected by a single study.

Another severe limitation of the LDRMD studies is the non-availability of data on risk factors other then radiation, especially of smoking data. Such risk factors may confound the results. Since, however, neither the LDRMD studies nor the analyses of the atomic bomb survivors take such risk factors into account, the risk ratios derived in the present paper may be less affected by the missing information than the risk estimates themselves.

A main limitation of the present analysis is the inclusion of results for different exposed groups and different groups of cancer types. Indeed, the relative risks among the atomic bomb survivors matching the conditions of the LDRMD studies vary by more than a factor of 2.5. There is no obvious way to avoid this limitation because the available single studies and even the large 15-countries pooled analysis do not have enough statistical power to allow conclusions as drawn in the present paper. However, the calculation of risk ratios for comparable conditions (groups of cancer types, male fraction, age at exposure, age attained, dose quantity used in the risk analysis, mortality or incidence data) in the present paper and the determination of a combined estimator for these ratios alleviate the problem with heterogeneous study conditions and endpoints.

Another limitation is the fact that published risk estimates were used instead of individual data from the included studies. Access to individual data from some of the excluded studies is possible via the Comprehensive Epidemiologic Data Resource (http://cedr.lbl.gov/). However, for the current analyses such extensive data acquisition and analysis could not be undertaken.

Finally, in the comparison of risks from protracted and acute exposures, the definition of age at exposure is problematic. In the present analysis, the average age at the start of follow-up has been used in the comparison. An older effective age at exposure would be more correct, but could not be estimated in this study. Using an older effective age at exposure would result in lower ERR-per-dose estimates for acute exposures and thus in even higher q_i values than obtained in the present analysis.

In summary, the value of the present study is a general estimation of implications of published studies rather than a quantitative risk evaluation.

Comparison with low-dose-rate, high-dose exposures

Two papers have been published in the past few years on large cohort studies of solid cancer risk due to low-dose-rate, but high-dose exposures.

One study included workers at the Mayak Production Association in the Southern Urals, Russia, which produced plutonium for the atomic weapons of the former Soviet Union.[13] These workers were exposed to external radiation and to plutonium which exposed mainly lungs, liver and bone. A first analysis of the cancer mortality with regard to other
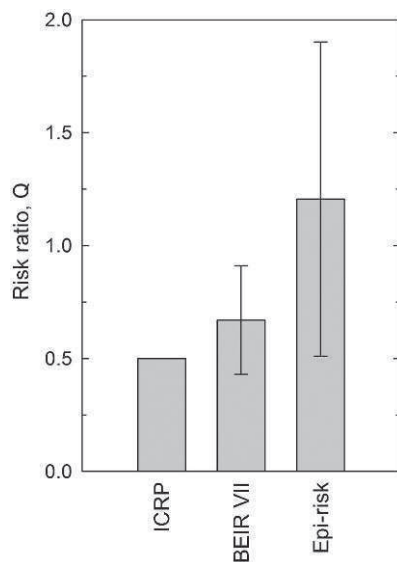
organs yielded an estimate of the ERR per external dose which was considerably lower than that for the atomic bomb survivors. It may, however, be noted that leukaemia risks per dose were quite comparable.

The second study included residents of northern Kazakhstan who were exposed to the fallout and also to external radiation from atomic bomb explosions performed at the nuclear Semipalatinsk test site.[12] The best estimate of the excess relative cancer mortality risk per dose was considerably higher than that for the atomic bomb survivors.

In summary, these high-dose studies do not provide contradictory evidence for the present evaluation of LDRMD exposure studies.

Comparison with BEIR VII and ICRP recommendations

According to BEIR VII, cancer risk after LDRMD exposure is expected to be by a factor of 1.5, according to the ICRP by a factor of 2, smaller than among atomic bomb survivors. However, the best estimates of the cancer risk in 11 of the 12 LDRMD studies are larger than both expectations (tables 3 and 4).

Due to low statistical power most single studies are consistent with the BEIR VII and ICRP recommendations: the 90% confidence ranges of 10 of the 12 risk ratios, q_i, include the value of 0.67, corresponding to the inverse $DDREF$ value used by BEIR VII; eight include the ICRP value of 0.5.

According to the main analysis in the present paper, the combined estimator of the risk ratio, Q, is compatible with the $DDREF$ used in BEIR VII, although the BEIR VII risk estimates are in the lower range (fig 3). The risk value recommended by the ICRP is smaller than the present result for LDRMD exposures. This result is borderline significant on the 90% confidence level.

The ICRP and BEIR VII base their $DDREF$s mainly on radiobiological results including animal data, which, in their majority, suggest a characteristically low risk for low-dose-rate exposures. It remains an open question as to why this characteristic is apparently not reflected in the human epidemiological data.

Implications

The recent epidemiological studies analysed here provide some evidence that cancer risks associated with LDRMD exposures to ionising radiation may be greater than those published by BEIR VII and the ICRP.

The ICRP rationale for radiation protection is based on three concepts: justification, dose limitation, and optimisation. The results of the new epidemiological studies highlight the need for justification of the use of radionuclides and ionising radiation in medicine, industry and research. Derivation of dose limits for radiation protection is a complex process including, for example, comparisons of occupational exposures with exposures to radiation from natural sources, or of radiation risks with other occupational health and mortality risks. Compared with earlier recommendations, the ICRP decided in 1991 to considerably reduce the recommended limit on effective dose for occupational exposures to 20 mSv per year, averaged over 5 years (100 mSv in 5 years).[26] Estimates of cancer risks related to exposures with cumulated doses of 100 mSv have been given in the Results section.

The ICRP has defined optimisation "as the source-related process to keep the likelihood of incurring exposures…, the number of people exposed, and the magnitude of individual doses as low as reasonably achievable, taking economic and societal factors into account".[2] The new epidemiological results

may influence optimisation procedures for future use of radionuclides and ionising radiation.

Probability-of-causation calculations play an important role in the adjudication of claims of compensations for cancer diseases after occupational radiation exposures. The computer code IREP made available by the US National Institute for Occupational Safety and Health (http://www.niosh-irep.com) is widely used for these calculations. The IREP includes a DDREF, which lowers the probability of causation for low-dose-rate exposures.[27] Use of such a factor in these calculations is questioned by the new epidemiological studies. Indeed, in the UK compensation scheme it is not assumed that low-dose exposures result in a lower risk per dose than acute, high-dose exposures.[28]

REFERENCES

1. **Cardis E,** Vrijheid M, Blettner M, et al. Risk of cancer after low doses of ionising radiation: retrospective cohort study in 15 countries. BMJ 2005;**331**:77–80.
2. **International Commission on Radiological Protection.** The 2007 Recommendations of the International Commission on Radiological Protection. ICRP Publication 103. Annals of the ICRP 37, Nos. 2–4, 2007.
3. **Committee to Assess Health Risks from Exposure to Low Levels of Ionizing Radiation, National Research Council.** Health risks from exposures to low levels of ionizing radiation. BEIR VII phase 2. Washington, DC: National Academies Press, 2006.
4. **Ivanov VK,** Tumanov KA, Kashcheev VV, et al. Mortality in Chernobyl clean-up workers: analysis of dose-effect relationship. Radiation and Risk 2006;**15**:11–22. (In Russian.)
5. **Stayner L,** Vrijheid M, Cardis E, et al. A Monte Carlo maximum likelihood method for estimating uncertainty arising from shared errors in exposures in epidemiological studies of nuclear workers. Radiat Res 2007;**168**:757–63.
6. **Muirhead CR,** O'Hagan JA, Haylock RGE, et al. Mortality and cancer incidence following occupational radiation exposure: third analysis of the National Registry for Radiation Workers. Brit J Cancer 2009;**100**:206–12.
7. **Atkinson WD,** Law DV, Bromley KJ, et al. Mortality of employees of the United Kingdom Atomic Energy Authority, 1946–97. Occup Environ Med 2004;**61**:577–85.
8. **Habib RR,** Abdallah AM, Law M, et al. Cancer incidence among Australian nuclear industry workers. J Occup Health 2006;**48**:358–65.
9. **Hwang SL,** Guo HR, Hsieh WA, et al. Cancer risks in a population with prolonged low dose-rate γ-radiation exposure in radiocontaminated buildings, 1983–2002. Int J Radiat Biol 2006;**82**:849–58.
10. **Sigurdson AJ,** Doody M, Rao RS, et al. Cancer incidence in the US radiologic technologists health study, 1983–1998. Cancer 2003;**97**:3080–9.
11. **Silver SR,** Daniels RD, Taulbee TD, et al. Differences in mortality by radiation monitoring status in an expanded cohort of Portsmouth Naval Shipyard workers. J Occup Environ Med 2004;**46**:677–90.
12. **Bauer S,** Gusev BI, Pivina LM, et al. Radiation exposure due to local fallout from Soviet atmospheric nuclear weapons testing in Kazakhstan: Solid cancer mortality in the Semipalatinsk historical cohort, 1960–1999. Radiat Res 2005;**164**:409–19.
13. **Shilnikova NS,** Preston DL, Ron E, et al. Cancer mortality risk among workers at the Mayak nuclear complex. Radiat Res 2003;**159**:787–98.
14. **Auvinen A,** Pukkala E, Hyvönen H, et al. Cancer incidence among Finnish nuclear reactor workers. J Occup Environ Med 2002;**44**:634–8.
15. **Jartti P,** Pukkala E, Uitti J, et al. Cancer incidence among physicians occupationally exposed to ionizing radiation in Finland. Scand J Work Environ Health 2006;**32**:368–73.
16. **Cardis E,** Vrijheid M, Blettner M, et al. The 15-country collaborative study of cancer risk among radiation workers in the nuclear industry: Estimates of radiation-related cancer risks. Radiat Res 2007;**167**:396–416.
17. **Preston DL,** Ron E, Tokuoka S, et al. Solid cancer incidence in atomic bomb survivors: 1958–1998. Radiat Res 2007;**168**:1–64.
18. **Boice JD,** Cohen SS, Mumma MT, et al. Mortality among radiation workers at Rocketdyne (Atomics International), 1948–1999. Radiat Res 2006;**166**:98–115.
19. **Telle-Lamberton M,** Samson E, Caer S, et al. External radiation exposure and mortality in a cohort of French nuclear workers. Occup Environ Med 2007;**64**:694–700.
20. **Wing S,** Richardson DB. Age at exposure to ionising radiation and cancer mortality among Hanford workers: follow up through 1994. Occup Environ Med 2005;**62**:465–72.
21. **Ivanov VK,** Gorski AI, Maksioutov MA, et al. Mortality among the Chernobyl emergency workers: estimation of radiation risks (preliminary analysis). Health Phys 2001;**81**:514–21.

Review

22. **Ivanov VK,** Gorski AI, Tsyb AF, *et al*. Solid cancer incidence among the Chernobyl emergency workers residing in Russia: estimation of radiation risks. *Radiat Environ Biophys* 2004;**43**:35–42.
23. **Krestinina LY,** Davis F, Ostroumova EV, *et al*. Solid cancer incidence and low-dose-rate radiation in the Techa River cohort: 1956–202. *Int J Epidemiol* 2007;**36**:1038–46.
24. **Krestinina LY,** Preston DL, Ostroumova EV, *et al*. Protracted radiation exposure and cancer mortality in the Techa River Cohort. *Radiat Res* 2005;**164**:602–11.
25. **Ivanov VK.** Late cancer and noncancer risks among Chernobyl emergency workers of Russia. *Health Phys* 2007;**93**:470–9.
26. **International Commission on Radiological Protection**. *1990 Recommendations of the International Commission on Radiological Protection*. ICRP Publication 60. Annals of the ICRP 21, Nos. 1–3, 1991.
27. **Land C,** Gilbert E, Smith JM. *Report of the NCI-CDC Working Group to revise the 1985 NIH radioepidemiological tables*. US Department of Health and Human Services, National Institutes of Health, Bethesda, 2003.
28. **Wakeford R,** Antell BA, Leigh WJ. A review of probability of causation and its use in a compensation scheme for nuclear industry workers in the United Kingdom. *Health Phys* 1998;**74**:1–9.
29. **Zankl M.** Personal dose equivalent for photons and its variation with dosimeter position. *Health Phys* 1999;**76**:162–70.
30. **International Commission on Radiological Protection**. *Conversion coefficients for use in radiological protection against external radiation*. ICRP Publication 74. Annals of the ICRP 26, Nos. 3/4, 1996.

APPENDIX 1: RELATION OF WHOLE BODY DOSE AND SKIN DOSE

The term "whole body dose", as used in a number of epidemiological studies of workers exposed to ionising radiation, relates to the dosimeter dose worn in front of the trunk of the worker. Values for this dose quantity are not available for the atomic bomb survivors. The main exposure of the atomic bomb survivors is due to Roentgen rays or gamma rays in the energy range of 100 keV to a few MeV. In this Appendix an organ is identified, for which dose values are available and which may serve as a surrogate for the whole body dose among atomic bomb survivors.

Zankl published conversion coefficients for the whole body dose, or more specifically for the personal dose equivalent, $H_p(10)$, per air kerma free in air, K_a (in Sv Gy^{-1}) for a typical dosimeter position, for monoenergetic photons incident in various irradiation geometries.[29] The ICRP published conversion coefficients of 15 organs in an anthropomorphic phantom per kerma free in air for monoenergetic photons incident in various irradiation geometries.[30]

We calculated the ratios of these two sets of conversion factors for two irradiation geometries: parallel from the front (anterior-posterior) and parallel from all horizontal directions (rotational invariant). For the photon energies and irradiation geometries of interest, the conversion coefficients for skin were found to be similar to the conversion coefficients for whole body dose: for both irradiation geometries and the whole energy range the coefficients agree within 10%.

29. Walsh L. Heterogeneity of variation of relative risk by age at exposure in the Japanese atomic bomb survivors. Radiat. Environ. Biophys. 48, 345-347, 2009

LETTER TO THE EDITOR

Heterogeneity of variation of relative risk by age at exposure in the Japanese atomic bomb survivors

Linda Walsh

The cohort of the atomic bomb survivors from Hiroshima and Nagasaki is unique due to: the large number of cohort members; the long follow-up period of more than 50 years; a composition that includes males and females, children and adults; whole-body exposures (which are more typical for radiation protection situations than the partial-body exposures associated with many medically exposed cohorts); a large dose ranges from natural to lethal levels; and an internal control group with negligible doses, i.e. those who survived at large distances (>3 km) from the hypocentres. There is a recent dataset on cancer incidence, for the follow-up time periods from 1958 to 1998, with the new dosimetry system DS02 (Young and Kerr 2005), available from the Radiation Effects Research Foundation (RERF). The incidence data are in grouped form and are categorised by: gender, city, age-at-exposure, age-attained, the calendar time period during which the health checks were made, and weighted survivor colon dose. This data-set provides an opportunity for conducting analyses of the data with various risk models, e.g., for radiation-induced all-solid-cancer incidence, as in BEIR VII (2006), Preston et al. (2007), Little (2009). Such analyses are extremely important as they form the basis for national and international radiation protection standards.

A recent paper on the Japanese atomic bomb survivors, by Preston et al. (2007) suggests that solid cancer relative risk exhibits a U-shaped relationship with age at exposure,

initially decreasing and then increasing at older exposure ages. This fascinating U-shape has prompted several investigators, including the author of a paper in this issue (Little 2009), and the current author, to take a closer look at the relevant analyses. The indication for this U-shape is based on just the two upper age-at-exposure categories [Fig. 6 on page 16 of Preston et al. (2007), but cited wrongly on page 13 as Fig. 7] from 50 to 60 years and beyond 60 years. The purpose of this letter is to report the author's reproduced analysis and own version of the Fig. 6 of Preston et al. (2007) as shown here in Figs. 1 and 2 with individual confidence intervals on each non-parametric excess relative risk (ERR) point. Figure 1 shows the age-at-exposure effects on solid cancer risks. The points are non-parametric category-specific estimates of the gender-averaged ERR at age 70 years after a dose of 1 Gy and correspond to those in Fig. 6 of Preston et al. (2007). These points have been recalculated with exactly the same model as applied in Preston et al. (2007). The confidence intervals are of the Wald type, based on an exponential re-parameterization and are for the 95% level. Figure 2 shows the same points but here the confidence intervals are based on likelihood profiles [computed with the BOUND command of the EPI-CURE package (Preston et al. 1993)] also based on an exponential re-parameterization and for the 95% level. Likelihood-based bounds are computed by direct exploration of the profile likelihood function using a constrained Newton–Raphson method. Figure 3 shows the same type of analysis for the most recent solid cancer mortality data (Preston et al. 2004) where the U-shape is less obvious.

The current author is not convinced that the U-shape is of much importance mainly because the risk at age at exposure 65 years is associated with a very large 95% confidence interval that spans most of the ordinate, and is not shown in the Fig. 6 of Preston et al. (2007). This effect is

L. Walsh (✉)
Department of Radiation Protection and Health,
Federal Office for Radiation Protection,
Ingolstaedter Landstr. 1, 85764 Oberschleissheim, Germany
e-mail: lwalsh@bfs.de
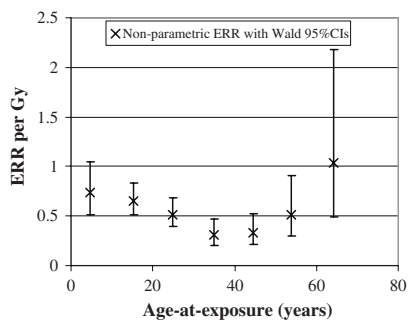
Fig. 1 Age-at-exposure effects on solid cancer incidence risks. The points are non-parametric category-specific estimates of the gender-averaged risk at age 70 years after a dose of 1 Gy. The confidence intervals are of the Wald type [computed with the CI command of the EPICURE package (Preston et al. 1993)] and are for the 95% level
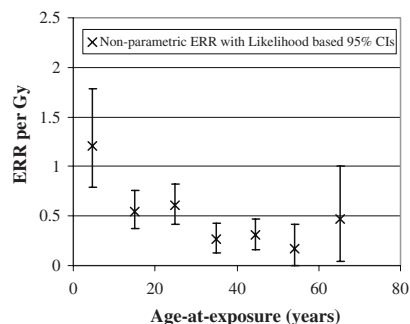
Fig. 3 Age-at-exposure effects on solid cancer mortality risks. The points are non-parametric category-specific estimates of the gender-averaged risk at age 70 years after a dose of 1 Gy. The confidence intervals are based on likelihood profiles [computed with the BOUND command of the EPICURE package (Preston et al. 1993)] and are for the 95% level
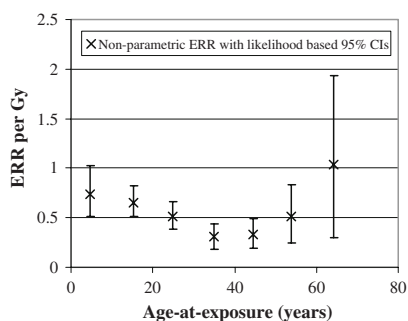
Fig. 2 Age-at-exposure effects on solid cancer incidence risks. The points are non-parametric category-specific estimates of the gender-averaged risk at age 70 years after a dose of 1 Gy. The confidence intervals are based on likelihood profiles [computed with the BOUND command of the EPICURE package (Preston et al. 1993)] and are for the 95% level

even more pronounced in Fig. 2 here, where the confidence intervals are likelihood-based, than in Fig. 1, where the confidence intervals are of the Wald type. Usually in such multi-dimensional optimisations the likelihood-based method for confidence interval determination is preferable to the Wald method.

In the original paper in this issue by Little (2009), the latest Japanese atomic bomb survivor solid cancer incidence (Preston et al. 2007) and mortality (Preston et al. 2004) data have been analysed with an extra stratification, where possible, by cancer sub-type (which is not usually applied in the official RERF analyses) and some parabolic functions of age at exposure. Both interesting additions to the modelling have been prompted by the U-shape mentioned above. Highly statistically significant ($p < 0.001$)

variations of relative risk by cancer type, and statistically significant variations by cancer type in the adjustments for sex ($p = 0.010$) and age at exposure ($p = 0.013$) to the relative risk were reported. However, no statistically significant ($p > 0.2$) variation by cancer type in the adjustment of relative risk for attained age was found. Figure 1 of the Little (2009) also gives a figure which is very similar to the above mentioned Fig. 6 in Preston et al. (2007) and the current author is pleased to see the error bars. However, Little has not made any comments on the issues of the statistical significance of the U-shape.

The current author believes that the three figures presented here will be useful additions in the assessment of the issue of the statistical significance of the U-shaped age-at-exposure effect modification of the ERR that has excited so much recent attention. This is especially true when one considers that epidemiological follow-up is already complete for the persons contributing to the age-at-exposure groups of more than 50 years. Consequently, no smaller error bars for this group can be expected with new data in the future.

References

Little MP (2009) Heterogeneity of variation of relative risk by age at exposure in the Japanese atomic bomb survivors. Radiat Environ Biophys (in press)

Preston DL, Lubin JH, Pierce DA (1993) Epicure user's guide. Hiro-Soft International Corporation, Seattle

Preston DL, Pierce DA, Shimizu Y, Cullings HM, Fujita S, Funamoto S, Kodama K (2004) Effects of recent changes in atomic bomb survivors dosimetry on cancer mortality risk estimates. Radiat Res 162:377–389

Preston DL, Ron E, Tokuoka S, Funamoto S, Nishi N, Soda M, Mabuchi K, Kodama K (2007) Solid cancer incidence in atomic bomb survivors: 1958–1998. Radiat Res 168:1–64

BEIR VII, United States National Research Council, Committee to Assess Health Risks from Exposure to Low Levels of Ionizing Radiation (2006) Health risks from exposure to low levels of ionizing radiation: BEIR VII—Phase 2. United States National Academy of Sciences. National Academy Press, Washington

Young R, Kerr GD (eds) (2005) DS02: reassessment of the atomic bomb radiation dosimetry for Hiroshima and Nagasaki, Dosimetry System 2002, DS02, vols 1, 2. Radiation Effects Research Foundation, Hiroshima

30. Schneider U & Walsh L. Cancer risk above 1 Gy and the impact for space radiation protection. Advances in Space Research. 44, 202-209, 2009

Cancer risk above 1 Gy and the impact for space radiation protection

Uwe Schneider [a,b,*], Linda Walsh [c]

[a] *University of Zürich, Vetsuisse Faculty, 8063 Zürich, Switzerland*
[b] *Hirslanden Medical Center, Institute for Radiotherapy, 5001 Aarau, Switzerland*
[c] *Department of Radiation Protection and Health, Federal Office for Radiation Protection, 85764 Oberschleissheim, Germany*

Abstract

Analyses of the epidemiological data on the Japanese A-bomb survivors, who were exposed to γ-rays and neutrons, provide most current information on the dose–response of radiation-induced cancer. Since the dose span of main interest is usually between 0 and 1 Gy, for radiation protection purposes, the analysis of the A-bomb survivors is often focused on this range. However, estimates of cancer risk for doses larger than 1 Gy are becoming more important for long-term manned space missions. Therefore in this work, emphasis is placed on doses larger than 1 Gy with respect to radiation-induced solid cancer and leukemia mortality. The present analysis of the A-bomb survivors data was extended by including two extra high-dose categories and applying organ-averaged dose instead of the colon-weighted dose. In addition, since there are some recent indications for a high neutron dose contribution, the data were fitted separately for three different values for the relative biological effectiveness (RBE) of the neutrons (10, 35 and 100) and a variable RBE as a function of dose. The data were fitted using a linear and a linear-exponential dose–response relationship using a dose and dose-rate effectiveness factor (DDREF) of both one and two. The work presented here implies that the use of organ-averaged dose, a dose-dependent neutron RBE and the bending-over of the dose–response relationship for radiation-induced cancer could result in a reduction of radiation risk by around 50% above 1 Gy. This could impact radiation risk estimates for space crews on long-term mission above 500 days who might be exposed to doses above 1 Gy. The consequence of using a DDREF of one instead of two increases cancer risk by about 40% and would therefore balance the risk decrease described above.

© 2009 COSPAR. Published by Elsevier Ltd. All rights reserved.

Keywords: Space radiation protection; Mars missions; Space flight; Radiation-induced cancer

1. Introduction

The health risk for astronauts and cosmonauts from space radiation is recognized as one of the limiting factors for long-term space missions. All cosmic radiation ultimately comes from two sources, the galactic cosmic rays (GCR), which originate outside the solar system, and the energetic solar wind and solar particle events (SPE), which are emitted by the sun. The GCR are ubiquitous in space and consist mainly of protons and ions with energies up to several hundred GeV, with peaks ranging from several hundred MeV up to around 1 GeV (Reitz, 2008). In low earth orbit the GCR contribute about 50% of the total dose equivalent received by astronauts and cosmonauts (Shiver, 2008). The relative contribution to the dose from GCR when traveling outside the Earth's magnetosphere, e.g. on Moon or Mars missions, is even greater. The solar wind, the energetic SPE and the cosmic ray intensity varies during the course of the approximately eleven year solar cycle. At times of high solar activity, solar wind and SPE present the most dangerous radiation environment whereas the cosmic ray intensity is at a minimum. Due to the GCR, crew members on space missions are exposed to an enhanced level of radiation, e.g. in deep space the dose-rate is about 1 mSv/day at solar maximum, which can increase up to lethal dose-rates of a hundred times higher than from

* Corresponding author. Address: University of Zürich, Vetsuisse Faculty, 8063 Zürich, Switzerland. Tel.: +41 44 4661369.
E-mail address: uschneider@vetclinics.uzh.ch (U. Schneider).

the GCR during energetic and transient SPE ranging from less than an hour to several days. It has been estimated that a human mission to Mars may take longer than 500 days (Shiver, 2008). Without considering radiation shielding, the personnel on such a mission might be exposed to a total effective dose of more than 1 Sv (Shiver, 2008).

The dose–response relationship for radiation carcinogenesis up to 1 Gy (usually up to 2 or 4 Gy) has been quantified in several major analyses of the atomic-bomb survivors data. Recent papers have been published, for example, by Preston et al. (2003, 2004) and Walsh et al. (2004a,b). This dose range is important for radiation protection purposes where low doses are of particular interest. However, it is also important to know the shape of the dose–response curve for radiation-induced cancer for doses larger than 1 Gy because it can impact the derivation of radiation risk factors relevant for long-term space travel.

Risk estimates for radiation protection in space are, among other factors, dependent on the shape of the dose–response curve for radiation-induced cancer, the neutron RBE (relative biological effectiveness) used for analyzing the A-bomb survivor data and the dose and dose-rate effectiveness factor (DDREF) which translates the risks obtained from the A-bomb survivors at high dose-rates to low dose-rates.

It is not clear whether cancer risk as a function of dose continues to be linear or decreases at high dose due to cell killing. Walsh et al. (2004a) found that the relative cancer risks of the A-bomb survivor mortality data support more curvature in the dose–response curve when extra follow-up (1950–1997) was taken into account. There has also been a study in which the shape of the dose–response curve at the high-dose end was presented. Schneider and Walsh (2008) analyzed the A-bomb survivor incidence data (1958–1998) with respect to absolute excess risk for cancer incidence and explicitly modeled the evident bending-over of the dose–response relationship for the cancer risk above 1 Gy.

The value of the neutron RBE traditionally applied in the analyses of the A-bomb survivors data is 10. However, there are some recently reported indications of a high neutron dose contribution (Kellerer et al., 2006; Rühm and Walsh, 2007). In this study, the impact of neutron RBE on space radiation protection was analyzed by using three different values for the relative biological effectiveness of neutrons (10, 35 and 100). In addition, a dose-dependent RBE_D for neutrons determined by Sasaki et al. (2006) was used.

There is new evidence that a DDREF for solid cancer risk of two as proposed by ICRP (2007) could be too large. In a recent meta-analysis (Jacob et al., submitted for publication), 12 studies on cancer risks from low dose-rate and moderate dose (LDRMD) exposures were compared to the risks from the A-bomb survivors. Overall, the ratio of the ERR per unit dose in the LDRMD dose studies to the corresponding quantity in the atomic-bomb survivors was 1.21 (90% CI: 0.51; 1.90). Consequently no indication was

found that the excess cancer risk for low dose-rate exposures is smaller than for acute, high-dose exposures, suggesting a DDREF of one. Therefore, in the present study both a DDREF of one and two were used to estimate space radiation risk.

The work presented here, aims to clarify the impact of dose–response shape, neutron RBE and DDREF on space radiation risk. For the relevant dose range, excess relative (ERR) and absolute risks (EAR) for solid cancer and leukemia mortality were fitted to the atomic-bomb survivors data from Hiroshima and Nagasaki, although the data pertaining to doses of over 4 Gy have not usually been included in previous analyses, due to the associated large uncertainties. Since NASA specifies the permissible space exposure limit for space flight radiation exposure in terms of the risk of exposure induced cancer death (REID), which shall not exceed 3% (NASA, 2007), the obtained ERR and EAR were used to calculate REID.

2. Materials and methods

2.1. Atomic-bomb survivors data

The most recent epidemiological data, for the follow-up period from 1950 to 2000, pertaining to solid cancer and leukemia mortality with DS02 doses were analyzed here (Preston et al., 2003). These data (filename: ds02can.dat) are publicly available from the Radiation Effects Research foundation – RERF, web site: www.rerf.or.jp. The data represent 10,127 solid cancer deaths and 296 leukemia deaths, among 86,607 subjects contributing 3.18 million person-years. Organ-averaged weighted doses were adopted as the main explanatory variable in the solid cancer risk models because reference to the colon dose, as supplied with the standard dataset, is known to underestimate the average dose to all organs (Kellerer and Walsh, 2001). Computations of leukemia risks were performed with respect to the weighted bone-marrow doses. A-bomb-survivors with doses larger than 4 Gy were also included in the analysis. There are 106 survivors with doses over 4 Gy with a maximum dose of about 13 Gy. Two extra dose categories for 4–6 Gy and 6–13 Gy absorbed dose were created. The method of Pierce et al. (1990a) was applied for dose adjustments to allow for random errors in dose estimates. Both types of models, excess relative risk (ERR) and excess absolute risk models (EAR), were optimized against the epidemiological data, by the method of maximum likelihood Poisson regression, with the EPICURE-AMFIT software (Pierce et al., 1990a).

2.2. ERR and EAR risk models

The ERR and EAR models applied here were the same as those already considered and explained in detail by Preston et al. (2003, 2004). Organ-averaged weighted dose D is here the sum of the γ-ray dose and the RBE weighted neutron dose. The differences between the previous (Preston

et al., 2003) and present work are: the input data include two extra high-dose categories; organ-average weighted doses are applied instead of colon-weighted doses (for solid cancers); a range of neutron weighting factors (RBEs) are considered; and a different form of dose–response relationship, more suitable for the high-dose data, a linear-exponential model, is employed.

The excess relative and absolute risk for solid cancer mortality, respectively, is factorized into a function of dose and a modifying function that depends on the variables gender (*s*), age at exposure (*e*) and age attained (*a*). A linear model was considered for the excess risk (ER – where ER is either EAR or ERR),

$$ER_S(D, e, a, s) = \beta D \mu(e, a, s) \tag{1}$$

as well as a linear-exponential approach,

$$ER_S(D, e, a, s) = \beta D \exp(-\alpha D) \mu(e, a, s), \tag{2}$$

where β is the initial slope, the subscript *S* denotes solid cancer risk and μ is the modifying function containing the population dependent variables:

$$\mu(e, a, s) = \exp\left\{ \gamma_e(e - 41) + \gamma_a \ln\left(\frac{a}{60}\right) \right\}$$
$$\times (1 + s) \quad \text{(+for females, } - \text{ for males)} \tag{3}$$

In this form the fit parameters are gender-averaged and centered at an age at exposure (*e*) of 41 years and an attained age (*a*) of 60 years, since the average age of astronauts is 41 (Souvestre and Landrock, 2007). However, the centering is not critical to the fitting procedure and the resulting risks can be scaled to gender-specific values for any values of the two age variables.

Since for leukemia, additive risk models are preferable, exclusively EAR was fitted to a linear-quadratic law,

$$EAR_L(D, e, a, s) = (\beta D + \delta D^2) \mu(e, a, s) \tag{4}$$

and to a linear-quadratic-exponential law,

$$EAR_L(D, e, a, s) = (\beta D + \delta D^2) \exp(-\alpha D) \mu(e, a, s) \tag{5}$$

where μ is defined by Eq. (3).

2.3. REID

According to NASA (2007) the permissible space exposure limit for space flight radiation exposure shall be specified in risk of exposure induced cancer death (REID). In this report the method of Kellerer et al. (2001) was applied to obtain REID from excess relative and absolute risks:

$$REID(e) = \int_e^{100} m_E(a) \frac{S(a, D)}{S(e, D)} da \tag{6}$$

where $S(a,D)$ and $S(e,D)$ represent the survival function of the population after exposure to dose *D* and $m_E(a)$ is the excess cancer mortality due to an exposure at age *a*. The excess radiation cancer mortality can be written as:

$$m_E(a) = \frac{0.5 ERR_S(a) m(a) + 0.5 EAR_S(a)/10,000}{DDREF}$$
$$+ EAR_L(a)/10,000 \tag{7}$$

where $m(a)$ is the spontaneous cancer mortality taken from Kellerer et al. (2001) and *ERR* and *EAR* are the excess relative and additive risks taken from Eqs. (1), (2), (4) and (5) and which are evenly weighted for solid cancer mortality. For leukemia risk, a purely additive model is used (NASA, 2005).

The most uncertain quantity in the definition of *REID* by Eq. (6) is the dose-dependent survival function $S(e, D)$. Survival after a substantial radiation exposure is diminished due to radiation-induced cancer and non-cancer mortality. At doses on the order of 1 Gy this also includes acute mortality. In addition studies among the A-bomb survivors show that there is late radiation-induced non-cancer mortality, such as cardiac mortality, but it remains difficult to quantify its dose dependence. An approach used by Kellerer et al. (2001) is applied here, where a linear relationship with a slope of $NCM = 0.1/\text{Gy}$ and a threshold of 0.5 Gy is used for the excess relative non-cancer mortality. A function describing the acute radiation-induced mortality (*ARM*) was taken from a publication of Anno et al. (2003):

$$ARM(D) = \frac{1}{2} erf\left(\frac{k + 7.133 \log(D)}{\sqrt{2}} + 1\right) \tag{8}$$

where $k = -5.6571$ if medical care is applied and $k = -4.4011$ if no medical care is applied. The dose-dependent survival function is then:

$$\frac{S(a, D)}{S(e, D)} = \frac{S(a)}{S(e)}(1 - NCM(D))(1 - ARM(D)), \tag{9}$$

where $S(a)$ is the survival function for the general population, i.e. the probability at birth to reach at least age *a*. The ratio $S(a)/S(e)$ is the conditional probability of a person alive at age *e* to reach at least age *a*. The survival function of an unexposed standard population was taken from Kellerer et al. (2001).

3. Results

Fitting the ERR and EAR models Eqs. (1)–(5) to the atomic survivor data, including the high-dose categories,

Table 1
Results of fitting a *linear* model to *solid cancer* excess *relative* mortality to the atomic-bomb at attained age 60 after exposure at age 41 applying the EPICURE-AMFIT code to the atomic survivor data.

RBE	γ_e	γ_a	β^*	*s*
10	−0.03542	−0.8655	0.2543	0.3171
35	−0.03499	−0.8356	0.2032	0.3256
100	−0.03454	−0.8016	0.1306	0.3333
Sasaki	−0.03466	−0.8514	0.2242	0.3153

* In Gy^{-1}.

Table 2

Results of fitting a *linear-exponential* model to *solid cancer* excess *relative* mortality to the atomic-bomb data at attained age 60 after exposure at age 41 applying the EPICURE-AMFIT code to the atomic survivor data.

RBE	γ_e	γ_a	β^*	α^*	s
10	−0.03542	−0.8655	0.2950	0.05920	0.3171
35	−0.03499	−0.8356	0.2466	0.05148	0.3256
100	−0.03454	−0.8016	0.1774	0.04501	0.3333
Sasaki	−0.03466	−0.8514	0.2489	0.04093	0.3153

* In Gy^{-1}.

Table 3

Results of fitting a *linear* model to *solid* cancer excess *absolute* mortality to the atomic-bomb data at attained age 60 after exposure at age 41 applying the EPICURE-AMFIT code to the atomic survivor data.

RBE	γ_e	γ_a	β^*	s
10	−0.02380	3.476	9.441	0.06163
35	−0.02336	3.494	7.522	0.07112
100	−0.02277	3.513	4.831	0.08263
Sasaki	−0.02317	3.486	8.271	0.06167

* In (10,000 PY Gy)$^{-1}$.

for the different neutron RBE values, yields the model fit parameters listed in Tables 1–6.

In Fig. 1 REID is plotted as a function of dose for the different dose–response and RBE models for a DDREF = 1. For low doses, the linear-exponential model yields a higher risk, on the contrary at higher doses (>2 Gy) the linear model shows a larger risk. However, model dependent risk differences are small. The impact of RBE is more intense, roughly doubling risk when using a RBE = 10 instead of 100. The application of a dose varying RBE leads to 15% lower risk when compared to the standard RBE of 10. This difference is nearly independent of dose.

Fig. 2 shows REID as a function of dose using the two different DDREF values, solid lines indicate a value of one, dotted lines a value of 2, respectively. REID is around 80% larger at low doses when using a DDREF of one when compared to a DREF of 2. This difference decreases with increasing dose to approximately 40%.

The dependence of REID on RBE is shown in Fig. 3 for 1 Gy dose and for maximum REID. Apparently REID decreases with increasing neutron RBE. A dose variable

Table 4

Results of fitting a *linear-exponential* model to *solid* cancer excess *absolute* mortality to the atomic-bomb data at attained age 60 after exposure at age 41 applying the EPICURE-AMFIT code to the atomic survivor data.

RBE	γ_e	γ_a	β^*	$\alpha^{\#}$	s
10	−0.02380	3.476	10.70	0.04964	0.06163
35	−0.02336	3.494	8.895	0.04396	0.07112
100	−0.02277	3.513	6.310	0.03825	0.08263
Sasaki	−0.02317	3.486	8.977	0.03197	0.06167

* In (10,000 PY Gy)$^{-1}$.
$^{\#}$ In Gy^{-1}.

Table 5

Results of fitting a *linear-quadratic* model to *leukemia* excess *absolute* mortality to the atomic-bomb data at attained age 60 after exposure at age 41 applying the EPICURE-AMFIT code to the atomic survivor data.

RBE	γ_e	γ_a	β^*	$\delta^{\#}$	s
10	0.03815	−1.395	1.288	1.203	−0.2348
35	0.03741	−1.346	1.573	0.4516	−0.2411
100	0.03663	−1.311	1.530	0.03386	−0.2499
Sasaki	0.03808	−1.393	0.8441	1.040	−0.2369

* In (10,000 PY Gy)$^{-1}$.
$^{\#}$ In 10,000 PY^{-1} Gy^{-2}.

Table 6

Results of fitting a *linear-quadratic-exponential* model to *leukemia* excess *absolute* mortality to the atomic-bomb data at attained age 60 after exposure at age 41 applying the EPICURE-AMFIT code to the atomic survivor data.

RBE	γ_e	γ_a	β^*	$\delta^{\#}$	α^+	s
10	0.03840	−1.442	0.05162	4.187	0.3784	−0.2452
35	0.03784	−1.413	0.1671	2.862	0.3315	−0.2470
100	0.03654	−1.312	1.528	−0.04470	−0.05343	−0.2499
Sasaki	0.03807	−1.421	−0.06387	2.932	0.2947	−0.2484

* In (10,000 PY Gy)$^{-1}$.
$^{\#}$ In 10,000 PY^{-1} Gy^{-2}.
$^+$ In Gy^{-1}.

RBE would reduce risk compared to the standard RBE of 10 by around 15–20%, dependent on age of exposure.

NASA specifies the permissible space exposure limit for space flight radiation exposure in risk of exposure induced cancer death (REID), which shall not exceed 3% (NASA, 2005, 2007). Hence, in Tables 7 and 8 the doses in cSv which correspond to a 3% REID are listed for different ages at exposure, all RBE regimes considered and for both dose–response models. In Table 7 the dose was calculated
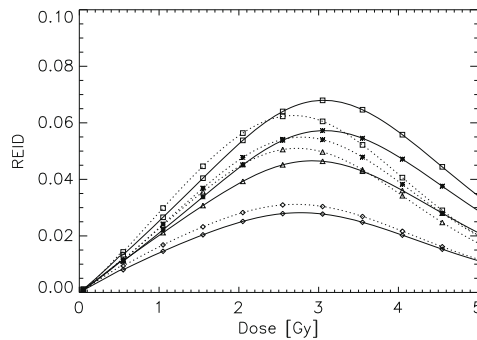
Fig. 1. REID plotted as a function of dose for a DDREF = 2. Acute radiation-induced mortality was considered without medical care. The solid curves show the results of the linear model, the dotted curves the linear-exponential model. Squares, triangles, diamonds and stars indicate RBE = 10, 35, 100 and a dose varying RBE, respectively. Data are plotted for an age at exposure $e = 41$.
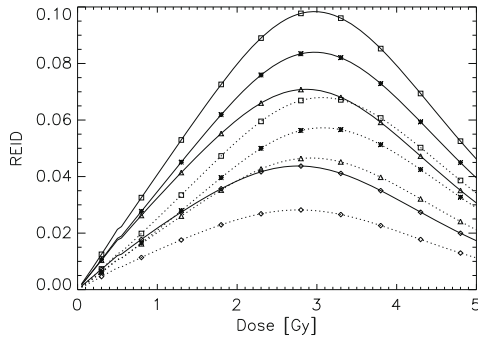
Fig. 2. REID plotted as a function of dose for the linear dose–response model. Acute radiation-induced mortality was considered without medical care. The dotted curves show the results using a DDREF = 1, the dotted curves DDREF = 2. Squares, triangles, diamonds and stars indicate RBE = 10, 35, 100 and a dose varying RBE, respectively. Data are plotted for an age at exposure $e = 41$.
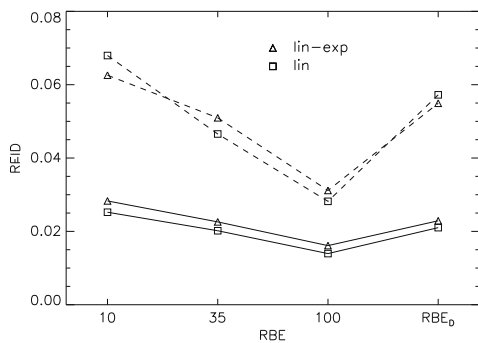
Fig. 3. REID plotted as a function of RBE for a DDREF = 2. Acute radiation-induced mortality was considered without medical care. Squares show the results of the linear model, triangles of the linear-exponential model. The solid lines represent REID at 1 Gy and the dashed lines maximum REID.

Table 7
Equivalent dose in cSv which corresponds to 3% REID calculated with a DDREF = 1 and acute radiation-induced mortality considered without medical care. Data are presented for males, the linear and linear-exponential model and for various RBEs.

Age	Males							
	Linear model				Linear-exponential			
	10	35	100	RBE$_D$	10	35	100	RBE$_D$
30	57	71	111	67	50	64	89	63
35	65	81	126	76	59	73	102	72
40	74	92	145	87	67	82	118	81
45	84	105	167	98	76	93	137	91
50	95	120	197	112	86	106	161	103
55	109	138	252	127	98	121	194	118

et al. (1996) for leukemia. Lower values are found in this work. It is interesting to note that the results of this work using a DDREF of one are only slightly larger than the NASA predictions with a DDREF = 2. This difference disappears completely when larger neutron RBEs are assumed. For a dose varying RBE for example, REID is 0.29, 3.8 and 4.0 for 0.084, 1.03 and 1.07 Sv, respectively (for males and a linear model).

The risk difference with respect to sex and DDREF is shown in Fig. 4 as a function of age at exposure. Females are at higher risk of about 30% at young ages (30 years), however this risk difference approaches zero when the exposure occurs at large ages.

Finally Fig. 5 shows the impact of medical care for acute radiation-induced mortality on REID. For doses up to around 2 Gy there is no difference between astronauts who receive medical care in case of acute exposure when compared to no medical care.

4. Discussion

The epidemiological data from the atomic-bomb survivors including the high-dose categories are associated with large errors. Nevertheless some basic conclusion can be tentatively drawn from the analysis presented here.

with a DDREF of one and Table 8 reproduces the same tabular form but for a DDREF of two.

NASA is considering various lunar and Mars missions as part of its exploration vision. An exploration concept is planned with missions to the Moon and Mars swingby and surface missions. Approximate characteristic doses for such missions used in the calculations are taken from NASA (2005) and NRC (2008) which were estimated at solar minimum and with a 5 g cm^{-2} aluminum shielding of the space craft. In Table 9 the risks for the different missions are listed with the corresponding effective doses. Values are compared with the estimates of NASA and NRC (NASA, 2005; NRC, 2008) which are based on the risk estimates of Preston et al. (2003) for solid cancers and Pierce

Table 8
Equivalent dose in cSv which corresponds to 3% REID calculated with a DDREF = 2 and acute radiation-induced mortality considered without medical care. Data are presented for males, the linear and linear-exponential model and for various RBEs.

Age	Males							
	Linear model				Linear-exponential			
	10	35	100	RBE$_D$	10	35	100	RBE$_D$
30	96	122	200	114	87	107	165	105
35	107	136	238	126	96	118	192	116
40	117	151	*	139	105	131	230	127
45	129	168	*	153	116	144	*	140
50	142	189	*	168	128	160	*	154
55	157	215	*	185	142	179	*	171

* = REID always smaller than 3%.

Table 9
REID in % for different mission types and doses. All data are for age at exposure 40 and RBE = 10.

Mission	E/Sv	REID-NASA	REID-linear	REID-lin-exp	REID-linear	REID-lin-exp
		DDREF = 2			DDREF = 1	
Males						
Lunar, long	0.084	0.34	0.20	0.18	0.34	0.35
Mars, swing	1.03	4.0	2.6	2.9	4.2	4.6
Mars, surface	1.07	4.2	2.7	3.0	4.4	4.8
Females						
Lunar, long	0.084	0.41	0.25	0.25	0.46	0.49
Mars, swing	1.03	4.9	3.0	3.3	5.3	5.8
Mars surface	1.07	5.1	3.1	3.4	5.5	6.1

4.1. Impact of using an organ-averaged dose analysis

The gender-averaged excess absolute and excess relative risk for all solid cancers determined in this work using a linear analysis and a RBE of 10 for a males at an age of exposure of 30 years and an attained age of 70 years is 20 per 10,000PY per Gy and 0.22 per Gy, respectively. This can be compared to the EAR and ERR obtained by Preston et al. (2003 listed in Table 6) who found 29 per 10,000PY per Gy and 0.35 per Gy. The analysis presented here results in an approximately 30% lower risk, although exactly the same modeling techniques were used. As already pointed out by Kellerer and Walsh (2001) part of the reason for this behaviour is the use of organ-averaged dose instead of the colon-weighted dose, which is known to underestimate the average dose to all organs.

4.2. Use of different neutron RBE models

The first question which arises when using large neutron RBE values is the feasibility of such an analysis. For an RBE of 10, the average doses in the two highest-weighted dose categories are 5.4 and 8.9 Sv and are increased for a RBE of 100 up to 12.7 and 22.1 Sv, respectively. Since

the data in these high-dose categories are subject to very large errors (standard deviation 0.8 Sv and 2.3 Sv for RBE = 10, and 6.1 Sv and 12.3 Sv for RBE = 100), it is not possible to assess the degree of dependability of the assumption of large neutron RBE values such as 100, if the mean doses in these dose categories are compared with the lethal doses for humans (LD50). Additionally, it is worth noting that the last dose category employed here has been omitted in all previous analyses of these data, since the small chance of survival suggests that estimates of doses in this upper group could possibly be too large (Pierce et al., 1990b). Using Sasaki's formulation of a neutron RBE, which is variable with dose, results in a moderate increase of 5.7 and 9.0 Sv in the two highest dose categories. This could be an additional indication for a dose-dependent neutron RBE. A dose-dependent RBE for neutrons, however, would have an impact on risk estimates for space flights, since above 1 Gy it would predict risks which are around 15–20% lower than compared to the traditional use of an RBE of 10 (Fig. 3).

4.3. Curvature in the dose–response curve

Surprisingly the shape of the dose–response does not have a large impact on the mortality risk estimates up to
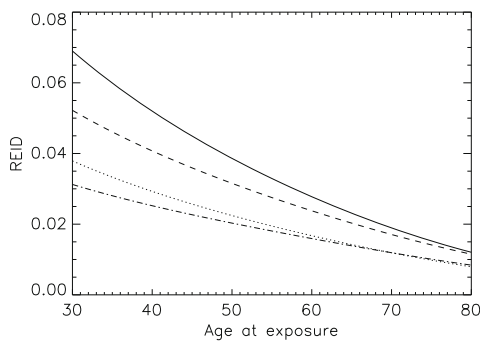
Fig. 4. REID at 1 Gy plotted as a function of age at exposure for a RBE = 10 and a linear model. Solid and dashed lines indicate a DDREF = 1 and dotted and dashed-dotted lines a DDREF = 2. Acute radiation-induced mortality was considered without medical care. Solid and dotted curves indicate data for females, dashed and dashed-dotted for males.
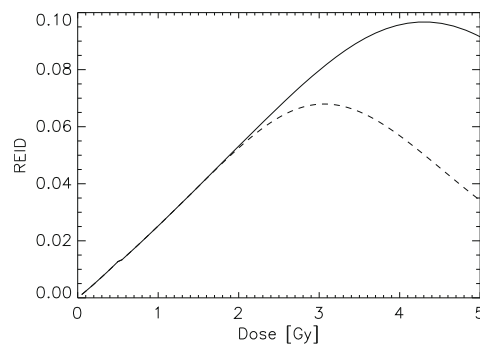
Fig. 5. REID as a function of dose for a linear model, a DDREF = 2, age at exposure 40, RBE = 10 and males. Acute radiation-induced mortality was considered without medical care represented by the dashed and with medical care by the solid line.

a dose of around 2 Gy. In Fig. 1 the linear and linear-exponential models are plotted as a function of dose and a strong dose dependence can be observed. At 1 and 2 Gy the risk differences between the models are around 10% and 5%, respectively.

It should be noted here, however, that the analysis of cancer incidence data (as opposed to mortality) shows a larger difference between the models used (Schneider and Walsh, 2008).

4.4. DDREF

The variation of a DDREF between one and two for solid cancer risk has a strong impact on the risk estimates. However, risk variation with DDREF is strongly dose dependent. While at low doses the difference can be as large as 80%, for the dose range which is of interest for long-term space missions, it is around 40%.

The present study implies that the use of organ-averaged dose, a dose-dependent neutron RBE and models which describe the bending-over of the dose–response relationship, fit the A-bomb survivor data well. As a consequence cancer risks above 1 Gy might be around 50% smaller than estimated with traditional radiation protection models. This could have an impact for radiation risk estimates for long-term mission space crews who might be exposed to doses above 1 Gy. However in a recent review on cancer risk from low dose-rate and moderate dose exposures, no indication was found that the excess cancer risk for low dose-rate exposures is smaller than for acute, high-dose exposures, suggesting a DDREF of one. A DDREF of one on the other hand would increase risk for the dose range relevant for space travel by about the same amount (40%) that it was reduced by the factors discussed above.

It must be noted here that the galactic cosmic radiation consists mainly of protons and heavy ions. In addition the dose-rate of the galactic cosmic radiation differs significantly from that of the A-bomb survivors. The data for carcinoma induction due to heavy ions are scarce and the estimation of risk factors for heavy particles is related to large uncertainties since the relative biological effectiveness of this kind of radiation is not well known. Such uncertainties may be larger than the uncertainties related to characteristics which were discussed in this report.

5. Conclusions

The results of this study imply that the use of organ-averaged dose, a dose-dependent neutron RBE and the bending-over of the dose–response relationship for radiation-induced cancer could impact radiation risk estimates for space crews on long-term mission above 500 days who might be exposed to doses above 1 Gy. The radiation risks estimated for this dose range could be 50% lower than obtained when applying traditional radiation protection models.

The above estimates were obtained applying a DDREF of two as recommended by ICRP. However, in recent publications a DDREF of one is suggested, which would increase cancer risk in the dose range of interest by about 40% and would therefore balance the risk decrease described above.

Acknowledgements

References

Anno, G.H., Young, R.W., Bloom, R.M., Mercier, J.R. Dose response relationships for acute ionizing-radiation lethality. Health Phys. 84, 565–574, 2003.

ICRP Recommendations of the International Commission on Radiological Protection. ICRP Publication 103. Ann ICRP 37, 2007.

Jacob, P., Rühm, W., Walsh, L., Blettner, M., Hammer, G., Zeeb, H., Cancer risk of radiation workers larger than expected?, submitted for publication.

Kellerer, A.M., Walsh, L. Risk estimation for fast neutrons with regard to solid cancer. Radiat. Res. 156, 708–717, 2001.

Kellerer, A.M., Nekolla, E.A., Walsh, L. On the conversion of solid cancer excess relative risk into lifetime attributable risk. Radiat. Environ. Biophys. 40 (4), 249–257, 2001.

Kellerer, A.M., Rühm, W., Walsh, L. Indications of the neutron effect contribution in the solid cancer data of the A-bomb survivors. Health Phys. 90 (6), 554–564, 2006.

NASA (National Aeronautics and Space Administration). Managing Lunar and Mars Mission Radiation Risks, Part I: Cancer Risks, Uncertainties, and Shielding Effectiveness. NASA/TP-2005-213164. NASA, Washington, DC, 2005.

NASA (National Aeronautics and Space Administration). NASA Space Flight Human Standard, vol. 1: Crew Health. NASA-STD-3001. NASA, Washington, DC, 2007.

NRC (National Research Council). Managing Space Radiation Risks in the New Era of Space Exploration. National Academy Press, Washington, DC, 2008.

Pierce, D.A., Shimizu, Y., Preston, D.L., Vaeth, M., Mabuchi, K. Studies of the mortality of atomic bomb survivors. Report 12, Part I: Cancer: 1950–1990. Radiat. Res. 146 (1), 1–27, 1996.

Pierce, D.A., Stram, D.O., Vaeth, M. Allowing for random errors in radiation dose estimates for the atomic bomb survivor data. Radiat. Res. 123, 275–284, 1990a.

Pierce, D.A., Stram, D.O., Vaeth, M. Allowing for random errors in radiation dose estimates for the atomic bomb survivor data. Radiat. Res. 123, 275–284, 1990b.

Preston, D.L., Shimizu, Y., Pierce, D.A., Suyama, A., Mabuchi, K. Studies of mortality of atomic bomb survivors. Report 13: Solid cancer and noncancer disease mortality: 1950–1997. Radiat Res 160 (4), 381–407, 2003.

Preston, D.L., Pierce, D.A., Shimizu, Y., Cullings, H.M., Fujita, S., Funamoto, S., Kodama, K. Effects of recent changes in atomic bomb survivor dosimetry on cancer mortality risk estimated. Radiat. Res. 162, 377–389, 2004.

Reitz, G. Characteristic of the radiation field in low earth orbit and in deep space. Z. Med. Phys. 18 (4), 234–243, 2008.

Rühm, W., Walsh, L. Current risk estimates based on the A-bomb survivors data – a discussion in terms of the ICRP recommendations on the neutron weighting factor. Radiat. Prot. Dosim. 126 (1–4), 423–431, 2007.

Sasaki, M.S., Endo, S., Ejima, Y., Saito, I., Okamura, K., Oka, Y., Hoshi, M. Effective dose of A-bomb radiation in Hiroshima and Nagasaki as assessed by chromosomal effectiveness of spectrum energy photons and neutrons. Radiat. Environ. Biophys. 45, 79–91, 2006.

Schneider, U., Walsh, L. Cancer risk estimates from the combined Japanese A-bomb and Hodgkin cohorts for doses relevant to radiotherapy. Radiat. Environ. Biophys. 47 (2), 253–263, 2008.

Shiver, L. Transport calculations and accelerator experiments needed for radiation risk assessment in space. Z. Med. Phys. 18 (4), 253–264, 2008.

Souvestre, P.A., Landrock, C. Biomedical performance monitoring and assessment of astronauts by means of an ocular–vestibular monitoring system. Acta Aeronaut. 60, 313–321, 2007.

Walsh, L., Rühm, W., Kellerer, A.M. Cancer risk estimates for X-rays with regard to organ specific doses, Part I: All solid cancers combined. Radiat. Environ. Biophys. 43, 145–151, 2004a.

Walsh, L., Rühm, W., Kellerer, A.M. Cancer risk estimates for γ-rays with regard to organ specific doses, Part II: Site specific solid cancers. Radiat. Environ. Biophys. 43, 225–231, 2004b.

31. Schmid E, Wagner FM, Romm H, Walsh L & Roos R. Dose-response relationship of dicentric chromosomes in human lymphocytes obtained for the fission neutron therapy facility MEDAPP at the research reactor FRM II. Radiat. Environ. Biophys. 48(1), 67-75, 2009

ORIGINAL PAPER

Dose–response relationship of dicentric chromosomes in human lymphocytes obtained for the fission neutron therapy facility MEDAPP at the research reactor FRM II

E. Schmid · F. M. Wagner · H. Romm ·
L. Walsh · H. Roos

Abstract The biological effectiveness of neutrons from the neutron therapy facility MEDAPP (mean neutron energy 1.9 MeV) at the new research reactor FRM II at Garching, Germany, has been analyzed, at different depths in a polyethylene phantom. Whole blood samples were exposed to the MEDAPP beam in special irradiation chambers to total doses of 0.14–3.52 Gy at 2-cm depth, and 0.18–3.04 Gy at 6-cm depth of the phantom. The neutron and γ-ray absorbed dose rates were measured to be 0.55 Gy min^{-1} and 0.27 Gy min^{-1} at 2-cm depth, while they were 0.28 and 0.25 Gy min^{-1} at 6-cm depth. Although the irradiation conditions at the MEDAPP beam and the RENT beam of the former FRM I research reactor were not identical, neutrons from both facilities gave a similar linear-quadratic dose–response relationship for dicentric chromosomes at a depth of 2 cm. Different dose–response curves for dicentrics were obtained for the MEDAPP beam at 2 and 6 cm depth, suggesting a significantly lower biological effectiveness of the radiation with increasing depth. No obvious differences in the dose–response curves for dicentric chromosomes estimated under interactive or additive prediction between neutrons or γ-rays and the experimentally obtained dose–response curves could be determined. Relative to ^{60}Co γ-rays, the values for the relative biological effectiveness at the MEDAPP beam decrease from 5.9 at 0.14 Gy to 1.6 at 3.52 Gy at 2-cm depth, and from 4.1 at 0.18 Gy to 1.5 at 3.04 Gy at 6-cm depth. Using the best possible conditions of consistency, i.e., using blood samples from the same donor and the same measurement techniques for about two decades, avoiding the inter-individual variations in sensitivity or the differences in methodology usually associated with inter-laboratory comparisons, a linear-quadratic dose–response relationship for the mixed neutron and γ-ray MEDAPP field as well as for its fission neutron part was obtained. Therefore, the debate on whether the fission-neutron induced yield of dicentric chromosomes increases linearly with dose remains open.

E. Schmid (✉) · H. Roos
Radiobiological Institute, University of Munich,
Schillerstraße 42, 80336 Munich, Germany
e-mail: Ernst.Schmid@lrz.uni-muenchen.de

F. M. Wagner
Forschungsneutronenquelle, Heinz-Maier-Leibnitz (FRM II)
Technische Universität München, 85747 Garching, Germany

H. Romm · L. Walsh
Federal Office for Radiation Protection,
85764 Oberschleißheim, Germany

Introduction

A considerable contribution to current knowledge on the relative biological effectiveness (RBE) of neutrons has been made by experimental studies on the induction of dicentric chromosomes (dicentrics) in human lymphocytes. From data on dicentrics compiled by the International Commission on Radiological Protection (ICRP) [1, 2], it is apparent that the RBE of neutrons increases with decreasing dose up to a constant value, denoted as maximum RBE (RBE$_M$), at doses where both the reference (X-rays or γ-rays) and the neutron dose–response curves are linear. Since two decades, our data on dicentrics induced by neutrons and photons of different energies have been obtained by using blood samples from the same donor. Thus, any inter-individual variations in sensitivity and differences in methodology usually associated with

inter-laboratory comparisons were avoided. Therefore, results of these systematic investigations are compiled in part by the ICRP [2] and the BEIR VII Report [3].

In earlier studies, the RBE of the mixed fission-neutron and γ-ray beam of the RENT neutron therapy facility at the former FRM I research reactor, to induce dicentrics in human lymphocytes was determined at different irradiation conditions, either free-in-air [4] or in a polymethylmeth-acrylate (PMMA) phantom [5]. From the analysis of metaphases of the first cell division after irradiation, linear-quadratic dose–response curves were obtained for both experiments, which did not differ significantly. The FRM I was shut down in 2000. The new FRM II research reactor started operation in March 2004. Since the beam characteristics of the new MEDAPP therapy facility at FRM II are similar to those of the former RENT facility [6], only limited efforts have been made so far to investigate the biological effectiveness of the new fission neutron beam. First, results on preclinical screening of the RBE have shown that the MEDAPP beam is subject to marked changes in biological effectiveness over defined depths of a polyethylene (PE) phantom that are relevant for the envisaged clinical target volumes [7]. The present experiments were designed to determine the RBE of the MEDAPP beam with respect to ^{60}Co γ-rays, for the induction of dicentrics in human lymphocytes from the same healthy donor who was also involved in the earlier experiments at the RENT beam [4, 5]. In the present study, the findings which have been obtained at different depths of a PE phantom are reported.

Materials and methods

Fresh peripheral blood samples were taken from the same healthy male donor whose blood was also used in the earlier experiments at the former RENT facility [4, 5], as well as in experiments investigating the reference radiation of ^{60}Co γ-rays [8, 9]. Whole blood samples were exposed to the mixed fission-neutron and γ-ray beam of the ME-DAPP beam in special irradiation chambers, which had also been used in the former RENT experiments. The chambers consisted of flat plastic (polyvinyl carbazol) rings (24 mm in diameter, 2.2 mm thick), which are closed by a 20-μm stretched Mylar foil (polyethylene terephthal-ate, PET) at top and bottom. Thus, the irradiation chambers contained 1 ml whole blood (thickness 2 mm).

Irradiation conditions

The technical features of the new MEDAPP therapy facility as well as the spectral and dosimetric data have already been described elsewhere [6, 10–12]. Briefly, the

irradiations were carried out at depths of 2 and 6 cm in a PE phantom (width 398 mm, height 335 mm and depth 200 mm), where the blood chambers were inserted into densely matching cavities. A large beam section of 230 mm × 230 mm was chosen, to guarantee a homogeneous dose distribution and a simultaneous irradiation of two blood chambers which were put in staggered at the different depths.

To measure the radiation dose in a mixed field, two ionization chambers with different sensitivities to the neutron and γ components of the radiation field are necessary. One chamber consists of the electrically conducting material A 150 (the so-called Shonka-plastic), which is tissue equivalent (TE), i.e., it radiologically approximates the properties of human muscle tissue. Whereas this chamber volume (1 cm^3) is flooded with TE gas on a methane basis, the second chamber is made of magnesium and flooded with argon gas. For both chambers, the Bragg–Gray condition for the determination of the energy dose is fulfilled. Due to the hydrogen in its structure material, the TE chamber is sensitive to neutrons; for a fission spectrum, the ratio of the sensitivities to the neutron- and the γ-component is 49:51. Hence, the TE-chamber current is essentially proportional to the total dose rate present. In contrast, the magnesium–argon chamber shows only little neutron sensitivity (2%). Thus, the doses from the neutron and γ components can be determined separately. With the standard filters (1 cm B$_4$C-epoxy and 3.5 cm Pb) used for the medical applications at the beam, the ratio of the neutron-to-photon doses decreases from 3.6 near to the surface of the phantom to unity at about 10 cm depth. For the present experiments, irradiation was carried out at depths of 2 and 6 cm in the PE phantom. The neutron and γ-ray absorbed dose rates of the MEDAPP beam were measured in the PE phantom to be 0.55 and 0.27 Gy min^{-1} at 2-cm depth, and 0.28 and 0.25 Gy min^{-1} at 6-cm depth [12]. Hence, the fast neutrons contributed 67% to the total dose rate at 2 cm, but only 52% at 6 cm.

Culture conditions and chromosome analysis

Immediately following irradiation of a blood sample with a particular dose (total doses of 0.14–3.52 Gy at 2-cm depth, and 0.18–3.04 Gy at 6-cm depth), two lymphocyte cultures containing 0.5 ml whole blood, 4.5 ml RPMI 1640 medium supplemented with 15% fetal calf serum, 2.5% phytohemagglutinin (PHA) and antibiotics (penicillin/streptomycin) were established. Colcemid (0.03 μg/ml) was present during the entire incubation period of 48 h. Chromosome preparation and Giemsa staining were performed according to standard procedures, and all slides were coded. These culture conditions ensured that the chromosome analysis could be performed exclusively in

metaphases of the first cell cycle in vitro. In the present study, only the data for dicentrics were used in the quantitative analysis, although the frequencies of centric rings and supernumerary acentric fragments were also determined. The background frequency of 1 dicentric in 3,000 cells obtained in the present experiment is not significantly different to that of 4 dicentrics in 12,000 cells obtained from the same donor for earlier studies with monoenergetic neutrons [13].

Results

The results of the analysis of dicentrics determined at the phantom depth of 2 cm are presented in Table 1. At the low dose levels of 0.14 and 0.27 Gy, the intercellular distribution of the dicentrics is significantly (at the 5% level) overdispersed when compared to a Poisson distribution. This can be deduced from the ratio of variance and mean (σ^2/y) and from the test quantity u [14]. Values of u greater than 1.96 indicate an overdispersion at the 5% level of significance. At the five higher dose levels, the intercellular distribution of the dicentrics shows no significant deviation

from a Poisson distribution. Accordingly, the dicentric data determined at a phantom depth of 6 cm are presented in Table 2. For two of seven doses, the intercellular distribution is significantly overdispersed when compared to a Poisson distribution.

As in our earlier studies with the mixed neutron and γ-ray RENT beam [4, 5], a weighted least-squares method was applied to fit the dicentric data to the linear-quadratic function given in Eq. 1.

$$y = c + \alpha D + \beta D^2, \tag{1}$$

where $c = 0.0003 \pm 0.0002$ represents the control value of the blood donor [13].

Reciprocals of the estimated variances were used as weights. Since the stated uncertainties of the doses were less than 5% and by far lower than the uncertainties of the dicentric data, only the standard deviation of the mean dicentric yields was taken into account in the fit and the RBE calculations. As a result, the coefficients ($\pm$SE) are $\alpha = 0.332 \pm 0.020$ Gy^{-1} and $\beta = 0.045 \pm 0.009$ Gy^{-2} at a depth of 2 cm, and $\alpha = 0.201 \pm 0.021$ Gy^{-1} and $\beta = 0.058 \pm 0.012$ Gy^{-2} at a depth of 6 cm (Table 3). The corresponding weighted least-squares regression curve

Table 1 Intercellular distribution of dicentrics (Dic) in human lymphocytes induced by the MEDAPP beam at a depth of 2 cm in the PE phantom

Dose (Gy)	Analyzed cells	Dic per cell	Intercellular distribution of dicentrics								σ^2/y	u-value
			0	1	2	3	4	5	6	7		
0	3,000	0.00033	2,999	1							1.0	0
0.14	1,500	0.0527	1,429	63	8						1.15	4.13
0.27	1,000	0.078	932	58	10						1.18	4.05
0.63	500	0.238	400	82	17	1					1.10	1.59
1.60	500	0.676	262	161	60	12	4	1			1.09	1.42
2.57	300	1.160	82	132	56	20	7	2	1		0.95	−0.59
2.96	200	1.405	37	73	52	29	3	1			1.11	1.06
3.52	200	1.685	39	58	56	30	12	2	2	1	1.04	0.35

Table 2 Intercellular distribution of dicentrics (Dic) in human lymphocytes induced by the MEDAPP beam at a depth of 6 cm in the PE phantom

Dose (Gy)	Analyzed cells	Dic per cell	Intercellular distribution of dicentrics							σ^2/y	u-value
			0	1	2	3	4	5	6		
0	3,000	0.00033	2,999	1						1.0	0
0.18	1,500	0.0373	1,448	48	4					1.11	2.96
0.40	1,000	0.101	906	89	6					1.02	0.42
1.03	500	0.250	393	90	16	1				1.06	0.89
1.63	400	0.420	269	103	20	7	1			1.14	2.01
1.91	300	0.617	164	95	34	6	1			1.01	0.17
2.28	300	0.830	142	90	49	17	1	0	1	1.15	1.79
3.04	200	1.130	71	63	45	14	4	3		1.12	1.23

Table 3 Dose–yield coefficients α and β for dicentrics in human lymphocytes induced by the MEDAPP beam or its fission neutron and γ-ray components at different depths in the PE phantom, and level of significance (P value) for coefficient β (d$f = 6$; $P = 0.05$; critical t value = 2.45; SE standard error)

Radiation quality	Phantom depth (cm)	Coefficient α	Coefficient β		
		$(\alpha \pm SE)$ Gy^{-1}	$(\beta \pm SE)$ Gy^{-2}	Calculated t value	P value
MEDAPP beam	2	0.332 ± 0.020	0.045 ± 0.009	5.24	<0.001
Neutron component	2	0.493 ± 0.029	0.087 ± 0.018	4.78	<0.002
γ-ray component	2	0.011 ± 0.001	0.056 ± 0.003	19.82	<0.001
MEDAPP beam	6	0.201 ± 0.021	0.058 ± 0.012	4.77	<0.002
Neutron component	6	0.371 ± 0.039	0.165 ± 0.043	3.84	<0.005
γ-ray component	6	0.014 ± 0.001	0.056 ± 0.003	19.82	<0.001
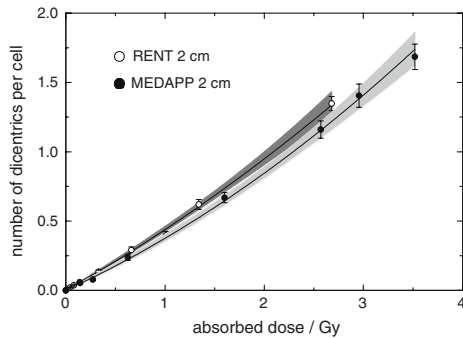
Fig. 1 Yield of dicentrics in human lymphocytes as a function of dose obtained for the RENT beam and the MEDAPP beam at a phantom depth of 2 cm, in a PMMA and a PE phantom, respectively. *Solid lines* show the weighted least-squares fit to the data with the *shadowed areas* representing the standard error bands. Standard errors of the mean are indicated by *vertical bars*

for a depth of 2 cm is shown in Fig. 1 as a solid line, together with the corresponding curve determined earlier at the same phantom depth for the RENT beam [5]. It must be noted that the irradiation conditions during the two experiments at FRM I and at FRM II were not identical. Apart from the fact that the dose rate at MEDAPP is approximately fourfold, the beam section at MEDAPP was about three times bigger, and a larger phantom (width 398 mm, height 335 mm and depth 200 mm) consisting of PE was used instead of the PMMA phantom of 160-mm side length at RENT. The difference between the two curves shown in Fig. 1 may result from the increased generation of secondary 2.2 MeV photons from the absorption of thermal neutrons by hydrogen in the MEDAPP phantom, and hence, in a slightly different neutron-to-γ-ray ratio when compared to that in the RENT experiment. Note that the photon contribution to the total absorbed dose was 25% for the RENT beam at a depth of 2 cm in the PMMA phantom [5], while it is measured to be

33 and 48% for the MEDAPP beam at a depth of 2 and 6 cm in the PE phantom.

As already stated in an earlier report on the RBE of mammography X-rays relative to conventional X-rays [15], the standard error bands of linear-quadratic dose–response curves should not be derived from the standard errors of the coefficients. Since the linear and the quadratic term of the dose–response are negatively correlated, their standard errors are not independent and cannot, therefore, be combined in the usual way, i.e., by summing the error squares, to quantify the uncertainty of the dicentric yields. Error bands for the dose–response relations must, therefore, be obtained by specific methods, e.g., in terms of orthogonal parameters which are suitably transformed to become uncorrelated. Since a recently described method simplifies the use of orthogonal parameters considerably [16], this method was applied here to derive the standard error bands of the dose–response curves obtained for the RENT and MEDAPP therapy facilities at a phantom depth of 2 cm. Figure 1 demonstrates that, although the mean dicentric yields at comparable dose levels of the MEDAPP beam are lower than those of the former RENT beam, the standard error bands (shadowed areas) of the derived dose–response curves overlap slightly, at low and high doses. Therefore, it can be assumed—with some restrictions—that both therapy facilities may induce comparable biological effects. As shown in Fig. 2, different dose–response curves for dicentrics were obtained for exposure of blood samples to the MEDAPP beam at phantom depths of 2 and 6 cm. This result is predominantly on the basis of the coefficient α, which is reduced by a factor of 40% at a depth of 6 cm when compared to that at a depth of 2 cm (Table 3).

A simultaneously performed experiment for the reference radiation, as usually required for estimating the RBE of any beam, was not performed in the present experiment. However, a standard reference dose–response curve [8] for ^{60}Co γ-rays, with the coefficients $\alpha = 0.011 \pm 0.004$ Gy^{-1} and $\beta = 0.056 \pm 0.003$ Gy^{-2}, established at a PMMA phantom depth of 1 cm and a dose rate of 0.5 Gy/min, was
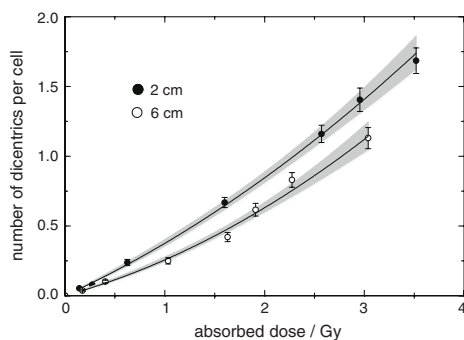
Fig. 2 Yield of dicentrics as a function of dose obtained for the MEDAPP beam at depths of 2 and 6 cm in the PE phantom. *Solid lines* show the weighted least-squares fit to the data with the *shadowed areas* representing the standard error bands. Standard errors of the mean are indicated by *vertical bars*

used instead. This linear-quadratic dose–response relationship had been obtained under comparable conditions, i.e., using similar dose rates, culture and evaluation conditions, and with blood from the same donor. For the induction of dicentrics in human lymphocytes at phantom depths of 2 and 6 cm, the RBE dose–response relationships for the MEDAPP beam relative to ^{60}Co γ-rays at a phantom depth of 1 cm are shown in Fig. 3. Within the analyzed dose ranges, the RBE of the MEDAPP beam decreases from 5.9 at 0.14 Gy to 1.6 at 3.52 Gy at 2 cm, and from 4.1 at 0.18 Gy to 1.5 at 3.04 Gy at 6 cm. The values of the RBE_M (which is equivalent to the ratio of the linear coefficients of the test and the standard reference dose–response curves) of the MEDAPP beam at the PE phantom
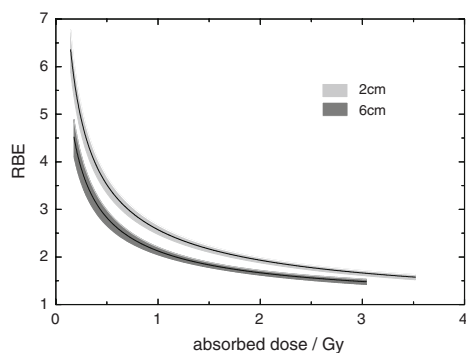
Fig. 3 RBE of the MEDAPP beam relative to the standard reference radiation of ^{60}Co γ-rays obtained at PE phantom depths of 2 and 6 cm. *Solid lines* show the weighted least-squares fit to the data with the *shadowed areas* representing the standard error bands

depths of 2 and 6 cm are 30.2 ± 11.1 and 18.3 ± 6.9, respectively.

Discussion

In the former experiments with the mixed neutron and γ-ray beam of the RENT therapy facility, the irradiation of the blood samples was carried out either free-in-air [4] or at a depth of 2 cm in a PMMA phantom [5]. Secondary charged-particle equilibrium was not established for the γ-ray component of the beam, for the free-in-air irradiation of thin blood samples (0.2 cm thickness). Consequently, results from earlier experiments with TE chambers of different wall thicknesses, which showed that the absorbed dose in 0.21 g/cm^2 tissue (equivalent to 0.2 cm of blood) amounts to about 70% of the absorbed dose (kerma) in charged-particle equilibrium [17], were used as a measure for the absorbed dose. Using these measured neutron kerma rates as a good approximation to dose, a linear-quadratic dose–response relationship for the yields of dicentrics was determined [4], which could be confirmed by irradiation experiments with the RENT beam in a PMMA phantom depth of 2 cm [5]. The existence of a significant quadratic coefficient β obtained in both irradiation experiments with the RENT beam [4, 5] was surprising, because all the dicentric data on fission spectra (with mean neutron energies from 0.40 to 2.13 MeV), which had been published up to that time, could be best fitted to a linear dependence on dose (reviewed by Lloyd and Edwards [18]).

Since this review only a few further studies that investigated the dose–response relationship of dicentrics in human lymphocytes following irradiation with fission neutrons were published. Using a degraded fission-neutron spectrum with a mean neutron energy of 210 keV (neutrons contributed 97% of the dose and γ-rays 3%) from a facsimile of the Hiroshima bomb ("Little-Boy" replica) assembled at Los Alamos, Dobson et al. [19] obtained a linear dose–response for dicentrics plus centric rings within a dose range from 0.02 to 2.92 Gy. Edwards et al. [20] examined a beam of predominately 24 keV neutrons (iron-filtered fission neutrons) with a γ-ray dose rate of about 17% of the neutron absorbed dose rate. The slope of the linear dose–response curve for dicentrics, they reported was very close to that observed in the same laboratory for a fission spectrum with a mean neutron energy of 700 keV [18]. It should be mentioned that all these linear dose–response curves for fission neutrons as well as the linear-quadratic dose–response curves for the RENT [4, 5] and MEDAPP beams (present data) were determined for acute irradiation conditions, which means that the exposure period was by far shorter than 1 h. Therefore, the absence of a quadratic component of the dose–response

relationship cannot be explained by a time-dependent influence.

To examine whether the γ-ray component of the RENT beam (about 25%) could have been responsible for the positive quadratic coefficient β [4], the dicentric yield attributable to γ-rays, as estimated from our dose–response curve for ^{60}Co γ-rays [8], was subtracted at each dose [4]. Provided that both the neutron and the γ-ray component of the beam acted completely independent, the remaining dicentric yields had been assumed to be due to the neutron component of the RENT beam. It was suggested that the quadratic contribution in the dicentric data could have been caused by the effect of released fast recoil protons with low linear energy transfer (LET), because a quadratic coefficient β that was significantly different from zero was still present for the neutron component of the beam after subtracting the corresponding γ-ray component. In a recent review of experimental data on the induction of dicentrics in human lymphocytes by neutrons and their interaction products [21], it was stated that if our former data [5], corrected for the γ-ray component of the RENT beam, "are fitted to a straight line, then it appears that a linear fit cannot be rejected". In contrast, however, according to our statistical analysis that involved testing the significance of the regression coefficients based on the t value, a significant positive value of the quadratic coefficient β was indeed induced by the RENT beam (calculated t value = 8.73 > critical t value = 2.37; P value $\ll 0.001$). Therefore, the existence of a statistically significant positive β value for fission neutrons still remains an open question. However, it should be taken into consideration that our former assumption that the coefficient β was induced by fast recoil protons with low LET is in good agreement with recent dicentric data obtained in track segment irradiation experiments with 16.5 MeV protons using blood of the same donor [22]. Applying a multi-layer array consisting of a blood chamber subdivided into three samples by Mylar foils, each containing 1 ml blood, linear-quadratic dose–response relationships for dicentric chromosomes were only obtained for protons with low LET (dose-averaged LET values of 3.5 and 5.3 keV/μm), whereas a linear dose–response relationship was obtained for protons with higher LET (dose-average LET of 19 keV/μm).

Recently, Sasaki et al. [23] measured dicentrics in human lymphocytes induced by different neutron spectra (mean neutron energies: 0.026, 0.747 and 1.285 MeV) at the YAYOI nuclear reactor facility. On the basis of the theory of dual radiation action [24, 25], they determined the dose–response relationship of dicentrics by fitting the data to a combined linear-quadratic curve. According to this theory, a biological system, which is simultaneously exposed to different radiation types, will show a larger biological effect than the sum of the independent effects of each radiation alone, due to an interaction of both radiation types. Such an interaction, sometimes called synergism, was also taken into account for the neutron and the γ-ray components of the MEDAPP beam, to determine the dose–response relationship for the dicentric data obtained in the present irradiation experiments with the MEDAPP beam. To be more specific, it was assumed that the two primary lesions induced by neutrons or γ-rays required to induce DNA double strand breaks which are generally accepted to be the most relevant basis for chromosomal rearrangements such as dicentrics would interact in the same way as two primary lesions induced by the same type of radiation. In addition, it is noteworthy that the mean of more than 20 values of the coefficient β available in the literature (including our own values)—over the wide range of photon energies from 100 keV to 20 MeV—was 0.054 Gy^{-2} [23]. Thus, it was justified to use the coefficient $\beta = 0.056 \pm 0.003$ Gy^{-2} from our standard reference dose–response curve for ^{60}Co γ-rays [8] as a constant for the γ-ray component of the MEDAPP beam, at both phantom depths of 2 and 6 cm. As it was originally derived for inter-track interaction of two primary lesions [25], a constant k (analogous to β) can be applied to both neutrons and γ-rays provided that comparable dose rates have been used. Therefore, on the basis of the assumption that both radiation components of the MEDAPP beam interact with each other, the dose–response relationship of dicentrics was determined by using the combined linear-quadratic function given in Eq. 2.

$$y = \alpha_n D_n + \alpha_\gamma D_\gamma + k(D_n + D_\gamma)^2, \qquad (2)$$

where $k = 0.056 \pm 0.003$ Gy^{-2} [8], D_n and D_γ are the doses in Gy from neutrons and γ-rays, and α_n and α_γ are the coefficients for the linear dose–response of neutrons and γ-rays, respectively.

On the basis of the assumption that both radiation components interact with each other, the resulting dose–response relationships for dicentrics at both phantom depths are shown as dashed lines in Fig. 4, while the solid lines represent the corresponding dose–response relationships based on the assumption that both radiation components act completely independently of one another (Eq. 3):

$$y = \alpha_n D_n + \alpha_\gamma D_\gamma + k\left(D_n^2 + D_\gamma^2\right). \qquad (3)$$

Figure 4 shows that there are no obvious differences between the dose–response relationship for dicentrics obtained by assuming an interaction between the radiation components, which assuming no interaction, and the standard error bands (shadowed areas) of the experimentally obtained dose–response relationships from Fig. 2. On the basis of these findings, it appeared justified to examine
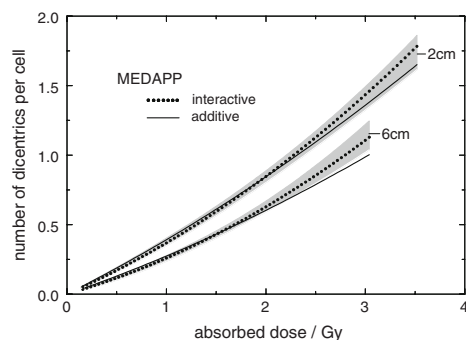
Fig. 4 Yield of dicentrics as a function of dose obtained for the MEDAPP beam at depths of 2 and 6 cm; *dashed line* interaction between the neutron and the γ-ray component included; *solid line* no interaction included, i.e., both components were assumed to act independently; the *shadowed areas* represent the standard error bands for the weighted least-squares fit to the measured data (also shown in Fig. 2)

whether a significant quadratic coefficient β could be determined for the fission neutron component of the MEDAPP beam. However, in contrast to the procedure applied earlier for the fission neutrons of the RENT beam [4, 5], a modified method was used taking into consideration both the well-known differential intercellular distribution of dicentrics induced either by γ-ray or neutron irradiation, as well as the recent findings on the depth-dependent induction of dicentrics in human lymphocytes by ^{60}Co γ-rays [26]. In our irradiation experiments with ^{60}Co γ-rays [8, 9, 13, 26, 27], a Poisson distribution of the induced dicentrics was observed, whereas in our irradiation experiments with several quasi-monoenergetic neutron energies from 36 keV to 60 MeV, an overdispersion was observed compared to Poisson [13, 27]. Therefore, for estimating the yield of dicentric aberrations attributable to the neutron component of the MEDAPP beam at phantom depths of 2 and 6 cm, at each dose level the corresponding γ-ray component of the beam was subtracted using the mean values of the dicentric yield and their Poisson distribution from appropriate linear-quadratic dose–response curves for ^{60}Co γ-rays. The construction of the linear and the quadratic term of these special dose–response curves are based on results which have recently been published [23, 26].

First, radiobiological evidence in terms of the induction of dicentrics in human lymphocytes shows that a significant depth-dependence of the RBE_M-value of ^{60}Co γ-rays in a cubic PMMA phantom of 30 cm edge length exists [26]. Either on the basis of Monte Carlo simulations for scattered photons with incident energies from 1 to 10 MeV [28] or on the basis of experiments where human

lymphocytes were irradiated by a ^{60}Co γ-source [26], it was demonstrated that, due to moderation of these photons in the phantom, the value of the coefficient α of a linear-quadratic dose–response curve is increased with increasing depth in the phantom. Therefore, for estimating the dicentric yields which may be induced by the γ-ray component of the MEDAPP beam, the coefficients $\alpha = 0.011 \pm 0.001$ Gy^{-1} and $\alpha = 0.014 \pm 0.001$ Gy^{-1} were used at phantom depths of 2 and 6 cm, respectively. Both values were obtained by an interpolation between several values of the coefficient α determined at phantom depths from 1 to 20 cm [26]. Although different phantom materials have been used (PMMA in the earlier experiments [26] and PE in the present experiments), this calculation of the depth dependence of the biological effectiveness of the γ-rays seems to be justified, because the hydrogen concentration in PMMA of 8% [28] is only slightly increased to 15.2% in PE [29]. Second, as discussed earlier, the coefficient β of 0.056 ± 0.003 Gy^{-2} from a standard reference dose–response curve for ^{60}Co γ-rays [8] was used for the γ-ray component of the MEDAPP beam at both phantom depths. For the remaining dicentric yields, which are attributed to the neutron component of the MEDAPP beam, linear-quadratic dose–response relationships could be determined for both phantom depths (Table 3). Applying the t test it was found that the calculated t values are always higher than the critical t values. The corresponding P values are far lower than 0.001 (Table 3). The present results for the MEDAPP beam and its neutron component are consistent with the earlier findings for the RENT beam and its neutron component suggesting the existence of a quadratic term of the dose–response relationship for dicentrics. However, it should be mentioned that the ratios of the linear and the quadratic terms of the dose–response curves, α/β, obtained for the MEDAPP beam at phantom depths of 2 and 6 cm are greater than the doses analyzed in the present experiments. Thus, the resulting values of 7.6 and 3.5 Gy, respectively, indicate a clear predominance of the linear term of the dose–response curves, at the investigated doses.

The dicentrics induced in human lymphocytes by the MEDAPP beam at a depth of 2 cm in the PE phantom confirm in principle the findings obtained for the RENT beam in the PMMA phantom [5]. This result is remarkable because, due to differences in the neutron therapy facilities at FRM I and FRM II, which include a larger size of the new facility and the used phantom, different phantom materials (PE instead of PMMA) which resulted in a larger hydrogen content of 7% fraction mass, the biological parameters of both beams such as the RBE need not necessarily be the same [12]. On the basis of the corresponding linear-quadratic dose–response relationships for dicentrics,

it can be calculated that, for doses between of 0.14 and 3.52 Gy, the RBE of the MEDAPP beam and that of the RENT beam decrease from 5.9 to 1.6 and from 6.5 to 1.6, respectively. The corresponding RBE_M values are 30.2 ± 11.1 and 36.4 ± 13.3, respectively. Therefore, in spite of the differences in the photon contribution to absorbed dose, there is no indication for differences in the biological effectiveness between the new MEDAPP therapy facility at FRM II and the former RENT therapy facility at FRM I.

Conclusions

Using the best possible conditions of biological consistency, e.g., avoiding the inter-individual variations in sensitivity by using blood samples from the same person, and avoiding differences in methodology usually associated with inter-laboratory comparisons by using identical measurement protocols, linear-quadratic dose–response relationships were obtained both for the mixed neutron and γ-ray RENT and MEDAPP beams, and for their fission neutron component (mean neutron energy: about 1.9 MeV). Since our earlier investigations on quasi-monoenergetic neutrons with energies from 36 keV to 60 MeV suggested linear dose–response relationships for the induction of dicentrics in human lymphocytes, the question of whether dicentrics induced by fission neutrons increase mainly linearly with dose remains open. At the phantom depths of 2 and 6 cm, the RBE of the MEDAPP beam decreases from 5.9 to 1.6 within the dose range from 0.14 to 3.52 Gy, and from 4.1 to 1.5 within the dose range from 0.18 to 3.04 Gy, respectively.

References

1. ICRP (1991) Recommendations of the International Commission on Radiological Protection. Publication 60. Pergamon Press, Oxford
2. ICRP (2003) Relative biological effectiveness (RBE), quality factor (Q), and radiation weighting factor (w_R). *Annals of the ICRP*, Publication 92. Pergamon Press, Oxford
3. BEIR VII Report (2006) Health risks from exposure to low levels of ionizing radiation. National Academies Press, Washington, DC
4. Bauchinger M, Koester L, Schmid E, Dresp J, Streng S (1984) Chromosome aberrations in human lymphocytes induced by fission neutrons. Int J Radiat Biol 45:449–457
5. Schmid E, Schraube H, Bauchinger M (1998) Chromosome aberration frequencies in human lymphocytes irradiated in a phantom by a mixed beam of fission neutrons and γ-rays. Int J Radiat Biol 73:263–267
6. Breitkreutz H, Wagner FM, Röhrmoser A, Petry W (2008) Spectral fluence rates of the fast reactor neutron beam MedApp at FRM II. Nucl Instrum Methods Phys Res A. doi:10.1016/j.nima.2008.05.008
7. Mogaddino V, Wagner FM, Kummermehr J (2007) Preclinical screening of the biological effectiveness of a therapeutic neutron beam at the FRM II. Exp Strahlenther Klin Strahlenbiol 16:129–131
8. Bauchinger M, Schmid E, Streng S, Dresp J (1983) Quantitative analysis of the chromosome damage at first division of human lymphocytes after ^{60}Co γ-irradiation. Radiat Environ Biophys 22:225–229
9. Schmid E, Regulla D, Guldbakke S, Schlegel D, Roos M (2002) Relative biological effectiveness of 144 keV neutrons in producing dicentric chromosomes in human lymphocytes compared with ^{60}Co gamma rays under head-to-head conditions. Radiat Res 157:453–460
10. Kampfer S, Wagner FM, Loeper-Kabasakal B, Kneschaurek P (2007) Die neue neutronentherapieanlage am FRM II in Garching. Strahlenther Onkol 183(1):72
11. Wagner FM, Bücherl Th, Kampfer S, Kastenmüller A, Waschkowski W (2007) Thermal neutron converter for irradiations with fission neutrons. Nuclear Phys Atomic Energy 3:30–36
12. Wagner FM, Kneschaurek P, Kampfer S, Kastenmüller A, Loeper-Kabasakal B, Waschkowski W, Breitkreutz H, Molls M, Petry W (2008) The Munich fission neutron therapy facility MEDAPP at FRM II. Strahlenther Onkol 184
13. Schmid E, Schlegel D, Guldbakke S, Kapsch RP, Regulla D (2003) RBE of nearly monoenergetic neutrons at energies of 36 keV–14.6 MeV for induction of dicentrics in human lymphocytes. Radiat Environ Biophys 42:87–94
14. Schmid E, Braselmann H, Nahrstedt U (1995) Comparison of γ-ray induced dicentric yields in human lymphocytes measured by conventional analysis and FISH. Mutat Res 348:125–130
15. Göggelmann W, Jacobsen C, Walsh L, Panzer W, Roos H, Schmid E (2003) The re-evaluation of the RBE of 29 kV X-rays (mammography X-rays) relative to 220 kV X-rays using neoplastic transformation. Radiat Environ Biophys 42:175–182
16. Kellerer AM (2003) Error bands for the linear-quadratic dose–effect relation. Radiat Environ Biophys 42:77–85
17. Koester L (1984) Applicability of reactor fission neutrons for radiation therapy of cancer. Nucl Sci Appl 2:79–96
18. Lloyd DA, Edwards AA (1983) Chromosome aberrations in human lymphocytes: effect of radiation quality, dose, and dose rate. In: Ishihara T, Sasaki MS (eds) Radiation-induced chromosome damage in man, Inc. AR Liss, New York, pp 22–49
19. Dobson RL, Straume T, Carrano AV, Minkler JL, Deaven LL, Littlefield LG, Awa AA (1991) Biological effectiveness of neutrons from Hiroshima bomb replica: results of a collaborative cytogenetic study. Radiat Res 128:142–149
20. Edwards AA, Lloyd DC, Prosser JS (1994) The induction of chromosome aberrations in human lymphocytes by 24 keV neutrons. Radiat Prot Dosimetry 31:265–268
21. Ballarini F, Biaggi M, Edwards AA, Ferrari A, Ottolenghi A, Pelliccioni M, Scannicchio D (2003) Estimating mixed field effects: an application supporting the lack of a non-linear component for chromosome aberration induction by neutrons. Radiat Prot Dosimetry 103:19–28
22. Schmid E, Roos H, Rimpl G, Bauchinger M (1997) Chromosome aberration frequencies in human lymphocytes irradiated in a multi-layer array by protons with different LET. Int J Radiat Biol 72:661–665
23. Sasaki MS, Endo S, Ejima Y, Saito I, Okamura K, Oka Y, Hoshi M (2006) Effective dose of A-bomb radiation in Hiroshima and Nagasaki as assessed by chromosomal effectiveness of spectrum energy photons and neutrons. Radiat Environ Biophys 45:79–91
24. Kellerer AM, Rossi HH (1972) The theory of dual radiation action. Curr Top Radiat Res Q 8:86–157
25. Kellerer AM, Rossi HH (1978) A generalized formation of dual radiation action. Radiat Res 75:471–488

26. Schmid E, Roos H, Kramer HM (2008) The depth-dependence of the biological effectiveness of ^{60}Co γ-rays in a large absorber determined by dicentric chromosomes in human lymphocytes. Radiat Prot Dosimetry 130:442–446

27. Nolte R, Mühlbradt KH, Meulders JP, Stephan G, Haney M, Schmid E (2005) RBE of quasi-monoenergetic 60 MeV neutron radiation for induction of dicentric chromosomes in human lymphocytes. Radiat Environ Biophys 44:201–209

28. Harder D, Petoussi-Henß N, Regulla D, Zankl M, Dietze G (2004) Spectra of scattered photons in large absorbers and their importance for the values of radiation weighting factor w_R. Radiat Prot Dosimetry 109:291–295

29. Hermann KP, Geworski L, Muth M, Harder D (1985) Polyethylene-based water-equivalent phantom material for X-ray dosimetry at tube voltages from 10 to 100 MeV. Phys Med Biol 30:1195–1200

32. Kreuzer M, Grosche B, Schnelzer M, Tschense A, Dufey F & Walsh L. Radon and risk of death from cancer and cardiovascular diseases in the German uranium miners cohort study: follow-up 1946-2003. Radiat. Environ. Biophys. 49 (2), 177-185, 2010

ORIGINAL PAPER

Radon and risk of death from cancer and cardiovascular diseases in the German uranium miners cohort study: follow-up 1946–2003

Michaela Kreuzer · B. Grosche · M. Schnelzer ·
A. Tschense · F. Dufey · L. Walsh

Abstract Data from the German uranium miners cohort study were analyzed to investigate the radon-related risk of mortality from cancer and cardiovascular diseases. The Wismut cohort includes 58,987 men who were employed for at least 6 months from 1946 to 1989 at the former Wismut uranium mining company in Eastern Germany. By the end of 2003, a total of 3,016 lung cancer deaths, 3,355 deaths from extrapulmonary cancers, 5,141 deaths from heart diseases and 1,742 deaths from cerebrovascular diseases were observed. Although a number of studies have already been published on various endpoints in the Wismut cohort, the aim of the present analyses is to provide a direct comparison of the magnitude of radon-related risk for different cancer sites and cardiovascular diseases using the same data set, the same follow-up period and the same statistical methods. A specific focus on a group of cancers of the extrathoracic airways is also made here, due to the assumed high organ doses from absorbed radon progeny. Internal Poisson regression was used to estimate the excess relative risk (ERR) per unit of cumulative exposure to radon in working level months (WLM) and its 95% confidence limits (CI). There was a statistically significant increase in the risk of lung cancer with increasing radon exposure (ERR/WLM = 0.19%; 95% CI: 0.17%; 0.22%). A smaller, but also statistically significant excess was found for cancers of the extrathoracic airways and trachea (ERR/WLM = 0.062%; 95% CI: 0.002%; 0.121%). Most of the remaining nonrespiratory cancer sites showed a positive relationship with increasing radon exposure, which, however, did not reach statistical significance. No increase in risk was noted for coronary heart diseases (ERR/WLM = 0.0003%) and cerebrovascular diseases (ERR/WLM = 0.001%). The present data provide clear evidence of an increased radon-related risk of death from lung cancer, some evidence for an increased radon-related risk of death from cancers of the extrathoracic airways and some other extrapulmonary cancers, and no evidence for mortality from cardiovascular diseases. These findings are consistent with the results of other miner studies and dosimetric calculations for radon-related organ doses.

M. Kreuzer (✉) · B. Grosche · M. Schnelzer · A. Tschense ·
F. Dufey · L. Walsh
Department of Radiation Protection and Health,
Federal Office for Radiation Protection,
Ingolstädter Landstr. 1, 85764 Neuherberg, Germany
e-mail: mkreuzer@bfs.de

Introduction

The radioactive noble gas radon was classified in 1988 as a known pulmonary carcinogen in humans by the International Agency for Research on Cancer (IARC 1988). Since then, several miner studies (Lubin et al. 1994; BEIR 1999; Laurier et al. 2004; Tomasek and Zarska 2004; Tomasek et al. 2008; Brüske-Hohlfeld et al. 2006; Grosche et al. 2006; Vacquier et al. 2008, 2009; Villeneuve et al. 2007a; Schubauer-Berigan et al. 2009) and residential radon studies (Lubin et al. 2004; Darby et al. 2005; Krewski et al. 2005) have consistently shown a significant relationship between exposure to radon and the risk of lung cancer. A few epidemiological studies have investigated a possible causal relationship between radon and cancers other than the lung (Darby et al. 1995; BEIR 1999; Laurier et al. 2004; Vacquier et al. 2008; Rericha et al. 2006; Moehner et al. 2006, 2008; Xuan et al. 1993; Tomasek et al. 1993) or

cardiovascular diseases (Villeneuve and Morrison 1997; Villeneuve et al. 2007b; Tomasek et al. 1994; Xuan et al. 1993), and most provided no clear evidence for an increased radon-related risk. This result is compatible with dosimetric calculations (Kendall and Smith 2002; Marsh et al. 2008) showing about 100–1,000 times higher organ doses from absorbed radon progeny for the lung and the extrathoracic airways compared to other organs.

The German uranium miners cohort study is currently the largest single study of radon-exposed miners worldwide, with almost 2 million person-years of observation based on 58,987 male former employees of the German Wismut uranium company in Eastern Germany. By the end of 1998, a total of 4,800 deaths from malignant cancer and 5,417 deaths from cardiovascular diseases had occurred (Grosche et al. 2006; Kreuzer et al. 2006). This number increased to 6,373 and 7,395 by the extension of the follow-up to 2003 (Kreuzer et al. 2009), respectively. Within the Wismut cohort study, the radon-related risk of death from lung cancer was published for the follow-up period 1946–1998 (Grosche et al. 2006) and 1946–2003 (Walsh et al. 2009); extrapulmonary cancer was published for the period 1960–2003 (Kreuzer et al. 2008) and that from cardiovascular disease for the period 1946–1998 (Kreuzer et al. 2006). The aim of the present analyses of the German cohort is to provide a direct comparison of the magnitude of radon-related risk for different cancer sites and cardiovascular diseases using the same data set, the same follow-up period and the same statistical methods. A specific focus on a group of cancers of the extrathoracic airways is also made here, due to the assumed high organ doses from absorbed radon progeny.

Materials and methods

Cohort

The cohort represents a stratified random sample of 58,987 males, who had been employed for at least 6 months between 1946 and 1989 at the former Wismut uranium company in East Germany. The first mortality follow-up period finished at the end of 1998 (Kreuzer et al. 2006; Grosche et al. 2006). The present analyses are based on an extension of the first follow-up by 5 years to December 31, 2003 (Kreuzer et al. 2008, 2009; Walsh et al. 2009). Information on the vital status of the cohort members was obtained from local registration offices. Copies of death certificates were obtained from several sources, not only from the responsible Public Health Administrative offices, but also from the central archives and the pathology archive of the Wismut Company. The underlying causes of

death from either the death certificates or the autopsy files were coded according to the 10th revision of the International Classification of Diseases (ICD-10).

Radiation exposure was estimated by using a detailed job-exposure matrix (JEM) (Lehmann et al. 1998; HVBG and BBG 2005). The JEM includes information on exposure to radon and its progeny in working level months (WLM), external γ radiation in mSv and long-lived radionuclides in kBqh m^{-3} for each calendar year, each place of work (surface, open pit mining, underground, milling), each mining facility and each type of job. One working level is defined as the concentration of short-lived radon daughters per liter of air that gives rise to 1.3×10^5 MeV of alpha energy. One WLM of cumulative exposure corresponds to exposure to 1 WL during 1 month (170 h) and is equivalent to 3.5 mJh m^{-3}. Radon (^{222}Rn) area measurements in the Wismut mines were carried out from 1955 onwards. Thus, for the period 1946–1954, radon concentrations were retrospectively estimated by an expert group based on measurements from 1955, taking into account ventilation rate, vein space, uranium content and other factors. Information on arsenic, dust and silica is based on a separate job-exposure matrix similar to that for radiation (HVBG and BBG 2005; Bauer 2000; Dahmann et al. 2008). The annual exposure values are given in dust years, where one dust year is defined as an exposure to 1 mg m^{-3} fine dust or silica dust and to 1 μg m^{-3} for arsenic over a time period of 220 shifts of 8 h.

Statistical methods

Internal Poisson regression was used to test for an association between mortality risk and cumulative radon exposure. Similar to previous analyses (Kreuzer et al. 2008; Walsh et al. 2009), a 5-year lag was used in calculating the cumulative exposure to radon for all outcomes except leukemia, where a zero-year lag was defined. Every cohort member contributes to the number of person-years starting 180 days after the date of first employment and ending at the earliest of date of loss to follow-up, date of death or end of follow-up (31.12.2003). Tabulations of person-years at risk and cancer deaths were created with the DATAB module of the EPICURE software (Preston et al. 1998). Cross-classifications were made by attained age, a, in 16 categories (<15, 15–19, 20–24,…, 85+ years), individual calendar year, y, in 58 categories and cumulative radon exposure, w, in 9 categories (0, >0–9, 10–49, 50–99, 100–199, 200–499, 500–999, 1,000–1,499, 1,500+ WLM). The tabulated data were fitted to the model in 1—if $r(a,y,w)$ is the age, year- and exposure-specific cancer mortality rate and $r_0(a,y) = r(a,y,0)$ is the baseline disease rate for non-exposed individuals ($w = 0$) then

$$r(a, y, w) = r_0(a, y) \times [1 + \text{ERR}(w)] \qquad (1)$$

where ERR is the excess relative risk.

A linear form for ERR$(w) = \beta w$ was used to investigate the exposure–response relationship. In addition, a categorical analysis of the form ERR$(w) = \Sigma_{j=1,9} \, \beta_j w_j$ was performed, where j refers to the exposure class. In order to test for the five potential confounders (long-lived radionuclides (LRN), external gamma radiation, fine dust, silica dust and arsenic), each of these variables z_i, $i = 1,..,5$ was added separately to the model (1) with ERR$(w,z_i) = \beta w + \gamma z_i$. Maximum likelihood with the AMFIT module of the EPICURE software (Preston et al. 1998) was used for the estimation of the fit parameters β, γ, β_j, $j = 1,..,9$ and the internal baseline rates in strata. Wald-type and likelihood-based confidence intervals were calculated and found to be very similar. Consequently, and for consistency with previous papers, all parameters are given here with their 95% Wald-type confidence intervals (CI).

According to previous analyses within the Wismut cohort, the following outcomes based on the ICD-10 classification were investigated: lung cancer (C34) (Grosche et al. 2006; Walsh et al. 2009), all other cancer sites with more than 35 cases as defined in Kreuzer et al. (2008), circulatory diseases (I00–I99), coronary heart diseases (I00–59), cerebrovascular diseases (I60–69) and acute myocardial infarction (I21) as in Kreuzer et al. (2006). In addition, here all cancers of the extrathoracic airways and trachea were combined including cancers of the oral cavity (C01–C06), pharynx (C09–C14), nasal cavity and paranasal sinus (C30–C31), larynx (C32) and trachea (C33).

Results

In the follow-up period from 1946 to 2003, a total of 58,987 persons were under observation (see Table 1), resulting in 1,996,959 person-years at risk and a mean duration of follow-up of 35 years. By the end of 2003, 35,294 (59.8%) men were alive, 20,920 (35.5%) had died, 2,773 (4.7%) were lost to follow-up. The underlying cause of death has been available for 19,588 (93.6%) of the deceased men, among them, 3,016 lung cancer deaths, 3,355 deaths from other malignant cancers and 7,395 deaths from cardiovascular diseases. A total of 50,773 (86.1%) individuals have been exposed to radon at some time during employment at the Wismut Company. Those exposed received a person-year-weighted mean cumulative exposure to radon of 218 WLM, a mean person-year-weighted cumulative exposure to external gamma radiation of 30 mSv and an average-weighted cumulative exposure to long-lived radionuclides of 3 kBqh m^{-3}.

Table 1 Characteristics of the German uranium miner cohort study, 1946–2003; WLM: Working Level Month

Variable	Number (%)
Total number of miners	58,987 (100%)
Person-years at risk	1,996,959
Mean duration of follow-up (years)	35
Year of begin of employment	
1946–1954	23,920 (40.6%)
1955–1970	17,944 (30.4%)
1971–1989	17,123 (29.0%)
Year of end of employment	
1946–1954	2,719 (4.6%)
1955–1970	28,121 (47.7%)
1971–1989	28,147 (47.7%)
Vital status	
Alive	35,294 (59.8%)
Deceased	20,920 (35.5%)
Lost to follow-up	2,773 (4.7%)
Year of death (% of available causes of death)	
<1960	236 (36.9%)
1960–1969	1,324 (62.7%)
1970–1979	3,255 (95.1%)
1980–1989	5,554 (96.7%)
1990–1999	7,538 (96.7%)
2000–2003	3,013 (96.9%)
Total	20,920 (93.6%)
Exposure to radon and its progeny	
Never (0 WLM)	8,214 (13.9%)
Ever (>0 WLM)	50,773 (86.1%)
Among exposed: mean (min–max)	
Cumulative exposure in WLM	280 (>0–3,224)
Age at first exposure in years	25 (14–67)
Duration of exposure in years	11 (1–44)

Figure 1 shows the number of radon-exposed cohort members by calendar year as well as the average cumulative radon exposure in WLM per year among exposed cohort members. With the introduction of ventilation measures from 1955 onwards, the radon concentration sharply dropped down, reaching levels of international radiation protection standards in the 1970s.

In Table 2 and Fig. 2, the excess relative risk per unit of cumulative radon exposure for morality from different cancer sites and cardiovascular diseases is given. A statistically significant increase in risk is observed for lung cancer (ERR/WLM = 0.19%; 95% CI: 0.17%; 0.22%) and all extrapulmonary cancers combined (ERR/WLM = 0.014%; 95% CI: 0.006%; 0.023%). Next to lung cancer, the highest excess is found for the group of cancers of the extrathoracic airways and trachea (ERR/WLM = 0.062%; 95% CI: 0.002%; 0.121%), with an excess of 0.16% for pharynx

Fig. 1 Number of radon-exposed cohort members and mean cumulative radon exposure per calendar year ($n = 50{,}773$)
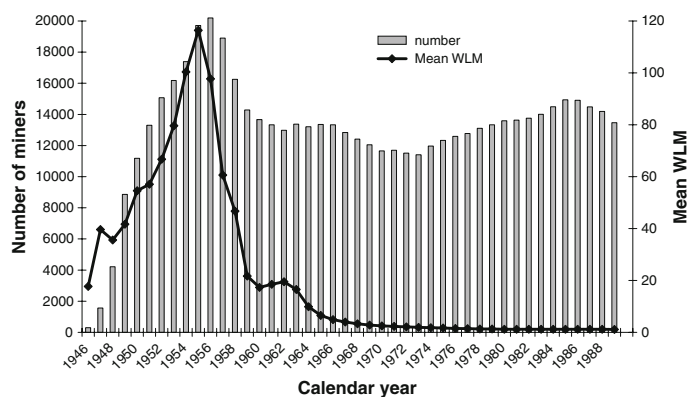
Table 2 Excess relative risk (ERR) per 100 WLM and 95% confidence limits for different causes of deaths from cancer and cardiovascular diseases in relation to cumulative radon exposure, 1946–2003

Cause of death (ICD-10 code)	Number of deaths	ERR/100 WLM	p value
Malignant cancer (C)			
Lung (C34)	3,016	0.194	<0.001
Extrapulmonary cancers (C00–32, C35–C97)	3,355	0.014	0.001
Extrathoracic airways and trachea (C01–C06, C09–C14, C30–C33)	177	0.062	0.042
Oral cavity (C01–C06)	38	0.047	0.481
Pharynx (C09–C14)	53	0.164	0.114
Larynx (C32)	75	0.020	>0.5
Nasal cavity, paranasal sinus (C30–31)	9	–	
Trachea (C33)	2	–	
Esophagus (C15)	126	−0.025	0.070
Stomach (C16)	595	0.020	0.055
Colon (C17–C18)	301	0.018	0.222
Rectum (C19–C21)	241	0.029	0.112
Liver (C22)	159	0.043	0.095
Gallbladder (C23–C24)	81	0.019	0.492
Pancreas (C25)	229	−0.001	>0.5
Prostate (C61)	264	−0.001	>0.5
Kidney (C64–C66)	171	0.018	0.371
Bladder (C67–C68)	177	0.019	0.306
Brain and other (C70–C72)	115	−0.018	0.271
Non-Hodgkin's disease (C82–C85, C91.4)	87	0.034	0.331
Myeloma (C90)	55	0.001	>0.5
Leukemia (C91–C95, excluding C91.4)	128	0.008	>0.5
Cardiovascular diseases (I)			
All (I00–I99)	7,395	0.001	>0.5
Coronary heart diseases (I00–I59)	5,141	0.000	>0.5
Acute myocardial infarction (I21)	2,074	0.008	0.114
Cerebrovascular diseases (I60–I69)	1,742	0.001	>0.5

cancer, 0.05% for cancers of the oral cavity and 0.02% for larynx cancer. Due to the small numbers of cases, however, only the excess of the combined group of extrathoracic

cancers reached statistical significance but none of the separate subgroups. Among the remaining cancer sites, borderline statistically significant excesses are present for death
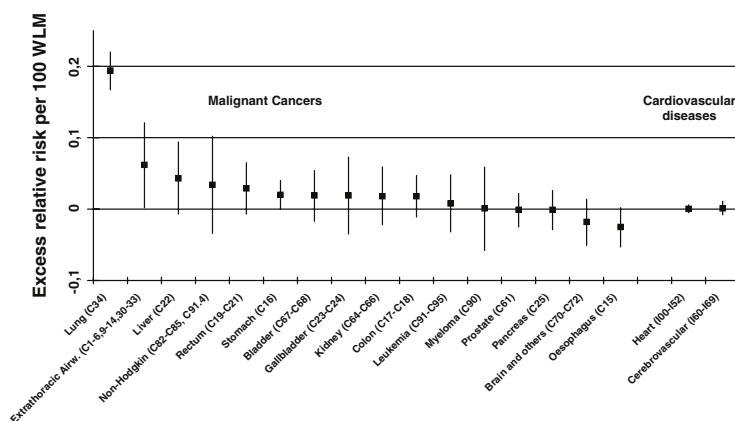
Fig. 2 Excess relative risk (ERR) per 100 WLM and 95% confidence limits for mortality from different cancer sites and cardiovascular diseases, 1946–2003

from cancers of the stomach (ERR/WLM = 0.02%, 95% CI: 0.000%; 0.040%) and liver (ERR/WLM = 0.043%; 95% CI: −0.007%; 0.094%). There is no association between leukemia and cumulative radon exposure apparent here. This is also true for all types of leukemia except chronic lymphatic leukemia, chronic lymphatic leukemia and acute myeloid leukemia.

Figure 3 presents the relative risks for death from lung cancer and cancers of the extrathoracic airways and trachea in nine categories of cumulative radon exposure along with the linear model. With respect to lung cancer, there is a clear steep increase in risk with increasing radon exposure, and all exposure categories above 50 WLM are associated with a statistically significant elevated relative risk. With respect to cancers of the extrathoracic airways and trachea, the two highest exposure categories (1,000–1,499 and 1,500+ WLM) were combined, because only two cases occurred in the exposure group with more than 1,500 WLM. The corresponding categorical analysis shows an approximately linear increase in the relative risk with increasing radon exposure up to the exposure category of about 1,000 WLM with nearly as high relative risks as observed for lung cancer mortality. The corresponding RR's, however, do not reach statistical significance. In the highest exposure category (>1,000 WLM), the relative risk drops down, indicating nonlinearity in the full exposure range.

No relationship between mortality from cardiovascular diseases overall and cumulative radon exposure is present (Table 2; Fig. 2). This holds true for the subgroups coronary heart diseases (ERR/WLM = 0.0003%) and cerebrovascular diseases (ERR/WLM = 0.001%) where no

increased relative risk was noted (Fig. 4), even in the high exposure categories (>1,500 WLM) of both subgroups. Analysis of deaths from acute myocardial infarction showed a quite small, but borderline statistically significant ERR/WLM of 0.008% (*p* value = 0.11), yet no clear increase in risk was observed in the categorical analysis (RR values of 1.00, 0.86, 0.91, 1.10, 0.93, 0.88, 0.96, 0.99, 1.14, in the exposure categories 0, 0–9, 10–49, 50–99, 100–199, 200–499, 500–999, 1,000–1,499, >1,500 WLM).

Potential confounding by occupational exposure to external gamma radiation, long-lived radionuclides, fine dust, silica dust or arsenic was examined for the individual cancer sites and cardiovascular diseases. Overall, there is low correlation between exposure to radon and exposure to external gamma radiation, long-lived radionuclides or arsenic ($R < 0.28$), while fine dust ($R = 0.57$) and silica dust ($R = 0.63$) are relatively highly correlated with radon exposure. The influence of adjustment for these potential confounders on the exposure–response relationship was found to be modest for all cancer sites and groups of cardiovascular diseases, except for stomach cancer, where a strong reduction in risk is observed.

Discussion

Dosimetric calculations indicate that the absorbed doses from radon and its progeny are highest for the respiratory tract including the lung, trachea and extrathoracic airways, while for the majority of other organs, the doses are lower by two orders of magnitude (Kendall and Smith 2002). In the present study, a statistically significant relationship
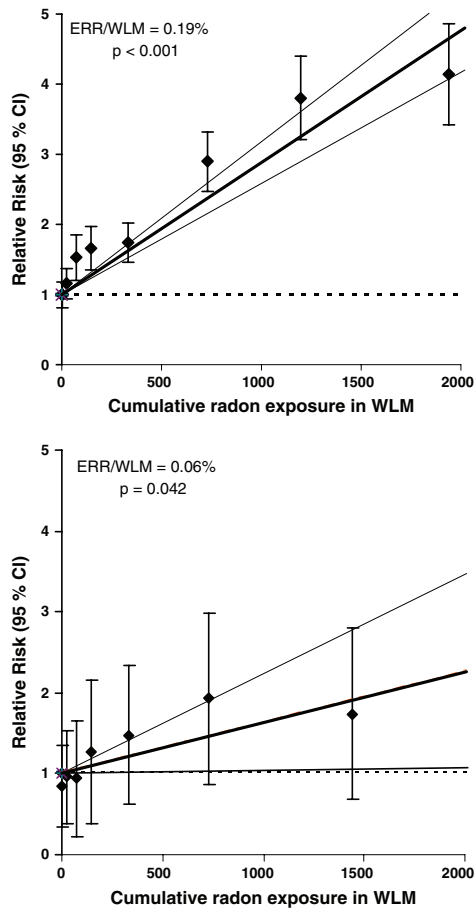
Fig. 3 Relative risk of death from lung cancer ($n = 3,016$) (*upper figure*) and cancers of the extrathoracic airways and trachea ($n = 177$) (*lower figure*) in relation to cumulative radon exposure in WLM, 1946–2003. Categorical analysis (0, 0–10, 10–49, 50–99, 100–199, 200–499, 500–999, 1,000–1,499, 1,500+), and simple linear model (*bold solid line*) and 95% confidence limits (*solid lines*). For cancers of the extrathoracic airways, the two highest exposure categories were combined

Fig. 4 Relative risk of death from heart diseases ($n = 5,141$) (*upper figure*) and cerebrovascular diseases ($n = 1,742$) (*lower figure*) in relation to cumulative radon exposure in WLM, 1946–2003. Categorical analysis (0, 0–10, 10–49, 50–99, 100–199, 200–499, 500–999, 1,000–1,499, 1,500+) and simple linear model (*bold solid line*) and 95% confidence limits (*solid lines*)

between cumulative radon exposure and mortality from lung cancer and cancers of the extrathoracic airways and trachea is observed. Most other cancer sites showed positive exposure–response relationships, but these were insignificant (Kreuzer et al. 2008). No evidence for a radon-related increased risk of deaths from cardiovascular diseases was noted. The epidemiological findings of the

present study thus largely confirm the findings of the bi-okinetic models.

Lung cancer

The simple ERR/WLM without adjustment for effect modifiers obtained here is 0.19% (95% CI: 0.17%; 0.22%) for the lung. Recent more detailed analyses using, for example, the BEIR VI exposure-age-concentration model

(BEIR VI 1999) showed that the ERR/WLM is additionally strongly modified by time since exposure, attained age and exposure rate, yielding a value of 0.57% at an age attained <55 years, time since exposure 5–14 years and 15 WL or more (Walsh et al. 2009). The risk decreases with increasing attained age, increasing time since exposure and decreasing exposure rate. The present results are largely compatible with those of the pooled 11 miners studies (BEIR VI 1999), however, with slightly lower risk estimates in the Wismut cohort. No major confounding by the other occupational risk factors was found (Walsh et al. 2009).

Cancer of the extrathoracic airways

In the present study, a statistically significant relation between cumulative radon exposure and cancers of the extrathoracic airways and trachea (ERR/WLM = 0.06%; 95% CI: 0.002%; 0.121%) is observed, which is only marginally modified after adjustment for the five potential confounders. It is unclear whether this association is causal, because the categorical analyses indicated a linear increase up to an exposure of 1,000 WLM and a leveling off at higher exposures. Several reasons could account for this decrease such as the healthy worker survivor effect or unconsidered modifying time-dependent variables, or potential confounders such as alcohol consumption. Since the radon-related lung cancer risk is strongly modified by factors such as time since exposure, attained age and exposure rate, these factors were additionally considered as exponential modifiers in the model for extrathoracic cancers. For this latter group of sites, however, no modifying effects were observed.

Because of the rare occurrence of cancers of the extrathoracic airways, only few other miners studies investigated the relationship between these cancers and exposure. Thus, for example, no results are available on the relationship of radon with pharyngeal cancer or cancers of the oral cavity, the cancer sites that showed the highest risk in the present study (ERR/WLM = 0.16 and 0.05%), respectively. If at all, these studies focused on laryngeal cancer. No relationship of laryngeal cancer with cumulative radon exposure was found in the pooled 11 miners study (Darby et al. 1995), but there were only 38 cases. In contrast, an elevated, but insignificantly increased Standardized Mortality Ratio (SMR) was observed in the French uranium miners study (SMR = 1.24, n = 29) (Vacquier et al. 2008). In contrast, a large case–control study on incidental larynx cancer among former German Wismut uranium miners, including 554 cases and 929 controls, provided no evidence for an association between exposure to short-lived radon progeny and laryngeal cancer (Moehner et al. 2008); even in the highest exposure

category (1,000 WLM+), there was only a slightly elevated risk (OR = 1.13; 95% CI: 0.75; 1.70).

Malignant cancers external to the respiratory tract

The present results, based on the follow-up period 1946–2003, do not differ much from those based on the earlier follow-up period 1960–2003 (Kreuzer et al. 2008), because very few cases occurred before 1960. A statistically significant excess was present for all extrapulmonary cancers combined (ERR/WLM = 0.014%; 95% CI: 0.006%; 0.023%). When considering only cancer sites external to the respiratory tract, the majority exhibited a positive exposure–response relationship. However, none of these individual cancer sites showed a statistically significant exposure–response relationship. Borderline significant excesses were observed for liver cancer and stomach cancer. Other miner studies have provided little evidence for a relationship between nonrespiratory cancers and exposure to radon progeny (Darby et al. 1995; Moehner et al. 2006; Tomasek et al. 1993; Vacquier et al. 2008). However, most of the previous studies may have been limited in statistical power.

Cardiovascular diseases

It is important to investigate radiation-related mortality from cardiovascular disease in the low-dose range, because a linear dose–response relationship between circulatory diseases and ionizing radiation in the dose range 0–4 Sv has already been observed in the Life Span Study cohort of Japanese atomic bomb survivors (Preston et al. 2003). However, the relevant results from other epidemiological studies are not consistent with each other (McGale and Darby 2005; Little et al. 2008, 2009), and there is currently little knowledge on the biological mechanism for inducing such effects. Inhalation of radon results in small doses of radon progeny only to the blood or arteries (Kendall and Smith 2002). Previous results from the Wismut cohort based on the follow-up period up to the end of 1998 (Kreuzer et al. 2006) provided no evidence of an increased risk of death from circulatory diseases overall, heart and cerebrovascular diseases. This result is confirmed here by the present analyses with updated data and also in other miner studies (Villeneuve and Morrison 1997; Villeneuve et al. 2007a, b; Xuan et al. 1993; Tomasek et al. 1994).

Strengths and limitations of the present study

The major strengths of the German Wismut uranium miner study are the large cohort size, the long follow-up period, the wide range of exposure to radon, and particularly the availability of information on other types of exposures in

the mines. These advantages meant that the Wismut study data could be applied in an independent replication of the analysis that had already been used for the 11 miner cohort studies (Darby et al. 1995; BEIR 1999; Lubin et al. 1994), which, although of similar size to the Wismut study, may have suffered from heterogeneity problems.

Potential limitations of the present study concern availability and validity of cause of death. Causes of death are missing for 6.4% of the deceased cohort members. The main reason for missing causes of death is the destroyed certificates of deaths. The validity of cause of death may vary between different types of cause of death. A higher validity can be expected for lung cancer compared to cardiovascular diseases in general and particularly in this medically monitored occupational group. Moreover, about 49.9% of the causes of death with lung cancer diagnosis are based on autopsy results, but only 21.5% of those for cancers of the extrathoracic airways and 17.8% of the cardiovascular diseases.

Exposure misclassification particularly in the early years of mining activities is another potential limitation. Previous analyses, however, demonstrated no major differences in the ERR/WLM for the cancer sites considered (Kreuzer et al. 2008; Walsh et al. 2009) when different time periods with different quality of exposure (1946–1954: no measurements available, 1955–1989: measurements in shafts available) were compared. For this reason, a major bias through misclassification of exposure is unlikely, but cannot be completely excluded. Low statistical power with respect to some of the individual cancer sites as well as missing information on other potential confounders such as alcohol consumption, smoking or asbestos are further potential limitations. Within a nested case–control study of lung cancer in the Wismut cohort, information on smoking was collected from miners, their relatives and the medical Wismut archive (Schnelzer et al. 2009). Most of the former Wismut employees had been smokers. Overall, there was a low correlation between smoking and cumulative radon exposure. Thus, it is unlikely that smoking is a major confounder. Additional support comes from a German case–control study on incident lung cancer among former Wismut miners, for which information on smoking was collected in detail by personal interviews (Brüske-Hohlfeld et al. 2006): The risk of lung cancer was only slightly modified to a higher risk after taking smoking into account.

Conclusion

The present study provides clear evidence of a linear relationship between lung cancer and cumulative radon exposure. There is some evidence of a positive relation between exposure to radon progeny and particularly

cancers of the extrathoracic airways and some other non-respiratory cancers. However, noncausal chance results due to uncontrolled confounding cannot be completely ruled out. There is no indication of a relationship between exposure to radon and cardiovascular diseases. Overall, the pattern of observed risk is compatible with dosimetric calculations for organ doses and confirms the results of other epidemiological studies on miners.

References

Bauer HD (2000) Studie zur retrospektiven Analyse der Belastungs-situation im Uranerzbergbau der ehemaligen SDAG Wismut mit Ausnahme der Strahlenbelastung für die Zeit von 1946 bis 1990. Hauptverband der gewerblichen Berufsgenossenschaften, Sankt Augustin

BEIR (1999) Committee on biological effects of ionizing radiation (BEIR VI). Health effects of exposure to radon—BEIR VI. National Academy Press, Washington DC

Brüske-Hohlfeld I, Schaffrath Rosario A, Wölke G, Heinrich J, Kreuzer M, Kreienbrock L, Wichmann HE (2006) Lung cancer risk among former uranium miners of the Wismut company in Germany. Health Phys 90:208–216

Dahmann D, Bauer HD, Stoyke G (2008) Retrospective exposure assessment for respirable and inhalable dust, crystalline silica and arsenic in the former German uranium mines of SAG/SDAG Wismut. Int Arch Occup Environ Health 81:949–958

Darby SC, Whitley E, Howe GR, Hutchings SJ, Kusiak RA, Lubin JH, Morrison HI, Tirmarche L, Tomásek L, Radford EP (1995) Radon and cancers other than lung cancer in underground miners: a collaborative analysis of 11 studies. J Natl Cancer Inst 87:378–384

Darby SC, Hill D, Auvinen A, Baysson H, Bochicchio F, Deo H, Falk R, Forastiere F, Hakama M, Heid I, Kreienbrock L, Kreuzer M, Lagarde F, Mäkeläinen I, Muirhead C, Oberaigner W, Pershagen G, Ruano-Ravina A, Ruosteenoja E, Rosario AS, Tirmarche M, Tomásek L, Whitley E, Wichmann HE, Doll R (2005) Radon in homes and risk of lung cancer: collaborative analysis of individual data from 13 European case-control studies. BMJ 330:223–227

Grosche B, Kreuzer M, Kreisheimer M, Schnelzer M, Tschense A (2006) Lung cancer risk among German male uranium miners: a cohort study, 1946–1998. Br J Cancer 95:1280–1287

HVBG, BBG (2005) Belastung durch ionisierende Strahlung, Staub und Arsen im Uranerzbergbau der ehemaligen DDR (Version

08/2005). Bergbau BG (BBG), Gera, Hauptverband der gewerblichen Berufsgenossenschaften (HVBG), St. Augustin (CD-Rom)

IARC (1988) Man-made mineral fibres and radon. IARC Monographs on the evaluation of carcinogenic risks to humans, vol 43. IARC, Lyon

Kendall GM, Smith TJ (2002) Doses to organs and tissues from radon and its decay products. J Radiol Prot 22:389–406

Kreuzer M, Kreisheimer M, Kandel M, Tschense A, Grosche B (2006) Mortality from cardiovascular diseases in the German uranium miners cohort study, 1946–1998. Radiat Environ Biophys 45:159–166

Kreuzer M, Walsh L, Schnelzer M, Tschense A, Grosche B (2008) Radon and risk of extrapulmonary cancers: results of the German uranium miners cohort study, 1960–2003. Br J Cancer 99:1946–1953

Kreuzer M, Schnelzer M, Tschense A, Walsh L, Grosche B (2009) Cohort profile: the German uranium miners cohort study (WISMUT cohort), 1946–2003. Int J Epidemiol online first doi:10.1093/ije/dyp216

Krewski D, Lubin JH, Zielinski JM, Alavanja M, Catalan VS, Field RW, Klotz JB, Létourneau EG, Lynch CF, Lyon JL, Sandler DP, Schoenberg JB, Steck DJ, Stolwijk JA, Weinberg C, Wilcox HB (2005) Residential radon and risk of lung cancer: a combined analysis of 7 North American case-control studies. Epidemiology 16:137–145

Laurier D, Tirmarche M, Mitton N, Valenty M, Richard P, Poveda S, Gelas JM, Quesne B (2004) An update of cancer mortality among the French cohort of uranium miners: extended follow-up and new source of data for causes of death. Eur J Epidemiol 19:139–146

Lehmann F, Hambeck L, Linkert KH, Lutze H, Reiber H, Renner HJ, Reinisch A, Seifert T, Wolf F (1998) Belastung durch ionisierende Strahlung im Uranerzbergbau der ehemaligen DDR. Hauptverband der gewerblichen Berufsgenossenschaften, Sankt Augustin

Little MP, Tawn EJ, Tzoulaki I, Wakeford R, Hildebrandt G, Paris F, Tapio S, Elliott P (2008) A systematic review of epidemiological associations between low and moderate doses of ionizing radiation and late cardiovascular effect, and their possible mechanisms. Radiat Res 169:99–109

Little MP, Tawn EJ, Tzoulaki I, Wakeford R, Hildebrandt G, Paris F, Tapio S, Elliott P (2009) Review and meta-analysis of epidemiological associations between low/moderate doses of ionizing radiation and circulatory disease risks, and their possible mechanisms. Radiat Environ Biophys. doi:10.1007/s00411-009-0250-z

Lubin JH, Boice JD, Edling C, Hornung RW, Howe G, Kunz E, Kusiak RA, Morrison HI, Radford EP, Samet JM, Tirmarche M, Woodward A, Xiang YS, Pierce DA (1994) Radon and lung cancer risk: a joint analysis of 11 underground miners studies. NIH, Washington DC

Lubin JH, Wang ZY, Boice JD Jr, Zy Xu, Blot WJ, De Wang L, Kleinerman RA (2004) Risk of lung cancer and residential radon in China: pooled results of two studies. Int J Cancer 109:132–137

Marsh JW, Bessa Y, Birchall A, Blanchardon E, Hofmann W, Nosske D, Tomasek L (2008) Dosimetric models used in the alpha-risk project to quantify exposure of uranium miners to radon gas and its progeny. Radiat Prot Dosimetry 130:101–106

McGale P, Darby SC (2005) Low doses of ionizing radiation and circulatory diseases: a systematic review of the published epidemiological evidence. Radiat Res 163:247–257

Moehner M, Lindtner M, Otten H, Gille HG (2006) Leukemia and exposure to ionizing radiation among German uranium miners. Am J Ind Med 49:238–248

Moehner M, Lindtner M, Otten H (2008) Ionizing radiation and risk of laryngeal cancer among German uranium miners. Health Phys 95:725–733

Preston DL, Lubin JH, Pierce DA, McConney ME (1998) Epicure, release 2.10. HiroSoft, Seattle

Preston DL, Shimizu Y, Pierce DA, Suyama A, Mabuchi K (2003) Studies of mortality of atomic bomb survivors. Report 13: solid cancer and noncancer disease mortality: 1950–1997. Radiat Res 160:381–407

Rericha V, Kulich M, Rericha R, Shore DL, Sandler DP (2006) Incidence of leukemia, lymphoma, and multiple myeloma in Czech uranium miners: a case-control study. Environ Health Perspect 114:818–822

Schnelzer M, Hammer G, Kreuzer M, Tschense A, Grosche B (2009) Accounting for smoking in the radon related lung cancer risk among German uranium miners: results of a nested case-control study. Health Phys (accepted for publication)

Schubauer-Berigan MK, Daniels RD, Pinkerton LE (2009) Radon exposure and mortality among white and American Indian uranium miners: an update of the Colorado Plateau Cohort. Am J Epidemiol 169:718–730

Tomasek L, Zarska H (2004) Lung cancer risk among Czech tin and uranium miners-comparison of lifetime detriment. Neoplasma 51:255–260

Tomasek L, Darby SC, Swerdlow AJ, Placek V, Kunz E (1993) Radon exposure and cancers other than lung cancer among uranium miners in West Bohemia. Lancet 341:919–923

Tomasek L, Swerdlow AJ, Darby SC, Placek V, Kunz E (1994) Mortality in uranium miners in west Bohemia: a long term cohort study. Occup Environ Med 51:308–315

Tomasek L, Rogel A, Tirmarche M, Mitton N, Laurier D (2008) Lung cancer in French and Czech uranium miners: radon-associated risk at low exposure rates and modifying effects of time since exposure and age at exposure. Radiat Res 169:125–137

Vacquier B, Caer S, Rogel A, Feurprier M, Tirmarche M, Luccioni C, Quesne B, Acker A, Laurier D (2008) Mortality risk in the French cohort of uranium miners: extended follow-up 1946–1999. Occup Environ Med 65:597–604

Vacquier B, Rogel A, Leuraud K, Caer S, Acker A, Laurier D (2009) Radon-associated lung cancer risk among French uranium miners: modifying factors of the exposure-risk relationship. Radiat Environ Biophys 48:1–9

Villeneuve PJ, Morrison HI (1997) Coronary heart disease mortality among Newfoundland fluorspar miners. Scand J Environ Health 23:221–226

Villeneuve PJ, Morrison HI, Lane R (2007a) Radon and lung cancer risk: an extension of the mortality follow-up of the Newfoundland fluorspar cohort. Health Phys 92:157–169

Villeneuve PJ, Lane R, Morrison HI (2007b) Coronary heart disease mortality and radon exposure in the Newfoundland fluorspar miners' cohort, 1950–2001. Radiat Environ Biophys 46:291–296

Walsh L, Tschense A, Schnelzer M, Dufey F, Grosche B, Kreuzer M (2009) The influence of radon exposures on lung cancer mortality in German uranium miners, 1946–2003. Radiat Res (accepted for publication)

Xuan XZ, Lubin JH, Li JY, Yang LF, Luo As, Lan Y, Wang JZ, Blot WJ (1993) A cohort study in southern China of tin miners exposed to radon and radon decay products. Health Phys 64:123–131

33. Walsh L, Tschense A, Schnelzer M, Dufey F, Grosche B & Kreuzer M. The Influence of radon exposure on lung cancer mortality in German uranium miners, 1946-2003. Radiat. Res. 173, 79-90, 2010

The Influence of Radon Exposures on Lung Cancer Mortality in German Uranium Miners, 1946–2003

Linda Walsh,[1] Annemarie Tschense, Maria Schnelzer, Florian Dufey, Bernd Grosche and Michaela Kreuzer

Federal Office for Radiation Protection, Department "Radiation Protection and Health", 85764 Oberschleissheim, Germany

Walsh, L., Tschense, A., Schnelzer, M., Dufey, F., Grosche, B. and Kreuzer, M. The Influence of Radon Exposures on Lung Cancer Mortality in German Uranium Miners, 1946–2003. Radiat. Res. 173, 79–90 (2010).

Extensive uranium extraction took place from 1946 until 1990 at the former Wismut mining company in East Germany. A total of 58,987 male former employees of this company form the largest single uranium miners cohort that has been followed up for causes of mortality occurring from the beginning of 1946 to the end of 2003. The purpose of this study was to investigate and evaluate different forms of models for the radon exposure-related lung cancer mortality risk based on 3,016 lung cancer deaths and 2 million person years. Other exposure covariables such as occupational exposure to external γ radiation, long-lived radionuclides, arsenic, fine dust and silica dust are available. The standardized mortality ratio for lung cancer is 2.03 (95% CI: 1.96; 2.10). The simple cohort excess relative risk (ERR/WLM) for lung cancer is estimated as 0.0019 (95% CI: 0.0016; 0.0022). The BEIR VI model produced risks similar to those obtained with a selected mathematically continuous ERR model for lung cancer. The continuous model is linear in radon exposure with exponential effect modifiers that depend on the whole range of age at median exposure, time since median exposure, and radon exposure rate. In this model the central estimate of ERR/WLM is 0.0054 (95% CI: 0.0040; 0.0068) for an age at median exposure of 30 years, a time since median exposure of 20 years, and a mean exposure rate of 3 WL. The ERR decreases by 5% for each unit of exposure-rate increase. The ERR decreases by 28% with each decade increase in age at median exposure and also decreases by 51% with each decade increase in time since median exposure. The method of determination of radon exposure (i.e., whether the exposures were estimated or measured) did not play an important role in the determination of the ERR. The other exposure covariables were found to have only minor confounding influences on the ERR/WLM for the finally selected continuous model when included in an additive way. © 2010 by Radiation Research Society

[1] Address for correspondence: Federal Office for Radiation Protection, Department "Radiation Protection and Health", Ingolstaedter Landstr. 1, 85764 Oberschleissheim, Germany; e-mail: lwalsh@bfs.de.

INTRODUCTION

Early indications of increased lung cancer mortality in miners working in uranium-containing mines [e.g. refs. (*1–3*)] are now known to have been well founded. Recent studies have shown that exposure to the radioactive gas radon (^{222}Rn) and its progeny increases the risk of lung cancer in underground miners exposed to radon (*4–18*). In 1999 the BEIR VI model (*7*) was developed for the analyses of the study of the 11 miner cohorts (*6*) and showed a linear increase in the relative risk of lung cancer with cumulative exposure to radon in working level months (WLM).[2] This proportionate increase was modified by time since exposure, attained age and either exposure rate [exposure-age-concentration (EAC) model] or duration of exposure [exposure-age-duration (EAD) model]. A version of the BEIR VI model (different from the original model in the treatment of the baseline rates; see the Discussion section) was also applied to the first mortality follow-up (1946–1998) of the German uranium miner cohort (*14*), which is of similar size to that of the study of the 11 miner cohorts. The EAC model fit better and produced more relevant results than the EAD model because the exposure rate modified the risk but the duration of exposure did not (*14*). Overall, the observed decrease of the excess relative risk per unit of exposure (ERR/WLM) with increasing attained age and exposure rate in the 11 miner cohorts was confirmed; however, the overall ERR/WLM was lower and the highest ERR/WLM was observed in the time window 15 to 24 years since exposure in contrast to 5 to 14 years in the BEIR VI study.

The Wismut mortality data set has recently been extended by 5 years to provide a second follow-up from 1.1.1946 to 31.12.2003 (*19*) that is based on 58,987 male former employees. This German cohort is currently the

[2] Exposure to radon and its progeny is expressed in WLM. One working level is defined as the concentration of short-lived radon daughters per liter of air that gives rise to 1.3×10^5 MeV of α-particle energy after decay; 1 WLM of cumulative exposure corresponds to exposure to 1 WL during 1 month (170 h) and is equivalent to 3.5 mJ h m^{-3}.

largest single cohort study, with 3,016 deaths occurring from lung cancer and almost 2 million person-years of observation. In the second follow-up, the proportion of individuals lost to follow-up and of missing causes of death was reduced compared to the first follow-up, and data on potential confounders such as exposure to γ radiation, long-lived radionuclides, fine dust, arsenic dust and quartz fine dust are now available (*20, 21*). The Wismut study also has a large number of non-radiation-exposed cohort members that provide a good internal comparison group for the reliable determination of baseline (spontaneous) cancer rates.

The aim of the present analyses of the German uranium miner cohort study is to investigate the shape of the relationship between cumulative radon exposure and lung cancer with age, time and exposure-rate effect modifiers based on the updated data of the second follow-up. For this purpose, the BEIR VI exposure-age-concentration (EAC) model, which was indicated as preferred for the first follow-up (*14*), is re-examined with the updated data. Refined models similar to those currently applied in the Czech and French cohort studies (*16, 17*) are also developed and applied. Effects of potential confounders and different periods with different methods for determination of radon exposure on the radon-induced risk for lung cancer are also examined.

MATERIAL AND METHODS

Cohort Definition, Periods and Mortality Follow-up

Full details of the selection of cohort members and the determination of radiation exposure quantities evaluated by means of a job-exposure matrix (JEM) have already been given (*14, 19, 20, 22*). Radon (^{222}Rn) area measurements in the Wismut mines were carried out from 1955 onward. For the period 1946–1954, radon concentrations were estimated by an expert group based on measurements from 1955, taking into account, for example, the ventilation rate, vein space and uranium content (*14, 23, 24*). The total duration of production for uranium mining by the Wismut company can be divided into three distinct periods (*25*). During the first period from 1946 to 1954, working conditions were characterized by dry drilling, the lack of forced ventilation, and an increasing exposure to radon. Working conditions improved and radon concentrations decreased due to improved ventilation and the replacement of dry drilling by wet drilling in the second period between 1955 and 1970. International radiation protection standards were introduced in the third period from after 1970 up to the company closure in 1990. Follow-up was conducted through local registration offices and district archives for information on vital status or through local health authorities for copies of death certificates. Information on the causes of death before 1989 was partly available from the Wismut pathology archives. Every cohort member contributes to the number of person years starting 180 days after the date of first employment and ending at the earliest of date of loss to follow-up, date of death or end of follow-up (31.12.2003). In the present analyses the former codes of the comparison external baseline rates for the German Democratic Republic were recoded to the 10th ICD code, which was applied throughout.

Analysis

Several types of risk evaluation methods and models based on Poisson regression have been applied here to test for an association between the lung cancer mortality risk and cumulative radon exposure and other agents. In common with other miner studies (*15–17*), a 5-year lag was used in calculating the cumulative exposure to radon for all types of models considered.

BEIR VI Report Model (internal comparison group)

The BEIR VI report exposure-age-concentration (EAC) model was applied here. In this categorical model, baseline rates were dealt with by stratification on attained age and calendar year. A previous analysis of the first follow-up data (*14*) applied a version of the BEIR VI model in which baseline rates were modeled as a parabolic function of attained age. For this reason, the first follow-up data have been reanalyzed here with stratification of the baseline rates as described above. The ERR model part included cumulative exposure, time since exposure, attained age and exposure rate. The latter was calculated as the total cumulative exposure, *w*, measured in working level months, WLM, divided by total duration (with a lag) at each attained age, on the assumption of 11 working months per year. The ERR/WLM was assessed by means of the exposure–response trend parameter, β, which was permitted to vary by categories of several cofactors. To assess effects of exposures occurring in various intervals prior to lung cancer death, cumulative exposure *w* was assigned to four exposure windows. This was done so that $w = w_{5-14} + w_{15-24} + w_{25-34} + w_{35}$, where w_{5-14}, w_{15-24}, w_{25-34} and w_{35} were exposures received 5–14, 15–24, 25–34 and more than 35 years before a given attained age, respectively. Modification to the ERR/WLM by attained age was achieved by considering four age groups with indicator variables, $acat_{<55}$, $acat_{55-64}$, $acat_{65-74}$ and $acat_{75}$, corresponding to <55, 55–64, 65–74 and 75+ years, respectively. Similarly, modification of the ERR/WLM by exposure rate was achieved by considering six groups with indicator variables $ercat_{<0.5}$, $ercat_{0.5-1}$, $ercat_{1-3}$, $ercat_{3-5}$, $ercat_{5-15}$ and $ercat_{15+}$, corresponding to <0.5, 0.5–1.0, 1.0–3.0, 3.0–5.0, 5.0–15.0 and 15+ WL, respectively. The notation of the relative risk (RR) model is

$$RR(w) = 1 + \beta \, w^* a^* E^* \qquad (1)$$

with

$$w^* = \theta_1 w_{5-14} + \theta_2 w_{15-24} + \theta_3 w_{25-34} + \theta_4 w_{35+},$$
$$a^* = \phi_1 \, acat_{<55} + \phi_2 \, acat_{55-64} + \phi_3 \, acat_{65-74} + \phi_4 \, acat_{75+},$$
$$E^* = \gamma_1 ercat_{<0.5} + \gamma_2 ercat_{0.5-1} + \gamma_3 ercat_{1-3} + \gamma_4 ercat_{3-5} + \gamma_5 ercat_{5-15} + \gamma_6 ercat_{15+},$$

where θ_k, $k = 2,\dots 4$ ϕ_l, $l = 2,\dots 4$, and γ_m, $m = 1,\dots 5$ were the fit parameters that can be used for obtaining the required ERR/WLM by adjusting the ERR/WLM at the fixed reference categories $\theta_1 = 1$, $\phi_1 = 1$ and $\gamma_6 = 1$, i.e. β. For example, the relative risk for a worker at 5 to 14 years since exposure, aged under 55 years, with a mean exposure rate between 0.5 and 1.0 WL would be predicted by the model with Eq. (1) as $1 + \beta \, \theta_1 w_{5-14} \phi_1 \gamma_2$.

Data analysis was conducted using Poisson regression with the DATAB and AMFIT modules of the EPICURE software (*26*). All parameters are given with their 95% Wald-type confidence bounds, computed by EPICURE's AMFIT module with exponential reparameterization to avoid range restrictions.

SMR Analysis (external comparison group)

Mortality rates observed in the cohort were compared with those of the general male population in Eastern Germany, formerly the German Democratic Republic. Since external rates were available only from 1960 onward, the standardized mortality ratio (SMR)

analysis was limited to the follow-up period 1960 to 2003, so 18 lung cancers deaths with the corresponding person-years prior to 1960 were excluded. The SMR analysis for lung cancer has been done here in exactly the same way as described previously for extra-pulmonary cancers (*19*).

ERR Parametric Risk Models (internal comparison group)

The rationale for conducting these additional analyses was based mainly on enabling a model-compatible comparison of risks between the Wismut cohort and the French and Czech cohorts (*16*) and obtaining a more parsimonious model than the BEIR VI report model, better suited to building in the other five exposure covariables. Tabulations of person-years at risk and cancer deaths were created with the DATAB module of the EPICURE software (*26*). Age at median exposure and time since median exposure were calculated with reference to median exposures, i.e., when half of the exposure cumulated up to a given date was reached. Cross-classifications were made by attained age, a, in 16 categories (<15, 15–19, 20–24,....., 85+ years), individual calendar year, y, in 58 categories, age at median exposure, e, in seven categories (<20, 20–24, 25–29, 30–34, 35–39, 40–44, >45 years), time since median exposure, t, in six categories (<5, 5–9, 10–14, 15–19, 20–24, >24 years), and cumulative radon exposure, w, in two sets of nine categories (0, >0–9, 10–49, 50–99, 100–199, 200–499, 500–999, 1,000–1,499, 1500+ WLM), with each set corresponding to different methods of exposure determination (referred to as measured, M, and estimated, E). Since the estimated component of exposure also contributes to total exposure beyond 1955, it was not possible to achieve the same components with just nine total exposure groups and a binary covariate (<1955, ≥1955). The exposure rate, er, calculated as the recomputed total cumulative WLM divided by total duration (with a lag) at each attained age, on the assumption of 11 working months per year, was also categorized into six groups (0–0.5, 0.5–1, 1–2, 2–4, 4–10, 10+ WL). The WLM categories were defined to be comparable with other studies (*16*) but with added categories at higher exposures. The tabulated data were fitted to the following model: If $r(a, y, w, er, e, t)$ is the age, year, exposure, exposure rate, age at median exposure and time since median exposure specific lung cancer mortality rate and $r_0(a, y) = r(a, y, 0, 0, 0, 0)$ is the baseline disease rate for non-exposed individuals, $w = 0$, $er = 0$, then

$$r(a, y, w, er, e, t) = r_0(a, y) \times \{1 + \text{ERR}(w, er, e, a, t)\}, \qquad (2)$$

where ERR is the excess relative risk factorized into a function of exposure and a modifying function:

$$\text{ERR}(w, er, e, a, t) = f(w, er) \cdot g(e, a, t). \qquad (3)$$

Several functions of radon exposure were considered, some of which were for direct comparison with the results in ref. (*16*):

$$f(w) = \beta_w \, w, \qquad (4a)$$

$$f(w_E, w_M) = \beta_{wE} w_E + \beta_{wM} w_M, \qquad (4b)$$

$$f(w) = \sum_{j=1,6} \beta_j w_j, \qquad (4c)$$

$$f(w) = \sum_{i=1,9} \beta_i w_i, \qquad (4d)$$

$$f(w, er) = \beta_w \, w \cdot \exp\,[\psi_w(er-3)], \qquad (4e)$$

where the total cumulated radon exposure w was considered as a continuous explanatory variable [Eq. (4a)], in two components, w_E and w_M [Eq. (4b)], where the subscripts indicate different methods

for exposure determination referred to as estimated (E, before 1955) and measured (M, from 1955) cumulative exposures, respectively, with the total exposure variable subdivided into six exposure rate categories [$j = 1$, 6 in Eq. (4c)]; and in nine exposure classes [$i = 1$, 9 in Eq. (4d)].

Similarly, a linear model with a continuous effect modifier for total exposure rate was considered [Eq. (4e)], where the model centering at an exposure rate of 3 WL was chosen to closely match the mean cohort value. Linear-quadratic functions of radon exposure were also considered but are not shown.

The modifying function $g(e, a, t)$ is either in terms of the attained-age model, $\text{ERR}(w, a) = f(w) \cdot g(a)$, the time-since-exposure model, $\text{ERR}(w, t)$, or the age-at-exposure model, $\text{ERR}(w, e)$. In common with previous analyses (*16*), e and t are calendar time-dependent variables, calculated with reference to the median time-lagged exposures, unless otherwise specified (since e = age at first exposure was also tested for goodness of fit). Prior to or in the absence of exposure, $t = 0$ and $e = a$. Three more complicated mixed models, which need to include only any two of the three time variables (a, e, t) because of the linear dependence, $a = e + t$ between them, e.g. $\text{ERR}(w, er, a, e)$, are also considered as alternatives. The preferred models can be determined by applying model selection criteria for nested and non-nested models (*27*), where the latter are defined in the Appendix. The functional form is exponential for age at median exposure and/or attained age and/or time since median exposure where the modifying factors are

$$g(e, a, t) = \exp\,[\alpha(e-30) + \delta(a-50) + \varepsilon(t-20)] \qquad (5)$$

and α, δ and ε are fit parameters. The model centering at an age at median exposure of 30 years, time since median exposure of 20 years, and an age of 50 years were chosen to closely match the mean cohort values and to be consistent with ref. (*16*). The age- and time-modifying patterns, with either one or two of the terms in Eq. (5), were applied to the exposure models given in Eqs. (4a) and (4b) [as in ref. (*16*)] and in Eqs. (4c) and (4e).

To test for the other five agents, external γ radiation, long-lived radionuclides, fine dust, arsenic or quartz, as potential confounders, each of these explanatory variables z_i, $i = 1$, 5, respectively, was added separately to the final preferred model given in Eq. (6), optimized, with fit parameter λ_i, and then removed, with

$$\text{ERR}(w, z_i) = \beta_w \, w \cdot \exp\,[\psi_w(er-3) + \alpha(e-30) + \varepsilon(t-20)]$$
$$+ h(\{\lambda_i z_i\}). \qquad (6)$$

To test for the best model overall, each of these variables z_i, $i = 1$, 5 was included additively to Eq. (6) one by one in a cumulative fashion.

Maximum likelihood with the AMFIT module of the EPICURE software (*26*) was used for estimation of the fit parameters and the internal baseline rates in 928 strata of attained age (16 categories) and individual calendar year (58 categories), chosen to match the grouping that was available in the external rates. Out of these 928 possible strata, 708 actually contained data.

RESULTS

The full cohort pertains to 58,987 cohort members who were male former employees of the Wismut company. Table 1 shows some main characteristics of the first and second follow-ups, which ended on 31.12.1998 and 31.12.2003, respectively. The completeness of the follow-up was improved between the two follow-ups. The observed percentage of cohort members lost to follow-up and the percentage of missing causes

TABLE 1
Details of Important Descriptive Statistics for the Current Second Follow-up (FU 2) Compared with the First Follow-up (FU 1) Period for the Wismut Cohort

End of mortality follow-up:	FU 1: 31.12.1998	FU 2: 31.12.2003
Total number of subjects	59,001	58,987
Total number of person-years	1,801,630	1,996,880
Mean duration of follow-up in years	30.5	34
Vital status		
Alive	39,255 (66.5%)	35,294 (59.8%)
Deceased	16,598 (28.1%)	20,920 (35.5%)
Lost to follow-up	3,148 (5.3%)	2,773 (4.7%)
Year of death (% of causes of death that are known)		
<1970	1,479 (50.6%)	1,560 (58.8%)
1970–1979	3,132 (90.0%)	3,255 (95.1%)
1980–1989	5,368 (91.4%)	5,554 (96.7%)
1990–1999	6,619 (93.3%)	7,538 (96.7%)
2000–2003	—	3,013 (96.9%)
Total	16,598 (88.2%)	20,920 (93.6%)

of deaths were reduced (Table 1). In addition, the number of lung cancer deaths increased from 2,388 to 3,016. The second follow-up is characterized by a vital status of 59.8% alive, 35.5% deceased, and 4.7% lost to follow-up, an average follow-up period of 34 years, a mean duration of employment of 12 years, 1,996,880 person-years of observation, and an average person-year weighted cumulative exposure to radon of 218 WLM.

Important data for other occupational exposure covariables are also available. These are (listed with person-year weighted mean, standard deviation, and maximum values): external γ radiation in units of effective dose in Sv (0.03, 0.06, 0.87), long-lived radionuclides in units of kBq h/m³ (3.0, 6.4, 132.2), fine dust in units of dust-years (31.7, 42.3, 315.2), arsenic in units of dust-years (30.4, 84.5, 1417.4), and quartz in units of dust-years (5.2, 7.4, 56.0), where 1 dust-year is defined as an exposure to 1 mg/m³ fine dust or silica dust and 1 µg/m³ for arsenic over 220 8-h shifts. Arsenic exposures occurred in Saxony mines but were absent in Thuringia mines, so data on arsenic exposure are available for 18,234 cohort members.

BEIR VI Report Model (internal comparison group)

The results presented here update the previous results (*14*) with an additional 5 years of follow-up and improved data collection. Considering just the EAC

model, it can be seen from Table 2 that the risks for the first and second follow-ups are highest 5–14 years after exposure. There are lower risks in the other three categories of time since exposure and the confidence limits for these three groups overlap. The results in Table 2 also show that the decline of risk with attained age is notable, the effect of concentration (or exposure rate) is very strong, and an inverse exposure-rate effect is indicated; i.e. the risk per unit of exposure increases with decreasing exposure rate. Considering the EAD model, the main results for the second follow-up are very similar to those presented previously (*14*) and therefore are not shown here: The ERR/WLM was not modified by duration of exposure, and the estimates for the other two parameters are only slightly different from those using the EAC model.

SMR Results (external comparison group)

The number of deaths (1960–2003) observed, corrected for missing causes of death for lung cancers (O*), was significantly higher than expected (E) from national rates (SMR* = O*/E = 2.03, 95% CI: 1.96; 2.10). A statistically significant cumulative radon exposure effect was observed (ERR/WLM=0.0024; 95% CI: 0.0023; 0.0026%).

ERR Parametric Risk Models (internal comparison group)

1. Cohort radon risk (no modifying factors)

A statistically significant cumulative radon exposure effect was observed (ERR/WLM = 0.0019; 95% CI: 0.0016; 0.0022). This excess risk is lower than that quoted in the last paragraph mainly due to the differences between the internal and external comparison groups; i.e., the external baseline rates were found to be lower than the internal baseline rates by 16.5% (95% CI: 9; 24%) on average.

Figure 1 shows the results of fitting an ERR model [Eq. (4d)] that is categorical in nine classes of cumulative radon exposure along with the linear model described above. It can be seen from this figure that there is an indication for a non-linear exposure response. However, as will be seen below, this indication is unfounded when all relevant effect modifiers are correctly accounted for.

2. Continuous risk models with effect-modifying factors

a. Time and age patterns

The time and age patterns are very similar for all of the different radon exposure models investigated [Table 3 and Eqs. (4a), (4b), (4c) and (4e)]. Numerical details for the preferred model selection are given in Tables A1 and A2 of the Appendix. The preferred

TABLE 2
Results (with 95% Confidence Intervals) for the BEIR VI EAC Model for Three Data Sets: the Wismut First Follow-up (FU 1, 1946–1998), the Wismut Second Follow-up (FU 2, 1946–2003), and the Pooled Data from the 11-Cohort Study that was used by BEIR VI (6, 7)

Data set	FU 1: to 31.12.1998	FU 2: to 31.12.2003	BEIR VI
Observed lung cancer cases	2,388	3,016	2,705
Estimated excess cases	1217.51 (51.0%)	1413.14 (46.9%)	–
%ERR/WLM	0.50 (0.18–0.83)	0.57 (0.24–0.90)	0.83
Time since exposure (years)			
5–14	1.0	1.0	1.0
15–24	0.69 (0.32–1.06)	0.71 (0.36–1.07)	0.78
25–34	0.49 (0.23–0.75)	0.49 (0.25–0.74)	0.51
35+	0.33 (0.13–0.53)	0.36 (0.16–0.55)	
Attained age (years)			
<55	1.0	1.0	1.0
55–64	0.49 (0.31–0.79)	0.46 (0.30–0.71)	0.57
65–74	0.32 (0.20–0.54)	0.31 (0.19–0.50)	0.29
75+	0.38 (0.19–0.76)	0.32 (0.17–0.59)	0.09
Exposure rate (WL)			
<0.5	6.14 (3.14–12.01)	4.64 (2.46–8.74)	9.09
0.5–1.0	3.56 (1.89–6.71)	2.84 (1.57–5.14)	4.45
1.0–3.0	2.76 (1.81–4.19)	2.24 (1.56–3.22)	3.36
3.0–5.0	2.35 (1.57–3.52)	2.01 (1.42–2.84)	2.91
5.0–15.0	1.98 (1.34–2.92)	1.69 (1.21–2.35)	1.55
15.0+	1.0	1.0	1.0

Notes. The EAC model estimates exposure related lung cancer risk using time since exposure, attained age and exposure rate (concentration) categories. The %ERR/WLM is the value taken at the reference categories of attained age, time since exposure and exposure rate (i.e. those with parameter values fixed at 1.0, which are for the categories for age attained <55 years, 5–14 years since exposure and for exposure rates of 15 WL+).

models include exponential effect modifiers that depend on any two of the three age/time parameters, chosen here to be age at median exposure and time since median exposure. In these models, the central estimate of ERR is always given for an age at median exposure of 30 years and a time since median exposure of 20 years. The estimated age at median exposure effect for the preferred models indicates that the ERR decreases by about 30% $[=1 - \exp(10\alpha)$, with parameter values from Table 3] with each decade of increase in age at median exposure. Similarly, the ERR decreases by about 50% with each decade increase in time since median exposure. The same patterns hold for a set of models analogous to those in Table A1 but with age at first exposure instead of age at median exposure and time since first exposure instead of time since median exposure (results not shown). However, the quality of model fit for this sequence of models relating to first exposures was found to be either similar or in most cases significantly worse compared to the sequence of models relating to median exposures. It is also possible in theory to use models based on last exposures; however, since radiation sensitivity tends to decrease with increasing age and since the safety standards in mining improve continually, there is more practical value in applying either age at first exposure or age at median exposure.

b. Measured and estimated radon exposure effects

The sequence of radon exposure models given by Eqs. (4a) and (4b) matches those investigated by Tomasek *et al.* (*16*). It can be seen from Table A1 in the Appendix by applying model selection techniques for non-nested models (i.e. AIC and BIC as defined in the Appendix) that the splitting of the exposures into two classes that correspond to measured and estimated exposure is not associated with a statistically significant improvement in the model.[3] This can also be seen from Table 3 since the ERR/WLM from estimated exposures, β_{wE}, is not significantly different from the ERR/WLM from measured exposures, β_{wM}. Consequently the separation into estimated and measured exposures was omitted in the final phase of model construction and selection. However, for completeness of comparison with the sequence of radon exposure scenarios investigated by Tomasek *et al.* (*16*), the fit parameters for the preferred models with effect modifiers are given in Table 3.

[3] Model f(w) · g(e, t) has an AIC of 26504.5 and model f(w_E, w_M) · g(e, t) has an AIC of 26503.7, i.e. ΔAIC = –0.8, and is only associated with the positive level of evidence for model improvement, in terms of the BIC goodness of fit criterion, in favor of the simpler model [i.e., the simpler model f(w) · g(e, t) has a BIC of 26522.6 and model f(w_E, w_M) · g(e, t) has a BIC of 26527.7, i.e. ΔBIC = +5.1].

FIG. 1. A categorical excess relative risk (ERR) model for lung cancers and radon exposure with no age and time effect modifiers. The exposure category ERR fit parameters are shown as crosses in the graph with ±2 SD and the central estimate (solid line) and 95% CI (dashed lines) from the model for the cohort risk (with internal comparison groups).

Since Fig. 1 indicated a non-linear radon exposure response, the sequence of models, checked for goodness of fit in Table A1, was repeated with the addition of an exposure squared term (equations not shown). This second sequence of models is not documented here but showed that the addition of the exposure squared term results in significant model improvement for all exposure models except when the exposure rate is explicitly included.

3. The final continuous model including exposure-rate effects

A finally selected ERR model that is clearly preferred among all the continuous models considered (see Table A2 and parameter values in Table 3) is linear in radon exposure with exponential effect modifiers that depend on age at median exposure, time since median exposure, and radon exposure rate. In this model the central estimate of ERR/WLM is 0.0054 (95% CI: 0.0040; 0.0068) for mean age at median exposure of 30 years, mean time since median exposure of 20 years, and an exposure rate of 3 WL. The estimated age at median exposure effect for the preferred model indicates that the ERR decreases by 28% [= 1 – exp(10α), with parameter values from Table 3] with each decade of increase in age at median exposure. This central ERR also decreases by 5% for each exposure-rate increase of 1 WL. Similarly, the ERR decreases by 51% with each decade of increase in time since median exposure. An alternative formulation of this model that has the same deviance but includes the attained age covariable instead of the age at median exposure covariable is given in Table A3 of the Appendix. Although the inclusion of an exposure-rate effect

modification in the best model is unequivocally indicated, it should be noted that the indication for the exponential nature of the exposure-rate effect modification is rather weak. An alternative model with a linear function for the exposure-rate effect modification fitted only slightly less well (with ΔAIC = +0.3). As a double check on radon exposure linearity in the final preferred model, a quadratic radon exposure parameter was added to this preferred continuous model, resulting in a deviance drop of only 1.1 and a small fit parameter for the quadratic term, which was not statistically significant ($P = 0.28$).

A model that is categorical in exposure rate [Eqs. (4c) and (5)] is also given in Table 3 and Fig. 2 and is useful for investigating the strength of the exposure-rate effect. Table 4 presents the finally selected preferred model optimized with the radon exposures cut off at several different upper limits of under 1500, 1000, 500, 200 and 100 WLM. It can be seen from Table 4 that the central value of ERR/WLM increases from 0.0054 to 0.0111 if only exposures under 100 WLM are considered. This trend is consistent with that seen in Fig. 2 for the model that is categorical in total exposure rate.

4. The finally selected continuous model with other exposure covariables

The potential confounding effects of external γ radiation, long-lived radionuclides, fine dust, arsenic and quartz exposures (z_i, i = 1, 5, respectively) on the central radon risk from the finally selected continuous model were investigated with the model given in Eq. (6) fitted to a restricted data set that excluded 310 cohort members with invalid values for dust exposure. However, the resulting parameter values (not shown in detailed tables) indicated that the central ERR/WLM estimate of 0.0059 for this restricted data set is not influenced to any notable degree by the additive inclusion of these covariables, i.e., the model-to-model variation in the radon ERR/WLM; i.e., the β_w central estimate ranged from 0.0055 to 0.0060. To test for the best model overall, each of these covariables z_i, i = 1, 5 was also added one by one in a cumulative fashion; the results indicated that ERR/WLM estimate is not influenced to any notable degree by the inclusion of these covariables, i.e., the model-to-model variation in the radon ERR/WLM; i.e., where the β_w central estimate ranged from 0.0059 to 0.0047, where the lower value resulted with the model with all exposure covariables, However, it should be noted that the highest correlation between exposure variables occurs between quartz and fine dust ($\rho = 0.92$), which results in a variance inflation factor (VIF) of over 10— an indication that both exposure variables should not really be included simultaneously in the same model; however, further work is required to clarify this. When the model with all exposure covariables was excluded, the corresponding range in the β_w central estimate was 0.0059 to 0.0055.

TABLE 3
**ERR Models for Radon Exposure, Simple Models without Adjustment for Age and Time Effects and the Preferred
Models from Table A1 with Exponential Age and Time Effect Modifiers and Linear Radon Exposures**

Model description	Parameter name	Fitted value	Mean exposure (WLM)
$f(w)$	β_w	0.19 (0.16; 0.21)	218
$f(w) \cdot g(e, t)$	β_w	0.40 (0.30; 0.50)	218
	$\exp(10\alpha)$	0.70 (0.58; 0.83)	
	$\exp(10\varepsilon)$	0.50 (0.42; 0.59)	
$f(w_\mathrm{E}, w_\mathrm{M}) \cdot g(e, t)$	$\beta_{w\mathrm{E}}{}^{a}$	0.34 (0.22; 0.45)	96
	$\beta_{w\mathrm{M}}{}^{a}$	0.45 (0.32; 0.57)	122
	$\exp(10\alpha)$	0.70 (0.58; 0.83)	
	$\exp(10\varepsilon)$	0.50 (0.42; 0.59)	
$f(w,er) \cdot g(e, t)$	β_w	0.54 (0.40; 0.68)	
	$\exp(\psi_w)$	0.95 (0.93; 0.96)	
	$\exp(10\alpha)$	0.72 (0.60; 0.87)	
	$\exp(10\varepsilon)$	0.49 (0.42; 0.58)	
$f(w) \cdot g(e, t)$	β_1	1.28 (0.53; 2.03)	0.13
	β_2	0.73 (0.32; 1.14)	0.72
	β_3	0.57 (0.35; 0.79)	1.48
	β_4	0.50 (0.35; 0.64)	2.98
	β_5	0.46 (0.34; 0.58)	6.34
	β_6	0.30 (0.21; 0.39)	13.5
	$\exp(10\alpha)$	0.71 (0.59; 0.85)	
	$\exp(10\varepsilon)$	0.49 (0.42; 0.59)	

Notes. The covariables are w, for total exposure, w_E, the estimate component of exposure, w_M, the measured component of exposure, er, exposure rate, e, age at median exposure and t, time since median exposure. The ERR fit parameters (i.e. the β's) are in units of %ERR/WLM, with model centering, where applicable, at an age at median exposure of 30 years [relevant parameter is $\exp(10\alpha)$] and a time since median exposure of 20 years [relevant parameter is $\exp(10\varepsilon)$] and at an exposure rate of 3 WL [relevant parameter is $\exp(\psi_w)$]. All fit parameters are quoted with 95% Wald-type confidence intervals.
[a] These parameter values are not significantly different from each other ($P = 0.20$).

DISCUSSION

This is an updated lung cancer risk analysis of the German uranium miner Wismut cohort. The main analyses have been done according to the methods used both in Tomasek *et al.* (*16*) and for the joint analysis of 11 radon-exposed miner cohorts (*7*). The Wismut cohort is comparable to these 11 jointly analyzed cohorts in size and in the number of lung cancer cases, but it has a longer duration of follow-up. Moreover, the cohort is more homogeneous than the group of 11 cohorts in several aspects: All cohort members have the same geographical and societal background, follow-up was conducted in the same manner, exposure estimates are based on the same JEM for all cohort members, and causes of deaths were coded by trained staff using ICD-10 (*28*).

The main strength of the Wismut study lies in its size and homogeneity, which allows the verification of current knowledge on lung cancer risk from underground occupational exposure to radon and its progeny based on an independent data set. The percentage of cohort members that have been lost to follow-up is small, which is particularly impressive taking into account the late start of the study in 1994. Exposure estimates are based on a job–exposure matrix, which gives best exposure estimates on a daily basis. The cohort also includes a large number of individuals with low radon exposures, allowing the estimation of lung cancer risk for levels close to those measured in a normal housing environment (*29*).

Limitations of the study are possible uncertainties in exposures, which are more pronounced for the early years of mining, and the lack of complete smoking information and other information on confounders such as diesel fumes and asbestos. The possible effect of smoking on the radon-associated lung cancer risk cannot be evaluated completely in the full cohort. Most of the former Wismut employees had been smokers. However, information on smoking was collected within a nested case–control study where the resulting radon-related lung cancer risks, calculated with and without adjustment for smoking, were very similar (*30*). An earlier case-control study on lung cancer in Wismut miners (*13*) reported a slight inverse correlation between radon exposure and smoking and only a minor confounding effect.

Another potential limitation of the study is that the ascertainment of cause of death was not very good (<60%) for the period before 1970 (Table 1). To test whether this potential limitation affected the results, a binary covariable (<1970, ≥1970) was used to multiply the main risk in the finally selected continuous model. The results are that the central estimate with 95% CI of 0.54 (0.40; 0.68) given in Table 3 becomes 0.43 (0.18; 0.68) and 0.57 (0.41; 0.73) for before and from 1970, respectively. The difference in these latter two risks is
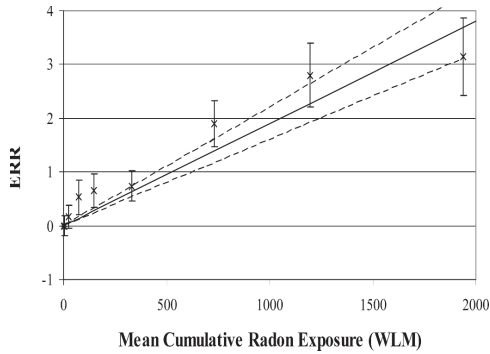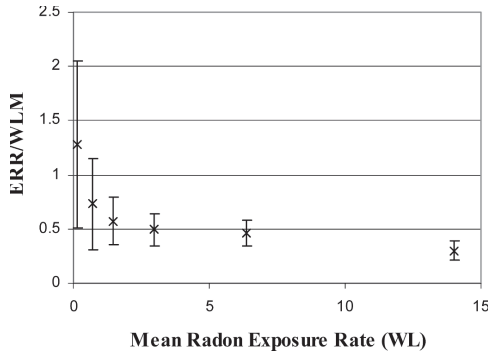
FIG. 2. A categorical excess relative risk (ERR) model for lung cancers and radon exposure rate with exponential age and time effect modifiers. The exposure rate category ERR fit parameters are shown as crosses in the graph with ±2 SD with model centering at an age at median exposure of 30 years and a time since median exposure of 20 years.

not statistically significant ($P = 0.37$), and the numerical values of the risk-modifying factors remain very stable between the two models.

There is a difference in the magnitude of the overall ERR/WLM (0.0019) from the parametric risk model (with an internal comparison group and no effect modifiers) and that presented in Table 2 for the second follow-up (0.0057) that is due to normalization. This difference arises because the former risk is for the whole cohort and is not centered or normalized to any specific values of age or time effect modifiers but the ERR/WLM in Table 2 is for age attained <55 years, 5–14 years since exposure and exposure rates of 15 WL+. It is also interesting to note that the continuous model that was preferred by model selection techniques from the many possible continuous modes investigated in Table A2 of the Appendix is not substantially different from the BEIR VI EAC model in the central risk estimates; however, the uncertainties associated with the latter model are somewhat larger.

Comparisons of Results with the 11-Cohort BEIR VI Analysis and the French and Czech Cohorts

The risks obtained here can be compared directly to those from the 11-cohort analysis with the EAC model, which was originally developed for the BEIR VI analysis (*7*). The ERR/WLM taken at the same reference categories as applied in BEIR VI was found here to be 0.57 (95% CI: 0.24; 0.90), which is close to the corresponding BEIR VI value of 0.83 (but no confidence interval was given). In common with the 11-cohort BEIR VI analysis, it has been shown that the risk is highest 5–14 years after exposure, while there are lower risks in the other three categories of time since exposure. These results for the second follow-up are now generally more consistent with BEIR VI than the earlier results for the first follow-up (*14*). Like the results from the first follow-up (*14*), the second follow-up results show that the decline of risk with attained age is notable, the effect of exposure rate is very strong with an inverse effect indicated, and the ERR/WLM from the EAD model was not modified by duration of exposure.

The results published previously for the first follow-up (*14*) were not computed in a way that was totally compatible with the BEIR VI model and the new second follow-up results in Table 2. This is because a parametric function (parabolic) of attained age was applied in the modeling of the baseline (spontaneous) lung cancer mortality rates in the previous study (*14*). BEIR VI and the FU2 employed stratification on attained age and calendar year for modeling the baseline rates. Table 2 contains the recomputed BEIR VI model for the first follow-up with the same stratification of the baseline rates. Comparison of the recomputed first follow-up results in Table 2 with those of the previous study (*14*) shows that the model parameters in Table 2 are much more consistent between the first follow-up and the second follow-up, and the highest ERR/WLM is now observed in the time window 5 to 14 years since exposure [instead of the 15- to 24-year window (*14*)]. The first follow-up results in Table 2 are also more consistent with BEIR VI than the results of the previous study (*14*) were.

TABLE 4
The Preferred WISMUT ERR Model for Radon Exposure with Different Values of Exposure Cut-off

Model description	Exposure cut-off (WLM)	Fitted value parameter β_w	$\exp(\psi_w)$	P value for $\exp(\psi_w)$	$\exp(10\alpha)$	$\exp(10\varepsilon)$
f(w, er) · g(e, t)	< 1500	0.55 (0.40; 0.70)	0.95 (0.93; 0.97)	< 0.001	0.73 (0.61; 0.89)	0.50 (0.41; 0.59)
f(w, er) · g(e, t)	< 1000	0.54 (0.37; 0.71)	0.94 (0.91; 0.97)	< 0.001	0.78 (0.62; 0.96)	0.48 (0.39; 0.59)
f(w, er) · g(e, t)	< 500	0.45 (0.25; 0.65)	0.83 (0.75; 0.92)	< 0.001	0.86 (0.63; 1.19)	0.39 (0.28; 0.54)
f(w, er) · g(e, t)	< 200	0.67 (0.23; 1.11)	0.74 (0.58; 0.95)	0.0193	0.71 (0.46; 1.09)	0.44 (0.29; 0.68)
f(w, er) · g(e, t)	< 100	1.11 (0.10; 2.11)	0.88 (0.60; 1.28)	0.492	0.64 (0.35; 1.16)	0.38 (0.20; 0.70)

Notes. The covariables are w, for total exposure, er, exposure rate, e, age at median exposure and t, time since median exposure. The ERR fit parameter, β_w is in units of %ERR/WLM, with model centering, at an age at median exposure of 30 years [relevant parameter is $\exp(10\alpha)$] and a time since median exposure of 20 years [relevant parameter is $\exp(10\varepsilon)$] and at an exposure rate of 3 WL [relevant parameter is $\exp(\psi_w)$]. All fit parameters are quoted with 95% Wald-type confidence intervals.

A joint analysis of the French and Czech cohorts of uranium miners, which are smaller than the Wismut cohort and are characterized by generally lower levels of exposure and lower exposure rates, was published in 2008 (16). In contrast to these most recent French and Czech results, where a ratio of the ERR with respect to estimated exposures to the ERR with respect to measured exposures of 0.22 (95% CI: 0.02–0.57) was quoted [Table 4 of ref. (16)], no difference in measured and estimated ERR risks was found here [corresponding ratio for the Wismut cohort = 0.76 (95% CI: 0.43; 1.08), see also Table 3].

The overall best estimate of ERR/WLM, centered at an age at median exposure of 30 years and a time since median exposure of 20 years from measured exposures for the combined analysis of the French and Czech cohorts of 0.042 (95% CI: 0.024–0.072) [Table 4 of ref. (16)], is much larger than the corresponding quantity from the finally selected continuous model (Table 3) of 0.0054 (0.0040; 0.0068). A possible explanation for this difference could be that the French and Czech cohorts have much lower average exposure rates and lower mean exposures than the Wismut cohort. In connection with this issue, it can be seen from Table 4 that the central ERR/WLM estimate shifts from 0.0054 to 0.0111 (95% CI: 0.0010; 0.0211) with an exposure cut-off at 100 WLM, and that the model that is categorical in exposure rate (Fig. 2) also has an upper 95% CI for ERR/WLM of over 0.02 for the lowest exposure-rate category. Another factor that could partially explain this discrepancy lies in the inherent differences in the baseline (spontaneous) cancer rates. The internal baseline rates for Wismut cohort members are significantly higher than the external (general population-based) baseline rates for East Germany. The French and Czech cohorts generally have a paucity of internal baseline cases and the analyses usually use the external rates; if such a difference were also present in the French and Czech cohorts, this could partially account for their higher excess risks.

The age at median exposure and time since median exposure effect modifiers given for the French and Czech cohorts [Table 4 of ref. (16)] are in good agreement with those in Table 3.

An analysis of the exposure-rate effect for the French and Czech cohorts (16) could be conducted only for the combined data due to the low number of cancers in the separate studies, and the results suggested no exposure-rate effect. This is in contrast to the results presented here where a parameter for the exposure-rate effect modification could be determined, was found to be statistically significant, and resulted in an effect modification to the central ERR that decreases by 5% for each unit of increase in exposure rate. It can be seen from Table 4 that this effect modification became stronger as the exposure cut-off was progressively

reduced until the exposure-rate effect finally became statistically insignificant. This lack of an inverse exposure-rate effect for data restricted to exposures below 100 WLM has been reported previously (7, 14).

The Effects of Other Exposure Covariables on the Radon Risk

Since dust and arsenic can be present in the working environment of the German uranium miners, a separate JEM for dust exposures is available. This made an assessment of the magnitude of the potential confounding effect of fine dust, arsenic and quartz possible. Gamma-ray exposure data are also available. These exposures are known to be a risk factor for lung cancer mortality from analyses on the Japanese atomic bomb survivors (31).

The finally selected continuous model was used to assess the confounding effects of five covariables mentioned above, first by assessing the additive inclusion of each exposure covariable in the finally selected continuous model one at a time. However, the central ERR/WLM estimate was not found to be influenced to any notable degree by the additive inclusion of these covariables. Second, the additive inclusion of each exposure covariable in the finally selected continuous model was considered in a cumulative fashion. Here also, the central ERR/WLM estimate was not found to be influenced to any notable degree. Other sets of analogous models were also optimized that had the exposure covariables inside the radon time and age effect modification; however, these models did not generally fit as well as the models mentioned above.

CONCLUSION AND PERSPECTIVES

The BEIR VI EAC categorical model and a finally selected continuous model both produce very similar central risk estimates that are compatible with the risks presented in the 11-cohort BEIR VI analysis (7). The clearly preferred (among the continuous models) and parsimonious "Wismut model", with only four parameters required to adequately model the ERR/WLM, has been developed and presented here. This model is linear in cumulative radon exposure and has exponential effect modifiers that depend on age at median exposure, time since median exposure, and radon exposure rate. The inverse exposure-rate effect has also been investigated by applying different exposure cut-off values to the Wismut model, and it was found to become stronger with decreasing cut-off, until finally disappearing with a 100 WLM cut-off. The potential confounding effects of five other exposure covariables, for which new data are available, were investigated, but no strong confounding effects were observed. The present study also stresses that the method of exposure determination in the

WALSH *ET AL.*

TABLE A1
Goodness-of-Fit Criteria for Radon Exposure Risk Models that are Linear in Exposure

Model description	Deviance	Number of parameters	AIC	BIC	ΔDeviance with respect to f(w)	ΔAIC = ΔBIC (P value for model improvement)	Bayesian evidence for model improvement
f(w)	26567.5	1	26569.5	26575.5	0.0		
f(w) · g(e)	26567.2	2	26571.2	26583.3	0.3	52.4 (< 0.05)	v. strong
f(w) · g(t)	26515.2	2	26519.2	26531.2	52.3	0.3 (>0.5)	weak
f(w) · g(a)	**26514.8**	2	**26518.8**	**26530.9**	52.7	*preferred model in group of 3*	
f(w) · g(e, t)ᵃ	**26498.5**	3	**26504.5**	**26522.6**	69.0		
f(w_E, w_M)	26563.9	2	26567.9	26580.0	3.6		
f(w_E, w_M) · g(e)	26563.7	3	26569.7	26587.7	3.8	51.7 (<0.05)	v. strong
f(w_E, w_M) · g(t)	26512.3	3	26518.3	26536.4	55.2	0.4 (>0.5)	weak
f(w_E, w_M) · g(a)	**26512.0**	3	**26518.0**	**26536.0**	55.5	*preferred model in group of 3*	
f(w_E, w_M) · g(e, t)ᵃ	**26495.7**	4	**26503.7**	**26527.7**	71.8		

Notes. The covariables are w, total exposure, w_E, the estimate component of exposure, w_M, the measured component of exposure, er, exposure rate, e, age at median exposure, t, time since median exposure, and a, attained age. The bold entries indicate the preferred model in each non-nested model set and the bold and underlined entries the preferred model overall.
ᵃ The deviance for model f(w) · g(e, t) is the same as that for models f(w) · g(a, t) and f(w) · g(a, e). The deviance for model f(w_M, w_E) · g(e, t) is the same as that for models f(w_M, w_E) · g(a, t) f(w_M, w_E) · g(a, e).

Wismut cohort is not an important factor that could influence results.

The risk analyses presented here in terms of radon exposures could also be performed with respect to organ doses, which are currently being quantified in the ALPHA-RISK project funded by the EU (*32*). Further work is also required to investigate the effects of radon combined with other exposure covariables such as occupational exposure to external γ radiation, long-lived radionuclides, arsenic, fine dust and silica dust.

APPENDIX

The general problem of choosing among non-nested models with different numbers of parameters has recently been reviewed (*27*). One approach involves an information theoretic extension of the maximum likelihood principle, as originally suggested by Akaike (*33, 34*). This approach amounts to maximizing the likelihood function separately for each model j, obtaining the likelihood M_j and then choosing the model that minimizes the Akaike Information Criterion (*AIC*),

$$AIC = -2\ln(M_j) + 2k_j, \tag{A1}$$

where k_j is the number of fit parameters in the model (i.e., the number of values that are estimated from the data) and the first term on the right hand side of Eq. (A1) is just the familiar deviance. Thus an arbitrary model A is considered to be an improvement of another model B with 95% probability if the *AIC* for model A is smaller than the *AIC* for model B by 5.9 points, i.e. $\Delta AIC = -5.9$

Another information criterion involves evaluating the leading term in the asymptotic expansion of the Bayes solution as suggested by Schwarz (*35*). Then the relevant procedure for model selection involves choosing the model that minimizes the Bayes Information Criterion (*BIC*), where the *BIC* is often defined to be minus twice the Schwarz criterion (*35*):

$$BIC = -2\ln(M_j) + k_j\ln(n), \tag{A2}$$

where n is the number of deaths from lung cancer, as proposed by Volinsky and Raftery (*36*). The evidence for model improvement is positive, strong or very strong, if the difference in the *BIC* values, between two competing models, lies in the ranges of 2 to 6, 6 to 10, and 10 and above, respectively.

ACKNOWLEDGMENTS

TABLE A2
Goodness-of-Fit Critera for Radon Exposure Risk Models that are Linear in Exposure with an Exponential Modifier for Exposure Rate

Model description	Deviance	Number of parameters	AIC	BIC	ΔDeviance with respect to f(w)	ΔAIC = ΔBIC (P value for model improvement)	Bayesian evidence for model improvement
f(w)	25740.5	1	25742.5	25748.6	0		
f(w, er)	25709.2	2	25713.2	25725.2	31.4		
f(w, er) · g(e)	25707.9	3	25713.9	25732.0	32.6	59.5 (<0.05)	v. strong
f(w, er) · g(t)	**25648.4**	3	**25654.4**	**25672.4**	92.1	*preferred model in group of 3*	
f(w, er) · g(a)	25657.3	3	25663.3	25681.4	83.2	8.9 (<0.05)	strong
f(w, er) · g(e, t)ᵃ	**25634.7**	4	**25642.7**	**25666.7**	105.9		

Notes. The covariables are w, total exposure, er, exposure rate, e, age at median exposure, t, time since median exposure, and a, attained age. The bold entries indicate the preferred model in each non-nested model set and the bold and underlined entries the preferred model overall.
ᵃ The deviance for model f(w, er) · g(e, t) is the same as that for models f(w, er) · g(a, t) and f(w, er) · g(a, e).

TABLE A3
Alternative Preferred Continuous ERR Model
for Radon Exposure, with Exponential Attained
Age and Time Effect Modifiers and Linear
Radon Exposures

Model description	Parameter name	Fitted value
$f(w, er) \cdot g(a, t)$	β_w	0.54 (0.40; 0.68)
	$\exp(\psi_w)$	0.95 (0.93; 0.96)
	$\exp(10\delta)$	0.72 (0.60; 0.87)
	$\exp(10\varepsilon)$	0.68 (0.58; 0.79)

Notes. The covariables are w, total exposure, er, exposure rate, a, attained age and t, time since median exposure. The ERR fit parameters (i.e. the β's are in units of %ERR/WLM, with model centering at an attained age of 50 years [relevant parameter is $\exp(10\delta)$] and a time since median exposure of 20 years [relevant parameter is $\exp(10\varepsilon)$] and at an exposure rate of 3 WL [relevant parameter is $\exp(\psi_w)$]. All fit parameters are quoted with 95% Wald-type confidence intervals.

REFERENCES

1. W. C. Hueper, *Occupational Tumors and Allied Diseases*, pp. 435–456. C C Thomas, Springfield, IL, 1942.

2. E. Lorenz, Radioactivity and lung cancer: A critical review of lung cancer in the mines of Schneeberg and Joachimsthal. *J. Natl. Cancer Inst.* **5**, 1 (1944).

3. V. E. Archer, H. J. Magnuson, D. A. Holaday and P. E. Lawrence, Hazards to health in uranium mining and milling. *J. Occup. Med.* **4**, 55–60 (1962).

4. R. W. Hornung and T. J. Meinhardt, Quantitative risk assessment of lung cancer in U.S. uranium miners. *Health Phys.* **52**, 417–430 (1987).

5. L. Tomasek, S. C. Darby, T. Fearn, A. J. Swerdlow, V. Placek and E. Kunz, Patterns of lung cancer mortality among uranium miners in West Bohemia with varying rates of exposure to radon and its progeny. *Radiat. Res.* **137**, 251–261 (1994).

6. J. H. Lubin, J. D. Boice, Jr., C. Edling, R. W. Hornung, G. Howe, E. Kunz, R. A. Kusiak, H. I. Morrison, E. P. Radford and S. X. Yao, Radon-exposed underground miners and inverse dose-rate (protraction enhancement) effects. *Health Phys.* **69**, 494–500 (1995).

7. National Research Council, Committee on the Biological Effects of Ionizing Radiation, *Health Effects of Exposure to Radon (BEIR VI)*. National Academy Press, Washington, DC, 1999.

8. R. W. Hornung, Health effects in underground uranium miners. *Occup. Med.* **16**, 331–344 (2001).

9. L. Tomasek, Czech miner studies of lung cancer risk from radon. *J. Radiol. Prot.* **22**, A107-1 (2002).

10. A. Rogel, D. Laurier, M. Tirmarche and B. Quesne, Lung cancer risk in the French cohort of uranium miners. *J. Radiol. Prot.* **22**, A101-6 (2002).

11. L. Tomasek and H. Zarska, Lung cancer risk among Czech tin and uranium miners-comparison of lifetime detriment. *Neoplasma* **51**, 255–260 (2004).

12. D. Laurier, M. Tirmarche, N. Mitton, M. Valenty, P. Richard, S. Poveda, J. M. Gelas and B. Quesne, An update of cancer mortality among the French cohort of uranium miners: extended follow-up and new source of data for causes of death. *Eur. J. Epidemiol.* **19**, 139–146 (2004).

13. I. Brüske-Hohlfeld, A. S. Rosario, G. Wolke, J. Heinrich, M. Kreuzer, L. Kreienbrock, and H. E. Wichmann, Lung cancer risk among former uranium miners of the WISMUT Company in Germany. *Health Phys.* **90**, 208–216 (2006).

14. B. Grosche, M. Kreuzer, M. Kreisheimer, M. Schnelzer and A. Tschense, Lung cancer risk among German uranium miners: a cohort study, 1946–1998. *Br. J. Cancer* **95**, 1280–1287 (2006).

15. P. J. Villeneuve, H. I. Morrison and R. Lane, Radon and lung cancer risk: an extension of the mortality follow-up of the Newfoundland fluorspar cohort. *Health Phys.* **92**, 157–169 (2007).

16. L. Tomasek, A. Rogel, M. Tirmarche, N. Mitton and D. Laurier, Lung cancer in French and Czech uranium miners: Radon-associated risk at low exposure rates and modifying effects of time since exposure and age at exposure. *Radiat. Res.* **169**, 125–137 (2008).

17. B. Vacquier, S. Caer, A. Rogel, M. Feurprier, M. Tirmarche, C. Luccioni, B. Quesne, A. Acker and D. Laurier, Mortality risk in the French cohort of uranium miners: extended follow-up 1946–1999. *Occup. Environ. Med.* **65**, 597–604 (2008).

18. M. K. Schubauer-Berigan, R. D. Daniels and L. E. Pinkerton, Radon exposure and mortality among white and American Indian uranium miners: An update of the Colorado Plateau Cohort. *Am. J. Epidemiol.* **169**, 718–730 (2009).

19. M. Kreuzer, L. Walsh, M. Schnelzer, A. Tschense and B. Grosche, Radon and risk of extrapulmonary cancers—Results of the German uranium miners cohort study, 1960–2003. *Br. J. Cancer* **99**, 1946–1953 (2008).

20. F. Lehmann, L. Hambeck, K. H. Linkert, H. Lutze, H. Meyer, H. Reiber, H. K. Renner, A. Reinisch, T. Seifert and F. Wolf, *Belastung durch ionisierende Strahlung im Uranerzbergbau der ehemaligen DDR*. Hauptverband der gewerblichen Berufsgenossenschaften, St. Augustin, 1998.

21. D. Dahmann, H-D. Bauer and G. Stoyke, Retrospective exposure assessment for respirable and inhalable dust, crystalline silica and arsenic in the former German uranium mines of SAG/SDAG Wismut. *Int. Arch. Occup. Environ. Health* **81**, 949–958 (2008).

22. M. Kreuzer, M. Schnelzer, A. Tschense, L. Walsh and B. Grosche, Cohort profile: The German uranium miners cohort study (WISMUT cohort), 1946–2003. *Int. J. Epidemiol.* Advanced Access published June 3, doi:10.1093/ije/dyp216 (2009).

23. M. Kreuzer, M. Kreisheimer, M. Kandel, A. Tschense and B. Grosche, Mortality from cardiovascular diseases in the German uranium miners cohort study, 1946–1998. *Radiat. Environ. Biophys.* **45**, 159–166 (2006).

24. M. Moehner, M. Lindtner, H. Otten and H. G. Gille, Leukemia and exposure to ionizing radiation among German uranium miners. *Am. J. Ind. Med.* **49**, 238–248 (2006).

25. M. Kreuzer, A. Brachner, F. Lehmann, K. Martignoni, H. E. Wichmann and B. Grosche, Characteristics of the German uranium miner cohort study. *Health Phys.* **83**, 26–34 (2002).

26. D. L Preston, J. H. Lubin, D. A. Pierce and M. E. McConney, *Epicure User's Guide*. HiroSoft, Seattle, WA, 1993.

27. L. Walsh, A short review of model selection techniques for radiation epidemiology. *Radiat. Environ. Biophys.* **46**, 205–213 (2007).

28. *International Statistical Classification of Diseases and Health Related Problems: The ICD-10 (German edition 1.3.1999).* WHO, Geneva, 1992.

29. S. Darby, D. Hill, A. Auvinen, J. M. Barros-Dios, H. Baysson, F. Bochicchio, H. Deo, R. Falk, F. Forastiere and R. Doll, Radon in homes and risk of lung cancer: collaborative analysis of individual data from 13 European case-control studies. *Br. Med. J.* **330**, 223–226 (2005).

30. M. Schnelzer, M. Kreuzer, A. Tschense, G. Hammer and B. Grosche, Accounting for smoking in the radon related lung cancer risk among German uranium miners: Results of a nested case-control study. *Health. Phys.*, in press.

31. D. L. Preston, Y. Shimizu, D. A. Pierce, A. Suyama and K. Mabuchi, Studies of the mortality of atomic bomb survivors. Report 13: Solid cancer and noncancer disease mortality: 1950–1997. *Radiat. Res.* **160**, 381–407 (2003).

32. European Commission, Alpha-Risk: Risks related to internal and external exposures. In *Euratom Research Projects and Training Activities*, Vol. II, pp. 26–27. EUR 21229, European Commission, Brussels, 2006. [Available online at http://ec.europa.eu/research/energy/pdf/nuclear_fission_2_en.pdf]

33. H. Akaike, Information theory and an extension of the maximum likelihood principle. In *Proceedings of the Second International Symposium on Information Theory* (B. N. Petrov and and F. Caski, Eds.), pp. 267–281. Akademiai Kiado, Budapest, 1973.

34. H. Akaike, A new look at the statistical model identification. *IEEE Trans. Autom. Control.* **19**, 716–723 (1974).

35. G. Schwarz, Estimating the dimension of a model. *Ann. Stat.* **6**, 461–464 (1978).

36. C. T. Volinsky and A. E. Raftery, Bayesian Information Criterion for censored survival models. *Biometrics* **56**, 256–262 (2000).

34. Walsh L, Dufey F, Tschense A, Schnelzer M, Grosche B & Kreuzer M. Radon and the risk of cancer mortality – Internal Poisson models for the German uranium miners cohort. Health Physics. 99(3), 292-300, 2010

RADON AND THE RISK OF CANCER MORTALITY—INTERNAL POISSON MODELS FOR THE GERMAN URANIUM MINERS COHORT

Linda Walsh, Florian Dufey, Annemarie Tschense, Maria Schnelzer, Bernd Grosche, and Michaela Kreuzer*

Abstract—Uranium mining occurred between 1946 and 1990 at the former Wismut mining company in East Germany. 58,987 male former employees form the largest single uranium miners cohort, which has been followed up for causes of mortality occurring from the beginning of 1946 to the end of 2003. The purpose of this paper is to present the radon exposure related cancer mortality risk based on 20,920 deaths, 2 million person-years, and 6,373 cancers. The latter include 3,016 lung cancers and 3,053 extrapulmonary solid cancers. Internal Poisson regression was used to estimate the excess relative risk (*ERR*) per unit of cumulative radon exposure in Working Level Months (WLM) for all major sites and for the follow-up period from 1946 to 2003. The simple cohort *ERR* WLM^{-1} for lung cancer is 0.20% [95% confidence interval (CI): 0.17%; 0.22%]. The *ERR* model for lung cancer is linear in radon exposure with exponential effect modifiers that depend on age at median exposure, time since median exposure, and radon exposure-rate. In this model the central estimate of *ERR* WLM^{-1} is 1.06% (95% CI: 0.69%; 1.42%) for an age at median exposure of 33 y, a time since median exposure of 11 y, and an exposure-rate of 2.7 WL. This central *ERR* decreases by 5% for each unit exposure-rate increase. The *ERR* decreases by 32% with each decade increase in age at median exposure and also decreases by 54% with each decade increase in time since median exposure. The *ERR* WLM^{-1} for all extrapulmonary solid cancers combined without effect modification is 0.014% (95% CI: 0.006%; 0.023%). The *ERR* model for extrapulmonary solid cancer is linear in radon exposure with an exponential effect modifier which depends on age-attained. In this model the central estimate of *ERR* WLM^{-1} is 0.040% (95% CI: −0.001%; 0.082%) for an age-attained of 44. The *ERR* decreases by 37% with each decade increase in age-attained. The highest *ERR* WLM^{-1}, after lung, is observed for cancers of the pharynx (0.16%), tongue/mouth (0.045%), and liver (0.04%).
Health Phys. 99(3):292–300; 2010

INTRODUCTION

RECENT STUDIES have shown an increase in the risk of lung cancer in underground miners exposed to the radioactive gas radon (^{222}Rn) and its progeny (e.g., Lubin et al. 1995; NRC 1999; Tomasek 2002; Laurier et al. 2004; Brüske-Hohlfeld et al. 2006; Grosche et al. 2006; Tomasek et al. 2008; Vacquier et al. 2008) and have indicated a possible link between extrapulmonary cancer and radon (Kreuzer et al. 2008). A large cohort of German uranium miners (described in Kreuzer et al. 2009) has recently provided updated data that are very suitable for analyses which could increase the current state of knowledge on general and specific cancer mortality after exposure to radon and other agents. These data are associated with the uranium mining that took place between 1946 and 1990 in the Saxony and Thuringia regions of East Germany at the Wismut company. Wismut is the German name for Bismuth and was used as a code name to cover up the real activity of the company during the early years of mining just after WWII. 58,987 male former employees of this company form the largest single uranium miners cohort, which has been followed up for causes of mortality occurring from the beginning of 1946.

The first follow-up of the Wismut mortality data (Grosche et al. 2006) has recently been extended by five years to 31 December 2003 (Kreuzer et al. 2008) and now includes 3,016 lung cancer deaths, 3,053 fatal extrapulmonary solid cancers, and almost 2 million person-years of observation. In the second follow-up, the number of miners either lost to follow-up or with missing causes of deaths was smaller than in the first follow-up. Data on potential confounders such as exposure to gamma radiation, long-lived radionuclides, fine dust, arsenic dust, and quartz fine dust are newly available in the second follow-up. The Wismut study also has a large number of

non-radiation exposed cohort members that contribute to a good internal comparison group for the reliable determination of spontaneous (baseline) cancer rates.

The aim of the present analyses of the German uranium miner's cohort study is to present models for the exposure-response relationship between cumulative radon exposure and either lung cancer or extrapulmonary solid cancers with age, time and exposure-rate effect modifiers based on the second follow-up. For this purpose, refined models, similar to those currently applied in the French and Czech cohort studies (Tomasek et al. 2008; Vacquier et al. 2008), are applied. Effects of potential confounders on the radon-induced risk for lung cancer and extrapulmonary solid cancers are also examined.

MATERIALS AND METHODS

Cohort definition, time periods, and mortality follow-up

Details of the selection of cohort members and the determination of radiation exposure quantities evaluated by means of a job-exposure matrix (JEM) have already been presented (Lehmann et al. 1998; Grosche et al. 2006; Kreuzer et al. 2008). Radon (^{222}Rn) area measurements in the Wismut mines were carried out from 1955 onwards. Radon concentrations were retrospectively estimated by an expert group for the period 1946–1954. These estimates were based on measurements made from 1955 onwards, taking factors such as ventilation rate, vein space, and uranium content into account (Grosche et al. 2006; Kreuzer et al. 2006; Moehner et al. 2006; HVBG, BBG 2005). The total production duration for uranium mining by the Wismut company can be divided into three distinct time periods (Kreuzer et al. 2002). Working conditions were characterized by dry drilling, the lack of forced ventilation, and an increasing exposure to radon during the first period from 1946 to 1954. During the second period between 1955 and 1970, radon concentrations decreased due to improved ventilation and wet drilling replacing dry drilling. Both of these measures directly led to improved working conditions. International radiation protection standards were introduced in the third time period after 1970 up to the company closure in 1990. Follow-up was conducted via local registration offices and district archives for information on vital status or via local health authorities for copies of death certificates. Information on the causes of death before 1989 was partly available from the Wismut pathology archives. Each cohort member contributes to the total number of person-years, starting 180 days after the date of first employment and ending at the earliest of date of loss to follow-up, date of death, or end of follow-up (31 December 2003). In the present analysis, the 10th ICD-code (WHO 1992) was applied throughout.

Analysis with excess relative risk (*ERR*) parametric risk models

Poisson regression risk evaluation methods and models have been applied here and used to test for an association between the cancer mortality risk and cumulative radon exposure and other agents. As in other miner studies (e.g., Tomasek et al. 2008; Vacquier et al. 2008), a 5-y lag was used in calculating the cumulative exposure to radon. Tabulations of person-years at risk and cancer deaths were created with the DATAB module of the EPICURE software (Preston et al. 1993). Age at exposure and time since exposure were calculated with reference to median exposures i.e., when half of the exposure cumulated up to a given date was reached. Cross-classifications were made by attained age, a, in 16 categories (<15, $15-<20$, $20-<25$, …, $85+$ y), individual calendar year, y, in 58 categories, age at median exposure, e, in 7 categories (<20, $20-<25$, $25-<30$, $30-35$, $35-<40$, $40-<45$, $45+$ y), time since median exposure, t, in 6 categories (<5, $5-<10$, $10-<15$, $15-<20$, $20-<25$, $25+$ y) and cumulative radon exposure, w, either in 7 categories (0, $>0-<50$, $50-<100$, $100-<500$, $500-<1,000$, $1,000-<1,500$, $1,500+$) for the simple cohort models (as in Kreuzer et al. 2008) or in 9 categories (0, $>0-<10$, $10-<50$, $50-<100$, $100-<200$, $200-<500$, $500-<1,000$, $1,000-<1,500$, $1,500+$ WLM†) for the models with time-dependent effect modifiers. The exposure-rate, er, was calculated as in the National Research Council, Committee on the Biological Effects of Ionizing Radiation (BEIR VI) definition (NRC 1999), i.e., recomputed total cumulative exposure (with a 5-y lag) divided by total duration (on the assumption of 11 working months per year) at each age-attained. The exposure-rate was also categorized into 6 groups ($0-<0.5$, $0.5-<1$, $1-<2$, $2-<4$, $4-<10$, $10+$ WL). The WLM categories were defined to be comparable with other studies (Tomasek et al. 2008), but with added categories at higher exposures. The tabulated data were fitted to the following model—if $r(a, y, w, er, e, t)$ is the age, year, exposure, exposure-rate, age at median exposure, and time since median exposure specific cancer mortality rate and $r_0(a, y) = r(a, y, 0, 0, 0, 0)$ is the baseline disease rate for non-exposed individuals, $w = 0$, $er = 0$, then

$$r(a, y, w, er, e, t) = r_0(a, y)[1 + ERR(w, er, e, a, t)],$$
$$(1)$$

where *ERR* is the excess relative risk factored into a function of exposure and a modifying function

$$ERR(w, er, e, a, t) = f(w, er) \times g(e, a, t). \quad (2)$$

[†] One WLM of cumulative exposure corresponds to exposure to 1 working level (WL) during one month (170 h) and is equivalent to 3.5 mJh m^{-3}.

A linear function of radon exposure was considered:

$$f(w) = \beta_w w \tag{3a}$$

$$f(w, er) = \beta_w w \exp[\psi_w(er - 2.7)]. \tag{3b}$$

where the total cumulative radon exposure w was considered: as a continuous explanatory variable (eqn 3a) and also non-parametrically in exposure with the total exposure variable subdivided into nine exposure classes.

Similarly, a linear model was also considered with a continuous effect modifier for total exposure-rate (eqn 3b), where the model centering at an exposure-rate of 2.7 WL was chosen to match the mean cohort value.

The modifying function $g(e, a, t)$ is either in terms of the age-attained model, $ERR(w, a) = f(w) \times g(a)$, the time since median exposure model, $ERR(w, t)$, or the age at median exposure model, $ERR(w, e)$. In common with previous analyses (Tomasek et al. 2008), e and t are calendar time-dependent variables, calculated with reference to the median time-lagged exposures, unless otherwise specified (since e = age at first exposure was also tested for goodness of fit). Prior to or in the absence of exposure, $t = 0$ and $e = a$. Three more complicated mixed models, which only need to include any two of the three time variables (a, e, t) because of the linear dependence, $a = e + t$, between them, e.g., $ERR(w, er, a, e)$, are also considered as alternatives. The preferred models can be determined by applying model selection criteria for nested and non-nested models (Walsh 2007). The functional form is exponential for age at median exposure and/or age-attained and/or time since median exposure where the modifying factors are

$$g(e, a, t) = \exp[\alpha(e - 33) + \delta(a - 44) + \varepsilon(t - 11)] \tag{4}$$

and α, δ, ε are fit parameters. The model centering at an age at median exposure of 33 y, time since median exposure of 11 y, and an age-attained of 44 y was chosen to match the mean Wismut cohort values—the choice of centering constants only served to change the risk by a factor and has no influence on the goodness of fit of a particular model. The age and time modifying patterns were applied to the exposure models given in eqns (3a) and (3b).

In order to test for the other two radiation agents, external gamma radiation and long-lived radionuclides, each of these explanatory variables z_i, $i = 1, 2$, respectively, was included additively and separately to the final relative risk (RR) model for lung cancer given in eqn (5a) or the final model for extrapulmonary solid cancer (eqn 5b), optimized, with fit parameter λ_i, and then removed:

$$RR(w, z_i) = 1 + \beta_w w \exp[\psi_w(er - 2.7)$$
$$+ \alpha(e - 33) + \varepsilon(t - 11)] + h[(\lambda_i z_i)] \tag{5a}$$

$$RR(w, z_i) = 1 + \beta_w w \exp[\delta(a - 44)] + h[(\lambda_i z_i)]. \tag{5b}$$

In order to test for the three non-radiation agents—fine dust, arsenic, or quartz—each of these explanatory variables z_i, $i = 3, 4, 5$, respectively, was included multiplicatively and separately to the final model for lung cancer given in eqn (6a) or the final model for extrapulmonary solid cancer (eqn 6b), optimized, with fit parameter λ_i, and then removed:

$$RR(w, z_i) = \{1 + \beta_w w \exp[\psi_w(er - 2.7)$$
$$+ \alpha(e - 33) + \varepsilon(t - 11)]\}\{1 + h[(\lambda_i z_i)]\} \tag{6a}$$

$$RR(w, z_i) = \{1 + \beta_w w \exp[\delta(a - 44)]\}\{1 + h[(\lambda_i z_i)]\}. \tag{6b}$$

Maximum likelihood with the AMFIT module of the EPICURE software (Preston et al. 1993) was used for estimation of the fit parameters and the internal baseline rates in 928 strata of age-attained (16 categories) and individual calendar year (58 categories). Out of these 928 possible strata, 708 actually contained data.

RESULTS

The full cohort pertains to 58,987 male former employees of the Wismut company. Table 1 shows a comparison of some main quantities between the first and second follow-up periods, which ended on 31 December 1998 and 31 December 2003, respectively. The

Table 1. Details of important descriptive statistics for the current second follow-up (FU 2) in comparison with the first follow-up (FU 1) period for the Wismut cohort.

End of mortality follow-up	FU 1: 31.12.1998	FU 2: 31.12.2003
Total number of subjects	59,001	58,987
Total number of person-years	1,801,630	1,996,880
Mean duration of follow-up in years	30.5	34
Vital status		
Alive	39,255 (66.5%)	35,294 (59.8%)
Deceased	16,598 (28.1%)	20,920 (35.5%)
Lost to follow-up	3,148 (5.3%)	2,773 (4.7%)
Year of death (% of causes of death that are known)		
<1970	1,479 (50.6%)	1,560 (58.8%)
1970–1979	3,132 (90.0%)	3,255 (95.1%)
1980–1989	5,368 (91.4%)	5,554 (96.7%)
1990–1999	6,619 (93.3%)	7,538 (96.7%)
2000–2003	—	3,013 (96.9%)
Total	16,598 (88.2%)	20,920 (93.6%)

observed percentage of cohort members lost to follow-up could be reduced from 5.3% to 4.7% and the percentage of missing causes of deaths could be reduced from 11.8% to 6.4%. It can be seen from Table 1 that the completeness of the follow-up has now been substantially improved. The number of lung cancer deaths increased from 2,388 to 3,016 cases (ICD-10, C34). The second follow-up is characterized by: 6,373 cancers (ICD-10, C00-97); 3,355 extrapulmonary cancers (ICD-10, C00-33, C35-97); 3,053 extrapulmonary solid cancers (ICD-10, C00-33, C35-80 and C97); a vital status of 59.8% alive, 35.5% deceased, 4.7% lost to follow-up; an average follow-up period of 34 y; a mean duration of employment of 12 y; 1,996,880 person-years of observation; and an average person-year weighted cumulative exposure to radon of 218 WLM.

Other occupational exposure covariables are also available. These are (listed with person-years weighted mean, standard deviation, and maximum values): external gamma radiation in units of effective dose in Sv (0.03, 0.06, 0.87); long-lived radionuclides in units of kBq m^{-3} (3.0, 6.4, 132.2); fine dust in units of dust-years (31.7, 42.3, 315.2); arsenic in units of dust-years (30.4, 84.5, 1417.4); and quartz in units of dust-years (5.2, 7.4, 56.0), where 1 dust-year is defined as an exposure to 1 mg m^{-3} fine dust or silica dust and 1 μg m^{-3} for arsenic over a time period of 220 shifts of 8 h. Arsenic exposures were only present in the Saxony mines and so data on this type of exposure are available for 18,234 cohort members. The correlations between radon and either gamma or long-lived radionuclides or arsenic are low with correlation coefficients of less than 0.4. However, higher correlations exist between radon and either fine dust or quartz with correlation coefficients of approximately 0.7.

ERR parametric risk models

Cohort radon risk (no modifying factors)

Fig. 1 shows the results of fitting an *ERR* model (eqn 3a) to sites with more than 35 cases. A statistically significant cumulative radon exposure effect was observed for lung cancer [*ERR* WLM^{-1} = 0.20%; 95% confidence interval (CI): 0.17%; 0.22%]. A small degree of numerical uncertainty in *ERR* WLM^{-1} is introduced by the two different grouping choices (with 7 and 9 categories) for radon exposure—this can be seen by comparing the value in Fig. 1 (0.20—calculated with 7 classes) and the value in Table 2 (0.19—calculated with 9 classes). There is a statistically significant increase in mortality from extrapulmonary cancers (shown in Fig. 1) and extrapulmonary solid cancers (not shown in Fig. 1) with cumulative radon exposure (*ERR* WLM^{-1} = 0.014%; 95% CI: 0.006%; 0.023%), where the risk is the same for both groups. When the remaining 18 individual cancer sites with more than 35 cases are considered, a statistically significant positive relation with radon is observed for stomach cancer (*ERR* WLM^{-1} = 0.02%; 95% CI: 0.001%; 0.04%), while excesses with borderline statistical significance were found for cancers of the pharynx (*ERR* WLM^{-1} = 0.16%; 95% CI: −0.04%; 0.37%) and liver (*ERR* WLM^{-1} = 0.04%; 95% CI: −0.01%; 0.1%). No evidence of an association between leukemia and cumulative radon exposure was found here. A previous work has already shown that the cohort *ERR*

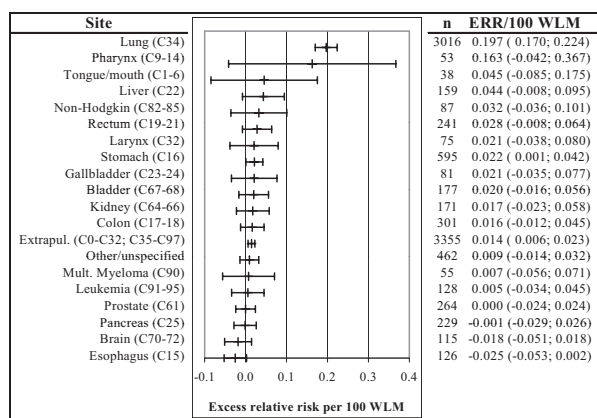| Site	n	ERR/100 WLM
Lung (C34)	3016	0.197 (0.170; 0.224)
Pharynx (C9-14)	53	0.163 (-0.042; 0.367)
Tongue/mouth (C1-6)	38	0.045 (-0.085; 0.175)
Liver (C22)	159	0.044 (-0.008; 0.095)
Non-Hodgkin (C82-85)	87	0.032 (-0.036; 0.101)
Rectum (C19-21)	241	0.028 (-0.008; 0.064)
Larynx (C32)	75	0.021 (-0.038; 0.080)
Stomach (C16)	595	0.022 (0.001; 0.042)
Gallbladder (C23-24)	81	0.021 (-0.035; 0.077)
Bladder (C67-68)	177	0.020 (-0.016; 0.056)
Kidney (C64-66)	171	0.017 (-0.023; 0.058)
Colon (C17-18)	301	0.016 (-0.012; 0.045)
Extrapul. (C0-C32; C35-C97)	3355	0.014 (0.006; 0.023)
Other/unspecified	462	0.009 (-0.014; 0.032)
Mult. Myeloma (C90)	55	0.007 (-0.056; 0.071)
Leukemia (C91-95)	128	0.005 (-0.034; 0.045)
Prostate (C61)	264	0.000 (-0.024; 0.024)
Pancreas (C25)	229	-0.001 (-0.029; 0.026)
Brain (C70-72)	115	-0.018 (-0.051; 0.018)
Esophagus (C15)	126	-0.025 (-0.053; 0.002)

Excess relative risk per 100 WLM

Fig. 1. Excess relative risk (*ERR*) per 100 WLM and 95% confidence limits for all cancer sites with more than 35 cases.

Table 2. *ERR* models for lung cancer and radon exposure, simple models without adjustment for age and time effects and the preferred models with exponential radon exposure, age, and time effect modifiers. The *ERR* fit parameters (i.e. the β's) are in units of *ERR* per 100 WLM, with model centering, where applicable, at an age at median (or first) exposure of 33 y [relevant parameter is $\exp(10\alpha)$] and a time since median (or first) exposure of 11 y [relevant parameter is $\exp(10\varepsilon)$] and at an exposure-rate of 2.7 WL [relevant parameter is $\exp(\psi_w)$]. All fit parameters are quoted with 95% Wald type confidence intervals.

Model description	Parameter name	Fitted value
$f(w)$	β_w	0.19 (0.16; 0.21)
$f(w, er) \times g(e, t)$ with age at	β_w	1.08 (0.69; 1.47)
first exposure and time since	$\exp(\psi_w)$	0.95 (0.93; 0.96)
first exposure	$\exp(10\alpha)$	0.66 (0.55; 0.79)
Deviance = 28,410.1	$\exp(10\varepsilon)$	0.50 (0.42; 0.59)
$f(w, er) \times g(e, t)$ with age at	β_w	1.06 (0.69; 1.42)
median exposure and time	$\exp(\psi_w)$	0.95 (0.93; 0.96)
since median exposure	$\exp(10\alpha)$	0.68 (0.57; 0.82)
Deviance = 28,398.2	$\exp(10\varepsilon)$	0.46 (0.39; 0.55)

Table 3. *ERR* models for extrapulmonary solid cancers and radon exposure, simple models without adjustment for age and time effects and the preferred models with an age-attained effect modifier. The *ERR* fit parameters (i.e. the β's) are in units of *ERR* per 100 WLM, with model centering, where applicable, at an age-attained of 44 y [relevant parameter is $\exp(10\delta)$]. All fit parameters are quoted with 95% Wald type confidence intervals.

Model description	Parameter name	Fitted value
$f(w)$	β_w	0.014 (0.005; 0.023)
$f(w) \times g(a)$	β_w	0.040 (−0.001; 0.082)
with age-attained	$\exp(10\delta)$	0.63 (0.37; 1.08)

WLM^{-1} for extrapulmonary, stomach, larynx, and liver cancers could be reduced to statistically insignificant values when adjusting additively for the five available covariables that are possible confounders (Kreuzer et al. 2008).

The Wismut risk models with effect modifying factors

Time and age patterns. The preferred model for lung cancer (Walsh et al. 2010) includes exponential effect modifiers that depend on any two of the three age/time parameters chosen here to be age at median exposure and time since median exposure. In this model, the central estimate of *ERR* is given in Table 2 for an age at median exposure of 33 y and a time since median exposure of 11 y. The estimated age at median exposure effect for the preferred models indicates that the *ERR* decreases by about 32% {= [1 − $\exp(10\alpha)$], with parameter values from Table 2} with each decade increase in age at median exposure. Similarly, the *ERR* decreases by about 54% with each decade increase in time since median exposure. Very similar patterns hold for a model with age at first exposure instead of age at median exposure and time since first exposure instead of time since median exposure (results also shown in Table 2). However the model relating to median exposures is an improvement of the model relating to first exposures with more than 95% probability because the Akaike Information Criterion (AIC) for the former model is smaller than the AIC for the latter model by more than 5.9 points (actual ΔAIC = −11.9) (see Walsh 2007 for model selection details).

A model for extrapulmonary solid cancer is presented here in Table 3 that depends on radon exposure

and attained-age. In this case, the model selection procedure is not so clear cut as it was for the lung cancer models. This is because the reference model with just radon exposure (i.e., eqn 3a) had a deviance of 25,713.06, the model inclusion of age at median exposure caused a deviance drop to 25,708.10 (4.96 points), the model with radon and time since median exposure had a deviance of 25,713.05 (0.1 points less than the reference), and the model with radon and age-attained had a deviance of 25,710.33 (2.73 points less than the reference). The model with age at median exposure causes the largest deviance drop but this model is not better than the model with age-attained (ΔAIC <5.9). Since age-attained is a much simpler covariable than age at median exposure it was decided to present the age-attained model here in Table 3 and Fig. 3. In this model the central estimate of *ERR* WLM^{-1} is 0.040% (95% CI: −0.001%; 0.082%) for an age-attained of 44 y. The *ERR* decreases by 37% with each decade increase in age-attained. The inclusion of two age/time covariables in the model for extrapulmonary solid cancers was not indicated by model selection techniques.

Exposure (linear or non-parametric) and exposure-rate effects. The preferred Wismut *ERR* model for lung cancer (Walsh et al. 2010) as shown in Fig. 2 (with parameter values in Table 2) is linear in radon exposure with exponential effect modifiers which depend on age at median exposure, time since median exposure, and radon exposure-rate. In this model the central estimate of *ERR* WLM^{-1} is 1.1% (95% CI: 0.7%; 1.4%) for mean age at median exposure of 33 y, mean time since median exposure of 11 y, and an exposure-rate of 2.7 WL. This central *ERR* decreases by 5% for each exposure-rate increase of 1 WL. The inclusion of an exposure-rate effect modification in the preferred model was unequivocally indicated, however there was no indication for model improvement if an exposure squared term was included in the model (Walsh et al. 2010). Fig. 2 also shows the results of fitting a model that is non-parametric

Fig. 2. Central estimate (solid line) and 95% CI (dashed lines) for an excess relative risk (*ERR*) model for lung cancers and radon exposure for a median age at exposure of 33 y, a time since exposure of 11 y, and an exposure-rate of 2.7 WL. The crosses indicate the non-parametric in exposure category *ERR* fit parameters (but also adjusted to a median age at exposure of 33 years, a time since exposure of 11 y, and an exposure-rate of 2.7 WL) and are shown in the graph with ±2 standard deviations. The largest effect from the other covariables was seen with the covariable quartz dust (shown here as a long dashed line).

in exposure category but which is also adjusted to a median age at exposure of 33 y, a median time since exposure of 11 y, and an exposure-rate of 2.7 WL.

The chosen model for extrapulmonary solid cancers did not include exposure-rate effects as there was no indication for model improvement if exposure-rate was included in the model. However, Fig. 3 also shows the results of fitting a model which is non-parametric in exposure category but which is also adjusted to an attained-age of 44 y.
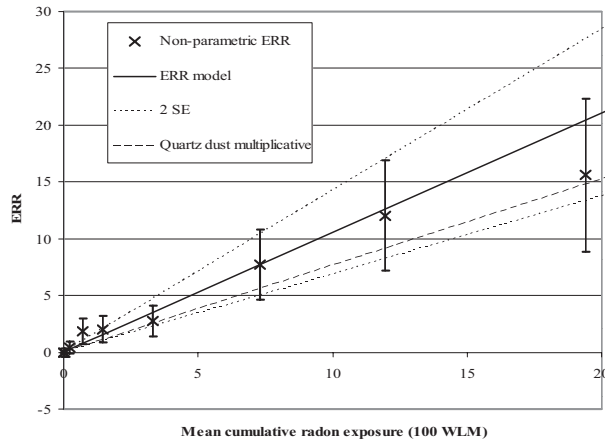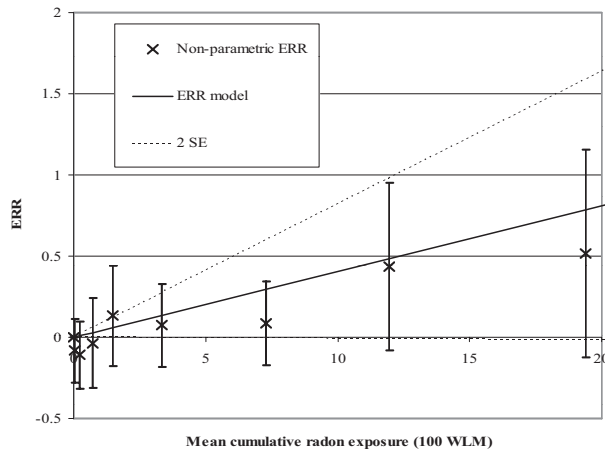

Fig. 3. Central estimate (solid line) and 95% CI (dashed lines) for an excess relative risk (*ERR*) model for extrapulmonary solid cancers and radon exposure for a median age-attained of 44 y. The crosses indicate the non-parametric in exposure category *ERR* fit parameters (but also adjusted to a median age-attained of 44 y) and are shown in the graph with ±2 standard deviations.

The Wismut preferred model with other exposure covariables

The confounding effects of external gamma radiation, long-lived radionuclides, fine dust, arsenic, and quartz exposures (z_i, $i = 1$–5, respectively) on the central radon risk from the two Wismut preferred models (shown in Figs. 2 and 3) were investigated with the models given in eqns (5a, 5b, 6a, and 6b) optimized against a restricted data set that excluded 310 cohort members with invalid values for dust exposure.

The resulting parameter values for the lung cancer model (shown in Table 4) indicated that the central *ERR* WLM^{-1} estimate, of 1.1% for this restricted dataset, is influenced to a notable degree only by the multiplicative inclusion of the covariable quartz (see also Fig. 2). In this case there is an approximately 25% reduction in the central risk estimate. The choice of additive model inclusion for the gamma radiation covariable and multiplicative inclusion for the non-radiation covariables is indicated by the data when applying model selection techniques in a preliminary analysis. However, in the case of models relating to radon and long-lived radionuclides, both additive and multiplicative models resulted in a similar goodness of fit.

The resulting parameter values for the extrapulmonary solid cancer model (shown in Table 5) indicated that

Table 4. *ERR* model for lung cancer and radon exposure model with exponential radon exposure, age, and time effect modifiers and with the inclusion of potential confounders. The *ERR* fit parameters (i.e. the β's) are in units of *ERR* per 100 WLM, with model centering, where applicable, at an age at median (or first) exposure of 33 y [relevant parameter is $\exp(10\alpha)$] and a time since median (or first) exposure of 11 y [relevant parameter is $\exp(10\varepsilon)$] and at an exposure-rate of 2.7 WL [relevant parameter is $\exp(\psi_w)$]. All fit parameters are quoted with 95% Wald type confidence intervals.

Model description	Parameter name	Fitted value
$f(w, er) \times g(e, t)$ with the covariable for γ effective dose in the model ADDITIVELY	β_w	1.02 (0.64; 1.41)
	$\exp(\psi_w)$	0.95 (0.94; 0.97)
	$\exp(10\alpha)$	0.66 (0.55; 0.81)
	$\exp(10\varepsilon)$	0.44 (0.36; 0.53)
$f(w, er) \times g(e, t)$ with the covariable for long-lived radionuclides in the model ADDITIVELY	β_w	1.07 (0.67; 1.47)
	$\exp(\psi_w)$	0.95 (0.93; 0.97)
	$\exp(10\alpha)$	0.66 (0.55; 0.81)
	$\exp(10\varepsilon)$	0.43 (0.36; 0.52)
$f(w, er) \times g(e, t)$ with the covariable for fine dust in the model MULTIPLICATIVELY	β_w	0.91 (0.56; 1.25)
	$\exp(\psi_w)$	0.95 (0.93; 0.97)
	$\exp(10\alpha)$	0.66 (0.54; 0.80)
	$\exp(10\varepsilon)$	0.43 (0.36; 0.52)
$f(w, er) \times g(e, t)$ with the covariable for quartz in the model MULTIPLICATIVELY	β_w	0.76 (0.45; 1.08)
	$\exp(\psi_w)$	0.95 (0.93; 0.97)
	$\exp(10\alpha)$	0.62 (0.50; 0.77)
	$\exp(10\varepsilon)$	0.40 (0.32; 0.49)
$f(w, er) \times g(e, t)$ with the covariable for arsenic in the model MULTIPLICATIVELY	β_w	1.00 (0.64; 1.36)
	$\exp(\psi_w)$	0.94 (0.92; 0.96)
	$\exp(10\alpha)$	0.69 (0.57; 0.83)
	$\exp(10\varepsilon)$	0.44 (0.37; 0.53)

the central *ERR* WLM^{-1} estimate, of 0.041% for this restricted dataset, is not influenced to a notable degree by inclusion of any of the potential confounders. The choice of additive or multiplicative model inclusion for the potential confounders is not indicated by the data when applying model selection techniques, since both additive and multiplicative models resulted in a very similar goodness of fit.

DISCUSSION

The main strength of the Wismut study lies in its homogeneity and large number of subjects, which allows the verification of current knowledge on lung cancer risk from underground occupational exposure to radon and its progeny based on an independent data set. The percentage of cohort members that have been lost to follow-up is small, which is particularly impressive taking into account the late start of the study in 1994. Exposure estimates are based on a job-exposure matrix, which gives best daily exposure estimates. The cohort also includes a large number of individuals with low radon exposures, allowing the estimation of lung cancer risk for levels close to those measured in a normal housing environment (Darby et al. 2005).

Limitations of the study include possible uncertainties in exposures, which are more pronounced for the early years of mining and the lack of complete smoking information and other information on possible confounders such as diesel fumes and asbestos. The possible effect of smoking on the radon associated lung cancer risk can not be completely evaluated in the full cohort. The majority of former Wismut employees had smoked. However, information on smoking was collected within a nested case-control study where the resulting radon related lung cancer risks, calculated with and without adjustment for smoking, were very similar (Schnelzer et al. 2010). Another, earlier case-control study of lung cancer in Wismut miners (Brüske-Hohlfeld et al. 2006) found a low inverse correlation between radon exposure and smoking and only a minor confounding effect.

Other miner cohort studies, mostly limited by small numbers of cases, have generally provided little evidence for an increased risk of cancers other than lung cancer due to radon (NRC 1999; Tomasek et al. 1993; Laurier et al. 2004; Vacquier et al. 2008). The results presented here confirm that lung cancer in humans is a site with sufficient evidence to be connected with radon exposures. There also appears to be evidence of a small but statistically significant risk of extrapulmonary cancers, but no apparent risk of leukemia, connected with radon—but chance results and confounding can not be completely ruled out. The evidence for the latter two cancer

Table 5. *ERR* model for extrapulmonary solid cancer and radon exposure with adjustment for attained-age and with the inclusion of potential confounders. The *ERR* fit parameters (i.e., the β's) are in units of *ERR* per 100 WLM, with model centering at an attained-age of 44 y [relevant parameter is $\exp(10\delta)$]. All fit parameters are quoted with 95% Wald type confidence intervals.

Model description	Parameter name	Fitted value
$f(w) \times g(a)$ with the covariable for γ effective dose in the model ADDITIVELY	β_w	0.043 (0.002; 0.084)
	$\exp(10\delta)$	0.64 (0.39; 1.06)
$f(w) \times g(a)$ with the covariable for long-lived radionuclides in the model ADDITIVELY	β_w	0.043 (0.002; 0.085)
	$\exp(10\delta)$	0.64 (0.39; 1.06)
$f(w) \times g(a)$ with the covariable for fine dust in the model MULTIPLICATIVELY	β_w	0.036 ($-$0.006; 0.078)
	$\exp(10\delta)$	0.59 (0.29; 1.18)
$f(w) \times g(a)$ with the covariable for quartz in the model MULTIPLICATIVELY	β_w	0.038 ($-$0.004; 0.081)
	$\exp(10\delta)$	0.61 (0.32; 1.16)
$f(w) \times g(a)$ with the covariable for arsenic in the model MULTIPLICATIVELY	β_w	0.040 ($-$0.002; 0.081)
	$\exp(10\delta)$	0.62 (0.36; 1.09)

groups could become stronger in the future, when the current results have been verified either with the next (third) follow-up or in terms of the relevant organ doses which are not yet available for the whole Wismut cohort.

The effects of other exposure covariables on the radon risk

The chosen Wismut models were used to assess the possible confounding effects of the other five covariables mentioned above. This was done by assessing the additive inclusion of each radiation exposure covariable in the preferred Wismut model one at a time and the multiplicative inclusion of the other three agents (fine dust, quartz, and arsenic). This division into additive and multiplicative groups was based on the radiobiological reasoning that it would not make sense to include other ionizing radiation covariables in a form that would multiply the radon risk. However the central *ERR* WLM^{-1} estimate for lung cancer was only found to be influenced to any notable degree, i.e., by an approximate 25% reduction, by the inclusion of the covariable for quartz dust. The central *ERR* WLM^{-1} estimate for extrapulmonary solid cancer was not found to be influenced to any notable degree by the inclusion of any of the covariables that were considered as potential confounders.

CONCLUSION AND PERSPECTIVES

Wismut models have been presented here that have only two and four parameters required to adequately model the *ERR* WLM^{-1} for extrapulmonary solid cancer and lung cancer, respectively. The preferred model for lung cancer is linear in cumulative radon exposure and has exponential effect modifiers which depend on age at median exposure, time since median exposure, and radon exposure-rate. The chosen model for extrapulmonary solid cancer is linear in cumulative radon exposure and has an exponential effect modifier which depends on

attained-age. These two Wismut models were also applied to investigate the possible confounding effects of five other exposure covariables, for which new data are available. However, the largest confounding effect (which caused a reduction of about 25% in the central risk estimate) was reported for lung cancer and exposure to quartz dust. A minor degree of numerical uncertainty in the lung cancer *ERR* WLM^{-1} was introduced by the two different grouping choices for radon exposure—this could be avoided in the future by direct modeling of the individual data.

Further work is required to more thoroughly investigate the combined effects of radon with other exposure covariables such as occupational exposure to external gamma radiation, long-lived radionuclides, arsenic, fine dust, and silica dust.

Future work will involve the recomputation of the risks presented here with the radon exposures included as their contribution to the total organ doses. Organ doses are currently being quantified in the ALPHA-RISK project funded by the European Commission (EC 2006). Data from the Wismut cohort study will soon be opened for interested scientists for further analysis. For more information please see http://www.bfs.de/en/bfs/forschung/Wismut.

REFERENCES

Brüske-Hohlfeld I, Rosario AS, Wolke G, Heinrich J, Kreuzer M, Kreienbrock L, Wichmann HE. Lung cancer risk among

former uranium miners of the WISMUT Company in Germany. Health Phys 90:208–216; 2006.

Darby S, Hill D, Auvinen A, Barros-Dios JM, Baysson H, Bochicchio F, Deo H, Falk R, Forastiere F, Hakama M, Heid I, Kreienbrock L, Kreuzer M, Lagarde F, Makelainen I, Muirhead C, Oberaigner W, Pershagen G, Ruano-Ravina A, Ruosteenoja E, Rosario AS, Tirmarche M, Tomasek L, Whitley E, Wichmann HE, Doll R. Radon in homes and risk of lung cancer: collaborative analysis of individual data from 13 European case-control studies. BMJ 330:223–226; 2005.

European Commission. Alpha-risk: risks related to internal and external exposures. In: Euratom research projects and training activities [online]. Brussels: EC; EUR 21229; 2006. Available at: http://ec.europa.eu/research/energy/pdf/nuclear_fission_2_en.pdf. Accessed 18 June 2010.

Grosche B, Kreuzer M, Kreisheimer M, Schnelzer M, Tschense A. Lung cancer risk among German uranium miners: a cohort study, 1946–1998. Br J Cancer 95:1280–1287; 2006.

HVBG, BBG. Belastung durch ionisierende Strahlung, Staub und Arsen im Uranerzbergbau der ehemaligen DDR (Version 08/2005). Gera: Bergbau BG (BBG), St. Augustin: Hauptverband der gewerblichen Berufsgenossenschaften (HVBG) (CD-ROM); 2005 (in German).

Kreuzer M, Brachner A, Lehmann F, Martignoni K, Wichmann HE, Grosche B. Characteristics of the German uranium miner cohort study. Health Phys 83:26–34; 2002.

Kreuzer M, Kreisheimer M, Kandel M, Tschense A, Grosche B. Mortality from cardiovascular diseases in the German uranium miners cohort study, 1946–1948. Radiat Environ Biophys 45:159–166; 2006.

Kreuzer M, Walsh L, Schnelzer M, Tschense A, Grosche B. Radon and risk of extrapulmonary cancers—results of the German uranium miners cohort study, 1960–2003. Br J Cancer 99:1946–1953; 2008.

Kreuzer M, Schnelzer M, Tschense A, Walsh L, Grosche B. Cohort profile: the German uranium miners cohort study (WISMUT cohort), 1946–2003. Int J Epidemiol 2009: doi:10.1093/ije/dyp216. Available at: http://ije.oxfordjournals.org/cgi/content/extract/dyp216v1. Accessed 18 June 2010.

Laurier D, Tirmarche M, Mitton N, Valenty M, Richard P, Poveda S, Gelas JM, Quesne B. An update of cancer mortality among the French cohort of uranium miners: extended follow-up and new source of data for causes of death. Eur J Epidemiol 19:139–146; 2004.

Lehmann F, Hambeck L, Linkert KH, Lutze H, Meyer H, Reiber H, Renner HK, Reinisch A, Seifert T, Wolf F.

Belastung durch ionisierende Strahlung im Uranerzbergbau der ehemaligen DDR. St. Augustin: Hauptverband der gewerblichen Berufsgenossenschaften; 1998 (in German).

Lubin JH, Boice Jr JD, Edling C, Hornung RW, Howe G, Kunz E, Kusiak RA, Morrison HI, Radford EP, Samet JM, Tirmarche M, Woodward A, Yao SX. Radon-exposed underground miners and inverse dose-rate (protraction enhancement) effects. Health Phys 69:494–500; 1995.

Moehner M, Lindtner M, Otten H, Gille HG. Leukemia and exposure to ionizing radiation among German uranium miners. Am J Ind Med 49:238–248; 2006.

National Research Council, Committee on the Biological Effects of Ionizing Radiation. Health effects of exposure to radon—BEIR VI. Washington, DC: National Academy Press; 1999.

Preston DL, Lubin JH, Pierce DA, McConney ME. EPICURE user's guide. Seattle: HiroSoft; 1993.

Schnelzer M, Hammer GP, Kreuzer M, Tschense A, Grosche B. Accounting for smoking in the radon related lung cancer risk among German uranium miners: results of a nested case-control study. Health Phys 98:20–28; 2010.

Tomasek L. Czech miner studies of lung cancer risk from radon. J Radiol Prot 22:A107–A112; 2002.

Tomasek L, Darby SC, Swerdlow AJ, Placek V, Kunz E. Radon exposure and cancer other than lung cancer among uranium miners in West Bohemia. The Lancet 34:919–923; 1993.

Tomasek L, Rogel A, Tirmarche M, Mitton N, Laurier D. Lung cancer in French and Czech uranium miners: radon-associated risk at low exposure rates and modifying effects of time since exposure and age at exposure. Radiat Res 169:125–137; 2008.

Vacquier B, Caer S, Rogel A, Feurprier M, Tirmarche M, Luccioni C, Quesne B, Acker A, Laurier D. Mortality risk in the French cohort of uranium miners: extended follow-up 1946–1999. Occup Environ Med 65:597–604; 2008.

Walsh L. A short review of model selection techniques for radiation epidemiology. Radiat Environ Biophys 46:205–213; 2007.

Walsh L, Tschense A, Schnelzer M, Dufey F, Grosche B, Kreuzer M. The influence of radon exposures on lung cancer mortality in German uranium miners, 1946–2003. Radiat Res 173:79–90; 2010.

World Health Organization. International statistical classification of diseases and health related problems: the ICD-10 (German Modification Version 2006—as of 1.10.2005). Geneva: WHO; 1992.

■ ■

35. Kreuzer M, Schnelzer M, Tschense A, Walsh L & Grosche B. Cohort profile: The German uranium miners cohort study (WISMUT cohort), 1946-2003. Int. J. Epidemiol. 39(4), 980-987, 2010

COHORT PROFILE

Cohort Profile: The German uranium miners cohort study (WISMUT cohort), 1946–2003

Michaela Kreuzer,* Maria Schnelzer, Annemarie Tschense, Linda Walsh and Bernd Grosche

How did the study come about?

Silver mining has been in existence since the 12th century in the Ore Mountains (Erzgebirge) located in the South of Eastern Germany in the Federal State of Saxony close to the border of the Czech Republic. In 1946, after World War II, the old silver mines were re-opened and the Soviet-Stock Corporation was founded with the code name WISMUT (i.e. the German name for bismuth).[1] The aim of this corporation was to produce as much uranium as possible for the Soviet nuclear weapon program. In the early years, from 1946 to about 1955, a large number of workers had been employed (about 100 000) under extremely bad working conditions. No worker-protection or radiation safety measures existed; consequently, exposures to radiation and dust were very high due to a lack of forced ventilation and the use of dry drilling. In 1954, the corporation was converted into the Soviet–German Stock Corporation. At that time mining was extended to the Federal State of Thuringia. In 1955, the first radon measurements were performed and from then onwards several worker-protection measures such as forced ventilation and wet drilling were introduced. Thus, from 1955 to 1970, the working conditions steadily improved and the number of employees was reduced to between 30 000 and 40 000. After 1970, international radiation protection standards were introduced, with provisions for individual radiation protection. The number of miners was stable at 20 000 and the working conditions had a high safety level. With the German reunification in 1990, mining was abandoned.

The Wismut company produced a total of 220 000 tons of uranium during its operation period from 1946 to 1990 and was the third-largest uranium producer worldwide. It is estimated that more than 400 000 persons worked at the company, most of whom were underground or in uranium-ore processing facilities.[2] Up to the end of 1990, more than 5000 of these workers were compensated for radiation induced cancers in the former German Democratic Republic (GDR). This number increased to 7695 by the end of 1999.[3] In 2004, the annual number of newly compensated cases was almost 200, though with a decreasing time trend.[4]

After German reunification, the German Federal Ministry of Environment (Bundesministerium für Umwelt, Naturschutz und Reaktorsicherheit/BMU) decided to preserve the health data that were stored at the Wismut Health Data Archives (Gesundheitsdatenarchiv Wismut/GDAW), which are now held by the Federal Office for Occupational Protection and Medicine (Bundesanstalt für Arbeitsschutz und Arbeitsmedizin/BAuA). These archives include paper files and histological material. The German Statutory Accident Insurance maintains records of all data relevant to the procedures for the compensation of occupational diseases. Payrolls are kept by the successor of the former Wismut company, the Wismut GmbH. Based on parts of the information held by these bodies, a cohort of former Wismut employees could be established,[5] with financial support from the BMU and the European Commission.

What does the study cover?

The Wismut cohort represents one of the largest occupationally radiation exposed collectives. The cohort forms the basis for investigations on the detrimental effects associated with: inhalation of radon and its progeny, inhalation of uranium dust, fine dust, silica dust and arsenic dust, and exposure to external gamma radiation and other risk factors. It is well known that occupational exposure to radon and its progeny increases the risk of lung cancer.[6–12] Uncertainty, however, still remains with regard to the exposure–response relationship at low levels of

Federal Office for Radiation Protection, Department of Radiation Protection and Health, Neuherberg, Germany

* Corresponding author. Federal Office for Radiation Protection, Department of Radiation Protection and Health, Ingolstaedter Landstrasse 1, Neuherberg, Germany.
  E-mail: mkreuzer@bfs.de

radon exposure, other risk or effect modifying factors (time since exposure, exposure rate, attained age, age at exposure, etc.) and the combined effects of radiation and dust, arsenic, smoking, etc. Another uncertainty concerns the radon-related risk for extra-pulmonary cancers[6,13–19] or cardiovascular diseases.[20–22]

Who is in the sample ?

Overall it is estimated that more than 400 000 workers may have been employed at the Wismut company during its operation period. Basic information on personal data and job history was available for about 130 000 workers from three files that allowed the establishment of a cohort study. Due to financial reasons it was decided to limit the size of the cohort to about 64 000 workers taken from the files of about 130 000 workers as a stratified random sample. In order to represent the different mining conditions at the Wismut company, the sample was stratified by the date of first employment (1946–54, 1955–70 and 1971–89), place of work (underground, milling/processing and surface) and area of mining (Saxony, Thuringia). Since it was assumed that, during the first years of production, women had also worked for at least some time underground, the sample was additionally stratified by gender. Moreover, all employees from one of the most important parts of the company (the so-called mining facility 'Object 09') who started working between 1955 and 1970 were included as well as any worker employed after 1970. Thus, the cohort is not representative of the entire Wismut workforce, but weighted towards those periods when exposures were medium to low in the selection of cohort members.

The following inclusion criteria were defined: (i) year of first employment between 1946 and 1989; (ii) minimum duration of employment 180 days;

(iii) year of birth after 1899; and (iv) men only. Females were excluded because it turned out that only a very small number of females had in fact worked underground. A total of 58 987 male former Wismut employees remained in the final cohort after exclusion of all persons who did not fulfil the inclusion criteria ($n = 5101$), were included twice in the data set ($n = 45$), had implausible data ($n = 22$), had an unknown radon exposure ($n = 97$) or with unclear identity ($n = 59$).

What has been measured?

The cohort includes individual information on year of birth, vital status, mortality, job history and occupational exposure to several factors (Table 1). Data on the job histories had been extracted from the payrolls, including information on the type of job, type of mining facility, area of work place, number of shifts and periods of absence on a daily basis. In a feasibility study, a lot of effort had been spent to retrieve complete information from the payrolls. For about 200 cohort members data had been extracted from Wismut files a second time. Some discrepancies led to an improved standardized data collection procedure for the main cohort study. During the whole data collection period detailed double plausibility checks had been performed at the German Statutory Accident Insurance (DGUV) and the Federal Office for Radiation Protection. Implausible, incomplete or unclear data were returned to DGUV, where the data were re-examined and corrected. Thus a high validity of these data can be assured.

A mortality follow-up for the complete cohort is performed every 5 years. The first and second mortality follow-up periods finished on December 31, 1998 and December 31, 2003, respectively. The main sources of information on the vital status are the local registration offices. Other sources are the Pathology

Table 1 Available information for WISMUT cohort members

• Job history at the Wismut company	On a daily basis for type of job and mining facility based on information from payrolls

• Occupational exposure to radiation
  – Radon and its progeny in WLM
  – External gamma radiation in mSv
  – Uranium dust in kBqh/m^3
	Annual cumulative exposure based on job-exposure matrix for radiation

• Occupational exposure to dust and arsenic
  – Fine dust in dust-years
  – Silica dust in dust-years
  – Arsenic in dust-years
	Annual cumulative exposure based on job-exposure matrix for dust and arsenic

• Smoking habits	Available only for 38% of the cohort, from 1970 onwards, based on annual medical examinations; very rough information
• Mortality data (vital status, year and cause of death)	Based on the mortality follow-up as of December 31, 2003; cause of death based on death certificates or in some cases on autopsy file
• Health data (occupational diseases, etc.)	For part of the cohort from last medical examination during employment

WLM = working level months.

Archive of the Wismut company and additional records on the health data and occupational compensation procedures of the Wismut company. The main sources of information on the causes of death are the Public Health Administrations and their corresponding archives, where copies of the death certificates are stored. Other sources were the Pathology Archive of the Wismut Company, where the autopsy files of former Wismut employees and their family members were kept, and the Wismut Health Data Archives located in Chemnitz. Currently, the possibility of an additional follow-up for incidence, at least for the years 1960–89, is under investigation.

Table 2 shows some main characteristics of the first and second mortality follow-up, which ended on December 31, 1998 and December 31, 2003, respectively. The completeness of the follow-up could be greatly improved during the time between the two follow-ups. The observed percentage of cohort members lost to follow-up of 5.3% was reduced to 4.7% and the percentage of missing causes of deaths could be reduced from 11.8 to 6.4%. The second follow-up has a total of 60% of the cohort members still alive, 35.5% deceased and 4.7% were lost-to follow-up. The cause of death is available for 93.6% of the deceased cohort members. Missing causes of deaths

Table 2 Characteristics of the mortality follow-ups of the WISMUT cohort

Mortality follow-up ending on	31 December, 1998	31 December, 2003
Total number	59 001	58 987
Person-years	1 801 630	1 997 041
Mean duration of follow-up in years	30.5	34
Vital status		
Alive	39 255 (66.5%)	35 294 (59.8%)
Deceased	16 598 (28.1%)	20 920 (35.5%)
Loss to follow-up	3148 (5.3%)	2773 (4.7%)
Year of death (% of available causes of death)		
<1970	1479 (50.6%)	1560 (58.8%)
1970–79	3132 (90.0%)	3255 (95.1%)
1980–89	5368 (91.4%)	5554 (96.7%)
1990–99	6619 (93.3%)	7538 (96.7%)
2000–03	–	3013 (96.9%)
Total	16 598 (88.2%)	20 920 (93.6%)
Cause of death (ICD-10)[a]		
AB Infectious diseases	82 (0.6%)	136 (0.7%)
C Malignant tumours	4800 (32.8%)	6373 (32.5%)
D Benign tumours	75 (0.5%)	104 (0.5%)
E Metabolic disorders	161 (1.1%)	276 (1.4%)
F Mental disorders	119 (0.8%)	165 (0.8%)
G Nervous system	91 (0.6%)	133 (0.7%)
H Eye diseases	1 (0.0%)	1 (0.0%)
I Cardiovascular diseases	5417 (37.0%)	7395 (37.8%)
J Respiratory diseases	1559 (10.6%)	1998 (10.2%)
K Digestive system	815 (5.6%)	1076 (5.5%)
L Diseases of the skin	2 (0.0%)	2 (0.0%)
M Musculoskeletal Diseases	33 (0.2%)	39 (0.2%)
N Genitourinary system	132 (0.9%)	171 (0.9%)
Q Malformations	2 (0.0%)	2 (0.0%)
R Others/unknown	73 (0.5%)	128 (0.7%)
ST Accidents/suicides,	1284 (8.8%)	1589 (8.1%)
Total	14 646 (100%)	19 588 (100%)

[a]ICD = International Classification of Diseases.

predominate for miners who died pre-1970, because death certificates were rarely stored for more than 30 years. In the second mortality follow-up, the most frequent cause of death was cardiovascular diseases (37.8%), followed by malignant cancers (32.5%) and respiratory diseases (10.2%). Overall, a total of 6373 malignant cancer deaths occurred. The most frequent type of cancer is lung ($n = 3016$) followed by stomach ($n = 595$), colon ($n = 291$), prostate ($n = 264$), pancreas ($n = 229$), rectum ($n = 222$), bladder ($n = 174$), liver ($n = 159$) and kidney ($n = 152$).

For all cohort members complete information on the job history is available on a daily basis. A large proportion of the cohort members (40.5%) started to work at the Wismut company before 1955, when radon exposures were high (Table 3), whereas nearly two-thirds of all cohort members were employed until 1990, when mining was abandoned. On average, the miners were 24 years old when they started to work at the Wismut company. The average duration of employment was 12 years. Total employment years apportion to 53.5% spent underground, 38.4% at the surface, 6.9% in processing/milling and 1.1% in open-pit mining.

Radiation exposure was estimated by using a detailed job-exposure matrix (JEM), which includes information on exposure to radon and its progeny in WLM, external γ radiation in mSv and long-lived radionuclides (^{235}U, ^{238}U) in kBqh/m^3. [23,24] The JEM provides exposure values for each calendar year of employment between 1946 and 1989, each place of work and each type of job. More than 900 different jobs and 500 different working places were evaluated for this purpose. Radon (^{222}Rn) measurements in the Wismut mines were carried out from 1955 onwards. Thus, for the period from 1946 to 1954, radon concentrations were estimated retrospectively by an expert group based on measurements from 1955, taking into account ventilation rate, vein space, uranium content, etc. In addition to exposure evaluation, work is currently in progress on the calculation of the individual doses to the various organs from radon, gamma radiation and long-lived radionuclides either separately or combined. [25] This work is part of the European collaborative research project ALPHA-RISK. [26] Information on arsenic, dust and silica is also based on a job-exposure matrix similar to that

for radiation. [24,27,28] Values are given in dust-years, where 1 dust-year is defined as an exposure to 1 mg/m^3 fine dust or silica dust and 1 μg/m^3 for arsenic over a time period of 220 shifts of 8 h. Differences in the number of shifts and daily working hours in the different calendar years were accounted for by multiplying with a correction factor. Arsenic exposures were present only in the mines of Saxony.

Figure 1 shows the number of radon-exposed cohort members by calendar year and the average cumulative radon exposure per year among exposed cohort members ($n = 50\,773$). With the introduction of ventilation measures from 1955 onwards, the radon concentration dropped sharply, reaching levels of international radiation protection standards in the 1970s. In contrast to this, external gamma radiation and long-lived radionuclides (LRN) show a different pattern (Figure 2a), because their concentration was not affected by the improved ventilation. Exposure to fine dust and silica dust (Figure 2b) had its peak between 1952 and 1955, after which time it steadily decreased with the implementation of wet drilling after 1955. A similar pattern is also observed for arsenic exposure (data not shown).

A summary description of the distribution of cumulative exposure to radon and its progeny, external gamma radiation, LRN, fine dust, silica and arsenic is given in Table 4. There is a wide range of radon
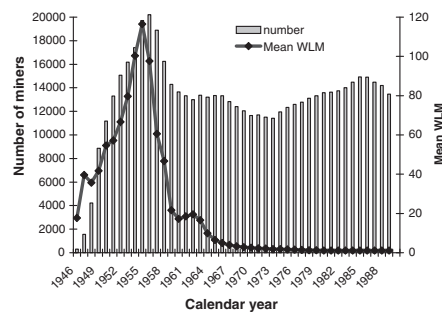
Figure 1 Number of radon-exposed cohort members and mean cumulative radon exposure per calendar-year ($n = 50\,773$)

Table 3 Job characteristics by year of start of employment, WISMUT cohort, 1946–2003

Year of start of employment	n (%)	Mean age at first employment in years (range)	Mean duration of employment in years (range)
1946–54	23 920 (40.5%)	27 (13–55)	17 (0.5– 44)
1955–70	17 944 (30.4%)	24 (14–65)	12 (0.5–35)
1971–89	17 123 (29.0%)	21 (13–68)	7 (0.5–19)
Total	58 987 (100%)	24 (13–68)	14 (0.5–44)

exposure levels, e.g. 8214 cohort members were unexposed; 27 739 members received <50 WLM, which represents the typical range for indoor radon levels; and 4698 subjects were exposed to >1000 WLM. The average duration of exposure was 11 years. Only 18 234 cohort members from the Saxony mines were occupationally exposed to arsenic.

No biological material is collected from the cohort members themselves, because the follow-up is passive

without personal contact to the cohort members. However, other procedures are currently being tested in order to establish a biobank containing samples from high- and low-radon-exposed former Wismut employees, including the same exposure information as in the cohort. Several thousands of former Wismut employees are regularly undergoing medical examinations that are offered by the Wismut company. During these visits additional blood will be collected for a sub-sample of former Wismut miners. Next to that, it is planned to isolate DNA from autopsy material of former Wismut employees who died from lung cancer.

What has already been found?

The WISMUT cohort data have already been primarily used to estimate the radon-related risk of death from lung cancer, extra-pulmonary cancers and cardiovascular diseases.[9,19,21] A linear relationship between radon and lung cancer was observed in the follow-up period 1946–98, with an Excess Relative Risk (ERR) per WLM of 0.21% [95% Confidence Interval (CI): 0.18;0.24].[9] The ERR/WLM was modified by time since exposure, attained age and exposure rate. Whereas a strong inverse exposure-rate effect was detected for high exposures, no such effect was detected at exposures <100 WLM. The ERR/WLM was not found to be modified by duration of exposure. Currently, these risk estimates are being updated by using more-refined models and extending the follow-up period to 2003.

The risk of extra-pulmonary cancers due to cumulative exposure to radon was evaluated for the follow-up period 1960–2003.[19] Based on internal regression, a statistically significant relation with cumulative radon exposure was observed for all extra-pulmonary cancers combined (ERR/WLM = 0.014%; 95% CI: 0.006%; 0.023%). The majority of individual sites investigated revealed a positive exposure–response relationship. However, these relations were either

Figure 2 (**a**) Mean annual exposure to external gamma radiation in mSv and LRN in kBqh/m^3 for exposed cohort members ($n = 50\,761$). (**b**) Mean annual exposure to fine dust ($n = 58\,695$) and silica dust ($n = 58\,658$) in dust-years for exposed cohort members

Table 4 Distribution parameters for exposure to radiation, dust and arsenic for the WISMUT cohort members, 1946–2003

	Cumulative exposure to					
	Radon and its progeny in WLM	External gamma radiation in mSv	LRN in kBqh/m^3	Fine dust in dust-years[a]	Silica dust in dust-years[a]	Arsenic in dust-years[b]
Missing information	0	0	0	292	292	43
Never exposed	8214	8226	8226	0	37	40 710
Ever exposed	50 773	50 761	50 761	58 695	58 658	18 234
Mean	280	47.5	4.1	36.6	5.9	121.2
Median	33	15.9	1.0	14.3	1.8	67.4
Max	3224	908.6	132.2	315.2	56.0	1 417.4

[a]Dust-year: 1 dust-year is defined as exposure to 1 mg/m^3 of fine dust or silica dust over 220 shifts each at 8 h.
[b]Dust-year is defined as exposure to 1 μg/m^3 for arsenic over 220 shifts each at 8 h.

not statistically significant or became insignificant after adjustment for potential confounders such as dust, arsenic, etc. Overall, the findings of the WISMUT cohort study provide some evidence for a relation between radon and extra-pulmonary cancers; however, chance and confounding cannot be ruled out.

The risk of cardiovascular diseases in relation to radiation was analysed based on the data of the first follow-up.[21] Overall, there was little evidence for a relationship with either cumulative exposure to radon, or external gamma radiation or LRN. This is also true for the sub-group cardial and cerebrovascular diseases. Low doses to the relevant organs and uncontrolled confounding, however, hamper interpretation.

Analyses based on part of the data of the WISMUT cohort together with data from the French and Czech uranium miner cohorts are currently being conducted within the European ALPHA-RISK project.[26] The main objective of this international collaboration is to evaluate the risk of mortality from lung cancer and other diseases by radon, with a focus on the low-exposure ranges. For this purpose the German cohort data were restricted to the follow-up period 1955–98. The feasibility of a pooled analysis of the three nested case–control studies on lung cancer from Germany, France and the Czech Republic is also under investigation.

A full list of papers arising on the WISMUT study, with links to the abstracts, can be found at the study website (http://www.bfs.de/de/bfs/forschung/Wismut).

What are the main strengths and weaknesses?

The WISMUT cohort is the largest single cohort study on uranium miners world wide. As well as to its size, the main strengths of the study are the long follow-up period (35 years and almost 2 million person-years); the small percentage of loss-to follow-up; the large number of deaths from cancer, cardiovascular and respiratory diseases and the wide range of exposure to radon and its progeny as well as the availability of detailed information on other occupational risk factors such as external gamma radiation, LRN, fine dust, quartz fine dust and arsenic.

Potential weaknesses of this study concern the accuracy of radiation exposure, particularly in the very early years of the WISMUT operation. Possible non-differential misclassification of radiation exposure and its effects on risk estimates are currently being investigated. Other potential limitations are the accuracy of causes of deaths, the proportion of missing causes of deaths as well as missing information on potential confounders such as smoking, asbestos exposure, exposure to diesel fumes, etc.

Several validity checks were completed for vital status ascertainment. First, the data on vital status

from the pathology archive (all deceased) were compared with the data received from the local registries ($n = 2382$). About 1% of the deceased cohort members of the pathology archive had falsely been specified as 'alive' by the local registries. A second strategy compared the data on vital status from all deceased persons according to the health records of the Wismut company (excluding those with additional information from the pathology archive) with the data received from the local registries ($n = 1905$). Only 2% had been wrongly classified by either the Wismut company or by the local registries. In all cases this was due to erroneous spelling or falsely identified persons (e.g. same name but different year of birth). Based on these data from the first follow-up, it was estimated that the vital status may be wrong for ~1% of the cohort. During the second follow-up this percentage had been further reduced.

Accuracy of the cause of death was checked by comparing persons for whom the cause of death was available both from autopsy files of the pathology archive and from certificates of death based on the clinical diagnosis without autopsy ($n = 1836$). With respect to lung cancer, 5.1% of the lung cancer cases had been wrongly classified as non-lung cancers by the clinical diagnoses and 1.7% of the non-lung cancers as lung cancer. Overall, a high validity for lung cancer as underlying cause of death is expected, because 49.8% of the lung cancer deaths are based on autopsy. This proportion is lower when all malignant cancers (35.8%) are considered.

With respect to potential confounders, some information is available on exposure to specific occupational risk factors (i.e. asbestos, weld smoke, solvents, noise, etc.) obtained from medical records. However, this information is selective and cannot be used for analyses. For 38% of the cohort members at least some very rough information is available with respect to smoking since 1971, when standardized and well-recorded medical check-ups were introduced. In order to obtain more information on smoking, a nested case–control study of lung cancer has been conducted. Additional information on smoking was collected from the miners themselves, their next of kin or the health archives for use within the case–control study. It was found that most of the miners were smokers. The correlation between smoking and cumulative radon exposure was rather low, rendering smoking to be an unlikely confounder in the cancer risk attributable to radon exposure.

How can I get hold of the data? Were can I find out more?

External collaborations are welcomed by the study management committee, which comprises BfS (Federal Office for Radiation Protection) staff members and an international advisory board. Mechanisms

exist for the submission of research proposals to BfS. Successful applicants will be instructed on how to use the data. The study website (http://www.bfs.de/de/bfs/forschung/Wismut) has been set up to describe these procedures for applicants; it provides full contact details, a list of relevant publications and access to the technical report that provides a detailed description of the cohort.

References

[1] Wismut. *Chronik der Wismut* (CD-ROM). Chemnitz: Wismut GmbH, 1999.

[2] Otten H, Schulz H. Wismut – an uranium exposure revisited. In: Stellmann JM (ed.). *Encyclopaedia of Occupational Health and Safety*. Geneva: International Labour Office, 1998, pp. 32.25–32.28.

[3] Schroeder C, Friedrich K, Butz M, Koppisch D, Otten H. Uranium mining in Germany: incidence of occupational diseases 1946-1999. *Int Arch Occup Environ Health* 2002;**75:** 235–42.

[4] Koppisch D, Hagemeyer O, Friedrich K, Butz M, Otten H. Das Berufskrankheitsgeschehen im Uranerzbergbau der 'Wismut' von 1946–2000. *Arbeitsmed Sozialmed Umweltmed* 2004;**39:**120–8.

[5] Kreuzer M, Brachner A, Lehmann F, Martignoni K, Wichmann HE, Grosche B. Characteristics of the German uranium miner cohort study. *Health Phys* 2002; **83:**26–34.

[6] BEIR. US National Academies, Nuclear and Radiation Studies Board, Committee on Biological Effects of Ionizing Radiation (BEIR VI). *Health effects of exposure to radon – BEIR VI*. National Academy Press: Washington DC, 1999.

[7] Laurier D, Tirmarche M, Mitton N *et al*. An update of cancer mortality among the French cohort of uranium miners: extended follow-up and new source of data for causes of death. *Europ J Epidemiol* 2004;**19:** 139–46.

[8] Brüske-Hohlfeld I, Schaffrath Rosario A, Wölke G *et al*. Lung cancer risk among former uranium miners of the Wismut company in Germany. *Health Phys* 2006;**90:** 208–16.

[9] Grosche B, Kreuzer M, Kreisheimer M, Schnelzer M, Tschense A. Lung cancer risk among German male uranium miners: a cohort study, 1946–1998. *Br J Cancer* 2006;**95:**1280–87.

[10] Vacquier B, Caer S, Rogel A *et al*. Mortality risk in the French cohort of uranium miners: extended follow-up 1946-1999. *Occup Environ Med* 2008;**65:**597–604.

[11] Villeneuve PJ, Morrison HI, Lane R. Radon and lung cancer risk: an extension of the mortality follow-up of the Newfoundland fluorspar cohort. *Health Phys* 2007; **92:**157–69.

[12] Tomasek L, Rogel A, Tirmarche M, Mitton N, Laurier D. Lung cancer in French and Czech uranium miners: radon-associated risk at low exposure rates and modifying effects of time since exposure and age at exposure. *Radiat Res* 2008;**169:**125–37.

[13] Darby SC, Whitley E, Howe GR *et al*. Radon and cancers other than lung cancer in underground miners: a collaborative analysis of 11 studies. *J Natl Cancer Inst* 1995;**87:** 378–84.

[14] Tomasek L, Darby SC, Swerdlow AJ, Placek V, Kunz E. Radon exposure and cancers other than lung cancer among uranium miners in West Bohemia. *Lancet* 1993; **341:**919–23.

[15] Laurier D, Valenty M, Tirmarche M. Radon exposure and the risk of leukemia: a review of epidemiological studies. *Health Phys* 2001;**81:**272–88.

[16] Tomasek L. Leukaemia among uranium miners – late effects of exposure to uranium dust? *Health Phys* 2004; **86:**426–27.

[17] Moehner M, Lindtner M, Otten H, Gille HG. Leukemia and exposure to ionizing radiation among German uranium miners. *Am J Ind Med* 2006;**49:**238–48.

[18] Rericha V, Kulich M, Rericha R, Shore DL, Sandler DP. Incidence of leukemia, lymphoma, and multiple myeloma in Czech uranium miners: a case-control study. *Environ Health Perspect* 2006;**114:**818–22.

[19] Kreuzer M, Walsh L, Schnelzer M, Tschense A, Grosche B. Radon and risk of extrapulmonary cancers – results of the German uranium miners cohort study, 1960–2003. *Br J Cancer* 2008;**99:**1946–53.

[20] Villeneuve PJ, Morrison HJ. Coronary heart disease mortality among Newfoundland fluorspar miners. *Scand J Work Environ Health* 1997;**23:**221–26.

[21] Kreuzer M, Kreisheimer M, Kandel M, Schnelzer M, Tschense A, Grosche B. Mortality from cardiovascular diseases in the German uranium miners cohort study, 1946–1998. *Radiat Environ Biophys* 2006;**45:**159–66.

[22] Villeneuve PJ, Lane RS, Morrison HI. Coronary heart disease mortality and radon exposure in the Newfoundland

fluorspar miners' cohort, 1950–2001. *Radiat Environ Biophys* 2007;**46**:291–96.

[23] Lehmann F, Hambeck L, Linkert KH *et al*. Belastung durch ionisierende Strahlung im Uranerzbergbau der ehemaligen DDR. Hauptverband der gewerblichen Berufsgenossenschaften: Sankt Augustin, 1998.

[24] HVBG, BBG. Belastung durch ionisierende Strahlung, Staub und Arsen im Uranerzbergbau der ehemaligen DDR (Version 08/2005). Gera: Bergbau BG (BBG), St. Augustin: Hauptverband der gewerblichen Berufs-genossenschaften (HVBG) (CD-Rom), 2005.

[25] Marsh JW, Bessa Y, Birchall A *et al*. Dosimetric models used in the alpha-risk project to quantify exposure of uranium miners to radon gas and its progeny. *Radiat Prot Dos* 2008;**130**:6–101.

[26] European Commission. Alpha-Risk: risks related to internal and external exposures. In Euratom Research Projects and Training Acitivities. 2005 ISBN 92-79-00064-0. EUR 21229. http://europa.ue.int/comm./research/energy/pdf/nuclear_fission_2_en.pdf (Volume 1).

[27] Bauer HD. Studie zur retrospektiven Analyse der Belastungssituation im Uranberzbergbau der ehemaligen SDAG Wismut mit Ausnahme der Strahlenbelastung für die Zeit von 1946 bis 1990. Hauptverband der gewer-blichen Berufsgenossenschaften: Sankt Augustin, 2000.

[28] Dahmann D, Bauer HD, Stoyke G. Retrospective exposure assessment for respirable and inhalable dust, crystalline silica and arsenic in the former German uranium mines of SAG/SDAG Wismut. *Int Arch Occup Environ Health* 2008;**81**:949–58.

36. Nekolla EA, Walsh L & Spiess H. Incidence of Malignant Diseases in Humans Injected with Radium-224, Radiat. Res. 174, 377-386, 2010

Incidence of Malignant Diseases in Humans Injected with Radium-224

Elke Anna Nekolla,[a,1] Linda Walsh[a] and Heinz Spiess[b]

[a] BfS Federal Office for Radiation Protection, 85764 Neuherberg, Germany; and [b] Children's Hospital, University of Munich, 80336 Munich, Germany

Nekolla, E. A., Walsh, L. and Spiess, H. Incidence of Malignant Diseases in Humans Injected with Radium-224. *Radiat. Res.* **174**, 377–386 (2010).

The "Spiess study" follows the health of 899 persons who received multiple injections of the short-lived α-particle emitter ^{224}Ra mainly between 1945 and 1955 for the treatment of tuberculosis, ankylosing spondylitis and some other diseases. In December 2007, 124 persons were still alive. The most striking health effect, observed shortly after ^{224}Ra injections, was a temporal wave of 57 malignant bone tumors. During the two most recent decades of observation, a significant excess of non-skeletal malignant diseases has become evident. Expected numbers of cases were computed from the age, gender and calendar year distribution of person years at risk and incidence rates from the German Saarland Cancer Registry. Poisson statistics were applied to test for statistical significance of the standardized incidence ratios. Up to the end of December 2007, the total number of observed malignant non-skeletal diseases was 270 (248 specified cases of non-skeletal solid cancers and 22 other malignant diseases, among these 16 malignant neoplasms of lymphatic and hematopoietic tissue, six without specification of site) compared to 192 expected cases. Accounting for a 5-year minimum latent period and excluding 13 cases of non-melanoma skin cancer, 231 non-skeletal solid cancers were observed compared to 151 expected cases. Significantly increased cancer rates were observed for breast (32 compared to 9.7), soft and connective tissue (11 compared to 1.0), thyroid (7 compared to 1.0), liver (10 compared to 2.4), kidney (13 compared to 5.0), pancreas (9 compared to 4.1), bladder (16 compared to 8.0), and female genital organs (15 compared to 7.8). © 2010 by Radiation Research Society

INTRODUCTION

During the 1940s and 1950s the pharmaceutical Peteosthor was administered to patients suffering from tuberculosis (TB), ankylosing spondylitis (AS), and some other diseases (e.g. multiple sclerosis or polyarthritis) and was claimed to be an effective treatment of such diseases by the physician Dr. Paul Troch.

¹ Address for correspondence: BfS Federal Office for Radiation Protection, Ingolstädter Landstraße 1, 85764 Neuherberg, Germany; e-mail: ENekolla@BfS.de.

Peteosthor was a mixture of the short-lived α-particle emitter radium-224 (^{224}Ra) and traces of the red dye eosin and colloidal platinum where the latter was supposed to "guide" the ^{224}Ra to the affected tissue. In 1948, the pediatrician Heinz Spiess evaluated the effectiveness of Peteosthor therapy and demonstrated that a suppression of the growth of the tubercle bacillus would require doses of ^{224}Ra that are lethal. Spiess found in animal experiments that the distribution of radium in the organism was the same for Peteosthor and for pure ^{224}Ra. In addition, he demonstrated that ^{224}Ra caused growth retardation in young rabbits. Repeated warnings about Peteosthor's very serious detrimental side effects were not heeded until Spiess succeeded in stopping the treatment of children in the 1950s. The treatment of adult AS patients with ^{224}Ra continued, although with much lower doses (1).

A cohort of 899 patients who received several injections of ^{224}Ra, mainly between 1945 and 1955, was established and followed up in the "Spiess study" (Fig. 1). The cohort includes most of the patients treated with high doses [mean bone surface dose: 30 Gy (2), mean specific activity: 0.66 MBq/kg] and almost all of those exposed during childhood or adolescence. The cohort members were treated mainly for either TB (455 patients including 214 children and juveniles), especially bone TB, or AS (393 patients who were mostly male adults) (Fig. 1, Table 1). Only the AS patients continued to be treated in the late 1950s and in the 1960s with ^{224}Ra.

The purpose of this paper is to quantify and report the cancer incidence in this cohort for the most recent follow-up period up to the end of December 2007. A total of 124 study persons (61 women, 63 men) were still alive (Table 1) with a mean attained age and a mean follow-up time of 71.5 years and 55 years, respectively. The cohort contributed 28,500 person years of observation.

MATERIALS AND METHODS

This research is exempt from review by the German Federal Commissioner for Data Protection and Freedom of Information because the human subjects all gave their explicit informed consent and approval for each follow-up period over the last 50 years, and the analysis uses only anonymized data. At the beginning of the study, each study cohort member received an ID number. The personal
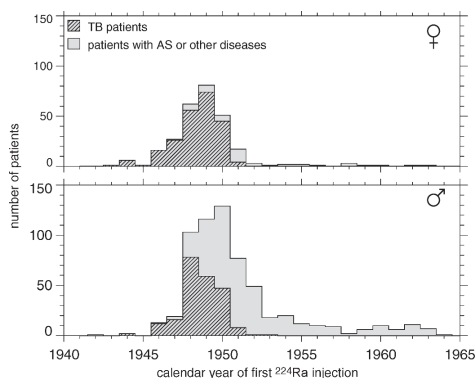
FIG. 1. The distribution of ^{224}Ra patients with respect to the calendar year of first ^{224}Ra injection, i.e., number of patients at specified calendar year (upper panel: female patients, lower panel: male patients). Hatched area: TB patients; gray area: other patients, i.e. predominantly the AS patients.

identifying information was discarded when the data were consolidated for the statistical analysis.

Information on the current health status of the patients was obtained at the beginning of the study by personal examination and in the last few decades from questionnaires sent to the patients and/or family doctors at intervals of 3 years. Causes of death were ascertained from death certificates, hospital records, reports of the public health department, civil registry, or doctor's or pathologist's reports. Diagnostic findings of malignant diseases were verified by hospital records, doctor's or pathologist's reports, or autopsy reports.

The expected numbers of cases were computed from the age, gender and calendar year distribution of person years at risk and the age-, gender- and calendar year-specific incidence rates from the German Saarland Cancer Registry. The German cancer registry of the state of Saarland was founded in 1967 and therefore has a long tradition in cancer registration. It covers a population of about 1.1 million and is considered to be complete and representative for the (West) German population. To account for secular trends in cancer baseline rates, it was decided to take data from the Saarland cancer registry where not only gender- and age-specific but also calendar year-specific rates are available for a long period. The expected numbers of cases were compared with the numbers of observed cases for various groups of malignant diseases. Poisson statistics was applied to test for statistical significance. Standardized incidence ratios (SIR), i.e., the quotients of the observed and the expected numbers of cases, and the two-sided 90% confidence intervals according to Poisson statistics, were calculated. A minimum latent (lag) period of 5 years for solid tumors and of 2 years for leukemia/lymphoma was assumed.

Where organ doses are quoted or SIRs for high- and low-dose groups are given, reference is made to the dosimetry of Henrichs *et al.* (*3*), and a relative biological effectiveness (RBE) of 20 for α-particle radiation is assumed. The dosimetric calculations of Henrichs *et al.* (*3*) are based on a preliminary biokinetic model that accounted for the biokinetics of radium in the human skeleton but had not yet been published by the International Commission on Radiological Protection (ICRP). The paper by Henrichs *et al.* provided dose conversion factors (DCFs) for ^{224}Ra for different ages (1, 5, 10 and 15 years and for adults) and nine different tissues standardized by the ICRP (*4*) (bone surface, red bone marrow, breast, kidney, urinary bladder, lungs, liver, upper and lower large intestine). Relative to the DCFs for adults, the DCFs for infants are about six to nine times higher and the DCFs for children and juveniles are about one to four times higher. In a more recent paper by Lassmann *et al.* (*5*), new dosimetric calculations were performed according to the final model proposed by the ICRP (*4*). Improved calculation algorithms were used that consider independent kinetics to determine the individual contributions of each daughter nuclide and account for the contributions of both low- and high-LET radiation to doses for all organs. Dose coefficients were given for a comprehensive set of organs but without dependence on age at exposure. In general, the former results (*3*) and the more recent results (*5*) are in good agreement. If the organ of interest was not included in the list of tissues considered by Henrichs *et al.* (*3*) but was included in the category "other tissues/organs" by the ICRP in the biokinetic model, age-dependent organ doses calculated by the DCFs for breast (which is part of "other tissues/ organs") were used here as the organ dose estimates.

In view of the fact that, especially for the TB patients, the administered activity was often correlated with the severity of disease, and a high percentage of severely ill patients died relatively early during the follow-up period, person-year weighted means of organ doses are given in the next section.

RESULTS AND DISCUSSION

Malignant Bone Tumors after ^{224}Ra Injection

The most prominent detrimental side effects of the ^{224}Ra injections were 57 malignant bone tumors that occurred in a temporal wave that peaked around 8 years after exposure. Based on cancer registry data, the expected number of malignant bone tumors in the study cohort would have been less than one over the entire observation period. Osteosarcoma was the major histological type of malignant bone tumor (approximately half) and fibrous-histiocytic sarcoma was the second most common (*2, 6*). The bone tumor excess has been described in several publications (e.g. *7–12*). A new analysis was performed in 2000 (*2*), because the dosimetry reassessment by Henrichs *et al.* (*3*) led to

TABLE 1
^{224}Ra Patients: Current Status (as of December 2007) and Distribution of Sexes, Ages at Exposure and Original Diseases

Total 899 (124)											
Females 278 (61)						Males 621 (63)					
Age at exposure ≤ 20 106 (39)			Age at exposure > 20 172 (22)			Age at exposure ≤ 20 111 (42)			Age at exposure > 20 510 (21)		
TB 105 (38)	AS–	O 1 (1)	TB 124 (20)	AS 24 (2)	O 24 (–)	TB 107 (40)	AS 1 (–)	O 3 (2)	TB 117 (8)	AS 368 (13)	O 25 (–)

Notes. TB: tuberculosis; AS: ankylosing spondylitis; O: other. The numbers in parentheses are the numbers of patients who are still alive.
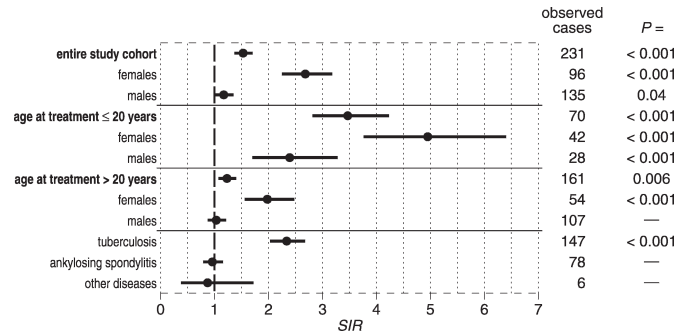
FIG. 2. Standardized incidence ratios (i.e. quotients of the observed and the expected numbers) for solid non-skeletal and soft tissue tumors (excluding non-melanoma skin cancer) with two-sided 90% confidence intervals (accounting for a 5-year lag period). SIRs are given for the entire ^{224}Ra cohort and for various subgroups of patients depending on gender, age at exposure and the original disease for which the ^{224}Ra was administered.

changed bone surface doses. The new dosimetric calculations indicated doses substantially smaller than those previously assumed for the patients exposed at a young age. Spiess had already suggested in 1969 that the bone tumor risk rises with decreasing age at ^{224}Ra injection (*13*). A later analysis concurred with this assumption but found that it did not reach statistical significance and that a better assessment of the dose to the skeleton was required (*12*). Subsequently, with the new dosimetric information (*3*), it was confirmed that there is a significant increase of bone tumor risk per unit dose with decreasing age at exposure (*2*).

In the earlier analysis (*12*), a reverse protraction factor (or inverse dose-rate effect) for the induction of bone tumors by the ^{224}Ra α particles was included in the risk estimates (i.e., higher bone tumor risk for patients with longer exposure times at equal total dose), an effect that has subsequently also been reported for lung cancers induced by the decay of radon and its daughters in the lungs of underground miners [see ref. (*14*)]. The analysis from 2000 (*2*) in terms of the new ^{224}Ra dosimetry (*3*) confirmed the reverse protraction factor for bone tumors and substantiated the suggestion that the dose-rate or duration modification of the excess bone tumor risk was effective only at higher doses, which is in agreement with general radiobiological experience and microdosimetric considerations.

Non-skeletal Malignant Diseases after ^{224}Ra Injections

Up to the end of December 2007, the total number of observed malignant diseases was 327 compared to 193 expected cases ($P < 0.001$). During the two most recent decades of the follow-up, a significant excess of non-skeletal malignant diseases has become apparent. Apart from the 57 malignant bone tumors, 248 specified cases

of non-skeletal solid cancers have been observed and 22 other malignant diseases, including six malignant neoplasms without specification of site, eight cases of leukemia, three non-Hodgkin lymphomas, and five multiple myelomas. Four of the 248 non-skeletal solid and soft tissue tumors occurred less than 5 years after the first ^{224}Ra injection. Assuming a lag period of 5 years and excluding 13 cases of non-melanoma skin cancer, mainly basaliomas, 231 cases were observed compared to 151 expected cases ($P < 0.001$).

In Fig. 2, the SIRs of non-skeletal solid and soft tissue tumors (excluding non-melanoma skin cancer) with 90% confidence intervals are given for the entire ^{224}Ra study cohort and for subgroups of patients according to gender, age at exposure or original disease. It can be seen from Fig. 2 that the observed number of cases for women is 2.7 times that expected, but the SIR for men is, although significantly increased ($P = 0.04$), closer to unity (SIR $= 1.2$). The rates are significantly increased both for women treated as adults and for women treated as children or juveniles. Especially for women exposed at younger ages, there is a marked excess: the number of observed cases is five times the number of expected cases. In this subgroup, 20 breast cancer cases (compared to 2.7) have been observed (see below). For males treated as children or juveniles, the SIR is 2.4. However, the observed number of malignant diseases in men exposed as adults is similar to that in a "normal" population; i.e., the cancer excess in men is due to additional cancer cases observed in those men treated as children or juveniles. The SIR in the subcohort of former TB patients is significantly increased as well because about half of these patients were below 21 years of age at the time of ^{224}Ra injections. However, in the subcohort of AS patients or of persons who suffered from other diseases, the number of cases is close to (or even less than) that expected.
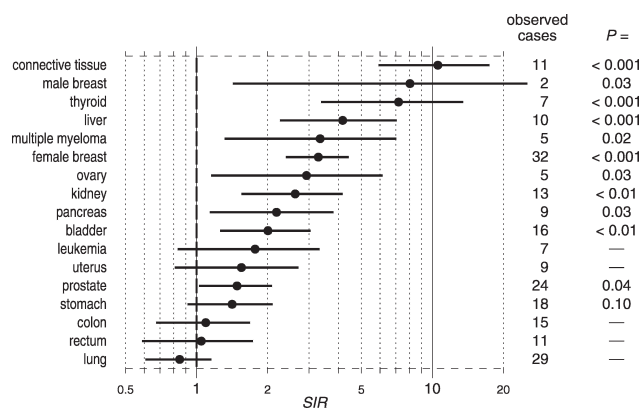
FIG. 3. Standardized incidence ratios for different sites of cancer with two-sided 90% confidence intervals (accounting for a 5-year lag period for solid cancers and malignant diseases of connective and soft tissue and a 2-year lag period for leukemia).

Figure 3 shows the SIRs for different sites of cancer with 90% confidence intervals and indicates an overall increase in the observed cancer rates relative to those expected from national rates. One of the most interesting and important results to emerge during the recent years of follow-up was the significant increase of female breast cancer incidence (32 cases observed compared to 9.7 cases expected). Remarkably, two cases of breast cancer also occurred in men (compared to 0.25 expected cases). Furthermore, a significant excess has also emerged for other sites: soft and connective tissue (11 compared to 1), thyroid (7 compared to 1), ovary (5 compared to 1.7), kidney (13 compared to 5.0), bladder (16 compared to 8.0), liver (10 compared to 2.4), pancreas (9 compared to 4.1), and prostate (24 compared to 16.1). Moreover, the number of multiple myeloma is significantly increased (5 compared to 1.5).

On the other hand, the observed number of lung cancer cases is lower than expected from a normal population (29 compared to 34.1, SIR = 0.85, 90% CI = 0.6, 1.2). The lung cancer "deficit" is restricted to the subgroup of AS patients (14 compared to 22.3) and is likely to be due to their low level of smoking (since respiratory impairment is a symptom of AS). A lower than average lung cancer risk has also been observed in another study on late effects of ^{224}Ra in which the ^{224}Ra was administered with lower doses for the treatment of AS (15). The assumption that non-radiation causes are responsible for the lower lung cancer risk in the ^{224}Ra cohort is also supported by the observation that the SIRs in the high-dose group (persons with organ doses to the lung higher than 2 Sv) and in the low-dose group (persons with organ doses lower than 2 Sv) are nearly the same: Ten lung cancer cases were registered in the

high-dose group (compared to 11.6; SIR = 0.9, 90% CI = 0.5, 1.5), whereas 19 lung cancer cases were observed in the low-dose group (compared to 21.2 expected cases; SIR = 0.9, 90% CI = 0.6, 1.3).

It might be argued that the lower than expected number of lung cancer cases is responsible for the "normal" SIR for men treated as adults given in Fig. 2. However, excluding the lung cancer cases from the number of observed cases as well as from the number of expected cases, the SIR for males treated as adults is 1.15, which is still a statistically nonsignificant increase (P = 0.1).

In the following sections, some details are given for certain cancer sites where enhanced rates have been observed.

1. Female breast cancer

Thirty-two cases were observed compared to 9.7 expected cases (SIR = 3.3, 90% CI = 2.4, 4.4; P < 0.001). In the sub-cohort of female ^{224}Ra patients treated as adults, breast cancer rates are nonsignificantly increased (12 compared to 7.1, SIR = 1.7, 90% CI = 0.98, 2.8). In the small subgroup of 106 female patients treated as children or juveniles, the excess is striking, 20 cases observed compared to 2.7 expected cases, the SIR being 7.5 (90% CI = 4.9, 10.8; P < 0.001).

Seven cases of breast cancer appeared relatively early, i.e. before the age of 45 years (Fig. 4). The youngest woman incurring breast cancer (age 28 at breast cancer diagnosis) was only 2 years old when treated with relatively high doses of ^{224}Ra.

The organ doses for breast tissue vary between 70 mSv and 11.9 Sv with a person-year weighted (pyw) mean of 2.7 Sv (pyw mean for cases: 3.1 Sv). Twelve cases were

FIG. 4. Breast cancer incidence in the subcohort of female ²²⁴Ra patients treated as adults (upper panel) and in the subcohort of those treated as children or juveniles (lower panel). The gray shaded area gives the number of patients under observation as a function of attained age (i.e. the person years at risk; left ordinate). The step function with the hatched range of standard errors represents the cumulative number of mammary carcinomas (right ordinate); the expected number of cases is indicated by the lower curve.

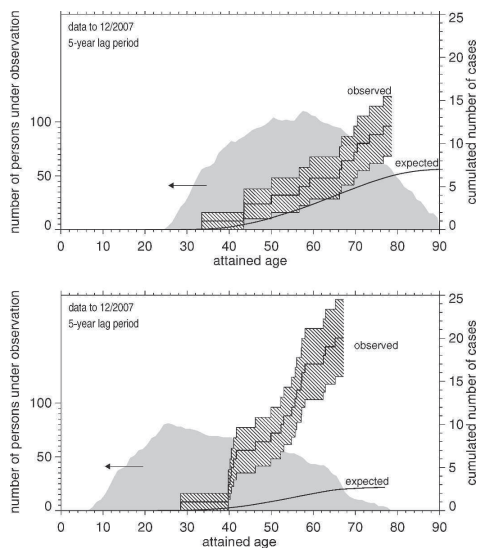observed with organ doses lower than 2 Sv (compared to 4.9 expected cases; SIR = 2.5, 90% CI = 1.4, 4.0) and 18 cases with higher organ doses (compared to 4.4; SIR = 4.1, 90% CI = 2.6, 6.0) (two cases with unknown dose). Age at exposure is a strong effect modifier. If only those women who were children or juveniles during the ²²⁴Ra treatment are considered, a more pronounced dose–effect relationship is suggested: seven breast cancer cases with organ doses lower than 2 Sv (compared to 1.4 expected cases; SIR = 5.0, 90% CI = 2.3, 9.4), 12 breast cancer cases with higher organ doses (compared to 1.2; SIR = 10.2, 90% CI = 5.9, 16.6), and one case with unknown dose.

As in other epidemiological studies of radiation-induced breast cancer, a clear age-at-exposure trend was observed. The risk estimates are of the same order of magnitude as those for the A-bomb survivors, where the ERR was estimated to be about 0.9 per Gy weighted breast dose for attained age 70 and exposure age 30 (16).

A control group was established to identify potential confounding factors such as chest X rays that might bias the breast cancer excess. The control group consists of TB patients who underwent conventional treatment that did not include ²²⁴Ra injections between the ages of 8

and 21 years at a German sanatorium in the 1940s. In the TB comparison group (114 women), a nonsignificant breast cancer excess was recorded (10 compared to 6.3). However, this excess is likely to be attributable to repeated fluoroscopic X-ray examinations in the course of a pneumothorax therapy. About 25% of control group patients received pneumothorax therapy, with correspondingly high numbers of fluoroscopies (on average 60 fluoroscopies per TB patient). The increased breast cancer incidence is much more pronounced in this subgroup (5 compared to 1.6, P = 0.02) whereas in the subgroup of women who did not receive pneumothorax therapy (on average eight fluoroscopies per TB patient) the number of observed breast cancer cases is close to normal (5 compared to 4.6). Another woman in the TB comparison group who was also treated by pneumothorax therapy was diagnosed with an angiosarcoma of the breast.

In the ²²⁴Ra cohort, TB patients were not treated by pneumothorax therapy. It is therefore presumed that the ²²⁴Ra injections are responsible for most of the breast cancer excess observed in the subcohort of those treated as children or juveniles.

2. Malignant diseases of connective and other soft tissues

Eleven cases were observed compared to 1.0 expected case (SIR = 10.5, 90% CI = 5.9, 15.5; P < 0.001). Three malignant diseases formerly classified as bone tumors are now included in the group of soft tissue cancer (two sarcomatoses, one myogenic sarcoma) due to a reclassification of the malignant bone tumors in the ²²⁴Ra cohort (17). The years of diagnosis for these cases date back several decades (to around 1955). In contrast, the other eight soft tissue malignancies were diagnosed in the 1980s or later (three leiomyosarcomas, one mesenchymal tumor, one neurofibrosarcoma, one neurilemoma, one fibrous histiocytoma and one soft tissue sarcoma). Even when these eight cases are considered separately, they amount to a significant excess (P < 0.001). Organ doses vary between 60 mSv and 17 Sv with a pyw mean of 2.4 Sv (pyw mean for cases: 3.0 Sv). Two cases were observed with organ doses lower than 2 Sv (compared to 0.6 expected cases; SIR = 3.5, 90% CI = 0.6, 10.9) and eight cases with higher organ doses (compared to 0.4; SIR = 18.8, 90% CI = 9.4, 34.0) (one case with unknown dose).

3. Thyroid cancer

Seven cases of thyroid cancer were observed compared to 1.0 expected case (SIR = 7.2, 90% CI = 3.4, 13.5; P < 0.001). It is noteworthy that most of the thyroid cancer patients were treated with ²²⁴Ra at younger ages; i.e., four of them were children during the ²²⁴Ra injections, and another two were in their early 20s when exposed (age at ²²⁴Ra injection on average:
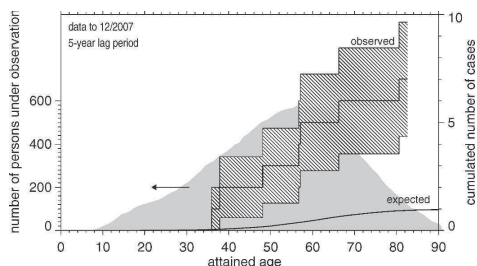
FIG. 5. Thyroid cancer incidence in the cohort of [224]Ra patients. The gray shaded area gives the person years at risk (left ordinate). The step function with the hatched range of standard errors represents the cumulative number of thyroid carcinomas (right ordinate); the expected number of cases is indicated by the lower curve.
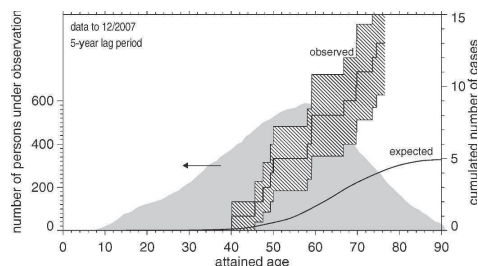
FIG. 6. Kidney cancer incidence in the cohort of [224]Ra patients. The gray shaded area gives the person years at risk (left ordinate). The step function with the hatched range of standard errors represents the cumulative number of kidney carcinomas (right ordinate); the expected number of cases is indicated by the lower curve.

17 years for thyroid cancer cases, 32 years for entire cohort). The SIR is estimated to be 17.6 in the subgroup of patients treated as children or juveniles (age at treatment ≤20 years) (90% CI = 6.0, 40.3) and 4.0 for those treated as adults (90% CI = 1.1, 10,4). Figure 5 gives the cumulative number of thyroid cancer cases in dependence on attained age.

Organ doses vary between 60 mSv and 17 Sv with a pyw mean of 2.4 Sv (pyw mean for cases: 3.0 Sv). Three cases were observed with organ doses lower than 2 Sv (compared to 0.5 expected cases; SIR = 5.7, 90% CI = 1.5, 14.6) and four cases with higher organ doses (compared to 0.4; SIR = 9.9, 90% CI = 3.4, 22.7).

The increased risk for thyroid cancer from exposure at young ages is in line with the original observation of Spiess for bone cancer due to the [224]Ra treatment (13), which was later substantiated (2) in terms of the current dosimetry (3). It is also in agreement with the high thyroid cancer risk in children exposed to the low-LET radiation from radioiodine after the Chernobyl accident (18) and with observations among the A-bomb survivors (16). The risk presented here is fully compatible with risks from the A-bomb survivors exposed when younger and risks for children exposed by the Chernobyl accident for a time since exposure of more than 10 years (18).

4. Female genital organs

In total, 15 malignant diseases of female genital organs were observed compared to 7.8 expected cases (SIR = 1.9, 90% CI = 1.2, 3.0; P = 0.01). On the one hand, there was a nonsignificant excess of uterus cancer (9 compared to 5.8; SIR = 1.6, 90% CI = 0.8, 2.7). On the other hand, the number of ovary cancers was significantly increased (5 compared to 1.7; SIR = 2.9, 90% CI = 1.2, 6.2; P = 0.03). This observation is in line with findings in other radioepidemiological studies, e.g. the study of the A-bomb survivors (16).

5. Cancers of urinary organs

Rates of bladder cancer and kidney cancer were significantly increased.

Sixteen cases of bladder cancer were observed (compared to 8.0 expected cases; SIR = 2.0, 90% CI = 1.3, 3.0; P < 0.01). Organ doses for bladder range from 67 mSv to 17 Sv with a pyw mean of 2.5 Sv (pyw mean for cases: 2.4 Sv). Eight cases were observed with organ doses lower than 2 Sv (compared to 4.8 expected cases; SIR = 1.7, 90% CI = 0.8, 3.0) and seven cases with higher organ doses (compared to 2.9; SIR = 2.4, 90% CI = 1.1, 4.5) (one case with unknown dose).

In the entire [224]Ra study cohort, 13 kidney cancer cases (compared to 5.0; SIR = 2.6, 90% CI = 1.6, 4.2; P = 0.002) were observed. For female patients, the kidney cancer excess is even more pronounced: 4 cases observed compared to 0.9 expected cases (SIR = 4.3, 90% CI = 1.5, 9.8; P = 0.02). The kidney cancers in the [224]Ra cohort were diagnosed at relatively young ages (59 years old on average; mean age at diagnosis in a normal population of comparable age distribution: 75 years, Fig. 6).

Again, it is striking that age at [224]Ra exposure is a strong effect modifier, i.e., that persons treated with [224]Ra as children or juveniles are at a considerably higher risk of incurring kidney cancer compared to those who were older at the time of [224]Ra injections. The SIR is estimated to be 7.5 (90% CI = 3.2, 14.7) for those exposed as children or juveniles (6 compared to 0.8). There is a nonsignificant excess for the older subgroup: 7 compared to 4.2 (SIR = 1.7, 90% CI = 0.8, 3.2). Organ doses for kidney range from 62 mSv to 16 Sv with a pyw mean of 2.3 Sv (pyw mean for cases: 4.0 Sv). Four cases were observed with organ doses lower than 2 Sv (compared to 2.9 expected cases; SIR = 1.4, 90% CI = 0.5, 3.2) and nine cases with higher organ doses (compared to 1.9; SIR = 4.8, 90% CI = [2.5,8.4]) (one case with unknown dose).

In the A-bomb survivor cohort, the number of kidney cancers is not large, and there was no significant excess of kidney cancer. However, there was a significant trend for increasing risk of kidney cancer with decreasing age at exposure as has been observed in the ^{224}Ra study cohort (16). Radioepidemiological data on kidney cancer are generally sparse; however, there are also two radiotherapy studies suggesting an increased kidney cancer risk after high radiation exposures (19, 20).

5. Prostate cancer

Twenty-four cases of prostate cancer were observed compared to 16.1 expected cases (SIR = 1.5, 90% CI = 1.0, 2.1; P = 0.04). No excess was found in the subcohort of AS patients; i.e., the excess was restricted to those who were treated with ^{224}Ra for TB or other diseases (13 compared to 5.2; SIR = 2.5, 90% CI = 1.5, 4.0; P < 0.01). This might be an indication that increased prostate cancer rates are associated mainly with higher radiation exposures since the subcohort of those treated for TB or other diseases received on average 50% higher doses compared to those treated for AS. Fourteen cases were observed with organ doses lower than 2 Sv (compared to 10.1 expected cases; SIR = 1.4, 90% CI = 0.8, 2.2) and 10 cases with higher organ doses (compared to 5.4; SIR = 1.8, 90% CI = 1.0, 3.1). In the atomic bomb survivor cohort, only a nonsignificantly increased prostate cancer rate was observed (16). However, in a radiotherapy study, a significant excess of prostate cancers occurred (19).

6. Liver cancer

Liver carcinomas developed in 10 patients compared to 2.4 cases expected (SIR = 4.2, 90% CI = 2.3, 7.1; P < 0.001). Eight of the 10 cases were observed in males (compared to 2.0; SIR = 4.0, 90% CI = 2.0, 7.2; P = 0.001). Organ doses to the liver are high and range from 0.2 Sv to 75 Sv with a pyw mean of 10.5 Sv (pyw mean for cases: 11.0 Sv). Six cases were observed with organ doses lower than 8 Sv (compared to 1.2 expected cases; SIR = 4.9, 90% CI = 2.1, 9.6) and four cases with higher organ doses (compared to 1.1; SIR = 3.7, 90% CI = 1.3, 8.5); i.e., there seems to be no dose–effect relationship.

However, liver cancer is frequently associated with pre-existing liver disease, and it is known that many ^{224}Ra patients suffered from hepatitis during the ^{224}Ra treatment. There are three known cases of liver cancer associated with pre-existing liver cirrhosis and one case with liver fibrosis.

7. Pancreas cancer

Nine cases of pancreas cancer were observed compared to 4.1 expected cases (SIR = 2.2, 90% CI = 1.1, 3.8; P = 0.03). Three cases were observed with organ doses lower than 2 Sv (compared to 2.5 expected cases; SIR = 1.2, 90% CI = 0.3, 3.1) and five cases with higher organ doses [compared to 1.5; SIR = 3.4, 90% CI = (1.3,7.1)] (one case with unknown dose). In the A-bomb survivor cohort, there was no indication of a statistically significant dose response for pancreas cancer; however, the excess relative risk was consistent with that for all solid cancers as a group (16). There are other radiobiological studies indicating that there is an association of radiation and an increased pancreas cancer rate (therapy studies) (21). In the ^{224}Ra cohort, the excess is restricted to females (6 compared to 1.0; SIR = 6.3, 90% CI = 2.7, 12.4; P < 0.001).

8. Leukemia

Leukemia has been observed in eight patients compared to 4.0 expected cases (P = 0.05, borderline statistical significance) with one acute myeloid leukemia (in an AS patient) diagnosed only 1.7 years after the first ^{224}Ra injection. Seven cases were observed compared to 3.9 (SIR = 1.8, 90% CI = 0.8, 3.3; P = 0.1) if a lag period of 2 years is assumed. On restricting attention to the subgroup of AS patients, five leukemia cases were observed compared to 2.2 expected (P = 0.07) (lag = 2 years: 4 compared to 2.2; P = 0.2). Two of the eight leukemia cases are of the chronic lymphocytic type, which is not generally assumed to be radiation inducible. Organ doses for red bone marrow range from 1.2 Sv to 410 Sv with a pyw mean of 51 Sv (pyw mean for cases: 49 Sv).

9. Multiple myeloma

Assuming a lag period of 2 years, five multiple myelomas were observed compared to 1.5 expected cases (SIR = 3.3, 90% CI = 1.3, 7.0; P = 0.02). There are very limited data from other radioepidemiological studies on multiple myeloma associated with radiation exposure. In the atomic bomb survivors study, a statistically significant dose response was observed based on the mortality data, but the incidence data showed little evidence of such an association (21).

Figure 7 gives an overview of the high-/low-dose group SIRs with 90% confidence intervals for those sites where SIRs for different dose groups were discussed above.

FINAL DISCUSSION AND CONCLUSION

There is no doubt that the follow-up of the health of the "Spiess study" participants has produced very important results connected with the detrimental side effects of ^{224}Ra injections. The study has been conducted by Spiess and coworkers over more than 60 years. The present results for the ^{224}Ra cohort represent an almost complete evaluation of late effects of ^{224}Ra treatment, since only about 15% of the cohort members were still alive at the end of the most recent follow-up period.
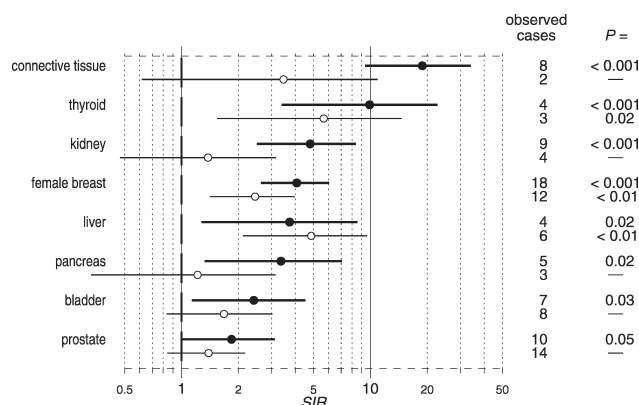
FIG. 7. Standardized incidence ratios, SIRs, for different sites of cancer with two-sided 90% confidence intervals (accounting for a 5-year lag period). For every site two SIRs are given: the thick line with solid dot represents the high-dose group, the thinner line with open dot the low-dose group. See the text for details.

In addition to the most striking *early* effect after ^{224}Ra injections, the 57 malignant bone tumors, a significant excess of *non-skeletal* malignant diseases has become evident during the two most recent observation decades. Overall, increased cancer rates are most prominent in females and especially in those treated at young ages. The increased rates of breast cancer, cancer of soft and connective tissue, and thyroid, kidney, pancreas and bladder cancer reported here are of particular importance.

The comparison of observed numbers of cancer cases in the ^{224}Ra cohort with expected numbers is based on cancer registry data. There are, of course, limitations in analyses like this that rely on external controls.

In the ^{224}Ra cohort, there were essentially two underlying medical conditions, i.e. ankylosing spondylitis and TB. There are other study groups of ankylosing spondylitis patients in which cancer risks after irradiation have been analyzed; the UK ankylosing spondylitis patients treated with X-ray therapy (19) and the German ankylosing spondylitis patients treated with lower doses of ^{224}Ra (15). In both groups, cancer mortality was lower than expected based on national rates among the nonirradiated patients. There are other study groups of former TB patients in which radiation-associated cancer risks have been studied: the Massachusetts TB patients (22) and the Canadian TB patients (23). In both cohorts, excess cancer cases/deaths were observed only in the exposed groups. A control group of former TB patients treated by conventional means that was established for those ^{224}Ra patients who were treated as children or juveniles also did not demonstrate higher than normal cancer risks, except for the subgroup treated by pneumothorax therapy, who had a high number of fluoroscopies. It can therefore be presumed that the baseline rates for the ^{224}Ra group are not higher than the population rates for reasons originating from the underlying diseases. The Saarland cancer registry is considered to be complete and representative of the German population. If biases do exist, they would result in the expected number of cancer cases, based on registry data, tending to be too high rather than too low. Thus the resulting SIR estimates can be considered as conservative.

Some comparisons of the results achieved from the ^{224}Ra study data were made, especially with results obtained from the A-bomb survivor data, i.e. a low-LET radiation study. However, no comparisons were performed with respect to other high-LET radiation studies. For example, there are some studies of patients who received intravascular injections of Thorotrast, a thorium-232 oxide preparation that concentrates in the liver, spleen and bone marrow. In the German Thorotrast patients, an extremely elevated mortality from liver cancer was observed, followed by cancers of the gallbladder and bile ducts. Most other cancer sites also showed increased mortality. However, due to the low numbers of observed cases for many cancer sites, several relative risks could not be confirmed statistically or could not be calculated at all (24). In the Danish Thorotrast patients, large excesses were seen for cancers of the liver, bile ducts and gallbladder and for leukemia other than CLL (cancer incidence). Similar findings were observed for the U.S. Thorotrast patients (cancer mortality). A marginally significant dose response was observed for the incidence of pancreatic cancer (25). In underground miners, an excess of lung cancer has been observed (26). In Mayak workers exposed to ^{239}Pu, mainly by inhalation, an excess of lung cancer has been found. Liver and bone cancers were also seen (27).

In the ^{224}Ra cohort, the risk of liver cancer is increased; however, as discussed, there is another risk factor for liver cancer present in the ^{224}Ra cohort that predisposes the study members for liver cancer, namely pre-existing liver cirrhosis. No excess of lung cancer has been observed in the ^{224}Ra study, presumably because of lower than average smoking habits. Finally, bone cancer in the ^{224}Ra cohort is a special issue that was not reanalyzed in the present study.

An increase of internal diseases such as kidney insufficiency, heart attack or coronary heart disease was recently reported by Spiess (28). Due to the lack of valid baseline rates of these internal diseases, this statement of a hypothesized increase is based on recent comparisons of living patients of similar age range in the exposed and the control cohort. Although one cannot exclude the possibility of biases, the increased rates of non-cancer diseases appear to become more important in the description of radiation late effects in the ^{224}Ra study.

REFERENCES

1. R. R. Wick, E. A. Nekolla, M. Gaubitz and T. L. Schulte, Increased risk of myeloid leukaemia in patients with ankylosing spondylitis following treatment with radium-224. *Rheumatology* **47**, 855–859 (2008).

2. E. A. Nekolla, M. Kreisheimer, A. M. Kellerer, M. Kuse-Isingschulte, W. Gössner and H. Spiess, Induction of malignant bone tumors in radium-224 patients. Risk estimates based on the improved dosimetry. *Radiat. Res.* **153**, 93–103 (2000).

3. K. Henrichs, L. Bogner, E. Nekolla, D. Noßke and T. Roedler-Vogelsang, Extended dosimetry for studies with ^{224}Ra patients. In *Health Effects of Internally Deposited Radionuclides: Emphasis on Radium and Thorium* (G. van Kaick, A. Karaoglou and A. M. Kellerer, Eds.), pp. 33–38. World Scientific, Singapore, 1995.

4. ICRP, *Age-dependent Doses to Members of the Public from Intake of Radionuclides: Part 2. Ingestion Dose Coefficients.* ICRP Publication 67, *Annals of the ICRP*, Vol. 23, nos. 3/4, Pergamon Press, Oxford, 1993.

5. M. Lassmann, D. Nosske and C. Reiners, Therapy of ankylosing spondylitis with ^{224}Ra-radium chloride: dosimetry and risk considerations. *Radiat. Environ. Biophys.* **41**, 173–178 (2002).

6. W. Gössner, Pathology of radium-induced bone tumors: New aspects of histopathology and histogenesis. *Radiat. Res.* **152** (Suppl.), S12–S15 (1999).

7. H. Spiess, Schwere Strahlenschäden nach der Peteosthor-Behandlung von Kindern (Serious radiation damage after Peteosthor treatment of children). *Dtsch. Med. Wschr.* **81**, 1053–1054 (1956).

8. H. Spiess and C. W. Mays, Bone cancers induced by ^{224}Ra (Th X) in children and adults. *Health. Phys.* **19**, 713–729 (1970).

9. C. W. Mays, H. Spiess, D. Chmelevsky and A. M. Kellerer, Bone sarcoma cumulative tumour rates in patients injected with ^{224}Ra. *Strahlentherapie Suppl.* **80**, 27–31 (1985).

10. D. Chmelevsky, A. M. Kellerer, H. Spiess and C. W. Mays, A proportional hazards analysis of bone sarcoma rates in German ^{224}radium patients. *Strahlentherapie Suppl.* **80**, 32–37 (1985).

11. A. M. Kellerer, H. Spiess and D. Chmelevsky, Dose and dose rate dependence for bone sarcomas in radium-224 patients. *Int. J. Radiat. Biol.* **58**, 864–866 (1990).

12. D. Chmelevsky, H. Spiess, C. W. Mays and A. M. Kellerer, The reverse protraction factor in the induction of bone sarcomas in radium-224 patients. *Radiat. Res.* **124** (Suppl.), S69–S79 (1990).

13. H. Spiess, Ra-224-induced tumors in children and adults. In *Delayed Effects of Bone-Seeking Radionuclides* (C. W. Mays, W. S. S. Jee, R. D. Lloyd, B. J. Stover, J. H. Dougherty and G. N. Taylor, Eds.), pp. 227–248. University of Utah Press, Salt Lake City, 1969.

14. J. H. Lubin, J. D. Boice, C. Edling, R. W. Hornung, G. Howe, E. Kunz, R. A. Kusiak, H. I. Morrison, E. P. Radford and D. A. Pierce, *Lung Cancer and Radon: A Joint Analysis of 11 Underground Miners Studies.* NIH Publication No. 94-3644, U.S. Department of Health and Human Services, National Institutes of Health, Bethesda MD, 1994.

15. R. R. Wick, M. J. Atkinson and E. A. Nekolla, Incidence of leukaemia and other malignant diseases following injections of the short-lived alpha-emitter ^{224}Ra into man. *Radiat. Environ. Biophys.* **48**, 287–294 (2009)

16. D. L. Preston, E. Ron, S. Tokuoka, S. Funamoto, N. Nishi, M. Soda, K. Mabuchi and K. Kodama, Solid cancer incidence in atomic bomb survivors: 1958–1998. *Radiat. Res.* **168**, 1–64 (2007).

17. W. Gössner, R. R. Wick and H. Spiess, Histopathological review of radium-224 induced bone sarcomas. In *Health Effects of Internally Deposited Radionuclides: Emphasis on Radium and Thorium* (G. van Kaick, A. Karaoglou and A. M. Kellerer, Eds.), pp. 255–259. World Scientific, Singapore, 1995.

18. L. Walsh, J. C. Kaiser and P. Jacob, Radiation risk modeling of thyroid cancer with special emphasis on the Chernobyl epidemiological data. *Radiat. Res.* **172**, 509–518 (2009).

19. H. A. Weiss, S. C. Darby and R. Doll, Cancer mortality following X-ray treatment for ankylosing spondylitis. *Int. J. Cancer* **59**, 327–338 (1994).

20. J. D. Boice, G. Engholm, R. A. Kleinerman, M. Blettner, M. Stovall, H. Lisco, W. C. Moloney, D. F. Austin, A. Bosch and B. MacMahon, Radiation dose and second cancer risk in patients treated for cancer of the cervix. *Radiat. Res.* **116**, 3–55 (1988).

21. National Research Council, Committee to Assess Health Risks from Exposure to Low Levels of Ionizing Radiation, *Health Risks from Exposure to Low Levels of Ionizing Radiation: BEIR VII Phase 2.* The National Academies Press, Washington, DC, 2006.

22. J. D. Boice Jr., D. Preston, F. G. Davis and R. R. Monson, Frequent chest X-ray fluoroscopy and breast cancer incidence among tuberculosis patients in Massachusetts. *Radiat. Res.* **125**, 214–222 (1991).

23. G. R. Howe and J. McLaughlin, Breast cancer mortality between 1950 and 1987 after exposure to fractionated moderate-dose-rate ionizing radiation in the Canadian fluoroscopy cohort study and a comparison with breast cancer mortality in the atomic bomb survivors study. *Radiat. Res.* **145**, 694–707 (1996).

24. N. Becker, D. Liebermann, H. Wesch and G. Van Kaick, Mortality among Thorotrast-exposed patients and an unexposed comparison group in the German Thorotrast study. *Eur. J. Cancer* **44**, 1259–1268 (2008).

25. L. B. Travis, M. Hauptmann, L. K. Gaul, H. H. Storm, M. B. Goldman, U. Nyberg, E. Berger, M. L. Janower, P. Hall and M. Andersson, Site-specific cancer incidence and mortality after cerebral angiography with radioactive Thorotrast. *Radiat. Res.* **160**, 691–706 (2003).

26. National Research Council, Committee on Health Risks of Exposure to Radon, *The Health Effects of Exposure to Indoor Radon (BEIR VI)*. National Academy Press, Washington, DC, 1999.

27. M. E. Sokolnikov, E. S. Gilbert, D. L. Preston, E. Ron, N. S. Shilnikova, V. V. Khokhryakov, E. K. Vasilenko and N. A. Koshurnikova, Lung, liver and bone cancer mortality in Mayak workers. *Int. J. Cancer* **123**, 905–911 (2008).

28. H. Spiess, Life span study on late effects of radium-224 in children and adults, 10th International Conference on the Health Effects of Incorporated Radionuclides, 10–14 May 2009, Santa Fe, New Mexico, USA. *Health Phys.* in press.

37. Walsh L, Radiation Protection in Occupational and Environmental settings, commissioned editorial, Occ. Env. Med (BMJ). 68, 387-388, 2011

Risks from nuclear accidents are still uncertain

Dana Loomis

As this issue of OEM goes to press, the situation at the Fukushima Daiichi nuclear power plant damaged by the March, 2011 earthquake and tsunami in Japan is classified at the highest level of severity on to the International Nuclear Event Scale—a value of 7, also given to the Chernobyl accident.[1] An editorial and a review article in this issue of the Journal[2 3] (*see pages 387 and 457*) and a complementary review and editorial we published in 2009[4 5] highlight both the progress that has been made in understanding the risks associated with exposure to ionising radiation and the considerable uncertainties that remain to be resolved.

Most of what we know about the health risks of ionising radiation comes from long-term studies of the survivors of the nuclear bombings at Hiroshima and Nagasaki and from follow-up of workers exposed to low levels of radiation over extended periods. Unfortunately, neither set of studies tells us enough about what to expect after a nuclear accident. One of the challenges is that major accidents occur rarely, so the database on their consequences is limited: the previous incidents at Three Mile Island and

Chernobyl may not have enough in common with the recent events in Japan to allow predictions to be made. Each accident also has its own uncertainties as it evolves, and workers who are trying to control an incident or respond to it are likely to be exposed under emergency conditions to hazards that are unknown and largely unpredictable.[6] Population exposures following an accident are also difficult to predict. Radioactive material from the Chernobyl accident travelled around the world (eg, Kurttio *et al*[7]) and radionuclides believed to be from Fukushima have already been detected as far away as the west coast of the USA, so the recent incident may result in exposures worldwide, as well as locally.

The challenges of identifying the health consequences of such exposures are many and significant. Doses must be reconstructed, cases must be ascertained, and analyses must be conducted with enough sensitivity to detect a subtle signal of exposure amid the effects of other risk factors. As the recent papers in the Journal indicate, this process is fraught with uncertainty even after exposures and disease events have occurred and are, at least in principle, measurable.

The much greater challenges of predicting the consequences of a complex incident as it unfolds speaks to the

limitations of exposure assessment and epidemiology as observational sciences, rather than predictive ones. Greater ability to use models to quickly forecast future events under a variety of scenarios could move the science forward and offer the potential for evidence-based decisions in emergency situations. Ultimately the reduction of uncertainty should lead to increased ability to protect workers and the public from the adverse effects of complex nuclear emergencies and their aftermath.

Competing interests None.

Correspondence to Dana Loomis, Department of Epidemiology, University of Nebraska, 984395 Nebraska Medical Center, Omaha, Nebraska, USA; dana.loomis@unmc.edu

REFERENCES

1. **International Atomic Energy Agency.** *Fukushima Nuclear Accident Update Log*. http://www.iaea.org/newscenter/news/tsunamiupdate01.html (accessed 19 Apr 2011).
2. **Walsh L.** Radiation protection in occupational and environmental settings. *Occup Environ Med* 2011;**68**:387—9.
3. **Daniels RD,** Schubauer-Berigan MK. A meta-analysis of leukaemia risk from protracted exposures to low-dose gamma radiation. *Occup Environ Med* 2011;**68**:457—64.
4. **Richardson DB.** Cancer risks and radiation. *Occup Environ Med* 2009;**66**:785—6.
5. **Jacob P,** Ruhm W, Walsh L, *et al*. Is cancer risk of radiation workers larger than expected? *Occup Environ Med* 2009;**66**:789—96.
6. **Sim MR.** Disaster response workers: are we doing enough to protect them? *Occup Environ Med* 2011;**68**:309—10.
7. **Kurttio P,** Pukkala E, Ilus T, *et al*. Radiation doses from global fallout and cancer incidence among reindeer herders and Sami in Northern Finland. *Occup Environ Med* 2010;**67**:737—43.

Radiation protection in occupational and environmental settings

Linda Walsh

The assessment of detrimental health risks for humans, due to exposures from ionising

Correspondence to Dr Linda Walsh, Federal Office for Radiation Protection, Department 'Radiation Protection and Health', Ingolstaedter Landstr 1, 85764 Oberschleissheim, Germany; lwalsh@bfs.de

radiation sources such as γ-rays, x-rays and neutrons, which penetrate deeply into the human body, has been an endeavour which has increased in magnitude and effort over the last century. Solid cancer and leukaemia incidence and mortality have emerged as having radiation as an important proven

risk factor from the many indicators of cellular damage and health effects that have been investigated to date. Studies on survivors of the World War II atomic bombings over Hiroshima and Nagasaki, who were exposed mainly to γ-rays and neutrons, continue to provide valuable radiation epidemiological data and quantitative assessments of the radiation related solid cancer and leukaemia risks.[1] The cohort of the atomic bomb survivors is unique and characterised by: the large number of cohort members (approximately 105 000); the long follow-up period of more than 50 years; a composition that includes males and females, children and adults; whole-body exposures (which are

more typical for radiation protection situations than the partial-body exposures associated with many medically exposed cohorts); a large dose range from natural to lethal levels; and an internal control group with negligible doses, that is, those who survived at large distances (>3 km) from the hypocentres. Results from this cohort have formed a basis in the construction of radiation protection guidelines that include the setting of various dose limits to the radiation received by occupationally exposed workers and the general public. Such dose limits come from assessments and recommendations that are issued and updated at regular intervals by international bodies, that is, the International Commission on Radiological Protection[2] and the United Nations Scientific Committee on the Effects of Atomic Radiation.[3]

Some of the major moot issues and sources of uncertainty related to the formulation of dose limit recommendations for radiation protection include the following points: first, the sensitivity of different organs to radiation and the relative tissue damaging effect of the various types of radiation are uncertain; second, the factors by which risks for children and young persons are higher than for adults; third, the shape and statistical significance of the cancer risk measure when plotted as a function of dose are not very well defined, particularly at the lower end of the dose range (where the associated error bars tend to be relatively wider than at higher doses); fourth, whether or not the cancer risks are similar for acute high-dose-rate exposures (as pertinent to the Japanese A-bomb survivors) and protracted low-dose-rate exposures (as relevant to a broad category of nuclear workers and the general population).

An important paper by Daniels and Schubauer-Berigan,[4] relevant to the last two of these issues with respect to leukaemia risks appears in this issue of OEM (*see page 457*). Daniels and Schu-bauer-Berigan have considered recent epidemiological evidence relevant to leukaemia mortality and incidence risks from protracted low dose and low-dose-rate exposures to γ-rays by making an extensive literature review of many studies on groups of people who were either occupationally or environmentally exposed. The reviewed studies are very interesting and include Chernobyl nuclear-accident clean-up workers, residents of apartments built in Taiwan with accidently contaminated metal support structures and a pooled study of nuclear workers in 15 countries. This initial liter-

ature review was narrowed down to 23 (20 occupational and three environmental) studies which fulfilled a predefined set of inclusion criteria related to study design and type of risk estimates reported. The individual risks were then analysed together by Daniels and Schubauer-Berigan in a meta-analysis; this basically involved constructing aggregated risks in the form of weighted means from the individual risk estimates for various subgroups of the 23 studies. The main advantage of conducting a meta-analysis is that the aggregated risks are then usually associated with smaller uncertainties than the uncertainties in the individual studies. Daniels and Schubauer-Berigan also carefully tested their aggregated results to find out if they were unduly influenced by bias or not. Sources of bias tested were: any particular individual study that may have unduly influenced the aggregated measure; an overlap of study participants between two or more studies; and the preferred publication of studies that reported a positive risk over those that found no risk. The main results reported for leukaemia pertain to mixed mortality and incidence effect sizes associated with a total radiation dose of 100 mGy. In order to obtain a perspective on this level of dose, it may be interesting to note that a total dose of 100 mGy is approximately 50—100 times larger than the annual natural background radiation and is roughly equivalent to five times the annual occupational limit that is currently in place in most European countries. The main risk measure value reported in the Daniels and Schubauer-Berigan paper, that is, the Excess Relative Risk, indicated that the spontaneous leukaemia risk (ie, for a group of unexposed persons) was found to be increased by 19% due to a dose of 100 mGy. The 19% increase was reported to agree well with the risk from acute exposure from the Japanese A-bomb survivors and is therefore an indication that leukaemia risks are similar for protracted and acute exposures. Moreover, the 95% CI associated with the 19% was found to range from 7% to 32%, which is reported to be narrower than a comparable interval for the Japanese A-bomb data.[5] This latter result is important for radiation protection because it presents narrower uncertainties than those associated with the A-bomb, acute exposure risks at this dose and also narrower uncertainties than those associated with the individual studies that contributed to the aggregated risk. Although Daniels and Schubauer-Berigan did not use the most recent A-bomb leukaemia risks[6 7] for

comparison, this does not affect their conclusions.

The main conclusions of the Daniels and Schubauer-Berigan paper are that protracted exposure to low-dose gamma radiation is significantly associated with leukaemia and that leukaemia risks are similar for protracted and acute exposures. These outcomes complement similar conclusions drawn for solid cancer in an analogous meta-analysis published in OEM last year[8] and add to the weight of evidence that is mounting up to indicate that cancer risks are similar for protracted and acute exposures for both solid cancer and leukaemia. This paper will undoubtedly find its way into international discussions as an important contribution to risk—benefit assessment of medical exposures and radiation protection in general, and specifically for the millions of persons worldwide working in jobs that involve low-level protracted exposure to ionising radiation.

REFERENCES

1. **Preston DL,** Ron E, Tokuoka S, et al. Solid cancer incidence in atomic bomb survivors: 1958—1998. *Radiat Res* 2007;**168**:1—64.
2. **International Commission on Radiological Protection.** The 2007 recommendations of the International Commission on Radiological Protection. ICRP_103. *Ann ICRP* 2007;**37**:1—332.
3. **United Nations.** Effects of ionizing radiation. *United Nations Scientific Committee on the Effects of Atomic Radiation UNSCEAR 2006 Report. Volume I. Annex A: Epidemiological Studies of Radiation and Cancer.* New York: United Nations, 2008.
4. **Daniels RD,** Schubauer-Berigan MK. A meta-analysis of leukaemia risk from protracted exposures to low-dose gamma radiation. *Occup Environ Med* 2011;**68**:457—64.
5. **Cardis E,** Vrijheid M, Blettner M, et al. Risk of cancer after low doses of ionising radiation: retrospective cohort study in 15 countries. *BMJ* 2005;**331**:77—82.
6. **Little MP,** Hoel DG, Molitor J, et al. New models for evaluation of radiation-induced lifetime cancer risk and its uncertainty employed in the UNSCEAR 2006 report. *Radiat Res* 2008;**169**:660—76.
7. **United States National Research Council.** *Committee to Assess Health Risks from Exposure to Low Levels of Ionizing Radiation. Health Risks from Exposure to Low Levels of Ionizing Radiation: BEIR VII—Phase 2.* Washington: United States National Academy of Sciences. National Academy Press, 2006.
8. **Jacob P,** Rühm W, Walsh L, et al. Is cancer risk of radiation workers larger than expected? *Occup Environ Med* 2009;**66**:789—96.

38. Walsh L & Kaiser JC. Multi-model inference of adult and childhood leukaemia excess relative risks based on the Japanese A-bomb survivors mortality data (1950-2000). Radiat. Environ. Biophys. 50, 21-35, 2011

ORIGINAL PAPER

Multi-model inference of adult and childhood leukaemia excess relative risks based on the Japanese A-bomb survivors mortality data (1950–2000)

Linda Walsh · Jan Christian Kaiser

Abstract Some relatively new issues that augment the usual practice of ignoring model uncertainty, when making inference about parameters of a specific model, are brought to the attention of the radiation protection community here. Nine recently published leukaemia risk models, developed with the Japanese A-bomb epidemiological mortality data, have been included in a model-averaging procedure so that the main conclusions do not depend on just one type of model or statistical test. The models have been centred here at various adult and young ages at exposure, for some short times since exposure, in order to obtain specially computed childhood Excess Relative Risks (ERR) with uncertainties that account for correlations in the fitted parameters associated with the ERR dose–response. The model-averaged ERR at 1 Sv was not found to be statistically significant for attained ages of 7 and 12 years but was statistically significant for attained ages of 17, 22 and 55 years. Consequently, such risks when applied to other situations, such as children in the vicinity of nuclear installations or in estimates of the proportion of childhood leukaemia incidence attributable to background radiation (i.e. low doses for young ages and short times since exposure), are only of very limited value, with uncertainty ranges that include zero risk. For example, assuming a total radiation dose to a 5-year-old child of 10 mSv and applying the model-averaged risk at 10 mSv for a 7-year-old exposed at 2 years of age would result in an ERR = 0.33, 95% CI: −0.51 to 1.22. One model (United Nations scientific committee on the effects of atomic radiation report. Volume 1. Annex A: epidemiological studies of radiation and cancer, United Nations, New York, 2006) weighted model-averaged risks of leukaemia most strongly by half of the total unity weighting and is recommended for application in future leukaemia risk assessments that continue to ignore model uncertainty. However, on the basis of the analysis presented here, it is generally recommended to take model uncertainty into account in future risk analyses.

Introduction

The assessment of detrimental health risks due to exposures from ionizing radiation has been an endeavour that has increased in magnitude and effort over the last century. Solid cancer and leukaemia incidence and mortality have emerged, from the many indicators of cellular damage and health effects investigated to date, as having radiation as an important and proven risk factor. Studies on survivors of the World War II atomic bombings over Hiroshima and Nagasaki continue to provide valuable radiation epidemiological data and quantitative assessments of the radiation-related solid cancer and leukaemia risks (Preston et al. 2003, 2004, 2007).

A related, recurring, research topic is whether increased risks for childhood leukaemia incidence exist in geographical regions near nuclear power stations or other installations related to the nuclear industry (Laurier et al. 2008). Nearly all of the 198 local nuclear site studies and 25 multi-site descriptive studies of leukaemia risk among children and young adults in the vicinity of nuclear facilities, recently reviewed (Laurier et al. 2008), have

L. Walsh (✉)
Department "Radiation Protection and Health",
Federal Office for Radiation Protection, Ingolstädter Landstr. 1,
85764 Oberschleissheim, Germany
e-mail: lwalsh@bfs.de

J. C. Kaiser
Institute of Radiation Protection, Helmholtz Zentrum München,
Ingolstädter Landstr. 1, 85764 Oberschleissheim, Germany

concluded that no significant leukaemia excesses exist. However, some local clusters of leukaemia cases are apparent and levels of concern rose recently, after a German study reported indications of a decreasing leukaemia incidence risk with distance from nuclear power plants among children under 5 years of age (Kaatsch et al. 2008). Another related issue involves estimates of the proportion of childhood leukaemia incidence that may be due to natural background ionizing radiation (e.g. about 15–20% in the United Kingdom according to Little et al. (2009), Wakeford et al. (2009)). Such estimates rely on the risk models developed with the Japanese A-bomb epidemiological data.

In view of these concerns, it is of interest to take a new detailed look at the models for leukaemia risks from ionizing radiation that have been fitted recently to data from the Japanese A-bomb Life Span Study (LSS) mortality studies. Although the modern studies mentioned earlier involve leukaemia incidence, whereas the LSS dataset considered here is for leukaemia mortality, it is assumed here that incidence and mortality are interchangeable for inter-study comparison purposes, because the treatment options were very limited in the past. A general review of recently published leukaemia models reveals here that—although existing models can be applied to young ages at exposure and short times since exposure of above 5–10 years—all published leukaemia models yield risks and uncertainties that are centred at adult age at exposure and middle-aged attained age, for several decades after exposure. The necessary calculations required to derive risks from these models at young ages at exposure and short times since exposure involve considerable difficulties and uncertainties associated with combining many fitted parameters, unpublished parameter correlations and very considerable model-to-model variations.

The purpose of the present paper is to re-examine and re-fit, under the same set of conditions, nine currently published leukaemia models (Preston et al. 2004; Little et al. 2008; UNSCEAR 2006; Schneider and Walsh 2009; Richardson et al. 2009; BEIR 7 phase 2 2006) that have been fitted to the most recent epidemiological mortality data (Preston et al. 2004) from the Japanese A-bomb survivors. This involved derivations of the overall Excess Relative Risks (ERR) of leukaemia mortality for the models, both as they currently stand in the literature and also with modifications to produce a degree of compatibility between models. Most of the models considered here have also been centred at various young ages at exposure and shorter times since exposure, in order to obtain specially computed childhood risks and uncertainties that account for correlations in the fitted parameters associated with the dose–response. Techniques of multi-model inference have also been applied to these nine models, and the

risks of leukaemia in adults aged 55 years and in young persons aged 7, 12, 17 and 22 years, which include model uncertainty, have been obtained.

Materials and methods

Model choice and multi-model inference statistics

Datasets in radiation epidemiology are observational and often involve numerous covariables that can be fitted to various forms of models. Consequently, assessing the preferred model by selection involving Akaike's information criterion is an important part of the inferential process (Akaike 1973, 1974; Walsh 2007). Akaike's information criterion is defined by AIC = −2log(MaxLikelihood) + 2 k, where k is the number of parameters in the model. Models with smaller values of AIC are favoured on the basis of fit and parsimony. However, using the data to choose a model and progressing to subsequent inference, assuming that the selected model has been chosen a priori, is a process that fails to acknowledge the uncertainties present in the model selection process (Chatfield 1995). Indeed, a large source of uncertainty for cancer risk evaluations associated with radiation exposure is model uncertainty. Neglecting this source is a serious shortcoming of previous evaluations. The modelling of leukaemia risks has been extended in this paper to take account of model uncertainties by allowing all currently circulating models (known to the authors) to contribute to risk estimation.

Recent statistical literature covers various approaches for model averaging (Hoeting et al. 1999; Posada and Buckley 2004; Claeskens and Hjort 2008). The work by Burnham and Anderson (1998, 2002) has been influential and has resulted in a major paradigm shift away from hypothesis testing as a tool for model choice. To average over all candidate models, a weight is assigned to each model, and then measures of interest are inferred across all weighted models. The introduction of AIC for model selection has been a positive contribution to the field of radiation epidemiology. In other fields, such as biology and ecology, the AIC weights for model averaging have already been providing an objective basis for model selection and multi-model inference (e.g. Zhang and Townsend 2009). Within the AIC framework, the weights (w_i, $i = 1, 2,…, m$) are computed for each model,

$$w_i = \exp[-0.5(\text{AIC}_i - \text{minAIC})] \bigg/ \sum_{j=1}^{m} \exp[-0.5(\text{AIC}_j - \text{minAIC})] \quad (1)$$

where m is the number of models and min AIC is the smallest AIC value among all models considered.

The minimum AIC is subtracted merely to avoid numerical problems caused by very high or very low arguments inside the exponential function. Individual w_i values can be interpreted to indicate the probability that the ith model is the best among the m models considered. A model-averaged estimator of a quantity, $\hat{\mu}$ (which is, in the practical terms of the analysis presented here, either the ERR/1 Sv or the low-dose limiting ERR/Sv or 100 ERR/ 10 mSv) can then be obtained as a weighted average of estimators, $\hat{\mu}_i$, from model i

$$\hat{\mu} = \sum_{i=1}^{m} w_i \hat{\mu}_i. \tag{2}$$

It is also possible to replace AIC in Eq. (1) either by the Bayesian Information Criterion (BIC) (see Walsh (2007) for an explanation of BIC) or other information criteria for special purposes (Claeskens and Hjort 2008). Approaches have also been developed to derive parameters of the distribution of $\hat{\mu}$ (Hoeting et al. (1999), Claeskens and Hjort (2008)).

The confidence intervals for the model averages $\hat{\mu}$ were calculated here by two methods. Method 1 involved evaluating Eq. 1 of Hoeting et al. (1999) (under the assumption that all models are equally likely a priori) with Monte-Carlo simulated sub-sets of realizations, i.e. one sub-set per model, where the size of each sub-set corresponded to its Akaike weight. Then, the sub-sets pertaining to separate models (e.g. 500, 300, or 200 realizations from models 1, 2 and 3 with Akaike weights of 0.5, 0,3 and 0.2, respectively) were merged to form a total set of 1,000 realizations. The realizations were then sorted, and the percentiles, corresponding to the level of confidence required, were located and adopted as upper and lower confidence intervals. Method 2 involved application of the following formula for the standard error (SE) of the model-averaged $\hat{\mu}$, from Burnham and Anderson (2004):-

$$SE(\hat{\mu}) = \sum_{i=1}^{m} w_i \sqrt{Var\left(\hat{\mu}\right) + \left(\hat{\mu}_i - \hat{\mu}\right)^2}. \tag{3}$$

Data on leukaemia mortality

The cohort of the atomic bomb survivors from Hiroshima and Nagasaki is unique owing to: the large number of cohort members; the long follow-up period of more than 50 years; a composition that includes males and females, children and adults; whole-body exposures (that are more typical for radiation protection situations than the partial-body exposures associated with many medically exposed cohorts); a large dose range from natural to lethal levels; and an internal control group with negligible doses, i.e. those who survived at large distances (>3 km) from the

hypocentres. The most recent dataset on cancer mortality for the follow-up time periods from 1950 to 2000 (Preston et al. 2004) (data file: DS02CAN.DAT from http://www.rerf.or.jp), with the new dosimetry system DS02 (Young and Kerr 2005), has been selected for most recently published leukaemia models. The mortality data are in a tabulated grouped form and are categorized by gender, city, age-at-exposure (5-year intervals), age-attained (5-year intervals), the calendar time period during which the health checks were made, and weighted survivor marrow dose.

Weighted doses

Weighted organ doses are defined by

$$d = d_\gamma + RBE\, d_n, \tag{4}$$

where d_γ and d_n are organ absorbed doses from γ-rays and neutrons, respectively. For RBE, the relative biological effectiveness of neutrons, the value 10 has been used. This value was chosen because it is used in most of the current analyses of the LSS data, although there are arguments that other values might be more appropriate (Rühm and Walsh 2007). Since this analysis involves currently published models for all types of leukaemia grouped together, weighted marrow doses have been applied with dose categories truncated to correspond to the 4-Gy kerma level. In common with previous analyses (e.g. Preston et al. 2004), statistical methods are used to reduce risk-estimation bias resulting from imprecision in individual dose estimates. The necessary adjustments for random errors in dosimetry applied to the dose term are already applied in the publicly available data, but a separate adjustment involving a multiplication factor to the dose-squared covariable should be done explicitly, according to either Pierce et al. (1990) (factor 1.12) or Pierce et al. (2008) (revised factor 1.15). Since most of the published analyses apply the factor 1.12, this has been adopted here.

The leukaemia models for A-bomb survivors

The risk models for radiation-induced leukaemia mortality applied here were selected by two criteria, i.e. that they were already published and based on the most recent leukaemia mortality dataset that is described earlier (Preston et al. 2004; Little et al. 2008; UNSCEAR 2006; Schneider and Walsh 2009; Richardson et al. 2009; BEIR 7 phase 2 2006). To the author's knowledge, the selection is complete by these two criteria. The first paper to report a leukaemia model, based on the then pre-release mortality data (1950–2000), was that of Preston et al. (2004). This was, however, an Excess Absolute Risk (EAR) model that has been recomputed here (refitted—in AMFIT) in the original parameter formulation, but as an ERR model (with fitted

parameters given in the Appendix Table 6) for inclusion in the model-averaging process. The paper by Little et al. (2008) reports on the models that were adopted in the UNSCEAR (2006) report. All models were identical between these latter two publications except the leukaemia ERR model that had a term adjusting for age at exposure in Little et al. (2008); this adjustment was not included in the UNSCEAR (2006) model, and therefore, both models are considered here. The models of Schneider and Walsh (2009), developed for assessing health risks to astronauts, are very similar to those in Little et al. (2008) and UNSCEAR (2006) even though they were developed independently at the same time, however, since they are very similar to previously published models for solid cancer (Preston et al. 2003), this is not surprising. The paper by Richardson et al. (2009) contains a model (in Table 3 of that paper) based on a cubic spline function of time since exposure but fitted to a dataset (not available to other members of the scientific community) that contains 14 additional leukaemia deaths and more detailed information on the types of leukaemia than the generally available data. For this reason, the model used by Richardson et al. (2009) for all types of leukaemia has been fitted here to the publicly available data for inclusion in the model-averaging process. Details of the latter model fitted to the publicly available data are presented here in the "Appendix" where Table 7 gives the fitted parameters and Fig. 2 shows a version of the Fig. 1 from Richardson et al. 2009 repeated for the parameters in Table 7. Table A1 in the "Appendix" of Richardson et al. (2009) also gives parameters for the BEIR 7 phase 2 (2006) model with two additional, similar, models that have also been fitted to the publicly available data; all three of these models were included in the model averaging here.

The present analysis, which is based on the models mentioned above, is gender averaged to facilitate the model-to-model comparisons. All models considered made use of a general rate (hazard) model of the form

$$\lambda(d, a, e, t, c, s, l) = \lambda_0(a, e, t, c, s, l)$$
$$\times [1 + \mathrm{ERR}(d, a, e, t, c, s, l)], \qquad (5)$$

for the ERR, where $\lambda_0(a, e, t, c, s, l)$ is the baseline cancer death rate, a is attained age, e is age at exposure, t is time since exposure, c is a two-level city indicator variable for Hiroshima and Nagasaki, s is a gender indicator variable and l is a two-level indicator variable for survivor location from the bomb hypocentre, i.e. proximal (<3 km) or distal.

The functional forms for the baseline model parts (i.e. to account for the spontaneous cancer rates that would have occurred in the absence of ionizing radiation) are given in Table 8 of the "Appendix" where it can be seen that seven models adopted a fully parametric approach and two dealt with baseline rates via stratification.
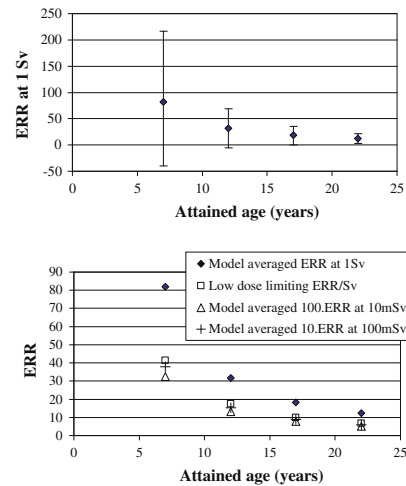
Fig. 1 Model-averaged ERR at 1 Sv values with Monte-Carlo simulated 95% CIs for various values of attained age in years from Table 4 (*top panel*) The *lower panel* shows the same ERR values again without confidence intervals for comparison with the low-dose limiting ERR/Sv and 100 and 10 times the model-averaged ERR at 10 and 100 mSv, respectively, from Table 5. Note the values at attained age 12, 17 and 22 years are for 10 years since exposure, and the value at attained age 7 is for 5 years since exposure

All models considered have an ERR form factorized into a function of dose and a modifying function that depends on some choice of a, e, t, c, s and l. The functional forms vary and are given in Table 1.

It is instructive here to explain, using an example, a property of the age and time risk centring constants that simplifies the computation of uncertainties. Consider splitting ERR(d, a, e) into ERR(d) * exp $(-\gamma (e-30) + \varepsilon \ln(a/55))$, where the ERR at unit dose is for an age at exposure of 30 years and an attained age of 55 years, and γ, ε are fitted parameters. The model centring at age at exposure of 30 years and an attained age of 55 years (or time since exposure of 25) serves as a reference for the main ERR dose–response, the fitted parameters and their uncertainties. In all but one of the nine models considered (i.e. the Richardson et al. (2009) model in Table 3 of that paper), different choices of centring values will not affect the overall quality of fit (the deviance value). Such a model can then be refitted at different centring ages, for example $e = 7$, $a = 17$, and the ERR at 1 Sv can be found by combining only the fitted parameters relevant to the dose–response. This is more efficient than having to combine all ERR fitted parameters for dose, age and time, and saves a considerable effort in the evaluation of the relevant uncertainties. Currently it is not possible to reliably

Table 1 Forms of excess relative risk models applied in the model-averaging procedure

Model reference	Form of ERR model
EAR model of Preston et al. (2004) (used here as an ERR model)	$(1 + \omega_s.s).\ (d + \theta.d^2).\ \exp\{\theta_{1-3}.\ ecat_{1-3} + \tau_{1-3}.\ ecat_{1-3}.\ \ln(t/25)\}$
BEIR VII, phase 2 (2006)	$(\beta_s.s).\ (d + \theta.d^2).\ \exp(\gamma\ e' + \delta\ \ln(t/25) + \phi\ e'\ln(t/25))$, where $e' = \min(0,(e-30)/10)$
Richardson et al. (2009) model 2, their Appendix Table A1	As BEIR VII, phase 2 (2006) ERR model above—(only differs in the baseline)
Schneider and Walsh (2009)	$(1 + \omega_s.s).\ (\beta.d + \alpha.d^2).\ \exp(-\gamma\ (e-30) + \varepsilon\ \ln(a/55))$ $(1 + \omega_s.s).\ (\beta.d + \alpha.d^2).\ v.\exp(d).\ \exp(-\gamma\ (e-30) + \varepsilon\ \ln(a/55))$
Little et al. (2008)	$(\beta.d + \alpha.d^2).\ \exp(\gamma\ \ln(e/30) + \varepsilon\ \ln(a/55))$
UNSCEAR (2006)	$(\beta.d + \alpha.d^2).\ \exp(\varepsilon\ \ln(a/55))$
Richardson et al. (2009) main model for all types of leukaemia, their Table 3	$(1 + \omega_c.c).\ (\beta.d + \alpha.d^2).\ \exp(\gamma\ e' + \phi_1\ e't + \phi_2\ e't^2 + \phi_3\ e't^3 + \phi_5\ e'(t-30)_+^3)$, where $e' = \min(0,(e-30)/10)$ and $(t-30)_+^3 = (t-30)^3$ if $t-30 > 0$, 0 otherwise.
Richardson et al. (2009) model 3, their Appendix Table A1	As BEIR VII, phase 2 (2006) ERR model above—(only differs in the baseline)

β_s and the other Greek symbols are fitted parameters, d is the weighted marrow dose, a is attained age, e is age at exposure, t is time since exposure, c is a two-level city indicator variable for Hiroshima and Nagasaki and s is a gender indicator variable. $ecat_{1-3}$ is a three-level indicator variable for three age at exposure groups (0–19, 20–39 and 40 + years)

compute such uncertainties from published information, even though all ERR fitted parameter estimates are published, because none of the papers on the nine models considered contain information on the parameter correlations. The re-evaluation of the models done here has applied this property of the centring constants that simplifies the computation of uncertainties, i.e. the models were re-centred (if necessary) at the ages of interest, i.e. for adults $a = 55$, $e = 30$, $t = 25$, and for children at a series of values $a = 2, 7, 12$ years (approximately in the middle of the data categories) for $t = 5$ and 10 years. The computation of the ERR and its uncertainty then involved the combination of only the dose–response parameters where the associated uncertainties were computed by Monte-Carlo simulations, which took the relevant elements of the full parameter correlation matrix (i.e. without fixing the baseline parameters) into account, using the Crystal-Ball software with 1,000 realizations per simulation.

Estimation of fitted parameters and statistical analysis

The maximum likelihood technique (Harrell 2001) was used to re-fit all the nine models here at the several combinations of age and time centring described in the last section. Best estimates, uncertainty ranges, which included both Wald-type and Likelihood-based confidence intervals, and correlations of the fitted parameters were determined as in the original publications by minimizing the deviance using the AMFIT module of EPICURE software (Preston et al. 1993).

Results

Epidemiological details

Since this work involves mainly a re-analysis of previously published models, most of the important epidemiological details, such as total number of subjects (86,611), total number of leukaemia deaths (296) or total person-years at risk (3.18 million), have already been given (Preston et al. 2004). However, since the models are re-centred at young ages at exposure and short times since exposure, it is important to report here, in Table 2, on the amount of data supporting this region of the dataset. Since the epidemiological follow-up did not begin until 5 years after the A-bombs, the youngest available attained age category is 5– < 10 years of age. It can be seen from Table 2 that this first available age category has four leukaemia deaths (cases) and 22,796 person-years (person-year-weighted mean weighted marrow dose and range, $d = 0.12$; 0–4.4 Sv (in the category) and 1.85; 1.31–4.13 Sv (for the cases in this category)) i.e. all four cases had very high doses. The minimum attained age is 7.37 years, and in the category of age at exposure <5 years, there were 13 deaths from leukaemia before the attained age of 20 years.

The quality of the model fit and associated values of parameters, information criterion and weights for model averaging

Table 3 gives the number of model parameters, the goodness of model fit to the data in terms of the deviance values,

Table 2 Details of the amount of data supporting the models at young ages at exposure and short times since exposure

Attained age category (years)	5–<10	10–<15	15–<20	20–<25
Number of leukaemia deaths	4	6	7	9
Number of person-years	22,796	70,167	106,226	154,253
Category-specific marrow dose; and range (Sv)	0.12; 0–4.4	0.12; 0–4.3	0.12; 0–4.5	0.13; 0–4.5
Case-specific marrow dose and range (Sv)	1.85; 1.31–4.13	0.08; 0–3.37	0.51; 0–4.28	0.29; 0.01–2.73

The last two rows give the mean marrow doses that have been weighted both by RBE as in Eq. 4 and also for person-years

Table 3 The number of parameters, deviance, AIC and model weighting, w_i, applied in the model-averaging procedure

Model reference	Number of parameters	Deviance	AIC	w_i
EAR model of Preston et al. (2004) (used here as an ERR model)	22	2,258.7	2,302.7	0
BEIR VII, phase 2 (2006)	19	2,255.2	2,293.2	0.001
Richardson et al. (2009) model 2, their Appendix Table A1	21	2,250.1	2,292.1	0.001
Schneider and Walsh (2009) LQ	13	2,258.0	2,284.0	0.069
Schneider and Walsh (2009) LQ-exp	14	2,253.9	2,281.9	0.198
Little et al. (2008)	11	2,259.7	2,281.7	0.219
UNSCEAR (2006)	10	2,260.0	2,280.0	0.512
Richardson et al. (2009) Main model for all types of leukaemia, their Table 3	448	1,915.5	2,811.5	0
Richardson et al. (2009) model 3, their Appendix Table A1	1,086	1,560.3	3,732.3	0

Individual w_i values can be interpreted to indicate the probability that the ith model is the best among the nine models considered. The models with w_i indicated as zero, actually had very small weights, of less than 0.0005, that have been rounded to zero. All of the models presented in this table were re-fitted to the same dataset, i.e. to DS02CAN.DAT from http://www.rerf.or.jp

and the Akaike weights assigned to each model. It is noteworthy that the UNSCEAR (2006) model attains the highest of all the Akaike weights of 0.512 and therefore, has the largest contribution to the model-averaged ERR at 1 Sv; as given in the last row of Table 4 and as a function of attained age in Fig. 1. The 95% confidence intervals for the model-averaged ERR at 1 Sv in Table 4 were computed with Method 1 involving Monte-Carlo simulations, but they were also calculated by Method 2 (Eq. 3) and found to be very similar, indicating that 1,000 realizations were adequate. Table 4 also gives the ERR at 1 Sv, for each attained age, age at exposure and time since exposure considered, computed from the parameter values given in Appendix Table 9. It can be seen that the model-averaged values are close to the values from the UNSCEAR (2006) model, due to its high weighting and the similarity of the other models with medium weights to this model. The model-averaged ERR at 1 Sv values for attained ages of 7 and 12 years, given in columns 3–5 of Table 4, are not statistically significant, with the highest central estimate occurring for attained age of 7 years (i.e. at the edge of the corresponding covariable range in the dataset). However, it is interesting to note that statistically significant model-averaged ERR at 1 Sv values are found in Table 4 for attained age 17 and 22 years and that the two risks for attained age of 17 years

are almost the same—indicating little difference in the risk at this age between exposure at age 7, 10 years later (model-averaged ERR at 1 Sv with 95% CI is 18.4 (0.6; 35.6)) and exposure at 12, 5 years later (model-averaged ERR at 1 Sv with 95% CI is 19.2 (0.1; 37.9)).

Model-averaged ERR at 100 and 10 mSv are given in Table 5. It is also theoretically possible to go through the model-averaging procedure for the low-dose limiting ERR/Sv (i.e. in Table 1, the fitted parameters β, β_s, θ_{1-3}). However, it was decided to present the low-dose limiting ERR/Sv for the UNSCEAR (2006) model as the best estimate in Table 5 for two reasons: (1) the UNSCEAR (2006) model is associated with a high weighting and (2) the lower likelihood-based 95% confidence bounds for β and β_s failed to be numerically found here in four of the models considered (i.e. the BEIR VII phase 2 model, the two modifications of this model in the Appendix Table A1 of Richardson et al. (2009), and the Schneider and Walsh (2009) linear quadratic exponential dose–response model). It can be seen from Table 5 and Fig. 1 (lower panel) that there is good agreement between the low-dose limiting ERR/Sv and the central estimates for the model-averaged ERR at 100 and 10 mSv when scaled to the same dose and that these scaled estimates are all approximately a factor two lower than the ERR at 1 Sv.

Table 4 ERR at 1 Sv with Monte-Carlo simulated 95% CIs for various values of attained age (a) and age at exposure (e) in years

Model reference	$a = 55$, $e = 30$, $t = 25$	$a = 7$, $e = 2$, $t = 5$	$a = 12$, $e = 2$, $t = 10$	$a = 12$, $e = 7$, $t = 5$	$a = 17$, $e = 7$, $t = 10$	$a = 17$, $e = 12$, $t = 5$	$a = 22$, $e = 12$, $t = 10$
EAR model of Preston et al. (2004) (used here as an ERR model)	2.72	27.9	11.3	27.9	11.3	27.9	11.3
	1.21; 4.24	8.0; 70.4	4.3; 21.9	8.0; 70.4	4.3; 21.9	8.0; 70.4	4.3; 21.9
BEIR VII, phase 2 (2006)	2.11	92.9	29.5	54.2	19.9	31.6	13.4
	−0.09; 2.98	−133.5; 249.5	−24.7; 61.3	−69.7; 126.6	−12.2; 37.9	−27.9; 64.4	−4.4; 22.0
Richardson et al. (2009) model 2, their Appendix Table A1	2.50	103.4	33.4	60.9	22.7	35.9	15.4
	−0.10; 3.59	−143.4; 302.0	−23.2; 71.2	−64.8; 147.9	−12.1; 43.8	−22.6; 74.2	−5.0; 26.8
Schneider and Walsh (2009) LQ	2.73	104.0	35.4	38.6	19.2	21.0	12.5
	1.60; 4.03	−72.7; 288.8	−7.3; 79.7	−11.0; 88.6	−0.6; 38.8	0.3; 41.6	2.3; 22.8
Schneider and Walsh (2009) LQ-exp	2.95	98.8	34.7	37.9	19.3	21.0	12.8
	1.51; 4.06	−40.2; 263.0	−2.4; 75.9	−4.5; 77.8	2.0; 36.5	3.1; 39.5	3.0; 21.4
Little et al. (2008)	2.78	75.9	29.0	34.4	18.5	19.9	12.6
	1.53; 4.04	−39.6; 194.2	−7.5; 62.6	−8.3; 77.0	0.2; 35.6	−1.2; 38.1	2.2; 22.3
UNSCEAR (2006)	2.71	74.9	31.4	31.4	17.9	17.9	11.8
	1.49; 3.88	−44.0; 190.9	−6.5; 70.0	−6.5; 70.0	0.9; 34.6	0.9; 34.6	2.6; 20.9
Richardson et al. (2009) Main model for all types of leukaemia, their Table 3	2.55	203.5	185.8	93.1	86.4	42.6	40.2
	1.12; 4.18	7.8; 4,654.6	16.7; 1,947.5	6.2; 1,149.1	12.1; 582.3	5.2; 295.1	8.1; 182.4
Richardson et al. (2009) model 3, their Appendix Table A1	2.72	212.1	47.9	111.6	31.0	58.6	20.1
	−0.46; 3.95	−5,527; 712.1	−56.3; 126.1	−207.3; 331.8	−32.6; 66.6	−76.9; 141.2	−16.9; 39.3
Model-averaged ERR at 1 Sv	2.77	81.9	31.8	33.9	18.4	19.2	12.23
	1.43; 3.84*	−40.1; 216.2#	−5.4; 68.9	−6.6; 74.1	0.6; 35.6	0.1; 37.9	2.7; 21.3

t is time since exposure in years. In the model of Preston et al. (2004), $e = 30$ refers to the age at exposure group 20–39 years, and the other values of e refer to the age at exposure group 0–19 years

, # independent calculation with the MECAN software (see "Discussion" section) yields 1.49; 3.96 and −64.5; 238#

Table 5 Model average values of ERR (10^{-2}) at 10 mSv and ERR (10^{-1}) at 100 mSv with Monte-Carlo simulated 95% CIs for various values of attained age (a) and age at exposure (e) in years

	$a = 55$, $e = 30$, $t = 25$	$a = 7$, $e = 2$, $t = 5$	$a = 12$, $e = 2$, $t = 10$	$a = 12$, $e = 7$, $t = 5$	$a = 17$, $e = 7$, $t = 10$	$a = 17$, $e = 12$, $t = 5$	$a = 22$, $e = 12$, $t = 10$
Low-dose limiting ERR/Sv (β) and 95% likelihood CI	1.50	41.5	17.4	17.4	9.9	9.9	6.6
	0.19; 3.2	3.9; 258.4	1.8; 73.8	1.8; 73.8	1.1; 33.4	1.1; 33.4	0.8; 18.8
Model-averaged ERR (10^{-2}) at 10 mSv	1.16	32.6	13.2	13.9	7.7	7.9	5.1
	−1.56; 2.78	−51.3; 122	−18.7; 41.4	−18.2; 46.3	−11.2; 22.6	−11.0; 24.0	−6.8; 14.7
Model-averaged ERR (10^{-1}) at 100 mSv	1.33	38.0	15.2	16.1	8.9	9.1	5.9
	−1.02; 2.92	−46.0; 122.3	−13.3; 43.8	−14.5; 47.2	−8.1; 23.3	−7.7; 24.3	−3.5; 14.7

t is time since exposure in years. Also given for comparison purposes are the best estimates of the low-dose limiting ERR/Sv (fitted parameter β in Table 1) for the model with the greatest Akaike weighting (the UNSCEAR (2006) model)

Discussion

Techniques of multi-model inference, involving model averaging with Akaike type weights, have been applied to nine recently published models fitted to the most recent, generally available, LSS leukaemia mortality data (1950–2000). Leukaemia risks including model uncertainty, in adults aged 55 years and in young persons aged 7, 12, 17 and 22 years, have been obtained. The procedure applied here appeals to Occam's razor, because it leads to an exclusion of complex models if they do not describe the data significantly better than their simpler counterparts (i.e. in the context of Table 3, models that are "excluded" have very small weights, which have been rounded to 0).

It has been shown that the model-averaged risks of leukaemia are influenced most strongly (51.2% of total weighting) by one model (UNSCEAR 2006) and that three other models, which are similar to this model (Little et al. 2008 and both models of Schneider and Walsh (2009)), have contributed the major part (48.6%) of the remaining weighting. As alluded to above, this is because the remaining five models have included several fitted parameters that were not indicated by the data to be necessary, and this has been numerically penalised in the model-averaging procedure. The model of Richardson et al. 2009, reproduced here in the penultimate lines of Tables 1 and 8 of the "Appendix", has two fitted parameters in the ERR model (see Appendix, Table 7) that are not statistically significant when fitted to the generally available dataset (deviance = 1,889.0, γ and ϕ_1, $p = 0.42$, 0.23, respectively). The fitted values and 90% confidence intervals quoted in the original publication, i.e. $\gamma = -1.06$ (−2.81; 0.74) and $\phi_1 = -0.20$ (−0.50; 0.07) for the special dataset with extra information of leukaemia sub-types, are also not statistically significant. According to calculations done here, with the generally available dataset, it is possible to leave out either γ or ϕ_1 from the model (with a reduction in deviance from full model of 0.7 and 1.6,

respectively, i.e. less than the critical value from the likelihood ratio test of 3.8 for $p = 0.05$ for keeping a parameter in a nested model) and so to arrive at two models where all fitted parameters are statistically significant. These two reduced models have some very different characteristics in the central estimate of ERR at 1 Sv for 10 years of age at exposure and for time since exposures of under 20 years, both when compared to each other and to the published sub-optimal model (see the lower panel of Fig. 2 in the "Appendix").

Similarly, the model of Preston et al. (2004), which was originally published as an EAR model and has been re-fitted here as an ERR model with the same parametric form, had several parameters that were not statistically significant (e.g. baseline parameters β_9, β_{10}, β_{11}, β_{12}, as in Appendix Table 8) both in the original EAR model and in the analogous ERR model described here. Since Preston et al. (2004) preferred to publish an EAR rather than an ERR model, because the EAR fitted the data somewhat better, it could be argued that the weights and the ERR estimates, which went into the multi-model inferences here, should have been calculated from the original model. However, the degree of model improvement is only small: where the EAR had a deviance of 2,254.8 (value quoted from http://www.rerf.or.jp, filename:DS02can.log), the analogous ERR model presented here had a deviance of 2,258.7; ΔAIC = 3.9. In such a pair-wise comparison, this latter value is smaller than a reference value of 5.9 for ΔAIC, which indicates that the model with the smaller AIC has a 95% chance of being correct (see Walsh 2007, and references therein, for an explanation).

None of the models that included gender-specific parameters, either in the baseline or in ERR model parts, indicated any statistically significant gender effects. This would indicate that it is not necessary to eliminate the female data and in so doing accept the resulting wider confidence intervals, when computing leukaemia risks from the A-bomb data for the purpose of comparison with cohorts

of male nuclear workers (e.g. as in Cardis et al. (2005)). Cardis et al. 2005 quoted an ERR/Sv based on the linear term of a linear quadratic dose–response model (i.e. the low-dose limiting ERR/Sv), for males aged 20–60, based on 83 leukaemia deaths excluding CLL, in the A-bomb cohort of 1.54 (95% CI −1.14 to 5.33). Cardis et al. 2005 also quoted a linear ERR/Sv for the same sub-group of 3.15 (95% CI 1.58 to 5.67) that is nevertheless statistically consistent with the model-averaged ERR at 1 Sv for adults aged 55 of 2.77 (95% CI 1.43; 3.84) found here.

A recent meta-analysis, which included results from 10 nuclear workers studies and adjusted for publication bias (Daniels and Schubauer-Berigan 2010, see also the editorial to this paper, Walsh 2010), found an ERR at 100 mGy of 0.19 (95% CI: 0.07; 0.32). They also used the linear term of a linear quadratic model as above (ERR at 100 mGy = 0.15 (95% CI −0.11 to 0.53)) for comparison with the A-bomb risks and conclude that the A-bomb estimates are not precise. However, the best comparison for this meta-analysis provided here by Table 5 (ERR at 100 mGy = 0.13 (95% CI −0.10 to 0.29)) is somewhat less uncertain even though model uncertainty is included. When applying leukaemia models derived from the LSS to nuclear worker studies, it should be considered that the exposure situations are very different, i.e. an almost instantaneous exposure compared to extended cumulative exposures; however, the good agreement in central risk estimates here could be taken as an indication of risk equivalence between protracted and acute exposures at the same dose.

In order to evaluate which time or age-dependent co-variables are most important for the risk modification, it is instructive to consider the one model (UNSCEAR 2006) that most strongly influenced the model-averaged risks of leukaemia. Little et al. 2009 assessed the model selection for this (UNSCEAR 2006) model in terms of all combinations of time or age-dependent covariables and concluded that attained age was more clearly indicated than age at exposure or time since exposure, or any two of these variables. Since only effect modification in terms of a power functional form was originally considered, both a linear and an exponential for the attained age modification were computed here, but were both found to fit the data less well (power function (deviance = 2,260.0; and reference model for ΔAIC computation); exponential function (deviance = 2,263.9; ΔAIC = 3.9); linear function (deviance = 2,266.6; ΔAIC = 6.6)). However, since the mean marrow dose of the four cases in the youngest age group available corresponding to 5 to <10 years was 1.85 Sv with a very high lower value of the dose range of 1.31 Sv, all the risk models considered here could have suffered from an ill-defined baseline risk at young attained ages under 10 years. Consequently, the preferred functional

form for age (i.e. power function) could be an artefact caused by the total lack of data for low exposures at ages under 10 years. In order to check this supposition, the same sequence of models was fitted to the data for attained age from 10 years. Again the linear and exponential function for the attained age modification were found to fit the data less well (power function (deviance = 2,231.2); exponential function (deviance = 2,233.8; ΔAIC = 2.6); linear function (deviance = 2,235.2; ΔAIC = 4.0)).

The model-averaging procedure applied here may not have treated the models with stratified baseline in the best possible way. Stratified baseline models are important because they may account for confounding factors in an indirect way or provide an alternative approach to parametric background modelling for treating highly collinear covariables (e.g. see Walsh et al. 2009). An adaptation of the method considered here could be to apply model averaging to the group of models with parametric baselines, and then separately to the group of models with stratified baselines, finally combining the two model-averaged estimates. However, at this stage, the theory necessary to do this has not been published and requires further work and development.

A further point, which has not received attention in the past, is the influence of the uncertainties in the baseline model parameters on the ERR parameters. Most radiation risks and uncertainties for various organs based on the A-bomb data have usually been identified with their linear dose–response fitted parameter (e.g. Preston et al. 2003). However, there is now new software developed by one of the authors (JCK) called MECAN that can account for uncertainties in parametric baseline parameters and is available on request. Table 4 also includes some examples of independent calculations of 95% confidence intervals that include parametric baseline uncertainties with the MECAN software. However, this method has not been applied globally in the model-averaging procedure here, for reasons of consistency, because it is not yet sufficiently well developed to deal with stratified baselines.

Results presented here for the model-averaged ERR at 1 Sv, which imply an increase with decreasing attained age, are not statistically significant for attained age 7 and 12 years, but are statistically significant for attained age 17 and 22. Given such results for the ERR at 1 Sv for young ages, which is a much higher radiation dose than natural background radiation (about 0.5–2.5 mSv per year), it can be assumed that any extrapolations of the ERR for children from high doses to the low doses relevant to background radiation are associated with even higher uncertainties. These uncertainties should be built into calculations of the percentage of childhood leukaemia incidence attributable to background radiation (which involve estimates of ERR and EAR), such as those recently presented for the United

Kingdom (Wakeford et al. 2009; Little et al. 2009). If this model uncertainty in ERR (or EAR) is explicitly built into such calculations, then the result could range from 0% to some much higher percentage, and thus it is difficult to see how the result of 15–20% (Wakeford et al. 2009; Little et al. 2009) could be statistically significant. Although these authors (Wakeford et al. 2009; Little et al. 2009) state that "the uncertainty associated with certain stages in the calculation is significant", no confidence intervals, for the 15–20% quoted, were given.

There are difficulties similar to those just mentioned, in extrapolating childhood leukaemia risks from the A-bomb data to obtain risks relevant to children under 5 years old living in the vicinity of nuclear power stations. Such children may have received annual doses in the order of a few μSv, in addition to the natural background radiation of 0.5–2.5 mSv. Assuming a total radiation dose to a 5-year-old of 10 mSv and applying the model-averaged risk at 10 mSv for a 7-year-old exposed at 2 years of age (found here from Table 5) would result in an ERR = 0.33, 95% CI: −0.51–1.22, which is a risk associated with large uncertainties. Generally, the greatest uncertainty in extrapolating from A-bomb data to other populations is associated with the children under the age of 10 years when exposed to the atomic bombs, 90% of whom are still alive (Preston et al. 2004). However, the follow-up relevant to the childhood leukaemia risks considered here was completed a long time ago.

Conclusion

Nine recently published leukaemia models have been included in a procedure, which has concentrated on applying model averaging, so that the main conclusions drawn from model selection do not depend on just one type of statistical test, which could be associated with stringent assumptions (e.g. nested models). This procedure led to an exclusion of complex models less supported by the data than their simpler counterparts. One model (UNSCEAR 2006) weighted model-averaged risks of leukaemia most strongly by half of the total unity weighting. Results presented here for the model-averaged ERR at 1 Sv are not statistically significant for attained ages of 7 and 12 years, but are statistically significant for attained ages of 17, 22 and 55 years. The most important risk-modifying factor implied is attained age, with a power functional increase in risk with decreasing age. Since the model-averaged ERR at 1 Sv at attained age 7 and 12 years are not statistically significant, risks applied to low doses for young ages and short times since exposure that are based on the A-bomb data are only of limited value. Consequently, such risks when applied to other situations such as children in the vicinity of nuclear installations, or in estimates of the proportion of childhood leukaemia incidence attributable to background radiation, should include a full discussion of confidence intervals that will be very wide and include zero risk. One model (UNSCEAR 2006) weighted model-averaged risks of leukaemia most strongly by half of the total unity weighting and is recommended for application in future leukaemia risk assessments that do not include model uncertainty. However, on the basis of the analysis presented here, it is generally recommended to take model uncertainty into account in future risk analyses.

The authors have attempted to bring some relatively new issues that augment the usual practice of ignoring model uncertainty when making inference about parameters of a specific model, to the attention of the radiation protection community. The application here of the Akaike weights is considered to be the simplest approach, mainly because it by-passes the need to specify Bayesian priors by assuming that all models are a priori equally likely. Although there is no doubt that model averaging using the Akaike weights can reduce bias due to model selection, the authors and one of the reviewers are not aware of any optimality theory concerning choice of model-averaging weights. A full Bayesian treatment may be more suitable for the present problem, given that the candidate models were developed with differing scientific goals in mind.

The authors would be very pleased if their initial efforts encourage more detailed analyses and more theoretical papers on model averaging in radiation protection, by much larger teams of experts. New methods for combining multi-model inferences with model predictive capability would also be very useful for radiation protection. The authors do not believe that this paper provides a benchmark for multi-model inference in radiation protection, it is merely a start in the right direction—there is still a lot of work to be done.

Appendix

This appendix contains fitted parameters for models that do not have fitted parameters already given in the literature because they were either fitted to a different dataset (as in Richardson (2009)) or because only EAR model forms were given previously (as in Preston et al. (2004)).

See Tables 6, 7, 8, 9, Fig. 2

Table 6 Main ERR model fitted here

Age at exposure group	Effect	Fit parameters with 95% Wald CI
0–19	*ERR/Sv exp(θ_1)	1.710 (0.529; 5.529)
	Time since exposure power, τ_1	−1.3 (−1.9; −0.7)
20–39	*ERR/Sv exp(θ_2)	1.375 (0.445; 4.249)
	Time since exposure power, τ_2	−0.7 (−1.4; 0.1)
40-	*ERR/Sv exp(θ_3)	1.200 (0.362; 3.975)
	Time since exposure power, τ_3	−0.2 (−1.2; 0.7)
All ages	Sex effect ω_s	0.04 (−0.29; 0.38)
All ages	Dose–response curvature θ	0.98 (−0.52; 2.48)

This model was originally fitted and given in the Table 8 of Preston et al. (2004) as an EAR model

* Note that these values are gender-averaged low-dose slopes at 25 years after exposure in a linear quadratic model. The parameter notation refers to Table 1 here and is not exactly the same notation as originally used in Preston et al. (2004)

Table 7 Main ERR model given in Table 3 of Richardson et al. (2009) for all types of leukaemia originally fitted to a special dataset with extra information on leukaemia sub-types, but re-fitted here to the publicly available data

Parameter	β	α	ω_c	γ	ϕ_1	ϕ_2	ϕ_3*	ϕ_5*
Fitted value	1.620	0.926	−0.461	−0.917	−0.214	0.0185	$-3.235 \cdot 10^{-4}$	$7.428 \cdot 10^{-4}$
95% Wald CI								
Lower	0.1845	0.1742	−0.872	−3.138	−0.562	0.000	$-6.144 \cdot 10^{-4}$	$9.651 \cdot 10^{-5}$
Upper	3.056	1.679	−0.050	1.305	0.134	0.037	$-3.249 \cdot 10^{-5}$	0.00139

The mathematical form of this model can also be seen in the penultimate lines of Tables 1 and 8 here

* Note that the precision originally given in Richardson et al. (2009) for these parameters was not high enough to either allow an independent reproduction of the original graphics in the Fig. 1 of that paper or to re-compute ERR central estimates at other required ages and times since exposure. The precision given here for these parameters is good enough to overcome these difficulties

Table 8 Forms of baseline models applied to account for the spontaneous leukaemia mortality in the ERR models considered in the model-averaging procedure

Model reference	Form of baseline model $\ln\{\lambda_o(a,e,s,c)\} =$
EAR model of Preston et al. (2004) (used here as an ERR model)	$\beta_{1-4}\,(s.c) + \beta_{5-6}\,s.\ln(a/70) + \beta_{7-8}\,s.\ln^2(a/70) + \beta_{9-10}\,s.\max^2(0, \ln(a/70)) + \beta_{11-12}\,s.(e-30) + \beta_{13-14}\,s.(e-30)^2$
BEIR VII, phase 2 (2006)	$\beta_0 + \beta_1\,s + \beta_2\,c + \beta_{3-4}\,s.\ln(a/70) + \beta_{5-6}\,s.\ln^2(a/70) + \beta_{7-8}\,s.\max^2(0, \ln(a/70)) + \beta_{9-10}\,s.(e-30) + \beta_{11-12}\,s.(e-30)^2$
Richardson et al. (2009) model 2, their Appendix Table A1	$\beta_0 + \beta_1\,s + \beta_{2-5}\,(c.l) + \beta_{6-7}\,s.\ln(a/70) + \beta_{8-9}\,s.\ln^2(a/70) + \beta_{10-11}\,s.\max^2(0, \ln(a/70)) + \beta_{12-13}\,s.(e-30) + \beta_{14-15}\,s.(e-30)^2$
Schneider and Walsh (2009) (both models)	$\beta_{1-4}\,(s.c) + \beta_5\,\ln(a/70) + \beta_6\,\ln^2(a/70) + \beta_7\,(e-30) + \beta_8\,(e-30)^2$
Little et al. (2008) and UNSCEAR (2006)	$\beta_0 + \beta_1\,s + \beta_2\,c + \beta_3\,\ln(a/70) + \beta_4\,\ln^2(a/70) + \beta_5(e-30) + \beta_6(e-30)^2$
Richardson et al. (2009) main model for all types of leukaemia, their Table 3	Stratification on categories of s, c, a, b and l
Richardson et al. (2009) model 3, their Appendix Table A1	Stratification on categories of s, c, a, e and l

β_{1-14} are fit parameters, a is attained age, e is age at exposure (applied here as a proxy variable for birth cohort, because exposure was momentary and at the same point in calendar time), c is a two-level city indicator variable for Hiroshima and Nagasaki, s is a gender indicator variable, and l is a two-level indicator variable for survivor location from the bomb hypocentre, i.e. proximal or distal, b, indexes birth cohort (<1895, 1895–1904, 1905–1914, 1915–1924, 1925–1945)

Table 9 The parameter values with Wald standard errors (SE) and likelihood-based 95% CI (Li 95% CI, but in some cases they were not found (NF)) as recomputed here under the same conditions for the models considered in the model-averaging procedure

EAR model of Preston et al. (2004) (used here as an ERR model)

Model reference and centring	θ1 (or θ2)	Wald SE	Li low 95% CI	Li up 95% CI	θ	Wald SE	Li low 95% CI	Li upper 95% CI	θ1 vs. θ
e = 0–<20; t = 25	0.54	0.60	−3.26	1.52	0.98	0.76	0.18	400.1	−0.89
e = 0–<20; t = 5	2.65	0.73	0.47	3.90	0.98	0.77	0.18	171.30	−0.74
e = 0–<20; t = 10	1.74	0.63	−4.12	2.77	0.98	0.77	0.18	171.30	−0.86
e = 20–<40; t = 25	(θ2) 0.32	0.58	−8.32	1.19	0.98	0.76	0.18	400.1	−0.90

BEIR VII, phase 2 (2006)

Model reference and centring	βm	Wald SE	Li low 95% CI	Li up 95% CI	βf	Wald SE	Li low 95% CI	Li up 95% CI	θ	Wald SE	Li low 95% CI	Li up 95% CI	θ vs. βm	θ vs. βf	βm vs. βf
e = 30; t = 25	1.06	0.59	0.09	2.60	1.18	0.65	0.11	2.89	0.88	0.66	0.16	15.27	−0.85	−0.84	0.80
e = 2; t = 5	46.63	51.55	NF	383.80	52.16	57.54	NF	430.00	0.88	0.66	0.16	15.25	−0.50	−0.49	0.95
e = 2; t = 10	14.80	12.22	NF	67.96	16.55	13.68	NF	76.47	0.88	0.66	0.16	15.25	−0.65	−0.63	0.91
e = 7; t = 5	27.18	25.71	NF	159.80	30.40	28.72	NF	179.30	0.88	0.66	0.16	15.25	−0.58	−0.56	0.93
e = 7; t = 10	9.98	7.35	NF	37.55	11.16	8.23	NF	42.30	0.88	0.66	0.16	15.25	−0.72	−0.70	0.89
e = 12; t = 5	15.86	12.83	NF	69.27	17.74	14.35	NF	77.88	0.88	0.66	0.16	15.25	−0.66	−0.63	0.91
e = 12; t = 10	6.74	4.46	NF	21.31	7.54	4.99	NF	24.04	0.88	0.66	0.16	15.25	−0.78	−0.76	0.86

Richardson et al. (2009) model 2, their Appendix Table A1

Model reference and centring	βm	Wald SE	Li low 95% CI	Li up 95% CI	βf	Wald SE	Li low 95% CI	Li up 95% CI	θ	Wald SE	Li low 95% CI	Li up 95% CI	θ vs. βm	θ vs. βf	βm vs. βf
e = 30; t = 25	1.42	0.75	0.26	3.43	1.59	0.83	0.30	3.82	0.66	0.48	0.10	5.32	−0.82	−0.80	0.79
e = 2; t = 5	58.76	63.59	NF	464.70	65.86	71.10	NF	521.10	0.66	0.48	0.10	5.32	−0.46	−0.45	0.95
e = 2; t = 10	18.96	15.12	2.75	83.77	21.26	16.95	3.13	94.54	0.66	0.48	0.10	5.32	−0.61	−0.59	0.91
e = 7; t = 5	34.62	31.87	NF	196.00	38.80	35.65	NF	220.10	0.66	0.48	0.10	5.32	−0.53	−0.51	0.93
e = 7; t = 10	12.89	9.10	2.01	46.74	14.45	10.20	2.28	52.82	0.66	0.48	0.10	5.32	−0.68	−0.65	0.88
e = 12; t = 5	20.40	15.93	3.14	85.96	22.86	17.84	3.56	96.78	0.66	0.48	0.10	5.32	−0.61	−0.59	0.90
e = 12; t = 10	8.77	5.52	1.44	26.80	9.83	6.18	1.64	30.32	0.66	0.48	0.10	5.32	−0.74	−0.71	0.85

Richardson et al. (2009) model 3, their Appendix Table A1

Model reference and centring	βm	Wald SE	Li low 95% CI	Li up 95% CI	βf	Wald SE	Li low 95% CI	Li up 95% CI	θ	Wald SE	Li low 95% CI	Li up 95% CI	θ vs. βm	βf vs. θ	βm vs. βf
e = 30; t = 25	1.51	0.85	0.24	3.86	1.60	0.87	0.27	3.97	0.75	0.55	0.13	6.72	−0.81	−0.80	0.74
e = 2; t = 5	117.80	175.20	NF	2,524.0	124.50	186.50	NF	2,753.0	0.75	0.55	0.13	6.72	−0.42	−0.40	0.96
e = 2; t = 10	26.62	27.76	NF	213.50	28.14	29.76	NF	231.50	0.75	0.55	0.13	6.72	−0.55	−0.53	0.93
e = 7; t = 5	61.99	77.06	NF	778.40	65.52	82.21	NF	848.70	0.75	0.55	0.13	6.72	−0.48	−0.46	0.95
e = 7; t = 10	17.21	15.48	NF	100.00	18.19	16.62	NF	108.40	0.75	0.55	0.13	6.72	−0.62	−0.59	0.90
e = 12; t = 5	32.56	33.37	NF	250.80	34.41	35.71	NF	273.30	0.75	0.55	0.13	6.72	−0.55	−0.53	0.92
e = 12; t = 10	11.14	8.63	NF	48.36	11.77	9.28	NF	52.36	0.75	0.55	0.13	6.72	−0.69	−0.66	0.87

Table 9 continued

	β	Wald SE	Li low 95% CI	Li up 95% CI	α	Wald SE	Li low 95% CI	Li up 95% CI	β vs. α
Little et al. (2008)									
$e = 30; t = 25$	1.53	0.76	0.18	3.31	1.25	0.42	0.42	2.22	−0.56
$e = 2; t = 5$	41.68	39.35	3.66	259.30	34.18	27.36	7.21	175.00	0.65
$e = 2; t = 10$	15.95	12.60	1.53	70.04	13.08	8.24	3.48	46.39	0.48
$e = 7; t = 5$	18.90	14.90	1.87	82.21	15.50	9.87	3.99	55.37	0.48
$e = 7; t = 10$	10.16	6.87	1.06	34.27	8.33	4.22	2.50	22.61	0.24
$e = 12; t = 5$	10.92	7.63	1.15	38.48	8.96	4.85	2.56	25.85	0.31
$e = 12; t = 10$	6.90	4.27	0.75	20.20	5.66	2.53	1.78	13.31	0.06
UNSCEAR (2006)									
$a = 55$	1.50	0.74	0.19	3.22	1.21	0.40	0.40	2.12	−0.58
$a = 7$	41.47	39.15	3.87	258.40	33.42	26.88	7.00	172.50	0.66
$a = 12$	17.40	13.43	1.82	73.76	14.03	8.65	3.75	48.57	0.46
$a = 17$	9.93	6.68	1.11	33.37	8.00	4.05	2.39	21.73	0.24
$a = 22$	6.55	3.98	0.76	18.84	5.28	2.29	1.68	12.15	0.03
Richardson et al. (2009) Main model for leukaemia, their Table 3.	Cannot be re-centred at different ages at exposure: see Appendix Table 7 for parameters								
Schneider and Walsh (2009) LQ									
$e = 30; t = 25$	1.45	0.74	0.14	3.19	1.28	0.41	0.46	2.23	−0.56943
$e = 2; t = 5$	55.21	55.70	3.92	396.50	48.83	42.30	9.39	291.10	0.69801
$e = 2; t = 10$	18.79	15.07	1.47	85.26	16.62	10.54	4.49	60.40	0.48879
$e = 7; t = 5$	20.48	16.66	1.62	95.05	18.12	11.78	4.76	68.17	0.50676
$e = 7; t = 10$	10.21	7.12	0.85	36.21	9.03	4.64	2.80	25.21	0.28181
$e = 12; t = 5$	11.12	7.85	0.93	40.12	9.84	5.19	2.98	28.35	0.30611
$e = 12; t = 10$	6.64	4.19	0.57	20.01	5.88	2.57	1.96	13.78	0.073231

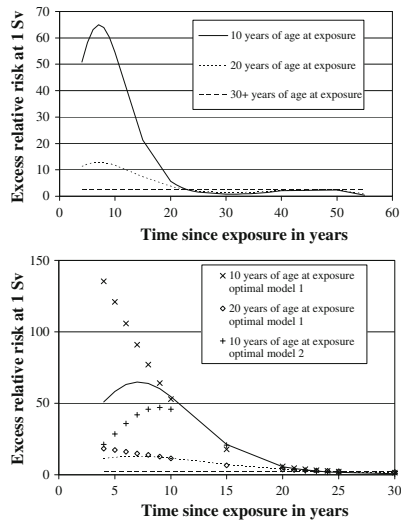| Schneider and Walsh (2009) LQexp	β	Wald SE	Li low 95% CI	Li up 95% CI	α	Wald SE	Li low 95% CI	Li up 95% CI	v	Wald SE	Li low 95% CI	Li up 95% CI	α vs. β	α vs. v	β vs. v
$e = 30; t = 25$	−0.35	1.04	NF	1.95	4.90	2.03	1.31	9.37	−0.43	0.17	−0.73	−0.02	−0.76	0.68	−0.89
$e = 2; t = 5$	−11.70	33.55	NF	152.60	163.90	127.10	32.10	885.00	−0.43	0.17	−0.73	−0.02	−0.38	0.66	−0.34
$e = 2; t = 10$	−4.13	11.84	NF	38.11	57.68	34.22	13.97	198.10	−0.43	0.17	−0.73	−0.02	−0.44	0.67	−0.50
$e = 7; t = 5$	−4.50	12.91	NF	42.11	62.90	37.95	15.03	221.70	−0.43	0.17	−0.73	−0.02	−0.44	0.67	−0.48
$e = 7; t = 10$	−2.29	6.60	NF	17.76	32.02	16.23	8.33	86.80	−0.43	0.17	−0.73	−0.02	−0.51	0.68	−0.62
$e = 12; t = 5$	−2.50	7.20	NF	19.53	34.92	17.92	9.00	96.60	−0.43	0.17	−0.73	−0.02	−0.50	0.68	−0.60
$e = 12; t = 10$	−1.52	4.39	NF	10.51	21.19	9.67	5.69	49.27	−0.43	0.17	−0.73	−0.02	−0.57	0.68	−0.72

Fig. 2 The *upper panel* shows a repeat of Fig. 1 in Richardson et al. 2009 (originally for the special dataset, with extra information of leukaemia sub-types) but fitted here to the publicly available leukaemia mortality data (1950–2000), with fitted model parameters from Table 7. The *lower panel* shows the same three lines as in the upper panel on a different scale and, where the main differences exist, the characteristics of the time since exposure effect obtained with optimal model 1 (i.e. with the ϕ_1 term omitted from the full model in the penultimate line of Table 1) and optimal model 2 (i.e. with the γ term from this full model omitted)

References

Akaike H (1973) Information theory and an extension of the maximum likelihood principle. In: Petrov BN, Caski F (eds) Proceedings of the second international symposium on information theory. Budapest, Hungary, Akademiai Kiado, pp 267–281

Akaike H (1974) A new look at the statistical model identification. IEEE Trans Autom Control 19(6):716–723

Burnham KP, Anderson DR (1998) Model selection and inference: a practical information-theoretic approach. Springer, New York

Burnham KP, Anderson DR (2002) Model selection and multimodel inference, 2nd edn. Springer, New York

Burnham KP, Anderson DR (2004) Multimodel inference. Understanding AIC and BIC in model selection. Sociol Meth Res 33(2): 261–304, see also Workshop on Model Selection, Amsterdam http://www2.fmg.uva.nl/modelselection/. Accessed March 2010

Cardis E, Vrijheid M, Blettner M, Gilbert E, Hakama M, Hill C, Howe G, Kaldor J, Muirhead CR, Schubauer-Berigan M, Yoshimura T, Bermann F, Cowper G, Fix J, Hacker C, Heinmiller B, Marshall M, Thierry-Chef I, Utterback D, Ahn Y-O, Amoros E, Ashmore P, Auvinen A, Bae J-M, Bernar Solano J, Biau A, Combalot E, Deboodt P, Diez Sacristan A, Eklof M, Engels H, Engholm G, Gulis G, Habib R, Holan K, Hyvonen H, Kerekes A, Kurtinaitis J, Malker H, Martuzzi M,

Mastauskas A, Monnet A, Moser M, Pearce MS, Richardson DB, Rodriguez-Artalejo F, Rogel A, Tardy H, Telle-Lamberton M, Turai I, Usel M, Veress K (2005) Risk of cancer after low doses of ionising radiation: retrospective cohort study in 15 countries. BMJ 331:77–82

Chatfield C (1995) Model uncertainty, data mining and statistical inference (with discussion). J R Stat Soc Ser A 158:419–466

Claeskens G, Hjort NL (2008) Model selection and model averaging. Cambridge University Press, Cambridge

Daniels RD, Schubauer-Berigan MK (2010) A meta-analysis of leukaemia risk from protracted exposures to low-dose gamma radiation. Accepted for publication in OEM

Harrell FE Jr (2001) Regression modeling strategies: with applications to linear models, logistic regression and survival analysis. Springer Series in Statistics

Hoeting JA, Madigan D, Raftery AE, Volinsky CT (1999) Bayesian model averaging: a tutorial. Stat Sci 14(4):382–417

Kaatsch P, Spix C, Schulze-Rath R, Schmiedel S, Blettner M (2008) Leukaemia in young children living in the vicinity of German nuclear power plants. Int J Cancer 122:721–726

Laurier D, Jacob S, Bernier MO, Leuraud K, Metz C, Samson E, Laloi P (2008) Epidemiological studies of leukaemia in children and young adults around nuclear facilities: A critical review. Radiat Prot Dosim 132:182–190

Little MP, Hoel DG, Molitor J Boice JD Jr, Wakeford R, Muirhead CR (2008) New models for evaluation of radiation-induced lifetime cancer risk and its uncertainty employed in the UNSCEAR 2006 report. Radiat Res 169:660–676

Little MP, Wakeford R, Kendall GM (2009) Updated estimates of the proportion of childhood leukaemia incidence in Great Britain that may be caused by natural background ionizing radiation. J Radiol Prot 29:467–482

Pierce DA, Stram DO, Vaeth M (1990) Allowing for random errors in radiation dose estimates for the atomic bomb survivor data. Radiat Res 123:275–284

Pierce DA, Vaeth M, Cologne J (2008) Allowance for random dose estimation errors in atomic bomb survivor studies: a revision. Radiat Res 170:118–126

Posada D, Buckley TR (2004) Model selection and model averaging in phylogenetics: advantages of Akaike information criterion and baysian approaches over likelihood ration tests. Syst Biol 53(5):793–808

Preston DL, Lubin JH, Pierce DA (1993) Epicure user's guide. HiroSoft International Corp, Seattle

Preston DL, Shimizu Y, Pierce DA, Suyama A, Mabuchi K (2003) Studies of the mortality of atomic bomb survivors. Report 13: solid cancer and noncancer disease mortality: 1950–1997. Radiat Res 160: 381–407

Preston DL, Pierce DA, Shimizu Y, Cullings HM, Fujita S, Funamoto S, Kodama K (2004) Effects of recent changes in atomic bomb survivors dosimetry on cancer mortality risk estimates. Radiat Res 162:377–389

Preston DL, Ron E, Tokuoka S, Funamoto S, Nishi N, Soda M, Mabuchi K, Kodama K (2007) Solid cancer incidence in atomic bomb survivors: 1958–1998. Radiat Res 168:1–64

Richardson D, Sugiyama H, Nishi N, Sakata R, Shimizu Y, Grant EJ, Soda M, Hsu WL, Suyama A, Kodama K, Kasagi F (2009) Ionizing radiation and leukemia mortality among Japanese atomic bomb survivors, 1950–2000. Radiat Res 172:368–382

Rühm W, Walsh L (2007) Current risk estimates based on the A-bomb survivors data inconsistent with ICRP recommendations on the neutron weighting factor. Radiat Prot Dosim 126:423–431

Schneider U, Walsh L (2009) Cancer risk above 1 Gy and the impact for space radiation protection. Adv Space Res 44:202–209

United Nations Effects of ionizing radiation (2006) United Nations scientific committee on the effects of atomic radiation

UNSCEAR 2006 report. Volume 1. Annex A: epidemiological studies of radiation and cancer. United Nations, New York (2008)

United States National Research Council, Committee to Assess Health Risks from Exposure to Low Levels of Ionizing Radiation (2006) Health risks from exposure to low levels of ionizing radiation: BEIR VII –phase 2. United States national academy of sciences. National Academy Press, Washington

Wakeford R, Kendall GM, Little MP (2009) The proportion of childhood leukaemia incidence in Great Britain that may be caused by natural background ionizing radiation. Leukemia 23:770–776

Walsh L (2007) A short review of model selection techniques for radiation epidemiology. Radiat Environ Biophys 46:205–213

Walsh L (2010) Radiation protection in occupational and environmental settings. Accepted for publication in OEM

Walsh L, Jacob P, Kaiser JC (2009) Radiation risk modeling of thyroid cancer with special emphasis on the chernobyl epidemiological data. Radiat Res 172:509–518

Young R, Kerr GD (eds) (2005) DS02: Reassessment of the atomic bomb radiation dosimetry for Hiroshima and Nagasaki, dosimetry system 2002, DS02, vol 1, 2. Radiation Effects Research Foundation, Hiroshima

Zhang Z, Townsend JP (2009) Maximum-likelihood model averaging to profile clustering of site types across discrete linear sequences. PLOS Comp Biol 5(6):e1000421

39. Walsh L, Dufey F, Möhner M, Schnelzer M, Tschense A & Kreuzer M. Differences in baseline lung cancer mortality between the German uranium miners cohort and the population of the former German Democratic Republic (1960–2003). Radiat. Environ. Biophys. 50, 57-66, 2011

ORIGINAL PAPER

Differences in baseline lung cancer mortality between the German uranium miners cohort and the population of the former German Democratic Republic (1960–2003)

Linda Walsh · Florian Dufey · Matthias Möhner ·
Maria Schnelzer · Annemarie Tschense ·
Michaela Kreuzer

Abstract A previous analysis of the radon-related lung cancer mortality risk, in the German uranium miners cohort, using Poisson modeling techniques, noted internal (spontaneous) rates that were higher on average than the external rates by 16.5% (95% CI: 9%; 24%). The main purpose of the present paper is to investigate the nature of, and possible reasons for, this difference by comparing patterns in spontaneous lung cancer mortality rates in a cohort of male miners involved in uranium extraction at the former Wismut mining company in East Germany with national male rates from the former German Democratic Republic. The analysis is based on miner data for 3,001 lung cancer deaths, 1.76 million person-years for the period 1960–2003, and national rates covering the same calendar-year range. Simple "age–period–cohort" graphical analyses were applied to assess the main qualitative differences between the national and cohort baseline lung cancer rates. Some differences were found to occur mainly at higher attained ages above 70 years. Although many occupational risk factors may have contributed to these observed age differences, only the effects of smoking have been assessed here by applying the Peto–Lopez indirect method for calculating smoking attributability. It is inferred that the observed age differences could be due to the greater prevalence of smoking and more mature smoking epidemic in the Wismut cohort compared to the general population of the former German Democratic Republic. In view of these observed differences between external population-based rates and internal (spontaneous) cohort baseline lung cancer rates, it is strongly recommended to apply only the internal rates in future analyses of uranium miner cohorts.

Introduction

The characteristics of the German "Wismut" uranium miners cohort have already been described elsewhere (Kreuzer et al. 2009a). It is currently the largest miners cohort study with 3,016 deaths occurring from lung cancer and almost 2 million person-years of observation for the full follow-up period from 1.1.1946 to 31.12.2003. Several analyses on this cohort, based on detrimental health effects' data pertaining to 58,987 male former employees, have recently been published (Kreuzer et al. 2008, 2009b; Schnelzer et al. 2010; Walsh et al. 2010a, b).

There are several occupational risk factors for detrimental health effects which are relevant to the cohort members, including exposure to radon, gamma radiation, long-lived radionuclides (Lehmann et al. 1998), fine dust, arsenic dust and quartz fine dust (Dahmann et al. 2008), diesel and asbestos (Brüske-Hohlfeld et al. 2006).

In radiation epidemiological cohorts assessed by cancer excess relative (or absolute) risk models, the baseline rates are defined as the cancer rates that would have occurred in the absence of radiation, i.e., spontaneously. The Wismut study includes a large number of non-radiation-exposed cohort members, contributing 25% and 21% of the total person-years for the full cohort and the sub-cohort from 1960, respectively. This substantial non-exposed

L. Walsh (✉) · F. Dufey · M. Schnelzer · A. Tschense ·
M. Kreuzer
Federal Office for Radiation Protection,
Department "Radiation Protection and Health",
Ingolstädter Landstr. 1, 85764 Oberschleissheim, Germany
e-mail: lwalsh@bfs.de

M. Möhner
Federal Institute for Occupational Safety and Health (BAuA),
Nöldnerstraße 40–42, 10317 Berlin, Germany

proportion forms a good contribution to the internal comparison group for a reliable determination of baseline cancer rates that can be compared with national rates for the former German Democratic Republic (GDR) that are available from 1960. Note, however, that the internally estimated baseline rates also contain a (statistical) contribution from the exposed cohort members. To illustrate this point further, 8% of the total lung cancers occur in the unexposed group, but a previous Poisson modeling analysis (Walsh et al. 2010a) found that 53% of the total lung cancers contributed to the baseline. This previous analysis of the lung cancer risk in German uranium miners, from exposure to radon, noted internal (spontaneous) rates that were higher on average than the external rates by 16.5% (95% confidence interval (CI): 9%; 24%) (Walsh et al. 2010a).

The aim of the present analyses is to investigate the nature and possible causes of this result by comparing spontaneous lung cancer mortality rates in cohort members, i.e., miners involved in uranium extraction at the former Wismut mining company in East Germany, with male national rates for the former GDR. Due to the limited availability of rates for the former GDR mentioned above, the analysis here is based on the subset of Wismut miner cohort data covering the period 1960–2003 and national rates for the same period. Simple "age–period–cohort" graphical analyses, which involve the mortality rates per 100,000 persons by age at death, period of death and birth cohort, are applied to assess the main qualitative differences between the national and cohort rates. An indirect procedure (the "Peto–Lopez method") for calculating the proportion of lung cancer deaths attributable to smoking via a smoking impact factor (SIF) (Peto et al. 1992, 1994 and Powles 2000) has also been applied. Methods are also applied, in the quantitative analyses involving standardized mortality ratios (SMR) and excess relative risk (ERR) models, to adjust the cohort rates for unknown causes of death because these rates show some systematic variation with calendar time, age at death and radon exposure class.

Materials and methods

Cohort definition, time periods and mortality follow-up

Full details of the cohort have already been given (Kreuzer et al. 2009b; Walsh et al. 2010a). Every cohort member contributes to the number of person-years starting 180 days after the date of first employment and ending at the earliest of date of loss to follow-up, date of death or end of follow-up (31.12.2003). In the present analyses, the former disease codes of the comparison of external baseline rates for the GDR were recoded via earlier ICD revisions to the 10th ICD code (WHO 1992), which was applied throughout. This recoding process was complicated by several revisions to ICD codes during the period of data coverage and German reunification. Population lung cancer rates are not available just for the relevant mining region of Turingia and Saxony. Consequently, the external rates applied here cover the total area of the former GDR (including East Berlin) during the time period 1960–1997; in contrast, from 1998, the rates pertain to the former GDR states and the whole of Berlin. The codes used here in the various time periods are as follows: 1960–1967: GDR code number 735 for trachea, bronchus and primary lung cancers; 1968–1979: ICD 8, code number 162; 1980–1997: ICD 9, code number 162; 1998–2003: ICD 10, code number C33, C34 all for trachea, bronchus and lung cancers.

Analysis

Three methods were applied that all require the tabulation of the individual data as described below and in previous analyses (Walsh et al. 2010a, b). Simple "age–period–cohort" graphical analyses, which involve the mortality rates per 100,000 persons by age at death, period of death and birth cohort, are applied to assess the main qualitative differences between the national rates and the baseline cohort rates (i.e., the spontaneous lung cancer mortality rates after the radon-related lung cancer rates have been accounted for). In this type of graphical analysis, it is necessary to match not only the calendar period of 1960–2003 but also the birth cohorts, i.e., the birth cohorts from 1875 to 1900 need to be excluded from the external rates because the miner cohort includes only the birth cohorts from 1900. Two quantitative risk evaluation methods based on a known association between the lung cancer mortality risk and cumulative radon exposure have also been applied here. These are the simple SMR model (considered both with and without an exposure response) and a previously published continuous Poisson regression ERR model (Walsh et al. 2010b) that contains all of the substantial age- and time-related radon exposure risk-modifying factors, in which a 5-year lag was used in calculating the cumulative exposure to radon. This ERR model for lung cancer is our preferred main model from many models assessed by model selection techniques and is linear in radon exposure with exponential effect modifiers that depend on age at median exposure, time since median exposure and exposure rate (with only minimal confounding e.g. by dust and arsenic).

Since the internally estimated background rates depend on the applied models, the simple SMR model served as a first indicator of differences between external and internal baseline rates and included overall and specific corrections

for missing causes of deaths. The preferred ERR model was then applied in the further detailed investigations into differences in internal to external baseline rates, by extracting the baseline rates from the strata in this model for a direct comparison, exterior to the modeling procedure, with the actual external rates. The preferred ERR model did not include a correction for missing causes of death.

Data tabulations

Tabulations of person-years at risk and cancer deaths were created with the DATAB module of the EPICURE software (Preston et al. 1993). Age at median exposure and time since median exposure were calculated with reference to median exposures, i.e., when half of the exposure cumulated up to a given date was reached. Cross-classifications were made by attained age, a, in 16 categories (<15, 15–<20, 20–<25, …, 85+ years), individual calendar year, y, in 58 categories, age at median exposure, e, in seven categories (<20, 20–<25, 25–<30, 30–<35, 35–<40, 40–<45, 45+ years), time since median exposure, t, in six categories (<5, 5–<10, 10–<15, 15–<20, 20–<25, 25+ years) and cumulative radon exposure, w, in nine categories (0,>0–<10, 10–<50, 50–<100, 100–<200, 200–<500, 500–<1,000, 1,000–<1,500, 1500+ WLM[1]). The exposure rate, er, calculated as the re-computed total cumulative working level months (WLM) divided by total duration (with a lag) at each attained age, on the assumption of 11 working months per year, was also categorized into six groups (0–<0.5, 0.5–<1, 1–<2, 2–<4, 4–<10, 10+ WL).

External rates and standardized mortality rates

Mortality rates observed in the cohort were compared with those of the general male population in Eastern Germany, formerly the GDR. Since external rates were only available from 1960 onwards, the SMR analysis was limited to the follow-up period 1960–2003. Therefore, 15 lung cancers deaths with the corresponding person-years prior to 1960 were excluded. The first stage of the SMR analysis for lung cancer has been done here in the same way as described previously for extra-pulmonary cancers (Kreuzer et al. 2009b) with some extensions that allow a comparison of internal (miner cohort) and external (former GDR) baseline (spontaneous) rates. Two finer methods for accounting for the unknown causes of death in the miners cohort were also used. The simplest SMR model relates the rates in the population of interest (the miners cohort) to a multiple of the rates from the external population (the former GDR). If

$\lambda^*(a, y)$ denotes the external rates as a function of age and calendar year and $\lambda(a, y)$ denotes the observed rates in the miners cohort, then the SMR model can be written as

$$\lambda(a, y) = \beta \cdot \lambda^*(a, y) \qquad (1)$$

where the β is a fit parameter and represents the SMR.

An SMR > 1 for the miners cohort is a known result (Walsh et al. 2010a). Therefore, it is instructive to fit a relative risk (RR) model

$$RR(a, y, w) = \beta_1 \cdot \lambda^*(a, y) \cdot (1 + \beta_2(w)) \qquad (2)$$

to estimate the radon exposure (w) effect, based on the GDR external rates, assuming that the SMR for the background rates is identically equal to 1, i.e., β_1 is fixed to unity during the optimization. In this case, β_2 is a fit parameter that then gives the simple ERR per unit of radon exposure relative to the external GDR rates. It is also possible to test whether the external GDR rates are different from the internal baseline rates in the miners cohort by simply freeing the parameter β_1 and repeating the optimization. The influence of missing causes of death has been investigated by fitting the models in Eqs. 1 and 2 with either no correction for missing causes of death or an average correction using one value of the proportion of causes of death that are known (Rittgen and Becker 2000) or a fine correction using the proportion of causes of death that are known either in each calendar-year period or in each Poisson cell. The Poisson cells here refer to the data elements obtained from tabulating the individual data into the groups described above. These methods assume that the missing lung cancers are evenly distributed throughout the covariable ranges in a way that is proportionate to the percentage of missing causes of death.

ERR parametric risk models (internal comparison group)

The tabulated data were fitted to the following model (Walsh et al. 2010b)—if $r(a, y, w, er, e, t)$ is the exposure-specific lung cancer mortality rate that depends on age, year, exposure, exposure rate, age at median exposure and time since median, and $r_0(a, y) = r(a, y, 0, 0, 0, 0)$ is the baseline disease rate for non-exposed individuals ($w = 0$, $er = 0$), then

$$r(a, y, w, er, e, t) = r_0(a, y) \times \{1 + ERR(w, er, e, t)\} \qquad (3)$$

where ERR is the excess relative risk factorized into a function of exposure and a modifying function:

$$ERR(w, er, e, t) = \beta_w w \, \exp[\psi_w (er - 2.7) + \alpha(e - 33) + \varepsilon(t - 11)] \qquad (4)$$

where and β_w, ψ_w, α and ε are fit parameters, w is the cumulated radon exposure and er is the exposure rate;

---

[1] One WLM of cumulative exposure corresponds to exposure to 1 WL during one month (170 h) and is equivalent to 3.5 mJh/m^{3}.

e and *t* are calendar time–dependent variables, calculated with reference to the median time-lagged exposures. The model-centering constants, at an age median exposure of 33 years and time since median exposure of 11 years, were chosen to match the mean Wismut cohort values—the choice of centering constants only serves to change the risk by a factor and has no influence on the goodness of fit of a particular model.

Maximum likelihood with the AMFIT module of the EPICURE software (Preston et al. 1993) was used for the estimation of the fit parameters and the internal baseline rates in 928 strata of age attained (16 categories) and individual calendar year (58 categories), chosen to match the grouping that was available in the external rates. Out of these 928 possible strata, 708 actually contained rate data that were extracted for direct comparison with the national rates for the former GDR.

Peto–Lopez indirect method for calculating deaths attributed to smoking

Since data on smoking habits are not available for the majority of Wismut cohort members, it is useful to have a method for estimating the effects of smoking directly from the baseline lung cancer mortality rates. As suggested by Sir Richard Peto FRS and colleagues (Peto et al. 1992, 1994 and Powles 2000), the prevalence of smoking can be estimated indirectly by comparing the lung cancer mortality rates of interest with the lung cancer rates among current smokers and never smokers in a large prospective cohort study conducted by the American Cancer Society (ACS) CPS-II study from the 1980s (see Thun et al. 2008, open access article for direct links to the data in EXCEL format and relevant references). The two main assumptions here are that: the CPS-II lung cancer mortality rates for current smoker and never smoker are a valid approximation of the (unobserved) smoking-specific lung cancer mortality rates pertaining to the two sets of rates of interest here (the Wismut baseline rates and the external lung cancer rates of the former GDR); and current lung cancer mortality provides a better measure of the effect of lifetime tobacco smoking than smoking prevalence.

Estimates of the fractions of tobacco-attributable deaths related to both the internal Wismut and external former GDR baseline rates were obtained by this indirect method. This was achieved by comparing both internal and external baseline lung cancer mortality rates with rates observed for current smokers or never smokers in the above-mentioned CPS-II cohort of men of European descent and deriving a 'smoking impact factor' (SIF).

The SIF was calculated according to the following formula that pertains to economically developed countries:

$$\text{SIF} = \text{Lung cancer death rate in excess of never smokers}$$
$$\text{in group of interest/Excess lung cancer death}$$
$$\text{rate for known reference group of current smokers}$$
$$= (C_{\text{LC}} - N_{\text{LC}})/(S_{\text{LC}}^{*} - N_{\text{LC}}^{*}), \tag{5}$$

where $C_{\text{LC}} = \lambda_{\text{B}}(a, y)$ or $\lambda^{*}(a, y)$, i.e., the lung cancer mortality (baseline) rates in the Wismut cohort or the external population rates (former GDR), respectively, N_{LC} is the lung cancer death rate among never smokers in the group of interest (assumed to be equal to N_{LC}^{*}), N_{LC}^{*} is the lung cancer death rate among never smokers in CPS-II and S_{LC}^{*} is the lung cancer mortality rate for smokers in CPS-II.

If the SIF is used to describe the age-specific or cumulative hazard of smoking, all calculated SIF values that exceed 1.0 (when $C_{\text{LC}} > S_{\text{LC}}^{*}$) are set equal to 1.0. Likewise, if SIR < 0 (which could happen if $C_{\text{LC}} < N_{\text{LC}}^{*}$, that might be the case for very young age-groups), the calculated values are set to 0. SIF is a measure that ranges from 0 to 1. An SIF of 1 is equivalent to a population comprised entirely of lifetime smokers (in the reference population), and an SIF of 0 is equivalent to a population comprised entirely of never smokers. Patterns in the age-specific SIF values indicate the maturity of the smoking epidemic in a given group: if the epidemic is in its early phases, the SIF values are high in the younger age-groups and low in the older; if the epidemic is 'mature', the elevated SIF values extend across the entire age range; and when the epidemic is declining, the SIF values are lower in the younger age-groups than in the older ones. The Peto–Lopez method is widely used in epidemiology and social science and is not effectively challenged by the tobacco industry (http://www.deathsfromsmoking.net).

Results

The absolute and cumulative number of lung cancer deaths in the full Wismut cohort (1946–2003) is shown in Fig. 1a and b as a function of calendar year from 1960 and age attained from 20 years. It can be seen from these figures that (a) the absolute number of lung cancers occurring reaches a maximum around 67 years of age, increases steadily from 1960 to 1980 and reaches a plateau thereafter; (b) the cumulative number of lung cancers has a sigmoid shape as a function of age attained, but with calendar year, there is a gradual non-linear increase up to 1970, which becomes linear thereafter.

On restricting the full data range available in the cohort (1946–2003) to match the availability of external lung cancer rates for the former GDR, i.e., by omitting the cohort data from 1946 to 1959, the main epidemiological
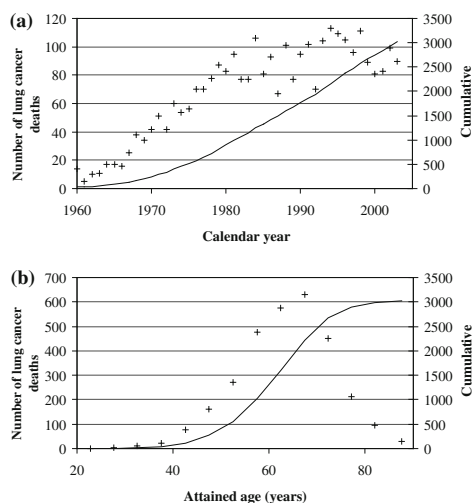
Fig. 1 **a** The number of lung cancer deaths in the Wismut cohort as a function of calendar year. The *left-hand* ordinate and crosses show the simple numbers, and the *right-hand* ordinate and *line* show the cumulative numbers. **b** The number of lung cancer deaths in the Wismut cohort as a function of age attained. The *left-hand* ordinate and crosses show the simple numbers, and the *right-hand* ordinate and *line* show the cumulative numbers

Table 1 ERR model for lung cancer and radon exposure, with exponential radon exposure rate, age and time effect modifiers (Eqs. 3 and 4)

Model description	Parameter name	Fitted value
$f(w,er) \cdot g(e, t)$	β_w	1.06 (0.69; 1.42)
	$\exp(\psi_w)$	0.95 (0.93; 0.96)
	$\exp(10\varkappa)$	0.68 (0.57; 0.82)
	$\exp(10\varepsilon)$	0.46 (0.39; 0.55)

The ERR fit parameters (i.e., the β's) are in units of ERR per 100 WLM, with model centering, where applicable, at an age at median exposure of 33 years (relevant parameter is $\exp(10\varkappa)$), a time since median exposure of 11 years (relevant parameter is $\exp(10\varepsilon)$), and an exposure rate of 2.7 WL (relevant parameter is $\exp(\psi_w)$). All fit parameters are quoted with 95% Wald-type confidence intervals

quantities of interest relevant to the analysis presented here are as follows: there are 3,001 lung cancers and 1.76 million person-years. The percentage of missing causes of deaths, based on 19,501 known causes of death and 1,183 missing causes of death, is 5.7%. A disproportionate number of the total missing causes of death (i.e., 494 of the total 1,183) occurred during the period 1960 to 1969. This is due to the late start of data collection for this cohort on 1.1.1999, linked with the fact that death certificates were rarely kept by the authorities for more than 30 years.

Qualitative age, period and cohort analysis

Qualitative differences between GDR external rates and internal birth cohort baseline rates were based on the latter obtained directly from the strata associated with a previously published (Walsh et al. 2010b) excess risk model (Eqs. 3 and 4), with the previously published parameters also given and described here in Table 1. This model is linear in radon exposure with exponential effect modifiers that depend on age at median exposure, time since median exposure and radon exposure rate. In this model, the central estimate of ERR/WLM is 1.06% (95% CI: 0.69%; 1.42%) for an age at median exposure of 33 years, a time since median exposure of 11 years and an exposure rate of

2.7 WL. This central ERR decreases by 5% for each unit of exposure rate increase. The ERR decreases by 32% with each decade increase in age at median exposure and also decreases by 54% with each decade increase in time since median exposure.

The results are presented in Fig. 2a (external rates) & b (internal strata) for the time period effects, and in Fig. 2c (external rates) & d (internal strata) for the birth cohort effects. A direct comparison of Fig. 2a and b shows that whereas the external rates tend to decline beyond age 70 years with increasing age in most time periods considered, the internal rates do not and are generally higher. A similar effect can also be seen by comparing Fig. 2c and d, for different birth cohorts. The earliest birth cohort available for the internal cohort is 1900–1904, and it can be seen from Fig. 2d that the variation in the death rates between attained-age categories is much greater for this group than for the later birth cohorts. This effect is caused by the relatively fewer person-years of observation available for this group.

Results for smoking impact factors from the Peto–Lopez indirect method

Estimates of the fraction of tobacco-attributable deaths from the internal and external baseline rates were obtained by the indirect method (proposed by Peto et al. 1992) described above.

The overall age-group-specific lung cancer rates for both the Wismut internal baseline and the former GDR are shown in Fig. 3 along with the lung cancer rates among smokers and non-smokers in the large prospective cohort study conducted by the American Cancer Society CPS-II study from the 1980s mentioned above. The age-specific SIFs are shown in Fig. 4 and indicate that the impact of smoking is greater in the Wismut baseline group for older ages, i.e., beyond 65 years, and lower for younger ages. Since the SIFs are decreasing with increasing age more
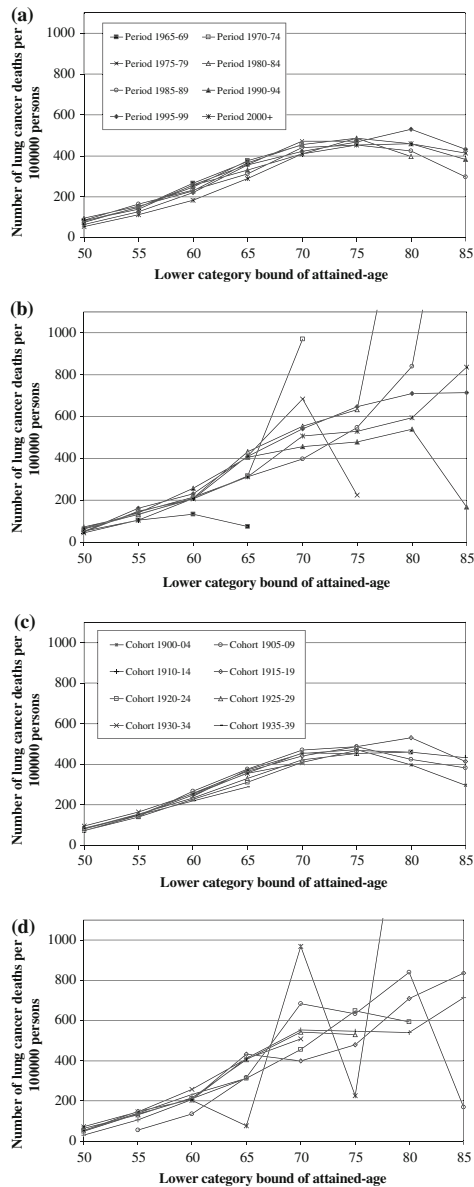
(a)

(b)

(c)

(d)

◀ **Fig. 2** **a** GDR external rates: The number of lung cancer deaths per 100,000 persons as a function of age attained in different time periods. **b** Internal cohort baseline rates: The number of lung cancer deaths per 100,000 persons as a function of age attained in different time periods. Note the *vertical scale* has not been extended to include two points with high rates of about 2,000 deaths per 100,000 persons, due to the very small number of person-years contributing to these spurious values. **c** GDR external rates: The number of lung cancer deaths per 100,000 persons as function of age attained in different birth cohorts. **d** Internal cohort baseline rates: The number of lung cancer deaths per 100,000 persons as a function of age attained in different birth cohorts. Note the vertical scale has not been extended to include two points with high rates of about 2,000 deaths per 100,000 persons, due to the very small number of person-years contributing to these spurious values
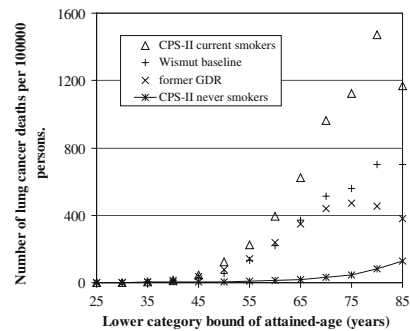

Fig. 3 Age-specific lung cancer mortality rates comparing: CPS-II male current smokers of European descent over six years of follow-up (1982–1988), CPS-II male never smokers over 22 years of follow-up (1982–1988), Wismut cohort internal baseline rates (1960–2003) and male rates for the population of the former GDR (1960–2003). The CPS-II data were accessed directly from (Thun et al. 2008 online tables S4 and S21)
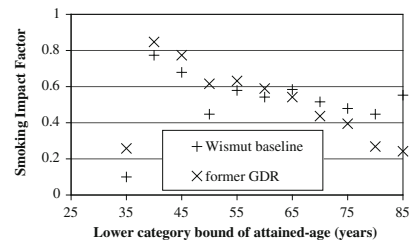

Fig. 4 Age-specific smoking impact factors (SIFs) computed as described in the main text applying the rates given in Fig. 3

SMR results (comparison with external rates)

The proportion of causes of death that are known, P, was also determined in each radon exposure class and for each calendar year (top panels of Figs. 5 and 6) and was found to show some non-random variation. Therefore, in the

strongly in the former GDR than in the Wismut group, it can be inferred that the smoking epidemic is more mature in the latter group.
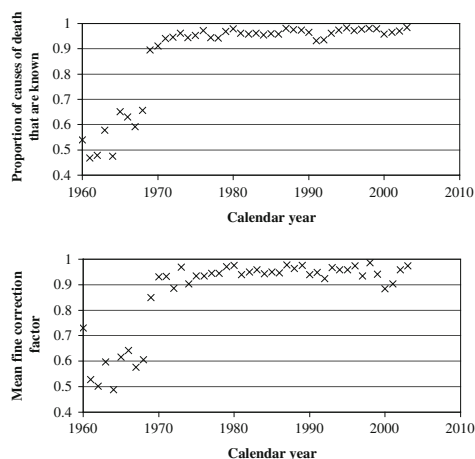
Fig. 5 *Top panel:* actual proportion of causes of death that are known in each calendar year between 1960 and 2003; *Bottom panel:* person-year-weighted average in each calendar year of the fine correction factor that was applied to each Poisson cell in the tabulated data
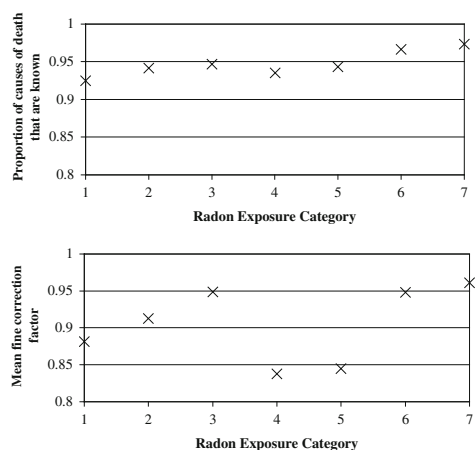

Fig. 6 *Top panel:* actual proportion of causes of death that are known in radon exposure category; *Bottom panel:* person-year-weighted average in each radon exposure category of the fine correction factor that was applied to each Poisson cell in the tabulated data

determination of SMR values, the observed number of deaths was applied: without adjustment, with adjustment for one mean cohort value of P and with an adjustment value of P obtained in each Poisson cell (bottom panels of Figs. 5 and 6). Since the Poisson cells are classified by calendar period, and age and exposure variables, which are

all related to calendar period, an additional adjustment to the observed number of deaths (O) made only by calendar period was tested.

It can be seen from Table 2 that the number of deaths (1960–2003) observed (O) was significantly higher than expected (E) from national rates. The fitted values of SMR (SMR $= O/E$) given in Table 2 depend slightly on whether a correction of O (uncorrected) to O^* (with a single average correction factor of 0.943, i.e., $O^* = O/0.943$) or to O^{**} (with a fine correction factor in each Poisson cell) was made for missing causes of death. The SMR values with 95% confidence intervals (CI) are 1.91 (1.85; 1.98), 2.03 (1.96; 2.10) or 2.06 (1.99; 2.14) for O, O^* and O^{**}, respectively. However, it can be seen from Table 2 that correction by calendar year produces results that are very similar to those obtained with the single average correction factor.

Simple ERR parametric cohort risk models
(comparisons with external and internal rates)

Statistically significant cumulative radon exposure effects in terms of ERR/WLM values and 95% CIs are also given in Table 2. These are: relative to the external GDR rates, 0.0022 (0.0021; 0.0024), 0.0025 (0.0023; 0.0026) and 0.0025 (0.0023; 0.0026) for O, O^* and O^{**}, respectively; and relative to the internal cohort baseline rates, 0.0019 (0.0017; 0.0022), 0.0019 (0.0017; 0.0022) and 0.0018 (0.0016; 0.0021) for O, O^* and O^{**}, respectively. As in the last section, it can be seen from Table 2 that correction by calendar year produces results that are very similar to those obtained with the single average correction factor.

Internal to external baseline comparison

Statistically significant differences were found in the ratio of internal to external baseline risks. These ratios and 95% CIs are also given in Table 2. These are 1.098 (1.027; 1.169), 1.165 (1.089; 1.240) and 1.200 (1.122; 1.278) for O, O^* and O^{**}, respectively. The result pertaining to O^* that the internal baseline rates were found to be greater than the external baseline rates by 16.5% has previously been reported (Walsh et al. 2010a). This result is an average value for the whole range of covariates, but a further analysis that recomputed this value for two age-groups of <70 and ≥70 years gives 1.097 (1.011; 1.184) and 1.34 (1.188; 1.499), respectively. This latter result that the internal baseline rates were found to be higher than the external baseline rates by 34% for ages over 70 years quantifies the qualitatively observed differences in Fig. 2a–d above. Since Fig. 5 indicates that the proportion of causes of death that are known are much lower for the time period 1960–1969 (i.e., at 0.63 with $O = 187$ lung cancers,

Table 2 Results of fitting the models for the standardized mortality ratios (SMR) given in Eqs. 1 and 2 of the main text

Correction mode for missing causes of death	Parameter name	Meaning	Fitted value	Parameter name	Meaning	Fitted value · $[10^{-2}]$
None	β	SMR	1.91 (1.85; 1.98)			
Average	β		2.03 (1.96; 2.10)			
By calendar year	β		2.03 (1.96; 2.10)			
Fine	β		2.06 (1.99; 2.14)			
None	β_1	*internal = external baseline*	fixed at 1	β_2	ERR/WLM *relative to external baseline*	0.223 (0.208; 0.238)
Average	β_1		fixed at 1	β_2		0.245 (0.229; 0.261)
By calendar year	β_1		fixed at 1	β_2		0.244 (0.229; 0.260)
Fine	β_1		fixed at 1	β_2		0.246 (0.230; 0.261)
None	β_1	*internal to external baseline ratio*	1.098 (1.027; 1.169)	β_2	ERR/WLM *relative to internal baseline*	0.192 (0.167; 0.216)
Average	β_1		1.165 (1.089; 1.240)	β_2		0.192 (0.167; 0.216)
By calendar year	β_1		1.163 (1.087; 1.239)	β_2		0.192 (0.167; 0.216)
Fine	β_1		1.200 (1.122; 1.278)	β_2		0.183 (0.159; 0.207)

Values given in parentheses represent 95% CI intervals

$O^* = 187/0.63 = 297$) than for later years, the internal to external baseline risk ratio was also computed for the data from 1970. Ratios and 95% confidence intervals for the data from 1970 are 1.123 (1.049; 1.198), 1.165 (1.087; 1.244) and 1.184 (1.105; 1.262) for O, O^* and O^{**}, respectively. Since there are only small differences between the ratios for the data from 1960 and the data from 1970, it can be inferred that the lower values for the proportion of causes of death that are known before 1970 have little influence on the observed differences in internal to external baseline risks.

Discussion

It is generally acknowledged in the field of radiation epidemiology that a cohort that is good for investigating the detrimental effects of ionizing radiation should have a substantial proportion of unexposed cohort members and that the unexposed cohort members form a more suitable group for assessing the radiation-associated disease rates than an external population group from the same geographical area. However, not many papers have actually investigated the detailed reasons for this generally accepted preference. The work presented here is aiming at filling this gap by examining systematic differences in the lung cancer mortality rates, which were found to exist when comparing the Wismut baseline group (i.e., the lung cancer rates remaining after accounting for the strong risk factor, radon) to the general population of the former GDR. There are several other risk factors for lung cancer, which are relevant to the Wismut cohort members at exposure levels that either do not apply at all to the general population or only apply at much lower levels. Such risk factors include exposure to gamma radiation, long-lived radionuclides,

fine dust, arsenic dust, quartz fine dust, asbestos and diesel fumes. All of these factors could have had some influence on the observed differences in lung cancer baseline rates. The analysis presented here should be repeated in the future when all of the other risk factors and their interactions have been fully evaluated. However, it is cautiously assumed now that there are two major factors that emerge from the many possible covariables that contribute to such differences in the current baseline rates, namely differences in the characteristics of routine medical screening programs (p. 666 Runge 1999) and differences in the prevalence of smoking as discussed below.

A screening program in the Wismut mining company was started in 1952, primarily because of the many observed cases of Silicosis and Tuberculosis. This was carried out initially as a pilot project, which was then extended to the general population of the former GDR in 1953/1954 with the primary aim of detecting tuberculosis. Initially, annual medical checks were carried out in the GDR that were later reduced to biennial checks (with chest X-rays for those over 40 years of age). At the Wismut company, the medical checks were supposed to be annual and independent of age and accumulated exposure. However, it is known that this regime was not strictly adhered to by the employees, since not turning up to medical examinations had no work-related consequences. It can therefore be assumed that, in the absence of symptoms of ill health, medical screening in the Wismut employees was only marginally more frequent than in the general population of the GDR. In contrast, Wismut employees with symptoms such as breathing difficulties were carefully monitored and given chest X-rays at short time intervals. Since there were about 20,000 confirmed cases of silicosis among Wismut employees up to 1990, treated by many associated medical

specialists for this disease, it is reasonable to assume that lung cancer was diagnosed at an earlier stage in Wismut employees than in the general population of the former GDR. This would not, however, explain the observed differences in the lung cancer mortality rates, although a minor part of these differences may be due to increased detection of lung cancers in the miner cohort, due to higher autopsy rates than in the general population of the former GDR.

The Wismut cohort data only include a very limited amount of smoking-related information and only for a small percentage of the subjects. Detailed smoking information has recently been collected for about 2000 cohort members and assessed in a nested case–control study that examined the influence of smoking on the radon-related lung cancer risk (Schnelzer et al. 2010). Since data on smoking are not available for the majority of Wismut cohort members, it is only possible to obtain indirect indications and apply methods for ascertaining the possible effects of smoking in this cohort. There have already been indications that the prevalence of smoking in the Wismut employees was higher than in the general population, from two case–control studies in the former GDR regions of Thuringia and Saxony. These two studies investigated the lung cancer risk due to radon and other risk factors, one concerning Wismut miners and the other excluding miners (Brüske-Hohlfeld et al. 2006; Wichmann et al. 1999). Based on standardized personal interviews that included detailed questions about smoking history, only 15.2% of male controls among the Wismut miners analyzed (Brüske-Hohlfeld et al. 2006) were classified as never having smoked, whereas the percentage in the other studies' control group of male non-miners was 26.5% (Wichmann et al. 1999).

It is also interesting to note that the former Soviet general director of the Wismut company, General Malzews, ordered additional remuneration and performance bonuses in the form of alcohol and tobacco products— "Every employee working in the mines or at ground level will receive 50 and 30 cigarettes per month, respectively. By above average performance an additional 50 cigarettes per 10 days are payable" (p. 780 Runge 1999). So, it was possible for Wismut employees to earn up to 200 cigarettes per month in addition to any they may have purchased—a large quantity by past and current standard—which can be compared to the average number of cigarettes consumed per month in the former GDR, which rose from 89 in 1960 to 154 in 1989 (Statistisches Bundesamt 2005). It can therefore be assumed that not only the smoking prevalence and the amount of tobacco consumed were higher, but also the age at the start of smoking was probably younger, than in the general population.

These earlier indications and the socially based evidence are corroborated by the analysis presented here in terms of the SIFs from the Peto–Lopez indirect method, which indicates that the smoking epidemic is more mature in the Wismut miners than in the general population of the GDR. A possible criticism of the SIF method could be that the lung cancer rates among lifelong non-smokers could have changed over time and may be different between countries. However, a recent analysis of 13 cohorts and 22 cancer registry studies (Thun et al. 2008) found no indication either that lung cancer rates have changed among never smokers in the age range 40–69 years in the US since the 1930s or that death rates have changed appreciably among never smokers from CPS-I (1959–1972) to CPS-II (1982–2004), where these latter two cohorts are the only cohorts currently available for assessing this point. The calculation of the SIFs involves the rates for current smokers; these rates were obtained over six years of follow-up of CPS-II (1982–1988) for men of European descent where this time period falls approximately in the middle of the time period for the Wismut cohort follow-up and GDR rates (1960–2003). The analyses for the age category–specific SIFs presented above were repeated for Wismut and GDR rates that were restricted to the 1982–1988 time period, but this restriction did not affect the main results to any notable degree. Other limitations to the SIF analysis might exist because factors relevant to the determination of lung cancer risk may have differed between the ACS cohort and the population and cohort studied here. Such factors include the daily amount and number of years smoked, exposure to second-hand smoke, brand of cigarette, age at initiation and inhalation habits.

Methods applied here for adjusting for missing causes of death associated with the data collection process for the Wismut cohort only indicated a minor effect of missing causes of death on both the differences in internal and external baseline rates and on the radon-related risk per unit of exposure. This is related to the fact that there are only about 6% of total deaths and 6% of total lung cancer deaths occurring in the period with the lowest proportion of causes of death that are known, i.e., between 1960 and 1970.

Conclusions

This work has shown that systematic differences in the lung cancer mortality rates exist when comparing the Wismut baseline (i.e., the lung cancer rates remaining after accounting for the strong risk factor, radon) to the lung cancer mortality of the general population of the former GDR. For this reason, it is generally recommended to apply the Wismut internal rates in preference to the external

mortality rates, for baseline lung cancer rate determination, in future detailed risk models of radiation-associated lung cancers in this cohort.

Even though the missing causes of death associated with the data collection process for the Wismut cohort show some non-random variation with calendar years and radon exposure category, they were found to have only a minor effect on both the differences in internal and external baseline rates, and on the radon-related risk per unit of exposure.

The Peto–Lopez method has been applied here and has indicated that the systematic differences in the lung cancer mortality rates between the internal and external baselines could be due to differences in the maturity of the smoking epidemic. In view of the current limitations, it is recommended that the analysis presented here should be repeated in the future and based on either a single or model-averaged preferred model that includes all of the other risk factors and their interactions. At this point in time, however, such risk factors have not yet been fully evaluated for the Wismut cohort.

References

Brüske-Hohlfeld I, Rosario AS, Wolke G, Heinrich J, Kreuzer M, Kreienbrock L, Wichmann HE (2006) Lung cancer risk among former uranium miners of the WISMUT Company in Germany. Health Phys 90:208–216

Dahmann D, Bauer HD, Stoyke G (2008) Retrospective exposure assessment for respirable and inhalable dust, crystalline silica and arsenic in the former German uranium mines of SAG/SDAG Wismut. Int Arch Occup Environ Health 81:949–958

Kreuzer M, Walsh L, Schnelzer M, Tschense A, Grosche B (2008) Radon and risk of extra-pulmonary cancers—Results of the German uranium miners cohort study, 1960–2003. Br J Cancer 99:1946–1953

Kreuzer M, Schnelzer M, Tschense A, Walsh L, Grosche B (2009a) Cohort profile: the German uranium miner cohort study (WISMUT cohort), 1946–2003. Int J Epidemiol. doi:10.1093/ije/dyp216

Kreuzer M, Grosche B, Schnelzer M, Tschense A, Dufey F, Walsh L (2009b) Radon and risk of death from cancer and cardiovascular diseases in the German uranium miners cohort study: follow-up 1946–2003. Radiat Environ Biophys 49(2):177–185

Lehmann F, Hambeck L, Linkert KH, Lutze H, Meyer H, Reiber H, Renner HK, Reinisch A, Seifert T, Wolf F (1998) Belastung durch ionisierende Strahlung im Uranerzbergbau der ehemaligen DDR. Hauptverband der gewerblichen Berufsgenossenschaften, St. Augustin

Peto R, Lopez AD, Boreham J, Thun M, Heath C Jr (1992) Mortality from tobacco in developed countries: indirect estimation from national vital statistics. Lancet 339:1268–1278

Peto R, Lopez AD, Boreham J, Thun MJ, Heath C Jr (1994) Mortality from smoking in developed countries, 1950–2000: indirect estimates from national vital statistics. Oxford University Press, Oxford. (Second edition available online at http://www.ctsu.ox.ac.uk/~tobacco/)

Powles J (2000) The Peto/Lopez indirect method for estimating the accumulated mortality hazard caused by smoking (GBD2000 protocol). Available from: http://www.phpc.cam.ac.uk/mst/phtop/peto_lopez_method_gbd2000.doc. Accessed 1 March 2010

Preston DL, Lubin JH, Pierce DA, McConney ME (1993) Epicure user's guide. HiroSoft, Seattle

Rittgen W, Becker N (2000) SMR Analysis of historical follow-up studies with missing death certificates. Biometrics 56:1164–1169

Runge W (editor in chief) (1999) Chronik der WISMUT, Wismut GmbH (2738 pages, in German)

Schnelzer M, Kreuzer M, Tschense A, Hammer G, Grosche B (2010) Accounting for smoking in the radon related lung cancer risk among German uranium miners: results of a nested case-control study. Health Phys 98:20–28

Statistisches Bundesamt (2005) Fachserie 14: Finanzen und Steuern, Reihe 9.1.1 Absatz von Tabakwaren, Abbildung 2.5.2: Jahrliche Pro-Kopf-Verbrauch (in Stück) an Zigaretten in Deutschland 1955 bis 2004

Thun MJ, Hannan LM, Adams-Campbell LL, Boffetta P, Buring JE, Feskanich D, Flanders WD, Jee SH, Katanode K, Kolonel LN, Lee IM, Marugame T, Palmer JR, Riboli E, Sobue T, Avila-Tang E, Wilkens LR, Samet JM (2008) Lung cancer occurrence in never-smokers: an analysis of 13 cohorts and 22 cancer registry studies. PLoS Med 5(9):1357–1371

Walsh L, Tschense A, Schnelzer M, Dufey F, Grosche B, Kreuzer M (2010a) The Influence of radon exposure on lung cancer mortality in German uranium miners, 1946–2003. Radiat Res 173:79–90

Walsh L, Dufey F, Tschense A, Schnelzer M, Grosche B, Kreuzer M (2010b) Radon and the risk of cancer mortality—Internal Poisson models for the German uranium miners cohort. Health Phys 99(3):292–300

WHO (1992) International statistical classification of diseases and health related problems: the ICD-10 (German edition 1.3.1999), Geneva

Wichmann HE, Gerken M, Wellmann J, Kreuzer M, Kreienbrock L, Keller G, Wölke G, Heinrich J (1999) Lungenkrebsrisiko durch Radon in der Bundesrepublik Deutschland (Ost)- Thuringen und Sachsen. ecomed, Landsberg. (in German)

40. Dufey F, Walsh L, Sogl M & Kreuzer M. Occupational doses of ionizing radiation and leukaemia mortality. Health Physics. 100(5), 548-550, 2011

OCCUPATIONAL DOSES OF IONIZING RADIATION AND LEUKEMIA MORTALITY

Dear Editors:

A RECENT paper (Möhner et al. 2010) has reported a weak association between risks for leukemia incidence and exposure to ionizing radiation. This paper has extended a previous case-control study (CCS) of uranium miners in the former German Democratic Republic (GDR) employed by the Wismut Company, with 377 cases and 980 controls (Möhner et al. 2006) to include medical exposures and organ doses to the red bone marrow (RBM). The purpose of this letter is to briefly present analogous results for leukemia mortality in a large cohort study of former employees of the Wismut Company (Kreuzer et al. 2010). The cohort comprises of about 59,000 men contributing 128 leukemia deaths and approximately 2 million person-years during the timespan 1946–2003. Besides its large size, the main strengths of the cohort study are the long follow-up period, the high percentage of causes of death for 93.6% of the deceased, and the low proportion (4.7%) of subjects lost to follow-up. Uranium mining was performed by the Wismut Company in East Germany from 1946 to 1989.

Both Möhner and colleagues and the authors have recently been involved in an EU project that has provided new software for calculating organ doses from the occupational radiation exposures (Marsh et al. 2008). Also the same job exposure matrix (Lehmann 2004; Lehmann et al. 1998; HVBG 2005) was used to assess exposure to radon, external gamma radiation and long-lived radionuclides. For these reasons, the quantification of dose in both studies is directly comparable.

While both studies considered leukemia in former employees in East German uranium mining, they differ markedly both in the definition of the source population and in whether incidence or mortality was considered:

- The source population for the CCS consists of male Wismut employees for whom medical records from Wismut or statutory insurance were available (approximately 360,000 men). Cases were identified by data linkage with the common cancer registry and the cancer control agency of the former GDR. This restricted the follow-up period of the study to 1950–1989. For the identification of controls, a sub-sample of individuals having no match in the cancer registry and stratified by year of birth, was drawn. Subsequently, controls were individually matched by year of birth.

- The cohort study is based on a stratified random sample of approximately 64,000 men drawn from about 130,000 persons for which sufficient information for follow-up and exposure data were available. Stratification criteria were gender, exposure status, place of work, and year of first employment (1946–1954, 1955–1970, 1971–1989). Final inclusion criteria were male gender, first employment between 1 January 1946 to 31 December 1989, year of birth after 1899, and a minimum employment time of 180 d. The second mortality follow-up covers the period from 1946 to 2003. Information on vital status and cause of death was obtained from local registration offices, autopsy files, and the Wismut Health Data Archives (Kreuzer et al. 2008, 2010; Walsh et al. 2010, 2010b).

In the cohort study, only 48 of a total of 128 deaths from leukemia occurred up to 1989, of which only 43 are also included in the 377 cases of the CCS. Thus the overlap of both studies is small. The mean doses in the cohort study are somewhat higher than in the CCS: absorbed RBM dose for the cohort study was 48.8 mGy (range 0 to 989 mGy), to which external gamma radiation contributed on the mean 40.9 mGy (range 0 to 909 mGy). This can be compared to the mean RBM dose for the CCS (for cases and controls taken together) of 23.6 mGy, of which 15.6 mGy were contributed on average by occupational gamma exposures.

The same absorbed RBM dose categories, lag-times (of 2 and 15 y) and confidence level (90%) as in Möhner et al. (2010) have been applied here in calculating the relative risks from the cohort data for direct comparison. The present comparison is based on the occupational doses, since the diagnostic doses have not yet been abstracted from the comprehensive medical records for the cohort study. Details of recent cohort analyses with other types of cancer or exposures have been described elsewhere (Kreuzer et al. 2008; Walsh et al. 2010a and b).

The dose category specific relative risks were calculated by Poisson regression with baseline stratification by age and calendar year with the AMFIT module of EPICURE (Preston et al. 1990). Results with respect to a lag time of 2 y (upper section of Table 1) give no possible hint of an excess leukemia mortality risk in the present study. This finding is in line with the results of Möhner

Table 1. Leukemia relative risk in the Wismut cohort (1946–2003) of German uranium miners by absorbed dose to the red bone marrow due to occupational exposure, time lag: 2 y.

Dose (mGy)	All leukemias (128 deaths)			CLL[a] (40 deaths)			Non-CLL[b] (88 deaths)		
	Deaths	RR[c]	90% CI	Deaths	RR[c]	90% CI	Deaths	RR[c]	90% CI
<0.4	29	1	—	12	1	—	17	1	—
0.4–<5.0	8	0.44	0.23–0.86	2	0.31	0.09–1.10	6	0.53	0.24–1.16
5.0–<25.6	31	0.76	0.50–1.18	9	0.59	0.28–1.22	22	0.89	0.52–1.53
25.6–<103.7	31	0.58	0.38–0.90	10	0.46	0.22–0.93	21	0.67	0.39–1.16
≥103.7	29	0.97	0.62–1.51	7	0.58	0.26–1.28	22	1.25	0.72–2.16
<5.0	37	1	—	14	1	—	23	1	—
5.0–<25.6	31	0.98	0.65–1.46	9	0.78	0.38–1.58	22	1.10	0.67–1.81
25.6–<103.7	31	0.74	0.49–1.11	10	0.60	0.30–1.19	21	0.83	0.50–1.38
≥103.7	29	1.24	0.82–1.88	7	0.77	0.35–1.66	22	1.54	0.93–2.55

[a] Chronic lymphatic leukemia.
[b] All leukemia, except CLL.
[c] Relative risk from a Poisson regression with baseline stratification by age and calendar year.

et al. Statistically significant and decreased relative risks for all types of leukemia combined are found in the categories 0.4 to <5 and 25.6 to <103.7 mGy in the upper section of Table 1. This pattern of decreased risks may be an artifact due to the low number of cases in the category with 0.4 to <5 mGy. This is supported by the observation that the significance of the decrease is not maintained (see the lower section of Table 1) when the first two lower dose categories are combined so that the under 5 mGy category becomes the reference category.

When assuming a lag time of 15 y, Möhner et al. (2010) found an increased odds-ratio of 1.78 (90% CI 1.09 to 2.91) only in the highest dose category for all leukemia types combined. The analogous results here (upper panel of Table 2), also presented with the first two dose categories combined due to the low number of cases in the second dose category (lower panel of Table 2), do not indicate an increased relative risk in the corresponding category, however (RR = 0.94; 90% CI 0.59 to 1.49). The difference of the estimators for long lag times may

be due to the longer follow-up time in the cohort study, which presumably also leads to a considerably longer mean time since exposure than in the CCS. With increasing mean time since exposure, the effect of a variation of the assumed lag-time on the risk estimators will diminish.

The linear trends in leukemia excess relative risk (ERR) per unit absorbed RBM dose were not significantly elevated statistically (ERR/Gy = 1.39, 90% CI −0.77 to 3.56, p = 0.28 and ERR/Gy = 0.80, 90% CI −1.38 to 2.98, p > 0.5 for lag-times of 2 and 15 y, respectively) in the present study and may be compared with the central estimate 2.06 (90% CI −0.86, 4.99) (lag time not specified) as reported by Möhner et al. (2010) with exposure including medical exposure. The two results are consistent given that their confidence intervals overlap strongly. They are also statistically compatible with values recently derived with techniques of multi-model inference for Japanese atomic bomb survivors (Walsh and Kaiser 2010, gender averaged ERR at 1 Sv = 2.8, 95% CI 1.4 to 3.8,

Table 2. Leukemia relative risk in the Wismut cohort of German uranium miners by absorbed dose to the red bone marrow due to occupational exposure, time lag: 15 y.

Dose (mGy)	All leukemias (128 deaths)			CLL[a] (40 deaths)			Non-CLL[b] (88 deaths)		
	Deaths	RR[c]	90% CI	Deaths	RR[c]	90% CI	Deaths	RR[c]	90% CI
<0.04	29	1	—	10	1	—	19	1	—
0.04–<3.4	12	0.88	0.49–1.57	4	0.81	0.30–2.16	8	0.93	0.45–1.93
3.4–<18.6	27	0.84	0.53–1.34	7	0.58	0.25–1.31	20	1.02	0.58–1.81
18.6–<74.9	31	0.71	0.45–1.12	12	0.64	0.32–1.31	19	0.76	0.42–1.36
≥74.9	29	0.94	0.59–1.49	7	0.53	0.23–1.21	22	1.23	0.69–2.20
<3.4	41	1	—	14	1	—	27	1	—
3.4–<18.6	27	0.88	0.58–1.34	7	0.62	0.29–1.32	20	1.05	0.63–1.74
18.6–<74.9	31	0.75	0.50–1.12	12	0.69	0.36–1.32	19	0.78	0.46–1.31
≥74.9	29	0.98	0.64–1.49	7	0.56	0.26–1.22	22	1.26	0.76–2.11

[a] Chronic lymphatic leukemia.
[b] All leukemia, except CLL.
[c] Relative risk from a Poisson regression with baseline stratification by age and calendar year.

for a 55-y-old exposed at age 30 y) and also with values from a meta-analysis of leukemia risk from protracted exposure to low-dose gamma radiation (Daniels and Schubauer-Berigan 2010), yielding an ERR at 100 mGy of 0.19, 95% CI 0.07 to 0.32.

The fraction of the different sub-types of leukemia differs somewhat between the two studies, as is to be expected given that the CCS analyzes incidence, while the cohort study is for mortality data. In the CCS, the percentage of CLL in the cases is 42.2%, while they contribute only 31.3% of the cases in the cohort study. A detailed comparison of the risk by sub-types of leukemia [chronic lymphatic leukemia (CLL) vs. others (non-CLL)] is hardly justified in the cohort study due to low statistical power. Nevertheless, it is noticeable that in the CCS, the reported estimators are generally higher for CLL than non-CLL, while in the cohort study the estimators for CLL are lower in all categories. A similar situation holds for the linear estimators: Möhner et al. (2010) found very similar values for the ERR/Gy of 1.95 and 2.14 for CLL and non-CLL, respectively, while in the cohort study the corresponding estimators are 0.33 (90% CI −2.83 to 3.50) and 2.08 (90% CI −0.84 to 4.99) assuming a lag time of 2 y.

Both the case-control and the cohort study are consistent in not finding a significant dose-response for the leukemia risk. In both studies, this may be due to restricted power and in the case of the cohort study also due to as yet uncollected information about the doses from medical exposures. It is planned to raise the medical exposure data for an embedded case-control study in the cohort, which will be based on an extended follow up-period ending with 2008.

FLORIAN DUFEY, LINDA WALSH, ANNEMARIE TSCHENSE, AND MICHAELA KREUZER

Federal Office for Radiation Protection
Department "Radiation Protection and Health"
Ingolstaedter Landstr. 1
85764 *Oberschleissheim, Germany*
fdufey@bfs.de

References

Daniels RD, Schubauer-Berigan MK. A meta-analysis of leukaemia risk from protracted exposure to low-dose gamma radiation. Occup Environ Med; 2010. Available online at http://dx.doi.org/10.1136/oem.2009.054684. Accessed on 16 March 2011.

Kreuzer M, Walsh L, Schnelzer M, Tschense A, Grosche B. Radon and risk of extrapulmonary cancers—results of the German uranium miners cohort study 1960-2003. Br J Cancer 99:1946–1953; 2008.

Kreuzer M, Schnelzer M, Tschense A, Walsh L, Grosche B. Cohort profile: The German uranium miners cohort study (WISMUT cohort), 1946-2003. Int J Epidemiol 39:980–987; 2010.

Lehmann F. Job-Exposure-Matrix Ionisierende Strahlung im Uranerzbergbau der ehemaligen DDR [Version 06/2003]. Erläuterungen zu einer lagerstätten-und schachtspezifischen Spezifizierung. Bergbau BG: Gera; 2004 [in German].

Lehmann F, Hambeck L, Linkert KH, Lutze H, Meyer H, Reiber H, Renner HK, Reinisch A, Seifert T, Wolf F. Belastung durch ionisierende Strahlung im Uranerzbergbau der ehemaligen DDR. Hauptverband der gewerblichen Berufsgenossenschaften: St. Augustin; 1998 [in German].

Marsh JW, Bessa Y, Birchall A, Blanchardon E, Hofmann W, Nosske D, Tomasek L. Dosimetric models used in the Alpha-Risk project to quantify exposure of uranium miners to radon gas and its progeny. Radiat Protect Dosim 130:101–106; 2008.

Möhner M, Gellissen J, Marsh JW, Gregoratto D. Occupational and diagnostic exposure to ionizing radiation and leukemia risk among German uranium miners. Health Phys 99:314–321; 2010.

Möhner M, Lindtner M, Otten H, Gille HG. Leukemia and exposure to ionizing radiation among German uranium miners. Am J Ind Med 49:238–248; 2006.

Preston DL, Lubin JH, Pierce DA. EPICURE: Risk regression and data analysis software. Seattle: Hirosoft International Corporation; 1990.

Walsh L, Dufey F, Tschense A, Schnelzer M, Grosche B, Kreuzer M. Radon and the risk of cancer mortality—internal Poisson models for the German uranium miners cohort. Health Phys 99:292–300; 2010a.

Walsh L, Tschense A, Schnelzer M, Dufey F, Grosche B, Kreuzer M. The influence of radon exposures on lung cancer mortality in German uranium miners, 1946–2003. Radiat Res 173:79–90; 2010b.

Walsh L, Kaiser J-C. Multi-model inference of adult and childhood leukaemia excess relative risks based on the Japanese A-bomb survivors mortality data (1950–2000). Radiat Env Biophys 50:21–35; 2010.

REPLY TO DUFEY AND COLLEAGUES

Dear Editors:

WE ARE grateful to Dufey and colleagues for their analysis of the relationship between occupational exposure to ionizing radiation and leukemia risk. In their comment, they describe some crucial differences between their cohort and our case-control study, which presumably lead to differences in important study characteristics such as mean cumulative exposure. In addition, the two studies use different endpoints; i.e., incidence and mortality.

In occupational studies we are trying to discover temporal relationships between certain exposure and disease onset, whereby disease onset is usually estimated

by the date of first diagnosis. The date of death is often used as a proxy, especially if incidence data are not available in the required quality and completeness. In this case, however, survival rates should also be considered. Given that a better prognosis for the disease under consideration results in a longer time span between diagnosis and death (i.e., the temporal reference points of the mortality and the incidence study diverge), the percentage of cases for which the disease is classified as the main cause of death decreases.

Remarkable progress in leukemia therapy was made over the study period, leading to an increase in the corresponding relative 5-y survival rate (5YSR) up to 55% in recent years (Stabenow et al. 2009). In addition, the various subtypes of leukemia differ in their 5YSR; while for chronic lymphatic leukemia (CLL) a 5YSR of 75% has already been achieved, for non-CLL it is only 45%. This explains the significantly higher percentage of CLL in the incidence study. It should also be noted that if the diagnosis was made during the subject's lifetime, the calculated absorbed dose to the red bone marrow continues to increase between time of diagnosis and death due to the previous exposure to long-lived radio-nuclides. In light of increasing survival rates, the temporal allocation of the exposure differs more and more between incidence and mortality studies.

The survival rate itself depends on a variety of factors such as the quality of health services. For the uranium miners, a comprehensive occupational health service staggered by exposure categories was already established in the 1950s. Consequently, it could be assumed that a disease such as leukemia would on average be detected earlier among miners than in the general population, which could possibly lead to a better prognosis for miners.

In summary, we believe that a possible relationship between radiation and leukemia could remain undetected in a study that is based on mortality data. Nevertheless, we welcome the embedded case-control study in the cohort planned by Dufey and colleagues and would like to encourage them to compare observed and expected cases of different leukemia subtypes under their cohort design. A detailed comparison of mortality cases with a match in the cancer registry in terms of registered leukemia subtype could also provide further insights into the validity of mortality diagnoses down to the fourth digit.

Matthias Möhner and Johannes Gellissen
Federal Institute for Occupational Safety and Health (BAuA)
Nöldnerstr. 40-42
D-10317 Berlin, Germany
Moehner.Matthias@baua.bund.de

Reference

Stabenow R, Streller B, Wilsdorf-Köhler H, Eisinger B. Cancer incidence and cancer mortality 2005–2006. Annual report of the Common Cancer Registry. Berlin: GKR; 2009 (in German).

■ ■

41. Walsh L. Radiation exposure and circulatory disease risk based on the Japanese A-bomb survivor mortality data (1950–2003) – neglect of the healthy survivor selection bias. Letter to the editor of BMJ, 2011 http://www.bmj.com/content/340/bmj.b5349.full/reply#bmj_el_260742

Research

Radiation exposure and circulatory disease risk: Hiroshima and Nagasaki atomic bomb survivor data, 1950-2003

Recent Rapid Responses

Rapid Responses are electronic letters to the editor. They enable our users to debate issues raised in articles published on bmj.com. Although a selection of rapid responses will be included as edited readers' letters in the weekly print issue of the BMJ, their first appearance online means that they are published articles. If you need the url (web address) of an individual response, perhaps for citation purposes, simply click on the response headline and copy the url from the browser window.

Radiation exposure and circulatory disease risk based on the Japanese A-bomb survivor mortality data (1950-2003) - neglect of the healthy survivor selection bias.

17 May 2011

A letter to the Editor of BMJ

Linda Walsh. Ph.D.

Federal Office for Radiation Protection, Department "Radiation Protection and Health", Ingolstaedter Landstr. 1, 85764 Oberschleissheim, Germany
E-mail: lwalsh@bfs.de

The recent paper by Shimizu et al (2010)(1) on radiation exposure and circulatory disease risk in the Hiroshima and Nagasaki atomic bomb survivor cohort for the follow-up 1950-2003, extended the work presented in the previous analysis by Preston et al (2003)(2) for the follow-up 1950 -1997. However the two papers place completely different emphasis and importance on the reported magnitude of the healthy survivor bias. This bias originates because survivors within 3km of the bomb hypocenters, called proximal survivors, were found to be initially healthier than the general population for reasons related to their selection from having survived the bombings (2,3). The Shimizu paper(1) is valuable to the field because it examined the effects of non-radiation factors such as smoking, alcohol intake, education, occupation, body mass index and diabetes on the association between cardiovascular disease and radiation risk. If such non -radiation factors are correlated with both radiation dose and circulatory disease mortality, they could indirectly be responsible for an apparent association between radiation risk and cardiovascular disease and are therefore called "potential confounding factors". The Results of Shimizu et al(1) suggest that "the associations of dose of radiation with mortality from stroke and heart disease is unlikely to be an artefact of confounding by major lifestyle, sociodemographic, or disease risk."

These potential confounding factors were unavailable for the earlier analysis by Preston et al(2)- where it was reported, for the non-cancer disease dose response, that "unless allowances are made, a substantial healthy survivor selection leads to spurious curvature in the dose response". The analysis of Preston et al(2) made allowances for the healthy survivor effect by restricting their analysis of cause specific non-cancer diseases risk estimates, such as stroke and heart disease, to proximal survivors for the follow-up between 1968 and 1997. Why did Shimizu and co-authors not also first perform a restricted analysis for the proximal survivors for the follow-up between 1968 and 2003, in order to account for the healthy survivor effect and for consistency with the previous analysis, and then additionally examine the non-radiation, lifestyle etc. potential confounding effects?

Even though Shimizu et al(1)report radiation risks per unit dose from models that are linear in radiation dose, they also report that the risk models that are purely quadratic in dose provided measures of goodness of fit (of the models to the data) that are only nominally better than the linear model for stroke and only nominally worse than the linear model for heart disease. In other words the preferred radiation risk models are either linear in dose or purely quadratic in dose and so the full follow-up data are consistent with relatively little radiation risk at lower doses, which according to the reasoning of Preston et al(2), is an artefact of the healthy survivor selection. This non-linearity is illustrated in the Shimizu paper figures 1 and 2 by the bold line of the linear quadratic model - which is not a preferred model by standard model selection techniques ($p=0.17$ and >0.5 for fit parameters multiplying the quadratic and linear radiation dose terms respectively for stroke and $p >0.5$ and $=0.11$ for fit parameters multiplying quadratic and linear radiation dose terms respectively for heart disease - according to the present authors calculations). Why was the purely quadratic in dose model not illustrated instead?

In the discussion section of Shimizu et al(1)they state that "some selection effects due to radiation dose related early mortality from the bombs may have occurred, although the impact of these is likely to be small" and they here reference Pierce et al (2007)(3) to justify this assertion. However Pierce et al(3) only indicates that it seems unlikely that the healthy survivor bias is large for cancer risk estimation. For non-cancer risk estimation Pierce et al(3) state that healthy survivor bias is considerably larger than it is for cancer risk estimation (increasing risks per unit dose by 47%). Since the grouped data for both follow-up periods are available at the Radiation Effects Research Foundation (RERF) web site, it should be easy enough for interested scientists to test these effects systematically for themselves. However since the data are grouped, with different grouping boundaries in both data-sets (e.g. there is no proximal/distal group and no boundary corresponding to 1968 in the grouped data that Shimizu used) - this is not possible. Shimizu et al(1) also state that the Poisson regression methods for the grouped data are "essentially identical" to the methods used by

Preston et al(2). However the functional forms for the baseline model parts (i.e. to account for the spontaneous disease rates that would have occurred in the absence of ionizing radiation) are different. Preston et al(2) adopted a fully parametric approach and Shimizu et al(1) dealt with baseline rates via stratification in categories of age-attained, age-at-exposure, city and gender. Different methods for the baselines can also lead to some differences in radiation risk estimates.

It would be helpful for interested scientists who may be external to the RERF and who then only have direct and quick access to the grouped data, if the grouping could be kept consistent from one follow-up to another. It would also be useful to be able to understand why completely different emphasis and importance on the reported magnitude of the healthy survivor bias is reported in the two papers mentioned above and why Pierce et al(3) appears to have been wrongly cited in Shimizu et al(1), to justify their apparent neglect of the healthy-survivor effect. Does the important suggestion from the results of Shimizu et al(1) (that associations of dose of radiation with mortality from stroke and heart disease are unlikely to be an artefact of confounding by major lifestyle, sociodemographic, or disease risk) still hold if the healthy survivor effect is also accounted for?

References

1. Shimizu Y, Kodama K, Nishi N, Kasagi F, Suyama A, Soda M, Grant EJ, Sugiyama, Sakata R,Moriwaki H, Hayashi M, Konda, M, Shore RE. Radiation exposure and circulatory disease risk: Hiroshima and Nagasaki atomic bomb survivor data, 1950-2003. BMJ 2010; 340: b5349.

2. Preston DL, Shimizu Y, Pierce DA, Suyama A, Mabuchi K (2003) Studies of the mortality of atomic bomb survivors. Report 13: solid cancer and noncancer disease mortality: 1950-1997. Radiat Res; 160: 381-407.

3. Pierce DA, Vaeth M and Shimizu Y Selection bias in cancer risk estimation from A-bomb survivours. Radiat Res 2007;167: 735-741.

Competing interests: None declared

Linda Walsh, Scientist
Federal Office for Radiation Protection, Germany

42. Walsh L, Dufey F, Tschense A, Schnelzer M, Sogl M & Kreuzer M. Prostate cancer mortality risk in relation to working underground in the Wismut cohort of German uranium miners (1970–2003). BMJ open, 2012;2:e001002. DOI: 10.1136/bmjopen-2012-001002, 2012

BMJ open
accessible medical research

Prostate cancer mortality risk in relation to working underground in the Wismut cohort study of German uranium miners, 1970–2003

Linda Walsh, Florian Dufey, Annemarie Tschense, Maria Schnelzer, Marion Sogl, Michaela Kreuzer

Department of "Radiation Protection and Health", Federal Office for Radiation Protection, Oberschleissheim, Germany

Correspondence to
Dr Linda Walsh;
lwalsh@bfs.de

ABSTRACT

Objective: A recent study and comprehensive literature review has indicated that mining could be protective against prostate cancer. This indication has been explored further here by analysing prostate cancer mortality in the German 'Wismut' uranium miner cohort, which has detailed information on the number of days worked underground.

Design: An historical cohort study of 58 987 male mine workers with retrospective follow-up before 1999 and prospective follow-up since 1999.

Setting and participants: Uranium mine workers employed during the period 1970–1990 in the regions of Saxony and Thuringia, Germany, contributing 1.42 million person-years of follow-up ending in 2003.

Outcome measure: Simple standardised mortality ratio (SMR) analyses were applied to assess differences between the national and cohort prostate cancer mortality rates and complemented by refined analyses done entirely within the cohort. The internal comparisons applied Poisson regression excess relative prostate cancer mortality risk model with background stratification by age and calendar year and a whole range of possible explanatory covariables that included days worked underground and years worked at high physical activity with γ radiation treated as a confounder.

Results: The analysis is based on miner data for 263 prostate cancer deaths. The overall SMR was 0.85 (95% CI 0.75 to 0.95). A linear excess relative risk model with the number of years worked at high physical activity and the number of days worked underground as explanatory covariables provided a statistically significant fit when compared with the background model (p=0.039). Results (with 95% CIs) for the excess relative risk per day worked underground indicated a statistically significant (p=0.0096) small protective effect of -5.59 (-9.81 to -1.36) $\times 10^{-5}$.

Conclusion: Evidence is provided from the German Wismut cohort in support of a protective effect from working underground on prostate cancer mortality risk.

ARTICLE SUMMARY

Article focus
■ Prostate cancer mortality in the Wismut cohort of German uranium miners in relation to time spent working underground and the time worked at high physical activity.

Key messages
■ Evidence is provided from the German Wismut cohort in support of a protective effect from working underground on prostate cancer mortality risk.

Strengths and limitations of this study
■ The Wismut study is currently the largest Uranium miner cohort.
■ There is detailed information on the time spent working underground and on other relevant occupational covariables.
■ However, there is no information on whether the shifts worked were early, late or at night.

INTRODUCTION

Prostate cancer is the second most common cancer diagnosed among men (after lung cancer) and is the sixth most common cause of cancer death among men worldwide.[1] In the European Union in 2006, prostate cancer was the most common form of incident cancer and the third most common form of cancer death in men (see table 3 of Ferlay et al[2]). Prostate cancer incidence in Germany has also become the most common form of incident cancer disease in men. It is notable that the prostate cancer mortality rates were approximately constant in the former eastern German Democratic Republic (GDR) between 1960 and 1980 but rose during the same time by 50% in West Germany.[3]

Prostate cancer is, in general, a slow-growing tumour with a long latency and an uncertain aetiology. The prevalence of latent microscopic prostate tumours has been

shown to be quite high in older people in most populations, that is, at least 50% in men over the age of 70.[4] Although there are only a few established risk factors for prostate cancer, such as age, race and a family history of prostate cancer,[5] there are also several mooted detrimental and protective associations.

The possible detrimental associations include early baldness,[6] shift work,[7] arsenic exposures,[8] diesel fume exposure[9] and oestrogen exposures.[10] Some evidence exists for radiation-related prostatic detrimental effects from studies on patients after diagnostic radiation procedures,[11] occupationally exposed British nuclear workers,[12] military and civil pilots and flight attendants,[13] and persons exposed by the Chernobyl accident.[14] There was little evidence of a prostate cancer risk radiation dose−response in the Japanese A-bomb survivors.[15] A recent meta-analysis of 24 cohort studies has concluded that an association of smoking with prostate cancer incidence and mortality exists.[16]

The possible protective associations include high sexual and/or androgenic levels,[17] ultraviolet and/or vitamin D,[18] high physical activity (PA)[19]—although some inconsistent results are observed for PA—and melatonin.[20−23] For a cohort of US male health professionals, Giovannucci et al[24] reported that for fatal prostate cancer, a recent smoking history, taller height, higher body mass index, family history and high intakes of total energy, calcium and α-linolenic acid were associated with a statistically significant increased risk, but higher vigorous PA level was associated with lower risk.

A recent Australian population-based case−control study and literature review[25] has indicated that mining could be protective against prostate cancer. Girschik et al[25] concluded that the relationship between mining and prostate cancer could possibly be connected to levels of either PA or changes in melatonin production caused by periods working underground and that these relationships deserve further investigation. Differential risk could not be reported in Girschik et al[25] because all but one of the studies reviewed did not report on working periods underground and overground. The main purpose of the present paper is to explore these indications further by analysing prostate cancer mortality risk in a cohort of male mine workers involved in uranium extraction at the former Wismut company in East Germany applying both external (national male rates for the former GDR) and internal backgrounds. New covariables for occupational PA and time spent underground have been specially created for this investigation. Simple standardised mortality ratio (SMR) analyses are complemented by refined analyses done entirely within the cohort.

The German 'Wismut' uranium mine workers' cohort has currently been followed up from 1 January 1946 to 31 December 2003, with almost 2 million person-years of observation and has already been described in detail.[26] It is currently the largest miners cohort study and several analyses of the detrimental health effects data pertaining

to the 58 987 male former employees have recently been published.[27−33]

There are several occupational risk factors for detrimental health effects, relevant to the cohort members, particularly with respect to lung cancer, including exposure to radon, γ radiation, long-lived radionuclides,[34] fine dust, arsenic dust and quartz dust,[35] asbestos[36] and diesel exposure. However, exposure covariables for the latter two quantities are not available in the cohort data. Previous analyses have shown that the mortality from prostate cancer in this cohort (1960−2006) is notably lower than in the comparison population of the former GDR (SMR=0.88, 95% CI 0.78 to 1.00[27]). The total absorbed dose to the prostate has not yet been calculated. However, since the absorbed dose to non-respiratory track organs is dominated by external γ radiation and the contributions of radon progeny, radon gas and particularly long-lived radionuclides are expected to be only a few per cent,[37] only the γ radiation is explicitly considered here, as a potential confounder. The effective γ doses have been converted into prostate organ dose via voxel model dose conversion factors.[38]

MATERIALS AND METHODS
Cohort definition, time periods and mortality follow-up
Full details of the cohort have already been given.[28 30] Every cohort member contributes to the number of person-years starting 180 days after the date of first employment and ending at the earliest of date of loss to follow-up, date of death or end of follow-up (31 December 2003). Due to the relatively high Percentage of Missing Causes of Death (PMCD) of 37.25% and the systematic variation of PMCD with calendar time from 1946 to 1969, the analyses here are based on the subset of Wismut miner cohort data covering the period 1970−2003 for which the PMCD is 3.56%. Consequently, no corrections for missing causes of death have been made. This difference in PMCD is due to the late start of data collection for this cohort on 1 January 1999, linked with the fact that death certificates were rarely kept by the authorities for more than 30 years.

National rates for the former GDR covering the same calendar year range are applied for the external comparisons. Former disease codes of the comparison external background rates for the GDR were re-coded via earlier ICD revisions to the 10th ICD code,[39] which was applied throughout. This recoding process was complicated by several revisions to ICD codes during the period of data coverage and German reunification. Population prostate cancer rates are not available just for the relevant mining region of Thuringia and Saxony. Consequently, the external rates applied here cover the total area of the former GDR (including East Berlin) during the time period 1970−1997; in contrast, from 1998, the rates pertain to the former GDR states and the whole of Berlin. The codes used here in the various time periods are as follows: 1970−1978 ICD 8, code number 185; 1979

ICD 8, code number 179−189 for the urogenital system; 1980−1997 ICD 9, code number 185; 1998−2003 ICD 10, code number C61, all for prostate cancer.

Analysis

The Poisson regression methods applied here require the tabulation of the individual data into grouped data records, as described below and in previous analyses.[30−32] This is because the input data for Poisson regression needs to consist of records containing the number of prostate cancer cases, the number of person-years and the mean values of the possible explanatory covariables. Poisson regression is a likelihood-based method for the quantitative analysis of such records or 'event-time tables',[40] whereby the rates to be modelled are computed as the ratios of prostate cancer cases to person-years for each record in the input data set. Descriptions of the background rates (ie, the spontaneous rates) were necessary to assess the excess risks, whereby such descriptions can either be based on models derived directly from the cohort data (internal comparisons) or from data on the GDR population rates (external comparisons).

Quantitative risk evaluation methods were based on the simple SMR model, where the SMR is the ratio of the observed number of prostate cancer deaths in the cohort to the number of prostate cancer deaths expected in the comparison population (see Breslow and Day, p65−68).[40] It is possible that an increased or decreased overall SMR could be a result of either an occupational or lifestyle exposure effect in the data. This can be tested directly by considering the simple SMR model with an exposure response to various possible explanatory covariables, for external and internal comparisons. In the case of the SMR model for external comparisons with an exposure response, a background SMR is computed (ie, the overall ratio of the observed background number of prostate cancer deaths in the cohort to the number of prostate cancer deaths expected in the comparison population) with an additional SMR that is linearly dependent on the covariable of interest.

The more refined analysis entirely within the cohort (internal comparisons) applied Poisson regression excess relative prostate cancer mortality risk model with background rate stratification by age and calendar year and a whole range of possible explanatory covariables: age (a), year (y), γ prostate dose (g), years at medium PA (mpa), years at high PA (hpa), days worked underground (u) and time since either first or last underground shift (t).

Data tabulations

Tabulations of person-years at risk and cancer deaths were created with the DATAB module of the EPICURE software[41] for the whole cohort data (1946−2003), so that the covariables of interest could be accumulated from the beginning of the cohort. The period of interest here was then selected to be 1970−2003 during the data analysis and model fitting procedures. Cross-classifications were made by attained age, a, in 16 categories (<15, 15 to <20, 20 to <25, …, 85+ years); individual calendar year, y, in 58 categories, and cumulative γ prostate doses, with a 5-year lag-time (eight categories: 0, >0 to <50, 50 to <100, 100 to <150, 150 to <200, 200 to <300, 300 to <400, 400+ mGy). For the current analysis, new covariables for occupational PA and time spent underground have been specially created. Exact shift information relating to daily underground and overground activities in each calendar year was used. The number of days worked underground in any one calendar year was then accumulated over calendar years of employment in eight categories (0, >0 to <1000, 1000 to <2000, 2000 to <3000, 3000 to <4000, 4000 to <5000, 5000 to <6000, 6000+ days). For the PA categories, information on the job type in each calendar year was extracted from the Wismut records. Each of the several hundred job types had already been classified into three levels of PA corresponding to different breathing rates for the purpose of organ dose calculations, for example, job types hewer, metal worker and lorry driver were classified as high, medium and low PA, respectively. The number of years worked in each of the high and medium PA classes were then accumulated over calendar years of employment, each in eight categories (0, >0 to <5, 5 to <10, 10 to <15, 15 to <20, 20 to <25, 25 to <30, 30+ years). Choice of units (years or days) reflects the quality of the information available in the mining records.

Standardised mortality ratios

Mortality rates observed in the cohort were compared with the GDR external rates. The first stage of the SMR analysis for prostate cancer has been done as described previously for extra-pulmonary cancers[28] with some extensions that allow a comparison of internal (miner cohort) and external (former GDR) background (spontaneous) rates. Justifications for the generally preferable internal comparison (done entirely within the cohort), connected with differences in the maturity of the smoking epidemic between the cohort and the GDR, have recently been given.[32] The simplest SMR model relates the rates in the population of interest (the miner cohort) to a multiple of the rates from the external population (the former GDR).

If $\lambda^*(a, y)$ denotes the external rates as a function of age and calendar year and $\lambda(a, y)$ denotes the observed rates in the miners cohort, then the SMR model can be written as

$$\lambda(a, y) = \beta \cdot \lambda^*(\alpha, y), \qquad (1)$$

where the β is a fit parameter and represents the SMR.

However, it is also possible to fit a RR model

$$RR(a, y, g) = \beta_1 \cdot \lambda^*(a, y) \cdot (1 + \beta_2(g)) \qquad (2)$$

to estimate the effects of various possible explanatory covariables, such as γ prostate dose (g), based on the

GDR external rates, assuming that the SMR for the background rates is identically equal to 1, that is, β_1 is fixed to unity during the optimisation. In this case, β_2 is a fit parameter that then gives the simple excess relative risk (ERR) per unit of exposure relative to the external GDR rates. It is also possible to test if the external GDR rates are different from the internal background rates in the miner cohort by simply freeing the parameter β_1 and repeating the optimisation. All of the parameters β, β_1 and β_2 can be multiplied by a two level categorical variable for either levels of PA or time spent underground.

Refined ERR models with background stratification by age and calendar year were employed—if $r(a, y, g, mpa, hpa, u, t)$ is the prostate cancer mortality rate and $r_0 (a, y)$ = r $(a,y,0,0,0,0,0)$ is the background disease rate for non-exposed individuals, $g =0$, $mpa =0$ … etc then

$$R(a, y, g, mpa, hpa, u, t) = \\ r_0(a,y) \cdot \{1 + ERR(g, mpa, hpa, u, a, t)\}, \quad (3)$$

where ERR is the excess relative risk factorised into a function of exposure, f(g, mpa, hpa, u) and a modifying function, h(a, t):

$$ERR(g, mpa, hpa, u, a, t) = \text{f}(g, mpa, hpa, u) \cdot \text{h}(a, t) \quad (4)$$

The γ prostate dose, years at medium PA, years at high PA and days worked underground were each included:

$$\text{singularly, f}(g) = \alpha \cdot g, \text{etc, and pairwise f}(g, mpa) \\ = \alpha_1 g + \alpha_2 mpa, \text{etc} \quad (5)$$

in the linear ERR model, both with and without the modifying function and assessed with model selection techniques to arrive at the model with the lowest deviance with respect to the background model, by forward selection. Backwards selection was also tested. Finally, the preferred linear model was tested for non-linearity, by adding quadratic terms for exposure covariables, and time or age effect modification (ie, adding h(a, t) functions to the model).

Maximum likelihood with the AMFIT module of the EPICURE software[41] was used for estimation of the SMR and ERR fit parameters associated with equations 1–5 above. CIs were computed at the 95% level and the Wald type CIs are given since, although very similar intervals were found with the profile likelihood-based CIs, some of the lower limits could not be numerically calculated with the latter method.

RESULTS
Of the total 58 987 cohort members in the complete follow-up period between 1946 and 2003, 55 435 members were included in the follow-up from 1970, specifically considered in the risk analysis presented here. In total, 20 920 persons were deceased (of which

1560 died before 1970), 35 294 were alive and 2773 were lost to follow-up (of which 1992 were lost before 1970). There were 263 prostate cancer deaths observed during 1.42 million person-years of observation between 1970 and 2003. The cumulative numbers of observed and expected prostate cancer deaths in this period are shown in figure 1A,B as a function of calendar year from 1970 and age attained from 40 years. The absolute number of prostate cancers occurring reaches a maximum in the category 75–80 years of age, due to the age distribution in the cohort, and increases steadily from 1970–2003 and the cumulative number of prostate cancers increases as a function of age attained and calendar year.

The mean values (and ranges) of age attained, mean number of days worked underground and mean number of years worked at high PA are 47 (14–103) years, 1649 (0–10 704) days and 3.5 (0–44) years, respectively. Table 1 gives the category-specific values for the number of prostate cancer deaths and person-years, for the number of years worked at high PA and days spent underground categories of mine workers.

SMR results (comparison of cohort rates with external rates)
The total number of deaths from prostate cancer (1970–2003) observed (O) was significantly lower (p<0.001) than expected (E) from national rates (equation 1). The SMR value with 95% CIs is 0.85 (0.75
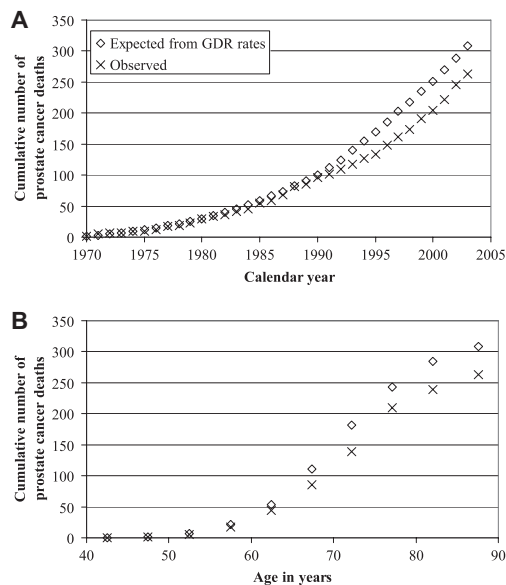

Figure 1 (A) The cumulative number of prostate cancer deaths observed in the Wismut cohort and expected from former German Democratic Republic (GDR) rates as a function of calendar year. (B) The cumulative number of prostate cancer deaths observed in the Wismut cohort and expected from GDR rates as a function of age attained.

Table 1 Category means and ranges for the number of days worked underground and the number of years worked at high physical activity (PA)

Category means (and ranges)	Number of prostate cancer deaths	Number of person-years	Mean γ prostate dose (mGy, with SD)
Mean number of days worked underground			
0	67	360 536	1.1 (4.4)
408 (2−999.9)	46	429 624	7.5 (9.9)
1466 (1000−1999.8)	30	184 782	24.5 (26.7)
2475 (2000−2999.8)	34	139 204	42.0 (44.2)
3465 (3000−3999.9)	24	97 808	68.3 (65.5)
4908 (4000−5999.9)	37	138 138	111.4 (93.9)
7236 (6000−10 704)	25	74 836	156.9 (127.4)
Mean number of years worked at high PA			
0	122	726 358	9.8 (28.1)
2.2 (1−4)	52	342 896	19.2 (33.1)
6.7 (5−9)	37	165 377	47.0 (46.9)
11.8 (10−14)	22	87 297	94.5 (73.5)
16.8 (15−19)	16	54 598	148.3 (94.2)
23.3 (20−29)	11	40 425	199.4 (123.1)
33.3 (30−42)	3	7978	238.3 (163.0)

In each category the number of deaths from prostate cancer mortality, the number of person-years at risk (rounded) and the mean cumulative person-year weighted γ prostate dose (with SD) are given.

to 0.95). Quantitative differences between GDR external rates and internal cohort rates can be assessed directly from a categorical SMR analysis in categories of attained age and calendar year. Some statistically significantly low categorical SMR values were found mainly in the age group 65−75 and in the calendar period from 1991 to 1995 (results not shown). The overall SMR with 95% CIs when recomputed by two categories of below and above mean time spent underground (1649 days) becomes 0.92 (0.76 to 1.07) and 0.79 (0.65 to 0.92), respectively. The SMR recomputed by two categories of below and above mean time worked at high PA (3.52 years) becomes 0.82 (0.69 to 0.94) and 0.91 (0.73 to 1.10), respectively.

Simple ERR parametric cohort risk models (comparison of cohort rates with external rates)

Cumulative exposure effects for various covariables in terms of ERR per unit exposure and 95% CIs are given in the first results column of table 2 (equation 2). The ERR per day worked underground, relative to the external GDR rates, is -4.44 (-7.11 to -1.76) $\times 10^{-5}$ and was found to be the statistically strongest exposure effect (p=0.001), that is, decreased for the number of days worked underground relative to the external rates. A similar value of -3.3 (-7.2 to 0.06) $\times 10^{-5}$ relative to the internal controls was found (table 2, third results column), although of reduced statistical significance (p=0.097). This latter result is connected with a background SMR of 0.93 (0.78 to 1.08) (table 2, second results column). The SMR model did not converge (NC) for the γ prostate dose relative to the external background rates. A statistically significant (p=0.03) decreased ERR/Gy for prostate γ doses, relative to the

internal background of -1.27 (-2.4 to -0.14), was also found (table 2, third results column).

Refined ERR parametric cohort risk models

The statistical significance of ERR/Gy for prostate γ doses reported with the simple analysis was not confirmed by the refined analysis (ERR/Gy=-1.18 (-2.4 to 0.02), see table 2, fourth results column) (equations 3−5). Although the coefficient for γ dose was of borderline statistical significance in the univariate model, the forward selection did not keep the γ prostate dose in the multivariate model. A preferred model by forward selection of the covariables γ prostate dose, g; years at medium PA, mpa; years at high PA, hpa, and days worked underground, u, taken linearly one or two at a time was found to be the model that included both hpa and u (table 3). This model had a reduction in deviance with respect to the stratified background model of 6.5 (p=0.04) by the likelihood ratio test. This model provided the results in the last column of table 2 (with 95% CIs) for the ERR per day worked underground, which indicates a statistically significant (p=0.01) small decreased effect of -5.59 (-9.81 to -1.36) $\times 10^{-5}$, and for the ERR per year worked at high PA, which indicates a statistically significant (p=0.04) small detrimental effect of 0.021 (0.001 to 0.040). The clinical significance of the results can be assessed by obtaining the number of deaths from prostate cancer prevented in this cohort from working underground, obtained from the fitted background and fitted excess number of cases in the preferred model. Depending on whether the slightly increased risk from high PA is accounted for or not, this number is either 14 or 22 prostate cancer deaths, respectively.

Table 2 Results of fitting the models

Covariable name (unit)	β_2, ERR/unit exposure relative to external background (ie, with β_1 fixed at unity)	β_1, free, internal-to-external background ratio	β_2, ERR/unit exposure relative to internal background (ie, with β_1 free)	α, ERR/unit exposure	α_1 and α_2, ERR/unit exposure
Gamma (Gy)	NC	0.90 (0.78 to 1.02) (p<0.001)	−1.27 (−2.4 to −0.14) (p=0.03)	−1.18 (−2.4 to 0.02) (p=0.055)	α_1=0.021 (0.001 to 0.040) (p=0.04); α_2=−5.59 (−9.81 to −1.36) (p=0.01)
Medium PA (years)	−0.010 (−0.019 to −0.001) (p=0.04)	0.87 (0.74 to 0.99) (p<0.001)	−0.003 (−0.17 to 0.01) (p>0.5)	−0.003 (−0.016 to 0.011) (p>0.5)	
High PA (years)	−0.003 (−0.016 to 0.010) (p>0.5)	0.81 (0.69 to 0.93) (p<0.001)	0.01 (−0.01 to 0.03) (p=0.26)	0.013 (−0.008 to 0.033) (p=0.24)	
Underground work (10^5 days)	−4.44 (−7.11 to −1.76) (p=0.001)	0.93 (0.78 to 1.08) (p<0.001)	−3.30 (−7.20 to 0.06) (p=0.097)	−3.07 (−7.12 to 0.99) (p=0.14)	

The first three numerical columns are for the standardized mortality ratios (SMR) (from equation 2). The interpretation of β_1 is that it represents the overall ratio of the observed background number of prostate cancers deaths in the cohort to the number of prostate cancer deaths expected in the comparison German Democratic Republic population, and β_2 is the additional incremental SMR that is linearly dependent on the covariable listed in the first column of the table, that is, an excess relative risk (ERR) per unit exposure of the covariable of interest. The fourth and fifth numerical columns are for the ERR internal regression models with background rates stratification on age and calendar year (from equations 3−5) for the univariate option in equation 5 (parameter α) and the multivariate option in equation 5 (parameters α_1 and α_2) models, respectively. Values given in parentheses represent 95% Wald type CIs, and the p values represent the statistical significance of the parameter values (and not the statistical significance of model improvement by their inclusion in the model). Models that did not converge are identified with NC. PA, physical activity.

Models that included just *hpa* or just *u* did not result in statistically significant risks (table 2, fourth results column) or lead to statistically significant model improvement (table 3). No evidence for an interaction between *hpa* and *u* was indicated by including a cross term in the preferred model (p>0.5). Testing of the quadratic or parabolic forms for *hpa* and *u* or testing risk effect modification by attained age (table 3) or time since first or last underground shift (results not shown) did not lead to statistically significant model improvement. The dose−response forms for the preferred model and the adjusted non-parametric risks with 95% CIs are shown in figure 2. It was not possible to confirm this result by backwards selection since the models with all six main covariables failed to converge.

DISCUSSION

The Wismut cohort is one of the largest single occupational cohorts and one of only a few cohorts with detailed information on the number of shifts worked underground. Although the number of shifts was documented, it is not known if these were early morning, daytime or night shifts. A substantial proportion (25%) of person-years are contributed by mine workers who did not work underground, which generally ensures the stability of analyses based on internal rates. The ERR per unit of various exposures have been modelled relative to the internal rates and relative to the external rates for the general population of the former GDR.

A statistically significant (p=0.001) negative response for the ERR per day worked underground, when modelled in relation to the general population of the former GDR, is reported here. There are some indications of unit exposure responses of the ERR which are decreased for γ prostate dose (p=0.03 and 0.055 for the simple and refined models, respectively) with respect to the internal rates. Rather than being decreased, the γ dose is a possible proxy variables for the number of days worked underground since there are moderate degrees of correlations between these covariables (ρ=0.68 for the correlation between time-dependent cumulative γ prostate doses and the number of days worked underground, see also table 1). Indication that the γ dose may be acting as a proxy was tested here directly by the creation of new categories of mine workers, with numbers of years worked at high or medium PA and the number of days worked underground and the application of model selection techniques.

The assumption is made in this paper that radon and long-lived radionuclides make only minor contributions to the total prostate dose. Previous analyses have shown that the ERR per 100 WLM of radon exposure, based on internal Poisson models, was not elevated for prostate cancer (ERR/100 WLM =0.000, 95% CI, −0.024 to 0.024).[31] None of the radiation covariables (ie, γ prostate dose but also including long-lived radionuclides and radon), when tested by inclusion singularly as linear risks in refined internal Poisson regression models, resulted in a deviance drop of more than three with respect to the

Table 3 Results of applying model selection techniques with the likelihood ratio test for variable selection

Covariables in model, form			Δ df	Δ Deviance	p Value
u, linear	**hpa, linear**		**2**	**6.47**	**0.039**
u, linear	*mpa*, linear	*hpa*, linear	3	7.25	0.064
u, linear	*hpa*, linear	*a*, exponential	3	7.23	0.065
u, linear	*hpa*, linear	*a*, power	3	7.15	0.067
u, linear	*hpa*, linear	*hpa*, squared	3	7.06	0.070
u, linear	*u*, squared	*hpa*, linear	3	6.75	0.080
u, squared	*hpa*, linear		2	5.04	0.080
	ERR/unit exposure (SE)				
g, linear	$-1.2\ (0.6) \times 10^{-3}$		1	2.61	0.107
u, linear	$-3.1\ (2.1) \times 10^{-5}$		1	1.88	0.171
hpa, linear	$1.3\ (1.1) \times 10^{-2}$		1	1.61	0.204
mpa, linear	$-2.8\ (7.0) \times 10^{-3}$		1	0.15	0.697

The changes in degrees of freedom (df) and deviance are all with respect to the stratified background model, which had a deviance of 3178.9 for a df of 555 433. *g*, *mpa*, *hpa*, *u* and *a* represent γ prostate dose, years at medium physical activity (PA), years at high PA, days worked underground and age attained, respectively. The top section represents a subset of seven models (preferred model in bold) from a complete sorted list of all models tested, for which the probability of model improvement with respect to the stratified background model had a p value under 0.10. The lower section represents the model selection results for all four models with single exposure covariables—none of which resulted in a statistically significant model improvement when compared with the background model.
ERR, excess relative risk.

background model which was stratified on age attained and calendar year.

A linear ERR model with the number of years worked at high PA and the number of days worked underground as explanatory covariables provided a statistically significant fit when compared with the background model (p=0.039). Results (with 95% CI) for the ERR per day worked underground indicated a statistically significant (p=0.01) small decreased effect at -5.59 (-9.81 to -1.36) $\times 10^{-5}$ and for the ERR per year worked at high PA, a statistically significant (p=0.04) small detrimental effect at 0.021 (0.001 to 0.040). This main result provides new evidence in support of the decreased effect of working underground which is manifested with respect to the internal and the external rates.

The number of days worked underground is connected with a particular hypothesis for reduced prostate cancer rates, for example, melatonin production rates (as described in detail in Girschik *et al*[25] and references therein). In summary, melatonin has been shown to have anti-cancer properties acting through several mechanisms.[20–23] The production of melatonin in the pineal gland is regulated by the natural diurnal light-level cycle, with suppressed production during the day, which is restored at night. Underground miners on day shifts would have a reduced exposure to visible light leading to an extended melatonin production period.

The relation between PA and prostate cancer risk was classified as 'probable' with respect to decreased risk, by the IARC in 2002,[42] but no definite mechanisms have been identified for a relation between PA and prostate cancer. Several plausible mechanisms have been postulated which include modulation of testosterone and vitamin D levels by PA, a link between physical inactivity and overweight/obesity and a beneficial modulation of immune function through exercise (see Lee *et al*[43] for a review). A recent systematic review and meta-analysis[44]

considered 13 studies with occupational PA, considered to be 'higher quality' studies and reported that nine studies gave a decreased risk, one study an increased risk and three studies reported no association. Two other studies have reported increased risks: Hosseini *et al*[45] found that intensity of occupational PA was associated with increased prostate cancer risk and Zeegers *et al*[46] reported an increased risk for obese men (body mass index over 30) who were physically active for more than 1 h/day and in men with high background energy intake.

A statistically significant increase in risk with increasing high PA is observed here, in contrast to the IARC classification and the majority of other studies. It is important to note that the variable PA here measures only part of the total PA and could be prone to misclassification. The PA variable is limited to the work period at the Wismut company (the mean duration of work at the company, 14 years) and no leisure time activities could be considered. The classification is simply based on job type without consideration of possible changes in PA in a specific job over time, for example, due to improved technical 'labour-saving' equipment. PA could also be an indicator of socioeconomic status because the jobs with low PA are more likely to be associated with higher education.

Another possible source of bias in the results based on external comparisons that should be considered is the selection bias known as the healthy worker effect. However, this effect, which can generally lead to occupational cohorts presenting mortality risks less than the general population, is not indicated since the risks are similar with respect to internal and external backgrounds. The occurrence of this form of bias could also be tested here by considering all solid cancer minus the sites that have already been linked to the main mine radiation exposure, that is, radon (lung, larynx, tongue,
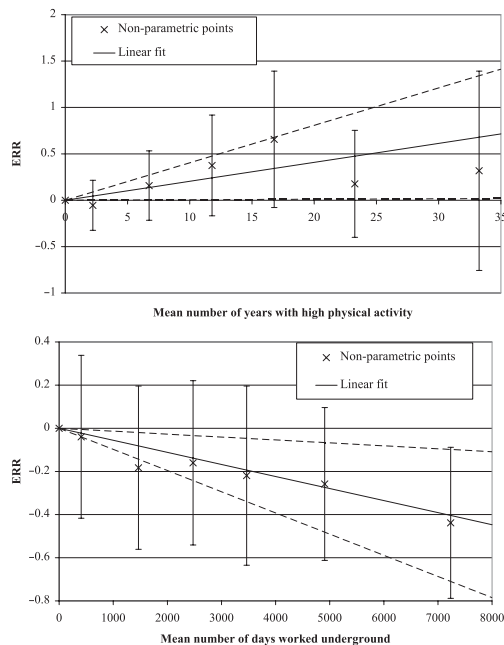
Figure 2 The upper panel shows the excess relative risk (ERR) and 95% CI as a function of mean number of years with high physical activity (PA) and corresponds to the risk given in the last column of table 2. The non-parametric points with 95% CI are adjusted for mean number of days worked underground. The lower panel shows the ERR and 95% CI as a function of mean number of days worked underground and corresponds to the risk given in the last column of table 2. The non-parametric points with 95% CI are adjusted for mean number of years with high PA.

mouth and pharynx). For this group of cancers, the SMR with 95% CI is 1.01 (0.97 to 1.04) also indicating that the healthy worker effect is not having a significant influence on the prostate cancer results in this cohort.

A further source of bias, possibly affecting the decrease in risk with increasing duration of working underground based on internal comparisons, could be the healthy worker survivor effect. Unhealthy workers may move from working underground to working at the surface. Consequently, the duration of working underground may be higher in the healthy group compared with the unhealthy group, leading to artificially decreased effects in relation to duration of working underground. However, this effect has been tested for by fitting the preferred model, which included both the number of days worked underground and number of years worked at high PA, to the subgroup of all solid cancers minus the sites that have already been linked to the main mine radiation exposure (lung, larynx, tongue, mouth and pharynx) and minus prostate. No significant trends were

found (p>0.5 for the linear trend of ERR with respect to the number of days worked underground and p=0.11 for the linear trend of ERR with number of years worked at high PA) indicating that the healthy worker survivor effect is not directly biasing the results for prostate cancer.

Although there is no general consensus as to whether radiation exposure is associated with prostate cancer risk,[47] an x-ray procedure risk doubling dose of about 20 mGy for prostate cancer incidence has been reported.[11] The magnitudes and ranges of the γ prostate doses in the Wismut study (with the prostate cancer mortality cases having a range up to 444 mGy and the cohort person-year weighted mean γ prostate dose of 34 mGy) should be large enough to find such an increased risk at the 20 mSv level, given the similar relative biological effect of x-rays and γ rays. However, a γ risk, at this 20 mSv level, has not been found in the Wismut cohort data for prostate cancer mortality.

Yang et al[8] reported that SMRs for prostate cancer declined gradually in an SW coastal district of Taiwan after the arsenic-contaminated artesian well drinking water supply was improved to a tap-water system. Since arsenic dust exposures are also available for the Wismut miners,[35] an arsenic covariable could be added to the preferred model for PA and time worked underground described above in a subsidiary analysis, but this only resulted in a deviance drop of 1.2 and a p value of 0.33 for the associated arsenic risk coefficient and did not confound the main risks from the preferred model.

An examination of the effects of smoking on the risk of prostate cancer mortality, as indicated in Huncharek et al,[16] could not be carried out for the Wismut cohort due to only a very limited amount of information on smoking being available.[29]

Although there were 264 prostate cancer deaths in the whole cohort, only one occurred before 1970, that is, during the period with a higher percentage of missing causes of death. This is consistent with prostate cancer generally being a type of cancer that occurs predominantly in old age coupled with the observation that—due to miners entering and leaving the cohort at various points in time during the follow-up period—the cohort aged, on average, at half the rate of any individual, that is, in 1960 and 2003, the mean ages of cohort members were 35 and 57 years, respectively. Consequently, it is very important to continue work on extending the current follow-up period.

CONCLUSIONS

This work has extended the evidence in support of a decreased, possibly protective, effect for prostate cancer mortality from working underground provided in[25] and could be interpreted as support for 'The Melatonin Hypothesis'. A linear internal excess RR model with the number of years worked at high PA and the number of days worked underground as explanatory covariables provided a statistically significant fit when compared with the background model (p=0.039).

Results (with 95% CI) for the ERR per day worked underground indicated a statistically significant (p=0.0096) small decreased, possibly protective, effect at -5.59 (-9.81 to -1.36) $\times 10^{-5}$. It is this main result that provides the new evidence in support of the protective effect of working underground which is also manifested with respect to the external rates. Additional computations made to examine the influence of biases due to the γ doses, the healthy worker selection effect and the healthy worker survivor effect indicate that the results are unbiased in these respects, but the effects of such biases cannot be entirely excluded.

REFERENCES

1. Baade PD, Youlden DR, Krnjacki LJ. International epidemiology of prostate cancer: Geographical distribution and secular trends. *Mol Nutr Food Res* 2009;53:171–84.
2. Ferlay J, Autier P, Boniol M, *et al.* Estimates of the cancer incidence and mortality in Europe in 2006. *Ann Oncol* 2007;18:581–92.
3. Becker N, Wahrendorf J. *Krebsatlas der Bundesrepublik Deutschland 1981–1990*, Vol. 3. Berlin: Springer, 1998.
4. Breslow N, Chan CW, Dhom G, *et al.* Latent carcinoma of prostate at autopsy in seven areas. *Int J Cancer* 1977;20:680–8.
5. Hsing AW, Devesa SS. Trends and patterns of prostate cancer: what do they suggest? *Epidemiol rev* 2001;23:3–13.
6. Yassa M, Saliou M, De Rycke Y, *et al.* Male pattern baldness and the risk of prostate cancer. *Ann Oncol* 2011;22:1824–7.
7. Foster RG, Wulff K. The rhythm of rest and excess. *Nat Rev Neurosci* 2005;6:407–14.
8. Yang CY, Chang CC, Chiu HF. Does arsenic exposure increase the risk for prostate cancer? *J Toxicol Environ Health A* 2008;71:1559–63.
9. Seidler A, Heiskel H, Bickeboller R, *et al.* Association between diesel exposure at work and prostate cancer. *Scand J Work Environ Health* 1998;24:486–94.
10. Margel D, Fleshner NE. Oral contraceptive use is associated with prostate cancer: an ecological study. *BMJ Open* 2011;1:e000311.
11. Myles P, Evans S, Lophatananon A, *et al.* Diagnostic radiation procedures and risk of prostate cancer. *Br J Cancer* 2008;98:1852–6.
12. Carpenter LM, Higgins CD, Douglas AJ, *et al.* Cancer mortality in relation to monitoring for radionuclide exposure in three UK nuclear industry workfaces. *Br J Cancer* 1998;78:1224–32.
13. Buja A, Lange JH, Perissinotto E, *et al.* Cancer incidence among military and civil pilots and flight attendants: an analysis on published data. *Toxicol Ind Health* 2005;21:273–82.
14. Vosianov AF, Romanenko AM, Zabarko LB, *et al.* Prostatic intraepithelial neoplasia and apoptosis in benign prostatic hyperplasia before and after Chernobyl accident in Ukraine. *Pathol Oncol Res* 1999;5:28–31.
15. Preston DL, Ron E, Tokuoka S, *et al.* Solid cancer incidence in atomic bomb survivors: 1958–1998. *Radiat Res* 2007;168:1–64.
16. Huncharek M, Haddock KS, Reid R, *et al.* Smoking as a risk factor for prostate cancer: a meta-analysis of 24 prospective cohort studies. *Am J Public Health* 2010;100:693–701.
17. Leitzmann MF, Platz EA, Stampfer MJ, *et al.* Ejaculation frequency and subsequent risk of prostate cancer. *JAMA* 2004;291:1578–86.
18. Hanchette CL, Schwartz GG. Evidence for a protective effect of ultraviolet radiation. *Cancer* 1992;70:2861–9.
19. Albanes D, Blair A, Taylor PR. Physical activity and risk of cancer in the NHANES I population. *Am J Public Health* 1989;79:744–50.
20. Schernhammer ES, Schulmeister K. Melatonin and cancer risk: does light at night compromise physiologic cancer protection by lowering serum melatonin levels? *Br J Cancer* 2004;90:941–3.
21. Feychting M, Osterlund B, Ahlbom A. Reduced cancer incidence among the blind. *Epidemiology* 1998;9:490–4.
22. Rimler A, Culig Z, Levy-Rimler G, *et al.* Melatonin elicits nuclear exclusion of the human androgen receptor and attenuates its activity. *Prostate* 2001;49:145–54.
23. Sainz RM, Mayo JC, Tan DX, *et al.* Melatonin reduces prostate cancer cell growth leading to neuroendocrine differentiation via a receptor and PKA independent mechanism. *Prostate* 2005;63:29–43.
24. Giovannucci E, Liu Y, Platz EA, *et al.* Risk factors for prostate cancer incidence and progression in the health professionals follow-up study. *Int J Cancer* 2007;121:1571–8.
25. Girschik J, Glass D, Ambrosini GL, *et al.* Could mining be protective against prostate cancer? A study and literature review. *Occup Environ Med* 2010;67:365–74.
26. Kreuzer M, Schnelzer M, Tschense A, *et al.* Cohort Profile: the German uranium miner cohort study (WISMUT cohort), 1946–2003. *Int J Epidemiol* 2010;39:980–7.
27. Kreuzer M, Walsh L, Schnelzer M, *et al.* Radon and risk of extra-pulmonary cancers - results of the German uranium miners cohort study, 1960–2003. *Br J Cancer* 2008;99:1946–53.
28. Kreuzer M, Grosche B, Schnelzer M, *et al.* Radon and risk of death from cancer and cardiovascular diseases in the German uranium miners cohort study: follow-up 1946–2003. *Radiat Environ Biophys* 2010;49:177–85.
29. Schnelzer M, Hammer GP, Kreuzer M, *et al.* Accounting for smoking in the radon-related lung cancer risk among German uranium miners: results of a nested case-control study. *Health Phys* 2010;98:20–8.
30. Walsh L, Tschense A, Schnelzer M, *et al.* The influence of radon exposure on lung cancer mortality in German uranium miners, 1946–2003. *Radiat Res* 2010;173:79–90.
31. Walsh L, Dufey F, Tschense A, *et al.* Radon and the risk of cancer mortality—Internal Poisson models for the German uranium miners cohort. *Health Phys* 2010;99:292–300.
32. Walsh L, Dufey F, Möhner M, *et al.* Differences in baseline lung cancer mortality between the German uranium miners cohort and the population of the former German Democratic Republic (1960-2003). *Radiat Env Biophys* 2011;50:57–66.
33. Dufey F, Walsh L, Tschense A, *et al.* Occupational doses of ionizing radiation and leukemia mortality. *Health Phys* 2011;100:548–50.
34. Lehmann F, Hambeck L, Linkert KH, *et al. Belastung durch ionisierende Strahlung im Uranerzbergbau der ehemaligen DDR.* St. Augustin: Hauptverband der gewerblichen Berufsgenossenschaften, 1998.
35. Dahmann D, Bauer HD, Stoyke G. Retrospective exposure assessment for respirable and inhalable dust, crystalline silica and arsenic in the former German uranium mines of SAG/SDAG Wismut. *Int Arch Occup Environ Health* 2008;81:949–58.
36. Brüske-Hohlfeld I, Rosario AS, Wölke G, *et al.* Lung cancer risk among former uranium miners from the Wismut company in Germany. *Health Phys* 2006;90:208–16.
37. Marsh JW, Harrison JD, Laurier D, *et al.* Dose conversion factors for radon: recent Developments. *Health Phys* 2010;99:511–16.
38. Petoussi-Henss N, Schlattl H, Zankl M, *et al.* Organ doses from environmental exposures calculated using voxel phantoms of adults and children. Submitted to *Phys Med Biol* 2012.

39. World Health Organisation. *International Statistical Classification of Diseases and Health Related Problems: The ICD-10 (German edition 1.3.1999)*. Geneva: WHO, 1992.

40. Breslow NE, Day NE. *Statistical Methods in Cancer Research, Vol. II. The Design and Analysis of Cohort Studies. IARC Scientific Publications No. 83*. Lyon: International Agency for Research on Cancer, 1988.

41. Preston DL, Lubin JH, Pierce DA, *et al. Epicure User's Guide*. Seattle, Washington: Hirosoft, 1993.

42. IARC. *Weight Control and Physical Activity*. Lyon, France: 6 IARC Press, 2002.

43. Lee IM, Sesso HD, Chen JJ, *et al.* Does physical activity play a role in the prevention of prostate cancer? *Epidemiol Rev* 2001;23:132−7.

44. Liu YP, Hu FL, Li DD, *et al.* Does physical activity reduce the risk of prostate cancer? A systematic review and meta-analysis. *European Urology* 2011;60:1029−44.

45. Hosseini M, Alinaghi SA, Mahmoudi M. A case-control study of risk factors for prostate cancer in Iran. *Acta Med Iran* 2010;48:61−6.

46. Zeegers MP, Dirx MJ, van den Brandt PA. Physical activity and the risk of prostate cancer in the Netherlands cohort study, results after 9.3 years of follow-up. *Cancer Epidemiol Biomarkers Prev* 2005;14:1490−5.

47. Health Protection Agency. *Risk of Solid Cancers Following Radiation Exposure: Documents of the HPA*. London: Health Protection Agency, 2011.

43. Schöllnberger H, Kaiser JC, Jacob P & Walsh L. Dose-responses from multi-model inference for the non-cancer disease mortality of atomic bomb survivors. Radiat. Environ. Biophys. 51, 165-178, 2012

ORIGINAL PAPER

Dose–responses from multi-model inference for the non-cancer disease mortality of atomic bomb survivors

H. Schöllnberger · J. C. Kaiser · P. Jacob · L. Walsh

Abstract The non-cancer mortality data for cerebrovascular disease (CVD) and cardiovascular diseases from Report 13 on the atomic bomb survivors published by the Radiation Effects Research Foundation were analysed to investigate the dose–response for the influence of radiation on these detrimental health effects. Various parametric and categorical models (such as linear-no-threshold (LNT) and a number of threshold and step models) were analysed with a statistical selection protocol that rated the model description of the data. Instead of applying the usual approach of identifying one preferred model for each data set, a set of plausible models was applied, and a sub-set of non-nested models was identified that all fitted the data about equally well. Subsequently, this sub-set of non-nested models was used to perform multi-model inference (MMI), an innovative method of mathematically combining different models to allow risk estimates to be based on several plausible dose–response models rather than just relying on a single model of choice. This procedure thereby produces more reliable risk estimates based on a comprehensive appraisal of model uncertainties. For CVD, MMI yielded a weak dose–response (with a risk estimate of about one-third of the LNT model) below a step at 0.6 Gy and a stronger dose–response at higher doses. The calculated risk estimates are consistent with zero risk below this threshold-dose. For mortalities related to cardiovascular diseases, an LNT-type dose–response was found with risk estimates consistent with zero risk below 2.2 Gy based on 90% confidence intervals. The MMI approach described here resolves a dilemma in practical radiation protection when one is forced to select between models with profoundly different dose–responses for risk estimates.

Keywords Risk assessment · Radiation · Cerebrovascular disease · Cardiovascular diseases · Threshold-dose · LNT

Introduction

One of the most important questions in radiation research relates to the shape of the dose–response for detrimental health effects at low doses, that is, whether any small dose of ionizing radiation adds to health risks, or whether there may be a threshold below which radiation may have no effect, or whether even protective effects may occur (Brenner et al. 2003; Averbeck 2009). This question bears essential relevance for our societies given, for example, the widespread use of medical imaging techniques such as CT scans, X-ray images, and mammography. It is also relevant for air crews and large worker populations who are exposed occupationally, for example, in nuclear installations. The possible risks of ionizing radiation are not limited to cancer but also relate to non-cancer diseases (Little et al. 2010). In that context, the question of a possible threshold or protective effects at low and/or medium doses is equally important as it is for cancer (Preston et al. 2003; Shimizu et al. 2010).

H. Schöllnberger (✉) · J. C. Kaiser · P. Jacob
Helmholtz Zentrum München, Department of Radiation Sciences, Institute of Radiation Protection, 85764 Neuherberg, Germany
e-mail: schoellnberger@helmholtz-muenchen.de

L. Walsh
BfS-Federal Office for Radiation Protection, Neuherberg, Germany

Springer

The mortality data from the Life Span Study (LSS), relating to the A-bomb survivors in Hiroshima and Nagasaki, are generally considered to be important for estimating the risk associated with ionizing radiation. Analyses of these data suggest a role of ionizing radiation in the formation of non-cancer diseases such as cerebrovascular disease (CVD)[1] and cardiovascular diseases excluding CVD[2] (Preston et al. 2003). Preston et al. (2003) concluded that the evidence for radiation effects on non-cancer mortality remains strong, with risks elevated by about 14% per Sv during the last 13 years of follow-up and that the best estimate for a threshold-dose is 0.2 Sv with an upper bound of about 0.7 Sv with no evidence against the linear-no-threshold hypothesis.

For protracted exposures, an important data set is the Mayak worker cohort (Azizova et al. 2008). The Mayak workers were exposed to low and medium doses at low dose rates. This together with the fact that these individuals did not have the threatening and traumatic experience of being exposed to the detonation of a nuclear bomb makes this data set especially valuable for risk estimations of general populations. Recently, statistically significant increasing trends in the incidence of cardiovascular and cerebrovascular diseases with external γ-ray dose have been reported for this cohort (Azizova et al. 2010a, b, 2011). Azizova et al. (2010a) found statistically significant increasing trends with both total external gamma-ray dose and internal liver dose in the incidence of ischaemic heart disease, a form of cardiovascular disease. They also reported statistically significant increasing trends in cerebrovascular disease incidence but not mortality with both total external γ-ray dose and internal liver dose from α-particle radiation (Azizova et al. 2010b, 2011).

In an extensive review, Little et al. (2010) present evidence for the epidemiological associations between lower-dose exposures and circulatory disease risks. They reviewed epidemiological data related to the atomic bomb survivors, low- and moderate-dose therapeutically exposed groups, and diagnostically, occupationally, and environmentally exposed groups. The authors conclude that the epidemiological evidence for an elevation of these diseases by moderate and low doses remains suggestive rather than persuasive (Little et al. 2010).

In the current study, various plausible dose–response curves (such as linear-no-threshold (LNT), linear quadratic, linear with threshold, step functions, hormesis-like dose–responses) were applied to the LSS data for CVD and cardiovascular diseases excluding CVD from Report 13 (Preston et al. 2003), and suitable quality-of-fit criteria were used to select the preferred models. A series of likelihood-ratio tests was used to obtain a set of preferable non-nested models. Multi-model inference (MMI), an innovative method to combine the estimates of several plausible non-nested models (Burnham and Anderson 2002; Claeskens and Hjort 2008), was then applied. The method resulted in a joint dose–response for each of the two biological endpoints. In the field of radiation epidemiology, MMI poses a fascinating new approach that avoids the danger of producing biased results from relying on just one single model of choice. Before the MMI method was introduced to radiation epidemiology by Walsh and Kaiser (2011), there was an earlier proposal to combine different probability distributions by assigning different probabilities to them regarding the possible existence of low-dose thresholds (Land 2002). This concept of Land (2002) can be regarded as a stimulating suggestion to apply MMI. For a further discussion of model selection criteria in radiation epidemiology, see the study by Walsh (2007).

An analysis of a more recent LSS data set with follow-up from 1950 to 2003 has also been performed (Shimizu et al. 2010). However, the question whether the dose–response is linear at low doses without threshold or whether nonlinear dose–response features are present is still unresolved. In the present study, it is shown that the shape of the dose–response curve cannot be found by exclusively using either the LNT or the linear threshold model, the approach used by Shimizu et al. (2010). The fact that several risk models yield plausible fits to the data is duly considered and accounted for here.

Materials and methods

Data on non-cancer disease mortality

The present analyses are based on two data sets for cerebrovascular disease (CVD; ICD-9 430–438) and cardiovascular diseases excluding CVD (ICD-9 390–429, 440–459) of LSS Report 13 (Preston et al. 2003; data fileR13MORT.DAT from http://www.rerf.or.jp). In the remainder of this publication, the ICD-9 codes 390–429, 440–459 are simply referred to as cardiovascular diseases. In the file R13MORT.DAT, the data are provided in a person-year table and are categorized by city, sex, age at exposure, age attained, calendar time period during which

---

[1] It is noted that Preston et al. (2003) and Shimizu et al. (2010) refer to the ICD-9 codes 430–438 as "stroke", while stroke is in fact a subgroup of ICD-9 430–438. The latter represents cerebrovascular disease.

[2] It is noted that Preston et al. (2003) and Shimizu et al. (2010) refer to the ICD-9 codes 390–429, 440–459 as "heart disease", while these ICD-9 codes are better described as cardiovascular diseases excluding CVD (Dr. Frauke Neff, Helmholtz Zentrum München, personal communication).

the mortality checks were made, and weighted survivor colon dose. For each data group, the data file contains person-year weighted means of age attained, age at exposure, colon dose with a weight of ten for the neutron contribution, the number of person-years, and the number of deaths cases.

The data were analysed with exactly the same restrictions applied by Preston et al. (2003): we used data with follow-up starting on 1 January 1968 and ending on 31 December 1997. Only proximal survivors were taken where proximal is taken to mean survivors who were within a radius of 3 km from the hypocenter at the time of bombing. That gives 50,364 individuals (19,467 men and 30,897 women), of whom 3,954 died from CVD (1,434 men and 2,520 women) and 4,477 died from cardiovascular diseases (1,614 men and 2,863 women). The number of person-years is 1200,991.8 (452,161.6 and 748,830.2 person-years for men and women, respectively). Data pertaining to men and women were fitted jointly.

Descriptive risk models

The mortality data for CVD and cardiovascular diseases from Report 13 of the LSS were analysed with the following parametric and categorical models for the risk that stems from radiation: the LNT model, the quadratic model and the linear-quadratic model, the linear-exponential model, the linear threshold model (often referred to as threshold model within this study), various step models, hormesis-like models and one categorical model. Altogether, eleven different dose–responses were tested (Fig. 1). All of them were implemented either as excess relative risk (ERR) models or as excess absolute risk (EAR) models. The general form of an ERR model is as follows: $h = h_0 \times (1 + ERR(D, s, a, e))$ where h is the total hazard function, h_0 is the baseline model and the function $ERR(D, s, a, e)$ describes the change of the hazard function with weighted colon dose D allowing for effects of sex (s), age at exposure (e) and attained age (a). It is $ERR(D, s, a, e) = err(D) \times \varepsilon(s, a, e)$. Here, $err(D)$ describes the shape of the dose–response function and $\varepsilon(s, a, e)$ contains the dose-effect modifiers sex, age attained, and age at exposure. The general form of an EAR model is $h = h_0 + EAR(D, s, a, e)$ where $EAR(D, s, a, e) = ear(D) \times \varepsilon(s, a, e)$. Mathematical details related to the effect modifiers are given in Sect. 3 of the Online Resource. For h_0, we first applied the Preston baseline model given in Eq. (A1) of the Online Resource (see file R13models.log at http://www.rerf.or.jp/library/dl_e/lss13.html, Preston et al. (2003)).

For $err(D)$ and $ear(D)$ the following dose–response models were used:

$$err(D) = err \times D \quad \text{LNT model, } \#1 \text{ in Fig.1}$$

$$err(D) = 1.12 \times err \times D^2 \quad \text{Quadratic model, } \#2 \text{ in Fig.1}$$

$$err(D) = err_1 \times D + 1.12 \times err_2 \times D^2$$
Linear - quadr. model, #3 in Fig.1

$$err(D) = (err_1 + err_2 D) \times \exp(-err_3 D^2)$$
Linear - expon. model, #4 in Fig.1

$$err(D) = \begin{Bmatrix} 0 & D < D_{th} \\ err(D - D_{th}) & D \geq D_{th} \end{Bmatrix}$$
Linear thresh. model, #5 in Fig.1

$$err(D) = 0.5 \times scale \times [\tanh(s(D - D_{th})) + 1]$$
Step model, #6 in Fig.1

$$err(D) = \begin{Bmatrix} 0 & D < D_{th} \\ err \times D & D \geq D_{th} \end{Bmatrix}$$
Step model with slope, #7 in Fig.1

$$err(D) = \begin{Bmatrix} 0 & D < D_{th} \\ err_1 + err_2(D - D_{th}) & D \geq D_{th} \end{Bmatrix}$$
Step model with slope, #8 in Fig.1

$$err(D) = \begin{Bmatrix} 0 & D < 0.005\,\text{Gy} \\ err_1 & 0.005\,\text{Gy} \leq D < D_{th} \\ err_2 & D \geq D_{th} \end{Bmatrix}$$
Hormesis - like model, #9 in Fig.1

$$err(D) = \begin{Bmatrix} 0 & D < 0.005\,\text{Gy} \\ err_1 & 0.005\,\text{Gy} \leq D < D_{th} \\ err_1 + err_2(D - D_{th}) & D \geq D_{th} \end{Bmatrix}$$
Hormesis - like with slope, #10 in Fig.1

$$err(D) = \begin{Bmatrix} err_1 & 0 \leq D < D_1 \\ err_2 & D_1 \leq D < D_2 \\ err_3 & D_2 \leq D < D_3 \\ err_4 & D \geq D_3 \end{Bmatrix}$$
3 - step categorical model, #11

The necessary adjustments for random errors in dosimetry applied to the dose term are already applied in the publicly available data, but a separate adjustment involving a multiplication factor to the dose-squared covariable should be done explicitly, either according to Pierce et al. (1990) (factor 1.12) or Pierce et al. (2008) (revised factor 1.15). Since most of the published analyses apply the factor 1.12, this has been adopted here for the quadratic and linear-quadratic models.

The Preston baseline model (given in Eq. (A1) of the Online Resource) was optimized here with series of likelihood-ratio tests. For nested models, the difference between their deviances (dev) is χ^2-distributed (Claeskens and Hjort 2008). A model is considered an improvement over another model with a 95% probability if the deviance is lowered by at least 3.84 points after adding of one parameter. A description of this streamlining process,

Fig. 1 Parametric (#1 to #8, #10) and categorical (#9, #11) models used to investigate the shape of the dose–responses related to the risk that stems from ionizing radiation. 1st row: LNT model, quadratic model, linear-quadratic model; 2nd row: linear-exponential model, linear threshold model (sometimes only referred to as threshold model, the threshold-dose is denoted by D_{th}), step model; 3rd row: step model with slope, another step model with slope, hormetic-like model; 4th row: hormetic-like model with slope; 3-step categorical model. Note that in both hormetic-like models the excess risk is set to zero for $D < 0.005$ Gy
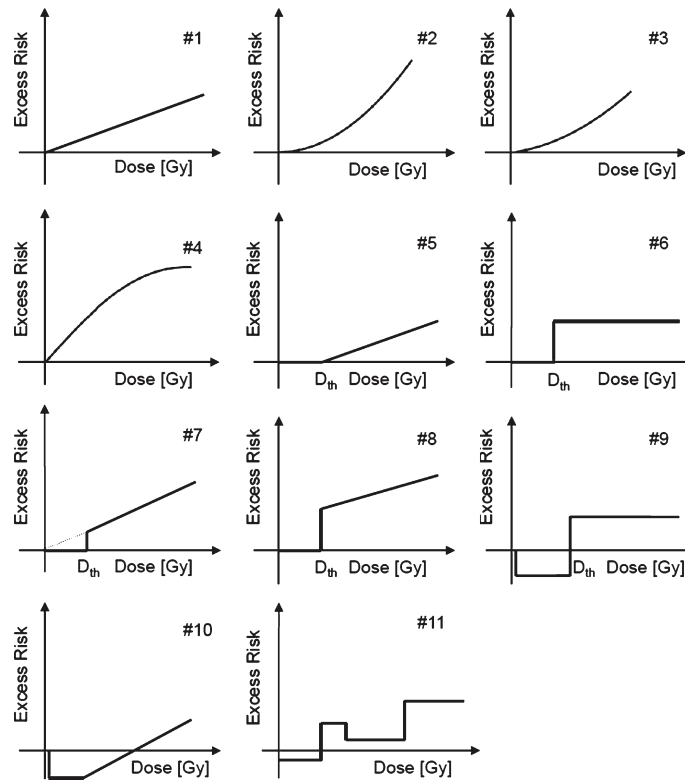
which has also been applied in a recent study on breast cancer risk in atomic bomb survivors (Kaiser et al. 2011), is given below.

Streamlining the Preston baseline model

Preston's fit to the LSS data for CVD (presented in Table 13 in Preston et al. (2003)) was reproduced in the first step. Preston et al. (2003) concluded that an LNT model implemented as ERR model fitted the data best. In order to reproduce this, the Preston baseline model given in Eq. (A1) of the Online Resource was combined with an LNT model, implemented as an ERR model and fitted to the joint data for CVD in men and women. This model is referred to as Preston's ERR-LNT model and contains 30 model parameters (dev = 3599.58, Table 1). Then, each of the 29 baseline parameters was tested for its significance at the 95% significance level by setting it to 0 and refitting all the other parameters. Rigorous testing led to a new set of statistically significant baseline parameters, with eight

parameters less than Preston et al. (2003) used within their baseline model [h_0 from Eq. (A1)]: the new model no longer contained four age at exposure dependences, the related three age knots, and one age attained dependence. In addition, it was found that the model fit significantly improved when two other age knots and one age at exposure knot were allowed to be free (for details consult Sect. 2 of the Online Resource). The streamlined baseline model for CVD, which was used in combination with the 11 models depicted in Fig. 1, therefore has 21 (29 − 8) model parameters (see Table S1 in the Online Resource).

For cardiovascular diseases, an analogous procedure was applied. Preston's best fit of the data for cardiovascular diseases was reproduced: the Preston baseline model given in Eq. (A1) of the Online Resource was combined with an LNT model, implemented as ERR model and fitted to the joint data for cardiovascular diseases. The results of fitting Preston's ERR-LNT model are given in Table 1: dev = 3709.71 with 30 model parameters. Then, each of the 29 baseline parameters was tested for its significance

Table 1 For both biological endpoints, the preferable final non-nested models are shown with related final deviances (dev), difference in final deviances (Δdev) with respect to the model with the smallest deviance, number of model parameters (N_{par}), AIC-values, difference in AIC-values (ΔAIC) with respect to the model with the smallest AIC-value, and Akaike weights

	dev	Δdev	N_{par}	AIC	ΔAIC	Weight
CVD (ICD-9 430–429)						
ERR-LNT model [#1]	3569.51	3.46	22	3613.51	1.46	0.2628
ERR-quadratic model [#2]	3570.14	4.09	22	3614.14	2.09	0.1918
ERR-step model [#6], $D_{th} = 0.62$ Gy	3566.05	0	23	3612.05	0	0.5454
Preston's ERR-LNT model	3599.58	33.53	30	3659.58	47.53	–
Cardiovascular diseases (390–429, 440–459)						
EAR-LNT model[a] [#1]	3693.73	0	17	3727.73	0	0.3619
ERR-quadratic model[a] [#2]	3694.05	0.32	17	3728.05	0.32	0.1918
EAR-threshold model [#5], $D_{th} = 2.0$ Gy	3695.0	1.27	17	3729.0	1.27	0.1379
EAR-step model [#6], $D_{th} = 2.19$ Gy	3695.66	1.93	17	3729.66	1.93	0.3084
Preston's ERR-LNT model	3709.71	15.98	30	3769.71	41.98	–

As a comparison, the values are also shown for Preston's ERR-LNT models. Note that for cerebrovascular disease the three preferable models are ERR models; for cardiovascular diseases, the four preferable non-nested models are EAR models. The numbers in brackets refer to the eleven dose–responses depicted in Fig. 1

[a] Contains an age-dependent dose-effect modifier

resulting in a streamlined baseline model with 14 model parameters less than the Preston baseline model, which also lost its city dependence (see Table S2 in the Online Resource). The streamlined baseline model no longer contained four age at exposure dependences, three age attained dependences, and the related five age knots. Furthermore, it was found that the model fit significantly improved when two other age knots were allowed to be free (for details consult Sect. 2 of the Online Resource). The streamlined baseline model for cardiovascular diseases therefore has 15 (29 − 14) model parameters (see Table S2 in the Online Resource).

Fitting the descriptive risk models

After having acquired two streamlined baseline models for CVD and cardiovascular diseases with the procedure described in the previous two paragraphs, all other models (i.e. models other than the LNT model that was already used for the streamlining process) depicted in Fig. 1 were also combined with the streamlined baseline models as either ERR model or EAR model and fitted to the data for CVD and cardiovascular diseases. For those parametric and categorical models that contain a threshold-dose D_{th}, the following set of different values for D_{th} was used to carefully investigate which value leads to the smallest deviance: 0.0001 Gy, 0.0002,…, 0.0005, 0.001, 0.005, 0.01, 0.02, …, 0.09, 0.1, 0.2, …, 0.9, 1, and 2 Gy. In the linear threshold model, however, D_{th} was adjusted in the model fit. The step model was replaced by a modified hyperbolic

tangent function as described below. Throughout this extensive approach, likelihood-ratio tests were applied to compare nested models with each other, to eliminate those nested models with inferior deviance values and to obtain two final sub-sets of non-nested models, one for each detrimental health outcome.

The step model (Fig. 1) was not implemented as a categorical model. Instead, the following modified hyperbolic tangent was used: $0.5 \times scale \times [\tanh(s(D − D_{th})) + 1]$. With appropriate values for *scale*, slope *s*, and D_{th}, this flexible function can accommodate various entirely different shapes, among them the step function as depicted in Fig. 1 (model #3). With the hyperbolic tangent, steps are not imposed a priori but are a result of a fit to the data. The advantage of this function is the fact that it generally allows an estimate of D_{th} to be obtained with greater accuracy by fitting the model to data, while in a categorical implementation a value of D_{th} has to be assumed for each fit.

It was also successively investigated whether or not any of the three dose-effect modifiers, that is, sex, age attained, and age at exposure improved the model fits significantly.

Data-fitting techniques and MMI

The MECAN software (Kaiser 2010) was applied to fit the EAR and ERR models to the data. This software uses Poisson regression (Schöllnberger et al. 2006) to estimate the values of the adjustable model parameters by fitting the model to the data. For the minimization of the Poisson deviance, MECAN applies Minuit2 (2008). Symmetric,

Wald-type standard errors are calculated for the parameter estimates.

The *ERR* and *EAR* risk estimates are calculated directly from the hazard function:

$$ERR = (h/h_0) - 1$$
$$EAR = h - h_0. \tag{1}$$

Confidence intervals (CI) for the risk estimates given in Eq. (A1) are calculated with Latin hypercube sampling (LHS) which accounts for uncertainties and correlations of all adjustable parameters. For a risk variable such as *ERR*, a probability density distribution of 10^4 realizations is generated, which is used to derive statistical descriptors such as mean, median, and percentiles. The MECAN software (Kaiser 2010) allows to perform Poisson regression, comparison of observed and expected cases, and simulation of uncertainty intervals within one run. The software package and all model-related input and result files are available from the authors upon request.

For both investigated detrimental health outcomes, the final non-nested models, which are presented in the "Results" section, were weighted according to the AIC (see below) and used to perform MMI, which is a method of mathematically superposing different non-nested models that all describe a certain data set almost equally well (Burnham and Anderson 2002). The method applies Akaike's Information Criterion (Akaike 1973, 1974): $AIC = dev + 2 N_{par}$, where N_{par} is the number of model parameters. For each model fit, an AIC-value is calculated. For a set of n non-nested models, the Akaike weight, p_m, is calculated for model m according to the following equation (Claeskens and Hjort 2008):

$$p_m = \frac{\exp(-\Delta AIC_m/2)}{\sum_{j=1}^{n} \exp(-\Delta AIC_j/2)}. \tag{2}$$

Here, $\Delta AIC_m = AIC_m - AIC_0$, where AIC_m is the AIC-value for model m and AIC_0 is the smallest AIC-value of all n models. The resulting weights, multiplied by a factor of 10^4, give the number of samples for risk estimates to be generated by LHS simulations. Then, for each set of preselected values of age attained, age at exposure, and dose, the created model-specific probability density functions (PDFs) are merged. The resulting probability density functions, each of size 10^4, represent all uncertainties arising within a model and from the superposition of the selected models. Statistical quantities such as mean, median, and percentiles are derived from the final PDFs.

Below, larger deviances compared to our best models (i.e. those with smallest AIC-values) are denoted by positive values of Δdev. The notation Δpar gives the difference in number of parameters compared to the models with smallest AIC.

Results

Using the approach outlined in the "Materials and methods" section, it was found that for CVD the following final three non-nested ERR models out-competed all other models and were included in the sub-set for MMI: an ERR-LNT model consisting of the streamlined baseline model with 21 significant baseline parameters combined with an LNT model via parameter *err* (Δdev = 3.46; Table 1), an ERR-quadratic model (Δdev = 4.09; Table 1), and an ERR-step model with $D_{th} = 0.62$ Gy (Δdev = 0; Table 1 and Fig. 1). Table 1 gives for these final three non-nested models all essential information obtained by fitting them to the CVD data. Table S1 in the Online Resource provides all related model parameters and related best estimates together with Wald-type standard errors: all three models contain 21 baseline parameters; the ERR-LNT model and the ERR-quadratic model each contain one radiation-related parameter (*err*); the ERR-step model has two radiation-related parameters (*scale*, D_{th}). As a comparison, Table 1 also includes the results for Preston's ERR-LNT model: Δdev = 33.53 and Δpar = 7, that is, even though Preston's ERR-LNT model has 7 parameters more than our ERR-step model, the latter still leads to a better fit than the Preston model by 33.53 deviance points. This improvement in fit is related to the free age knots and age at exposure knots described in the "Materials and methods" section.

For cardiovascular diseases, the MMI sub-set consisted of four non-nested EAR models: an EAR-LNT model (Δdev = 0), an EAR-quadratic model (Δdev = 0.32), an EAR-threshold model with $D_{th} = 2.0$ Gy (Δdev = 1.27), and an EAR-step model with $D_{th} = 2.19$ Gy (Δdev = 1.93). The first two models both include a dose-effect modifier that depends on age attained. The step model was implemented as a hyperbolic tangent function. Table 1 gives, for each of the final four models, all essential information obtained by fitting them to the data for cardiovascular diseases. Refer to Table S2 (Online Resource) for all related model parameters (baseline and radiation related), their best estimates and Wald-type standard errors. It is noted that for younger ages the significant dose-effect modifier in the EAR-LNT model leads to smaller slopes than the one depicted in Fig. 3 (see Sect. 3 of the Online Resource for details). As a comparison, Table 1 also includes the results for Preston's ERR-LNT model: Δdev = 15.98 and Δpar = 13, that is, although Preston's ERR-LNT model has 13 parameters more than our EAR-LNT model, the latter fits the data for cardiovascular diseases by 15.98 deviance points better than Preston's ERR-LNT model (Table 1).

The related AIC-values are shown in Table 1 together with the Akaike weights p_m (2). The latter were used to perform MMI as described in the "Materials and methods"

section. The results are shown in Figs. 2 and 3. For CVD, the deviance of 3566.57 (Δdev = 0.49) related to MMI is easily obtained, since the dose–response contains no dose–effect modifiers. The MMI predicts a very low ERR for doses below the threshold, because of the contribution from the ERR-step model with a threshold-dose of 0.62 Gy, and the 95% CIs include zero risk (Table 2). Therefore, the MMI risk estimates for CVD presented here are consistent with zero risk below the threshold of 0.62 Gy. The results for cardiovascular diseases follow a similar pattern: based on the 90% CI, the MMI implies zero risk up to 2.24 Gy.

The striking improvements of the deviances presented here compared with those from Preston's ERR-LNT fits (Table 1) were mainly achieved by streamlining the baseline models. Therefore, better matches of observed and predicted cases were expected mainly in the group of "unexposed" survivors (i.e. individuals with doses below 5 mGy). To test this assumption, it was investigated which categories of dose and age attained contribute most to the decrease in deviance, found here with the preferred models, when compared to Preston's ERR-LNT fits. For CVD, the preferred model according to AIC is the ERR-step model, for cardiovascular diseases it is the EAR-LNT model (Table 1). Using the related best estimates from Tables S1 and S2, forward calculations were performed with the data sets stratified into several groups of weighted colon dose and age attained. For CVD in men, the strongest contribution of 8.3 points to the improvement in deviance stems from individuals in dose category $0.1 < D \leq 0.5$ Gy with
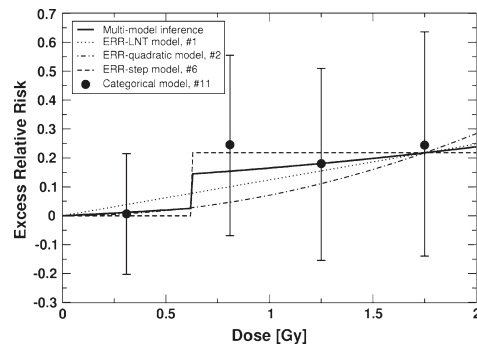

Fig. 3 *EAR* for cardiovascular diseases versus weighted colon dose for the final four non-nested EAR models and the multi-model inference (refer to Table 1). Also shown are point estimates and related 90% CI for a 3-step categorical ERR model that divides the dose range into four categories: $D < 0.75$ Gy, 0.75 Gy $\leq D < 1.5$ Gy, 1.5 Gy $\leq D < 2.19$ Gy, and $D \geq 2.19$ Gy. The 90% CI for the MMI are provided in Table 3 for an absorbed dose of 1 Gy. The figure is valid for men and women of both cities. The preselected values for age at exposure and age attained are 30 and 70 years, respectively

ages attained of 40 years and higher. For women, the strongest contribution of 19.8 points is related to dose categories $0.005 < D \leq 0.1$ Gy and $0.5 < D \leq 1$ Gy with ages attained of 40 years and higher. For cardiovascular diseases, the strongest contribution of 12 points stems from women in dose categories $0.1 < D \leq 0.5$ Gy and $0.5 < D \leq 1$ Gy at ages of 60 and higher, while men hardly improve the final deviance compared to the fit with Preston's ERR-LNT model (1915.21 versus 1915.88). Detailed results can be seen in Tables S3, S4, and S5 in the Online Resource.

For both detrimental health outcomes, the risk estimates *ERR* and *EAR* were calculated for the multi-model inferences and for the non-nested models listed in Table 1. The results are given in Tables 2 and 3 for a dose of 1 Gy and for different values of age attained (50 and 70 years) and age at exposure. For CVD and cardiovascular diseases, the mean age of the cases (i.e. of individuals who died from these diseases) was about 77 and 78 years, respectively. Because of the threshold at 0.62 Gy for CVD, for this disease *ERR* and *EAR* were also calculated for 0.2 Gy. The risk estimates from Preston et al. (2003) and Shimizu et al. (2010) are also provided. For CVD, the *EAR* depends on city and sex because it is calculated from ERR models and because the streamlined baseline model presented here depends on city and sex. Therefore, the *EAR*-values for MMI and for the single models #1, #2, and #6 in Table 2 are only valid for men from Hiroshima. For cardiovascular diseases, the *ERR* depends on sex because it is calculated

Fig. 2 *ERR* for cerebrovascular disease versus weighted colon dose for the final three non-nested ERR models and the multi-model inference (MMI) (Table 1). Also shown are point estimates and related 90% CI for a 3-step categorical ERR model that divides the dose range into four categories: $D < 0.62$ Gy, 0.62 Gy $\leq D < 1$ Gy, 1 Gy $\leq D < 1.5$ Gy, and $D \geq 1.5$ Gy. The 90% CI for the MMI are provided in Table 2 for absorbed doses of 0.2 and 1 Gy. The figure is valid for men and women of both cities. The preselected values for age at exposure and age attained are 30 and 70 years, respectively
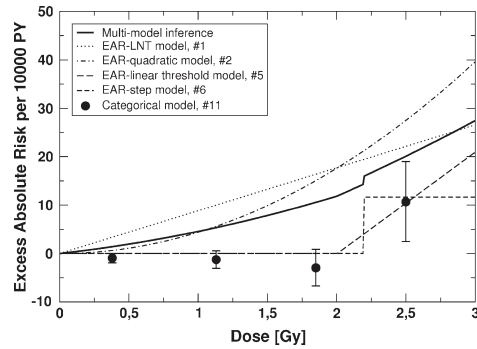
Table 2 Values for *ERR* and *EAR* for cerebrovascular disease calculated with the multi-model inference, the ERR-LNT model, the ERR-quadratic model, and the ERR-step model for 0.2 and 1 Gy and different values of age at exposure (*e*) and age attained (*a*)

	ERR	EAR [per 10^4 PY]
CVD		
Multi-model inference		
0.2 Gy		
$e = 20$, $a = 50$	0.007 (0, 0.035)	0.05 (0, 0.23)
$e = 20$, $a = 70$	0.007 (0, 0.035)	0.17 (0, 0.84)
$e = 30$, $a = 70$	0.007 (0, 0.035)	0.3 (0, 1.4)
$e = 50$, $a = 70$	0.007 (0, 0.035)	0.8 (0, 3.8)
1 Gy		
$e = 20$, $a = 50$	0.165 (0.033, 0.32)	1.10 (0.22, 2.1)
$e = 20$, $a = 70$	0.165 (0.033, 0.32)	3.97 (0.78, 7.7)
$e = 30$, $a = 70$	0.165 (0.033, 0.32)	6.6 (1.3, 13)
$e = 50$, $a = 70$	0.165 (0.033, 0.32)	18.0 (3.6, 35)
Single models		
0.2 Gy, $e = 30$, $a = 70$		
ERR-LNT model [#1]	0.0248 (0.0055, 0.044)	0.98 (0.22, 1.7)
ERR-quadratic model [#2]	2.84×10^{-3} (4.0×10^{-4}, 5.3×10^{-3})	0.114 (0.016, 0.21)
ERR-step model [#6], $D_{th} = 0.62$ Gy	0	0
1 Gy, $e = 30$, $a = 70$		
ERR-LNT model [#1]	0.124 (0.028, 0.22)	4.9 (1.1, 8.7)
ERR-quadratic model [#2]	0.071 (0.010, 0.13)	2.85 (0.40, 5.3)
ERR-step model [#6], $D_{th} = 0.62$ Gy	0.22 (0.093, 0.34)	8.7 (3.7, 14)
Preston ERR-LNT model (Preston et al. 2003)	0.12 (0.02, 0.22)	5.0[a] (1.0, 8.9)
ERR-LNT model (Shimizu et al. 2010)	0.09 (0.01, 0.17)[b]	2.3 (0.4, 4.4)[b]

The 90% confidence intervals are provided. The risk values from Preston et al. (2003) and Shimizu et al. (2010) are also shown. The numbers in brackets refer to the eleven dose–responses depicted in Fig. 1. The *EAR*-values for MMI and for the single models #1, #2, and #6 are only valid for men in Hiroshima. The city-averaged *EAR*-values for men can be calculated by multiplication with a factor of 1.1 (see Sect. 6 of the Online Resource for mathematical details). The *EAR*-values for women can be calculated by multiplying with a factor of 0.6

[a] Not given by Preston et al. (2003); calculated from Preston's ERR-LNT model

[b] This is the 95% CI

from EAR models and because the applied streamlined baseline model depends on sex (details are given in Sect. 5 of the Online Resource).

Discussion

In the present study, the dose–responses of the LSS non-cancer mortality data for CVD and cardiovascular diseases were investigated using different parametric and categorical models (Fig. 1). Two sub-sets of final, preferable, non-nested models were identified, one for each detrimental health outcome. These models are summarized in Table 1. They all describe the data about equally well: only relatively small differences in deviances and AIC-values were found.

For CVD, the ERR-step model (model #6 in Fig. 1; with the step smoothed by the hyperbolic tangent function) with

a threshold-dose of $D_{th} = 0.62$ Gy has the lowest AIC. The LNT model and the quadratic model are also included in the MMI (Fig. 2), resulting in a weak dose–response below the threshold (with a risk estimate of about one-third of that from the LNT model) and a stronger dose–response for higher doses. MMI results in a small excess relative risk below the threshold. The 90% confidence intervals are compatible with no risk up to 0.62 Gy (Table 2). This is confirmed by a fit using a categorical model: the risk estimate in the lowest dose group is not significantly different from zero (Fig. 2).

An analogous argument holds for the analysis of the LSS data for cardiovascular diseases (Fig. 3). Again, the MMI does not contain any threshold-dose but the lower bound of the related 90% CI at 1 Gy is zero (Table 3). The MMI is in fact consistent with zero risk up to 2.24 Gy. In that context, it is notable that a fit with a categorical model infers a *U*-shaped dose–response, that is, negative excess

Table 3 Values for *ERR* and *EAR* for cardiovascular diseases calculated with the multi-model inference, the EAR-LNT model, the EAR-quadratic model, the EAR-threshold model, and the EAR-step model for 1 Gy and different values of age at exposure (*e*) and age attained (*a*)

	ERR	EAR [per 10^4 PY]
Cardiovascular diseases		
Multi-model inference		
$e = 20$, $a = 50$	0.10 (0, 0.35)	0.8 (0, 2.7)
$e = 20$, $a = 70$	0.12 (0, 0.35)	5 (0, 13)
$e = 30$, $a = 70$	0.09 (0, 0.25)	5 (0, 13)
$e = 50$, $a = 70$	0.07 (0, 0.18)	5 (0, 13)
Single models		
$e = 30$, $a = 70$		
EAR-LNT model [#1]	0.171 (0.078, 0.27)	8.8 (4.2, 14)
EAR-quadratic model [#2]	0.084 (0.026, 0.14)	4.4 (1.4, 7.4)
EAR-threshold model [#5], $D_{th} = 2.0$ Gy	0	0
EAR-step model [#6], $D_{th} = 2.19$ Gy	0	0
Preston's ERR-LNT model, Preston et al. (2003)	0.17 (0.08, 0.26)	9.1[a] (4.2, 13.9)
ERR-LNT model, Shimizu et al. (2010)	0.14 (0.06, 0.23)[b]	3.2 (1.3, 5.2)[b]

The 90% confidence intervals are provided. The risk values from Preston et al. (2003) and Shimizu et al. (2010) are also shown. The numbers in brackets refer to the eleven dose–responses depicted in Fig. 1. The ERR-values for MMI and for the single models #1, 2, 5, and #6 are only valid for men. The ERR-values for women can be calculated by multiplication with a factor of 1.8

[a] Not given by Preston et al. (2003); calculated from Preston's ERR-LNT model

[b] This is the 95% CI

absolute risk in the lower-dose regimes with a statistically significant negative risk in the lowest dose group (Fig. 3). The increasing risk with attained age (via the age-dependent dose-effect modifier) produces a markedly higher risk in the EAR-LNT model with 94 excess cases in contrast to 9 cases in the EAR-threshold model and the EAR-step model, where the effect modifier was not statistically significant. Consequently, the dose–response curve from MMI also predicts a strongly reduced risk for death from cardiovascular diseases due to radiation. In the context of the results presented here, it is interesting to point out a recent low-dose study in which ApoE null mice were used. This mouse model system spontaneously develops atherosclerosis when fed a normal low-fat diet. In these mice, the effects of single doses of 25–500 mGy, given at either early or late stage disease, were distinctly nonlinear with dose and were generally protective for various measures of

the disease. In that animal model, most effects occurred below about 100 mGy, and many of the endpoints measured showed maximum protective effects at 25-50 mGy (Mitchel et al. 2011).

Related to Fig. 3, the *EAR* risk estimates for the EAR-LNT model, the EAR-quadratic model and for the MMI seem to be inconsistent with those calculated for the categorical fit, especially at the lower three doses. It is emphasized that this seeming inconsistency stems from the significant dose-effect modifier in the EAR-LNT model and the EAR-quadratic model (see Table S2 in the Online Resource). Figure 3 relates to an age attained of 70 years. For lower ages, the *EAR*-values for the EAR-LNT model are markedly decreased (numerical details are provided in Sect. 3 of the Online Resource). Consequently, this reduction also decreases the *EAR*-values for the MMI.

It is noted that for both diseases the categorical model (#11 in Fig. 1), a non-nested model, was not used for MMI because of its negligible contributions to the AIC-weights (Walsh 2007, Hoeting et al. 1999). Because of its similarity to the shape implied by the categorical model fit (Fig. 3), we also used the Gompertz curve to fit the excess absolute risk associated with the data for cardiovascular diseases. Again, it was found that the ΔAIC-based weight was too small to be used for MMI. For details, see Sect. 7 of the Online Resource.

Because of the well-known gender differences in cardiovascular disease mortality (Roger et al. 2011), it was investigated whether the data for men and women needed to be fitted separately. Model fits of the data for men and women were performed using an ERR-LNT model. For CVD, some differences were noted for the slope parameters ($err = 0.109044$ Gy^{-1} for men versus $err = 0.13524$ Gy^{-1} for women). However, comparing the related final deviances with the one from the joint fit (Table 1: dev = 3569.51 using 22 parameters) clearly showed that fitting the data for men and women separately does not lead to a significantly improved fit (men: dev = 1779.58 using 11 parameters; women: dev = 1788.24 using 13 parameters; sum = 3567.82). A similar result was found for cardiovascular diseases.

Preston et al. (2003) based their study on the use of the following five models: an LNT model, a linear-quadratic and a purely quadratic model, a linear threshold model, and categorical models implemented as either ERR model or EAR model. While Preston et al. (2003) report that there is no direct evidence of radiation effects for doses less than about 0.5 Sv, they conclude that radiation effects on LSS non-cancer mortality can be adequately described by a linear dose–response model. A data set on circulatory disease mortality with 6 years of additional follow-up has been publicly available since the end of 2010. Those data were analysed recently by Shimizu et al. (2010) with the

LNT model and the linear threshold model (model #5 in Fig. 1) for a wide range of possible values of threshold-dose D_{th}. They used differences in maximum likelihood to compare nested models and the AIC for non-nested models. For CVD, they report that the best estimate of a threshold-dose was 0.5 Gy but that this value was not statistically significant so that no threshold-dose may exist. For cardiovascular diseases, their best estimate of a threshold-dose was 0 Gy (Shimizu et al. 2010). In the present study, the earlier studies have been extended by using several additional possible dose–responses and by combining the results to obtain dose–responses and uncertainty ranges that are not based on assumptions made in a single model.

In their previous study, Preston et al. (2003) carefully explain why they did not use the full available data with follow-up starting in 1950. They state that characterization of the dose–response is complicated by a healthy survivor selection effect on non-cancer disease death rates. For a few years after the bombings, baseline (zero dose) non-cancer disease death rates for proximal survivors were markedly lower than those for distal survivors. The difference diminished steadily over the first two decades of follow-up, by which time it had largely vanished. This statistically significant pattern suggests that proximal survivors included in the LSS were initially healthier than the general population for reasons related to their selection by having survived the bombings. Analyses of the LSS non-cancer mortality data indicate that in 1950 baseline death rates for proximal survivors were 15% lower than those for distal survivors. The difference decreased to about 2% in the late 1960s (Preston et al. 2003). It has been illustrated by Preston et al. (2003) that a substantial healthy survivor selection leads to spurious curvature in the dose–response. According to Preston et al. (2003), the healthy survivor effect can be dealt with by restricting the analyses to proximal survivors and to the later period of follow-up, that is, 1968–1997. Unfortunately, the latest analysis of the LSS non-cancer data was done for the full cohort and for the full period of follow-up, that is, 1950–2003 (Shimizu et al. 2010). Concern related to the fact that Shimizu et al. (2010) place completely different emphasis and importance on the reported magnitude of the healthy survivor bias has been raised by Walsh (2011). Note that the downloadable grouped data by Shimizu et al. (2010) do not contain the same grouping boundaries as the data used in the present study: there is no proximal/distal group and no boundary corresponding to follow-up starting on 1 January 1968. A preliminary analysis of exactly the same mortality data for CVD that Shimizu et al. (2010) used (i.e. follow-up 1950–2003) using a streamlined Preston baseline model showed that an ERR-LNT model is preferable. It is interesting to note that when analysing the Shimizu CVD data

for the follow-up 1971-2003 (and thereby including most of the original Preston et al. 2003 data plus the additional 6 years of follow-up plus the distal survivors), the present authors found confirmation for the threshold-dose of 0.6 Gy obtained in the current study. The Shimizu CVD data for the follow-up 1971–2003 were analysed in the same way as the Preston et al. (2003) data. The Preston baseline model [Eq. (A1) of the Online Resource] was combined with an ERR-LNT model and fit to the data for CVD. The Preston baseline model was then streamlined using the likelihood-ratio test and then combined with the step model from Fig. 1 as an ERR model. The related best estimates and Wald-type standard errors (in parenthesis) are as follows: $D_{th} = 0.64$ Gy $(< 1\%)$, $scale = 0.204$ (0.081) with a fixed value for the slope s: 10^5/Gy (compare with Table 1 in the Online Resource). However, because of the above-mentioned incompatibility of the Shimizu et al. (2010) data with the data used by Preston et al. (2003), the analysis of the publicly available data set was not continued. Instead, the present authors are planning to pursue the analysis of a more suitable data set with a time cut-point at 1 January 1968 and an added indicator to distinguish proximal from distal survivors to be created by the Radiation Effects Research Foundation (RERF) in Japan.

Application of the AIC criterion for model selection exacts a rigorous application of parameter parsimony, since model weights are very sensitive to differences in AIC. The authors do not claim to have identified the optimal models. There is a potential to detect better parameterizations by fitting nonparametric models to the baseline death rates. However, the introduction of nonparametric baseline models into MMI requires further theoretical investigations by a larger number of experts. The present study leads to streamlined fully parametric baseline models (with significantly lower deviances despite the smaller number of model parameters) compared to the Preston baseline model (Preston et al. 2003). However, the risk estimates presented here with LNT models almost exactly correspond to those of Preston et al. (2003) (Tables 2 and 3).

In addition to these observed threshold-doses, another important difference from the earlier work of Preston et al. (2003) and Shimizu et al. (2010) is that the analyses presented here for the radiation influence on cardiovascular diseases actually favour EAR-risk models. The other authors prefer ERR models but renounced the rigorous application of quality-of-fit criteria.

In a review of published low-/moderate-dose epidemiological data sets on circulatory diseases, Little et al. (2010) list in their Table 1 14 studies related to the following exposed populations: atomic bomb survivors, low- and moderate-dose therapeutically exposed groups, diagnostically exposed groups, occupationally and environmentally exposed groups. Here, the dose–response

models applied in these 14 studies are briefly reviewed. The two papers analysing LSS non-cancer data are by Preston et al. (2003) and Yamada et al. (2004). The study of Preston et al. (2003) made use of four different dose–response models and has already been summarized above. Yamada et al. (2004) assumed an additive linear dose–response model: $RR_{ij} = 1 + \beta d_{ij} \exp(\alpha_k(Z_k))$, where RR_{ij} is the relative risk due to radiation dose associated with the jth exposure level, d_{ij} is the jth dose level in stratum i, β is the excess risk per Sievert averaged over all strata, and Z_k represents the effect modifiers (Yamada et al. 2004). They also tested linear-quadratic and purely quadratic models. For circulatory disease-related endpoints, such as hypertension, ischaemic heart disease, myocardial infarction and stroke, Yamada et al. (2004) did not find a statistically significant dependence on radiation exposure. Little et al. (2010) additionally included the following three studies related to low-dose radiotherapy and medical diagnostics. Carr et al. (2005) fitted a generalized linear model to a cohort of 3,719 peptic ulcer disease patients treated with radiotherapy or by other means. In the studies by Darby et al. (1987) and Davis et al. (1989), the standardized mortality ratio (SMR; number of observed cases divided by number of expected) as a precursor to modelling dose–response curves was calculated. The following eight occupational studies were also reviewed by Little et al. (2010). Ashmore and colleagues analysed the mortality from cancer and non-cancer diseases within a large cohort of Canadian radiation workers comprising 206,620 individuals. They used a relative risk model with risk increasing linearly with dose (Ashmore et al. 1998). Azizova and Muirhead (2009) modelled the ERR in the Mayak worker cohort by a linear trend with external or internal dose. In their analysis of 61,017 Chernobyl emergency workers, Ivanov et al. (2006) used a linear dependence of risk on dose as did Kreuzer et al. (2010) in their analysis of cancer and cardiovascular diseases in the German uranium miners cohort study. Non-cancer mortality was analysed in a large cohort of employees in the UK nuclear industry by McGeoghegan et al. (2008) using the following model for ERR: $R_{(b, a, r, i, s)} = \lambda_{(b, a, r, i, s)} [1 + ERR(d)]$. Here, R is the cause-specific mortality rate and λ is the background mortality rate in the absence of any effects from radiation exposure. The subscripts b, a, r, i, and s refer respectively to birth cohort, attained age, radiation exposure status, employment status, and site of employment. $ERR(d)$ is a function of lagged cumulative external dose (d) describing the excess relative risk (McGeoghegan et al. 2008). Muirhead et al. (2009) performed the latest analysis of the UK National Registry for Radiation Workers comprising a total number of 174,541 persons. They analysed among other biological endpoints the mortality from all circulatory diseases by modelling the

ERR as a linear function of dose. In their analysis of the associations between low-level exposure and mortality (including mortality from ischaemic heart disease) among workers at Oak Ridge National Laboratory Richardson and Wing (1999) applied a relative risk model of the form $\lambda(Z, z, y) = \exp(Z\alpha + \beta x + \delta y)$, where the mortality rate (λ) was considered in terms of a vector of covariates (Z), the radiation dose accumulated before age 45 (x), and the radiation dose accumulated after age 45 (y). This is a generalized linear model. In the IARC 15-country study of radiation workers, Vrijheid et al. (2007) found increasing trends with dose for some biological endpoints and decreasing trends for others, although none were statistically significant. In that context, we point out that Vrijheid et al. (2007) based their analyses on a linear relative risk Poisson model, in which the relative risk is of the form $1 + \beta Z$, where Z is the lagged cumulative dose in Sv and β is the excess relative risk per Sievert. Vrijheid et al. (2007) state that this model has been used commonly in analyses of nuclear workers studies and radiation risk estimation, and reference ICRP (1991) and US NRC (2006). Detailed results for the ERR found within these eight occupational studies have been summarized by Little et al. (2010). Talbott et al. (2003) reported a decreasing trend in heart disease mortality with dose for men and women exposed as a result of the accident at the Three Mile Island nuclear power station. For women, the decreasing trend was significant. The authors performed logistic regression fitting multiplicative relative risk models of the form $\lambda(t) = \lambda_0(t)\exp(x(t)\beta)$ (i.e. a generalized linear model) to the cohort rates (Talbott et al. 2003). This comprises the 14 studies reviewed by Little et al. (2010) including the study on environmental exposure by Talbott et al. (2003). The authors of the current study are convinced that dose–response analyses and related risk estimations should not be based on the application of only one model (for which usually a linear increase of risk with increasing dose is assumed) unless this one model is clearly preferred by model selection techniques. In the present study, it has been demonstrated that the use of a large variety of dose–response curves leads to a better and more realistic description of dose–response curves for non-cancer vascular diseases than the use of LNT models.

MMI is a form of Bayesian model averaging (BMA; Hoeting et al. 1999). It can be shown that the formula used to perform BMA (Eq. 1 in Hoeting et al. 1999) reduces to (2) for the Akaike weights p_m when one assumes that a priori all models are equally likely. This is the approach chosen here with respect to the models shown in Fig. 1. The present study did not aim to find the true model but the one which fits the data best. In this case, Burnham and Anderson (2002) (p. 77) argue for equal model priors (i.e. equal prior probabilities for the models to be tested) under

a so-called information-theoretic approach. A recent criticism by Richardson and Cole (2012) of applying the MMI technique in radiation epidemiology has been answered by Walsh et al. (2011).

The present study showed that the application of the MMI technique to non-cancer data of Report 13 on the atomic bomb survivors leads to distinctly nonlinear dose–response curves and related threshold-doses. This provides strong evidence that low and medium doses of ionizing radiation may have different effects than high doses. Such findings may stimulate the development of mechanistic models, which explain dose–responses based on radiobiological cellular processes. Biologically based mechanistic models are important for estimating at which stages of the disease process radiation may act (see, for example, the work of Little et al. (2009)). Motivated by the results of the present analysis, it is promising to include into mathematical models biological mechanisms (such as, for example, possible anti-inflammatory effects of low and medium doses of ionizing radiations) that may lead to distinct nonlinearities in the related dose–response curves. How this works for the biological endpoint of cancer induction after exposure to low doses of ionizing radiation at low dose rates has been shown by Schöllnberger et al. (2004, 2005) using deterministic and stochastic multi-stage models with clonal expansion.

Conclusions

Summarizing, it can be said that the present analyses of the non-cancer mortality data from Report 13 on the atomic bomb survivors predict a strongly reduced risk for death from CVD and cardiovascular diseases excluding CVD due to ionizing radiation. For CVD, MMI yielded a weak dose–response (with a risk estimate of about one-third of the LNT model) below a step at 0.6 Gy and a stronger dose–response at higher doses. Based on 90% confidence intervals, the calculated risk estimates are consistent with zero risk below this threshold-dose. For mortalities related to cardiovascular diseases excluding CVD, an LNT-type dose–response was found with risk estimates consistent with zero risk below 2.2 Gy based on 90% confidence intervals. Great care must be taken when analysing the shape of dose–responses for non-cancer mortalities. In addition to LNT and linear threshold models, other dose–responses must also be considered and tested. Non-standard dose–response curves derived from the rigorous application of a statistical protocol may stimulate the development of mechanistic models that explain dose–responses based on radiobiological cellular processes. Analysing the shape of dose–responses by testing a series of different empirical models, as it has been done in the present study using MMI, provides valuable information for the mechanistic modelling. In practical radiation protection, MMI is an important tool for risk assessment, especially at low doses. It allows different models to be combined, leading to a more comprehensive characterization of the uncertainty of risk estimates. This conclusion also holds for other detrimental health effects such as cancer.

References

Akaike H (1973) Information theory and an extension of the maximum likelihood principle. In: Petrov BN, Caski F (eds) Proceedings of the second international symposium on information theory. Akademiai Kiado, Budapest, pp 267–281

Akaike H (1974) A new look at the statistical model identification. IEEE Trans Autom Control 19:716–723

Ashmore JP, Krewski D, Zielinski JM, Jiang H, Semenciw R, Band PR (1998) First analysis of mortality and occupational radiation exposure based on the National Dose Registry of Canada. Am J Epidemiol 148:564–574

Averbeck D (2009) Does scientific evidence support a change from the LNT model for low-dose radiation risk extrapolation? Health Phys 97:493–504

Azizova TV, Muirhead CR (2009) Epidemiological evidence for circulatory diseases—occupational exposure. EU Scientific Seminar 2008. Emerging evidence for radiation induced circulatory diseases. In: Proceedings of a scientific seminar held in Luxembourg on 25 November 2008. Radiation Protection, vol 158, pp 33–46. http://ec.europa.eu/energy/nuclear/radiation_protection/doc/publication/158.pdf

Azizova TV, Day RD, Wald N, Muirhead CR, O'Hagan JA, Sumina MV, Belyaeva ZD, Druzhinina MB, Teplyakov II, Semenikhina NG, Stetsenko LA, Grigoryeva ES, Krupenina LN, Vlasenko EV (2008) The "clinic" medical-dosimetric database of Mayak production association workers: structure, characteristics and prospects of utilization. Health Phys 94:449–458

Azizova TV, Muirhead CR, Druzhinina MB, Grigoryeva ES, Vlasenko EV, Sumina MV, O'Hagan JA, Zhang W, Haylock RG, Hunter N (2010a) Cardiovascular diseases in the cohort of workers first employed at Mayak PA in 1948–1958. Radiat Res 174:155–168

Azizova TV, Muirhead CR, Druzhinina MB, Grigoryeva ES, Vlasenko EV, Sumina MV, O'Hagan JA, Zhang W, Haylock RG, Hunter N (2010b) Cerebrovascular diseases in the cohort of workers first employed at Mayak PA in 1948–1958. Radiat Res 174:851–864

Azizova TV, Muirhead CR, Moseeva MB, Grigoryeva ES, Sumina MV, O'Hagan J, Zhang W, Haylock RJ, Hunter N (2011) Cerebrovascular diseases in nuclear workers first employed at the Mayak PA in 1948–1972. Radiat Environ Biophys 50:539–552

Brenner DJ, Doll R, Goodhead DT, Hall EJ, Land CE, Little JB, Lubin JH, Preston DL, Preston RJ, Puskin JS, Ron E, Sachs RK, Samet JM, Setlow RB, Zaider M (2003) Cancer risks attributable to low doses of ionizing radiation: assessing what we really know. Proc Natl Acad Sci USA 100:13761–13766

Burnham KP, Anderson DR (2002) Model selection and multimodel inference, 2nd edn. Springer, New York

Carr ZA, Land CE, Kleinerman RA, Weinstock RW, Stovall M, Griem ML, Mabuchi K (2005) Coronary heart disease after radiotherapy for peptic ulcer disease. Int J Radiat Oncol Biol Phys 61:842–850

Claeskens G, Hjort NL (2008) Model selection and model averaging. Cambridge University Press, Cambridge

Darby SC, Doll R, Gill SK, Smith PG (1987) Long term mortality after a single treatment course with X-rays in patients treated for ankylosing spondylitis. Br J Cancer 55:179–190

Davis FG, Boice JD Jr, Hrubec Z, Monson RR (1989) Cancer mortality in a radiation-exposed cohort of Massachusetts tuberculosis patients. Cancer Res 49:6130–6136

Hoeting JA, Madigan D, Raftery AE, Volinsky CT (1999) Bayesian model averaging: a tutorial. Statist Sci 14:382–417

ICRP (International Commission on Radiological Protection) (1991) Recommendations of the International Commission on Radiological Protection, ICRP Report 60: Publication 60. Ann ICRP 49:1–3

Ivanov VK, Maksioutov MA, Chekin SY, Petrov AV, Biryukov AP, Kruglova ZG, Matyash VA, Tsyb AF, Manton KG, Kravchenko JS (2006) The risk of radiation-induced cerebrovascular disease in Chernobyl emergency workers. Health Phys 90:199–207

Kaiser JC (2010) MECAN. A software package to estimate health risks in radiation epidemiology with multi-model inference. User manual. Version 0.2, Helmholtz Zentrum München, Neuherberg

Kaiser JC, Jacob P, Meckbach R, Cullings HM (2012) Breast cancer risk in atomic bomb survivors from multi-model inference with incidence data 1958–1998. Radiat Environ Biophys 51:1–14

Kreuzer M, Grosche B, Schnelzer M, Tschense A, Dufey F, Walsh L (2010) Radon and risk of death from cancer and cardiovascular diseases in the German uranium miners cohort study: follow-up 1946–2003. Radiat Environ Biophys 49:177–185

Land CE (2002) Uncertainty, low-dose extrapolation and the threshold hypothesis. J Radiol Prot 22:A129–A135

Little MP, Gola A, Tzoulaki I (2009) A model of cardiovascular disease giving a plausible mechanism for the effect of fractionated low-dose ionizing radiation exposure. PLoS Comput Biol 5(10):e1000539

Little MP, Tawn EJ, Tzoulaki I, Wakeford R, Hildebrandt G, Paris F, Tapio S, Elliott P (2010) Review and meta-analysis of epidemiological associations between low/moderate doses of ionizing radiation and circulatory disease risks, and their possible mechanisms. Radiat Environ Biophys 49:139–153

McGeoghegan D, Binks K, Gillies M, Jones S, Whaley S (2008) The non-cancer mortality experience of male workers at British Nuclear Fuels plc, 1946–2005. Int J Epidemiol 37:506–518

Minuit2 Minimization Package (2008) [V. 5.20.00] http://seal.web.cern.ch/seal/snapshot/work-packages/mathlibs/minuit/

Mitchel REJ, Hasu M, Bugden M, Wyatt H, Little MP, Gola A, Hildebrandt G, Priest ND, Whitman SC (2011) Low-dose radiation exposure and atherosclerosis in ApoE −/− mice. Radiat Res 175:665–676

Muirhead CR, O'Hagan JA, Haylock RGE, Phillipson MA, Willcock T, Berridge GLC, Zhang W (2009) Mortality and cancer incidence following occupational radiation exposure: third analysis of the National Registry for Radiation Workers. Br J Cancer 100:206–212

Pierce DA, Stram DO, Vaeth M (1990) Allowing for random errors in radiation dose estimates for the atomic bomb survivor data. Radiat Res 123:275–284

Pierce DA, Vaeth M, Cologne J (2008) Allowance for random dose estimation errors in atomic bomb survivor studies: a revision. Radiat Res 170:118–126

Preston DL, Shimizu Y, Pierce DA, Suyama A, Mabuchi K (2003) Studies of mortality of atomic bomb survivors. Report 13: solid cancer and noncancer disease mortality: 1950–1997. Radiat Res 160:381–407

Richardson DB, Cole SR (2012) Model averaging in the analysis of leukemia mortality among Japanese A-bomb survivors. Radiat Environ Biophys 51:93–95

Richardson DB, Wing S (1999) Radiation and mortality of workers at Oak Ridge National Laboratory: positive associations for doses received at older ages. Environ Health Perspect 107:649–656

Roger VL, Go AS, Lloyd-Jones DM, Adams RJ, Berry JD, Brown TM, Carnethon MR, Dai S, de Simone G, Ford ES, Fox CS, Fullerton HJ, Gillespie C, Greenlund KJ, Hailpern SM, Heit JA, Ho PM, Howard VJ, Kissela BM, Kittner SJ, Lackland DT, Lichtman JH, Lisabeth LD, Makuc DM, Marcus GM, Marelli A, Matchar DB, McDermott MM, Meigs JB, Moy CS, Mozaffarian D, Mussolino ME, Nichol G, Paynter NP, Rosamond WD, Sorlie PD, Stafford RS, Turan TN, Turner MB, Wong ND, Wylie-Rosett J, On behalf of the American Heart Association Statistics Committee and Stroke Statistics Subcommittee (2011) Heart disease and stroke statistics—2011 update: a report from the American Heart Association. Circulation 123:e18–e209

Schöllnberger H, Stewart RD, Mitchel REJ, Hofmann W (2004) An examination of radiation hormesis mechanisms using a multi-stage carcinogenesis model. Nonlin Biol Toxicol Med 2:317–352

Schöllnberger H, Stewart RD, Mitchel REJ (2005) Low-LET-induced radioprotective mechanisms within a stochastic two-stage cancer model. Dose–Response 3:508–518

Schöllnberger H, Manuguerra M, Bijwaard H, Boshuizen H, Altenburg HP, Rispens SM, Brugmans MJ, Vineis P (2006) Analysis of epidemiological cohort data on smoking effects and lung cancer with a multistage cancer model. Carcinogen 27:1432–1444

Shimizu Y, Kodama K, Nishi N, Kasagi F, Suyama A, Soda M, Grant EJ, Sugiyama H, Sakata R, Moriwaki H, Hayashi M, Konda M, Shore RE (2010) Radiation exposure and circulatory disease risk: Hiroshima and Nagasaki atomic bomb survivor data, 1950–2003. Brit Med J 340:b5349

Talbott EO, Youk AO, McHugh-Pemu KP, Zborowski JV (2003) Long-term follow-up of the residents of the Three Mile Island accident area: 1979–1998. Environ Health Perspect 111:341–348

US NRC (2006) Committee on the biological effects of ionizing radiation. Health risks from exposures to low levels of ionizing radiation, BEIR VII

Vrijheid M, Cardis E, Ashmore P, Auvinen A, Bae J-M, Engels H, Gilbert E, Gulis G, Habib RR, Howe G, Kurtinaitis J, Malker H, Muirhead CR, Richardson DB, Rodriguez-Artalejo F, Rogel A, Schubauer-Berigan M, Tardy H, Telle-Lamberton M, Usel M, Veress K (2007) Mortality from diseases other than cancer following low doses of ionizing radiation: results from the 15-Country Study of nuclear industry workers. Int J Epidemiol 36:1126–1135

Walsh L (2007) A short review of model selection techniques for radiation epidemiology. Radiat Environ Biophys 46:205–213

Walsh L (2011) Radiation exposure and circulatory disease risk based on the Japanese A-bomb survivor mortality data (1950–2003)—neglect of the healthy survivor selection bias. Brit Med J. http://www.bmj.com/content/340/bmj.b5349?tab=responses

Walsh L, Kaiser JC (2011) Multi-model inference of adult and childhood leukaemia excess relative risks based on the Japanese A-bomb survivors mortality data (1950–2000). Radiat Environ Biophys 50:21–35

Walsh L, Kaiser JC, Schöllnberger H, Jacob P (2012) Response to "model averaging in the analysis of leukaemia mortality among Japanese A-bomb survivors" by Richardson and Cole. Radiat Environ Biophys 51:97–100

Yamada M, Wong FL, Fujiwara S, Akahoshi M, Suzuki G (2004) Noncancer disease incidence in atomic bomb survivors, 1958–1998. Radiat Res 161:622–632

ERRATUM

Erratum to: Dose–responses from multi-model inference for the non-cancer disease mortality of atomic bomb survivors

H. Schöllnberger · J. C. Kaiser · P. Jacob · L. Walsh

Erratum to: Radiat Environ Biophys (2012) 51:165–178
DOI 10.1007/s00411-012-0410-4

The original publication of this paper contained some errors. The correct details are given below.

In Table 1, line 1, the ICD-9 numbers for CVD were printed incorrectly. It should correctly read "CVD (ICD-9 430-438)".

In Table 1, line 8, related to cardiovascular diseases excluding CVD it is stated incorrectly that an ERR-quadratic model was used. It should correctly read "EAR-quadratic model[a] [#2]".

In Table 1, right column headed by "Weight", three of the Akaike weights were incorrectly assigned to the models given in the left most column. The correct assignment of the Akaike weights to the models is as follows:

H. Schöllnberger (✉) · J. C. Kaiser · P. Jacob
Helmholtz Zentrum München, Department of Radiation Sciences, Institute of Radiation Protection, 85764 Neuherberg, Germany
e-mail: schoellnberger@helmholtz-muenchen.de

L. Walsh
BfS-Federal Office for Radiation Protection, Neuherberg, Germany

Published online: 15 November 2012

🌱 Springer

Table 1 For both biological endpoints, the preferable final non-nested models are shown with related final deviances (dev), difference in final deviances (Δdev) with respect to the model with the smallest deviance, number of model parameters (N_{par}), AIC-values, difference in AIC-values (ΔAIC) with respect to the model with the smallest AIC-value, and Akaike weights

	dev	Δdev	N_{par}	AIC	ΔAIC	Weight
CVD (ICD-9 430-438)						
ERR-LNT model [#1]	3569.51	3.46	22	3613.51	1.46	0.2628
ERR-quadratic model [#2]	3570.14	4.09	22	3614.14	2.09	0.1918
ERR-step model [#6], $D_{th} = 0.62$ Gy	3566.05	0	23	3612.05	0	0.5454
Preston's ERR-LNT model	3599.58	33.53	30	3659.58	47.53	–
Cardiovascular diseases excluding CVD (390–429, 440–459)						
EAR-LNT model[a] [#1]	3693.73	0	17	3727.73	0	0.3619
EAR-quadratic model[a] [#2]	3694.05	0.32	17	3728.05	0.32	0.3084
EAR-threshold model [#5], $D_{th} = 2.0$ Gy	3695.0	1.27	17	3729.0	1.27	0.1918
EAR-step model [#6], $D_{th} = 2.19$ Gy	3695.66	1.93	17	3729.66	1.93	0.1379
Preston's ERR-LNT model	3709.71	15.98	30	3769.71	41.98	–

As a comparison, the values are also shown for Preston's ERR-LNT models. Note that for cerebrovascular disease, the three preferable models are ERR models; for cardiovascular diseases excluding CVD, the four preferable non-nested models are EAR models. The numbers in brackets refer to the eleven dose–responses depicted in Fig. 1

[a] Contains an age-dependent dose-effect modifier

44. Walsh L, Kaiser JC, Schöllnberger H & Jacob P. Response to "model averaging in the analysis of leukaemia mortality among Japanese A-bomb survivors" by Richardson and Cole. Radiat. Environ. Biophys. 51, 97-100, 2012

LETTER TO THE EDITOR

Response to "model averaging in the analysis of leukaemia mortality among Japanese A-bomb survivors" by Richardson and Cole

L. Walsh · J. C. Kaiser · H. Schöllnberger · P. Jacob

We would like to thank Drs. Richardson and Cole (Richardson and Cole 2011) for taking an interest in a recent paper on multi-model inference (MMI) based on the Japanese A-bomb data for leukaemia mortality from members of our group of research collaborators (Walsh and Kaiser 2011). We also appreciate the time that they took to consider our methodology. This methodology has been successfully applied in many other fields of research—physics, biology, environmental science, etc.,—where one can find a large number of papers (e.g. Liddle et al. 2006; Zhang and Townsend 2009; Lavoué and Droz 2009). However, we consider the application to be new in the field of radiation epidemiology and are particularly interested in refining and improving our initial approach. We prefer to use the MMI terminology rather than "model averaging" since model averaging implies that the related uncertainties from model combinations are reduced—in reality with MMI, the uncertainties are increased to account for uncertainties between several models that describe the data almost equally well.

Richardson and Cole correctly state in their comments that "model averaging is one approach to characterizing uncertainty in risk estimates in epidemiological studies in which there is low statistical power to discriminate between alternative model forms." Therefore, we are very surprised and concerned that they caution against our approach in general and state that both of our recommendations concerning the choice of models for risk assessment should be viewed cautiously. Their arguments are based on two examples: one using two models from the appendix of Richardson et al. (2009) and another offering a simply constructed hypothetical numerical illustration of how our approach can lead to biased results. We will consider these two points below and also a third point that illustrates how our initial approach can be improved.

Example 1: using two models in the appendix A2 of Richardson et al. (2009)

Richardson et al. (2009) specifically addressed the distinction between a modelling approach that they consider to minimize bias in estimation of an association and an approach that focuses on overall goodness of fit. In their analysis of the A-bomb leukaemia mortality data, they adjusted for proximal versus distal location while previous analyses, which did not seem to be cited, had not. Their adjustment was achieved with a four-level variable in the baseline function, which indicated proximal compared to distal location at the time of bombing in each city. The present authors have reproduced the fit of this model and found that the two location parameters for Nagasaki were not statistically significant (p-value = 0.23, 0.15).

Richardson and Cole noted that "prior research *suggested* that location was a potential confounder of the radiation dose-leukemia association, because rural (i.e. distal) location was a determinant of estimated DS02 dose and rural cohort members *may have* different mortality risks than urban." They state that "adjustment for this variable did not substantially improve overall model

L. Walsh (✉)
Federal Office for Radiation Protection,
85764 Neuherberg, Germany
e-mail: lwalsh@bfs.de

J. C. Kaiser · H. Schöllnberger · P. Jacob
Department of Radiation Sciences,
Institute of Radiation Protection,
Helmholtz-Zentrum München,
85764 Neuherberg, Germany

goodness of fit, but failure to adjust for it led to a *sub-stantial* change in estimate of the association of primary interest." We point out that changes in "estimates of the association of primary interest" (i.e. combinations of fit parameters) can only be taken to indicate bias (rather than random effects or some unknown combination of bias and random effects), if the fit parameters represent "what would be obtained in a sample so large that random error was negligible" (Greenland 2008). After examining the parameters in Richardson et al. (2009) table A1, page 378, we cannot agree that there were *substantial* changes in the association of primary interest (see Table 1). We observe that β_M changes from 1.1 (95% CI, 0.1; 2.6) in model 1 to 1.4 (95% CI, 0.3; 3.4) in model 2, which is not substantial given the relatively large confidence intervals (CIs) (see Table 1). An analogous argument holds for parameter β_F (Table A1 in Richardson et al. 2009 or Table 1).

Let us take the association of primary interest to be the female ERR at 1 Gy, 25 years after exposure at the age of 30 years. The central estimate for this quantity is arrived at by combining parameters β_F and θ (i.e. $\beta_F \times (1 + \theta)$) given in their table A1, page 378, with 95% CIs. For model 1 (without a location binary indicator variable), it can be seen from Table 1 here that this is 2.26 [=1.2 × (1 + 0.88)], (95% CI: −0.18; 3.53), and for model 2 (with the location binary indicator) 2.66 [=1.6 × (1 + 0.66)], (95% CI: −0.26; 4.02), that is, a 15% change in central estimate. It can be seen from Table 1 that there is an analogous 11% change for the corresponding male quantity. We do not consider these changes of 15 and 11%, or the changes in the parameters between models 1 and 2 (see Table 1), to be substantial, and we cannot rule out that such shifts in risk estimates are caused by random effects. This can also be

seen from the gender-averaged ERR at 1 Gy, 25 years after exposure at the age of 30 years given in Table 4 of Walsh and Kaiser (2011) and repeated here in Table 1, last row, for the same two models. Here, the difference in risk central estimate between models 1 and 2 corresponds to a shift that is only about 10% of the 95% CI span and therefore again not substantial.

It is also noteworthy that both original models also contain a gender effect (via β_M and β_F) in the excess risk part of the model (see Table A1 in Richardson et al. 2009) that is not supported by the data (note the strongly over-lapping CIs in Table 1). Also several baseline parameters are included in these two models: two parameters for a gender-specific spline join at the age of 70 years and two parameters for a gender-specific secular trend that are also not supported by the data (p-values of 0.3, >0.5, 0.4, 0.2). We also note two misprints in the table A1 of Richardson et al (2009) whereby the heading for models 2 and 3 should have been "Estimate (95% CI)" and not "Estimate (90% CI)" as printed. Therefore, the claim of Richardson and Cole that our approach would discount their model 2 when compared to a model that omitted adjustment for location is irrelevant; their model 2 is rejected based on the numerical arguments pointed out above.

We caution against adding possible explanatory covariables (such as distal/proximal location), that are not supported by the data, to a model required for radiation protection, just because of a *suggestion* of a mortality risks that *may be* different. Our MMI approach in Walsh and Kaiser (2011) was intended to lead to a focus on predictive modelling of the outcome, which is indeed the primary goal for researchers (and BEIR, UNSCEAR and ICRP commit-tees) interested in providing a good model for radiation

Table 1 Comparisons of possible associations of primary interest, reproduced from table A1 of Richardson et al. (2009) and Walsh and Kaiser (2011)

Association of primary interest	Model 1 from table A1 Richardson et al (2009)	95% Confidence interval	Model 2 from table A1 Richardson et al. (2009)	95% Confidence interval	Change (%)
β_M	1.1	0.1, 2.6	1.4	0.3, 3.4	21
β_F	1.2	0.1, 2.9	1.6	0.3, 3.8	25
Θ	0.88	0.16, 15.27	0.66	0.1, 5.32	−33
ERR at 1 Gy: males, 25 years since exposure at the age of 30 years = $\beta_M (1 + \theta)$	2.07	−0.30, 3.01	2.32	−0.16, 3.69	11
ERR at 1 Gy females, 25 years since exposure at the age of 30 years = $\beta_F (1 + \theta)$	2.26	−0.18, 3.53	2.66	−0.26, 4.02	15
Gender-averaged ERR at 1 Gy 25 years since exposure at the age 30 years from table 4 (Walsh and Kaiser 2011)	2.11	−0.09, 2.98	2.5	−0.10, 3.59	16

The 95% CIs for the ERR given below have been simulated by the current authors from Wald-type standard errors and parameter correlations, where the correlations between β_M and θ and β_F and θ were high (with correlation coefficients of approximately 0.8)

To find the risks given in the last row below in the original publication, refer to models "BEIR VII, phase 2" with ERR = 2.11 and "Richardson et al. (2009) model 2" with ERR = 2.50 in table 4 of Walsh and Kaiser 2011)

protection purposes. In obtaining a good model for radiation protection, a parsimonious model, with only the explanatory variables that are supported by the data, is usually associated with smaller uncertainties than a model containing many extra (possibly) explanatory covariables that are not supported by the data. Of course, if one is then interested in non-significant effects, one can examine these by including them in the preferred parsimonious model to put an upper or lower limit on the central estimates. This is particularly useful for meta-analyses where a study with either non-significant risks or non-significant risk effect modifiers can then be included numerically and with CIs. In the USA, compensation claims for cancer from occupational exposure are often based on the 99% CIs of the probability of causation (Kocher et al. 2008). In this situation, an accurate determination of uncertainties is crucial. We argue that this can be best achieved by applying MMI to the risk estimates of carefully selected parsimonious models.

Example 2—a simply constructed numerical illustration: the hypothetical example

Richardson and Cole offered a simple hypothetical example of how our approach can lead to biased results. We agree that averaging their simple models 1 and 2 (as provided in their comments, Richardson and Cole 2011) is misleading. Unfortunately, Richardson and Cole did not provide the Akaike Information Criterion (AIC) of the baseline model, which is necessary to put the results into perspective. Therefore, we have numerically reproduced their logistic regression analysis. We agree with odds ratios of 1.24 (p-value = 0.35) for their crude model 1 with X and 1.01 (p-value > 0.5) for their adjusted model 2 with X and Z. But since the AIC of the baseline model is 678.1, we do not consider neither the crude model 1 (AIC = 679.1) nor the adjusted model 2 (we calculate AIC = 678.7 in line with weights of 45% for crude model 1 and 55% for adjusted model 2) an improvement in fit, which is good enough to lead to an inclusion in an independently constructed MMI. In particular, contrary to the claim of Richardson and Cole, the adjusted model 2 does not explain the data adequately. We will illustrate our point more rigorously in the next section, by applying dedicated model selection criteria.

Example 3: using the hypothetical example to demonstrate an improved methodology for model selection

The hypothetical data in Table 1 of Richardson and Cole (2011) have been generated with a known "true" model that can easily be reconstructed. In this exceptional case,

the true model can be used as an additional criterion to assess the adequacy of several candidate models for MMI. In reality, the true model is not known and risk inference from a group of several plausible models appears justified. The selection of models for this so-called group of Occam (Hoeting et al. 1999; Kaiser et al. 2011) can be done in different ways. In Walsh and Kaiser (2011), we chose published risk models and simply ranked them according to their AIC. We are aware that parameter parsimony was not always a key issue for the authors of these models. Thus, application of the AIC criterion on hindsight might have discarded good candidate models. On the other hand, models with unsupported features might have been considered instead. A selection of leukaemia risk models based on rigorous selection rules has not yet been performed.

In two recent risk studies with A-bomb survivors data on breast cancer incidence (Kaiser et al. 2011) and on mortality for non-cancer diseases (Schöllnberger et al. 2011), we attempted to partly make up for these shortcomings. We proposed a protocol to select only those models for Occam's group that possess features relevant for cancer (respectively non-cancer) aetiology. It is based on a series of pair-wise likelihood ratio tests (LRT) to eliminate nested models. The tests were carried out on a high level of 95% probability to exclude spurious properties of risk estimates with weak statistical support. As suggested by Richardson and Cole, the selection protocol is "focused on a comparison of models that employed an identical approach to confounder control" since actually all confounders are judged by the same assessment criteria. We will demonstrate the selection protocol with Poisson regression by assuming that this example can be used to calculate the outcome rates for the four data groups with different combinations of the X, Z covariables and an observation period of 1 year (see Table 2). In Poisson regression, the excess relative risk ERR = OR − 1 is the quantity of interest. For a rare disease (number of cases ≪ number of persons at risk), the odds ratio from logistic regression is a good approximation of the odds ratio from Poisson regression. For logistic regression, the results for the true model are given below in addition to the modelling results of the previous section.

The selection protocol involves a series of LRTs to improve a simple baseline model with additional parameters (for details see Kaiser et al. 2011). A parameter is accepted as an improvement with a probability of 95%, if the deviance is lowered by at least 3.84 points. We have applied LRTs to a number of models, including models that correspond to the original models 1 and 2 of Richardson and Cole (see Table 2). The sole model eligible for Occam's group applies an adjustment factor $2Z − 1$ to the excess relative risk ERR_X. It explains the data almost completely with a deviance of 0.01 and two adjustable

Table 2 Number of parameters, Poisson deviance and excess cases caused by exposure X for six candidate models of the hypothetical example

Model	No. of parameters	Poisson deviance	Excess cases
bsl	1	6.17	0.0
$\text{bsl} \times (1 + \text{ERR}_X \times X)$[a]	2	5.22	9.7
$\text{bsl} \times (1 + \text{ERR}_Z \times Z)$	2	3.10	0.0
$\text{bsl} \times (1 + (2Z - 1) \times \text{ERR}_X \times X)$[c]	2	0.01	10.4
$\text{bsl} \times (1 + \text{ERR}_X \times X + \text{ERR}_Z \times Z)$[b]	3	3.03	−3.5
$(1 - Z) \times \text{bsl}_0 \times (1 + \text{ERR}_{X_0} \times X) + Z \times \text{bsl}_1 \times (1 + \text{ERR}_{X_1} \times X)$	4	0.00	10.3

[a] Corresponds to crude model 1 of Richardson and Cole (2011) with AIC = 679.1

[b] Corresponds to adjusted model 2 of Richardson and Cole (2011) with AIC = 678.7

[c] "True" model

parameters bsl and ERR_X. The estimates are 0.409 for ERR_X and 0.0956 for bsl. The model has been identified correctly by the selection protocol, and model averaging is not required. Due to a non-negligible correlation coefficient of 0.03 to outcome Y, 10 of the 106 cases are caused by exposure X (Table 2). For a moderate correlation coefficient of 0.53 between exposure X and covariate Z, Poisson regression is able to separate their effects. We also applied the selection protocol in logistic regression with models corresponding to those of Table 2. Minor differences in the deviance distance from the baseline deviance were caused by slightly different definitions of the odds ratio for logistic regression compared to Poisson regression. But the (almost) true model $\text{bsl} + (2Z - 1) \times \ln(\text{OR}_X) \times X$ for logistic regression has been identified with a deviance of 6.6 points lower than the baseline model (deviance 676.1) with the estimates of 0.107 for $\exp(\text{bsl})$ and 1.49 for OR_X.

Concluding remarks

Model selection bias can be defined as the bias introduced by using the data to select a single preferred model from a multiplicity of models employing many predictor variables. For any one model, attempting to minimize all small implications on the risk estimate, which could be due to either confounding bias and/or random effects—in an unknown way, leads to an increase in that models uncertainty. We chose to avoid this and prefer to account for the possibly large model selection bias via MMI. After careful consideration, in this reply, of the points made by Richardson and Cole (2011), we stand by and reinforce the approach and recommendations given in Walsh and Kaiser (2011).

We agree with Richardson and Cole that our method discounted models that employed a background stratified approach to adjustment for confounding factors. The discussion section in Walsh and Kaiser (2011) fully acknowledged this and identified this as an area needing

more research. We hope that interesting alternatives, including a hierarchical regression approach, can be useful here and would be very interested in seeing the results of applying such a method to the data-set that we considered.

References

Greenland S (2008) Invited commentary: variable selection versus shrinkage in the control of multiple confounders. Am J Epidemiol 167(5):523–529; Discussion 30–31

Hoeting JA, Madigan D, Raftery AE, Volinsky CT (1999) Bayesian model averaging: a tutorial. Stat Sci 14(4):382–417

Kaiser JC, Jacob P, Meckbach R, Cullings HM (2011) Breast cancer risk in atomic bomb survivors from multi-model inference with incidence data 1958–1998. Radiat Environ Biophys 56(23): 365–379. doi:10.1007/s00411-011-0387-4

Kocher D, Apostoaei AI, Henshaw RW, Hoffman FO, Schubauer-Berigan MK, Stancescu DO, Thomas BA, Trabalka JR, Gilbert ES, Land CE (2008) Interactive radioepidemiological program (IREP): a web-based tool for estimating probability of causation/assigned share of radiogenic cancers. Health Phys 95(1):119–147

Lavoué J, Droz PO (2009) Multimodel inference and multimodel averaging in empirical modeling of occupational exposure levels. Ann Occup Hyg 53(2):173–180

Liddle AR, Mukherjee P, Parkinson D, Wang Y (2006) Present and future evidence for evolving dark energy. Phys Rev D 74:123506

Richardson D, Cole BS (2011) Model averaging in the analysis of leukaemia mortality among Japanese A-bomb survivors. Radiat Environ Biophys 56(23):136–158. doi:10.1007/s00411-011-0395-4

Richardson D, Sugiyama H, Nishi N, Sakata R, Shimizu Y, Grant EJ, Soda M, Hsu WL, Suyama A, Kodama K, Kasagi F (2009) Ionizing radiation and leukemia mortality among Japanese atomic bomb survivors, 1950–2000. Radiat Res 172(3):368–382

Schöllnberger H, Kaiser JC, Walsh L, Jacob P (2011) Dose responses from multi-model inference for the non-cancer disease mortality of atomic bomb survivors (submitted)

Walsh L, Kaiser JC (2011) Multi-model inference of adult and childhood leukaemia excess relative risks based on the Japanese A-bomb survivors mortality data (1950–2000). Radiat Environ Biophys 50(1):21–35

Zhang Z, Townsend JP (2009) Maximum-likelihood model averaging to profile clustering of site types across discrete linear sequences. PLOS Comp Biol 5(6):e1000421

45. Sogl M, Taeger D, Pallapies D, Brüning T, Dufey F, Schnelzer M, Straif K, Walsh L & Kreuzer M. Quantitative relationship between silica exposure and lung cancer mortality in German Uranium miners, 1946–2008, Br. J. Cancer. 107, 1188-1194, 2012

Quantitative relationship between silica exposure and lung cancer mortality in German uranium miners, 1946–2003

M Sogl*,1, D Taeger2, D Pallapies2, T Brüning2, F Dufey1, M Schnelzer1, K Straif3, L Walsh1 and M Kreuzer1

[1]Department of Radiation Protection and Health, BfS, Federal Office for Radiation Protection, Neuherberg 85764, Germany; [2]Institute for Prevention and Occupational Medicine of the German Social Accident Insurance, Institute of the Ruhr University Bochum (IPA), Bochum 44789, Germany; [3]IARC, International Agency for Research on Cancer, Lyon 69372, France

BACKGROUND: In 1996 and 2009, the International Agency for Research on Cancer classified silica as carcinogenic to humans. The exposure–response relationship between silica and lung cancer risk, however, is still debated. Data from the German uranium miner cohort study were used to further investigate this relationship.

METHODS: The cohort includes 58 677 workers with individual information on occupational exposure to crystalline silica in $mg\,m^{-3}$-years and the potential confounders radon and arsenic based on a detailed job-exposure matrix. In the follow-up period 1946–2003, 2995 miners died from lung cancer. Internal Poisson regression with stratification by age and calendar year was used to estimate the excess relative risk (ERR) per dust-year. Several models including linear, linear quadratic and spline functions were applied. Detailed adjustment for cumulative radon and arsenic exposure was performed.

RESULTS: A piecewise linear spline function with a knot at $10\,mg\,m^{-3}$-years provided the best model fit. After full adjustment for radon and arsenic no increase in risk $< 10\,mg\,m^{-3}$-years was observed. Fixing the parameter estimate of the ERR in this range at 0 provided the best model fit with an ERR of 0.061 (95% confidence interval: 0.039, 0.083) $> 10\,mg\,m^{-3}$-years.

CONCLUSION: The study confirms a positive exposure–response relationship between silica and lung cancer, particularly for high exposures.

British Journal of Cancer (2012) **107,** 1188–1194. doi:10.1038/bjc.2012.374   www.bjcancer.com
Published online 28 August 2012
© 2012 Cancer Research UK

Keywords: epidemiology; silica; lung cancer; dose–response relationship; uranium miners

In 1996, the International Agency for Research on Cancer (IARC) classified crystalline silica, inhaled in the form of quartz from occupational sources, as carcinogenic to humans (group 1) with the lung as target organ (IARC, 1997). However, IARC noted a lack of extensive exposure–response data from epidemiological studies, differences in exposure metrics between the studies as well as inconsistencies in the exposure–response relationship across the studies. Since then, a number of individual studies (Ulm *et al*; 1999; Rice *et al*, 2001; Pukkala *et al*, 2005; Chen *et al*, 2007; Mundt *et al*, 2011; Vacek *et al*, 2011) on the relationship between occupational inhaled crystalline silica and lung cancer risk have been published, in addition to a series of meta- or pooled analyses (Brüske-Hohlfeld *et al*, 2000; Steenland *et al*, 2001; Kurihara and Wada, 2004; Lacasse *et al*, 2009; Erren *et al*, 2011) and reviews (Soutar *et al*, 2000; Pelucchi *et al*, 2006; Brown, 2009). In 2012 the IARC reconfirmed the classification of silica (IARC, 2012). However, there is still a debate on the shape of the exposure–response relationship, especially in the low exposure range.

The two most recent and currently largest analyses addressing the shape of the relationship between cumulative silica exposure and lung cancer are a pooled analysis of 10 cohort studies by Steenland *et al* (2001) and a meta-analysis of 4 cohort and 6 case–control studies by Lacasse *et al* (2009). The meta-analysis showed a statistically significant increased risk $> 1.8\,mg\,m^{-3}$-years with a plateau $> 6\,mg\,m^{-3}$-years. The interpretation of these findings is limited by differences in the quality of silica exposure assessment reported in the original studies and heterogeneity across studies (Lacasse *et al*, 2009). The pooled analysis by Steenland *et al* (2001) included 65 980 workers and 1079 lung cancer deaths over several industrial settings. There was a considerable heterogeneity between the various studies. An increase in risk with the natural logarithm of cumulative silica concentration was observed.

The German uranium miner cohort (Wismut cohort) study has a comparable size (nearly 60 000 members) to the pooled analysis (Steenland *et al*, 2001); it includes a large number of lung cancer deaths ($n = 2995$) and provides a long follow-up with almost 2 million person-years. Individual information on occupational exposure to crystalline silica is available, which allows a detailed investigation of the shape of the dose–response relationship with particular focus on the low-dose range in a single study. Individual information on other known occupational carcinogens such as exposure to radon and arsenic dust is available and can be accounted for in the risk analyses. In addition, there is some information about smoking from a nested case–control study on lung cancer in the Wismut cohort (Schnelzer *et al*, 2010), which allows the evaluation of potential confounding by smoking. The aim of the present analyses is to investigate the shape of the exposure–response relationship between crystalline silica exposure and lung cancer mortality and the combined effect of silica and radon.

Epidemiology

MATERIALS AND METHODS

Cohort definition and mortality follow-up

The Wismut cohort has been described in detail (Grosche *et al*, 2006; Kreuzer *et al*, 2008, 2010a, b; Walsh *et al*, 2010a, b). In brief, the cohort includes 58 987 males employed for at least 180 days between 1946 and 1989, selected as a random sample stratified by date of first employment, place of work and area of mining. Every cohort member contributes to the time at risk starting at the date of employment plus 180 days and ending at the earliest of date of death, date of loss to follow-up or the end of the follow-up period (31 December 2003). Information on the vital status of individuals was obtained from local registration offices, whereas death certificates were obtained from the responsible Public Health Administrations and the pathology archive of the Wismut company.

Information on exposure to dust and radiation

The silica and respirable fine dust content in the Wismut mines varied between time periods and mining regions and also between different mines within a given district, and even between regions within a specific mine (Dahmann *et al*, 2008). In the early period (1946–1954) the situation in mines was aggravated by poor industrial hygiene (i.e., dry drilling) and also by extremely low ventilation rates, i.e., air velocities $<0.1\,\mathrm{m\,s}^{-1}$ (Bauer, 1997; Dahmann *et al*, 2008). Thus, the dust exposures for the Wismut miners show high shift concentration averages for crystalline silica of well $>2\,\mathrm{mg\,m}^{-3}$ in many mines in the early times. After 1955 the situation improved continuously with the introduction of wet drilling and increasing mine ventilation rates up to about $0.3\,\mathrm{m\,s}^{-1}$. This resulted in a decrease of dust concentrations by $>97\%$ (Bauer, 1997; Dahmann *et al*, 2008) as illustrated in Figure 1.

From 1960, systematic measurements of silica and fine dust concentrations performed by the Wismut company were available. Major efforts were undertaken to retrospectively quantify exposures to silica and fine dust before 1960, including reconstruction of historical workplaces and simulating ventilation conditions (Bauer, 1997; Dahmann *et al*, 2008). Using these estimates and measurements, a detailed job-exposure matrix (JEM) was developed (HVBG and BBG, 2005). This JEM provides annual exposure values for each calendar year, each place of work and job type (>900 different jobs and several mining facilities). Annual and cumulative exposures are given in units of dust-years that are $1\,\mathrm{mg\,m}^{-3}$ silica dust or fine dust over a time period of 220 shifts of 8 h. Differences in the number of shifts and daily working hours in the different calendar years were accounted for. Figure 1 shows the mean annual exposure values for silica dust in the cohort. Silica dust is a proportion of the total measured respirable fine dust and therefore highly correlated with fine dust exposure ($r>0.95$). Consequently, the variable respirable fine dust is excluded from all risk analyses.

Arsenic exposure occurred only in mines located in Saxony (Dahmann *et al*, 2008). The arsenic content in the deposit and data on dust exposure were used as proxy variables to estimate the arsenic exposure within the JEM because only a few measurements of arsenic levels in air were available. The cumulative exposure to arsenic dust is quantified in dust-years, where 1 dust-year equals an exposure of $1\,\mu\mathrm{g\,m}^{-3}$ over 220 shifts of 8 h (HVBG and BBG, 2005).

Information on exposures to ionising radiation is based on a separate JEM similar to that for dust. This JEM includes information on exposure to radon and its progeny in working level month (WLM), external gamma radiation in mSv and long-lived radionuclides in $\mathrm{kBq\,h\,m}^{-3}$ (HVBG and BBG, 2005; Lehmann *et al*, 1998). Estimates for radon exposure were based on
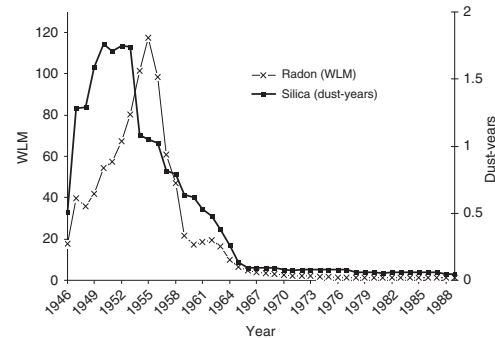

Figure 1 Mean annual exposure to silica dust in $\mathrm{mg\,m}^{-3}$-years and radon and its progeny in WLM among exposed cohort members with respect to silica ($n=58\,677$) and radon ($n=50\,468$).

systematic measurements in the air from 1955 onwards, and on detailed expert rating in the years before (HVBG and BBG, 2005). A WL is defined as $1.3\times10^{3}\,\mathrm{MeV}$ of potential alpha energy per litre of air. One WLM corresponds to exposure to 1 WL during 1 month, i.e., 170 working hours. The annual very high mean exposure values for radon and its progeny in the early years decreased after 1955 due to the introduction of ventilation measures (see Figure 1). Exposures to external gamma and long-lived radionuclides are not considered in the risk analyses due to negligible doses to the lung compared with the radon progeny.

Statistical methods

Several RR models based on internal Poisson regression have been applied here to investigate the shape of the relationship between cumulative silica dust exposure and lung cancer mortality risk and its interaction with radon. The confidence intervals (CIs) were of the Wald-type at the 95% level. Age was stratified in 5-year groups and individual calendar year in 58 categories. Analogously to previous analyses on lung cancer (Grosche *et al*, 2006; Walsh *et al*, 2010a, b) a 5-year lag was used in calculating the cumulative exposures to allow for a latent period between exposure and death. Lag times of 0, 10 and 15 years were also considered. Information on silica and arsenic dust was missing for 310 individuals of the cohort. Therefore, these individuals were excluded from all analyses leaving 58 677 miners out of 58 987 and 2995 out of 3016 lung cancer deaths. All models were fitted with the AMFIT module of the EPICURE software (Preston *et al*, 1998).

Main models for risk of lung cancer and silica In a first step, the RR of lung cancer death was estimated by a simple model with silica dust in categories. The following *a priori* defined cut-points were used for cumulative silica dust in $\mathrm{mg\,m}^{-3}$-years (0–0.5, 0.5–2, 2–5, 5–10, 10–20, 20–30 and 30+). In a second step, several excess relative risk (ERR) models with baseline stratification by age and calendar year were used. If $r(a, y, \mathrm{sil, rn, ars})$ is the specific lung cancer mortality rate for age, a; year, y; silica, sil; radon, rn; arsenic, ars; and $r_0(a, y) = r(a, y, 0, 0, 0)$ is the baseline disease rate for non-exposed individuals, then

$$r(a, y, \mathrm{sil, rn, ars}) = r_0(a, y) \cdot \{1 + \mathrm{ERR(sil, rn, ars)}\}.$$

Here, *ERR* is the excess RR for which several different functions of sil were tested:

Epidemiology

1. A linear function ERR (sil) $= \beta \cdot$ sil, where sil is the total cumulative exposure to silica dust in $mg\,m^{-3}$-years.
2. A piecewise linear spline function with one knot.

$$ERR\,(sil) = \begin{cases} \beta_1 \cdot sil & sil \leqslant sil_k \\ \beta_1 \cdot sil + \beta_2 \cdot (sil - sil_k) & sil > sil_k \end{cases}$$

Different locations of the knots $sil_k \in \{5, 7, 8, 9, 10, 11, 12, 15\}$ in $mg\,m^{-3}$-years were tested. A model in which β_1 was fixed at zero was also fitted.

3. Quadratic as well as linear–quadratic functions of cumulative silica exposure.

To adjust for potential confounding in the models above, the cumulative radon and arsenic exposures were first included as continuous variables in a linear way. Previous analyses on the relationship between lung cancer and cumulative radon exposure in the Wismut cohort provided evidence for a model that is linear in radon exposure with the exponential effect modifiers age at median exposure (or attained age), time since median exposure and radon exposure rate (Walsh *et al*, 2010a, b). Therefore, these three exponential effect modifiers of radon exposure were then additionally included to achieve better adjustment for the major confounder radon. The preferred models were identified by applying model techniques for nested models, i.e., the likelihood ratio test (see Walsh, 2007 for an explanation). Adjustment for confounders was performed in an additive and in a multiplicative way. As the additive model provided a better fit, only these results are shown.

Effect modification   Effect modification by age, time and exposure rate was present in the radon-induced lung cancer risk. These factors may also modify the effect of the silica-induced lung cancer risk. Therefore, all possible combinations of effect modification on silica and radon were tested. The effect modifiers were calculated in analogy to the calculations for radon (Walsh *et al*, 2010b). The aim was to obtain the best suited and most parsimonious model to describe the combined effect of silica and radon.

Quantification of the combined effect of silica and radon   In a first step, the combined effect of silica and radon on the risk of lung cancer death was described by simple categorical analyses with combinations of radon (<50, $50-1000$ and >1000 WLM) and silica dust (<10, $10-20$, $20-30$ and $30+$ $mg\,m^{-3}$-years) without consideration of arsenic and risk effect modifiers. To gain more insight into the form (additive or multiplicative) of the interaction between silica and radon, a geometric mixture model that is piecewise linear in silica (with a knot at $10\,mg\,m^{-3}$-years) and linear in radon with effect modifiers for silica and radon and adjustment for arsenic, as described above, was fitted:
$1 + ERR_{mix} = (1 + ERR_{mult})^{\lambda} \, (1 + ERR_{add})^{1-\lambda}$

The mixing parameter λ ($0 \leqslant \lambda \leqslant 1$) was first set to 0.0 (additive) and was then enhanced up to 1.0 (multiplicative) in 0.1-length steps.

RESULTS

Among the 58 677 cohort members, 20 748 died overall between 1946 and 2003 while 2995 died from lung cancer. The cause of death was available for 93.6% of the miners. In all, 4.7% were lost to follow-up. The cohort members contributed 1 984 687 person-years with an average follow-up period of 34 years, and the mean duration of employment was 14 years. All cohort members were exposed to silica dust at some time, because silica occurred not only underground but also in appreciably lower concentrations at the surface (Table 1).

In Table 2 the risk of lung cancer death in relation to cumulative silica dust exposure is given. A positive trend could be observed.

Table 1 Exposures of the Wismut cohort, 1946–2003

Cumulative exposure to	Exposed (%)	Mean	Median	Max	s.d.
Silica ($mg\,m^{-3}$-years)	100	5.9	1.8	56	8.0
Radon (WLM)	86	280	33	3224	445
Arsenic ($\mu g\,m^{-3}$-years)	31	121	67	1417	145

Abbreviation: WLM = working level months.

Without adjustment for radon and arsenic a statistically significant increased RR, compared with the reference category of $0-0.5\,mg\,m^{-3}$-years was present in all categories except for the category $0.5-2\,mg\,m^{-3}$-years (see also Figure 2A). After adjustment for the major confounder radon, all estimates decreased markedly, but remained statistically significant in the exposure categories $10-20$, $20-30$ and $30-56\,mg\,m^{-3}$-years. Additional adjustment for cumulative arsenic exposure led to a significant improvement of the model fit quality, but only to a small decrease of the RR (Table 2). More detailed adjustment for radon including the effect modifiers age at median exposure, time since median exposure and radon exposure rate, led to a further decrease of the silica-induced risk, showing a statistically significant increased risk only in the categories $20-30$ and $30-56\,mg\,m^{-3}$-years.

As the categorical analyses indicated a non-linear exposure response relationship (Figure 2A), two-line spline models with different knots were applied and compared by model selection procedures (Walsh, 2007). Models with silica dust as linear spline with one knot at 7, 8, 9 and $10\,mg\,m^{-3}$-years yielded in statistically better fits compared with the pure linear model. After adjustment for radon and arsenic a spline model with a knot at $10\,mg\,m^{-3}$-years provided the best fit. Table 3 provides information on the risk estimates for the model parameters β_1 and β_2 and the corresponding RRs at 5 and $15\,mg\,m^{-3}$-years based on the spline model, with a knot at $10\,mg\,m^{-3}$-years. Without adjustment for radon and arsenic, the RR was 1.34 (95% CI: 1.20; 1.47) at $5\,mg\,m^{-3}$-years and 2.44 (95% CI: 1.96; 2.61) at $15\,mg\,m^{-3}$-years compared with 0 dust-years. The RRs decreased after simple adjustment for radon and arsenic. After more detailed adjustment for radon, i.e., inclusion of the three exponential effect modifiers the silica risk estimates further decreased to 0.97 (95% CI: 0.86; 1.08) at $5\,mg\,m^{-3}$-years and 1.24 (95% CI: 0.98; 1.49) at $15\,mg\,m^{-3}$-years, but yielded significant RRs for cumulative exposures $>16\,mg\,m^{-3}$-years (Figure 2B). As β_1 decreased to -0.006 (-0.028; 0.015) after full adjustment, a model in which β_1 was fixed at zero was fitted additionally. The preferred model was achieved after detailed adjustment for the confounder radon (with effect modifiers) and arsenic and β_1 fixed at zero between 0 and $10\,mg\,m^{-3}$-years. Quadratic and linear quadratic models of cumulative silica exposure did not result in an improvement in goodness of fit.

The best suited and most parsimonious model, to describe both effects of silica and radon and their corresponding time- and dose-rate-related effect modifiers, was piece-wise linear in cumulative silica dust with one knot at $10\,mg\,m^{-3}$-years, with the initial slope fixed at 0 below $10\,mg\,m^{-3}$-years including attained age as exponential effect modifier. Table 3 shows that the preferred model had a deviance of 30 592.5 and one parameter less than the model with the optimised initial slope (deviance = 30 592.3). It was linear in radon with exponential effect modifiers that depend on time since median exposure and radon-exposure rate. The silica-induced lung cancer risk decreases with increasing attained age (Table 3).

In Table 4 the results of the categorical analyses on the combined effect of radon and silica are shown. There was an increase of the RR of silica (see increase in columns), and an increase of the RR of radon (see rows). The risk in the highest silica and radon exposure category ($>30\,mg\,m^{-3}$-years and

Table 2 Risk of death from lung cancer by cumulative silica dust exposure in mg m^{-3}-years by categories, 1946–2003

Silica dust in mg m^{-3}-years	Mean	Person-years	# of cases	RR 95% CI unadjusted	RR 95% CI adjusted for radon	RR 95% CI adjusted for radon, arsenic	RR 95% CI adjusted for radon, arsenic with effect modifiers
0–0.5	0.1	681 780	137	1.00 Reference	1.00 Reference	1.00 Reference	1.00 Reference
0.5–2	1	394 559	283	1.12 (0.89–1.35)	1.09 (0.86–1.31)	1.08 (0.86–1.31)	0.95 (0.77–1.12)
2–5	3	274 523	356	1.26 (1.00–1.51)	1.15 (0.91–1.38)	1.13 (0.89–1.37)	0.96 (0.78–1.13)
5–10	7	238 032	430	1.38 (1.10–1.66)	1.07 (0.83–1.30)	1.05 (0.81–1.28)	0.86 (0.67–1.04)
10–20	14	264 140	936	2.45 (1.98–2.92)	1.53 (1.19–1.88)	1.47 (1.13–1.81)	1.14 (0.87–1.40)
20–30	24	108 502	664	3.76 (3.02–4.49)	2.19 (1.64–2.75)	2.05 (1.51–2.60)	1.51 (1.08–1.94)
30–56	34	23 151	189	4.71 (3.62–5.80)	2.91 (1.96–3.83)	2.79 (1.87–3.70)	2.02 (1.28–2.75)
Total	5.9	1 984 687	2995				

Abbreviations: Adj. = adjusted; CI = confidence interval; RR = relative risk. RR, baseline stratified on age in 5-year groups and individual calendar year in 58 categories. RR adj. for radon (last-but-two column), for radon and arsenic (next-to-last column) and for radon with exponential inclusion of the effect modifiers age at median exposure, time since median exposure and radon exposure rate and arsenic (last column) as continuous variables in an additive way.
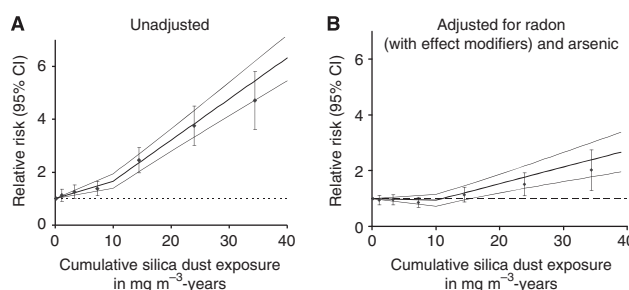

Figure 2 RR of death from lung cancer ($n = 2995$) in relation to cumulative silica dust without adjustment (**A**) and with additive adjustment for radon (with the effect modifiers age at median exposure, time since median exposure and radon exposure rate) and arsenic (**B**). Categorical analysis (0–0.5, 0.5–2, 2–5, 5–10, 10–20, 20–30 and 30 +) and linear spline model (bold line) with 95% confidence limits (fine lines).

> 1000 WLM) is 4.6-fold (95% CI: 3.7–5.4) higher compared with the risk in the reference category (< 10 mg m^{-3}-years and < 50 WLM). With the geometric mixture model, the form of the interaction between silica and radon was further investigated. The purely additive model provided a statistically significant better fit compared with the multiplicative model. These results indicate that the effects of silica and radon exposure are more likely to be additive rather than multiplicative.

DISCUSSION

The analysis of the Wismut uranium miner cohort study showed a statistically significant positive exposure–response relationship between silica and lung cancer for high cumulative silica exposures. Analyses on the combined effects of radon and silica provided evidence for a more additive rather than multiplicative relationship of both effects.

In contrast to other studies, beside silica a strong second risk factor – radon – was present in the cohort. Both variables correlate over time ($r = 0.79$) with high exposures in the very early years and low exposures later (Figure 1). Thus, the major challenge in the statistical analyses was to fully account for this strong confounder. The large size of the cohort and the detailed information on both risk factors enabled this adjustment. Owing to the relatively high correlation of radon and dust over time and the fact that radon is a stronger risk factor than silica, it cannot be ruled out that adjustment for radon including the three effect modifiers may have led to some over adjustment. Therefore, a small increase in risk even in the range < 10 mg m^{-3}-years cannot be ruled out.

Arsenic exposure was high in the early years and decreased later, however, the correlation with silica was low ($r = 0.46$), and arsenic itself a weak risk factor. The decrease in the silica-induced lung cancer risk was small after adjustment for arsenic. Restriction of the cohort data to individuals without any arsenic exposure ($n = 40\,753$) showed a very similar exposure–response pattern (RR at 15 mg m^{-3}-years = 1.35; 95% CI: 1.17–1.53) compared with the non-restricted data (RR = 1.31; 95% CI: 1.20–1.42) for the fully adjusted model.

The preferred model indicated that attained age modifies the silica-induced risk. With increasing attained age, the risk for silica-induced lung cancer decreases. Again, owing to the high timely correlation of both factors and the fact that radon is a stronger risk factor, it cannot be resolved whether there could be other modifying factors for the silica-induced lung cancer risk.

Limitations

A possible limitation of this study could be misclassification of the silica exposure in the early years from 1946 to 1960 when no measurements for silica were available. A very detailed expert assessment had been performed with simulated, remodelled historical exposure settings using historic equipments, model calculations and expert rating (Dahmann et al, 2008). Thus, misclassification, if present, should be small.

A further limitation is the lack of individual information on the potential confounder smoking. In a nested case–control study on lung cancer some information on smoking based on data from the medical archives or from relatives was obtained for 439 cases and 550 controls (Schnelzer et al, 2010). No statistically significant

Epidemiology

Table 3 Risk of lung cancer death by cumulative silica exposure in a linear spline model with one knot at $10 \, mg \, m^{-3}$-years, 1946–2003

Model	β_1[a] 95% CI	β_2[b] 95% CI	Deviance	RR[c] 95% CI $5 \, mg \, m^{-3}$-years	RR 95% CI $15 \, mg \, m^{-3}$-years
Unadjusted	0.067 (0.039; 0.094)	0.088 (0.058; 0.119)	30 768.1	1.34 (1.20; 1.47)	2.44 (1.96; 2.61)
Adjusted for radon [d]	0.015 (−0.008; 0.038)	0.072 (0.042; 0.102)	30 692.1	1.08 (0.96; 1.19)	1.59 (1.09; 2.08)
Adjusted for radon and arsenic [e]	0.012 (−0.011; 0.035)	0.068 (0.038; 0.098)	30 688.2	1.06 (0.95; 1.18)	1.52 (1.24; 1.79)
Adjusted for radon (with exponential	−0.006 (−0.028; 0.015)	0.066 (0.038; 0.094)	30 604.2	0.97 (0.86; 1.08)	1.24 (0.98; 1.49)
effect modifiers [f]) and arsenic	0.000 (fixed[g])	0.061 (0.039; 0.083)	30 604.5	1.00 (fixed)	1.31 (1.20; 1.42)
0-year lag	0.000 (fixed)	0.061 (0.039; 0.083)		1.00 (fixed)	1.31 (1.20;1.42)
10-year lag	0.000 (fixed)	0.060 (0.037; 0.082)	not comparable	1.00 (fixed)	1.30 (1.19; 1.41)
15-year lag	0.000 (fixed)	0.062 (0.039; 0.085)		1.00 (fixed)	1.31 (1.20; 1.43)
Silica with exponential effect modifier	0.000 (fixed)	0.073 (0.046; 0.100)	30 592.5	1.00 (fixed)	1.37 (1.23; 1.50)
attained age (centred at 64 years)	0.002 (−0.014; 0.018)	0.073 (0.043; 0.100)	30 592.3	1.01 (0.93; 1.09)	1.39 (1.16; 1.63)
adjusted for radon (with exponential modifiers [h]) and arsenic					
50 years attained age	0.007 (−0.040; 0.057)	0.223 (0.142; 0.322)	30 592.3	1.04 (0.80; 1.29)	2.21 (1.43; 3.02)
60 years	0.003 (−0.019; 0.025)	0.105 (0.066; 0.134)	30 592.3	1.15 (0.90; 1.13)	1.55 (1.30; 1.84)
70 years	0.001 (0.008; 0.011)	0.045 (0.021; 0.068)	30 592.3	1.01 (0.96; 1.06)	1.24 (1.07; 1.39)
80 years	0.001 (−0.004; 0.005)	0.020 (0.004; 0.035)	30 592.3	1.00 (0.98; 1.03)	1.11 (1.02; 1.20)

Abbreviations: CI = confidence interval; ERR = excess relative risk. [a,b]β_1 and β_2 describe the ERR in the following way, $sil_k = 10$:

$$\text{ERR}(\text{sil}) = \begin{cases} \beta_1 \cdot \text{sil} & \text{sil} \leqslant \text{sil}_k \\ \beta_1 \cdot \text{sil} + \beta_2 \cdot (\text{sil} - \text{sil}_k) & \text{sil} > \text{sil}_k \end{cases}$$

[c]Relative risk with 95% CI for a cumulative exposure of $5 \, mg \, m^{-3}$-years compared with 0. [d]Adjusted for cumulative radon exposure in a linear way. [e]Adjusted for cumulative radon and arsenic exposure in a linear way. [f]Exponential effect modifiers age at median exposure, time since median exposure and radon exposure rate. [g]Parameter β_1 is fixed at 0. [h]Exponential effect modifiers, time since median exposure and radon exposure rate.

Table 4 Combined effect of cumulative exposure to silica and radon on the risk of death from lung cancer, Wismut cohort, 1946–2003

	Radon						
	<50 WLM		50–1000 WLM		>1000 WLM		
Silica dust $mg \, m^{-3}$-years	*n*	RR (95% CI)	*n*	RR (95% CI)	*n*	RR (95% CI)	Total
<10	609	1.0 Reference	585	1.52 (1.34–1.69)	12	1.95 (0.83–3.07)	1206
10–20	54	1.10 (0.79–1.41)	663	2.45 (2.17–2.73)	219	3.11 (2.62–3.61)	936
20–30	6	1.33 (0.26–2.41)	238	3.11 (2.63–3.60)	420	4.29 (3.64–4.74)	664
30+	0	—	42	4.75 (3.25–6.25)	147	4.56 (3.72–5.41)	189
Total	669		1528		798		2995

Abbreviations: CI = confidence interval; RR = relative risk; WLM = working level month.

trend in the proportion of smokers with increasing silica exposure for both lung cancer cases and controls was observed (two-sided test for trend: $P = 0.31$ for cases, $P = 0.52$ for controls; Figure 3). Pukkala *et al* (2005) observed no increased risk of lung cancer in their preferred model in the category $1.0–9.9 \, mg \, m^{-3}$-years (RR = 0.97; 95% CI: 0.91–1.03) compared with $0 \, mg \, m^{-3}$-years and a statistically significant risk $>10 \, mg \, m^{-3}$-years (RR = 1.42; 95% CI: 1.20–1.70) after adjustment for smoking on aggregate level. This is similar to results given in Table 2 and therefore possibly further evidence that smoking is not a major confounder in this study. However, residual confounding by smoking cannot be fully excluded, because data on duration and amount of smoking are incomplete.

Silicosis is debated as possible effect modifier of the silica-induced lung cancer risk (Hnizdo *et al*, 1997; Ulm *et al*, 1999; Soutar *et al*, 2000; Pelucchi *et al*, 2006; Taeger *et al*, 2008; Brown, 2009; Erren *et al*, 2011) and the carcinogenic role of silica in the absence of silicosis is still debated. There is consistent evidence of an increased lung cancer risk among silicotics, whereas studies restricted to non-silicotics or those with 'unknown silicotic status' mainly show no increased risk of lung cancer. Many studies, however, suffer from insufficient information on silicosis status (e.g., Steenland *et al*, 2001; Attfield and Costello, 2004; Lacasse
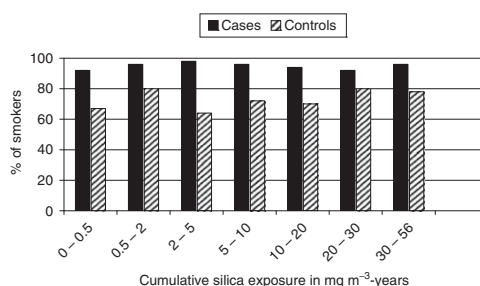
Figure 3 Percentages of smokers within cases (n = 439) and controls (n = 550) from a nested case–control study (Schnelzer *et al*, 2010) on lung cancer among the Wismut miners. A smoker is defined as a person who ever smoked in the last 20 years before death (for cases) or the reference case's death (for controls).

et al, 2009) or missing quantitative data on silica exposure. In the Wismut cohort selective data on silicosis are available. For a total of 3645 cohort members silicosis was noted on the death

Table 5 Risk of death from lung cancer by cumulative silica dust exposure in mg m^{-3}-years by categories after exclusion of known silicotics, 1946–2003

Silica dust in mg m^{-3}-years	Cohort excluding known silicotics				'Known' silicotics	
	Person-years	# of lung cancer deaths	RR 95%CI adjusted for radon and arsenic	RR 95%CI adjusted for radon and arsenic with effect modifiers	Person-years	# of lung cancer deaths
0–0.5	665 199	137	1.00 Reference	1.00 Reference	16 497	0
0.5–2	390 539	276	1.12 (0.86–1.31)	0.98 (0.79–1.18)	4019	7
2–5	267 161	333	1.12 (0.88–1.36)	0.97 (0.78–1.17)	7361	23
5–10	223 766	379	1.06 (0.82–1.30)	0.88 (0.69–1.07)	14 146	51
10–20	219 248	675	1.44 (1.10–1.78)	1.16 (0.89–1.43)	44 600	261
20–30	66 313	308	1.64 (1.13–2.15)	1.31 (0.92–1.70)	41 874	356
30–56	11 864	68	1.87 (0.98–2.77)	1.31 (0.63–1.99)	11 192	121
Total	1 844 090	2176			139 692	819

Abbreviations: CI = confidence interval; RR = relative risk. RR adjusted for radon and arsenic (forth column) and for radon with exponential inclusion of the effect modifiers age at median exposure, time since median exposure and radon exposure rate and arsenic (fifth column) as continuous variables in an additive way

certificates, the autopsy protocols or the protocols of the medical archive of the Wismut company. It is unclear how valid this information is. For the remaining 55 032 cohort members, the silicosis status is unknown. Categorical risk analyses excluding the 3645 known' silicotics (Table 5) show elevated RR's in the silica exposure categories > 10 mg m^{-3}-years after full adjustment. The corresponding estimate for the parameter β_2 (> 10 mg m^{-3}-years) was 0.034 (95% CI: 0.013; 0.055), which is appreciably lower compared with that in the full data set ($\beta_2 = 0.061$; 95% CI: 0.039; 0.083). It is unclear whether this excess is real or due to residual confounding (misclassified non-silicotics). Moreover, the statistical power is reduced, because the majority of highly radon- and silica-exposed cohort members were excluded as silicotics.

Comparison with other epidemiological studies

The increase in risk with increasing exposure in this study is consistent with other studies (Checkoway et al, 1997; Brüske-Hohlfeld et al, 2000; Rice et al, 2001; Steenland et al, 2001; Pukkala et al, 2005; Lacasse et al, 2009). On the other hand, a few single studies concluded that there was no evidence that crystalline silica acts as a risk factor for lung cancer (Steenland and Brown, 1995; Ulm et al, 1999; Graham et al, 2004; Chen et al, 2007; Mundt et al, 2011; Vacek et al, 2011). Exposures in some of these studies (Graham et al, 2004; Vacek et al, 2011) or parts of the study (Chen et al, 2007) have been quite low or subjects with silicosis had been omitted (Ulm et al, 1999).

Steenland et al (2001) pooled 10 cohort studies from a variety of industries and countries. The pooled study included 65 980 workers and 1079 lung cancer deaths. The logarithm of cumulative exposure with a 15-year lag showed a statistically significant positive trend with lung cancer risk. Categorical analyses by quintiles of cumulative silica exposure resulted in odds ratios of 1.0, 1.0 (95% CI, 0.85–1.3), 1.3 (95% CI, 1.1–1.7), 1.5 (95% CI, 1.2–1.9) and 1.6 (95% CI, 1.3–2.1) for cumulative silica exposure of < 0.4, 0.4–2.0, 2.0–5.4, 5.4–12.8 and > 12.8 mg m^{-3}-years, respectively. The risks for high exposures are approximately comparable to the present results, however, slightly shifted with a RR in this study of 1.51 (95% CI: 1.08–1.94) in the category 20–30 mg m^{-3}-years. The odds ratios of the lower exposure categories are appreciably higher compared with the fully adjusted

risks presented here, but the CIs overlap in both studies. No adjustment for smoking and other confounders was made. Furthermore, there was a considerable heterogeneity between the various studies in this pooled analysis.

The meta-analysis of Lacasse et al (2009) included four cohort studies and six case–control studies having quantitative measurements of crystalline silica exposure and adjustment for smoking. An increase in risk of lung cancer was observed with increasing cumulative silica exposure. Differences in the quality of silica exposure assessment of the original studies and significant heterogeneity across the studies limit its interpretation.

In conclusion, results indicate an elevated lung cancer risk at higher cumulative silica exposures. No increase in risk in the range < 10 mg m^{-3}-years was found, but a small increase cannot be ruled out. It is unclear whether these results can be applied to other industrial settings than uranium mining. In this study, even in the absence of known silicotics some increase in the silica-induced lung cancer risk was observed, however, this result has to be treated with caution due to possibly incomplete data on silicotics. Overall, the findings of this study support the evaluation of the IARC to classify silica as carcinogenic to humans with the lung as target organ (1997, 2012). The extension of the follow-up period to the end of 2008 will allow more detailed analyses of the low exposure range with alternative models.

REFERENCES

Attfield MD, Costello J (2004) Quantitative exposure-response for silica dust and lung cancer in Vermont granite workers. *Am J Ind Med* **45**: 129–138

Bauer H-D (1997) Staubbelastungen in untertägigen Betrieben der ehemaligen Wismut während der Frühphase der Uranerzgewinnung nach dem 2. Weltkrieg. *Gefahrstoffe – Reinhaltung der Luft* **57**: 349–354

Epidemiology

Brown T (2009) Silica exposure, smoking, silicosis and lung cancer – complex interactions. *Occup Med* **59:** 89–95

Brüske-Hohlfeld I, Möhner M, Pohlabeln H, Ahrens W, Bolm-Audorff U, Kreienbrock L, Kreuzer M, Jahn I, Wichmann H-E, Jöckel K-H (2000) Occupational lung cancer risk for men in Germany: results from a pooled case-control study. *Am J Epidemiol* **151:** 384–395

Checkoway H, Heyer NJ, Seixas NS, Welp E, Demers P, Hughes J, Weill H (1997) Dose-response associations of silica with non-malignant respiratory disease and lung cancer mortality in the diatomaceous earth industry. *Am J Epidemiol* **145:** 680–688

Chen W, Bochmann F, Sun Y (2007) Effects of work related confounders on the association between silica exposure and lung cancer: a nested case-control study among Chinese miners and pottery workers. *Int Arch Occup Environ Health* **80:** 320–326

Dahmann D, Bauer HD, Stoyke G (2008) Retrospective exposure assessment for respirable and inhalable dust, crystalline silica and arsenic in the former German uranium mines of SAG/SDAG Wismut. *Int Arch Occup Environ Health* **81:** 949–958

Erren TC, Morfeld P, Glende C, Piekarski C, Cocco P (2011) Meta-analyses of published epidemiological studies, 1979–2006, point to open causal questions in silica-silicosis-lung cancer research. *Med Lav* **102**(4): 321–335

Graham WG, Costello J, Vacek PM (2004) Vermont granite mortality study: an update with an emphasis on lung cancer. *J Occup Eviron Med* **46:** 459–466

Grosche B, Kreuzer M, Kreisheimer M, Schnelzer M, Tschense A (2006) Lung cancer risk among German male uranium miners: a cohort study, 1946–1998. *Br J Cancer* **95:** 1280–1287

Hnizdo E, Murray J, Klempman S (1997) Lung cancer in relation to exposure to silica dust, silicosis and uranium production in South African gold miners. *Thorax* **52:** 271–275

HVBG and BBG (2005) *Belastung durch ionisierende Strahlung, Staub und Arsen im Uranerzbergbau der ehemaligen DDR (Version 08/2005).* Bergbau BG (BBG): St. Augustin, Hauptverband der gewerblichen Berufsgenossenschaften (HVBG) (CD-Rom): Gera

International Agency for Research on Cancer (1997) *IARC Monographs on the Evaluation of Carcinogenic Risks to Humans, Vol 68, Silica, Some Silicates, Coal Dust and Para-Aramid Fibrils.* International Agency for Research on Cancer: Lyon

International Agency for Research on Cancer (2012) *IARC Monographs on the Evaluation of Carcinogenic Risks to Humans, Vol 100C, Arsenic, Metals, Fibres, and Dust.* International Agency for Research on Cancer: Lyon

Kreuzer M, Grosche B, Schnelzer M, Tschense A, Dufey F, Walsh L (2010b) Radon and risk of death from cancer and cardiovascular diseases in the German uranium miners cohort study, 1946–2003. *Radiat Environ Biophys* **49:** 177–185

Kreuzer M, Schnelzer M, Tschense A, Walsh L, Grosche B (2010a) Cohort profile: the German uranium miners cohort study (Wismut cohort), 1946–2003. *Int J Epidemiol* **39:** 980–987

Kreuzer M, Walsh L, Schnelzer M, Tschense A, Grosche B (2008) Radon and risk of extrapulmonary cancers: results of the German uranium miners cohort study, 1960–2003. *Br J Cancer* **99:** 1946–1953

Kurihara N, Wada O (2004) Silicosis and smoking strongly increase lung cancer risk in silica-exposed workers. *Ind Health* **42:** 303–314

Lacasse Y, Martin S, Gagné D, Lakhal L (2009) Dose-response meta-analysis of silica and lung cancer. *Cancer Causes Control* **20:** 925–933

Lehmann F, Hambeck L, Linkert KH, Lutze H, Reiber H, Renner HJ, Reinisch A, Seifert T, Wolf F (1998) *Belastung durch ionisierende Strahlung im Uranerzbergbau der ehemaligen DDR. Hauptverband der gewerblichen Berufsgenossenschaften: Sankt Augustin*

Mundt K, Kenneth A, Birk T, Parsons W, Borsch-Galetke E, Siegmund K, Heavner K, Guldner K (2011) Respirable crystalline silica exposure-response evaluation of silicosis morbidity and lung cancer mortality in the German porcelain industry cohort. *J Occup Environ Med* **53:** 282–289

Pelucchi C, Pira E, Piolatto G, Coggiola M, Carta P, La Vecchia L (2006) Occupational silica exposure and lung cancer risk: a review of epidemiological studies 1996–2005. *Ann Oncol* **17:** 1039–1050

Preston DL, Lubin JH, Pierce DA, McConney ME (1998) *Epicure, release 2.10.* HiroSoft: Seattle

Pukkala E, Guo J, Kyyrönen P, Lindbohm M-L, Sallmén M, Kauppinen T (2005) National job-exposure matrix in analyses of census-based estimates of occupational cancer risk. *Scand J Work Environ Health* **31:** 97–107

Rice FL, Park R, Stayner L, Smith R, Gilbert S, Checkoway H (2001) Crystalline silica exposure and lung cancer mortality in diatomaceous earth industry workers: a quantitative risk assessment. *Occup Environ Med* **58:** 38–45

Schnelzer M, Hammer GP, Kreuzer M, Tschense A, Grosche B (2010) Accounting for smoking in the radon-related lung cancer risk among German uranium miners: results of a nested case-control study. *Health Phys* **98:** 20–28

Soutar C, Robertson A, Miller B, Searl A, Bignon J (2000) Epidemiological evidence on the carcinogenicity of silica: factors in scientific judgement. *Ann Occup Hyg* **44:** 3–14

Steenland K, Brown D (1995) Mortality study of gold miners exposed to silica and nonasbestiform amphibole minerals: an update with 14 more years of follow-up. *Am J Ind Med* **27:** 217–229

Steenland K, Mannetje A, Boffetta P, Stayner L, Attfield M, Chen J, Dosemeci M, DeKlerk N, Hnizdo E, Koskela R, Checkoway H (2001) Pooled exposure-response analysis and risk assessment for lung cancer in 10 cohorts of silica-exposed workers: an IARC multicentre study. *Cancer Causes Control* **12:** 773–784; Erratum: *Cancer Causes Control* 2002; **13:** 777

Taeger D, Krahn U, Wiethege T, Ickstadt K, Johnen G, Eisenmenger A, Wesch H, Pesch B, Brüning T (2008) A study on lung cancer mortality related to radon, quartz, and arsenic exposures in German Uranium Miners. *J Toxicol Environ Health* **71:** 859–865

Ulm K, Waschulzik B, Ehnes H, Guldner K, Thomasson B, Schwebig A, Nuss H (1999) Silica and lung cancer in the German stone, quarrying, and ceramics industries: results of a case–control study. *Thorax* **54:** 347–351

Vacek P, Verma D, Graham W, Callas P, Gibbs G (2011) Mortality in Vermont granite workers and its association with silica exposure. *Occup Environ Med* **68:** 312–318

Walsh L (2007) A short review of model selection techniques for radiation epidemiology. *Radiat Environ Biophys* **46:** 205–213

Walsh L, Dufey F, Tschense A, Schnelzer M, Grosche B, Kreuzer M (2010b) Radon and the risk of cancer mortality – internal Poisson models for the German Uranium miners cohort. *Health Phys* **99:** 292–300

Walsh L, Tschense A, Schnelzer M, Dufey F, Grosche B, Kreuzer M (2010a) The influence of radon exposure on lung cancer mortality in German uranium miners, 1946–2003. *Radiat Res* **173:** 79–90

Epidemiology

46. Walsh L & Schneider U. A method for calculating weights for excess relative risk and excess absolute risk in calculations of lifetime risk of cancer from radiation exposure. Radiat. Environ. Biophys. *accepted* October 2012, DOI: 10.1007/s00411-012-0441-x

CONTROVERSIAL ISSUE

A method for determining weights for excess relative risk and excess absolute risk when applied in the calculation of lifetime risk of cancer from radiation exposure

Linda Walsh · Uwe Schneider

Abstract Radiation-related risks of cancer can be transported from one population to another population at risk, for the purpose of calculating lifetime risks from radiation exposure. Transfer via excess relative risks (ERR) or excess absolute risks (EAR) or a mixture of both (i.e., from the life span study (LSS) of Japanese atomic bomb survivors) has been done in the past based on qualitative weighting. Consequently, the values of the weights applied and the method of application of the weights (i.e., as additive or geometric weighted means) have varied both between reports produced at different times by the same regulatory body and also between reports produced at similar times by different regulatory bodies. Since the gender and age patterns are often markedly different between EAR and ERR models, it is useful to have an evidence-based method for determining the relative goodness of fit of such models to the data. This paper identifies a method, using Akaike model weights, which could aid expert judgment and be applied to help to achieve consistency of approach and quantitative evidence-based results in future health risk assessments. The results of applying this method to recent LSS cancer incidence models are that the relative EAR weighting by cancer solid cancer site, on a scale of 0–1, is zero for breast and colon, 0.02 for all solid, 0.03 for lung, 0.08 for liver, 0.15 for thyroid, 0.18 for bladder and 0.93 for stomach. The EAR weighting for female breast cancer increases from 0 to 0.3, if a generally observed change in the trend between female age-specific breast cancer incidence rates and attained age, associated with menopause, is accounted for in the EAR model. Application of this method to preferred models from a study of multi-model inference from many models fitted to the LSS leukemia mortality data, results in an EAR weighting of 0. From these results it can be seen that lifetime risk transfer is most highly weighted by EAR only for stomach cancer. However, the generalization and interpretation of radiation effect estimates based on the LSS cancer data, when projected to other populations, are particularly uncertain if considerable differences exist between site-specific baseline rates in the LSS and the other populations of interest. Definitive conclusions, regarding the appropriate method for transporting cancer risks, are limited by a lack of knowledge in several areas including unknown factors and uncertainties in biological mechanisms and genetic and environmental risk factors for carcinogenesis; uncertainties in radiation dosimetry; and insufficient statistical power and/or incomplete follow-up in data from radio-epidemiological studies.

Keywords Lifetime attributable risk · A-bomb survivors · Risk projection

L. Walsh (✉)
Federal Office for Radiation Protection, Department of Radiation Protection and Health, Ingolstädter Landstr. 1,
85764 Oberschleissheim, Germany
e-mail: lwalsh@bfs.de

L. Walsh
The Faculty of Medical and Human Sciences,
University of Manchester, Manchester, UK

U. Schneider
Vetsuisse Faculty, University of Zurich, Zurich, Switzerland

U. Schneider
Radiotherapy Hirslanden AG, Aarau, Switzerland

Introduction

Assessments of detrimental health risks due to exposures from ionizing radiation are often based on studies on survivors of the World War II atomic bombings over Hiroshima and Nagasaki. The life span study (LLS) of these

A-bomb survivors continues to provide valuable radiation epidemiological data and quantitative assessments of the radiation-related solid cancer, site-specific and leukemia risks (Preston et al. 2003, 2004, 2007; Ozasa et al. 2012). Results from this cohort have formed a basis for the construction of radiation protection guidelines that include the setting of various dose limits and reference values to the radiation received by occupationally exposed workers and the general public. Such limits and values have come from assessments and recommendations that are issued and updated at regular intervals by national and international bodies, that is, the International Commission on Radiological Protection (ICRP), the United Nations Scientific Committee on the Effects of Atomic Radiation (UNSCEAR), Biological Effects of Ionizing Radiation, U.S.A. (BEIR) and the Environmental Protection Agency, U.S.A. (EPA).

Choices for risk models applied in reports produced by such bodies (UNSCEAR, BEIR VII, EPA and ICRP) are often mainly based upon the Japanese atomic bomb survivor data. Although the specific choice of risk models for risk versus dose–responses and the lifetime risk calculations differ between regulatory groups, there is also disparity in applications of the weights to be applied to excess relative risk (ERR) or excess absolute risk (EAR) models when used in the calculation of lifetime risks. These weights were, up to now, invariably chosen in a qualitative way based on expert opinion. Owing to this process of decision making based on expert judgement, the numerical values of weights to be applied to ERR and EAR models when used in the calculation of lifetime risks vary both between reports produced at different points in time by the same body and also between reports produced at similar points in time by different bodies.

The purpose of this paper is to propose and illustrate a quantitative method for obtaining such weights. It is suggested that this method could be a useful addition and an aid to the qualitative decisions made by experts (which have often been quantified based only on qualitative judgement in the past) by providing additional quantitative results, such that decisions can also be based on measures of evidence specifically linked to the choice of ERR and EAR models. Although this technique is applicable to all measures of lifetime risk, the simplest measure called lifetime attributable risk (LAR) is considered here to illustrate the proposed weighting technique.

Materials and methods

Lifetime risks and the relative weighting of ERR and EAR models used in the calculations

Lifetime attributable risk (LAR—see e.g., Kellerer et al. (2001), (2002) and Vaeth and Pierce (1990)) has a linear

dose–response for a linear ERR or linear EAR model. Separate evaluations of LAR can be made using both an EAR model and an ERR model or a mixture of the two. For a person exposed at age e, to a radiation dose, D the LAR is

$$\text{LAR}(D, e) = \int_{e+L}^{a_{\max}} M(D, e, a) S(a)/S(e) \, \mathrm{d}a \qquad (1)$$

where $M(D, e, a)$ is the EAR at an age attained, a, after an exposure at age e. $S(a)$ is the survival curve, that is, the probability of surviving to age a, and L is the minimum latency period (e.g., 2 years for leukemia, 5 years for solid cancers). The ratio $S(a)/S(e)$ is the conditional probability of a person alive at age e to reach at least age a. (In Eq. (1) there is an assumed dependence of population statistics on gender). The LAR approximates the probability of a premature incidence of primary cancer from radiation exposure and is a weighted sum (over attained ages up to $a_{\max}$) of the age-specific excess probabilities of radiation-induced cancer incidence, $M(D, e, a)$ can be defined in three alternative ways:

$$M(D, e, a) = \text{EAR}(D, e, a); \qquad (2a)$$

$$M(D, e, a) = \text{ERR}(D, e, a) \cdot m(a); \qquad (2b)$$

or a weighted arithmetic sum of both-

$$M(D, e, a) = w_1 \text{EAR}(D, e, a) + (1 - w_1)(\text{ERR}(D, e, a) \cdot m(a)). \qquad (2c)$$

where $m(a)$ is the spontaneous cancer incidence rate in a pre-defined population or subpopulation at risk, w_1 is a weighting between 0 and 1, and $S(a)$ is the survival function for the unexposed population. This makes the LAR differ from the quantity REID (risk of exposure-induced death) as used by UNSCEAR because REID has an exposure-dependent survival function. However, LAR and REID coincide at lower doses under about 0.5 Gy (see Fig. 1 of Kellerer et al. 2001).

Model weighting from multi-model inference statistics

An important part of the inferential process in radiation epidemiology and other fields is assessing the preferred model for a dataset by selection involving Akaike's information criterion (AIC) (Akaike 1973, 1974; Walsh 2007). The introduction of AIC for model selection has been a positive contribution to the field of radiation epidemiology. Akaike's information criterion is defined by AIC $= -2\log(\text{MaxLikelihood}) + 2k$, where k is the number of parameters in the model and the first term on the right-hand side is just the deviance. Models with smaller values of AIC are favored on the basis of fit and parsimony. Model uncertainty contributes a large fraction of the total

uncertainty for cancer risk evaluations associated with radiation exposure. Assessing this source of uncertainty in a qualitative way or even neglecting this source of uncertainty altogether is a serious shortcoming of previous evaluations.

Recent statistical literature covers various approaches for combining information from different models fitted to the same data via multi-model inference (MMI) (Hoeting et al. 1999; Posada and Buckley 2004; Chatfield 1995; Claeskens and Hjort 2008; Burnham and Anderson 1998, 2002, 2004). To average over candidate models, a weight is assigned to each model and then measures of interest are inferred across all weighted models. The Akaike weights for model averaging have already been applied in radiation epidemiology to provide an objective basis for model selection and MMI (e.g., Walsh and Kaiser 2011). Within this framework, the Akaike weights (w_i, $i = 1, 2, \ldots, m$) are computed for each model,

$$w_i = \exp[-0.5(\text{AIC}_i - \text{minAIC})]$$
$$/ \sum_{j=1}^{m} \exp[-0.5(\text{AIC}_j - \text{minAIC})], \quad (3)$$

where m is the number of models and min AIC is the smallest AIC value among all models considered. The probability that the ith model is the best among the m models considered is quantified by the individual w_i values.

A model-averaged estimator of a quantity, $\hat{\mu}$, can then be obtained as a weighted average of estimators, $\hat{\mu}_i$, from model i (i.e., in the practical terms of the analysis presented here, either the right-hand sides of Eq. (2a) or (2b))

$$\hat{\mu} = \sum_{i=1}^{m} w_i \hat{\mu}_i. \quad (4)$$

Consequently, the weights w_1 and $1 - w_1$ in Eq. (2c) can be obtained from w_1 and w_2 in a two model ($m = 2$, one EAR and one ERR) MMI procedure.

EAR and ERR risk models for cancer incidence of various sites and leukemia mortality

Recent site-specific and all solid cancer incidence models for the follow-up 1958–1998 (Preston et al. 2007) (data file: lssinc07.csv, results files: lss07solmod.log, lss07siteahs.log, lss07sitemod.log from www.rerf.or.jp) and preferred leukemia mortality models for the follow-up 1950–2003 selected form a comprehensive MMI study (Kaiser and Walsh 2012), have been selected here for illustration. These results files contain information on model fit parameters and goodness of fit measures obtained from optimizing the models to the data via Poisson regression. The results files were generated with the AMFIT module of the EPICURE software (Preston et al. 1993) and were made available on the internet by Preston and co-workers, after the publication of Preston et al. (2007).

Since the forms of the EAR and ERR models, chosen to illustrate the weighting technique, have been described in Preston et al. 2007 (for all solid cancer and site-specific cancer incidence) and Kaiser and Walsh (2012) (for leukemia mortality), they will not be given explicitly here. The all solid cancer ERR and EAR models (linear in neutron weighted colon dose) and seven site-specific models (linear in neutron weighted organ dose) are fully parametric and all have exponential effect modifiers for age at exposure and effect modification for age attained via power functions even if they are not statistically significant. The preferred leukemia models from Kaiser and Walsh (2012) apply a dose–response with both a quadratic and an exponential dose term, modified by a power function of attained age. The exponential term has the effect of damping the quadratic dose–response to a small extent at higher doses. All solid cancer models documented in the RERF results files are gender-averaged models (except in the cases of sex-specific sites, that is, female breast cancer).

The nine sites considered here to illustrate the weighting technique are—all solid cancer, female breast, lung, colon, stomach, liver, bladder, thyroid cancer and leukemia. The solid cancer sites have both ERR and EAR models available in the results files. Other sites (oral cavity, esophagus, rectum, gall bladder, pancreas, renal cell, central nervous system, uterus, ovary and prostate) only have ERR models documented in the results files, that are linear in organ dose, but with no age-related effect modifiers. In fact, all that is required to apply this new application of the MMI technique is the deviance of the model fit and the number of fit parameters in the model. This information has been extracted from the original results files and is documented in Table 1.

However, many of the fit parameters given in the original RERF results files are not statistically significant. A justification for this general RERF approach was given in Pierce et al. (1996) where it was explained that as follow-up continues, risk modifications such as a sex effect will increase in statistical significance and so fit parameters that represent such risk modifications are included even if they are not statistically significant at the time of analysis.

Since small differences in model specifications can lead to differences in LAR projection results, it is more appropriate to consider here the optimized models. In the original paper by Preston et al. (2007), the models for all solid cancer seem to have been applied for the site-specific models considered here with little attention to model selection techniques so that approximately one-third of the original parameters were associated with large p-values much greater than 0.1. Consequently, the fit parameters that corresponded to $p > 0.1$ in the original Preston et al. 2007

models were removed, and the models re-optimized before the model weights were calculated. This means that both the baseline risks and the age and gender effect modifications in the excess risk part of the model were more appropriately represented and differences in the statistical significance of age or gender effect modifications between EAR and ERR models were taken into account with model selection techniques.

Results

The results of applying this technique to the sites considered here using the original models of Preston et al. (2007), from the computer files on the RERF website, are shown in Table 1. It can be seen, from the last column of Table 1, that the relative EAR weighting, (w_1), by cancer incidence site is zero for breast, 0.11 for colon, 0.12 for all solid and thyroid, 0.19 for lung, 0.22 for bladder, 0.25 for liver and 0.79 for stomach.

Table 2 shows the results of applying this technique to the sites considered here with the optimized models where the fit parameters that corresponded to $p > 0.1$ in the original Preston et al. (2007) models were removed and the models re-optimized. The weights obtained with the choice of $p > 0.1$ are very similar to those obtained if $p > 0.05$ is

Table 1 Quantification of the relative ERR and EAR weights to apply in the calculation of lifetime risks

Site/datafile	Model type	Deviance	Number of optimized parameters	AIC	Weights: $1 - w_1$ (ERR) w_1 (EAR)
All solid/	ERR	14736.0	19	14774.0	0.88
lss07solmod.log	EAR	14739.9	19	14777.9	0.12
Thyroid/	ERR	3038.0	20	3078.0	0.88
lss07siteahs.log	EAR	3042.0	20	3082.0	0.12
Fem. Breast/	ERR	3295.2	13	3321.2	1
lss07sitemod.log	EAR	3307.1	13	3333.1	0
Stomach/	ERR	8943.6	19	8981.6	0.21
lss07sitemod.log	EAR	8941.0	19	8979.0	0.79
Colon/	ERR	4561.2	19	4599.2	0.89
lss07sitemod.log	EAR	4565.3	19	4603.3	0.11
Liver/	ERR	4795.2	19	4833.2	0.75
lss07sitemod.log	EAR	4797.4	19	4835.4	0.25
Lung/	ERR	5326.6	19	5364.6	0.81
lss07sitemod.log	EAR	5329.5	19	5367.5	0.19
Bladder/	ERR	2418.1	19	2456.1	0.78
Lss07sitemod.log	EAR	2420.6	19	2458.6	0.22
Leukemia/	ERR	2258.7	22	2302.7	0.12
DS02can.log[a]	EAR	2254.8	22	2298.8	0.88

In this table w_1 and $1 - w_1$ correspond to the weights in Eq. (2c). The named files, from which the deviance and number of fit parameters were taken, are available from www.rerf.or.jp

[a] Note for leukemia: only an EAR model was published by Preston et al. (2004), the deviance value for the ERR model was calculated in Walsh and Kaiser (2011)

Table 2 Quantification of the relative ERR and EAR weights to apply in the calculation of lifetime risks

Site	Model type	Deviance	Number of optimized parameters	AIC	Weights: $1 - w_1$ (ERR) w_1 (EAR)
All solid	ERR	14,741.0	14	14,769.0	0.98
	EAR	14,748.4	14	14,776.4	0.02
Thyroid	ERR	3,048.7	12	3,072.7	0.85
	EAR	3,052.2	12	3,076.2	0.15
Fem. Breast	ERR	3,300.0	7	3,314.0	1
	EAR	3,312.3	8	3,328.3	0
Stomach	ERR	8,949.8	13	8,975.8	0.07
	EAR	8,944.6	13	8,970.6	0.93
Colon	ERR	4,562.5	13	4,588.5	1.0
	EAR	4,576.9	13	4,602.9	0.0
Liver	ERR	4,800.7	10	4,820.7	0.92
	EAR	4,803.6	11	4,825.6	0.08
Lung	ERR	5,330.4	13	5,356.4	0.97
	EAR	5,339.6	12	5,363.6	0.03
Bladder	ERR	2,423.6	11	2,445.6	0.82
	EAR	2,426.6	11	2,448.6	0.18
Leukemia	ERR	2,670.9	10	2,690.9	1.0
Kaiser and Walsh (2012)	EAR	2,677.7	12	2,701.7	0

In this table, w_1 and $1 - w_1$ correspond to the weights in Eq. (2c). The solid cancer models in Table 1 have been re-optimized, with only those parameters retained that had p-values ≤ 0.1, before re-calculating the weights. For the leukemia models from Kaiser and Walsh (2012), the optimization was based on models with p-values ≤ 0.05, using the Report 14 data for the follow-up period 1950–2003, from Ozasa et al. (2012)

used. It can be seen, from the last column of Table 2, that the relative EAR weighting, (w_1), by cancer incidence site, is zero for breast and colon, 0.02 for all solid, 0.03 for lung, 0.08 for liver, 0.15 for thyroid, 0.18 for bladder and 0.93 for stomach. The latter results are preferred here because they have been obtained from models in which differences in the statistical significance of age or gender effect modifications between EAR and ERR models were fully and correctly accounted for by standard model selection techniques. For example, in the original liver cancer models of Preston et al. (2007), none of the age and gender excess risk modifiers were statistically significant in the ERR model (the gender and age at exposure effect modifiers both had $p > 0.5$ and the age-attained effect modifier had $p = 0.21$) but the age attained ($p = 0.008$) and gender ($p = 0.04$) risk modifiers were statistically significant in the EAR model.

There is one important refinement to the breast cancer models described on page 34 of Preston et al. (2007), but not explicitly included in the computer files on the RERF website, that should also be considered here. That is explicitly allowing, in the EAR model, for the generally observed change in the trend between female age-specific breast cancer incidence rates and attained age, associated with menopause that is sometimes called Clemmesen's hook (Clemmesen 1948). Modeling Clemmesen's hook is just done by allowing effect modification of the EAR by the logarithm of age in the functional form of a quadratic spline with a knot at age 50 years. If Clemmesen's hook is explicitly accounted for, the EAR weighting increases from 0 to 0.3.

Table 3 compares the central risk estimates obtained with the original solid cancer models of Preston et al. (2007) with the central risk estimates obtained from the optimized models considered here. The central estimates are very similar for all sites, indicating that the further model optimization undertaken by the current authors, only had a minor impact on the central risk estimates.

The leukemia model of Preston et al. (2004), which was originally published only as an EAR model, had a deviance of 2254.8 (value quoted from www.rerf.or.jp, file-name:ds02can.log), the analogous ERR model has only been presented recently (Walsh and Kaiser 2011) and had a

deviance of 2258.7 with the same number and type of fit parameters. Applying this technique to these models for leukemia mortality results in an EAR weighting of 0.88 (Table 1). However, the MMI procedures of Walsh and Kaiser (2011) and Kaiser and Walsh (2012) identified leukemia models with much higher model weights than the leukemia model of Preston et al. (2004). Application of the preferred models from Kaiser and Walsh (2012) with the follow-up data covering the period (1950–2003), as applied in the analysis by Ozasa et al. (2012), results in an EAR weighting of 0.

From these results, it can be seen that, for the sites considered here, lifetime risk transfer is most highly weighted by EAR only for stomach cancer.

Discussion

In radiation-related cancer risk assessment for a subpopulation at risk, one is often required to transfer the risk obtained from the LSS of atomic bomb survivors to the actual subpopulation at risk. Due to a process of decision making based on expert judgement, the numerical values of weights to apply to ERR and EAR models, when used in the calculation of lifetime cancer risks, vary both between reports produced at different times by the same body and also between reports produced at similar times by different bodies.

In transporting risk estimates from Japan to the U.S.A., BEIR V (1990) assumed a multiplicative model. In contrast to this, BEIR VII/phase2 (2006) applied a weight, $wB7$ of 0.7 for the estimate obtained using ERR transport for sites other than breast, thyroid, and lung, and a complementary weight of 0.3 for the estimate obtained using EAR transport. This choice was justified in BEIR VII/phase2 (Chapter 10), by acknowledging that there is somewhat greater support for relative risk than for absolute risk transport. However, the BEIR VII/phase 2 (2006) weighting was done on a logarithmic scale. The LAR values were calculated separately based on preferred EAR and ERR models and then combined using a weighted geometric mean, whereby $LAR_{B7} = LAR_{ERR}^{wB7} \cdot LAR_{EAR}^{(1-wB7)}$. The BEIR VII report acknowledges that the choice of $wB7$ values "clearly involves subjective judgment". This geometric mean (GM) approach is not consistent with Eq. (4) and the current literature on MMI (some of which is cited in the materials and methods section of this paper).

The EPA (1994) report also adopted a GM approach stating that this "reflects a judgment regarding the distribution of uncertainty associated with the transportation of risk". However, the later EPA (2011) report (see also Pawel and Puskin 2012) made two points against the weighted GM approach stating, "First, it is difficult to

Table 3 Central risk estimates with standard Wald-type errors, for the models applied in Table 1 (from Preston et al. 2007) and Table 2 (the models from Preston et al. 2007 but re-optimized with the fit parameters with p-values > 0.1 removed)

Site/datafile	Model type	Central risk estimate (±1SE) Preston et al. (2007)	Central risk estimate (±1SE) with optimized model
All solid/	ERR	0.467 ± 0.044	0.461 ± 0.043
lss07solmod.log	EAR	51.63 ± 4.98	51.85 ± 4.97
Thyroid/	ERR	0.58 ± 0.26	0.67 ± 0.26
lss07siteahs.log	EAR	1.23 ± 0.51	1.37 ± 0.46
Fem. Breast/	ERR	0.88 ± 0.21	0.86 ± 0.20
lss07sitemod.log	EAR	9.26 ± 1.58	9.45 ± 1.57
Stomach/	ERR	0.336 ± 0.080	0.340 ± 0.074
lss07sitemod.log	EAR	9.52 ± 2.44	9.97 ± 2.08
Colon/	ERR	0.53 ± 0.16	0.57 ± 0.15
lss07sitemod.log	EAR	7.95 ± 2.15	8.80 ± 2.13
Liver/	ERR	0.30 ± 0.13	0.41 ± 0.12
lss07sitemod.log	EAR	4.23 ± 1.66	3.77 ± 1.33
Lung/	ERR	0.81 ± 0.16	0.90 ± 0.15
lss07sitemod.log	EAR	7.55 ± 1.68	8.71 ± 1.35
Bladder/	ERR	1.24 ± 0.41	1.15 ± 0.37
Lss07sitemod.log	EAR	3.23 ± 1.16	2.45 ± 0.75

The ERR is given per unit dose (1 Gy) and the EAR is given as the number of cases per 10,000 person–years per Gy

explain how a projection based on the GM should be interpreted. Second, the GM is not additive in the sense that: the GM of two risk projections for the combined effect of separate exposures is generally not equal to the sum of the GM projections for the exposures." For these reasons, EPA (2011) employed a weighted arithmetic mean to combine ERR and EAR projections, but still applied the numerical ERR weighting value of 0.7.

ICRP 103 (2007) projections were based on a weighted arithmetic average of ERR and EAR risk model projections. For most sites, ICRP 103 used a "subjective probability" weight (w_{ICRP}) of 0.5 for the ERR model; exceptions include breast, bone, and leukemia cancers ($w_{ICRP} = 0$), thyroid cancer ($w_{ICRP} = 1$) and lung cancer ($w_{ICRP} = 0.3$).

UNSCEAR (2006) projections (see also Little et al. 2008) were done separately for EAR and ERR transport. Methods for combining site-specific ERR and EAR risk projections for the risk transport problem were not recommended.

Excess relative risks models, often referred to as multiplicative, are appropriate if radiation risks are proportional to baseline rates, and EAR models (additive) are an alternative if radiation risks add to baseline rates. Since the gender and age patterns are often markedly different between EAR and ERR models, the Akaike model weights can help to determine the relative goodness of fit of the two types of models to the data. It can be seen from the results section that lifetime risk transfer is most highly weighted by EAR only for stomach cancer. The resulting Akaike model weights could be applied directly, if the projections are done from the LSS to a population at risk with similar genetic and environmental characteristics and similar baseline risks (e.g., the Japanese subpopulation at risk after the Fukushima nuclear power plant radiation release in 2011).

However, such projections are also required when large differences are observed in comparisons of baseline risks between the subpopulation at risk and the LSS for some site-specific cancers. For example, baseline risks for cancers of the colon, lung and female breast are higher in the USA than in the LSS, whereas according EPA (2011), ICRP 103 (2011) and UNSCEAR (2006) baseline risks for cancers of the stomach and liver are much higher in the LSS than in the USA.

In these cases, estimates based on relative and absolute risk can differ substantially and additional considerations are necessary. These include (a) comparisons of radiation risks from epidemiological studies on non-Japanese populations with the LSS results, (b) evaluations of the interaction of radiation and other factors that contribute to differences in baseline rates and (c) considerations of biological mechanisms of carcinogenesis. If inter-population and non-Japanese and interaction studies are sparse for particular cancer sites with large differences in comparisons of baseline risks between the subpopulation at risk and the LSS, then just applying the LSS Akaike weights may lead to misleading results and caution is required.

For example, the UNSCEAR (2006) stomach cancer estimates for the population of the USA based on absolute risk transport are approximately an order of magnitude larger than those based on relative risk transport (and inter-population and interaction studies are sparse for stomach cancer). In this extreme case, a direct additive transfer mode of the LSS EAR (EAR_{LSS}) to the much lower USA baseline rates would lead to a proportionately very high radiation risk. It is currently not known if the EAR_{LSS} for stomach cancer should then be 1) applied directly to the USA baseline rates (BL_{USA}) or 2) scaled first and then applied, that is, applied as $EAR_{LSS} *(BL_{USA}/BL_{LSS})$ or 3) applied as an ERR that has been calculated using the parameters from the preferred LSS EAR model. Due to lack of knowledge on the interactions of radiation and other factors that contribute to differences in baseline rates, especially in the case of stomach cancer, there is no evidence-based reason for preferring transfer mode 1, 2 or 3.

Weights from one radio-epidemiology study may be different from those obtained in a different study for the same cancer site. Some examples of this for breast and thyroid cancer are given later in this section. Another consideration—as pointed out in the BEIR VII/phase 2 (2006) report—is that ERR models used to obtain relative risk transport estimates may be less vulnerable to possible bias from under ascertainment of cases. A further consideration is that since one in six cancers is caused by infections (de Martel et al. 2012), (e.g., Helicobacter pylori: stomach cancer and hepatitis B and C viruses: liver cancer)—a result that the ERR model describes the variation of radiation-associated risks in LSS with age-at-exposure and attained age better or worse than the EAR model, may only partially explain how radiation-associated liver cancer or stomach cancer risks compare between the LSS and the subpopulation at risk (i.e., between Japan and for example the USA). A high prevalence of infection with hepatitis may act as a confounding factor in the LSS (UNSCEAR 2006). In such cases, genetic or environmental risk factors need additional assessment prior to the calculation of LAR. Usually, the computation of LAR is done either for a typical exposed individual person or an exposed population, under a set of assumptions concerning genetic or environmental risk factors, that is, it is assumed that the typical exposed individual is also typical with respect to genetic susceptibility or that the pattern of baseline cancers in an exposed population is not atypical (i.e., through a population susceptibility to a certain type of cancer (e.g., adult T cell leukemia is endemic Nagasaki (Arisawa et al. 2002))). Preliminary work on testing a set of assumptions

concerning genetic or environmental risk factors should be done and based on expert opinion, prior to the LAR calculations.

Clearly, even after consideration of such points, unless one adopts the UNSCEAR (2006) approach, there is a need for a method that is based on the current statistical literature on MMI and quantitative weighting founded on evidence-based techniques, rather than subjective probabilities. The suggested application of the technique presented here, aims to help to fulfill this need and it is recommended with the cautions as already explained, as an additional aid to expert opinion for future health risk assessments.

The next few paragraphs consider some of the model-based evidence obtained from the literature for leukemia, breast, thyroid and lung cancer in order to see if the LSS results from the approach presented here can be validated.

Model-based evidence obtained from the literature for leukemia

Little et al. (1999) found that relative risk models which account for leukemia sub-type provide a reasonable fit to data on A-bomb survivors, cervical cancer patients and spondylitis patients. Little (2008) presented leukemia risk models for childhood radiation exposure to the LSS data and data from several medical studies and found that "a relative risk transfer may be more appropriate than an absolute risk transfer between the Japanese A-bomb survivors and these three childhood populations". Little et al. (2008) presented two optimal models for leukemia risk models employed in UNSCEAR (2006). From the goodness of fit parameters in Table 2 of Little et al. (2008), the ERR weights are 0.98 and 0.97 for the two optimal models with the linear-quadratic dose–response and the linear-quadratic-exponential dose–response, respectively. The proposed method produces very similar results using information from all of these papers and leads to the conclusion that, for leukemia, projections should be primarily based on the ERR model (ERR weight = 1.0).

Model-based evidence obtained from the literature for female breast cancer

Preston et al. (2002) derived breast cancer risks in eight different cohorts and, although their findings did not provide a clear answer to the question of how risk projection should be done, recommend that either EAR estimates or a scaling of the attained age ERR model by the ratio of the baseline rates in Japan to those in the population of interest should be used. Preston et al. (2002) also stated that "Formal statistical comparison of the fits of the excess relative risk and absolute excess rate models was not possible. An informal comparison of the deviance values for the various fitted models considered suggested that, while deviances for the ERR models tend to be slightly smaller than those for the EAR models, both types of models provide comparable fits to these data" (page 231, 2nd column, 2nd paragraph from the top). However, there is enough information on the deviance of the final pooled data models of Preston et al. (2002) to compute the relative goodness of fit. One can continue to read further in Preston et al. (2002) that "final ERR model has deviance = 5849.3 and final EAR model has deviance of 5854.7 with two parameters more". From this information, the change in Akaike Information Criterion (AIC) is 9.4 which gives a calculated evidence ratio in favor of the ERR model over the EAR of 110 corresponding to a probability of model improvement of 0.991, that is, see Table 2 of Walsh (2007). In this type of comparison of the fits, an ERR weight of 0.99 can be calculated which is similar to the results presented here in Table 2 (ERR weight of 1 or 0.7, if Clemmesen's hook is accounted for). Both sets of weights lead to the conclusion that projections should be primarily based on the ERR model. This conclusion is also supported by a recent MMI analysis of breast cancer incidence in A-bomb survivors by Kaiser et al. (2012), whereby none of the EAR models could be included in the protocol selected set of models considered for MMI, due to the poor quality of their fit to the data relative to ERR and mechanistic type models.

Little and Boice (1999) provided a detailed comparison of breast cancer risks in the A-bomb survivors to those in the Massachusetts Tuberculosis Fluoroscopy (MTBF) cohort. Applying the goodness of fit parameters from Tables 2 and 3 of Little and Boice (1999), it is possible to calculate weights for the earlier A-bomb incidence dataset with follow-up: 1958–1987 as described in Thompson et al. (1994) (ERR weight = 1) and the MTBF cohort (ERR weight = 0.35). This discrepancy in the ERR weights could be related to different molecular subgroup types of breast cancer, possibly with different sensitivities to radiation, occurring with different frequencies in the USA and Japan—since breast cancer has been shown by Curtis et al. (2012) to be divisible into 10 novel molecular subgroups based on the impact of somatic copy number aberrations. Such discrepancies indicate that the weights for breast cancer risk transfer may need to be chosen more specifically for the population of interest, that is, a 35 % ERR, 65 % EAR transfer may be more appropriate for calculating LAR of breast cancer for a USA or western population and a 100 % (or 70 %, if Clemmesen's hook is accounted for) ERR transfer may be more appropriate for calculating LAR of breast cancer for a Japanese or Asian population. An alternative evidence-based method, for applying discrepant weighting results from different cohorts with a

known similarity of cancer sub-types, could be to apply an outer weighting (by some appropriate measure of study size) to the individual study weights.

Model-based evidence obtained from the literature for thyroid cancer

A pooled study on thyroid cancer risks from seven individual studies has been presented by Ron et al. (1995). In Table 6 of Ron et al. (1995), there is enough information given to calculate the weights for the earlier LSS incidence data, and three cohort studies on children irradiated for various maladies (see Table 4). Models for two studies (the largest study, based on 309 thyroid cancers in children irradiated for enlarged tonsils in Chicago and a study of 60 thyroid cancers in children treated for Tinea capitis) result in an EAR weighting of 0. However, models for the study on children irradiated for an enlarged thymus gland, based on 38 thyroid cancers, results in an EAR weighting of 0.88.

Consideration of the goodness of fit of models from a study of children affected by the Chernobyl nuclear power plant accident (Table 1 of Jacob et al. 2006, gives parameters for an EAR and an ERR model with the same AIC as each other, that is, ΔAIC $= 0.007$) results in an ERR weighting of 0.5. Another study on children affected by the Chernobyl nuclear power plant accident, Likhtarov et al. (2006), provides goodness of fit parameters required for the calculation of the weights in Tables 6 and 7 of Likhtarov et al. (2006) for models 1–4 of that study. These four models are for a baseline plus linear dose–response (model 1), whereby the interaction of dose with either gender (model 2), age in 1986 (model 3) or calendar year period (model 4) was also given. Models 1–3 indicate a ERR weight of 1 but model 4 indicated an EAR weight of 1 (but failed to provide converged EAR risk estimates—see Table 4). The general conclusion is that, for thyroid cancer, projections should be based on a mixed model that is most heavily weighted toward the ERR (ERR weight = 0.85, EAR weight = 0.15).

Model-based evidence obtained from the literature for lung cancer

A recent lung cancer analysis (Furukawa et al. 2010) indicated a complicated interaction between lung cancer and smoking based on an analysis applying the ERR model, that is, they applied generalized joint effect models, which they called "generalized additive and multiplicative ERR interaction models" and found stronger evidence than an earlier analysis (Pierce et al. 2003) against the additive approach. This indication partially supports the proposed method which provides the conclusion that, for lung cancer, projections should be based on the ERR model (ERR weight = 0.97).

Table 4 Collection of thyroid cancer studies from which the relative weights for ERR and EAR can be calculated

Thyroid study	Number of incident thyroid cancers	w_1 (EAR)	$1 - w_1$ (ERR)	Age at exposure
This work (LSS, FU:1958–1998)	471	0.15	0.85	All ages
[R]LSS, FU:1958–1987	169	0.32	0.68	$\geq$15 years
[R]LSS, FU:1958–1987	56	0.11	0.89	<15 years
[R]Chicago tonsils (MRH)	309	0	1.0	<15 years
[R]Tinea capitis	60	0	1.0	<15 years
[R]Thymus	38	0.88	0.12	<15 years
Chernobyl (Jacob et al. 2006)	1089	0.5	0.5	$\leq$18 years
[L]Chernobyl, Model 1 (dose)	232	0	1.0	$\leq$18 years
[L]Chernobyl, Model 2 (dose*gender)	232	0	1.0	$\leq$18 years
[L]Chernobyl, Model 3 (dose*age in 1986)	232	0	1.0	$\leq$18 years
[L]Chernobyl, Model 4 (dose*calendar year)	232	1.0[a]	0	$\leq$18 years

The studies marked with a superscript R are cited in and taken from the pooled study by Ron et al. (1995), where the goodness of fit parameters required for the calculation of the weights presented here have been taken from Table 6 of Ron et al. (1995). The models marked with a superscript L are taken from the study by Likhtarov et al. (2006), where the goodness of fit parameters required for the calculation of the weights presented here have been taken from Tables 6 and 7 of Likhtarov et al. (2006) for models 1–4 of that study which are for a baseline plus linear dose–response (model 1), whereby the interaction of dose with either gender (model 2), age in 1986 (model 3) or calendar year period (model 4) was also given. Follow-up (FU) period for the LSS is given

[a] However, no actual EAR values could be determined for model 4 due to the convergence problems reported in Likhtarov et al. (2006)

Other methods applied to assign qualitative weights

Projection of risks for purposes of radiation protection makes the assumption that the LSS risk estimates can be applied to other exposed populations. In order to assess the evidence for this assumption, it is useful to consider data from different populations in the few pooled analyses that exist, such as Preston et al. (2002) and Ron et al. (1995) for breast and thyroid cancer, respectively. Comparisons are often made

between the actual values of individual study EAR and ERR risks given in such pooled analyses to assess for overall agreement. It can be seen from Table 6 in Ron et al. (1995) that the individual study EAR central risks estimates agree with each other much better than the corresponding ERR risks (i.e., in four of the cohort studies, for persons exposed under 15 years of age, the ERR per unit dose (range, with 95 % CI 2.5 (0.6; 20.0)–32.5 (14.0; 57.1)/Gy) differed by a factor of 13 compared to a factor of 3 for the EAR unit dose (range, with 95 % CI 2.6 (1.7; 3.6)–7.6 (2.7; 13.0)/10^4 person–years Gy)—although in both cases the confidence intervals of the upper and lower range values overlap. Similarly Preston et al. (2002) noted a better agreement between the individual study EAR central estimates than between ERR central estimates. The latter observation for breast cancer was considered in the assignment of expert judgment weights for the EAR of 100 % in ICRP 103 (2007). An additional consideration here is that although consistency in risk estimates may be observed in some projections of the multi-dimensional LSS EAR (and/or ERR) models with models (or point estimates) from other studies—the degree of observed consistency may change between different model projections. ICRP 103 (2007) also pointed out that the use of EAR models for predicting cancer risks in sites generally associated with regular screening is problematic because variation in screening intensity will have a marked effect on the rate of identified radiation-associated cancers. The results obtained from the proposed quantitative method of determining weights with the LSS data are mostly consistent with this concern of ICRP 103 (2007), but not with the results regarding inter-study agreements in central risk estimates for thyroid and breast cancer.

The main aim of the work presented here is to describe a quantitative method that could aid expert opinion in future transfers of radiation risks from one population to another. Further work is required to expand on the calculations presented here and to perform an exhaustive analysis of weights calculated from results currently available in the literature. It is recommended here that, in future analyses of cohort data relating to radiation risks, the goodness of fit parameters for parsimonious ERR and EAR models, obtained with a thorough modeling of baseline rates, could also be provided as an aid to determining whether the additive or multiplicative models fit the data best. Such parsimonious models could be considered even if authors publish and actually prefer a categorical model based on many subgroups of explanatory co-variables as their main results. Finally, it is noted that the transfer of radiation risks from one population to another is not limited to a mixture of just one ERR and one EAR model—in future a full MMI procedure could be applied instead, so that model uncertainty is account for more completely.

Conclusion

In the transport of radiation risks from one population (i.e., the LSS of atomic bomb survivors) to another population at risk, transfer via ERR or EAR or a mixture of both has been performed in the past in a qualitative and inconsistent way. This paper identifies an approach that could aid expert judgment and could be applied, with the cautions given, to help achieve consistency of approach and evidence-based results and therefore contribute to future health risk assessments.

However, it is important to state that definitive conclusions, regarding the appropriate method for transporting cancer risks, are limited by a lack of knowledge in several areas. Such areas include, but are not limited to, unknown factors and uncertainties in biological mechanisms and genetic and environmental risk factors for carcinogenesis, uncertainties in radiation dosimetry and insufficient statistical power and/or incomplete follow-up in data from radio-epidemiological studies. It is also particularly important to acknowledge that the generalization and interpretation of radiation effect estimates based on the LSS cancer data, when projected to other populations, are particularly uncertain for cancer sites where considerable differences exist between site-specific baseline rates in the LSS and the other populations of interest.

References

Akaike H (1973) Information theory and an extension of the maximum likelihood principle. In: Petrov BN, Caski F (eds) Proceedings of the second international symposium on information theory. Akademiai Kiado, Budapest, pp 267–281

Akaike H (1974) A new look at the statistical model identification. IEEE Trans Autom Control 19(6):716–723

Arisawa K, Soda M, Shirahama S, Saito H, Takamura N, Yamaguchi M, Odagiri K, Nakagoe T, Suyama A, Doi H (2002) Geographic distribution of the incidence of adult T-cell leukemia/lymphoma and other malignancies in Nagasaki Prefecture, Japan. Jpn J Clin Oncol 32:301–306

Burnham KP, Anderson DR (1998) Model selection and inference: a practical information-theoretic approach. Springer, New York

Burnham KP, Anderson DR (2002) Model selection and multimodel inference, 2nd edn. Springer, New York

Burnham KP, Anderson DR (2004) Multimodel inference. Understanding AIC and BIC in model selection. Sociol Methods Res 33(2):261–304, see also Workshop on model selection, Amsterdam http://www2.fmg.uva.nl/modelselection/ (Accessed Nov 2011)

Chatfield C (1995) Model uncertainty, data mining and statistical inference (with discussion). J R Stat Soc Series A 158:419–466

Claeskens G, Hjort NL (2008) Model selection and model averaging. Cambridge University Press, Cambridge

Clemmesen J (1948) Carcinoma of the breast. Br J Radiol 21(252): 583–590

Curtis C, Shah SP, Chin SF, Gulisa Turashvili G, Rueda OM, Dunning MJ, Speed D, Lynch AG, Samarajiwa S, Yuan Y, Gräf S, Gavin H, Haffari G, Bashashati A, Russell R, McKinney S, METABRIC Group, Langerød A, Green A, Provenzano E, Wishart G, Pinder S, Watson P, Markowetz F, Murphy L, Ellis I, Purushotham A, Børresen-Dale AL, Brenton JD, Tavare S, Caldas C, Aparicio S (2012) The genomic and transcriptomic architecture of 2,000 breast tumours reveals novel subgroups. Nature. doi:10.1038/nature10983

de Martel C, Ferlay J, Franceschi S, Vignat J, Bray F, Forman D, Plummer M (2012) Global burden of cancers attributable to infections in 2008: a review and synthetic analysis. The Lancet Oncology, Early Online Publication, doi:10.1016/S1470-2045 (12)70137-7

EPA (1994) (Environmental Protection Agency). Estimating radiogenic cancer risks. EPA Report 402-R-93-076, Washington, DC: US EPA

EPA (2011) Radiogenic cancer risk models and projections for the US population, EPA 402-R-11-001, US. Environmental protection agency office of radiation and indoor air Washington, DC 20460

Furukawa K, Preston DL, Lonn S, Funamoto S, Yonehara S, Matsuo T, Egawa H, Tokuoka S, Ozasa K, Kasagi F, Kodama K, Mabuchi K (2010) Radiation and smoking effects on lung cancer incidence among atomic bomb survivors. Radiat Res 174:72–82

Hoeting JA, Madigan D, Raftery AE, Volinsky CT (1999) Bayesian model averaging: a tutorial. Stat Sci 14(4):382–417

International Commission on Radiological Protection (2007) The 2007 recommendations of the international commission on radiological protection. ICRP_103. Ann ICRP 7:2–4

Jacob P, Bogdanova TI, Buglova E, Chepurniy M, Demidchik Y, Gavrilin Y, Kenigsberg J, Meckbach R, Schotola C, Shinkarev S, Tronko MD, Ulanovski A, Vavilov S, Walsh L (2006) Thyroid cancer risk in areas of Ukraine and Belarus affected by the chernobyl accident. Radiat Res 165:1–8

Kaiser JC, Walsh L (2012) Independent analysis of the radiation risk for leukaemia in children and adults with mortality data (1950–2003) of the Japanese A-bomb survivors. Radiat Environ Biophys (accepted). doi:10.1007/s00411-012-0437-6

Kaiser JC, Jacob P, Meckbach R, Cullings HM (2012) Breast cancer risk in atomic bomb survivors from multi-model inference with incidence data 1958–1998. Radiat Environ Biophys 51:1–14

Kellerer AM, Nekolla E, Walsh L (2001) On the conversion of solid cancer excess relative risk into lifetime attributable risk. Radiat Environ Biophys 40:249–257

Kellerer AM, Walsh L, Nekolla EA (2002) Risk coefficient for γ-rays with regard to solid cancer. Radiat Environ Biophys 41:113–123

Likhtarov L, Kovgan L, Vavilov S, Chepurny M, Ron E, Lubin J, Bouville A, Tronko N, Bogdanova T (2006) Post-chornobyl thyroid cancers in Ukraine, Report 2: risk analysis. Radiat Res 166:375–386

Little MP (2008) Leukemia following childhood radiation exposure in the Japanese atomic bomb survivors and in medically exposed groups. Radiat Prot Dosim 132(2):156–165

Little MP, Boice JD Jr (1999) Comparison of breast cancer incidence in the Massachusetts tuberculosis fluoroscopy cohort and in the Japanese atomic bomb survivors. Radiat Res 151:218–224

Little MP, Weiss HA, Boice JD Jr, Darby SC, Day NE, Muirhead CR (1999) Risks of leukemia in Japanese atomic bomb survivors, in women treated for cervical cancer, and in patients treated for ankylosing spondylitis. Radiat Res 152:280–292

Little MP, Hoel DG, Molitor J, Boice JD Jr, Wakeford R, Muirhead CR (2008) New models for evaluation of radiation-induced lifetime cancer risk and its uncertainty employed in the UNSCEAR 2006 report. Radiat Res 169:660–676

Ozasa K, Shimizu Y, Suyama A, Kasagi F, Soda M, Grant EJ, Sakata R, Sugiyama H, Kodama K (2012) Studies of the mortality of atomic bomb survivors, report 14, 1950–2003: an overview of cancer and noncancer diseases. Radiat Res 177(3):229–243

Pawel DJ, Puskin JS (2012) U.S. Environmental protection agency radiogenic risk models and projections for the U.S. population. Health Phys 102(6):646–656

Pierce DA, Shimizu Y, Preston DL, Vaeth M, Mabuchi K (1996) Studies of the mortality of atomic bomb survivors. report 12, Part I. Cancer: 1950–1990. Radiat Res 146:1–27

Pierce DA, Sharp GB, Mabuchi K (2003) Joint effects of radiation and smoking on lung cancer risk among atomic bomb survivors. Radiat Res 159:511–520

Posada D, Buckley TR (2004) Model selection and model averaging in phylogenetics: advantages of Akaike Information Criterion and Bayesian approaches over likelihood ratio tests. Syst Biol 53(5):793–808

Preston DL, Lubin JH, Pierce DA (1993) Epicure user's guide. HiroSoft International Corp, Seattle

Preston DL, Mattsson A, Holmberg E, Shore R, Hildreth NG, Boice JD (2002) Radiation effects on breast cancer risk: a pooled analysis of eight cohorts. Radiat Res 158:220–235

Preston DL, Shimizu Y, Pierce DA, Suyama A, Mabuchi K (2003) Studies of the mortality of atomic bomb survivors. Report 13: solid cancer and noncancer disease mortality: 1950–1997. Radiat Res 160:381–407

Preston DL, Pierce DA, Shimizu Y, Cullings HM, Fujita S, Funamoto S, Kodama K (2004) Effects of recent changes in atomic bomb survivors dosimetry on cancer mortality risk estimates. Radiat Res 162:377–389

Preston DL, Ron E, Tokuoka S, Funamoto S, Nishi N, Soda M, Mabuchi K, Kodama K (2007) Solid cancer incidence in atomic bomb survivors: 1958–1998. Radiat Res 168:1–64

Ron E, Lubin JH, Shore RE, Mabuchi K, Modan B, Pottern LM, Schneider AB, Tucker MA, Boice JD Jr (1995) Thyroid cancer after exposure to external radiation: a pooled analysis of seven studies. Radiat Res 141:259–277

Thompson DE, Mabuchi K, Ron E, Soda M, Tokunaga S, Ochikubo S, Sugimoto S, Ikeda T, Terasaki M (1994) Cancer incidence in atomic bomb survivors. Part II: solid tumors, 1958–1987. Radiat Res 137(Suppl):S17–S67

United Nations (2006) Effects of ionizing radiation. United Nations scientific committee on the effects of atomic radiation UNSCEAR 2006 Report. Volume I. Annex A: Epidemiological studies of radiation and cancer. United Nations, New York, 2008

United States National Research Council, Committee to Assess Health Risks from Exposure to Low Levels of Ionizing Radiation (1990) Health effects of exposure to low levels of ionizing

radiation: BEIR V. United States National Academy of Sciences. National Academy Press, Washington

United States National Research Council, Committee to Assess Health Risks from Exposure to Low Levels of Ionizing Radiation (2006) Health risks from exposure to low levels of ionizing radiation: BEIR VII—Phase 2. United States National Academy of Sciences. National Academy Press, Washington

Vaeth M, Pierce D (1990) Calculating lifetime risk in relative risk models. Environ Health Perspect 87:83–94

Walsh L (2007) A short review of model selection techniques for radiation epidemiology. Radiat Environ Biophys 46:205–213

Walsh L, Kaiser JC (2011) Multi-model inference of adult and childhood leukaemia excess relative risks based on the Japanese A-bomb survivors mortality data (1950–2000). Radiat Environ Biophys 50:21–35

47. Walsh L, Neutron relative biological effectiveness for solid cancer incidence in the Japanese A-bomb survivors – an analysis considering the degree of independent effects from γ-ray and neutron absorbed doses with hierarchical partitioning. Radiat. Environ. Biophys (*online first*). 2012, DOI: 10.1007/s00411-012-0445-6

ORIGINAL ARTICLE

Neutron relative biological effectiveness for solid cancer incidence in the Japanese A-bomb survivors: an analysis considering the degree of independent effects from γ-ray and neutron absorbed doses with hierarchical partitioning

Linda Walsh

Abstract It has generally been assumed that the neutron and γ-ray absorbed doses in the data from the life span study (LSS) of the Japanese A-bomb survivors are too highly correlated for an independent separation of the all solid cancer risks due to neutrons and due to γ-rays. However, with the release of the most recent data for all solid cancer incidence and the increased statistical power over previous datasets, it is instructive to consider alternatives to the usual approaches. Simple excess relative risk (ERR) models for radiation-induced solid cancer incidence fitted to the LSS epidemiological data have been applied with neutron and γ-ray absorbed doses as separate explanatory covariables. A simple evaluation of the degree of independent effects from γ-ray and neutron absorbed doses on the all solid cancer risk with the hierarchical partitioning (HP) technique is presented here. The degree of multi-collinearity between the γ-ray and neutron absorbed doses has also been considered. The results show that, whereas the partial correlation between the neutron and γ-ray colon absorbed doses may be considered to be high at 0.74, this value is just below the level beyond which remedial action, such as adding the doses together, is usually recommended. The resulting variance inflation factor is 2.2. Applying HP indicates that just under half of the drop in deviance resulting from adding the γ-ray and neutron absorbed doses to the baseline risk model comes from the *joint* effects of the neutrons and γ-rays—leaving a substantial proportion of this deviance drop accounted for by *individual* effects of the neutrons and γ-rays. The average ERR/Gy γ-ray absorbed dose and the ERR/Gy neutron absorbed dose that have been obtained here directly for the first time, agree well with previous indirect estimates. The average relative biological effectiveness (RBE) of neutrons relative to γ-rays, calculated directly from fit parameters to the all solid cancer ERR model with both colon absorbed dose covariables, is 65 (95 %CI: 11; 170). Therefore, although the 95 % CI is quite wide, reference to the colon doses with a neutron weighting of 10 may not be optimal as the basis for the determination of all solid cancer risks. Further investigations into the neutron RBE are required, ideally based on the LSS data with organ-specific neutron and γ-ray absorbed doses for all organs rather than the RBE weighted absorbed doses currently provided. The HP method is also suggested for use in other epidemiological cohort analyses that involve correlated explanatory covariables.

Introduction

Studies on survivors of the World War II atomic bombings over Hiroshima and Nagasaki have been crucial to assessments of the detrimental health risks due to exposures from ionising radiation. The life span study (LSS) of A-bomb survivors continues to provide valuable radiation epidemiological data and quantitative assessments of the radiation-related detrimental health risks (Preston et al. 2003, 2004, 2007; Ozasa et al. 2012). The radiation

L. Walsh (✉)
Department Radiation Protection and Health, Federal Office for Radiation Protection, Ingolstädter Landstr. 1, 85764 Oberschleissheim, Germany
e-mail: lwalsh@bfs.de

L. Walsh
The Faculty of Medical and Human Sciences, University of Manchester, Manchester, UK

🍨 Springer

absorbed doses in the LSS have been determined from information on the mixed γ-ray and neutron field and survivor location at the time of the bombings using the most recent dosimetry system DS02 (Young and Kerr 2005). However, in nearly all past LSS health risk analyses, it has been assumed that the neutron and γ-ray absorbed doses are too highly correlated to be able to separate out the detrimental health effects due to neutrons and γ-rays independently (e.g., Hunter and Charles 2002). Consequently, the widely adopted practice, in nearly all recent analyses, had been to base risk estimates on weighted absorbed doses, that is, γ-ray organ absorbed dose plus a weighting factor for the neutrons multiplied by the organ neutron absorbed dose. However, since the release of the most recent data for all solid cancer incidence which, with 17,448 first primary cancer cases, represents an increase in statistical power over previous datasets (i.e., 8,613 first primary incident solid cancers in Thompson et al. 1994: 9,335 deaths from solid cancer in Preston et al. 2003; and 10,929 deaths from solid cancer in Ozasa et al. 2012), it is instructive to consider alternatives to the usual approach.

Recent developments in the application of information theory and multi-model inference to radiation epidemiology have aided the inferential process by reducing uncertainty associated with model-selection and accounting for increased uncertainties when a multiplicity of models fit the data almost equally well (Walsh 2007; Walsh and Kaiser 2011). However, these approaches focus on comparisons among alternative models and not on the relative importance of the explanatory variables included in the models. Once, a preferred model or set of models has been identified, radiation epidemiologists would often like to know which of the various possibly explanatory covariables included in the models has the strongest influence on the risk response variable.

The purpose of this paper is two fold. The first purpose is to propose and give details of a quantitative technique for obtaining a measure of the relative importance of several main and possibly explanatory covariables in the assessment of detrimental health risks in epidemiological cohorts using the method of hierarchical partitioning (HP) (Chevan and Sutherland 1991). Hierarchical partitioning is considered here because this method has been shown by Murray and Conner (2009) to be the best method for application when correlations between the explanatory variables are present. It is suggested here to apply HP more widely in the field of radiation epidemiology cohort analysis because correlations of concern are often present in the data. The second purpose is to illustrate the application of HP to the covariables for the γ-ray and neutron absorbed doses in the assessment of risks for all solid cancer in the publically available LSS data to see if any extra information regarding

the average effectiveness of neutrons relative to γ-rays can be extracted from the data.

Materials and methods

Determination of the degree of independent effects via HP

Hierarchical partitioning represents an add-on to any technique that yields a measure of goodness of fit of a model to a dataset (e.g., the deviance in Poisson regression). It is similar to a technique called "dominance analysis" in other fields of research (e.g., Budescu 1993). The objective of applying HP to multivariate regression is to partition a measure of association, R (e.g., the deviance) between each independent component, I, and a joint component, J, such that $R = I + J$. The requirements of HP are as follows: an initial measure of fit when no independent variable is present; a final measures of fit when all considered independent variables are present; and all intermediate models with various combinations of independent variables. Given a dependent variable (y) and k explanatory variables ($x_1, x_2,…, x_k$), the independent effect of covariable x_1 represents the average contribution of covariable x_1 to the variance in y over all 2^k possible models. Through the process of HP, the independent effect of each covariable is calculated by comparing the fit of all models containing a particular variable to the fit of all nested models lacking that variable. Although the idea behind HP is simple, the equations illustrating the method can be somewhat abstruse and the application computationally intensive. Therefore, a qualitative description of HP, similar to that provided in German by Dormann and Kühn (2009), has been opted for here.

Consider three independent variables, that is, the explanatory additive covariables A, B and C, resulting in $2^3 = 8$ simple linear models: no covariable (N), A, B, C, $A + B, A + C$ and $B + C$ and $A + B + C$. This set of models can be considered to have four hierarchical levels (0, 1, 1, 1, 2, 2, 2, 3), respectively. In order to study the effect of A, one considers all models without A, then one adds A to each of these models and computes each of the resulting changes in goodness of fit measure: A versus N, $A + B$ versus B, $A + C$ versus C, $A + B + C$ versus $B + C$. In the next step, the resulting changes in goodness of fit measure are averaged for each hierarchical level. Finally, these hierarchical level-specific averages are further averaged over all hierarchical levels. The result of this averaging procedure is the *independent* effect, I, of A on the dependent variable. The *joint* effects, J, of A can be calculated from the difference in goodness of fit measure of

the complete model and the partial model. The application made here is for the simpler case of only two independent variables which are the γ-ray and neutron absorbed doses in the LSS data.

Correlations among explanatory covariables

Problems with multi-collinearity (high levels of correlation) between independent variables include instability of fit-parameter estimates, inflated standard errors for model fit parameters with concomitant increases in Type II errors and false rankings of variable importance (see for example Zar 1999; Belsley et al. 2004). Degrees of multi-collinearity can be assessed with variance inflation factors (VIFs) or tolerance values (TOLs) between two (or more) correlated explanatory covariables (x_1, x_2). Calculation of TOLs and VIFs does not vary based on the type of multivariate analysis to be applied because multi-collinearity concerns the relationship between the independent variables, rather than the relationship of the independent variables to the dependent variable. VIFs can be obtained by a linear regression (even if performing Poisson regression) of one covariable onto the other, that is, if $x_1 = \beta x_2$ is defined as the regression function and r^2 is the coefficient of determination in this linear regression model, then VIF = $1/(1 - r^2)$ = 1/TOL, see Fig. 1. The VIF indicates how much the estimated variances of the regression coefficients associated with x_1 and x_2 are increased above what they would be if $r^2 = 0$. Although suggested cut-off values for the pair-wise correlation coefficient (r) requiring remedial action vary widely, remedial methods are generally not recommended unless $r > 0.80$ (p 90, Katz 2011), see Fig. 1. According to Katz (2011), TOLs <0.25 are worrisome, <0.10 are serious; VIFs >2.5 may be problematical,
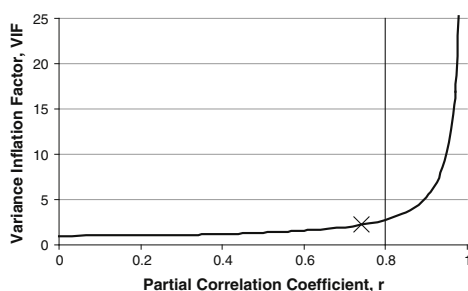
and >10 are serious. There are also "rules of thumb" for indicating excessive multi-collinearity associated with the VIF—most commonly the rule of 10—sometimes the rule of 4. O'Brien (2007) has given a thorough review of such rules and elucidated reasons for caution in applying such rules.

Risk models and dataset

The most recent all solid cancer incidence data for the follow-up 1958–1998 (Preston et al. 2007, data file: ds02can. dat, results file: ds02can.log from www.rerf.or.jp), have been used. The risk models applied here, for radiation-induced solid cancer incidence, are very similar to those already considered and explained in detail in Preston et al. 2007. Use is made of a general rate (hazard) model of the form

$$\lambda(d_\gamma, d_n, a, e, s, c, \text{nic}) = \lambda_0(a, e, s, c, \text{nic}) \cdot [1 + \text{ERR}(d_\gamma, d_n)], \quad (1)$$

for the excess relative risk (ERR), where $\lambda_0(a, e, s, c, \text{nic})$ is the baseline cancer death rate, at age attained, a, age at exposure e, with indicator variables for gender, s (M = male, F = female), city, c (H = Hiroshima, N = Nagasaki) and "not in either city at the time of the bombs", nic. The organ absorbed doses from γ-rays and neutrons are d_γ, d_n, respectively. Organs with separate γ-ray and neutron absorbed doses given in the dataset considered here are colon, liver and marrow (for the other organs only the weighted absorbed doses are available).

Although the baseline rates can be dealt with by stratification, a fully parametric model is adopted here:

$$\begin{aligned}\lambda_0(a, e, s, c, \text{nic}) = \exp\{&\beta_{0,M} + \beta_{1,F} + \beta_{2,N} + \beta_{3,H\_\text{nic}} \\ &+ \beta_{4,N\_\text{nic}} + \beta_{5,M}\ln(a/70) + \beta_{6,F}\ln(a/70) \\ &+ \beta_{7,M}\max^2(0, \ln(a/70)) \\ &+ \beta_{8,F}\max^2(0, \ln(a/70)) + \beta_{9,M}(e-30) \\ &+ \beta_{10,F}(e-30)\}, \quad (2)\end{aligned}$$

where $\beta_{0,M}, \ldots, \beta_{10,F}$ are fit parameters.

This is a simplified version of the model of Preston et al. (2007) because some terms associated with p values >0.05, including a city parameter relating to differences in baseline cancer rates between Hiroshima and Nagasaki, were not considered here. This was because an application of the likelihood ratio test for nested models indicated that the extra terms did not significantly improve the fit in the current analysis.

The ERR models considered were of the form ERR(d_γ, d_n) = $\alpha_1 d_\gamma + \alpha_2 d_n$. A set of four models for HP was considered for the main analysis: a baseline model with ERR($d_\gamma = 0$, $d_n = 0$); ERR(d_γ, $d_n = 0$); ERR($d_\gamma = 0$, d_n);

Fig. 1 The variance inflation factor (VIF) as a function of the degree of correlation (r), between two explanatory covariables. The *vertical line* shows the level below which remedial actions are typically not recommended. The *cross* indicates the value from Table 3, for the correlation between the neutron and γ-ray absorbed doses in the Japanese epidemiological incidence data (Preston et al. 2007)

and ERR(d_γ, d_n). Additional terms in d_γ^2 and d_n^2 were also included and tested in the ERR model to determine if they resulted in a statistically significant improvement in goodness of fit of the model to the data. This approach differs from the usual application of ERR(d), $d = d_\gamma + \text{RBE} \cdot d_n$, that is, the organ absorbed doses weighted by the relative biological effectiveness (RBE) of neutrons relative to γ-rays. The value of 10 for RBE has been widely used in the past for weighting the organ absorbed doses in spite of indication for larger values (Kellerer et al. 2006, Rühm and Walsh 2007). In the present work, adjustments in the ERR relating to the explanatory covariables of gender, age attained and age-at-exposure are omitted so that the resulting risks are gender and age averages. This was done because there is clearly a limit to the statistical power associated with this data and so the model was chosen to be parsimonious for the main purpose, that is, the determination of separate average γ-ray and neutron risk estimates, from which an average RBE can be determined.

Model fit parameters and goodness of fit measures were obtained by optimising the models to the data via Poisson regression with the AMFIT module of the EPICURE software (Preston et al. 1993).

Results

The results of applying this technique are shown in Table 1 which gives the deviances of the set of four ERR models for hierarchical partitioning, that is, just baseline model with ERR($d_\gamma = 0$, $d_n = 0$), ERR(d_γ, $d_n = 0$), ERR($d_\gamma = 0$, d_n) and ERR(d_γ, d_n). R (i.e., R_γ and R_n) is a measure of the zero-order association between the dependent variable (ERR) and the subscripted independent variable, I is the *independent* component of R and J is the *joint* component of R, where $R = I + J$. It can be seen from Table 1 that the joint effect of d_γ, and d_n is less than the independent effects and only accounts for just less than half of the total effects (R). The total deviance drop from adding the covariables d_γ, d_n in a linear ERR model relative to the baseline model was 324.4. This deviance drop partitions into an *independent* contribution from the γ-rays of 177.8 (54.8 %) and an *independent* contribution from the neutrons of 146.6 (45.2 %), thus providing also a rank of the importance of the dose covariables. The addition of quadratic d_γ or d_n terms to the ERR model did not lead to either a statistically significant improvement in overall goodness of fit or statistically significant fit parameters ($p > 0.5$, by the score test) in both cases. The goodness of fit of purely quadratic dose models was much worse than for the linear dose models.

Table 2 gives the all solid cancer ERR/Gy of γ-ray absorbed dose and the ERR/Gy of neutrons for the three organ absorbed doses that are included with the dataset applied, that is, colon, liver and marrow. The fit-parameter correlation coefficients between the ERR/Gy of γ-ray absorbed dose and the ERR/Gy of neutrons are -0.826, -0.817 and -0.813 for the risks with respect to colon, liver

Table 1 Deviances of the ERR models with respect to (wrt) colon doses, that is, just the baseline model (BL) with ERR($d_\gamma = 0$, $d_n = 0$), ERR(d_γ, $d_n = 0$), ERR($d_\gamma = 0$, d_n), ERR(d_γ, d_n)

Covariables in ERR model	Deviance	Change in deviance, Δdev
BL	15,168.6	(wrt BL)
d_γ	14,850.6	$R_\gamma = 318.0$
d_n	14,881.7	$R_n = 286.9$
d_γ, d_n	14,844.3	324.4
Models without neutron doses	Add neutron dose effect	Δdev, between models in same row
Effect of neutrons, d_n		
BL	d_n	286.9
d_γ	d_γ, d_n	6.3
Mean *independent* contribution of neutrons, I_n		$I_n = 146.6$ (i.e., average of above two numbers)
Models without γ-ray doses	Add γ-ray dose effect	Δdev, between models in same row
Effect of γ-rays, d_γ		
BL	d_γ	318.0
d_n	d_n, d_γ	37.5
Mean *independent* contribution of γ-rays I_γ		$I_\gamma = 177.8$ (i.e., average of above two numbers)
Joint contribution $J_{n,\gamma}$		$J_{n,\gamma} = 140.3$

R (i.e., R_γ and R_n) is a measure of the zero-order association between the dependent variable (ERR) and the subscripted independent variable, I is the *independent* component of R and J is the *joint* component of R

Table 2 Excess relative risk (ERR) for all solid cancer for various models with respect to either the colon, liver or marrow absorbed doses

Model	ERR/Gy of γ-rays with 95 % CI	ERR/Gy of neutrons with 95 % CI
With respect to colon absorbed dose		
ERR(d_γ, $d_n = 0$)	0.64 (0.56; 0.74)	
ERR($d_\gamma = 0$, d_n)		96.2 (82.0; 111.2)
ERR(d_γ, d_n)	0.47 (0.31; 0.63)	30.4 (6.5; 55.3)
With respect to liver absorbed dose		
ERR(d_γ, $d_n = 0$)	0.61 (0.53; 0.70)	
ERR($d_\gamma = 0$, d_n)		57.7 (49.1; 66.82)
ERR(d_γ, d_n)	0.46(0.31; 0.61)	17.3 (3.1; 32.1)
With respect to marrow absorbed dose		
ERR(d_γ, $d_n = 0$)	0.58 (0.50; 0.66)	
ERR($d_\gamma = 0$, d_n)		42.9 (36.4.0; 49.7)
ERR(d_γ, d_n)	0.44 (0.30; 0.58)	12.6 (2.2; 23.5)

and marrow absorbed doses, respectively. Using these parameter correlations and the ERR/Gy with uncertainty ranges in Table 2, the RBE of neutrons with respect to γ-rays and the corresponding uncertainty ranges were calculated with Monte-Carlo simulation using 1,000 realizations. The results are RBE values of 65 (95 % confidence interval (CI): 11; 170), 38 (95 % CI: 4; 97) and 29 (95 % CI: 5; 75) when calculated from the fit parameters with respect to colon, liver and marrow absorbed doses, respectively (Table 3).

Table 3 gives the person-year weighted mean absorbed doses and the partial correlation (r) between the neutron and γ-ray absorbed doses. The correlation between neutron and γ-ray colon absorbed doses is $r = 0.74$. The corresponding VIF is 2.2 and therefore much lower than the commonly assumed threshold values, beyond which remedial measures are often taken (see also Fig. 1). The neutron fraction of the organ absorbed dose, defined as neutron organ absorbed dose/(neutron organ absorbed dose + γ-ray organ absorbed dose) has also been calculated and given in Table 3 for the three types of organ absorbed doses considered here. The mean neutron absorbed dose fractions in per cent are 0.46, 0.69 and 0.86, with respect to colon, liver and marrow absorbed doses, respectively.

Discussion

Hierarchical partitioning is not the only method currently available to quantify covariable importance. A recent study by Murray and Conner (2009) has compared six different measures commonly used; zero-order correlations, partial correlations, semi-partial correlations, standardised regression coefficients, Akaike weights, and independent effects (HP) using simulated test data that included correlated explanatory variables and a spurious variable. Once spurious variables had been identified and eliminated, hierarchical partitioning was found by Murray and Conner (2009) to be the best method for application when correlation between the explanatory variables was included in the test model. For this reason, the HP technique was considered here suitable for application to the LSS epidemiological data that have correlated neutron and γ-ray absorbed doses.

The partial correlation between the LSS neutron and γ-ray colon absorbed doses may be considered to be high at 0.74, but this value is just below the level, beyond which remedial action is usually recommended (see Fig. 1). The resulting VIF is 2.2 and also below levels often assumed to indicate the need for the application of measures for reducing multi-collinearity (such as combining two or more independent variables into a single variable). Applying HP it was found that only just under half of the drop in deviance, resulting from adding the γ-ray and

Table 3 Mean person-year weighted colon, liver and marrow absorbed doses

Dose type	Mean absorbed dose (Gy) (person-year weighted) and range	Correlation coefficient	VIF	Neutron absorbed dose fraction (%)	RBE (95 % CI)
Colon d_γ	0.083 (0, 3.07)	0.742*	2.23	0.46	65 (11; 170)
Colon d_n	0.00038 (0, 0.097)				
Liver d_γ	0.087 (0, 3.09)	0.743	2.23	0.69	38 (4; 97)
Liver d_n	0.0006 (0, 0.139)				
Marrow d_γ	0.092 (0, 3.17)	0.739	2.20	0.86	29 (5; 75)
Marrow d_n	0.0008 (0, 0.183)				

The correlation between γ-ray and neutron absorbed doses with the corresponding variance inflation factors (VIF) are also tabulated. The neutron fraction of the absorbed organ dose, defined as neutron organ absorbed dose/(neutron organ absorbed dose + γ-ray organ absorbed dose), is also given

* This value corresponds to a similar value from regressing d_γ on to d_n of 0.744, resulting in a VIF of 2.23

neutron absorbed doses to the baseline risk model, comes from the *joint* effects of the neutrons and γ-rays. Hence, a substantial proportion of this deviance drop is accounted for by *individual* effects of the neutrons and γ-rays. It is the presence of this substantial proportion of individual effects that leads to a reliable determination of separate neutron and γ-ray risks and hence average RBE determinations. Under these conditions, average *RBE* values of 65 (95 % CI: 11; 170), 38 (95 % CI: 4; 97) and 29 (95 % CI: 5; 75) when calculated from the risks (Table 2) correlate inversely with the neutron absorbed dose fractions of 0.46, 0.69 and 0.86 %, where both sets of values are with respect to colon, liver and marrow absorbed doses, respectively. Although the 95 % CIs are quite wide, this pattern in the central estimates of average RBE values is consistent with the physics of the neutron shielding by the human body— that is, the organs with less body shielding have larger neutron absorbed dose fractions because the neutrons are attenuated more than the γ-rays by body shielding (Kellerer et al. 2006).

The calculations of all solid cancer risks with reference to the colon, as adopted in most recent LSS analyses such as Preston et al. (2003, 2004, 2007) and Ozasa et al. (2012) with the assumed RBE weight of 10, apply an RBE that is at about the lower 95 % confidence limit of the RBE determined here of 65 (95 % CI: 11; 170). Also, the level of correlation between the γ-ray and neutron absorbed doses is not high enough to indicate that the linear combination of these absorbed doses into organ-weighted absorbed doses is absolutely necessary on the grounds of remedy for multi-collinearity.

An important qualification with respect to the partial correlation between the LSS neutron and γ-ray colon absorbed doses of 0.74 should be considered here. A large part of the inhomogeneity between neutron and γ-ray absorbed doses is due to a systematic difference between Hiroshima and Nagasaki. The partial correlations for the two cities are 0.89 and 0.94 for Hiroshima and Nagasaki, respectively. Consequently, it is a possibility that the portion of any dose–response difference between neutron and γ-ray absorbed doses that is due to the difference in neutron versus γ-ray absorbed doses in the two cities could be confounded with a city effect due to other factors, such as a city-specific genetic predisposition to one type of cancer (e.g., it is known that adult T cell leukaemia is endemic in Nagasaki (Arisawa et al. 2002)). However, the author is not aware of any such factors that could have confounded the current analysis based on all solid cancers.

A previous method (Kellerer and Walsh 2001, 2002) uncoupled the solid cancer mortality risk coefficient for neutrons from the low dose estimates of the RBE of neutrons and the γ-ray risk coefficient. This was achieved by relating the solid cancer risk in terms of organ-averaged absorbed doses—rather than the colon absorbed doses—to two directly assessable quantities, namely the excess relative risk (ERR_1) due to an intermediate reference dose $D_1 = 1$ Gy of γ-rays and the RBE of neutrons, R_1, against this reference dose. It was concluded that the neutrons have caused 18 or 35 % of the total effect at 1 Gy for tentatively assumed R_1 values between 20 and 50. The corresponding solid cancer mortality ERR for neutrons was found to be between 8/Gy and 16/Gy of organ-averaged absorbed dose. The latter risks are more numerically compatible with the ERR/Gy of neutrons presented here based on liver absorbed dose (17.3, 95 %CI: 3.1; 32.1) and marrow absorbed dose (12.6, 95 %CI: 2.2; 23.5) than central risk estimates based on colon absorbed dose (30.4, 95 %CI: 6.5; 55.3). Also, the average RBE values of 65 (95 % CI: 11; 170), 38 (95 % CI: 4; 97) and 29 (95 % CI: 5; 75) obtained with reference to the colon, liver and marrow, respectively, are, if one equates R_1 to the average RBE, more compatible numerically for average RBE values based on liver and marrow absorbed doses. The average RBE values of 38 and 29 based on liver and marrow absorbed doses, respectively, are also more compatible with ICRP 103 (2007) (neutron weighting factor values in the range of 5–20 depending on energy), the results of Rühm and Walsh (2007) and biological experiments (RBE in the range 5–50, e.g., Edwards 1999) than the average RBE value of 65 based on colon absorbed doses. Therefore, reference to the colon may not be the best organ on which to base all solid cancer risk estimates. Reference to either a less shielded organ than the colon or organ-specific doses may be more appropriate.

The application of organ-specific doses to the grouped, publicly available LSS solid cancer data for the purpose of determining the all solid cancer risk per unit dose is not entirely trivial. Pierce et al. (1996) noted that "It is impossible to use more specific organ doses for solid cancers as a class, since there is no designated organ for those not dying of cancer." However, this difficulty has been resolved (Walsh et al. 2004) by treating each person as a set of a number of sub-units at risk, where each sub-unit belongs to one organ category.

Kellerer et al. (2006) presented indications for a higher neutron RBE with respect to γ-rays, than previously assumed. Kellerer et al. (2006) obtained organ-specific ERRs relative to the RBE weighted organ absorbed dose, ERR/Gy. These risks were then plotted against the neutron fraction of the absorbed organ dose, which decreases with the depth of the organ in the human body. It was found that the risks calculated with RBE = 10 are larger for organs closer to body surface and that this trend, although inconspicuous, was highly statistically significant. This trend can be explained by underestimation of the neutron RBE since the statistical significance of the trend was found to decrease for larger RBE values.

It is noted that whereas the LSS incidence data analysed by Preston et al. (2007) contains organ-specific γ-ray and neutron absorbed doses for the three types of organ absorbed doses considered here (colon, liver and marrow), the publicly available data for the LSS mortality follow-up period 1950–2003, analysed by Ozasa et al. (2012) is limited by only including RBE = 10 weighted absorbed doses. Therefore, further research into the neutron RBE, based on the Ozasa et al. 2012 publically available dataset, is precluded due to this limitation.

Only the grouped data can be made publicly available because Japanese human rights protection laws, related to the extremely important issue of privacy for the atomic bomb survivors, understandably require a rigorous programme of de-identifying and assuring the security of individual data at the Radiation Effects Research Foundation (RERF) before allowing it to be shared with outside investigators. Currently the RBE weighted absorbed doses, with a weight of 10, for all organs of interest are included in the publically available data. Further investigations into the neutron RBE with the publically available grouped LSS data are limited by a lack of availability of organ-specific neutron and γ-ray absorbed doses for all organs of interest. Additional improvements in the precision by which the average neutron RBE could be determined, although they may not be substantial, could also come from a direct application of the methods described here to the ungrouped epidemiological data. Indications from Kellerer and Walsh (2001), Kellerer et al. (2006) and the present study deserve further investigation and should be treated seriously since, for example, some proton therapy patients receive an additional neutron dose as an unwanted by-product (FP-7-EU-ANDANTE for more information see http://www.sciencenet-mv.de/index.php/kb_746/io_2905/io.html). For these reasons, the author would like to encourage RERF scientists with access to the individual data to improve the precision on current average neutron RBE determinations as far as scientifically possible.

Conclusion

A simple evaluation of the degree of independent effects from γ-ray and neutron absorbed doses on the all solid cancer risk with the HP technique is presented here. The HP method is also generally recommended for use in other epidemiological cohort analyses that involve correlated explanatory covariables. The degree of correlation between the γ-ray and neutron absorbed doses has also been considered. The partial correlation between the neutron and γ-ray colon absorbed doses ($r = 0.74$) and the resulting VIF (2.2) are both below the levels beyond which remedial action is usually recommended. Applying HP to the models,

it was found that just under half of the drop in deviance resulting from adding the γ-ray and neutron absorbed doses to the baseline risk model, comes from the *joint* effects of the neutrons and γ-rays—leaving a substantial proportion of the deviance drop accounted for by *individual* effects. The average ERR/Gy γ-ray absorbed dose and the average ERR/Gy neutron absorbed dose obtained directly here for the first time, agree well with previous indirect estimates. The average RBE of neutrons relative to γ-rays, calculated from fit parameters to the ERR all solid cancer model with both colon absorbed dose covariables is 65 (95 %CI: 11; 170). Therefore, the determination of all solid cancer risks based on reference to the colon absorbed doses with a neutron weighting of 10 may not be optimal, and this practice should be reviewed. Any future improvements in neutron RBE precision could have important public-health consequences, for example, for the types of proton therapy that produce unwanted by-product neutron doses.

References

Arisawa K, Soda M, Shirahama S, Saito H, Takamura N, Yamaguchi M, Odagiri K, Nakagoe T, Suyama A, Doi H (2002) Geographic distribution of the incidence of adult T-cell leukemia/lymphoma and other malignancies in Nagasaki Prefecture, Japan. Jpn J Clin Oncol 32:301–306

Belsley DA, Kuh E, Welsch RE (2004) Regression diagnostics: identifying influential data and sources of collinearity. Wiley, Hoboken

Budescu DV (1993) Dominance analysis: a new approach to the problem of relative importance of predictors in multiple regression. Psychol Methods 8:542–551

Chevan A, Sutherland M (1991) Hierarchical Partitioning. The American Statistician 45(2):90–96

Dormann CF, Kühn I (2009) Angewandte Statistik für die biologischen Wissenschaften 2. durchgesehene, aktualisierte, überarbeitete und erweiterte Auflage 2009

Edwards AA (1999) Neutron RBE values and their relationship to judgements in radiological protection. J Radiol Prot 19(2):93–105

Hunter N, Charles MW (2002) The impact of possible modifications to the DS86 dosimetry on neutron risk and relative biological effectiveness. J Radiol Protect 22(4):357

International Commission on Radiological Protection (2007) the 2007 recommendations of the international commission on radiological protection. ICRP_103 Annals of the ICRP 37:2–4

Katz MH (2011) Multivariable analysis: a practical guide for clinicial and public health researchers, 3rd edn. Cambridge University Press, New York

Kellerer AM, Walsh L (2001) Risk estimation for fast neutrons with regard to solid cancer. Radiat Res 156:708–717

Kellerer AM, Walsh L (2002) Solid cancer risk coefficient for fast neutrons, in terms of effective dose. Radiat Res 158:61–68

Kellerer AM, Rühm W, Walsh L (2006) Indications of the neutron effect contribution in the solid cancer data of the A-bomb survivors. Health Phys 90(6):554–564

Murray K, Conner M (2009) Methods to quantify variable importance: implications for the analysis of noisy ecological data. Ecology 90(2):348–355

O'Brien RM (2007) A caution regarding rules of thumb for variance inflation factors. Qual Quant 41:673–690

Ozasa K, Shimizu Y, Suyama A, Kasagi F, Soda M, Grant EJ, Sakata R, Sugiyama H, Kodama K (2012) Studies of the mortality of atomic bomb survivors, report 14, 1950–2003: an overview of cancer and noncancer diseases. Radiat Res 177(3):229–243

Pierce DA, Shimizu Y, Preston DL, Vaeth M, Mabuchi K (1996) Studies of the mortality of atomic bomb survivors. Report 12, Part 1. Cancer 1950–1990. Radiat Res 146:1-27

Preston DL, Lubin JH, Pierce DA (1993) Epicure user's guide. HiroSoft International Corp, Seattle

Preston DL, Shimizu Y, Pierce DA, Suyama A, Mabuchi K (2003) Studies of the mortality of atomic bomb survivors. Report 13: solid cancer and noncancer disease mortality: 1950–1997. Radiat Res 160:381–407

Preston DL, Pierce DA, Shimizu Y, Cullings HM, Fujita S, Funamoto S, Kodama K (2004) Effects of recent changes in atomic bomb survivors dosimetry on cancer mortality risk estimates. Radiat Res 162:377–389

Preston DL, Ron E, Tokuoka S, Funamoto S, Nishi N, Soda M, Mabuchi K, Kodama K (2007) Solid cancer incidence in atomic bomb survivors: 1958–1998. Radiat Res 168:1–64

Rühm W, Walsh L (2007) Current risk estimates based on the A-bomb survivors data—a discussion in terms of the ICRP recommendations on the neutron weighting factor. Proceedings of the Tenth Symposium on Neutro Dosimetry, Uppsala, Sweden. June 12–16, 2006. Radiat Prot Dosim 126(1–4): 423–431

Thompson DE, Mabuchi K, Ron E, Soda M, Tokunaga M, Ochikubo S, Sugimoto S, Ikeda T, Terasaki M, Izumi S, Preston DL (1994) Cancer incidence in atomic bomb survivors. Part II: solid Tumors, 1958–1987. Radiat Res 137:S17–S67

Walsh L (2007) A short review of model selection techniques for radiation epidemiology. Radiat Environ Biophys 46:205–213

Walsh L, Kaiser JC (2011) Multi-model inference of adult and childhood leukaemia excess relative risks based on the Japanese A-bomb survivors mortality data (1950–2000). Radiat Environ Biophys 50:21–35

Walsh L, Rühm W, Kellerer AM (2004) Cancer risk estimates for γ-rays with regard to organ specific doses, part I: all solid cancers combined. Radiat Environ Biophys 43:145–151

Young R, Kerr GD (eds) (2005) DS02: Reassessment of the atomic bomb radiation dosimetry for Hiroshima and Nagasaki, Dosimetry System 2002, DS02 vols 1 and 2, Radiation Effects Research Foundation, Hiroshima

Zar JH (1999) Biostatistical analysis. Prentice Hall, Upper Saddle River

48. Kaiser JC & Walsh L. Independent analysis based on the radiation risk for leukaemia in children and adults with mortality data (1950–2003) of Japanese A-bomb survivors. Radiat. Environ. Biophys (*online first*). 2012, DOI: 10.1007/s00411-012-0437-6

ORIGINAL PAPER

Independent analysis of the radiation risk for leukaemia in children and adults with mortality data (1950–2003) of Japanese A-bomb survivors

Jan Christian Kaiser · Linda Walsh

Abstract A recent analysis of leukaemia mortality in Japanese A-bomb survivors has applied descriptive models, collected together from previous studies, to derive a joint excess relative risk estimate (ERR) by multi-model inference (MMI) (Walsh and Kaiser in Radiat Environ Biophys 50:21–35, 2011). The models use a linear-quadratic dose response with differing dose effect modifiers. In the present study, a set of more than 40 models has been submitted to a rigorous statistical selection procedure which fosters the parsimonious deployment of model parameters based on pairwise likelihood ratio tests. Nested models were consequently excluded from risk assessment. The set comprises models of the excess absolute risk (EAR) and two types of non-standard ERR models with sigmoidal responses or two line spline functions with a changing slope at a break point. Due to clearly higher values of the Akaike Information Criterion, none of the EAR models has been selected, but two non-standard ERR models qualified for MMI. The preferred ERR model applies a purely quadratic dose response which is slightly damped by an exponential factor at high doses and modified by a power function for attained age. Compared to the previous analysis, the present study reports similar point estimates and confidence intervals (CI) of the ERR from MMI for doses between 0.5 and 2.5 Sv. However, at lower doses, the point estimates are markedly reduced by factors between two and five, although the reduction was not statistically significant. The 2.5 % percentiles of the ERR from the preferred quadratic-exponential model did not fall below zero risk in exposure scenarios for children, adolescents and adults at very low doses down to 10 mSv. Yet, MMI produced risk estimates with a positive 2.5 % percentile only above doses of some 300 mSv. Compared to CI from a single model of choice, CI from MMI are broadened in cohort strata with low statistical power by a combination of risk extrapolations from several models. Reverting to MMI can relieve the dilemma of needing to choose between models with largely different consequences for risk assessment in public health.

J. C. Kaiser (✉)
Helmholtz Zentrum München, German Research Centre for Environmental Health, Institute of Radiation Protection, 85764 Oberschleissheim, Germany
e-mail: christian.kaiser@helmholtz-muenchen.de

L. Walsh
Department Radiation Protection and Health, Federal Office for Radiation Protection, 85764 Oberschleissheim, Germany

L. Walsh
The Faculty of Medical and Human Sciences, University of Manchester, Manchester, UK

Introduction

In a recent analysis of leukaemia mortality in the Japanese life span study (LSS) cohort of A-bomb survivors, a joint radiation risk has been derived from a group of several models by applying the technique of multi-model inference (MMI) (Walsh and Kaiser 2011). Reduction of bias from relying on a single model for risk assessment constitutes the main virtue of MMI. Application of MMI can produce more reliable point estimates and improves the characterisation of uncertainties (Burnham and Anderson 2002).

Walsh and Kaiser (2011) have chosen models for a so-called group of Occam, after a review of the relevant literature in radio-epidemiology. The group contained those models which were deemed adequate for joint risk inference (Hoeting et al. 1999; Kaiser et al. 2012). They were then ranked according to the Akaike Information Criterion (AIC) which penalises models with many parameters. A joint risk estimate is given by the mean of model-specific estimates with AIC-based weights, and confidence intervals (CI) are calculated by approximate methods.

For the models discussed in Walsh and Kaiser (2011), parameter parsimony was not always the main concern of model authors so that highly parametrised models had received negligible weights in the weighting process. This intrinsic feature of MMI was criticised by Richardson and Cole (2012). They argued that models with explanatory variables which *may* have an impact on the radiation risk are not considered adequately. In their reply, Walsh et al. (2012) cautioned against the use of model parameters which are not sufficiently supported by the data. Based on the hypothetical problem posed by Richardson and Cole (2012), Walsh et al. (2012) illustrated that models, which contain parameters with weak statistical support, may cause misleading point estimates of the risk. In other examples, over-parametrised models may have little impact on point estimates but can still inflate uncertainty ranges artificially. This side-effect contorts risk assessment in radiation protection if an accurate determination of uncertainties is desired. Such desire is brought forward in court cases related to compensation claims for detrimental health effects from occupational radiation exposure (Niu et al. 2010). For example, decisions in USA courts are sometimes based on the 99 % CI of the probability of causation for cancer in a specific organ (Kocher et al. 2008).

Thus, the criterion for the choice of models for MMI in the study of Walsh and Kaiser (2011) has been changed here, so that the advice of Walsh et al. (2012) is taken seriously. Instead of picking models from peer-reviewed literature without further qualifications, potential candidate models are now submitted to a rigorous statistical selection protocol. Such a protocol has been introduced by Kaiser et al. (2012) and applied to the selection of both descriptive and mechanistic breast cancer models for joint risk inference.

All models considered in Walsh and Kaiser (2011) include a linear-quadratic dose response with different combinations of explanatory variables such as sex, age at exposure and attained age to modify the dose response of the risk. A linear-quadratic response is also preferred in the LSS studies on leukaemia incidence (Preston et al. 1994) and mortality (Preston et al. 2004). It is recommended by committees BEIR VII (NRC 2006), ICRP (Valentin 2007) and UNSCEAR (2008) after consideration of a sizeable number of leukaemia risk studies.

Although the linear-quadratic response can be regarded as the accepted standard in the radio-epidemiology of leukaemia, a number of non-standard responses have been tested motivated by earlier investigations. Little et al. (1999) found that a quadratic-exponential response yielded optimal fits when applied to LSS leukaemia incidence data. Preston et al. (1994) applied a model of two linear dose responses, represented by two line spline functions with a changing slope at a break point, as an alternative to the linear-quadratic response. Explicitly, nonlinear dose responses with sigmoidal forms have also been investigated. They are well-known in toxicology (Hodgson 2010) and are applied in radiation biology to describe normal tissue damage, i.e., of the skin (Hall 2006).

It is emphasised here that the choice of candidate models is on no account exhaustive and that a possible inclusion of non-standard models into Occam's group is mainly justified by goodness-of-fit criteria.

The assignment of weights to risk models is also practised to transport organ-specific risk estimates from the LSS cohort to western populations, if no information on the radiation risk in Caucasian cohorts is available. However, committees BEIR VII (NRC 2006) and ICRP (Valentin 2007) support different approaches to combine an excess absolute risk (EAR) model and an excess relative risk (ERR) model with weights quantified by expert judgement. In any case, adequate transfer models must provide a good description of the risk in the population of origin. The relevance of this statistical criterion for risk transfer concerning leukaemia will be highlighted by the present study.

Past studies of the leukaemia risk at low doses for young attained ages and ages at exposure were performed for settlements in the vicinity of nuclear power stations (NPP) (Laurier et al. 2008; Kaatsch et al. 2008) and to estimate the proportion of cases induced by computer tomography (CT) scans (Pearce et al. 2012) or natural background radiation (Wakeford et al. 2009; Little et al. 2009; Kendall et al. 2012). Investigations in these fields and, additionally, ongoing risk assessment for residents near the Japanese Fukushima Daiichi NPP may benefit from both risk estimates with stronger support of the data and a more comprehensive quantification of uncertainties, which are the aim of the present study.

Materials and methods

Epidemiological data set

The present study is closely related to the study of Walsh and Kaiser (2011) which used LSS mortality data from

1950 to 2000. After it appeared, the LSS data have been updated with an extended follow-up to 2003 in Report 14 (Ozasa et al. 2012). To provide an analysis with the most recent data set, all results reported by the present study are based on LSS Report 14. The updated data set comprises 86,611 subjects, 318 leukaemia deaths (including 22 cases in 2001–2003) and 3,294,282 person years (including 109,927 person years in 2001–2003). The person-year weighted means are 22 year for age at exposure, 50 year for attained age, 58 year for age of cases and 134 mSv for the weighted dose to bone marrow with a factor of ten for the relative biological effectiveness (RBE) of neutrons. The RBE value depends on the radiation field and the detrimental health effect under observation. For leukaemia, an estimation is difficult and produces very large CI (Little 1997; Hunter and Charles 2002). The LSS cohort data in file lss14.csv are available for download from the website of the Radiation Effects Research Foundation (RERF) in Japan (http://www.rerf.or.jp).

The MECAN software package

The analysis has been performed with the MECAN software package which is available from the corresponding author by request (Kaiser 2010). A user manual, regression control files and an executable to repeat the present analysis are included. MECAN is executed in a terminal on a command line under Linux or Windows. To implement risk models other than those applied here, a minimal knowledge of the C++ programming language is required. The code includes the C++ library MINUIT2 (Moneta and James 2010) from CERN which minimises the Poisson likelihood. Pre-processing of the grouped data, regression, comparison of observed and expected cases, and simulation of uncertainty intervals can all be performed in one run. The calculation of risk estimates from MMI is automated with shell script files which contain the set of required commands.

Results from MECAN for the preferred models of the present study and of the study by Walsh and Kaiser (2011) have been cross-checked by independent calculations with the EPICURE package (Preston et al. 1993). Deviances from the two packages differed by around 10^{-3} points. Relative differences of estimates for model parameters, Wald-type standard errors and CI from the likelihood profile fell below 10^{-2}. Relative differences in the entries of the parameter correlation matrices exceeded one per cent in some cases.

Baseline model

The model for the baseline mortality rates

$$h_0(s,c,a,e) = \exp\{b_0 + b_s s + b_c c \\ + b_{a_1} \ln(a/55) + b_{a_2} \ln^2(a/55) \\ + b_{e_1}(e-30) + b_{e_2}(e-30)^2\} \quad (1)$$

applies the same functional form as the models of the UNSCEAR committee and of Little et al. (2008) (see Table 8 of Walsh and Kaiser 2011). The parameter b_0 represents a constant factor, parameters b_s and b_c account for rate differences by sex (males $s = -1$ and females $s = +1$) and city, i.e. Hiroshima ($c = -1$) and Nagasaki ($c = +1$). Parameters b_{a_1} and b_{a_2} quantify variations of the rates with attained age. Parameters b_{e_1} and b_{e_2} depend on age at exposure which for the acute exposure of the A-bomb survivors serves as a surrogate for dependence on birth cohort to account for secular trends in baseline rates. The present baseline model consumes seven adjustable parameters.

Model selection protocol

The selection protocol of Kaiser et al. (2012) has been applied here. It starts with step-by-step attempts to optimise the baseline model in Eq. (1) with exposure-related features contained in a set of candidate models. Parameters are added individually or in groups and retained, if the nested model with the additional parameter(s) survived a likelihood ratio test (LRT) against the model of origin. For nested models, the difference between their deviances is χ^2-distributed (Claeskens and Hjort 2008; Walsh 2007). The number of degrees of freedom for the difference is equal to the difference in the number of parameters. A model with one additional parameter is considered an improvement over the model without this parameter with a 95 % probability if the deviance is lowered by at least 3.84 points. The probability threshold is set relatively high to avoid inclusion of spurious features in risk models (Anderson et al. 2001; Walsh et al. 2012).

In the first round, various versions of the dose response are tested which are shown schematically in the flow chart of Fig. 1. To retain clarity, not all tested models are shown. A second round would involve improvements with dose effect modifications by explanatory variables such as sex, age at exposure or attained age, an example is given in Eq. (4). After passing an LRT, a model is kept for further rounds of testing. It may join Occam's group, if improvements are no longer possible. Defeated models are rejected for risk assessment. In Fig. 1, a defeated model is identified by at least one arrow pointing away from it. Models surviving the last round of tests 'see' only arrowheads. More details of the protocol are given in Kaiser et al. (2012).

In the present analysis, an additional selection criterion prevents the overpopulation of Occam's group with models
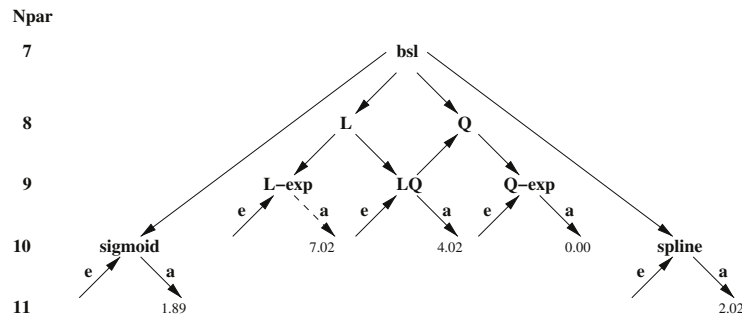
Fig. 1 Flow chart of model selection. Models are grouped in rows pertaining to equal number of model parameters N_{par}. The protocol starts with the baseline model bsl (*top*), arrows point to models which survived a pairwise LRT on the 95 % level. Dose effect modifiers are annotated as *e* for age at exposure and as *a* for attained age. AIC differences to the preferred model Q-exp with dose effect modifier for *a* are given for all models surviving the last round of tests. Model L-exp with dose effect modifier for *a* is discarded because its ΔAIC exceeded 5.99 (*dashed arrow line*)

of negligible influence. Based on the Akaike Information (Akaike 1973; Burnham and Anderson 2002)

$$AIC = dev + 2\,N_{par}, \tag{2}$$

where *dev* denotes the Poisson deviance and N_{par} denotes the number of parameters, a weight $1/[1 + \exp(-\Delta AIC_k/2)]$ can be constructed for the pairwise comparison of the preferred model with AIC_0 and model k with AIC_k, where $\Delta AIC_k = AIC_k - AIC_0$. If this weight fell below 5 % (or ΔAIC_k exceeds 5.99), the corresponding model k was not used for risk assessment (Hoeting et al. 1999; Walsh 2007). Note, that the second criterion does not constitute a statistical test (Burnham and Anderson 2002, p 84). After its application, the L-exp model with dose effect modifier for attained age has been discarded (see Fig. 1).

At the end of the selection procedure, Occam's group of non-nested risk models with enough relevance for risk assessment has been established for use in the MMI$_{SP}$ analysis.[1]

Candidate models for Occam's group

From the outset, the dose response of candidate models is constrained to yield a zero excess risk at zero dose and to rise monotonously with an increasing dose. Models with hormetic dose responses have not been tested but would have been admitted into Occam's group if they qualified. Apart from these preconditions, admission to Occam's group is achieved solely by sufficient goodness-of-fit.

---

[1] The present study is named MMI$_{SP}$ study, since models are chosen by a *S*election *P*rotocol. For a better distinction, the study of Walsh and Kaiser (2011) is named here MMI$_{PM}$ study, since it was based on previously *P*ublished *M*odels.

Improvements of the baseline model from Eq. (1) have been attempted with three types of dose responses 'LQ-exp', 'sigmoid' and 'spline' (see Fig. 1) for both EAR and ERR models. The complete dose response of the LQ-exp model took the form $(\alpha\,d + \beta\,d^2)\exp(-\gamma\,d)$. To account for random errors, the dose-squared covariable has been multiplied by a factor of 1.12 (Walsh and Kaiser 2011; Pierce et al. 1990). Sub-models with all seven possible combinations of the dose–response parameters α, β and γ have been tested but only the two parameter combinations α, β (sub-model LQ for linear-quadratic) and β, γ (sub-model Q-exp for quadratic-exponential) survived the series of LRTs. Cubic-exponential or quadratic-exponential models did not yield better fits than the Q-exp model. But a model with a sigmoidal response (which progresses from small beginnings and levels off at high doses) and a model with two linear dose responses, connected by a break point at dose d_k (termed spline model), could also be added to Occam's group.

To perform valid LRTs, two continuous derivatives (i.e. a C2 condition) of the Poisson deviance with respect to the model parameters are required (Schervish 1997). All but one model apply parametric functions which are twice continuously differentiable. For the spline model, it is not obvious that the C2 condition is fullfilled for derivatives with respect to the break point d_k. Therefore, the region around the minimum of the Poisson likelihood as a function of d_k has been scanned numerically by fixing d_k at different values and re-fitting the remaining parameters. The scan revealed a slightly tilted paraboloid so that both derivatives are indeed continuous. The minimum is reached at $d_k = 0.36$Sv (σ CI$_{LP}$ 0.28; 0.52). The CI$_{LP}$ are calculated from the likelihood profile with the

MINOS routine of MINUIT2. A graphical evaluation of the numerical scan yielded the same values.

Dose effect modifiers of sex s, age at exposure e and attained age a have been tested separately and in combination but only the modifier $\exp\left(\varepsilon \ln \frac{a}{55}\right)$ has been accepted in all three types of dose responses shown in Fig. 1. The difference between males and females was not significant for all selected ERR models in contrast to the results of the (discarded) EAR models.

Determination of model-specific risk estimates and confidence intervals

A best risk estimate for a single model is calculated with the set of parameter estimates which minimises the likelihood. To determine the corresponding CI, a probability density function (pdf) with 10,000 entries is generated by Monte-Carlo simulation which accounts for uncertainty ranges and pairwise correlations of all adjusted parameters. Two percentiles, corresponding to the required level of confidence (i.e. 95 %), are adopted as upper and lower CI.

To meet the requirement of a symmetric parameter correlation matrix as the backbone of the Monte-Carlo simulation, each parameter-specific pdf must ideally follow a Gaussian distribution. As a necessary precondition, the σ CI$_{LP}$, calculated from the likelihood profile, should lie symmetrically around the best parameter estimate. The precondition is fulfilled for the baseline model given in Eq. (1) which is used by the models of Occam's group. All parameters of the ERR in the LQ and the Q-exp model show symmetric CI$_{LP}$ to a good approximation if models are centred at $e = 30$ and $a = 55$ (see Table 1). However, models centred at young ages at exposure and attained ages exhibit markedly skewed CI$_{LP}$ for the linear and the quadratic term in the $ERR(d)$. The ERR parameters a and b of the sigmoid model possess asymmetric CI$_{LP}$ with ratios of 0.7 and 2 between lower and upper bound but the asymmetry did not disappear for centring at different values. The spline model had symmetric CI$_{LP}$ for the two linear risk coefficients but the break point d_k showed asymmetric CI$_{LP}$ for all tested combinations of centring. To calculate CI with Monte-Carlo simulation for all five combinations of e and a, the models have been centred at $e = 30$ and $a = 55$. Although the precondition of symmetric parameter CI$_{LP}$ is not fully met for two ERR parameters of the sigmoid model and one parameter of the spline model, one expects that Monte–Carlo simulations of uncertainties for these two models yield results with a moderate bias.

Centring does not change the quality of fit, i.e., the value of the Poisson deviance and the best risk estimates. Walsh and Kaiser (2011) exploited this fact and centred the risk models at seven pairs of a and e for a more convenient calculation of uncertainties. Especially at young ages, their

Table 1 Best parameter estimates, symmetric Wald-type ΔCI from a parabolic approximation around the minimum of the likelihood function, and ΔCI$_{LP}$ from the actual likelihood profile for the preferred Q-exp model; to facilitate the assessment of symmetry, ΔCI are given as distances from the best parameter estimate in the standard σ range

Name	Unit	Best estim.	Wald-type ΔCI	ΔCI$_{LP}$
b_0	–	-9.50	0.10	-0.11; 0.10
b_s	–	-0.322	0.057	-0.057; 0.057
b_c	–	-0.140	0.065	-0.066; 0.064
b_{a_1}	–	2.11	0.27	-0.27; 0.27
b_{a_2}	–	1.08	0.21	-0.21; 0.20
b_{e_1}	10^{-3} year^{-1}	6.4	-0.46	-0.46; 0.46
b_{e_2}	10^{-4} year^{-2}	-7.2	2.3	-2.3; 2.2
β	Sv^{-2}	4.3	1.2	-1.1; 1.4
γ	Sv^{-1}	-0.38	0.13	-0.13; 0.13
ϵ	–	-1.62	0.35	-0.36; 0.34

approach (implemented in their Method 1) yielded symmetric CI in the Monte-Carlo simulations even if the correct CI$_{LP}$ from the profile likelihood were highly asymmetric. To partly make up for this bias, the simulation of CI in their MMI$_{PM}$ analysis has been repeated with their models centred at $e = 30$ and $a = 55$ with approx. symmetric CI$_{LP}$. Moreover, the complete parameter correlation matrix was used now to simulate parameter uncertainties instead of the fraction that pertained to the ERR part of the model. In the repeated analysis, only the four models with the highest weights (see Table 3 of Walsh and Kaiser (2011)) were applied to the data set of LSS report 14 (Ozasa et al. 2012). Now the 2.5 % percentiles of the ERR for the UNSCEAR model do not drop below zero in contrast to the results reported in Table 4 of Walsh and Kaiser (2011).

Multi-model inference

The surviving models are ranked according to their AIC, defined in Eq. (2), and to each model k an AIC-related weight

$$p_k = \frac{\exp\left(-\frac{1}{2}\Delta\text{AIC}_k\right)}{\sum_{j=0}^{M-1} \exp\left(-\frac{1}{2}\Delta\text{AIC}_j\right)} \tag{3}$$

has been assigned.

The central risk estimate from MMI is given by the AIC-weighted mean of best estimates from the models in Occam's group. The CI of the MMI mean are derived from a joint pdf with 10,000 entries which is obtained by merging the model-specific pdf with sizes corresponding to the AIC-weight (i.e. 5,301, 2,062, 1,927 and 710 realisations from models Q-exp, sigmoid, spline and LQ, see Table 2). From the joint pdf, an approximation of the unconditional sampling variance [see Burnham and Anderson 2002, Eq. (4.3)]

Table 2 Parametric dose dependence for the ERR models of Occam's group used in MMI, the AIC-weight is calculated from Eq. (3)

Model name	Form of $ERR(d)$	N_{par}	Deviance	AIC-Weight
Q-exp	$\beta d^2 \exp(\gamma d)$	10	2,670.890	0.5301
Sigmoid	$\frac{A}{B+d^c}$	11	2,670.778	0.2062
Spline	$\begin{cases} \alpha_1 d & \text{for} \quad d < d_k \\ \alpha_2(d-d_k) & \text{for} \quad d \geq d_k \end{cases}$	11	2,670.914	0.1927
LQ	$\alpha\, d + \beta\, d^2$	10	2,674.910	0.0710

can be obtained. Implicitly, this pdf also accounts for model correlations.

Results

For a total of 26 ERR and 16 EAR candidate models, lists of Poisson deviances, number of parameters and AIC values are given in the online resource as a PDF excerpt of an EXCEL workbook (ESM1). The AIC of the preferred EAR model was still about 11 points away from the AIC of the preferred ERR model. Thus, no EAR model fell within Occam's group.

For the four selected models, files with model-specific data on the quality of fit, parameter estimates and CI (from both the parabolic approximation of the likelihood minimum and from the likelihood profile), the parameter correlation matrix and tables to compare observed and expected cases are added to the online resource in PDF format. The data provided allow a repetition of the MMI_{SP} analysis without re-fitting the corresponding models.

Table 2 presents the four ERR models in Occam's group. Only the dose dependence $ERR(d)$ is shown there, the final form

$$\mathrm{ERR}(d,a) = \mathrm{ERR}(d) \exp\left(\varepsilon \ln \frac{a}{55}\right) \qquad (4)$$

additionally applies a power function for attained age a centred at 55 year.

Compared to the previous analysis, the baseline function of both the LQ model and LQ-exp model from Schneider and Walsh (2009) was replaced by Eq. (1) with one parameter less which increased the deviance by only about one point. Accounting for the explanatory variables of sex and age at exposure yielded no significant improvements of their models so they were discarded. With these modifications, the LQ model of Schneider and Walsh (2009) morphed into the LQ model of the present analysis, which is equivalent to the UNSCEAR model considered in Walsh and Kaiser (2011). With the same modifications, and after elimination of the linear term, the LQ-exp model of Schneider and Walsh

(2009) became the preferred Q-exp model of the present analysis with parameter estimates given in Table 1. The model of Little et al. (2008) was excluded from Occam's group because the dependence on age at exposure did not survive the LRT with the UNSCEAR model.

The UNSCEAR model (termed LQ model in the present analysis) dominated the MMI_{PM} risk estimate in Walsh and Kaiser (2011) with a weight of 51 % (see their Table 5), but here its contribution is reduced to only 7 %. Now the Q-exp model is preferred with a weight of 53 % with a four points lower deviance than the LQ model. Inspection of tables, which compare observed and expected cases in model-specific result files (here ESM3 and ESM2) of the online resource, suggests that the Q-exp model produced slightly better fits to the data at young ages of exposure and attained ages. For example, for Poisson strata (numbered 0, 10, 20 in the result files) with person-year weighted means of $e \simeq 5$ year, $a \simeq 15$ y the contribution to the Poisson deviance of the Q-exp model is about 2.5 points lower compared to the LQ model. Such exposure scenarios are of enhanced interest for radiation protection and here the Q-exp model yields lower (and better supported) risk estimates than models with a linear-quadratic dose response.

The quadratic term of the Q-exp model determines the response at doses <0.5 Sv, damping by the exponential term becomes important above >2.5 Sv. In the intermediate range between 0.5 and 2.5 Sv, the response is well approximated by a linear relationship (see Fig. 2). Between 2.5 and 3 Sv, nine cases have been recorded and there are only two cases above 3 Sv. The markedly different risk estimates for high doses are caused by the low statistical power in the corresponding cohort strata.
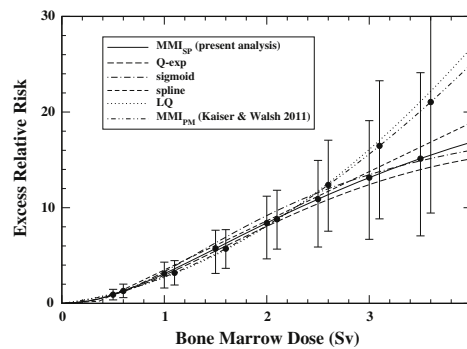

Fig. 2 Excess relative risk (AIC-weighted mean or best estimate for separate models, with 95 % CI) for a 55-year old adult exposed at age 30 from MMI_{SP} (present analysis), the preferred Q-exp model, the sigmoid model, the spline model, the LQ model and from the repeated MMI_{PM} analysis with the four top-ranking models of Walsh and Kaiser (2011)
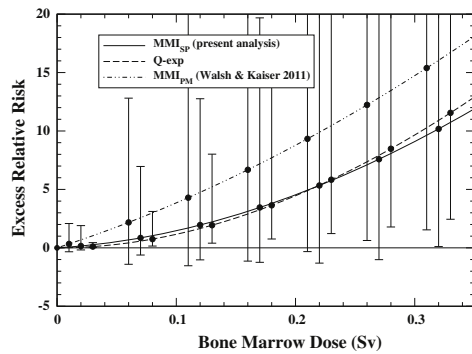
Fig. 3 Excess relative risk (AIC-weighted mean or best estimate for model Q-exp, with 95 % CI) for a 7-year old child exposed at age 2 from MMI$_{SP}$ (present analysis), the preferred Q-exp model and from the repeated MMI$_{PM}$ analysis with the four top-ranking models of Walsh and Kaiser (2011)

The ERR at low doses for a 7-year-old child exposed at age 2 is shown in Fig. 3. Compared to the previous analysis, the AIC-weighted mean of the ERR from MMI$_{SP}$ is reduced, i.e.,. by a factor of two at 100 mSv, although the reduction is not statistically significant. The effect of any one model is directly visible in the MMI dose response if it has a weight of more than fifty per cent. The AIC-weighted mean from MMI$_{SP}$ closely follows the best estimate of the preferred Q-exp model. The additional three models cause a sizeable increase of the CI especially at low doses where

a determination of the ERR implies an extrapolation to cohort strata with almost no cases (see Table 2 of Walsh and Kaiser 2011). In these regions, CI from a single model of choice underestimate the risk uncertainty by wide margins (see also Tables 3, 4).

Tables 3, 4 and 5 present the ERR from the four models of Occam's group separately and from MMI$_{SP}$ of the present analysis and of the MMI$_{PM}$ analysis by Walsh and Kaiser (2011) at 10 mSv, 100 mSv and 1 Sv. At exposure of 1 Sv, both MMI analyses and all separate models yield similar estimates and CI for children, adolescents and adults.

The situation changes at 100 mSv. Now the new preferred Q-exp model predicts a four times lower risk than the previously chosen UNSCEAR (here LQ) model. Compared to the repeated MMI$_{PM}$ analysis with the four top-ranking models of Walsh and Kaiser (2011), estimates from the present MMI$_{SP}$ analysis differ by a factor of 2.5 and the CI are markedly reduced.

At 10 mSv, the AIC-weighted mean of the present study no longer approximates the best estimate of the preferred Q-exp model. The mean is strongly influenced by a 30 times higher estimate of the LQ model which on the other hand acquires the lowest weight in MMI$_{SP}$. To avoid this effect and to preserve the similarity between the point estimates from the preferred model and from MMI, Kaiser et al. (2012) recommend to replace the AIC-weighted mean by the median of the joint pdf, which is given in brackets in Table 3.

At doses of 10 mSv and 100 mSv, the 2.5 % percentiles from the present MMI$_{SP}$ analysis include a zero risk due to the uncertainty of the spline model.

Table 3 ERR (10^{-2}) at 10 mSv for five combinations of age at exposure e and attained age a

Model name or MMI result	$e = 2$ $a = 7$	$e = 2$ $a = 12$	$e = 7$ $a = 17$	$e = 12$ $a = 22$	$e = 30$ $a = 55$
MMI$_{PM}$	33.5	13.7	7.80	5.12	1.14
Walsh and Kaiser (2011)*	−33.5; 208	−12.4; 61.7	−7.24; 28.5	−4.78; 16.4	−1.22; 2.77
LQ	40.4	16.8	9.48	6.22	1.39
UNSCEAR (2008)	−0.753; 215	−0.370; 64.0	−0.237; 29.2	−0.167; 16.5	−0.0402; 2.80
Spline	17.7	7.34	4.15	2.72	0.609
	−36.3; 153	−12.9; 46.1	−6.98; 22.0	−4.36; 12.8	−1.00; 2.19
Sigmoid	0.851	0.358	0.204	0.135	0.0310
	1.2×10^{-3}; 41.2	5.5×10^{-4}; 14.9	3.2×10^{-4}; 7.92	2.2×10^{-4}; 5.06	5.8×10^{-5}; 1.04
Q-exp	1.20	0.501	0.285	0.188	0.0427
(preferred model)	0.246; 5.02	0.140; 1.50	0.0953; 0.699	0.0696; 0.398	0.0184; 0.0667
MMI$_{SP}^{\dagger}$	7.09 (1.41)	2.94 (0.568)	1.67 (0.317)	1.09 (0.206)	0.245 (0.0463)
(present study)	−9.02; 92.7	−3.67; 31.8	−2.01; 16.3	−1.34; 9.89	−0.323; 1.99

AIC-weighted mean for MMI or model-specific best estimate in first row, 95 % CI from Monte-Carlo simulation in second row, for MMI$_{SP}$ the mean is calculated with the model-specific weights of Table 2

† median of joint pdf from MMI$_{SP}$ in brackets

* Point estimates and CI from repeated analysis (see text)

Table 4 ERR (10^{-1}) at 100 mSv for five combinations of age at exposure e and attained age a

AIC-weighted mean for MMI or model-specific best estimate in first row, 95 % CI from Monte-Carlo simulation in second row, for MMI_{SP} the mean is calculated with the model-specific weights of Table 2

* Point estimates and CI from repeated analysis (see text)

Model name or MMI result	$e = 2$ $a = 7$	$e = 2$ $a = 12$	$e = 7$ $a = 17$	$e = 12$ $a = 22$	$e = 30$ $a = 55$
MMI_{PM}	38.5	15.7	8.92	5.86	1.31
Walsh and Kaiser (2011)*	−15.5; 219	−6.19; 64.7	−3.61; 29.8	−2.49; 17.0	−0.642; 2.84
LQ	43.9	18.2	10.3	6.76	1.51
UNSCEAR (2008)	2.37; 227	1.18; 66.5	0.745; 30.3	0.513; 17.2	0.125; 2.88
Spline	17.7	7.34	4.15	2.72	0.609
	−36.3; 153	−12.9; 46.1	−6.98; 22.0	−4.36; 12.8	−1.00; 2.19
Sigmoid	9.58	4.03	2.30	1.52	0.348
	0.298; 91.9	0.145; 31.4	0.0889; 15.7	0.0620; 9.56	0.0164; 1.89
Q-exp (preferred model)	11.6	4.84	2.76	1.82	0.413
(preferred model)	2.39; 48.2	1.37; 14.4	0.932; 6.67	0.683; 3.79	0.182; 0.633
MMI_{SP}	14.6	6.10	3.47	2.28	0.515
(present study)	−8.60; 103	−3.58; 34.0	−1.97; 17.6	−1.31; 10.5	−0.312; 2.07

Table 5 ERR at 1 Sv for five combinations of age at exposure e and attained age a

AIC-weighted mean for MMI or model-specific best estimate in first row, 95 % CI from Monte-Carlo simulation in second row, for MMI_{SP} the mean is calculated with the model-specific weights of Table 2

* Point estimates and CI from repeated analysis (see text)

Model name or MMI result	$e = 2$ $a = 7$	$e = 2$ $a = 12$	$e = 7$ $a = 17$	$e = 12$ $a = 22$	$e = 30$ $a = 55$
MMI_{PM}	81.8	32.9	18.7	12.3	2.76
Walsh and Kaiser (2011)*	17.0; 356	10.2; 97.7	6.24; 44.2	5.28; 24.9	1.60; 3.90
LQ	78.6	32.6	18.4	12.1	2.71
UNSCEAR (2008)	17.2; 348	10.2; 100	7.16; 44.9	5.48; 24.8	1.59; 3.81
Spline	101	42.0	23.8	15.6	3.49
	22.8; 423	13.8; 121	9.83; 54.2	7.60; 30.1	2.27; 4.69
Sigmoid	91.1	38.3	21.9	14.5	3.31
	18.7; 345	10.9; 102	7.61; 46.5	5.77; 26.3	1.56; 4.37
Q-exp (preferred model)	82.4	34.4	19.6	12.9	2.94
(preferred model)	18.2; 322	10.8; 94.4	7.45; 43.1	5.55; 24.3	1.54; 3.91
MMI_{SP} (present study)	87.6	36.6	20.8	13.7	3.10
(present study)	19.7; 343	11.4; 101	7.95; 46.2	5.94; 25.9	1.60; 4.31

Discussion

Little et al. (1999) analysed the dose response for three subtypes of acute myeloid leukaemia (AML), chronic myeloid leukaemia (CML) and acute lymphocytic leukaemia (ALL) separately and for all subtypes combined. Their analysis was carried out with LSS incidence data, and with two other data sets of women treated for cervical cancer (incidence) and UK patients treated for ankylosing spondilitis (mortality). From a list of 13 ERR models, using similar versions of the general LQ-exp response with dose effect modifiers, the Q-exp response has been preferred for yielding the optimal fit. They used already LRTs to discard models with statistically insignificant features. Their estimates of the coefficients β for the dose squared and γ for the exponential damping were 5.8 (95 % CI 2.7; 11) Sv^{-2} and −0.49 (95 % CI −0.76; −0.22) Sv^{-1}, respectively (see their Table 5). Risk estimates for leukaemia incidence are expected to exceed those for mortality. Comparison with estimates in Table 1 shows that this relation is realised for dose $\lesssim$ 3 Sv, albeit without statistical significance.

Separate estimates for the other two data sets produced no significant risk (women with cervical cancer) or a ten times larger coefficient β (patients with ankylosing spondilitis). Comparison of risks in these different populations is complicated by the consideration that the LSS subjects were not under observation because of known diseases whereas members of the two other data sets were.

Basic tenets of MMI might be extended to address questions of risk transfer between populations which are discussed in reports of committees BEIR VII (NRC 2006) and ICRP (Valentin 2007). BEIR VII propose to transfer risks for solid cancer sites (except breast and thyroid) and for leukaemia from the LSS cohort to the US population with a linear combination of an ERR model and an EAR model. They recommend point estimates as weighted means obtained under the two models. For leukaemia and solid cancer sites (except breast, thyroid and lung), the weights of

0.7 (ERR) and 0.3 (EAR) are chosen by expert judgement based on the observation 'that there is a somewhat greater support for relative risk than for absolute risk transport' (see p. 276). Inconsistent with BEIR VII, ICRP recommend to apply only the EAR model of Preston et al. (1994) for leukaemia incidence.

In general, the consensus on a risk transfer model is based on a complex mix of factors, but a comprehensive consideration is beyond the scope of the present study. However, any adequate transfer model should provide a good description of the risk in the population of origin. Would goodness-of-fit criteria be allowed to assess the adequacy of a model, EAR models of leukaemia mortality would not contribute to the transfer. The best EAR model exceeds the AIC of the preferred Q-exp model by about 11 points which leads to a negligible AIC-weight. A second criterion of Bayesian information ($BIC = dev + N_{par} \ln(n_{cases})$) is often used as an alternative to the AIC because it favours more parsimonious models (Claeskens and Hjort 2008). It is 18 points higher which constitutes strong evidence (Kass and Raftery 1995) for the rejection of the EAR model. Likewise, Little (2008) recommends to drop EAR models, but with a different rationale. Based on a comparison of risks for childhood exposure between the LSS cohort and three medically exposed groups in Europe, he observed that heterogeneity in cohort-specific EAR estimates is much higher than in ERR estimates.

A recent risk study of leukaemia (and brain tumours) after childhood exposure by CT scans reports an ERR of 36 (95 % CI 5; 120) Sv^{-1} from a purely linear model for age at exposure <22 year, dose range between 0 and 100 mSv and follow-up of 23 year (Pearce et al. 2012). The same linear model applied to the LSS incidence data (Preston et al. 1994) produced an ERR of 37 (95 % CI 14; 127) Sv^{-1} for age at exposure <20 year, dose range between 0 and 4 Sv and follow-up of 20 year (see Table 8 of the supplement to Pearce et al. (2012)).

The authors of the present study fitted a purely quadratic model to the LSS incidence data for all dose ranges which increased the deviance by 4.8 points compared to the linear model. If the overlap of dose ranges was improved by a reduction to 0–500 mSv for the LSS data, the quadratic model yielded a slightly better fit. The deviance decreased by 2.4 points compared to the linear model. Improved fits of a quadratic model at lower doses are in line with findings of the present study (mortality) and the study of Little et al. (1999) (incidence). With a coefficient of 61 (95 % CI 22; 185) Sv^{-2} for the quadratic model, the ERR at 100 mSv is six times lower than for the linear model. Using both models in MMI would still yield a reduction of the ERR by a factor of three compared to the linear model.

Nevertheless, Pearce et al. (2012) report 'little evidence of nonlinearity of the dose response, using either linear-quadratic or linear-exponential forms of departure from linearity', but purely quadratic responses appear not to have been tested. At this point, the present authors suggest a comparison of the CT risk with the LSS quadratic response. Should alternative dose responses, such as purely quadratic, fit the data comparably well, an even fairer comparison might account for model uncertainty in the CT cohort. In this case, reverting to MMI can relieve the dilemma of needing to choose between models with largely different consequences for issues of public health, e.g., for assessing the risk-to-benefit ratio related to a CT scan. In a wider context, MMI might be of use for statistical analysis in a number of cohort studies of CT exposure and cancer incidence which will be completed in the near future (Einstein 2012).

Conclusions

Only models with a linear-quadratic dose response were included in the MMI analysis of Walsh and Kaiser (2011). The present analysis introduced three models with non-standard dose responses which produced significantly better fits to the data. All considered models yield very similar point estimates and uncertainties in the dose range 0.5–2.5 Sv, i.e., in cohort strata with a sufficient number of cases. Divergent predictions appear in strata with almost no cases for children and adolescents exposed to very low doses of 100 mSv and below (see Table 2 of Walsh and Kaiser 2011). Yet for purposes of radiation protection, these exposure scenarios are of increased interest. Compared to the study of Walsh and Kaiser (2011), the present MMI analysis predicts markedly lower risks with factors of two around 100 mSv and up to five for lower doses. These point estimates are considered as more reliable since they were produced with models, which describe the data slightly better notably for children and adolescents.

Besides the improvement of point estimates, a second benefit of MMI has been demonstrated. Several plausible models can be included in a more comprehensive (though not exhaustive) determination of uncertainties. Again, the benefit becomes noticeable in the above-mentioned cohort strata with low statistical power, where the risk is determined by extrapolation. Now uncertainty ranges are mainly determined by the *spread* of model-specific point estimates, whereas the model-specific uncertainty ranges are rather small. Hence, inferring uncertainties from a single model of choice may lead to a substantial underestimation. In this context, the present MMI study provides significant risks only above some three hundred mSv, whereas the

95 % CI of the preferred Q-exp model do not include a zero risk for all considered exposure scenarios.

The impact of pertinent sources of uncertainty, such as the 'healthy survivor effect', errors in dosimetry or misdiagnosis of cases on risk estimates has been discussed extensively in the literature, for the LSS cohort see, e.g., Little et al. (1999), Preston et al. (2003), Preston et al. (2004). Already Little et al. (1999) preferred ERR models with a Q-exp response. They did, however, not consider the additional contribution to the uncertainty which is induced by including models with other plausible dose responses into the risk analysis. In this developing field of research in radiation epidemiology, the present MMI study aims to be of help.

The model selection bias cannot be eliminated by MMI but can be markedly reduced. The bias is transferred from the level of picking a single model of choice to picking a set of candidate models. In the present analysis, this set included more than 40 models with different forms of dose responses, of which four models have been admitted to Occam's group. Under the given rules for model selection, it appears unlikely that by broadening the basis of candidate models a considerable number of new models would enter Occam's group. Even if new models appeared, their impact on risk estimates would be contained by the original models.

References

Akaike H (1973) Information theory and extension of the maximum likelihood principle. In: Petrov N, Caski F (eds) Proceedings of the second international symposium on information theory. Budapest, Hungary, Akademiai Kiado, pp 267–281

Anderson DR, Burnham KP, Gould WR, Cherry S (2001) Concerns about finding effects that are actually spurios. Wildl Soc Bull 29(1):311–316

Burnham KP, Anderson DR (2002) Model selection and multimodel inference, 2nd edn. Springer, New York

Claeskens G, Hjort NL (2008) Model selection and model averaging. Cambridge University Press, Cambridge

Einstein AJ (2012) Beyond the bombs: cancer risks of low-dose medical radiation. The Lancet 380:455–457

Hall EJ (2006) *Radiobiology for the radiologist*, chapter dose-relationships for model normal tissues, 6th edn. Lippincott, New York

Hodgson E (ed) (2010) A textbook of modern toxicology, 4th edn. Wiley, New York

Hoeting JA, Madigan D, Raftery AE, Volinsky CT (1999) Bayesian model averaging: a tutorial. Stat Sci 14(4):382–417

Hunter N, Charles MW (2002) The impact of possible modifications to the DS86 dosimetry on neutron risk and relative biological effectiveness. J Radiol Prot 22(4):357–370

Kaatsch P, Spix C, Schulze-Rath R, Schmiedel S, Blettner M (2008) Leukaemia in young children living in the vicinity of German nuclear power plants. Int J Cancer 122:721–726

Kaiser JC, Jacob P, Meckbach R, Cullings HM (2012) Breast cancer risk in atomic bomb survivors from multi-model inference with incidence data 1958–1998. Radiat Environ Biophys 51:1–14

Kaiser JC (2010) MECAN-A software package to estimate health risks in radiation epidemiology with multi-model inference. User Manual, Version 0.2

Kass RE, Raftery AE (1995) Bayes factors. J Am Stat Assoc 90(430):773–795

Kendall GM, Little MP, Wakeford R, Bunch KJ, Miles JCH, Vincent TJ, Meara JR, Murphy MFG (2012) A record–based case–control study of natural background radiation and the incidence of childhood leukaemia and other cancers in Great Britain during 1980–2006. Leukemia doi:10.1038/leu.2012.151

Kocher DC, Apostoaei AI, Henshaw RW, Hoffman FO, Schubauer-Berigan MK, Stancescu DO, Thomas BA, Trabalka JR, Gilbert ES, Land CE (2008) Interactive radioepidemiological program (IREP): a web-based tool for estimating probability of causation/assigned share of radiogenic cancers. Health Phys 95(1):119–147

Laurier D, Jacob S, Bernier MO, Leuraud K, Metz C, Samson E, Laloi P (2008) Epidemiological studies of leukaemia in children and young adults around nuclear facilities: a critical review. Radiat Prot Dosim 132:182–190

Little MP (1997) Estimates of neutron relative biological effectiveness derived from the Japanese atomic bomb survivors. Int J Radiat Biol 72(6):715–726

Little MP (2008) Leukaemia following childhood radiation exposure in the Japanese atomic bomb survivors and in medically exposed groups. Radiat Prot Dosim 132(2):156–165

Little MP, Weiss HA, Jr. Boice JD, Darby SC, Day NE, Muirhead CR (1999) Risks of leukemia in Japanese atomic bomb survivors, in women treated for cervical cancer, and in patients treated for ankylosing spondylitis. Radiat Res 152:280–292

Little MP, Hoel DG, Molitor J, Boice JD, Wakeford R, Muirhead CR (2008) New models for evaluation of radiation-induced lifetime cancer risk and its uncertainty employed in the UNSCEAR 2006 report. Radiat Res 169:660–676

Little MP, Wakeford R, Kendall GM (2009) Updated estimates of the proportion of childhood leukaemia incidence in Great Britain that may be caused by natural background ionizing radiation. J Radiol Prot 29:467–482

Moneta L, James F (2012) Minuit2 minimization package. http://seal.web.cern.ch/seal/snapshot/work-packages/mathlibs/minuit, April 2010. v. 5.27.02, Accessed 20 Feb

Niu S, Deboodt P, Zeeb H, (eds) (2010) Approaches to attribution of detrimental health effects to occupational ionizing radiation exposure and their application in compensation programmes for cancer—a practical guide, volume 73 of *Occupational Safety and Health Series*. International Labour Organization (ILO), Geneva. ISBN 978-92-2-122413-6

NRC (2006) *Health risks from exposure to low levels of ionizing radiation: BEIR VII—phase 2*. United States National Academy

of Sciences, National Academy Press, Washington, DC. United States National Research Council, Committee to assess health risks from exposure to low levels of ionizing radiation

Ozasa K, Shimizu Y, Suyama A, Kasagi F, Soda M, Grant EJ, Sakata R, Sugiyamaa H, Kodama K (2012) Studies of the mortality of atomic bomb survivors, report 14, 1950–2003: an overview of cancer and noncancer diseases. Radiat Res 177:229–243

Pearce MS, Little MP, Salotti JA, McHugh K, Lee C, Kim KP, Howe NL, Ronckers CM, Rajaraman P, Sir AW Craft, Parker L, Berrington de González A (2012) Radiation exposure from CT scans in childhood and subsequent risk of leukaemia and brain tumours: a retrospective cohort study. The Lancet 380:499–505

Pierce DL, Væth M, Stram DO (1990) Allowing for random errors in radiation dose estimates for the atomic bomb survivor data. Radiat Res 170:118–126

Preston DL, Lubin JH, Pierce DA (1993) Epicure user's guide. HiroSoft International Corp., Seattle

Preston DL, Kusumi S, Tomonaga M, Izumi S, Ron E, Kuramoto A, Kamada N (1994) Cancer incidence in atomic bomb survivors. Part III: leukemia, lymphoma and multiple myeloma, 1950–1987. Radiat Res 137:S68–S97

Preston DL, Pierce DA, Shimizu Y, Cullings HM, Fujita S, Funamoto S, Kodama K (2004) Effects of recent changes in atomic bomb survivors dosimetry on cancer mortality risk estimates. Radiat Res 162:377–389

Preston DL, Shimizu Y, Pierce DA, Suyama A, Mabuchi K (2003) Studies of mortality of atomic bomb survivors. Report 13: solid cancer and noncancer disease mortality: 1950–1997. Radiat Res 160:381–407

Richardson DB, Cole SR (2012) Model averaging in the analysis of leukemia mortality among Japanese A-bomb survivors. Radiat Environ Biophys 51:93–95

Schervish MJ (1997) *Theory of statistics*. Springer series in statistics, 2nd edn. Springer, New York

Schneider U, Walsh L (2009) Cancer risk above 1 Gy and the impact for space radiation protection. Adv Space Res 44:202–209

UNSCEAR (2008) *2006 REPORT*, volume I, effects of ionizing radiation, report to the general assembly annex a: epidemiological studies of radiation and cancer. United Nations, New York

Valentin J (ed) (2007) The 2007 Recommendations of the international commission on radiological protection. Annals of the ICRP. Elsevier, Publication 103

Wakeford R, Kendall GM, Little MP (2009) The proportion of childhood leukaemia incidence in Great Britain that may be caused by natural background ionizing radiation. Leukemia 23:770–776

Walsh L (2007) A short review of model selection techniques for radiation epidemiology. Radiat Environ Biophys 46:205–213

Walsh L, Kaiser JC (2011) Multi-model inference of adult and childhood leukaemia excess relative risks based on the Japanese A-bomb survivors mortality data (1950*-2000). Radiat Environ Biophys 50:21–35

Walsh L, Kaiser JC, Schöllnberger H, Jacob P (2012) Reply to Drs Richardson and cole: model averaging in the analysis of leukaemia mortality among Japanese A-bomb survivors. Radiat Environ Biophys 51:97–100

49. Kreuzer M, Sogl M, Dufey F, Schnelzer M, Straif K & Walsh L, Cardiovascular diseases in relation to gamma exposures in German uranium miners, 1946–2008. Radiat. Env. Biophys. *accepted* November 2012, DOI: 10.1007/s00411-012-0446-5

External gamma radiation and mortality from cardiovascular diseases in the German WISMUT uranium miners cohort study, 1946–2008

M. Kreuzer (✉), F. Dufey, M. Sogl, M. Schnelzer, L. Walsh

Federal Office for Radiation Protection, Department of Radiation Protection and Health, Ingolstädter Landstr. 1, 85764 Neuherberg, Germany.

E-mail: mkreuzer@bfs.de

Tel.: +49-18333-2250

Fax.: +49-18333-2205

Abstract   It is currently unclear whether exposure of the heart and vascular system, at lifetime accumulated dose levels relevant to the general public (<500 mGy), is associated with an increased risk of cardiovascular disease. Therefore, data from the German WISMUT cohort of uranium miners were investigated for evidence of a relationship between external gamma radiation and death from cardiovascular diseases. The cohort comprises 58,982 former employees of the Wismut company. There were 9,039 recorded deaths from cardiovascular diseases during the follow-up period from 1946 to 2008. Exposures to external gamma radiation were estimated using a detailed job-exposure matrix. The exposures were based on expert ratings for the period 1946-1954 and measurements thereafter. The Excess Relative Risk (ERR) per unit of cumulative gamma dose was obtained with internal Poisson regression using a linear ERR model with baseline stratification by age and calendar year. The mean cumulative gamma dose was 47 mSv for exposed miners (86%), with a maximum of 909 mSv. No evidence for an increase in risk with increasing

cumulative dose was found for mortality from all cardiovascular diseases (ERR/Sv = -0.13; 95% confidence interval (CI): -0.38; 0.12) and ischemic heart diseases (n=4,613; ERR/Sv = -0.03; 95% CI: -0.38, 0.32). However, a statistically insignificant increase (n=2,073; ERR/Sv = 0.44; 95% CI: -0.16, 1.04) for mortality from cerebrovascular diseases was observed. Data on smoking, diabetes and overweight are available for sub-groups of the cohort, indicating no major correlation with cumulative gamma radiation. Confounding by these factors or other risk factors, however, cannot be excluded. In conclusion, the results provide weak evidence for an increased risk of death due to gamma radiation only for cerebrovascular diseases.

Introduction

There is emerging evidence that low-dose ionizing radiation may increase the risk of cardiovascular diseases (Little et al. 2008; 2009; 2012; UNSCEAR 2008). However, results from epidemiological studies on the relationship between cardiovascular diseases and total doses below 500 mGy (absorbed dose to the heart/brain or uniform whole body dose) are not conclusive (Yamada et al. 2004; Kreuzer et al. 2006; Ivanov et al. 2006; Vrijheid et al. 2007; Villeneuve et al 2007; McGeoghegan et al. 2008; Muirhead et al. 2009; Azizova et al. 2010a,b; 2011; 2012; Shimizu et al. 2010; Nusinovici et al. 2010; Lane et al. 2010; Laurent et al. 2010; Grosche et al. 2011; Takahashi et al. 2012; Guseva Canu et al. 2012). The majority of these studies show positive relationships, which are statistically significant in only a few of these studies and for specific sub-groups of the disease (Ivanov et al. 2006; McGeoghegan et al. 2008; Azizova et al. 2010a,b; 2011, 2012; Shimizu et al. 2010*;* Laurent al. 2010; Nusinovici et al. 2010; Takahashi et al. 2012). Such inconclusive results could be due to either low statistical power or the absence of a true effect or uncontrolled confounding for major risk factors such as e.g. tobacco, high blood pressure, overweight, hyperlipidemia and diabetes (Kromhout et al. 2001). Studies based on incidence data for cardiovascular diseases are rare (Yamada et al. 2004; Ivanov et al. 2006; Azizova et al. 2010a,b; 2011; 2012, Takahashi et al. 2012). A recent meta-analysis of epidemiological studies with exposure to uniform low and moderate external whole-body doses (<5 Gy) showed statistically significant excess relative risks (ERR) for the subgroups of ischemic heart diseases, cerebrovascular diseases, and non-ischemic heart diseases and circulatory diseases apart from

heart and cerebrovascular disease. There was significant heterogeneity across the individual studies particularly for non-cardiac outcomes (Little et al. 2012).

The Wismut uranium miner cohort study is a large cohort with detailed individual information on external gamma radiation, the major source of ionizing radiation with respect to organs related to cardiovascular diseases, and a large number of deaths from cardiovascular diseases. No relationship between external gamma radiation and all cardiovascular diseases, and the sub-groups of heart or cerebrovascular diseases was observed in the Wismut cohort for the follow-up period to the end of 1998 (Kreuzer et al. 2006). Since this latter analysis, the follow-up period has been extended by 10 years up to the end of 2008, increasing the number of deaths from cardiovascular diseases from 5,417 to 9,039, and the number of person-years from 1,801,626 to 2,180,639. The purpose of this paper is to further investigate the exposure-response relationship between total gamma dose and all circulatory diseases and several subgroups such as ischemic heart diseases and cerebrovascular diseases, and to investigate potential confounding by overweight, diabetes and smoking.

Materials and Methods

Cohort and endpoints

The cohort includes 58,982 males employed for at least 180 days between 1946 and 1989 at the Wismut company. Cohort member selection was via random sampling from personnel files on approximately 130,000 former employees with sufficient information on working history and data for follow-up, and was stratified by date of first employment, place of work and area of mining (Kreuzer et al. 2010a). Follow-up was from date of first employment plus 180 days to first date of death, emigration, loss-to-follow-up or 31 Dec 2008. Information on the vital status was obtained via local registration offices. By the end of 2008, 25,438 men had died (43.1%), 31,406 (53.2%) were alive, 535 (0.9%) had emigrated and 1,603 (2.7%) were lost to follow-up. Information on the cause of death was based on death certificates obtained from the responsible Public Health Administrations and the pathology archive of the Wismut company. The underlying cause of death from either the certificates of death or the autopsy files was available for

23,939 (94.1%) of the deceased men, and was coded according to the 10th revision of the International Classification of Diseases (ICD-10). In order to achieve consistency with previous studies (Little et al. 2010; 2012) the following causes of death are investigated: all circulatory diseases (ICD-10 code: I00-I99); ischemic heart disease (I20-I25), with the subgroup acute myocardial infarction (I21); and cerebrovascular diseases (I60-I69).

Radiation and dust exposure

The Wismut employees were exposed to radon and its progeny, long-lived radionuclides from the uranium dust, and external gamma radiation, with particularly high values of radon progeny in the very early years up to 1958, i.e. before artificial ventilation was available. In contrast to this, external gamma exposure, which is hardly affected by ventilation measures, had maximum values between 1957 and 1968 probably due to the high uranium ore content in these years. Figure 1 shows the quartiles of external gamma exposure by calendar year among the exposed cohort members (n=50,756). In addition to radiation, the workers were exposed to fine dust, silica dust and arsenic dust, again with higher values in the very early years when dry drilling instead of wet drilling was performed. Exposure to radiation and dust was estimated from detailed job-exposure-matrices (JEMs) that provide annual values for each calendar year, place of work and type of job (Kreuzer et al. 2010a; HVBG and BBG 2005). Radon exposures, external gamma radiation doses and long-lived radionuclide exposures are from a JEM based on measurements in the Wismut mines, which had been carried out from 1955 onwards for radon and gamma radiation and from 1967 onwards for long-lived radionuclides. Radiation exposures prior to these years were estimated by an expert group from the first available measurements by taking factors such as ventilation rate, vein space and uranium content into account (HVBG and BBG 2005).

Recently a software program was established to calculate the total absorbed organ doses for each of the cohort members (Marsh et al. 2008). Unfortunately, no calculations of organ doses for heart, brain, and the vascular system have been made so far. In contrast to the extremely high total lung doses due to inhalation of radon progeny, doses to other organs are appreciably lower and

dominated by external gamma radiation. The average total absorbed liver dose for example - which is estimated to be roughly comparable to the doses for the heart or arteries - was 50 mGy among exposed cohort members. The main contribution was from external gamma radiation (47 mGy). Previous analyses in the Wismut cohort on the relationship between cumulative exposure to radon progeny or long-lived radionuclides and death from cardiovascular diseases (Kreuzer et al. 2006; 2010b) provided no evidence for an increased risk of death from cardiovascular diseases or its subgroups. This holds true for the present data. The present paper thus focuses only on external gamma radiation as relevant radiation source for the heart, brain and vascular system.

Estimates of dust concentrations were based on another JEM containing systematic measurements taken by the Wismut company from 1960 onwards or, prior to this, from expert estimations (Kreuzer et al. 2010a). Cumulative exposures are given in dust-year units, defined as an exposure to 1 mg/m^3 fine dust or silica dust and 1 μg/m^3 for arsenic over a time period of 220 shifts of 8 hours.

Information on potential confounders

Information on potential confounders such as smoking, diabetes and overweight was collected in subgroups of the cohort via different sources. In a nested case-control study on lung cancer some information on smoking habits was collected for 439 cases and 550 controls from medical archives or the relatives (Schnelzer et al. 2010). Smoking was roughly categorized into "smokers" (current smokers or those who stopped smoking less than 20 years ago) and "non-smokers" (never smokers or workers who stopped smoking more than 20 years ago). In the group of deceased cohort members with known underlying cause of death (n=23,939) for 18,528 individuals additional information on accompanying diseases was available based on copies of the certificate of death or autopsy protocols. For this group information was extracted on whether diabetes had been mentioned or not. For 25,118 cohort members medical information from the last occupational medical examination during Wismut employment including data on bodyweight (in form of overweight yes/no) has been documented, mainly for the years after 1980.

Statistical analyses

Internal Poisson regression models were used to investigate the relationship between cumulative external gamma radiation and mortality from cardiovascular diseases. The simple model for the excess relative risk (ERR) had the following form:

$$r(a,y,d) = r_0(a,y) \, [1 + ERR(d)]$$

where r is the cause-specific mortality rate and r_0 is the baseline mortality rate (i.e. without radiation exposure). The covariables a and y refer to attained age in 16 categories [0-15, 15-20, .., 85+ years] and individual calendar year in 63 categories. The excess relative risk, $ERR(d)$ is defined as a linear function of lagged cumulative external gamma dose, d. For reasons of consistency with the majority of other published studies, a lag-time of 10 years was applied (Vrijheid et al. 2007; Muirhead et al. 2009; Azizova et al. 2010a,b; 2011; 2012; Grosche et al. 2011; Laurent et al. 2010). In addition, categorical analyses with the following a priori defined categories of cumulative dose were performed: (0, >0-50, 50-100, 100-150, 150-200, 200-300, 300-400, 400+ mSv). All models were fitted with the AMFIT module of the EPICURE software (Preston et al. 1998). Ninety-five percent confidence limits were provided.

Several sensitivity analyses were conducted: 1) In order to account for possible higher uncertainty in the classification of the underlying cause of death at older ages, the date of end of follow-up was fixed to attained age 80, 85 or 90 years; 2) In order to investigate the so-called healthy worker survivor effect, additional stratification for duration of employment was performed in two (<10, 10+ years) and three categories (<10, 10-20, 20+ years). A negative bias due to this effect could occur when workers who are healthier and therefore have lower mortality rates, stay in employment longer and may accumulate higher doses; 3) Different lag times (2, 5, 10 and 15 years) were applied to investigate the effect of lag time.

The association between cumulative external gamma radiation categories (0, -50, -100, -200, -300, 300+) and the binary variables of presence of overweight, diabetes (separately for individuals with and without underlying cause of death from cardiovascular diseases) or smoking status (separately for lung cancer cases and controls) was investigated, to get at least some hint on possible confounding of these factors. The two-sided Cochran-Armitage trend-test was used to test for a statistically significant trend with cumulative exposure to gamma radiation.

Results

By the end of 2008, a total of 9,039 deaths from cardiovascular diseases (with a total of 2,180,639 person-years) were recorded with a mean age at death of 70 years and a range from 18 to 100 years (Table 1). The two most frequent subtypes of circulatory deaths were ischemic heart diseases (51%) and cerebrovascular diseases (22.9%) with a mean age at death of 69 and 72 years, respectively (Table 1). A total of 50,756 cohort members had been exposed at some time to external gamma radiation (mainly underground workers) with a mean cumulative exposure of 47 mSv among the exposed. Around 5.2% (n=3,075) and 0.8% (n=517) of all cohort members experienced a total dose of more than 200 and 400 mSv, respectively. The maximum was 909 mSv, the median 16 mSv. The mean duration of exposure to gamma radiation among the exposed was 11 years, ranging from 1 to 44 years. The mean age at first exposure was 25 years, ranging from 14 to 67 years. A total of 50, 189, and 2,204 individuals had their first gamma exposure at age 14, 15, and 16, respectively.

Concerning other occupational exposures, around 86% of the cohort members had been exposed to radon progeny or long-lived radionuclides at some time, with mean cumulative exposure values of 280 Working Level Months (WLM) (max=3,224 and 4.1 kBqh/m^3 (max=132) among the exposed, respectively. A percentage of 31% of the cohort members were exposed to arsenic exposure at some time with a mean cumulative exposure of 121 µg/m^3-years (max=1,417), while practically all cohort members were exposed to fine dust with a mean cumulative exposure of 37 mg/m^3-years (max = 315).

Table 2 provides information on the risk of death from cardiovascular diseases by cumulative exposure to external gamma radiation. When all deaths from cardiovascular diseases were considered, there was a decrease in risk with increasing total gamma exposure which was not statistically significant (ERR/Sv = -0.13; 95% CI: -0.38; 0.12). In the highest exposure category (400 and more mSv) the relative risk was 0.89 (95% CI: 0.69; 1.09) compared to the exposure category 0 mSv. No increase in risk was observed for the sub-group of ischemic heart diseases (ERR/Sv = -0.03; 95% CI: -0.38; 0.32), while a non-significant increase in the risk was present for cerebrovascular diseases (ERR/Sv = 0.44; 95% CI: -0.16; 1.04). Death from acute myocardial infarction showed no significant increase in risk (ERR/Sv = 0.08; 95% CI: -0.41; 0.57) (data not shown).

Table 3 shows the association between the potential confounders smoking, diabetes and overweight with external gamma radiation. Data from the nested case-control study on lung cancer showed that generally most Wismut miners smoked at some time (95% of the cases and 73% of the controls). There was no statistically significant positive or negative trend in the smoking prevalence across external gamma exposure categories for cases and controls. Diabetes was mentioned as accompanying disease on the certificate of death or the autopsy protocols for 19% or 12% of the deceased individuals with or without an underlying cause of death of cardiovascular diseases. This percentage varied only slightly in the respective categories of total gamma exposure in both groups. Overweight was noted at the last medical examination during employment at the Wismut in 18% of these people. Again, the percentage was comparable in all gamma exposure categories (around 21%), except in the category >0-50 mGy (15.8%), leading to a statistically significant test for heterogeneity. It can be assumed that people in this low dose category were on average relatively young when they left the Wismut company and thus had a lower probability of being overweight, compared to those with no exposure (mixture of all ages) and those with higher cumulative exposure, who were likely to be employed for a longer time period and thus older.

Discussion

Our findings provide little evidence for a relationship between mortality from cardiovascular diseases and external gamma radiation at such low doses as received by uranium miners. A small excess of death from cardiovascular diseases, and here particularly cerebrovascular diseases, in the order of magnitude as observed in studies of moderate dose ranges (Ivanov et al. 2006; Azizova et al. 2010b; 2011; Shimizu et al. 2010), however, cannot be ruled out. Major advantages of the present cohort are (a) the large cohort size, (b) more than 60 years of time of follow-up (average duration of follow-up is 38 years), (c) the large number of deaths from cardiovascular diseases, (d) the almost complete information on vital status (96%) and causes of death (94%), and (e) a detailed assessment of exposure to external gamma radiation. The miners were exposed to chronic low-level external gamma doses mostly in the range 0-500 mSv, the range of public health concern with regard to medical diagnostic exposure and occupational radiation exposure.

Comparison with other studies

Overall, currently available studies focussing on the low dose (majority of doses below 500 mGy) or moderate dose range (up to a few Grays) of uniform whole body exposure provide inconsistent results (Table 4). A statistically significant relationship between total dose and cerebrovascular diseases was demonstrated mainly in studies with moderate dose ranges (Ivanov et al. 2006; Azizova et al. 2010b; 2011; Shimizu et al. 2010; Takahashi et al. 2012) and here mostly for incidence (Ivanov et al. 2006; Azizova et al. 2010b; 2011; Takahashi et al. 2012). With respect to ischemic heart diseases statistically significant quantitative relationships are limited to moderate dose studies with incidence data (Ivanov et al. 2006; Azizova et al. 2010a; 2012) and one low-dose mortality study (McGeoghegan et al. 2008), where heterogeneity across exposure and employment status was of concern. The most recent meta-analysis by Little et al. (2012) that included low- and moderate-dose studies showed a statistically significant ERR for ischemic heart diseases (ERR/Sv=0.10; 95% CI: 0.05; 0.15) and cerebrovascular diseases (ERR/Sv=0.20; 95% CI: 0.14; 0.25). Heterogeneity among studies, however, affected the latter results. In addition, the possibility of

uncontrolled confounding could not be ruled out. The confidence limits of the corresponding risk estimates in the present study overlap (ERR/Sv = -0.03; 95% CI: -0.38, 0.32) and (ERR/Sv= 0.44; 95% CI: -0.16; 1.04).

It is unclear whether the few statistically significant relationships in the moderate-dose studies are mainly driven from the doses above 500 mSv and whether a threshold may exist. A recent re-analysis of the data of the LSS on mortality from cerebrovascular diseases by multi-model inference, revealed a weak dose-response below a step at 0.6 Gy (Schöllnberger et al. 2012) that was consistent with zero risk below this threshold-dose. In the extended study of Mayak Plutonium workers (Azizova et al. 2011; 2012), no increase was present for mortality from cerebrovascular diseases (RR=0.90; 95% CI: 0.76, 1.07) or ischemic heart diseases (RR=0.96, 95% CI: 0.84; 1.09) in the dose category 200-500 Gy compared to that with less than 200 mGy using a lag-time of 10 years. This result is compatible with the present findings (RR=1.17; 95% CI: 0.96; 1.37 and RR=1.00; 95% CI: 0.88; 1.11, respectively).

Adjustment for duration of employment had the effect of increasing the radiation-induced excess risk due to the so-called "healthy worker survivor effect", in the 15-country nuclear worker study (Vrijheid et al. 2007), but a similar adjustment led to a decrease of the effect in the UK NRRW worker study (Muirhead et al. 2009). These authors argued that some feature of long-term radiation work other than radiation itself might influence cardiovascular disease risk (Muirhead et al. 2009). In the present study stratification for duration of employment (Table 5) led to an increase in the risk from mortality from all cardiovascular diseases and the subgroup ischemic heart diseases, indicating a small "healthy worker survivor effect". In contrast to this, a substantial decrease in risk was observed in the subgroup for cerebrovascular diseases. This could be a spurious finding or an effect related to some feature of long-term work that is independent of radiation.

Other radiation exposures

Previous analyses on the relationship between cumulative radon exposure and death from circulatory diseases provided mostly negative results (Lane et al. 2010; Kreuzer et al. 2006, Villeneuve et al. 2007). One exception is the French

uranium miner cohort (Nusinovici et al. 2010) that reported a significant excess risk only for the subgroup of cerebrovascular diseases, however based on a small numbers of deaths. In the present study no increased ERR with cumulative radon exposure was observed for all circulatory diseases (ERR/100 Working Level Months (WLM) = 0.002; 95% CI: -0.003;0.006), ischemic heart diseases (ERR/100 WLM=0.006; 95% CI: -0.001; 0.012) or cerebrovascular diseases (ERR/100 WLM=0.000; 95% CI: -0.008; 0.009). The same holds true for cumulative exposure to long-lived radionuclides. The corresponding risk estimates (ERR per 100 kBqh/m^3) were -0.13 (95% CI: -0.37; 0.12), -0.03 (95% CI: 0.37; 0.32), and 0.12 (95% CI: -0.41; 0.65), respectively.

Limitations

A potential limitation of the present study is the lack of complete individual information on potential confounders such as e.g. smoking, cholesterol level, blood pressure, and diabetes. Nearly all cohort members are "blue collar" workers with equal socio-economic status. This high level of socio-economic homogeneity of the cohort should limit potential confounding associated with lifestyle factors. The analyses on smoking, diabetes and overweight for subgroups of the cohort with available information, indicated no major association with cumulative external gamma radiation. However, the information available is relatively rough and might be selectively reported. Therefore residual confounding cannot be excluded. Additional medical radiation exposure of the Wismut miners due to regularly performed x-ray examinations for purposes of screening for silicosis has been mentioned by Möhner et al. (2010). This information is presently not available in the cohort. The correlation of medical radiation exposure with silica exposure is expected to be high, whereas the correlation with external occupational gamma radiation is assumed to be low. However, confounding by medical radiation exposure cannot be excluded.

Potential occupational confounding factors may concern exposure to arsenic (Navas-Acien et al. 2005) and dust (Landen et al. 2011). Both variables were not associated with an increased risk in relation to cardiovascular diseases in the present study. The ERR for all cardiovascular diseases per cumulative exposure

to arsenic in dust-years was 0.00002 (95% CI: -0.00017; 0.00021) and -0.00016 (95% CI: -0.00061; 0.00028) for fine dust,.

Misclassification of cardiovascular disease as the underlying cause of death is likely to have occurred and may differ over time and could be dependent on age at diagnosis. Sensitivity analyses using the ages 80, 85 and 90 years as date of end of follow-up, provided risk estimates similar to those obtained without restriction on age for all sub-groups of cardiovascular diseases (Table 4), indicating no major age-related misclassification bias. A percentage of 15.6% of all deaths from cardiovascular diseases was based on autopsy. Analyses with different lag-times showed higher risks with increasing lag-time. This finding is consistent to those from the 15-country nuclear worker study published by Vrijheid et al. (2007) and the Life Span study of Japanese A-bomb survivors, where effects of cardiovascular diseases appeared for the first time more than 20 years after exposure (Preston et al. 2003).

Uncertainty in the assessment of exposure to external gamma radiation is another issue. The assessment used here was based on external expert rating before 1955, while from 1955 onwards measurement data in the respective shafts were used and weighted by the type of job. Restriction of the cohort to those who were first employed after 1954 (n=35,060) led to a reduction of the number of cardiovascular diseases from 9,039 to 2,448 deaths and to a reduction of the mean cumulative gamma exposure from 47 mSv to 34 mSv. The ERR/Sv was 0.27 (95% CI: -0.42; 0.96) for all cardiovascular diseases, and 0.55 (95% CI: -0.46; 1.57) and 0.23 (95% CI: -1.33; 1.80) for ischemic heart diseases and cerebrovascular diseases, respectively. Thus the results are compatible with the overall results.

Conclusion

The results presented here for the Wismut cohort, provide no evidence for an increased risk of death from all cardiovascular diseases due to external gamma radiation exposure among uranium miners. However, a hint of a possible increase in mortality from cerebrovascular diseases was observed which could

be associated with external gamma radiation exposure. Despite the large size of the Wismut study and the large number of deaths from cardiovascular diseases, the range of doses is quite low and low statistical power to detect a small effect is an issue. Results based on rough data on smoking, diabetes and overweight do not indicate any large correlation with cumulative external exposure to gamma radiation. Confounding by these and other risk factors, however, cannot be excluded. Overall, the results presented here are broadly consistent with those of other epidemiological studies, and a small effect in the order of magnitude already observed in the meta-analyses and moderate-dose studies cannot be ruled out. Further research on the possible biological mechanism as well as molecular epidemiological studies with a focus on the low and moderate dose range are necessary.

References

Azizova TV, Muirhead CR, Druzhinina MB, Grigoryeva ES, Vlasenko EV, Sumina MV, O'Hagan J, Zhang W, Haylock RGE, Hunter N (2010a) Cardiovascular diseases in the cohort of workers first employed at Mayak PA in 1948-1958. Radiat Res 174:155-168

Azizova TV, Muirhead CR, Druzhinina MB, Grigoryeva ES, Vlasenko EV, Sumina MV, O'Hagan J, Zhang W, Haylock RGE, Hunter N (2010b) Cerebrovascular diseases in the cohort of workers first employed at Mayak PA in 1948-1958. Radiat Res 174:851-64

Azizova TV, Muirhead CR, Moseeva MB, Grigoryeva ES, Sumina MV, O'Hagan J, Zhang W, Haylock RGE, Hunter N (2011) Cerebrovascular diseases in nuclear workers first employed at the Mayak PA in 1948-1972. Radiat Environ Biophys 50:539-552

Azizova TV, Muirhead CR, Moseeva MB, Grigoryeva ES, Vlasenko EV, Hunter N, Haylock GE, O'Hagan J (2012) Ischemic heart diseases in nuclear workers first employed at the Mayak PA in 1948-1972. Health Phys 103:3-14

Grosche B, Lackland DT, Land CE, Simon SL, Apsalikov KN, Pivina LM, Bauer S, Gusev BI (2011) Mortality from cardiovascular diseases in the Semipalatinsk Historical cohort, 1960-1999, and its relationship to radiation exposure. Radiat Res 176:660-9

Guvesa Canu I, Garsi JP, Caer-Lorho S, Jacob S, Collomb P, Acker A, Laurier D (2012) Does uranium induce circulatory diseases? First results from a French cohort of uranium workers. Occup Environ Med 69; 404-9

HVBG, BBG (2005) Belastung durch ionisierende Strahlung, Staub und Arsen im Uranerzbergbau der ehemaligen DDR (Version 08/2005). Gera: Bergbau BG (BBG), St. Augustin: Hauptverband der gewerblichen Berufsgenossenschaften (HVBG), 2005 (CD-Rom)

Ivanov VK, Maksioutov MA, Chekin SY, Petrov AV, Biryukov AP, Kruglova ZG, Matyash VA, Tsyb AF, Manton KG, Kravchenko JS (2006) The risk of

radiation-induced cerebrovascular disease in Chernobyl emergency workers. Health Phys 90: 199-207

Kreuzer M, Kreisheimer M, Kandel M, Schnelzer M, Tschense A, Grosche B (2006) Mortality from cardiovascular diseases in the German uranium miners cohort study, 1946-1998. Radiat Environ Biophys 45: 159-166

Kreuzer M, Schnelzer M, Tschense A, Walsh L, Grosche B (2010a) Cohort profile: the German uranium miners cohort study (WISMUT cohort), 1946-2003. Int J Epidemiol 39:980-987

Kreuzer M, Grosche B, Schnelzer M, Tschense A, Dufey F, Walsh L (2010b) Radon and risk of death from cancer or cardiovascular diseases in the German uranium miners cohort study, follow up 1946–2003. Radiat Environ Biophys 49:177-185

Kromhout D (2001) Epidemiology of cardiovascular diseases in Europe. Public Health Nutr 4:441-57

Landen DD, Wassell JT, McWilliams L, Patel A (2011) Coal dust exposure and mortality from ischemic heart disease among a cohort of U.S. coal miners. Am J Ind Med 54:727-733

Lane R, Frost SE, Howe GR, Zablotska LB (2010) Mortality (1950-1999) and cancer incidence (1969-1999) in the cohort of Eldorado uranium workers. Radiat Res 174: 773-85

Laurent O, Metz-Flamant C, Rogel A, Hubert D, Riedel A, Garcier Y, Laurier D (2010) Relationship between occupational exposure to ionizing radiation and mortality at the French electricity company, period 1961-2003. Int Arch Occup Environ Health 83:935-44

Little MP, Tawn EJ, Tzoulaki I, Wakeford R, Hildebrandt G, Paris F, Tapio S, Elliott P (2008) A systematic review of epidemiological associations between low and moderate doses of ionizing radiation and late cardiovascular effects, and their possible mechanisms. Radiat Res 169: 99-109

Little MP, Tawn EJ, Tzoulaki I, Wakeford R, Hildebrandt G, Paris F, Tapio S, Elliott P (2010) Review and meta-analysis of epidemiological associations between low/moderate doses of ionizing radiation and circulatory disease risks, and their possible mechanisms. Radiat Environ Biophys 49:139-153

Little MP, Azizova TV, Bazyka D, Bouffler SD, Cardis E, Chekin S, Chumak VV, Cucinotta FA, de Vathaire F, Hall P, Harrison JD, Hildebrandt G, Ivanov V, Kashcheev VV, Klymenko SV, Kreuzer M, Laurent O, Ozasa K, Schneider T, Tapio S, Taylor AM, Tzoulaki I, Vandoolaeghe WL, Wakeford R, Zablotska LB, Zhang W, Lipshultz SE (2012) Systematic review and meta-analysis of circulatory disease from exposure to low-level ionizing radiation and estimates of potential population mortality risks. Environ Health Persp 120:1503-1511

Marsh JW, Bessa Y, Birchall A, Blanchardon E, Hofmann W, Nosske D, Tomasek L (2008) Dosimetric models used in the alpha-risk project to quantify exposure of uranium miners to radon gas and its progeny. Radiat Prot Dos 130:101-106

McGeoghegan D, Binks K, Gillies M, Jones S, Whaley S (2008) The non-cancer mortality experience of male workers at British Nuclear Fuels plc, 1946-2005. Int J Epidemiol 37: 506-518

Möhner M, Gellissen J, Marsh J, Gregoratto D (2010) Occupational and diagnostic exposure to ionizing radiation and leukemia risk among German uranium miners. Health Phys 99:314-321

Muirhead CR, O'Hagan JA, Haylock RGE, Phillipson MA, Willcock T, Berridge GLC, Zhang W (2009) Mortality and cancer incidence following occupational radiation exposure: third analysis of the National Registry for Radiation Workers. Br J Cancer 100: 206-212

Navas-Acien A, Sharrett R, Silbergeld EK, Schwartz BS, Nachman KE, Burke TA, Guallar E (2005) Arsenic exposure and cardiovascular disease: A systematic review of the epidemiological evidence. Am J Epidemiol 162:1037-1049

Nusinovici S, Vacquier B, Leurand K, Metz-Flamant C, Caer-Lorho S, Acker A, Laurier D (2010) Mortality from circulatory system diseases and low –level radon exposure in the French cohort study of uranium miners, 1946-1999. Scand J Work Environ Health 36:373-83

Preston DL, Lubin JH, Pierce DA (1998) Epicure, release 2.10, HiroSoft: Seattle

Preston DL, Shimizu Y, Pierce DA, Suyama A, Mabuchi K (2003) Studies of mortality of atomic bomb survivors. Report 13: Solid cancer and non-cancer disease mortality: 1950-1997. Radiat Res 160:381-407

Schnelzer M, Hammer GP, Kreuzer M, Tschense A, Grosche B (2010) Accounting for smoking in the radon-related lung cancer risk among German uranium miners: results of a nested case-control study. Health Phys 98:20-28

Schöllnberger H, Kaiser JC, Jacob P, Walsh L (2012) Dose-responses from multi-modell inference for the non-cancer disease mortality of atomic bomb survivors. Radiat Environ Biophys 51:165-178

Shimizu Y, Kodama K, Nishi N, Kasagi F, Suyama A, Soda M, Grant EJ, Sugiyama H, Sakata R, Moriwaki H, Hayashi M, Konda M, Shore RE (2010) Radiation exposure and circulatory disease risk: Hiroshima and Nagasaki atomic bomb survivor data, 1950-2003. Brit Med J 340:b5349

Takahashi I, Abbott RD, Ohshita T, Takahashi T, Ozsasa K, Akahoshi M, Fujiwara S, Kodama K, Matsumoto M (2012) A prospective follow-up study of the association of radiation exposure with fatal and non-fatal stroke among atomic bomb survivors in Hiroshima and Nagasaki (1980-2003). Brit Med J Open 2(1):e000654

United Nations Scientific Committee on the Effects of atomic radiation. UNSCEAR 2006 report. New York: United Nations; 2008

Villeneuve PJ, Lane RS, Morrison HI (2007) Coronary heart disease mortality and radon exposure in the Newfoundland fluorspar miners' cohort; 1950-2001. Radiat Environ Biophys 46:291-6

Vrijheid M, Cardis E, Ashmore P, Auvinen A, Bae JM, Engels H, Gilbert E, Gulis
G, Habib RR, Howe G, Kurtinaitis J, Malker H, Muirhead CR, Richardson
DB, Rodriguez-Artalejo F, Rogel A, Schubauer-Berigan M, Tardy H, Telle-
Lamberton M, Usel M, Veress K (2007) Mortality from diseases other than
cancer following low doses of ionizing radiation: results from the 15-Country
Study of nuclear industry workers. Int J Epidemiol 36: 1126-1135

Yamada M, Wong FL, Fujiwara S, Akahoshi M, Suzuki G (2004) Non cancer
disease incidence in the atomic bomb survivors, 1958-1998. Radiat Res
161: 622-632

Table 1: Description of the deaths from cardiovascular diseases in the Wismut cohort, 1946-2008

Characteristics	n	%
Total	9,039	100.0
Age at death in years		
< 50	481	5.3
50-59	1,129	12.5
60-69	2,547	28.2
70-79	3,142	34.8
80-89	1,561	17.3
>90	179	2.0
Year of death		
< 1969	165	1.8
1970 – 1979	968	10.7
1980 – 1989	2,132	23.6
1990 – 1999	3,098	34.3
2000 – 2008	2,676	29.6
Subgroups of cause of death		
I00 – I09 Acute or chronic rheumatic fever	69	0.8
I10 – I15 Hypertensive diseases	366	4.0
I20 – I25 Ischemic heart diseases	4,613	51.0
I26 – I28 Pulmonary heart disease of pulmonary circulation	319	3.5
I30 – I52 Other forms of heart diseases	1,022	11.3
I60 – I69 Cerebrovascular diseases	2,073	22.9
I70 – I79 Diseases of arteries, arterioles and capillaries	472	5.2
I80 – I89 Diseases of veins, lymphatic vessels and lymph nodes, not elsewhere classified	103	1.1
I90 – I99 Other and unspecified disorders of the circulatory system	2	0.0

ICD 10, 10th revision of the International classification of diseases

Table 2: Risk of death from circulatory diseases by cumulative exposure to external gamma radiation in mSv, among the Wismut cohort, 1946-2008; data were analyzed based on a relative risk model using Poisson regression stratified by age and calendar year; ERR. Excess relative risk; CI: confidence limit; p-value relates to the significance of the ERR/Sv

Cum. exp. to external gamma radiation in mSv	Mean	Person-years	All cardiovascular diseases (I00-I99)			Ischemic heart diseases (I20-I25)			Cerebrovascular diseases (I60-I69)		
			# of deaths	Relative Risk	95% CI	# of deaths	Relative Risk	95% CI	# of deaths	Relative Risk	95 % CI
0	0	779,190	1,485	1.00	-	742	1.00	-	335	1.00	-
>0 – 50	12	1,120,200	5,430	1.00	0.94; 1.06	2,746	0.97	0.89, 1.05	1,236	1.08	0.95; 1.21
50 – 100	71	134,231	945	0.96	0.88; 1.04	484	0.94	0.83, 1.05	232	1.12	0.93, 1.31
100 – 150	122	53,940	388	0.98	0.87; 1.09	213	1.02	0.86, 1.17	81	1.02	0.77, 1.27
150 – 200	173	30,107	216	0.92	0.79; 1.06	124	1.01	0.81, 1.20	43	0.90	0.61, 1.18
200 – 300	246	37,489	334	1.01	0.89; 1.13	166	0.94	0.78, 1.10	94	1.41	1.08; 1.74
300 – 400	342	17,319	157	0.97	0.81; 1.13	95	1.09	0.85, 1.32	27	0.87	0.53, 1.21
400 – 909	465	8,164	84	0.89	0.69; 1.09	43	0.86	0.59, 1.12	25	1.35	0.80, 1.90
ERR/Sv		2,180,639	9,039	-0.13 (-0.38; 0.12) p = 0.30		4,613	-0.03 (-0.38; 0.32) p > 0.50		2,073	0.44 (-0.16; 1.04) p = 0.13	

Table 3: Investigation of possible confounding by smoking, diabetes or overweight. Association between categories of cumulative exposure to gamma radiation in mSv and (1) percentage of smokers based on data from a nested case-control study, (2) percentage of individuals with accompanying disease diabetes among deceased cohort members and (3) percentage of individuals being overweight based on data from medical examinations; [a] two-sided Cochran-Armitage Trend-Test; [b] Current smokers or workers who stopped smoking less than 20 years ago; CVD: cardiovascular diseases

	Cumulative gamma exposure in mSv	0	>0-50	100	-200	-300	300+	Total	p-value trend [a]
Smoking	Nested case-control study on lung cancer (Schnelzer et al. 2010)								
	Lung cancer cases								
	Total number	21	154	78	88	51	47	439	p = 0.65
	% of smokers [b]	90.5	96.1	92.3	93.1	98.0	95.7	94.8	
	Controls								
	Total number	55	269	90	63	33	40	550	p = 0.20
	% of smokers	65.5	71.7	72.2	82.5	81.8	67.5	72.7	
Diabetes	Deceased individuals in the cohort								
	Underlying cause of death CVD								
	Total number	1,211	4,328	773	475	271	204	7,262	p = 0.63
	% with diabetes as accompanying disease	19.2	18.5	20.3	21.3	19.2	22.5	19.2	
	Underlying cause of death not CVD								
	Total number	1,399	6,436	1,377	1,042	576	436	11,266	p = 0.13
	% with diabetes as accompanying disease	14.0	11.6	12.5	12.5	12.0	11.9	12.1	
Overweight	Data from the last medical examination at the Wismut for part of the cohort								
	Total number	2,410	15,356	3,229	2,128	952	1,043	25,118	
	% being overweight	21.9	15.8	20.5	21.4	22.7	21.7	18.0	p < 0.05

Table 4: Published studies providing quantitative data on the relationship between external whole-body uniform exposure and cardiovascular diseases in the low (majority of doses below 500 mGy) or moderate (up to a few Grays) dose range;
[a] 90% CI; [b] all settlements with dose estimates (table 6c of Grosche et al 2011) ;
[c] relative risk at 100 mSv; [d] analyses based on colon dose; [e] analyses based on stomach dose;
[f] BNFL: British nuclear fuels Limited; ERR – excess relative risk; [g] fixed effect models

Cohort	Cohort size	Mean total dose	Mortality /Incidence	Lag period	Cerebrovascular diseases		Ischemic heart diseases	
					No of deaths	ERR (95% CI)	Deaths	ERR (95% CI)
Low-dose studies								
15-country nuclear worker study (Vrijheid et al. 2007)	275,312	21 (<0.1% >500 mGy)	Mortality	10 y	1,224	0.88 (-0.67; 3.16)	5,821	-0.01 (-0.59; 0.69)
UK BNFL[f] nuclear worker (McGeoghegan et al. 2008)	42,426	53 (1% > 590 mSv)	Mortality	15 y	1,018	0.43 (-0.10; 1.12)	3,567	0.70 (0.33; 1.11)[a]
UK National Registry for radiation workers (Muirhead et al. 2009)	174,541	25 (6% > 100 mSv)	Mortality	10 y	1,817	0.16 (-0.42; 0.91)	7,168	0.26 (-0.05; 0.61)
German uranium miners, 1946-98 (Kreuzer et al. 2006)	58,987	41 (0.2% > 500 mSv)	Mortality	5 y	1,297	0.09 (-0.6; 0.8)	n.a.	n.a.
German uranium miners, 1946-2008 Present analyses	58,982	41 (0.2% > 500 mSv)	Mortality	10 y	2,073	0.44 (-0.16; 1.04)	4,613	-0.03 (-0.38; 0.32)
Semipalatinsk cohort (Grosche et al. 2011)	19,545	90 (0 – 630 mSv)	Mortality	10 y	839[b]	-0.06 (-0.65; 0.54)	1,554	0.03 (-0.44; 0.50)
Eldorado uranium miners (Lane et al. 2010)	17,660	52	Mortality	2 y	244	-0.29 (<-0.3; 0.27)	1,235	0.15 (-0.14; 0.58)
French electric worker (Laurent et al. 2010)	22,393	22 (5% > 100 mSv)	Mortality	10 y	22	2.7[c] (p = 0.019)	79	1.41[c] (p = 0.17)
Moderate-dose studies								
Chernobyl liquidators (Ivanov et al. 2006)	61,017	109	Incidence		12,832	0.45 (0.11; 0.80)	10,942	0.41 (0.05; 0.78)
Mayak worker, 1948-1958 (Azizova et al. 2010b, 2011)	12,210	840 (1% > 3 Gy)	Mortality Incidence	10 y	744 4,418	-0.02 (-0.12;0.08) 0.45 (0.34; 0.56)	1,461 3,133	0.07 (-0.02; 0.15) 0.12 (0.05; 0.19)
Mayak worker, 1948-1972 (Azizova et al. 2010a, 2012)	18,763	630 (22% > 1 Gy)	Mortality Incidence	10 y	1,480 6,590	0.04 (-0.06; 0.13) 0.40 (0.30; 0.49)	2,583 5,301	0.06 (-0.01;0.13) 0.11 (0.05; 0.18)
Japanese Life Span study, 1950-2003 (Shimizu et al. 2010)	86,572	200[d] (0 – 4 Gy)	Mortality	5 y	9,622	0.09 (0.01; 0.17)	3,252	0.02 (-0.10; 0.15)
Japanese Adult Health Study (ADH) (Yamada et al. 2004)	10,339	570 (0 – 4Gy)[e]	Incidence	13 y	729	0.07 (-0.08; 0.24)	1,546	0.05 (-0.05; 0.16)
Meta-analyses								
Little et al. 2012	-	Low and moderate doses	Mortality and incidence		9[g] studies	0.20 (0.14; 0.25)	8 studies	0.10 (0.05; 0.15)

Table 5: Excess relative risk (ERR) per unit cumulative external gamma radiation in Sv from all cardiovascular diseases and the subgroups of ischemic heart diseases and cerebrovascular diseases, 1946-2008;
[a]: ICD 10: International Classification of disease; CI: confidence interval

	All cardiovascular diseases (I00-I99)[a]			Ischemic heart diseases (I20-I25)			Cerebrovascular (I60-I69)		
	Deaths	ERR/Sv	95 % CI	Deaths	ERR/Sv	95% CI	Deaths	ERR/Sv	95 % CI
Overall	9,039	-0.13	-0.37; 0.13	4,613	-0.03	-0.38; -0.32	2,073	0.44	-0.16; 1.04
Lag-time									
2 y	9,039	-0.19	-0.43; 0.05	4,613	-0.10	-0.43; 0.24	2,073	0.37	-0.21; 0.95
5 y	9,039	-0.18	-0.42; 0.06	4,613	-0.08	-0.42; 0.26	2,073	0.38	-0.21; 0.96
10 y	9,039	-0.13	-0.37; 0.13	4,613	-0.03	-0.38; 0.32	2,073	0.44	-0.14; 1.08
15 y	9,039	-0.09	-0.35; 0.18	4,613	0.01	-0.36; 0.38	2,073	0.51	-0.12; 1.15
Stratification by									
duration of employment									
<10, 10+ y	9,039	-0.10	-0.37; 0.17	4,613	-0.03	-0.41; 0.35	2,073	0.15	-0.45; 0.74
<10,-20, 20+ y	9,039	-0.04	-0.32; 0.24	4,613	-0.01	-0.39; 0.38	2,073	0.20	-0.42; 0.82
Cutting age at									
80 y	7,301	-0.18	-0.45; 0.08	3,853	-0.06	-0.43; 0.32	1,582	0.53	-0.15; 1.21
85 y	8,321	-0.15	-0.41; 0.10	4,315	-0.06	-0.42; 0.30	1,876	0.52	-0.12; 1.15
90 y	8,900	-0.16	-0.41; 0.09	4,550	-0.05	-0.40; 0.30	2,041	0.40	-0.20; 1.00

50. Dufey F, Walsh L, Sogl M, Tschense A & Kreuzer M. Radiation dose dependent risk of liver cancer mortality in the German uranium miners cohort 1946–2003 J. Radiol. Prot. *accepted* November 2012

Radiation dose dependent risk of liver cancer mortality in the German uranium miners cohort 1946–2003

F Dufey, L Walsh, M Sogl, A Tschense, M Schnelzer and M Kreuzer

Department "Radiation Protection and Health"
Federal Office for Radiation Protection
Ingolstädter Landstr. 1
85764 Oberschleissheim, Germany

E-mail: `fdufey@bfs.de`

Abstract. An increased risk of mortality from primary liver cancers among uranium miners has been observed in various studies. An analysis of the data from the German uranium miner cohort (the "Wismut cohort") was used to assess the relationship with ionizing radiation. To that end the absorbed organ dose due to high and low linear energy transfer radiation was calculated for 58 987 miners with complete information on radiation exposure from a detailed job-exposure matrix. 159 deaths from liver cancer were observed in the follow-up period from 1946 to 2003. Relative risk models with either linear or categorical dependence on high and low linear energy transfer radiation liver doses were fitted by Poisson regression, stratified on age and calendar year. The linear trend of excess relative risk in a model with both low and high linear transfer radiation is -0.8 (95 % confidence interval (CI): -3.7, 2.1) Gy^{-1} and 48.3 (95 % CI: -32.0, 128.6) Gy^{-1} for low and high linear energy transfer radiation, respectively, and thus not statistically significant for either dose. The increase of excess relative risk with equivalent liver dose is 0.57 (95 % CI:-0.69, 1.82) Sv^{-1}. Adjustment for arsenic only had a negligible effect on the radiation risk. In conclusion there is only weak evidence for an increase of liver cancer mortality with increasing radiation dose in the German uranium miners cohort. However both a lack of statistical power and potential misclassification of primary liver cancer are issues.

1. Introduction

Primary liver cancer (PLC) is estimated to be the second most common cause of death from cancer in men worldwide and the sixth most common cause in women (Ferlay *et al* 2010) with both incidence and mortality varying strongly between nations. In Germany in 2003, the age adjusted mortality rate due to PLC was 4.8 per 100 000 for men as compared to 143.7 for all cancers combined (Becker and Wahrendorf 1998). The high geographical variability in incidence and mortality reflects the spread of the main risk factors for PLC, namely infections with hepatitis virus B (HVB) and C (HVC) (Bosch *et al* 1999). Other risk factors include alcohol consumption (Bosch *et al* 1999) and, of lower importance,

smoking (Bosch *et al* 1999, IARC 2004), obesity and diabetes. Several chemicals also have been found to induce liver cancer (Bosch *et al* 1999) of which arsenic (Liu and Waalkes 2008, Chiu *et al* 2004, Tapio and Grosche 2006, IARC 2011) may be of relevance in the cohort. Radiation is a known risk factor for PLC (UNSCEAR 2008), however, the results from different populations and exposures are inconsistent: Significantly increased risks, for the incidence of PLC, have been observed in the Life Span Study (LSS) of atomic bomb survivors (ERR(1 Gy)=0.32 (90 % CI: 0.12; 0.60)) (Preston *et al* 2007) who were exposed to gamma radiation and neutrons while studies on both incidence and mortality among X-ray radiotherapy patients (Weiss *et al* 1994, Kleinerman *et al* 1995, Mattsson *et al* 1997, Carr *et al* 2002) did not find an increase of risk with radiation dose. Another set of studies (Andersson *et al* 1995, Mori *et al* 1999, van Kaick *et al* 1999) where an increased risk of PLC mortality was found as a result of exposure to ionizing radiation includes persons administered with the radioactive contrast medium "thorotrast". In contrast to the studies already mentioned the major contribution to the radiation dose in thorotrast patients is due to high linear energy transfer (high-LET) alpha radiation.

The German miners study, comprising nearly 60 thousand miners, is one of the largest miner cohorts world wide. The study can, therefore, make a valuable contribution to knowledge about the PLC risk due to radiation as the cohort comprises both a large number of persons and cases which are exposed to both low-LET (mainly external gamma radiation) and high-LET radiation (due to mainly alpha-radiation of radon, radon progeny and long lived radionuclides) in the interesting low dose range. Only a few analyses of PLC in miner cohorts have been published: Darby *et al* (1995) reported a significantly increased standardized mortality ratio (SMR) in a pooled cohort of 11 miner studies while Laurier *et al* (2004) and Vacquier *et al* (2008) found no significantly increased SMR compared to national rates. Kreuzer *et al* (2008) reported a significantly increased SMR in the German uranium miners cohort and a borderline significant increase of risk with cumulative radon progeny exposure (Kreuzer *et al* 2008, Kreuzer *et al* 2010). Since that first analysis, a program for the calculation of organ radiation doses has been developed (Marsh *et al* 2008, Marsh *et al* 2011) so that it has become possible to analyze directly the relationship of PLC with radiation dose, also separately for both high- and low-LET doses.

2. Materials and methods

2.1. Cohort

The cohort has already been described in detail (Grosche *et al* 2006, Kreuzer *et al* 2010); the main characteristics are summarized in table 1. It represents a stratified random sample of 58 987 males, employed for at least 6 months between 1946 and 1989 at the former Wismut uranium mining company in East Germany. The present analyses use information gathered in the second follow-up which extends to December 31st, 2003 (Kreuzer *et al* 2008, Kreuzer *et al* 2010, Walsh *et al* 2011). Information on the vital status of the cohort members was obtained from local registration offices. Copies of death certificates were obtained from

several sources, not only from the responsible Public Health Administrative offices, but also from the central archives and the pathology archive of the Wismut Company. The underlying causes of death from either the death certificates or the autopsy files were coded according to the 10th revision of the International Classification of Diseases (ICD-10) with PLC having ICD-10 C22.–. Information on histological subtype was usually only available when an autopsy had been performed.

2.2. Exposure assessment and dose calculation

Radiation exposure was estimated by using a detailed job-exposure matrix (JEM) (Lehmann *et al* 1998, HVBG and BBG 2005). The JEM includes information on exposure to radon progeny in working level months (WLM), external gamma radiation in mSv and long-lived radionuclides (LLR) in $kBq\,h\,m^{-3}$ for each calendar year (1946–1989), each place of work (surface, open pit mines, underground, milling), each mining facility and each type of job.

One working level is defined as any concentration of short lived radon daughters (^{218}Po, ^{214}Po, ^{214}Pb, ^{214}Bi) which gives rise to a potential alpha energy concentration of $1.3{\times}10^5$ MeV per liter of air. One WLM corresponds to an exposure to one working level for 180 h or $3.54{\times}10^{-3}\,J\,h\,m^{-3}$. Area measurements of radon (^{222}Rn) in the Wismut mines were carried out from 1955 onwards. Thus, for the period 1946–1954, radon concentrations were retrospectively estimated by an expert group based on simulations and posterior measurements, taking into account ventilation rate, vein space, uranium content and other factors. Similarly exposure measurements of γ-radiation and of LLR started in 1955 and 1967 whence values for years preceding these dates are also based on expert rating. For the calculation of doses to the liver in miners a dedicated dosimetric program "Alphaminer" (Marsh *et al* 2008, Marsh *et al* 2011) was used. Specific scenarios were assumed depending on the job type (hewer or not), the ventilation status in the mine (poor, medium and good), the type of drilling (dry and wet) and the use of diesel machinery in order to assign values for aerosol parameters such as median diameter, unattached fraction and equilibrium factor for each exposure scenario. For the calendar year periods 1946–1958, 1959–1963 and $\geq$1964 equilibrium factor values of 0.5, 0.3 and 0.2 were assumed, respectively. Job types were classified into three physical activity classes with corresponding breathing rates of $1.4\,m^3$/h, $1.2\,m^3$/h and $1.0\,m^3$/h.

The calculation of absorbed doses to the liver as a result of inhalation of radon, its progeny and LLR is based on biokinetic and dosimetric models of the International Commission on Radiological Protection (ICRP) (ICRP 1994, ICRP 1979). On output, absorbed doses (in mGy) to the liver are provided by source (radon progeny, radon gas and LLR) and by type of radiation (low- and high LET radiation).

Information on arsenic is based on a separate job-exposure matrix (HVBG and BBG 2005, Bauer 2000, Dahmann *et al* 2008) similar to that for radiation. The annual exposure values are given in dust years, where one dust year is defined as an exposure to $1\,\mu g\,m^{-3}$ arsenic over a time period of 220 shifts of 8 h.

2.3. Statistical methods

Internal Poisson regression was used to test for an association between mortality risk and the lagged radiation doses or cumulative arsenic exposure. Here, a lag time of 5 years was assumed for all doses and cumulative exposure. Every cohort member contributes to the number of person-years starting 180 days after the date of first employment and ending at the earliest of date of loss to follow-up, date of death or end of follow-up (31.12.2003). Tabulations of person-years at risk and cancer deaths were created with the DATAB module of the EPICURE software (Preston *et al* 1998). Cross-classifications were made by attained age, *a*, in 16 categories ([0, 15], [15, 20), [20, 25), ..., [85, 103] years), individual calendar year, *y*, in 58 categories, cumulative arsenic dust D_a in 8 categories (unknown, [0, 0], (0, 25), [25, 50), [50, 100), [100, 200), [200, 500), [500, 1417] dust-years), cumulative high-LET liver dose D_h in 7 categories ([0, 0], (0, 0.5), [0.5, 1), [1, 2.5), [2.5, 5), [5, 10), [10, 29.2] mGy) and cumulative low-LET liver dose D_l in 7 categories ([0, 0], (0, 10), [10, 25), [25, 50), [50, 100), [100, 250), [250, 1914] mGy). These categories were also used in the categorical analysis. In all analyses including arsenic, the miners for which information was not available ($n = 310$) were excluded from the analysis, including one liver cancer death.

The tabulated data were fitted to the model

$$r(a, y, D) = r_0(a, y)\left[1 + \mathrm{ERR}(D)\right] \tag{1}$$

where $r(a, y, D)$ is the liver cancer mortality rate which depends on age *a*, year *y* and dose or exposure (generically called "*D*", here) and $r_0(a, y) = r(a, y, 0)$ is the baseline disease rate for non-exposed individuals ($D = 0$). A linear form for $\mathrm{ERR}(D) = \beta D$ was used to model the dose-response relationship. In addition, a categorical analysis of the form $\mathrm{RR} = 1 + \mathrm{ERR}(D) = 1 + \sum_j \beta_j D_j$ was performed, where $D_j(D)$ is a window function which is 1 if *D* falls in class *j* and 0 otherwise. RR is the relative risk. Hence the RR for the persons in an arbitrary category is the risk relative to the persons in the reference category of the unexposed persons.

Additionally models which include both low-LET dose D_l and high-LET dose D_h simultaneously were considered where either both entered linearly or one of the two categorically and the other one linearly:

$$r(a, y, D_l, D_h) = r_0(a, y)(1 + \beta_l D_l + \beta_h D_h) \tag{2}$$

Maximum likelihood method performed with the AMFIT module of the EPICURE software (Preston *et al* 1998) was used for the estimation of the fit parameters β of the stratified Poisson regression. All parameters are given here with their 95 % Wald-type confidence intervals (CI). For the parametric models also likelihood-profile CI's were calculated where possible, although their computation frequently did not converge. The confidence intervals did not differ much from the Wald intervals so that only the latter are reported.

3. Results

The cohort comprises 58 987 miners which contributed 2 million person-years in the time span from 1946 to 2003. 86 % of the miners were exposed at any time to low-LET and high-LET with an average absorbed liver dose of 47.9 mGy and 2.4 mGy, respectively (cf. table 2). The yearly mean dose rates and mean doses due to high- and low-LET for exposed miners in the cohort are expounded in figure 1. The pronounced temporal difference between the high- and low-LET doses is due to the high-LET doses (mainly α-radiation) depending only on the exposures to radon, its progeny and LLR, while the low-LET is mainly due to external γ-radiation. In contrast to the exposure to the latter, the exposure to radon, its progeny and LLR was strongly reduced with the introduction of effective ventilation systems in the late nineteen-fifties. While the high-LET doses are on average much lower than the low-LET doses, they may nevertheless be of comparable importance for health risk as the relative biological effectiveness is usually higher (Valentin 2003). With respect to arsenic dust, only 18 234 miners were ever exposed (exposure occurred in Saxonian mines, only). The mean cumulative arsenic dust exposure was 121.2 dust-years. 20 920 persons died from any cause; 159 from liver cancer. The mean (minimum, maximum) age at death from PLC was 65.4 (33.1, 87.9) years. In 37 % of the PLC deaths, liver cirrhosis was documented on the death certificate.

First the risk estimates for each single dose or exposure parameter without further adjustment are presented: In the case of low-LET the ERR/D_l [Gy^{-1}] 0.57, 95 % CI: −1.40; 2.55 was not significantly increased and also the categorical analysis (table 3) showed no systematic variation of risk with dose. In the case of high-LET the ERR/D_h [Gy^{-1}] 32.5 (95 % CI: −23.5; 88.6) was also not significantly increased although its absolute value and range was considerably higher than that for low-LET. The categorical analysis (table 4) showed again no systematic variation of risk with dose. No significant increase of risk of liver cancer was observed in dependence on cumulative arsenic dust exposure (ERR/D_{As} [(100 dust-years)$^{-1}$]= −0.04 (95 % CI: −0.17; 0.09)).

Next, models which contained both radiation doses at the same time were considered: Joint inclusion in a linear fashion of both low-LET and high-LET dose—equivalent to a mutual adjustment of one factor on the other—increased the ERR per unit of dose in the case of high-LET (ERR/D_h [Gy^{-1}] 48.3, 95 % CI:−32.0, 128.6) and led to a decreasing ERR with low-LET dose (ERR/D_l [Gy^{-1}] −0.80, 95 % CI:−3.69, 2.10), however with neither of the two parameters reaching statistical significance. The CI's are not much larger than for models with only one parameter which is in line with the correlation between the two doses being moderate ($r = 0.70$) so that considerable variance inflation is not to be expected. Also a linear adjustment of the categorical analyses on high-LET dose categories by low-LET did not lead to a qualitative change of the categorical estimates (table 4). On the other hand linear adjustment of low-LET categorical analysis by high-LET decreased the risk estimates in the highest low-LET categories considerably (table 3).

Finally, the increase of ERR with equivalent dose $D_{eq} = D_l + 20D_h$ (Valentin 2003) was estimated as ERR/D_{eq} [Sv^{-1}] 0.57, 95 % CI:−0.69, 1.82.

4. Discussion

One of the big advantages of the German uranium miners study is—beside its size—the very detailed information on exposure to radon progeny, long lived radionuclides and external gamma radiation. With the information from the corresponding JEM's, it was possible to calculate organ doses for the different ionizing radiation quantities (low- and high-LET) and estimate separate risk estimates for each of them.

For either type of radiation (low- or high-LET) taken separately, a positive dose-risk relation (ERR/$D_l = 0.57\,\mathrm{Gy}^{-1}$ and ERR/$D_h = 32.5\,\mathrm{Gy}^{-1}$) is found though neither of them is statistically significant. As far as the combined influence of both radiation quantities is concerned, the absence of liver cancer risk due to low-LET dose (ERR/$D_l = -0.80\,\mathrm{Gy}^{-1}$) is consistent with the null result of several studies on liver cancers following X-ray radiotherapy (Weiss *et al* 1994, Kleinerman *et al* 1995, Mattsson *et al* 1997, Carr *et al* 2002). Although in the case of high-LET the adjusted estimate of ERR/$D_h = 48.3\,\mathrm{Gy}^{-1}$ is also not significant, its large value would be in line with the strong increase of PLC with dose due to incorporated alpha emitters as found in the Thorotrast studies (Andersson *et al* 1995, Mori *et al* 1999, van Kaick *et al* 1999). For comparison purposes and radiation protection it is desirable to condense the radiation risk due to both high- and low-LET into a single number. With a weighting factor of 20 for high-LET radiation relative to low-LET radiation, as assumed in the definition of equivalent dose D_{eq} (Valentin 2003), a not statistically significant estimate ERR/$D_{eq} = 0.57\,\mathrm{Sv}^{-1}$ was found.

In miner studies (Darby *et al* 1995, Kreuzer *et al* 2008) quite consistently an increased risk of PLC among miners as compared to the general population is observed. Kreuzer *et al* (2008) found the ratio of observed PLC deaths in the Wismut cohort O[*] corrected for missing causes of death to expected ones E based on the mortality in the East German population in the time span from 1960 to 2003 as O[*]/E=1.26 (95 % CI: 1.07; 1.48). The present results suggest that this observed increase can—at least in this study—not be fully explained by radiation effects but is likely attributable to other risk factors such as increased alcohol consumption in the cohorts. For example in the Wismut cohort alcohol formed part of the miner's remuneration in the very early years.

As in previous analyses (Kreuzer *et al* 2008, Kreuzer *et al* 2010) a lag time of 5 years was assumed. Other times (0, 10, 15, 20 years) were tested, too, but no significant differences were found.

Although the present study comprises a considerable number of PLC deaths ($n = 159$), the liver doses are rather small with a mean of only 48 mGy in case of low-LET radiation and even lower mean for high-LET radiation. Power calculations (cf. UNSCEAR (2008, Annex A, Appendix A)) indicate that numbers of deaths need to be an order of magnitude larger to obtain a power of 80 %. Extension of follow-up and pooling with other cohorts may be future strategies to achieve higher power.

4.1. Misclassification of disease

The epidemiology of PLC faces specific difficulties in comparison with other cancer types, namely the frequent misclassification of PLC (UNSCEAR 2008): "Mortality data [for PLC] are unreliable because the liver is one of the most frequent sites for metastatic cancer. Up to 50 % of liver cancers reported on death certificates are metastatic rather than primary [...]". This makes it quite difficult to assess the radiation dependent risk despite PLC being—at least word wide—a rather common cancer. In the German cohort, about a quarter of all deaths and one third of the PLC deaths were confirmed by autopsy. Thus the problem of misclassification can directly be addressed as for most autopsies a comparison with the causes of death from the clinical report was possible. Deaths in the cohort for which both the clinical result and the result from autopsy were available ($n = 4086$), among them 46 PLC cases, showed (c.f. the 2×2 contingency table 5) that 8 out of 18 deaths with a clinical diagnose of PLC turned out to be other diseases (ICD 10 codes: C16.9, C25.2, C25.9, C34.2, C34.9, K26.4, K74.6, K81.9) among them also 2 cases of lung cancer for which a strong dose-effect relation is well established. This misclassification of lung cancer as liver cancer might constitute an alternative explanation for the rather large ERR per unit of high-LET dose given that the high-LET radiation is a known risk factor for lung cancer (UNSCEAR 2008) and that the lung dose is orders of magnitude higher (mean high-LET lung dose among exposed: 1542.6 mGy) than that of the liver (mean high-LET liver dose among exposed: 2.4 mGy). For low-LET dose, such a bias is not to be expected, as doses are quite comparable (mean low-LET lung dose among exposed: 78.3 mGy; mean liver dose: 47.9 mGy).

The misclassification also occurs in the direction of liver cancers wrongly being diagnosed as other diseases: only 26 % of actual liver cancer cases ($n = 46$) for which both autopsy and clinical result was available, were correctly (or fully) identified on the clinical report. The cases which had not been correctly identified were mainly classified as other hepatic diseases (K70–K77, $n = 16$), unspecified neoplasms (C76.2, C80, $n = 6$), or other types of cancer ($n = 6$).

It is possible that the level of misclassification inferred from this comparison exaggerates the situation actually prevalent in the full cohort as: a) it is likely that autopsies are preferentially performed when the cause of death is uncertain; b) The rate of autopsies was very high (51.7 %) before German re-unification in 1990 but low (7.4 %) afterwards (compare also table 1) so that in the early years the mortality data are mainly based on reliable autopsies; c) Diagnostic progress may have increased the validity of death certificates (La Vecchia *et al* 2000) in the course of time.

4.2. Possible confounding

The prevalence of the main risk factors for PLC, namely infections with HVB and HVC and alcoholism in the cohort could not be assessed quantitatively. The prevalence of HVB and C infections is rather low in Germany (Thierfelder *et al* 2001) as compared to the global mean and the mortality from PLC in the East German population shows very little variation with calendar period, so that larger waves of infections with HVB or C can probably be excluded.

Furthermore, it is hard to imagine a plausible mechanism to generate a correlation of the prevalence of HVB or C and the radiation dose so that it is rather unlikely that these infections constitute strong confounders.

In the case of alcohol, selective information is available on some death certificates ($n = 896$) on alcohol abuse, among them are 13 PLC cases. Table 6 shows the percentage of deaths with documented alcoholism in all deaths with known cause ($n = 19\,588$) in the cohort by high- and low-LET categories. Alcoholism seems to be less frequent in categories with higher doses ($P = 0.049$ for low-LET and $P < 0.0001$ for high-LET; from Cochran–Armitage test (Agresti 2002)) so that confounding would rather result in an underestimation of the radiation risks.

Additive adjustment of low- and high-LET for arsenic hardly changed the ERR/D [Gy^{-1}] estimators to 1.22 (95 % CI: −0.85, 3.29) and to 30.0 (95 % CI: −27.9; 87.8), respectively. Although there is accumulating evidence for a carcinogenic effect of arsenic for liver cancer (Bosch *et al* 1999, Liu and Waalkes 2008, Chiu *et al* 2004, Tapio and Grosche 2006, IARC 2011), this assessment is based mainly on either animal studies or ecological studies on arsenic in drinking water. In the Wismut mines, arsenic dust was composed mainly of badly soluble arsenides (HVBG and BBG 2005), which makes it hard to compare with these kind of studies. In summary major confounding due to arsenic exposure seems unlikely.

Because non-radiation-exposed individuals (workers at the surface) may differ with respect to their lifestyle from exposed individuals, risk analysis was also performed on miners excluding those who had never been exposed in the whole follow up, including 25 PLC deaths. The corresponding adjusted ERR/D_l [Gy^{-1}] is −1.00 and the ERR/D_h [Gy^{-1}] is 67.4 with both estimates not being statistically significant.

5. Conclusion

The German uranium miners cohort study is one of the largest occupational cohorts with information on liver doses due to both high- and low-LET radiation in the low-dose range. It comprises detailed information on both radiation dose and exposure to arsenic. While a statistically insignificant increase of risk with high-LET dose was observed, no such increase was observed with low-LET dose. Hence this cohort provides only weak evidence for an increased PLC mortality risk due to high-LET radiation and no evidence for a risk due to low-LET radiation. The negative outcome may also be the result of the restricted power due to the rather low radiation doses despite the relatively large number of liver cancer deaths ($n = 159$). While confounding by arsenic seems to be only of little importance, possible confounding by alcohol consumption may rather lead to an underestimation of the radiation risk. Misclassification of PLC and of secondary cancer diagnoses, based only on death certificates, are an issue.

Acknowledgments

References

Agresti A 2002 *Categorical Data Analysis* Wiley Series in Probability and Statistics John Wiley & Sons.

Andersson M, Carstensen B and Storm H H 1995 *Radiat. Res.* **142**(3), 305–320.

Bauer H D 2000 *Studie zur retrospektiven Analyse der Belastungssituation im Uranerzbergbau der ehemaligen SDAG Wismut mit Ausnahme der Strahlenbelastung für die Zeit von 1946 bis 1990* Hauptverband der Gewerblichen Berufsgenossenschaften.

Becker N and Wahrendorf J 1998 *Krebsatlas der Bundesrepublik Deutschland 1981–1990. Continuation in the Internet: www.krebsatlas.de* Springer Berlin, Heidelberg, New York.

Bosch F, Ribes J, Borras J *et al* 1999 *Semin. Liver Dis.* **19**(3), 271–85.

Carr Z A, Kleinerman R A, Stovall M, Weinstock R M, Griem M L and Land C E 2002 *Radiat. Res.* **157**(6), 668–677.

Chiu H, Ho S, Wang L, Wu T and Yang C 2004 *J. Toxicol. Environ. Health, Part A* **67**(19), 1491–1500.

Dahmann D, Bauer H D and Stoyke G 2008 *Int. Arch. Occup. Environ. Health* **81**, 949–958.

Darby S C, Whitely E, Howe G R, Hutchings S J, Kusiak R A, Lubin J H, Morrison H I, Tirmarche M, Tomasek L, Radford E P, Roscoe R J, Samet J M and Yao S X 1995 *J. Natl. Cancer Inst.* **87**(5), 378–384.

Ferlay J, Shin H R, Bray F, Forman D, Mathers C and Parkin D M 2010 *Int. J. Cancer* **127**(12), 2893–2917.

Grosche B, Kreuzer M, Kreisheimer M, Schnelzer M and Tschense A 2006 *Br. J. Cancer* **95**(9), 1280–1287.

HVBG and BBG, ed. 2005 *Belastung durch ionisierende Strahlung, Staub und Arsen im Uranerzbergbau der ehemaligen DDR (CD-ROM, Version 8/2005)* Hauptverband der Gewerblichen Berufsgenossenschaften HVBG, St. Augustin and Bergbau BG (BBG), Gera.

IARC, ed. 2004 *Tobacco Smoke and Involuntary Smoking* Vol. 83 of *IARC Monographs on the Evaluation of Carcinogenic Risks to Humans* IARC (International Agency for Research on Cancer) Lyon, France.

IARC, ed. 2011 *A Review of Human Carcinogens. Part C: Arsenic, Metals, Fibres, and Dusts* Vol. 100C of *IARC Monographs on the Evaluation of Carcinogenic Risks to Humans* IARC (International Agency for Research on Cancer) Lyon, France.

ICRP (International Commission on Radiological Protection) 1979 *Ann. ICRP* **2**(3–4), 30–34.

ICRP (International Commission on Radiological Protection) 1994 *Ann. ICRP* **24**(1–3), 1–482.

Kleinerman R A, Boice J D, Storm H H, Sparen P, Andersen A, Pukkala E, Lynch C F, Hankey B F and Flannery J T 1995 *Cancer* **76**(3), 442–452.

Kreuzer M, Grosche B, Schnelzer M, Tschense A, Dufey F and Walsh L 2010 *Radiat. Environ. Biophys.* **49**(2), 177–185.

Kreuzer M, Schnelzer M, Tschense A, Walsh L and Grosche B 2010 *Int. J. Epidemiol* **39**(4), 980–987.

Kreuzer M, Walsh L, Schnelzer M, Tschense A and Grosche B 2008 *Br. J. Cancer* **99**(11), 1946–1953.

La Vecchia C, Lucchini F, Franceschi S, Negri E and Levi F 2000 *Eur. J. Cancer* **36**(7), 909–915.

Laurier D, Tirmarche M, Mitton N, Valenty M, Richard P, Poveda S, Gelas J and Quesne B 2004 *Eur. J. Epidemiol.* **19**(2), 139–146.

Lehmann F, Hambeck L, Linkert K, Lutze H, Meyer H, Reiber H, Reinisch A, Renner H, Seifert T and Wolf F 1998 *Belastung durch ionisierende Strahlung im Uranerzbergbau der ehemaligen DDR: Abschlussbericht zu einem Forschungsvorhaben* Hauptverband der Gewerblichen Berufsgenossenschaften St. Augustin.

Liu J and Waalkes M P 2008 *Toxicol. Sci.* **105**(1), 24–32.

Marsh J W, Bessa Y, Birchall A, Blanchardon E, Hofmann W, Nosske D and Tomasek L 2008 *Radiat. Prot. Dosimetry* **130**(1), 101–106.

Marsh J W, Blanchardon E, Gregoratto D, Hofmann W, Karcher K, Nosske D and Tomášek L 2011 *Radiat. Prot. Dosimetry* **149**(4), 371–383.

Mattsson A, Hall P, Rudén B I and Rutqvist L E 1997 *Radiat. Res.* **148**(2), 152–160.

Mori T, Kido C, Fukutomi K, Kato Y, Hatakeyama S, Machinami R, Ishikawa Y, Kumatori T, Sasaki F and Hirota Y 1999 *Radiat. Res.* **152**(6s), 84–87.

Preston D L, Lubin J H, Pierce D A and McConney M E 1998 Epicure Release 2.10 Technical report HiroSoft International Seattle.

Preston D L, Ron E, Tokuoka S, Funamoto S, Nishi N, Soda M, Mabuchi K and Kodama K 2007 *Radiat. Res.* **168**(1), 1–64.

Tapio S and Grosche B 2006 *Mutat. Res.* **612**(3), 215–246.

Thierfelder W, Hellenbrand W, Meisel H, Schreier E and Dortschy R 2001 *Eur. J. Epidemiol.* **17**, 429–435.

UNSCEAR (United Nations Scientific Committee on the Effects of Atomic Radiation), ed. 2008 *Effects of ionizing radiation: UNSCEAR 2006 report to the General Assembly, with scientific annexes* Vol. I United Nations Pubs.

Vacquier B, Caer S, Rogel A, Feurprier M, Tirmarche M, Luccioni C, Quesne B, Acker A and Laurier D 2008 *Occup Environ Med* **65**(9), 597–604.

Valentin J 2003 *Ann. ICRP* **33**(4), 1–121.

van Kaick G, Dalheimer A, Hornik S, Kaul A, Liebermann D, Lührs H, Spiethoff A, Wegener K and Wesch H 1999 *Radiat. Res.* **152**(6s), S64–S71.

Walsh L, Dufey F, Möhner M, Schnelzer M, Tschense A and Kreuzer M 2011 *Radiat. Environ. Biophys* **50**(1), 57–66.

Weiss H A, Darby S C and Doll R 1994 *Int. J. Cancer* **59**(3), 327–338.

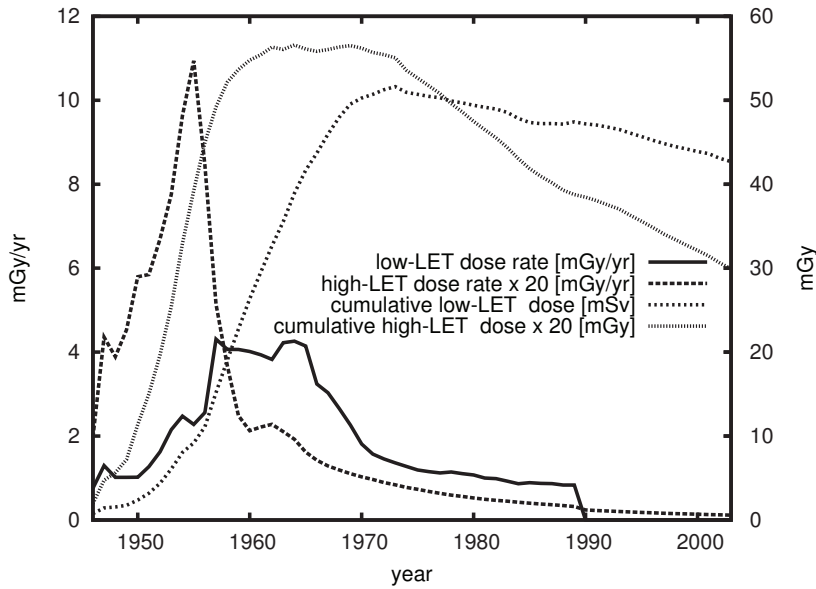**Figure 1.** Distribution of the mean absorbed liver dose rates and cumulative doses due to high- and low-LET radiation by calendar year for radiation exposed miners in the Wismut cohort. High-LET doses are only due to radon, radon progeny and long lived radionuclide exposure while low-LET dose is mainly due to external gamma radiation. Both high-LET doses and dose rates have been scaled by a factor of 20 for better visibility.

Table 1. Main characteristics of the cohort and distribution of liver cancer deaths by calendar year and age categories, 1946–2003.

Number of subjects	58 987
Person-years	1 996 959
Deceased miners	20 920
Alive	35 294
Loss to follow-up	2 773
Causes of death available	19 588
Liver cancer deaths	159
Mean (min, max) duration of follow up [yrs]	34 (0, 58)
Mean (min, max) duration of employment [yrs]	14 (0.5, 46)
Mean (min, max) age at first employment [yrs]	24 (13, 68)

Period	# PLC[a] / # PLC by autopsy
1946–1969	5 / 3
1970–1979	15 / 13
1980–1989	33 / 23
1990–1999	73 / 12
2000–2003	33 / 2

Age at death [yrs]	# PLC
<55	21
55–64	54
65–74	53
≥75	31

[a]PLC: Primary liver cancer.

Table 2. Mean and maximal cumulative exposure or liver dose for high-LET[a], low-LET, radon progeny, long lived radionuclides, gamma radiation and arsenic dust among exposed cohort members, 1946–2003.

exposure or dose	# of exposed[b]	mean	maximum
high-LET [mGy]	50 772	2.4	29.2
low-LET [mGy]	50 772	47.9	913.5
Radon progeny [WLM[c]]	50 773	280	3 224
Radon progeny [mGy]	50 772	1.1	16.2
Radon Gas [mGy]	50 772	1.0	10.8
Long lived radionuclides [kBq h m^{-3}]	50 761	4	132
Long lived radionuclides [mGy]	50 671	0.8	23.0
Gamma radiation [mSv]	50 761	47	909
Arsenic dust [dust-years[d]]	18 234	121.2	1 417.4

[a]LET: linear energy transfer.

[b]Differences in the number of exposed persons and persons with nonzero dose are due to exposure values having to be rounded to 3 decimals on input to the dosimetry software which results in some persons with minimal exposures to get zero dose.

[c]WLM: working level month.

[d]dust-year: one dust year of arsenic corresponds to an exposure to 1 μg of arsenic during 220 shifts of 8 h.

Table 3. Relative risk for liver cancer death by low-LET[a] dose categories and linear increase in ERR[b] with low-LET dose; also adjusted for high-LET dose.

low-LET category [mGy]	mean low-LET [mGy]	person time [1000 years]	# deaths	RR[c] (95 % CI[d])	RR adjusted for high-LET (95 % CI)
[0, 0]	0.0	505	25	1	1
(0, 10)	3.8	633	35	0.80 (0.39, 1.22)	0.77 (0.36, 1.17)
[10, 25)	16.4	306	25	0.84 (0.37, 1.32)	0.72 (0.27, 1.17)
[25, 50)	35.8	218	30	1.12 (0.52, 1.72)	0.95 (0.36, 1.53)
[50, 100)	70.4	159	16	0.76 (0.28, 1.24)	0.52 (0.02, 1.02)
[100, 250)	156.8	123	18	1.01 (0.39, 1.63)	0.54 (0[e], 1.18)
[250, 1 914]	342.9	52	10	0.99 (0.25, 1.72)	0.44 (0[e], 1.31)
[0, 1 914]	31.8	1 997	159	–	–
ERR/D_l[f] [Gy^{-1}]				0.57 (−1.40, 2.55)	−0.80 (−3.69, 2.10)

Poisson regression stratified on age and calendar year.

[a]LET: linear energy transfer.

[b]ERR: excess relative risk.

[c]RR: relative risk.

[d]CI: confidence interval.

[e]Lower Wald bounds are < 0.

[f]ERR/D_l: linear variation of excess relative risk with low-LET dose.

Table 4. Relative risk for liver cancer death by high-LET[a] dose categories and linear increase in ERR[b] with high-LET dose; also adjusted for low-LET dose.

high-LET category [mGy]	mean high-LET [mGy]	person time [1000 years]	# deaths	RR[c] (95 % CI[d])	RR adjusted for low-LET (95 % CI)
[0, 0]	0.00	505	25	1.00	1.00
(0, 0.5)	0.14	699	32	0.83 (0.39, 1.28)	0.84 (0.39, 1.28)
[0.5, 1)	0.72	162	18	0.99 (0.39, 1.60)	1.01 (0.40, 1.62)
[1, 2.5)	1.63	220	14	0.50 (0.17, 0.83)	0.54 (0.19, 0.89)
[2.5, 5)	3.63	184	22	0.87 (0.37, 1.38)	0.91 (0.38, 1.45)
[5, 10)	7.07	166	36	1.39 (0.67, 2.12)	1.54 (0.72, 2.37)
[10, 29.2]	12.83	60	12	0.94 (0.28, 1.59)	1.16 (0.27, 2.04)
[0, 29.2]	1.59	1 997	159	–	–
ERR/D_h[e] [Gy^{-1}]				32.52 (−23.51, 88.56)	48.30 (−32.00, 128.60)

Poisson regression stratified on age and calendar year.
[a]LET: linear energy transfer.
[b]ERR: excess relative risk.
[c]RR: relative risk.
[d]CI: confidence interval.
[e]ERR/D_h: Linear variation of excess relative risk with high-LET dose.

Table 5. 2×2 contingency table showing the distribution of primary liver cancer diagnoses among those deaths for which both a clinical result and the result of autopsy are documented.

		autopsy		row sum
		yes	no	
clinical	yes	10	8	18
result	no	33	4035	4068
column sum		43	4043	4086

Table 6. Number of deaths with known cause and documented alcoholism and total number of deaths with known cause by high- and low-LET[a] categories.

low-LET category [Gy^{-1}]	# alcoholics/ # all	%	high-LET category [Gy^{-1}]	# alcoholics/ # all	%
[0, 0]	113/ 2 872	3.93	[0, 0]	113/ 2 872	3.93
(0, 10)	270/ 4 325	6.24	(0, 0.5)	322/ 3 840	8.39
[10, 25)	161/ 3 290	4.89	[0.5, 1)	97/ 1 721	5.64
[25, 50)	113/ 3 146	3.59	[1, 2.5)	136/ 2 907	4.68
[50, 100)	100/ 2 535	3.94	[2.5, 5)	75/ 2 827	2.65
[100, 250)	85/ 2 306	3.69	[5, 10)	98/ 3 521	2.78
[250, 1 914]	54/ 1 114	4.85	[10, 29.2]	55/ 1 900	2.89
[0, 1 914]	896/ 19 588	4.57	[0, 29.2]	896/ 19 588	4.57

[a]LET: linear energy transfer.

APPENDIX.

Copies of the candidate's degree certificates

THE VICTORIA
UNIVERSITY OF MANCHESTER

Degree of

Doctor of Philosophy

It is hereby certified that

Linda Grimshaw

has been duly admitted as a DOCTOR OF PHILOSOPHY of this University.

K. E. Kitchen ———— Registrar.

(The Doctor is requested to sign here.) *Linda Grimshaw*

November 7th. 1985

THE VICTORIA
UNIVERSITY OF MANCHESTER

Degree of

Master of Science

in the Faculty of Science

It is hereby certified that

Linda Grimshaw

has been duly admitted as a MASTER OF SCIENCE of this University.

K. S. Kitchen   Registrar.

(The Master is requested to sign here.)   *Linda Grimshaw.*

December 11th, 1980.

37253-5-77

THE VICTORIA
UNIVERSITY OF MANCHESTER

Degree of

Bachelor of Science

in the Faculty of Science

It is hereby certified that

Linda Grimshaw

has satisfied the Examiners in the Final Examination in the Honours

School of _Physics_ for the above-

named Degree, being placed in the Second Class, Division _Two_, and

has been duly admitted as a BACHELOR OF SCIENCE in the Faculty of

Science of this University.

Registrar.

(The Bachelor is requested to sign here.) _Linda Grimshaw._

July 9th. 1979

37286.5-77